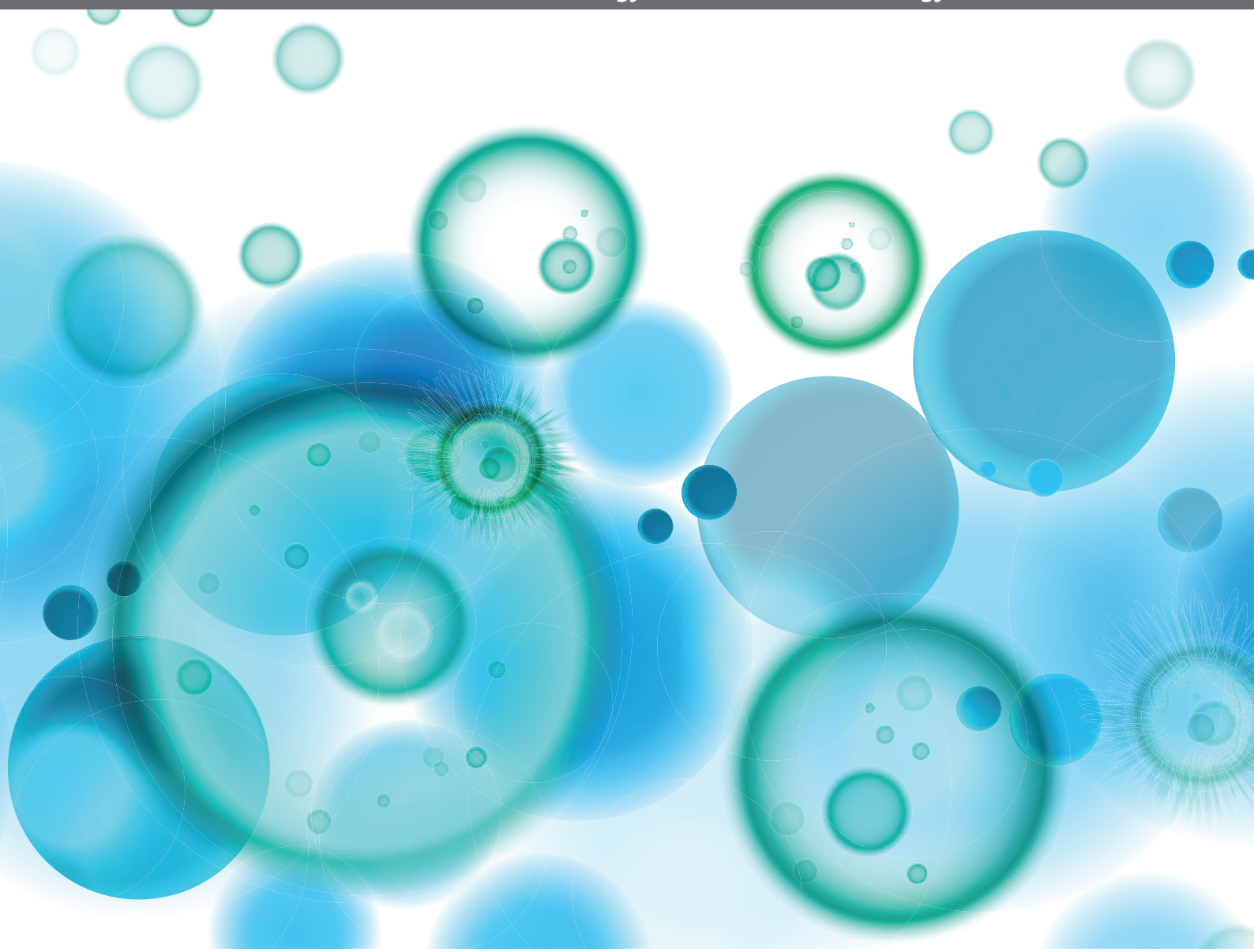
CANCER VACCINES: TIME TO THINK DIFFERENTLY!

EDITED BY: Stephanie E. B. McArdle, Alan Graham Pockley, Pål Johansen and Graham Pawelec

PUBLISHED IN: Frontiers in Immunology and Frontiers in Oncology



frontiers Research Topics



frontiers

Frontiers eBook Copyright Statement

The copyright in the text of individual articles in this eBook is the property of their respective authors or their respective institutions or funders. The copyright in graphics and images within each article may be subject to copyright of other parties. In both cases this is subject to a license granted to Frontiers.

The compilation of articles constituting this eBook is the property of Frontiers.

Each article within this eBook, and the eBook itself, are published under the most recent version of the Creative Commons CC-BY licence. The version current at the date of publication of this eBook is CC-BY 4.0. If the CC-BY licence is updated, the licence granted by Frontiers is automatically updated to the new version.

When exercising any right under the CC-BY licence, Frontiers must be attributed as the original publisher of the article or eBook, as applicable.

Authors have the responsibility of ensuring that any graphics or other materials which are the property of others may be included in the CC-BY licence, but this should be checked before relying on the CC-BY licence to reproduce those materials. Any copyright notices relating to those materials must be complied with.

Copyright and source acknowledgement notices may not be removed and must be displayed in any copy, derivative work or partial copy which includes the elements in question.

All copyright, and all rights therein, are protected by national and international copyright laws. The above represents a summary only. For further information please read Frontiers' Conditions for Website Use and Copyright Statement, and the applicable CC-BY licence.

ISSN 1664-8714
ISBN 978-2-88971-729-3
DOI 10.3389/978-2-88971-729-3

About Frontiers

Frontiers is more than just an open-access publisher of scholarly articles: it is a pioneering approach to the world of academia, radically improving the way scholarly research is managed. The grand vision of Frontiers is a world where all people have an equal opportunity to seek, share and generate knowledge. Frontiers provides immediate and permanent online open access to all its publications, but this alone is not enough to realize our grand goals.

Frontiers Journal Series

The Frontiers Journal Series is a multi-tier and interdisciplinary set of open-access, online journals, promising a paradigm shift from the current review, selection and dissemination processes in academic publishing. All Frontiers journals are driven by researchers for researchers; therefore, they constitute a service to the scholarly community. At the same time, the Frontiers Journal Series operates on a revolutionary invention, the tiered publishing system, initially addressing specific communities of scholars, and gradually climbing up to broader public understanding, thus serving the interests of the lay society, too.

Dedication to Quality

Each Frontiers article is a landmark of the highest quality, thanks to genuinely collaborative interactions between authors and review editors, who include some of the world's best academicians. Research must be certified by peers before entering a stream of knowledge that may eventually reach the public - and shape society; therefore, Frontiers only applies the most rigorous and unbiased reviews.
Frontiers revolutionizes research publishing by freely delivering the most outstanding research, evaluated with no bias from both the academic and social point of view. By applying the most advanced information technologies, Frontiers is catapulting scholarly publishing into a new generation.

What are Frontiers Research Topics?

Frontiers Research Topics are very popular trademarks of the Frontiers Journals Series: they are collections of at least ten articles, all centered on a particular subject. With their unique mix of varied contributions from Original Research to Review Articles, Frontiers Research Topics unify the most influential researchers, the latest key findings and historical advances in a hot research area! Find out more on how to host your own Frontiers Research Topic or contribute to one as an author by contacting the Frontiers Editorial Office: frontiersin.org/about/contact

CANCER VACCINES: TIME TO THINK DIFFERENTLY!

Topic Editors:
Stephanie E. B. McArdle, Nottingham Trent University, United Kingdom
Alan Graham Pockley, Nottingham Trent University, United Kingdom
Pål Johansen, University of Zurich, Switzerland
Graham Pawelec, University of Tübingen, Germany

Citation: McArdle, S. E. B., Pockley, A. G., Johansen, P., Pawelec, G., eds. (2021). Cancer Vaccines: Time to Think Differently!. Lausanne: Frontiers Media SA.
doi: 10.3389/978-2-88971-729-3

Table of Contents

05 ***Editorial: Frontiers' Research Topic "Cancer Vaccines: Time to Think Differently!"***
Stephanie E. B. McArdle, Graham Pawelec, Alan Graham Pockley and Pål Johansen

07 ***Treatment and Prevention of Lung Cancer Using a Virus-Infected Reprogrammed Somatic Cell-Derived Tumor Cell Vaccination (VIReST) Regime***
Zhe Zhang, Shuangshuang Lu, Louisa S. Chard Dunmall, Zhizhong Wang, Zhenguo Cheng, Zhongxian Zhang, Wenli Yan, Yongchao Chu, Dongling Gao, Na Wang, Yang Li, Jiwei Wang, Yuenan Li, Yupei Ji, Danyang Shan, Keke Li, Panpan Wang, Yunshu Dong, Jianzeng Dong, Nick R. Lemoine, Duanqing Pei, Lirong Zhang and Yaohe Wang

24 ***Mature Dendritic Cells May Promote High-Avidity Tuning of Vaccine T Cell Responses***
Adarsh Kumbhari, Colt A. Egelston, Peter P. Lee and Peter S. Kim

38 ***Induction of Progenitor Exhausted Tissue-Resident Memory CD8$^+$ T Cells Upon* Salmonella *Typhi Porins Adjuvant Immunization Correlates With Melanoma Control and Anti-PD-1 Immunotherapy Cooperation***
Ricardo A. León-Letelier, Daniel I. Castro-Medina, Oscar Badillo-Godinez, Araceli Tepale-Segura, Enrique Huanosta-Murillo, Cristina Aguilar-Flores, Saraí G. De León-Rodríguez, Alejandra Mantilla, Ezequiel M. Fuentes-Pananá, Constantino López-Macías and Laura C. Bonifaz

59 ***Tumor-Specific Antibody, Cetuximab, Enhances the* In Situ *Vaccine Effect of Radiation in Immunologically Cold Head and Neck Squamous Cell Carcinoma***
Won Jong Jin, Amy K. Erbe, Ciara N. Schwarz, Abigail A. Jaquish, Bryce R. Anderson, Raghava N. Sriramaneni, Justin C. Jagodinsky, Amber M. Bates, Paul A. Clark, Trang Le, Keng-Hsueh Lan, Yi Chen, KyungMann Kim and Zachary S. Morris

75 ***Photochemical Internalization Enhanced Vaccination Is Safe, and Gives Promising Cellular Immune Responses to an HPV Peptide-Based Vaccine in a Phase I Clinical Study in Healthy Volunteers***
Tone Otterhaug, Sylvia Janetzki, Marij J. P. Welters, Monika Håkerud, Anne Grete Nedberg, Victoria Tudor Edwards, Sanne Boekestijn, Nikki M. Loof, Pål Kristian Selbo, Hans Olivecrona, Sjoerd H. van der Burg and Anders Høgset

91 ***Thymoproteasome-Expressing Mesenchymal Stromal Cells Confer Protective Anti-Tumor Immunity* via *Cross-Priming of Endogenous Dendritic Cells***
Jean-Pierre Bikorimana, Nehme El-Hachem, Abed El-Hakim El-Kadiry, Jamilah Abusarah, Natasha Salame, Riam Shammaa and Moutih Rafei

103 ***Enhancing the Efficacy of Tumor Vaccines Based on Immune Evasion Mechanisms***
Jianyu Chen, Honghao Zhang, Lijuan Zhou, Yuxing Hu, Meifang Li, Yanjie He and Yuhua Li

117 ***In-Depth Analysis of the Impact of Different Serum-Free Media on the Production of Clinical Grade Dendritic Cells for Cancer Immunotherapy***
João Calmeiro, Luís Mendes, Iola F. Duarte, Catarina Leitão, Adriana R. Tavares, Daniel Alexandre Ferreira, Célia Gomes, João Serra, Amílcar Falcão, Maria Teresa Cruz, Mylène A. Carrascal and Bruno Miguel Neves

134 ***Discordance Between the Predicted Versus the Actually Recognized CD8+ T Cell Epitopes of HCMV pp65 Antigen and Aleatory Epitope Dominance***
Alexander A. Lehmann, Ting Zhang, Pedro A. Reche and Paul V. Lehmann

148 ***Dendritic Cell-Based Immunotherapy in Lung Cancer***
Dieter Stevens, Joline Ingels, Sandra Van Lint, Bart Vandekerckhove and Karim Vermaelen

174 ***Cancer Vaccines: Adjuvant Potency, Importance of Age, Lifestyle, and Treatments***
Stefania Cuzzubbo, Sara Mangsbo, Divya Nagarajan, Kinana Habra, Alan Graham Pockley and Stephanie E. B. McArdle

199 ***Prophylactic Cancer Vaccines Engineered to Elicit Specific Adaptive Immune Response***
Davis W. Crews, Jenna A. Dombroski and Michael R. King

213 ***Cancer Vaccines, Adjuvants, and Delivery Systems***
Samantha J. Paston, Victoria A. Brentville, Peter Symonds and Lindy G. Durrant

234 ***Immune Modulation Plus Tumor Ablation: Adjuvants and Antibodies to Prime and Boost Anti-Tumor Immunity* In Situ**
Renske J. E. van den Bijgaart, Fabian Schuurmans, Jurgen J. Fütterer, Marcel Verheij, Lenneke A. M. Cornelissen and Gosse J. Adema

248 ***Clinical Experience and Recent Advances in the Development of* Listeria-*Based Tumor Immunotherapies***
Mariam Oladejo, Yvonne Paterson and Laurence M. Wood

266 ***A Novel HAGE/WT1-ImmunoBody® Vaccine Combination Enhances Anti-Tumour Responses When Compared to Either Vaccine Alone***
Rukaia Almshayakhchi, Divya Nagarajan, Jayakumar Vadakekolathu, Barbara-Ann Guinn, Stephen Reeder, Victoria Brentville, Rachael Metheringham, A. Graham Pockley, Lindy Durrant and Stephanie McArdle

frontiers in Immunology

EDITORIAL
published: 15 October 2021
doi: 10.3389/fimmu.2021.771319

Editorial: Frontiers' Research Topic "Cancer Vaccines: Time to Think Differently!"

Stephanie E. B. McArdle[1,2*], *Graham Pawelec*[3,4], *Alan Graham Pockley*[1,2] *and Pål Johansen*[5]

[1] John Van Geest Cancer Research Centre, Nottingham Trent University, Nottingham, United Kingdom, [2] Centre for Health, Ageing and Understanding Disease (CHAUD), School of Science and Technology, Nottingham Trent University, Nottingham, United Kingdom, [3] Department of Immunology, Institute for Cell Biology, University of Tuebingen, Tuebingen, Germany, [4] Cancer Solutions Program, Health Sciences North Research Institute (HSNRI), Sudbury, ON, Canada, [5] Department of Dermatology, University Hospital Zurich, Zurich, Switzerland

Keywords: combined immunotherapies, cancer vaccine combination, novel approach, dendritic cells, PD1 and PDL1

Editorial on the Research Topic:

Cancer Vaccines: Time to Think Differently!

Although the advent of checkpoint inhibitors has revolutionised immunotherapy, the surge of optimism has been quickly dampened by the fact that only some cancers and only a proportion of cancer patients truly benefit from these treatments when they are administered as a monotherapy. The era of combined therapy is now upon us and many clinical trials are now combining drugs, vaccines and checkpoint inhibitors with the aim to amplify the ability of the immune system to recognize and eradicate cancer. This Frontiers Research Topic entitled "Cancer vaccines: Time to think differently!" has collated 16 contributions from experts who are exploring a range of novel treatment approaches that are centred on vaccine-based approaches for triggering protective anti-cancer immunity in pre-clinical animal models and patients.

In a mouse model of head and neck squamous cell carcinoma, Jin et al. show that combining radiation and cetuximab (an epidermal growth factor receptor inhibitor) increased intra-tumoral infiltration of NK cells and $CD8^+$ T cell and enhanced the expression of PD-L1 (checkpoint pathway ligand) by tumour cells. As a consequence, this heightened the susceptibility of the tumour to PD-L1 antibody treatment and thereby increased durable tumour regression and the survival of mice when all three treatments were combined. However, this is only one example of many new and different strategies that are currently being investigated, as has been highlighted in the review article by Chen et al. Although the current focus is very much on 'checkpoint blockade', there is no doubt that future combination strategies are likely to include metabolic and epigenetic therapies to circumvent immune escape mechanisms and block intricate immunosuppressive mechanisms in the tumour microenvironment (TME), as discussed by Chen et al. or the use of *in situ* ablation, as discussed by van den Bijgaart et al.

The successful application of platforms employing mRNA-based cancer vaccine technology to SARS-CoV-2 vaccines and the remarkable success of these mRNA-based formulations against COVID-19 has once again highlighted the potency of this novel approach in cancer. This success has reawakened awareness of the potential potency of earlier approaches to vaccines such as the use of dendritic cells (DCs), as shown by Kumbhari et al. who has used a theoretical approach which applies a mathematical model and simulations to demonstrate how vaccine-induced avidity selection

OPEN ACCESS

Edited and reviewed by:
Denise L. Doolan, James Cook University, Australia

***Correspondence:**
Stephanie E. B. McArdle
stephanie.mcardle@ntu.ac.uk

Specialty section:
This article was submitted to Vaccines and Molecular Therapeutics, a section of the journal Frontiers in Immunology

Received: *06 September 2021*
Accepted: *13 September 2021*
Published: *15 October 2021*

Citation:
McArdle SEB, Pawelec G, Pockley AG and Johansen P (2021) Editorial: Frontiers' Research Topic "Cancer Vaccines: Time to Think Differently!" Front. Immunol. 12:771319. doi: 10.3389/fimmu.2021.771319

can influence tumour clearance. They showed that treatment with immature DCs has the potential to promote the selective expansion of high-avidity cytotoxic T lymphocytes (CTLs) and lead to tumour regression. "Classical" approaches to the generation of DCs for use in immunotherapy may also still leave room for improvement, as discussed by Calmeiro et al. Alternatively, using delivery systems such as the DNA-based ImmunoBody® which directly targets immature DCs *in vivo* offers the opportunity to simultaneously trigger immunity to two antigens, HAGE and WT1, as described by Almshayakhchi et al. Although predicted epitopes derived from vaccines can be used to monitor $CD8^+$ T cell responses *ex vivo* in clinical trial settings as a means to gauge the success of T cell vaccines, Lehmann et al. showed that there was no correlation between the ranking of epitopes on the prediction scale and their actual immune dominance. One would therefore need to screen large vaccine-derived peptide pools to increase the accuracy of the targeted response.

Data from murine models presented by Bikorimana et al. demonstrate that thymoproteasome-based proteasomal alterations can trigger potent T cell immunity when used as part of an engineered mesenchymal stromal cell-based vaccine. Although vaccination led to the recruitment of macrophages and DCs, the immunotherapeutic effect was mediated by cross-priming-dependent DCs. It was also noted that an interaction between vaccine and monocytes/macrophages impaired T cell activation, as a consequence of which the depletion of monocytes/macrophages prior to vaccination increased efficacy. In an additional article on the use of DC-based vaccines, Stevens et al. review nearly 20 years of DC-based immunotherapy in lung cancer. They conclude that combining DC-based immunotherapy with other cancer therapies, such as chemotherapy, radiotherapy and/or checkpoint inhibition may potentially improve vaccine efficacy. Clinical studies testing these hypotheses are underway.

Alternative new and previously considered cancer vaccine delivery approaches are also being (re)-evaluated and discussed in the field. Oladejo et al. consider *Listeria monocytogenes* as a vaccine vector. They discuss recent clinical experience with Listeria-based immunotherapies and recent advances in the development of improved Listeria-based vaccine platforms and their utilization. In an elegant approach by Otterhaug et al., a subunit cancer vaccine is combined with a photochemical compound in a so-called photochemical internalisation (PCI). The intradermal administration of the vaccine is followed by its uptake into skin antigen presenting cells (APCs). Subsequent light treatment disrupts vaccine-containing endosomes and triggers the release of antigen to the cytosol for presentation to major histocompatibility (MHC) class I molecules and stimulation of $CD8^+$ T cell responses. This first-in-human phase I study in healthy volunteers assessed safety, tolerability, and immune responses to PCI vaccination in combination with the adjuvant poly-ICLC. Another approach to cancer vaccination is presented by Zhang et al. who describe a personalized vaccination regime that could be applied for both the therapeutic and prophylactic treatment of lung cancer. This is based on the derivation of lung cancer cells from induced pluripotent stem cells (iPSCs), which are modified to express Cre-dependent tumour antigens. Subsequent viral delivery (e.g. *via* Adenovirus) of Cre activated exogenous driver mutations and resulted in the transformation of lung cancer cells. This "Virus-Infected Reprogrammed Somatic cell-derived Tumour cell vaccination" (VIReST), primed tumour-specific T cell responses that significantly prolonged survival in mouse models of lung cancer.

Finally, a vaccine cannot be better than its adjuvant. Especially in the context of cancer vaccines, the strength and quality of adjuvants is essential if one is to overcome the self-tolerance barrier of barely immunogenic tumour antigens. As discussed by Cuzzubo et al., the use of carefully selected adjuvants to improve vaccine potency in older patients becomes crucial and although some cancers can be completely protected against by vaccinating early in life, as discussed by Crews et al., the majority will rely on the use of adjuvants capable of inducing efficient and long lasting T_{RM} cells. These may have a progenitor exhausted phenotype such as the one described by León-Letelier et al., which have been shown to control the disease and lead to better responses to PD-1 immunotherapy. Adjuvants may also offer a means to overcome the immune suppressive TME, as discussed by Paston et al.

Cancer develops over many years during which time cells have accumulated numerous genetic alterations and been continuously "sculpted"/modified by the immune system. This leads to the emergence of one fully malignant escapee which then goes on to form a tumour having an immunosuppressive TME. However, although one fully malignant cell represents the origin of tumour growth and spread, many other cells at different stages of potential disease progression remain even if the tumour has been cured. Hence, in addition to the challenging task of eliminating the primary tumour to prevent metastasis and relapse, future treatments will have to take this into consideration. There is no longer any doubt that our lifestyle and age will affect our immune system and the entirety of the soma, all of which will influence our ability to respond to novel combinatorial treatments such as those detailed in this Research Topic. It is our firm belief that we will not be able to cure/eradicate cancer unless we are able to harness ways to implement a more holistic approach to cancer treatments (and cancer prevention in the first place).

AUTHOR CONTRIBUTIONS

All authors listed have made a substantial, direct, and intellectual contribution to the work and approved it for publication.

Conflict of Interest: The authors declare that the research was conducted in the absence of any commercial or financial relationships that could be construed as a potential conflict of interest.

Publisher's Note: All claims expressed in this article are solely those of the authors and do not necessarily represent those of their affiliated organizations, or those of the publisher, the editors and the reviewers. Any product that may be evaluated in this article, or claim that may be made by its manufacturer, is not guaranteed or endorsed by the publisher.

Copyright © 2021 McArdle, Pawelec, Pockley and Johansen. This is an open-access article distributed under the terms of the Creative Commons Attribution License (CC BY). The use, distribution or reproduction in other forums is permitted, provided the original author(s) and the copyright owner(s) are credited and that the original publication in this journal is cited, in accordance with accepted academic practice. No use, distribution or reproduction is permitted which does not comply with these terms.

frontiers in Immunology

ORIGINAL RESEARCH
published: 13 August 2020
doi: 10.3389/fimmu.2020.01996

Treatment and Prevention of Lung Cancer Using a Virus-Infected Reprogrammed Somatic Cell-Derived Tumor Cell Vaccination (VIReST) Regime

Zhe Zhang[1], Shuangshuang Lu[2], Louisa S. Chard Dunmall[3], Zhizhong Wang[2], Zhenguo Cheng[2], Zhongxian Zhang[2], Wenli Yan[2], Yongchao Chu[2], Dongling Gao[2], Na Wang[2], Yang Li[2], Jiwei Wang[2], Yuenan Li[2], Yupei Ji[2], Danyang Shan[2], Keke Li[2], Panpan Wang[2], Yunshu Dong[4], Jianzeng Dong[5], Nick R. Lemoine[2,3], Duanqing Pei[6], Lirong Zhang[7] and Yaohe Wang[2,3]**

[1] National Center for International Research in Cell and Gene Therapy, Sino-British Research Centre for Molecular Oncology, School of Basic Medical Sciences, Academy of Medical Sciences, Zhengzhou University, Zhengzhou, China, [2] National Center for International Research in Cell and Gene Therapy, Sino-British Research Centre for Molecular Oncology, Academy of Medical Sciences, Zhengzhou University, Zhengzhou, China, [3] Centre for Biomarkers and Biotherapeutics, Barts Cancer Institute, Queen Mary University of London, London, United Kingdom, [4] CAS Key Laboratory of Infection and Immunity, Institute of Biophysics, Chinese Academy of Sciences, Beijing, China, [5] Department of Cardiology, Beijing Anzhen Hospital, Capital Medical University, Beijing, China, [6] CAS Key Laboratory of Regenerative Biology, South China Institute for Stem Cell Biology and Regenerative Medicine, Guangzhou Institutes of Biomedicine and Health, Chinese Academy of Sciences, Guangzhou, China, [7] School of Basic Medical Sciences, Academy of Medical Sciences, Zhengzhou University, Zhengzhou, China*

OPEN ACCESS

Edited by:
Alan Graham Pockley, Nottingham Trent University, United Kingdom

Reviewed by:
Bart Vandekerckhove, Ghent University, Belgium
Munitta Muthana, The University of Sheffield, United Kingdom

***Correspondence:**
Lirong Zhang
lrzhang@zzu.edu.cn
Yaohe Wang
yaohe.wang@qmul.ac.uk

Specialty section:
This article was submitted to Cancer Immunity and Immunotherapy, a section of the journal Frontiers in Immunology

Received: *23 March 2020*
Accepted: *23 July 2020*
Published: *13 August 2020*

Citation:
Zhang Z, Lu S, Dunmall LSC, Wang Z, Cheng Z, Zhang Z, Yan W, Chu Y, Gao D, Wang N, Li Y, Wang J, Li Y, Ji Y, Shan D, Li K, Wang P, Dong Y, Dong J, Lemoine NR, Pei D, Zhang L and Wang Y (2020) Treatment and Prevention of Lung Cancer Using a Virus-Infected Reprogrammed Somatic Cell-Derived Tumor Cell Vaccination (VIReST) Regime. Front. Immunol. 11:1996. doi: 10.3389/fimmu.2020.01996

Lung cancer is one of the most commonly diagnosed cancer and despite therapeutic advances, mortality remains high. The long period of clinical latency associated with lung cancer provides an ideal window of opportunity to administer vaccines to at-risk individuals that can prevent tumor progression and initiate long-term anti-tumor immune surveillance. Here we describe a personalized vaccination regime that could be applied for both therapeutic and prophylactic prevention of lung cancer, based on the derivation of lung cancer cells from induced pluripotent stem cells. Stem cells from healthy mice were modified to express Cre-dependent $KRAS^{G12D}$ and $Trp53^{R172H}$ prior to differentiation to lung progenitor cells. Subsequent viral delivery of Cre caused activation of exogenous driver mutations, resulting in transformation and development of lung cancer cells. iPSC-derived lung cancer cells were highly antigenically related to lung cancer cells induced in LSL-$KRAS^{G12D/+}$; $Trp53^{R172H/+}$ transgenic mice and were antigenically unrelated to original pluripotent stem cells or pancreatic cancer cells derived using the same technological platform. For vaccination, induced lung cancer cells were infected with oncolytic Adenovirus or Vaccinia virus, to act as vaccine adjuvants, prior to delivery of vaccines sequentially to a murine inducible transgenic model of lung cancer. Application of this Virus-Infected, Reprogrammed Somatic cell-derived Tumor cell (VIReST) regime primed tumor-specific T cell responses that significantly prolonged

survival in both subcutaneous post-vaccine challenge models and induced transgenic models of lung cancer, demonstrating that stem cell-derived prophylactic vaccines may be a feasible intervention for treatment or prevention of lung cancer development in at-risk individuals.

Keywords: lung cancer, vaccine, induced pluripotent stem cells, KRAS, TP53, adenovirus, Vaccinia virus, neo-antigen

INTRODUCTION

Lung cancer remains one of the most fatal malignant tumors. The 2018 GLOBOCAN report suggested that lung cancer is the most commonly diagnosed cancer (11.6% of total cases) and the leading cause of cancer death (18.4% of total cancer deaths) (1) and despite advances in therapeutic approaches, the 5 year survival rate is 16% for the majority of patients whose tumor is not diagnosed at an early, localized stage (2).

Recent immunotherapeutic approaches for the treatment of lung cancer have investigated therapeutic vaccination as a method of controlling disease progression. Theoretically, vaccination strategies are a promising therapeutic option as they can provoke an anergic immune system to activation against one or more tumor cell antigens, resulting in a long-term immune response against the tumor. The majority of these approaches have their basis in targeting specific tumor associated antigens (TAAs) such as epidermal growth factor receptor (EGFR), over-expressed in over half of lung cancer cases, which has been targeted using Cimavax-EGF, an immunogenic recombinant protein vaccine or Mucin-1 (MUC1), also over-expressed in non-small cell lung cancer using Simuvax, a liposomally delivered MUCI peptide. Despite promising early data, these agents have yet to meet primary endpoints in late phase trials (3, 4). TG4010, an alternative MUCI-based vaccine, delivered using a Vaccinia virus (VV) platform is more promising, and evidence of epitope spreading beyond the primary target epitope has been observed clinically (5). The targeting of multiple epitopes will be crucial for successful vaccination strategies to prevent tumor escape from control, however a phase III study investigating a whole cell allogeneic vaccination approach has also failed to demonstrate improved survival (6). The paucity of success of therapeutic vaccination strategies across all cancers can be ascribed to a suboptimal vaccine design, in which inappropriate antigens are targeted or adjuvants are ineffective at breaking immunological tolerance to tumor antigens, and their application in advanced stage disease in which the tumor microenvironment is highly immunosuppressive and refractory to intervention (7). Targeting early pre-malignant lesions, however, may demonstrate more success. These lesions are heavily infiltrated by both adaptive and innate immune cells, with activated phenotypes, suggesting on-going immune responses. Furthermore, immunosuppressive cells are rare at this stage (7).

Recent data suggests a long period of clinical latency of at least 20 years before clinical detection of lung cancer (8). Analysis of the accrual of mutations during lung cancer evolution suggests that lung adenocarcinomas may be particularly suited for early intervention using prophylactic, as opposed to therapeutic vaccination strategies as accrual of known non-synonymous mutations, particularly driver mutations, occur as early molecular events, and 76% of all mutations were detected in all regions of the tumor (9).

We have recently presented a novel, personalized prophylactic vaccination strategy for the prevention of pancreatic ductal adenocarcinoma (PDAC) development in which induced pluripotent stem cells (iPSCs) were induced to PDAC cells via stable knock-in of inactive $KRAS^{G12D}$ and $p53^{R172H}$ prior to lineage differentiation and transformation (10). Importantly, we found that the derived murine tumor cells displayed high antigenic similarities to PDAC cell lines derived from the related KPC or KC transgenic mouse model, demonstrating that the process we used to generate autologous vaccination material was sufficient to model neo-antigen accrual, based on the genetic and epigenetic profile of autologous stem cells, during the earliest stages of tumorigenesis. When pre-infected with replicating oncolytic Adenovirus (AdV) and Vaccinia virus (VV), to act as potent immune adjuvants, and administered to pre-malignant animals in a prime-boost Virus-Infected Reprogrammed Somatic cell-derived Tumor cell vaccination (VIReST) regime, we were able to significantly delay disease development in a robust transgenic mouse model of disease, extending life-span of prophylactically vaccinated animals by up to 51%. Given the latency associated with lung cancer development, in addition to the early and homogenous accrual of truncal mutations, we reasoned that lung cancer would also be particularly responsive to prophylactic therapy. Here we present a VIReST regime targeting lung cancer, in which iPSCs from healthy animals were modified to express inactivated common driver mutations $KRAS^{G12D}$ and $p53^{R172H}$ (11), prior to differentiation into lung progenitor cells and transformation to tumor cells. The iPSC derived lung cancer cell line was able to mimic the characteristics of the lung cancer cell line established from an early-stage lung cancer model. Pre-infection of these cells with AdV and VV prior to delivery into pre-malignant animals was able to induce potent anti-tumor immune responses that safely delayed tumor development when administered prophylactically using a subcutaneous murine model of lung cancer and when administered prior to disease detection in a complex transgenic model of disease. These data suggest VIReST as an effective alternative to autologous whole cancer cell vaccines, that can be delivered prior to or early in disease development, is antigenically compatible with each patient and can engage immune surveillance mechanisms to detect initiation of lung malignancies.

MATERIALS AND METHODS

Cells and Viruses

Murine embryonic fibroblasts (MEFs) from E13.5 WT mice were cultured using Dulbecco's modified Eagles medium (DMEM) supplemented with 10% fetal bovine serum (FBS). MEF feeder cells were inactivated by mitomycin C (MMC) (10 μg/ml for 2.5 h) (MedChemExpress, HY-13316) treatment. iPSCs were cultured using mES medium (DMEM supplemented with 15% FBS (Gemini, 900–108), leukemia inhibitory factor (LIF) (10 ng/ml) (Thermo Fisher Scientific, PMC9484), β-mercaptoethanol (0.1 mM) (Sigma Aldrich, 60-24-2), 1x non-essential amino acids (NEAA) (Thermo Fisher Scientific, 11140050), 1x Glutamax (Thermo Fisher Scientific, 35050061), Sodium pyruvate (1 mM) (Thermo Fisher Scientific, 11360070).

The LC cell lines KPL 160302S and KPL 160424S were cultured from LSL-KRASG12D/+; Trp53R172H/+ mice that had developed lung cancer after Ad-Cre inhalation. These were maintained in DMEM supplemented with 10% FBS. CV1 (African monkey kidney) cells and JH293 cells were obtained from the American Type Culture Collection (ATCC, VA, USA) and maintained in DMEM containing 10% FBS. KP-LC cells were maintained in DMEM containing 10% FBS. The PDAC cell line TB11381 was cultured from LSL-KRASG12D/+; Trp53R172H/+; Pdx-1-Cre mice that had developed PDAC (12). This was kindly provided by David Tuveson (Cancer Research UK Cambridge Institute, now at Cold Spring Harbor Laboratory) and maintained in DMEM supplemented with 10% FBS. Mouse Ovarian Surface Epithelial Cell Line (MOSEC) was provided by Prof Iain McNeish at Barts Cancer Institute and maintained in DMEM supplemented with 10% FBS. All cell lines were routinely tested for the presence of mycoplasma. Cell lines used or created during this study are listed in **Table S1**.

The thymidine kinase (TK)-deleted Lister strain Vaccinia virus (VVL15) was described previously (13). VVL15 was further modified by *XhoI/EcoRI*-mediated removal of the LacZ open reading frame (ORF) from the VV TK shuttle vector pSC65 (GenBank: HC193923.1), which was replaced with red fluorescent protein (RFP) derived by *NheI/AflII* digestion of pCMV-dsRED-Express (Clontech). The virus was produced as previously described (14). Ad-Cre non-replicative virus was purchased from Vector Biolabs and propagated in our laboratory. Wild-type Adenovirus serotype 5 (Ad5) was described previously (15).

Teratoma Test

A total 1×10^7 of LSL-KRAS$^{G12D/+}$; LSL-Trp53$^{R172H/+}$ iPSCs were implanted subcutaneously into the right flank of nude male mice. After 2 weeks and 4 days, with diameter of <1.5 cm, tumors were surgically dissected, formalin-fixed, paraffin-embedded, and stained using hematoxylin and eosin (H&E).

Induction of LSL-KRAS$^{G12D/+}$; LSL-Trp53$^{R172H/+}$ iPSCs to Lung Cancer Cells

LSL-KRAS$^{G12D/+}$; LSL-Trp53$^{R172H/+}$ iPSCs were cultured on mouse embryonic fibroblasts (MEF) in-mES medium. iPSCs were treated with 0.25% trypsin for 5 min, and the differential adhesion method was used to remove MEF. The basic medium of induction was serum-free differentiation (SFD) media of DMEM/F12 (3:1) (Thermo Fisher Scientific, 11765054) supplemented with N2 (Thermo Fisher Scientific, 17502048), B27 (Thermo Fisher Scientific, 12587010), ascorbic acid (50 μg/ml) (Sigma Aldrich), Glutamax (2 mM) (Thermo Fisher Scientific, 35050061), monothioglycerol (0.4 μM) (Sigma Aldrich, 96-27-5), 0.05% bovine serum albumin (BSA) (Sangon Biotech, 9048-46-8), 1% penicillin-streptomycin. iPSCs were plated onto six-well plates coated by 1% agar to form embryoid bodies in the media of SFD with Y-27632 (10 μM) (R&D Systems, 129830-38-2) and mouse BMP4 (3 ng/ml) (R&D Systems, 5020-BP) for 24 h. Embryoid bodies were induced to endoderm in SFD with Y27632 (10 μM), mouse BMP4 (0.5 ng/ml), mouse bFGF (2.5 ng/ml) (R&D Systems, 3139-FB), mouse Activin A (100 ng/ml) (PeproTech, 120-14) for 72 h on low-adherence plates. Half of the old media was removed, and half new media was added every 36 h. Endodermal cells were then induced to anterior foregut endoderm. Cells were cultured on 0.2% Gelatin-coated, 24-well plates (100,000–150,000 cells/well) in SFD with Dorsomorphin dihydrochloride (1.5 μM) (R&D Systems, 1219168-18-9) and SB431542 (10 μM) (R&D Systems, 301836-41-9) for 24 h, followed by SFD with SB431542 (10 μM) and IWP2 (1 μM) (R&D Systems,686770-61-6) for 24 h. Cells were induced to lung progenitors in the medium of SFD with CHIR99021 (3 μM) (Stemgent,04-0004-10), mouse FGF10 (10 ng/ml) (R&D Systems, 6224-FG-025), mouse FGF7 (10 ng/ml) (R&D Systems, 5028-KG-025), mouse BMP4 (10 ng/ml) (R&D Systems, 5020-BP), and *all-trans* retinoic acid (ATRA) (1 μM) (Sigma, 302-79-4) for 9 days. The differentiation protocol was based on a previous report (16). On the 10th day of lung progenitor differentiation, non-replicative Ad5-Cre was added at 50 PFU/cell to remove the LSL cassette. After continuous passage, lung progenitors transformed into lung cancer cells. The changes in cell morphology at each stage of induced differentiation were photographed using the light microscope.

Immunofluorescence

At each differentiation stage, cells were fixed with 4% PFA for 15 min at room temperature then washed three times with PBS. The slides of cells were permeabilized with PBS + 0.5% Triton X-100 for 20 min and washed three times with PBS. Slides were blocked with 10% goat serum for 30 min and incubated with the primary antibodies at 4°C overnight (>16 h) diluted in PBS. Following incubation, the slides were rinsed with PBS and incubated with secondary antibodies at 37°C for 1 h. The slides were rinsed with PBS and the cell nucleus was stained with DAPI (Sigma Aldrich). The images were visualized using an Olympus BX41 fluorescence microscope. Dilutions and Catalog numbers for primary antibodies were as follows: Anti-Oct4 antibody (1:200 dilution) (Abcam, ab18976), Anti-Nanog antibody (1:200 dilution) (Abcam, ab80892), Anti-FOXA2 antibody (1:300 dilution) (Abcam, ab108422), Anti-SOX17 antibody (1:50 dilution) (Abcam, ab191699), Human/Mouse/Rat SOX2 antibody (1:200 dilution) (R&D Systems, AF2018),

Anti-TTF1 antibody (1:200 dilution) (Abcam, ab76013), Anti-SOX9 antibody (1:200 dilution) (Abcam, ab26414). The secondary antibody: Goat Anti-Rabbit IgG H&L (Alexa Fluor 488) (1:500 dilution) (Abcam, ab150077), Rhodamine (TRITC)-conjugated AffiniPure Bovine Anti-Goat IgG (H+L) (1:100 dilution) (Jackson ImmunoResearch, 805-025-180).

Quantitative Real-Time PCR

At each differentiation stage, total RNA was extracted using Trizol (Invitrogen) and cDNA was synthesized by HiScript Q Select RT SuperMix for qPCR (+gDNA wiper) kit (Vazyme, R133-01). qPCR was carried out using the ABI STEPONE PLUS system and the AceQTM qPCR SYBR Green Master Mix (Vazyme, Q111-02). The primers used are listed in **Table S2**.

Identification of Loxp-Stop-Loxp Cassette Removal After Ad5-Cre Addition

Cells were collected and digested in 500 μl/ tube digestion buffer [distilled water + 50 mM Tris-HCl (PH 8.0) + 100 mM EDTA (PH8.0) + 100 mM NaCl + 1% SDS] + 0.1 mg/ml proteinase K for 30 min at 55° C. Cells were then added 250 μl/ tube saturated NaCl solution and 100 μl chloroform and centrifuged 13,523 g at 4° C for 10 min. The upper supernatant was transferred to another tube and 500 μl isopropanol added prior to centrifugation at 13,523 g for 10 min. The supernatant was discarded and 250 μl 70% alcohol was added for 10 min. The tubes were centrifuged 13,523 g for 5 min. The supernatant was discarded and distilled water was added to dissolve the DNA. DNA concentration was measured using the Nanodrop (Thermo Fisher).

Primers on the both sides of LSL cassette were designed. The bands of activated mutations of KRAS/Trp53 were longer than the bands of wide type with one loxp. The fragments with the complete LSL cassettes cannot be amplified in this PCR system.

Primers for KRAS identification: F: 5′-ATATCCAGTCAACAA AGAATACC-3′, R: 5′-TCCGAATTCAGTGACTACAGATGT ACAGAG-3′
Primers for p53 identification: F: 5′-AGCCTGCCTAGCTTCC TCAGG-3′, R: 5′-CTTGGAGACATAGCCACACTG-3′.

Karyotype Analysis

WT iPSC/KP-LC/KPL 160302S/KPL 160424S were cultured to a density of about 80–90%, and treated with colchicine (0.2 μg/ml) for 3 h. Cells were digested with trypsin and collected into centrifuge tubes, pipetted into single cell suspensions, centrifuged at 250 g for 5 min and the supernatant was discarded. Five milliliters 37°C preheated KCl solution (0.075 mol/L) was added. The cell suspensions were mixed uniformly, and the hypotonic treatment performed in the 37°C water bath for 30 min. The cell suspensions were centrifuged and the supernatant discarded. The cell pellets were resuspended with a little residual liquid. One milliliter fixative solution (methanol: glacial acetic acid = 3: 1) was added slowly along the tube wall. The cell suspensions were mixed while dropping, and left to stand for 5 min. Afterwards, the cell suspensions were centrifuged, and the supernatant was discarded. Three milliliters fixative solution was added, and left to stand for 30 min. Again, the cell suspensions were centrifuged, and the supernatant was discarded. Three milliliters fixative solution was added, and left to stand for 30 min. The cell suspensions were centrifuged, and the supernatant was discarded. One milliliter fixative solution was added, and the cells were pipetted to make cell suspensions. The cell suspension was aspirated with a pipette and dropped on cold glass slides at high altitude. The slides were baked in an oven at 80°C for 2 h, digested by preheating trypsin for 30 s, stained by Giemsa for 10 min, rinsed with water, and dried. Finally, the slides were observed and pictured with oil lens.

Transcriptome Sequencing

Cell transcriptomes were sequenced in BGI. Tec, Shenzhen, China. RNA libraries were prepared using an Illumina TruSeq RNA Sample Prep Kit. Briefly, 200 ng total RNA sample was purified by oligo-dT beads, then poly (A)-containing mRNA were fragmented into small pieces with Elute, Prime, Fragment mix. First-strand cDNA was generated by First Strand Master Mix and Super Script II (Invitrogen) reverse transcription. The Second Strand Master Mix was added to synthesize second-strand cDNA (16°C for 1 h). The purified fragmented cDNA was combined with end-repair mix and incubated at 30°C for 30 min. The end-repaired DNA was purified using Ampure XP Beads (AGENCOURT). A-Tailing Mix was then added and samples were incubated at 37° C for 30 min. These samples were incubated with RNA Index Adapter and Ligation Mix at 30° C for 10 min. The end-repaired DNA was purified using Ampure XP Beads (AGENCOURT). Several rounds of PCR amplification with a PCR Primer Cocktail and PCR Master Mix were performed to enrich the cDNA fragments. The PCR products were finally purified with Ampure XP Beads (AGENCOURT).

After the libraries were obtained, they were amplified on cBot to generate a cluster on the flowcell (TruSeq PE Cluster Kit V3–cBot–HS, Illumina). The amplified flowcell was sequenced using the HiSeq 2000 System (TruSeq SBS KIT-HS V3, Illumina) with a read length of 100 bp, producing on average 24M paired-end sequence reads per sample. Sequencing reads were aligned to the mouse genome build mm10/GRCm38 with the HISAT2 aligner (17). The number of reads uniquely aligned (mapping quality score $q > 10$) to the exonic region of each gene were counted using HTSeq (18), based on GENCODE version 9 mouse gene annotation. Only genes that achieved at least one count per million (CPM) mapped reads in at least one sample were included, leading to 15,687 filtered genes in total. Read counts were further normalized using the conditional quantile normalization (cqn) method (19), accounting for gene length and GC content, with the FPKM (Fragments Per Kilobase of transcript per Million mapped fragments) values derived for genes across the eight samples. The overall gene expression correlations between samples were subsequently calculated. The data of transcriptome sequencing has been uploaded to GEO, the series entry number is GSE151813. The genes expressed at higher levels in KP-LC compared to WT-iPSCs or KP-LC compared to KPL 160424S were analyzed. Tumor-associated antigens such as CTA, CEA were searched among them. Meanwhile, GO analysis was applied to determine highly expressed genes in KP-LC using the https://david.ncifcrf.gov/summary.jsp~website.

Cytotoxicity Assay

Cells were seeded at 4×10^3 to 6×10^3 cells per well in 96-well plates and infected with Ad5/ VVL15-RFP 14–18 h later at starting multiplicity of infection (MOI) of 1,000 PFU/cell. Cells were incubated at 37°C, 5% CO_2 incubator for 6 days after viral infection. Cell survival was detected by SpectraMax M5e microplate reader.

Viral Replication Assay

Cells were seeded at 2×10^5 cells per well in 24-well plates. Fourteen to eighteen hours later, cells from three wells were harvested with trypsin and cell number per well-determined. Cells were infected with Ad5 (MOI:10 PFU/cell) for 4 h or VVL15-RFP (MOI: 1 PFU/cell) for 2 h. Twenty-four wells were then switched to DMEM + 10% FBS. The other 24 wells were switched to DMEM + 10% FBS + 200 μg/ml MMC for 2.5 h, and then DMEM + 10% FBS. Cells were collected in triplicate at 24-h intervals up to 96 h after infection, freeze-thawed three times and titrated on JH293 cells for Ad5 or CV1 cells for VVL15-RFP. The Reed-Muench mathematical method was used to calculate the 50% tissue culture infective dose (TCID50) value for each sample (20). Viral burst titers were converted to PFU per cell based on the number of cells present at viral infection.

Cell Proliferation and Plate Colony Formation of KP-LC With Ad5/VVL15-RFP Infection and MMC Treatment

Cells were seeded at 3,000 cells per well in 96-well plates. Fourteen to eighteen hours later, cells were infected with Ad5 (MOI: 50 PFU/cell) for 4 h/VVL15-RFP (MOI: 1 PFU/cell) for 2 h. Then the medium was switched to DMEM + 10% FBS + 200 μg/ml MMC for 2.5 h, and then DMEM + 10% FBS. Cell survival 24 or 72 h after MMC treatment was determined by MTS assay by SpectraMax M5e microplate reader.

In six-well plates, 2.5×10^5 cells per well were seeded. After 14–18 h, cells in 3 wells were digested with trypsin and the average number of cells in each well was calculated. Cells in the remaining wells were infected with Ad5 (MOI: 50 PFU/cell) for 4 h or VVL15-RFP (MOI: 1 PFU/cell) for 2 h. After that, the medium was changed to DMEM + 10% FBS + 200 μg/ml MMC and incubated for 2.5 h, and then the medium was changed to DMEM + 10% FBS. Forty-eight and ninety-six hours after MMC treatment, cells were digested with trypsin and the average number of cells per well was calculated. After counting, the cells were seeded in new six-well plates for plate colony formation experiments. Meanwhile, KP-LC without virus infection and MMC treatment was seeded into six-well plates at 300 or 600 cells per well as a normal control. Six days later, cells of the normal control group grew into visible colonies. The six-well plates were fixed with 4% paraformaldehyde at room temperature for 15 min, and washed twice with PBS. The wells were stained with crystal violet for 20 min, rinsed with tap water and photographed.

Cell Growth Curve

6×10^4 cells/well were cultured in 96-well plates for 5 days in DMEM + 10% FBS. Cell counts were carried out using Incucyte every 2 h.

Soft Agar Colony Formation Assay

Two percent agar and DMEM + FBS were mixed to a final concentration of 0.5% agar and 20% FBS, and the mixture placed in to 24-well plates as a base layer. Cells were trypsinized and suspended in DMEM + 20% FBS. 0.5% agar and cells suspension were mixed to a final concentration of 0.2% agar and added over the solid base layer. DMEM + 10% FBS was added after top layer was solidified. Plates were incubated at 37°C for 2 weeks. Colonies of each well were visualized using an Olympus IX51 microscope, counted and colony forming efficiency (total number of colonies/initial number of cells) was calculated.

Plate Formation Assay

50/100/200 cells/well were seeded in 96-well plates in DMEM + 10% FBS. The plates were then put into Incucyte to take pictures. Two weeks later, colonies of each well were counted, averaged and colony forming efficiency calculated as above.

Wound Healing Assay

3×10^4 cells/well were cultured in 96-well plates for 1 day. Plates were then scratched with the 96 well pin block and put into Incucyte. Pictures were taken every 2 h and relative wound density was calculated.

Western Blot

Cells were seeded at 1×10^6 cells per well in six-well plates. Fourteen to eighteen hours later the cell number per well was determined. Cells were infected with Ad5 (MOI: 50 PFU/cell) for 4 h/VVL15-RFP (MOI: 1 PFU/cell) for 2 h. The medium was switched to DMEM + 10% FBS + 200 μg/ml MMC for 2.5 h, and then DMEM + 10% FBS. Cells were collected at 24 and 72 h after MMC treatment. Cells were lysed by RIPA lysis buffer + PMSF (Solarbio, R0020), and concentration of protein was detected by BCA kit (Solarbio, PC0020). Protein was separated by SDS-PAGE gel (CWBIO, CW0022S), and transferred to a piece of PVDF membrane (BEIJING DINGGUO CHANGSHENG BIOTECHNOLOGY CO., XLL094-2). The membrane was blocked with 10% skim milk for 1 h and incubated with the primary antibodies at 4°C overnight diluted in 5% skim milk.

Following incubation, the membrane was rinsed with TBST 3 times and incubated with secondary antibodies diluted in 5% skim milk at room temperature for 1 h. The membrane was rinsed 3 times with TBST and ECL added (Thermo Scientific, NC15079) prior to exposure (GE Amersham Imager 600). Dilutions and catalog numbers for primary antibodies were as follows: Adenovirus Type 5 E1A Ab-1, Mouse Monoclonal Antibody (1:300 dilution) (Thermo, MS-587-P1), Vaccinia virus (Polyclonal Antibody) (1:300 dilution) (AbD Serotec, 9503-2057), GAPDH Antibody (Mouse Monoclonal) (1:5,000 dilution) (Proteintech, 60004-1-Ig). The secondary antibody: Peroxidase-Conjugated Goat anti-Mouse IgG (1:5,000 dilution) (ZSGB-BIO, ZB-2305), Peroxidase-Conjugated Goat anti-Rabbit IgG (1:5,000 dilution) (ZSGB-BIO, ZB-2301).

In vivo Experiments

All animal procedures were approved by the Animal Welfare and Research Ethics Committee of Zhengzhou University (Zhengzhou, China). Mice were housed in groups in accordance with the regulations for mouse welfare and ethics of Zhengzhou University with 12 h dark-light cycles and free access to food and water.

LSL-KRAS$^{G12D/+}$; LSL-Trp53$^{R172H/+}$ (KP) mice were kindly provided by David Tuveson. Genotyping was performed using the following primers; KRAS F: 5′-CCATGGCTTGAGTAAG TCTGC-3′ KRAS R 5′-CGCAGACTGTAGAGCAGCG-3′ (550 bp); P53_F: 5′-AGCTAGCCACCATGGCTTGAGTAAGTCTG CA-3′ P53_R: 5′-CTTGGAGACATAGCCACACTG-3′ (270 bp). This model is modified heterozygous KRAS^{G12D} and Trp53^{R172H} on 129 mouse background. These two point mutations were silenced by a loxp-stop-loxp (LSL) cassette in the absence of Cre. 2.5×10^7 PFU Ad-Cre was delivered to 10–12 week (20–28 g) male mice intranasally. After the intranasal inhalation of Ad-Cre, the two mutations were activated and lung cancer developed gradually. To acquire lung cancer cell lines from this model, lungs of KP mice that had been infected with Ad-Cre were surgically dissected at 8 and 16 weeks, and rinsed in PBS twice. Lungs were dissected in a small amount of PBS + 10% BSA and the cells cultured in ACL-4 media (RPMI 1640 with 20 μg/ml insulin, 10 μg/ml transferrin, 25 nM sodium selenite, 50 nM hydrocortisone, 1 ng/ml epidermal growth factor, 10 μM ethanolamine, 10 μM phosphorylethanolamine, 100 pM triiodothyronine, 2 mg/ml bovine serum albumin, 0.5 mM HEPES, 0.5 mM sodium pyruvate and 2 mM glutamine). After 2 passages, ACL-4 media was switched to DMEM + 10% FBS.

Male C57/BL6 mice and nude mice were purchased from Vitalriver.com, Beijing, China.

In subcutaneous tumor models, 4 to 5-weeks old, 16–18 g male mice were randomly assigned to treatment groups and tumor growth was measured using electronic calipers [tumor volume = (length × width^2 × π)/6] until tumor volume reached 2,500 mm^3 or ulcerated, at which point the animal was sacrificed. For KP lung cancer models, animals were assigned randomly to treatment groups and animal survival was monitored by assessment of animal well-being every other day. In the survival experiments, the animal was sacrificed when one of the following situations occurred: animal was curled up motionlessly, hair became fluffy and messy, animal showed no response to external stimuli, weight loss exceeding 2 g in 2 days. Lung tissue was collected from each mouse to confirm, using H&E staining, that all mice developed lung cancer. Animal caretakers were blinded to treatment groups in all cases.

Statistical analysis was carried out using Graph Pad Prism 5 and SPSS 19.0 software. The results were represented as mean ± standard or deviation (SD) or ± standard error of the mean (SEM). Differences between groups were analyzed using Students' unpaired *T*-tests or Kaplan–Meier survival analysis. Differences were considered statistically significant when the $p < 0.05$.

VIReST Vaccinations for Subcutaneous Tumor Experiments

KP-LC cells were infected with Ad5 at an MOI of 50 PFU/cell in serum-free DMEM for 4 h. Following infection, medium was switched to DMEM + 10% FBS + 200 μg/ml mitomycin C (MMC) (Meilun Biotechnology, 50-07-7) and cells incubated at 37°C for 2.5 h. Cells were washed with PBS twice, harvested with trypsin and diluted with PBS to 2×10^6 cells/100 μl. Ad5-infected cells were injected subcutaneously (s.c) as a prime vaccination using 100 μl per inoculation in the right flank of male KP littermates. KP-LC cells were infected with VVL15 at an MOI of 1 PFU/cell for 2 h and then MMC-treated as for AdV-infected cells. Four weeks after prime vaccination, cells treated with VVL15-MMC were injected s.c in the same side as a booster vaccination. Two weeks after boost, KPL160302S/KPL 160424S cells were injected s.c in 100 μl (2×10^6 cells) per inoculation, in the right flank and tumor growth was monitored.

Immunohistochemistry

The tissues were collected at different time points, dipped in isopentane and frozen at −80°C. Tissues were cut into 6 μm sections by freezing microtome (Leica, CM1950). The sections were fixed with −20°C acetone for 10 min, washed three times with PBS. Then the slides were incubated with 3% H_2O_2 for 8 min, washed twice with PBS and slides blocked with 10% goat serum for 30 min. Slides were incubated with the primary antibodies at 4°C overnight diluted in PBS. Following incubation, the slides were rinsed 3 times with PBS. Polink-2 plus polymer HRP detection system for rat primary antibody (ZSGB-BIO, PV-9004) and DAB kit (ZSGB-BIO, ZLI-9018) were used. The slides were flushed using tap water thoroughly, dyed by hematoxylin, flushed by tap water, differentiated by hydrochloric acid alcohol, dehydrated, and sealed. The images were visualized using an Olympus BX41 microscope. Dilutions and catalog numbers for primary antibodies were as follows: CD4 antibody (1:100 dilution) (BioLegend, 100402), CD8 antibody (1:100 dilution) (BioLegend, 100702).

Ten high-power fields (HPF) were randomly selected from each group to count lymphocytes, three mice per group at each time point. Statistical graphs show the mean ± standard error of the mean (SEM) of each group and compared using independent *T*-test.

Establishment of Orthotopic Lung Cancer Model

Ad-Cre was intranasally delivered to KRAS$^{LSL-G12D/+}$; p53$^{LSL-R172H/+}$ (KP) mice between 10 and 12 weeks of age. DMEM + Ad5-Cre + 10 mM $CaCl_2$ were incubated at room temperature for 20 min to form calcium phosphate precipitates. Meanwhile, mice were anesthetized using avertin at 0.45 mg/g body weight for males via intra-peritoneal injection. A total volume of 75 μl containing 2.5×10^7 PFU per mouse was delivered as previously described (21).

Vaccinations for Survival Experiments

Ad5-infected KP-LC, KPL 160302S, or KPL 160424S cells produced as described above were injected s.c, using 100 μl per inoculation, in the right flank of male KP mice 2 weeks 4 days after Ad-Cre inhalation, as a prime. Four weeks later, cells treated with VVL15-MMC were injected subcutaneously in the same side as a boost. For analysis of α-PD1 combination, 600 μg α-PD1 (Bioxcell) was administered to mice intra-peritoneally (i.p.) 2 weeks post-prime and 1 and 3 weeks post-booster injection.

Flow Cytometric Analysis

Splenocytes of three mice vaccinated by KP-LC and 3 mice vaccinated by PBS were stained with CD3e (FITC) (eBioscience, 11-0031-86), CD4 (APC) (eBioscience, 17-0041-82), CD8a (PE) (eBioscience, 12-0081-85), CD44 (eFluor 450) (eBioscience, 48-0441-80), CD62L (PerCP-Cyanine5.5) (eBioscience, 4300748) for 30 min at 4°C. After washing, stained cells were analyzed on an ACEA NovoCyte flow cytometer.

IFNγ Expression Induced by Vaccination

Spleens of three mice vaccinated using KP-LC and three mice vaccinated using PBS 3 weeks after boost were harvested under sterile conditions. Spleens were mashed through 70 μm cell strainers (BIOFIL, CSS010070), centrifuged at and re-suspended in 5 ml of RBC lysis buffer, washed with PBS, centrifuged and re-suspended with T cell media (TCM) (RPMI-1640 + 10% FBS + 1% streptomycin/ penicillin + 1% sodium pyruvate + 1% non-essential amino acids) to a final concentration of 5×10^6 cells/ml.

KP-LC, KPL 160302S, KPL160424S, KPL-234S, and MOSEC as stimulator cells were incubated with TCM + 0.2 mg/ml MMC for 2.5 h. The cells were washed twice with PBS, trypsinized and re-suspended in TCM to a final concentration of 5×10^5 cells/ml. Peptides of K-RAS (GADGVGKSA) (GL Biochem, 492748), B8R (TSYKFESV) (GL Biochem, 492745), OVA(SIINFEKL) (GL Biochem, 492746) were diluted in TCM to 100 μg/ml.

One hundred microliters of each of the splenocyte suspensions were co-cultured with 100 μl of stimulator cell suspension or peptide in a round bottomed 96 well plate. Background contained 5×10^5 splenocytes in 200 μl TCM. The plates were incubated at 37° C, 5% CO_2 for 3 days. The plates were centrifuged at 512 g for 5 min. The concentration of IFNγ in supernatants was measured using mouse IFNγ ELISA Ready-SET-Go kit (eBioscience, 88-7314-88).

In vivo CD8+ or CD4+ T Cell Depletion

α-CD8 (TIB2100) or α-CD4 (GK1.5) (Provided by Professor Shengdian Wang, the Chinese Academy of Sciences, Institute of Biophysics) was injected into the abdominal cavity of the KP mice 1 day before prime and two times/week in the interval between prime and boost, and 4 weeks after boost at 200 μg/mouse/time point. CD8+ or CD4+ T cell depletion was confirmed using flow cytometric analysis throughout the experiment.

Mouse Anti-nuclear Antibody ELISA

Three mice vaccinated using KP-LC and three mice vaccinated using PBS had blood collected from tail tips 3 weeks after boost. The blood was coagulated at 37°C for 15 min and centrifuged 20 min at 845 g. Supernatant was serum, and the concentration of anti-nuclear antibody in serum was measured using mouse anti-nuclear antibody kit (Nanjing Senbeijia Biological Technology Co., SBJ-MO134-96T).

Statistical Analysis

GraphPad Prism 6 was used for comparative statistical analysis. Dual condition comparisons were made using the unpaired student *T*-test. For more than one condition or for an additional variable such as time, one or two-way ANOVAs, respectively were performed, with *post-hoc* Tukey tests to compare treatment pairs. Survival data was represented by Kaplan-Meier plots with log rank analyses to delineate whether any differences between specific treatment pairs were statistically significant. $^*p < 0.05$, $^{**}p < 0.01$, and $^{***}p < 0.001$.

RESULTS

Lineage Differentiation and Transformation of iPSCs Provides an Antigenically Compatible Whole Cell Lung Cancer Vaccine

We have previously generated a wide type iPS cell line from 129J/C57/BL6 male mice and modified the genome with Cre-dependent LSL-KRASG12D/+; LSL-Trp53R172H/+, to create WT-KP iPSCs. The introduction of driver mutations prior to lineage differentiation had no impact on the pluripotency of iPSCs as demonstrated by the ability to form characteristic teratoma when inoculated into nude mice (**Figure 1A**). WT-KP iPSCs were directed to differentiation to lung progenitor cells following the protocol shown in **Figure 1B**. To confirm effective induction, markers of iPSC, endoderm, anterior foregut endoderm (AFE), and lung progenitors (LP) were detected by immunofluorescence (**Figure 1C**) and RT-qPCR (**Figure S1A**). iPSC-derived LP cells were then infected with non-replicating Ad5 vector expressing Cre (AdCre) to induce mutant $KRAS^{G12D}$ and $p53^{R172H}$ expression and transformation to lung cancer cells (KP-LC) (**Figure 1D**). Genotyping confirmed the presence of mutant KRAS in the KP-LC cell line and KPL 160302S and KPL160424S cell lines [lung adenocarcinoma cell lines derived from the lung cancer KP transgenic mouse model (21)], but not in LP cells that were not infected with AdCre. Similarly, mutant p53 was detected in KP-LC cell line but not in the AdCre uninfected lung progenitor (LP) cells that do not express mutated p53 (**Figure S1B**). Furthermore, KP-LC and KPL 160302S, KPL 160424S all had abnormal chromosome profiles (**Figure S1C**). These three lung cancer cell lines had similar growth rate *in vitro* (**Figure S1D**). Investigations into the tumorigenicity of iPSC-derived KP-LC cells demonstrated these cells were able to develop into subcutaneous tumors when inoculated into the flank of KP transgenic littermate mice or C57/BL6 mice that had no pre-disposition to cancer (**Figure 1E** and **Figure S1E**), forming tumors pathologically similar to those formed after inoculation of KPL 160302S and KPL 160424S tumor cells derived from the induced KP transgenic lung cancer model (**Figure 1E** and

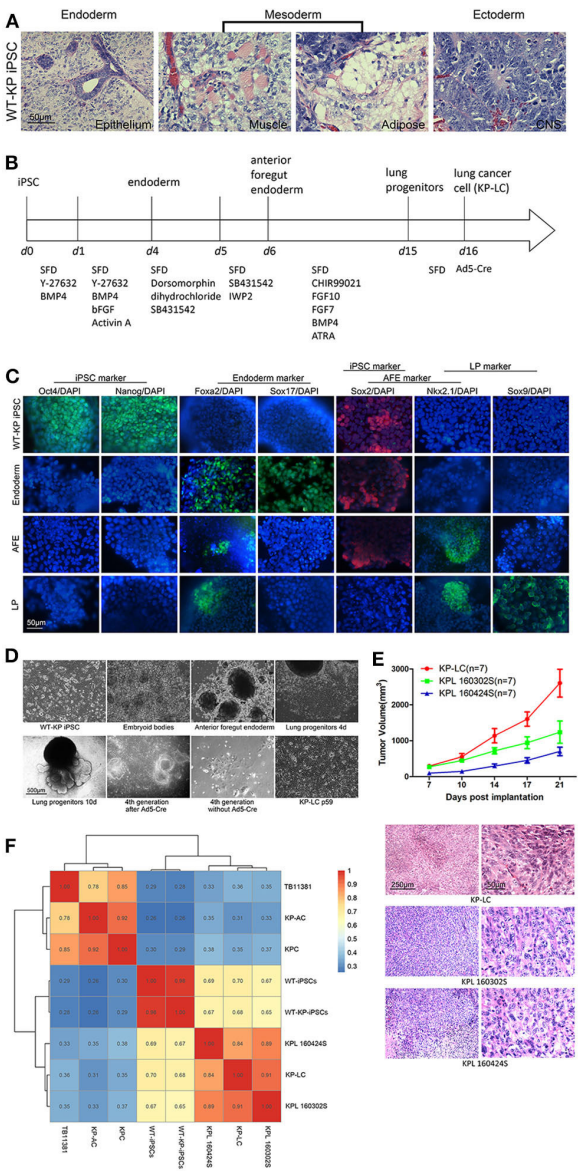


FIGURE 1 | Antigenically relevant lung cancer cells can be derived from murine iPSCs. **(A)** H&E staining of tissues derived after LSL-KRAS$^{G12D/+}$; LSL-Trp53$^{R172H/+}$ iPSCs were subcutaneously injected into nude mice to form teratoma. **(B)** Schematic of the protocol employed for stepwise differentiation of LSL-KRAS$^{G12D/+}$; LSL-Trp53$^{R172H/+}$ iPSCs to lung cancer cells. **(C)** Immunofluorescence images to examine expression of markers indicative of stages of induction of lung progenitor cells from iPSC. DAPI was used to stain for nuclear content. **(D)** Morphology of WT-KP iPSCs, embryoid bodies, anterior foregut endoderm, lung progenitors, and KP-LC. On the 10th day of lung progenitors, cells displayed structures akin to lung buds. Tubular structures could be observed at the 4th generation after infection of Ad5-Cre. Without the infection of Ad5-Cre, lung progenitors gradually became senescent. After serial passage post-infection of Ad5-Cre, cells transformed to lung cancer cells. **(E)** Subcutaneous tumor growth curve of KP littermates bearing KP-LC, KPL 160302S, and KPL 160424S tumors with the initial dose of 2 × 10^6 cells/ mouse. Mean ± SEM is shown. $N = 7$/group. H&E staining of subcutaneous tumors at day 21 is shown beneath the growth curve. **(F)** Indicated cell lines were subjected to RNA deep sequencing and a transcriptome expression correlation matrix, based on 15,687 filtered genes, was generated.

Figure S1E). Scratch assays to examine *in vitro* invasion of cells demonstrated that over 90% of the wound of KPL 160424S cells, from an advanced lung cancer model, healed 16 h after scratch. At the same time point, the wound in KPL 160302S cells, which came from an early stage lung cancer model, demonstrated healing at <20% and KP-LC cells showed a 40% heal from scratch (**Figure S1F**). Both KP-LC and KPL 160302S were able to form colonies in the soft agar (**Figure S1G**) and plate colony formation assay (**Figure S1H**). Most importantly, analysis of the transcriptome of KP-LC cells demonstrated a high similarity between KP-LC cells derived from iPSCs and the cell lines derived from the transgenic mouse model (KPL 160302S and KPL 160424S) (**Figure 1F**). KP-LC cells had the highest similarity with KPL 160302S which came from the early stage lung cancer model (91%), followed by KPL 160424S which came from the advanced lung cancer model (84%). We speculate that KP-LC derived from iPSC retained more neoantigens/tumor-associated antigens similar to cells from early staged lung cancer model because it had not been screened by the immune system. Similarity between KP-LC and untransformed iPSCs (WT iPSC derived from KPC transgenic mice with wild-type KRAS and p53 or WT-KP iPSCs derived from littermate mice with stable insertion of KRAS^{G12D} and p53^{R172H}) was lower, demonstrating the limitations of vaccination strategies based on the use of unmodified iPSCs as previously reported (22). Cancer associated genes such as MageE1, Morc2b, Morc4, Cage1, Brdt, IL13ra1, were expressed at significantly higher levels in KP-LC than WT-iPSCs (**Figure S2A**) and these genes were enriched in several pathways associated with cancer, including the PI3K-Akt signaling pathway, cancer proteoglycans, the Ras signaling pathway, cancer associated MicroRNAs, the Rap1 signaling pathway, HTLV-1 infection, the MAPK signaling pathway and ECM-receptor interactions (**Figure S2C**). Furthermore, when compared to KPC or KP-AC iPSCs, which were derived in the same way, using the same driver mutations, but induced to pancreatic lineage tumor cells, and TB11381 cells derived from the transgenic pancreatic cancer model with the same driver mutations, concordance was low. This demonstrates that the lineage specific genetic and epigenetic profiles and not the driver mutation *per se* drive the accumulation of neo-antigens or/and tumor-associated antigens (**Figure 1F**).

Oncolytic Viruses Can Successfully Infect and Express Viral Proteins in KP-LC Cells

Lack of immunogenicity plays a central role in therapeutic tumor vaccine failure, thus provision of an effective adjuvant is critical for inducing robust anti-tumor immune activity, even within the pre-malignant environment. Virus-infected cell vaccines, whereby tumor cells are pre-infected with replicating tumor tropic virus prior to delivery as a vaccine, has previously been shown to induce strong anti-tumor immune reactions (23), and we have demonstrated that replicating oncolytic Vaccinia virus (VV) and Adenovirus (AdV) can induce the necessary danger signals and inflammatory environment required for anti-tumor immune induction (10). To validate their use in a lung cancer vaccination regime, we investigated the ability of VV and AdV to replicate in and kill iPSC-derived KP-LC cells *in*

vitro. Both viruses were significantly more cytotoxic in KP-LC cells compared to KPL160302S cells derived from the induced transgenic mouse model (**Figure 2A**). Consistent with previous reports (15), Ad5 replicated poorly in murine cells, including KP-LC (**Figure 2B**), but viral protein expression was detected after infection (**Figure 2F**). VV replicated and expressed viral protein efficiently in KP-LC cells (**Figures 2B,F**). In order to ensure safety of the vaccination protocol, we completely inhibited ongoing cell proliferation and virus replication using mitomycin-C (MMC) (**Figures 2B–E**). This had the effect of preventing both cell proliferation and viral replication, but viral protein expression, required for adequate stimulation of anti-tumor immune responses, persisted for at least 72 h post-infection (**Figure 2F**).

A VIReST Regime Using OV-Infected iPSC-Derived KP-LC Cells Prevents Tumor Growth in Immunocompetent Mice

To demonstrate the principle of prophylactic vaccination, the efficacy of a Virus Infected, Reprogrammed Somatic cell-derived Tumor cell (VIReST) vaccination regime was examined using subcutaneous models of lung cancer in immunocompetent mice. As detailed in **Figure 3A**, KP littermates that are not disposed to cancer development were immunized at day 0 using AdV-infected, MMC-treated KP-LC cells. Four weeks after prime vaccination, VV-infected, MMC-treated KP-LC cells were injected subcutaneously as a boost. Two weeks following this booster vaccination, lung cancer cell lines KPL 160302S (**Figure 3B**) or KPL 160424S (**Figure 3F**) were inoculated into the flank of immunized mice to form subcutaneous tumor and tumor growth measured. While prophylaxis did not completely prevent the growth of tumors after challenge, it was able to delay and impair growth after challenge with a large number of tumor cells compared to PBS vaccination. To determine the mechanisms responsible for efficacy, tumors were analyzed using immunohistochemistry (IHC) at day 24 (KPL 160302S) or 31 (KPL 160424S) after re-challenge. The numbers of $CD8^+$ and $CD4^+$ T cells infiltrating the tumors were analyzed (**Figures 3C–E,G–I**). In both models, prophylactic vaccination using the KP-LC VIReST regime resulted in a heavier infiltration of both CD8+ and CD4+ T cells, demonstrating that vaccination can induce adaptive immune responses capable of homing to the site of tumor development to impede growth.

VIReST Using iPSC-Derived Lung Cancer Cells Evokes Anti-tumor Immune Responses in an Induced Transgenic Model of Lung Cancer

We next investigated the KP-LC-based VIReST regime in a more pathologically relevant model of lung cancer using the lung cancer transgenic mouse model previously described (21). $KRAS^{LSL-G12D/+}$; $Trp53^{LSL-R172H/+}$ mice were intra-nasally (i.n.) infected with Ad-Cre to induce $KRAS^{G12D}$ and $P53^{R172H}$ expression within the lung and drive carcinogenesis. H&E staining of lung sections carried out 3–28 weeks after AdCre delivery demonstrated that early lesions could not be detected 3 weeks post-infection (**Figure S3**) suggesting that disease had not yet developed in these animals or was at an early stage, undetectable by histopathology examination. After 8 weeks, tumors with enlarged nuclei with prominent nucleoli were observed. In contrast, KP mice that were not infected with AdCre did not develop signs of lung carcinogenesis at any age (**Figure S3**). Based on the observed progression, mice were treated 2 weeks and 4 days post-AdCre infection with a prime-boost VIReST regime as shown in **Figure 4A**.

One, two, and three weeks following booster injection, CD4+ and CD8+ T cell infiltration into the lungs was observed (**Figures 4B–D**). CD8+ T cell infiltration into lung tissues was significantly enhanced by VIReST treatment at each timepoint. CD4+ T cell infiltration was also significantly enhanced by treatment, but this advantage was lost 3 weeks post-booster vaccination, although it should be noted that both anti-tumor CD4+ populations and TReg inhibitory CD4+ populations will be detected using this method. Of note, the immune response caused by KP-LC vaccination was similar to that induced by KPL 160302S vaccination using the same regime for they both elicited more CD8+ T cells infiltration 1–3 weeks post-booster vaccination and more CD4+ T cells infiltration 1–2 weeks post-booster vaccination. To further investigate the breadth of anti-tumor immunity, splenocytes from immunized mice were gathered 3 weeks post-boost and the T cell effector phenotype (**Figures 4E,F**) and *ex vivo* responses to several lung cancer cell lines and specific antigens were determined (**Figure 4G**). KP-LC VIReST induced more effector CD8+ T cell populations compared to PBS vaccination (**Figures 4E,F**). In addition, KP-LC VIReST resulted in significantly enhanced IFNγ responses to all lung cancer cell lines and the KRAS epitope (**Figure 4G**). Of note, IFNγ responses induced by KPL 160424S cells, which was derived from the advanced lung cancer model and had the same driver mutations as KP-LC, was significantly lower compared to other lung cancer cell lines stimulation. KP-LC VIReST also resulted in significantly enhanced IFNγ responses to a mouse ovarian surface epithelial cell line (MOSEC). However, the production of IFNγ induced by MOSEC is significantly lower than KP-LC (**Figure 4G**). This phenomenon may be caused by some antigenic similarity between MOSEC and mouse lung cancer cell lines and warrants further investigation into shared antigens. Together these results demonstrate the ability of KP-LC VIReST to induce potent anti-tumor immune reactions within the emerging tumor microenvironment (TME) in a physiologically relevant model of lung cancer.

VIReST Can Delay Tumor Development in an Induced Transgenic Lung Cancer Model in a CD8+ and CD4+ T Cell Dependent Manner

To determine treatment efficacy, animals were immunized following the regime shown in **Figure 4A** and the progression and survival was monitored. The lung tissues of mice were collected 10.5 and 15.5 weeks after Ad-Cre infection. The tumors of the KP-LC VIReST group were significantly smaller than PBS group (**Figures 5A,B**). KP-LC VIReST was able to delay

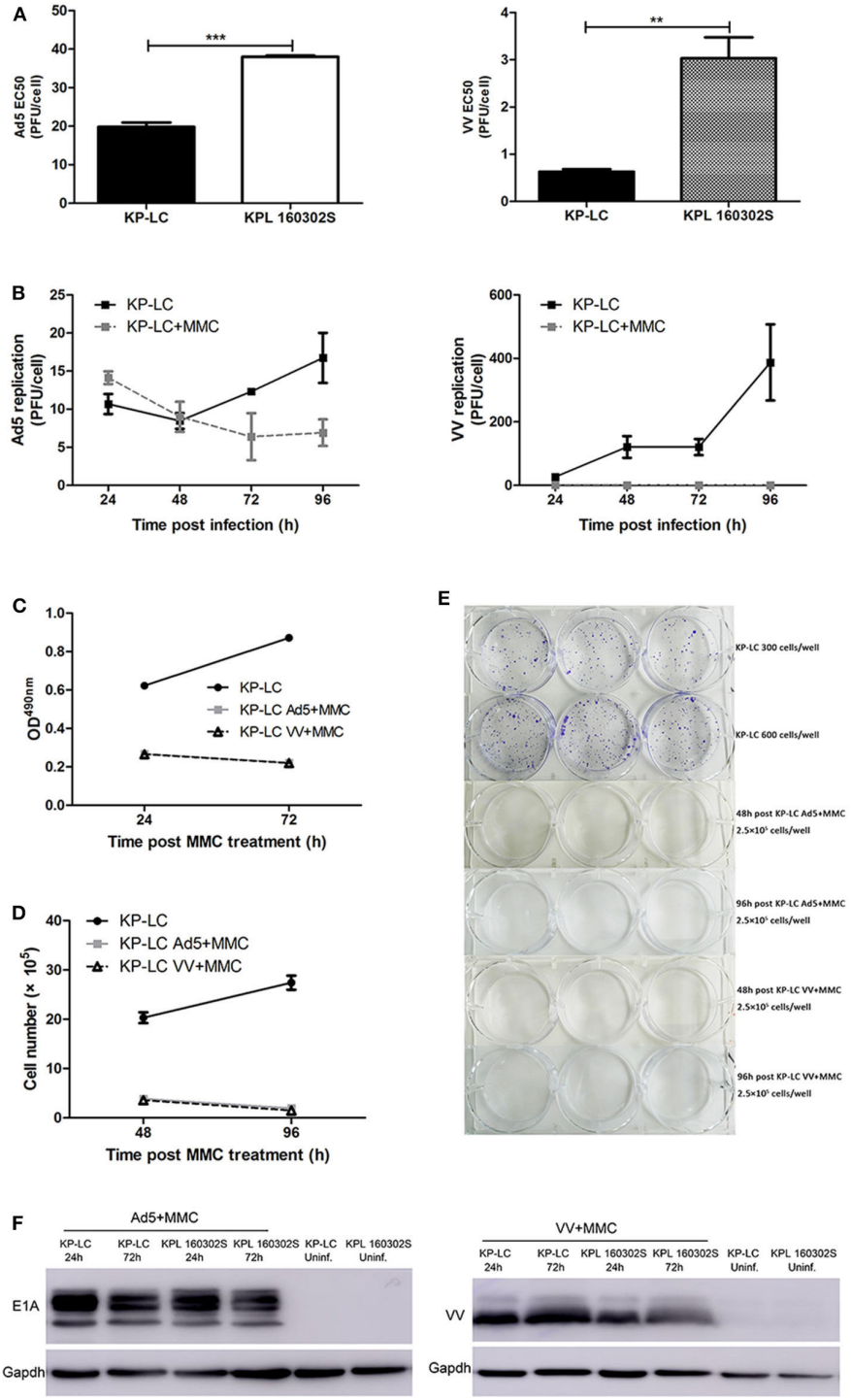


FIGURE 2 | AdV and VV can infect and replicate in transformed iPSCs and mitomycin-C treatment inhibits ongoing replication and tumor cell proliferation. **(A)** Cytotoxicity of Ad5 or VV on iPSC-derived KP-LC cells and KPL 160302S lung tumor cells. Cell death was determined by MTS assay 144 h post-infection. Mean EC50 values ± SEM are shown. **(B)** Production of infectious Ad5 or VV virions in KP-LC cells. Cells were infected with virus and were untreated or treated with mitomycin C. Mean viral replication ± SEM was determined at 24 h intervals for 96 h by TCID50 assay. JH293 cells for Ad5 or CV1 cells for VVL15-RFP. **(C)** Cell proliferation of KP-LC cells after infection and mitomycin-C treatment was determined using MTS assay at 24 and 72 h post-mitomycin C treatment. Mean OD^{490}nm values ± SEM are shown. $n = 3$/group. **(D)** Cell proliferation of KP-LC cells after infection and mitomycin-C treatment was determined by cell counting at 48 and 96 h post-mitomycin C treatment. $n = 3$/group. **(E)** Plate colony formation of KP-LC cells after infection and mitomycin-C treatment. **(F)** Viral protein expression was determined in KP-LC or KPL 160302S cells at 24 and 72 h post-infection +/− mitomycin C treatment of cells. Anti-E1A was used to confirm AdV protein expression. Anti-VV coat protein was used to confirm VV protein expression. GAPDH was used as a loading control. $^{**}p < 0.01$ and $^{***}p < 0.001$.

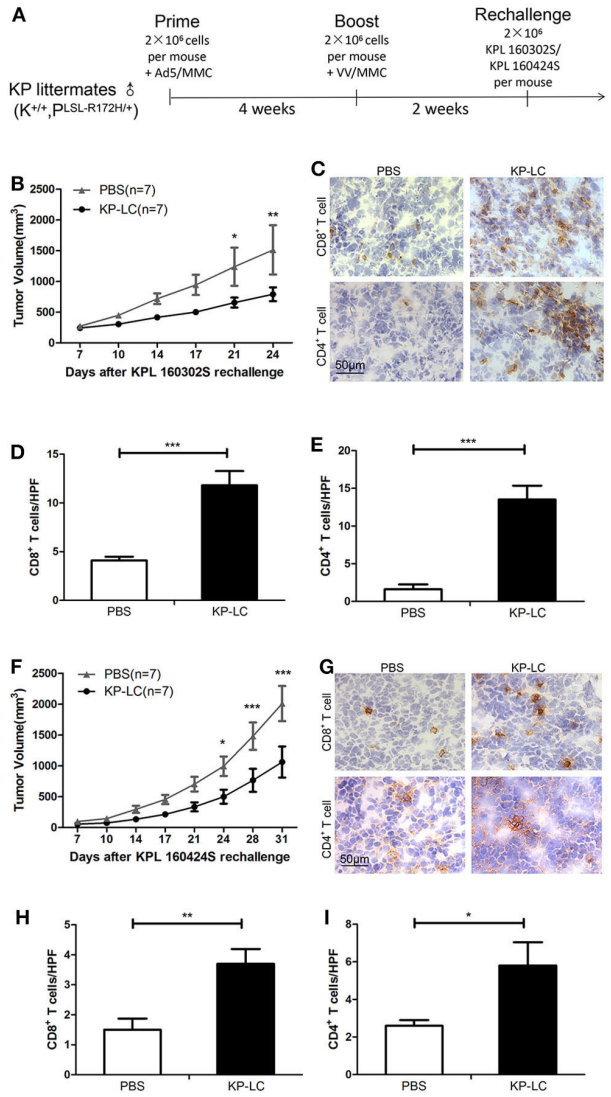


FIGURE 3 | A KP-LC VIReST immunization regime can protect against tumor growth in a subcutaneous lung cancer model. **(A)** KP littermates were immunized with AdV-infected KP-LC cells, followed by a booster immunization using VV-infected KP-LC cells 4 weeks later. Two weeks after boost, mice were challenged using 2×10^6 KPL 160302S or KPL 160424S cells. **(B)** Mice were treated using the regime shown in **(A)** and KPL 160302S tumor growth monitored. Mean subcutaneous tumor sizes ± SEM are shown for each group and compared using a 2-way ANOVA with Bonferroni *post-hoc* testing (n = 7/group). **(C)** Representative images of immuno-histochemical staining for CD8+ and CD4+ T cells in subcutaneous tumors derived from **(B)** 24 days post-inoculation. **(D,E)** Lymphocytes were counted in 10 high power fields (HPFs) randomly selected from each group. Mean ± SEM are shown for each group of CD8+ T cells **(D)** or CD4+ T cells **(E)** and compared using an independent T-test. **(F)** KP littermates ($K^{+/+}$, $P^{LSL-R172H/+}$) immunized as in **(A)** were re-challenged using KPL 160424S tumor cells (n = 7/group). Mean subcutaneous tumor sizes ± SEM are shown for each group and compared using a 2-way ANOVA with Bonferroni *post-hoc* testing. **(G)** Representative images of immuno-histochemical staining for CD8+ and CD4+ T cells in subcutaneous tumors derived from **(F)** 31 days post-inoculation. **(H,I)** Lymphocytes were counted in 10 HPFs randomly selected from each group of CD8+ T cells **(H)** or CD4+ T cells **(I)**. Mean ± SEM are shown for each group and compared using an independent T-test. $^*p < 0.05$, $^{**}p < 0.01$, and $^{***}p < 0.001$.

disease onset and mortality in this model compared to treatment with PBS, increasing median survival time by 17% (**Figure 5C** and **Figure S4**). Furthermore, KPL 160302S vaccination also protected this model, increasing median survival time by 21%, but vaccination using KPL 160424S cells did not have a protective function (**Figure 5C** and **Figure S4**). This difference may be attributed to the fact that KP-LC and KPL 160302S had a higher similarity at the transcriptome level (**Figure 1F**) and elicited similar immune responses (**Figures 4B–D**). MageE1, a cancer-testis antigen (CTA), was expressed at significantly higher levels in KP-LC compared to KPL 160424S (**Figure S2B**) and as previously, genes differentially expressed by KP-LC and KPL 160424S were enriched in several pathways associated with cancer (**Figure S2D**). This may form part of the reason why the efficacy of KP-LC is higher than KPL 160424S. Depletion of both CD8+ (**Figure 5D**) and CD4+ (**Figure 5E**) T cells reduced the survival advantage afforded by KP-LC VIReST treatment (**Figure S5**), demonstrating that the induction of adaptive immune responses is vital for treatment efficacy. Given the sensitivity of some lung tumors to immune checkpoint inhibition (ICI), coupled with an impressive induction of adaptive T cell immunity after vaccination, we reasoned that combination treatment of VIReST with ICI may improve overall mortality. Interestingly however, when induced transgenic mice were treated with α-PD1 antibody, no synergy with VIReST treatment was observed and the efficacy was not enhanced (**Figure 5F** and **Figure S5**), although the PD1 blockade did improve the survival of animals compared to untreated control animals. This suggests that treatment failure in this model may not be due to PD1-PDL1-mediated T cell anergy and alternative immunotherapeutic approaches may be considered as synergistic partners.

Of note, an important concern in the development of vaccines derived from "self"-somatic cells is the possibility of breaking immune tolerance against self-antigens. However, none of the immunized mice developed any evident signs of autoimmune disorders and there was no difference in the amount of circulating anti-nuclear antibodies (ANA) detected between immunized and unimmunized mice (**Figure 5G**), suggesting that the VIReST regimen was not associated with significant risk of induction of autoimmunity. In addition, no tumor formation was detected at the site of inoculation, demonstrating VIReST as a safe approach for prophylactic prevention of lung cancer as depicted in **Figure 6**.

DISCUSSION

Vaccination strategies for lung cancer have historically been unsuccessful, with no positive reports through large, late stage clinical trials over the last decade. However, our improved understanding of the fundamental processes underlying the cancer-immunity cycle has led to a resurgence of interest in developing cancer vaccination strategies, which will be underpinned by rational approaches to selection of tumor antigen targets and prevention of immune suppression. We have recently described a novel vaccination strategy for pancreatic cancer that overcomes current limitations of antigen selection by

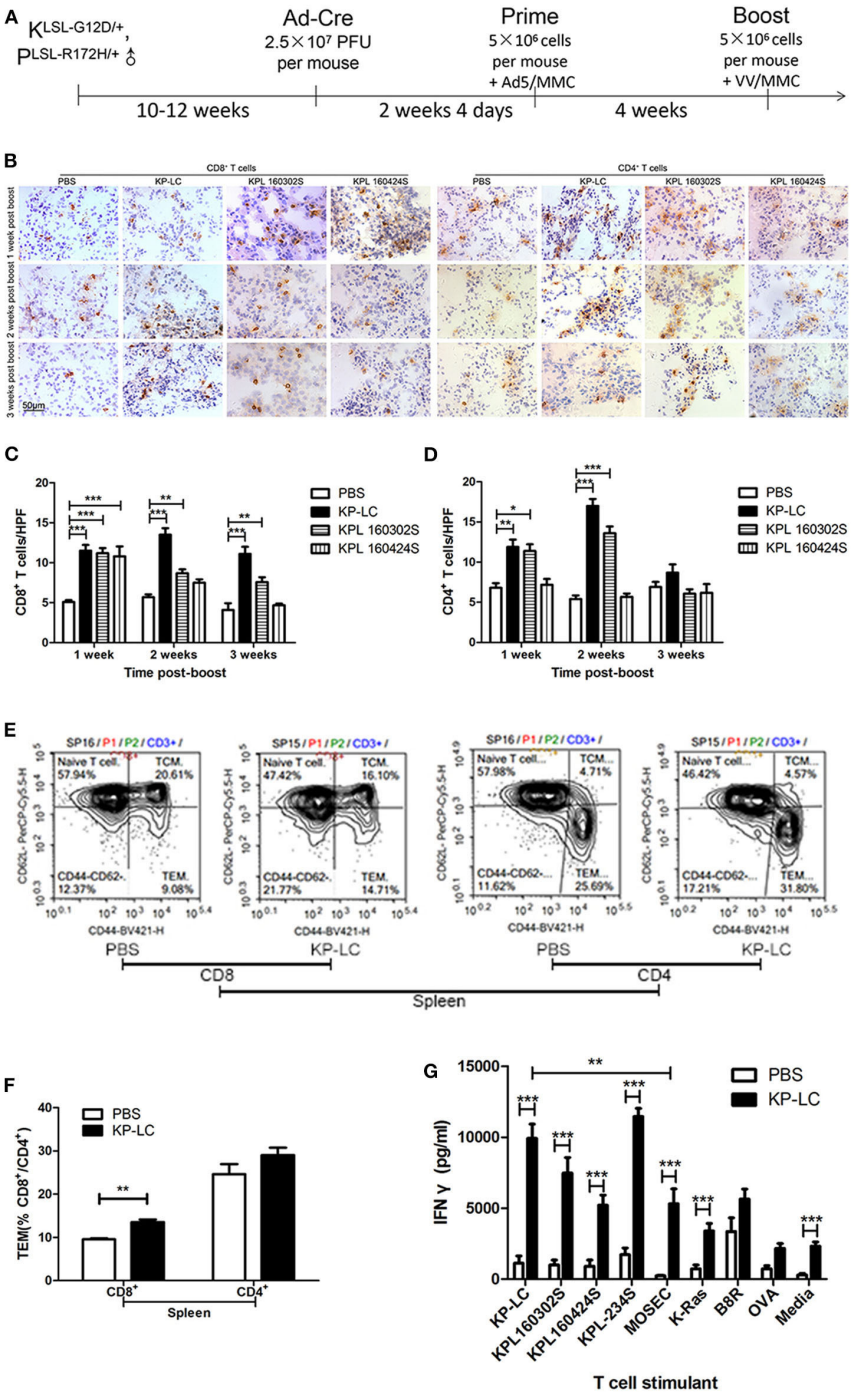


FIGURE 4 | A VIReST regime using induced KP-LC tumor cells induces potent anti-tumor immune responses. **(A)** Schematic representing the immunization protocol. LSL-KRAS$^{G12D/+}$; LSL-Trp53$^{R172H/+}$ mice were infected with Ad-Cre to induce lung cancer development. Two weeks 4 days later, mice were immunized with AdV-infected, mitomycin C-treated KP-LC iPSC-derived tumor cells, KPL 160302S, lung tumor cells, or KPL 160424S lung tumor cells. Four weeks later, a booster of VV-infected, mitomycin C-treated KP-LC, KPL 160302S, KPL 160424S cells were subcutaneously given. Control animals were treated with PBS at the same time points. **(B)** Representative images of immunohistochemical staining for CD8+ or CD4+ T cells in lung tissues from immunized cre-infected KP mice 1, 2, and 3 weeks post-boost. **(C,D)** Lymphocytes were counted in 10 high power fields (HPFs) randomly selected from each group of CD8+ T cells **(C)** or CD4+ T cells **(D)**. Three mice per time point per group were used. Mean ± SEM are shown for each group and compared using a one-way ANOVA with Tukey post-test. **(E)** Spleens of KP-LC immunized mice were collected 3 weeks post-boost and stained for CD3, CD8, CD4, CD44, and CD62L. Representative images of flow cytometry were shown. **(F)** The percentages of effector memory T cells (TEM) (CD44^{hi}; CD62L^{lo}) of **(E)** are shown (n = 3/group). Mean ± SEM are shown for each group and compared using an independent t-test. **(G)** Three weeks post-booster vaccination, splenocytes were re-stimulated *ex-vivo* with growth-arrested lung cancer cells as shown, or mouse ovarian surface epithelial cells (MOSEC) or K-RAS or B8R or OVA peptides or media and IFNγ production measured using ELISA. Three mice per group were analyzed in triplicate and the mean IFNγ production ± SEM is shown. Significance was analyzed using an independent T-test. $^{*}p < 0.05$, $^{**}p < 0.01$, and $^{***}p < 0.001$.

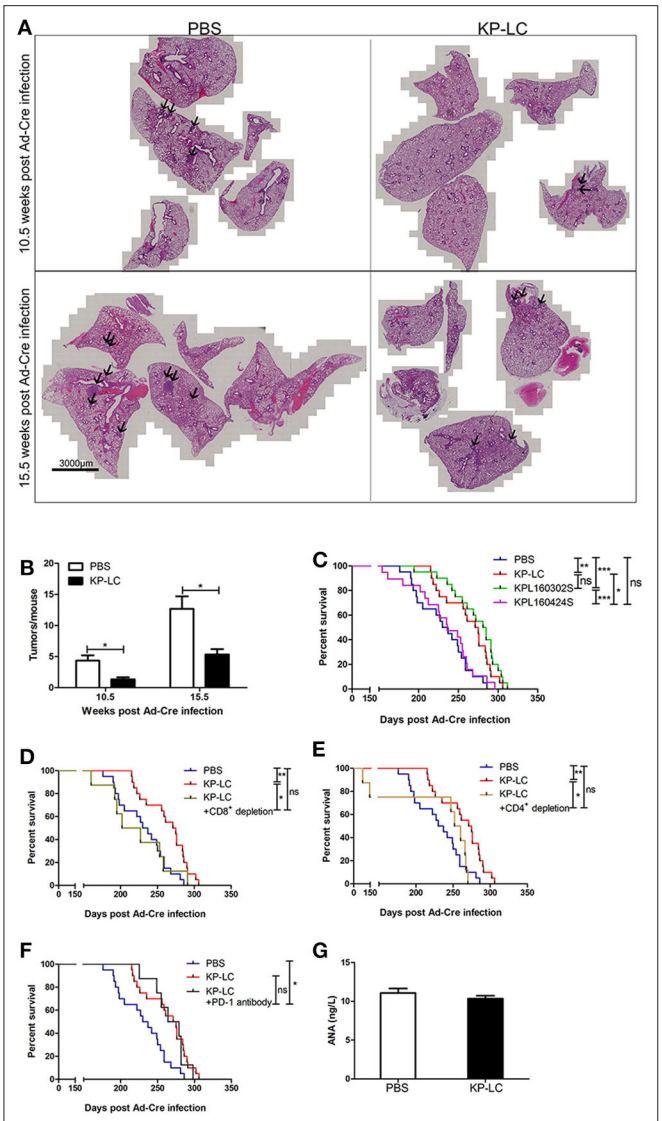


FIGURE 5 | A VIReST regime using iPSC-derived lung tumor cells delays mortality in an induced transgenic model of lung cancer. Ten to twelve week-old KP transgenic mice were immunized using a VIReST regime as shown in **Figure 4A**. **(A)** Lung tissues of mice 10.5 or 15.5 weeks post-Ad-Cre infection were collected. Representative images of H&E staining are shown. Tumor tissue is indicated by the arrows. **(B)** Tumors present in the H&E stained sections were counted. Significance was analyzed using a student's independent *T*-test. **(C)** After treatment with PBS/KP-LC/KPL 160302S/KPL 160424S vaccination ($n = 20$/group for PBS or KP-LC or KPL 160302S; $n = 19$/group for KPL 160424S), long term survival was monitored. Kaplan-Meier survival analysis followed by Log rank (Mantel-Cox) tests was used to determine significance. **(D)** KP mice were treated with the KP-LC VIReST regime with or without CD8+ T cell depletion and survival monitored as above ($n = 20$/group for PBS or KP-LC; $n = 8$/group for depletion). **(E)** KP mice were treated with the KP-LC VIReST regime with or without CD4+ T cell depletion and survival monitored as above ($n = 20$/group for PBS or KP-LC; $n = 8$/group for depletion). **(F)** KP mice were treated with the KP-LC VIReST regime with or without additional α-PD1 treatment and survival monitored as above ($n = 20$/group for PBS or KP-LC; $n = 8$/group for α-PD1 treatment). Kaplan-Meier survival analysis followed by Log rank (Mantel-Cox) tests was used to determine significance. **(G)** Sera of immunized mice and control mice were analyzed by ELISA for presence of ANAs. $^{*}p < 0.05$, $^{**}p < 0.01$, $^{***}p < 0.001$, and ns, no significance.

creating autologous cancer vaccines directly from stem cells (10). Using two common driver mutations, $KRAS^{G12D}$ and $P53^{R172H}$, we were able to replicate the transcriptome profile of cancer cells isolated from transgenic mice in our stem cell derived pancreatic cancer cells. Here, we extend this protocol to lung cancer and importantly demonstrate that despite the use of the same, albeit ubiquitous, driver mutations, the antigenic profile of subsequent tumor cell lines was highly identical to lung cancer cell lines from induced transgenic models, but not related to pancreatic cancer cells derived in the same manner. This demonstrates that the initiating mutations are less relevant to the ensuing accrual of passenger mutations than the epigenetics and lineage specialization of individual tumors. As driver mutations can be expected to have low immunogenicity, these passenger mutations must be key targets if vaccination strategies are to be successful (10, 24). One of the most important aspects of this vaccination regime is the ability to apply entirely autologous vaccines early, or even prior to, disease development. Early application will be the key to vaccine success, as antigen-specific T cell induction can occur prior to selection of MHCI loss of heterogeneity (LOH) variants, common in the evolution of many cancers (25). It has previously been shown that a large proportion of neoantigens were observed to bind to lost MHCI haplotypes (26). Furthermore, recent evidence supports a model of branched evolution in cancers that leads to variable, but potentially considerable intra-tumoral heterogeneity in different tumor types (27–29). This factor may be less relevant for lung cancer vaccination strategies, as recent analysis suggests that 76% of all mutations can be detected in all region of the tumor (9). However, this characterization also revealed that accrual of non-synonymous mutations occur as early events in the evolution of cancer, thus early treatment potentially targets a large number of immunogenic antigens, prior to immune suppression or evasion, setting up an immune system capable of long-term control of disease.

Early disease management is also vital for avoiding the strongly immunosuppressive environment that occurs later in disease evolution. Indeed, early pre-malignant lesions are heavily infiltrated by immune cells with an activated phenotype suggesting an ongoing anti-tumor response. At this stage, immunosuppressive cells are considered rare (7). To maximize the immunogenicity of the vaccine at this stage, we developed a VIReST protocol, in which the stem cell derived cancer cells were pre-infected with either AdV or VV prior to administration in a prime-boost vaccination regime. Virus-infected cell vaccines, whereby tumor cells are pre-infected with replicating tumor tropic virus prior to delivery as a vaccine, has been shown to provoke high levels of anti-tumor immunity that was not achieved when cells were delivered without infection (23), suggesting that replicating viruses can provide relevant danger signals required for vaccine immunogenicity. We have previously demonstrated that replicating viruses can provide adjuvant danger signals and that sequential application of oncolytic AdV followed by VV provides superior efficacy compared to use of either virus alone or in the reverse order when administered as therapeutics in animal tumor models (15) or as vaccine adjuvants (10). We have also previously shown that the VIReST

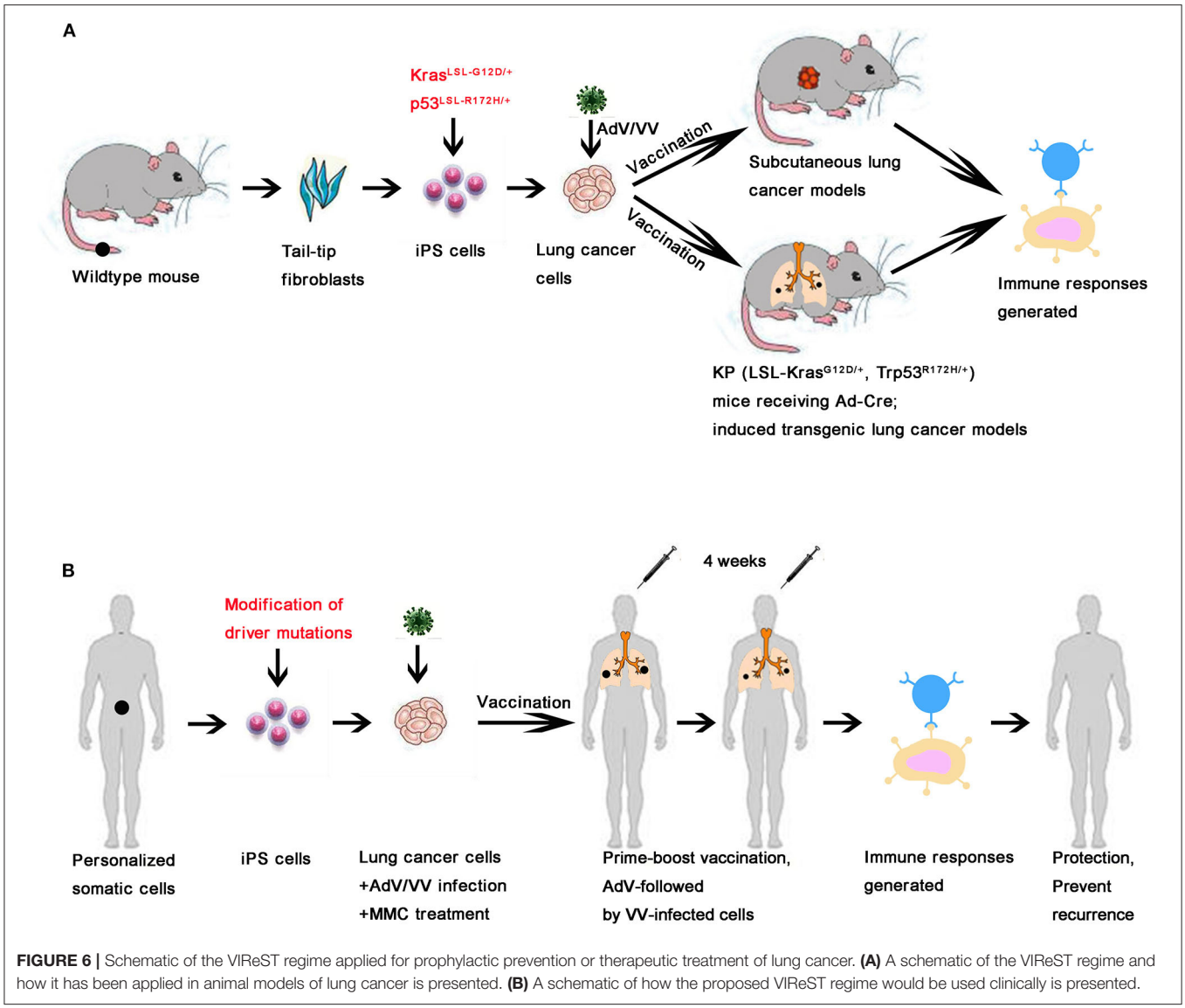


FIGURE 6 | Schematic of the VIReST regime applied for prophylactic prevention or therapeutic treatment of lung cancer. **(A)** A schematic of the VIReST regime and how it has been applied in animal models of lung cancer is presented. **(B)** A schematic of how the proposed VIReST regime would be used clinically is presented.

regime is ineffective in a pancreatic cancer model when stem cell-derived cancer cells are delivered without concomitant viral infection (10).

Given that vaccine efficacy will be most prominent in early stage or pre-malignant disease, a patient selection issue arises. Lung cancers symptoms rarely appear until tumors are at an advanced, often incurable stage. However, a number of developments have led to the introduction of screening techniques that can be applied to high risk individuals, including Low-Dose Cat Scans (LCDT) that have been endorsed for annual use to detect early signs of cancer (30, 31). In this regard, use of personalized vaccine as an adjuvant to surgical removal of pre-cancerous lesions can be envisaged. In addition, circulating tumor DNA can be detected in the early-stage lung cancers based on driver mutations (32, 33), and changes in gene expression levels in the bronchial airway can be identified before tumorigenesis (34, 35). These latter advances may also make it possible to more accurately tailor VIReST to the individual, by identification of driver mutations specific to the individual that can be used to derive the lung cancer cells from iPSCs. Patient tailored treatments will be vital for induction of long-term efficacy, considering the role that environmental factors play in the induction of lung tumors through a range of driver mutations.

The results presented here suggest that it is feasible to create personalized cancer cells from iPSCs without the need for specimens from surgical biopsy, and these induced cancer cells can mimic the original tumor, or potential tumor, to a great extent. In addition to its use as an early-stage, or even prophylactic, vaccine we also expect a role for this technology in the detection of drug sensitivity of specific cancers *in vitro*.

To increase the efficiency of manufacture, it is possible to source iPSCs with matched HLA molecules from iPSC stocks (36) and safety concerns are addressed by preventing ongoing cell

division using MMC treatment prior to application. No tumor growth was observed at the inoculation site in any experiment conducted and circulating ANA levels suggest no autoimmunity was induced by the treatment.

In this study, we showed that KP-LC vaccine evokes anti-tumor T cell responses using both subcutaneous tumor and induced transgenic models of disease (**Figure 6A**) and significantly extended the survival time of KP-LC vaccinated mice, although notably did not prevent disease related death. This suggests scope for improvement of the regime, that should include optimizing the number of prime-boost cycles applied to the patient and more specific tailoring of iPSCs by introduction of other driver mutations, particularly those associated with genetic inheritance, including EGFR amongst others (37). It is worth noting that vaccination produced by the lung cancer cell line KP-LC derived from iPS cells or the lung cancer cell line KPL 160302S derived from early lung cancer models can both significantly prolong the survival of lung cancer mice, and their effect on CD8+ T cells and CD4+ T cells infiltration are similar. These two cell lines showed the highest similarities at the transcriptome level and so we inferred that the lung cancer cell line induced by iPS cells can largely mimic lung cancer cell lines from early stage tumors. Interestingly, vaccination produced by the lung cancer cell line KPL 160424S derived from advanced lung cancer models cannot prolong the survival of mice and we speculate that lung cancer cells derived from iPS cells or early staged lung cancer had more immunogenic neo-antigens because they had not been significantly screened or edited by the immune system compared with the lung cancer cells from advanced lung cancer. Interestingly, at the transcriptome level, several genes enriched in cancer associated pathways were expressed more highly in KP-LC than KPL 160424S. Thus, iPS cells can be used as a source of cells for individualized preventive or therapeutic vaccination and for the latter case will be extremely valuable when it is difficult to obtain sufficient tumor cells from early stage cancers to create personalized treatments. Further bioinformatical analysis of the transcriptome data generated from this research may prove invaluable in determining important antigen targets for future vaccination strategies.

Immune checkpoint inhibition (ICI) has emerged as a promising and powerful tool for cancer therapy and some lung cancers have been shown to be sensitive to treatment with ICI therapies clinically. Here we were unable to induce synergy when combining VIReST with α-PD1 antibody therapy, suggesting that ultimate treatment failure in our model was not due to PD1-PD-L1-mediated T cell anergy. Indeed, while immune checkpoint inhibition has been adopted for treatment of non-small cell lung cancer (NSCLC), in fact only a small subset of patients respond to treatment (38). Objective responses have been noted to correlate with higher mutational burdens (39) or as a result of involvement of specific driver mutations that result in induction of PD-L1 expression within the TME (40). Thus, genetic analysis of early stage disease may select patient populations expected to respond more effectively to the combination of VIReST and immune checkpoint blockade. There are however, a number of alternative or complementary avenues for further exploration of combination treatments that may improve regime efficacy, including targeting TIM-3 and Lag-3, additional co-inhibitory receptors known to be clinically significant in lung cancer escape from immune control (41) or inhibition of TReg (42) and MDSC suppressive cells (43) within the developing TME.

In summary, we have described a technological platform for the development of highly antigenically related lung cancer cells from iPSCs of healthy individuals and an effective vaccination regime for prevention and treatment of lung cancer (**Figure 6B**). These tumor cells were developed via introduction of common tumor driver mutations, but the resulting antigenic profile was not dependent on the driver mutation introduced, suggesting that the epigenetics of an individual, specific to tissue lineage, account for the pattern of neo-antigens expressed. Clearly the situation in human patients is far more complex than reflected in the mouse model used in this study and driving tumorigenesis by introducing further driver mutations, to tailor iPSCs even more accurately, is possible. This technology also has potential for therapeutic use, after tumor resection where adequate viable autologous material is not recovered, as a mechanism to prevent tumor recurrence and metastasis after surgery. Determination of patients for primary prophylactic use is more complex, however identified high-risk individuals would be an obvious population for targeted vaccination strategies. Ultimately, the VIReST provides a safe and effective platform upon which to create robust preventative vaccines that are personalized to be most effective at preventing development or eliminating nascent tumors and preventing their recurrence.

DATA AVAILABILITY STATEMENT

The datasets presented in this study can be found in online repositories. The names of the repository/repositories and accession number(s) can be found in the article/ **Supplementary Material**.

ETHICS STATEMENT

This animal study was reviewed and approved by the Animal Welfare and Research Ethics Committee of Zhengzhou University.

AUTHOR CONTRIBUTIONS

YW conceived and supervised this study. YW and LZ were responsible for all aspects of study design and managed the project. ZheZ and SL designed and conducted most of the experiments and the analysis of results with LD. ZheZ, NW, and WY did *in vitro* and *in vivo* characterization of reprogrammed tumor cells and immune assays. SL supervised the iPS differentiation *in vitro*. ZheZ, ZW, ZhoZ, YaL, JW, YuL, KL, YJ, DS, and PW did animal experiments. ZC and DG performed histopathology studies. YC made oncolytic Adv and VV virus. ZW and YD did the bioinformatics analysis for RNA sequencing. JD and NL participated in interpretation of some experiments and critically reviewed the manuscript. LD, ZheZ, SL, and YW

interpreted all results and wrote the manuscript. All authors contributed to the article and approved the submitted version.

FUNDING

This project was supported by the National Key R&D program of China (2016YFE0200800), the Nature Sciences Foundation of China (81272525 and 81771776), and the core funding for development of the Cell and Gene Therapy Programme by Zhengzhou University. LD was funded by the MRC (MR/M015696/1).

ACKNOWLEDGMENTS

We are grateful to Prof. David Tuveson, Professor Iain McNeish, and Professor Istvan Fodor for providing materials for this study.

SUPPLEMENTARY MATERIAL

The Supplementary Material for this article can be found online at: https://www.frontiersin.org/articles/10.3389/fimmu.2020.01996/full#supplementary-material

REFERENCES

1. Bray F, Ferlay J, Soerjomataram I, Siegel RL, Torre LA, Jemal A. Global cancer statistics 2018: GLOBOCAN estimates of incidence and mortality worldwide for 36 cancers in 185 countries. *CA Cancer J Clin*. (2018) 68:394–424. doi: 10.3322/caac.21492
2. Mascaux C, Tomasini P, Greillier L, Barlesi F. Personalised medicine for nonsmall cell lung cancer. *Eur Respir Rev*. (2017) 26:170066. doi: 10.1183/16000617.0066-2017
3. Butts C, Socinski MA, Mitchell PL, Thatcher N, Havel L, Krzakowski M, et al. Tecemotide (L-BLP25) versus placebo after chemoradiotherapy for stage III non-small-cell lung cancer (START): a randomised, double-blind, phase 3 trial. *Lancet Oncol*. (2014) 15:59–68. doi: 10.1016/S1470-2045(13)70510-2
4. Tagliamento M, Rijavec E, Barletta G, Biello F, Rossi G, Grossi F, et al. CIMAvax-EGF, a therapeutic non-small cell lung cancer vaccine. *Expert Opin Biol Ther*. (2018) 18:829–35. doi: 10.1080/14712598.2018.1492539
5. Quoix E, Lena H, Losonczy G, Forget F, Chouaid C, Papai Z, et al. TG4010 immunotherapy and first-line chemotherapy for advanced non-small-cell lung cancer (TIME): results from the phase 2b part of a randomised, double-blind, placebo-controlled, phase 2b/3 trial. *Lancet Oncol*. (2016) 17:212–23. doi: 10.1016/S1470-2045(15)00483-0
6. Giaccone G, Bazhenova LA, Nemunaitis J, Tan M, Juhasz E, Ramlau R, et al. A phase III study of belagenpumatucel-L, an allogeneic tumour cell vaccine, as maintenance therapy for non-small cell lung cancer. *Eur J Cancer*. (2015) 51:2321–9. doi: 10.1016/j.ejca.2015.07.035
7. Finn OJ. The dawn of vaccines for cancer prevention. *Nat Rev Immunol*. (2018) 18:183–94. doi: 10.1038/nri.2017.140
8. de Bruin EC, McGranahan N, Mitter R, Salm M, Wedge DC, Yates L, et al. Spatial and temporal diversity in genomic instability processes defines lung cancer evolution. *Science*. (2014) 346:251–6. doi: 10.1126/science.1253462
9. Zhang J, Fujimoto J, Zhang J, Wedge DC, Song X, Zhang J, et al. Intratumor heterogeneity in localized lung adenocarcinomas delineated by multiregion sequencing. *Science*. (2014) 346:256–9. doi: 10.1126/science.1256930
10. Lu S, Zhang Z, Du P, Chard LS, Yan W, El Khouri M, et al. A virus-infected, reprogrammed somatic cell-derived tumor cell (VIReST) vaccination regime can prevent initiation and progression of pancreatic cancer. *Clin Cancer Res*. (2020) 26:465–76. doi: 10.1158/1078-0432.CCR-19-1395
11. Herbst RS, Morgensztern D, Boshoff C. The biology and management of non-small cell lung cancer. *Nature*. (2018) 553:446. doi: 10.1038/nature25183
12. Hingorani SR, Wang L, Multani AS, Combs C, Deramaudt TB, Hruban RH, et al. Trp53R172H and KRASG12D cooperate to promote chromosomal instability and widely metastatic pancreatic ductal adenocarcinoma in mice. *Cancer Cell*. (2005) 7:469–83. doi: 10.1016/j.ccr.2005.04.023
13. Denes B, Yu J, Fodor N, Takatsy Z, Fodor I, Langridge WH. Suppression of hyperglycemia in NOD mice after inoculation with recombinant vaccinia viruses. *Mol Biotechnol*. (2006) 34:317–27. doi: 10.1385/MB:34:3:317
14. Tysome JR, Briat A, Alusi G, Cao F, Gao D, Yu J, et al. Lister strain of vaccinia virus armed with endostatin-angiostatin fusion gene as a novel therapeutic agent for human pancreatic cancer. *Gene Ther*. (2009) 16:1223–33. doi: 10.1038/gt.2009.74
15. Tysome JR, Li X, Wang S, Wang P, Gao D, Du P, et al. A novel therapeutic regimen to eradicate established solid tumors with an effective induction of tumor-specific immunity. *Clin Cancer Res*. (2012) 18:6679–89. doi: 10.1158/1078-0432.CCR-12-0979
16. Huang SX, Islam MN, O'Neill J, Hu Z, Yang YG, Chen YW, et al. Efficient generation of lung and airway epithelial cells from human pluripotent stem cells. *Nat Biotechnol*. (2014) 32:84–91. doi: 10.1038/nbt.2754
17. Kim D, Langmead B, Salzberg SL. HISAT: a fast spliced aligner with low memory requirements. *Nat Methods*. (2015) 12:357–60. doi: 10.1038/nmeth.3317
18. Anders S, Pyl PT, Huber W. HTSeq–a Python framework to work with high-throughput sequencing data. *Bioinformatics*. (2015) 31:166–9. doi: 10.1093/bioinformatics/btu638
19. Hansen KD, Irizarry RA, Wu Z. Removing technical variability in RNA-seq data using conditional quantile normalization. *Biostatistics*. (2012) 13:204–16. doi: 10.1093/biostatistics/kxr054
20. Reed LJ, Muench H. A simple method of estimating fifty percent endpoints. *Am J Hyg*. (1938) 27:493–7. doi: 10.1093/oxfordjournals.aje.a118408
21. Dupage M, Dooley AL, Jacks T. Conditional mouse lung cancer models using adenoviral or lentiviral delivery of Cre recombinase. *Nat Protoc*. (2009) 4:1064–72. doi: 10.1038/nprot.2009.95
22. Kooreman NG, Kim Y, De Almeida PE, Termglinchan V, Diecke S, Shao N-Y, et al. Autologous iPSC-based vaccines elicit anti-tumor responses *in vivo*. *Cell Stem Cell.* (2018) 22:501–13.e7. doi: 10.1016/j.stem.2018.01.016
23. Lemay CG, Rintoul JL, Kus A, Paterson JM, Garcia V, Falls TJ, et al. Harnessing oncolytic virus-mediated antitumor immunity in an infected cell vaccine. *Mol Ther*. (2012) 20:1791–9. doi: 10.1038/mt.2012.128
24. Schoenberger SP. Is it possible to develop cancer vaccines to neoantigens, what are the major challenges, and how can these be overcome? Targeting the right antigens in the right patients. *Cold Spring Harb Perspect Biol*. (2018) 10:a028837. doi: 10.1101/cshperspect.a028837
25. Garrido F, Aptsiauri N, Doorduijn EM, Garcia Lora AM, Van Hall T. The urgent need to recover MHC class I in cancers for effective immunotherapy. *Curr Opin Immunol*. (2016) 39:44–51. doi: 10.1016/j.coi.2015.12.007
26. McGranahan N, Rosenthal R, Hiley CT, Rowan AJ, Watkins TBK, Wilson GA, et al. Allele-specific HLA loss and immune escape in lung cancer evolution. *Cell.* (2017) 171:1259-71.e11. doi: 10.1016/j.cell.2017.10.001
27. Navin N, Kendall J, Troge J, Andrews P, Rodgers L, Mcindoo J, et al. Tumour evolution inferred by single-cell sequencing. *Nature*. (2011) 472:90–4. doi: 10.1038/nature09807
28. Sottoriva A, Spiteri I, Piccirillo SG, Touloumis A, Collins VP, Marioni JC, et al. Intratumor heterogeneity in human glioblastoma reflects cancer evolutionary dynamics. *Proc Natl Acad Sci USA*. (2013) 110:4009–14. doi: 10.1073/pnas.1219747110
29. Cancer Genome Atlas Research Network. Integrated genomic characterization of pancreatic ductal adenocarcinoma. *Cancer Cell.* (2017) 32:185–203.e13. doi: 10.1016/j.ccell.2017.07.007
30. Midthun DE. Early detection of lung cancer. *F1000Res.* (2016) 5:F1000. doi: 10.12688/f1000research.7313.1
31. Heuvelmans MA, Oudkerk M. Appropriate screening intervals in low-dose CT lung cancer screening. *Transl Lung Cancer Res*. (2018) 7:281–7. doi: 10.21037/tlcr.2018.05.08
32. Izumchenko E, Chang X, Brait M, Fertig E, Kagohara LT, Bedi A, et al. Targeted sequencing reveals clonal genetic changes in the progression of early

lung neoplasms and paired circulating DNA. *Nat Commun*. (2015) 6:8258. doi: 10.1038/ncomms9258
33. Cohen JD, Li L, Wang Y, Thoburn C, Afsari B, Danilova L, et al. Detection and localization of surgically resectable cancers with a multi-analyte blood test. *Science*. (2018) 359:926–30. doi: 10.1126/science.aar3247
34. Gustafson AM, Soldi R, Anderlind C, Scholand MB, Qian J, Zhang X, et al. Airway PI3K pathway activation is an early and reversible event in lung cancer development. *Sci Transl Med*. (2010) 2:26ra25. doi: 10.1126/scitranslmed.3000251
35. Kensler TW, Spira A, Garber JE, Szabo E, Lee JJ, Dong Z, et al. Transforming cancer prevention through precision medicine and immune-oncology. *Cancer Prev Res*. (2016) 9:2–10. doi: 10.1158/1940-6207.CAPR-15-0406
36. Inoue H, Nagata N, Kurokawa H, Yamanaka S. iPS cells: a game changer for future medicine. *EMBO J*. (2014) 33:409–17. doi: 10.1002/embj.201387098
37. Yamamoto H, Yatabe Y, Toyooka S. Inherited lung cancer syndromes targeting never smokers. *Transl Lung Cancer Res*. (2018) 7:498–504. doi: 10.21037/tlcr.2018.06.01
38. Santini FC, Hellmann MD. PD-1/PD-L1 axis in lung cancer. *Cancer J*. (2018) 24:15–9. doi: 10.1097/PPO.0000000000000300
39. Rizvi NA, Hellmann MD, Snyder A, Kvistborg P, Makarov V, Havel JJ, et al. Cancer immunology. Mutational landscape determines sensitivity to PD-1 blockade in non-small cell lung cancer. *Science*. (2015) 348:124–8. doi: 10.1126/science.aaa1348
40. Akbay EA, Koyama S, Carretero J, Altabef A, Tchaicha JH, Christensen CL, et al. Activation of the PD-1 pathway contributes to immune escape in EGFR-driven lung tumors. *Cancer Discov*. (2013) 3:1355–63. doi: 10.1158/2159-8290.CD-13-0310
41. Datar IJ, Sanmamed MF, Wang J, Henick BS, Choi J, Badri T, et al. Expression analysis and significance of PD-1, LAG-3 and TIM-3 in human non-small cell lung cancer using spatially-resolved and multiparametric single-cell analysis. *Clin Cancer Res*. (2019) 25:4663–73. doi: 10.1158/1078-0432.CCR-18-4142
42. Akimova T, Zhang T, Negorev D, Singhal S, Stadanlick J, Rao A, et al. Human lung tumor FOXP3+ Tregs upregulate four "Treg-locking" transcription factors. *JCI Insight*. (2017) 2:e94075. doi: 10.1172/jci.insight.94075
43. Weber R, Fleming V, Hu X, Nagibin V, Groth C, Altevogt P, et al. Myeloid-derived suppressor cells hinder the anti-cancer activity of immune checkpoint inhibitors. *Front Immunol*. (2018) 9:1310. doi: 10.3389/fimmu.2018.01310

Conflict of Interest: SL, ZheZ, and YW are inventors of a filed patent in the relevant field.

The remaining authors declare that the research was conducted in the absence of any commercial or financial relationships that could be construed as a potential conflict of interest.

Copyright © 2020 Zhang, Lu, Dunmall, Wang, Cheng, Zhang, Yan, Chu, Gao, Wang, Li, Wang, Li, Ji, Shan, Li, Wang, Dong, Dong, Lemoine, Pei, Zhang and Wang. This is an open-access article distributed under the terms of the Creative Commons Attribution License (CC BY). The use, distribution or reproduction in other forums is permitted, provided the original author(s) and the copyright owner(s) are credited and that the original publication in this journal is cited, in accordance with accepted academic practice. No use, distribution or reproduction is permitted which does not comply with these terms.

frontiers in Immunology

HYPOTHESIS AND THEORY
published: 30 October 2020
doi: 10.3389/fimmu.2020.584680

Mature Dendritic Cells May Promote High-Avidity Tuning of Vaccine T Cell Responses

Adarsh Kumbhari[1†], *Colt A. Egelston*[2†], *Peter P. Lee*[2‡] *and Peter S. Kim*[1*‡]

[1] School of Mathematics and Statistics, University of Sydney, Sydney, NSW, Australia, [2] Department of Immuno-Oncology, Beckman Research Institute, City of Hope, Duarte, CA, United States

Therapeutic vaccines can elicit tumor-specific cytotoxic T lymphocytes (CTLs), but durable reductions in tumor burden require vaccines that stimulate high-avidity CTLs. Recent advances in immunotherapy responses have led to renewed interest in vaccine approaches, including dendritic cell vaccine strategies. However, dendritic cell requirements for vaccines that generate potent anti-tumor T-cell responses are unclear. Here we use mathematical modeling to show that, counterintuitively, increasing levels of immature dendritic cells may lead to selective expansion of high-avidity CTLs. This finding is in contrast with traditional dendritic cell vaccine approaches that have sought to harness ex vivo generated mature dendritic cells. We show that the injection of vaccine antigens in the context of increased numbers of immature dendritic cells results in a decreased overall peptide:MHC complex load that favors high-avidity CTL activation and expansion. Overall, our results provide a firm basis for further development of this approach, both alone and in combination with other immunotherapies such as checkpoint blockade.

Keywords: T-cell avidity, DC vaccines, cancer vaccines, immature DCs, mathematical model

OPEN ACCESS

Edited by:
Graham Pawelec, University of Tübingen, Germany

Reviewed by:
Markus Philipp Radsak, Johannes Gutenberg University Mainz, Germany
Michele De Palma, École Polytechnique Fédérale de Lausanne, Switzerland

***Correspondence:**
Peter S. Kim
peter.kim@sydney.edu.au

†These authors share first authorship

‡These authors have contributed equally to this work

Specialty section:
This article was submitted to Vaccines and Molecular Therapeutics, a section of the journal Frontiers in Immunology

Received: *17 July 2020*
Accepted: *05 October 2020*
Published: *30 October 2020*

Citation:
Kumbhari A, Egelston CA, Lee PP and Kim PS (2020) Mature Dendritic Cells May Promote High-Avidity Tuning of Vaccine T Cell Responses. Front. Immunol. 11:584680. doi: 10.3389/fimmu.2020.584680

INTRODUCTION

In principle, the immune system can eliminate cancer cells by the activation and expansion of cancer-specific cytotoxic T lymphocytes (CTLs). Immune checkpoint blockade (ICB) immunotherapies, which release T cells from various negative regulatory pathways, have demonstrated impressive clinical successes and have become standard-of-care for many malignancies (1). However, the response to ICB seems to require the pre-existence of anti-tumor T cells (2). Vaccine approaches to generate tumor-specific T cells offer a potential solution towards generating a sufficient anti-tumor T cell response. Dendritic cell (DC) vaccines in particular, offer a means to activate and expand tumor-specific T cells (3). Here we discuss the impact of DC maturation status on vaccine design strategies.

CTLs detect cancer cells by T cell receptor (TCR) recognition of peptides displayed by a major histocompatibility complex (pMHC) on the surface of target cancer cells. Each TCR-pMHC interaction occurs at a particular strength–*affinity*–with multiple TCR-pMHC interactions occurring for each CTL-target cell interaction. While affinity is a measure of individual TCR-pMHC bonds, *avidity* is an overall measure of the strength of the TCR-pMHC interaction and as such, depends on the amount of

pMHC expressed by antigen presenting cells (4). Importantly, T cell avidity determines the likelihood of successful lysis (5).

Therapeutic peptide vaccines aim to capitalize on the cancer-killing ability of CTLs. Initial results of peptide-based vaccines showed the ability to elicit significant numbers of antigen-specific CTLs, but often lacked measurable clinical successes (6–8). Recent progress in vaccine construction and combinatorial strategies with other immunotherapy agents has shown renewed promise for therapeutic peptide vaccines (3). Our work suggests that the dose and modality of peptide vaccines are key considerations for the design of future clinical interventions.

Early studies of cancer-specific CTLs showed that high-avidity TCRs are necessary to effectively lyse cancer cells that express native antigens at low levels (9). Preferentially selecting for high-avidity CTLs, however, is difficult. Regarding vaccines targeting cancer-associated antigens (CAA), thymic education of CTLs may likely have removed high-avidity T cells from the T-cell repertoire *via* negative selection (10). As a result, primarily low-avidity CTLs are left to respond to CAA-targeting vaccines. Beyond CAA, recent therapeutic vaccine efforts have focused on targeting somatic mutation-derived neo-antigens (11, 12). As yet, neo-antigen vaccines have largely focused on peptides sought to elicit high affinity TCR responses but have not yet explored the impact of dosage on T-cell repertoire response to the vaccine (13, 14). For both CAA and neo-antigen targeting vaccines, standard dosages typically involve high antigen loads that may non-discriminately favor the expansion of both high and low avidity CTLs. However, lowering the dosage of peptides for vaccination yields sub-therapeutically relevant levels of CTL (15). Together, this highlights the need for further understanding of antigen dosage and context for efficacious vaccine design.

We previously showed that therapeutic vaccine designs were sensitive to DC-associated parameters (16). Given that DCs, which present antigen on their cell surface along with co-stimulatory molecules, facilitate CTL activation, we hypothesized that modulation of DC and peptide dosing could enhance an anti-cancer immune response. We show that by increasing the number of immature DCs (iDCs), the average DC antigen load is lowered, which in turn selects for the expansion of high-avidity CTLs. This observation suggests traditional DC vaccine approaches that intravenously inject ex vivo matured DCs (mDCs) may need to be reconsidered in favor of an injection of iDCs paired with injection of peptide and adjuvant (3, 17). Our work suggests that combinatorial therapy with vaccine antigens and increased immature DCs, either by ex vivo generation or stimulated *in vivo*, may have efficacy. Thus, our findings suggest an approach that could improve already existing immune-based cancer therapies for increased and more durable clinical responses.

MATERIAL AND METHODS

We previously developed a mathematical model to study how vaccine-induced avidity selection affects tumor clearance (16). This model was calibrated to ex vivo human data from Chung et al. (18) and then validated against data from (19, 20). Here, we extend this model to show that induction of immature DCs may improve current treatments by eliciting high-avidity CTLs. What follows is a brief description of our previously published model. We primarily use parameter estimates from the literature (see **Table 1** and the references therein) and estimates generated from our prior analysis of ex vivo human data.

Basic Model

The model consists of three major components: the activation and maturation of DCs (Eqs 1–8); the activation and proliferation of T cells (Eqs 9–16); and the lysis and trogocytosis-mediated MHC stripping of cancer cells by effector CTLs (Eqs 23–25). **Figure 1** depicts a schematic of these interactions.

Dendritic Cells

To model the activation and maturation of DCs at the injection site (the volume of which is V_{tissue}), we consider several populations: P, the concentration of vaccine peptides; A, the concentration of vaccine adjuvant; I, the concentration of immature DCs; S, the concentration of semi-mature or "tolerizing" DCs; and M_j, the concentration of maturing DCs presenting j vaccine-associated pMHCs, where j can vary between zero and N. In modelling the interactions between these populations, we assume that immature DCs become semi-mature in the presence of peptide antigen, various danger signals, and tissue-derived immunogenic signals (57, 58). Once in this semi-mature state, we assume DC maturation occurs as a result of vaccine adjuvant. DC maturation signals may in turn affect T-cell priming and activation (19). As a simplifying assumption, we assume that the strategy to optimize DC maturation is successful. That is, we do not model the pharmacodynamics of the vaccine adjuvant. Next, we model the interactions between these populations with an ODE system:

Change in vaccine peptide concentration:

$$\frac{dP}{dt} = \underbrace{u(t)}_{\substack{\text{Vaccine}\\ \text{injection}}} - \underbrace{d_P P}_{\text{Vaccine turnover}} - \underbrace{k_{Pi} PI}_{\text{Uptake by iDCs}} - \underbrace{k_P P \sum_{j=0}^{N} M_j}_{\text{Uptake by mDCs}} - \underbrace{k_{P\phi} P,}_{\substack{\text{Turnover due to}\\ \text{macrophage uptake}}} \quad (1)$$

Change in adjuvant concentration:

$$\frac{dA}{dt} = \underbrace{a(t)}_{\text{Adjuvant injection}} - \underbrace{k_{Pi} AI}_{\text{Uptake by iDCs}} - \underbrace{d_A A}_{\text{Adjuvant washout}} - \underbrace{k_{P\phi} A,}_{\substack{\text{Turnover due to}\\ \text{macrophage uptake}}} \quad (2)$$

Change in immature DC concentration:

$$\frac{dI}{dt} = \underbrace{s_D}_{\text{iDC supply}} - \underbrace{\delta_D I}_{\text{iDC turnover}} - \underbrace{k_D \frac{P}{\chi + P} I,}_{\text{iDC activation}} \quad (3)$$

Change in semi-mature/tolerized DC concentration:

$$\frac{dS}{dt} = \underbrace{k_D \frac{P}{\chi + P} I}_{\text{iDC activation}} - \underbrace{d_D S}_{\text{Turnover}} - \underbrace{k_S \frac{A}{A + A_0} S,}_{\substack{\text{Maturation due to}\\ \text{adjuvant}}} \quad (4)$$

TABLE 1 | Estimates that are characterized by human data are marked with a superscript H, while estimates based on murine data are marked with a superscript M.

Parameter	Description	Estimate	Reference
d_p	Peptide decay rate [V]	6.16/day	(21)
k_P	Mature DC uptake rate [HV]	3×10^{-2} $(k/\mu L)^{-1}$/day	(22)
k_{Pi}	Immature DC uptake rate [MV]	6.84×10^{-2} $(k/\mu L)^{-}$/day	(23)
$k_{P\phi}$	Vaccine clearance rate due to tissue macrophages [MV]	3.1875/day	(24)
δ_D	Immature DC decay rate [HV]	5×10^{-2}/day	(25)
S_D	Immature DC supply rate	$\delta_D I$ (0)	Steady state
$I(0)$	Immature DC concentration	5.9976 k/μL	(26)
d_A	Adjuvant washout rate [M]	0.396/day	(27)
k_S	Semi-matured/tolerized DC maturation rate	5×10^6/day	Estimate
A_0	Adjuvant saturation constant	10^4 ng/mL	Estimate
d_D	Mature DC decay rate [HV]	0.33/day	(25)
χ	Concentration of non-vaccine-associated proteins [H]	7×10^7 ng/mL	(28)
k_D	Mature DC presentation rate [MV]	2.4×10^5 pMHCs/day	(29, 30)
d_m	pMHC degradation rate [MV]	2.9/day	(31)
N	(Computational) maximum number of vaccine-associated pMHCs on a maturing DC	700	(16)
J	Number of avidity levels	20	(16)
$d_N N(0)$	Naive CTL supply rate		Steady state
S_H	Naive helper T cell supply rate	$d_{NH} N^H(0)$	Steady state
S_R	Naive nTreg supply rate	$d_{NR} N_R(0)$	Steady state
d_N	Naive CTL egress rate [M]	1.2/day	(32)
d_{NH}	Naive helper T cell egress rate [M]	2.2/day	(32)
d_{NR}	Naive nTreg turnover rate [M]	2.2×10^{-3}/day	(33)
$N(0)$	Initial naive CTL concentration [M]	7.6×10^{-3} k/μL	(34–37)
$N^H(0)$	Initial naive helper T cell concentration [M]	0.0571 k/μL	(34, 38)
$N_R(0)$	Initial naive nTreg concentration [M]	$0.05 \times N^H(0)$	(39)
R_{LH}	Ratio of low-high avidity naive CTLs	100	Assumption
n_R	Number of nTreg divisions [HV]	6	(40)
k_{DC}	Naive CTL-DC interaction rate [M]	0.4 $(k/\mu L)^{-1}$/day	(34)
τ_m	DC migration time [M]	0.75 days	(34)
V_{tissue}	Volume of tissue site	1000 μL	(16)
V_{LN}	Volume of lymph node [M]	4.2 μL	(34)
n_H	Number of helper T cell divisions [HV]	10	(41)
τ_a	T cell division time [M]	1 day	(38, 42)
d_H	Effector helper T cell decay rate [H]	0.008/day	(43)
n_T	Number of CTL divisions [M]	15	(42, 44–47)
d_T	Effector CTL decay rate [H]	0.009/day	(43)
φ_0	Antigen saturation constant	5×10^3 ng/mL	(16)
r_1	Secretion rate of growth signal by CTLs	0.1/day	(16)
r_2	Secretion rate of growth signal by helper T cells	1/day	(16)
d_G	Growth factor decay rate [H]	144.4/day	(48)
k_G	T cell-growth factor interaction rate	0.1 $(k/\mu L)^{-1}$/day	(16)
k_R	iTreg differentiation rate	0.2/day	(16)
d_R	iTreg decay rate [H]	0.083/day	(49, 50)
d_{RN}	Effector nTreg decay rate [H]	0.063/day	(50)
μ	CTL-Treg interaction rate [H]	5 $(k/\mu L)^{-1}$/day	(16)
K	(Computational) maximum number of cognate pMHCs expressed on cancer cell	295	(16)
γ	Growth rate of melanomas [H]	0.0185/day	(51–53)
κ	Carrying capacity of melanomas [M]	736 k/μL	(54)
α	pMHC regeneration rate [MV]	8.4/day	(55, 56)
k_T	Tumor-CTL interaction rate [HV]	16.1 $(k/\mu L)^{-1}$/day	Estimate
p_T	Probability of trogocytosis [HV]	0.7	Estimate
ω_1	Lysis likelihood for lowest avidity ($j = 1$) CTL [HV]	0.28	Estimate
ω_J	Lysis likelihood for highest avidity ($j = J$) CTL [HV]	0.96	Estimate
C_{init}	Initial cancer concentration	0.05 k/μL	(16, 18)

Additionally, estimates that are based on cell culture data are marked with a superscript V. Finally, the unit 'k' denotes 10^3 cells.

Change in mature DC concentration:

$$\frac{dM_0}{dt} = -k_D \frac{P}{\chi + P} M_0 + d_m M_1 - d_D M_0, \tag{5}$$

$$\frac{dM_1}{dt} = \underbrace{k_S \frac{A}{A + A_0} S}_{\text{Maturation due to adjuvant}} + \underbrace{k_D \frac{P}{\chi + P} (M_0 - M_1)}_{\text{pMHC presentation}} + \underbrace{d_m (2M_2 - M_1)}_{\text{pMHC turnover}} - \underbrace{d_D M_1}_{\text{mDC turnover}}, \tag{6}$$

$$\frac{dM_j}{dt} = \underbrace{k_D \frac{P}{\chi + P} \left(M_{j-1} - M_j\right)}_{\text{pMHC presentation}} + \underbrace{d_m \left((j+1)M_{j+1} - jM_j\right)}_{\text{pMHC turnover}} - \underbrace{d_D M_j}_{\text{mDC turnover}}, \tag{7}$$

$$\text{for } j = 2, \ldots, N-1,$$

$$\frac{dM_N}{dt} = k_D \frac{P}{\chi + P} M_{N-1} - N d_m M_N - d_D M_N \,. \tag{8}$$

In Equation 1, vaccine peptides are injected intramuscularly at rate $u(t)$, decay at rate d_p, taken up by immature DCs at rate k_{Pi}, taken up by mature DCs at rate k_p, and are competitively diminished due to consumption by tissue macrophages at rate $k_{P\phi}$ (note that we do not model these macrophages in our study). Here, we assume that iDCs have a greater antigen uptake rate than mDCs (59, 60). In Equation 2, vaccine adjuvants are injected intramuscularly at rate $a(t)$, taken up by immature

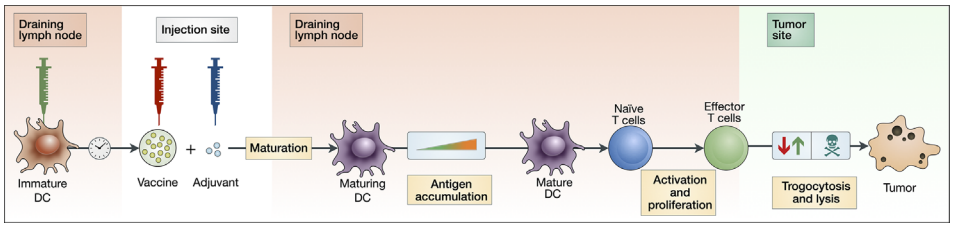


FIGURE 1 | Block diagram depicting key aspects of our theoretical vaccination model. An injection of peptide vaccine is given intramuscularly with adjuvant. Immature DCs are injected intranodally, prompting an accumulation of antigen by maturing DCs. These maturing DCs then migrate and activate naive T cells in the lymph node, which then proliferate into effector T cells. Effector T cells can both strip peptides off the surface of cancer cells *via* trogocytosis and kill cancer cells.

DCs at rate k_{Pi}, washed out at rate d_A, and are lost due to consumption by splenic macrophages at rate $k_{P\phi}$. In Equation 3, immature DCs are supplied at rate s_D, decay at rate δ_D and become semi-mature and acquire vaccine peptides at rate $k_D \frac{P}{\chi+P}$. Here, k_D is the rate of peptide presentation, χ is the concentration of non-vaccine peptides, and $\frac{P}{\chi+P}$ is the proportion of peptides presented that are vaccine specific.

In Equation 4, we assume that semi-mature DCs, S, turnover at a rate comparable to mature DCs d_D, and mature due to adjuvant at rate $k_S \frac{A}{A+A_0}$. Here, k_S is the maturation rate due to adjuvant and A_0 is a adjuvant-saturation constant that ensures that for large adjuvant doses, the DC maturation tapers off. In the absence of adjuvant, however, these semi-mature DCs are unlikely to produce a functional T cell response (61). Thus, for the purposes of this study we do not track T cells that become tolerized as a result of these semi-mature/tolerized DCs.

In Eqs 5 and 6, newly matured DCs initially enter the mature DC population presenting one vaccine peptide with subsequent peptides presented at rate $k_D \frac{P}{\chi+P}$ as described above. Additionally, surface peptides degrade at rate d_m, which is proportional to the number of presented peptides, j. Finally, mature DCs decay at rate d_D. Here, we assume that mature DCs decay faster than iDCs (62).

T Cells

To model the activation and proliferation of T cells both at the lymph node (the volume of which is V_{LN}) and at the tumor site, we first model avidity as a spectrum that varies from j=1 to j=J, corresponding to the lowest and highest avidity states respectively. We then consider several populations: N_j, the concentration of naive CTLs of avidity j; N_j^H, the concentration of naive helper T cells of avidity j; N_R, the concentration of naive natural regulatory T cells; T_j, the concentration of effector CTLs of avidity j; H_j, the concentration of effector helper T cells of avidity j; R, the concentration of induced regulatory T cells; R_N, the concentration of effector natural regulatory T cells; and G, the concentration of positive growth factors. The interactions between these populations are then modelled with an ODE system:

Change in naive helper T cell concentration:

$$\frac{dN_j}{dt} = \underbrace{\rho_j s_T}_{\text{Supply}} - \underbrace{d_N N_j}_{\text{Turnover}} - \underbrace{\frac{V_{\text{tissue}}}{V_{\text{LN}}} e^{-d_D\tau_m} \sum_{k=1}^{N} (k_{\text{DC}} p_{j,k}) N_j M_k(t-\tau_m)}_{\text{Activation}}, \quad (9)$$

Change in naive killer T cell concentration:

$$\frac{dN_j^H}{dt} = \underbrace{\rho_j s_H}_{\text{Supply}} - \underbrace{d_{NH} N_j^H}_{\text{Turnover}} - \underbrace{\frac{V_{\text{tissue}}}{V_{\text{LN}}} e^{-d_D\tau_m} \sum_{k=1}^{N} (k_{\text{DC}} p_{j,k}) N_j^H M_k(t-\tau_m)}_{\text{Activation}}, \quad (10)$$

Change in naive natural regulatory T cell concentration:

$$\frac{dN_R}{dt} = \underbrace{s_R}_{\text{Supply}} - \underbrace{d_{NR} N_R}_{\text{Turnover}} - \underbrace{\frac{V_{\text{tissue}}}{V_{\text{LN}}} e^{-d_D\tau_m} \sum_{k=1}^{N} \sum_{j=1}^{J} (k_{\text{DC}} p_{j,k}) N_R M_k(t-\tau_m)}_{\text{Activation}}, \quad (11)$$

Change in effector killer T cell concentration:

$$\frac{dT_j}{dt} = \overbrace{e^{-d_N\tau_a} \varphi(P) 2^{n_T} e^{-d_D\tau_m} \sum_{k=1}^{N} (k_{DC} p_{j,k}) \quad N_j(t-\tau_a) M_k(t-\tau_m-\tau_a)}^{\text{T cell induction}} \quad (12)$$

$$- \overbrace{d_T T_j}^{\text{Turnover}} - \overbrace{\mu R T_j}^{\text{iTreg suppression}} - \underbrace{\mu R_N T_j}_{\text{nTreg suppression}} + \underbrace{k_G G T_j}_{\text{Growth due to growth factors}},$$

Change in effector helper T cell concentration:

$$\frac{dH_j}{dt} = \overbrace{e^{-d_{NH}\tau_a} 2^{n_H} e^{-d_D\tau_m} \sum_{k=1}^{N} (k_{DC} p_{j,k}) \quad N_j^H(t-\tau_a) M_k(t-\tau_m-\tau_a)}^{\text{Tcellinduction}}$$

$$\text{Differentiation into iTregs} \quad \overbrace{k_R H_j}^{\text{iTreg supression}} - \overbrace{\mu R H_j}^{\text{nTreg supression}} - \underbrace{\mu R_N H_j}_{\text{Turnover}} + \underbrace{d_H H_j}_{\text{Growth due to growth factors}} \underbrace{k_G G H_j}, \quad (13)$$

Change in natural regulatory T cell concentration:

$$\frac{dR_N}{dt} = \underbrace{e^{-d_{NR}\tau_a} 2^{n_R} e^{-d_D\tau_m} \sum_{k=1}^{N} \sum_{j=1}^{J} (k_{\text{DC}} p_{j,k}) N_R(t-\tau_a) M_k(t-\tau_m-\tau_a)}_{\text{nTreg induction}} - \underbrace{d_{RN} R_N}_{\text{Turnover}}, \quad (14)$$

Change in induced regulatory T cell concentration:

$$\frac{dR}{dt} = \underbrace{k_R \sum_{j=1}^{J} H_j}_{\substack{\text{Differentiated} \\ \text{helper T cells}}} - \underbrace{d_R R}_{\text{Turnover}}, \tag{15}$$

Change in concentration of positive growth factors:

$$\frac{dG}{dt} = \underbrace{r_1 \sum_{j=1}^{J} T_j}_{\substack{\text{Secretion} \\ \text{by CTLs}}} + \underbrace{r_2 \sum_{j=1}^{J} H_j}_{\substack{\text{Secretion by} \\ \text{helper T cells}}} \underbrace{- k_G G \sum_{j=1}^{J} \left(T_j + H_j\right)}_{\substack{\text{Consumption} \\ \text{by T cells}}} - \underbrace{d_G G}_{\text{Turnover}}. \tag{16}$$

In Equation 9, naive CTLs in the lymph node of avidity j are supplied at rate $\rho_j s_T$, where ρ_j is the proportion supplied that have avidity j. These naive CTLs also exit the lymph node at rate d_N. The rate at which naive CTLs are activated by mature DCs that have migrated into the lymph node is

$$\frac{V_{\text{tissue}}}{V_{\text{LN}}} e^{-d_D \tau_m} \sum_{k=1}^{N} \left(k_{\text{DC}} p_{j,k}\right) N_j M_k(t - \tau_m). \tag{17}$$

Migration is modelled with a fixed delay of τ_m, with $e^{-d_D \tau_m}$ being the proportion that survives migration. For intranodal injections, the value of τ_m is set to zero. The kinetic interaction rate between naive CTLs of avidity j and mature DCs presenting k vaccine-peptides is k_{DC} with $p_{j,k}$ being the probability of an interaction leading to successful activation. This means the *net* kinetic rate, $k_{\text{DC}} p_{j,k}$, depends on both T cell avidity, j, and the number of pMHCs presented on a DC, k. Finally, the leading term $\frac{V_{\text{tissue}}}{V_{\text{LN}}}$ accounts for the volume change between the injection site and the lymph node. However, for intranodal injections, this ratio is set to one as there will be no change in volume. In Equation 10, which is similar to Equation 9, naive helper T cells of avidity j are supplied at rate $\rho_j s_H$, decay at rate d_{NH}, and are activated at the net rate of

$$\frac{V_{\text{tissue}}}{V_{\text{LN}}} e^{-d_D \tau_m} \sum_{k=1}^{N} \left(k_{\text{DC}} p_{j,k}\right) N_j^H M_k(t - \tau_m). \tag{18}$$

In Equation 11, which is similar to Eqs 9 and 10, naive natural regulatory T cells (nTregs) are supplied at rate s_R, decay at rate d_{NR}, and are activated at the net rate of

$$\frac{V_{\text{tissue}}}{V_{\text{LN}}} e^{-d_D \tau_m} \sum_{k=1}^{N} \sum_{j=1}^{J} \left(k_{\text{DC}} p_{j,k}\right) N_R M_k(t - \tau_m). \tag{19}$$

As we do not account nTregs of different avidities, we sum over the variable j.

Equations 12–16 describe interactions within the tumor site. In Equation 12, naive CTLs undergo n_T divisions. The division program is modelled with a fixed delay of τ_a, with $e^{d_N \tau_a}$ being the proportion that effectively activate and traffic to the tumor site. As a consequence, not all T cells that exit the lymph node arrive as effector T cells at the tumor site. These assumptions equate to a net supply rate of

$$e^{-d_N \tau_a} 2^{n_T} k_{\text{DC}} e^{-d_D \tau_m} \sum_{k=1}^{N} p_{j,k} N_j(t - \tau_a) M_k(t - \tau_m - \tau_a). \tag{20}$$

To account for T-cell hyporesponsiveness, we multiply Equation 20 by $\varphi(P) = \frac{\varphi_0}{\varphi_0 + \int_0^t P(s)\, ds}$. This ensures that antigen accumulation results in diminished effector CTL expansion. We also assume effector CTLs: decay at rate d_T; expand due to interactions with positive growth factors at rate k_G; and are suppressed by interactions with induced regulatory T cells at rate μ. Given that induced regulatory T cells (iTregs) and effector nTregs have similar suppression rates (63, 64), we assume that nTregs suppress effector CTLs at an identical rate of μ.

In Equation 13, naive helper T cells undergo n_H divisions. Following a similar argument to that in Equation 12, the net supply rate of effector helper T cells is

$$e^{-d_{NH} \tau_a} 2^{n_H} k_{\text{DC}} e^{-d_D \tau_m} \sum_{k=1}^{N} p_{j,k} N_j(t - \tau_a) M_k(t - \tau_m - \tau_a). \tag{21}$$

These effector helper T cells differentiate into induced regulatory T cells at rate k_R; are suppressed by both iTregs and nTregs at rate μ; decay at rate d_H; and expand due to interactions with positive growth factors at rate k_G.

In Equation 14, following a similar argument to that in Equation 12, effector nTregs enter the system at rate

$$e^{-d_{NR} \tau_a} 2^{n_R} e^{-d_D \tau_m} \sum_{k=1}^{N} \sum_{j=1}^{J} (k_{DC} p_{j,k}) N_R(t - \tau_a) M_k(t - \tau_m - \tau_a), \tag{22}$$

and decay at rate d_{RN}. In Equation 15, iTregs enter the system as differentiated effector helper T cells and decay at rate d_R. Finally, in Equation 16, effector CTLs and helper T cells secrete growth factors such as IL-2 at rates r_1 and r_2. These growth factors are assumed to decay at rate d_G.

Cancer Cells

To model the lysis of cancer cells and trogocytosis of cancer cell MHC by effector CTLs, we consider a population of cancer cells presenting k vaccine-associated peptides, C_k, where k varies from zero to K. The interactions between these cancer cells and effector CTLs are modelled with an ODE system:

$$\frac{dC_0}{dt} = \gamma(1 - C_{total}/\kappa)(C_0 + C_1) - \alpha C_0 + k_T \left(\sum_{j=1}^{N} T_j\right) \left(\sum_{m=1}^{K} C_m q_{m,m}\right), \tag{23}$$

For $k = 1, \cdots, K-1$,

$$\overbrace{\frac{dC_0}{dt} = \gamma(1 - C_{total}/\kappa)(-C_k + 2C_{2k} + C_{2k-1} + C_{2k+1})}^{\text{Growth}} + \overbrace{\alpha(C_{k-1} - C_k)}^{pMHC\ \ regeneration} + \underbrace{k_T\left(\sum_{j=1}^{N} T_j\right)\left(\left(\sum_{m=k+1}^{K} C_m q_{m-k,m}\right) - C_k(1-q_{0,k})\right)}_{Trogocytosis} - \underbrace{k_T \sum_{j=1}^{N} \lambda_{j,k} T_j C_k}_{Lysis}, \quad (24)$$

$$\frac{dC_k}{dt} = \gamma C_k(1 - C_{total}/\kappa) + \alpha C_{K-1} - k_T\left(\sum_{j=1}^{N} T_j\right) C_k(1-q_{0,k}) - k_T \sum_{j=1}^{N} \lambda_{j,k} T_j C_k\,. \quad (25)$$

In Eqs 23–25, the total cancer population, $C_{total} = \Sigma_{k=0}^{K} C_j$, grows logistically at rate γ and with carrying capacity κ. As a simplifying assumption, we assume that the number of surface peptides is halved after mitosis, resulting in a net compartmental growth rate of

$$\gamma\left(1 - \frac{C_{total}}{\kappa}\right)(-C_k + C_{2k} + C_{2k-1} + C_{2k+1}), \quad (26)$$

for the population of cancer cells presenting k peptides, C_k. We also assume that surface peptides are regenerated at rate α. To model trogocytosis-mediated MHC stripping, we assume that CTLs and cancer cells presenting k peptides interact at rate k_T and additionally assume the number of peptides stripped during this interaction is binomially distributed with probability p_T. For brevity we let $q_{m,n} = \binom{n}{m} p_T^m (1-p_T)^{n-m}$ denote the probability that a CTL will trogocytose m MHC:peptides off a cancer cell presenting n surface peptides. This allows us to describe the trogocytosis rate as

$$k_T(\Sigma_{j=1}^{N} T_j)\left((\Sigma_{m=k+1}^{K} C_m q_{m-k,m}) - C_k(1-q_{0,k})\right). \quad (27)$$

Finally, to model lysis, we let $\lambda_{j,k}$ denote the lysis probability between a cancer cell presenting k peptides and an effector CTL of avidity j and assume that these interactions occur at rate k_T. This implies the net kinetic interaction rate depends on both T cell avidity and the amount of pMHC presented by a cancer cell. To model the lysis probability, we assume that the probability of lysis increases with cognate pMHCs but is also modulated by CTL avidity. This can be modelled by assuming a probability function of the form

$$1 - e^{-r_j k},$$

where r_j is an avidity-dependent rate parameter chosen so that the lysis probability at maximal levels of cognate pMHC expression, i.e., $\lambda_{j,k}$ varies linearly from ω_1 for the lowest avidity CTL to ω_J for the highest avidity CTL.

Functional Forms

Peptide Vaccine Injection Rate

Here, we assume that the vaccine is injected systemically at a fixed dose, u_0, and at a regular interval of ζ, which corresponds to the functional form

$$u(t) = u_0 \sum_{a=0}^{\infty} \delta(t - \zeta a)\,.$$

Vaccine Adjuvant Injection Rate

We assume that the vaccine adjuvant is injected at a clinically-relevant fixed dose of $5{\times}10^5$ ng/mL (19), and at a regular interval of η, corresponding to the functional form

$$a(t) = (5 \times 10^5 \text{ng/ml}) \times \sum_{n=0}^{\infty} \delta(t - n\eta)\,.$$

Peptide Uptake Rates

We previously used ex vivo human data from (22) to estimate a mature DC uptake rate, k_P, of 3×10^{-2} (k/μL)$^{-1}$/day. It is generally understood that immature DCs, relative to mature DCs, have a greater uptake rate (59, 60). To estimate the uptake rate by iDCs, we use *in vitro* murine data from (23), who note that antigen internalization (as quantified by staining for the antibody YAe) in iDCs is 2.28 times greater than in mDCs. Thus, we assume that the uptake by iDCs, k_{Pi}, is $2.28 \times k_P = 6.84 \times 10^{-2}$ (k/μL)$^{-1}$/day. To account for vaccine clearance by splenic macrophage, we first note the steady-state concentration of non-activated macrophages in mice is estimated to be 1.25×10^{-1} k/μL (24). In (24), the authors also estimate the rate of phagocytosis by non-activated macrophages to be 25.2 (k/μL)$^{-1}$/day. Together, these correspond to a splenic macrophage associated vaccine clearance rate, $k_{P\phi}$, of 25.2 (k/μL)$^{-1}$/day × 0.125 k/μL = 3.1875/day.

Activation Probability

The probability of a mature DC presenting k vaccine-associated pMHCs activating a naive T cell of avidity j, $p_{j,k}$, is modelled with a switch:

$$p_{j,k} = \begin{cases} 1, & \text{if } \left|\frac{j-1}{J-1} - \left(1 - \frac{k-1}{N_c-1}\right)\right| \le \nu \quad and\, k < N_c \\ 1, & \text{if } j = 1 \quad and\, k \ge N_c \\ 0, & otherwise\,. \end{cases}$$

Here, $1/(N_c - 1)$ and $1/(J - 1)$ map j and k from their respective domains to [0,1]. The dimensionless parameter $\nu = 0.05$ determines how sensitive our switching function is to pMHC expression. This characterization ensures that and high pMHC levels on DCs stimulate both high- and low-avidity CTLs (20, 65–69) and by contrast, low pMHC expression stimulates mostly high-avidity CTLs (10, 70–72). To reflect this, we assumed that beyond a critical number of pMHCs, N_c, only low-avidity CTLs were stimulated. We set $N_c = N / 2 = 350$, implying that DCs must have a surface antigen density *below* 50% to stimulate high-avidity CTLs.

Initial Conditions

We assume that the vaccine is first administered at $t = 0$, i.e., $P(0) = u_0$, where u_0 is the vaccine dose. Our model assumes a large number of immature DCs preexist at the injection site. In (73), the total DC population at steady-state conditions in the dermis is estimated to be approximately 23.4 k/μL. Around 92.74% of this population is expected to immature (74), equating to an initial iDC concentration at the injection site of 21.7 k/μL. Similarly, 7.26% of the total DC population is expected to be mature (74), equating to a total mDC concentration of 1.7 k/μL. For intravenous injections, we use a total DC concentration of 25 DCs/μL (75), and assume that 90% of this population is immature, equating to an iDC concentration of 22.5 DCs/μL and total mDC concentration of 2.5DCs/μL. Finally, for intranodal injections, we use a pre-existing LN iDC count of 25,190 cells, and an mDC count of 32,920 cells (26), which for a control volume of V_{LN}, equates to an iDC concentration of 5.9976 k/μL, and a total mDC concentration of 7.8381 k/μL. Moreover, we assume that within this mature DC population, pMHCs are normally distributed with mean $\mu = 100$ and variance $\sigma^2 = 25$ (76). As a simplifying assumption, we assume the initial concentration of semi-mature/tolerizing DCs is zero.

To model the scarcity of high-avidity naive T cells, we assume that their availability decreases exponentially. Specifically, we assume $N_j(0) = \rho_j N(0)$ and $N_j^H(0) = \rho_j N^H(0)$, where $\rho_j = ae^{-bj}$. Here, the model parameters a and b are chosen so that $\Sigma_{j=1}^{J}\rho_j = 1$ and ρ_1/ρ_J, i.e., the ratio low-avidity to high-avidity T cells, equates to the model parameter R_{LH}. In our simulations, we set R_{LH} to 100, which means that for one high-avidity T cell there are 100 low-avidity T cells. Moreover, naive natural regulatory T cells, N_R, make up roughly 5% of the naive helper T cell population (39), thus, we set $N_R(0) = 0.05 \times N^H(0)$.

Prior to vaccination, tumor-specific effector T cells exist, albeit at low concentrations (approximately 0.12% of the total CD8+ count) (77). Assuming a total CD8+ count of 600 cells/μL (78), this equates to an initial tumor-specific effector CTL concentration of 0.72 cells/μL. To estimate the initial tumor-specific effector helper T cell concentration, we assume a comparable percentage (i.e., 0.12%) also exists before vaccination. Using a circulating helper T cell concentration of 10^3 cells/μL (79), this corresponds to an initial tumor-specific effector helper T cell concentration of 1.2 cells/μL. Moreover, approximately 1.5% of this helper T cell pool expresses the natural regulatory T cell phenotype (39), which equates to an initial effector natural regulatory T cell concentration of $R_N(0) = 1.8 \times 10^{-2}$ cells/μL. As a simplification, we assume that initially there are no induced regulatory T cells, i.e., $R(0) = 0$, and that the concentration of growth factor is zero, i.e., $G(0) = 0$. Finally, to account for the scarcity of high-avidity T cells, we multiply the concentrations of effector CTLs and effector helper T cells by ρ_j (defined in the above paragraph). Mathematically, $T_j(0) = \rho_j \times 0.72$ cells/μL and $H_j(0) = \rho_j \times 1.2$ cells/μL. In other words, initially, for every high-avidity tumor-specific effector T cell, there are 100 low-avidity tumor-specific effector T cells.

Finally, we assume that the total cancer cell concentration is C_{init}, with cognate pMHC being normally distributed with mean $\mu = 148$ and variance $\sigma^2 = 49$. Mathematically, if $f_k = \frac{1}{\sigma\sqrt{2\pi}}\exp\left(-\frac{(k-\mu)^2}{2\sigma^2}\right)$, then $C_k(0) = C_{init} \times \frac{f_k}{\Sigma_{k=1}^{K} f_k}$.

Sensitivity Analysis

To understand how DC maturation status affects parameter sensitivity, we conduct sensitivity analysis on our modified model. We account for non-linear interactions between parameters by varying all parameters simultaneously using Latin hypercube sampling (n=250) over the ranges shown in **Table 2**, and measure sensitivity by calculating Spearman's rank correlation coefficient (SRCC), ρ, for each parameter against the fold decrease. These simulations use a peptide vaccine dosage of 7×10^5 ng fortnightly, with an iDC dosage of 10^6 cells/μL injected at the same time as the peptide vaccine. **Table 2** shows SRCC ρ for each parameter.

In our previous model, a sensitivity analysis identified antigen presentation by DCs as a key variable for the beneficial

TABLE 2 | Spearman's rank correlation coefficient between modified model parameters and fold decreases of simulations when varied simultaneously.

Parameter	Description	Range	SRCC
d_p	Peptide decay rate	± 50%	0.0575
k_p	Mature DC uptake rate	± 50%	0.0283
k_{Pi}	Immature DC uptake rate	± 50%	-0.0825
$k_{P\phi}$	Clearance rate due to splenic macrophages	± 50%	-0.0342
k_D	Mature DC presentation rate	± 50%	-0.0274
χ	Concentration of non-vaccine-associated proteins	± 50%	-0.0530
δ_D	Immature DC decay rate	± 50%	0.0198
d_A	Adjuvant washout rate	± 50%	0.1015
d_D	Mature DC decay rate	± 50%	0.0989
k_S	Semi-matured/tolerized DC maturation rate	± 50%	0.0505
d_m	pMHC degradation rate	± 50%	-0.0322
d_N	Naive CTL egress rate	± 50%	-0.1761
d_{NH}	Naive helper T cell egress rate	± 50%	-0.0490
d_{NR}	Naive nTreg turnover rate	± 50%	-0.0285
τ_m	DC migration time	± 50%	0.0717
k_{DC}	Naive CTL-DC interaction rate	± 50%	-0.1214
V_{tissue}	Volume of tissue site	± 50%	0.0427
V_{LN}	Volume of lymph node	± 50%	-0.0591
R_{LH}	Ratio of low-high avidity naive CTLs	10-500	-0.0630
τ_a	T cell division time	± 50%	0.0536
Φ_0	Antigen saturation constant	± 50%	-0.0239
n_T	Number of CTL divisions	10-20	0.4981
n_H	Number of helper T cell divisions	4-10	-0.0036
n_R	Number of nTreg divisions	± 50%	-0.2096
d_R	iTreg decay rate	± 50%	0.0907
d_{RN}	Effector nTreg decay rate	± 50%	-0.1181
d_T	Effector CTL decay rate	± 50%	0.0497
μ	CTL-Treg interaction rate	± 50%	-0.2410
k_G	T cell-growth factor interaction rate	± 50%	-0.0841
k_R	iTreg differentiation rate	± 50%	0.0951
d_H	Effector helper T cell decay rate	± 50%	-0.0119
r_1	Secretion rate of growth signal by CTLs	± 50%	0.0557
r_2	Secretion rate of growth signal by helper T cells	± 50%	0.0508
d_G	Growth factor decay rate	± 50%	0.0774
γ	Growth rate of melanomas	3×10^{-3} to 8.7×10^{-2}/day	-0.7318
κ	Carrying capacity of melanomas	48.7 to 2360 k/μL	0.0260
α	pMHC regeneration rate	± 50%	0.0925
k_T	Tumor-CTL interaction rate	± 50%	0.0998
p_T	Probability of trogocytosis	± 50%	-0.1336
ω_1	Lysis likelihood for lowest avidity (j = 1) CTL	± 50%	0.0588

therapeutic value of vaccines. Here, we amend our model with the induction of immature DCs, resulting in supraphysiological levels of DCs. The resulting scale difference reduces the power of DC-associated parameters. Additionally, the model is now sensitive to the tumor growth rate, γ, suggesting that characteristics such as proliferative and apoptotic cell rates may affect the clinical response to the therapeutic vaccine.

RESULTS

Modified Mathematical Model

We previously found that the rate of antigen presentation by DCs determined the therapeutic value of an anti-tumor CTL response (16). Here, we hypothesize that inducing high levels of immature DCs would preferentially stimulate naive high-avidity CTLs by increasing the total concentration of mature DCs while lowering the average antigen density per DC. To test this proposed approach, we change Equation 2 in our original model (see Materials and Methods) to include a source term, $\nu(t)$, which describes the elicitation of immature DCs, either by injection of ex vivo derived DCs or by recruitment of DC progenitors from the bone marrow *via* cytokine stimulation:

$$\frac{dI}{dt} = s_D + \nu(t) - \delta_D I - k_D \frac{P}{\chi + P} I \,. \tag{23}$$

As a simplifying assumption, we assume that induced immature DCs (iDCs) are given at a fixed dose ν_0, and at dosing intervals of ξ hours *after* the injection of the peptide vaccine, which leads to the functional form:

$$\nu(t) = \nu_0 \sum_{a=0}^{\infty} \delta(t - \xi a) \,. \tag{24}$$

Figure 1 uses a block diagram to depict the key interactions of our model.

Increased immature DC levels yields lower peptide:MHC levels and tumor cell reduction

In our example, we assume our tumor is a melanoma and assume that our vaccine either targets either neo-antigen peptides or classical antigens such as MART1. Initially, we simulate the DC context of the vaccine while leaving the peptide dosage fixed at the previously optimized value of 100 ng daily. Using this low peptide dosing, we effectively fix the pMHC levels on DCs to be low. To assess the robustness of our modified model, we next simulated iDC doses ranging from 10^3 cells/μL to 10^{12} cells/μL, with dosing intervals that range from 0 to 24 hours *after* a peptide injection. For these simulations, we assume that our vaccine adjuvant is delivered at a dose of 10^5 ng simultaneously with the peptide vaccine.

A global sweep of iDC dosages within these ranges identified multiple iDC induction magnitudes as being optimal, i.e., inducing a >90% decrease in tumor burden (**Figure 2A**). For example, an iDC induction magnitude of 10^6 iDCs/μL given at the same time as the peptide vaccine, induced a 97% decrease in tumor burden. Importantly, the substantial reduction in tumor concentration we observed is neither dose dependent nor time dependent within our parameters, with a wide range of iDC concentrations and dosing intervals achieving a high degree of tumor reduction. Indeed, for iDC doses between 10^2 to 10^7 k/μL, the *percentage decrease* in tumor concentration varies minimally from the local optimum regardless of the dosing interval used. We thus find that the temporal robustness of this system centered around iDC induction and high-avidity T cell induction potentially allows for the possibility of introducing other combinatorial therapeutic strategies that may synergize with vaccine strategies, including checkpoint blockade and inducers of immunogenic cell death.

Our initial results demonstrated that increased iDC levels, rather than increased mDC levels, favor robust tumor clearing. We next set to determine if similar results could be recapitulated with clinically relevant vaccine dosages, rather than the 100 ng daily peptide dose identified by our previous model. We first compared pMHC levels in three therapeutic variations: peptide with either no DCs, induction of iDCs, or induction of mDCs with around 6×10^6 DCs (which, for a control volume of V_{LN} =4.2 μL, equates to a concentration of 1.43×10^3 k/μL), a dosing concentration similar to previously used in a clinical setting and within optimal concentrations found in our global sweep above (80). We assume that within this population of ex vivo matured DCs (mDCs), pMHCs are normally distributed with mean μ=100 and variance σ^2 = 25 (76). Additionally, we compare peptide dosing concentrations for both an ideal 100 ng daily and a clinically relevant 7×10^5 ng every 2 weeks (20). Our model shows that at both peptide doses, induction of iDCs results in increased pMHC-low mature DCs as compared to no DC or mDC conditions (**Figure 2B**). This reduced antigen density in the context of the same peptide injection concentrations is due to the significantly increased numbers of mDCs generated by inducing iDCs (**Figure 2B**). These increased numbers are due to the longer half-life of iDCs as compared to mDCs, which are thought to rapidly decay upon maturation. As a result, the same peptide concentration dispensed over a larger number of DCs results in lower pMHC levels per DC.

Immature DCs Promote High-Avidity T Cells and Tumor Clearance in Clinically Relevant Dosing Schemes

Previously, we showed lower levels of pMHC competitively favor the expansion of high-avidity T cells rather than low-avidity T cells (16). As expected, we find that at both peptide dosing schemes induction of iDCs significantly favors the generation of high-avidity T cells compared to mDCs (**Figure 3A**). The optimal low dose of 100 ng daily of peptide significantly favors the development of high-avidity T cells, but even with the clinically relevant dosing of 7×10^5 ng every 2 weeks, the induction of iDCs significantly shifts the balance of T cell composition to favor high-avidity T cells. This highlights that while traditional mDC or peptide-only vaccination strategies do increase T-cell induction, they do so at the expense of high-avidity T cells. In reflection of increased expansion of high-avidity T cells, our simulations further demonstrate that iDC induction results in improved cancer cell lysis (**Figure 3B**).

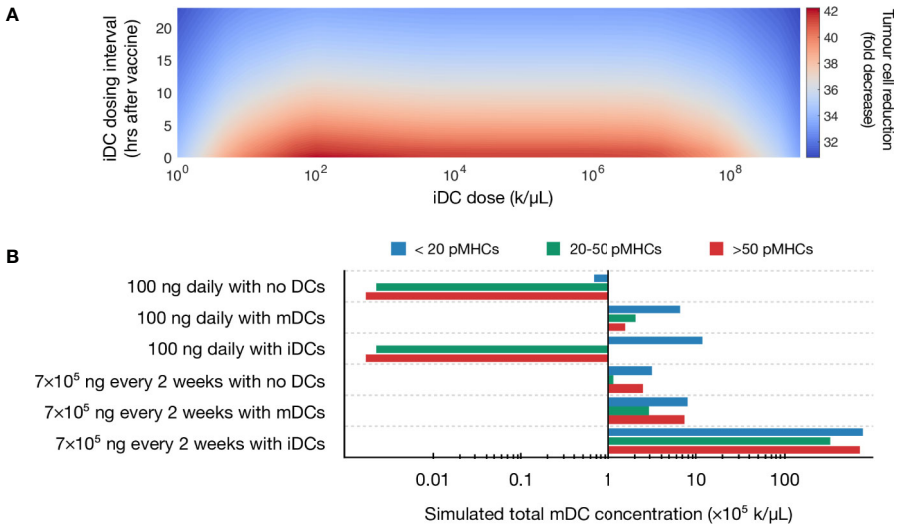


FIGURE 2 | Simulated induction of iDCs favors tumor reduction. **(A)** Heatmap depicts predicted tumor cell reduction (fold change) for different iDC dosages when given with 100 ng of peptide daily. Here, the unit 'k' denotes 10^3 cells. **(B)** Stacked bar chart visualizing the predicted distribution of antigen on mature DCs for various vaccine protocols.

Finally, we compared vaccine responses in three different delivery routes: intramuscular, intravenous, and intranodal. For intramuscular case, at most, only 4% of DCs are expected to arrive at the LN (81). To model this, we multiply the source terms (described by Eqs 17–20) by 4%. To model intravenous delivery, we modify our initial conditions so that DCs in our model are characterized by blood DC data (75). Finally, to model intranodal delivery, we assume there is no migratory delay between the injection site and the LN (i.e., $\tau_m = 0$), and that there is no volume change between DC compartment and the LN compartment. Our simulations suggest that in the context of avidity-selection and tumor clearance (see **Figure 3C**), DC vaccination route is a critical consideration for maximizing vaccine efficiency. iDCs intranodal injections followed by intravenous injection were both preferable over intradermal DC injections. This data highlights the importance of high iDC cell numbers accumulating in the LN in our vaccination model.

DISCUSSION

Cancer immunotherapy is now a routine means of successfully treating tumors of various types in the clinic. However, improved immunotherapies to benefit greater numbers of patients with increased durability are still needed. Despite its tremendous successes, ICB therapy only benefits less than the majority of patients treated (82–84) and presents significant risks for adverse side-effects (85–87). Therapeutic peptide vaccines can robustly induce a tumor-specific CTL response with limited side effects due to induction of an antigen-specific immune response rather than broad immune activation (20). Preferential development of high avidity anti-tumor CTLs enables enhanced tumor cell killing (9, 18). Previously, we showed that vaccine dosages could be optimized to preferentially elicit high-avidity CTLs, unlike standard dosages that elicit low-avidity CTLs (16). In that study, we showed that the efficacy of a dosage-optimized approach depended on DC-related parameters, which motivated us to explore how we could harness immature DCs to boost anti-tumor activity.

High peptide antigen doses have been shown experimentally to result in low avidity and T cell responses (88, 89). However dosing timing strategy has been shown to have a significant effect on the average avidity of a T cell population (90, 91). Other work has shown that modulation of antigen presenting cells is a key component of the induction of high avidity T cells (92). We hypothesized that increasing the magnitude of iDCs given with a dosage-optimized peptide vaccine may enhance CTL responses. It is important to stress that this approach is conceptually different from traditional DC vaccines in which ex vivo matured DCs are injected (3, 17). To assess this approach, we extended our previous model to account for a hypothetical induction of iDCs. We show that induction of iDCs, and not mDCs, can significantly reduce tumor burden, improving upon the performance of a peptide vaccine. A key assumption of our model is that iDCs will have a longer half-life and inducing iDCs will result in a larger overall pool of DCs as compared to the injection of mDCs, which are known to have a shorter half-life (62). Our simulations show that these effects are tied to the increased half-life of iDCs and therefore increased DC levels in general, which results in a lower average antigen density per DC. As such, induction of iDCs favors the preferential stimulation of high-avidity CTLs and tumor cell clearance. In support of our findings, increased circulating DC levels have been associated with increased survival in certain malignancies (93–95). Further experimental or clinical evidence of the relationship between circulating DC levels and vaccination efficacy is needed.

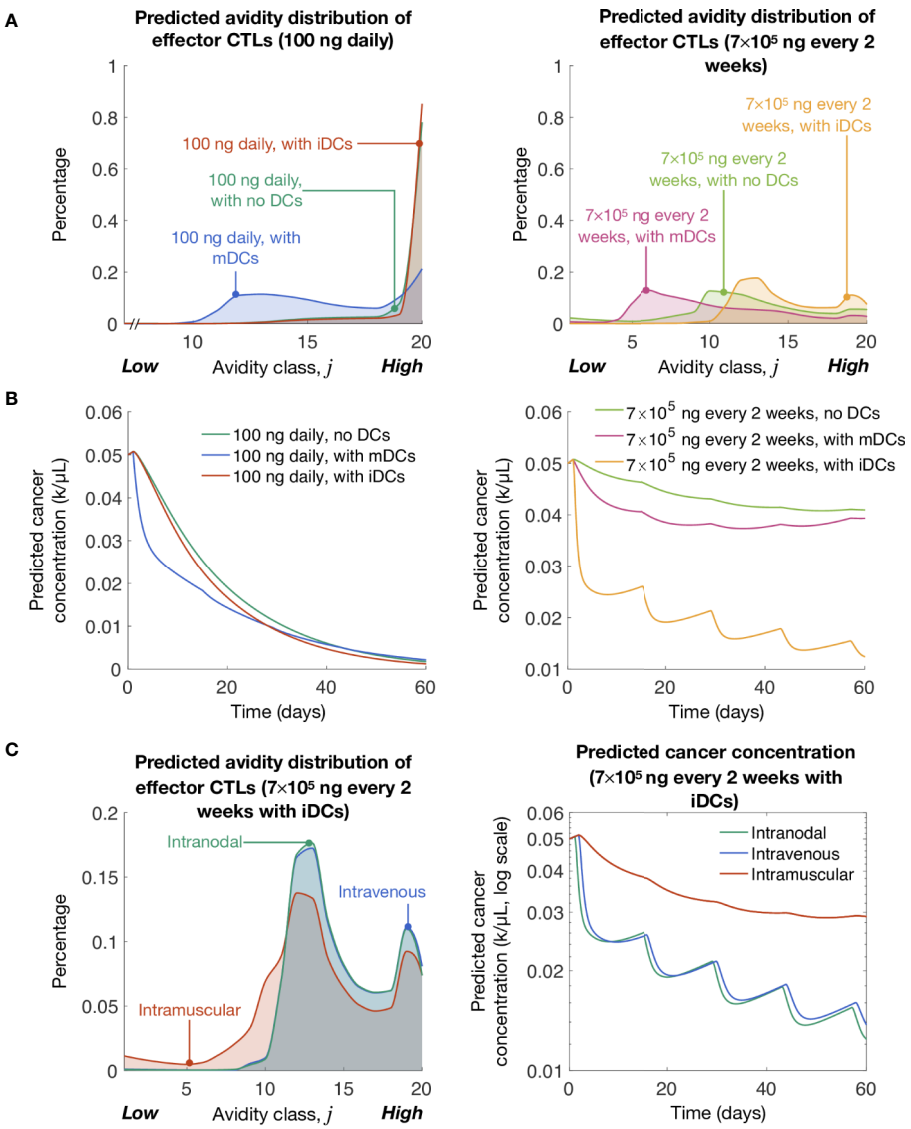


FIGURE 3 | Simulated induction of iDCs at clinically relevant vaccination doses yields significant tumor cell clearance. **(A)** Simulated avidity distribution of effector T cells for various vaccine protocols. **(B)** Simulated cancer concentrations over time for various vaccine protocols. **(C)** Simulated avidity distribution of effector T cells and tumor cell reduction (fold change) for different delivery routes. The unit 'k' denotes 10^3 cells.

Early cancer vaccines targeting over-expressed CAAs such as MART-1, MAGE, NYE-ESO-1, HER2, and MUC-1 demonstrated mediocre clinical results. Evidence suggests that the T cell repertoire capable of responding to these antigens are primarily composed of low-avidity T cells due to central tolerance of T cells specific for self-antigens (96). Recently, there has been renewed interest in cancer vaccines due to promising results for those targeting neoantigens (97–100). Additionally, encouraging preliminary clinical results have recently been observed in therapeutic approaches combining DC vaccines with checkpoint blockade (101). Our findings suggest that inducing increased iDC levels would benefit vaccines targeting either over-expressed CAAs or neoantigens, as the expansion of high-avidity CTLs would favor clinical responses in both scenarios.

Initial DC vaccines, such as Sipuleucel-T, were major milestones for immunotherapy-based treatments of cancer and demonstrated modest, but meaningful, clinical results (102). While DC vaccines have not achieved widespread therapeutic success, it is unclear if this is a result of targeting TAAs, the influence of previously unknown immunosuppression mechanisms in the tumor microenvironment, or difficult in manufacturing cell products (103). While traditional DC vaccines have been based on ex vivo antigen loading and maturation of autologous DCs, our model finds that injecting iDCs results in a maximal anti-tumor response. We find that intranodal injection, as compared to intradermal or intravenous injection, results in the most T cell activation as it ensures high

numbers of DCs are loaded with low pMHC levels. Although repeated intranodal injection of iDCs is not an ideal clinical scenario, it highlights the importance of recent bioengineering efforts to localize tumor antigen vaccination to lymph node sites (104). However, intravenous injection of iDCs did result in substantial tumor burden reduction. We suggest that other alternatives to iDC generation and injection, such as mobilization of bone marrow DC precursors, is an attractive possibility for future consideration in tumor vaccine design. Treatments with cytokines such as Fms-like tyrosine kinase 3 ligand (Flt3L) has demonstrated efficacy in increasing levels of circulating DCs (105–107). Our model suggests that elevated levels of iDCs, rather than mDCs, favors a longer half-life of the circulating DC compartment and results in lower average pMHC levels that would then favor high-avidity T cell generation. Therefore, induction of iDCs by any of several means followed by peptide vaccination and adjuvant for *in vivo* DC maturation would favor tumor clearance. While our model simplistically accounts for adjuvant as a necessary requirement for DC maturation and activation of T cells, we acknowledge that different adjuvant choices may have highly variable effects on DC activation and downstream T cell differentiation (108, 109).

Our work addresses an important and less appreciated element of cancer vaccines – how vaccine design and administration can select for and enhance the proliferation of high-avidity CTLs. However, there remain many barriers to efficacy with a combination strategy that our model does not consider. For example, we do not account for potential intra-tumoral heterogeneity of antigen expression, factors influencing CTL trafficking to tumor sites, or a multitude of potential immune suppression mechanisms found within tumor microenvironments. Additionally, in modelling the T cell activation we do not *explicitly* model TCR signaling. Future work will involve incorporating existing validated models of TCR signaling (110), and calibrating these models to avidity data from (111, 112). Defining the minimum complexity of the immune system is challenging, and the model used in this study does not, nor does it aim to account for all known immune interactions.

The mathematical model presented here proposes that increasing the magnitude of iDCs with an optimized peptide vaccine may improve tumor clearance. The model highlights the relative importance of antigen loads on DCs, which facilitate the selective expansion of high-avidity CTLs. While pre-clinical experimental validation of our findings are necessary, our model suggests previously unappreciated aspects of vaccine design that may be necessary for the development of effective cancer treatments.

DATA AVAILABILITY STATEMENT

All datasets presented in this study are included in the article.

AUTHOR CONTRIBUTIONS

AK performed the simulations and formal analysis. AK and CE wrote the first draft of the manuscript. All authors contributed to the article and approved the submitted version.

FUNDING

This work was supported by an Australian Government Research Training Program Scholarship; an Australian Research Council Discovery Project [DP180101512]; and by the US Department of Defense Breast Cancer Research Program [W81XWH-11–1–0548].

REFERENCES

1. Zappasodi R, Merghoub T, Wolchok JD. Emerging Concepts for Immune Checkpoint Blockade-Based Combination Therapies. *Cancer Cell* (2018) 33 (4):581–98. doi: 10.1016/j.ccell.2018.03.005
2. Trujillo JA, Sweis RF, Bao R, Luke JJ. T Cell-Inflamed versus Non-T Cell-Inflamed Tumors: A Conceptual Framework for Cancer Immunotherapy Drug Development and Combination Therapy Selection. *Cancer Immunol Res* (2018) 6(9):990–1000. doi: 10.1158/2326-6066.CIR-18-0277
3. Saxena M, Bhardwaj N. Re-Emergence of Dendritic Cell Vaccines for Cancer Treatment. *Trends Cancer* (2018) 4(2):119–37. doi: 10.1016/j.trecan.2017.12.007
4. Jandus C, Usatorre AM, Vigano S, Zhang L, Romero P. The Vast Universe of T Cell Diversity: Subsets of Memory Cells and Their Differentiation. *Methods Mol Biol* (2017) 1514:1–17. doi: 10.1007/978-1-4939-6548-9_1
5. Abbas AK, Lichtman AHH, Pillai S. *Cellular and Molecular Immunology*. Philadelphia, Pennsylvania, USA: Elsevier Health Sciences (2014).
6. Slingluff CL. The present and future of peptide vaccines for cancer: single or multiple, long or short, alone or in combination? *Cancer J* (2011) 17(5):343–50. doi: 10.1097/PPO.0b013e318233e5b2
7. Lollini PL, Cavallo F, Nanni P, Forni G. Vaccines for tumour prevention. *Nat Rev Cancer* (2006) 6(3):204–16. doi: 10.1038/nrc1815
8. Mougel A, Terme M, Tanchot C. Therapeutic Cancer Vaccine and Combinations With Antiangiogenic Therapies and Immune Checkpoint Blockade. *Front Immunol* (2019) 10:467. doi: 10.3389/fimmu.2019.00467
9. Stuge TB, Holmes SP, Saharan S, Tuettenberg A, Roederer M, Weber JS, et al. Diversity and recognition efficiency of T cell responses to cancer. *PloS Med* (2004) 1(2):e28. doi: 10.1371/journal.pmed.0010028
10. McMahan RH, Slansky JE. Mobilizing the low-avidity T cell repertoire to kill tumors. *Semin Cancer Biol* (2007) 17(4):317–29. doi: 10.1016/j.semcancer.2007.06.006
11. Hu Z, Ott PA, Wu CJ. Towards personalized, tumour-specific, therapeutic vaccines for cancer. *Nat Rev Immunol* (2018) 18(3):168–82. doi: 10.1038/nri.2017.131
12. Schumacher TN, Schreiber RD. Neoantigens in cancer immunotherapy. *Science.* (2015) 348(6230):69–74. doi: 10.1126/science.aaa4971
13. Pan RY, Chung WH, Chu MT, Chen SJ, Chen HC, Zheng L, et al. Recent Development and Clinical Application of Cancer Vaccine: Targeting Neoantigens. *J Immunol Res* (2018) 2018:4325874. doi: 10.1155/2018/4325874
14. Speiser DE, Baumgaertner P, Voelter V, Devevre E, Barbey C, Rufer N, et al. Unmodified self antigen triggers human CD8 T cells with stronger tumor reactivity than altered antigen. *Proc Natl Acad Sci USA* (2008) 105(10):3849–54. doi: 10.1073/pnas.0800080105
15. Kittlesen DJ, Thompson LW, Gulden PH, Skipper JC, Colella TA, Shabanowitz J, et al. Human melanoma patients recognize an HLA-A1-restricted CTL epitope from tyrosinase containing two cysteine residues: implications for tumor vaccine development. *J Immunol* (1998) 160(5):2099–106.
16. Kumbhari A, Kim PS, Lee PP. Optimisation of anti-cancer peptide vaccines to preferentially elicit high-avidity T cells. *J Theor Biol* (2019) 486:110067. doi: 10.1016/j.jtbi.2019.110067

17. Perez CR, De Palma M. Engineering dendritic cell vaccines to improve cancer immunotherapy. *Nat Commun* (2019) 10(1):5408. doi: 10.1038/s41467-019-13368-y
18. Chung B, Stuge TB, Murad JP, Beilhack G, Andersen E, Armstrong BD, et al. Antigen-specific inhibition of high-avidity T cell target lysis by low-avidity T cells via trogocytosis. *Cell Rep* (2014) 8(3):871–82. doi: 10.1016/j.celrep.2014.06.052
19. Hailemichael Y, Dai Z, Jaffarzad N, Ye Y, Medina MA, Huang X-F, et al. Persistent antigen at vaccination sites induces tumor-specific CD8+ T cell sequestration, dysfunction and deletion. *Nat Med* (2013) 19(4):465–72. doi: 10.1038/nm.3105
20. Rezvani K, Yong ASM, Mielke S, Jafarpour B, Savani BN, Le RQ, et al. Repeated PR1 and WT1 peptide vaccination in Montanide-adjuvant fails to induce sustained high-avidity, epitope-specific CD8+ T cells in myeloid malignancies. *Haematologica* (2011) 96(3):432–40. doi: 10.3324/haematol.2010.031674
21. Harndahl M, Rasmussen M, Roder G, Dalgaard Pedersen I, Sorensen M, Nielsen M, et al. Peptide-MHC class I stability is a better predictor than peptide affinity of CTL immunogenicity. *Eur J Immunol* (2012) 42(6):1405–16. doi: 10.1002/eji.201141774
22. Sallusto F, Cella M, Danieli C, Lanzavecchia A. Dendritic cells use macropinocytosis and the mannose receptor to concentrate macromolecules in the major histocompatibility complex class II compartment: downregulation by cytokines and bacterial products. *J Exp Med* (1995) 182(2):389–400. doi: 10.1084/jem.182.2.389
23. Platt CD, Ma JK, Chalouni C, Ebersold M, Bou-Reslan H, Carano RA, et al. Mature dendritic cells use endocytic receptors to capture and present antigens. *Proc Natl Acad Sci USA* (2010) 107(9):4287–92. doi: 10.1073/pnas.0910609107
24. Maree AF, Komba M, Dyck C, Labecki M, Finegood DT, Edelstein-Keshet L. Quantifying macrophage defects in type 1 diabetes. *J Theor Biol* (2005) 233(4):533–51. doi: 10.1016/j.jtbi.2004.10.030
25. Kaplan G, Nusrat A, Witmer MD, Nath I, Cohn ZA. Distribution and turnover of Langerhans cells during delayed immune responses in human skin. *J Exp Med* (1987) 165(3):763–76. doi: 10.1084/jem.165.3.763
26. Di Girolamo W, Coronato S, Portiansky E, Laguens G. Profile of immune cells in lymph nodes draining human malignant tumors. *Med (B Aires)* (2008) 68(6):423–7.
27. Dupuis M, McDonald DM, Ott G. Distribution of adjuvant MF59 and antigen gD2 after intramuscular injection in mice. *Vaccine* (1999) 18(5-6):434–9. doi: 10.1016/s0264-410x(99)00263-7
28. Leeman M, Choi J, Hansson S, Storm MU, Nilsson L. Proteins and antibodies in serum, plasma, and whole blood-size characterization using asymmetrical flow field-flow fractionation (AF4). *Anal Bioanal Chem* (2018) 410(20):4867–73. doi: 10.1007/s00216-018-1127-2
29. Delamarre L, Holcombe H, Mellman I. Presentation of exogenous antigens on major histocompatibility complex (MHC) class I and MHC class II molecules is differentially regulated during dendritic cell maturation. *J Exp Med* (2003) 198(1):111–22. doi: 10.1084/jem.20021542
30. Henrickson SE, Mempel TR, Mazo IB, Liu B, Artyomov MN, Zheng H, et al. T cell sensing of antigen dose governs interactive behavior with dendritic cells and sets a threshold for T cell activation. *Nat Immunol* (2008) 9(3):282–91. doi: 10.1038/ni1559
31. Wilson NS, El-Sukkari D, Villadangos Je A. Dendritic cells constitutively present self antigens in their immature state in vivo and regulate antigen presentation by controlling the rates of MHC class II synthesis and endocytosis. *Blood.* (2004) 103(6):2187–95. doi: 10.1182/blood-2003-08-2729
32. Mandl JN, Liou R, Klauschen F, Vrisekoop N, Monteiro Ja o P, Yates AJ, et al. Quantification of lymph node transit times reveals differences in antigen surveillance strategies of naive CD4+ and CD8+ T cells. *Proc Natl Acad Sci* (2012) 109(44):18036–41. doi: 10.1073/pnas.1211717109
33. Rubtsov YP, Niec RE, Josefowicz S, Li L, Darce J, Mathis D, et al. Stability of the regulatory T cell lineage in vivo. *Science* (2010) 329(5999):1667–71. doi: 10.1126/science.1191996
34. Catron DM, Itano AA, Pape KA, Mueller DL, Jenkins MK. Visualizing the first 50 hr of the primary immune response to a soluble antigen. *Immunity.* (2004) 21(3):341–7. doi: 10.1016/j.immuni.2004.08.007
35. Pittet MJ, Valmori D, Dunbar PR, Speiser DE, Lienard D, Lejeune F, et al. High frequencies of naive Melan-A/MART-1–specific CD8+ T cells in a large proportion of human histocompatibility leukocyte antigen (HLA)-A2 individuals. *J Exp Med* (1999) 190(5):705–16. doi: 10.1084/jem.190.5.705
36. Williams H, Sarapata E, Caldwell T, dePillis L. Mathematical modeling of regulatory T cell effects on renal cell carcinoma treatment. *Discrete Continuous Dyn Syst Ser B* (2013) 18: (4):915–43. doi: 10.3934/dcdsb.2013.18.915
37. Speiser DE, Colonna M, Ayyoub M, Cella M, Pittet MJ, Batard P, et al. The activatory receptor 2B4 is expressed in vivo by human CD8+ effector alpha beta T cells. *J Immunol* (2001) 167(11):6165–70. doi: 10.4049/jimmunol.167.11.6165
38. Homann D, Teyton L, Oldstone MBA. Differential regulation of antiviral T-cell immunity results in stable CD8+ but declining CD4+ T-cell memory. *Nat Med* (2001) 7(8):913–9. doi: 10.1038/90950
39. Valmori D, Merlo A, Souleimanian NE, Hesdorffer CS, Ayyoub M. A peripheral circulating compartment of natural naive CD4 Tregs. *J Clin Invest* (2005) 115(7):1953–62. doi: 10.1172/JCI23963
40. Litjens NH, Boer K, Zuijderwijk JM, Klepper M, Peeters AM, Prens EP, et al. Allogeneic Mature Human Dendritic Cells Generate Superior Alloreactive Regulatory T Cells in the Presence of IL-15. *J Immunol* (2015) 194(11):5282–93. doi: 10.4049/jimmunol.1402827
41. Geiger R, Duhen T, Lanzavecchia A, Sallusto F. Human naive and memory CD4+ T cell repertoires specific for naturally processed antigens analyzed using libraries of amplified T cells. *J Exp Med* (2009) 206(7):1525–34. doi: 10.1084/jem.20090504
42. Murali-Krishna K, Altman JD, Suresh M, Sourdive DJ, Zajac AJ, Miller JD, et al. Counting antigen-specific CD8 T cells: a reevaluation of bystander activation during viral infection. *Immunity* (1998) 8(2):177–87. doi: 10.1016/s1074-7613(00)80470-7
43. Hellerstein M, Hanley MB, Cesar D, Siler S, Papageorgopoulos C, Wieder E, et al. Directly measured kinetics of circulating T lymphocytes in normal and HIV-1-infected humans. *Nat Med* (1999) 5(1):83–9. doi: 10.1038/4772
44. Obst R. Timing T cell priming cycling. *Front Immunol* (2015) 6:563. doi: 10.3389/fimmu.2015.00563
45. Butz EA, Bevan MJ. Massive expansion of antigen-specific CD8+ T cells during an acute virus infection. *Immunity* (1998) 8(2):167–75. doi: 10.1016/s1074-7613(00)80469-0
46. Gerlach C, Rohr JC, Perie L, van Rooij N, van Heijst JW, Velds A, et al. Heterogeneous differentiation patterns of individual CD8+ T cells. *Science* (2013) 340(6132):635–9. doi: 10.1126/science.1235487
47. Buchholz VR, Flossdorf M, Hensel I, Kretschmer L, Weissbrich B, Graf P, et al. Disparate individual fates compose robust CD8+ T cell immunity. *Science* (2013) 340(6132):630–5. doi: 10.1126/science.1235454
48. Lotze MT, Matory YL, Ettinghausen SE, Rayner AA, Sharrow SO, Seipp CA, et al. In vivo administration of purified human interleukin 2. II. Half life, immunologic effects, and expansion of peripheral lymphoid cells in vivo with recombinant IL 2. *J Immunol* (1985) 135(4):2865–75.
49. Borghans J AM, Tesselaar K, de Boer RJ. Current best estimates for the average lifespans of mouse and human leukocytes: reviewing two decades of deuterium-labeling experiments. *Immunol Rev* (2018) 285(1):233–48. doi: 10.1111/imr.12693
50. Vukmanovic-Stejic M, Zhang Y, Cook JE, Fletcher JM, McQuaid A, Masters JE, et al. Human CD4+ CD25hi Foxp3+ regulatory T cells are derived by rapid turnover of memory populations in vivo. *J Clin Invest* (2006) 116(9):2423–33. doi: 10.1172/JCI28941
51. Carlson JA. Tumor doubling time of cutaneous melanoma and its metastasis. *Am J Dermatopathol* (2003) 25:291–9. doi: 10.1097/00000372-200308000-00003
52. Eskelin S, Pyrhonen S, Summanen P, Hahka-Kemppinen M, Kivela T. Tumor doubling times in metastatic malignant melanoma of the uvea: tumor progression before and after treatment. *Ophthalmology.* (2000) 107:1443–9. doi: 10.1016/S0161-6420(00)00182-2
53. Ollila DW, Stern SL, Morton DL. Tumor doubling time: a selection factor for pulmonary resection of metastatic melanoma. *J Surg Oncol* (1998) 69:206–11. doi: 10.1002/(SICI)1096-9098(199812)69:4<206::AID-JSO3>3.0.CO;2-N
54. Sarapata EA, de Pillis LG. A comparison and catalog of intrinsic tumor growth models. *Bull Math Biol* (2014) 76(8):2010–24. doi: 10.1007/s11538-014-9986-y

55. Carreno BM, Hansen TH. Exogenous peptide ligand influences the expression and half-life of free HLA class I heavy chains ubiquitously detected at the cell surface. *Eur J Immunol* (1994) 24(6):1285–92. doi: 10.1002/eji.1830240607
56. Christinck ER, Luscher MA, Barber BH, Williams DB. Peptide binding to class I MHC on living cells and quantitation of complexes required for CTL lysis. *Nature.* (1991) 352(6330):67–70. doi: 10.1038/352067a0
57. Coffman RL, Sher A, Seder RA. Vaccine adjuvants: putting innate immunity to work. *Immunity.* (2010) 33(4):492–503. doi: 10.1016/j.immuni.2010.10.002
58. Gardner A, Ruffell B. Dendritic Cells and Cancer Immunity. *Trends Immunol* (2016) 37(12):855–65. doi: 10.1016/j.it.2016.09.006
59. Mellman I, Steinman RM. Dendritic cells: specialized and regulated antigen processing machines. *Cell.* (2001) 106(3):255–8. doi: 10.1016/S0092-8674(01)00449-4
60. Trombetta ES, Mellman I. Cell biology of antigen processing in vitro and in vivo. *Annu Rev Immunol* (2005) 23:975–1028. doi: 10.1146/annurev.immunol.22.012703.104538
61. Steinman RM, Hawiger D, Nussenzweig MC. Tolerogenic dendritic cells. *Annu Rev Immunol* (2003) 21:685–711. doi: 10.1146/annurev.immunol.21.120601.141040
62. De Smedt T, Pajak B, Muraille E, Lespagnard L, Heinen E, De Baetselier P, et al. Regulation of dendritic cell numbers and maturation by lipopolysaccharide in vivo. *J Exp Med* (1996) 184(4):1413–24. doi: 10.1084/jem.184.4.1413
63. Benson MJ, Pino-Lagos K, Rosemblatt M, Noelle RJ. All-trans retinoic acid mediates enhanced T reg cell growth, differentiation, and gut homing in the face of high levels of co-stimulation. *J Exp Med* (2007) 204(8):1765–74. doi: 10.1084/jem.20070719
64. Dons EM, Raimondi G, Cooper DK, Thomson AW. Induced regulatory T cells: mechanisms of conversion and suppressive potential. *Hum Immunol* (2012) 73(4):328–34. doi: 10.1016/j.humimm.2011.12.011
65. Alexander-Miller MA, Leggatt GR, Berzofsky JA. Selective expansion of high- or low-avidity cytotoxic T lymphocytes and efficacy for adoptive immunotherapy. *Proc Natl Acad Sci* (1996) 93(9):4102–7. doi: 10.1073/pnas.93.9.4102
66. Bullock TNJ, Mullins DW, Colella TA, Engelhard VH. Manipulation of Avidity to Improve Effectiveness of Adoptively Transferred CD8+ T Cells for Melanoma Immunotherapy in Human MHC Class I-Transgenic Mice. *J Immunol* (2001) 167(10):5824–31. doi: 10.4049/jimmunol.167.10.5824
67. Kedl RM, Schaefer BC, Kappler JW, Marrack P. T cells down-modulate peptide-MHC complexes on APCs in vivo. *Nat Immunol* (2002) 3(1):27. doi: 10.1038/ni742
68. Kedl RM, Rees WA, Hildeman DA, Schaefer B, Mitchell T, Kappler J, et al. T cells compete for access to antigen-bearing antigen-presenting cells. *J Exp Med* (2000) 192(8):1105–14. doi: 10.1084/jem.192.8.1105
69. Kroger CJ, Amoah S, Alexander-Miller MA. Cutting edge: Dendritic cells prime a high avidity CTL response independent of the level of presented antigen. *J Immunol* (2008) 180(9):5784–8. doi: 10.4049/jimmunol.180.9.5784
70. Sandberg JK, Franksson L, Sundback J, Michaelsson J, Petersson M, Achour A, et al. T cell tolerance based on avidity thresholds rather than complete deletion allows maintenance of maximal repertoire diversity. *J Immunol* (2000) 165(1):25–33. doi: 10.4049/jimmunol.165.1.25
71. van den Boorn JG, Le Poole IC, Luiten RM. T-cell avidity and tuning: the flexible connection between tolerance and autoimmunity. *Int Rev Immunol* (2006) 25(3-4):235–58. doi: 10.1080/08830180600743081
72. Vigano S, Utzschneider DT, Perreau M, Pantaleo G, Zehn D, Harari A. Functional avidity: a measure to predict the efficacy of effector T cells? *Clin Dev Immunol* (2012) 2012:153863. doi: 10.1155/2012/153863
73. Bauer J, Bahmer FA, Worl J, Neuhuber W, Schuler G, Fartasch M. A strikingly constant ratio exists between Langerhans cells and other epidermal cells in human skin. A stereologic study using the optical disector method and the confocal laser scanning microscope. *J Invest Dermatol* (2001) 116(2):313–8. doi: 10.1046/j.1523-1747.2001.01247.x
74. Ferdousi M, Romanchuk K, Mah JK, Virtanen H, Millar C, Malik RA, et al. Early corneal nerve fibre damage and increased Langerhans cell density in children with type 1 diabetes mellitus. *Sci Rep* (2019) 9(1):8758. doi: 10.1038/s41598-019-45116-z
75. Haller Hasskamp J, Zapas JL, Elias EG. Dendritic cell counts in the peripheral blood of healthy adults. *Am J Hematol* (2005) 78(4):314–5. doi: 10.1002/ajh.20296
76. Walseng E, Furuta K, Bosch B, Weih KA, Matsuki Y, Bakke O, et al. Ubiquitination regulates MHC class II-peptide complex retention and degradation in dendritic cells. *Proc Natl Acad Sci USA* (2010) 107(47):20465–70. doi: 10.1073/pnas.1010990107
77. Gannon PO, Baumgaertner P, Huber A, Iancu EM, Cagnon L, Abed Maillard S, et al. Rapid and Continued T-Cell Differentiation into Long-term Effector and Memory Stem Cells in Vaccinated Melanoma Patients. *Clin Cancer Res* (2017) 23(13):3285–96. doi: 10.1158/1078-0432.CCR-16-1708
78. Murphy K. *Janeway's Immunobiology (Immunobiology: The Immune System (Janeway))*. New York, New York, USA: Garland Science (2011).
79. Beers MH, Berkow R, Bogin RM, Fletcher AJ, Nace BA, Moy DE, et al. *The Merck manual of diagnosis and therapy*. Whitehouse Station, NJ: Merck (1999). Available at: http://www.merck.com/pubs/mmanual/.
80. Schreibelt G, Bol KF, Westdorp H, Wimmers F, Aarntzen EH, Duiveman-de Boer T, et al. Effective Clinical Responses in Metastatic Melanoma Patients after Vaccination with Primary Myeloid Dendritic Cells. *Clin Cancer Res* (2016) 22(9):2155–66. doi: 10.1158/1078-0432.CCR-15-2205
81. Verdijk P, Aarntzen EH, Lesterhuis WJ, Boullart AC, Kok E, van Rossum MM, et al. Limited amounts of dendritic cells migrate into the T-cell area of lymph nodes but have high immune activating potential in melanoma patients. *Clin Cancer Res* (2009) 15(7):2531–40. doi: 10.1158/1078-0432.CCR-08-2729
82. Camacho LH. CTLA-4 blockade with ipilimumab: biology, safety, efficacy, and future considerations. *Cancer Med* (2015) 4(5):661–72. doi: 10.1002/cam4.371
83. Mahoney KM, Freeman GJ, McDermott DF. The Next Immune-Checkpoint Inhibitors: PD-1/PD-L1 Blockade in Melanoma. *Clin Ther* (2015) 37(4):764–82. doi: 10.1016/j.clinthera.2015.02.018
84. Ott PA, Hodi FS, Robert C. CTLA-4 and PD-1/PD-L1 blockade: new immunotherapeutic modalities with durable clinical benefit in melanoma patients. *Clin Cancer Res* (2013) 19(19):5300–9. doi: 10.1158/1078-0432.CCR-13-0143
85. Bertrand A, Kostine M, Barnetche T, Truchetet ME, Schaeverbeke T. Immune related adverse events associated with anti-CTLA-4 antibodies: systematic review and meta-analysis. *BMC Med* (2015) 13:211. doi: 10.1186/s12916-015-0455-8
86. Corsello SM, Barnabei A, Marchetti P, De Vecchis L, Salvatori R, Torino F. Endocrine side effects induced by immune checkpoint inhibitors. *J Clin Endocrinol Metab* (2013) 98(4):1361–75. doi: 10.1210/jc.2012-4075
87. Gelao L, Criscitiello C, Esposito A, Goldhirsch A, Curigliano G. Immune checkpoint blockade in cancer treatment: a double-edged sword cross-targeting the host as an "innocent bystander". *Toxins (Basel)* (2014) 6(3):914–33. doi: 10.3390/toxins6030914
88. Andersson B. Studies on the regulation of avidity at the level of the single antibody-forming cell. The effect of antigen dose and time after immunization. *J Exp Med* (1970) 132(1):77–88. doi: 10.1084/jem.132.1.77
89. Billeskov R, Lindenstrom T, Woodworth J, Vilaplana C, Cardona PJ, Cassidy JP, et al. High Antigen Dose Is Detrimental to Post-Exposure Vaccine Protection against Tuberculosis. *Front Immunol* (2017) 8:1973. doi: 10.3389/fimmu.2017.01973
90. Carretero-Iglesia L, Couturaud B, Baumgaertner P, Schmidt J, Maby-El Hajjami H, Speiser DE, et al. High Peptide Dose Vaccination Promotes the Early Selection of Tumor Antigen-Specific CD8 T-Cells of Enhanced Functional Competence. *Front Immunol* (2019) 10:3016. doi: 10.3389/fimmu.2019.03016
91. Narayan S, Choyce A, Fernando GJ, Leggatt GR. Secondary immunisation with high-dose heterologous peptide leads to CD8 T cell populations with reduced functional avidity. *Eur J Immunol* (2007) 37(2):406–15. doi: 10.1002/eji.200535688
92. Oh S, Hodge JW, Ahlers JD, Burke DS, Schlom J, Berzofsky JA. Selective induction of high avidity CTL by altering the balance of signals from APC. *J Immunol* (2003) 170(5):2523–30. doi: 10.4049/jimmunol.170.5.2523
93. Della Bella S, Gennaro M, Vaccari M, Ferraris C, Nicola S, Riva A, et al. Altered maturation of peripheral blood dendritic cells in patients with breast cancer. *Br J Cancer* (2003) 89(8):1463–72. doi: 10.1038/sj.bjc.6601243
94. Hirooka S, Yanagimoto H, Satoi S, Yamamoto T, Toyokawa H, Yamaki S, et al. The role of circulating dendritic cells in patients with unresectable pancreatic cancer. *Anticancer Res* (2011) 31(11):3827–34.

95. Pinzon-Charry A, Ho CS, Maxwell T, McGuckin MA, Schmidt C, Furnival C, et al. Numerical and functional defects of blood dendritic cells in early- and late-stage breast cancer. *Br J Cancer* (2007) 97(9):1251–9. doi: 10.1038/sj.bjc.6604018
96. Pedersen SR, Sorensen MR, Buus S, Christensen JP, Thomsen AR. Comparison of vaccine-induced effector CD8 T cell responses directed against self- and non-self-tumor antigens: implications for cancer immunotherapy. *J Immunol* (2013) 191(7):3955–67. doi: 10.4049/jimmunol.1300555
97. Carreno BM, Magrini V, Becker-Hapak M, Kaabinejadian S, Hundal J, Petti AA, et al. Cancer immunotherapy. A dendritic cell vaccine increases the breadth and diversity of melanoma neoantigen-specific T cells. *Science* (2015) 348(6236):803–8. doi: 10.1126/science.aaa3828
98. Ott PA, Hu Z, Keskin DB, Shukla SA, Sun J, Bozym DJ, et al. An immunogenic personal neoantigen vaccine for patients with melanoma. *Nature* (2017) 547(7662):217–21. doi: 10.1038/nature22991
99. Sahin U, Derhovanessian E, Miller M, Kloke BP, Simon P, Lower M, et al. Personalized RNA mutanome vaccines mobilize poly-specific therapeutic immunity against cancer. *Nature* (2017) 547(7662):222–6. doi: 10.1038/nature23003
100. Schumacher T, Bunse L, Pusch S, Sahm F, Wiestler B, Quandt J, et al. A vaccine targeting mutant IDH1 induces antitumour immunity. *Nature* (2014) 512(7514):324–7. doi: 10.1038/nature13387
101. Wilgenhof S, Corthals J, Heirman C, van Baren N, Lucas S, Kvistborg P, et al. Phase II Study of Autologous Monocyte-Derived mRNA Electroporated Dendritic Cells (TriMixDC-MEL) Plus Ipilimumab in Patients With Pretreated Advanced Melanoma. *J Clin Oncol* (2016) 34(12):1330–8. doi: 10.1200/JCO.2015.63.4121
102. Kantoff PW, Higano CS, Shore ND, Berger ER, Small EJ, Penson DF, et al. Sipuleucel-T immunotherapy for castration-resistant prostate cancer. *N Engl J Med* (2010) 363(5):411–22. doi: 10.1056/NEJMoa1001294
103. Mastelic-Gavillet B, Balint K, Boudousquie C, Gannon PO, Kandalaft LE. Personalized Dendritic Cell Vaccines-Recent Breakthroughs and Encouraging Clinical Results. *Front Immunol* (2019) 10:766. doi: 10.3389/fimmu.2019.00766
104. Liu H, Moynihan KD, Zheng Y, Szeto GL, Li AV, Huang B, et al. Structure-based programming of lymph-node targeting in molecular vaccines. *Nature* (2014) 507(7493):519–22. doi: 10.1038/nature12978
105. Anandasabapathy N, Breton G, Hurley A, Caskey M, Trumpfheller C, Sarma P, et al. Efficacy and safety of CDX-301, recombinant human Flt3L, at expanding dendritic cells and hematopoietic stem cells in healthy human volunteers. *Bone Marrow Transplant* (2015) 50(7):924–30. doi: 10.1038/bmt.2015.74
106. Maraskovsky E, Daro E, Roux E, Teepe M, Maliszewski CR, Hoek J, et al. In vivo generation of human dendritic cell subsets by Flt3 ligand. *Blood* (2000) 96(3):878–84. doi: 10.1182/blood.V96.3.878.015k15_878_884
107. Pulendran B, Banchereau J, Burkeholder S, Kraus E, Guinet E, Chalouni C, et al. Flt3-ligand and granulocyte colony-stimulating factor mobilize distinct human dendritic cell subsets in vivo. *J Immunol* (2000) 165(1):566–72. doi: 10.4049/jimmunol.165.1.566
108. Obeid J, Hu Y, Slingluff CLJr. Vaccines, Adjuvants, and Dendritic Cell Activators–Current Status and Future Challenges. *Semin Oncol* (2015) 42(4):549–61. doi: 10.1053/j.seminoncol.2015.05.006
109. Palucka K, Banchereau J, Mellman I. Designing vaccines based on biology of human dendritic cell subsets. *Immunity.* (2010) 33(4):464–78. doi: 10.1016/j.immuni.2010.10.007
110. Lever M, Maini PK, van der Merwe PA, Dushek O. Phenotypic models of T cell activation. *Nat Rev Immunol* (2014) 14(9):619–29. doi: 10.1038/nri3728
111. Irving M, Zoete V, Hebeisen M, Schmid D, Baumgartner P, Guillaume P, et al. Interplay between T cell receptor binding kinetics and the level of cognate peptide presented by major histocompatibility complexes governs CD8+ T cell responsiveness. *J Biol Chem* (2012) 287(27):23068–78. doi: 10.1074/jbc.M112.357673
112. Naeher D, Daniels MA, Hausmann B, Guillaume P, Luescher I, Palmer E. A constant affinity threshold for T cell tolerance. *J Exp Med* (2007) 204(11):2553–9. doi: 10.1084/jem.20070254

Conflict of Interest: The authors declare that the research was conducted in the absence of any commercial or financial relationships that could be construed as a potential conflict of interest.

Copyright © 2020 Kumbhari, Egelston, Lee and Kim. This is an open-access article distributed under the terms of the Creative Commons Attribution License (CC BY). The use, distribution or reproduction in other forums is permitted, provided the original author(s) and the copyright owner(s) are credited and that the original publication in this journal is cited, in accordance with accepted academic practice. No use, distribution or reproduction is permitted which does not comply with these terms.

frontiers in Immunology

ORIGINAL RESEARCH
published: 06 November 2020
doi: 10.3389/fimmu.2020.583382

Induction of Progenitor Exhausted Tissue-Resident Memory CD8$^+$ T Cells Upon *Salmonella* Typhi Porins Adjuvant Immunization Correlates With Melanoma Control and Anti-PD-1 Immunotherapy Cooperation

Ricardo A. León-Letelier[1,2], Daniel I. Castro-Medina[1], Oscar Badillo-Godinez[3†], Araceli Tepale-Segura[1], Enrique Huanosta-Murillo[1], Cristina Aguilar-Flores[1], Saraí G. De León-Rodríguez[1,4], Alejandra Mantilla[5], Ezequiel M. Fuentes-Pananá[6], Constantino López-Macías[1] and Laura C. Bonifaz[1]*

[1] Unidad de Investigación Médica en Inmunoquímica, UMAE Hospital de Especialidades, Centro Médico Nacional Siglo XXI, Instituto Mexicano del Seguro Social, Mexico City, Mexico, [2] Posgrado en Ciencias Biomédicas, Universidad Nacional Autónoma de México, Mexico City, Mexico, [3] Centro de Investigación Sobre Enfermedades Infecciosas, Instituto Nacional de Salud Pública, Cuernavaca, Mexico, [4] Posgrado en Ciencias Biológicas, Universidad Nacional Autónoma de México, Mexico City, Mexico, [5] Servicio de Patología, Hospital de Oncología, Centro Médico Nacional Siglo XXI, Instituto Mexicano del Seguro Social, Mexico City, Mexico, [6] Unidad de Investigación en Virología y Cáncer, Hospital Infantil de México Federico Gómez, Mexico City, Mexico

Immunotherapy has improved the clinical response in melanoma patients, although a relevant percentage of patients still cannot be salvaged. The search for the immune populations that provide the best tumor control and that can be coaxed by immunotherapy strategies is a hot topic in cancer research nowadays. Tumor-infiltrating TCF-1$^+$ progenitor exhausted CD8$^+$ T cells seem to grant the best melanoma prognosis and also efficiently respond to anti-PD-1 immunotherapy, giving rise to a TIM-3$^+$ terminally exhausted population with heightened effector activity. We tested Porins from *Salmonella* Typhi as a pathogen associated molecular pattern adjuvant of natural or model antigen in prophylactic and therapeutic immunization approaches against murine melanoma. Porins induced protection against melanomas, even upon re-challenging of tumor-free mice. Porins efficiently expanded IFN-γ-producing CD8$^+$ T cells and induced central and effector memory in lymph nodes and tissue-resident (Trm) T cells in the skin and tumors. Porins induced TCF-1$^+$ PD-1$^+$ CD8$^+$ Trm T cells in the tumor stroma and the presence of this population correlated with melanoma growth protection in mice. Porins immunization also cooperated with anti-PD-1 immunotherapy to hamper melanoma growth. Importantly, the potentially protective Trm populations induced by Porins in the murine model were also observed in melanoma patients in which their presence also correlated with disease control. Our data support the use of cancer vaccination to sculpt the tumor stroma with efficient and lasting Trm T cells with effector activities, highlighting the use of Porins as an

OPEN ACCESS

Edited by:
Graham Pawelec,
University of Tübingen, Germany

Reviewed by:
María Moreno,
Universidad de la República, Uruguay
Eyad Elkord,
University of Salford, United Kingdom

***Correspondence:**
Laura C. Bonifaz
labonifaz@yahoo.com

†Present address:
Oscar Badillo-Godinez, Department of Immunology, Genetics and Pathology, Rudbeck Laboratory, Uppsala University, Uppsala, Sweden

Specialty section:
This article was submitted to Cancer Immunity and Immunotherapy, a section of the journal Frontiers in Immunology

Received: *14 July 2020*
Accepted: *14 October 2020*
Published: *06 November 2020*

Citation:
León-Letelier RA, Castro-Medina DI, Badillo-Godinez O, Tepale-Segura A, Huanosta-Murillo E, Aguilar-Flores C, De León-Rodríguez SG, Mantilla A, Fuentes-Pananá EM, López-Macías C and Bonifaz LC (2020) Induction of Progenitor Exhausted Tissue-Resident Memory CD8$^+$ T Cells Upon Salmonella Typhi Porins Adjuvant Immunization Correlates With Melanoma Control and Anti-PD-1 Immunotherapy Cooperation. Front. Immunol. 11:583382. doi: 10.3389/fimmu.2020.583382

adjuvant. Furthermore, our data place CD8$^+$ Trm T cells with a progenitor exhausted phenotype as an important population for melanoma control, either independently or in cooperation with anti-PD-1 immunotherapy.

Keywords: melanoma, immunotherapy, adjuvant, tissue-resident memory T cells, progenitor exhausted T cells, anti-PD-1 Ab

INTRODUCTION

Melanoma is the most aggressive form of skin cancer, and even though it only accounts for 1%, it is the cause of the majority of the skin cancer-related deaths. The incidence rate of melanoma has risen rapidly in the last three decades, but its mortality has decreased (1), perhaps because of the immunotherapy strategies that have revolutionized melanoma treatment. Since immunotherapy aims to strengthen anti-tumoral activities, successful responses depend on the state of the immune system and in the density of tumor-infiltrating lymphocytes (TILs), particularly of T cells (2). Thus, melanomas often do not respond to immunotherapy due to lack of T cell infiltration, or because T cells have acquired dysfunctional phenotypes (3). Dissecting the specific T cell subsets responsible for anti-tumoral effector functions and understanding the mechanisms that lead them to mediate healthy immunotherapy responses are central objectives of the revolutionary way in which we treat cancer nowadays.

Immunotherapy has helped to better understand the tumor stroma population dynamics pointing out to T cells with and without anti-tumor activity. Long-lasting immune anti-tumoral responses depend on formation of memory T cells, central (Tcm), effector (Tem), and tissue-resident memory (Trm). Trm T cells are long-lived in tissues that have undergone antigenic challenge. Indeed, solid tumors are often infiltrated by CD8$^+$ Trm T cells that are critical to eliminate tumor cells (4, 5). Trm T cells are characterized by the stable expression of CD69 and CD103, which signal for retention in tissues and for rapid effector function (4, 6). However, not all T cells infiltrating the tumor stroma seem to be able to display effector functions, with some populations exhibiting exhausted phenotypes, and Trm T cells can express high levels of PD-1 (7). Exhausted populations were first defined because of expression of this check-point marker, and were originally associated with T cell dysfunction due to chronic antigen stimulation (8). However, based on murine models of chronic viral infection, we are now beginning to understand the different PD-1$^+$ subsets conforming the exhausted T cells, for instance, those recognized as "progenitor exhausted" with a TCF-1$^+$ PD-1$^+$ phenotype, and the "terminally exhausted" TIM-3$^+$ PD-1$^+$ (9, 10). The relevance to separate these subtypes lies in that only the progenitor exhausted T CD8$^+$ population proliferates after anti-PD-1 therapy, resulting in immune control of the chronic viral infection (11–13). Recently, these two subtypes of exhausted CD8$^+$ T cells have been also identified in the infiltrate of murine melanoma (9, 14), and in melanoma, kidney and lung cancer patients (14–16). Similar to the chronic viral model, only the progenitor exhausted CD8$^+$ cells proliferated in response to anti-PD-1 therapy (9). Indeed, a human equivalent population of exhausted CD8$^+$ TCF-7$^+$ (the human ortholog of TCF-1) T cells have been found to predict positive responses to anti-PD-1 immunotherapy and enhanced survival of melanoma patients (17). Although this progenitor exhausted T cells do not display effector functions upon PD-1 blockade, they differentiate into terminally exhausted T cells with potent anti-tumor activities, such as IFN-γ secretion (18, 19). Thus, while both progenitor and terminally exhausted phenotypes are essential, the former seems to sense and trigger anti-PD-1-induced T cell effector functions (9, 10).

One mechanism to induce anti-tumor immune responses and provide long-lasting protection against relapse is by fostering T cell responses through immunization with cancer vaccines, a strategy that potentially could also synergize with immune check-point inhibitors. To achieve an efficient immunization, it is crucial not only to choose the proper antigen, but also a suitable adjuvant (20). Some adjuvants based on pathogen associated molecular patterns (PAMP) have shown protection against tumor growth and enhancement of the immune check-point inhibitors efficacy (21–24), but the synergic mechanisms of these adjuvants with the inhibitors is not completely understood. One adjuvant with a potent effect in a melanoma model is the nontoxic Cholera B subunit (CTB), a non-classical PAMP that activates the immune cells through NLRP3 and FcRγ-CARD9 (25, 26). We have previously demonstrated that an intradermal (i.d.) immunization with CTB and a model antigen promotes an efficient IFN-γ$^+$ CD4$^+$ T-cell response (27), that increase the survival of mice challenged with melanoma associated with a CD4$^+$ Trm response (28–30). However, the participation of CD8$^+$ T cells was not evaluated.

We have also studied the adjuvant capacity of highly purified outer membrane proteins (Porins) from Salmonella enterica serovar Typhi (*S.* Typhi). Porins are a classical PAMP that induce a potent antibody and T cell specific immune response in mice and humans (31, 32). We have previously reported that Porins were capable to increase the expression of the costimulatory molecules CD86 and CD40 on dendritic cells (DCs) through TLR2 and TLR4 (33). Moreover, Porins were also able to induce Porin-specific CD8$^+$ and CD4$^+$ T cells and antigen-specific CD4 response when used as an adjuvant (31, 34–36). Nevertheless, the capacity of Porins as an adjuvant to induce

Abbreviations: CTB, nontoxic Cholera B subunit; GZMB, Granzyme B; MAA, melanoma associated antigen; Porins, highly purified outer membrane proteins; *S.* Typhi, *Salmonella* enterica serovar Typhi; Tcm, central memory T cell; Tem, effector memory T cell; TIL, tumor-infiltrating lymphocyte; Trm, tissue-resident memory.

antigen-specific CD8s has not been tested, nor has the Porins adjuvant strength in a tumor model.

Different skin immunization strategies are able to induce long-lasting $CD8^+$ Trm anti-tumoral responses (37, 38). The capacity of Porins to activate DCs and T cell responses points it out as a good candidate to test in a tumor model. In this study, we designed different immunization strategies aiming to induce Trm responses able to control melanoma initiation and progression. We observed that Porins gave rise to a $CD8^+$ Trm PD-1^+ T cell population that also express TCF-1, whose generation marked mice with better control of melanoma growth. Although it is known that Trm with effector functions can be induced in the tumor (38), our data argue that the choice of adjuvant in cancer vaccination can lead to formation of progenitor exhausted $CD8^+$ Trm T cells, and that formation of this population correlates with the capacity to control melanoma cells independently and in cooperation with anti-PD-1 immunotherapy. Remarkably, the populations induced by Porins immunization were also identified in human melanoma patients associated with disease control.

MATERIALS AND METHODS

Mice

Wild-type C57BL/6 mice were obtained from Unidad de Medicina Experimental, UNAM animal facility. The OT-IxCD45.1^+ mice were kindly provided by Dr. J.C. Crispín, Instituto Nacional de Ciencias Médicas y Nutrición Salvador Zubirán (INCMNSZ), and OT-IIxCD45.1^+ were kindly provided by Dr. G. Soldevila, Instituto de Investigaciones Biomédicas, UNAM animal facility. All mice were male and age (8–12 weeks)-matched. All animal experiments were performed following the Institutional Ethics Committee and the Mexican national regulations on animal care and experimentation (R-2015-785-008).

Porins Purification

Porins were purified from *S.* Typhi 9,12, Vi:d. ATCC 9993 (Omp-C and Omp-F) using the method previously published (32). Briefly, *S.* Typhi was grown in glucose- supplemented minimal A medium and Porins were extracted from the bacteria using buffer with sodium dodecyl sulfate. Proteins were purified by molecular exclusion chromatography using a Sephacryl S-200 column. Chromatographically purified proteins were analyzed by sodium dodecyl sulfate-polyacrylamide gel electrophoresis. Lipopolysaccharide content was evaluated using a Limulus Amoebocyte Lysate Assay (Endosafe KTA, Charles River Endosafe Laboratories), and all batches used in the study were negative (detection limit, 0.2 ng LPS/mg protein). Western blot analysis using anti-LPS polyclonal sera confirmed that LPS was not detectable.

Melanoma Culture and Tumor Challenge

B16-F10 or B16-F10-OVA (MO4) melanoma cells were cultured in DMEM containing 10% FBS, 0.1% penicillin/ streptomycin, 0.2% l-glutamine, 0.05% 2-mercaptoethanol, 0.01% sodium pyruvate, 0.1% HEPES, and 0.1% nonessential amino acids. Melanoma tumors were established by subcutaneous (s.c.) injection of 2.5×10^5 cells in the left flank. The tumors width and length were measured using a caliper every 2 days starting at day 7. The tumor volume was calculated as $4/3\pi$ (1/2 width)^2(1/2 length), in mm^3. Tumor appearance was scored daily through manual palpation, and mice with no evidence of tumor by the end of the following period were scored as tumor-free.

Prophylactic Immunization

For prophylactic experiments, mice were challenged with MO4 7 days after the immunization with 30 μg of ovalbumin (OVA) plus adjuvant: 10 μg of Porins or 10 μg of CTB (Sigma-Aldrich), injected s.c. in the left flank. As controls, mice were s.c. injected with OVA, Porins, CTB or PBS. For the re-challenge experiment, the tumor-free OVA + Porins immunized mice at day 28 were re-challenged with MO4 and followed up for 100 days from the first immunization. For the melanoma-associated antigen (MAAs) experiment, mice were injected with 70 nmol of the human/mouse recombinant peptides TRP-2 (AnaSpec) and gp100 (MyBioSource), with or without Porins, 10 and 3 days before challenge with the B16-F10 melanoma cells (39, 40).

Therapeutic Immunization

For therapeutic experiments the MO4 challenge was 7 days prior the immunization (explained above) and followed up for 21 days. The therapeutic immunization was also executed with or without intraperitoneal (i.p.) injection of 100 μg anti-PD-1 monoclonal antibody (mAb) (BioLegend Cat# 114102, RRID:AB_313573), at days 19, 21, and 23, only for the immunized group, followed up for 28 days.

Circulating Lymphocyte Depletion Experiment

OVA + Porins immunized mice received i.p. 100 μg of anti-CD8 mAb (TIB105, Clone 53-6.72, in house) or 250 μg of anti-CD4 mAb (GK1.5, in house) or 250 μg of control mAb (III-10, in house) as follows: 1 day before MO4 challenge, on the day of MO4 challenge and every 3 days after, with the last two injections 4 days apart, up to day 12 or 21, specified in each experiment. The OVA + Porins immunization was 7 or 28 days, or 28 days/ boost before the MO4 challenge. At the end of the experiment, tumors and blood were harvested for Trm T cells and circulating lymphocyte identification, respectively.

$CD8^+$ and $CD4^+$ OVA-Specific T Cell Enrichment and Adoptive Transfer

Skin-draining lymph nodes (SDLN), mesenteric lymph nodes and spleen were collected from OT-IxCD45.1^+ and OT-IIxCD45.1^+ mice and worked separately as described elsewhere (28). Briefly: recovered cells (see below) were incubated for 30 min on ice with homemade rat hybridoma supernatants, for OT-IxCD45.1^+ T cells: against CD4, B cells, MHCII-expressing cells, macrophages and NK cells; for OTI-IIxCD45.1^+ T cells: against CD8, B cells, MHCII-expressing cells, macrophages and NK

cells. Next, cells were poured into Petri dishes previously coated with rat anti-IgG, and non-adherent cells were recovered for injection through the retro orbital vein. Congenic mice received 3×10^6 OT-IxCD45.1$^+$ cells and 3×10^6 OT-IIxCD45.1$^+$ cells intravenously (i.v.). After 24 h, anesthetized mice were i.d. immunized in both ears with 15 μg of OVA with the adjuvant: 5 μg Porins or 5 μg CTB.

Skin and Skin-Draining Lymph Node Processing

Mice were sacrificed at 7 or 28 days post-immunization in the ear, to collect SDLN and skin. SDLN were macerated and filtered, and skin-infiltrating lymphocytes were obtained as previously described (28). Briefly: Skin cell suspensions were obtained by enzymatic digestion with Liberase TL and DNAse, then chopped and incubated under the same conditions. Next, enzymatic digestion was stopped, and cell suspensions were filtered followed by the addition of DNAse. Finally, cells were washed with PBS, counted and stained. SDLN cells were re-stimulated as previously reported (28). Briefly: Cells were incubated for 48 h with 1 mg/ml of SIINFEKL (InvivoGen) and OVA peptide 323–339 (InvivoGen), followed by cell stimulation cocktail plus protein transport inhibitor for 4 h at 37°C. Then the lymphocytes were collected, washed, and stained.

Tumor Processing

At the end of the tumor growth experiments, tumors were harvested and divided in two fractions that were analyzed by immunofluorescence and flow cytometry. TILs were obtained with the method previously documented (21). Briefly: The tumor was chopped and incubated with Collagenase D and DNAse. Finishing the enzymatic reaction, the cell suspension was filtered, followed by the addition of DNAse. The lymphocyte interface from the centrifuged 40/90 Percoll solution was collected, washed, counted and stained.

Flow Cytometry

Cells were stained with anti-CD45-PECy7 (BioLegend Cat# 157613, RRID:AB_2832559), and DAPI (ThermoFisher), mixed with CountBright absolute counting beads (ThermoFisher) and acquired for flow cytometry. Cell surface staining was performed first blocking with FACS and then adding the following antibodies: anti-CD45-PB (BioLegend Cat# 103126, RRID:AB_493535) or -PECy7, anti-CD45.1-Percp-Cy5.5 (BD Biosciences Cat# 560580, RRID:AB_1727489), anti-CD8-FITC (BioLegend Cat# 100705, RRID:AB_312744, Clone 53-6.70), -APC (BD Biosciences Cat# 553035, RRID:AB_398527) or -APC-Cy7 (BioLegend Cat# 100714, RRID:AB_312753), anti-CD4-APC-Cy7 (BioLegend Cat# 100526, RRID:AB_312727), anti-CD44-BV510 (BioLegend Cat# 103043, RRID:AB_2561391), anti-CD62L-PE-Cy7 (BioLegend Cat# 104418, RRID:AB_313103), anti-CD103-PECy7 (BioLegend Cat# 121426, RRID:AB_2563691), anti-CD69-PE (BioLegend Cat# 104507, RRID:AB_313110), anti-PD-1-APC (BioLegend Cat# 135209, RRID:AB_2251944), and anti-TIM-3-PE/Dazzle^{TM}594 (BioLegend Cat# 134014, RRID:AB_2632738). LIVE/DEAD Fixable Aqua (Thermofisher) staining was included. To achieve intracellular staining, cell surface staining was first performed, followed by fixation and permeabilization using the intracellular fixation and permeabilization buffer set (Thermofisher), according to the manufacturer's instructions. Intracellular staining included anti-IFN-γ-APC (BioLegend Cat# 505810, RRID:AB_315404) and anti-TCF-1/7-AF488 (Cell Signaling Technology Cat# 6444, RRID:AB_2797627). Cells were acquired in a BD FACSCanto II or BD FACSAria cytometer (Becton, Dickinson and company). Data obtained from the cytometer was analyzed with FlowJo software (Tree Star, Inc.).

Mice Immunofluorescence Assay

Tumoral tissue was embedded in Tissue-Tek (Sakura) and sections (5 μm) were cut onto charged glass slides (Superfrost Plus Yellow) and rehydrated. Antigen retrieval was performed in citrate buffer pH 6.0 (sodium citrate 10 μM) at 90°C for 20 min. The sections were permeabilized (bovine serum albumin 10 mg/ml, horse serum 5%, Triton 0.5%, and sodium azide 0.02%) for 2 h and incubated with anti-CD8-FITC (BioLegend Cat# 100705, RRID:AB_312744), anti-CD103 (BioLegend Cat# 121426, RRID:AB_2563691), anti-PD-1-APC (BioLegend Cat# 135209, RRID:AB_2251944), anti-TIM-3-PE/Dazzle (BioLegend Cat# 134014, RRID:AB_2632738), anti-GZMB (BioLegend Cat# 372222, RRID:AB_2728389), anti-IFNγ-PE and anti-TCF-1 primary antibodies at room temperature (RT) for 18 h. The anti-CD103, anti-GZMB and anti-TCF-1/7 mAbs were revealed with a secondary antibody, either AF-647 (Jackson ImmunoResearch Labs Cat# 711-585-152, RRID:AB_2340621) or AF-594 (Jackson ImmunoResearch Labs Cat# 711-605-152, RRID:AB_2492288). The nuclei were counterstained with Hoechst (Invitrogen) for 10 min. The sections were mounted with Vectashield (Vector Laboratories).

Human Samples of Melanoma and Skin Control

Twelve paraffin blocks from resection procedures of confirmed melanoma patients were obtained from the Pathology department of Hospital de Oncología Centro Médico Nacional Siglo XXI, and seven healthy control skin samples were obtained from a repository of biological tissues derived from non-cancerous surgical procedures. Both melanoma and skin samples were obtained with approval of our Institutional Scientific and Ethics Board of Reviews (protocol R-2019-785-05). After 2 years of clinical follow up, the melanoma patients were classified as "metastatic" when patients showed cancer spreading to other organs ($N = 5$) or "disease-free" when there was no tumor evidence after this period of time ($N = 7$) (**Supplementary Table 1**).

Immunofluorescence Assays of Human Samples

Fifteen μm control skin or tumor sections were placed in charged glass slides (Superfrost Plus Green). Slides were placed into a stove (70°C) for 40 min in order to remove the paraffin excess. Tissues were rehydrated with a Xylene/ Ethanol train of solvents.

Antigen retrieval was performed using citrate buffer pH 6.0 (sodium citrate 10 μM) at 120°C for 20 min. Skin samples were permeabilized for 3 h with a perm solution that contained 10mg/ml bovine serum albumin, 5% horse serum, 0.02% sodium azide, and 0.4% Triton. Following permeabilization the tissues were incubated with different primary antibodies: anti-CD8 (Bio-Rad Cat# MCA351G, RRID:AB_877504), anti-CD103 (LifeSpan, Cat# LS-C45284, RRID:AB_2296301), anti-PD-1 (Abcam, Cat# ab175391, RRID: AB_2868534), anti-CD69 (Abcam Cat# ab52587, RRID: AB_881954), or anti-TCF-1/7-AF-488 (Cell Signaling Technology Cat# 6444, RRID:AB_2797627) for 18 h. Incubation with secondary mAb AF-488 (Jackson ImmunoResearch Labs Cat# 711-545-152, RRID:AB_2313584), AF-594 (Jackson ImmunoResearch Labs Cat# 712-585-150, RRID:AB_2340688), and AF-647 (Jackson ImmunoResearch Labs Cat# 715-605-150, RRID:AB_2340862) was performed for 2 h. When specified, fluorescent conjugated antibody anti-IFN-γ-FITC (SONY BIOTECHNOLOGY, Cat# 3132520, RRID: AB_2868456) was incubated for 2 h. Nuclei were stained with Hoechst (Invitrogen) for 10 min. Sections were mounted with Vectashield (Vector Laboratories) and stored at 4°C. Quantification of positive $CD8^+$ $CD103^+$ $CD69^+$ and $CD8^+$ $CD103^+$ $TCF1^+$ cells was performed in highly infiltrated areas. A total of 100 cells were counted in each infiltrated area, registering positive cells. This process was repeated in three different tissue areas and the mean percentage of triple positive cells was obtained from each patient.

Confocal Microscopy

Micrographs were obtained on a Nikon Ti Eclipse inverted confocal microscope (Nikon Corporation) using NIS Elements v.4.50. Imaging was performed using a 20x (dry, NA 0.8) objective lens. Zoom was performed at 3.4x and Digital Zoom was performed when specified. Images were analyzed using FIJI ImageJ Software (ImageJ software, National Institutes of Health; http://rsbweb.nih.gov/ij/).

Statistics

Statistical analysis was performed using Prism 6.0 (GraphPad Software Inc., La Jolla, CA, USA). Statistical significance was calculated using unpaired two-tailed Student's t-test for two groups, and one-way or two-way ANOVA with Tukey's multiple comparison test for more than two groups. Statistical significance for tumor-free percentage was calculated using Log-rank (Mantel-Cox) test. Statistical significance was defined as * $p < 0.05$, ** $p < 0.01$, *** $p < 0.001$, **** $p < 0.0001$.

RESULTS

Immunization With Porins Elicits Prophylactic and Therapeutic Melanoma Control

We first determined whether the *S.* Typhi Porins could be used as a PAMP-adjuvant in a murine melanoma model using two different vaccination strategies exemplifying prophylactic and therapeutic approaches. Mice were immunized s.c. in the left flank with the model antigen OVA and the Porins as adjuvant. The same immunization conditions were used for the control groups: OVA-alone, Porins-alone and PBS. In the prophylactic approach, mice were challenged s.c. at the same place with the OVA-expressing B16-F10 melanoma cell line (MO4) 7 days post-immunization and the mice were followed for up to 21 days. The results showed that a prophylactic immunization with OVA + Porins powerfully suppressed tumor growth, with 60% of immunized mice clear of tumor and the rest bearing tumors under 2 mm^3 in size (**Figure 1A**). Meanwhile all control mice had established large tumors.

Effective therapeutic responses are substantially more challenging, and we sought to assess whether the prophylactic protection of Porins was also capable to control already established tumors. For this, mice were first inoculated s.c. with MO4, and 7 days later immunized s.c. with the conditions mentioned above. Again, the combination of OVA + Porins was able to significantly control the tumor growth (**Figure 1B**). We then tested whether Porins could induce a protective immune memory. Since in the therapeutic experiment all OVA + Porins immunized mice developed small tumors, we evaluated memory in the prophylactic scheme, re-challenging tumor-free mice at day 28 with another MO4 inoculation. We observed that by the end of the 100 days following period, three out of four of the re-challenged mice were still tumor-free (**Figure 1C**). Altogether, these results support that the Porins from *S.* Typhi are an efficient prophylactic and therapeutic PAMP-adjuvant, also inducing a long-lasting protective memory against melanoma.

Porins Elicit Circulatory and Tissue-Resident Memory T Cells

To better understand the adjuvant mechanism of Porins, we evaluated its capacity to generate T cell memory subsets that are essential for tumor control. For this, we tracked the immune response of OVA-specific T cells using the well-studied adoptive transfer model of OT-I and OT-II $CD45.1^+$ T cells, which express transgenic TCRs specific for the CD8 and CD4 OVA epitopes, respectively, in CD45.2 mice that were immunized with OVA + Porins 1 day after the adoptive transfer. We observed a 25-fold expansion of $CD45.1^+$ cells in the OVA + Porins group by day 7 that consisted of both OT-I and OT-II T cells (**Figure 2A**). The OT-I frequency in skin-draining lymph nodes (SDLN) at day 7 and 28 was significantly higher for OVA + Porins compared with PBS (**Figure 2B**), while OT-II cells were only significantly increased at day 7 (**Supplementary Figure 1A**). When we evaluated the two main types of circulating memory in SDLN, we observed Tcm ($CD44^+$ $CD62L^+$) and Tem ($CD44^+$ $CD62L^-$) cells only in the OVA + Porins immunized mice, both types by day 7, and mostly Tcm cells by day 28 (**Figure 2C**). Both OT-I (**Figure 2C**) and OT-II (**Supplementary Figure 1B**) observed a similar pattern of memory formation. No memory cells were observed in the control groups (data not shown). We also tested the induced T cells to produce IFN-γ by re-stimulating them ex

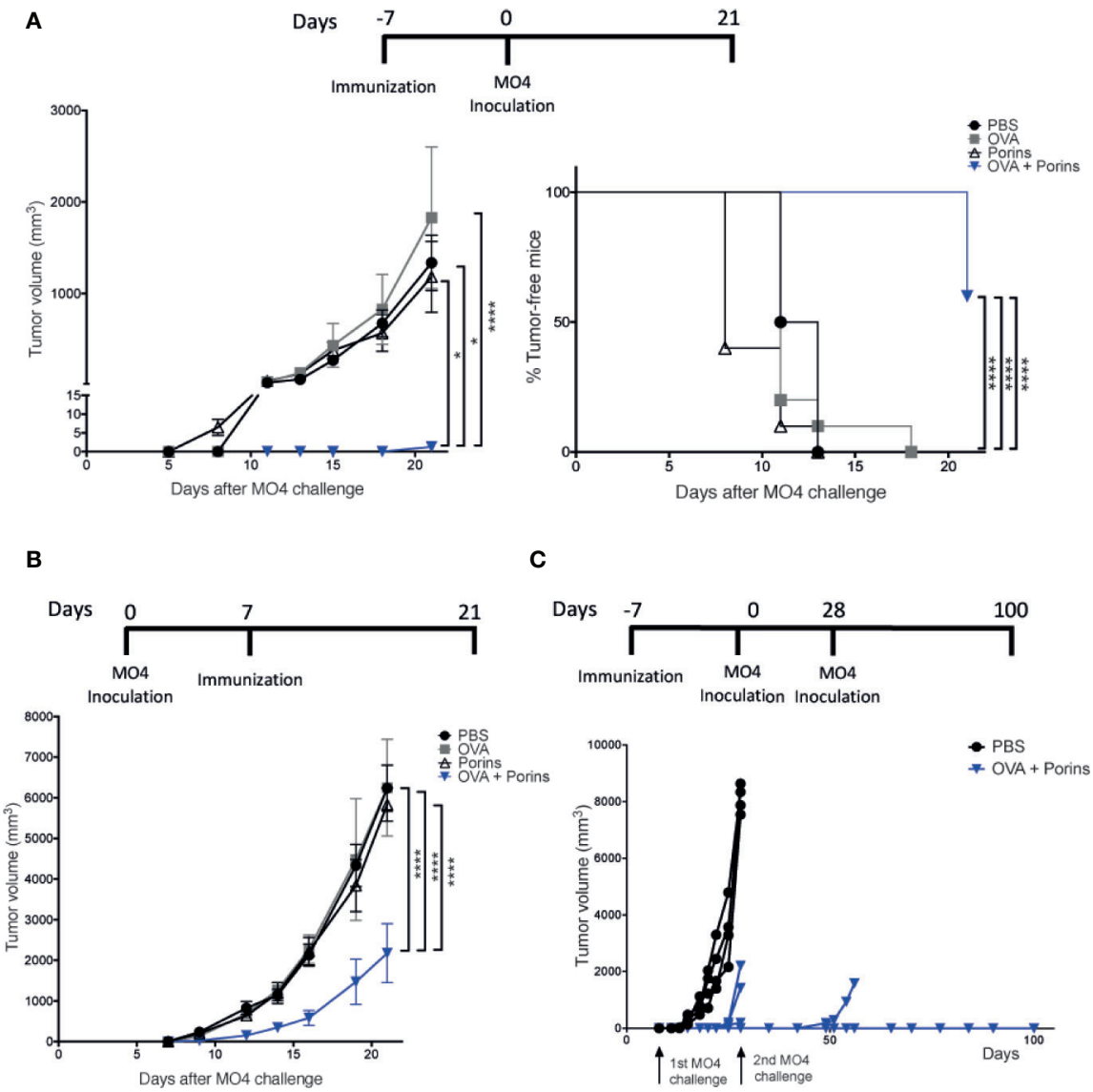


FIGURE 1 | Porins as adjuvant induce an effective prophylactic and therapeutic anti-tumoral response. **(A)** C57BL/6 mice were immunized s.c. in the left back, with OVA + Porins or single inoculated with OVA, Porins or PBS, as control groups. Seven days later, 2.5 x 10^5 MO4 cells were inoculated s.c. in the same place as the immunization. The tumor volume and the tumor-free mice were scored every 3 days starting on day 7 until day 21. **(B)** C57BL/6 mice were challenged with MO4 and 7 days later were immunized with OVA + Porins or inoculated with OVA, Porins or PBS. **(C)** Mice were immunized with either OVA + Porins (N = 7) or PBS and challenged with MO4 cells [as in **(A)**], and mice that were tumor-free by day 28 (N = 4) were re-challenged with a new dose of MO4 cells. Statistical data were pooled from three independent experiments with three mice per experimental condition. *p < 0.05, ****p < 0.0001.

vivo with CD8 and CD4 specific OVA peptides. IFN-γ–producing cells comprised 25% and 60% of OT-I T cells by days 7 and 28, respectively (**Figure 2D**). Likewise, we observed IFN-γ^+ OT-II T cells (**Supplementary Figure 1C**), although it was significantly lower than the OT-I response, particularly by day 28 (**Supplementary Figure 1D**).

Since Porins facilitate formation and expansion of circulating memory cells in the SDLN, we also evaluated its capacity to induce Trm T cells (CD103$^+$ CD69$^+$) in the skin, perhaps the most relevant population for melanoma control. We used the same adoptive transfer and immunization strategy explained above, again observing that only the OVA + Porins mice harbored CD45.1$^+$ cells in the skin 7 and 28 days after immunization (**Figures 2E, F**). Both OT-I and OT-II T cells were able to form Trm T cells (**Figures 2E, G**; **Supplementary Figure 1E**), but again with significant reduced percentage for OT-II cells (**Supplementary Figure 1F**). Thus, Porins reinforce the formation of IFN-γ-producing T cells and a pool of early and lasting Tcm and Tem CD8$^+$ T cells at draining lymph nodes and Trm CD8$^+$ T cells at the site of immunization.

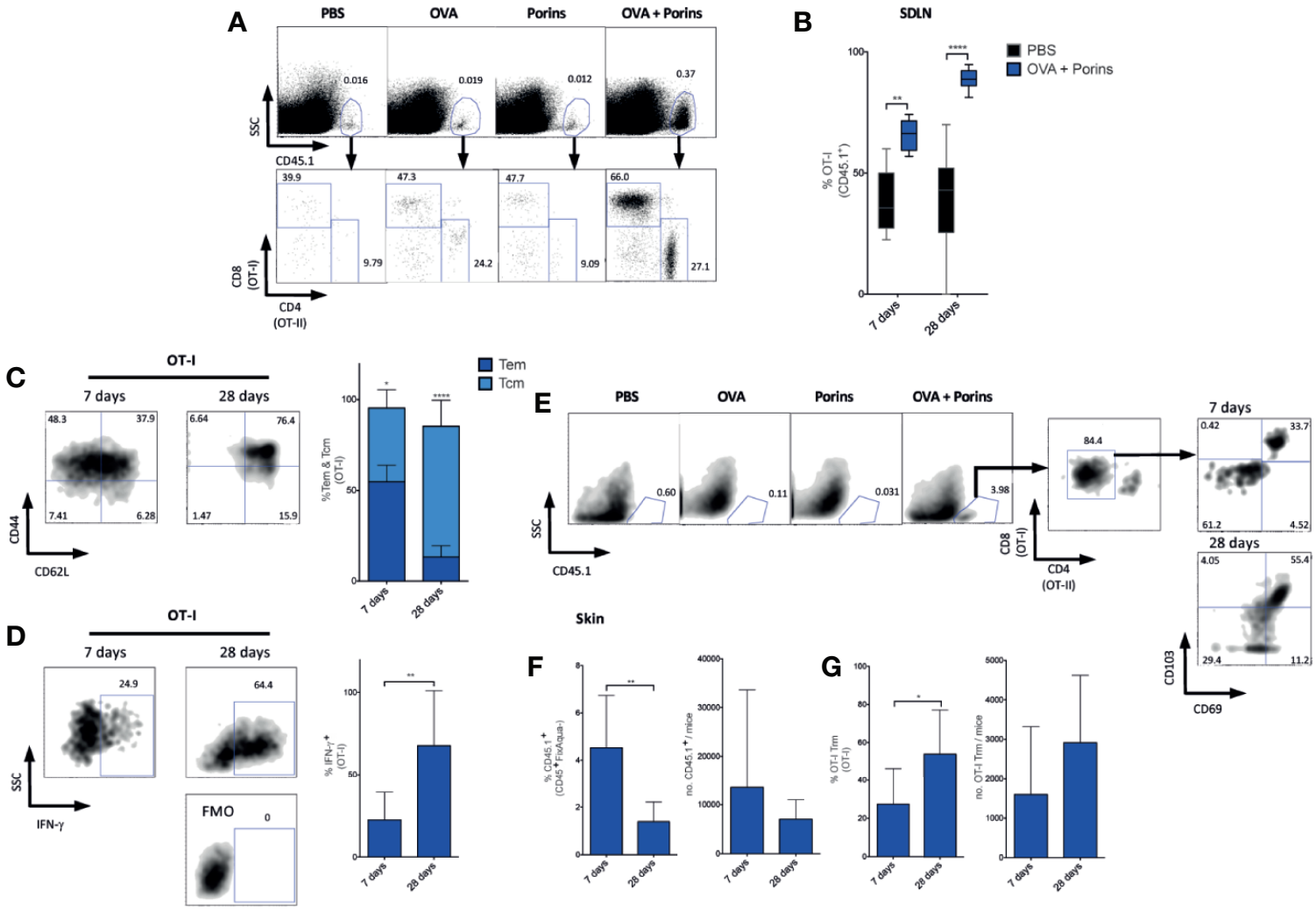


FIGURE 2 | Porins induce circulating and tissue-resident memory T cells. C57BL/6 mice were i.v. transferred with OVA-specific $CD8^+$ $CD45.1^+$ T cells (OT-I) and $CD4^+$ $CD45.1^+$ T cells (OT-II) and a day later, i.d. immunized in both ears with OVA + Porins, and OVA, Porins or PBS as controls. Generation of the following populations was analyzed by flow cytometry in skin-draining lymph nodes (SDLN) **(A–D)** and skin **(E–G)** 7 and 28 days post-immunization as marked in the specific figure. **(A)** OVA-specific $CD45.1^+$, OT-I and OT-II cells. **(B)** Comparison of SDLN OT-I frequencies induced by the immunization and PBS groups. **(C)** OT-I Tcm ($CD44^+$ $CD62L^+$) and OT-I Tem ($CD44^+$ $CD62L^-$). **(D)** IFN-γ positive OT-I cells from SDLN cells re-stimulated with OVA peptides (SIINKFEL and 323-339). **(E)** OT-I Trm T cells ($CD103^+$ $CD69^+$), with percentage and absolute numbers of $CD45.1^+$ **(F)** and OT-I Trm T cells **(G).** Statistical data were pooled from three independent experiments with 3 mice per experimental condition. *$p < 0.05$, **$p < 0.01$, ****$p < 0.0001$.

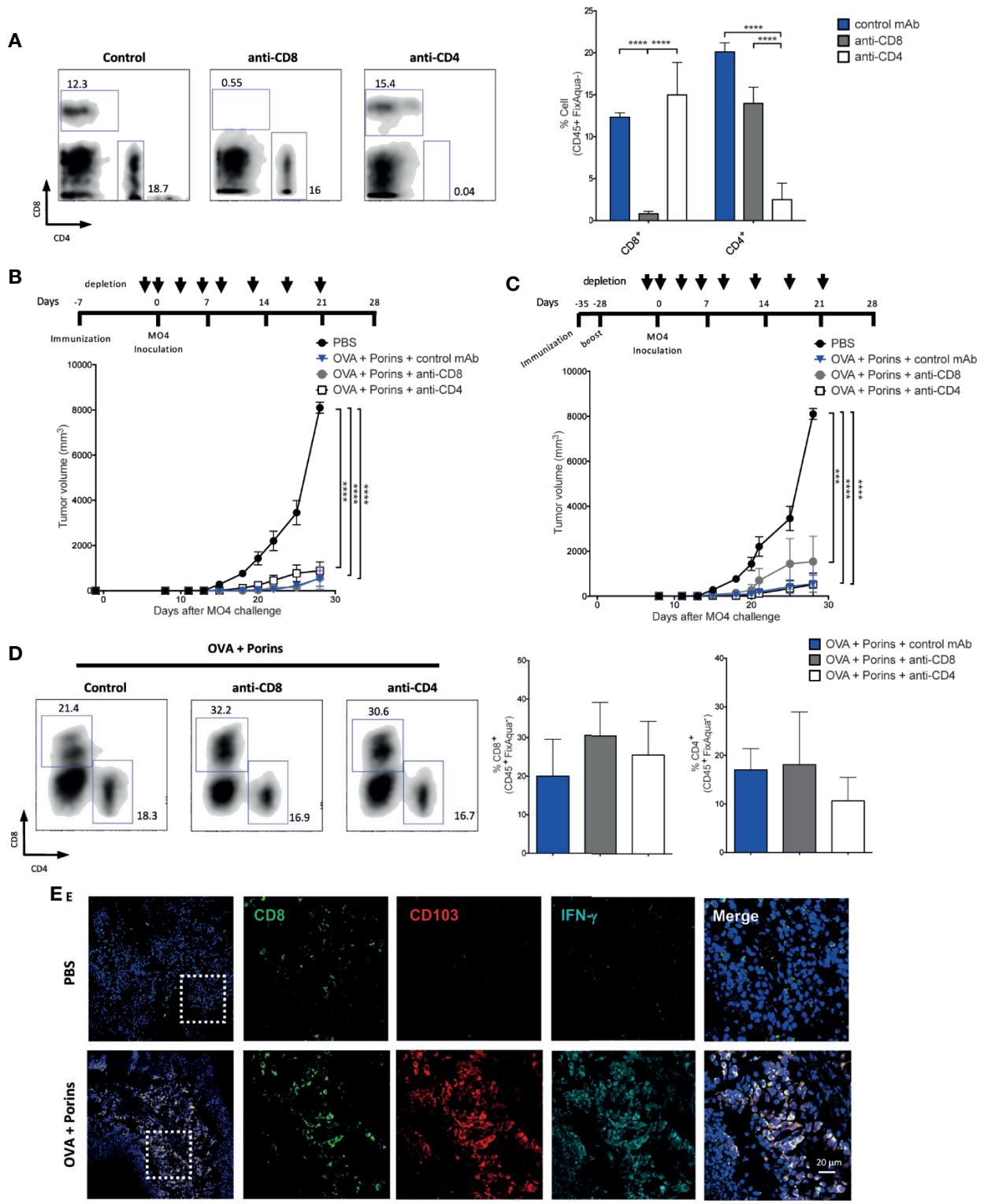


FIGURE 3 | Porins induce functional tumor-infiltrating Trm T cells that correlate with tumor growth control. Immunized mice were depleted of $CD8^+$ and $CD4^+$ T cells **(A)**, and tumor control was assessed after two different immunization schemes, 7 days before MO4 inoculation **(B)** or 35 days before with boosting at day -28 **(C)**. Arrows indicate the anti-CD8 and anti-CD4 mAb injection days. **(D)** Flow cytometry charts and plots of the frequency of $CD8^+$ and $CD4^+$ TILs. **(E)** $CD103^+$ (red) $CD8^+$ (green) T cells expressing IFN-γ (cyan) from tumor of the prime/boost immunization scheme (representative immunofluorescence micrographs from a zoomed area) (Scale bar = 20µm). Statistical data were pooled from three independent experiments with 3–4 mice per experimental condition. ***$p < 0.001$, ****$p < 0.0001$.

Formation of Functional Trm T Cells Correlates With Melanoma Protection

To address the individual contributions of different memory T cell populations for protection against melanoma growth, we eliminated the circulating $CD8^+$ or $CD4^+$ T cells injecting i.p. eight doses of anti-CD8 or anti-CD4 mAbs. For this, we tested two immunization schemes: 1) 7 days before the MO4 melanoma cell challenge, and 2) 35 days before challenge with one boost at day -28. Similar experimental approaches have previously documented that skin and tumor-infiltrating Trm T cells are resistant to antibody-dependent depletion (38, 41). The efficiency of circulating T cell depletion is shown in **Figure 3A** and the immunization and T cell depletion schemes in **Figures 3B, C** (top). We observed tumor growth control in spite of depletion of circulating $CD8^+$ or $CD4^+$ T cells (**Figures 3B, C**, bottom), seen also by the percentage of tumor-free mice (**Supplementary Figures 2A, B**). Indeed, we corroborated that tumor-infiltrating $CD8^+$ and $CD4^+$ T cells were not affected by depletion of circulating T cells in the OVA + Porins-immunized mice 21 days post MO4 inoculation (**Figure 3D**). Worth mentioning, an immunization scheme 28 days before challenge and with no additional boost was not able to control the tumor growth in the absence of the circulating T cells (**Supplementary Figure 2C**). In order to evaluate Trm formation in the tumor stroma after a prime/boost immunization we evaluate the presence and function of Trm T cells by immunofluorescence (IF) microscopy. As it can be observed in **Figure 3E**, there is an increased infiltration of $CD8^+$ T cells that express CD103 in the immunized mice compared with control mice. Importantly, the Trm T cell population in the tumor stroma express IFN-γ (**Figure 3E**) and granzyme B (GZMB) (**Supplementary Figure 3A**). The Trm formation in the tumors is also not affected by depletion of circulating T cells (**Supplementary Figure 3B**). Taken together, these data support that Porins strongly shape a tumor stroma Trm T cell milieu associated with the control of tumor growth, that can be explained by an early seeding of functional Trm T cells that need to be reinforced to be protective at late time points.

To assess the extent of the Porins-induced melanoma protective T cell populations, we tested the Porins adjuvant capacity against two melanoma-associated antigens (MAA), TRP-2 and gp100, previously reported as critical antigens in cancer vaccine development (42). For this, mice were immunized at day -10 before challenge with the B16-F10 melanoma cell line, according to previously published immunization strategies (39, 40). A boost was executed 7 days after the first immunization, when a Trm population is already established (**Figure 2E**). We observed better control of melanoma in mice immunized with MAA + Porins than MAA-alone or PBS (**Figure 4A**). Here, Porins-alone with the boosting scheme showed efficient protection and no clear differences were found with MAA + Porins, suggesting the induction of protective responses by the exogenous antigens but also by tumor endogenous melanoma antigens. Considering that the tumor growth control is independent of circulating T cells and seems to be dependent of T cells seeded in the tumor stroma (**Figure 3**), we next evaluated the presence of TILs in the immunized mice. Even though in the MAA + Porins group a higher percentage of $CD8^+$ TILs was observed, the tumor-density of total $CD8^+$ T cells was similar among all groups (**Figures 4B, C**). We did not observe differences among the groups in the total $CD4^+$ T cells (**Supplementary Figures 4A, B**). Importantly, we observed the $CD8^+$ Trm T cell formation only in the MAA + Porins immunization and the Porins-alone, which are the groups that could control the tumor growth (**Figures 4A, D**), this was similar with the $CD4^+$ Trm TILs (**Supplementary Figures 4A, C**) although its frequency was significantly lower (**Supplementary Figure 4D**). These results illustrate the extent of the use of the Porins as an adjuvant of tumor associated antigens as well as the high correlation of Trm T cells formation with the tumor growth control.

Porins Induce Enhanced Adjuvant Protection More Than the Cholera Toxin B Subunit

To put in context the anti-tumor adjuvant capacity of Porins (classical PAMP), we compared it against the CTB (non-classical PAMP), an adjuvant that also promotes the formation of protecting Trm T cells against melanoma (28). Mice were again immunized with each adjuvant and inoculated with MO4 melanoma cells 7 days later (**Figure 5A**, top). We observed that Porins and CTB exhibit prophylactic protection delaying tumor growth compared with control groups. However, there was a significantly better protection with OVA + Porins than with any other treatment, measured as tumor volume and percentage of tumor free mice (**Figure 5A**, left and right graphs, respectively). To gain insights into the relevance of the induced memory T cell populations, we compared the capacity of both CTB and Porins to generate $CD8^+$ Trm T cells anticipating to observed more in the OVA + Porins mice correlating with the better protection. We also looked for early signals of exhaustion in this skin-infiltrating population by assessing PD-1 expression. For this, $CD45.1^+$ OT-I and OT-II cells were tracked after adoptive transfer experiments similar to the ones for **Figures 2A–C**. We observed a greater expansion of skin-infiltrating $CD45.1^+$ cells in OVA + CTB than in OVA + Porins mice at day 7 and 28 (**Supplementary Figures 5A–C**). Still, we observed a higher efficiency of formation of OT-I Trm in the OVA + Porins immunization group compared with the OVA + CTB (**Figures 5B, C**), but that was not reflected in absolute numbers because of the greatest expansion of $CD45.1^+$ cells in OVA + CTB mice (**Supplementary Figure 5B**). Remarkably, we found that the OVA + Porins-induced OT-I Trm have a lower percentage and number of PD-1 positive cells (**Figure 5D**), also observed with a lower MFI (**Figure 5E**). Similar data were obtained when cells were harvested 28 days post immunization (**Figures 5F–H**), suggesting that the enhanced protection conferred by OVA + Porins may be due to the low numbers of $CD8^+$ Trm $PD\text{-}1^+$ T cells. Somehow different, the OT-II Trm T cell frequency was greater for OVA + Porins than OVA + CTB, but induced-OT-II Trm T cells with both adjuvants have similar

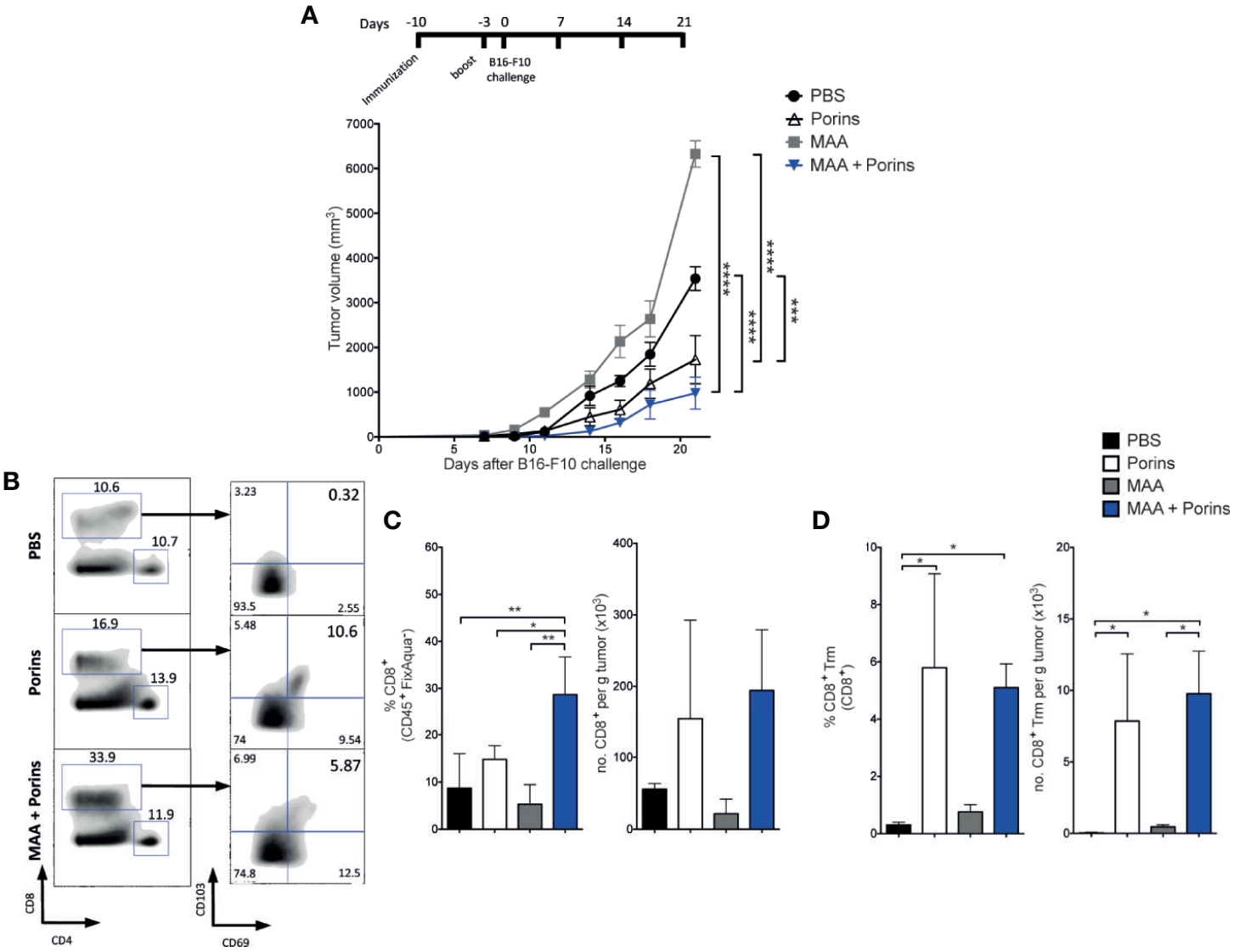


FIGURE 4 | Porins induce protection against native melanoma antigens. **(A)** Mice were immunized s.c. with Porins, TRP-2 and gp100, two melanoma-associated antigens (MAA), 10 and 3 days before B16-F10 challenge and the control groups: Porins-alone, MAA-alone and PBS. **(B)** Flow cytometry analysis of $CD8^+$ TILs assessing the Trm phenotype 21 days after melanoma challenge. Frequencies and absolute numbers per tumor mass are given of $CD8^+$ T cells **(C)** and $CD8^+$ Trm T cells **(D)**. Statistical data were pooled from two independent experiments with 5 mice per experimental condition. *$p < 0.05$, **$p < 0.01$, ***$p < 0.001$, ****$p < 0.0001$.

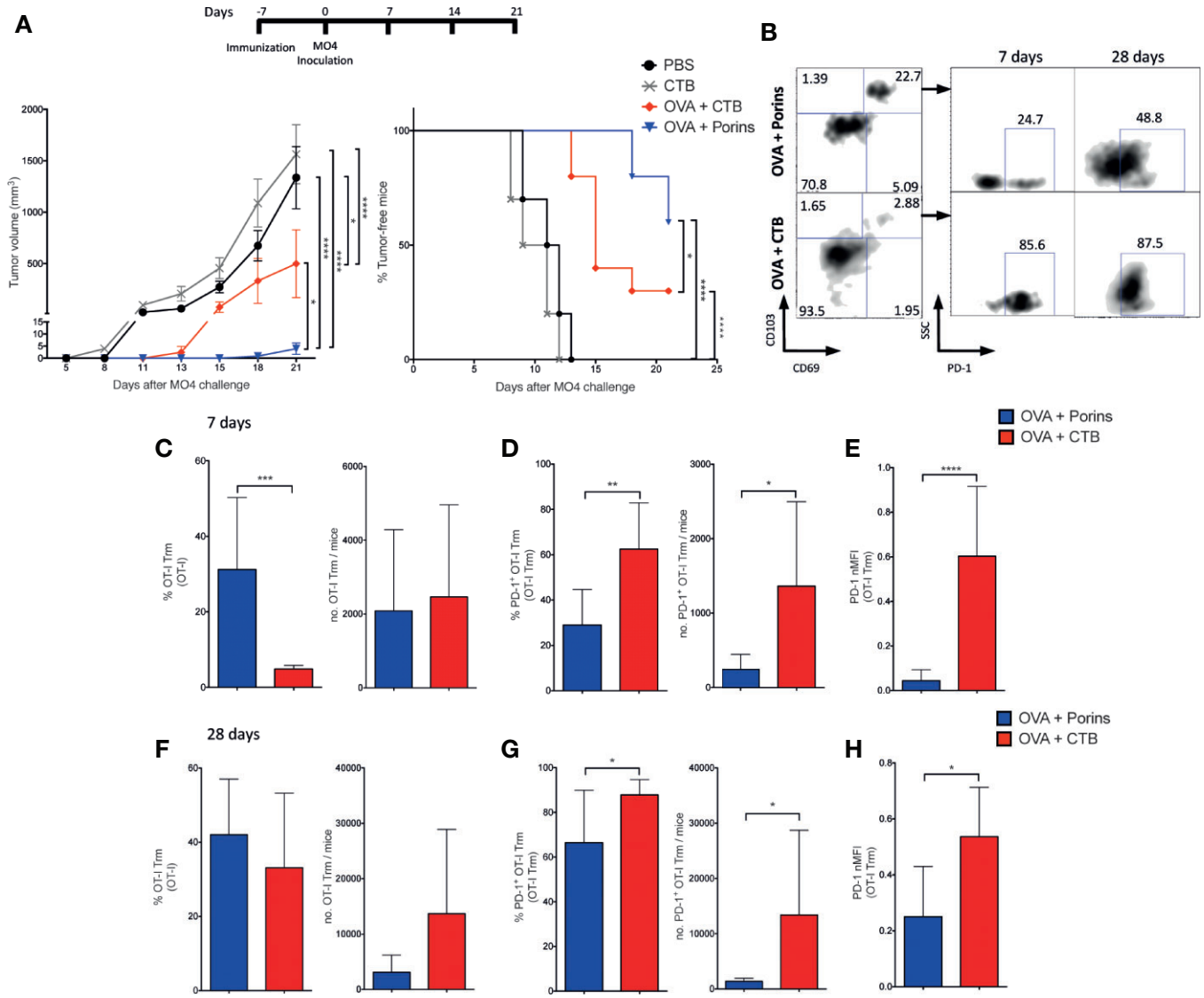


FIGURE 5 | Porins induce better adjuvant protection than the B subunit of the Cholera toxin. **(A)** Mice were immunized subcutaneously with OVA + Porins or OVA + CTB and controls, challenged with MO4 cells and tumor volume and tumor-free mice were scored. Mice were adoptively transferred and immunized as in **Figure 2**, comparing the OVA + Porins against OVA + CTB immunization. **(B)** OT-I Trm T cells and PD-1$^+$ cells at day 7 and 28. Percentage and absolute numbers of OT-I Trm T cells **(C)**, OT-I Trm T cells PD-1 positive **(D)** and the PD-1 normalized MFI from OT-I Trm T cells **(E)** at day 7; and the same analysis at day 28 **(F–H)**. Statistical data were pooled from three independent experiments with 3–4 mice per experimental condition. *p < 0.05, **p < 0.01, ***p < 0.001, ****p < 0.0001.

percentages of PD-1 positive cells at day 7 (**Supplementary Figure 5D**), which became more abundant in the OVA + Porins by day 28 (**Supplementary Figure 5E**). In summary, even though CTB can promote a superior expansion of OVA-specific T cells in the skin, Porins are capable to promote a greater and more stable population of $CD8^+$ Trm T cells with lower PD-1 expression as an early exhaustion signature, and perhaps because of that, Porins promoted a more efficient control of melanoma.

Porins-Induced Progenitor Exhausted Trm T Cell Population Correlates With an Enhanced Protection

Since CTB and Porins immunization provides a suitable model to compare induced populations with protection, we compared the capacity of both adjuvants to induced native T cell populations without the constraint of a T cell adoptive transfer (28). For this, we first compared the therapeutic protection rendered by OVA + CTB and OVA + Porins in MO4 melanoma, observing again a more proficient protection with the latter (**Figure 6A**). Next, we assessed whether Porins were also able to induce functional T cells evaluating the formation of IFN-γ-producing T cells. Indeed, we observed IFN-γ-producing $CD8^+$ TILs in both immunizations, but lacking in the PBS control (**Figure 6B**). Flow cytometry analysis of $CD8^+$ TILs showed a greater frequency of PD-1^+ cells in OVA + CTB immunization that is not reflected in absolute numbers (**Figures 6C, D**). When we assessed the presence of potential terminally exhausted T cells, we were able to observe $CD8^+$ TILs co-expressing PD-1 and TIM-3 in both immunizations with no difference in TIM-3 expression (**Figures 6E, F**). Importantly, we confirmed the functionality of $CD8^+$ TIM-3^+ TILs through expression of IFN-γ and GZMB, although there were no differences between both immunizations (**Supplementary Figures 6A, B**). IFN-γ secretion has previously been associated with terminally exhausted T cells (9, 10). Thus, this potentially terminally exhausted phenotype was also evaluated in mice immunized with MAA + Porins and with Porins-alone, observing in $CD8^+$ and in $CD8^+$ Trm TILs the co-expression of TIM-3 and PD-1 exclusively for the MAA + Porins immunization condition (**Supplementary Figures 7A, B**), these phenotypes have already been described in previous studies (43, 44). Nevertheless, the presence of TIM-3^+ $CD8^+$ Trm TILs did not correlate with tumor growth control (see **Figure 4A** and **Supplementary Figure 7B**).

Considering that the TIM-3^+ PD-1^+ $CD8^+$ TILs induced by Porins did not show correlation with protection, we evaluated the tumor-infiltrating $CD8^+$ T cells with a TCF-1^+ progenitor exhausted phenotype. Immunofluorescence staining of the tumor stroma showed $CD8^+$ TCF-1^+ cells, solely in the OVA + Porins immunization (**Figure 7A**). An increase in the TCF-1 MFI in the $CD8^+$ and $CD8^+$ PD-1^+ TILs was also observed by flow cytometry in the OVA + Porins condition, but did not reach a statistically difference compared with OVA + CTB (**Figure 7B**). Considering the higher TCF-1 expression of the OVA + Porins-induced $CD8^+$ TILs, we evaluated if the progenitor exhausted phenotype was derived from a Trm population. We observed a greater infiltrate of $CD8^+$ Trm T cells in OVA + Porins-immunized mice than in OVA + CTB (**Figures 7C, D**). The same was observed with the percentage and tumor-infiltrate density of the PD-1^+ $CD8^+$ Trm T cells (**Figures 7C, E**). Interestingly, among tumor-infiltrating cells the population that expressed TCF-1 corresponded to the PD-1^+ $CD8^+$ Trm T cells, only noticed in the tumors from OVA + Porins-immunized mice (**Figures 7F, G**; **Supplementary Figure 8**), which is also supported by the greater TCF-1 MFI of the $CD8^+$ Trm T cells and the PD-1^+ subset (**Figure 7H**). These results indicate that Porins induce a progenitor exhausted Trm T cell population that correlates with tumor growth control.

Porins-Induced Progenitor Exhausted Trm T Cell Population Correlates With Anti-PD-1 Immunotherapy Cooperation

Because the tumor-infiltrating progenitor exhausted TCF-1^+ PD-1^+ $CD8^+$ T cells are documented to be the population that responds to the anti-PD-1 immunotherapy (9, 17), we administrated three doses of anti-PD-1 mAb at days 19, 21, and 23 in mice therapeutically immunized with either OVA + CTB or OVA + Porins (**Figure 8A**, top) (9). For this experiment, the anti-PD-1 immunotherapy was carried out only in mice harboring tumors of similar size from both immunization protocols to level the starting point of tumor growth, in which we were going to evaluate the response to immunotherapy. We observed that while progression of tumors in OVA + CTB mice was not altered by the anti-PD-1 mAb, immunotherapy halted further tumor growth in the OVA + Porins mice (**Figure 8A**, bottom). These data support that Porins promote the formation of a $CD8^+$ Trm T cell population with a progenitor exhausted phenotype and function. A clear difference between the immunization conditions tested was the greater capacity of Porins to generate a PD-1-expressing $CD8^+$ Trm T cells that also express TCF-1 (**Figures 7F, G**; **Supplementary Figure 8**). Thus, we also evaluated the formation of the TCF-1^+ populations in the mice immunized with Porins treated or not with anti-PD-1 mAb. We observed the formation of TCF1$^+$ PD-1^+ $CD8^+$ T cells clusters (**Figure 8B**), as well as an increase in the TCF-1^+ $CD103^+$ $CD8^+$ T cells (**Figure 8C**) in the tumor stroma of mice treated with Porins and anti-PD-1 mAb, suggesting the expansion of this population after the immunotherapy. In contrast the frequency of TIM-3^+ PD1$^+$ $CD8^+$ T cell population after the PD-1 blockade was similar that in untreated Porin-immunized mice (**Supplementary Figure 9**). Altogether these results argue for an important role of the progenitor exhausted Trm T cell population for control of melanoma growth, independently or in cooperation with anti-PD-1 immunotherapy.

Progenitor Exhausted Trm T Cells in the Tumor Stroma of Melanoma Patients Also Correlate With Disease Control

We determined whether the Trm T cell populations observed after Porin immunization could also be present in human

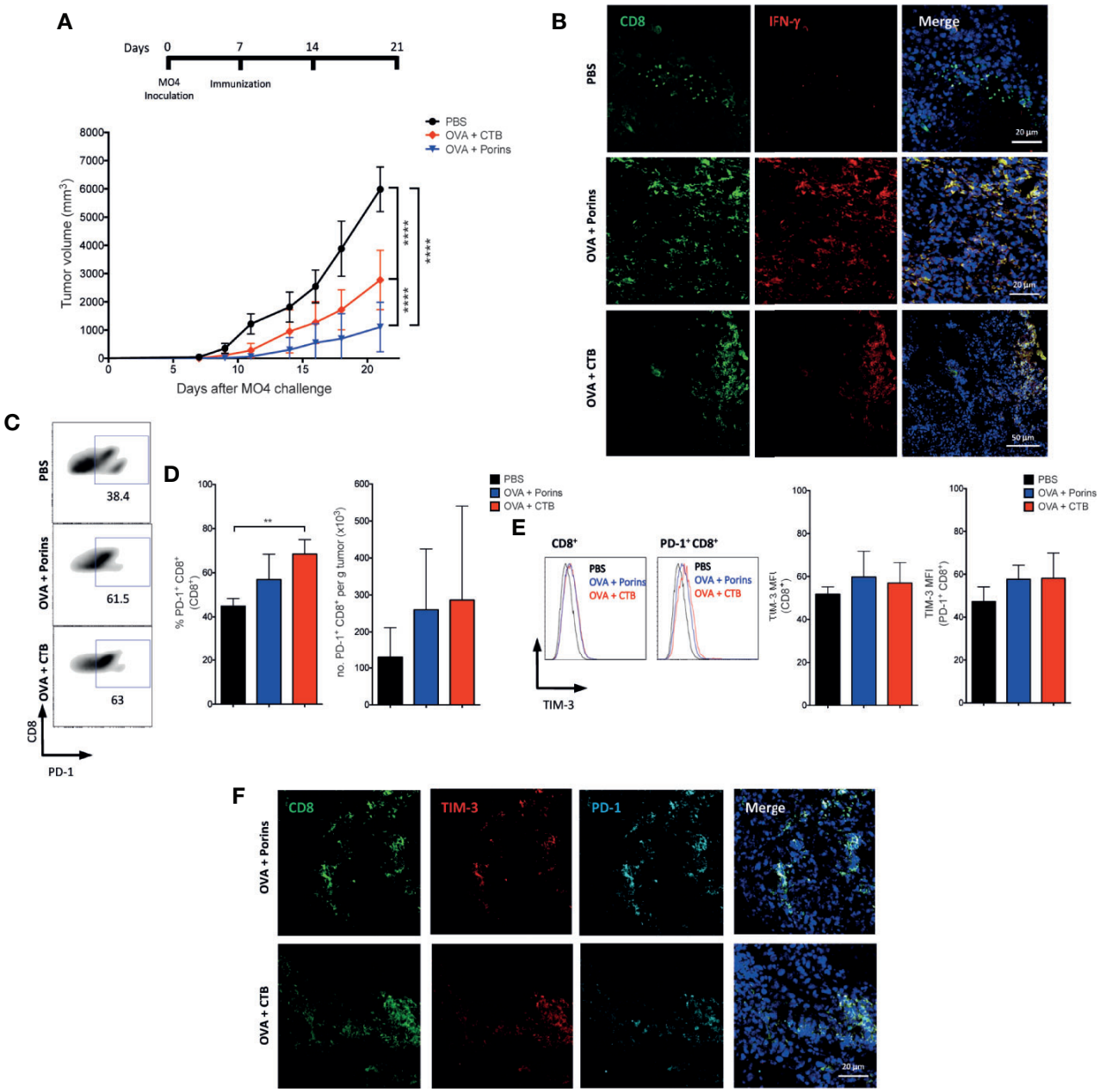


FIGURE 6 | Porins induce functional TIM-3$^+$ PD-1$^+$ CD8$^+$ T cells in a therapeutic scheme. **(A)** Mice were inoculated with MO4 cells and immunized s.c. with OVA + Porin, OVA + CTB or PBS control, data is presented 21 days after the melanoma challenge. **(B)** CD8$^+$ (green) T cells expressing IFN-γ (red) from tumors (representative immunofluorescence micrographs from a zoomed area). **(C)** Flow cytometry of CD8$^+$ PD-1$^+$ TILs and **(D)** their percentages. **(E)** TIM-3 medium fluorescent intensity (MFI) from CD8$^+$ and CD8$^+$ PD-1$^+$ TILs. **(F)** CD8$^+$ (green) T cells expressing TIM-3 (red) and PD-1 (cyan) from tumors (representative immunofluorescence micrographs from a zoomed area) (Scale bar = 20µm). Statistical data were pooled from three independent experiments with three mice per experimental condition. **p < 0.01, ****p < 0.0001.

melanoma tumors. For this, we assessed resection products of five metastatic and seven disease-free melanoma patients after a 2 years follow-up (**Supplementary Table 1**). We observed an increase of CD103$^+$ CD69$^+$ CD8$^+$ T cells in the tumor stroma of disease-free patients compared with metastatic patients and healthy control skin (CS) (**Figures 9A, B**; **Supplementary Figure 10A**). Importantly, the Trm CD8$^+$ TILs of melanoma patients expressed IFN-γ; which were increased in disease-free patients compared with metastatic patients (**Figure 9C**; **Supplementary Figure 10B**). We also evaluated the presence of progenitor exhausted T cells. As shown in **Figure 10A**, there was an increment of TCF-7$^+$ PD-1$^+$ CD8$^+$ T cells in melanoma

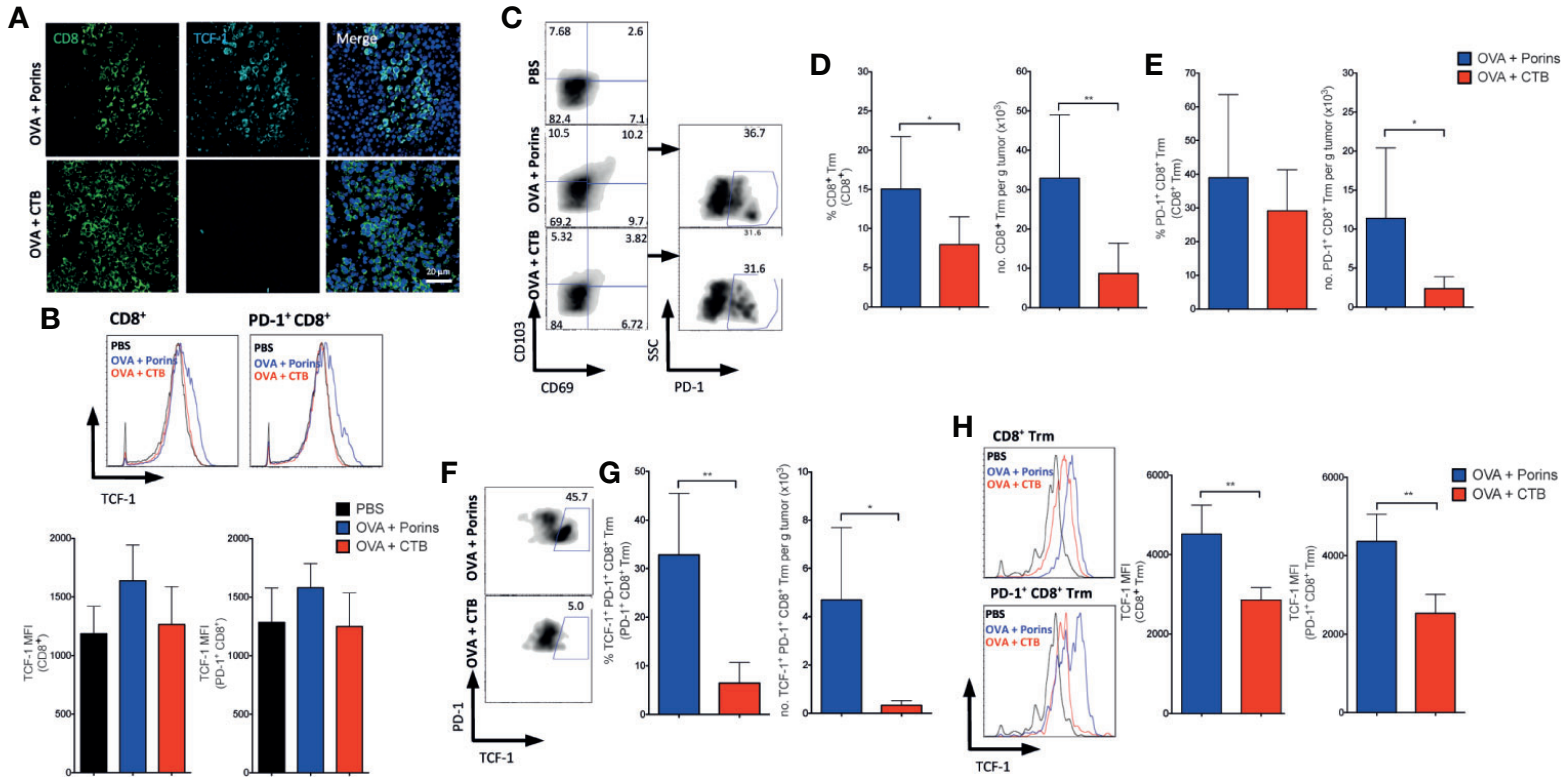


FIGURE 7 | Porins-induced tumor-infiltrating TCF-1$^+$ Trm CD8$^+$ T cell correlates with melanoma protection. Vaccination scheme as in **Figure 6A**, data is presented 21 days after the melanoma challenge. **(A)** CD8$^+$ (green) T cells expressing TCF-1 (cyan) from tumors (representative immunofluorescence micrographs from a zoomed area) (Scale bar = 20μm). **(B)** TCF-1 medium fluorescent intensity (MFI) from CD8$^+$ and PD-1$^+$ CD8$^+$ TILs. **(C)** Flow cytometry of PD-1$^+$ expressing CD8$^+$ Trm T cells. Frequencies and absolute numbers of CD8$^+$ Trm **(D)** and PD-1$^+$ CD8$^+$ Trm **(E)**. **(F)** Flow cytometry of CD8$^+$ Trm T cells expressing PD-1$^+$ and TCF-1$^+$. **(G)** Frequencies and absolute numbers of TCF-1$^+$ PD-1$^+$ CD8$^+$ Trm T cells. **(H)** TCF-1 MFI from CD8$^+$ Trm and PD-1$^+$ CD8$^+$ Trm. Statistical data were pooled from three independent experiments with 3–4 mice per experimental condition. *$p < 0.05$, **$p < 0.01$.

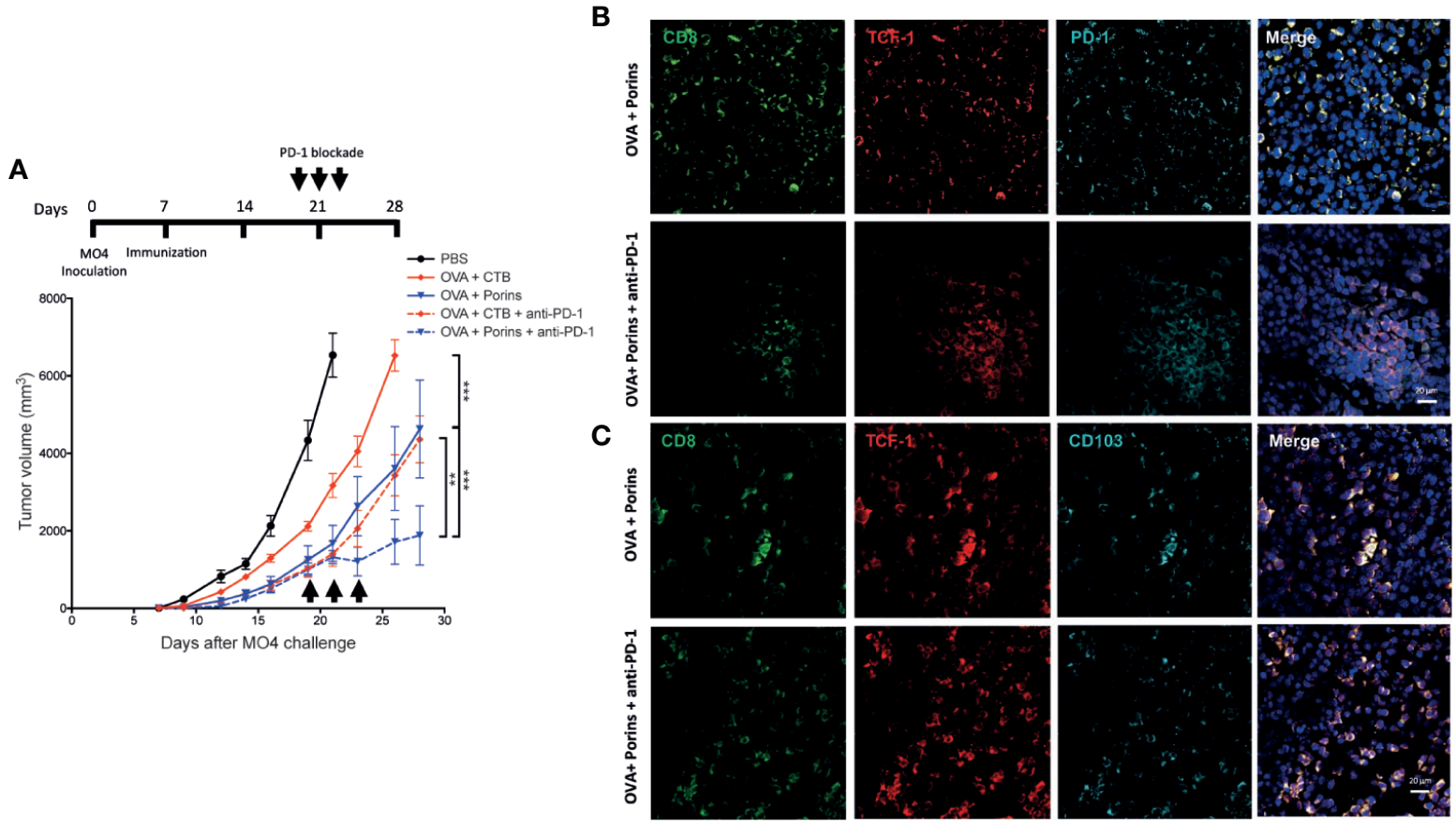


FIGURE 8 | Porins-induced progenitor exhausted Trm $CD8^+$ T cells correlate with enhanced response to anti-PD-1 immunotherapy. **(A)** Mice immunized and challenged as in **Figure 6A** were treated with anti-PD-1 immunotherapy (arrows), and tumors were harvested at day 28. Analysis of $TCF\text{-}1^+$ (red) $CD8^+$ (green) T cells expressing PD-1 (cyan) **(B)** or CD103 (cyan) **(C)** from the tumors of OVA + Porins-immunized mice with or without anti-PD-1 mAb, representative immunofluorescence micrographs from a zoomed area (Scale bar = 20μm). Statistical data were pooled from three independent experiments with 3-4 mice per experimental condition. $^{**}p < 0.01$, $^{***}p < 0.001$.

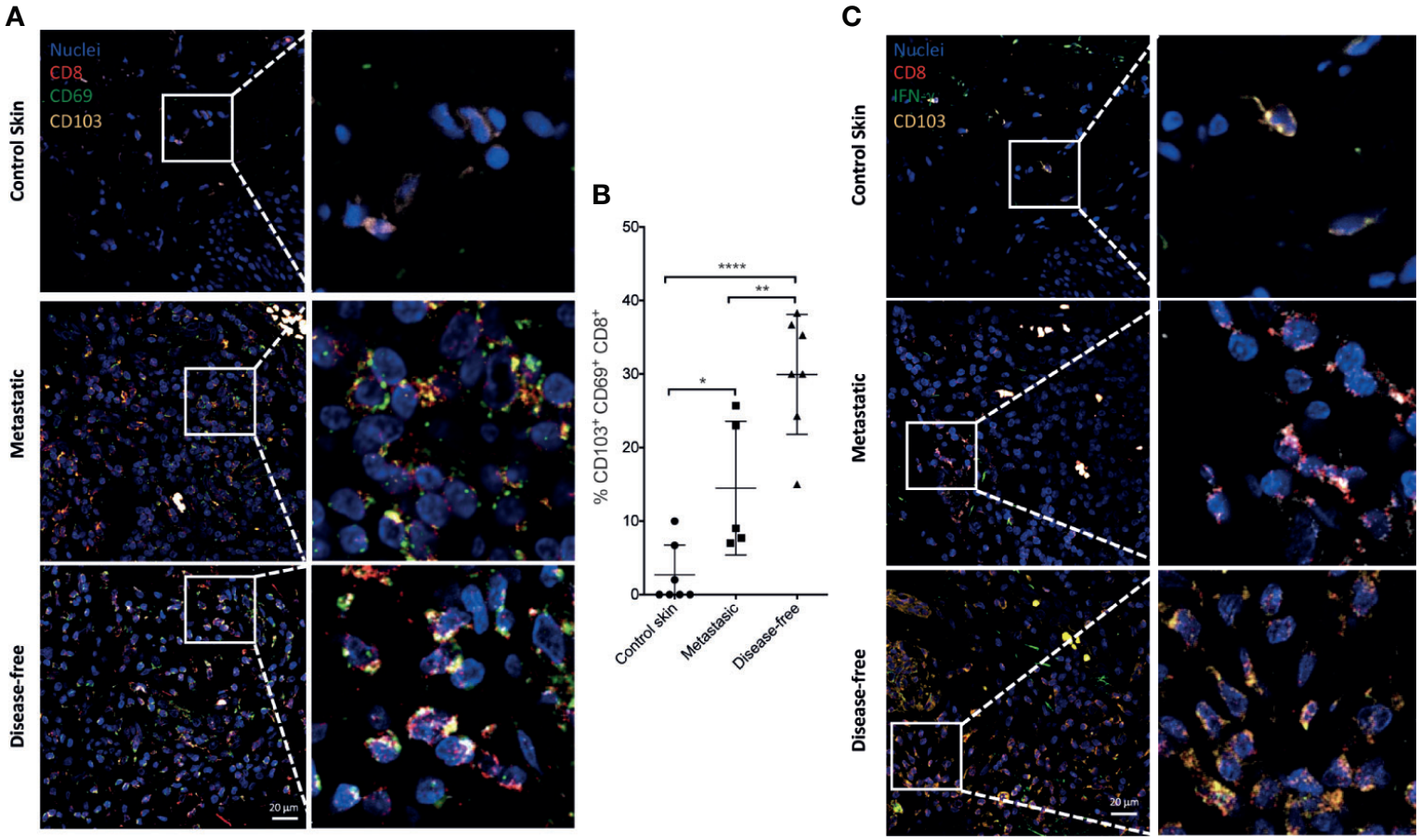


FIGURE 9 | IFN-γ-producing Trm $CD8^+$ TILs correlate with disease control in melanoma patients. Merged images of $CD103^+$ (yellow) $CD69^+$ (green) $CD8^+$ (red) **(A)** and $CD103^+$ (yellow) IFN-γ^+ (green) $CD8^+$ (red) **(C)** TILs from healthy control skin or from melanoma derived from metastatic or disease-free patients (representative immunofluorescence micrographs from a zoomed area) (Scale bar = 20 µm). **(B)** Percentages of $CD103^+$ $CD69^+$ $CD8^+$ T cells are shown. Statistical data were pooled from a comparison of healthy skin (*N* = 7), and metastatic (*N* = 5) and disease-free melanoma patients (N = 7). *p < 0.05, **p < 0.01, ****p < 0.0001.

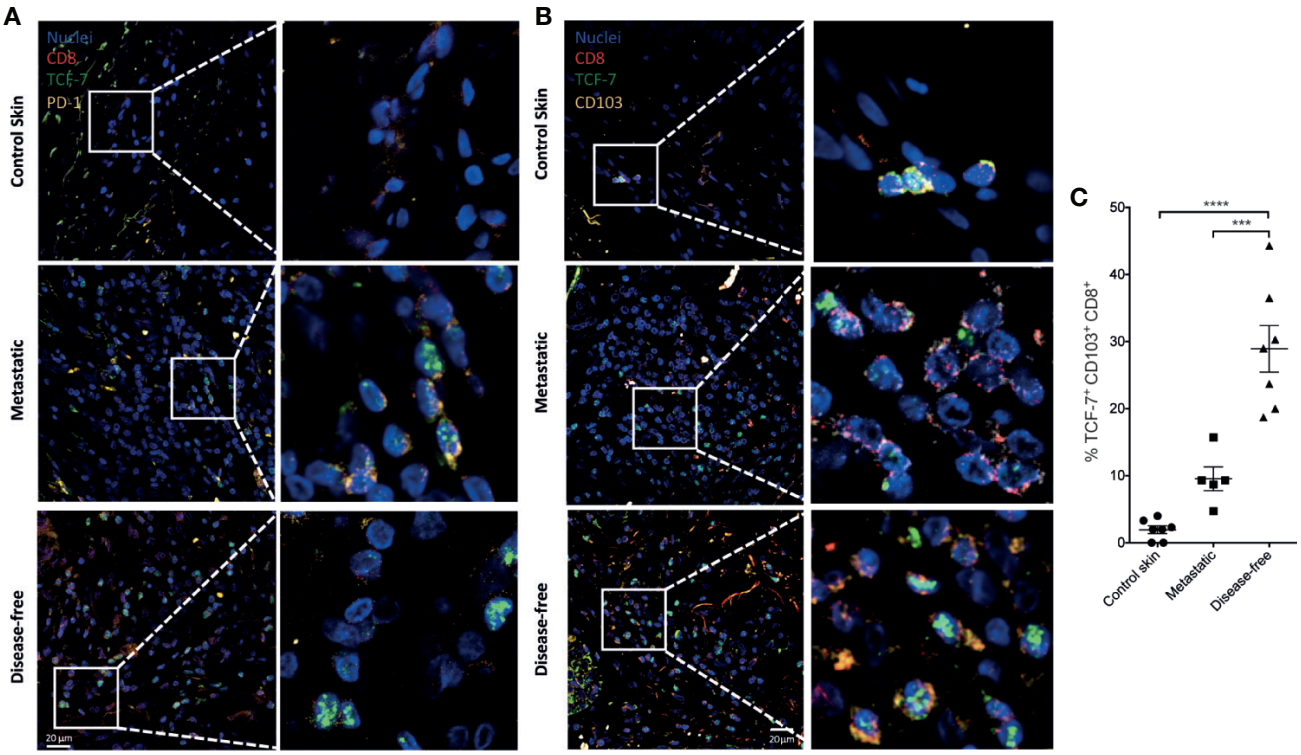


FIGURE 10 | TCF-7$^+$ progenitor exhausted Trm CD8$^+$ TILs correlates with disease control in melanoma patients. Merged images of TCF-7$^+$ (green) PD-1$^+$ (yellow) CD8$^+$ (red) **(A)** and TCF-1$^+$ (green) CD103$^+$ (yellow) CD8$^+$ (red) **(B)** TILs from healthy control skin or from tumor stroma derived from metastatic or disease-free melanoma patients (representative immunofluorescence micrographs from a zoomed area) (Scale bar = 20µm). **(C)** Percentages of TCF-7$^+$ CD103$^+$ CD8$^+$ T cells are shown. Statistical data were pooled from a comparison of healthy skin (N = 7), and metastatic (N = 5) and disease-free melanoma patients (N = 7). ***p < 0.001, ****p < 0.0001.

patients compared with CS (**Figure 10A**; **Supplementary Figure 11A**). Remarkably, there is also a significant increment of CD103$^+$ CD8$^+$ TILs that express TCF-7 in disease-free patients compared with CS and metastatic patients (**Figures 10B, C**; **Supplementary Figure 11B**). Altogether, these results indicate that the populations induced by Porins immunization are present in human melanoma, in which they also seem to correlate with disease control, supporting the findings observed in the B16-F10 melanoma model and indicating the relevance of the induction or expansion of this population by cancer vaccination strategies.

DISCUSSION

A CD8$^+$ T cell signature has traditionally marked good prognosis in many types of cancers (45), but it is only more recently that we are beginning to appreciate the great complexity of T cell subpopulations inhabiting the tumor stroma and the infiltrating lymph nodes. Successful immune-based therapies should expand and rescue effector functions of those populations with the most anti-tumor activity. We showed here that *S.* Typhi Porins are an effective adjuvant conferring prophylactic and therapeutic protection against melanoma bearing a model antigen (OVA) or native MAAs (TRP-2/gp100) indicating the large spectrum of protection and that includes endogenous antigens. In agreement, Porins were able to induce IFN-γ-producing T cells, Tcm and Tem cells in SDLN as well as the formation of Trm T cells in the skin and in the melanoma stroma.

We observed an early induction of Trm T cells that correlated with tumor protection (37, 38), contrary to studies in which Trm maturation took at least 4 weeks (46). Other authors support circulating CD4$^+$ and CD8$^+$ T cell memory formation as early as 3–5 days after antigen encounter (47–49). We were also able to induce a lasting Trm population, but to achieve an effective anti-tumoral response independently of circulating memory T cells (37, 38), it required a prime/boost scheme most likely to sustain the numbers of Trm cells required for protection (28, 43, 50, 51). Furthermore, we also observed a long-lasting protective memory when we re-challenged tumor free mice, which remained healthy for additional 70 days. Therefore, protection is most likely explained by the expansion of antigen-specific memory T cells in the lymph nodes, which develop into functional Trm T cells seeded in the tumor stroma. Although we did not formally prove that protection is dependent on CD4$^+$ and CD8$^+$ Trm, we have previously reported that protection using the B16-F10

melanoma model is highly dependent on $CD8^+$ T cells, and in a lesser extent also on $CD4^+$ T cells (52). Here, tumor protection was still observed after depletion of circulating T cells but in the presence of functional Trm T cells, suggesting that $CD4^+$ and $CD8^+$ Trm T cells were responsible for protection. Although Tem cells can be present in the tumor stroma, these cells still maintain the potential to recirculate (28, 37). Previous reports also support that Trm T cells are highly relevant for tumor control (4, 5, 37, 43). However it is possible that in the absence of sustain functional Trm, other memory T cell populations could be relevant in tumor protection (37, 38). Supporting the findings in the B16-F10 murine model, we present evidence of the presence of functional IFN-γ-producing Trm T cells in melanoma patients, which are also associated with disease control. This is consistent with previous work correlating infiltrating Trm T cells and survival in immunized melanoma patients (53).

The search for measures to foster cancer control, as with vaccination or immunotherapy, has propelled the hunt for biomolecules that condition T cell effector functions, the identity of the populations that express them, and for strategies to restore their positive responses. $CD8^+$ populations co-expressing markers of exhaustion, memory, effector functions and stemness have been often observed in tumor infiltrates, conceptually framing the idea of an ontogenic flow of exhausted memory cells sustained at the base by those with progenitor potential. Sade-Feldman M et al., defined at least six subpopulations after single cell RNA sequencing of tumor $CD8^+$ T cells from melanoma patients. T cell populations expressing TCF-7 were enriched in immunotherapy responding patients (17). TCF-7^+ progenitor exhausted T cells also seem to be the best marker of good prognosis, mainly documented for melanoma, but also for kidney and lung cancer patients (9, 15–17). In addition, the equivalent TCF-1^+ exhausted population in mice has the potential to generate a terminally exhausted TIM-3^+ population with functional effector function (9, 10). We document here that Porins induce IFN-γ- and GZMB-producing TIM-3^+ $CD8^+$ T cells in the tumor stroma; however, we were unable to correlate the density of TIM-3^+ cells with neither enhanced or reduced protection. In contrast, the importance of the TCF-1^+ Trm T cell populations was highlighted in the comparison between Porins and CTB. Although both Porins and CTB induced $CD8^+$ Trm T cells in the tumor stroma, Porins were highly efficient to form TCF-1^+ $CD8^+$ Trm, contrary to CTB. This difference may be at least in part explained by their mechanisms to activate DCs, since Porins induce a transient and CTB a sustained activation (28, 33).

Our findings are also supported by a previous study, in which tumor-infiltrating TCF-1^+ PD-1^+ $CD8^+$ T cells were capable to control the tumor in response to vaccination (54). Recently, it was determined in mice that one of the TCF-1^+ exhausted subsets also express CD69, a tissue-resident memory marker, which is in agreement with our data (14). We also identified a TCF-7^+ $CD103^+$ $CD8^+$ progenitor exhausted T cell population in the tumor stroma of human melanoma, which seems to be the equivalent to the progenitor exhausted Trm identified in mice. To the best of our knowledge, this is the first evidence of a $CD8^+$ Trm T cell with a progenitor exhausted phenotype. Furthermore, this human progenitor exhausted Trm T cell also correlated with disease control in melanoma patients. Also relevant is that this protective population can be induced or expanded by immunization strategies that result in better melanoma control, such as the one we tried here with Porins as a cancer vaccine adjuvant.

Although our data support the existence of $CD8^+$ Trm T cells that express the progenitor marker TCF-1, it has been previously reported that in virus and tumor models $CD8^+$ Trm T cells express Blimp-1 (54–56), a transcriptional repressor of the *Tcf7* gene that encodes TCF-1. The capacity of Blimp-1 to promote terminally exhausted T cells has been previously documented (16, 57). On the contrary, Blimp-1 has also been associated with stemness, pluripotency, efficient memory T cell response, and lineage decisions in hematopoietic stem cells and in more mature immune cells (55, 58, 59), supporting the co-existence of this transcription factor and TCF-1 in cells that maintain progenitor potential. In this scenario, the studies mentioned above did not evaluate TCF-1 protein expression, and perhaps Blimp-1 only modulates *Tcf7* expression to open the way to form downstream populations, which while maintaining progenitor competence also start turning on additional terminal effector functions (56). In future studies, it would be important to determine Blimp-1 expression in the progenitor exhausted Trm $CD8^+$ T cells induced by cancer vaccines.

There are several immunization strategies that induce an effective anti-tumoral response, but only few have been documented to cooperate with anti-PD-1 immunotherapy (21–24). Moreover, the strategies for recovery of TCF-1^+ exhausted T cell populations that explain the cooperative mechanisms with PD-1 blockade are only beginning to be elucidated (54). Porins promoted formation of TCF-1^+ PD-1^+ $CD8^+$ Trm T cells, leading us to assess whether they could also respond to anti-PD-1 immunotherapy. Indeed, we observed that Porins seem to sensitize mice for better control of melanoma growth upon immunotherapy. Worth mentioning, we observed a positive response even though we carried the anti-PD-1 immunotherapy at later times than in most melanoma murine models, when the tumor had already reached a considerable size. These data further highlight the efficacy of the early generation and expansion of progenitor exhausted Trm T cells in the tumor stroma as central for melanoma control independently of anti-PD-1 immunotherapy, but also priming it for additional strategies looking to reinforce anti-tumoral responses. It is interesting how these progenitor exhausted T cells converge as an important population for cancer control in both immunization and immunotherapy strategies. Understanding how these T cell populations are formed and modulated will be decisive for strategies of cooperative therapies, particularly because of the high number of patients with tumors refractory to immunotherapy or that relapse after an initial positive response (3, 60, 61).

In summary, our data highlight the importance of adjuvants in cancer vaccines to sculpt the tumor microenvironment with

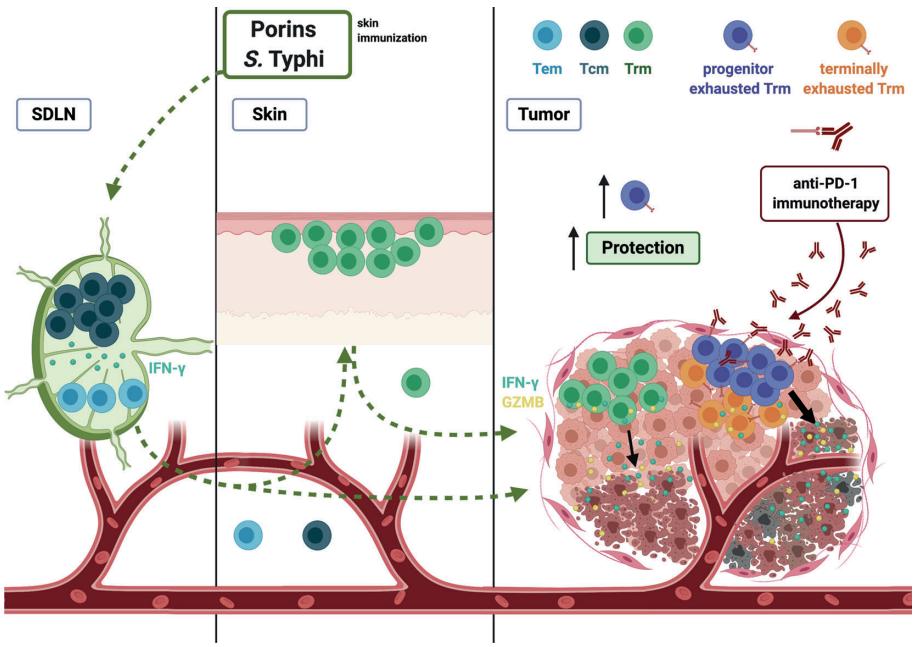


FIGURE 11 | Model of vaccination strategy protecting against melanoma using *Salmonella* Typhi Porins. Depicted are the circulating from skin-draining lymph nodes (SDLN), skin and tumor-infiltrating Trm T cell response induced by Porin immunization. Porins as an adjuvant induce a circulating memory T cell response. In addition, the immunization induces a Trm response in the skin and a formation of functional Trm T cells in the tumor. A Porins immunization is capable to induce tumor-infiltrating TIM-3$^+$ PD-1$^+$ CD8$^+$ Trm T cells (potential terminally exhausted Trm) and importantly TCF-1$^+$ PD-1$^+$ CD8$^+$ Trm T cells (progenitor exhausted Trm), being the latter associated with tumor growth control and anti-PD-1 immunotherapy cooperation. Created with BioRender.com.

the appropriate tumor-fighting populations, placing Porins as an adjuvant with the capacity to seed and expand CD8$^+$ Trm T cells with a progenitor exhausted phenotype, which are very proficient to control melanoma growth and display responsiveness to anti-PD-1 immunotherapy (**Figure 11**). A combination of vaccination and immunotherapy strategies would help patients with aggressive cancers that are not benefited by traditional treatment schemes.

DATA AVAILABILITY STATEMENT

The raw data supporting the conclusions of this article will be made available by the authors, without undue reservation.

ETHICS STATEMENT

The studies involving human participants were reviewed and approved by Institutional Scientific and Ethics Board of Reviews (protocol R-2019-785-051). Written informed consent for participation was not required for this study in accordance with the national legislation and the institutional requirements. The animal study was reviewed and approved by Institutional Ethics Committee and the Mexican national regulations on animal care and experimentation (R-2015-785-008).

AUTHOR CONTRIBUTIONS

RL-L performed the majority of the experiments, interpreted the data and drafted the manuscript. D-CM helped with the immunization experiments and tissue processing. O-BG helped with the tumor processing to obtain TILs. AT-S helped with the tissue processing and skin analysis. EH-M performed the IF of the mice tumors and CA-F and SD-R performed the IF of human melanoma tumors. AM selected the patients and performed the histological assays to identify the tumor infiltrating areas. E-FP discussed and revised the results and thoroughly revised the manuscript. CL-M produced Porins and conceived its use as adjuvants, helped with the design of the study and revised the manuscript. LB conceived, designed, directed the study and wrote the manuscript. All authors contributed to the article and approved the submitted version.

FUNDING

RL-L is a doctoral student from the Programa de Doctorado en Ciencias Biomédicas, Universidad Nacional Autónoma de México (UNAM) and has received Consejo Nacional de Ciencia y Tecnología (CONACyT) fellowship 631989. This study was funded by CONACyT, grant number: SRE-CONACYT 263683 and SEP-CONACYT CB-2015-256402 (to CL-M), and principally by the Instituto Mexicano del

Seguro Social (IMSS), R-2019-785-051 FIS/IMSS/PROT/PRIO/19/125 and R-2015-785-008 FIS/IMSS/PROT/G16/1606 (to LB).

ACKNOWLEDGMENTS

We thank the staff of the animal facility at the Experimental Medicine Unit, Faculty of Medicine, UNAM, and at the INSP, SS, for providing expert animal care, specially to MVZ MC Anayántzin Paulina Heredia Antúnez. We thank Dr. Jose Carlos Crispin from Instituto Nacional de Ciencias Médicas y Nutrición Salvador Zubirán (INCMNSZ) for providing OT-IxCD45.1$^+$ mice, and Dr. Gloria Soldevila from the Instituto de Investigaciones Biomédicas (IIB), UNAM, for providing OT-IIxCD45.1$^+$ mice. Finally, we extend our gratitude to the Flow Cytometry core facility, the Coordinación de Investigación en Salud, the CMN S XXI, and the IMSS, for their instrumental and technical support.

SUPPLEMENTARY MATERIAL

The Supplementary Material for this article can be found online at: https://www.frontiersin.org/articles/10.3389/fimmu.2020.583382/full#supplementary-material

REFERENCES

1. American Cancer Society. Cancer Facts & Figures. *Atlanta American Cancer Society* (2020) 1–76.
2. Spranger S, Luke JJ, Bao R, Zha Y, Hernandez KM, Li Y, et al. Density of immunogenic antigens does not explain the presence or absence of the T-cell–inflamed tumor microenvironment in melanoma. *Proc Natl Acad Sci* (2016) 113:E7759–68. doi: 10.1073/pnas.1609376113
3. León-Letelier RA, Bonifaz LC, Fuentes-Pananá EM. OMIC signatures to understand cancer immunosurveillance and immunoediting: Melanoma and immune cells interplay in immunotherapy. *J Leukocyte Biol* (2019) 161:1. doi: 10.1002/JLB.MR0618-241RR
4. Amsen D, Gisbergen KPJM, Hombrink P, Lier RAW. Tissue-resident memory T cells at the center of immunity to solid tumors. *Nat Immunol* (2018) 19:1–9. doi: 10.1038/s41590-018-0114-2
5. Molodtsov A, Turk MJ. Tissue Resident CD8$^+$ Memory T Cell Responses in Cancer and Autoimmunity. *Front Immunol* (2018) 9:2810. doi: 10.3389/fimmu.2018.02810
6. Schenkel JM, Fraser KA, Beura LK, Pauken KE, Vezys V, Masopust D. Resident memory CD8$^+$ T cells trigger protective innate and adaptive immune responses. *Science* (2014) 346:98–101. doi: 10.1126/science.1254536
7. Hartana CA, Ahlén Bergman E, Broomé A, Berglund S, Johansson M, Alamdari F, et al. Tissue-resident memory T cells are epigenetically cytotoxic with signs of exhaustion in human urinary bladder cancer. *Clin Exp Immunol* (2018) 194:39–53. doi: 10.1111/cei.13183
8. Wherry EJ, Kurachi M. Molecular and cellular insights into T cell exhaustion. *Nat Publishing Group* (2015) 15:486–99. doi: 10.1038/nri3862
9. Miller BC, Sen DR, Abosy Al R, Bi K, Virkud YV, LaFleur MW, et al. Subsets of exhausted CD8$^+$ T cells differentially mediate tumor control and respond to checkpoint blockade. *Nat Immunol* (2019) 20:1–18. doi: 10.1038/s41590-019-0312-6
10. Shan Q, Hu S, Chen X, Danahy DB, Badovinac VP, Zang C, et al. Ectopic Tcf1 expression instills a stem-like program in exhausted CD8$^+$ T cells to enhance viral and tumor immunity. *Cell Mol Immunol* (2020). doi: 10.1038/s41423-020-0436-5
11. Utzschneider DT, Charmoy M, Chennupati V, Pousse L, Ferreira DP, Calderon-Copete S, et al. T Cell Factor 1-Expressing Memory-like CD8$^+$ T Cells Sustain the Immune Response to Chronic Viral Infections. *Immunity* (2016) 45:415–27. doi: 10.1016/j.immuni.2016.07.021
12. Im SJ, Hashimoto M, Gerner MY, Lee J, Kissick HT, Burger MC, et al. Defining CD8$^+$ T cells that provide the proliferative burst after PD-1 therapy. *Nature* (2016) 537:417–21. doi: 10.1038/nature19330
13. Blackburn SD, Shin H, Freeman GJ, Wherry EJ. Selective expansion of a subset of exhausted CD8$^+$ T cells by αPD-L1 blockade. *Proc Natl Acad Sci* (2008) 105:15016–21. doi: 10.1073/pnas.0801497105
14. Beltra JC, Manne S, Abdel Hakeem MS, Kurachi M, Giles JR, Chen Z, et al. Developmental Relationships of Four Exhausted CD8$^+$ T Cell Subsets Reveals Underlying Transcriptional and Epigenetic Landscape Control Mechanisms. *Immunity* (2020) 52:825–41.e8. doi: 10.1016/j.immuni.2020.04.014
15. Jansen CS, Prokhnevska N, Master VA, Sanda MG, Carlisle JW, Bilen MA, et al. An intra-tumoral niche maintains and differentiates stem-like CD8$^+$ T cells. *Nature* (2019) 576:465–70. doi: 10.1038/s41586-019-1836-5
16. Brummelman J, Mazza EMC, Alvisi G, Colombo FS, Grilli A, Mikulak J, et al. High-dimensional single cell analysis identifies stem-like cytotoxic CD8$^+$ T cells infiltrating human tumors. *J Exp Med* (2018) 215:2520–35. doi: 10.1084/jem.20180684
17. Sade-Feldman M, Yizhak K, Bjorgaard SL, Ray JP, de Boer CG, Jenkins RW, et al. Defining T Cell States Associated with Response to Checkpoint Immunotherapy in Melanoma. *Cell* (2018) 175:998–1013.e20. doi: 10.1016/j.cell.2018.10.038
18. Shahbaz S, Dunsmore G, Koleva P, Xu L, Houston S, Elahi S. Galectin-9 and VISTA Expression Define Terminally Exhausted T Cells in HIV-1 Infection. *J Immunol* (2020) 204:2474–91. doi: 10.4049/jimmunol.1901481
19. LaFleur MW, Nguyen TH, Coxe MA, Miller BC, Yates KB, Gillis JE, et al. PTPN2 regulates the generation of exhausted CD8$^+$ T cell subpopulations and restrains tumor immunity. *Nat Immunol* (2019) 20:1–20. doi: 10.1038/s41590-019-0480-4
20. Lizee G, Overwijk WW, Radvanyi L, Gao J, Sharma P, Hwu P. Harnessing the Power of the Immune System to Target Cancer. *Annu Rev Med* (2013) 64:71–90. doi: 10.1146/annurev-med-112311-083918
21. Salmon H, Idoyaga J, Rahman A, Leboeuf M, Remark R, Jordan S, et al. Expansion and Activation of CD103$^+$ Dendritic Cell Progenitors at the Tumor Site Enhances Tumor Responses to Therapeutic PD-L1 and BRAF Inhibition. *Immunity* (2016) 44:924–38. doi: 10.1016/j.immuni.2016.03.012
22. Takeda Y, Kataoka K, Yamagishi J, Ogawa S, Seya T. Matsumoto M. A TLR3-Specific Adjuvant Relieves Innate Resistance to PD-L1 Blockade without Cytokine Toxicity in Tumor Vaccine Immunotherapy. *Cell Rep* (2017) 19:1874–87. doi: 10.1016/j.celrep.2017.05.015
23. Wang S, Campos J, Gallotta M, Gong M, Crain C, Naik E, et al. Intratumoral injection of a CpG oligonucleotide reverts resistance to PD-1 blockade by expanding multifunctional CD8$^+$ T cells. *Proc Natl Acad Sci* (2016) 113:E7240–9. doi: 10.1073/pnas.1608555113
24. Wang H, Hu S, Chen X, Shi H, Chen C, Sun L, et al. cGAS is essential for the antitumor effect of immune checkpoint blockade. *Proc Natl Acad Sci* (2017) 114:1637–42. doi: 10.1073/pnas.1621363114
25. Orimo T, Sasaki I, Hemmi H, Ozasa T, Fukuda-Ohta Y, Ohta T, et al. Cholera toxin B induces interleukin-1β production from resident peritoneal macrophages through the pyrin inflammasome as well as the NLRP3 inflammasome. *Int Immunol* (2019) 31:657–68. doi: 10.1093/intimm/dxz004
26. Phongsisay V, Iizasa E, Hara H, Yoshida H. Evidence for TLR4 and FcRγ–CARD9 activation by cholera toxin B subunit and its direct bindings to TREM2 and LMIR5 receptors. *Mol Immunol* (2015) 66:463–71. doi: 10.1016/j.molimm.2015.05.008
27. Meza Sánchez D, Pérez Montesinos G, Sánchez García J, Moreno J, Bonifaz LC. Intradermal immunization in the ear with cholera toxin and its non-toxic β subunit promotes efficient Th1 and Th17 differentiation dependent on migrating DCs. *Eur J Immunol* (2011) 41:2894–904. doi: 10.1002/eji.201040997

28. Antonio-Herrera L, Badillo-Godinez O, Medina-Contreras O, Tepale-Segura A, García-Lozano A, Gutierrez-Xicotencatl L, et al. The Nontoxic Cholera B Subunit Is a Potent Adjuvant for Intradermal DC-Targeted Vaccination. *Front Immunol* (2018) 9:2212. doi: 10.3389/fimmu.2018.02212
29. Shankaran V, Ikeda H, Bruce AT, White JM, Swanson PE, Old LJ, et al. IFNγ and lymphocytes prevent primary tumour development and shape tumour immunogenicity. *Nature* (2001) 410(6832):1107–11. doi: 10.1038/35074122
30. Muranski P, Restifo NP. Does IL-17 promote tumor growth? *Blood* (2009) 114:231–2. doi: 10.1182/blood-2009-04-215541
31. Moreno-Eutimio MA, Tenorio-Calvo A, Pastelin-Palacios R, Perez-Shibayama C, Gil-Cruz C, López-Santiago R, et al. Salmonella Typhi OmpS1 and OmpS2 porins are potent protective immunogens with adjuvant properties. *Immunology* (2013) 139:459–71. doi: 10.1111/imm.12093
32. Salazar-González RM, Maldonado-Bernal C, Ramírez-Cruz NE, Rios-Sarabia N, Beltrán-Nava J, Castañón-González J, et al. Induction of cellular immune response and anti-Salmonella enterica serovar typhi bactericidal antibodies in healthy volunteers by immunization with a vaccine candidate against typhoid fever. *Immunol Lett* (2004) 93:115–22. doi: 10.1016/j.imlet.2004.01.010
33. Cervantes-Barragán L, Gil-Cruz C, Pastelin-Palacios R, Lang KS, Isibasi A, Ludewig B, et al. TLR2 and TLR4 signaling shapes specific antibody responses to Salmonella typhi antigens. *Eur J Immunol* (2009) 39:126–35. doi: 10.1002/eji.200838185
34. Diaz-Quinonez A, Martin-Orozco N, Isibasi A, Ortiz-Navarrete V. Two Salmonella OmpC Kb-Restricted Epitopes for $CD8^+$-T-Cell Recognition. *Infect Immun* (2004) 72:3059–62. doi: 10.1128/IAI.72.5.3059-3062.2004
35. Perez-Shibayama C, Gil-Cruz C, Pastelin-Palacios R, Cervantes-Barragán L, Hisaki E, Chai Q, et al. IFN-γ-producing $CD4^+$ T cells promote generation of protective germinal center-derived IgM+ B cell memory against Salmonella Typhi. *J Immunol* (2014) 192:5192–200. doi: 10.4049/jimmunol.1302526
36. Pérez-Toledo M, Valero-Pacheco N, Pastelin-Palacios R, Gil-Cruz C, Perez-Shibayama C, Moreno-Eutimio MA, et al. Salmonella Typhi Porins OmpC and OmpF Are Potent Adjuvants for T-Dependent and T-Independent Antigens. *Front Immunol* (2017) 8:230. doi: 10.3389/fimmu.2017.00230
37. Enamorado M, Iborra S, Priego E, Cueto FJ, Quintana JA, Martinez-Cano S, et al. Enhanced anti-tumour immunity requires the interplay between resident and circulating memory $CD8^+$ T cells. *Nat Commun* (2017) 8:1–11. doi: 10.1038/ncomms16073
38. Gálvez-Cancino F, López E, Menares E, Díaz X, Flores C, Cáceres P, et al. Vaccination-induced skin-resident memory $CD8^+$ T cells mediate strong protection against cutaneous melanoma. *OncoImmunology* (2018) 7:1–12. doi: 10.1080/2162402X.2018.1442163
39. Ly LV, Sluijter M, Versluis M, Luyten GPM, van der Burg SH, Melief CJM, et al. Peptide Vaccination after T-Cell Transfer Causes Massive Clonal Expansion, Tumor Eradication and Manageable Cytokine Storm. *Cancer Res* (2010) 70:8339–46. doi: 10.1158/0008-5472.CAN-10-2288
40. Ly LV, Sluijter M, van der Burg SH, Jager MJ, van Hall T. Effective cooperation of monoclonal antibody and peptide vaccine for the treatment of mouse melanoma. *J Immunol* (2013) 190:489–96. doi: 10.4049/jimmunol.1200135
41. Gebhardt T, Whitney PG, Zaid A, Mackay LK, Brooks AG, Heath WR, et al. Different patterns of peripheral migration by memory $CD4^+$ and $CD8^+$ T cells. *Nature* (2011) 477:1–6. doi: 10.1038/nature10339
42. Tagliamonte M, Petrizzo A, Tornesello ML, Buonaguro FM, Buonaguro L. Antigen-specific vaccines for cancer treatment. *Hum Vaccines Immunother* (2014) 10:3332–46. doi: 10.4161/21645515.2014.973317
43. Nizard M, Karaki S, Tran T, Voron T, Dransart E, Sandoval F, et al. Induction of resident memory T cells enhances the efficacy of cancer vaccine. *Nat Commun* (2017) 8:1–11. doi: 10.1038/ncomms15221
44. Djenidi F, Adam J, Goubar A, Durgeau A, Meurice G, de Montpréville V, et al. $CD8^+$ $CD103^+$ Tumor–Infiltrating Lymphocytes Are Tumor-Specific Tissue-Resident Memory T Cells and a Prognostic Factor for Survival in Lung Cancer Patients. *J Immunol* (2015) 194:3475–86. doi: 10.4049/jimmunol.1402711
45. Durgeau A, Virk Y, Corgnac S, Mami-Chouaib F. Recent Advances in Targeting $CD8^+$ T-Cell Immunity for More Effective Cancer Immunotherapy. *Front Immunol* (2018) 9:14. doi: 10.3389/fimmu.2018.00014
46. Harrington LE, Janowski KM, Oliver JR, Zajac AJ, Weaver CT. Memory $CD4^+$ T cells emerge from effector T-cell progenitors. *Nature* (2008) 452:356–60. doi: 10.1038/nature06672
47. Obar JJ, Lefrançois L. Early Signals during $CD8^+$ T Cell Priming Regulate the Generation of Central Memory Cells. *J Immunol* (2010) 185:263–72. doi: 10.4049/jimmunol.1000492
48. Knudsen ML, Ljungberg K, Kakoulidou M, Kostic L, Hallengärd D, García-Arriaza J, et al. Kinetic and phenotypic analysis of CD8+ T cell responses after priming with alphavirus replicons and homologous or heterologous booster immunizations. *J Virol* (2014) 88:12438–51. doi: 10.1128/JVI.02223-14
49. Mackay LK, Rahimpour A, Ma JZ, Collins N, Stock AT, Hafon ML, et al. The developmental pathway for $CD103^+$ $CD8^+$ tissue-resident memory T cells of skin. *Nat Immunol* (2013) 14:1–10. doi: 10.1038/ni.2744
50. Zhou AC, Wagar LE, Wortzman ME, Watts TH. Intrinsic 4-1BB signals are indispensable for the establishment of an influenza-specific tissue-resident memory $CD8^+$ T-cell population in the lung. *Nat Mucosal Immun* (2017) 10:1294–309. doi: 10.1038/mi.2016.124
51. Behr FM, Parga-Vidal L, Kragten NAM, Dam TJP, Wesselink TH, Sheridan BS, et al. Tissue-resident memory $CD8^+$ T cells shape local and systemic secondary T cell responses. *Nat Immunol* (2020) 21(9):1070–81. doi: 10.1038/s41590-020-0723-4
52. Bonifaz LC, Bonnyay DP, Charalambous A, Darguste DI, Fujii SI, Soares H, et al. In Vivo Targeting of Antigens to Maturing Dendritic Cells via the DEC-205 Receptor Improves T Cell Vaccination. *J Exp Med* (2004) 199:815–24. doi: 10.1084/jem.20032220
53. Murray T, Fuertes Marraco SA, Baumgaertner P, Bordry N, Cagnon L, Donda A, et al. Very Late Antigen-1 Marks Functional Tumor-Resident $CD8^+$ T Cells and Correlates with Survival of Melanoma Patients. *Front Immunol* (2016) 7:573. doi: 10.3389/fimmu.2016.00573
54. Siddiqui I, Schaeuble K, Chennupati V, Marraco SAF, Calderon-Copete S, Ferreira DP, et al. Intratumoral $Tcf1^+$ $PD\text{-}1^+$ $CD8^+$ T Cells with Stem-like Properties Promote Tumor Control in Response to Vaccination and Checkpoint Blockade Immunotherapy. *Immunity* (2019) 50:195–211.e10. doi: 10.1016/j.immuni.2018.12.021
55. Rutishauser RL, Martins GA, Kalachikov S, Chandele A, Parish IA, Meffre E, et al. Transcriptional Repressor Blimp-1 Promotes $CD8^+$ T Cell Terminal Differentiation and Represses the Acquisition of Central Memory T Cell Properties. *Immunity* (2009) 31:296–308. doi: 10.1016/j.immuni.2009.05.014
56. Mackay LK, Minnich M, Kragten NAM, Liao Y, Nota B, Seillet C, et al. Hobit and Blimp1 instruct a universal transcriptional program of tissue residency in lymphocytes. *Science* (2016) 352:459–63. doi: 10.1126/science.aad2035
57. Wu T, Ji Y, Moseman EA, Xu HC, Manglani M, Kirby M, et al. The TCF1-Bcl6 axis counteracts type I interferon to repress exhaustion and maintain T cell stemness. *Sci Immunol* (2016) 1:eaai8593–eaai8593. doi: 10.1126/sciimmunol.aai8593
58. Wang D, Zhuang L, Gao B, Shi C-X, Cheung J, Liu M, et al. The Blimp-1 gene regulatory region directs EGFP expression in multiple hematopoietic lineages and testis in mice. *Transgenic Res* (2007) 17:193–203. doi: 10.1007/s11248-007-9140-9
59. Kallies A, Xin A, Belz GT, Nutt SL. Blimp-1 Transcription Factor Is Required for the Differentiation of Effector $CD8^+$ T Cells and Memory Responses. *Immunity* (2009) 31:283–95. doi: 10.1016/j.immuni.2009.06.021
60. Pawelec G. Immune correlates of clinical outcome in melanoma. *Immunology* (2017) 153:415–22. doi: 10.1111/imm.12870
61. Pawelec G. Immune signatures predicting responses to immunomodulatory antibody therapy. *Curr Opin Immunol* (2018) 51:91–6. doi: 10.1016/j.coi.2018.03.003

Conflict of Interest: CL-M is listed as inventor on a patent related to the use of Salmonella Porins as adjuvants and vaccines.

The remaining authors declare that the research was conducted in the absence of any commercial or financial relationships that could be construed as a potential conflict of interest.

Copyright © 2020 León-Letelier, Castro-Medina, Badillo-Godinez, Tepale-Segura, Huanosta-Murillo, Aguilar-Flores, De León-Rodríguez, Mantilla, Fuentes-Pananá, López-Macías and Bonifaz. This is an open-access article distributed under the terms of the Creative Commons Attribution License (CC BY). The use, distribution or reproduction in other forums is permitted, provided the original author(s) and the copyright owner(s) are credited and that the original publication in this journal is cited, in accordance with accepted academic practice. No use, distribution or reproduction is permitted which does not comply with these terms.

frontiers in Immunology

ORIGINAL RESEARCH
published: 12 November 2020
doi: 10.3389/fimmu.2020.591139

Tumor-Specific Antibody, Cetuximab, Enhances the *In Situ* Vaccine Effect of Radiation in Immunologically Cold Head and Neck Squamous Cell Carcinoma

*Won Jong Jin[1], Amy K. Erbe[1], Ciara N. Schwarz[1], Abigail A. Jaquish[1], Bryce R. Anderson[1], Raghava N. Sriramaneni[1], Justin C. Jagodinsky[1], Amber M. Bates[1], Paul A. Clark[1], Trang Le[2], Keng-Hsueh Lan[1], Yi Chen[2], KyungMann Kim[2] and Zachary S. Morris[1]**

[1] Department of Human Oncology, University of Wisconsin, Madison, WI, United States, [2] Department of Biostatistics and Medical Informatics, University of Wisconsin, Madison, WI, United States

OPEN ACCESS

Edited by:
Alan Graham Pockley,
Nottingham Trent University,
United Kingdom

Reviewed by:
Franz Rödel,
University Hospital Frankfurt, Germany
Udo S. Gaipl,
University Hospital Erlangen, Germany

***Correspondence:**
Zachary S. Morris
zmorris@humonc.wisc.edu

Specialty section:
This article was submitted to Cancer Immunity and Immunotherapy, a section of the journal Frontiers in Immunology

Received: 03 August 2020
Accepted: 19 October 2020
Published: 12 November 2020

Citation:
Jin WJ, Erbe AK, Schwarz CN, Jaquish AA, Anderson BR, Sriramaneni RN, Jagodinsky JC, Bates AM, Clark PA, Le T, Lan K-H, Chen Y, Kim K and Morris ZS (2020) Tumor-Specific Antibody, Cetuximab, Enhances the In Situ Vaccine Effect of Radiation in Immunologically Cold Head and Neck Squamous Cell Carcinoma. Front. Immunol. 11:591139. doi: 10.3389/fimmu.2020.591139

In head and neck squamous cell carcinoma (HNSCC) tumors that over-expresses huEGFR, the anti-EGFR antibody, cetuximab, antagonizes tumor cell viability and sensitizes to radiation therapy. However, the immunologic interactions between cetuximab and radiation therapy are not well understood. We transduced two syngeneic murine HNSCC tumor cell lines to express human EGFR (MOC1- and MOC2-huEGFR) in order to facilitate evaluation of the immunologic interactions between radiation and cetuximab. Cetuximab was capable of inducing antibody-dependent cellular cytotoxicity (ADCC) in MOC1- and MOC2-huEGFR cells but showed no effect on the viability or radiosensitivity of these tumor cells, which also express muEGFR that is not targeted by cetuximab. Radiation enhanced the susceptibility of MOC1- and MOC2-huEGFR to ADCC, eliciting a type I interferon response and increasing expression of NKG2D ligands on these tumor cells. Co-culture of splenocytes with cetuximab and MOC2-huEGFR cells resulted in increased expression of IFNγ in not only NK cells but also in CD8+ T cells, and this was dependent upon splenocyte expression of FcγR. In MOC2-huEGFR tumors, combining radiation and cetuximab induced tumor growth delay that required NK cells, EGFR expression, and FcγR on host immune cells. Combination of radiation and cetuximab increased tumor infiltration with NK and CD8+ T cells but not regulatory T cells. Expression of PD-L1 was increased in MOC2-huEGFR tumors following treatment with radiation and cetuximab. Delivering anti–PD-L1 antibody with radiation and cetuximab improved survival and resulted in durable tumor regression in some mice. Notably, these cured mice showed evidence of an adaptive memory response that was not specifically directed against huEGFR. These findings suggest an opportunity to improve the treatment of HNSCC by combining radiation and cetuximab to engage an innate anti-tumor immune response that may prime an effective adaptive immune response when combined with immune checkpoint

blockade. It is possible that this approach could be extended to any immunologically cold tumor that does not respond to immune checkpoint blockade alone and for which a tumor-specific antibody exists or could be developed.

Keywords: head and neck squamous cell carcinoma, EGFR, resistance, *in situ* vaccination, immunotherapy, immune checkpoint, cetuximab, radiation

INTRODUCTION

Head and neck squamous cell carcinoma (HNSCC) carries a poor prognosis in patients with metastatic or recurrent disease (1, 2). Up to 90% of HNSCC tumors express the epidermal growth factor receptor (EGFR) (3, 4) and EGFR signaling plays a pivotal role in HNSCC cell proliferation (5, 6). Cetuximab is an antibody that binds to the extracellular domain of EGFR where it inhibits EGFR signaling and cell cycle progression and promotes apoptosis in HNSCC tumor cells (7, 8). Clinical studies demonstrate that cetuximab improves survival in patients with metastatic or recurrent HNSCC when combined with chemotherapeutics (9). Cetuximab also intrinsically sensitizes HNSCC cells to radiation therapy (10), and improves survival in patients with locally advanced HNSCC when used in combination with radiation (11, 12). Yet, most HNSCC patients respond only temporarily to cetuximab (9, 13, 14). This results from acquired resistance, despite persistent cetuximab binding to EGFR that is expressed on the tumor cell surface (15, 16). While acquired resistance limits the clinical benefit of cetuximab currently, an improved understanding of the impact of cetuximab on immune recognition of EGFR-expressing tumor cells may lead to development of novel therapeutic combinations for treating HNSCC patients.

Recent clinical data demonstrate that immune checkpoint inhibition with anti–PD-1 improves survival among patients with recurrent or metastatic HNSCC (17). With this treatment, a small percentage of patients with metastatic HNSCC may experience complete and durable tumor response. These results raise the possibility of dramatically improving survival and more consistently achieving curative outcomes for HNSCC patients by developing approaches to increase the rate and depth of response to anti–PD-1 immunotherapy. Immune checkpoint inhibitors are not typically effective in patients with immunologically "cold" tumors, characterized by low levels of T cell infiltrate and/or few mutation-created neo-antigens (18). In order to improve the response to immune checkpoint blockade in such cold tumors, others and we have been developing *in situ* cancer vaccine approaches (19). *In situ* vaccination is a therapeutic strategy that seeks to convert a patient's own tumor into a nidus for enhanced presentation of tumor-specific antigens in a way that will stimulate and diversify an anti-tumor T cell response. The goal is localized destruction of a tumor to enable the destroyed cancer cells to function as a potent immune stimulus and personalized source of antigenicity for tumor-specific adaptive T cell immunity that is able to eradicate metastatic tumors.

Local radiation therapy can serve as a method of *in situ* vaccination. Recently, numerous case reports and retrospective studies have suggested safety and the potential for enhanced systemic anti-tumor response with combinations of radiation therapy and immune checkpoint blockade (20–27). Several prospective trials have also investigated the combination of radiation therapy and immune checkpoint blockade (28–32). These studies have further supported the safety of combining radiation and immune checkpoint inhibition and have demonstrated that radiation therapy can elicit an *in situ* vaccine effect when combined with immune checkpoint blockade clinically. For most tumor types, however, it remains to be determined whether and how radiation therapy can be used to elicit a clinically meaningful improvement in the duration, depth, or rate of response to immune checkpoint blockade. In the setting of head and neck cancer, a recently reported study randomized patients with metastatic HNSCC to receive either anti–PD-1 checkpoint blockade alone or in combination with radiation therapy to a single lesion (9 Gy × 3 fractions). The primary endpoint of objective response rate in non-irradiated lesions was not improved with combination therapy in that study (32).

Here, we evaluate a combined modality treatment approach to improve the *in situ* vaccine effect of radiation in HNSCC. To achieve this we combine: 1) radiation to enhance tumor cell immunogenicity, 2) the tumor-specific mAb, cetuximab, to enhance tumor destruction and antigen presentation by immune cells that express Fc-γ receptor (FcγR) including NK cells and macrophages, and 3) anti–PD-L1 immune checkpoint inhibition to augment and propagate an adaptive anti-tumor immune response.

MATERIAL AND METHODS

Cell Lines and Preparation

Wild-type (WT) MOC1 and MOC2 cells were a kind gift from Dr. Ravindra Uppaluri. huEGFR-expressing cells were generated by transduction of human EGFR (NM_005228.3) along with the puromycin resistance gene *via* lentivirus using pLV vectors designed in VectorBuilder. Stably transduced MOC1/2-huEGFR cells were selected with puromycin (4 μg/ml, Sigma-Aldrich) and single-cell cloned. MOC1/2-huEGFR cells were cultured in Dulbecco's Modified Eagle Medium (DMEM; Corning)/Ham's F12 (Corning) at a 2:1 mixture with 5% fetal bovine serum (Life Technologies), 1% penicillin/streptomycin (Life Technologies), 5 ng/ml epidermal growth factor (EGF; Gibco), 400 ng/ml hydrocortisone (Sigma-Aldrich), and 5 μg/ml insulin (Sigma-Aldrich). The human HNSCC cell line, SCC6, was cultured in DMEM containing 10% fetal bovine serum, 1 μg/

ml hydrocortisone, and 1% penicillin/streptomycin. All cells were cultured in a humidified incubator at 37°C in an atmosphere of 5% carbon dioxide. ATCC guidelines were followed for authentication of all cell lines by monitoring morphology, growth curve analysis, and testing for mycoplasma (33).

Cytotoxicity Assay

In vitro ^{51}chromium (^{51}Cr)-release cytotoxicity assay was performed as previously described (34). Briefly, "target" MOC1/2 and MOC1/2-huEGFR cells were labeled with ^{51}Cr for 2 h and then washed and cultured with or without peripheral blood mononuclear cell (PBMC) "effectors" at indicated ratios (50:1, 40:1, 12.5:1, 10:1) in the presence or absence of cetuximab (0.5 μg/ml). After a 4 h incubation, the media was collected and the presence of ^{51}Cr from lysed target cells was quantified using a beta counter (Packard Matrix 9600). The percent of lysis among target cells was calculated as 100 × (cetuximab treated − spontaneous)/(detergent lysed maximum − spontaneous).

Clonogenic Assay of Radiation Sensitivity

We used a standard clonogenic assay to evaluate for effects of cetuximab on the radiosensitivity of MOC2-huEGFR cells. For this, we followed techniques that others have used to demonstrate the effect of cetuximab in sensitizing in HNSCC cells to radiation (10). Briefly, tumor cells were cultured for 24 h to allow the cells to adhere and then irradiated with indicated doses (0, 2, 4, and 8 Gy). The cells were then replated in the presence of non-specific human IgG or cetuximab (0.5 μg/ml) and allowed to grow for 5-7 days until the 0 Gy control group began forming colonies. The cells were then washed with PBS and stained using 0.5% crystal violet in methanol. Colonies consisting of 50 or more cells were counted, and the surviving fraction was determined as the (number of colonies)/(number of plated cells × plating efficiency).

Murine Tumor Models

Mice were housed in accordance with the Guide for Care and Use of Laboratory Mice and treatments were performed under a protocol approved by the University of Wisconsin Institutional Animal Care and Use Committee. Mice aged 6–8 weeks were purchased from Taconic (C57BL/6, FcγR deficient C57BL/6.129P2-Fcer1g^{tm1Rav} N12).

MOC2 or MOC2-huEGFR tumor cells were engrafted by subcutaneous flank injection of $2x10^6$ tumor cells in 100 μl of PBS. Tumor sizes were measured using digital calipers and tumor volume was calculated as (width^2 × length)/2. Treatment began when group tumor size reached 150 to 200 mm^3, about 8 to 10 days after tumor cell implantation. The initial day of radiation treatment was defined as "day 1" for all experiments and for tumor response and survival curves. Intratumoral (IT) injections of non-specific human IgG (Sigma-Aldrich) or cetuximab (Eli Lilly) were administrated (50 μg/mouse) in 100 μl of PBS daily from day 6 to 10. Anti–PD-L1 antibody (B7-H1, BioXcell, 200 μg/mouse) was given *via* intraperitoneal (35) injection at days 0, 4, and 7. Animals were sacrificed when tumor volume exceeded a pre-determined maximum diameter (20 mm). To deplete NK cells, IP injections of 50 μg NK1.1 mAb (PK136, BioXcell) were given at days 0, 5, and 10.

Radiotherapy

Radiation was delivered to tumor-bearing mice using a cabinet orthovoltage X-ray biological irradiator, X-RAD 320 (Precision X-Ray, Inc.). Local radiation to the tumor site was delivered after immobilization and shielding of mice using custom lead jigs that exposed only the tumor + ~5 mm margin. Radiation for *in vitro* experiments was delivered using an RS225 (Xstrahl) cabinet orthovoltage irradiator and was performed at least 24 h after plating the cells. Media was replaced immediately after radiation delivery.

Immunohistochemistry and Cytokine Analysis

Mice engrafted and treated as above were sacrificed 48 h after treatment completion, and tumor specimens were collected. The tumors were embedded in OCT, flash frozen in liquid nitrogen, cryosectioned and placed on microscope slides. Tumor sections were fixed in cold acetone, rehydrated and blocked using 10% goat serum (Sigma-Aldrich) for 45 min. After washing, sections were incubated with mAb [CD8 (clone 53-6.7), NKG2A/C/E (clone 20d5), and FOXP3 (clone FJK-15s; all from eBioscience)] overnight in 1% goat serum. Following a wash, antigen-antibody complexes were labeled using an anti-rat IgG ImmPRESS kit (Vector Laboratories). The slides were developed with DAB substrate kit (Cell Signaling) for 60 s, counterstained with Mayer's hematoxylin (Rowley Biochemical) for 30 s, then mounted with Permount (Fisher Chemical). All labeling was performed with primary control IgG antibody as a negative control. Digital pictures of the stained sections were taken at 200× magnification, and analyzed using ImageJ software. A minimum of three high-power field images were captured per tumor sample (n = 4–5 tumors/group). A blinded observer quantified positive labeled cells in each image.

Additional portions of tumor specimens were minced with a surgical blade and disaggregated using 5 mg of collagenase (Sigma-Aldrich) and 500 μg of DNase (Sigma-Aldrich) in 37°C incubator with shaking at 150 RPM for 30 min. Disaggregated tumor cells was strained through a 70 μm filter with 5 ml of RPMI. The samples were centrifuged at 2000 RPM for 5 min and the supernatants were collected. Using ELISA kits and following the manufacturer's guidelines, cytokine concentrations IFNγ (BioLegend) in disaggregated tumor supernatants were measured using SpectraMax i3 at 450 nm absorbance.

Cell Sorting and Flow Cytometry

Spleens from C57BL/6 mice were harvested, minced, and strained through a 70 μm filter in RPMI-1640 (Corning). Mice peripheral blood was collected from the submandibular vein. Red Blood Cell Lysing Buffer (Sigma-Aldrich) was added to the splenocytes to lyse erythrocytes. NK cells were sorted *via* negative selection using a magnetic-activated cell sorting (MACS) bead isolation kit (Miltenyi Biotec). To test intracellular IFNγ expression in splenocytes, MOC2-huEGFR

cell (5×10^4) were plated in 48-well plates for 24 h. The cells were radiated (8 Gy) and further cultured for 3 days. Splenocytes (1×10^6) from WT or FcγR KO mouse were cocultured with radiated MOC2-huEGFR in the presence of cetuximab (2 μg/ml) for 24 h. The cells were treated GolgiStop™ protein transport inhibitor (BD Bioscience) for 5 h before antibodies staining. Total cells were harvested and treated CD16/32 antibody (BioLegend) for tumor cell non-specific binding.

Flow cytometry was performed using fluorescent beads (UltraComp Beads eBeads, Invitrogen, #01-2222-42) to determine compensation and fluorescence minus one (FMO) methodology to determine gating. Live cell staining was performed using Ghost Red Dye 780 (Tonbo Biosciences) according to the manufacturer's instruction. Antibodies used for flow cytometry include: anti-CD45-PE-Cy7 (BioLegend), anti-CD3-FITC (BioLegend), anti-NK1.1-BV605 (BioLegend), anti-CD274 (PD-L1)-PE (BD Pharmingen), anti-IFNγ-APC (BioLegend) and Pan Rae1-APC (Miltenyi Biotec). In addition, human IgG (Sigma-Aldrich), cetuximab (Eli Lilly), calreticulin (ThermoFisher), and ULBP (ThermoFisher) were used as primary antibodies and anti-human IgG-PE (eBioscience), anti-rabbit IgG-PE (eBioscience), and anti-goat hamster IgG-PE (eBioscience) were used as a secondary antibody. After live-dead staining, a single cell suspension was labeled with the surface antibodies at 4°C for 30 min, washed three times using flow buffer (2% FBS + 2 mM EDTA in PBS). For intracellular staining, the cells were fixed and stained internal IFNγ with permeabilization solution according to the instruction (BD Cytofix/Cytoperm™). Flow cytometry was performed using an Attune NxT Flow Cytometer (ThermoFisher). Data was analyzed using FlowJo Software.

Real-Time Quantitative PCR

After euthanizing mice, tumor specimens were collected and transferred to tubes containing ceramic beads (Fisher Brand) with 1 ml of Trizol reagent (ThermoFisher). Tumor tissue was homogenized using a Bead Ruptor Elite (OMNI) for 30 s. RNA was isolated using Qiagen's RNeasy Mini Kit according to the manufacturer's instructions. The RNA concentrations were determined using a Nanodrop 1000 spectrophotometer (ThermoScientific) and 2 μg of RNA was used to make cDNA using a QuantiTect Reverse Transcriptase Kit (Qiagen). Synthesized cDNA was diluted 1:10 with distilled water and qPCR was performed with 2 μl of diluted cDNA per reaction using the CFX96 Real-Time System (Bio-Rad) with PowerUp SYBR Green master mix (Applied Biosystems). Relative mRNA expression levels of target genes were determined according to the $2^{-\Delta\Delta CT}$ method using HPRT as a reference gene (36). Primer sequences are listed in **Table 1**.

TABLE 1 | List of primers.

Murine Genes	Primer sequences 5' -3'	
	Forward	**Reverse**
PD-L1	CCAGCCACTTCTGAGCATGA	CTTCTCTTCCCACTCACGGG
IFNβ	CCCTATGGAGATGACGGAGA	CTGTCTGCTGGTGGAGTTCA
IFNγ	AGCAAGGCGAAAAAGGATGC	TCATTGAATGCTTGGCGCTG
MHCI	TGTTCCCTGTGAGCCTATGG	GGAAGGGAAGACAGAGCAGT
MILL1	TCCCGAGATACAGGATTTCTGC	GCTGTGATCATTTTAGGCTGGC
MILL2	GTTGATCTTAGGGCTGCTCCTT	TGCTGGAACCATGAACCTCC
Rae1α	ATGGATACACCAACGGGCTG	TCCACTAAGCACTTCGCTTCA
Rae1δ	AAGAGGGGTGGCGATTTCAG	CTGGGCCCTCAGGGACTATT
H60b	GGTATTCGCTTGGTGTATGCTG	CTCCCCAGCACAGCTTGTTA
H60c	TCAACAAATCGTCGCCACAC	CCATCAAAGGGGCTGGACTT
ULBP1	TTGACAGTGCCTGAGACGTG	TCGTCTGAAGTCAACAGCACA
HPRT	AGCCTAAGATGAGCGCAAGT	GGCCACAGGACTAGAACACC
Human Genes	**Primer sequences 5' -3'**	
	Forward	**Reverse**
IFNβ	AAGGCCAAGGAGTACAGT	ATCTTCAGTTTCGGAGGTAA
HPRT	TATGGCGACCCGCAGCCCT	CATCTCGAGCAAGACGTTCAG

Immunoblot and Cell Viability Assay

WT MOC1 and MOC2, MOC1- and MOC2-huEGFR, and SCC6 cells (5×10^5 cells/well) were cultured in a 6-well plate in the absence or presence of human IgG or cetuximab (0.5 μg/ml) for 3 days and stimulated with EGF (30 ng/ml) for 5 min. To check γH2AX expression, cells were incubated with non-specific human IgG control or cetuximab (0.5 μg/ml) for 2 h and then irradiated (8 Gy). After 10 min, the cells were lysed and a Western blot was performed as previously described (37). Antibodies including anti-phospho-ERK (#9101), anti-ERK (#9102), anti-γH2AX (#9718), anti-GAPDH (#2118), and HRP-linked secondary antibodies were obtained from Cell Signaling Technologies.

To evaluate cell viability *in vitro*, cells (1×10^3 cells/well) were cultured in a 96-well plate in the presence of varied concentrations of cetuximab or 1 μM of ERK inhibitor (Sigma-Aldrich). Conditions were repeated in triplicate. At indicated time points, viable cells were quantified using the Cell Counter Kit 8 (CCK-8, Enzo Life Sciences) according to the manufacturer's instructions. Absorbance was measured at 450 nm using SpectraMax i3.

Statistical Analysis

Tumor response curves were generated by plotting mean tumor volume and standard deviation. Log-transformed tumor growth over time were modeled and compared between treatment groups using linear mixed-effects models and Tukey method was used to adjust for p values in *post hoc* pairwise comparison. Surviving fraction was analyzed using a linear mixed model with logarithm base 10 transformation of survival colonies, in which individual samples were modeled as a random effect, while treatment group and radiation dose and their interaction were modeled as fixed effects. The *post hoc* pairwise comparison analysis was conducted with Tukey adjustment for p-values of the two-way interaction effect between radiation dose and treatment. Observed differences among groups from IHC, qPCR and flow cytometry were analyzed using ANOVA and Tukey's method for multiple comparison was used to adjust for p values in *post hoc* pairwise comparison. Student's t test was used for two-sample comparison. Mouse survival curves were generated using the Kaplan-Meier method. BH's method for p values adjustments was used to assess the multiple comparisons of survival curves. All statistical tests were two-sided, and 5% ($p <$

0.05) was set as the level of significance. Statistical analysis was done in R 3.4.2. All experiments were replicated to confirm reported observations and data from the first of replicate studies is shown.

RESULTS

Murine HNSCC Cells That Express huEGFR at the Plasma Membrane Are Resistant to Cetuximab Effects on Cell Viability and EGFR Signaling

To enable testing of the potential immune-based effects of cetuximab (anti-huEGFR antibody) against HNSCC tumor cells, we generated syngeneic murine models of HNSCC that express huEGFR. Because cetuximab does not recognize or antagonize murine EGFR, we expected that these models would be resistant to the effects from cetuximab that are dependent on blockade of EGFR signaling. We hypothesized, therefore, that syngeneic murine HNSCC tumor models expressing huEGFR would enable us to evaluate immune-mediated effects of cetuximab, such as ADCC, without the potentially confounding effects of cetuximab on tumor cell viability and radiation sensitivity.

To begin, we generated huEGFR-expressing MOC1 and MOC2 cell lines by viral transduction. MOC1 and MOC2 have been described previously, with MOC2 being more immunologically "cold" compared to MOC1 and characterized by low MHC1 expression and low levels of tumor infiltrating lymphocytes with a predominance of suppressive regulatory T cells (Tregs) (38, 39). Following transduction to express huEGFR, we confirmed that cetuximab was capable of binding MOC1- and MOC2-huEGFR cells, whereas cetuximab did not bind to WT MOC1 and MOC2 cells (**Figure 1A**). We observed that expression of huEGFR did not affected the viability of MOC1- and MOC2-huEGFR cells compared to WT MOC1 and MOC2 (**Figure 1B**). Given that cetuximab can inhibit the viability of huEGFR-expressing HNSCC cells (10), we tested whether cetuximab antagonized the viability of MOC1- or MOC2-huEGFR. We observed that the viability of MOC1- and MOC2-huEGFR tumor cells was not affected by cetuximab (**Figure 1C**). In contrast, using these same approaches we confirmed that cetuximab binds to and antagonizes the

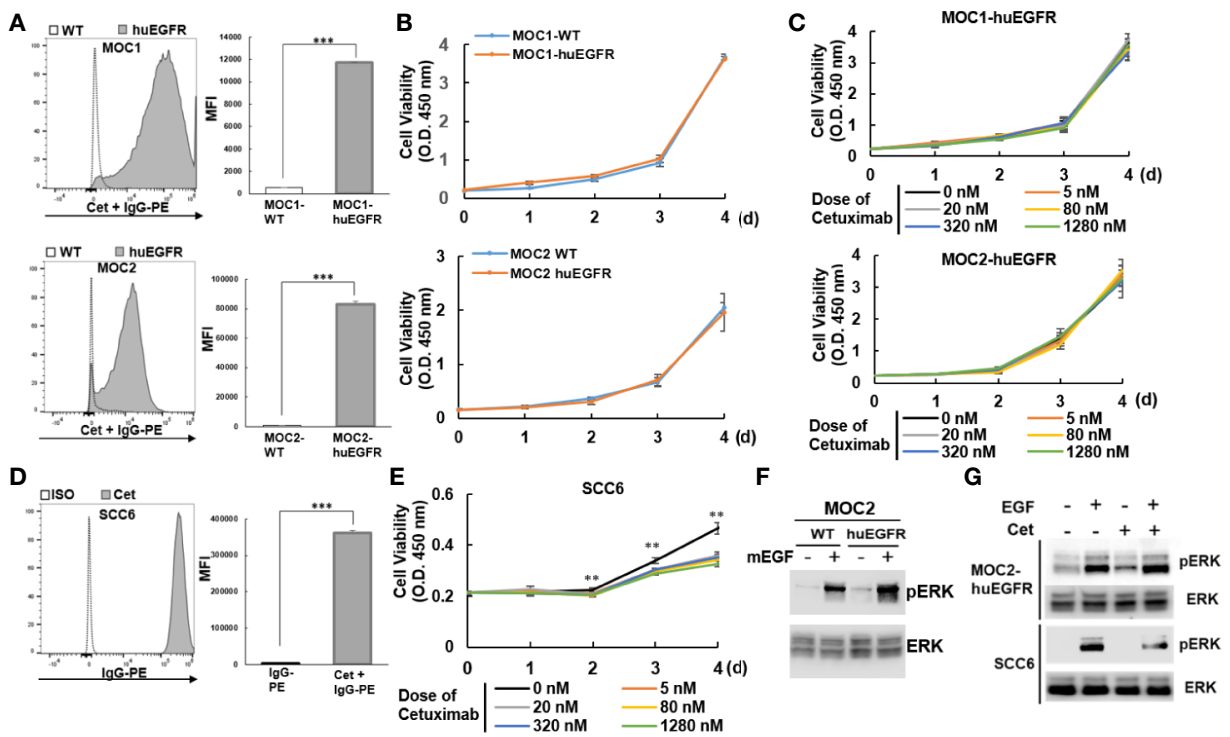


FIGURE 1 | Murine MOC1 and MOC2 HNSCC cell lines expressing huEGFR at the plasma membrane are resistant to cetuximab effects on cell viability and EGFR signaling. **(A)** Cell surface expression of huEGFR in the MOC1 and MOC2 murine HNSCC cell lines (MOC1-, MOC2-huEGFR) was detected by flow cytometry using cetuximab (anti-huEGFR mAb). **(B)** Expression of huEGFR did not altered cell viability of MOC1 and MOC2 compared to parental cells (WT). **(C)** Cetuximab did not affect the viability of huEGFR-expressing MOC1 and MOC2. **(D)** The human HNSCC cell line, SCC6, over-expresses huEGFR at a level comparable to that of our murine models, as detected by flow cytometry using cetuximab as a primary antibody. **(E)** In contrast with our huEGFR-expressing murine HNSCC cells, treatment with cetuximab reduced the viability of human SCC6 cells. **(F)** Expression of huEGFR modestly increased mEGF-induced ERK phosphorylation in MOC2 cells. **(G)** Cetuximab did not affect mEGF-mediated ERK phosphorylation in MOC2-huEGFR, whereas cetuximab inhibited ERK phosphorylation in SCC6. (*$p < 0.05$, **$p < 0.01$, ***$p < 0.001$, at least two independent experiments).

viability of human SCC6 HNSCC cells, which endogenously overexpress huEGFR (**Figures 1D, E**).

Next, we tested the effect of cetuximab on the activation of ERK, a downstream target of EGFR signaling (40, 41). We observed that expression of huEGFR in MOC2 cells resulted in a modest increase in murine EGF ligand-induced ERK phosphorylation compared to WT MOC2 (**Figure 1F**). While cetuximab suppressed EGF-stimulated ERK phosphorylation in human SCC6 cells as expected, it did not inhibit EGF-induced ERK phosphorylation on MOC2-huEGFR (**Figure 1G**), consistent with persistent mEGFR signaling in these cells in the presence of cetuximab. In similarly designed studies, we confirmed that mEGF increased ERK phosphorylation in MOC1-huEGFR cells compared to WT MOC1 (**Supplementary Figure 1A**). We further confirmed that despite no effect of cetuximab on the viability of MOC1- and MOC2-huEGFR, these cells remain sensitive to targeted inhibition of the EGFR signaling pathway when using a small molecule ERK inhibitor (**Supplementary Figure 1B**). These results suggest that because of endogenous expression of mEGFR, cetuximab binding to huEGFR does not affect EGF-induced mitogenic signaling in MOC1- and MOC2-huEGFR cells.

huEGFR-Expressing Murine HNSCC Cells Are Not Sensitized to Radiation by Cetuximab but Upregulate Type I Interferon and NKG2D Ligands Following Radiation

We evaluated the potential impact of cetuximab on the intrinsic radiosensitivity of MOC1- and MOC2-huEGFR cells. We did not detect any effect of cetuximab on the sensitivity of MOC1- or MOC2-huEGFR cells (**Figures 2A, B**) or on WT MOC1 and MOC2 cells (**Supplementary Figure 2**). Consistent with prior reports (10), cetuximab increased the radiosensitivity of human SCC6 cells (**Figure 2C**). These observations support the critical role of EGFR signaling blockade in the known effect of cetuximab on DNA damage response and on tumor cell sensitivity to radiation (10). Consistent with this, we observed that cetuximab does not affect the production of γH2AX, a marker of DNA double-strand breaks (15), following radiation of MOC2-huEGFR cells (**Supplementary Figure 1C**).

Activation of a type I interferon response in tumor cells following radiation is critical to the role of radiation in enhancing response to immunotherapies including anti–PD-1/PD-L1 checkpoint blockade (42). To evaluate radiation-induced effects on the immunogenicity of HNSCC cells *in vitro*, we used qPCR to

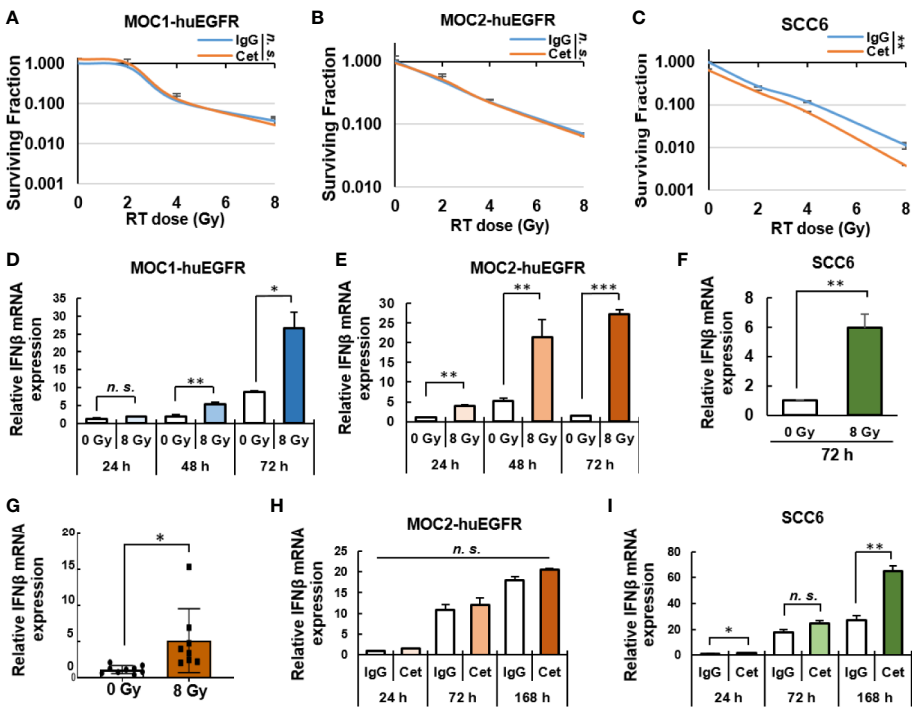


FIGURE 2 | Cetuximab does not affect the radiosensitivity of MOC1- and MOC2-huEGFR cells but radiation induces a type I interferon response in these cells. **(A–C)** Cetuximab did not affect the radiosensitivity on huEGFR-expressing MOC1 and MOC2 but does in SCC6, as measured by *in vitro* clonogenic assays performed in the presence of human-IgG control or cetuximab (0.5 μg/ml). **(D–F)** 8 Gy radiation induced *Ifnβ* expression in MOC1- and MOC2-huEGFR cells and in SCC6 cells *in vitro* as determined *via* qPCR at 24, 48, and 72 h after radiation. **(G)** In MOC2-huEGFR tumors, local radiation (8 Gy) increased bulk tumor mRNA expression of *Ifnβ* compared to 0 Gy sham radiation. **(H)** In MOC2-huEGFR cells treated with 8 Gy radiation *in vitro*, cetuximab did not impact the magnitude or time course of radiation-induced *Ifnβ* expression. **(I)** In SCC6 cells, however, cetuximab did increase the effect of radiation in inducing *Ifnβ* expression at 24 and 168 h after radiation. (mean ± SEM, $^*p < 0.05$, $^{**}p < 0.01$, $^{***}p < 0.001$, *n. s.*, not significant, Student T-test, at least two independent experiments).

measure changes in the expression of *Ifnβ* in murine MOC1- and MOC2-huEGFR and human SCC6 cells exposed to 8 Gy of radiation. We observed that radiation significantly increased *Ifnβ* expression in each of these cell lines compared to non-radiated controls (**Figures 2D–F**). We similarly evaluated the effect of radiation on the expression of *Ifnβ* in MOC2-huEGFR tumors *in vivo*. For this, mice bearing MOC2-huEGFR tumors (200 mm^3) were treated with 8 Gy or sham radiation. After 5 days, the tumors were resected, mRNA was isolated, and gene expression was quantified by qPCR. Consistent with prior reports on the effects of radiation therapy in other tumor models (42, 43), we detected increased *Ifnβ* expression in MOC2-huEGFR tumors treated with 8 Gy as compared to the non-radiated controls (**Figure 2G**). We observed no effect of cetuximab on the induction of *Ifnβ* expression in MOC2-huEGFR cells following 8 Gy radiation delivered *in vitro* (**Figure 2H**). In contrast, cetuximab increased the induction of *Ifnβ* expression in human SCC6 cells following 8 Gy radiation *in vitro* (**Figure 2I**), suggesting that the radiosensitizing effects of cetuximab may further enhance the type I interferon response induced by radiation in tumor cells that are sensitive to cetuximab-mediated blockade of EGFR signaling.

Cetuximab and Radiation Cooperate to Enhance the ADCC Anti-Tumor Immune Response

We hypothesized that despite the lack of cetuximab effect on viability or radiosensitivity of MOC1- and MOC2-huEGFR cells, the expression of huEGFR at the plasma membrane of these cells (**Figure 1A**) could render them susceptible to cetuximab-mediated ADCC. Furthermore, given the potential for type I IFN to enhance the activity of ADCC effector cells (44–46), we hypothesized that radiation might augment cetuximab-mediated ADCC. Importantly the MOC1- and MOC2-huEGFR HNSCC models allow us to test for such a cooperative interaction in the absence of confounding effects of cetuximab on tumor cell viability and radiosensitivity. WT or huEGFR-expressing MOC1 and MOC2 cells were co-cultured with PBMCs and examined using a ^{51}Cr-release assay to evaluate for tumor-specific ADCC elicited by cetuximab (**Figure 3A**). Cetuximab induced ADCC against huEGFR-expressing MOC1 and MOC2 cells, and this effect was not seen with WT MOC1 or MOC2 cells. These effects correlated with an increase in IFNγ production in sorted NK cells when co-cultured with MOC2-huEGFR and cetuximab or with positive control lipopolysaccharide (LPS), but not when NK cells were co-cultured with cetuximab alone or with MOC2-huEGFR cells alone (**Figure 3B**).

Importantly, we observed that irradiation of MOC2-huEGFR cells enhanced the capacity of cetuximab to elicit ADCC against these targets compared to non-radiated MOC2-huEGFR cells (**Figure 3C**). In agreement with this, we observed increased NK cell expression of the activation marker *Ifnγ* following co-culture of sorted NK cells with cetuximab and radiated MOC2-huEGFR cells, compared to co-culture with cetuximab and non-radiated MOC2-huEGFR cells (**Figure 3D**).

We evaluated potential mechanisms whereby radiation might contribute to an enhanced ADCC response. Radiation is known to induce immunogenic tumor cell death (47, 48). We evaluated the plasma membrane translocation of calreticulin as a marker of radiation-induced immunogenic cell death (49) in MOC2-huEGFR cells treated with radiation and/or cetuximab using flow cytometry (**Figure 3E**). Consistent with prior studies, we observed that radiation increased the expression of calreticulin at the cell surface in MOC2-huEGFR cells. However, in these cells, in which cetuximab does not affect viability or radiosensitivity, we did not observe an effect of cetuximab on this marker of immunogenic cell death either alone or with radiation. Many tumors express NKG2D ligands and these are upregulated by cell stress and enhance the susceptibility of cells to elimination by cytotoxic NK cells (50, 51). We therefore tested whether the enhanced ADCC response observed against MOC2-huEGFR cells following radiation might be associated with increased expression of NKG2D ligands. Following 8 Gy radiation of MOC2-huEGFR, *Rae1α/δ*, *Mill1/2*, *H60b/c*, and *Ulbp1* all exhibited significantly increased gene transcription by qPCR (**Figure 3F**) and we confirmed increased expression of RAE1 and ULBP1 proteins at the plasma membrane in these cells by flow cytometry (**Figure 3G**). Transcription of other NKG2D ligands including *Rae1β*, *Rae1γ*, and *H60a* was not detected in MOC2-huEGFR tumors. These data indicate that radiation promotes cetuximab-mediated ADCC and this may result in part from a novel effect of radiation enhancing the susceptibility of tumor cells to NK cell-mediated cytotoxicity by increasing expression of NKG2D ligands.

NK Cell-Dependent Increase in the Local Anti-Tumor Effect of Radiation Therapy by Cetuximab

To test for cooperative immune-mediated anti-tumor effects of radiation and cetuximab, we implanted MOC2-huEGFR tumors in C57BL/6 mice. When the average tumor volume reached 150-200 mm^3, tumors were treated with local radiation (8 Gy) or sham radiation and daily IT injections of cetuximab or non-specific control human IgG antibody (50 μg/injection) on days 6–10 after radiation (**Figure 4A**). Cetuximab alone showed no significant effect on tumor growth compared to non-specific control human IgG and local radiation alone resulted in mild tumor growth delay (**Figure 4B**). Compared to these treatments, the combination of radiation and cetuximab resulted in significantly increased tumor growth delay and improved overall survival (**Figure 4B**). We evaluated the potential impact of different routes of cetuximab delivery on this cooperative therapeutic interaction with radiation. Both intraperitoneal (35) and IT injections of cetuximab delayed the tumor growth and were not significantly different from one another (**Figure 4C**).

To assess differences in the tumor immune infiltrate among mice receiving radiation and/or cetuximab, tumor tissue was collected on day 12 after radiation from a separate cohort of mice and immunohistochemistry was performed. Consistent with prior studies, we observed a modest increase in CD8+ T cells in tumors treated with radiation alone (19), and this effect was enhanced in tumors treated with the combination of radiation and cetuximab (**Figure 4D**). In contrast, radiation and

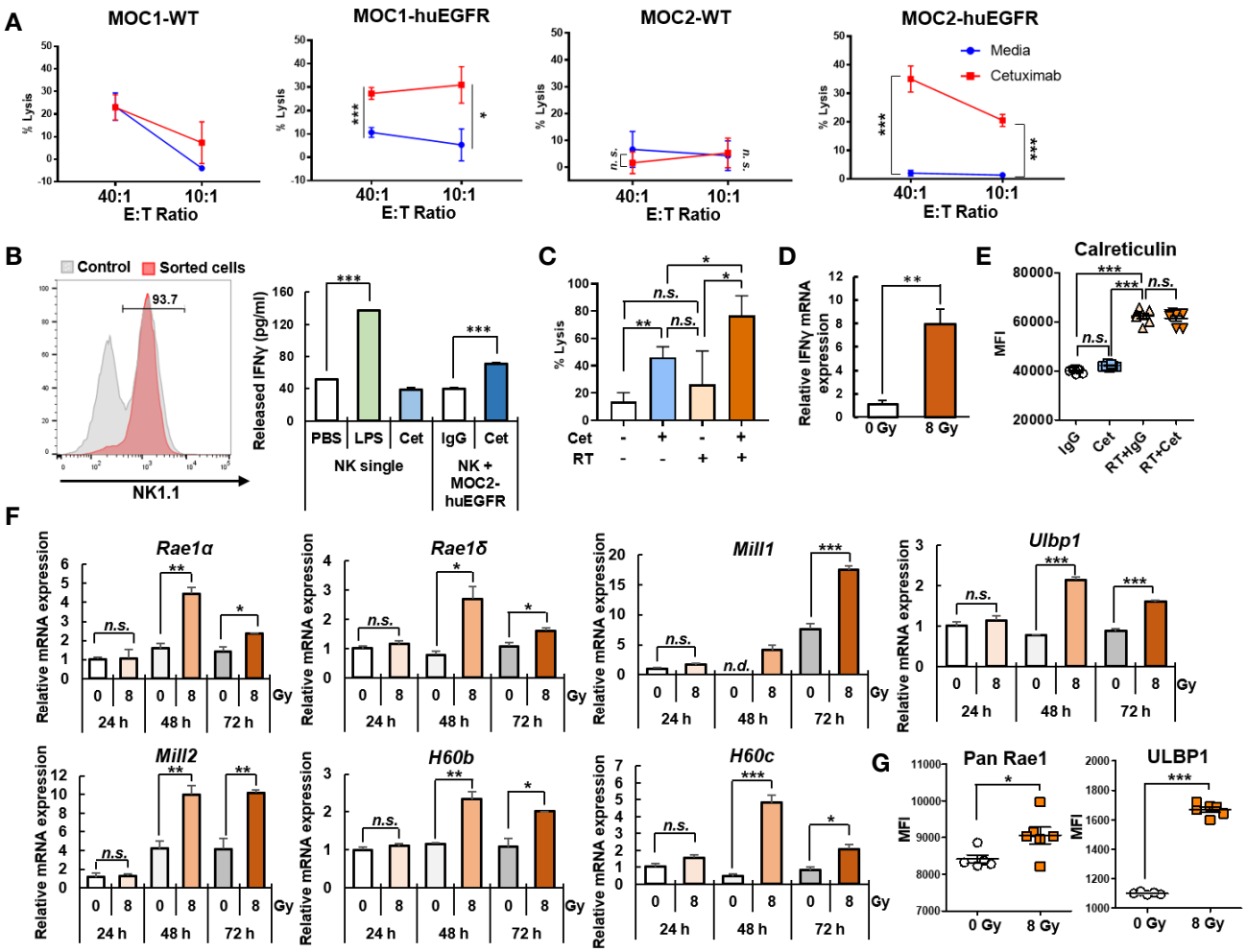


FIGURE 3 | Radiation enhances cetuximab-mediated ADCC and activation of NK cells. **(A)** Cetuximab (0.5 μg/ml) induced ADCC against huEGFR-expressing MOC1 and MOC2 cells but not against WT MOC1 and MOC2 cells in a ^{51}Cr-release assay. Percent of lysis among target tumor cells is presented. **(B)** Cetuximab increased IFNγ release in media collected after 24 h co-culture of murine NK cells (sorted from splenocytes by MACS) and MOC2-huEGFR in the presence of cetuximab, but not in the presence of non-specific human IgG, as measured by ELISA. Cetuximab alone did not affect IFNγ production compared to PBS (negative control), whereas LPS (positive control) did. **(C)** Cetuximab-mediated ADCC response was significantly increased against MOC2-huEGFR cells treated with 8 Gy radiation, compared to non-radiated MOC2-huEGFR cells, as determined by ^{51}Cr-release assay on day 3 after radiation or sham radiation. In contrast, radiation did not significantly alter cytotoxicity when combined with non-specific IgG control. **(D)** mRNA expression of *Ifnγ* was increased in NK cells sorted from murine spleen and co-cultured for 12 h with radiated (8 Gy) MOC2-huEGFR cells in the presence of cetuximab (0.5 μg/ml), as compared to non-radiated (0 Gy) MOC2-huEGFR cells in the presence of cetuximab, as determined by qPCR. **(E)** As measured by flow cytometry, radiation increased calreticulin expression at the plasma membrane of MOC2-huEGFR 72 h after radiation, but cetuximab (0.5 μg/ml) did not alter the level of calreticulin at the plasma membrane in these cells, either in with or without radiation (8 Gy). **(F, G)** 8 Gy radiation induced increased mRNA expression of multiple NKG2D ligands by qPCR (after 48 h to 72 h) and protein expression of the NKG2D ligands RAE1 and ULBP1 at the plasma membrane by flow cytometry (after 72 h of culture) in MOC2-huEGFR tumor cells. (mean ± SEM, $*p < 0.05$, $**p < 0.01$, $***p < 0.001$, *n. s.*, not significant, *n. d.*, not detectable, Student T-test, at least two independent experiments).

cetuximab treatments alone did not affect tumor infiltration by NK cells, but the combination of cetuximab and radiation significantly increased tumor infiltration by NK cells (**Figure 4E**). These results demonstrate that pairing cetuximab with radiation increases MOC2-huEGFR tumor response, despite no effect of cetuximab on the viability or radiosensitivity of this tumor model (**Figures 1B** and **2B**) and this augmented response is associated with increased tumor infiltration by both CD8+ T cells and NK cells in MOC2-huEGFR tumors.

Previous studies indicate that in some settings three fractions of 8 Gy radiation may be more effective in activating a type I IFN response and anti-tumor immune response compared to a single 8 Gy fraction (42). We evaluated the impact of cetuximab when combined with an 8 Gy × 3 fraction radiation regimen (**Figure 4F**). We observed that this combination treatment resulted in enhanced tumor regrowth delay and a significant increase in overall survival compared to cetuximab alone or 8 Gy × 3 fractions of radiation alone (**Figure 4G**) as well as significantly increased tumor

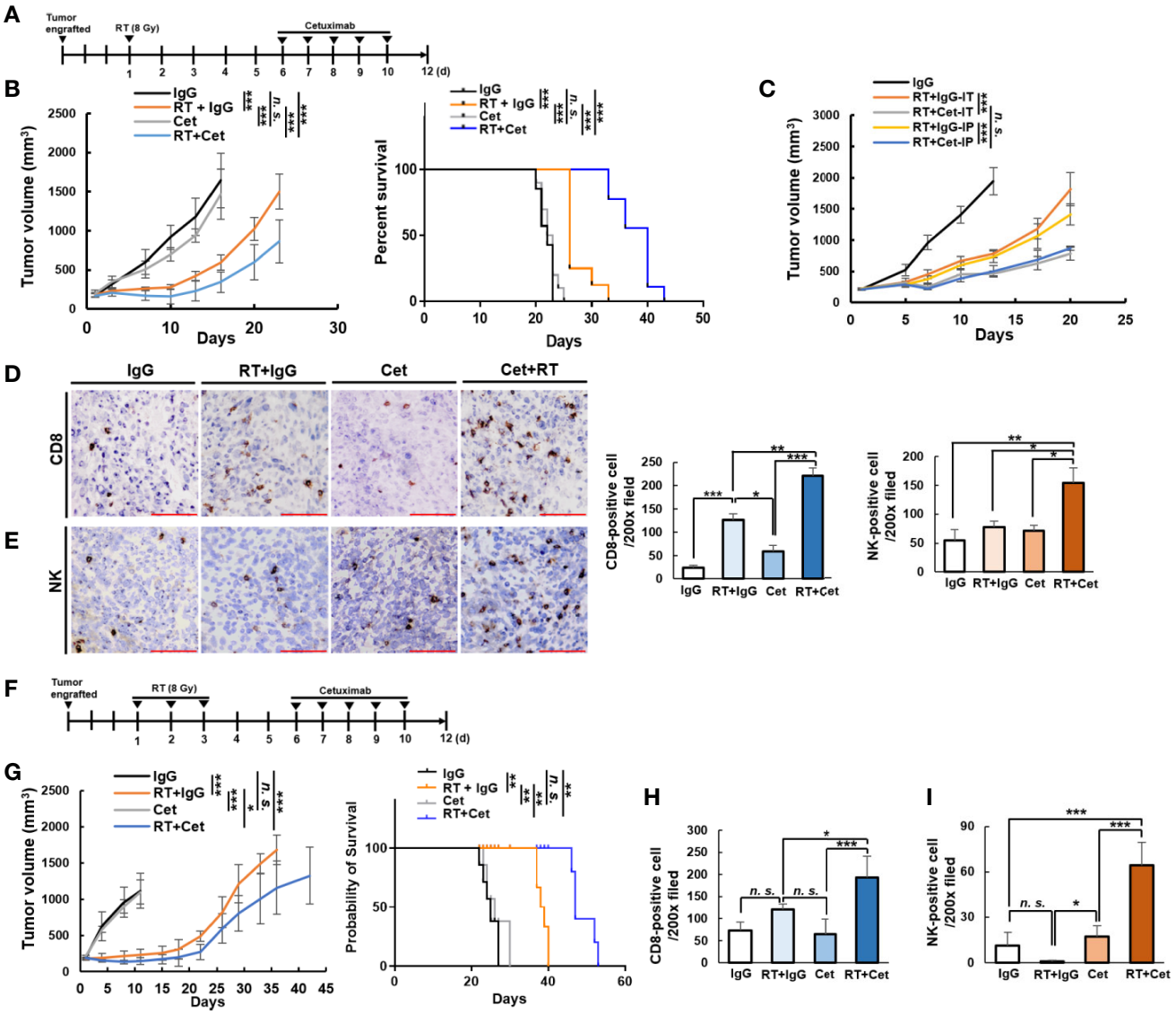


FIGURE 4 | Cooperative therapeutic interaction between cetuximab and radiation in the MOC2-huEGFR model. **(A)** Mice bearing MOC2-huEGFR tumors were treated with radiation (8 Gy) or sham radiation (0 Gy), and non-specific human IgG or cetuximab (50 μg) were injected IT on days 6–10 after radiation. **(B)** Cetuximab alone showed no effect on tumor growth compared to non-specific control IgG and radiation slightly delayed tumor growth. When given together, radiation + cetuximab significantly increased this delay in tumor growth and increased overall survival (n = 7–10/group). **(C)** No difference was observed in tumor response using either systemic delivery of cetuximab by IP injection or local delivery by IT injection when MOC2-huEGFR tumor-bearing mice were treated with 8 Gy tumor radiation or sham radiation on day 1 and non-specific human IgG or cetuximab (50 μg) on days 6–10 (n = 4/group). **(D, E)**, Tumor infiltrating CD8+ T cells and NK cells were detected by immunohistochemistry in tumors harvested on day 12 after 8 Gy radiation or sham radiation. Scale bar indicates 100 μm. **(F)** Mice bearing MOC2-huEGFR tumors were treated with 8 Gy radiation daily from days 1 to 3. Non-specific human IgG or cetuximab (50 μg) were injected IT on days 6–10 after radiation. **(G)** Radiation (8 Gy × 3 fractions) + cetuximab significantly increased tumor growth delay and increased overall survival (n = 5/group). **(H, I)** Tumor infiltrating CD8+ T cells and NK cells were increased following combined radiation (8 Gy × 3 fractions) + cetuximab, however the degree of NK infiltrate in tumors appeared to be reduced at this time point compared with 8 Gy × 1 fraction in E. (mean ± STDEV, $^*p < 0.05$, $^{**}p < 0.01$, $^{***}p < 0.001$, *n. s.*, not significant, multiple comparison by ANOVA with *post hoc* Tukey, at least three independent animal experiments).

infiltration by CD8+ T cell and NK cells (**Figures 4H, I**). However, the number of tumor-infiltrating NK cells was lower in cohorts treated with 8 Gy × 3 compared to 8 Gy × 1 (**Figures 4E, I**). Interestingly, we observed that upregulation of NKG2D ligands in MOC2-huEGFR tumors following 8 Gy × 3 fractions of radiation was comparable to or greater than that achieved by a single 8 Gy fraction (**Supplementary Figures 3A, B**). However, expression of MHCI, which is inhibitory to NK cells, was increased to a greater extent following 8 Gy × 3 fractions as compared to a single 8 Gy fraction (**Supplementary Figures 3C, D**).

NK Cells, Host FcγR, and huEGFR Are Required for the Cooperative Interaction of Radiation and Cetuximab Therapy

We hypothesized that the effect of cetuximab in augmenting anti-tumor response to local radiation in MOC2-huEGFR tumors was mediated, at least in part, by NK cells. To test this, we treated mice bearing MOC2-huEGFR tumors with 8Gy and daily IT injections of cetuximab as in **Figure 4A** and compared the effect of this treatment with that observed in a cohort of mice depleted of NK cells (**Figure 5A**). We confirmed that IP administration of anti-NK1.1 antibody depleted NK cells but not CD3+ cells (**Figures 5B, C**). Depletion of NK cells resulted in a complete loss of the cooperative therapeutic interaction between cetuximab and radiation in treating MOC2-huEGFR tumors (**Figures 5D, E**). Similarly, we tested the necessity of tumor cell expression of huEGFR in this cooperative therapeutic interaction by treating mice bearing WT MOC2. We observed no differences between treatment with radiation and cetuximab versus radiation and non-specific control human IgG in these tumors, indicating that huEGFR expression was necessary for the cooperative therapeutic interaction between cetuximab and radiation *in vivo* (**Figure 5F**). Using FcγR-deficient C57BL/6

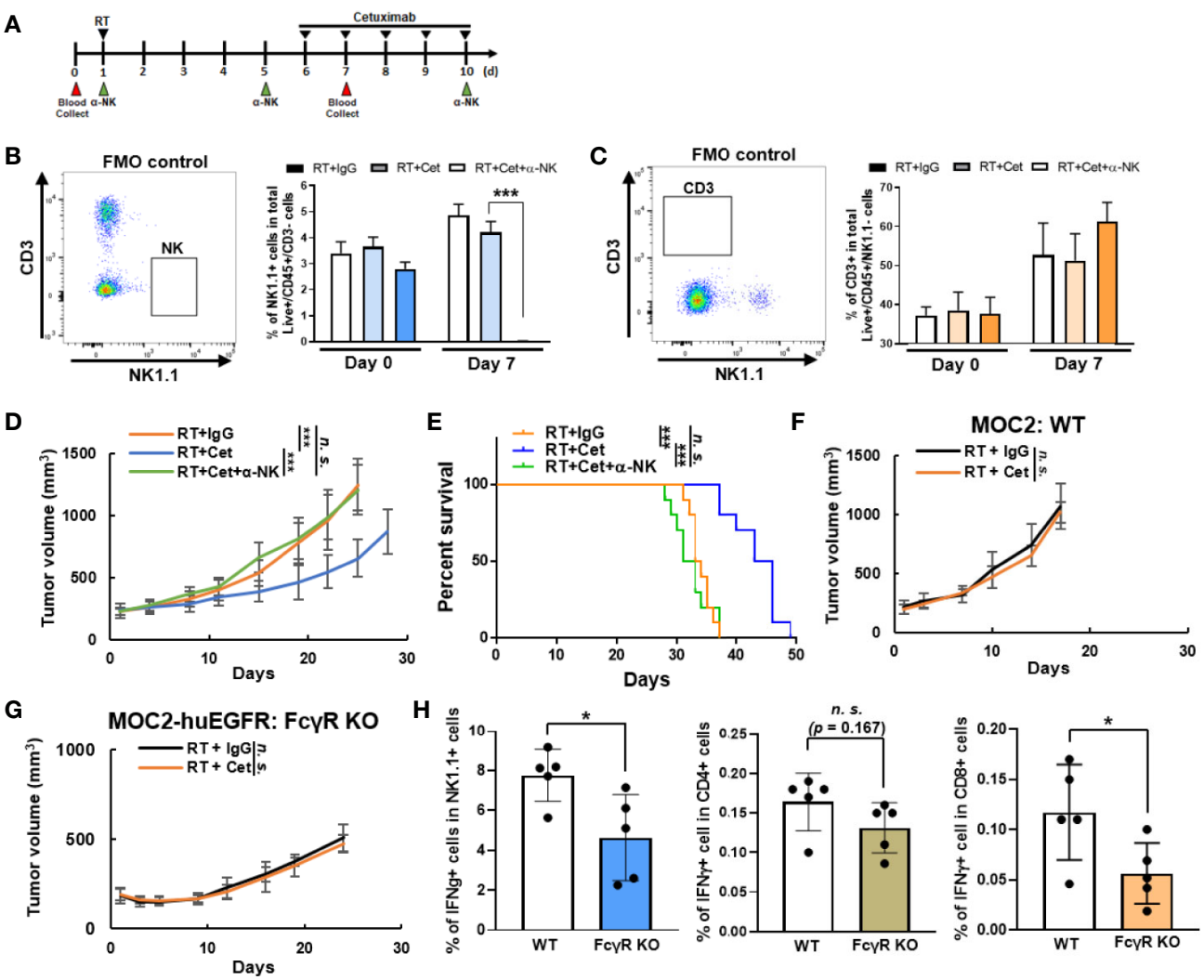


FIGURE 5 | The cooperative therapeutic interaction between radiation and cetuximab in MOC2-huEGFR tumors requires huEGFR, host expression of FcγR, and NK cells. **(A)** Intratumoral cetuximab treatments, with or without intraperitoneal anti–NK1.1 antibody (50 μg), were administrated on indicated day after tumor radiation. **(B, C)**, Peripheral blood was collected to confirm the selective depletion of NK cells (mean ± STDEV, $*p < 0.05$, $**p < 0.01$, $***p < 0.001$, Student T-test). **(D, E)** The combination of cetuximab and radiation did not improve anti-tumor response or overall survival in mice depleted of NK cells ($n = 10$/group). **(F, G)**, Treatment was administered as per **Figure 4A** ($n = 4$–5/group). **(F)** Expression of huEGFR was required to elicit anti-tumor response to combined radiation (8 Gy) and cetuximab treatment. **(G)** Combined radiation (8 Gy) and cetuximab did not improve response compared to radiation alone in MOC2-huEGFR tumors when delivered in host syngeneic mice that were lacking FcγR expression. **(H)** Co-culture of splenocytes from WT or FcγR KO mice with radiated MOC2-huEGFR (8 Gy) in the presence of cetuximab (2 μg/ml) for 24 h results in increased expression of IFNγ in NK and CD8+ T cells among WT but not FcγR-deficient splenocytes. Expression of IFNγ was analyzed using flow cytometry (mean ± STDEV, $*p < 0.05$, $***p < 0.001$, *n. s.*, not significant, Student T-test, at least three independent animal experiments).

mice, we also confirmed that the cooperative therapeutic effects of radiation and cetuximab require expression of FcγR on the host-animal's immune cells (**Figure 5G**). Notably, co-culture of splenocytes with radiated MOC2-huEGFR cells in the presence of cetuximab resulted in increased expression of IFNγ in not only NK cells but also in CD8+ T cells (**Figure 5H**). This activation of both NK and T cells was dependent upon splenocyte expression of FcγR (**Figure 5H**). This indicates that although radiation induced NKG2D ligand expression in MOC2-huEGFR, direct effector engagement of these cells *via* antibody-FcγR binding is required to activate NK cells. This further suggests that *in vitro* activation of innate FcγR-expressing cells could secondarily activate adaptive effector T cells, which do not express FcγR. Collectively, these results demonstrate an NK-cell mediated, FcγR-dependent, cooperative therapeutic interaction between to local radiation and cetuximab in huEGFR-expressing tumors.

Radiation Combined With Cetuximab Augments Response to Anti–PD-L1 Checkpoint Inhibition

In MOC2-huEGFR tumors treated with combined cetuximab and radiation, we evaluated markers of immune activation and suppression. Even though combination therapy promoted CD8+ T cell and NK cell infiltration compared to radiation alone (**Figure 4D**), we observed no differences in Ifnγ gene expression or IFNγ cytokine production in tumors treated with radiation alone or radiation plus cetuximab (**Figure 6A**). We hypothesized that suppressive features in the immunologically "cold" MOC2-huEGFR tumor microenvironment or on these tumor cells might be blunting the activation of adaptive anti-tumor immunity among the increased number of tumor-infiltrating lymphocytes observed after combined radiation and cetuximab.

By immunohistochemistry we quantified FOXP3+ cells, which include regulatory T cells (Tregs), but we identified only a non-significant trend toward an increase in this population at day 12 following radiation or radiation plus cetuximab (**Figure 6B**). Following *in vitro* radiation of MOC2-huEGFR cells, however, we did identify a significant increase in the mRNA expression of programed death-ligand 1 (Pd-l1) (**Figure 6C**). This resulted in a radiation-induced increase in the cell surface expression of PD-L1 and this was not altered when radiation was delivered in the presence of cetuximab (**Figure 6D**). We hypothesized that this radiation-induced expression of PD-L1 on tumor cells might blunt the activation of an adaptive anti-tumor immune response *in vivo* following combined treatment with radiation and cetuximab. To test this, we administered systemic anti–PD-L1 therapy (200 μg IP, days 0, 4 and 7 after radiation) in combination with radiation and cetuximab in syngeneic mice bearing MOC2-huEGFR tumors. We observed enhanced tumor regression and increased overall survival in mice treated with the combination of radiation, cetuximab, and anti–PD-L1 antibody as compared to mono- or dual combinations of these treatments (**Figures 6E, F**). This combined treatment led to complete tumor regression in 30% (n = 3/10) of mice bearing the immunologically cold, MOC2-huEGFR tumor, whereas no complete response was observed in tumor-bearing naive mouse (**Figure 6G**).

Among these mice rendered disease-free, we tested for an adaptive anti-tumor memory response by re-engrafting these mice and age-matched naïve controls with MOC2 and MOC2-huEGFR in the upper right flank and upper left flank (both outside of the prior treatment field), respectively. We observed that all disease-free mice rejected both the MOC2 and MOC2-huEGFR cells compared with 100% engraftment among control mice. These data suggest a potent adaptive anti-tumor memory response against antigen(s) shared by MOC2-huEGFR and MOC2, consistent with an *in situ* vaccination effect.

DISCUSSION

We generated huEGFR-expressing syngeneic murine models of HNSCC for the purpose of evaluating immune-mediated therapeutic interactions between radiation and the anti-huEGFR antibody, cetuximab. These murine models uniquely enable evaluation of such immune-mediated mechanisms because they are not sensitive to the potentially confounding effects of cetuximab on tumor cell viability or radiosensitivity. This results from the inability of cetuximab to bind and antagonize mEGFR. In their persistent expression of huEGFR at the plasma membrane but lack of sensitivity to anti-proliferative and radiosensitizing effects of cetuximab, these huEGFR-expressing murine tumor models are phenotypically analogous to human HNSCC tumor cells with acquired cetuximab resistance (52, 53). We acknowledge many differences between our murine models and clinically acquired resistance to cetuximab in human HNSCC. Notably, acquired resistance to cetuximab often results from activation of alternative ErbB family signaling pathways leading to persistent ERK activation (35). In contrast, our murine models achieve this through persistent ERK activation downstream of mEGFR. However, with an understanding of such limitations, these huEGFR-expressing syngeneic murine tumor models can serve as a unique tool for evaluating immune-mediated mechanisms of cetuximab and the interaction of these mechanisms with radiation or other therapeutic modalities in syngeneic mice. Given the known and potentially confounding effects of cetuximab in inhibiting EGFR+ HNSCC tumor cell viability and in sensitizing these cells to radiation (7, 8, 10), we are not aware of any alternative syngeneic HNSCC model that would allow for testing of the interaction between radiation and cetuximab-mediated ADCC.

In patients with HNSCC, an adaptive immune cell tumor infiltrate is associated with improved treatment outcomes (54–56). Here, we observe that cetuximab alone does not alter NK cell infiltration of the MOC2-huEGFR tumor or reduce growth of this tumor, but is capable of eliciting ADCC against HNSCC tumor cells independent of its roles in blocking EGFR signaling or enhancing radiosensitivity. When combined with local

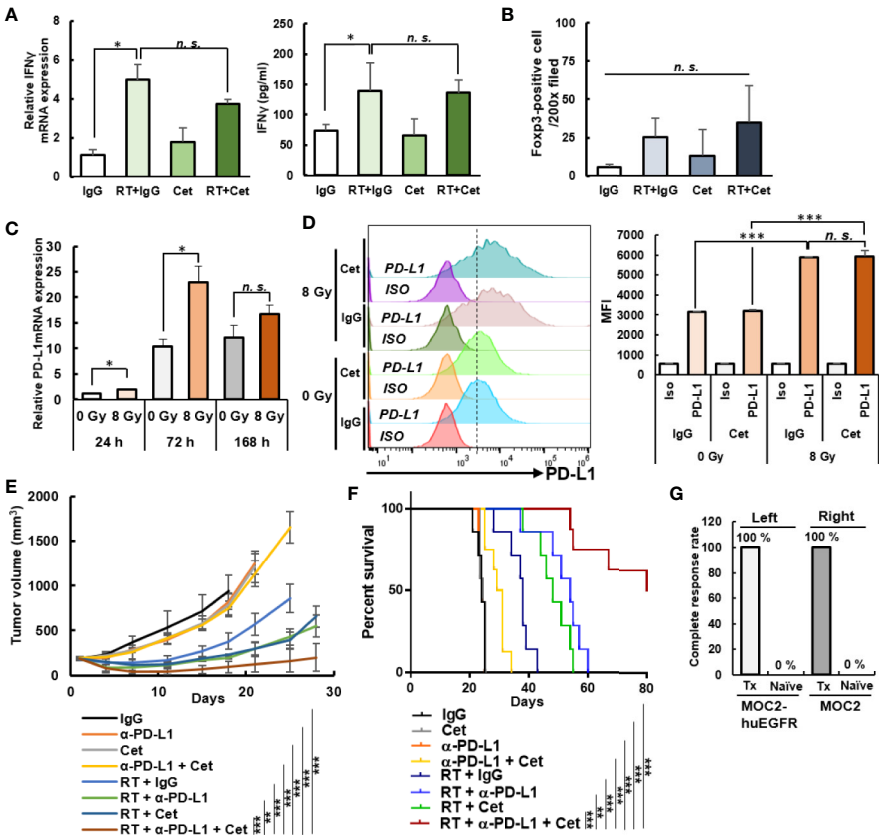


FIGURE 6 | Anti-tumor immune response to anti–PD-L1 immune checkpoint blockade is enhanced by combined treatment with radiation and cetuximab in MOC2-huEGFR tumors. **(A)** Combined radiation (8 Gy) and cetuximab therapy did not increase *Ifnγ* expression in bulk tumor compared to radiation alone on day 12 after radiation as determined by qPCR (left) and ELISA (right)—despite greater infiltration of these tumors by NK and T cells (see **Figure 4D**) (mean ± STDEV, $^{*}p < 0.05$, $^{**}p < 0.01$, $^{***}p < 0.001$, multiple comparison by ANOVA with *post hoc* Tukey). **(B)** FOXP3+ cells were analyzed from tumor immunohistochemistry of **Figure 4D**. A non-significant trend was observed toward an increase in FOXP3+ cells among tumors treated with radiation or radiation plus cetuximab (mean ± STDEV, $^{*}p < 0.05$, $^{**}p < 0.01$, $^{***}p < 0.001$, multiple comparison by ANOVA with *post hoc* Tukey). **(C)** Radiation induced *Pd-l1* expression in MOC2-huEGFR cells treated with 8 Gy, as measured by qPCR (mean ± SEM, $^{*}p < 0.05$, $^{**}p < 0.01$, $^{***}p < 0.001$, Student T-test). **(D)** MOC2-huEGFRs were treated with 8 Gy radiation and stimulated with non-specific human IgG or cetuximab (2 μg/ml) 3 days before flow cytometry analysis. PD-L1 expression was observed to increase following radiation with no effect noted from cetuximab on this response (mean ± STDEV, $^{*}p < 0.05$, $^{**}p < 0.01$, $^{***}p < 0.001$, multiple comparison by ANOVA with *post hoc* Tukey). **(E)** Anti–PD-L1 antibody increased anti-tumor response elicited by radiation and cetuximab in MOC2-huEGFR tumor-bearing mice resulting in tumor regression and **(F)** a durable survival benefit with this triple combination compared to single or dual agent control treatments (n = 7–10/group). **(G)** Naïve (n = 3) and disease-free mice (Tx, n = 3) were rechallenged by subcutaneous right flank MOC2 cell injection and left flank MOC2-huEGFR cell injection. The percentage of complete response is shown ($^{*}p < 0.05$, $^{**}p < 0.01$, $^{***}p < 0.001$, *n. s.*, not significant, at least three independent animal experiments).

radiation, cetuximab increased both NK cell and CD8+ T cell tumor infiltration *in vivo* and enhanced ADCC response to cetuximab *in vitro*. This may result from effects of radiation that enhance the susceptibility of tumor cells to ADCC, including activation of a type I IFN response, induction of immunogenic cell death in neighboring tumor cells, and increased expression of NKG2D ligands. We observed that radiation gradually increased IFNβ in MOC2-huEGFR out to 168 h and this effect was not modified by the presence of cetuximab. Therefore, *in vivo*, we hypothesized that the susceptibility of radiated tumor cells to ADCC would be highest at a delayed time point (when the type I IFN response was maximal). This expectation was also influence by our prior observations testing the timing of radiation and tumor specific antibody response, where we observed greater anti-tumor immune effect when tumor-specific antibody delivery was delayed rather than concurrent with radiation (19). Indeed, when we combined radiation and delayed administration of cetuximab (days 6–10 after radiation) *in vivo* for treatment of our MOC2-huEGFR HNSCC model, we observed improved tumor response and overall survival.

We did not observe curative treatment effects from combined radiation and cetuximab in the spontaneously metastatic MOC2-huEGFR HNSCC model. This suggests that radiation and cetuximab did not fully stimulate activation of tumor-specific T cells, perhaps due to simultaneous activation of suppressive mechanisms. Indeed, we observed increased *Pd-l1* expression in MOC2-huEGFR cells following this treatment regimen *in vivo* (**Figure 6C**). Studies examining tumor surface PD-L1 expression

have suggested that IFNβ and IFNγ produced from immune cells stimulate PD-L1 expression on tumors (57, 58). Another group observed that radiation elicits PD-L1 expression on melanoma and glioblastoma (59). In the present study, we observed that radiation increases IFNβ and PD-L1expression in murine models of HNSCC. We hypothesize that in these tumor models IFNβ production, induced in tumor cells by radiation, increases PD-L1 expression through autocrine and/or paracrine signaling mechanisms. Consequently, increased PD-L1 in these tumors may blunt to development or effect of an adaptive immune response following radiation and cetuximab. This may explain the benefit of anti–PD-L1 therapy when added to this radiation and cetuximab combination treatment, despite no apparent therapeutic efficacy of anti–PD-L1 when used alone in this immunologically "cold" tumor model.

PD-1/PD-L1 engagement is a well-known immune checkpoint for T cells and recent studies also show inhibitory effects of PD-1/PD-L1 on NK cell activation and viability (60). Inhibition of the PD-1/PD-L1 axis in HNSCC has resulted in a ~20% response rate and improved overall survival and anti–PD-1 therapy is now approved for frontline treatment of recurrent or metastatic HNSCC (17). In the immunologically "cold" MOC2-huEGFR model (39), we found that anti–PD-L1 monotherapy does not elicit an anti-tumor response (**Figure 4C**), despite gradually increased endogenous *Pd-l1* expression on growing tumor. However, by enhancing tumor cell susceptibility to NK cell killing and by increasing tumor infiltration and activation of NK cells, the combination of radiation and cetuximab therapy triggers recruitment and activation of CD8+ T cells, priming an adaptive response to "cold" tumors and enabling durable tumor eradication when combined with anti–PD-L1 therapy. With this combination treatment, 100% of mice exhibited anti-tumor response and 30% were cured. Unlike the combination of radiation and cetuximab alone, the adaptive immune response unleashed by combination with anti–PD-L1 conveyed immunologic memory to those mice that were cured and this adaptive response was equally effective against huEGFR+ or huEGFR-deficient variants of the eradicated tumor line. We speculate that we do not observe 100% cure among mice treated with radiation, cetuximab, and anti–PD-L1 checkpoint blockade due to the effects of additional mechanisms of immune inhibition, potentially including alternative immune checkpoint receptor-ligand interactions, and we will further evaluate approaches to overcoming these in future studies.

In support of the generalizability of our observations, we have previously reported preclinical studies demonstrating a therapeutic interaction between radiation and tumor-specific anti-GD2 antibody in murine models of melanoma and neuroblastoma (19). That effect was also NK-cell dependent. However, anti-GD2 antibody is not commonly delivered in conjunction with radiotherapy. On the other hand, cetuximab is the only tumor-specific antibody that is specifically approved for concurrent use with radiotherapy. This is based on a prior randomized clinical study that demonstrated improved overall

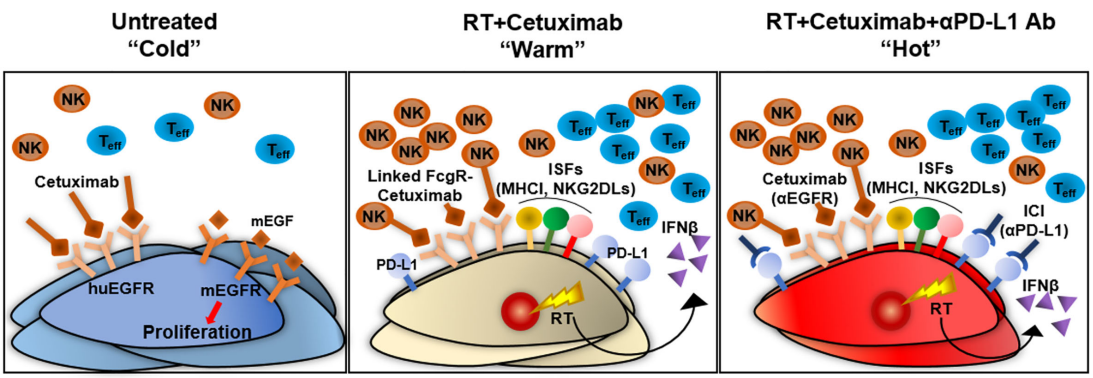


FIGURE 7 | Summary of an *in situ* vaccine regimen combining radiation and cetuximab for the treatment of an immunologically "cold" HNSCC murine tumor model. Our huEGFR-expressing syngeneic murine HNSCC tumor models enable evaluation of immune-mediated mechanisms whereby cetuximab may elicit immune-dependent therapeutic effects because cetuximab is able to bind the huEGFR on these cells but does not antagonize mEGFR that is endogenously expressed. This eliminates experimentally confounding effects of cetuximab on EGFR signaling pathways. The MOC2-huEGFR tumor model is phenotypically analogous to an immunologically "cold" human HNSCC tumor with acquired cetuximab resistance. Cetuximab is capable of binding huEGFR on these cells but this does not affect cell viability or radiosensitivity. However, cetuximab is able to elicit ADCC against MOC2-huEGFR cells and this is enhanced when the tumor cells have been radiated. Radiotherapy alone can act as an *in situ* vaccination and induces tumor infiltration by CD8+ T cells and NK cells and increases surviving tumor cell susceptibility to both T and NK cell recognition and killing by increasing tumor cell expression of type I interferon and immune susceptibility markers including NKG2D ligands. This *in situ* vaccine effect of radiation is increased by combination with cetuximab, although this combination alone does not lead to durable tumor control. This results at least in part from increased expression of PD-L1 in the tumor following combined radiation and cetuximab treatment. Addition of anti–PD-L1 immune checkpoint inhibitor therapy to the combination of radiation and cetuximab overcomes this limitation and enables curative response with evidence of adaptive anti-tumor memory in some mice. These results indicate that the *in situ* vaccine effect of radiation may be augmented by combination with tumor-specific antibodies through more effective engagement of innate immune effectors that convert an immunologically cold tumor microenvironment to one that is immunologically "warm" and responsive to immune checkpoint blockade. ICI, immune checkpoint inhibitor; IFNβ, interferon beta; ISFs, immune susceptibility factors; mEGF, murine epidermal growth factor; MHCI, major histocompatibility complex I; NK, natural killer cells; RT, radiation; Teff, effector T cells.

survival in patients with locally advanced HNSCC treated with cetuximab and radiation, as compared to radiation alone (11). This effect has been thought to result predominantly from effects of cetuximab on tumor cell viability and radiosensitivity (10, 61–64). Our data now suggest that at least a component of this proven cooperative therapeutic effect may be immune-mediated.

In our prior study of the interaction of radiation and anti-GD2 antibodies (19), we did also evaluate the interaction of radiation and cetuximab, demonstrating a therapeutic effect against cetuximab-resistant human HNSCC tumor cells that expressed huEGFR at the cell surface. However, due to a lack of suitable syngeneic murine models at that time, those studies were performed in immunodeficient nude mice that have NK cells but lack T cell immunity. This precluded evaluation of the potential mechanisms of interaction between innate and adaptive immunity following combined treatment with radiation and cetuximab and did not allow for testing of the potential benefit of combining this approach with additional immunotherapies including PD-1/PD-L1 checkpoint blockade. We developed the MOC1- and MOC2-huEGFR tumor models specifically to overcome these limitations and to enable these preclinical investigations of therapeutic mechanisms whereby the combination of radiation and cetuximab might elicit a more robust *in situ* vaccine effect and prime adaptive response to immune checkpoint blockade.

Our results are consistent with previous studies showing that FcγR is required to activate NK cells (44). Although some studies have demonstrated that stimulation of NKG2D can trigger activation of NK cells even in the absence of FcγR (45), we observed that in FcγR-deficient NK cells the exposure to cetuximab and radiated tumor cells did not effectively activate IFNγ expression, despite up-regulation of NKG2D ligands on the radiated tumor cells. Our data suggest that the increased production of IFNγ in NK cells exposed to cetuximab and radiated tumor cells may contribute to activation of CD8+ T cells, as this effect that was dependent upon antibody and FcγR expression. This suggests that cetuximab and potentially other tumor-specific antibodies may augment the *in situ* vaccine effect of radiation therapy (23, 30). Given the availability of tumor-specific antibodies for a wide variety of tumor types, this portends tremendous translational potential for combining radiation and tumor-specific antibodies to achieve greater local and systemic tumor control.

Early phase clinical data has suggested safety for the combination of radiation, cetuximab, and anti–PD-1 checkpoint blockade (65), albeit with a fractionated approach to radiation therapy. Our results suggest that patients with metastatic HNSCC may benefit from treatment with combinations of radiation, cetuximab, and immune checkpoint blockade, including those patients with immunologically "cold" tumors not responding to anti–PD-1 therapy alone and those with acquired resistance to cetuximab but persistent tumor cell expression of huEGFR (**Figure 7**). This observation will lead an opportunity to optimize such treatment combinations, through future studies evaluating the varied dose-dependency of radiation effects on tumor cell expression of type I interferon, NKG2D ligands, PD-L1, and other markers of tumor cell susceptibility to innate and adaptive anti-tumor immunity.

DATA AVAILABILITY STATEMENT

The original contributions presented in the study are included in the article/**Supplementary Material**, further inquiries can be directed to the corresponding author.

ETHICS STATEMENT

The animal study was reviewed and approved by the University of Wisconsin-Madison, Institutional Animal Care and Use Committee.

AUTHOR CONTRIBUTIONS

WJ was responsible for the primary conception and design of the experiments input from AE, CS, AJ, and ZM. Primary investigator ZM determined the experimental direction and provided study funding. CS, AJ, and JJ assisted with *in vitro* experiments for all studies. AE conducted gene transduction, ADCC, and tumor cell line quality check. BA, RS, and PC assisted with animal experiments including tumor measurements, survival rate, and IHC. Data analysis and interpretation were provided by AB, TL, YC, and KK. All authors contributed to the article and approved the submitted version.

FUNDING

The authors would like to thank the NIH funding support from P30 CA014520, P50 DE026787, 1DP5OD024576, U01CA233102, T32GM008692 and TL1TR002375.

ACKNOWLEDGMENTS

The authors wish to acknowledge Dr. Ravi Uppaluri for provision of MOC1 and MOC2. The authors also thank the expert assistance from UWCCC flow cytometry and histology/pathology core personnel.

SUPPLEMENTARY MATERIAL

The Supplementary Material for this article can be found online at: https://www.frontiersin.org/articles/10.3389/fimmu.2020.591139/full#supplementary-material

REFERENCES

1. Rubin Grandis J, Melhem MF, Gooding WE, Day R, Holst VA, Wagener MM, et al. Levels of TGF-alpha and EGFR protein in head and neck squamous cell carcinoma and patient survival. *J Natl Cancer Inst* (1998) 90(11):824–32. doi: 10.1093/jnci/90.11.824
2. Hirsch FR, Varella-Garcia M, McCoy J, West H, Xavier AC, Gumerlock P, et al. Increased epidermal growth factor receptor gene copy number detected by fluorescence *in situ* hybridization associates with increased sensitivity to gefitinib in patients with bronchioloalveolar carcinoma subtypes: a Southwest Oncology Group Study. *J Clin Oncol* (2005) 23(28):6838–45. doi: 10.1200/JCO.2005.01.2823
3. Ishitoya J, Toriyama M, Oguchi N, Kitamura K, Ohshima M, Asano K, et al. Gene amplification and overexpression of EGF receptor in squamous cell carcinomas of the head and neck. *Br J Cancer* (1989) 59(4):559–62. doi: 10.1038/bjc.1989.113
4. Grandis JR, Tweardy DJ. Elevated levels of transforming growth factor alpha and epidermal growth factor receptor messenger RNA are early markers of carcinogenesis in head and neck cancer. *Cancer Res* (1993) 53(15):3579–84.
5. Sacco AG, Worden FP. Molecularly targeted therapy for the treatment of head and neck cancer: a review of the ErbB family inhibitors. *Onco Targets Ther* (2016) 9:1927–43. doi: 10.2147/OTT.S93720
6. Cassell A, Grandis JR. Investigational EGFR-targeted therapy in head and neck squamous cell carcinoma. *Expert Opin Invest Drugs* (2010) 19(6):709–22. doi: 10.1517/13543781003769844
7. Yarden Y. The EGFR family and its ligands in human cancer. signalling mechanisms and therapeutic opportunities. *Eur J Cancer* (2001) 37(Suppl 4): S3–8. doi: 10.1016/s0959-8049(01)00230-1
8. Mehra R, Cohen RB, Burtness BA. The role of cetuximab for the treatment of squamous cell carcinoma of the head and neck. *Clin Adv Hematol Oncol* (2008) 6(10):742–50. doi: 10.1007/s11912-008-0027-6
9. Vermorken JB, Mesia R, Rivera F, Remenar E, Kawecki A, Rottey S, et al. Platinum-based chemotherapy plus cetuximab in head and neck cancer. *N Engl J Med* (2008) 359(11):1116–27. doi: 10.1056/NEJMoa0802656
10. Huang SM, Bock JM, Harari PM. Epidermal growth factor receptor blockade with C225 modulates proliferation, apoptosis, and radiosensitivity in squamous cell carcinomas of the head and neck. *Cancer Res* (1999) 59 (8):1935–40.
11. Bonner JA, Harari PM, Giralt J, Azarnia N, Shin DM, Cohen RB, et al. Radiotherapy plus cetuximab for squamous-cell carcinoma of the head and neck. *N Engl J Med* (2006) 354(6):567–78. doi: 10.1056/NEJMoa053422
12. Bonner JA, Harari PM, Giralt J, Cohen RB, Jones CU, Sur RK, et al. Radiotherapy plus cetuximab for locoregionally advanced head and neck cancer: 5-year survival data from a phase 3 randomised trial, and relation between cetuximab-induced rash and survival. *Lancet Oncol* (2010) 11(1):21–8. doi: 10.1016/S1470-2045(09)70311-0
13. Vermorken JB, Trigo J, Hitt R, Koralewski P, Diaz-Rubio E, Rolland F, et al. Open-label, uncontrolled, multicenter phase II study to evaluate the efficacy and toxicity of cetuximab as a single agent in patients with recurrent and/or metastatic squamous cell carcinoma of the head and neck who failed to respond to platinum-based therapy. *J Clin Oncol* (2007) 25(16):2171–7. doi: 10.1200/JCO.2006.06.7447
14. Chen LF, Cohen EE, Grandis JR. New strategies in head and neck cancer: understanding resistance to epidermal growth factor receptor inhibitors. *Clin Cancer Res* (2010) 16(9):2489–95. doi: 10.1158/1078-0432.CCR-09-2318
15. Wheeler DL, Huang S, Kruser TJ, Nechrebecki MM, Armstrong EA, Benavente S, et al. Mechanisms of acquired resistance to cetuximab: role of HER (ErbB) family members. *Oncogene* (2008) 27(28):3944–56. doi: 10.1038/onc.2008.19
16. Saki M, Toulany M, Rodemann HP. Acquired resistance to cetuximab is associated with the overexpression of Ras family members and the loss of radiosensitization in head and neck cancer cells. *Radiother Oncol* (2013) 108 (3):473–8. doi: 10.1016/j.radonc.2013.06.023
17. Ferris RL, Blumenschein GJr., Fayette J, Guigay J, Colevas AD, Licitra L, et al. Nivolumab for Recurrent Squamous-Cell Carcinoma of the Head and Neck. *N Engl J Med* (2016) 375(19):1856–67. doi: 10.1056/NEJMoa1602252
18. Park JA, Cheung NV. Limitations and opportunities for immune checkpoint inhibitors in pediatric malignancies. *Cancer Treat Rev* (2017) 58:22–33. doi: 10.1016/j.ctrv.2017.05.006
19. Morris ZS, Guy EI, Francis DM, Gressett MM, Werner LR, Carmichael LL, et al. In Situ Tumor Vaccination by Combining Local Radiation and Tumor-Specific Antibody or Immunocytokine Treatments. *Cancer Res* (2016) 76 (13):3929–41. doi: 10.1158/0008-5472.CAN-15-2644
20. Haymaker CL, Kim D, Uemura M, Vence LM, Phillip A, McQuail N, et al. Metastatic Melanoma Patient Had a Complete Response with Clonal Expansion after Whole Brain Radiation and PD-1 Blockade. *Cancer Immunol Res* (2017) 5(2):100–5. doi: 10.1158/2326-6066.CIR-16-0223
21. Alomari AK, Cohen J, Vortmeyer AO, Chiang A, Gettinger S, Goldberg S, et al. Possible Interaction of Anti-PD-1 Therapy with the Effects of Radiosurgery on Brain Metastases. *Cancer Immunol Res* (2016) 4(6):481–7. doi: 10.1158/2326-6066.CIR-15-0238
22. Postow MA, Callahan MK, Barker CA, Yamada Y, Yuan J, Kitano S, et al. Immunologic correlates of the abscopal effect in a patient with melanoma. *N Engl J Med* (2012) 366(10):925–31. doi: 10.1056/NEJMoa1112824
23. Twyman-Saint Victor C, Rech AJ, Maity A, Rengan R, Pauken KE, Stelekati E, et al. Radiation and dual checkpoint blockade activate non-redundant immune mechanisms in cancer. *Nature* (2015) 520(7547):373–7. doi: 10.1038/nature14292
24. Bang A, Wilhite TJ, Pike LRG, Cagney DN, Aizer AA, Taylor A, et al. Multicenter Evaluation of the Tolerability of Combined Treatment With PD-1 and CTLA-4 Immune Checkpoint Inhibitors and Palliative Radiation Therapy. *Int J Radiat Oncol Biol Phys* (2017) 98(2):344–51. doi: 10.1016/j.ijrobp.2017.02.003
25. von Reibnitz D, Chaft JE, Wu AJ, Samstein R, Hellmann MD, Plodkowski AJ, et al. Safety of combining thoracic radiation therapy with concurrent versus sequential immune checkpoint inhibition. *Adv Radiat Oncol* (2018) 3(3):391–8. doi: 10.1016/j.adro.2018.05.001
26. Ahmed KA, Stallworth DG, Kim Y, Johnstone PA, Harrison LB, Caudell JJ, et al. Clinical outcomes of melanoma brain metastases treated with stereotactic radiation and anti-PD-1 therapy. *Ann Oncol* (2016) 27(3):434–41. doi: 10.1093/annonc/mdv622
27. Shaverdian N, Lisberg AE, Bornazyan K, Veruttipong D, Goldman JW, Formenti SC, et al. Previous radiotherapy and the clinical activity and toxicity of pembrolizumab in the treatment of non-small-cell lung cancer: a secondary analysis of the KEYNOTE-001 phase 1 trial. *Lancet Oncol* (2017) 18 (7):895–903. doi: 10.1016/S1470-2045(17)30380-7
28. Tang C, Welsh JW, de Groot P, Massarelli E, Chang JY, Hess KR, et al. Ipilimumab with Stereotactic Ablative Radiation Therapy: Phase I Results and Immunologic Correlates from Peripheral T Cells. *Clin Cancer Res* (2017) 23 (6):1388–96. doi: 10.1158/1078-0432.CCR-16-1432
29. Antonia SJ, Villegas A, Daniel D, Vicente D, Murakami S, Hui R, et al. Durvalumab after Chemoradiotherapy in Stage III Non-Small-Cell Lung Cancer. *N Engl J Med* (2017) 377(20):1919–29. doi: 10.1056/NEJMoa1709937
30. Formenti SC, Rudqvist NP, Golden E, Cooper B, Wennerberg E, Lhuillier C, et al. Radiotherapy induces responses of lung cancer to CTLA-4 blockade. *Nat Med* (2018) 24(12):1845–51. doi: 10.1038/s41591-018-0232-2
31. Theelen W, Peulen HMU, Lalezari F, van der Noort V, de Vries JF, Aerts J, et al. Effect of Pembrolizumab After Stereotactic Body Radiotherapy vs Pembrolizumab Alone on Tumor Response in Patients With Advanced Non-Small Cell Lung Cancer: Results of the PEMBRO-RT Phase 2 Randomized Clinical Trial. *JAMA Oncol* (2019) 5(9):1276–82. doi: 10.1001/jamaoncol.2019.1478
32. McBride SM, Sherman EJ, Tsai CJ, Baxi SS, Aghalar J, Eng J, et al. A phase II randomized trial of nivolumab with stereotactic body radiotherapy (SBRT) versus nivolumab alone in metastatic (M1) head and neck squamous cell carcinoma (HNSCC). *J Clin Oncol* (2018) 36(15_suppl):6009. doi: 10.1200/JCO.2018.36.15_suppl.6009
33. Uphoff CC, Drexler HG. Detection of Mycoplasma contamination in cell cultures. *Curr Protoc Mol Biol* (2014) 106:28.4.1–14. doi: 10.1002/0471142727.mb2804s106
34. Connor JP, Felder M, Hank J, Harter J, Gan J, Gillies SD, et al. Ex vivo evaluation of anti-EpCAM immunocytokine huKS-IL2 in ovarian cancer. *J Immunother* (2004) 27(3):211–9. doi: 10.1097/00002371-200405000-00005
35. Yonesaka K, Zejnullahu K, Okamoto I, Satoh T, Cappuzzo F, Souglakos J, et al. Activation of ERBB2 signaling causes resistance to the EGFR-directed therapeutic antibody cetuximab. *Sci Transl Med* (2011) 3(99):99ra86. doi: 10.1126/scitranslmed.3002442

36. Livak KJ, Schmittgen TD. Analysis of relative gene expression data using real-time quantitative PCR and the 2(-Delta Delta C(T)) Method. *Methods* (2001) 25(4):402–8. doi: 10.1006/meth.2001.1262
37. Li C, Huang S, Armstrong EA, Francis DM, Werner LR, Sliwkowski MX, et al. Antitumor Effects of MEHD7945A, a Dual-Specific Antibody against EGFR and HER3, in Combination with Radiation in Lung and Head and Neck Cancers. *Mol Cancer Ther* (2015) 14(9):2049–59. doi: 10.1158/1535-7163.MCT-15-0155
38. Judd NP, Winkler AE, Murillo-Sauca O, Brotman JJ, Law JH, Lewis JSJr., et al. ERK1/2 regulation of CD44 modulates oral cancer aggressiveness. *Cancer Res* (2012) 72(1):365–74. doi: 10.1158/0008-5472.CAN-11-1831
39. Judd NP, Allen CT, Winkler AE, Uppaluri R. Comparative analysis of tumor-infiltrating lymphocytes in a syngeneic mouse model of oral cancer. *Otolaryngol Head Neck Surg* (2012) 147(3):493–500. doi: 10.1177/0194599812442037
40. Ercan D, Xu C, Yanagita M, Monast CS, Pratilas CA, Montero J, et al. Reactivation of ERK signaling causes resistance to EGFR kinase inhibitors. *Cancer Discov* (2012) 2(10):934–47. doi: 10.1158/2159-8290.CD-12-0103
41. Leung DW, Tompkins C, Brewer J, Ball A, Coon M, Morris V, et al. Phospholipase C delta-4 overexpression upregulates ErbB1/2 expression, Erk signaling pathway, and proliferation in MCF-7 cells. *Mol Cancer* (2004) 3:15. doi: 10.1186/1476-4598-3-15
42. Vanpouille-Box C, Alard A, Aryankalayil MJ, Sarfraz Y, Diamond JM, Schneider RJ, et al. DNA exonuclease Trex1 regulates radiotherapy-induced tumour immunogenicity. *Nat Commun* (2017) 8:15618. doi: 10.1038/ncomms15618
43. Sharabi AB, Nirschl CJ, Kochel CM, Nirschl TR, Francica BJ, Velarde E, et al. Stereotactic Radiation Therapy Augments Antigen-Specific PD-1-Mediated Antitumor Immune Responses *via* Cross-Presentation of Tumor Antigen. *Cancer Immunol Res* (2015) 3(4):345–55. doi: 10.1158/2326-6066.CIR-14-0196
44. Hokland P, Berg K. Interferon enhances the antibody-dependent cellular cytotoxicity (ADCC) of human polymorphonuclear leukocytes. *J Immunol* (1981) 127(4):1585–8.
45. Fan S, Fehr HG, Adams D. Activation of macrophages for ADCC *in vitro*: effects of IL-4, TNF, interferons-alpha/beta, interferon-gamma, and GM-CSF. *Cell Immunol* (1991) 135(1):78–87. doi: 10.1016/0008-8749(91)90255-a
46. Arase H, Arase N, Saito T. Interferon gamma production by natural killer (NK) cells and NK1.1+ T cells upon NKR-P1 cross-linking. *J Exp Med* (1996) 183(5):2391–6. doi: 10.1084/jem.183.5.2391
47. Apetoh L, Ghiringhelli F, Tesniere A, Obeid M, Ortiz C, Criollo A, et al. Toll-like receptor 4-dependent contribution of the immune system to anticancer chemotherapy and radiotherapy. *Nat Med* (2007) 13(9):1050–9. doi: 10.1038/nm1622
48. Golden EB, Apetoh L. Radiotherapy and immunogenic cell death. *Semin Radiat Oncol* (2015) 25(1):11–7. doi: 10.1016/j.semradonc.2014.07.005
49. Golden EB, Frances D, Pellicciotta I, Demaria S, Helen Barcellos-Hoff M, Formenti SC. Radiation fosters dose-dependent and chemotherapy-induced immunogenic cell death. *Oncoimmunology* (2014) 3:e28518. doi: 10.4161/onci.28518
50. Nausch N, Cerwenka A. NKG2D ligands in tumor immunity. *Oncogene* (2008) 27(45):5944–58. doi: 10.1038/onc.2008.272
51. Lanier LL. NKG2D Receptor and Its Ligands in Host Defense. *Cancer Immunol Res* (2015) 3(6):575–82. doi: 10.1158/2326-6066.CIR-15-0098
52. Rebucci M, Peixoto P, Dewitte A, Wattez N, De Nuncques MA, Rezvoy N, et al. Mechanisms underlying resistance to cetuximab in the HNSCC cell line: role of AKT inhibition in bypassing this resistance. *Int J Oncol* (2011) 38(1):189–200. doi: 10.3892/ijo_00000838
53. Leblanc O, Vacher S, Lecerf C, Jeannot E, Klijanienko J, Berger F, et al. Biomarkers of cetuximab resistance in patients with head and neck squamous cell carcinoma. *Cancer Biol Med* (2020) 17(1):208–17. doi: 10.20892/j.issn.2095-3941.2019.0153
54. Uppaluri R, Dunn GP, Lewis JSJr. Focus on TILs: prognostic significance of tumor infiltrating lymphocytes in head and neck cancers. *Cancer Immun* (2008) 8:16.
55. Thurlow JK, Pena Murillo CL, Hunter KD, Buffa FM, Patiar S, Betts G, et al. Spectral clustering of microarray data elucidates the roles of microenvironment remodeling and immune responses in survival of head and neck squamous cell carcinoma. *J Clin Oncol* (2010) 28(17):2881–8. doi: 10.1200/JCO.2009.24.8724
56. Snyderman CH, Heo DS, Chen K, Whiteside TL. Johnson JT. T-cell markers in tumor-infiltrating lymphocytes of head and neck cancer. *Head Neck* (1989) 11(4):331–6. doi: 10.1002/hed.2880110408
57. Garcia-Diaz A, Shin DS, Moreno BH, Saco J, Escuin-Ordinas H, Rodriguez GA, et al. Interferon Receptor Signaling Pathways Regulating PD-L1 and PD-L2 Expression. *Cell Rep* (2017) 19(6):1189–201. doi: 10.1016/j.celrep.2017.04.031
58. Thiem A, Hesbacher S, Kneitz H, di Primio T, Heppt MV, Hermanns HM, et al. IFN-gamma-induced PD-L1 expression in melanoma depends on p53 expression. *J Exp Clin Cancer Res* (2019) 38(1):397. doi: 10.1186/s13046-019-1403-9
59. Derer A, Spiljar M, Baumler M, Hecht M, Fietkau R, Frey B, et al. Chemoradiation Increases PD-L1 Expression in Certain Melanoma and Glioblastoma Cells. *Front Immunol* (2016) 7:610. doi: 10.3389/fimmu.2016.00610
60. Liu Y, Cheng Y, Xu Y, Wang Z, Du X, Li C, et al. Increased expression of programmed cell death protein 1 on NK cells inhibits NK-cell-mediated anti-tumor function and indicates poor prognosis in digestive cancers. *Oncogene* (2017) 36(44):6143–53. doi: 10.1038/onc.2017.209
61. Liang K, Ang KK, Milas L, Hunter N, Fan Z. The epidermal growth factor receptor mediates radioresistance. *Int J Radiat Oncol Biol Phys* (2003) 57(1):246–54. doi: 10.1016/s0360-3016(03)00511-x
62. Bonner JA, Maihle NJ, Folven BR, Christianson TJ, Spain K. The interaction of epidermal growth factor and radiation in human head and neck squamous cell carcinoma cell lines with vastly different radiosensitivities. *Int J Radiat Oncol Biol Phys* (1994) 29(2):243–7. doi: 10.1016/0360-3016(94)90269-0
63. Huang SM, Harari PM. Modulation of radiation response after epidermal growth factor receptor blockade in squamous cell carcinomas: inhibition of damage repair, cell cycle kinetics, and tumor angiogenesis. *Clin Cancer Res* (2000) 6(6):2166–74.
64. Milas L, Mason K, Hunter N, Petersen S, Yamakawa M, Ang K, et al. In vivo enhancement of tumor radioresponse by C225 antiepidermal growth factor receptor antibody. *Clin Cancer Res* (2000) 6(2):701–8.
65. Ferris RL, Gillison ML, Harris JW, Colevas AD, Mell LK, Kong CS, et al. Safety evaluation of nivolumab (Nivo) concomitant with cetuximab-radiotherapy for intermediate (IR) and high-risk (HR) local-regionally advanced head and neck squamous cell carcinoma (HNSCC): RTOG 3504. *J Clin Oncol* (2018) 36(15_Suppl):6010–6010. doi: 10.1200/JCO.2018.36.15_suppl.6010

Conflict of Interest: The authors declare that the research was conducted in the absence of any commercial or financial relationships that could be construed as a potential conflict of interest.

Copyright © 2020 Jin, Erbe, Schwarz, Jaquish, Anderson, Sriramaneni, Jagodinsky, Bates, Clark, Le, Lan, Chen, Kim and Morris. This is an open-access article distributed under the terms of the Creative Commons Attribution License (CC BY). The use, distribution or reproduction in other forums is permitted, provided the original author(s) and the copyright owner(s) are credited and that the original publication in this journal is cited, in accordance with accepted academic practice. No use, distribution or reproduction is permitted which does not comply with these terms.

frontiers in Immunology

CLINICAL TRIAL
published: 08 January 2021
doi: 10.3389/fimmu.2020.576756

Photochemical Internalization Enhanced Vaccination Is Safe, and Gives Promising Cellular Immune Responses to an HPV Peptide-Based Vaccine in a Phase I Clinical Study in Healthy Volunteers

Tone Otterhaug[1], Sylvia Janetzki[2], Marij J. P. Welters[3], Monika Håkerud[1,4], Anne Grete Nedberg[1,4], Victoria Tudor Edwards[1,4], Sanne Boekestijn[3], Nikki M. Loof[3], Pål Kristian Selbo[4], Hans Olivecrona[1], Sjoerd H. van der Burg[3] and Anders Høgset[1]**

[1] PCI Biotech AS, Oslo, Norway, [2] ZellNet Consulting, Inc., Fort Lee, NJ, United States, [3] Department of Medical Oncology, Oncode Institute, Leiden University Medical Center, Leiden, Netherlands, [4] Department of Radiation Biology, Institute for Cancer Research, The Norwegian Radium Hospital, Oslo University Hospital, Oslo, Norway

OPEN ACCESS

Edited by:
Stephanie E. B. McArdle, Nottingham Trent University, United Kingdom

Reviewed by:
Thomas Kündig, University Hospital Zürich, Switzerland
Eric Tartour, Hôpital Européen Georges-Pompidou (HEGP), France

***Correspondence:**
Tone Otterhaug
tone@pcibiotech.no
Anders Høgset
anders.hogset@pcibiotech.no

Specialty section:
This article was submitted to Vaccines and Molecular Therapeutics, a section of the journal Frontiers in Immunology

Received: 26 June 2020
Accepted: 20 November 2020
Published: 08 January 2021

Citation:
Otterhaug T, Janetzki S, Welters MJP, Håkerud M, Nedberg AG, Edwards VT, Boekestijn S, Loof NM, Selbo PK, Olivecrona H, van der Burg SH and Høgset A (2021) Photochemical Internalization Enhanced Vaccination Is Safe, and Gives Promising Cellular Immune Responses to an HPV Peptide-Based Vaccine in a Phase I Clinical Study in Healthy Volunteers. Front. Immunol. 11:576756. doi: 10.3389/fimmu.2020.576756

Background and Aims: Photochemical internalization (PCI) is a technology for inducing release of endocytosed antigens into the cell cytosol *via* a light-induced process. Preclinical experiments have shown that PCI improves MHC class I antigen presentation, resulting in strongly enhanced CD8+ T-cell responses to polypeptide antigens. In PCI vaccination a mixture of the photosensitizing compound fimaporfin, vaccine antigens, and an adjuvant is administered intradermally followed by illumination of the vaccination site. This work describes an open label, phase I study in healthy volunteers, to assess the safety, tolerability, and immune response to PCI vaccination in combination with the adjuvant poly-ICLC (Hiltonol) (ClinicalTrials.gov Identifier: NCT02947854).

Methods: The primary objective of the study was to assess the safety and local tolerance of PCI mediated vaccination, and to identify a safe fimaporfin dose for later clinical studies. A secondary objective was to analyze the immunological responses to the vaccination. Each subject received 3 doses of HPV16 E7 peptide antigens and two doses of Keyhole Limpet Hemocyanin (KLH) protein. A control group received Hiltonol and vaccine antigens only, whereas the PCI groups in addition received fimaporfin + light. Local and systemic adverse effects were assessed by standard criteria, and cellular and humoral immune responses were analyzed by ELISpot, flow cytometry, and ELISA assays.

Results: 96 healthy volunteers were vaccinated with fimaporfin doses of 0.75–50 μg. Doses below 17.5 μg were safe and tolerable, higher doses exhibited local tolerability issues in some study subjects, mainly erythema, and pain during illumination. There were few, and only mild and expected systemic adverse events. The employment of PCI increased the number of subjects exhibiting a T-cell response to the HPV peptide vaccine

about 10-fold over what was achieved with the antigen/Hiltonol combination without PCI. Moreover, the use of PCI seemed to result in a more consistent and multifunctional CD8+ T-cell response. An enhancement of the humoral immune response to KLH vaccination was also observed.

Conclusions: Using PCI in combination with Hiltonol for intradermal vaccination is safe at fimaporfin doses below 17.5 µg, and gives encouraging immune responses to peptide and protein based vaccination.

Keywords: photochemical internalization, vaccine delivery, peptide vaccines, immunologic adjuvant, multifunctional T-cells, phase I study photochemical enhancement of T-cell responses

INTRODUCTION

T-cell-mediated immunity is important for the control of cancer and infections by viruses, intracellular bacteria and parasites. Hence, vaccines against such diseases should be designed to induce proper T-cell responses. T-cell responses can readily be induced by vaccines based on viral vectors and nucleic acids. In contrast, subunit vaccines based on polypeptide antigens are generally good at generating antibody responses, but cellular immune responses, and especially CD8+ T-cell responses, are often inadequate. An important reason for this may be insufficient presentation of exogenously added vaccine antigens on MHC class I molecules on antigen presenting cells (APCs). Such presentation generally requires that the antigen is present in the cytosol of the APCs. Although some specialized dendritic cells has the ability to translocate antigens to the cytosol [reviewed in (1)], in most APCs the antigens stay inside intracellular vesicles in the APC with poor access to the cytosol.

Photochemical internalization (PCI) is a technology where endocytosed molecules can be released into the cell cytosol *via* a light-induced process (2). The endosomal escape induced by PCI results in enhanced access for antigens to the MHC class I presentation pathway (3, 4), as well as strongly enhanced CD8+ T-cell responses in mice (3–9). Vaccination with PCI is based on the utilization of an amphiphilic membrane-docking photosensitizing molecule ($TPCS_{2a}$ or fimaporfin) (10) in combination with the vaccine antigen. After endocytosis, the PCI-photosensitizer and the antigen co-localizes to endosomes and lysosomes. Light-controlled activation of the photosensitizer results in reactions with molecular oxygen (O_2) and generation of reactive oxygen species (ROS) (11). These ROS species can induce lipid peroxidation and permeabilization of the vesicle membranes, ultimately leading to the release of the endosomal content into the cytosol [reviewed in (12, 13)]. The fimaporfin photosensitizer is also used to enhance the efficacy of cytotoxic drugs, and is under clinical development for cancer therapy (14).

In addition to proper antigen presentation, the upregulation of co-stimulatory molecules and the production of cytokines are necessary signals for a proper priming of CD8+ T-cells (15). For polypeptide-based vaccination the two latter signals can be provided by immunological adjuvants inducing activation and maturation of APCs (16). Certain adjuvants can also to some degree induce cross presentation of peptide and protein antigens on MHC class I (17), but this effect is often not sufficient for a proper priming of CD8+ T-cells after vaccination. It therefore seemed logical to combine the enhanced MHC class I presentation provided by PCI with an adjuvant with a strong APC activating effect. As shown in pre-clinical experiments, combining PCI with poly(IC) based adjuvants gives a strong synergistic effect on the CD8+ T-cell response to vaccination (Selbo *et al*., manuscript in preparation). Somewhat surprisingly, in these experiments it also was found that PCI also improved helper T-cell and antibody responses

Here we present results from a phase I clinical study in healthy volunteers, showing that PCI-based peptide and protein vaccination with a poly(IC) based adjuvant is safe and results in enhanced cellular and humoral immune responses, similar to what has been observed in animal studies.

MATERIALS AND METHODS

Study Design and Participants

This was an open label, phase I study to assess safety, tolerability, and immune response to vaccination with fimaporfin-induced PCI with antigens and adjuvant in healthy volunteers. The clinical study was done at Covance Clinical Research Unit Ltd., Leeds, UK and participants were recruited through their subject database and *via* advertisement on the Covance website and in social media. All subjects gave written informed consent and the trial was conducted in accordance with the principles of the Declaration of Helsinki and Good Clinical Practice. The study was approved in the UK by Medicines and Healthcare Products Regulatory Agency (CTA 34788/0006/001-0015) and the North East–York Research Ethics Committee (16/NE/0198). The ClinicalTrials.gov Identifier was NCT02947854.

The primary objective of the study was to assess the safety of PCI mediated vaccination. The safety endpoints were: Adverse events (graded according to the National Cancer Institute (NCI) Common Terminology Criteria for Adverse Events (CTCAE v4.03); laboratory safety evaluations; vital sign assessments; and local tolerance as assessed by pain, erythema, edema, induration, and ulceration. The secondary objective of the study was to analyze the immunological responses to PCI-mediated vaccination, with endpoints of: induction of antigen-specific T-cells measured by enzyme-linked ImmunoSpot

(ELISpot) quantification of interferon-gamma (IFN-γ) releasing cells; and induction of KLH-specific antibodies.

The inclusion criteria included: Caucasian males or females, between 18 and 55 years of age, body mass index between 18.0 and 32.0 kg/m^2, body weight between 50 and 100 kg, and evaluated to be in good health. In addition, because the HPV16 E7 peptide antigens used are known to contain HLA-A2 restricted epitopes (18), subjects had to be human leukocyte antigen A2 (HLA-A2) positive to be included in the fimaporfin dose-finding part of the study (not a criterion in the safety run-in part, see below). The exclusion criteria included: i) known previous exposure to KLH or HPV16; ii) pregnancy or breastfeeding; iii) any medication (including steroids) within 14 days of the first dose administration, that could interfere with the study procedures or compromise safety.

Materials

The PCI photosensitizer fimaporfin [meso-tetraphenyl chlorin disulfonate ($TPCS_{2a}$)] was obtained from PCI Biotech (Oslo, Norway). Fimaporfin was provided at 30 mg/ml in 3% polysorbate 80, 2.8% mannitol, 50 mM Tris, pH 8.5 (Amphinex formulation) and was kept light protected at 2–8°C. The adjuvant poly-ICLC (Hiltonol) is a synthetic double-stranded RNA complex of poly(IC) stabilized with poly-L-lysine polylysine and carboxymethylcellulose (19). Hiltonol 2 mg/ml was purchased from Oncovir (Washington DC, USA) and kept at 2–8°C (when aliquoted it was used within 14 days). The vaccine antigens employed in the clinical study were: Human papillomavirus type 16 (HPV16) oncoprotein $E7_{1-35}$: MHGDTPTLHEYMLDLQPETTDLYCYEQLNDSSEEE and HPV16 $E7_{62-98}$: DSTLRLCVQSTHVDIRTLEDLLMGTLG IVCPICSQKP both produced according to Good Manufacturing Practice by PepScan (Lelystad, Netherlands). The HPV16 E7 peptides were stored at -70°C. Keyhole Limpet Hemocyanin 1 mg/ml (KLH: Immucothel®) was obtained from Biosyn Arzneimittel GmbH (Fellbach, Germany) and stored at 15–20°C.

Study Procedures

The vaccine components were mixed at the bedside within 15 min prior to injection using sterile, endotoxin-free 0.9% NaCl as diluent: 1) KLH Mix consisted of Hiltonol (50 μg), KLH (100 mg), and fimaporfin (0.75–50 μg); 2) HPV16 E7 Mix consisted of Hiltonol (50 μg), HPV16 $E7_{1-35}$ (100 μg), HPV16 $E7_{62-98}$ (100 μg), and fimaporfin (0.75–50 μg). After gentle mixing by hand, 150 μl was aspirated into a 0.3 ml syringe with a 30G needle (BD MicroFine® 39, Becton Dickinson, Franklin Lakes, USA) and injected intradermally (ID) to the subjects. 20 h (± 4 h) later, each injection site was exposed to 652 nm red light, delivered from a CE-marked PCI Biotech laser (produced by Modulight, Tampere, Finland). When not illuminated, the injection sites were covered by dark clothing, a bandage or dressing, for 14 days after the injections.

As is outlined in **Figure 1** the clinical study was conducted in two parts, the first part being a safety run-in to select the fimaporfin starting dose for the dose-finding part of the study. The run-in part was a sequential group, fimaporfin dose-reduction study to evaluate the safety and tolerability (pain and local reactions) of the components of PCI (fimaporfin and light), in the absence of antigen, when administered alone and in combination with Hiltonol. The fimaporfin doses tested (50 and 100 μg) were selected as they are known to be effective in mice and tolerable in minipigs (data not shown). Eight subjects were enrolled in two fimaporfin dose groups (**Table 1**); four subjects received 100 μg and four subjects received 50 μg. On day 1, each subject received a single ID dose of fimaporfin and a single ID dose of a mixture of Hiltonol and fimaporfin, at 2 separate injection sites. The illumination dose of 1 J/cm^2 was fixed, however the irradiance regimen was different in each fimaporfin subgroup, where two subjects received the dose as 5 mW/cm^2 for 200 s and the other two as 10 mW/cm^2 for 100 s.

Subsequently, a fimaporfin dose-finding part was performed to evaluate the safety, tolerability and immune responses when PCI was combined with the vaccine antigens and adjuvant. An antigen-adjuvant control group was included to enable a comparison of effects with and without PCI. The starting dose of fimaporfin and illumination was determined based on results from the safety run-in part of the study and fimaporfin doses of 0.75–50 μg were tested with a light dose of 1 J/cm^2. Overall, each subject received two doses of the KLH vaccine and three doses of HPV16 E7 vaccine (unless safety concerns or stopping criteria were met) given at separate, rotating injection sites in the upper arms and on the belly. The vaccine mixes were given as ID injections with 2 weeks between vaccinations.

Blood samples were drawn pre-treatment, 14 days after each vaccination and at the end of the study, 4 weeks after the last vaccination. Clinical assessments for safety as well as immunology endpoints were performed before and after each vaccination. Participants remained in the clinic from the day before dosing and for 24 h post ID dosing (control group), or 6 h post light exposure on day 2, 16, and 30, and returned for non-residential visits the following day and up to 4 weeks after last dosing.

Safety Measures in the Study

For safety reasons a sequential-group, sentinel dosing design was chosen for the dose-finding part of the study, as the impact of antigens and adjuvant in the presence of the photosensitizer fimaporfin and illumination was unknown. This part was conducted with two sentinel subjects, dosing cohorts of 1, 1 and 4 subjects on different days. Available safety data from the first sentinel subject ≥ 40 h post light dosing was evaluated by the investigator before dosing started for the second sentinel subject, and available safety data from the second sentinel (≥ 40 h post light dosing) was evaluated before dosing started for the remaining four subjects in the dose group. Similar evaluations of available safety data were done prior to the second and third dosing occasions for the second sentinel subject and the remaining four subjects within each dose group.

Prior to the second and third dosing of each individual, available safety data from the previous dosing in the individual was evaluated. If there were safety concerns in individual subjects, subsequent doses of one or both antigen/adjuvant combinations were not given to that particular subject. Subjects were withdrawn from dosing if they experienced a serious adverse event (SAE) or

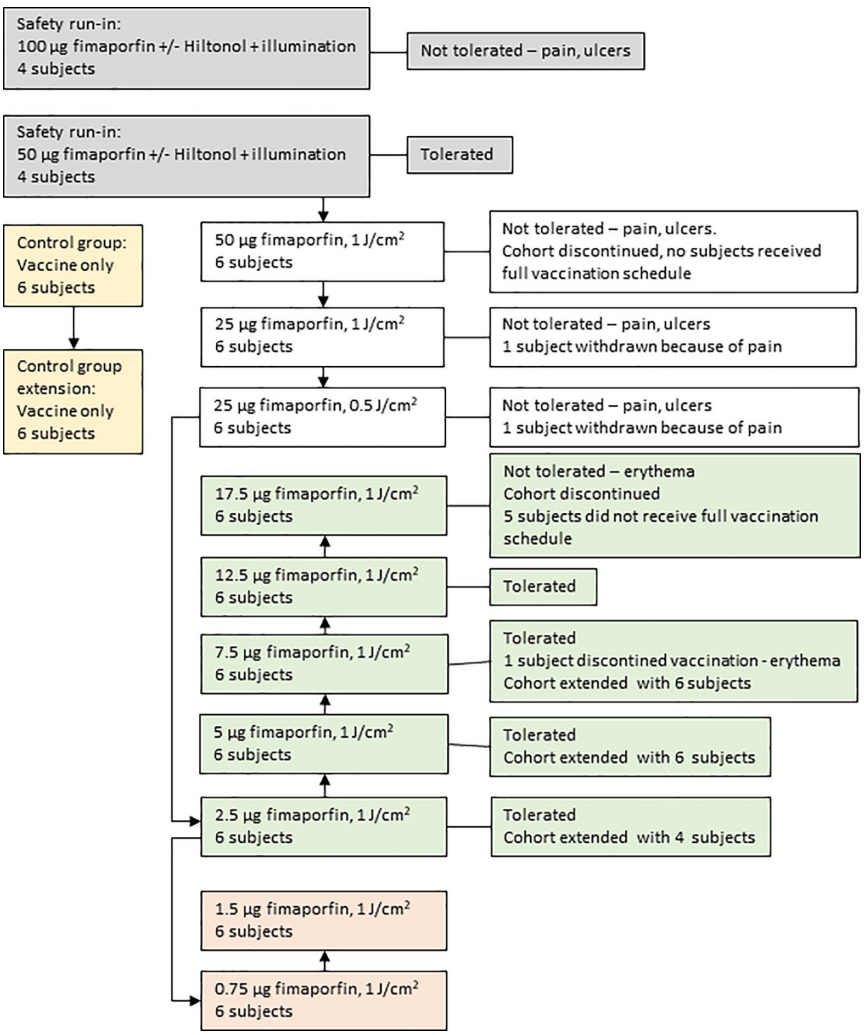


FIGURE 1 | Patient disposition. The flow of study subjects through the different phases of the study is outlined. Each study subject participated in one group only. The arrows depict the temporal relationships for the consecutive treatment of the different groups. As described in detail in the main text the study started with a safety run-in part (gray boxes) where a dose of 50 µg fimaporfin was found to be tolerated. The main study (white boxes) was then started with this dose, but because of the appearance of vaccination site ulcers in some subjects the dose was reduced to 25 µg. Also this dose was not tolerated, due to the occurrence of ulcers and pain during illumination. The fimaporfin dose was therefore reduced to 2.5 µg. This dose was well tolerated, and the dose was escalated (green boxes) up to 17.5 µg, which was not tolerated due to the development of erythema of a size that exceeded the cohort stopping criteria. Due to initial promising signs of immune responses in the 2.5 µg dose cohort, also the lower doses of 0.75 and 1.5 µg fimaporfin were included in the study (light red boxes). In parallel with the first dose cohorts a control group, receiving the vaccine without fimaporfin, was performed (yellow boxes). Based on the results obtained during the study the control group and several of the fimaporfin dose groups were extended with six or four additional study subjects (as indicated on the figure), meaning the at the end of the study a total of 12 subjects had been treated in the control group and 10, 12 and 12 in the 2.5, 5 and 7.5 µg dose groups, respectively.

TABLE 1 | Safety run-in treatment doses.

Subjects	**50 µg fimaporfin**				**100 µg fimaporfin**			
	n=2		**n=2**		**n=2**		**n=2**	
Injection site	1	2	1	2	1	2	1	2
Hiltonol (µg)	0	50	0	50	0	50	0	50
Irradiance (mW/cm^2)	5	5	10	10	5	5	10	10
Illumination duration (s)	200	200	100	100	200	200	100	100

Each subject received 2 ID doses of fimaporfin, with and without the addition of Hiltonol. Four subjects received the same fimaporfin dose where two subjects received same light irradiance and illumination duration.

had clinical signs of hypersensitivity reaction or cytokine release syndrome grade 3 or above considered to be possibly related to study treatment, or if they had grade 3 local administration site reactions or the presence of local administration site ulceration [as defined by the CTCAE criteria (Version 4.03 or later)].

Between each dose cohort, a Safety Review Committee (SRC) consisting of a minimum of the investigator, a sponsor representative, an independent immunologist, and a medical monitor, reviewed safety and tolerability data from a minimum of four subjects in the last dose group (up to at least 40 h after second dosing). An interim safety report, summarising results from all required safety assessments, was provided, and any clinically significant results were discussed before next dose cohort. Separate dose escalation decisions were made for each antigen. A minimum of 7 days separated the dosing of the last subject receiving their second dose in one group and dosing of the first subject in the next group.

Dose escalation would stop, or a lower dose be selected if ≥ 1 grade 3, or ≥ 2 grade 2, AEs of a similar nature within a dose group was considered related to the study drug. In addition, if ≥ 2 subjects in a group had grade 3 local administration site reactions (as defined above), presence of local administration site ulceration, or were not able to tolerate the complete light application, the dose would not be escalated. When the stopping criteria for a dose cohort were met, all subjects in that cohort discontinued further treatment. Doses where the stopping criteria were not met were regarded as safe and tolerable.

Safety Assessments

Safety monitoring included vital signs and clinical laboratory evaluations, physical examinations and 12-lead ECGs. Any adverse event (AE) and remedial actions required were recorded, and any clinically significant abnormalities identified during the course of the study were followed up until they returned to normal or could be clinically explained. Local tolerability at the dosing sites was assessed prior to and after each ID injection and light application (2, 6, 24, and 48 h post ID and light dosing), and involved evaluation of pain, erythema, edema, induration, and ulceration following individual scales for each measure. Local tolerability events of grade 3 included: *Pain*: Prevents daily activity or necessitated repeated use of narcotic pain reliever; *Erythema*: More than 100 mm; *Edema*: More than 100 mm; *Induration*: height: >1 mm. Local tolerability ratings of ≥ Grade 3 and/or the presence of ulceration were recorded as adverse events. Assessment of pain intensity at the injection site before, during, and after light exposure was assessed using a visual analogue scale (VAS) from 0 to 100 mm.

Immune Monitoring Analysis

Peripheral Blood Mononuclear Cells Isolation and Storage

Blood was collected in sodium heparin tubes from subjects prior to the vaccination (day 1) and post-vaccination on days 15, 29, 43, and 56. Peripheral blood mononuclear cells (PBMCs) for immune monitoring were isolated within 8 h of venipuncture by standard density gradient centrifugation using Histopaque (Sigma-Aldrich, St. Louis, USA). PBMCs were cryopreserved in Cell recovery (ThermoFisher, Waltham, USA) or CTL ABC (CTL, Shaker Heights, USA) freezing medium using Mr. Frosty (Sigma-Aldrich, St. Louis, USA). Cells were initially frozen at -80°C and transferred to liquid N_2 within 18–48 h.

ELISpot Analysis

To assess cellular immunity, an interferon-γ (IFN-γ) ELISpot assay was done to determine responses to HPV16 E7 and KLH. Cryopreserved PBMC samples were thawed in a 37°C water bath until a small piece of ice remained. The PBMCs were then immediately transferred to a 15 ml Falcon tube, and 10 ml (37°C) AIM-V medium (Thermo Fisher Scientific, Waltham, USA) containing 0.5 U/ml benzonase nuclease (Sigma-Aldrich, St. Louis, USA) was added drop-wise. Cells were centrifuged 10 min at 450 × g at room temperature (RT) and re-suspended in 10 ml AIM-V (37°C) (without benzonase). After a new centrifugation, cells were re-suspended in AIM-V (37°C) at $2x10^6$ cells/ml, split into 5 ml aliquots in 50 ml tubes (with the cap not completely closed to enable CO_2 exchange) and maintained overnight (20–24 h) in a cell incubator with a humidified atmosphere containing 5% CO_2 at 37°C (20, 21). Counting of viable cells was performed using trypan blue staining.

For the IFN-γ ELISpot assay the Human IFN-γ ELISpot^{PLUS} (ALP) kit (3420-4ALP-10, Mabtech, Nacka Strand, Sweden) was used according to the manufacturer's instructions. Shortly, the overnight rested cells were resuspended, and an aliquot was removed for cell counting. Cells were centrifuged at 450 g and re-suspended in AIM-V medium (37°C) at $2x10^6$ viable cells/ml. Then, 100 µl of each sample was added to the wells in the precoated ELISpot plate, 100 µl of AIM-V (37°C) containing concentrated stimulants was added for triplicate testing per condition and the plates were incubated for 20–22 h at 37°C. The HPV16 E7 peptides (the same as used for the vaccination) were dissolved in DMSO and added to the cell samples for a final concentration of 10 µg/ml, with a final DMSO concentration of 1.2%.

KLH was reconstituted in sterile solvent supplied in the kit and added to cell samples for a final concentration of 100 µg/ml. Concanavalin A (1 µg/ml final; Sigma-Aldrich, St. Louis, USA) and CEFx peptides (1 µg/ml final) (JPT Peptide Technologies Berlin, Germany) were added to the samples in separate wells as positive controls, while cells incubated with medium only served as a negative control. Each batch of tested subjects (typically 3 subjects at a time) was accompanied by testing the same PBMCs from a healthy donor (reference sample) against medium, CEFx, and ConA. Testing results of this reference control revealed robust and similar antigen and mitogen responses at all testing dates. The next day cells were removed from the plate and the wells were washed 5 times with PBS before the addition of 100 µl 1 µg/ml biotinylated monoclonal Antibody 7-B6-1 working solution. Following incubation at RT for 2 h and 5 washes, the plates were incubated with Streptavidin-ALP for 1 h before washing again. The plates were developed until spots emerged (usually around 3 min) using the substrate BCIP/NBT dissolved in deionized water. Plates were left to dry in the dark and spots

were enumerated at ZellNet Consulting Inc. (Fort Lee, USA) with a KS ELISpot reader (Zeiss, Thornwood, USA), using Software version KS ELISpot 4.9.16 following the International harmonization guidelines for ELISpot plate evaluation (22).

The Limit of Detection (LOD) in the ELISpot assay was determined from the actual trial subjects tested. Using the spot counts in the negative control wells from all the samples, the median spot count was calculated to be 5. Therefore, using a signal: noise ratio of 3:1 for defining the LOD, 15 spots was considered the LOD for this study. This LOD was used as the basis for calculations of response rates.

Two definitions for an antigen-specific response were used: i) A statistical Distribution-Free Resampling (DFR) test in the setting where triplicate wells were available for all antigens (23). The DFR test provides two results: I. for any statistical difference [DFR(eq) testing results, less stringent], and II. for statistical differences which are at least 2-fold above the negative control [DFR(2x), more stringent testing] ii) An empirical rule of 2-fold or greater difference between the mean antigen spot counts compared to the mean negative control spot counts. For both tests, the average antigen spot count had to be greater than or equal to the global LOD of 15 spots to be considered a response.

The response to treatment was defined with the following rules: i) If there was no pre-existing response measured on day 1), but there was a response, measured at any of the following time points ii) If there was a pre-existing response, a response measured at any of the following time points had to be at least 2x as high as the response measured on day 1.

Flow Cytometry Analyses

To assess functional responses of CD4+ and CD8+ T-cells in response to stimulation with HPV16 E7 peptide pools, flow cytometry analysis was performed. Thawed PBMC samples were resuspended in Iscove's Modified Dulbecco's Medium (IMDM, Lonza, Basel, Switzerland), supplemented with 2mM L-glutamine, 100 U/ml penicillin, 100 µg/ml streptomycin (all from Life Technologies, Waltham, USA), and 10% human serum albumin (Albuman®; Sanquin Plasma Products BVAmsterdam, Netherlands) and plated in 6-wells plates (days 29, 43, and 57 were separately put into culture). The cells were stimulated with peptide pools consisting of HPV16 E7 1-35 (35-mer) + E7 61-82 (22-mer) + E7 64-98 (35-mer). The next day T-cell growth factor (TCGF; ZeptoMetrix, Buffalo NY, USA) and Interleukin-15 (IL-15; Peprotech, London, UK) was added to the bulk cultures as described previously (24, 25). The cells were cultured for 10 days (only medium with Albumin was added when required, mostly on day 7). Thawed PBMC samples (1–4 x 10^6 cells/ml) from the corresponding day 15 samples were used for monocyte adherence in 48-wells plates (0.5 ml/well) to be used as APCs. These monocytes were cultured in X-vivo 15 medium (Lonza, Basel, Switzerland) and incubated with 800 IU/ml Granulocyte-macrophage colony stimulating factor (GM-CSF; Invitrogen, Waltham, USA) for 3 days and subsequently loaded overnight separately with the following peptide pools: i) HPV16 E7 1-35 (10-mer peptides): 1-10, 2-11, 5-14, 7-16, 10-19, 11-20, 15-24, 20-29, 26-35; ii) HPV16 E7 62-98 (10-mer peptides): 62-71, 63-72, 70-79, 73-82, 77-86, 78-87, 80-89, 82-91, 85-94, 89-98; iii) HPV16 E7 (22-mer peptides): 1-22, 11-32, 21-42, 61-82, 71-92, 77-98. Monocytes loaded with Staphylococcus enterotoxin B (SEB, Sigma) served as a positive control, and monocytes in X-vivo 15 medium only as a negative control. The 10-days cultured PBMCs were harvested, resuspended in IMDM with Albumin (2 x 10^6 cells/ml) and added to the peptide loaded monocytes (0.5 ml/well). Brefeldin A was added after 1 h (final concentration 10 µg/ml) to prevent cytokine secretion, and the cells were after overnight stimulation harvested and subjected to intracellular cytokine staining (24, 25). Staining was done for the following markers: T-cell markers CD3, CD4, and CD8; cytokines IFN-γ, TNF-α and IL-2; and activation markers CD154 and CD137. A time-gate was set to exclude any regions of sheath flow fluctuations that could result in false-positive or false-negative events (gating tree shown in **Supplementary Figure 1**). To determine whether samples were reactive to HPV16 E7 (or the positive control SEB), measured T-cell responses were considered positive if they consisted of ≥10 events within the gate, and their frequency was at least twice that in the matched negative control (medium only). Reported results are background-subtracted except if noted otherwise.

KLH IgG Antibody Analysis

Serum samples collected from subjects before vaccination, 14 days after each vaccination and at the end of the study (6 weeks after last KLH vaccination) were analyzed for anti-KLH IgG using an ELISA assay (Alpha Diagnostics, San Antonio, USA). The ELISAs were performed with dilutions of positive and naïve anti-KLH IgG human serum samples and the subject samples were tested in 5 dilutions. The ELISA plate was read using a Spectramax 340PC plate reader at 450 nm. The anti-KLH IgG in a sample was determined using an antibody cut titration method. The concentration of each sample was calculated, and the average of diluted samples was determined.

RESULTS

Subject Disposition

As outlined in **Figure 1**, In total 96 healthy volunteers participated in this study; 8 in the safety run-in part and 88 in the fimaporfin dose-finding part of the study. In this dose-finding part, 12 of the 88 subjects were enrolled in the control group and 76 subjects were treated with different doses of fimaporfin (**Figure 1** and **Table 2**). The 8 subjects in the safety run-in part received fimaporfin alone or in combination with Hiltonol as shown in **Table 1**. In the 100 µg fimaporfin dose group, four adverse events of grade 1 local ulceration in three patients were reported, in addition to injection site paresthesia (one event) and extravasation (one event) all being suspected as related to study treatment (**Table 3**). In the 50 µg group, no ulcerations or other prominent local reactions were observed, and 50 µg was therefore selected as the starting dose for the fimaporfin dose-finding part of the study. There were no apparent differences in safety events between subjects receiving

TABLE 2 | Baseline characteristics and dose groups assignment of subjects in the fimaporfin dose-finding part.

Dose group		Control (N=12)	Low (N=46)	Intermediate (N=6)	High (N=6)	Non-tolerated (N=18)	Overall (N=88)	Safety run-in (N=8)
Fimaporfin dose		0 µg	0.75– 7.5 µg	12.5 µg	17.5 µg	25–50 µg	0– 50 µg	50– 100 µg
Age, years (median, range)		33 (19–55)	34–42 (19–53)	44 (21–52)	44 (25–55)	30–47 (19–55)	36 (19–55)	45 (21–55)
Sex	Male	9 (75.0%)	37 (80.4%)	5 (83.3%)	4 (66.7%)	12 (66.7%)	67 (76.1%)	4 (50.0%)
	Female	3 (25.0%)	9 (19.6%)	1 (16.7%)	2 (33.3%)	6 (33.3%)	21 (23.9%)	4 (50.0%)
Race	White	12 (100.0%)	46 (100.0%)	6 (100.0%)	6 (100.0%)	18 (100.0%)	88 (100.0%)	8 (100.0%)
Ethnicity	Not Hispanic or Latino	11 (91.7%)	46 (100.0%)	6 (100.0%)	6 (100.0%)	17 (94.4%)	86 (97.7%)	8 (100.0%)
	Hispanic or Latino	1 (8.3%)	0 (0.0%)	0 (0.0%)	0 (0.0%)	1 (5.6%)	2 (2.3%)	0 (0.0%)

Median (range) or number of subject (with percentage) are given for the different characteristics.

TABLE 3 | Any Related TEAEs reported in Safety Run-In part.

Dose group	50 µg fimaporfin (N=4)		100 µg fimaporfin(N=4)	
Preferred Term	**Mild**	**Moderate**	**Mild**	**Moderate**
Any related TEAE	–	1 (25.0%) [1]	4 (100.0%) [6]	–
Local TEAE	–	–	4 (100.0%) [6]	–
IS ulcer	–	–	3 (75.0%) [4]	–
IS extravasation	–	–	1 (25.0%) [1]	–
IS paresthesia	–	–	1 (25.0%) [1]	–
Systemic TEAE	–	1 (25.0%) [1]	–	–
Syncope	–	1 (25.0%) [1]	–	–

AEs were considered to be local symptoms were anywhere the MedDRA Preferred Term contained the term 'Injection site'. For Related to Study Treatment this counts all TEAE that have been recorded as having a suspected relationship to study treatment with and/or without red light. N, Number of subjects studied; (), Percentage of subjects with adverse events; [], Number of adverse events. Events were coded using MedDRA (Version 19.0).

illumination at 5 mW/cm^2 and subjects being illuminated with 10 mW/cm^2; and an irradiance of 5 mW/cm^2 for 200 s, giving an illumination dose of 1 J/cm^2, was chosen for the dose-finding part of the study. Although there were few patients in this safety run-in part of the study, the results indicated that the local reactions observed were mainly due to the photochemical treatment with fimaporfin, since there was no clear difference between the injection sites with or without Hiltonol.

As shown in **Figure 1** the subjects enrolled into the fimaporfin dose-finding part were divided over 10 cohorts, each consisting of 6–12 healthy volunteers, who received fimaporfin doses from 0.75 µg to 50 µg. The control group (n=12) received Hiltonol and vaccine antigens only, whereas the fimaporfin groups received PCI (fimaporfin + light) in addition to Hiltonol and vaccines. All groups received the same dose of Hiltonol and vaccine antigens, and up to five injections (**Figure 2**).

Safety and Tolerability of PCI Mediated Vaccination

ID vaccination with PCI was safe and well tolerated (**Table 4**), and no SAEs were reported in the study. Overall, 27 of the 88 subjects (30.7%) in the dose-finding part reported 53 treatment emergent AEs (TEAEs), of which 34 were local symptoms and 19 were systemic reactions. The majority of the reported events were classified as mild, but 4 subjects in the highest dose groups (25 µg and 50 µg fimaporfin) reported five moderate TEAEs that were classified as related to the study treatment; four of these events were local reactions at the injection site. Systemic AEs related to study treatment were all mild except 1 moderate event of procedural site reaction (25 µg). Only 2 of the reported systemic symptoms (headache and procedural reaction) were reported by ≥ 2 subjects. There were 13 more different systemic AEs, each one reported by one subject, and only at one time-point. All laboratory abnormalities were classified as not related to the study intervention.

In the 50 µg dose group stopping criteria were met, as two subjects developed injection site ulceration grade 2 at one or both injection sites (three events) (**Tables 5** and **6**). The dose was therefore reduced to 25 µg, which significantly decreased the side effects. Although stopping criteria were not met, this dose was deemed as poorly tolerated with regards to pain during illumination. Two subjects at this dose were not able to receive the full light dose at one or both injection sites (one of the subjects was withdrawn from the study due to pain during illumination). Because of the pain issue with the 25 µg fimaporfin cohort, the fimaporfin dose was substantially reduced, to 2.5 µg, and a dose escalation was performed from this dose level. The 2.5 µg dose was well tolerated, as were doses of 5, 7.5 and 12.5 µg. At 17.5 µg three subjects developed local administration site reactions of erythema that were generally

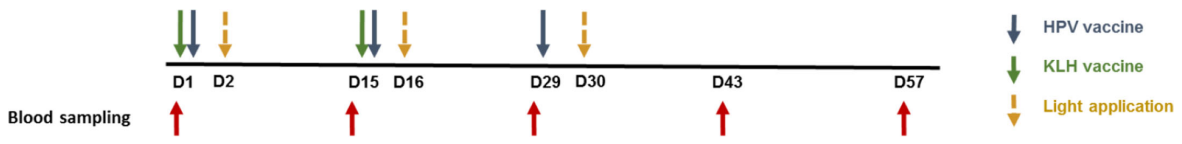


FIGURE 2 | Treatment and blood sampling schedule. Subjects could receive three doses of HPV vaccine, and two doses of KLH vaccine given at 2 weeks intervals. Blood samples were collected pre- and post-vaccination at the time points indicated by red arrows.

TABLE 4 | Any TEAEs related to study treatment reported by ≥ 2 subjects.

Dose group Fimaporfin dose	Control (N=12) 0 µg		Low (N=46) 0.75–7.5 µg		Intermediate (N=6) 12.5 µg		High (N=6) 17.5 µg		Non-tolerated (N=18) 25–50 µg		Overall (N=88) 0–50 µg	
Preferred Term	**Mild**	**Moderate**	**Mild**	**Moderate**	**Mild**	**Moderate**	**Mild**	**Moderate**	**Mild**	**Moderate**	**Mild**	**Moderate**
Any related TEAE	4 (33%) [4]	–	6 (13%) [7]	–	1 (17%) [1]	–	5 (83%) [13]	–	9 (50%) [23]	4 (22%) [5]	25 (28%) [48]	4 (5%) [5]
Local TEAE	3 (25%) [3]	–	5 (11%) [6]	–	1 (17%) [1]	–	5 (83%) [12]	–	6 (33%) [8]	3 (17%) [4]	20 (23%) [30]	3 (3%) [4]
IS vesicles	–	–	2 (4%) [2]	–	–	–	3 (50%) [7]	–	2 (11%) [2]	–	7 (8.%) [11]	–
IS pruritus	3 (25%) [3]	–	2 (4%) [2]	–	–	–	–	–	2 (11%) [4]	–	7 (8.%) [9]	–
IS pain	–	–	–	–	1 (17%) [1]	–	1 (17%) [1]	–	1 (6%) [1]	1 (6%) [1]	3 (3%) [3]	1 (1%) [1]
IS ulcer	–	–	–	–	–	–	–	–	1 (6%) [1]	2 (11%) [3]	1 (1%) [1]	2 (2%) [3]
IS reaction	–	–	1 (2%) [2]	–	–	–	1 (17%) [1]	–	–	–	2 (2%) [3]	–
IS erythema	–	–	–	–	–	–	2 (33%) [2]	–	–	–	2 (2%) [2]	–
IS scab	–	–	–	–	–	–	1 (17%) [1]	–	–	–	1 (1%) [1]	–
Systemic TEAE	1 (8%) [1]	–	1 (2%) [1]	–	–	–	1 (17%) [1]	–	8 (44%) [15]	1 (6%) [1]	11 (13%) [18]	1 (1%) [1]
Headache	1 (8%) [1]	–	–	–	–	–	–	–	3 (17%) [3]	–	4 (5%) [4]	–
Procedural site reaction	–	–	–	–	–	–	1 (17%) [1]	–	–	1 (6%) [1]	1 (1%) [1]	1 (1%) [1]

AEs considered to be local symptoms were anywhere the MedDRA Preferred Term contained the term Injection site (IS)'. For Related to Study Treatment this counts all TEAEs that have been recorded as having a suspected relationship to study treatment with and/or without red light. N, Number of subjects studied; (), Percentage of subjects with adverse events; [], Number of adverse events. Events were coded using MedDRA (Version 19.0).

TABLE 5 | Total 14 subjects discontinued dosing either due to development of AEs or Dose stopping criteria being met in the cohort.

Fimaporfin dose	Subject	Reason for discontinued treatment
50 µg	207	Cohort discontinued
	208	Cohort discontinued
	209	Ulceration (Stopping criteria met)
	210	Cohort discontinued
	211	Cohort discontinued
	212	Ulceration (Stopping criteria met)
25 µg	215	Unable to tolerate light dose[1]
	224	Unable to tolerate light dose[2]
17.5 µg	250	Cohort discontinued
	251	Cohort discontinued
	252	Erythema (Stopping criteria met)[3]
	253	Cohort discontinued
	254	Erythema (Stopping criteria met)[3]
7.5 µg	264	Local reaction/erythema[3]

When the stopping criteria for a dose cohort was met, all subjects in that cohort discontinued further treatment. [1]withdrawn after second ID dosing due to pain (completed 2 KLH doses but only one HPV dose), [2]withdrawn due to pain during first dosing (physician decision), [3]local erythema ≥10 cm in ≥2 subjects.

mild, but exceeded 10 cm (**Figure 3**), thereby meeting the dose stopping criteria.

Although pain was generally not a problem at doses lower than 25 µg fimaporfin, pain scores during illumination were variable between subjects, and mild pain was also observed in some subjects in the lower dose groups. The pain usually vanished immediately after the end of light application.

As will also be apparent from **Figure 1**, altogether 14/88 (15.9%) subjects in the fimaporfin dose-finding part discontinued dosing; seven subjects discontinued due to AEs (all being local injection site events) and seven subjects due to their study cohort reaching predefined stopping criteria (50 and 17.5 µg dose groups) (**Tables 5** and **6**). Discontinuation AEs were ulcerations (moderate) in two subjects in the highest dose group (50 µg), mild erythema in three subjects [17.5 µg (n=2) and 7.5 µg (n=1)], and pain during light application in two subjects [not able to receive the full light dose (25 µg)]. None of the subjects in the 50 µg dose completed the full HPV or KLH vaccination regimen, and in the 17.5 µg dose group, one subject received only one HPV dose, four subjects received two doses and only one subject completed all three HPV doses. In addition, one subject in the 7.5 µg dose group did not receive the third HPV dose.

Taken together, PCI could be safely applied to intradermal vaccination in humans, with no unexpected and mostly mild systemic AEs. At higher dose levels there were some local tolerability issues, but doses below 17.5 µg fimaporfin were well tolerated and are suitable for use in later studies.

Immune Responses to KLH and HPV16 E7 Peptide Vaccination

The humoral response to KLH was measured in the control and 2.5-12.5 µg fimaporfin dose groups. The titer of circulating KLH-specific IgG antibodies increased in all the study subjects after the second vaccination. However, as compared to the control group, the response in vaccinated patients co-treated with PCI at a fimaporfin dose of 12.5 µg displayed a >3-fold higher KLH antibody titer at days 28 [p=0.039, t-test (unpaired, two-tailed)]

TABLE 6 | Subject Treatment Disposition.

Fimaporfin dose	Subjects	Completed all vaccinations		Completed HPV vaccinations			Completed KLH vaccinations	
	(N=)	HPV	KLH	1st dose	2nd dose	3rd dose	1st dose	2nd dose
0	12	12 (100%)	12 (100%)	12 (100%)	12 (100%)	12 (100%)	12 (100%)	12 (100%)
0.75 µg	6	6 (100%)	6 (100%)	6 (100%)	6 (100%)	6 (100%)	6 (100%)	6 (100%)
1.5 µg	6	6 (100%)	6 (100%)	6 (100%)	6 (100%)	6 (100%)	6 (100%)	6 (100%)
2.5 µg	10	10 (100%)	10 (100%)	10 (100%)	10 (100%)	10 (100%)	10 (100%)	10 (100%)
5 µg	12	12 (100%)	12 (100%)	12 (100%)	12 (100%)	12 (100%)	12 (100%)	12 (100%)
7.5 µg	12	11 (92%)	12 (100%)	12 (100%)	12 (100%)	11 (92%)	12 (100%)	12 (100%)
12.5 µg	6	6 (100%)	6 (100%)	6 (100%)	6 (100%)	6 (100%)	6 (100%)	6 (100%)
17.5 µg	6	1 (17%)	5 (83%)	6 (100%)	5 (83%)	1 (17%)	6 (100%)	5 (83%)
25 µg	12	10 (83%)	11 (92%)	11 (92%)	10 (83%)	10 (83%)	11 (92%)	11 (92%)
50 µg	6	0 (0%)	2 (33%)	6 (100%)	2 (33%)	0 (0%)	6 (100%)	2 (33%)

*Subjects in the fimaporfin dose-finding part could receive up to 3 doses with HPV and 2 doses with KLH, Subjects in the highest dose groups discontinued treatment due to cohort stopping criteria being met or for safety reasons (see **Table 5**).*

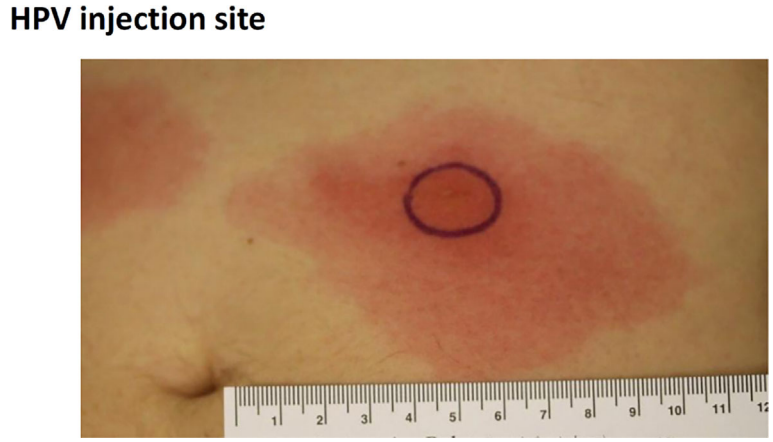


FIGURE 3 | Development of vaccination site erythema induced discontinuation of treatment in the 17.5 µg dose cohort. The figure shows an example of erythema > 10 cm developed after PCI-mediated vaccination in the 17.5 µg fimaporfin dose group. Vaccination was performed on the belly, and the picture was taken after the second vaccination, 24 h after illumination. The black circle denotes the illuminated area.

and 43 (p=0.030) (**Figure 4A**). Notably, the response in the 12.5 µg fimaporfin group was more consistent with strong responses observed in all subjects, while a rather weak antibody response (< 5000 units) was observed in two of the six subjects in the control group (**Figure 4B**).

Antigen specific T-cells responses were analyzed by IFN-γ ELISpot as well as by multiparametric flow cytometry. Vaccination in the absence, or with low doses, of fimaporfin did not result in mean HPV-specific T-cell reactivity detectable above the LOD (15 spots per 200,000 cells, see *Materials and Methods*) in the ELISpot assay (**Figure 5**). However, a T-cell response was detected in the groups receiving co-treatment with 12.5 and 17.5 µg fimaporfin, amounting to mean spot count between 20 and 30 spots per 200,000 cells. The PCI enhanced response to HPV peptide vaccination was first observed 14 days after the second vaccination (day 29), reached a peak 2 weeks after the third vaccination (day 43), and declined at day 57 (28 days after the third vaccination). The HPV reactivity in the 17.5 µg dose group seems to taper off to a larger degree than in the 12.5 µg group, which is likely due to the missing third vaccination dose in five of six subjects the 17.5 µg fimaporfin group. In the 25 and 50 µg dose groups the ELISpot results did not seem to differ from what was observed in the control group. Thus, there seem to be a peak of immune enhancement in the 12.5–17.5 µg dose range.

Using the response criterion defined in *Materials and Methods*, the number of responders to HPV vaccination in the different dose groups was assessed based on the ELISpot results. As can be seen from **Figure 6A**, PCI co-treatment at doses of 12.5 or 17.5 µg fimaporfin strongly increased the number of subjects responding to vaccination. While only 8% of the control subjects showed a response, the response rate in the 12.5 and 17.5 µg dose groups was 83% and 67%, respectively. **Figure 6B** shows the kinetics of the responses, indicating that a considerable number of responses were seen already after two vaccinations, but that adding a third vaccination further increased the response rate. The number of responders to vaccination with KLH was also assessed by ELISpot. There was a significant

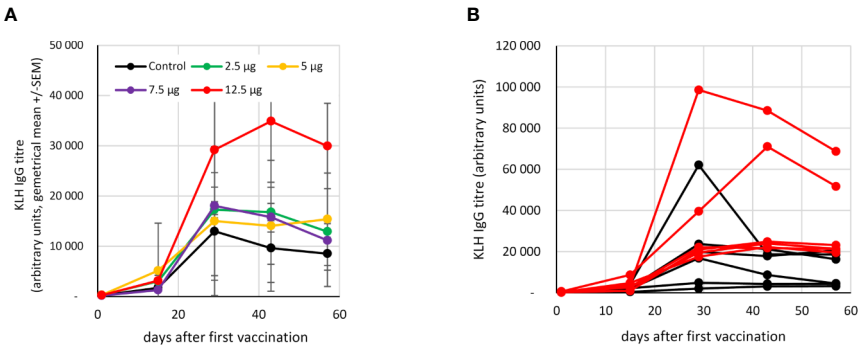


FIGURE 4 | Antibody response to KLH vaccination. The presence of anti-KLH IgG was analysed by ELISA as described under *Materials and Methods*. Vaccinations were performed at days 1 and 15. **(A)** Geometrical mean (+/- SEM) of IgG titres in different fimaporfin dose groups. **(B)** IgG titres at the different time points in single study subjects in the control (black lines) and the 12.5 µg fimaporfin (red lines) groups.

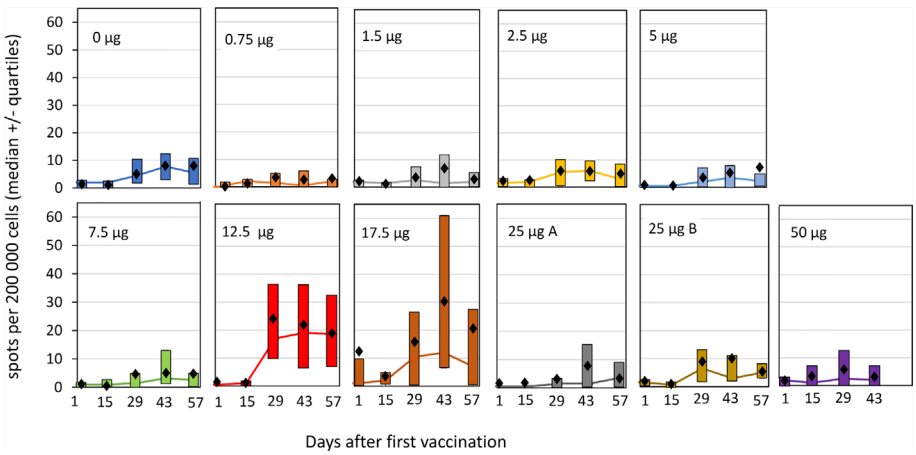


FIGURE 5 | ELISpot responses against HPV16 E7 by cohorts and timepoint. PBMCs from the study subjects were isolated before and at different time points after vaccination, and subjected to ELISpot analysis after re-stimulation with the HPV E7 peptides used for the vaccination, as described under *Materials and Methods*. The spot counts for each sample were background corrected for simplified interpretation by subtracting the mean of the negative control wells from each donor from each antigen measurement from that donor. If the difference was <0, it was set to a value of 0. Each panel shows the result for an individual dose group. The lines indicate median values with the upper and lower quartiles indicated by the boxes. Mean values are shown as black diamonds. Group 25 µg A received the normal light dose of 1 J/cm^2 at an irradiance of 5 mW/cm^2, group 25 µg B received a light dose of 0.5 J/cm^2 at an irradiance of 2.5 mW/cm^2.

response rate in all study groups, including 50% of the control group. However, this was increased to 100% when PCI co-treatment with 12.5 and 17.5 µg fimaporfin was given (**Supplementary Figure 2**).

In order to determine the phenotype of the T-cells responding to vaccination, PBMCs from the control group, the 2.5 µg and the 12.5 µg fimaporfin dose groups were stimulated *in vitro* and re-stimulated with different HPV16 E7 peptide mixes before being evaluated by multiparametric flow cytometry The 2.5 µg fimaporfin group was selected in addition to the control group and the 12.5 µg fimaporfin group since CD8 responses have been observed already at this dose level in mouse studies (Høgset, unpublished). The functional markers analyzed were the cytokines IFN-γ, IL-2 and TNF-α as well as the activation markers CD137 and CD154. Since the cell expansion step employed in this assay introduces possibilities for skewing of the samples, we did not use this assay for performing exact quantitative comparisons of differences in response, but rather a qualitative assessment of T-cell reactivity was performed.

The flow cytometry analysis revealed HPV-specific CD4+ T-cell responses in all tested subjects, with the exception of a borderline response in one of the control subjects (#205; **Supplementary Figure 3**). Thus, with this very sensitive assay there was no obvious difference in CD4+ T-cell responses between the control and the PCI treated groups, in contrast to what was observed with the more stringent *ex vivo* ELISpot assay.

The results also indicate that a significant fraction of the CD4+ T-cells co-express multiple functional markers, and

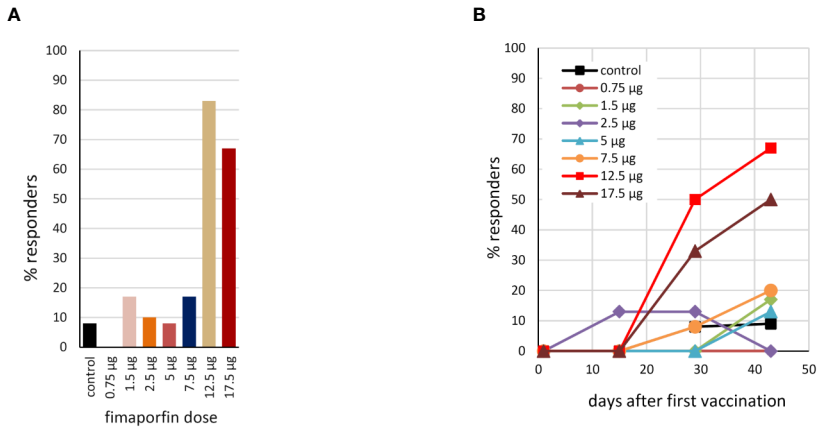


FIGURE 6 | Percentage of responders to HPV16 E7 vaccination. **(A)** Based on the IFN-γ ELISpot analysis (re-stimulation with the HPV16 E7 peptides used for vaccination), the percentage of responders to the vaccination within each dosage group was calculated using as response definition: HPV response at any time after day 1; no pre-existing response. 2-fold empirical rule with median sport counts > 20 spots per 200,000 cells (see also *Materials and Methods*). **(B)** The kinetics of the response for each dose group, using the DFR(2x) response criterion (see *Materials and Methods*).

following stimulation with HPV16 E7 22-mer, the proportion of cells simultaneously expressing all four functions (CD154, IFN-γ, IL-2, and TNF-α) or the combinations of CD154, IFN-γ and TNF-α and CD154, IL-2 and TNF-α appears to be larger in the 2.5 and 12.5 µg dose groups, as compared to the control group (**Supplementary Figure 4**).

CD8+ T-cell responses to the positive control SEB were relatively consistent across time-points for individual subjects for the production of IFN-γ, TNF-α, and CD154, with the expression of IL-2 and CD137 being less consistent (**Supplementary Figure 5**). There seemed to be a lower reactivity to the SEB antigen in some of the subjects in the 12.5 µg dose group (notably subjects 244, 245, and 248). This might indicate a lower quality of the cells in these samples, but the fact that some of these samples show an HPV E7 response for functional markers (**Figure 7**) may indicate that the low response seen with the SEB positive control was due to natural individual variations in the SEB response rather than an impairment of the cell samples. A CD8+ T-cell response to the HPV16 E7 22-mer peptides at least at one time-point was detected in three of the six tested control subjects and in 6/6 and 4/6 subjects in the 2.5 µg and 12.5 µg fimaporfin groups, respectively (**Figure 7**). While no subjects in the control groups developed a response at two or more timepoints, such responses were observed for 3/6 subjects both in the 2.5 and in the 12.5 µg dose groups (**Figure 7**). Furthermore, 1/6 and 2/6 subjects exhibited HPV E7 22-mer-specific responses at all 3 time-points tested in the 2.5 and 12.5 µg dose groups, respectively (**Figure 7**).

While the cells in the control group samples produced only CD154 or IFN-γ, samples from the 2.5 µg dose group exhibited any of the four functional markers (IFN-γ, IL-2, TNF-α, CD154), with subject 225 (d43) producing both IFN-α and IL-2, and subject 228 (d43) producing both IFN-γ and TNF-α. Samples from the 12.5 µg dose groups showed production of any of the four functional markers, in some cases with co-production of IFN-γ and CD154 (243 d43), IL-2 and CD154 [subject 243 (d57)], or even IFN-γ, TNF-α, and CD154 [subject 243 (d29), subject 244 (d29)].

The multifunctionality of the CD8+ T-cell response to HPV E7 22-mer stimulation was further analyzed using pie charts highlighting all the possible combinations of functional markers measured. **Figure 8A** illustrates the resulting pie charts for those samples that yielded a positive response (see **Figure 7**). The **Figure 8A** pie charts appear to have a higher diversity of responses than the **Figure 7** histograms might indicate; this is due to the fact that the pie chart data is not background-subtracted. The results indicate that at least some of the cells co-express multiple functional markers, as visualized by the turquoise-to-red pie segments. Such multi-functional cells represent a larger proportion of total responding CD8+ T-cells in subjects that were treated with PCI (2.5 and 12.5 µg dose groups) than in control subjects, with the proportion of cells expressing any combination of three or four functional markers being about 4 times higher in the 12.5 µg dose group than in the control group (**Figure 8B**).

DISCUSSION

It has previously been shown that the PCI technology with the photosensitizing compound fimaporfin ($TPCS_{2a}$) gives a strong enhancement of MHC class I presentation of peptide antigens in antigen presenting cells *in vitro* (4), and that this effect can be exploited to improve the CD8+ T-cell response to peptide and protein vaccination in mice (3–9). The present work represents the first study to translate these pre-clinical findings into the clinical setting, through a phase I dose-finding study using the PCI technology for vaccination with peptide and protein

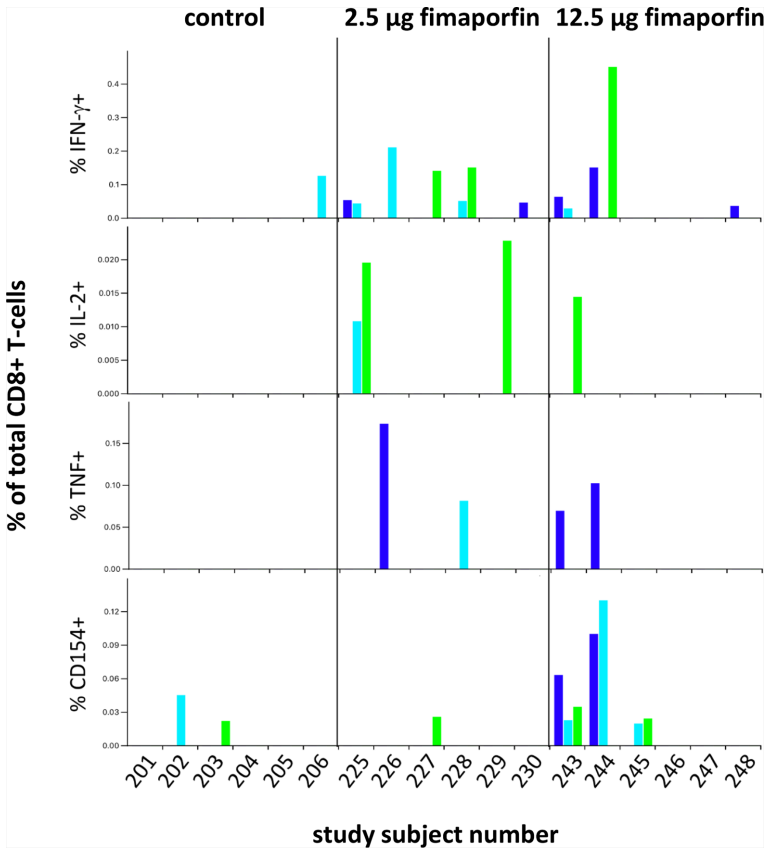


FIGURE 7 | CD8+ T-cell responses to HPV16 E7 peptides. The expression of IFN-γ, IL-2, TNF-α, and CD154 was assessed in CD8+ T-cells following stimulation with HPV16 E7 22-mer peptides (described under *Materials and Methods*) for each analyzed sample. Results for the three time-points [d(ay)29, d43, d57] are indicated by the colored bars: d29 dark blue, d43 light blue, and d57 green. All measurements have been background-subtracted.

antigens in combination with the adjuvant poly-ICLC (Hiltonol). The primary objective of the study was to assess the safety of intradermal vaccination with PCI in combination with Hiltonol, and to define a fimaporfin dose suitable for use in later clinical studies. The results showed that the use of the PCI/Hiltonol combination in humans was safe, with generally mild adverse events localized at the site of vaccination, and identified fimaporfin doses lower than 17.5 µg as well tolerated, with higher doses being less tolerable due to local reactions. The secondary objective of the study was to assess immune responses induced by PCI-mediated vaccination, and the results indicated that the employment of PCI increased the number of subjects that exhibited a T-cell response to an HPV long peptide vaccine over what was achieved with the antigen/Hiltonol combination without PCI. Moreover, the use of PCI seemed to result in a more consistent and multifunctional CD8+ T-cell response.

It is well established that photodynamic therapy of e.g. skin cancer can induce substantial pain in a significant fraction of the patients and that high dose photochemical treatment doses can induce skin ulcers (26). Thus, in the clinical study we first conducted a safety run-in part in order to define a photochemical dose that would be tolerable as the starting dose for the main study part (fimaporfin dose-finding part). For the run-in study, a starting dose of 100 µg fimaporfin was selected, as this dose has been shown to induce immune responses in mice; and also had good tolerability in minipigs. However, in the present study, the highest doses of fimaporfin (50 and 100 µg) were not tolerated due to development of ulcers at the injection site. Ulcerations have also been reported with other vaccination technologies using adjuvants (27) and is not uncommon e.g. in a setting of therapeutic cancer vaccination. Although the local tolerability was significantly better at the 25 µg dose, it was still not deemed acceptable due to pain during illumination in some of the study subjects. The starting dose for the fimaporfin dose escalations was therefore reduced to 2.5 µg, which was well tolerated, as were doses of 5, 7.5, and 12.5 µg. Development of mild erythema was seen at 17.5 µg and dose escalation stopping criteria for the study were met as these exceeded 10 cm in longest diameter. Fimaporfin doses of 0.5 and 1.5 µg fimaporfin were also tested, and as could be expected these doses exhibited excellent tolerability, with only mild local reactions and negligible pair being observed.

Local tolerability events increasing with the fimaporfin dose levels was the only safety issue observed with the PCI vaccination regimen tested, systemic adverse reactions were generally mild

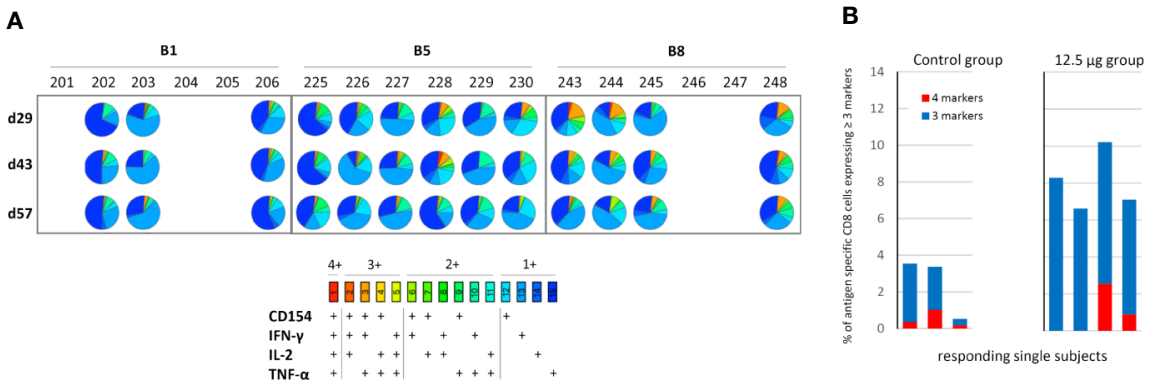


FIGURE 8 | Analysis of CD8+ T-cell multifunctionality. PBMCs were incubated with pools of HPV peptides for 10 days, re-stimulated with HPV E7 22-mer peptides, stained with antibodies recognizing various surface and functional markers (CD3, CD4, CD8, IFN-γ, TNF-α, IL-2, CD154), and analysed by flow cytometry as described under *Materials and Methods*. **(A)** Assessment of the co-expression of CD154, IFN-γ, IL-2, and TNF-α. The pie charts illustrate the relative representation of cells co-expressing all four, different combinations of three, different combinations of two, or only a single of these functional markers within total functional cells (i.e. all cells that are positive for CD154 and/or IFN-γ and/or IL-2 and/or TNF), for those samples that had measurable CD8+ T-cell responses to HPV16 E7 peptide re-stimulation as defined in *Materials and Methods*. The data are not background-subtracted. **(B)** Percentage of CD8-cells expressing multiple (≥3) functional markers. Results are shown for each subject defined as a responder under the criteria described in *Materials and Methods*.

and of a character that is expected in a vaccination study. Thus, PCI-mediated vaccination with fimaporfin doses below 17.5 µg can safely be further explored in humans.

As the secondary objective of the study we assessed various aspects of the immune response to PCI-mediated vaccination. Here, the most interesting finding was that PCI vaccination with a fimaporfin dose of 12.5 µg led to an almost 10-fold increase in the percentage of study subjects exhibiting a T-cell response to HPV16 E7 peptide vaccination, as compared to a control group receiving the same vaccine without PCI. A positive effect was seen also in the 17.5 µg group despite that only 1/6 subjects in this group received the full HPV peptide vaccination schedule.

It is known that HPV E7 synthetic long peptide vaccination leads to strong CD4+ T-cell responses, but that with such antigens it is much more difficult to induce CD8+ T-cell responses (25, 28, 29). Thus, the enhanced overall T-cell response (IFN-γ ELISpot) observed in the 12.5 and 17.5 µg fimaporfin groups probably to a large degree represents an effect on the magnitude of the HPV-specific CD4+ type 1 T-cell response. The occurrence of CD4+ T-cell responses were also corroborated by the more sensitive, but less stringent, flow cytometry analysis, where most subjects in the analyzed groups (except one subject in the control group) exhibited strong CD4+ T-cell responses. Increased antigen-specific CD4+ T-cell responses after PCI treatment have also been observed in pre-clinical studies with protein antigens (Selbo *et al.*, manuscript in preparation).

In the present work also a significant increase in the IgG antibody response to the KLH protein antigen was observed. A similar effect has been observed in several pre-clinical studies with protein and long peptide antigens used in combination with poly(IC) (Selbo *et al.*, manuscript in preparation). The mechanism behind the stimulation of antibody responses may include an enhancement of CD4+ T-cell responses, potentially stimulating B-cells to produce antibodies (30).

The main cellular effect of the PCI technology is inducing endosomal permeabilization, among other things leading to enhanced MHC class I antigen presentation (4, 5). Given that endocytic vesicles are important in the MHC class II presentation pathway, it may seem counter-intuitive that PCI should enhance CD4+ T-cell responses. There may however be several explanations for this. Firstly, during illumination there will be a light dose gradient downwards and sideways in the tissue. This means that APCs located at different locations in the tissue will receive different "doses of PCI". Thus, the situation in the vaccination area may well be that some APCs (near to the light source) will receive a high "PCI dose" permeabilizing all endocytic vesicles and leading mainly to MHC class I presentation in these cells (maybe at the expense of class II presentation). Other cells will receive an intermediate "PCI dose" giving both MHC class I and II presentation in the same cell, and some cells located "far away" from the injection/illumination site (e.g. deeper in the tissue), may receive antigen, adjuvant and fimaporfin but only a small light dose, meaning that the "default" MHC class II presentation will dominate in these cells. Furthermore, PCI-induced stimulation of CD4+ T-cell responses may occur through several mechanisms. i) The photochemical treatment in itself can have a general immunostimulatory effect e.g. by the induction of cytokine production [e.g. IL-6 (5);] and by the upregulation of activation markers on APCs (4). ii) A substantial fraction of MHC class II presentation may take place by pathways involving antigen localization in the cytosol (31), and presentation mediated by such pathways may be enhanced by PCI, because of increased availability of antigens in the cytosol. iii) Various forms of photochemical treatments have been shown to induce autophagy (32), and autophagy is known to be involved in some types of MHC class II antigen presentation (33, 34).

Taken together, the aggregated effects, measurable in blood samples, of these possible different processes may lead to a

stimulation both of CD8+ T-cell, CD4+ T-cell and antibody responses. In most vaccination settings stimulation of all these branches of the immune system would be highly advantageous.

In contrast to the finding of an enhanced antibody response observed in the present study, earlier studies on PCI-mediated immunization with adjuvant-free particle- (6) or liposome- (7) based vaccines have indicated that PCI may have a negative effect on humoral immune responses to the ovalbumin (OVA) antigen, and also that that the effect of PCI on CD8+ T-cell responses is independent of CD4+ T-cells (9). The reason for the seemingly different effects of PCI on antibody production has so far not been elucidated, but one possibility is that it may be related to the use of poly(IC) based adjuvants in the studies showing av positive effect of PCI on antibody production.

Earlier clinical experience with HPV16 E7 peptide vaccination have shown that it is difficult to induce CD8+ T-cell responses to HPV16 E7 peptides in humans, with response rates of 11% (25) and 50% (28) being reported using vaccines containing nine HPV16 E6 plus four HPV16 E7 peptides. Thus, as discussed above it was expected that the IFN-γ response detected by ELISpot analysis in the present study using only two HPV16 E7 peptides was mostly contributed by CD4+ T-cells. Therefore, the flow cytometry analysis was employed to explore the effect of the PCI treatment specifically on CD8+ T-cell responses. Samples from three selected study groups were selected for this analysis, which was performed using the same methodology as used in the above cited studies (25, 28). As could be expected from previous studies with HPV E7 peptides (24, 27) in general the CD8+ T-cells responses observed in the present study were weak (<0.5% positive cells), while the CD4+ T-cell responses seemed much more robust, with up to 15% positive cells in same samples. The flow cytometry analyses revealed HPV-specific CD8+ T-cell responses in 50% of the subjects in the control group, however, such responses were likely to be weak since they could be detected at only one time point. In comparison, for the CD8+ T-cell responses the groups of subjects co-treated with fimaporfin had a tendency of a higher overall response rate, and exhibited more robust responses, with responses seen at several time points and to more than one of the analyzed markers. Apparently, these responses were of better quality than the responses in the control group, as reflected in the multifunctionality of the responses measured. A similar effect on functionality has been observed also in several animal studies (Selbo *et al.*, manuscript in preparation). Given the importance of the functionality of the CD8+ T-cells for effective immune responses to tumors and viral infections (35–37) this finding is very encouraging for the future exploration of PCI-mediated vaccination in therapeutic vaccination settings.

In conclusion, this clinical study demonstrates that the use of PCI in combination with a poly(IC) based adjuvant is safe and can enhance both cellular and humoral immune responses to ID vaccination over what is achieved with a vaccine given without PCI. As shown in animal studies the properties of the PCI technology may be especially useful for enhancing the effect of polypeptide based therapeutic cancer vaccines (Selbo *et al.*, manuscript in preparation), and based on the positive clinical results in the present study, this will be explored in further clinical studies.

DATA AVAILABILITY STATEMENT

The raw data supporting the conclusions of this article will be made available by the authors, without undue reservation.

ETHICS STATEMENT

The studies involving human participants were reviewed and approved by North East–York Research Ethics Committee, UK (16/NE/0198). The patients/participants provided their written informed consent to participate in this study.

AUTHOR CONTRIBUTIONS

TO and AH contributed to conception and design of the clinical study including immune monitoring analysis plan, immune data interpretation, wrote the first draft of the manuscript and final manuscript. TO was the project manager for the clinical study. SJ contributed to ELISpot assay design, ELISpot data analysis and interpretation, flow cytometry analysis and data interpretation as well as to the manuscript. MW contributed to flow cytometry analysis and data interpretation as well as to the manuscript. MH, AN, and VE contributed to data acquisition by ELISpot analysis. SBo and NL contributed to data acquisition by flow cytometry and analysis. PS provided scientific input and contributed to manuscript writing and final approval of manuscript. SvdB contributed to data interpretation and to the manuscript. HO contributed to design of the clinical study and safety monitoring. All authors contributed to the article and approved the submitted version.

FUNDING

The study was funded by PCI Biotech AS. PCI Biotech has received funding from the Norwegian Research Council for a Project (Project no. 269817) including the present study.

SUPPLEMENTARY MATERIAL

The Supplementary Material for this article can be found online at: https://www.frontiersin.org/articles/10.3389/fimmu.2020.576756/full#supplementary-material

REFERENCES

1. Gros M, Amigorena S. Regulation of Antigen Export to the Cytosol During Cross-Presentation. *Front Immunol* (2019) 10:41. doi: 10.3389/fimmu.2019.00041
2. Berg K, Selbo PK, Prasmickaite L, Tjelle TE, Sandvig K, Moan J, et al. Photochemical internalization: a novel technology for delivery of macromolecules into cytosol. *Cancer Res* (1999) 59(6):1180–3.
3. Hakerud M, Waeckerle-Men Y, Selbo PK, Kundig TM, Hogset A, Johansen P. Intradermal photosensitisation facilitates stimulation of MHC class-I restricted CD8 T-cell responses of co-administered antigen. *J Control Release* (2014) 174:143–50. doi: 10.1016/j.jconrel.2013.11.017
4. Haug M, Brede G, Hakerud M, Nedberg AG, Gederaas OA, Flo TH, et al. Photochemical Internalization of Peptide Antigens Provides a Novel Strategy to Realize Therapeutic Cancer Vaccination. *Front Immunol* (2018) 9:650. doi: 10.3389/fimmu.2018.00650
5. Waeckerle-Men Y, Mauracher A, Hakerud M, Mohanan D, Kundig TM, Hogset A, et al. Photochemical targeting of antigens to the cytosol for stimulation of MHC class-I-restricted T-cell responses. *Eur J Pharm Biopharm* (2013) 85(1):34–41. doi: 10.1016/j.ejpb.2013.02.002
6. Bruno C, Waeckerle-Men Y, Hakerud M, Kundig TM, Gander B, Johansen P. Photosensitizer and Light Pave the Way for Cytosolic Targeting and Generation of Cytosolic CD8 T Cells Using PLGA Vaccine Particles. *J Immunol* (2015) 195 (1):166–73. doi: 10.4049/jimmunol.1500431
7. Hjalmsdottir A, Buhler C, Vonwil V, Roveri M, Hakerud M, Wackerle-Men Y, et al. Cytosolic Delivery of Liposomal Vaccines by Means of the Concomitant Photosensitization of Phagosomes. *Mol Pharm* (2016) 13(2):320–9. doi: 10.1021/acs.molpharmaceut.5b00394
8. Hakerud M, Selbo PK, Waeckerle-Men Y, Contassot E, Dziunycz P, Kundig TM, et al. Photosensitisation facilitates cross-priming of adjuvant-free protein vaccines and stimulation of tumour-suppressing CD8 T cells. *J Control Release* (2015) 198:10–7. doi: 10.1016/j.jconrel.2014.11.032
9. Varypataki EM, Hasler F, Waeckerle-Men Y, Vogel-Kindgen S, Hogset A, Kundig TM, et al. Combined Photosensitization and Vaccination Enable CD8 T-Cell Immunity and Tumor Suppression Independent of CD4 T-Cell Help. *Front Immunol* (2019) 10:1548. doi: 10.3389/fimmu.2019.01548
10. Berg K, Nordstrand S, Selbo PK, Tran DT, Angell-Petersen E, Hogset A. Disulfonated tetraphenyl chlorin (TPCS2a), a novel photosensitizer developed for clinical utilization of photochemical internalization. *Photochem Photobiol Sci* (2011) 10(10):1637–51. doi: 10.1039/c1pp05128h
11. Agostinis P, Berg K, Cengel KA, Foster TH, Girotti AW, Gollnick SO, et al. Photodynamic therapy of cancer: an update. *CA Cancer J Clin* (2011) 61 (4):250–81. doi: 10.3322/caac.20114
12. Jerjes W, Theodossiou TA, Hirschberg H, Hogset A, Weyergang A, Selbo PK, et al. Photochemical Internalization for Intracellular Drug Delivery. From Basic Mechanisms to Clinical Research. *J Clin Med* (2020) 9(2):528–79. doi: 10.3390/jcm9020528
13. Sosic L, Selbo PK, Kotkowska ZK, Kundig TM, Hogset A, Johansen P. Photochemical Internalization: Light Paves Way for New Cancer Chemotherapies and Vaccines. *Cancers (Basel)* (2020) 12(1):165–87. doi: 10.3390/cancers12010165
14. Sultan AA, Jerjes W, Berg K, Hogset A, Mosse CA, Hamoudi R, et al. Disulfonated tetraphenyl chlorin (TPCS2a)-induced photochemical internalisation of bleomycin in patients with solid malignancies: a phase 1, dose-escalation, first-in-man trial. *Lancet Oncol* (2016) 17(9):1217–29. doi: 10.1016/S1470-2045(16)30224-8
15. Mescher MF, Curtsinger JM, Agarwal P, Casey KA, Gerner M, Hammerbeck CD, et al. Signals required for programming effector and memory development by CD8+ T cells. *Immunol Rev* (2006) 211:81–92. doi: 10.1111/j.0105-2896.2006.00382.x
16. Khong H, Overwijk WW. Adjuvants for peptide-based cancer vaccines. J Immunother. *Cancer* (2016) 4:56. doi: 10.1186/s40425-016-0160-y
17. Datta SK, Redecke V, Prilliman KR, Takabayashi K, Corr M, Tallant T, et al. A subset of Toll-like receptor ligands induces cross-presentation by bone marrow-derived dendritic cells. *J Immunol* (2003) 170(8):4102–10. doi: 10.4049/jimmunol.170.8.4102
18. Ressing ME, Sette A, Brandt RM, Ruppert J, Wentworth PA, Hartman M, et al. Human CTL epitopes encoded by human papillomavirus type 16 E6 and E7 identified through in vivo and in vitro immunogenicity studies of HLA-A*0201-binding peptides. *J Immunol* (1995) 154(11):5934–43.
19. Houston WE, Crabbs CL, Stephen EL, Levy HB. Modified polyriboinosinic-polyribocytidylic acid, an immunological adjuvant. *Infect Immun* (1976) 14 (1):318–9. doi: 10.1128/IAI.14.1.318-319.1976
20. Wegner J, Hackenberg S, Scholz CJ, Chuvpilo S, Tyrsin D, Matskevich AA, et al. High-density preculture of PBMCs restores defective sensitivity of circulating CD8 T cells to virus- and tumor-derived antigens. *Blood* (2015) 126(2):185–94. doi: 10.1182/blood-2015-01-622704
21. Santos R, Buying A, Sabri N, Yu J, Gringeri A, Bender J, et al. Improvement of IFNg ELISPOT Performance Following Overnight Resting of Frozen PBMC Samples Confirmed Through Rigorous Statistical Analysis. *Cells* (2014) 4 (1):1–18. doi: 10.3390/cells4010001
22. Janetzki S, Price L, Schroeder H, Britten CM, Welters MJ, Hoos A. Guidelines for the automated evaluation of Elispot assays. *Nat Protoc* (2015) 10(7):1098–115. doi: 10.1038/nprot.2015.068
23. Moodie Z, Price L, Gouttefangeas C, Mander A, Janetzki S, Lower M, et al. Response definition criteria for ELISPOT assays revisited. *Cancer Immunol Immunother* (2010) 59(10):1489–501. doi: 10.1007/s00262-010-0875-4
24. Welters MJ, Kenter GG, de Vos van Steenwijk PJ, Lowik MJ, Berends-van der Meer DM, Essahsah F, et al. Success or failure of vaccination for HPV16-positive vulvar lesions correlates with kinetics and phenotype of induced T-cell responses. *Proc Natl Acad Sci USA* (2010) 107(26):11895–9. doi: 10.1073/pnas.1006500107
25. van Poelgeest MI, Welters MJ, Vermeij R, Stynenbosch LF, Loof NM, Berends-van der Meer DM, et al. Vaccination against Oncoproteins of HPV16 for Noninvasive Vulvar/Vaginal Lesions: Lesion Clearance Is Related to the Strength of the T-Cell Response. *Clin Cancer Res* (2016) 22 (10):2342–50. doi: 10.1158/1078-0432.CCR-15-2594
26. Borgia F, Giuffrida R, Caradonna E, Vaccaro M, Guarneri F, Cannavo SP. Early and Late Onset Side Effects of Photodynamic Therapy. *Biomedicines* (2018) 6(1):12–28. doi: 10.3390/biomedicines6010012
27. Petrovsky N. Comparative Safety of Vaccine Adjuvants: A Summary of Current Evidence and Future Needs. *Drug Saf* (2015) 38(11):1059–74. doi: 10.1007/s40264-015-0350-4
28. Welters MJ, Kenter GG, Piersma SJ, Vloon AP, Lowik MJ, Berends-van der Meer DM, et al. Induction of tumor-specific CD4+ and CD8+ T-cell immunity in cervical cancer patients by a human papillomavirus type 16 E6 and E7 long peptides vaccine. *Clin Cancer Res* (2008) 14(1):178–87. doi: 10.1158/1078-0432.CCR-07-1880
29. Kenter GG, Welters MJ, Valentijn AR, Lowik MJ, Berends-van der Meer DM, Vloon AP, et al. Vaccination against HPV-16 oncoproteins for vulvar intraepithelial neoplasia. *N Engl J Med* (2009) 361(19):1838–47. doi: 10.1056/NEJMoa0810097
30. Parker DC. T cell-dependent B cell activation. *Annu Rev Immunol* (1993) 11:331–60. doi: 10.1146/annurev.iy.11.040193.001555
31. Leung CS. Endogenous Antigen Presentation of MHC Class II Epitopes through Non-Autophagic Pathways. *Front Immunol* (2015) 6:464. doi: 10.3389/fimmu.2015.00464
32. Kessel D. Apoptosis, Paraptosis and Autophagy: Death and Survival Pathways Associated with Photodynamic Therapy. *Photochem Photobiol* (2019) 95 (1):119–25. doi: 10.1111/php.12952
33. Vyas JM, Van der Veen AG, Ploegh HL. The known unknowns of antigen processing and presentation. *Nat Rev Immunol* (2008) 8(8):607–18. doi: 10.1038/nri2368
34. Munz C. Antigen Processing for MHC Class II Presentation via Autophagy. *Front Immunol* (2012) 3:9. doi: 10.3389/fimmu.2012.00009
35. Seder RA, Darrah PA, Roederer M. T-cell quality in memory and protection: implications for vaccine design. *Nat Rev Immunol* (2008) 8(4):247–58. doi: 10.1038/nri2274
36. Wimmers F, Aarntzen EH, Duiveman-deBoer T, Figdor CG, Jacobs JF, Tel J, et al. Long-lasting multifunctional CD8(+) T cell responses in end-stage melanoma patients can be induced by dendritic cell vaccination. *Oncoimmunology* (2016) 5(1):e1067745. doi: 10.1080/2162402X.2015.1067745
37. Panagioti E, Klenerman P, Lee LN, van der Burg SH, Arens R. Features of Effective T Cell-Inducing Vaccines against Chronic Viral Infections. *Front Immunol* (2018) 9:276. doi: 10.3389/fimmu.2018.00276

Conflict of Interest: TO and AH are employees of PCI Biotech AS and own shares and share options in the Company. AH and PS are inventors on several patents and patent Applications on the PCI Technology. HO and SJ work as consultants for PCI Biotech, and SJ is working for ZellNet Consulting, Inc. VE is an employee of PCI Biotech.

The remaining authors declare that the research was conducted in the absence of any commercial or financial relationships that could be construed as a potential conflict of interest.

Copyright © 2021 Otterhaug, Janetzki, Welters, Håkerud, Nedberg, Edwards, Boekestijn, Loof, Selbo, Olivecrona, van der Burg and Høgset. This is an open-access article distributed under the terms of the Creative Commons Attribution License (CC BY). The use, distribution or reproduction in other forums is permitted, provided the original author(s) and the copyright owner(s) are credited and that the original publication in this journal is cited, in accordance with accepted academic practice. No use, distribution or reproduction is permitted which does not comply with these terms.

frontiers in Immunology

ORIGINAL RESEARCH
published: 19 January 2021
doi: 10.3389/fimmu.2020.596303

Thymoproteasome-Expressing Mesenchymal Stromal Cells Confer Protective Anti-Tumor Immunity *via* Cross-Priming of Endogenous Dendritic Cells

Jean-Pierre Bikorimana[1], *Nehme El-Hachem*[2,3], *Abed El-Hakim El-Kadiry*[4], *Jamilah Abusarah*[5], *Natasha Salame*[6], *Riam Shammaa*[7,8,9*] *and Moutih Rafei*[1,4,5,10*]

[1] Department of Microbiology, Infectious Diseases and Immunology, Université de Montréal, Montreal, QC, Canada, [2] Centre Hospitalier Universitaire (CHU) Ste-Justine Research Center, Université de Montréal, Montreal, QC, Canada, [3] Genomics Institute of Precision Medicine, American University of Beirut, Beirut, Lebanon, [4] Department of Pharmacology and Physiology, Université de Montréal, Montreal, QC, Canada, [5] Department of Microbiology and Immunology, McGill University, Montreal, QC, Canada, [6] Department of Biomedical Sciences, Université de Montréal, Montreal, QC, Canada, [7] Department of Family and Community Medicine, University of Toronto, Toronto, ON, Canada, [8] Canadian Centers for Regenerative Therapy, Toronto, ON, Canada, [9] Intellistem Technologies Inc., Toronto, ON, Canada, [10] Molecular Biology Program, Université de Montréal, Montreal, QC, Canada

OPEN ACCESS

Edited by:
Stephanie E. B. McArdle, Nottingham Trent University, United Kingdom

Reviewed by:
Izumi Ohigashi, Tokushima University, Japan
Severine Loisel, Université de Bretagne Occidentale, France

***Correspondence:**
Moutih Rafei
moutih.rafei.1@umontreal.ca
Riam Shammaa
riam.shammaa@ccrttoronto.ca

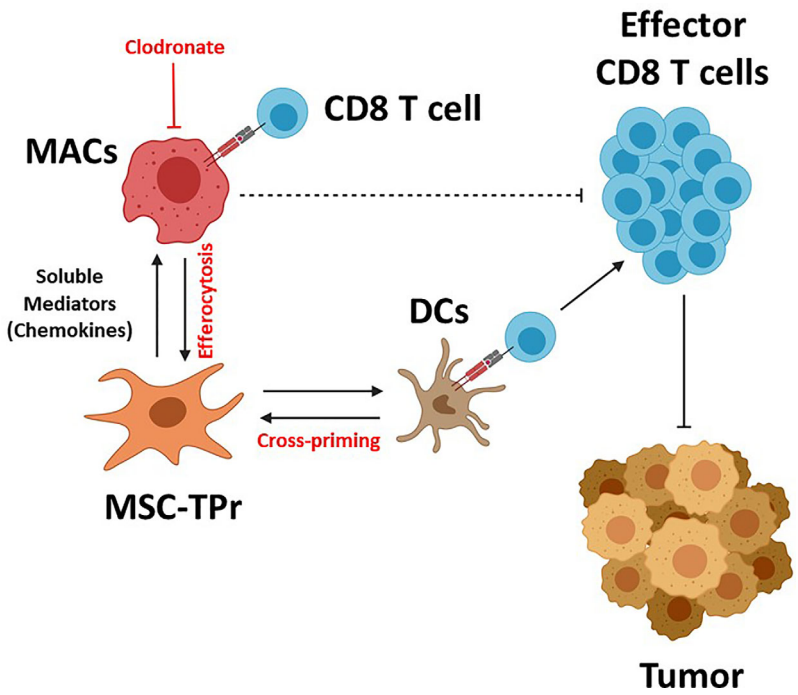
Specialty section:
This article was submitted to Cancer Immunity and Immunotherapy, a section of the journal Frontiers in Immunology

Received: 19 August 2020
Accepted: 14 December 2020
Published: 19 January 2021

Citation:
Bikorimana J-P, El-Hachem N, El-Kadiry AEH, Abusarah J, Salame N, Shammaa R and Rafei M (2021) Thymoproteasome-Expressing Mesenchymal Stromal Cells Confer Protective Anti-Tumor Immunity via Cross-Priming of Endogenous Dendritic Cells. Front. Immunol. 11:596303. doi: 10.3389/fimmu.2020.596303

Proteasomes are complex macromolecular structures existing in various forms to regulate a myriad of cellular processes. Besides degrading unwanted or misfolded proteins (proteostasis), distinct immune functions were ascribed for the immunoproteasome and thymoproteasome (TPr) complexes. For instance, antigen degradation during ongoing immune responses mainly relies on immunoproteasome activity, whereas intrathymic CD8 T-cell development requires peptide generation by the TPr complex. Despite these substantial differences, the functional contribution of the TPr to peripheral T-cell immunity remains ill-defined. We herein explored whether the use of mesenchymal stromal cells (MSCs) engineered to exhibit altered proteasomal activity through *de novo* expression of the TPr complex can be exploited as a novel anti-cancer vaccine capable of triggering potent CD8 T-cell activation. Phenotypic and molecular characterization of MSC-TPr revealed a substantial decrease in MHCI (H2-K^b and H2-D^d) expression along with elevated secretion of various chemokines (CCL2, CCL9, CXCL1, LIX, and CX3CL1). In parallel, transcriptomic analysis pinpointed the limited ability of MSC-TPr to present endogenous antigens, which is consistent with their low expression levels of the peptide-loading proteins TAP, CALR, and PDAI3. Nevertheless, MSC-TPr cross-presented peptides derived from captured soluble proteins. When tested for their protective capacity, MSC-TPr triggered modest anti-tumoral responses despite efficient generation of effector memory CD4 and CD8 T cells. In contrast, clodronate administration prior to vaccination dramatically enhanced the MSC-TPr-induced anti-tumoral immunity clearly highlighting a refractory role mediated by phagocytic cells. Thus, our data elute to a DC cross-priming-dependant pathway in mediating the therapeutic effect of MSC-TPr.

Keywords: mesenchymal stromal cell, thymoproteasome, cancer vaccine, antigen cross-presentation, cross-priming, efferocytosis, clodronate



GRAPHICAL ABSTRACT | MSC-TPr administration to immunocompetent mice leads to the recruitment of myeloid cells (macrophages and DCs) *via* a myriad of soluble mediators including chemokines. Although DC recruitment and cross-priming is beneficial to trigger anti-tumoral immunity, the interaction between MSC-TPr and monocytes/macrophages impairs T-cell activation. Depletion of macrophages by clodronate re-establishes full anti-tumoral immunity leading to complete protection.

INTRODUCTION

Initially, the proteasomal machinery was believed to strictly coordinate proteolysis *via* the degradation of aberrant cytoplasmic proteins (1). This perception quickly evolved with the emergence of additional proteasomal functions including the regulation of transcriptional activities, cell cycle and division, DNA repair, immunity, development/differentiation as well as organelle biogenesis (1–4). In contrast to yeast, which harbors a single proteasomal form, mammals can express three types of proteasomes: i) the constitutive proteasome (CPr: β1, β2, and β5), ii) the immunoproteasome (IPr: β1i, β2i, and β5i), and iii) the thymoproteasome (TPr: β1i, β2i, and β5t) (1, 5). Whereas the CPr complex is expressed in all eukaryotic cells, the IPr subunits are constitutively detected in antigen-presenting cells or assembled *de novo* in eukaryotic cells following interferon (IFN)-gamma stimulation. Compared to the CPr, the proteolytic activity of the IPr readily generates peptides fitting snugly in major histocompatibility (MHC)I grooves, which ensures efficient immune surveillance and pathogen clearance by CD8 T cells (1). TPr biogenesis, on the other hand, is restricted to cortical thymic epithelial cells (cTECs) (1, 6, 7). Its role is vital for positive selection of CD8 thymocytes as mice deficient in *β5t* exhibit aberrant CD8 T-cell development (CD4 T cells are not affected) despite normal thymic architecture and MHCI expression on cTECs (7, 8). The latter observations in *β5t*-deficient mice led to the conclusion that the unique and poor chymotrypsin-like activity of the TPr provides a set of MHCI-associated peptides completely distinct from those generated by the CPr or IPr complexes and dedicated to CD8 T-cell development (7, 8). It is however unclear whether the benefits of TPr are merely limited to the development of functional CD8 T cells or can also be exploited in immunotherapy to activate peripheral CD8 T cells. Additional studies are therefore required to investigate whether molding of peripheral CD8 T-cell immunity can be mediated by the TPr.

To this extent, we opted for culture-adapted non-hematopoietic mesenchymal stromal cells (MSCs) as a working model since they: i) can be harvested by a simple low volume aspirate from mice, ii) exhibit rapid *in vitro* proliferation, iii) require minimal culture conditions, iv) display minimal senescence through multiple passages, and v) are highly permissive to a variety of genetic engineering methods (9, 10). Besides, MSCs can switch gears and behave as conditional antigen-presenting cell upon IFN-gamma licensing, buttressing their rationale use in the context of antigen presentation (11). We show in this study that TPr-expressing MSCs (MSC-TPr) can indeed capture and cross-present peptides derived from soluble antigens. This acquired antigen presentation potential confers decent anti-tumor protection in immunocompetent mice. However, these elicited anti-tumor responses result from a delicate balance between phagocyte-mediated efferocytosis and endogenous DC cross-priming.

MATERIALS AND METHODS

Animals and Ethics

All female C57BL/6NCrl and Balb/c mice (6–8 weeks old) were purchased from the Jackson Laboratory (Bar Harbor, ME, USA) and housed in a pathogen-free environment at the animal facility of the Institute for Research in Immunology and Cancer (IRIC). All experimental procedures and protocols were approved by the Animal Ethics Committee of Université de Montréal.

Cell Lines and Reagents

The EG.7 T-cell lymphoma, the AP2 retroviral plasmid and the 293-GP2 packaging system were kindly provided by Dr. Jacques Galipeau (University of Wisconsin-Madison, WI, USA). The A20 B-cell lymphoma was purchased from ATCC (Manassas, VA). All cell culture media and reagents were purchased from Wisent Bioproducts (St-Jean-Baptiste, QC, Canada). All flow-cytometry antibodies were purchased from BD Biosciences (San Jose, CA, USA). These include PE anti-CD11b (clone KH95, catalog no. 553574), PE anti-CD11c (clone HL3; catalog no. 557401), PE anti-CD31 (clone MEC 13.3; catalog no. 553373), APC anti-CD44 (clone IM7; catalog no. 561862), PE anti-CD45 (clone 30-F11; catalog no. 553081), PerCP-Cy^{TM}5.5 anti-CD62L (clone MEL-14; catalog no. 560513), PE anti-CD73 (clone TY/23; catalog no. 550741), anti-CD90.1 (clone OX-7; catalog no. 551401), PE anti-CD105 (clone MJ7/18; catalog no. 562759), PE anti-H2-K^{b} (clone AF6-88.5; catalog no. 553570), PE anti-H2-D^{b} (clone KH95; catalog no. 553574), PE anti-I-A^{b} (clone AF6-120.1; catalog no. 553552), PE anti-CD80 (clone 16-10A1; catalog no. 553769), PE anti-CD86 (clone GL1; catalog no. 553692), and PE anti-PD-L1 (clone MIH5; catalog no. 558091). All ELISA kits and western blot antibodies were purchased from R&D Systems (Minneapolis, MN, USA). The 25-D1.16 antibody was purchased from Biolegend (San Diego, CA, USA). PolyFect and the RNeasy mini kit were purchased from Qiagen (Toronto, ON, Canada). The chicken egg white ovalbumin (OVA) protein, Cell Lytic^{TM} lysis buffer, lipopolysaccharide (LPS) and Accutase$^{®}$ were purchased from Sigma-Aldrich (St-Louis, MI, USA). Recombinant GM-CSF was purchased from PeproTech (Rocky Hill, NJ, USA). Polybrene was purchased from Cedarlane (Burlington, ON, Canada). The OVA Alexa Fluor^{TM} 647 Conjugate was purchased from ThermoFisher (Mississauga, ON, Canada). The SIINFEKL peptide was synthesized by Genscript (Piscataway, NJPiscataway, NJ, USA). The chemokine array was purchased from RayBiotech (Peachtree Corners, GA, USA). The CD8 T-cell isolation kit was purchased from StemCell Technologies (Vancouver, BC, Canada). The Bradford reagent was purchased from Bio-Rad (Hercules, CA, USA). Liposomes and liposome-Clodronate were purchased from Liposoma Research (Amersterdam, The Netherlands).

Generation of Bone Marrow–Derived Dendritic Cells

To generate dendritic cells (DCs), the tibia/femur bones of 8 weeks old C57BL/6 female mice were flushed. Collected bone marrow (BM) cells were plated in 10-cm Petri dishes containing 10 ml of complete RPMI 1640 medium (10% fetal bovine serum (FBS), 1% sodium pyruvate, 1% HEPES, 1% non-essential amino acids, 1% l-glutamine, 1% penicillin-streptomycin, and 5 μM β-mercaptoethanol) supplemented with 50 ng/ml of recombinant GM-CSF (PeproTech). The media was changed at days 3 and 6 of culture prior to the induction of DC maturation using 1 ng/ml of LPS (Sigma) added at day 8 for 12 h.

Generation of BM-Derived MSCs

In order to generate MSCs, femurs of 6–8 weeks old female C57BL/6 mice were isolated and flushed with Alpha Modification of Eagle's Medium (AMEM) supplemented with 10% FBS, and 50 U/ml of penicillin-streptomycin in a 10 cm cell culture dish (CellStar), then incubated at 37°C. Two days later, non-adherent cells were removed and the media was replaced every 3 to 4 days until the cells reached 80% confluency. Adherent cells were detached using 0.05% trypsin and expanded until a uniform MSC population is obtained. Generated MSCs were validated by flow-cytometry for the expression of CD31, CD44, CD45, CD73, CD90, and CD105.

Engineering MSCs to Express the TPr Subunits

The AP2 retroviral construct, containing the green fluorescent protein (eGFP) as a marker for retroviral expression, was designed to contain the genes coding for the three murine TPr subunits (β1i, β2i, and β5t) separated by the viral T2A sequence (**Figure 1A**) (12). Both AP2 and pVSV-G (encoding the viral envelop protein) were used to co-transfect the GP2-293 packaging cell line using PolyFect (Qiagen) according to the manufacturer's protocol. Supernatants containing the virus were collected 48 h post-transfection and centrifuged at 1,500 rpm for 5 min at 4°C to remove cell debris. An ultracentrifugation at 25,000 rpm for 90 min at 4°C was then conducted to concentrate the virus 10-fold. Passage 5 MSCs were plated at 50–60% and transduced with the concentrated virus in a minimal volume containing 5 μg/ml of Polybrene (Cedarlane). Transduction efficiency was confirmed by eGFP expression and immunoblotting of the TPr subunits. Similar steps were followed using the empty AP2 construct backbone to generate control (Ctl) MSCs.

Cytokine and Chemokine Analyses

For cytokine and chemokine profiling, 15 cm culture petri dishes containing 80–90% confluent MSC-β5t or Ctl MSCs were grown in serum-free media for 24 h at 37°C. Collected supernatants were then analyzed using luminex by Eve Technologies (Calgary, AB, CA) or commercially-available chemokine arrays (RayBiotech) according to manufacturer's instructions.

RNA Extraction and Sequencing

Total RNA was isolated from 10^{6} cells using RNeasy$^{®}$ mini kit (QIAGEN) according to manufacturer's instructions. Following total RNA quantification by QuBit (ABI), 500 ng of total RNA was used for library preparation. Quality of total RNA was assessed with the BioAnalyzer Nano (Agilent) and all samples

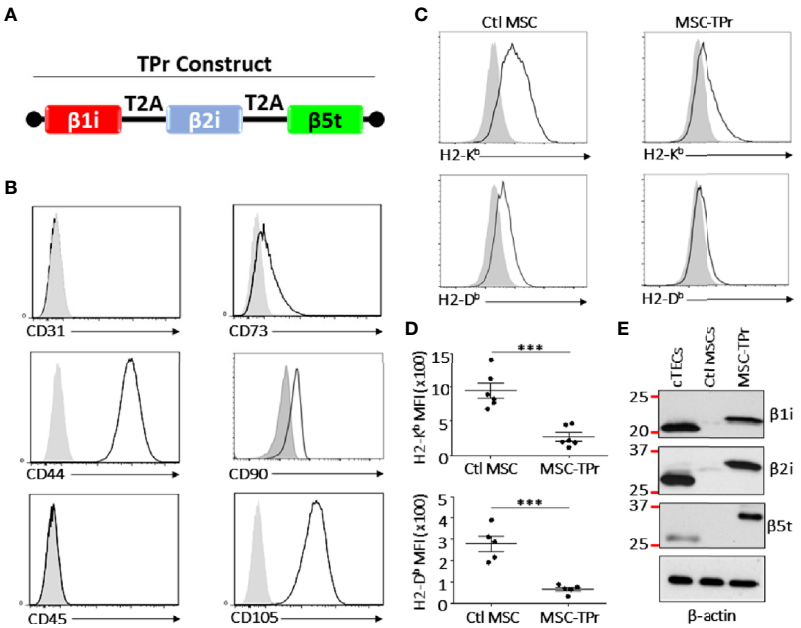


FIGURE 1 | Engineering and characterizing MSC-TPr. **(A)** A cartoon representing the cloning strategy used to generate the TPr retroviral construct. **(B)** Phenotypic analysis of MSC-TPr after gene-modification. **(C, D)** Comparative analysis for the expression levels of MHCI molecules on Ctl MSC versus MSC-TPr. **(E)** Representative Western-blot depicting the expression of the three TPr subunits in 1) cTECs (positive control), 2) Ctl MSCs, and 3) MSC-IPr. For the experiment in **(D)**, n = 6/group with ***P < 0.001.

had a RIN above 8. Library preparation was done with the KAPA mRNAseq stranded kit (KAPA, Cat no. KK8420). Ligation was made with 9 nM final concentration of Illumina index and 10 PCR cycles was required to amplify cDNA libraries. Libraries were quantified by QuBit and BioAnalyzer. All librairies were diluted to 10 nM and normalized by qPCR using the KAPA library quantification kit (KAPA; Cat no. KK4973). Libraries were pooled to equimolar concentration. Sequencing was performed with the Illumina Hiseq2000 using the Hiseq Reageant Kit v3 (200 cycles, paired-end) using 1.7 nM of the pooled library. Around 40 M paired-end PF reads were generated per sample. Library preparation and sequencing was made at the IRIC Genomics Platform.

Bioinformatics Analysis

Raw RNA-seq counts from reads aligned to the mouse genome (mm10 assembly) were generated with Htseq-count (PMID: 25260700). Differentially expressed genes between TPr and Ctl MSCs were calculated by DESeq2 (PMID: 25516281). Pre-ranked gene set enrichment was performed as recommended for RNA-seq data (PMID: 16199517). Custom R scripts were used to filter highly redundant biological processes. A false discovery rate of 0.05 was considered as an acceptable threshold for further investigation. All analyses were conducted in R (v3.6) or Python (v3.7) programming language. The ggplot2, ClusterProfiler and dplyr packages were used for data visualization. Student's *t-test* was performed for normally distributed data to compute the *p*-value and the Benjamini-Hochberg procedure was used for adjusting the statistical inference of multiple comparisons.

Detection of MHC-Peptide Complexes on the Surface of Pulsed MSC-TPr

To detect the SIINFEKL/MHC-I complex at the cell surface, MSC-TPr or Ctl MSCs were pulsed with the OVA protein (5 mg/ml) or the SIINFEKL peptide (2.5 μg/ml) at 37°C for different time points. The supernatants were discarded and the cells were washed twice with PBS prior to adding fresh medium. The signal for SIINFEKL/MHCI complex on cell surface was monitored by flow-cytometry at 1, 3, 6, 9, and 24 h post-pulsing using the 25-D1.16 antibody (Biolegend). To detect the increase in peptide-MHCI complex formation on H2-K^b and H2-D^d molecules, the cells were pulsed with OVA (5 mg/ml) for 1 h prior to detection of the H2-K^b/H2-D^b levels by flow-cytometry at 1, 3, 6 and 24 h post-washing (chase).

Monitoring Antigen Uptake and Processing

To evaluate the cells ability to up-take antigens, MSC-TPr or Ctl MSCs were seeded at 4×10^4 cells/well in a 12 well plate (Corning) and incubated with 1 μg/ml of Alexa Fluor®647-conjugated OVA. At the end of incubation time, treated cells were then detached and washed four times with cold PBS containing 2% FBS. Fluorescence was detected by BD FACS Diva on CANTOII and analyzed by FlowJoV10.

Antigen Presentation Assay

For the antigen cross-presentation assay *in vitro*, Ctl MSCs or MSC-TPr cells were seeded at 25×10^3 cells per well in a 24-well plate (Corning). The following day, plated cells were washed and pulsed with 5 mg/ml of OVA or 2.5 μg/ml of the SIINFEKL peptide. At the end of the pulsing period, the cells were washed prior to their co-culture with 10^6/ml CD8 T-cells purified from the spleen of OT-I mouse or immunized mice using the CD8α$^+$ positive isolation kit according to the manufacturer's protocol. The supernatants were collected three days later to quantify IFN-gamma levels by ELISA.

Peritoneal Lavage and CellTrace™ Analysis

To specifically assess *in vivo* efferocytosis, 10^6 CellTrace™-labelled MSC-TPr were *intraperitoneally (IP)*-injected in immunocompetent 6–8 weeks old female *C57BL/6 mice* (n = 3/group). Clodronate or control liposomes (50μl/20g mouse) were delivered the day before (13). Four hours following MSC admninistration, mice were sacrificed and peritoneal lavage was conducted using 30 ml of serum-free RPMI. Collected cells were centrifuged at 1 500 rpm for 10 min and the cell pellets washed twice with PBS. Recovered cells were then analyzed by flow-cytometry to detect CD11b$^+$ cells exhibiting a positive CellTrace™ signal.

Generation of Heat-Killed MSCs

Ctl MSCs and MSC-TPr were heat-killed as previously described (13). Briefly, ready for injection MSCs (re-suspended in sterile PBS) were incubated in a water bath at 50°C for 15 min. Cell death was confirmed by annexin-V and the absence of peptide-MHC complexes on their cell surface.

Cancer Cell Lysate Preparation

To prepare the A20 cell lysate, 50×10^6 cells were collected by centrifugation at 1 500 rpm for 10 min and the cell pellets washed twice with PBS to remove traces of FBS. The pellets underwent 5 cycles of freeze and thaw using liquid nitrogen and boiling water respectively. After removing large particles using 70 μM cell strainers followed by an additional filtration with a 0.45 μM filter, the lysate was quantified using Bradford reagent then aliquoted and stored at -80°C until use.

Immunization and Tumor Challenge

For all prophylactic vaccination studies, 6–8 weeks old female C57BL/6 mice (n = 10/group) or Balb/c mice (n = 10/group) were IP-injected at day 0 and 14 with OVA- (5 mg/ml) or tumor lysate- (1 mg/ml) pulsed MSC-TPr versus Ctl MSCs. Two weeks following the second vaccination, mice were subcutaneously (SC) challenged with 5×10^5 EG.7 or A20 cells and tumor growth was assessed two to three times per week. To detect memory CD4 and CD8 T cells, blood samples isolated from immunized mice were stained with CD44 and CD62L and analyzed by flow-cytometry.

To block efferocytosis during immunization, 6–8 weeks old female C57BL/6 mice (n = 10/group) were IP-injected with liposome-clodronate or control liposome one day prior to immunization (50μl/20g mouse) (13). Two weeks later, the same process was repeated, followed by tumor challenge (5×10^5 EG.7 cells) one week following the second immunization. All tumor-free mice were then re-challenged 10 weeks later (total of two EG.7/A20 challenges). A similar approach was followed to block DC cross-priming except that animals were IP-injected with 30 μg of anti-CD11c antibodies or isotype control.

Statistical Analysis

P-values were calculated using the one-way analysis of variance (ANOVA) for most experiments unless otherwise mentioned. Statistical significance is represented with asterisks: *P < 0.05, **P < 0.01, ***P < 0.001. Statistical tests used for bioinformatic analysis are described in their corresponding sections.

RESULTS

Phenotypic Characterization of TPr-Expressing MSCs

Although genetic modification of MSCs to express the TPr subunits (β1i, β2i, and β5t; **Figure 1A**) did not alter their original mesenchymal phenotype (**Figure 1B**; **Figure S1**), lower levels of H2-K^b and H2-D^b were detected on the surface of MSC-TPr in comparison to Ctl MSCs (**Figures 1C, D**). In addition, expression of the TPr by MSCs (**Figure 1E**) did not induce MHCII (I-A^b), CD80, CD86 or PD-L1 expression (**Figure S2**), nor caused unusual alterations in their responsiveness to IFN-gamma treatment (**Figure S3**). When analyzed for their secretome profile, MSC-TPr expressed higher levels of VEGF (**Figure 2A**), in addition to CCL2, CCL9, CXCL1, LIX, and CX3CL1 while CXCL12 was decreased (**Figures 2B, C**). These results indicate that TPr expression in MSCs alters their MHCI expression and secretion of various soluble immune mediators.

TPr Expression May Limit the Ability of MSCs to Process and Present Endogenous Antigens

Given the pleiotropic functions mediated by the proteasome, we next questioned the impact of *de novo* TPr expression on the overall transcriptional profile of MSCs. In sum, 885 and 1042 genes were significantly down- and up-regulated respectively (**Figure 3A**) affecting various biological processes (**Figure 3B**) and pathways as shown by pre-ranked Gene Set Enrichment Analysis (**Figure 3C**). Given our interest in antigen presentation, we mainly focused on pathways related to protein degradation (**Figure 3D**) and observed enhanced expression of genes encoding for the alpha and beta subunits of the 20S proteasomal complex (*Psma1, Psma3-7*, *Psmb3*, *Psmb7*, and *Psmb10*). Interestingly, most of these genes are associated with the proteasome ubiquitin-independent protein catabolism pathway, which was recently reported to depend on β5t expression (14). This may suggest that in MSC-TPr, degradation of various client proteins may preferentially occur *via* the ubiquitin-independent pathway especially with the observed decrease in the expression of several genes regulating

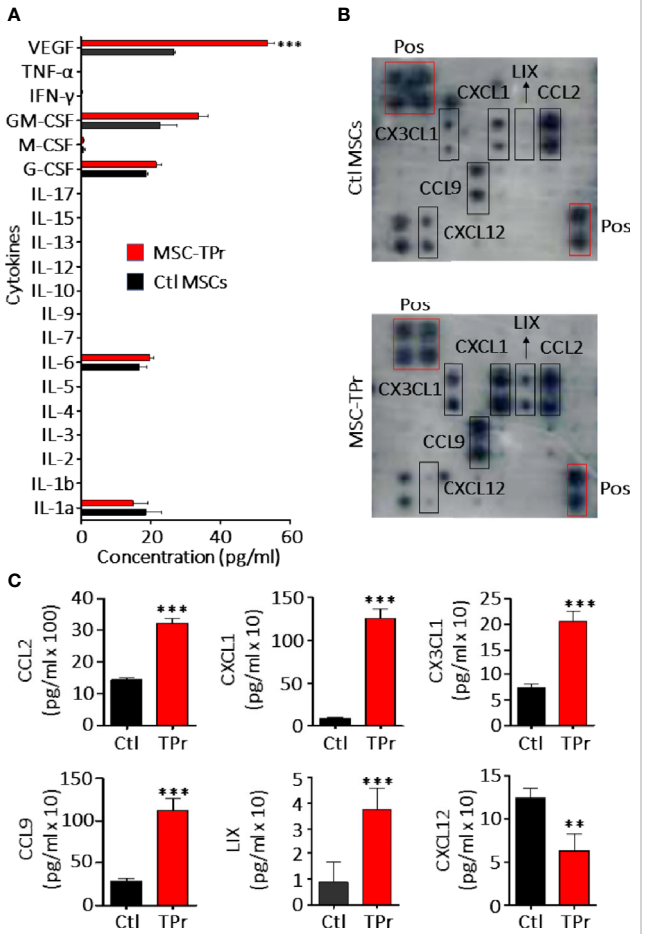


FIGURE 2 | Analysis of MSC-TPr secretome. **(A)** Luminex quantification of various cytokines secreted by Ctl (black) or MSC-TPr (red). **(B)** Analysis of various chemokines secreted by Ctl versus TPr-expressing MSCs using commercial chemokine arrays. **(C)** Quantification of chemokines selected from **(B)**. For **(A, C)**, n = 6/group with $^{**}P < 0.01$ and $^{***}P < 0.001$.

protein poly-ubiquitination (*Birc2*, *Birc3*, *Papr10*, and *Ubr5*; **Figure 3D**). These observations are also in agreement with the decreased ability of the MSC-TPr in processing and presenting endogenous antigens and the low expression levels of various genes involved in the endoplasmic reticulum-associated protein degradation (ERAD) pathway (**Figure 3D**). The relevance and/or significance for the existence of such ubiquitin-independent degradation pathway in MSC-TPr is unclear. However, this catabolic pathway may be a default mechanism for the degradation of various endogenous proteins involved in DNA and chromatin structure, metabolism, immunity, cell cycle and apoptosis, which may not require a fast-adaptive response for their proteostasis control (15). Overall, transcriptomic analysis suggests that TPr expression negatively impacts endogenous protein catabolism and presentation by MSCs, which explains the previously observed decrease in MHCI on their cell surface (**Figures 1C, D**).

MSC-TPr Can Present Peptides Derived From Exogenous Soluble Proteins

The intriguing observation of diminished endogenous antigen processing and presentation led us to quantify the expression of various genes involved in the peptide-loading machinery (16). With the exception of tapasin (*Tapbp*), expression of the transporter associated with antigen processing (*Tap*)*1* and *Tap2*, Protein-disulfide Isomerase-associated (*Pdai*)*3* and calreticulin (*Calr*) were down-regulated in MSC-TPr (**Figure 4A**). We next monitored the kinetics of SIINFEKL-H2-K^b complex formation at the cell surface of MSC-TPr following SIINFEKL or OVA pulsing. Although SIINFEKL pulsing increased the formation of the peptide-MHCI complex on the surface of MSC-TPr in a timely fashion (**Figure 4B**), the same SIINFEKL-MHC complex was undetected following OVA pulsing (**Figure 4C**) despite efficient protein uptake (**Figure S4A**). These observations are consistent with the impaired OT-I T-cell activation using OVA-pulsed MSC-TPr (**Figure 4D**). Since SIINFEKL is a strong and stable peptide immunogen unlikely to be generated by the poor chymotrypsin-like activity of the TPr complex, we hypothesized that CD8 T cells isolated from animals immunized using OVA-pulsed MSC-TPr would respond to other OVA-derived peptides without avail (**Figure 4E**). Given these unexpected data, we next validated the ability of MSC-TPr to present other OVA-derived peptides by assessing their cell surface level of MHCI molecules following protein pulsing (reflecting formation of MHC-peptide complexes). A pulse-chase experiment revealed the progressive appearance of H2-K^b/H2-D^b levels on the surface of OVA-pulsed MSC-TPr (**Figure 4F**), which was substantially higher than Ctl MSCs (**Figure S4B**). Collectively, these results suggest that TPr expression in MSCs instills a distinct peptide repertoire unlikely to trigger peripheral CD8 T-cell activation.

Prophylactic Vaccination of Macrophage-Depleted Animals Confers Potent Long-Term Protection Against T-Cell Lymphoma

Since MSC-TPr can efficiently uptake and process soluble OVA, yet are unable to activate CD8 T cells *in vitro*, we next interrogated their therapeutic utility against the E.G7 (OVA-expressing EL4 thymoma) T-cell lymphoma model (**Figure 5A**). In contrast to OVA-pulsed Ctl MSCs, which failed in providing a meaningful anti-tumor effect, prophylactic vaccination using OVA-pulsed MSC-TPr significantly delayed tumor growth with a 30% survival rate reached beyond 120 days (**Figures 5B, C**). To define the basis of this prolonged survival, we next quantified the levels of effector ($CD44^{hi}CD62L^{-}$) and central memory ($CD44^{hi}CD62L^{+}$) T cells in treated animals. The level of effector memory CD4 and CD8 T cells in the blood of mice vaccinated using OVA-pulsed MSC-TPr was 9 and 16%, respectively, in comparison with 4.8 and 9.2% in mice vaccinated using OVA-pulsed Ctl MSCs and 6 and 5.6% in un-vaccinated mice (**Figures 5D, E**).

The fact that MSC-TPr can elicit modest anti-tumor responses without any apparent ability to activate CD8 T cells *in vitro* strongly indicates cross-priming of "bystander" immune cells *in vivo*. Although the immunomodulatory function of MSCs

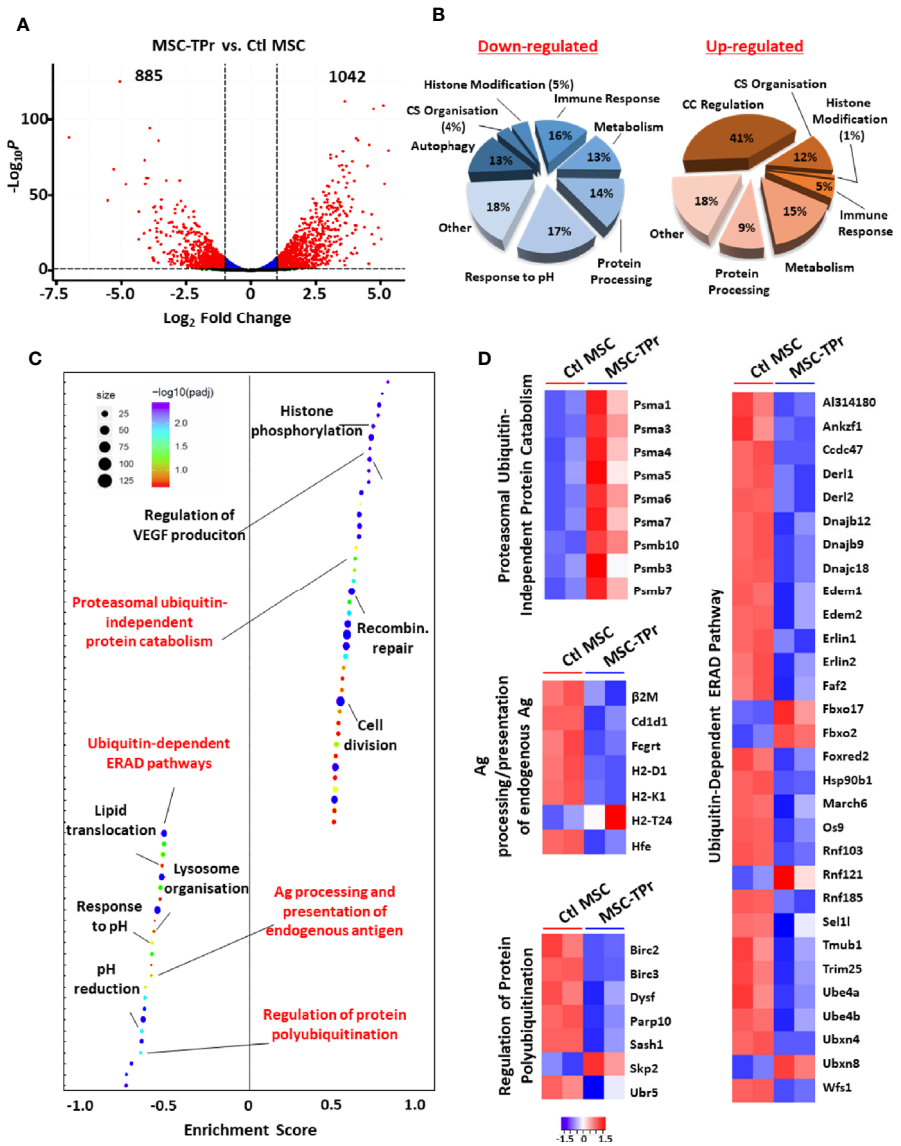


FIGURE 3 | Transcriptomic analysis of MSC-TPr. **(A)** Volcano plot showing the estimated fold changes (x-axis) versus the minus log10 of the adjusted *p*-values (y-axis) from DEseq analysis. Significant genes with absolute value of log2 fold-changes greater or equal to 0.5 are shown in red. **(B)** Major biological processes groups modulated in MSC-TPr compared to Ctl MSCs. CS refers to cytoskeleton whereas CC means cell cycle. **(C)** Plot showing the enriched GO biological processes from an unbiased GSEA analysis of the differentially expressed genes between MSC-TPr and Ctl MSCs. The FDR threshold is set to 0.05. Features are ranked by the enrichment score from the KS test (x-axis). **(D)** A series of heat-maps representing the z-scored expression level of the differentially expressed genes from various processes. Up-regulated and down-regulated genes are highlighted in red and blue respectively.

is mostly driven by soluble mediators and/or contact factors (13, 17–19), previous pre-clinical studies revealed the importance of macrophages in supporting MSC-mediated immunosuppression either through efferocytosis of apoptotic MSCs or *via* IL-10 secretion in response to MSCs-derived chemokine interactome (13, 20). Considering the pivotal role of macrophages in promoting MSCs immunosuppression, we next examined the impact of MSC-TPr vaccination following monocyte/macrophage depletion by clodronate administration (**Figure 5F**). Indeed, phagocyte depletion enhanced the anti-tumor response induced by OVA-pulsed MSC-TPr in both syngeneic (**Figures 5G, H**) and allogeneic models (**Figures 5I, J**) despite secondary re-challenges. These data thus confirm a major suppressive role mediated by phagocytic cells in response to MSC-TPr vaccination.

DC Cross-Priming Is Indispensable to the Anti-Tumor Effect of MSC-TPr

Since clodronate administration enhances dramatically the anti-tumor response elicited by MSC-TPr, we next validated efferocytosis

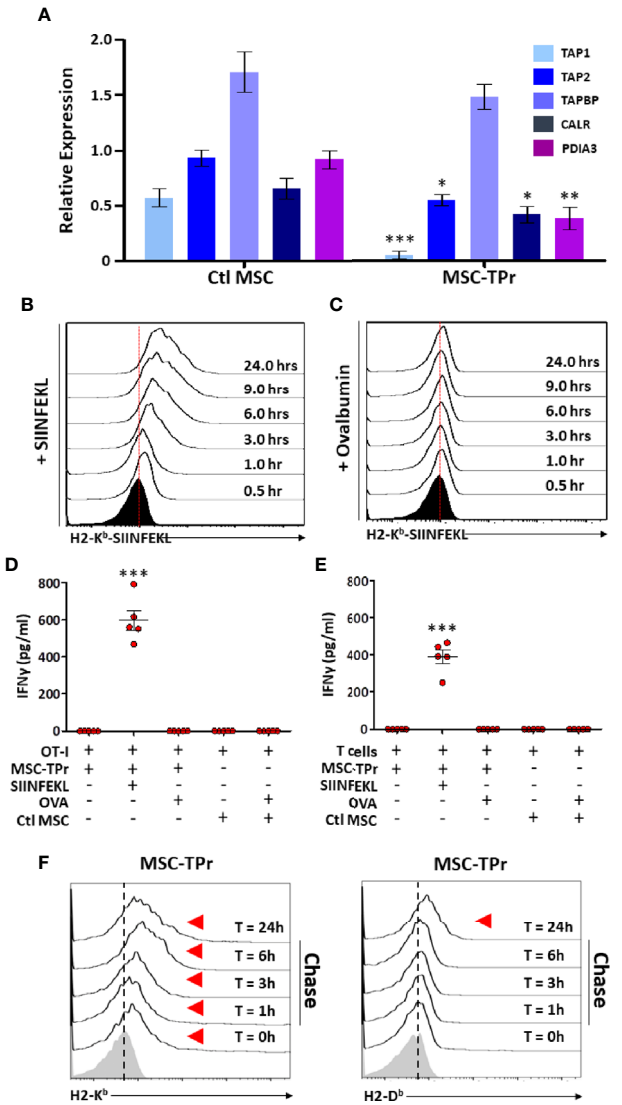


FIGURE 4 | Evaluating the antigen cross-presentation ability of MSC-TPr. **(A)** Transcript quantification of genes involved in antigen presentation. **(B, C)** Representative flow-cytometry analysis of the SIINFEKL/H2-K^b complex following pulsing with the SIINFELK peptide **(B)** or OVA protein **(C)**. Black histograms represent the population in question without peptide/protein pulsing (t=0). The red dotted lines represent the threshold level according to non-pulsed controls. **(D, E)** An antigen-presentation assay conducted using MSC-TPr following pulsing with the SIINFEKL peptide (2.5 µg/ml) or OVA protein (5 mg/ml). Quantification of IFN-gamma production was conducted following MSC-TPr co-culturing with OT-I CD8 T cells **(D)** or CD8 T cells isolated from mice immunized using OVA-pulsed MSC-TPr. **(F)** Flow-cytometry analysis of H2-K^b and H2-D^b following OVA pulsing. For **(A, D, E)**, n = 5/group with *P < 0.05, **P < 0.01 and ***P < 0.001.

of injected cells directly *in vivo*. Hence, an experiment was designed in which CellTrace^{TM}-labelled MSC-TPr were injected into immunocompetent syngeneic mice undergoing control liposome or clodronate injection followed by a peritoneal lavage (**Figure 6A**). Analysis of collected cells 4 h later confirmed the absence of myeloid cells in clodronate-treated animals but revealed the presence of two distinct CD11b$^+$ cell populations in control liposome-treated mice (**Figure 6B**) with only CD11b^{hi} cells staining positive for CellTrace^{TM} (**Figure 6C**). This salient observation led us to formulate the hypothesis that the therapeutic efficiency of MSC-TPr relies on a balance between efferocytosis and cross-priming of professional antigen-presenting cells. Indeed, OVA-pulsed BM-derived DCs successfully activated CD8 T cells derived from MSC-TPr-vaccinated animals, which was further enhanced if clodronate-treated donor mice are used (**Figure 6D**). Given that phosphatidylserine (PIS) can serve as an "eat-me" signal to monocytes/macrophages, we next quantified the levels of PIS on the surface of live versus heat-killed MSC-TPr (21). The basal level of PIS on live MSC-TPr was substantially higher than that on Ctl MSCs and further enhanced after heat-killing (**Figure 6E**) along with a loss in H2-K^b detection on the cell surface (**Figure 6F**). These observations served as impetus to compare the anti-tumor ability of heat-killed MSC-TPr (dead cells with high PIS cell surface levels but no chemokines) versus live MSC-TPr delivered to mice pre-treated with anti-CD11c antibodies as a means to functionally impair DC cross-priming (22). Both treatments impaired the anti-tumor efficacy of the vaccine (**Figure 6G**) clearly indicating that the fate of the immune response induced by MSC-TPr results from a delicate balance between efferocytosis mediated by a subset of CD11^{hi} phagocytes known for mediating immune-suppression, and DC cross-priming responsible for eliciting a pro-inflammatory response.

DISCUSSION

The discovery of a unique and conserved TPr complex despite constant evolution of adaptive immunity has offered an altered and well accepted peptide model for intrathymic positive selection of competent CD8 T cells (23, 24). However, the impact of the TPr on the proteome and/or transcriptome to pervasively affect given cellular functions besides providing a unique set of MHCI peptides remains a matter of debate (14, 25). Here, we report for the first time the therapeutic use of the TPr complex to mount protective anti-tumor responses using both syngeneic and allogeneic MSCs. Although TPr expression in MSCs did not alter their original mesenchymal phenotype, a wide landscape of transcriptional changes affecting various biological functions including endogenous antigen presentation was observed. We further highlight key roles for host-derived phagocytes and professional antigen-presenting cells in orchestrating the balance for MSC-TPr effector functions (**Graphical Abstract**).

Our results are in agreement with the notion that the TPr complex provides a unique peptide repertoire exhibiting low affinity to the CD8 T-cell receptor (26). This is best exemplified by the inability of MSC-TPr to activate CD8 T cells derived from transgenic or vaccinated animals (26). The impaired activation capacity of MSC-TPr could not be due to an absent OVA-derived peptide repertoire as OVA pulsing enhanced MHCI levels on the surface of MSC-TPr indicating *de novo* peptide-MHCI complex formation. If we presume that the peptide repertoire generated

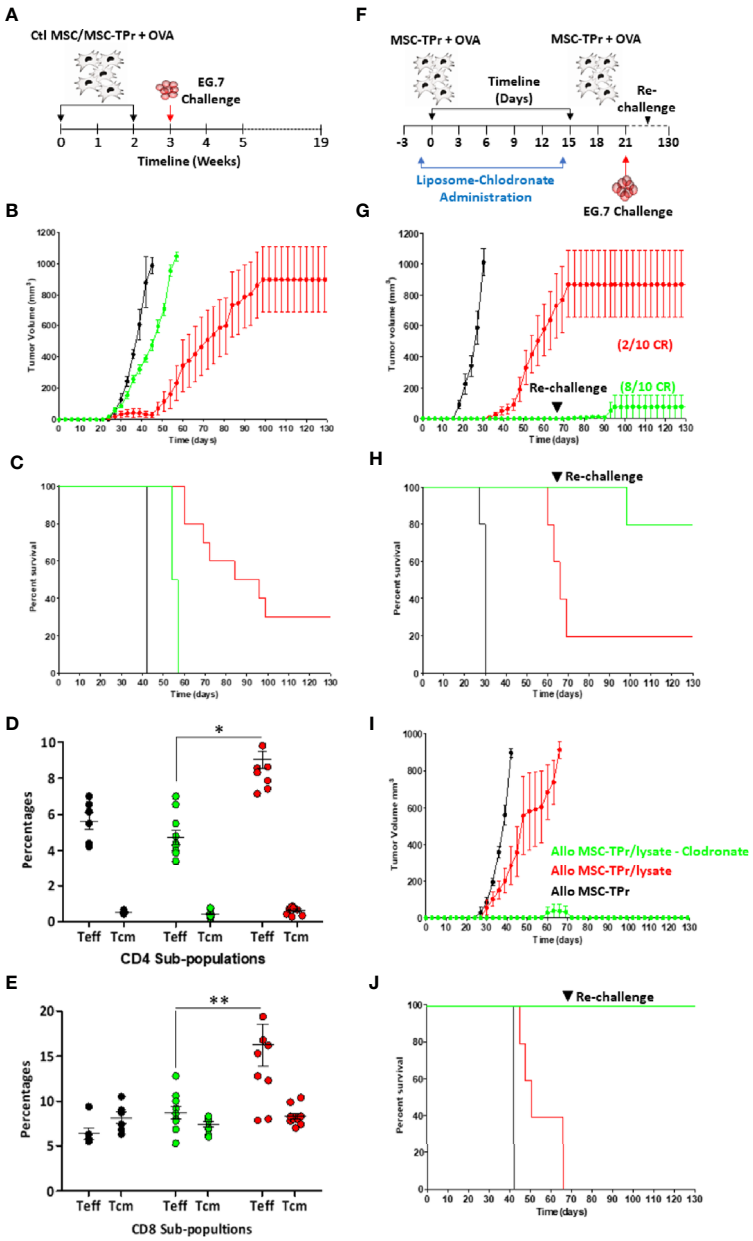


FIGURE 5 | Testing the protective efficacy of MSC-TPr against T-cell lymphoma. **(A)** Schematic diagram representing the prophylactic vaccination schedule. **(B)** Prophylactic vaccination against EG.7 cells. C57BL/6 mice were vaccinated using OVA-pulsed Ctl MSCs (green) or MSC-TPr (red). Non-immunized animals injected with the EG.7 tumor cells are shown in black. **(C)** Kaplan-Meier survival curve of the experiment shown in **(B)**. **(D, E)** Flow-cytometry assessment of effector and central memory CD4 **(D)** and CD8 **(E)** T cells. Ctl mice are shown in black, Ctl MSCs in green and MSC-TPr in red. The main bars represent the mean ± SEM. **(F)** Schematic diagram representing clodronate use with prophylactic vaccination. **(G)** Prophylactic vaccination against EG.7 cells. Vaccinated C57BL/6 mice receiving liposome are shown in red whereas clodronate-treated mice are shown in green. Non-immunized control animals injected with the EG.7 tumor cells are shown in black. **(H)** Kaplan-Meier survival curve of the experiment shown in **(G)**. **(I)** Prophylactic vaccination against A20 cells. Vaccinated Balb/c mice receiving liposome are shown in red whereas clodronate-treated mice are shown in green. Non-immunized Ctl animals injected with the A20 tumor cells are shown in black. **(H)** Kaplan-Meier survival curve of the experiment shown in **(I)**. For **(B. C, G, J)**, n = 10/group. For **(D, E)** n = 7/group with *P < 0.05 and **P < 0.01.

by MSC-TPr is mainly composed of weak agonists or antagonist peptides, then DC-based activation of CD8 T cells derived from MSC-TPr-vaccinated animals shed light on a "bystander" role for MSC-TPr instead of their direct involvement in antigen presentation *in situ*.

Clearance of dying cells by phagocytes (efferocytosis) have recently sparked significant interest in the controversial field of *in vivo*-mediated effector functions of MSCs (20). This concept stipulates the need for the induction of MSC apoptosis *in vivo* in an MHC/HLA-independent fashion but requiring the paracrine

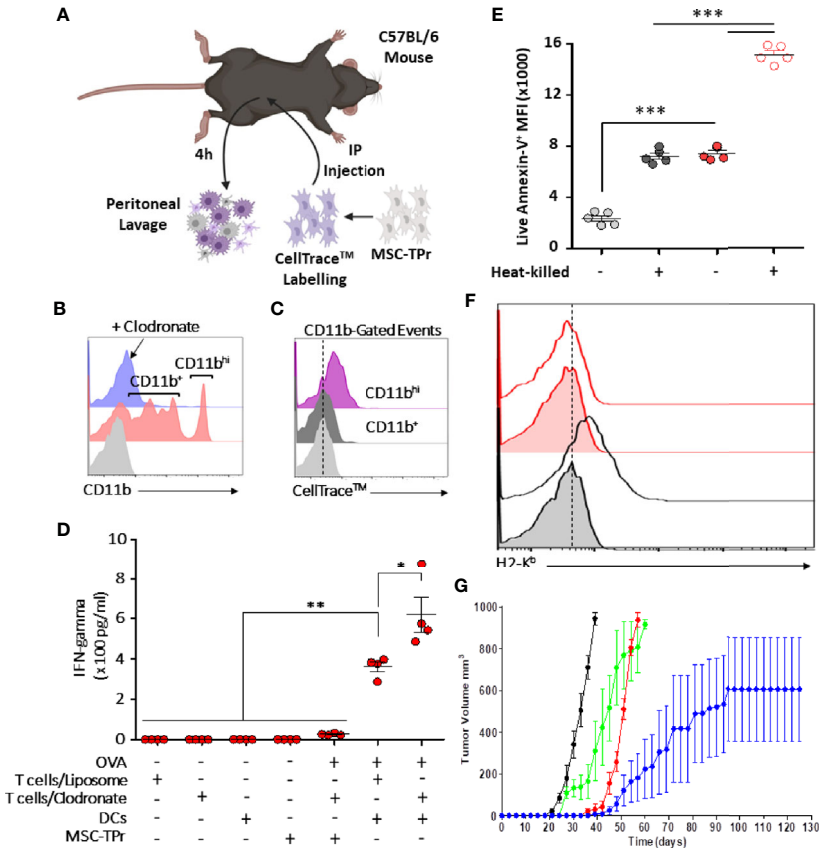


FIGURE 6 | Evaluating the cross-priming ability of MSC-TPr. **(A)** Schematic diagram representing the experimental design for efferocytosis analysis. **(B)** Analysis of $CD11b^+$ cells collected from the peritoneum of vaccinated mice. **(C)** Flow-cytometry assessment of $CD11b^+$ exhibiting a CellTrace™ signal. **(D)** An antigen presentation assay conducted using DCs and CD8 T cells isolated from liposome-/clodronate-treated and vaccinated mice. **(E)** Quantification of the Annexin-V signal on live versus heat-killed Ctl (gray) or MSC-TPr (red). **(F)** Flow-cytometry assessment of $H2\text{-}K^b$ on the surface of live (gray) versus heat-killed (red) MSC-TPr. **(G)** Prophylactic vaccination against EG.7 cells. C57BL/6 mice (n = 6/group) were vaccinated using OVA-pulsed heat-killed MSC-TPr (green) or following administration of CD11c to deplete DCs (red). Ctl MSCs are shown in black and OVA-pulsed MSC-TPr in blue. For **(D, E)**, n = 5/group with $^*P < 0.05$, $^{**}P < 0.01$ and $^{***}P < 0.001$.

effect of granules released by activated cytotoxic cells (20). This concept of inflammation-induced MSC-TPr apoptosis is inconsistent with our syngeneic model as we administered MHC-matched MSCs to naïve animals with no apparent signs of inflammation. An alternative explanation may, in part, involve the higher PIS content on the surface of MSC-TPr, which can serve as an "eat-me" flag signal especially if combined with enhanced recruitment of myeloid cells (phagocytes and DCs) *via* specific chemokines such as CCL2, CX3CL1, and CCL9 (13, 21). This is consistent with the improved anti-tumor responses observed in phagocyte-depleted animals and the lack of therapeutic effects using heat-killed MSC-TPr. If phagocytes impair the anti-tumor response of the vaccine and MSC-TPr cannot behave as an antigen-presenting cell *in vivo*, then how can animals develop a protective OVA-specific CD8 T-cell response? The simplest explanation lies in endogenous DC cross-priming as animals undergoing anti-CD11c treatment are incapable of mounting protective anti-tumor responses (22). Besides, the loss of function observed with heat-killed MSC-TPr also indicate the need for metabolically-fit cells secreting specific chemokines and perhaps other soluble growth factor to recruit and cross-prime endogenous DCs.

CONCLUSION

Our findings provide clear evidence that TPr-based proteasomal alterations can trigger potent T-cell immunity when used as part of an engineered MSC-based vaccine. By modulating the antigen processing activity and chemokine secretion profile of MSCs, TPr expression coordinates an indirect but efficient pro-inflammatory response exploiting MSCs as a "living vector with a therapeutic payload" potentially delivering antigen fragments to host-derived DCs. Investigating the nature and exact involvement of the "eat-me" signals as well as the role played by individual chemokines would further define the molecular landscape of this interaction.

DATA AVAILABILITY STATEMENT

The datasets presented in this study are available online, under repository: GEO accession GSE161773.

ETHICS STATEMENT

The animal studies including all experimental procedures and protocols were reviewed and approved by the Animal Ethics Committee of Université de Montréal.

AUTHOR CONTRIBUTIONS

J-PB designed most of the study, carried-out most of the experiments, analyzed the data and prepared the figures. NE-H conducted the bioinformatics analysis for the RNA-Seq. AE-K, JA, NS and RS designed some experiments and wrote some sections of the manuscript. MR designed the study, discussed the results with all authors and wrote the manuscript. All authors contributed to the article and approved the submitted version.

FUNDING

This work was supported by a Discovery Grant from the National Sciences and Engineering Research Council of Canada (RGPIN/06101-2014).

ACKNOWLEDGMENTS

We are grateful to the Institute for Research in Immunology and Cancer genomics and animal care facility staff for their assistance. JA is a Vanier Scholar. MR holds a Fonds de la Recherche en Santé du Québec Junior II Award.

SUPPLEMENTARY MATERIAL

The Supplementary Material for this article can be found online at: https://www.frontiersin.org/articles/10.3389/fimmu.2020.596303/full#supplementary-material

REFERENCES

1. Murata S, Takahama Y, Kasahara M, Tanaka K. The immunoproteasome and thymoproteasome: functions, evolution and human disease. *Nat Immunol* (2018) 19(9):923–31. doi: 10.1038/s41590-018-0186-z
2. Princiotta MF, Finzi D, Qian SB, Gibbs J, Schuchmann S, Buttgereit F, et al. Quantitating protein synthesis, degradation, and endogenous antigen processing. *Immunity* (2003) 18(3):343–54. doi: 10.1016/S1074-7613(03)00051-7
3. López-Otín C, Blasco MA, Partridge L, Serrano M, Kroemer G. The hallmarks of aging. *Cell* (2013) 153(6):1194–217. doi: 10.1016/j.cell.2013.05.039
4. de Verteuil DA, Rouette A, Hardy MP, Lavallée S, Trofimov A, Gaucher É., et al. Immunoproteasomes shape the transcriptome and regulate the function of dendritic cells. *J Immunol* (2014) 193(3):1121–32. doi: 10.4049/jimmunol.1400871
5. de Verteuil D, Muratore-Schroeder TL, Granados DP, Fortier MH, Hardy MP, Bramoulle A, et al. Deletion of immunoproteasome subunits imprints on the transcriptome and has a broad impact on peptides presented by major histocompatibility complex I molecules. *Mol Cell Proteomics* (2010) 9(9):2034–47. doi: 10.1074/mcp.M900566-MCP200
6. Takahama Y, Ohigashi I, Murata S, Tanaka K. Thymoproteasome and peptidic self. *Immunogenetics* (2019) 71(3):217–21. doi: 10.1007/s00251-018-1081-3
7. Xing Y, Jameson SC, Hogquist KA. Thymoproteasome subunit-β5T generates peptide-MHC complexes specialized for positive selection. *Proc Natl Acad Sci USA* (2013) 110(17):6979–84. doi: 10.1073/pnas.1222244110
8. Nitta T, Murata S, Sasaki K, Fujii H, Ripen AM, Ishimaru N, et al. Thymoproteasome shapes immunocompetent repertoire of CD8+ T cells. *Immunity* (2010) 32(1):29–40. doi: 10.1016/j.immuni.2009.10.009
9. Tschöpe C, Miteva K, Schultheiss HP, Linthout SV. Mesenchymal stromal cells: a promising cell source for the treatment of inflammatory cardiomyopathy. *Curr Pharm Des* (2011) 17(30):3295–307. doi: 10.2174/138161211797904136
10. Hao L, Sun H, Wang J, Wang T, Wang M, Zou Z. Mesenchymal stromal cells for cell therapy: besides supporting hematopoiesis. *Int J Hematol* (2012) 95(1):34–46. doi: 10.1007/s12185-011-0991-8
11. Stagg J, Pommey S, Eliopoulos N, Galipeau J. Interferon-gamma-stimulated marrow stromal cells: a new type of nonhematopoietic antigen-presenting cell. *Blood* (2006) 107(6):2570–7. doi: 10.1182/blood-2005-07-2793
12. Galipeau J, Li H, Paquin A, Sicilia F, Karpati G, Nalbantoglu J. Vesicular stomatitis virus G pseudotyped retrovector mediates effective in vivo suicide gene delivery in experimental brain cancer. *Cancer Res* (1999) 59(10):2384–94.
13. Giri J, Das R, Nylen E, Chinnadurai R, Galipeau J. CCL2 and CXCL12 Derived from Mesenchymal Stromal Cells Cooperatively Polarize IL-10+ Tissue Macrophages to Mitigate Gut Injury. *Cell Rep* (2020) 30(6):1923–34.e4. doi: 10.1016/j.celrep.2020.01.047
14. Ohigashi I, Tanaka Y, Kondo K, Fujimori S, Kondo H, Palin AC, et al. Trans-omics Impact of Thymoproteasome in Cortical Thymic Epithelial Cells. *Cell Rep* (2019) 29(9):2901–16.e6. doi: 10.1016/j.celrep.2019.10.079
15. Sánchez-Lanzas R, Castaño JG. Proteins directly interacting with mammalian 20S proteasomal subunits and ubiquitin-independent proteasomal degradation. *Biomolecules* (2014) 4(4):1140–54. doi: 10.3390/biom4041140
16. Barral DC, Brenner MB. CD1 antigen presentation: how it works. *Nat Rev Immunol* (2007) 7(12):929–41. doi: 10.1038/nri2191
17. Galipeau J, Sensébé L. Mesenchymal Stromal Cells: Clinical Challenges and Therapeutic Opportunities. *Cell Stem Cell* (2018) 22(6):824–33. doi: 10.1016/j.stem.2018.05.004
18. Rafei M, Campeau PM, Aguilar-Mahecha A, Buchanan M, Williams P, Birman E, et al. Mesenchymal stromal cells ameliorate experimental autoimmune encephalomyelitis by inhibiting CD4 Th17 T cells in a CC chemokine ligand 2-dependent manner. *J Immunol* (2009) 182(10):5994–6002. doi: 10.4049/jimmunol.0803962
19. Rafei M, Hsieh J, Fortier S, Li M, Yuan S, Birman E, et al. Mesenchymal stromal cell-derived CCL2 suppresses plasma cell immunoglobulin production via STAT3 inactivation and PAX5 induction. *Blood* (2008) 112(13):4991–8. doi: 10.1182/blood-2008-07-166892
20. Galleu A, Riffo-Vasquez Y, Trento C, Lomas C, Dolcetti L, Cheung TS, et al. Apoptosis in mesenchymal stromal cells induces in vivo recipient-mediated immunomodulation. *Sci Transl Med* (2017) 9(416):eaam7828. doi: 10.1126/scitranslmed.aam7828
21. Zhou Y, Fei M, Zhang G, Liang WC, Lin W, Wu Y, et al. Blockade of the Phagocytic Receptor MerTK on Tumor-Associated Macrophages Enhances P2X7R-Dependent STING Activation by Tumor-Derived cGAMP. *Immunity* (2020) 52(2):357–73.e9. doi: 10.1016/j.immuni.2020.01.014
22. Wu J, Wu H, An J, Ballantyne CM, Cyster JG. Critical role of integrin CD11c in splenic dendritic cell capture of missing-self CD47 cells to induce adaptive

immunity. *Proc Natl Acad Sci U S A* (2018) 115(26):6786–91. doi: 10.1073/pnas.1805542115
23. Kondo K, Ohigashi I, Takahama Y. Thymus machinery for T-cell selection. *Int Immunol* (2019) 31(3):119–25. doi: 10.1093/intimm/dxy081
24. Kasahara M, Flajnik MF. Origin and evolution of the specialized forms of proteasomes involved in antigen presentation. *Immunogenetics* (2019) 71 (3):251–61. doi: 10.1007/s00251-019-01105-0
25. Apavaloaei A, Brochu S, Dong M, Rouette A, Hardy MP, Villafano G, et al. PSMB11 Orchestrates the Development of CD4 and CD8 Thymocytes via Regulation of Gene Expression in Cortical Thymic Epithelial Cells. *J Immunol* (2019) 202(3):966–78. doi: 10.4049/jimmunol.1801288
26. Sasaki K, Takada K, Ohte Y, Kondo H, Sorimachi H, Tanaka K, et al. Thymoproteasomes produce unique peptide motifs for positive selection of CD8(+) T cells. *Nat Commun* (2015) 6:7484. doi: 10.1038/ncomms8484

Conflict of Interest: RS is the founder of IntelliStem Technologies Inc. (Toronto, ON, Canada).

The remaining authors declare that the research was conducted in the absence of any commercial or financial relationships that could be construed as a potential conflict of interest.

Copyright © 2021 Bikorimana, El-Hachem, El-Kadiry, Abusarah, Salame, Shammaa and Rafei. This is an open-access article distributed under the terms of the Creative Commons Attribution License (CC BY). The use, distribution or reproduction in other forums is permitted, provided the original author(s) and the copyright owner(s) are credited and that the original publication in this journal is cited, in accordance with accepted academic practice. No use, distribution or reproduction is permitted which does not comply with these terms.

frontiers in Oncology

REVIEW
published: 03 February 2021
doi: 10.3389/fonc.2020.584367

Enhancing the Efficacy of Tumor Vaccines Based on Immune Evasion Mechanisms

Jianyu Chen[1], *Honghao Zhang*[1], *Lijuan Zhou*[1], *Yuxing Hu*[1], *Meifang Li*[1], *Yanjie He*[1] *and Yuhua Li*[1,2*]

[1] *Department of Hematology, Zhujiang Hospital, Southern Medical University, Guangzhou, China,* [2] *Bioland Laboratory (Guangzhou Regenerative Medicine and Health Guangdong Laboratory), Guangzhou, China*

Tumor vaccines aim to expand tumor-specific T cells and reactivate existing tumor-specific T cells that are in a dormant or unresponsive state. As such, there is growing interest in improving the durable anti-tumor activity of tumor vaccines. Failure of vaccine-activated T cells to protect against tumors is thought to be the result of the immune escape mechanisms of tumor cells and the intricate immunosuppressive tumor microenvironment. In this review, we discuss how tumor cells and the tumor microenvironment influence the effects of tumor infiltrating lymphocytes and summarize how to improve the efficacy of tumor vaccines by improving the design of current tumor vaccines and combining tumor vaccines with other therapies, such as metabolic therapy, immune checkpoint blockade immunotherapy and epigenetic therapy.

Keywords: tumor vaccines, immune evasion, tumor microenvironment, combination therapies, immunotherapy

OPEN ACCESS

Edited by:
Graham Pawelec,
University of Tübingen, Germany

Reviewed by:
Sadhak Sengupta,
Triumvira Immunologics, Inc., United States
William J. Magner,
University at Buffalo, United States

***Correspondence:**
Yuhua Li
liyuhua1974@outlook.com
orcid.org/0000-0002-0982-6680

Specialty section:
This article was submitted to Cancer Immunity and Immunotherapy, a section of the journal Frontiers in Oncology

Received: *17 July 2020*
Accepted: *22 December 2020*
Published: *03 February 2021*

Citation:
Chen J, Zhang H, Zhou L, Hu Y, Li M, He Y and Li Y (2021) Enhancing the Efficacy of Tumor Vaccines Based on Immune Evasion Mechanisms. Front. Oncol. 10:584367. doi: 10.3389/fonc.2020.584367

INTRODUCTION

Immunotherapy aims to initiate or reinitiate the self-sustaining cycle of tumor immunity, and there is great expectation that this approach will cure various tumor types. Many tumor-targeting approaches exist, but few tumor therapies induce as durable activity as immunotherapy. Safe and robust tumor vaccines have held great promise for tumor immunotherapy.

Tumors are known for their accumulation of genetic alterations and loss of normal cellular regulatory processes (1). These events can lead to the expression of tumor antigens, resulting in peptides that bind to major histocompatibility class I (MHC-I) molecules on the surface of tumor cells (2). These tumor specific peptide-MHC-I complexes can be recognized by $CD8^+$ T cells (3). The aim of tumor vaccines is to expand the tumor-specific T cell pool from the naïve pool and reactivate existing tumor-specific T cells in dormant or unresponsive states. Despite tremendous potential of tumor vaccines for tumor immunotherapy, the clinical outcomes in some patients remain suboptimal. In the past, this may be attributed to the selection of tumor antigen, as traditional tumor vaccines mainly target tumor-associated antigens (TAAs), which can be detected on both tumor cells and normal cells (4, 5). Currently, the development of sequencing technologies and different bioinformatics algorithms have accelerated the identification of neoantigens and the construction of neoantigen tumor vaccines (6, 7). Neoantigens are highly immunogenic because they are only expressed on tumor cells and do not present in normal cells, hence bypassing central thymic tolerance (4). Clinical trials have shown that neoantigen vaccine strategies successfully

increase the frequency and activity of tumor-specific cytotoxic T lymphocytes (CTLs) (8, 9). However, tumor development is a dynamic progression. Owing to the immune suppression and escape mechanisms of tumor tissues, neoantigen vaccines alone may not be able to apply expected anti-tumor protection, even if host immune systems have been activated, for the reason that the vaccine alone fails to ensure that the activated T cells home to the tumor bed and exert anti-tumor effects within the tumor.

In fact, the immune response in tumors is precisely regulated in a cancer-immunity cycle. First, the tumor antigens should be released and presented by antigen presenting cells (APCs) to T cells through the T cell receptor (TCR) in order to prime and activate the tumor-specific effector T cells. Second, activated effector T cells must be trafficked to tumor bed and infiltrate into the tumors to specifically recognize the tumor cells. Last, the effector T cells kill the tumor cells (10). Tumor vaccines should go through the above immunity cycle to produce a tumor killing effect. Unfortunately, many tumor specific T cells have become victims of immune suppression and immune escape mechanisms, which means that the vaccine-activated T cells become exhausted or dysfunctional before they exert tumor-killing effects. This is one of the most important reasons for tumorigenesis, recurrence and metastasis in relation to both tumor cell-intrinsic factors and the tumor microenvironment (TME). In this review, we mainly focus on the key aspects of how tumor specific T cells are controlled by the tumor cells and tumor microenvironment and are manipulated to enhance the anti-tumor immunity of tumor vaccines to implement new clinical strategies.

MODULATION OF T CELL FUNCTION BY TUMORS

Tumor evasion immunity comprises both tumor cell-intrinsic alterations and TME modification. These components form a complex immunosuppressive network in tumors, which together limits the activation of and induces the dysfunction of T cells. **Figure 1** shows how tumors influence the function of effector T cells.

Inhibition of Recognition, Priming, and Activation

Tumorigenesis is the process of continuous tumor cell evolution. A series of changes may occur in tumor cells to evade the recognition of immune cells. MHC-I molecules presented on the surface of tumor cells are key proteins for $CD8^+$ T cell recognition. However, MHC-I molecule abnormalities have been found to occur at a relatively high frequency in tumor cells, including the loss or downregulation of MHC-I molecules (11, 12). This leads to the conclusion that alterations of MHC-I molecules stand for a common immune-escape mechanism of tumor cells (13). Actually, the expression of MHC-I molecules is the result of a proper antigen processing machinery (APM) and any alterations in the APM may lead to the deficiency of antigen processing and cause immune escape. For example, transporter associated with antigen processing (TAP) plays an important role in the transportation of proteins and the alteration of TAP can induce a sharp decrease of the MHC-I/b2m-peptide complexes expressed on tumor cells (14, 15). Indeed, the deficiency of TAP can be found in a variety of tumors such as head and neck carcinoma, gastric cancer and cervical carcinoma (14–17). Apart from the above gene regulatory mechanisms, the presentation of tumor antigens can be affected by other tumor cell biological processes. For example, the expression of TAP, latent membrane protein (LMP), Tapasin and MHC-I molecules are recovered after histone deacetylase inhibitor (HDACi) treatment, suggesting that epigenetic repression is also involved in the mechanism of tumor MHC-I molecules loss (18).

In addition to the intrinsic tumor cell factors, a series of factors in the TME, such as regulatory T cells (Tregs), disrupt the antigen presentation process, leading to insufficient T cell activation. Cross-presentation of tumor antigens by dendritic cells (DCs) is considered important in the early stage of tumor immune recognition because DCs acquire, process, and present tumor antigens to TCR and provide co-stimulatory factors to prime and boost the $CD8^+$ T cells. However, CTLA-4 expressed on Tregs can suppress such immune response through the interaction with co-stimulation factors CD80 and CD86 expressed on DCs. When combined, the expression of CD80 and CD86 on DCs will be downregulated, thus impairing DC function and inhibiting T cell stimulation (19, 20). Moreover, a novel study uncovered that the antigen-specific Tregs activated by DCs can form a strong interaction with DCs. Such strong binding can remove the peptide-major histocompatibility complex class II (pMHCII) complexes from the surface of DCs and thereby decrease the antigen presentation efficiency of DCs (21). The upregulation of lymphocyte activation gene-3 (LAG-3) expression on activated Tregs is also a factor that acts as an immune regulatory protein (22).

Other components in TME may also influence the activation of effector T cells. Metabolic stress, including hypoxia and glucose deficiency, can cause downregulation of MHC-I molecules on tumor cells. Such alteration is accompanied by the loss of sensitivity of tumor cells to the upregulation of MHC molecules mediated by interferon (IFN)-γ (23). Programmed cell death 1 ligand (PD-L1) and Programmed cell death 2 ligand (PD-L2) expressed on tumor cells and other cells are also indispensable factors that inhibit proliferation and cytokine production of programmed cell death (PD)-1 expressing T cells (24).

Inhibition of Trafficking and Infiltration to Tumor Bed

Chemokines and cytokines regulate the trafficking and infiltration of immune cells into the TME. Researchers have found that in tumors lacking in the infiltration of $CD8^+$ T cells, the expression of chemokines involved in the recruitment of effector T cells was significantly reduced (25), implying their critical roles in tumor progression. On the one hand, chemokine expression is regulated by environmental cues in the TME. In transplanted melanoma mouse model, Barreira da Silva et al. showed that the dipeptidylpeptidase

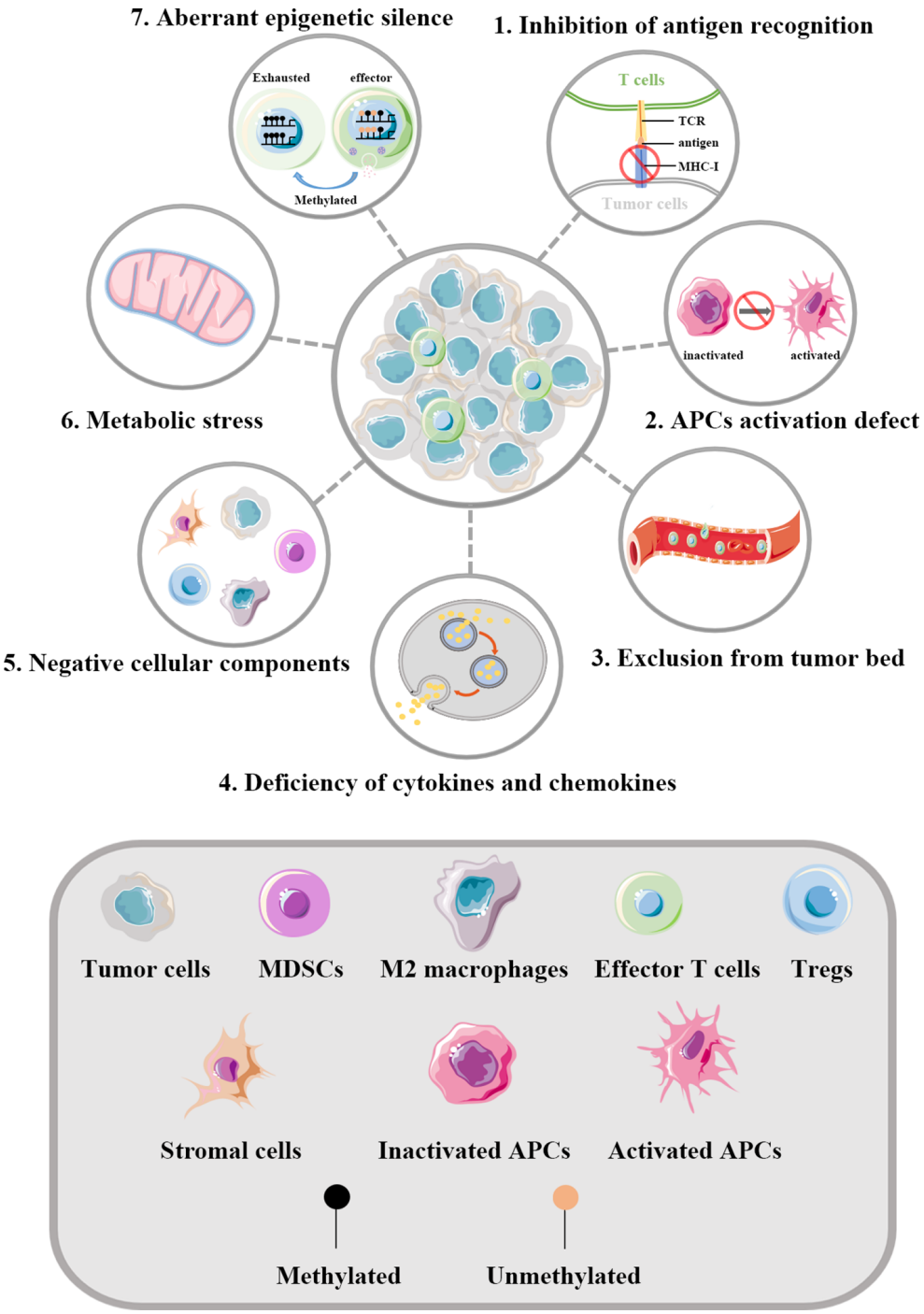


FIGURE 1 | Regulation of T cells by tumors. The key aspects of how tumors influence the function of effector T cells are illustrated. 1) Abnormal alterations of MHC-I molecules in tumor cells can help evade the recognition of T cells. 2) A series of factors in TME can inhibit the maturation of APCs, thus defecting the priming and activating of effector T cells. 3) Tumor blood vessels act as physical barriers affecting the infiltration of T cells into the tumor bed. The vascular endothelial growth factors generated by tumor derived blood vessels can result in multiple changes within the vessels and thereby drive T cells depletion. 4) Abnormal cytokines and chemokines in TME can influence the infiltration of T cells. In tumors lacking in the infiltration of effector T cells, the expression of chemokines involved in the recruitment of T cells are significantly reduced. 5) Negative cellular components are key cellular mediators reshaping the immunosuppressive TME. 6) Dysregulated metabolism pathways in tumor cells can lead to insufficient nutrients in TME. What's more, the specialized metabolism of tumor cells establishes an unfriendly TME to effector T cells, which further increases the living stress of effector T cells. 7) Effector T cells infiltrating in TME are frequently in exhaustion state and accumulating evidence implies such reprogramming to be the consequence of aberrant epigenomes such as methylated. TCR, T cell receptor; MHC-I, major histocompatibility class I molecules; APCs, antigen presenting cells; MDSCs, myeloid-derived suppressor cells; Tregs, regulatory T cells.

(DPP4) produced by stromal cells within the tumor inactivated chemokine CXCL10, leading to the reduction of T cell infiltration (26). On the other hand, chemokine expression can be regulated by tumor cell-intrinsic epigenetic and genetic mechanisms. Tumor epigenetic silencing often includes zeste homologue2 (EZH2)-mediated histone modifications and DNA methyltransferase 1 (DNMT1)-mediated DNA methylation. Using the ovarian cancer mouse models, researchers found repression of T helper 1 (Th1)-type chemokines CXCL9 and CXCL10 produced by tumor cells caused by the above epigenetic silencing. The finding indicates that there exists a negative association between tumor-infiltrating $CD8^+$ T cells and epigenetic silencing (27). A similar change was found in C-C motif chemokine ligand (CCL)5, where DNA methylation reduced the expression of CCL5 and caused tumor-infiltration lymphocyte desertification (28). Moreover, using a genetically engineered mouse melanoma model, researchers found that oncogenic pathway is another approach displayed by tumor cells to control chemokine expression. In the melanoma model, the activation of β-catenin resulted in poor expression of CCL4, which is important for the migration of $CD103^+$ DCs, and subsequently limited the activation and infiltration of effector T cells (29).

Another reason accounting for the defective T cell infiltration to the tumor sites could be the presence of physical barriers. Like normal tissues, tumors need to obtain nutrients and oxygen and excrete metabolic wastes to maintain their survival, and the generation of tumor-associated neo-vasculature can meet these needs. However, such blood vessels are produced under the condition of an unbalanced mix of proangiogenic signals (1) and can act as physical barriers to the transportation of T cells into the tumor bed. When T cells enter the tumor vessels, a series of changes in the tumor vasculature repress T cell activity and induce T cell exhaustion. First, intercellular adhesion molecule-1 (ICAM-1) and vascular cell adhesion molecule-1 (VCAM-1) are needed for the extravasation of T cells and upregulation of ICAM-1 has been associated with good prognosis of cancer patients (30–33). However, tumor-derived blood vessels can generate vascular endothelial growth factors (VEGF) to inhibit the expression of adhesion molecules and thus prevent T cells from infiltrating into the tumor (34). Second, as within the tumor, inhibitory regulatory molecules such as PD-L1, PD-L2, galectin-9, indoleamine 2,3-dioxygenase 1 (IDO-1), and human B7 homolog 3 (B7-H3) (35–39) can be upregulated on vascular endothelial cells to directly inhibit T cell activity. VEGF-α can also induce the expression of thymocyte selection-associated high mobility group box (TOX) protein in T cells, thereby driving T cell depletion (40). Third, Fas-L expressed on tumor endothelial cells can directly cause T cell apoptosis (41). Finally, tumor blood vessels are known for their unique characteristics, such as slow and irregular blood flow, microvascular disorders, lack of basement membranes and abnormally thick membranes in blood vessels (42), which together result in insufficient oxygen supply in blood vessels and the accumulation of metabolic waste, leading to the impairment of T cells. What's more, these factors would trigger the release and activation of pro-angiogenic growth factors (43) and further deepen the damage to T cells, as demonstrated above.

Impairment of T Cell Function and the Induction of Dysfunctional T Cells

Tumor cells rely on metabolic networks to maintain their proliferation, and various metabolism pathways are dysregulated in tumor cells due to their irregulated genetic landscape. Like tumor cells, having enough nutrients is essential for normal metabolic activity and anti-tumor immune response of T cells. However, the competition for nutrients between tumor cells and T cells can affect the immune response, and depletion of nutrients in the TME can also lead to insufficient immune response and tumor progression. Glucose is a major energy source, and it plays an important role in maintaining normal cellular functions and supporting cellular bioenergy. Even when oxygen is sufficient, tumor cells utilize glucose *via* glycolysis, which is called the Warburg effect (44). The glycolytic enzyme hexokinase 2 (HK2) overexpressed in tumor cells ensures the high efficiency of glycolysis in tumor cells and at the same time inhibits the glucose uptake of T cells (45, 46). Long-term glucose deficiency results in low T cell response and impairs the production of cytokines, allowing tumors to acquire immune escape properties. In addition to glucose, amino acids and lipids are also metabolic sources competed for by tumor cells and T cells. For example, IDO is expressed in many tumors and can catabolize tryptophan (47). Lower concentrations of tryptophan in extracellular environment can inhibit the proliferation of $CD8^+$ T cells and promote the differentiation of Tregs by activating general control nonderepressible 2 (GCN2) kinase (48). Lipid rafts in the cell membrane of T cells are required to form immune synaptic tissues (49), while the growing tumor cells also need fatty acids to synthesize cell membranes or other molecules (50). The disturbance of lipid homeostasis may therefore result in a reduction of effector T cells.

In addition to nutrient depletion, the specialized metabolism of tumor cells also establishes a hypoxic, acidic TME (44) that is unfriendly to the anti-tumor immune response. In other words, besides promoting the growth of tumor cells, the unique metabolic programs can also prevent the development of an effective anti-tumor response. For example, the reduced blood flow and Warburg effect can result in a hypoxia state in the TME. Earlier studies have indicated that hypoxia can lead to the deficiency of mTOR signaling in T cells which can drive the anergy of effector T cells (51, 52) while promoting the development of Tregs (53). The aberrant Warburg effect of tumor cells produces lactic acid to be exported into the extracellular space, which can result in an acidic TME. The resultant acidification of TME can induce the apoptosis of T cells and suppress T cell function by the inhibition of nuclear factor of activated T cells (NFAT) upregulation and the inhibition of p38 and JNK/c-Jun activation (54, 55). Lactic acid has also been shown to interfere with the maturation of DCs (56) and increase the frequency of forkhead box P3 $(FoxP3)^+$ Tregs (57). Research has shown an increased expression of PD-L1 on tumor cells by the accumulation of lactic acid (58).

In addition to tumor cells, MDSCs and Tregs are two key cellular mediators in the immunosuppressive TME. The function of Tregs has been described above. Here, we discuss how MDSCs shape the intra-tumoral immune landscape to impair the function of T cells.

MDSCs deplete amino acids in the TME that are essential for T cell function. MDSCs are characterized by the expression of enzyme arginase 1 (Arg1) (59). L-arginine is the substrate of Arg1, and excessive Arg1 leads to the depletion of L-arginine in the TME, which is of significant importance for the maturation of T cell receptor ζ-chain (TCRζ) and can therefore result in impaired T cell growth and differentiation (59). Moreover, MDSCs can deplete the extracellular cysteine pool to limit the activation of T cells (60). Inducible nitric oxide synthase-2 (iNOS2) produced by MDSCs can release high level of nitrogen monoxide (NO), which can interrupt T cell function by interfering with T cell JAK/STAT signaling proteins and can induce T cell apoptosis (61). MDSCs can also induce the proliferation of Tregs by secreting soluble factor IL-10 to further downregulate the activation and expansion of T cells (62).

Tumor vaccines can potentially induce efficient antitumor immunity by recruiting and activating immune cells. However, the mechanisms demonstrated above can be utilized by tumors to turn effector T cells into exhausted ones, which can be characterized by the deficiency of response to TCR stimulation, the production of cytokines and the upregulation of inhibitory factors. This condition can be associated with the loss of tumor growth control. In the following section, we consider how different strategies can modulate tumor vaccine function to better boost antitumor immunity.

STRATEGIES TO IMPROVE TUMOR VACCINE EFFICACY

Currently, strategies have been used in pre-clinical experiments and clinical trials to improve the anti-tumor efficacy of tumor vaccines. Here, we discuss how these strategies influence the responsiveness of tumor vaccines against tumors. **Table 1** shows the related strategies.

IMPROVE THE DESIGN OF CURRENT TUMOR VACCINES

Vaccines Based on Both MHC-I–Specific Tumor Antigens and MHC-II Specific Tumor Antigens

At present, most tumor immunotherapy is aimed at activating $CD8^+$ T cells. With improved understanding of the immunology, recent studies have highlighted the role of $CD4^+$ T cells in tumor clearance. The activation of an effective anti-tumor immune response not only needs helper T cells to recruit the killer T cells but also needs them induce killer T cells into the activation state in which they are capable of killing tumor cells (63, 64). In

TABLE 1 | Strategies enhancing the anti-tumor efficacy of tumor vaccines.

Strategies	Target steps[a]	Effect on tumor vaccines	Challenges
1. Improve the design of tumor vaccines.			
Vaccines based on both MHC-I specific tumor antigens and MHC-II specific tumor antigens	Inhibition of T cell priming and activation	$CD4^+$ T cells help activate $CD8^+$ T cells and help them mature into CTLs; more efficient uptake and presentation; cytokines secreted by $CD4^+$ T cells dictate the quality of CTLs.	Loss of MHC-II molecules expression on tumor cells; few of found MHC-II restricted tumor antigens due to current prediction algorithms
Re-assembling tumor vaccines with nanoparticles	Inhibition of T cell priming and activation; inhibition of trafficking and infiltration to tumor bed; impairment of T cell function and the induction of dysfunctional T cells	Vectors for different molecules that synergize with tumor vaccines; stabilize the loaded adjuvants; reshape immunosuppressive TME; promote the production of CTLs.	The safety of chosen material compositions; optimize the physical properties of nanoparticles.
2. Combine tumor vaccines with other therapies.			
Tumor vaccines plus metabolic therapy	Impairment of T cell function and the induction of dysfunctional T cells	Switch to metabolisms beneficial to T cell function; magnify the metabolic plasticity defect of tumor cells.	Side effects caused by the dysfunctional normal cell metabolisms; intrinsic toxicity.
Tumor vaccines plus CAR-T therapy	inhibition of tumor antigen recognition	Recognize antigen on any HLA background; target tumor cells that downregulate MHC-I molecules.	Increased toxicity.
Tumor vaccines plus ICBs therapy	Inhibition of T cell priming and activation; impairment of T cell function and induction of dysfunctional T cells	Reinvigorate exhausted T cells; evoke tumor immunogenicity.	Induction of dysfunctional cell subsets; injection sequence.
Tumor vaccines plus OVs therapy	Inhibition of tumor antigen recognition; inhibition of T cell priming and activation; inhibition of trafficking and infiltration to tumor bed	Help reverse the down-regulation of MHC-I molecules; induce the maturation and function of DCs; reshape the immunosuppressive TME.	Balancing the antitumor immune response and antiviral immune response; more appropriate clinical indicators.
Tumor vaccines plus epigenetic therapy	Inhibition of tumor antigen recognition; inhibition of T cell priming and activation; inhibition of trafficking and infiltration to tumor bed; impairment of T cell function and the induction of dysfunctional T cells	Help restore APM expression; increase immune infiltration; directly reinvigorate exhausted T cells.	Intrinsic toxicity; balancing the pro-immunogenic and immunosuppressive functions.

[a]*According to Modulation of T Cell Function by Tumors section, how tumors influence the function of T cells can be briefly concluded into the following steps: inhibition of tumor antigen recognition, inhibition of T cell priming and activation, inhibition of trafficking and infiltration to tumor bed, impairment of T cell function and the induction of dysfunctional T cells. This list mainly focuses on which steps the strategy targets to improve the function of tumor vaccines. MHC, major histocompatibility class; CTLs, cytotoxic T cells; TME, tumor microenvironment; ICBs, immune checkpoint blockage; APM, antigen processing machinery.*

other words, killer T cells should synergize with the helper T cells to activate a robust and durable immune protection.

Studying mouse models of human tumors, researchers found that vaccines act more effectively when both helper and killer T cells are activated. Using the KP9025 sarcoma mice model, researchers indicated that the administration of vaccines with a mixture of KP.mLAMA4 (MHC-I specific tumor antigen) and KP.mITGB1 (MHC-II specific tumor antigen) provided more effective protection against tumor challenge than administration of each the antigen alone. What's more, spleen from mice vaccinated with the mixture antigens contained more functional $CD8^+$ T cells than the mice receiving only MHC-I specific tumor antigen. These results demonstrated the crucial role of $CD4^+$ T cell in activating $CD8^+$ T cells and helping them mature into CTLs (65), which may be the results of more efficient uptake and presentation by APCs (66, 67). In another study using the B16F10 tumor-bearing mice models, MHC class II-restricted neo-epitope-encoding RNA vaccines were injected into the mice. Compared with the control group, MDSCs and $FoxP3^+$ Tregs were markedly reduced in the experimental group, indicating that the induction of $CD4^+$ T cells could help overcome tumor-associated immune suppression, which in turn resulted in a more efficacious tumor control (68).

In fact, $CD4^+$ T cells can indirectly promote anti-tumor responses, as the cytokines and co-stimulatory factors secreted by $CD4^+$ T cells largely dictate the quality of CTLs. For example, IL-2 secreted by Th1 is essential for maintaining the growth and proliferation of $CD8^+$ T cells (69). Moreover, Th1 can help promote the recruitment and infiltration of $CD8^+$ T cells through the secretion of IFN-γ (70). Furthermore, tumor-specific $CD4^+$ T cells can also secrete IL-4 to recruit macrophages as well as establish long-term memory immune responses to tumors (71, 72). In fact, immunotherapy based on mutation-specific $CD4^+$ T cells has been proven effective in clinical trials. In patient 3737 experiencing widely metastatic cholangiocarcinoma, tumor infiltrating lymphocytes (TILs) containing approximately 25% mutation-specific Th1 cells were transferred, and the patient received tumor regression and experienced disease stabilization (NCT01174121) (73). *Patrick A. Ott* enrolled ten patients with previously untreated high-risk melanoma in a phase I study. In the study, they used long peptides leading to the activation of both $CD8^+$ and $CD4^+$ T cells. Of six patients treated with the vaccines, four had no recurrence at the follow up of 25 months after vaccination, while the two patients experiencing recurrent disease subsequently received anti-PD-1 therapy and achieved complete tumor regression (NCT 01970358) (8).

In conclusion, $CD4^+$ T cells can help promote the effector function of CTLs and reshape the TME to overcome negative regulation, both of which can amplify the anti-tumor response of T cells. The reasons why tumor vaccines targeting $CD4^+$ T cells are difficult to synthesize can be summarized into the following aspects. First, most tumors lack the expression of MHC-II molecules (68). Another factor may be the specificity of neoantigens in tumor cells. At present, most tumor neoantigens capable of stimulating effector T cells belong to MHC-I restricted molecules, and they can only be recognized by effector T cells. In contrast, few MHC-II restricted tumor neoantigens have been found. One of the obstacles is that the existing MHC-II antigen prediction algorithms find it difficult to identify MHC-II restricted tumor-specific antigens that function as neoantigens for $CD4^+$ T cells (74).

Thinking of the importance of $CD4^+$ T cells in antitumor immunity, it is urgent for us to deepen the understanding of the underlying principles of immunology and overcome technical difficulties before applying such vaccines into clinical practice.

Re-Assembling Tumor Vaccines With Nanoparticles to Enhance the Immunogenicity

Due to the intricate immunosuppressive TME, the therapeutic effects of a majority of tumor vaccines are quite limited. The immunosuppressive TME inhibits not only the antigen uptake and presentation but also the activation and infiltration of lymphocytes *in vivo*. Therefore, new methods are expected to improve the effectiveness of current immunotherapies, and thus, nanoparticles have been in extensive use in recent years. Compared to traditional tumor vaccines, re-assembled tumor vaccines are armed with the following advantages brought by nano-materials.

First, nanoparticles can be loaded with different adjuvants and molecules, making them novel vectors for different types of tumor vaccines, such as peptide vaccines, RNA vaccines (75, 76). Molecules such as chemical drugs and immune checkpoint inhibitors can be loaded into the vectors with the vaccines to achieve synergistic antitumor effects. Liu X. et al. constructed a tumor nano-vaccine composed of antigenic peptide, CpG-ODN, and cationic polymer nanoparticle. Using breast carcinoma 4T1 models, they found that the injection of the nano-vaccine significantly promoted the infiltration of CTLs in the tumor and could help prevent tumor recurrence and pulmonary metastasis (77). Xie X. et al. developed a novel therapeutic vaccine co-encapsulating epitope peptide and PD-1 antibody with self-healing microcapsule. With the synergism of epitope peptide, PD-1 antibody, and the unique self-healing feature of the microcapsule, a single dose of the vaccine led to the recruitment of activated APCs and significantly improved the infiltration of tumor-specific CTLs. The results indicated that such new vaccine platform could serve as a promising immunotherapy modality for anti-tumor treatment (78).

Second, nanoparticles serve as safeguards to protect the adjuvants from being degraded in the biological environment and precisely deliver the therapeutic ingredients to a particular place to improve the immune response (79). Some particles may also release the coated ingredients according to the conditions of the environment, such as pH and oxygen content, to better adapt to the harsh TME. *Keman Cheng* developed a therapeutic peptide assembling nanoparticle that can sequentially respond to the tumor microenvironment. The basic of the nano-vaccine was a short D-peptide antagonist of programmed cell death-ligand 1 (^{D}PPA-1), an inhibitor of idoleamine 2,3-dioxygenase (NLG919). When exposed to the acidic tumor microenvironment, the

material became swollen. The material would soon collapse due to the cleavage of the peptide substrate by matrix metalloproteinase 2 (MMP-2), which is upregulated in tumor stroma. Such a subtle design guarantees the controllable release of the ingredient and provides a favorable circumstance for CTLs to survival and become activated (80).

Third, nano-materials can serve as an immunotherapeutic platform that can reshape immunosuppressive TME (81, 82). The low response rate of current tumor immunotherapy can partly account for the immunosuppressive factors in TME. To better overcome this, *Chanyoung Song* developed an injectable immunotherapeutic nanogel. The nanogel was injected in the dissected empty space after removing approximately 90% of the primary tumor by surgery in 4T1 triple-negative breast cancer and TC1 cervical cancer mice models. Compared with the groups without injected the nanogel, the original immunosuppressive TME of the experimental group was reverted into the immunogenic one, including increased levels of infiltrating CTLs and upregulated expression of cytokines. Moreover, the percentage of immunosuppressive cells such as MDSCs and M2 macrophages decreased after treatment (83).

Lastly, because the size of the nanoparticles is similar to that of the pathogens, the injection of the nanoparticles can promote the presentation of antigens, which can in turn induce the production of more effective, long-lasting tumor specific CTLs (84). Altogether, the modified tumor vaccines can effectively activate the host immune response and induce the death of tumor cells. The re-assembled tumor vaccines distributed in tumors reprogram the immunosuppressive networks and increase immune cells infiltration.

In spite of the fact that nanoparticles have enhanced the anti-tumor immune response in preclinical models, there remains difficulties before fully applying them to clinical use. One of the most important factors may be the selection of material compositions. The safety of the materials should achieve the certifications of the FDA. The materials should be biodegradable and their degradants must also be non-toxic to humans without leading to biological immune rejection. In addition to safety, the physical properties of these materials such as cation density and surface activity, need to be further optimized to better enhance the antitumor effect of the immune system.

THE COMBINATION OF TUMOR VACCINES AND OTHER THERAPIES

The Combination of Tumor Vaccines and Metabolic Therapy

Both tumor cells and T cells are in desperate need of anabolic and energetic to maintain their survival and growth. Tumor cells are known to have unique metabolisms, and differences in cellular metabolism between tumor cells and immune cells can serve as a basis to better improve the antitumor effect.

The unique Warburg effect of tumor cells causes hypoglycemia and hypoxia in the TME (44). TILs must adapt to this environment to survive and exert anti-tumor function. By analyzing the $CD8^+$ T cell metabolism 30 days after vaccine treatment in melanoma-bearing mice, Zhang et al. found that the intensity of glycolysis metabolites declined in $CD8^+$ TILs while the peroxisome proliferator-activated receptor (PPAR)-a signaling and fatty acid (FA) catabolism metabolites increased, implying that $CD8^+$ TILs switched to these modes of metabolism to preserve their effector functions under the pressure of hypoglycemia and hypoxia in TME. They further confirmed this conclusion by adding fenofibrate, a PPAR-a agonist, to increase FA catabolism. Indeed, the addition of fenofibrate largely improved the antitumor function of vaccines compared to the vaccinated, tumor-bearing group (85). Glutamine has long been used for metabolism therapy due to its crucial role in cell metabolism (86, 87). 6-diazo-5-oxo-L-norleucine (DON) is the most widely studied broad-spectrum glutamine antagonist and has been used in clinical trials (88, 89). However, DON was then abandoned as an antitumor agent due to its toxicity, especially gastrointestinal symptoms (88, 90). *Robert D. Leone* then developed a prodrug of DON, JHU083, which could only be activated in the TME. Blocking of glutamine metabolism led to the inhibition of wide-ranging metabolism and the disruption of NADP(H) homeostasis while robustly enhancing the function and effectiveness of TILs and acquiring a long-lived, highly activated phenotype. This difference may be due to the lack of plasticity in tumor metabolism (91).

In conclusion, metabolism is integrated in cellular processes and determines the fate of both tumor cells or immune cells. Deeper insights into the mechanisms of the differences between tumor cell and immune cell metabolism will help yield new targets for therapy.

The Combination of Tumor Vaccines and Chemeric Antigen Receptor T Cells Therapy

CAR-T therapy is another successful attempt at immunotherapy. At present, dramatic clinical responses have been achieved in non-Hodgkin's lymphoma (NHL), adult and pediatric patients with relapsed and refractory (R/R), B-cell acute lymphoblastic leukemia (B-ALL), and chronic lymphocytic leukemia (CLL) (92–94). However, relapse has become one of the obstacles that hinders the development of such therapy. It is well known that engraftment and persistence of CAR-T *in vivo* are the keys to successful tumor eradication. However, the frequency of CAR-T cells declined *in vivo* after transfer (95). The combination of tumor vaccine and CAR-T therapy will be a leap forward for tumor immunotherapy, as the combination can complement the shortcomings of each therapy alone and synergistically enhance anti-tumor ability. For example, unlike effector T cells activated by tumor vaccines which engage HLA-peptide complexes, CAR-T cells have the ability to recognize antigen on any HLA background and are therefore more broadly applicable to patient populations with diverse HLA background (96). They can also target tumor cells that downregulate MHC-I molecules, which is a major mechanism that contributes to tumor escape from vaccine therapy (97). Likewise, the administration of tumor vaccine improves the engraftment and persistence of CAR-T cells to partly overcome CAR-T cell exhaustion in the TME. Actually, a large number of studies have proved that this combination strategy is feasible.

K. Reinhard recently reported claudin (CLDN) 6 as a target for CAR-T cell therapy. In the study, the researchers designed 2nd generation CLDN6-CAR engineered human T cells as well as a liposomal CLDN6-encoding RNA vaccine. Their data established that the addition of tumor vaccine induced a profound expansion of circulation CAR-T cells and showed complete rejection of tumors with higher median survival. The administration of tumor vaccine enabled tumor control at lower CAR-T cell doses (98).Similar results have been shown in other studies using WT1-specific CAR-T cells combined with DC vaccine pulsed with $WT1_{236Y}$ peptide (99) and CMV/CD19 bispecific T cells combined with CMV peptide vaccine (100). In each study, the post-transfer of vaccine enhanced the therapeutic efficacy of CAR-T cells targeting tumor antigens *via* CAR-T cell expansion and activation. An important goal of immunotherapy is to establish immune memory to protect against tumor recurrence. In addition to the enhancement in anti-tumor ability, vaccines have been shown to increase the numbers of memory T cells and decrease the number of terminally differentiated T cells, implying that vaccines can promote immunologic memory in CAR-T cells (101). *Clare* rechallenged the long-term surviving mice with tumor cells in the contralateral site 100 days after the initial treatment, and they found that the mice were completely resistant to rechallenge with the same tumor cells, suggesting that the administration of vaccine did generate a memory response in the surviving mice (102).

The concept of the combination of tumor vaccine and CAR-T cell therapy to specifically eradicate malignant cells has been repeatedly demonstrated in animal models but was sometimes questioned due to the results of trials in humans. In a phase 1/2 study of $WT1_{236Y}$ peptide vaccine involving 26 patients, a patient suffered from an immune-related, but manageable, adverse event (103). Therefore, there remains the possibility that the synergism of tumor vaccine and CAR-T therapy may be associated with increased toxicity. The combination of vaccine and CAR-T therapy has been applied in a relapsed pediatric acute lymphoblastic leukemia clinical trial (NCT01195480). In the CD19CAR CTL therapy with irradiated EBV transformed lymphoblastoid cell lines (LCL) vaccination cohort, four of six patients had detectable CAR-T cells in the blood until 1–3 months after infusion and showed a significantly improved persistence compared with the cohort without vaccination. However, while the usage of vaccine improved the persistence of CAR-T cells somewhat, it was inadequate to induce the proliferation of CAR19 CTLs needed for an effective antitumor response (104). Such results require us to take how to mitigate such risks into more careful consideration and to refine the combination therapeutic strategies, including the doses of tumor vaccine and CAR-T cells in combination therapy, the injection time and the injection sequence.

The Combination of Tumor Vaccines and Immune Checkpoint Blockade Immunotherapy

Growing preclinical and clinical trials have combined tumor vaccines with ICBs in the attempt to reinvigorate exhausted T cells, and many support the assumption that the combination of ICBs and tumor vaccines have the ability to synergistically improve the clinical outcome (105–108). The immune checkpoint pathway plays an important role in maintaining immune tolerance and deciding the fate and function of T cells (109). Herein is discussed the optimal timing and sequencing of the combination of ICBs and tumor vaccines to obtain the maximum therapeutic benefits.

Because the preparation of tumor vaccines will take a long period of time, ICBs have always been the priority selection in the clinic, followed by tumor vaccines. However, studies have shown that the initial state of T cells is one of the main reasons affecting the effect of combination treatment. Vivek Verma et al. (110) uncovered the phenomenon that when PD-1 was blocked first, the anti-tumor effect of the tumor vaccines was abrogated due to the decrease rate of $CD8^+$ T cells and defective T cell activation. The blockade of PD-1 under sub-optimally activated $CD8^+$ T cell conditions would lead to the presence of dysfunctional $PD\text{-}1^+CD38^{hi}CD8^+$ T cells, resulting in the failure of antigenic stimulation response and defective effector functions (111). Researchers have found that such populations of T cells are associated with resistance to anti-PD-1 therapy. If treated appropriately with tumor vaccines before PD-1 inhibitors, the resistance to the PD-1 inhibitors will be resolved. This finding implies that proper sequencing of immunomodulatory agents is necessary for ideal clinical outcomes. In a therapeutic strategy for the clinical use of PD-1 inhibitors combined with tumor vaccines, it may be better to use tumor vaccines before PD-1 inhibitors, or at least use them at the same time. However, we come to a totally opposite conclusion in another experiment using ARF-Fc anti-CTLA-4 mAb where if anti-CTLA-4 mAb was given with the peptide vaccines simultaneously, not only the $CTLA\text{-}4^+$ Tregs but also the $CTLA\text{-}4^+CD8^+$ T cells were depleted. Giving the anti-CTLA-4 mAb treatment several days before the vaccine stimulation resulted in the depletion of Tregs and the expansion of antigen-specific $CD8^+$ T cells *in vitro* and led to an enhanced anti-tumor effect *in vivo* (112). Whether all the ICBs would undergo the above changes when combined with the tumor vaccines needs to be further confirmed. However, these reports do provide unique insights into the normalization of the combined immunomodulatory agents.

In conclusion, correct timing and sequence of ICBs treatment and tumor antigen vaccines are important factors influencing the effect of tumor immunotherapy. Such normalization should be based on the kinetics of immune checkpoints and effector T cell activation.

The Combination of Tumor Vaccines and Oncolytic Viruses

To better improve the antitumor efficacy of tumor vaccines, the ability to alter the immunosuppressive TME is the most attractive feature. When compared with other immunotherapies, OVs seem to be more ideal antitumor immunity inducers. OVs have been shown to overcome the issues regarding immunosuppressive TME, which often encountered by T cell therapies.

OVs can promote antitumor T cell responses through multiple mechanisms. First, OVs can promote T cell priming. Due to the defective antiviral responses, tumor cells are

susceptible to virus infection. The enzymes and factors required for rapid cell division are often highly expressed in tumor cells, providing viruses with a replicative advantage in the tumor cells (1). Once the infection is established, continuous replication of viruses will at last lead to oncolysis. When the tumor cells are broken, the damage associated molecular patterns and tumor antigens will be released into the TME, which can contribute to the maturation and function of DCs, leading to the priming of tumor-specific T cell response (113, 114). Second, OVs induce a pro-inflammatory TME that can increase T cell trafficking and infiltration. Chemokines and cytokines regulate the trafficking and infiltration of immune cells into the TME. Studies have shown that the infection of OVs elicits potent type I interferon responses (115, 116), which can stimulate the production of T cell recruiting chemokines. Inflammatory factors such as tumor necrosis factor (TNF) and interleukin-1β (IL-1β) can also be induced by OVs, which in turn upregulate the expression of selectin on endothelial cells and provide an important signal for T cell infiltration (117–119). The presence of physical barriers is another critical reason accounting for the defective T cell infiltration. However, Ilkow et al. found that the vesicular stomatitis virus (VSV) can selectively destroy cancer-associated fibroblasts (CAFs), which are key components of immunosuppressive tumor stroma (120). Their depletion can represent yet another means by which OVs increase the infiltration of T cells. Last, OVs improve the recognition of tumor cells. To avoid T cell recognition, tumor cells can downregulate MHC class I expression and other components involved in the antigen processing and presentation pathway. OVs have the ability to reverse these effects, likely by inducing type I interferon production (121, 122).

Bringing together the above concepts, combined treatment with OVs can be a promising strategy for reverting immunosuppressive TME and enhancing the antitumor capabilities of tumor vaccines. In B16-OVA melanoma mouse models, combination treatment of VSV-GP, a chimeric vesicular stomatitis virus (VSV) pseudotyped with the glycoprotein (GP) of the lymphocytic choriomeningitis virus, with an ovalbumin (OVA) peptide-loaded dendritic cell (DC) vaccine (DCVacc) significantly increased the numbers of tumor-infiltrating, highly activated T cells while relatively reducing the number of Tregs. Researchers observed that several proinflammatory cytokines increased in the VSV-GP-treated group (123). Using a pre-clinical ovarian cancer mouse model, the combination of vaccine and antigen-armed oncolytic Maraba virus elicited robust tumor-specific $CD8^+$ T cell responses and led to unique immunological changes that correlated with improved clinical outcome of ovarian cancer patients (124). These findings pointed to a key role of OVs to help exert systemic immunologic effects and improve survival. OVs can also serve as adjuvants for tumor vaccines. Erkko Ylösmäki et al. physically attached tumor-specific peptides onto the viral envelope of the virus and found that by coating the viral envelope with therapeutic peptides, the antitumor immunity in the tumor microenvironment can be significantly enhanced (125).

In conclusion, the synergism of tumor vaccine and OVs can combine the advantages of both approaches. The viruses activate the immune response and reshape the TME, and the therapeutic antitumor vaccine direct the immune response towards the neoantigens. Currently, numerous oncolytic viruses have been applied in early phase clinical trials (126–128). Unlike standard drugs, such live viruses have unique challenges. They are live viruses and can proliferate during clinical administration, making it difficult to establish safe and effective dosing guidelines. Moreover, the immune response induced by OVs can be further divided into antitumor immune response and antiviral immune response. On the one hand, viruses help induce immune response against tumor cells. On the other hand, the response to neutralize virus toxicity may block virus replication and the ongoing infection of tumor cells (129). Hence, more careful attention should be taken in the establishment of this combination therapeutic regimen to balance the immune responses and maximize the advantages of the combination therapy. Moreover, compared to agents that directly kill tumor cells, immune-mediated antitumor responses will be much slower. Therefore, more appropriate clinical indicators are needed to capture therapeutic responses of the combination therapy.

The Combination of Tumor Vaccines and Epigenetic Therapy

Immune cells infiltrating in the TME are frequently in an exhaustion state and accumulating evidence indicates that such reprogramming can partly be the consequence of aberrant epigenomes. As a result, epigenetic therapy has the potential to reverse the exhausted immune T cells caused by aberrant epigenomes. At present, histone deacetylase inhibitors (HDACi) and hypomethylating agents have been approved by the FDA and have brought epigenetic therapy to the front of tumor therapies. Collectively, the synergistic effect of epigenetic drugs on tumor vaccines can be concluded in the following points.

First, epigenetic therapy helps restore the HLA class-I antigen processing machinery expression on tumors. For example, hypomethylating agents have been shown to have the ability to upregulate tumor antigens as well as antigen processing and presentation genes (130, 131). Similarly, in the glioma implantation mouse model, Ting Sun et al. found upregulated expression of antigen processing and presenting associated molecules on the surface of the glioma tumor cells in the HDACi-treated group, such as TAP1, TAP2, and MHC-I, thereby enhancing the specific lysing efficacy of the immune cells and in turn potentiating the immune response (132). Interestingly, Ailsa et al. (133) uncovered that HDACi mediated tumor cells apoptosis could stimulate the uptake by APCs and that the combination of HDACi and immune-activating antibodies to promote the function of APCs could enhance the proliferation and survival of cytotoxic T cells. Second, epigenetic therapy can modulate the immunosuppressive TME. Both hypomethylating agents and HDACi have been shown to increase the number of natural killer (NK) cells in the tumor bed while reducing the percentage of tumor-infiltrating MDSCs and Tregs (134–136). Tumor cells can epigenetically silence the expression of chemokines to impair the

infiltration activity of immune cells. However, pharmacological inhibition of histone deacetylase in tumor cells was shown to increase the expression of chemokines, thus attracting peripheral infiltrating T cells to the tumor bed (27). Last, apart from regulating T cell extrinsic factors, epigenetic therapy can act on TILs directly by re-invigorating exhausted T cells (137) and decreasing the activation induced cell death in TILs (138). However, it is worth mentioning that epigenetic therapy can also suppress the immune response. For example, the administration of hypomethylating agents prior to allogeneic transplantation can relieve graft versus-host disease (GVHD) through inducing the production of Tregs (139), which implies that it is necessary to balance the pro-immunogenic and immunosuppressive functions in clinical use.

Generally, clinical agents that can be used in conjunction with tumor vaccines should have the characteristics below. First, they act directly upon the T cells to enhance the adaptive anti-tumor immune response. Second, they relieve the tumor-induced immunosuppression, which in turn provides a suitable immune microenvironment for anti-tumor immune cells to help them work properly. Considering the fact that some drugs may also produce cytotoxic effect on immune cells, it is critical to ensure that appropriate dosages are used in the combination therapy.

DISCUSSION

In the TME, T cells are key cellular components that extensively crosstalk with tumor cells. Recent successes have fueled interest in improving the durable anti-tumor ability of tumor vaccines. Advances in the understanding of immune regulation mechanisms provide solid foundation for the development of novel tumor vaccine combination therapy strategies. However, the occurrence and development of tumors is a dynamic evolution process characterized by genetic instability (1). Due to the immune escape mechanism of tumor cells, tumor vaccines alone may not exert expected tumor killing effects, which is one of the factors that hinders the application of tumor vaccines. In the upcoming era, the application of tumor vaccines should be combined with other therapies such as chemotherapy, radiation therapy, molecular targeted drugs and other immunotherapies to produce a more durable anti-tumor immune response and improve the prognosis of cancer patients.

Although combined treatments have achieved anti-tumor effects and prolonged survival time in pre-clinical animal models, questions exist in clinical translation. The most important point is that the immune background of the animal models is quite different from that of humans. Although patient-derived tumor xenograft (PDX) models have been widely applied in tumor immunology research, the dosage and usage in animal models still require a long time to verify their feasibility in human beings, which greatly extends the time for clinical translation. Second, due to the complexity of tumor immunotherapy and the heterogeneity of patients in the clinic, more precise predictive biomarkers still need to be explored to better identify the standard to combine for different treatments. They can also help to determine which treatments are suitable for patients in early clinical diagnosis to develop personal treatment options for different patients. The occurrence and development of tumors is a complex process. Under the pressure of immune survival, a series of changes will happen in tumor cells to avoid immune responses. These lead to challenges in clinical work of how to adjust the combined treatment regimen in time according to different biological changes in tumor cells to maximize the effect of combined treatment. Third, like predictive biomarkers, appropriate indicators should also be developed in the clinic to assess the effect of combination therapy. Finally, a perfect combination treatment regimen needs to be developed based on the cancer immunity cycle to decide which treatment should be included. In other words, such regimens should include activating the endogenous immune response, promoting immune cell infiltration, increasing tumor sensitivity to therapy, reducing tumor burden and maintaining long-term immunity. This requires clinicians to have an accurate grasp of the combination treatment regimen. Continuous studies on tumor immune mechanism and clinical translation are needed to overcome the questions of how to combine different treatments; whether each of the treatment should be added sequentially or concurrently; and whether each of the treatments should be added continuously of intermittently. In general, the biological toxicity of each treatment should be minimized while the synergistic effects of each treatment should be maximized.

AUTHOR CONTRIBUTIONS

JC, HZ, LZ, and YHu reviewed relevant literatures and drafted the manuscript. ML, YHe, and YL analyzed and revised the manuscript. All authors contributed to the article and approved the submitted version.

FUNDING

This work was funded by the Frontier Research Program of Bioland Laboratory (Guangzhou Regenerative Medicine and Health Guangdong Laboratory) [grant number 2018GZR110105014], the Natural Science Foundation of Guangdong Province, China [grant number 2018B030311042], Science and Technology Program of Guangzhou, China [grant number 201704020216], Clinical Research Startup Program of Southern Medical University by High-level University Construction Funding of Guangdong Provincial Department of Education [grant number LC2016ZD027], and President Foundation of Zhujiang Hospital, Southern Medical University [grant number yjjj2019qn07].

REFERENCES

1. Hanahan D, Weinberg RA. Hallmarks of cancer: the next generation. *Cell* (2011) 144(5):646–74. doi: 10.1016/j.cell.2011.02.013
2. De Plaen E, Lurquin C, Van Pel A, Mariame B, Szikora JP, Wolfel T, et al. Immunogenic (tum-) variants of mouse tumor P815: cloning of the gene of tum- antigen P91A and identification of the tum- mutation. *Proc Natl Acad Sci U S A* (1988) 85(7):2274–8. doi: 10.1073/pnas.85.7.2274
3. Boon T, Cerottini JC, Van den Eynde B, van der Bruggen P, Van Pel A. Tumor antigens recognized by T lymphocytes. *Annu Rev Immunol* (1994) 12:337–65. doi: 10.1146/annurev.iy.12.040194.002005
4. Xing Y, Hogquist KA. T-cell tolerance: central and peripheral. *Cold Spring Harb Perspect Biol* (2012) 4(6):a006957. doi: 10.1101/cshperspect.a006957
5. Aleksic M, Liddy N, Molloy PE, Pumphrey N, Vuidepot A, Chang KM, et al. Different affinity windows for virus and cancer-specific T-cell receptors: implications for therapeutic strategies. *Eur J Immunol* (2012) 42(12):3174–9. doi: 10.1002/eji.201242606
6. van Buuren MM, Calis JJ, Schumacher TN. High sensitivity of cancer exome-based CD8 T cell neo-antigen identification. *Oncoimmunology* (2014) 3:e28836. doi: 10.4161/onci.28836
7. Yadav M, Jhunjhunwala S, Phung QT, Lupardus P, Tanguay J, Bumbaca S, et al. Predicting immunogenic tumour mutations by combining mass spectrometry and exome sequencing. *Nature* (2014) 515(7528):572–6. doi: 10.1038/nature14001
8. Ott PA, Hu Z, Keskin DB, Shukla SA, Sun J, Bozym DJ, et al. An immunogenic personal neoantigen vaccine for patients with melanoma. *Nature* (2017) 547(7662):217–21. doi: 10.1038/nature22991
9. Sahin U, Derhovanessian E, Miller M, Kloke BP, Simon P, Lower M, et al. Personalized RNA mutanome vaccines mobilize poly-specific therapeutic immunity against cancer. *Nature* (2017) 547(7662):222–6. doi: 10.1038/nature23003
10. Chen DS, Mellman I. Oncology meets immunology: the cancer-immunity cycle. *Immunity* (2013) 39(1):1–10. doi: 10.1016/j.immuni.2013.07.012
11. Seliger B. Molecular mechanisms of MHC class I abnormalities and APM components in human tumors. *Cancer Immunol Immunother* (2008) 57 (11):1719–26. doi: 10.1007/s00262-008-0515-4
12. Garrido F, Algarra I, Garcia-Lora AM. The escape of cancer from T lymphocytes: immunoselection of MHC class I loss variants harboring structural-irreversible "hard" lesions. *Cancer Immunol Immunother* (2010) 59(10):1601–6. doi: 10.1007/s00262-010-0893-2
13. Garcia-Lora A, Algarra I, Garrido F. MHC class I antigens, immune surveillance, and tumor immune escape. *J Cell Physiol* (2003) 195(3):346–55. doi: 10.1002/jcp.10290
14. Abele R, Tampe R. Modulation of the antigen transport machinery TAP by friends and enemies. *FEBS Lett* (2006) 580(4):1156–63. doi: 10.1016/j.febslet.2005.11.048
15. Einstein MH, Leanza S, Chiu LG, Schlecht NF, Goldberg GL, Steinberg BM, et al. Genetic variants in TAP are associated with high-grade cervical neoplasia. *Clin Cancer Res* (2009) 15(3):1019–23. doi: 10.1158/1078-0432.CCR-08-1207
16. Leibowitz MS, Andrade Filho PA, Ferrone S, Ferris RL. Deficiency of activated STAT1 in head and neck cancer cells mediates TAP1-dependent escape from cytotoxic T lymphocytes. *Cancer Immunol Immunother* (2011) 60(4):525–35. doi: 10.1007/s00262-010-0961-7
17. Marincola FM, Jaffee EM, Hicklin DJ, Ferrone S. Escape of human solid tumors from T-cell recognition: molecular mechanisms and functional significance. *Adv Immunol* (2000) 74:181–273. doi: 10.1016/s0065-2776(08)60911-6
18. Khan AN, Gregorie CJ, Tomasi TB. Histone deacetylase inhibitors induce TAP, LMP, Tapasin genes and MHC class I antigen presentation by melanoma cells. *Cancer Immunol Immunother* (2008) 57(5):647–54. doi: 10.1007/s00262-007-0402-4
19. Chattopadhyay G, Shevach EM. Antigen-specific induced T regulatory cells impair dendritic cell function via an IL-10/MARCH1-dependent mechanism. *J Immunol* (2013) 191(12):5875–84. doi: 10.4049/jimmunol.1301693
20. Wing K, Onishi Y, Prieto-Martin P, Yamaguchi T, Miyara M, Fehervari Z, et al. CTLA-4 control over Foxp3+ regulatory T cell function. *Science* (2008) 322(5899):271–5. doi: 10.1126/science.1160062
21. Akkaya B, Oya Y, Akkaya M, Al Souz J, Holstein AH, Kamenyeva O, et al. Regulatory T cells mediate specific suppression by depleting peptide-MHC class II from dendritic cells. *Nat Immunol* (2019) 20(2):218–31. doi: 10.1038/s41590-018-0280-2
22. Andrews LP, Marciscano AE, Drake CG, Vignali DA. LAG3 (CD223) as a cancer immunotherapy target. *Immunol Rev* (2017) 276(1):80–96. doi: 10.1111/imr.12519
23. Marijt KA, Sluijter M, Blijleven L, Tolmeijer SH, Scheeren FA, van der Burg SH, et al. Metabolic stress in cancer cells induces immune escape through a PI3K-dependent blockade of IFNgamma receptor signaling. *J Immunother Cancer* (2019) 7(1):152. doi: 10.1186/s40425-019-0627-8
24. Chemnitz JM, Parry RV, Nichols KE, June CH, Riley JL. SHP-1 and SHP-2 associate with immunoreceptor tyrosine-based switch motif of programmed death 1 upon primary human T cell stimulation, but only receptor ligation prevents T cell activation. *J Immunol* (2004) 173(2):945–54. doi: 10.4049/jimmunol.173.2.945
25. Bedognetti D, Spivey TL, Zhao Y, Uccellini L, Tomei S, Dudley ME, et al. CXCR3/CCR5 pathways in metastatic melanoma patients treated with adoptive therapy and interleukin-2. *Br J Cancer* (2013) 109(9):2412–23. doi: 10.1038/bjc.2013.557
26. Barreira da Silva R, Laird ME, Yatim N, Fiette L, Ingersoll MA, Albert ML. Dipeptidylpeptidase 4 inhibition enhances lymphocyte trafficking, improving both naturally occurring tumor immunity and immunotherapy. *Nat Immunol* (2015) 16(8):850–8. doi: 10.1038/ni.3201
27. Peng D, Kryczek I, Nagarsheth N, Zhao L, Wei S, Wang W, et al. Epigenetic silencing of TH1-type chemokines shapes tumour immunity and immunotherapy. *Nature* (2015) 527(7577):249–53. doi: 10.1038/nature15520
28. Dangaj D, Bruand M, Grimm AJ, Ronet C, Barras D, Duttagupta PA, et al. Cooperation between Constitutive and Inducible Chemokines Enables T Cell Engraftment and Immune Attack in Solid Tumors. *Cancer Cell* (2019) 35(6):885–900.e10. doi: 10.1016/j.ccell.2019.05.004
29. Spranger S, Bao R, Gajewski TF. Melanoma-intrinsic beta-catenin signalling prevents anti-tumour immunity. *Nature* (2015) 523(7559):231–5. doi: 10.1038/nature14404
30. Fujihara T, Yashiro M, Inoue T, Sawada T, Kato Y, Ohira M, et al. Decrease in ICAM-1 expression on gastric cancer cells is correlated with lymph node metastasis. *Gastric Cancer* (1999) 2(4):221–5. doi: 10.1007/s101200050067
31. Maeda K, Kang SM, Sawada T, Nishiguchi Y, Yashiro M, Ogawa Y, et al. Expression of intercellular adhesion molecule-1 and prognosis in colorectal cancer. *Oncol Rep* (2002) 9(3):511–4.
32. Piali L, Fichtel A, Terpe HJ, Imhof BA, Gisler RH. Endothelial vascular cell adhesion molecule 1 expression is suppressed by melanoma and carcinoma. *J Exp Med* (1995) 181(2):811–6. doi: 10.1084/jem.181.2.811
33. Afanasiev OK, Nagase K, Simonson W, Vandeven N, Blom A, Koelle DM, et al. Vascular E-selectin expression correlates with CD8 lymphocyte infiltration and improved outcome in Merkel cell carcinoma. *J Invest Dermatol* (2013) 133(8):2065–73. doi: 10.1038/jid.2013.36
34. Wu X, Giobbie-Hurder A, Liao X, Lawrence D, McDermott D, Zhou J, et al. VEGF Neutralization Plus CTLA-4 Blockade Alters Soluble and Cellular Factors Associated with Enhancing Lymphocyte Infiltration and Humoral Recognition in Melanoma. *Cancer Immunol Res* (2016) 4(10):858–68. doi: 10.1158/2326-6066.CIR-16-0084
35. Shin SJ, Jeon YK, Cho YM, Lee JL, Chung DH, Park JY, et al. The Association Between PD-L1 Expression and the Clinical Outcomes to Vascular Endothelial Growth Factor-Targeted Therapy in Patients With Metastatic Clear Cell Renal Cell Carcinoma. *Oncologist* (2015) 20(11):1253–60. doi: 10.1634/theoncologist.2015-0151
36. Seeber A, Klinglmair G, Fritz J, Steinkohl F, Zimmer KC, Aigner F, et al. High IDO-1 expression in tumor endothelial cells is associated with response to immunotherapy in metastatic renal cell carcinoma. *Cancer Sci* (2018) 109 (5):1583–91. doi: 10.1111/cas.13560
37. Lim WC, Olding M, Healy E, Millar TM. Human Endothelial Cells Modulate CD4(+) T Cell Populations and Enhance Regulatory T Cell Suppressive Capacity. *Front Immunol* (2018) 9:565. doi: 10.3389/fimmu.2018.00565
38. Nambiar DK, Aguilera T, Cao H, Kwok S, Kong C, Bloomstein J, et al. Galectin-1-driven T cell exclusion in the tumor endothelium promotes immunotherapy resistance. *J Clin Invest* (2019) 129(12):5553–67. doi: 10.1172/JCI129025

39. Kraan J, van den Broek P, Verhoef C, Grunhagen DJ, Taal W, Gratama JW, et al. Endothelial CD276 (B7-H3) expression is increased in human malignancies and distinguishes between normal and tumour-derived circulating endothelial cells. *Br J Cancer* (2014) 111(1):149–56. doi: 10.1038/bjc.2014.286
40. Kim CG, Jang M, Kim Y, Leem G, Kim KH, Lee H, et al. VEGF-A drives TOX-dependent T cell exhaustion in anti-PD-1-resistant microsatellite stable colorectal cancers. *Sci Immunol* (2019) 4(41):eaay0555. doi: 10.1126/sciimmunol.aay0555
41. Sata M, Walsh K. TNFalpha regulation of Fas ligand expression on the vascular endothelium modulates leukocyte extravasation. *Nat Med* (1998) 4 (4):415–20. doi: 10.1038/nm0498-415
42. Jain RK. Normalization of tumor vasculature: an emerging concept in antiangiogenic therapy. *Science* (2005) 307(5706):58–62. doi: 10.1126/science.1104819
43. Wigerup C, Pahlman S, Bexell D. Therapeutic targeting of hypoxia and hypoxia-inducible factors in cancer. *Pharmacol Ther* (2016) 164:152–69. doi: 10.1016/j.pharmthera.2016.04.009
44. Warburg O. On the origin of cancer cells. *Science* (1956) 123(3191):309–14. doi: 10.1126/science.123.3191.309
45. Chang CH, Qiu J, O'Sullivan D, Buck MD, Noguchi T, Curtis JD, et al. Metabolic Competition in the Tumor Microenvironment Is a Driver of Cancer Progression. *Cell* (2015) 162(6):1229–41. doi: 10.1016/j.cell.2015.08.016
46. Ho PC, Bihuniak JD, Macintyre AN, Staron M, Liu X, Amezquita R, et al. Phosphoenolpyruvate Is a Metabolic Checkpoint of Anti-tumor T Cell Responses. *Cell* (2015) 162(6):1217–28. doi: 10.1016/j.cell.2015.08.012
47. Munn DH, Shafizadeh E, Attwood JT, Bondarev I, Pashine A, Mellor AL. Inhibition of T cell proliferation by macrophage tryptophan catabolism. *J Exp Med* (1999) 189(9):1363–72. doi: 10.1084/jem.189.9.1363
48. Fallarino F, Grohmann U, You S, McGrath BC, Cavener DR, Vacca C, et al. The combined effects of tryptophan starvation and tryptophan catabolites down-regulate T cell receptor zeta-chain and induce a regulatory phenotype in naive T cells. *J Immunol* (2006) 176(11):6752–61. doi: 10.4049/jimmunol.176.11.6752
49. Pallett LJ, Schmidt N, Schurich A. T cell metabolism in chronic viral infection. *Clin Exp Immunol* (2019) 197(2):143–52. doi: 10.1111/cei.13308
50. Currie E, Schulze A, Zechner R, Walther TC, Farese RVJr. Cellular fatty acid metabolism and cancer. *Cell Metab* (2013) 18(2):153–61. doi: 10.1016/j.cmet.2013.05.017
51. Walton ZE, Patel CH, Brooks RC, Yu Y, Ibrahim-Hashim A, Riddle M, et al. Acid Suspends the Circadian Clock in Hypoxia through Inhibition of mTOR. *Cell* (2018) 174(1):72–87.e32. doi: 10.1016/j.cell.2018.05.009
52. Zheng Y, Delgoffe GM, Meyer CF, Chan W, Powell JD. Anergic T cells are metabolically anergic. *J Immunol* (2009) 183(10):6095–101. doi: 10.4049/jimmunol.0803510
53. Battaglia M, Stabilini A, Roncarolo MG. Rapamycin selectively expands CD4+CD25+FoxP3+ regulatory T cells. *Blood* (2005) 105(12):4743–8. doi: 10.1182/blood-2004-10-3932
54. Mendler AN, Hu B, Prinz PU, Kreutz M, Gottfried E, Noessner E. Tumor lactic acidosis suppresses CTL function by inhibition of p38 and JNK/c-Jun activation. *Int J Cancer* (2012) 131(3):633–40. doi: 10.1002/ijc.26410
55. Brand A, Singer K, Koehl GE, Kolitzus M, Schoenhammer G, Thiel A, et al. LDHA-Associated Lactic Acid Production Blunts Tumor Immunosurveillance by T and NK Cells. *Cell Metab* (2016) 24(5):657–71. doi: 10.1016/j.cmet.2016.08.011
56. Gottfried E, Kunz-Schughart LA, Ebner S, Mueller-Klieser W, Hoves S, Andreesen R, et al. Tumor-derived lactic acid modulates dendritic cell activation and antigen expression. *Blood* (2006) 107(5):2013–21. doi: 10.1182/blood-2005-05-1795
57. Comito G, Iscaro A, Bacci M, Morandi A, Ippolito L, Parri M, et al. Lactate modulates CD4(+) T-cell polarization and induces an immunosuppressive environment, which sustains prostate carcinoma progression via TLR8/miR21 axis. *Oncogene* (2019) 38(19):3681–95. doi: 10.1038/s41388-019-0688-7
58. Feng J, Yang H, Zhang Y, Wei H, Zhu Z, Zhu B, et al. Tumor cell-derived lactate induces TAZ-dependent upregulation of PD-L1 through GPR81 in human lung cancer cells. *Oncogene* (2017) 36(42):5829–39. doi: 10.1038/onc.2017.188
59. Szefel J, Danielak A, Kruszewski WJ. Metabolic pathways of L-arginine and therapeutic consequences in tumors. *Adv Med Sci* (2019) 64(1):104–10. doi: 10.1016/j.advms.2018.08.018
60. Srivastava MK, Sinha P, Clements VK, Rodriguez P, Ostrand-Rosenberg S. Myeloid-derived suppressor cells inhibit T-cell activation by depleting cystine and cysteine. *Cancer Res* (2010) 70(1):68–77. doi: 10.1158/0008-5472.CAN-09-2587
61. Waldron TJ, Quatromoni JG, Karakasheva TA, Singhal S, Rustgi AK. Myeloid derived suppressor cells: Targets for therapy. *Oncoimmunology* (2013) 2(4):e24117. doi: 10.4161/onci.24117
62. Serafini P, Mgebroff S, Noonan K, Borrello I. Myeloid-derived suppressor cells promote cross-tolerance in B-cell lymphoma by expanding regulatory T cells. *Cancer Res* (2008) 68(13):5439–49. doi: 10.1158/0008-5472.CAN-07-6621
63. Zhu Z, Cuss SM, Singh V, Gurusamy D, Shoe JL, Leighty R, et al. CD4+ T Cell Help Selectively Enhances High-Avidity Tumor Antigen-Specific CD8+ T Cells. *J Immunol* (2015) 195(7):3482–9. doi: 10.4049/jimmunol.1401571
64. Borst J, Ahrends T, Babala N, Melief CJM, Kastenmuller W. CD4(+) T cell help in cancer immunology and immunotherapy. *Nat Rev Immunol* (2018) 18(10):635–47. doi: 10.1038/s41577-018-0044-0
65. Alspach E, Lussier DM, Miceli AP, Kizhvatov I, DuPage M, Luoma AM, et al. MHC-II neoantigens shape tumour immunity and response to immunotherapy. *Nature* (2019) 574(7780):696–701. doi: 10.1038/s41586-019-1671-8
66. Bennett SR, Carbone FR, Karamalis F, Miller JF, Heath WR. Induction of a CD8+ cytotoxic T lymphocyte response by cross-priming requires cognate CD4+ T cell help. *J Exp Med* (1997) 186(1):65–70. doi: 10.1084/jem.186.1.65
67. Bennett SR, Carbone FR, Karamalis F, Flavell RA, Miller JF, Heath WR. Help for cytotoxic-T-cell responses is mediated by CD40 signalling. *Nature* (1998) 393(6684):478–80. doi: 10.1038/30996
68. Kreiter S, Vormehr M, van de Roemer N, Diken M, Lower M, Diekmann J, et al. Mutant MHC class II epitopes drive therapeutic immune responses to cancer. *Nature* (2015) 520(7549):692–6. doi: 10.1038/nature14426
69. Greenberg PD. Adoptive T cell therapy of tumors: mechanisms operative in the recognition and elimination of tumor cells. *Adv Immunol* (1991) 49:281–355. doi: 10.1016/s0065-2776(08)60778-6
70. Bos R, Sherman LA. CD4+ T-cell help in the tumor milieu is required for recruitment and cytolytic function of CD8+ T lymphocytes. *Cancer Res* (2010) 70(21):8368–77. doi: 10.1158/0008-5472.Can-10-1322
71. Quezada SA, Simpson TR, Peggs KS, Merghoub T, Vider J, Fan X, et al. Tumor-reactive CD4(+) T cells develop cytotoxic activity and eradicate large established melanoma after transfer into lymphopenic hosts. *J Exp Med* (2010) 207(3):637–50. doi: 10.1084/jem.20091918
72. Xie Y, Akpinarli A, Maris C, Hipkiss EL, Lane M, Kwon EK, et al. Naive tumor-specific CD4(+) T cells differentiated in vivo eradicate established melanoma. *J Exp Med* (2010) 207(3):651–67. doi: 10.1084/jem.20091921
73. Tran E, Turcotte S, Gros A, Robbins PF, Lu YC, Dudley ME, et al. Cancer immunotherapy based on mutation-specific CD4+ T cells in a patient with epithelial cancer. *Science* (2014) 344(6184):641–5. doi: 10.1126/science.1251102
74. Andreatta M, Trolle T, Yan Z, Greenbaum JA, Peters B, Nielsen M. An automated benchmarking platform for MHC class II binding prediction methods. *Bioinformatics* (2018) 34(9):1522–8. doi: 10.1093/bioinformatics/btx820
75. Liu L, Wang Y, Miao L, Liu Q, Musetti S, Li J, et al. Combination Immunotherapy of MUC1 mRNA Nano-vaccine and CTLA-4 Blockade Effectively Inhibits Growth of Triple Negative Breast Cancer. *Mol Ther* (2018) 26(1):45–55. doi: 10.1016/j.ymthe.2017.10.020
76. Shan W, Zheng H, Fu G, Liu C, Li Z, Ye Y, et al. Bioengineered Nanocage from HBc Protein for Combination Cancer Immunotherapy. *Nano Lett* (2019) 19(3):1719–27. doi: 10.1021/acs.nanolett.8b04722
77. Liu X, Feng Z, Wang C, Su Q, Song H, Zhang C, et al. Co-localized delivery of nanomedicine and nanovaccine augments the postoperative cancer immunotherapy by amplifying T-cell responses. *Biomaterials* (2020) 230:119649. doi: 10.1016/j.biomaterials.2019.119649
78. Xie X, Hu Y, Ye T, Chen Y, Zhou L, Li F, et al. Therapeutic vaccination against leukaemia via the sustained release of co-encapsulated anti-PD-1 and

a leukaemia-associated antigen. *Nat BioMed Eng* (2020). doi: 10.1038/s41551-020-00624-6
79. Leleux J, Roy K. Micro and nanoparticle-based delivery systems for vaccine immunotherapy: an immunological and materials perspective. *Adv Healthc Mater* (2013) 2(1):72–94. doi: 10.1002/adhm.201200268
80. Cheng K, Ding Y, Zhao Y, Ye S, Zhao X, Zhang Y, et al. Sequentially Responsive Therapeutic Peptide Assembling Nanoparticles for Dual-Targeted Cancer Immunotherapy. *Nano Lett* (2018) 18(5):3250–8. doi: 10.1021/acs.nanolett.8b01071
81. Ye X, Liang X, Chen Q, Miao Q, Chen X, Zhang X, et al. Surgical Tumor-Derived Personalized Photothermal Vaccine Formulation for Cancer Immunotherapy. *ACS Nano* (2019) 13(3):2956–68. doi: 10.1021/acsnano.8b07371
82. Musetti S, Huang L. Nanoparticle-Mediated Remodeling of the Tumor Microenvironment to Enhance Immunotherapy. *ACS Nano* (2018) 12 (12):11740–55. doi: 10.1021/acsnano.8b05893
83. Song C, Phuengkham H, Kim YS, Dinh VV, Lee I, Shin IW, et al. Syringeable immunotherapeutic nanogel reshapes tumor microenvironment and prevents tumor metastasis and recurrence. *Nat Commun* (2019) 10 (1):3745. doi: 10.1038/s41467-019-11730-8
84. Xu J, Wang H, Xu L, Chao Y, Wang C, Han X, et al. Nanovaccine based on a protein-delivering dendrimer for effective antigen cross-presentation and cancer immunotherapy. *Biomaterials* (2019) 207:1–9. doi: 10.1016/j.biomaterials.2019.03.037
85. Zhang Y, Kurupati R, Liu L, Zhou XY, Zhang G, Hudaihed A, et al. Enhancing CD8(+) T Cell Fatty Acid Catabolism within a Metabolically Challenging Tumor Microenvironment Increases the Efficacy of Melanoma Immunotherapy. *Cancer Cell* (2017) 32(3):377–91.e9. doi: 10.1016/j.ccell.2017.08.004
86. Altman BJ, Stine ZE, Dang CV. From Krebs to clinic: glutamine metabolism to cancer therapy. *Nat Rev Cancer* (2016) 16(11):749. doi: 10.1038/nrc.2016.114
87. Scalise M, Pochini L, Galluccio M, Console L, Indiveri C. Glutamine Transport and Mitochondrial Metabolism in Cancer Cell Growth. *Front Oncol* (2017) 7:306. doi: 10.3389/fonc.2017.00306
88. Magill GB, Myers WP, Reilly HC, Putnam RC, Magill JW, Sykes MP, et al. Pharmacological and initial therapeutic observations on 6-diazo-5-oxo-1-norleucine (DON) in human neoplastic disease. *Cancer* (1957) 10(6):1138–50. doi: 10.1002/1097-0142(195711/12)10:6<1138::aid-cncr2820100608>3.0.co;2-k
89. Li MC, Whitmore WFJr., Golbey R, Grabstald H. Effects of combined drug therapy on metastatic cancer of the testis. *JAMA* (1960) 174:1291–9. doi: 10.1001/jama.1960.03030100059013
90. A CLINICAL study of the comparative effect of nitrogen mustard and DON in patients with bronchogenic carcinoma, Hodgkin's disease, lymphosarcoma, and melanoma. *J Natl Cancer Inst* (1959) 22(2):433–9.
91. Leone RD, Zhao L, Englert JM, Sun IM, Oh MH, Sun IH, et al. Glutamine blockade induces divergent metabolic programs to overcome tumor immune evasion. *Science* (2019) 366(6468):1013–21. doi: 10.1126/science.aav2588
92. Brentjens RJ, Davila ML, Riviere I, Park J, Wang X, Cowell LG, et al. CD19-targeted T cells rapidly induce molecular remissions in adults with chemotherapy-refractory acute lymphoblastic leukemia. *Sci Transl Med* (2013) 5(177):177ra38. doi: 10.1126/scitranslmed.3005930
93. Cruz CR, Micklethwaite KP, Savoldo B, Ramos CA, Lam S, Ku S, et al. Infusion of donor-derived CD19-redirected virus-specific T cells for B-cell malignancies relapsed after allogeneic stem cell transplant: a phase 1 study. *Blood* (2013) 122(17):2965–73. doi: 10.1182/blood-2013-06-506741
94. Kochenderfer JN, Somerville RPT, Lu T, Yang JC, Sherry RM, Feldman SA, et al. Long-Duration Complete Remissions of Diffuse Large B Cell Lymphoma after Anti-CD19 Chimeric Antigen Receptor T Cell Therapy. *Mol Ther* (2017) 25(10):2245–53. doi: 10.1016/j.ymthe.2017.07.004
95. Maude SL, Frey N, Shaw PA, Aplenc R, Barrett DM, Bunin NJ, et al. Chimeric antigen receptor T cells for sustained remissions in leukemia. *N Engl J Med* (2014) 371(16):1507–17. doi: 10.1056/NEJMoa1407222
96. Sadelain M, Brentjens R, Riviere I. The basic principles of chimeric antigen receptor design. *Cancer Discov* (2013) 3(4):388–98. doi: 10.1158/2159-8290.CD-12-0548
97. Zhou G, Levitsky H. Towards curative cancer immunotherapy: overcoming posttherapy tumor escape. *Clin Dev Immunol* (2012) 2012:124187. doi: 10.1155/2012/124187
98. Reinhard K, Rengstl B, Oehm P, Michel K, Billmeier A, Hayduk N, et al. An RNA vaccine drives expansion and efficacy of claudin-CAR-T cells against solid tumors. *Science* (2020) 367(6476):446–53. doi: 10.1126/science.aay5967
99. Akahori Y, Wang L, Yoneyama M, Seo N, Okumura S, Miyahara Y, et al. Antitumor activity of CAR-T cells targeting the intracellular oncoprotein WT1 can be enhanced by vaccination. *Blood* (2018) 132(11):1134–45. doi: 10.1182/blood-2017-08-802926
100. Wang X, Wong CW, Urak R, Mardiros A, Budde LE, Chang WC, et al. CMVpp65 Vaccine Enhances the Antitumor Efficacy of Adoptively Transferred CD19-Redirected CMV-Specific T Cells. *Clin Cancer Res* (2015) 21(13):2993–3002. doi: 10.1158/1078-0432.CCR-14-2920
101. Wu M, Zhang L, Zhang H, Ning J, Tu S, He Y, et al. CD19 chimeric antigen receptor-redirected T cells combined with epidermal growth factor receptor pathway substrate 8 peptide-derived dendritic cell vaccine in leukemia. *Cytotherapy* (2019) 21(6):659–70. doi: 10.1016/j.jcyt.2019.03.313
102. Slaney CY, von Scheidt B, Davenport AJ, Beavis PA, Westwood JA, Mardiana S, et al. Dual-specific Chimeric Antigen Receptor T Cells and an Indirect Vaccine Eradicate a Variety of Large Solid Tumors in an Immunocompetent, Self-antigen Setting. *Clin Cancer Res* (2017) 23(10):2478–90. doi: 10.1158/1078-0432.CCR-16-1860
103. Ueda Y, Ogura M, Miyakoshi S, Suzuki T, Heike Y, Tagashira S, et al. Phase 1/2 study of the WT1 peptide cancer vaccine WT4869 in patients with myelodysplastic syndrome. *Cancer Sci* (2017) 108(12):2445–53. doi: 10.1111/cas.13409
104. Rossig C, Pule M, Altvater B, Saiagh S, Wright G, Ghorashian S, et al. Vaccination to improve the persistence of CD19CAR gene-modified T cells in relapsed pediatric acute lymphoblastic leukemia. *Leukemia* (2017) 31 (5):1087–95. doi: 10.1038/leu.2017.39
105. Duraiswamy J, Kaluza KM, Freeman GJ, Coukos G. Dual blockade of PD-1 and CTLA-4 combined with tumor vaccine effectively restores T-cell rejection function in tumors. *Cancer Res* (2013) 73(12):3591–603. doi: 10.1158/0008-5472.CAN-12-4100
106. Karyampudi L, Lamichhane P, Scheid AD, Kalli KR, Shreeder B, Krempski JW, et al. Accumulation of memory precursor CD8 T cells in regressing tumors following combination therapy with vaccine and anti-PD-1 antibody. *Cancer Res* (2014) 74(11):2974–85. doi: 10.1158/0008-5472.CAN-13-2564
107. Gibney GT, Kudchadkar RR, DeConti RC, Thebeau MS, Czupryn MP, Tetteh L, et al. Safety, correlative markers, and clinical results of adjuvant nivolumab in combination with vaccine in resected high-risk metastatic melanoma. *Clin Cancer Res* (2015) 21(4):712–20. doi: 10.1158/1078-0432.CCR-14-2468
108. Massarelli E, William W, Johnson F, Kies M, Ferrarotto R, Guo M, et al. Combining Immune Checkpoint Blockade and Tumor-Specific Vaccine for Patients With Incurable Human Papillomavirus 16-Related Cancer: A Phase 2 Clinical Trial. *JAMA Oncol* (2019) 5(1):67–73. doi: 10.1001/jamaoncol.2018.4051
109. Boussiotis VA. Molecular and Biochemical Aspects of the PD-1 Checkpoint Pathway. *N Engl J Med* (2016) 375(18):1767–78. doi: 10.1056/NEJMra1514296
110. Verma V, Shrimali RK, Ahmad S, Dai W, Wang H, Lu S, et al. PD-1 blockade in subprimed CD8 cells induces dysfunctional PD-1(+)CD38(hi) cells and anti-PD-1 resistance. *Nat Immunol* (2019) 20(9):1231–43. doi: 10.1038/s41590-019-0441-y
111. Philip M, Fairchild L, Sun L, Horste EL, Camara S, Shakiba M, et al. Chromatin states define tumour-specific T cell dysfunction and reprogramming. *Nature* (2017) 545(7655):452–6. doi: 10.1038/nature22367
112. Ha D, Tanaka A, Kibayashi T, Tanemura A, Sugiyama D, Wing JB, et al. Differential control of human Treg and effector T cells in tumor immunity by Fc-engineered anti-CTLA-4 antibody. *Proc Natl Acad Sci U S A* (2019) 116 (2):609–18. doi: 10.1073/pnas.1812186116
113. Brown MC, Holl EK, Boczkowski D, Dobrikova E, Mosaheb M, Chandramohan V, et al. Cancer immunotherapy with recombinant poliovirus induces IFN-dominant activation of dendritic cells and tumor antigen-specific CTLs. *Sci Transl Med* (2017) 9(408):eaan4220. doi: 10.1126/scitranslmed.aan4220
114. Kaufman HL, Kohlhapp FJ, Zloza A. Oncolytic viruses: a new class of immunotherapy drugs. *Nat Rev Drug Discov* (2016) 15(9):660. doi: 10.1038/nrd.2016.178

115. Di Paolo NC, Miao EA, Iwakura Y, Murali-Krishna K, Aderem A, Flavell RA, et al. Virus binding to a plasma membrane receptor triggers interleukin-1 alpha-mediated proinflammatory macrophage response in vivo. *Immunity* (2009) 31(1):110–21. doi: 10.1016/j.immuni.2009.04.015
116. Glorioso JC, Cohen JB, Goins WF, Hall B, Jackson JW, Kohanbash G, et al. Oncolytic HSV Vectors and Anti-Tumor Immunity. *Curr Issues Mol Biol* (2020) 41:381–468. doi: 10.21775/cimb.041.381
117. Bridle BW, Stephenson KB, Boudreau JE, Koshy S, Kazdhan N, Pullenayegum E, et al. Potentiating cancer immunotherapy using an oncolytic virus. *Mol Ther* (2010) 18(8):1430–9. doi: 10.1038/mt.2010.98
118. Vestweber D. How leukocytes cross the vascular endothelium. *Nat Rev Immunol* (2015) 15(11):692–704. doi: 10.1038/nri3908
119. Wakimoto H, Ikeda K, Abe T, Ichikawa T, Hochberg FH, Ezekowitz RA, et al. The complement response against an oncolytic virus is species-specific in its activation pathways. *Mol Ther* (2002) 5(3):275–82. doi: 10.1006/mthe.2002.0547
120. Ilkow CS, Marguerie M, Batenchuk C, Mayer J, Ben Neriah D, Cousineau S, et al. Reciprocal cellular cross-talk within the tumor microenvironment promotes oncolytic virus activity. *Nat Med* (2015) 21(5):530–6. doi: 10.1038/nm.3848
121. Gujar SA, Marcato P, Pan D, Lee PW. Reovirus virotherapy overrides tumor antigen presentation evasion and promotes protective antitumor immunity. *Mol Cancer Ther* (2010) 9(11):2924–33. doi: 10.1158/1535-7163.MCT-10-0590
122. Gujar SA, Lee PW. Oncolytic virus-mediated reversal of impaired tumor antigen presentation. *Front Oncol* (2014) 4:77. doi: 10.3389/fonc.2014.00077
123. Koske I, Rossler A, Pipperger L, Petersson M, Barnstorf I, Kimpel J, et al. Oncolytic virotherapy enhances the efficacy of a cancer vaccine by modulating the tumor microenvironment. *Int J Cancer* (2019) 145 (7):1958–69. doi: 10.1002/ijc.32325
124. McGray AJR, Huang RY, Battaglia S, Eppolito C, Miliotto A, Stephenson KB, et al. Oncolytic Maraba virus armed with tumor antigen boosts vaccine priming and reveals diverse therapeutic response patterns when combined with checkpoint blockade in ovarian cancer. *J Immunother Cancer* (2019) 7 (1):189. doi: 10.1186/s40425-019-0641-x
125. Ylosmaki E, Malorzo C, Capasso C, Honkasalo O, Fusciello M, Martins B, et al. Personalized Cancer Vaccine Platform for Clinically Relevant Oncolytic Enveloped Viruses. *Mol Ther* (2018) 26(9):2315–25. doi: 10.1016/j.ymthe.2018.06.008
126. Ribas A, Dummer R, Puzanov I, VanderWalde A, Andtbacka RHI, Michielin O, et al. Oncolytic Virotherapy Promotes Intratumoral T Cell Infiltration and Improves Anti-PD-1 Immunotherapy. *Cell* (2018) 174(4):1031–2. doi: 10.1016/j.cell.2018.07.035
127. Downs-Canner S, Guo ZS, Ravindranathan R, Breitbach CJ, O'Malley ME, Jones HL, et al. Phase 1 Study of Intravenous Oncolytic Poxvirus (vvDD) in Patients With Advanced Solid Cancers. *Mol Ther* (2016) 24(8):1492–501. doi: 10.1038/mt.2016.101
128. Mahalingam D, Wilkinson GA, Eng KH, Fields P, Raber P, Moseley JL, et al. Pembrolizumab in Combination with the Oncolytic Virus Pelareorep and Chemotherapy in Patients with Advanced Pancreatic Adenocarcinoma: A Phase Ib Study. *Clin Cancer Res* (2020) 26(1):71–81. doi: 10.1158/1078-0432.CCR-19-2078
129. Twumasi-Boateng K, Pettigrew JL, Kwok YYE, Bell JC, Nelson BH. Oncolytic viruses as engineering platforms for combination immunotherapy. *Nat Rev Cancer* (2018) 18(7):419–32. doi: 10.1038/s41568-018-0009-4
130. James SR, Link PA, Karpf AR. Epigenetic regulation of X-linked cancer/germline antigen genes by DNMT1 and DNMT3b. *Oncogene* (2006) 25 (52):6975–85. doi: 10.1038/sj.onc.1209678
131. Roulois D, Yau HL, De Carvalho DD. Pharmacological DNA demethylation: Implications for cancer immunotherapy. *Oncoimmunology* (2016) 5(3): e1090077. doi: 10.1080/2162402X.2015.1090077
132. Sun T, Li Y, Yang W, Wu H, Li X, Huang Y, et al. Histone deacetylase inhibition up-regulates MHC class I to facilitate cytotoxic T lymphocyte-mediated tumor cell killing in glioma cells. *J Cancer* (2019) 10(23):5638–45. doi: 10.7150/jca.34471
133. Christiansen AJ, West A, Banks KM, Haynes NM, Teng MW, Smyth MJ, et al. Eradication of solid tumors using histone deacetylase inhibitors combined with immune-stimulating antibodies. *Proc Natl Acad Sci U S A* (2011) 108(10):4141–6. doi: 10.1073/pnas.1011037108
134. Gang AO, Frosig TM, Brimnes MK, Lyngaa R, Treppendahl MB, Gronbaek K, et al. 5-Azacytidine treatment sensitizes tumor cells to T-cell mediated cytotoxicity and modulates NK cells in patients with myeloid malignancies. *Blood Cancer J* (2014) 4:e197. doi: 10.1038/bcj.2014.14
135. Wang L, Amoozgar Z, Huang J, Saleh MH, Xing D, Orsulic S, et al. Decitabine Enhances Lymphocyte Migration and Function and Synergizes with CTLA-4 Blockade in a Murine Ovarian Cancer Model. *Cancer Immunol Res* (2015) 3(9):1030–41. doi: 10.1158/2326-6066.CIR-15-0073
136. Shen L, Ciesielski M, Ramakrishnan S, Miles KM, Ellis L, Sotomayor P, et al. Class I histone deacetylase inhibitor entinostat suppresses regulatory T cells and enhances immunotherapies in renal and prostate cancer models. *PloS One* (2012) 7(1):e30815. doi: 10.1371/journal.pone.0030815
137. Ghoneim HE, Fan Y, Moustaki A, Abdelsamed HA, Dash P, Dogra P, et al. De Novo Epigenetic Programs Inhibit PD-1 Blockade-Mediated T Cell Rejuvenation. *Cell* (2017) 170(1):142–57.e19. doi: 10.1016/j.cell.2017.06.007
138. Cao K, Wang G, Li W, Zhang L, Wang R, Huang Y, et al. Histone deacetylase inhibitors prevent activation-induced cell death and promote anti-tumor immunity. *Oncogene* (2015) 34(49):5960–70. doi: 10.1038/onc.2015.46
139. Ehx G, Fransolet G, de Leval L, D'Hondt S, Lucas S, Hannon M, et al. Azacytidine prevents experimental xenogeneic graft-versus-host disease without abrogating graft-versus-leukemia effects. *Oncoimmunology* (2017) 6(5):e1314425. doi: 10.1080/2162402x.2017.1314425

Conflict of Interest: The authors declare that the research was conducted in the absence of any commercial or financial relationships that could be construed as a potential conflict of interest.

Copyright © 2021 Chen, Zhang, Zhou, Hu, Li, He and Li. This is an open-access article distributed under the terms of the Creative Commons Attribution License (CC BY). The use, distribution or reproduction in other forums is permitted, provided the original author(s) and the copyright owner(s) are credited and that the original publication in this journal is cited, in accordance with accepted academic practice. No use, distribution or reproduction is permitted which does not comply with these terms.

frontiers in Immunology

ORIGINAL RESEARCH
published: 05 February 2021
doi: 10.3389/fimmu.2020.593363

In-Depth Analysis of the Impact of Different Serum-Free Media on the Production of Clinical Grade Dendritic Cells for Cancer Immunotherapy

João Calmeiro[1,2], Luís Mendes[3], Iola F. Duarte[3], Catarina Leitão[4], Adriana R. Tavares[1,2], Daniel Alexandre Ferreira[5], Célia Gomes[5,6], João Serra[7], Amílcar Falcão[1,8], Maria Teresa Cruz[1,2], Mylène A. Carrascal[7†] and Bruno Miguel Neves[4*†]*

[1] Faculty of Pharmacy, University of Coimbra, Coimbra, Portugal, [2] Center for Neuroscience and Cell Biology (CNC), University of Coimbra, Coimbra, Portugal, [3] CICECO, Aveiro Institute of Materials, Department of Chemistry, University of Aveiro, Aveiro, Portugal, [4] Department of Medical Sciences and Institute of Biomedicine (iBiMED), University of Aveiro, Aveiro, Portugal, [5] Coimbra Institute for Clinical and Biomedical Research (iCBR), Faculty of Medicine, University of Coimbra, Coimbra, Portugal, [6] Center for Innovation in Biomedicine and Biotechnology (CIBB), University of Coimbra, Coimbra, Portugal, [7] Tecnimede Group, Sintra, Portugal, [8] Coimbra Institute for Biomedical Imaging and Translational Research (CIBIT), University of Coimbra, Coimbra, Portugal

OPEN ACCESS

Edited by:
Graham Pawelec, University of Tübingen, Germany

Reviewed by:
Gerty Schreibelt, Radboud University Nijmegen, Netherlands
Georgi Guruli, Virginia Commonwealth University, United States

***Correspondence:**
Bruno Miguel Neves
bruno.neves@ua.pt
Mylène A. Carrascal
mylenecarrascal87@gmail.com

†These authors have contributed equally to this work

Specialty section:
This article was submitted to Cancer Immunity and Immunotherapy, a section of the journal Frontiers in Immunology

Received: *10 August 2020*
Accepted: *17 December 2020*
Published: *05 February 2021*

Citation:
Calmeiro J, Mendes L, Duarte IF, Leitão C, Tavares AR, Ferreira DA, Gomes C, Serra J, Falcão A, Cruz MT, Carrascal MA and Neves BM (2021) In-Depth Analysis of the Impact of Different Serum-Free Media on the Production of Clinical Grade Dendritic Cells for Cancer Immunotherapy. Front. Immunol. 11:593363. doi: 10.3389/fimmu.2020.593363

Dendritic cell (DC)-based antitumor vaccines have proven to be a safe approach, but often fail to generate robust results between trials. Translation to the clinic has been hindered in part by the lack of standard operation procedures for vaccines production, namely the definition of optimal culture conditions during *ex-vivo* DC differentiation. Here we sought to compare the ability of three clinical grade serum-free media, DendriMACS, AIM-V, and X-VIVO 15, alongside with fetal bovine serum-supplemented Roswell Park Memorial Institute Medium (RPMI), to support the differentiation of monocyte-derived DCs (Mo-DCs). Under these different culture conditions, phenotype, cell metabolomic profiles, response to maturation stimuli, cytokines production, allogenic T cell stimulatory capacity, as well as priming of antigen-specific $CD8^+$ T cells and activation of autologous natural killer (NK) cells were analyzed. Immature Mo-DCs differentiated in AIM-V or X-VIVO 15 presented lower levels of CD1c, CD1a, and higher expression of CD11c, when compared to cells obtained with DendriMACS. Upon stimulation, only AIM-V or X-VIVO 15 DCs acquired a full mature phenotype, which supports their enhanced capacity to polarize T helper cell type 1 subset, to prime antigen-specific $CD8^+$ T cells and to activate NK cells. $CD8^+$ T cells and NK cells resulting from co-culture with AIM-V or X-VIVO 15 DCs also showed superior cytolytic activity. 1H nuclear magnetic resonance-based metabolomic analysis revealed that superior DC immunostimulatory capacities correlate with an enhanced catabolism of amino acids and glucose. Overall, our data highlight the impact of critically defining the culture medium used in the production of DCs for clinical application in cancer

immunotherapy. Moreover, the manipulation of metabolic state during differentiation could be envisaged as a strategy to enhance desired cell characteristics.

Keywords: cancer immunotherapy, dendritic cells vaccines, clinical grade serum-free media, metabolic activity, dendritic cell differentiation, CTL priming, dendritic cell-NK cell crosstalk

INTRODUCTION

Dendritic cells (DCs) comprise several subsets of highly specialized professional antigen-presenting cells with superior capacity to acquire, process and present antigens to naïve T-lymphocytes (T-cells) (1). Considering their capacity to elicit strong antitumor immune responses, DCs have been extensively used in immunotherapeutic strategies to fight cancer (2, 3). Currently, there are four main approaches exploring DCs in oncologic treatments: 1) non-targeted protein and nucleic acid-based vaccines captured by DCs *in vivo;* 2) direct targeting of antigens to DCs *in vivo*; 3) vaccines composed of *ex vivo* produced DCs, matured and loaded with tumor antigens; 4) biomaterial based platforms to recruit and program endogenous DCs (4). Among these approaches, *ex vivo* generated DCs are used in nearly 97% of the registered clinical trials, leukapheresis-isolated $CD14^+$ monocytic precursors being the primary source to produce monocyte-derived DCs (Mo-DCs) (5).

Notwithstanding the good safety profile of DC antitumor vaccines, the rate of success in inducing clear therapeutic outcomes has been inconstant, with effective responses observed in less than 15% of the cases (5). Several factors have been suggested to explain this outcome: patients with a severely compromised immune system; the multitude of tumor immunosuppressive mechanisms that actively dampen DC functionality; the antigens selected as targets; the limited immunostimulatory abilities of Mo-DCs; and the lack of clinical standard operating procedures (cSOPs) for DCs production (6, 7).

The nonexistence of cSOPs for *ex vivo* manipulation of DCs results in a plethora of protocols that differ in the source of precursors, differentiation and maturation stimuli, antigen nature and loading procedures and, finally, route of administration (5). While extensive research has been performed on the impact of cytokines and growth factors used for DC differentiation and maturation, the relevance of culture media to these processes has been underestimated. Evidence has emerged demonstrating that the metabolism influences DC differentiation, with several connections established between cell metabolic state and their functional specialization [reviewed in (8)]. Hence, it is reasonable to expect that the culture media used during Mo-DCs production may impact their metabolism and inherently their phenotype and functional capacities. Most of our knowledge on *ex vivo* Mo-DC differentiation comes from culture settings comprising fetal bovine serum (FBS). However, for clinical purposes it is crucial to substitute serum or serum components of animal origin, in order to avoid immune reactions and transmission of infectious diseases (9). The use of autologous human serum (HS) can also be undesirable, as many factors that influence DC differentiation and maturation differ between patients and thus contribute to cell product variability (10, 11).

To overcome these limitations, several clinical grade serum-free media (SFM), have become commercially available, allowing to operate according to good manufacturing practice (GMP) conditions. Despite the extensive use of these SFM in the production of clinical grade DCs, very few studies directly compare them for their ability to influence differentiation and cell functional abilities (12–15). In this study, we analyzed the impact of three different SFM (DendriMACS, AIM-V, and X-VIVO 15) on the production of Mo-DCs. We show that the distinct media impact the phenotype, response to maturation stimuli and consequently the immunostimulatory capacities of produced cells. When compared to DendriMACS, immature DCs (iDCs) produced in X-VIVO 15 or AIM-V express higher levels of CD11c, CD86, and major histocompatibility complex (MHC)-I, while presenting lower levels of CD1a and CD1c. Upon stimulation with alpha cytokine cocktail, AIM-V and X-VIVO 15 DCs presented higher expression of CD86, C-C chemokine receptor 7 (CCR7) and superior production of interleukin (IL)-12p70. Such characteristics enable these DCs to polarize $CD4^+$ T cells toward T helper cell type 1 (Th1) subset, prime antigen-specific $CD8^+$ T cells, and activate natural killer (NK) cells in a superior way. The observed phenotypical and functional differences correlate with the cell's metabolic status, as revealed by combined metabolomics profiling of culture media and intracellular extracts.

Abbreviations: BCAA, brain chain amino acids; CCL19, chemokine ligand 19; CCL21, chemokine ligand 21; CCR, C-C chemokine receptor; CFSE, carboxyfluorescein succinimidyl ester; CSOP, clinical standard operating procedures; CTL, cytotoxic T-lymphocyte; CXCR4, C-X-C chemokine receptor type 4; DC, dendritic cell; ES, effect size; FBS, fetal bovine serum; FOXP3, forkhead-box-P3; GAPDH, glyceraldehyde 3-phosphate dehydrogenase; GM-CSF, granulocyte-macrophage colony-stimulating factor; GMP, good manufacturing practice; HIF-1α, hypoxia-inducible factor-1α; HLA, human leucocyte antigen; HMDB, human metabolome database; HS, human serum; iDC, immature dendritic cell; IFN-γ, interferon γ; IL, interleukin; IPST, Portuguese Blood and Transplantation Institute; LDH, lactate dehydrogenase; mDC, mature dendritic cell; MFI, mean fluorescence intensity; MHC, major histocompatibility complex; MLR, mixed leucocyte reaction; Mo-DC, monocyte-derived dendritic cell; mTOR, mammalian target of rapamycin; mTORC1, mammalian target of rapamycin complex 1; NK, natural killer; NMR, nuclear magnetic resonance; OXPHOS, oxidative phosphorylation; PBMCs, peripheral blood mononuclear cells; PBS, phosphate-buffered saline PCA, principal component analysis; PGE2, prostaglandin E2; Poly-I:C, polyinosinic: polycytidylic acid; PPARγ, peroxisome proliferator-activated receptor γ; qPCR, quantitative real-time polymerase chain reaction; RPMI, Roswell Park Memorial Institute Medium; SEM, standard error of the mean; SFM, serum-free media; T-bet, T-box protein expressed in T-cells; TCA, tricarboxylic acid; T cell, T-lymphocyte cell; TGFB1, transforming growth factor beta 1; Th1, T helper cell type 1; TNF, tumor necrosis factor; Treg, regulatory T cells.

Hence, this study highlights the need of rationally selecting the medium used in the production of clinical grade DCs according to the desired immunostimulatory abilities and therapeutic goals.

METHODS

Culture Media

Four culture media were tested in this study: AIM-V (Gibco, Waltham, MA USA), X-VIVO 15 (Lonza, Basel, Switzerland), DendriMACS (Miltenyi Biotec, Bergisch Gladbach, Germany) and Roswell Park Memorial Institute Medium (RPMI) 1640 (Gibco, MA, USA). AIM-V, X-VIVO 15 and DendriMACS are SFM, used in clinical DC-based immunotherapy. RPMI is the most used culture medium in pre-clinical DC research and it was supplemented with 10% heat-inactivated fetal bovine serum (FBS), 100 U/ml penicillin, and 100 μg/ml streptomycin, 2 mM glutamax, 1 mM sodium pyruvate, and 1× MEM non-essential amino acids (all from Gibco).

Cell Isolation and Culture

To obtain human monocytes and T cells, peripheral blood mononuclear cells (PBMCs) were isolated by Ficoll-Paque (GE Healthcare, Chalfont St. Giles, UK) gradient centrifugation from buffy coats of healthy volunteers. Buffy coats were provided by the Portuguese Blood and Transplantation Institute (IPST) following an established protocol allowing access to buffy coats for scientific research with academic purposes only. The buffy coats were not specifically obtained for the present study and were provided without any personal detail from the donor.

Monocytes and T cells were isolated by positive selection using CD14 and CD3 antibody-coated magnetic beads (Miltenyi Biotec), respectively, as described by the manufacturer. T cells were maintained in RPMI medium until co-cultured with DCs. Monocytes were cultured at a density of 1×10^6 cells/ml in the different culture media supplemented with 250 U/ml of IL-4 (Peprotech, London, UK) and 400 U/ml of granulocyte-macrophage colony-stimulating factor (GM-CSF) (Peprotech), for differentiation into immature DCs (iDCs). Each medium was refreshed every 2 days and DCs maturation was induced at day 6 of culture, by adding 50 ng/ml of tumor necrosis factor (TNF)-α (Biolegend), 25 ng/ml of IL-1β (Biolegend), 20 ng/ml of polyinosinic:polycytidylic acid (Poly-I:C) (Novus Biologicals, Abingdon, UK), and 100 ng/ml of interferon (IFN)-γ (Peprotech).

Flow Cytometry

Cell staining was performed using fluorescence-conjugated antibodies, specifically CD1a-Alexa Fluor 488, CD14-PE, CD11c-APC, CD1c-FITC, CD16-APC, CD86-Alexa Fluor 488, CD83-PE, CD80-PerCP/Cy5.5, CD40-APC, human leucocyte antigen (HLA)-DR-Alexa Fluor 488, HLA-ABC-APC, CCR C-C chemokine receptor 1 (CCR1)-Alexa Fluor 488, CCR2-PerCP/Cy5.5, CCR5-APC, CCR7-PerCP/Cy5.5, chemokine receptor (CXCR4)-PE, CD3-PE, CD4-PerCP/Cy5.5, CD8-APC, CD69-FITC, CD25-APC, forkhead-box-P3 (FoxP3)-FITC, T-box protein expressed in T-cells (T-bet)-PE (all from Biolegend). Isotype-matched antibodies were used as controls. Briefly, 0.2×10^6 monocytes, DCs or T cells were washed and stained with 3 μl of fluorescence-conjugated antibodies in phosphate-buffered saline (PBS) + 1% FBS for 30 min at 4°C, in the dark. Cells were subsequently washed, resuspended in PBS + 1% FBS and analyzed in an Accuri C6 flow cytometer (BD Bioscience, San Jose, CA, USA). For intracellular staining, Fix&Perm (Thermo FisherScientific, Waltham, MA, USA), a fixation and cell permeabilization kit, was used as described by the manufacturer. Data were analyzed with FlowJo™ software (version 10) and results presented as percentage of positive cells or mean fluorescence intensity (MFI) after subtraction of isotype control values.

Phagocytosis Assay

The human bladder cancer cell line, UM-UC3 (ATCC, Manassas, VA, USA), was labeled with 0.75 μM carboxyfluorescein succinimidyl ester (CFSE) in PBS, during 20 min at 37°C. Excess dye was quenched by adding culture medium containing 10% FBS and then cell-washed twice with PBS. Cell death was induced by heating cells at 60°C for 30 min and then apoptotic/necrotic cells were added for 2 h at 37°C, in a 2:1 ratio to iDCs differentiated with the different media. After co-culture, iDCs were labeled with APC-conjugated anti-HLA-DR antibody and their phagocytic capacity was assessed by flow cytometry as the percentage of HLA-DR^+ DCs positive for CFSE fluorescence.

Cytokine Analysis

The transcriptional levels of *IL12B*, *TNF, IL10*, and transforming growth factor beta 1 (*TGFB1)* genes were analyzed by quantitative real-time polymerase chain reaction (qPCR) on DCs differentiated and maturated in the different media. RNA was extracted with NZY Total RNA Isolation kit (Nzytech, Lisbon, Portugal), according to the manufacturer's instructions. RNA concentration was measured by OD260 using a NanoDrop spectrophotometer (ThermoScientific, Wilmington, DE, USA) and samples were kept in RNA Storage Solution (Ambion, Foster City, CA, USA) at −80 °C until further use. cDNA was obtained by reverse transcription of 1 μg of total RNA using the NZY First-Strand cDNA Synthesis Kit (Nzytech). qPCR reactions were performed on a Bio-Rad CFX Connect equipment (Bio-rad, Hercules, CA, USA) and gene transcription changes were analyzed using the built-in CFX Maestro software, as previously described (16). Results were normalized using glyceraldehyde 3-phosphate dehydrogenase (*GAPDH*) as a reference gene, experimentally determined with Genex software (MultiD Analyses AB, Göteberg, Sweden) as the most stable for the used treatment conditions. Primer sequences (Supplementary Table 1) were designed using Beacon Designer software version 7.7 Premier Biosoft International (Palo Alto, CA, USA) and thoroughly tested.

The secretion of IL12p70 by mature DCs and IFNγby T cells after co-culture with matured DCs was analyzed by ELISA Max

Deluxe Kits (Biolegend, London, UK), according to the manufacturer instructions.

Mixed Leukocyte Reaction (MLR)

To assess T cell proliferation, allogenic T cells were stained with CFSE before being co-cultured with matured DCs for 5 days at 10:1 ratio. All co-cultures were carried out in U-bottomed 96-well plates with a final volume of 200 µl of RPMI medium. The percentage of positive T cell subtypes and their activation and proliferation was analyzed by flow cytometry.

At the end of the co-culture period, cells were stained with anti-CD4 and anti-CD8 antibodies. Additionally, anti-T-bet, anti-Foxp3, and anti-CD25 were also used to evaluate Th1 and T regulatory lymphocytes (Treg) subsets. To measure T cell activation, allogenic T cells were co-cultured with matured DCs for 18 h at a 10:1 ratio and then stained for CD4, CD8 and CD69 activation marker.

Cytolytic Assays

To address the capacity of DCs to prime and expand antigen-specific CD8+ T cells, autologous HLA-A2$^+$ CD8$^+$ and CD4$^+$ T cells were co-cultured for fourteen days at 10:1:1 ratio with matured DCs previously loaded with short (ELAGIGILTV) or long (GHGHSYTTAEELAGIGILTVILGVL) Melan-A peptides. All co-cultures were carried out in 24-well plates with a final volume of 1 ml of X-VIVO 15 supplemented with 10% FBS. The percentage of Melan-A-specific CD8$^+$ T cells was analyzed by flow cytometry, using Pro5 HLA-A*02:01 – ELAGIGILTV Pentamer – Biotin (Proimmune, Oxford, UK) as described by the manufacturer. The cytolytic activity was evaluated after 24 h of co-culture of these stimulated T cells and Melan-A-loaded H1650 lung cancer cell line at 50:1 ratio by lactate dehydrogenase (LDH) release assay (Biolegend), as described by the manufacturer.

To assess the effect of each medium in the capacity of DCs to activate NK cells, autologous HLA-A2$^+$ NK cells were co-cultured with matured DCs for 24 h at 5:1 ratio. These co-cultures were carried out in U-bottomed 96-well plates with a final volume of 200 µl of RPMI medium. DC-NK cell bidirectional crosstalk was addressed by analyzing the impact of cell interaction on the DC expression levels of CD86, MHC-I and MHC-II and on the NK cell expression levels of CD69 and CD25. The NK cytolytic activity was evaluated after 24 h of co-culture of these stimulated NK cells and H1650 lung cancer cell line or Panc1 pancreatic cancer cell line at 10:1 ratio by LDH release assay.

Metabolomic Analysis

At the end of the DC differentiation period, medium was collected and centrifuged at 300*g* for 5 min to collect floating cells. Supernatants were stored at −80°C for further extraction and cells were washed 3 times with cold PBS and immediately extracted using a biphasic extraction protocol with methanol/chloroform/water (1:1:0.7), as previously described (17). The resulting polar extracts were dried under vacuum in a SpeedVac concentrator (Eppendorf, Hamburg, Germany) and stored at −80°C until analysis. Cell conditioned media was thawed and subjected to a protein-precipitation procedure as described elsewhere (18). The resulting supernatants were vacuum dried and stored at −80°C until nuclear magnetic resonance (NMR) acquisition. Respective cell-free medium was processed in the same conditions and used to assess metabolite consumption and excretion by cells.

For NMR analysis, the dried samples were resuspended in 600 µl of deuterated PBS (100 mM, pH 7.4) containing 0.1 mM 3-(trimethylsilyl) propanoic acid (TSP-d_4), and 550 µl of each sample were transferred to 5 mm NMR tubes. All samples were analyzed in a Bruker Avance III HD 500 NMR spectrometer (University of Aveiro, Portuguese NMR Network), operating at 500.13 MHz for ^{1}H observation, at 298 K, using a 5 mm TXI probe. Standard 1D ^{1}H spectra with water presaturation (pulse program "noesypr1d" from Bruker library) were acquired and processed as previously described (19). Metabolite assignment was based on matching spectral information to reference spectra available in Chenomx (Edmonton, Canada), BBIOREFCODE-2–0–0 (Bruker Biospin, Rheinstetten, Germany) and the Human Metabolome Database (HMDB) (20).

Principal Component Analysis (PCA) was carried out in SIMCA-P 11.5 (Umetrics, Umeå, Sweden) to identify sample clusters, while signal integration, performed in Amix-Viewer 3.9.15 (Bruker Biospin, Rheinstetten, Germany), was employed to provide quantitative information on metabolite levels and variations. For media samples, only statistically significant variations ($p < 0.05$) with an absolute effect size larger than 1 (calculated as described in ref (21)) were considered.

Statistical Analysis

Results are presented as mean ± standard error of the mean (SEM) of the indicated number of experiments. Comparisons between two groups were made by the two-sided unpaired Student's t test and multiple group comparisons by one-way ANOVA analysis, with a Tukey multiple comparison post-test. Statistical analysis was performed using GraphPad Prism, version 6 (GraphPad Software, San Diego, CA, USA). Significance levels are as follows: *p <0.05, **p <0.01, ***p <0.001, ****p <0.0001

RESULTS

Different SFM Distinctly Impact the Phenotype of iDCs

Monocytes were cultured with GM-CSF and IL-4 in three different SFM, specifically AIM-V, X-VIVO-15, and DendriMACS, or with FBS-supplemented RPMI. After 6 days of differentiation, iDCs were analyzed for their morphological appearance and expression levels of CD14, CD16, CD1a, CD1c, and CD11c. The yield of differentiation as well as the viability (>80%) was similar between all four tested media (data not shown). Cells cultured in X-VIVO 15, AIM-V, or DendriMACS were found to be adherent and with elongated shape, in contrast to iDCs differentiated in RPMI that were rounder and mainly non- or loosely adherent (**Figure 1**). Differentiation of monocytes toward an iDC phenotype was observed for all the

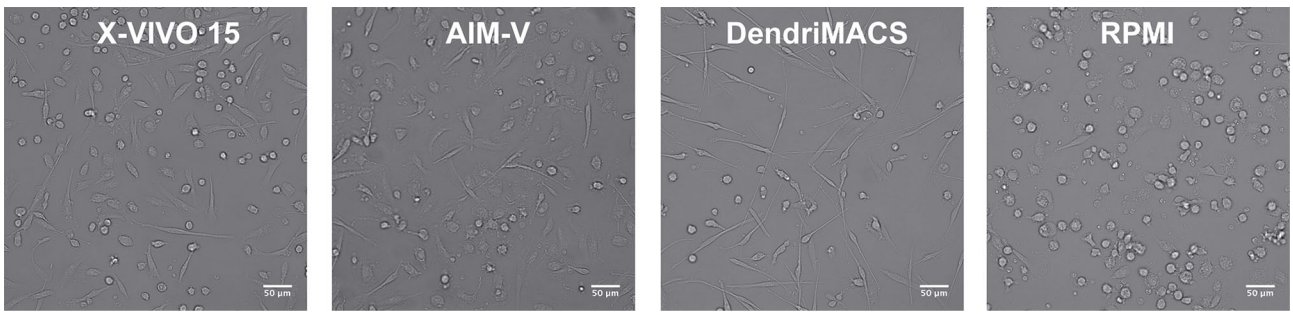


FIGURE 1 | Representative images of immature dendritic cells (iDCs) at day 6 of culture. Monocytes were cultured with GM-CSF and IL-4 in three different serum-free media (SFM)—AIM-V, X-VIVO-15, and DendriMACS—and with FBS-supplemented RPMI, for 6 days. Human iDCs differentiated in SFM are adherent and present a similar elongated morphology, while DCs differentiated in RPMI present a round shape with decreased cell adherence. X-VIVO 15, AIM-V, DendriMACS, RPMI. Images were obtained by wild-field microscope Zeiss AXIO Observer. Magnification: 100×. Scale = 50 µm.

tested media, as proved by the downregulation of CD14 and CD16 and the increased expression of the DC markers CD1a, CD1c, and CD11c (**Figure 2**). Graphics for mean fluorescence intensity (MFI) as well as statistical analysis are provided in **Figure S1**. However, the expression levels of DC markers are quantitatively different between media. Cells cultured in RPMI present a significant higher expression of CD1a, CD1c, and CD11c, when compared to SFM-iDCs (**Figure S1**). Of all SFM, DendriMACS elicited the highest levels of CD1c and CD1a, while X-VIVO 15 and AIM-V cultured cells presented an increased expression of CD11c. Importantly, all the three SFM induced two distinct populations regarding the expression levels of CD11c, with this output being particularly evident for cells differentiated in X-VIVO 15 (**Figure 2**).

The capacity of DCs to endocyte extracellular material, such as apoptotic/necrotic tumor cells, is critical for their role in antitumor immunity and is an indicator of functional quality of *ex-vivo* differentiated DCs. Therefore, we tested the impact of the different GMP SFM and of RPMI on iDCs capacity to endocyte apoptotic-labeled cancer cells, as previously described (22). The results indicate that iDCs produced with the three SFM present a similar capacity to internalize apoptotic/necrotic tumor cells. After 2 h of co-culture, 23,5% ±5,6 (AIM-V), 30,6% ±3,5 (X-VIVO 15) and 32,2% ±4,1 (DendriMACS) of iDCs presented engulfed material (**Figure S2**). However, these values are significantly lower ($p<0,05$; $p<0,01$) than the ones observed for iDCs produced in serum-supplemented RPMI (89,4%). These results clearly indicate that the absence of serum during DC differentiation negatively modulates their endocytic capacity.

Culture Media Used during DC Differentiation Affects Their Response to Maturation Stimuli

To address whether culture media used during DC differentiation impacts their response to maturation stimuli, cells obtained with the different media were treated with a maturation cocktail frequently used in clinical trials, comprising TNF-α, IL-1β, poly I:C, and IFN-γ. Cell maturation profile was subsequently assessed by analyzing the expression levels of: CD40, CD80, CD83, CD86, MHC-I, and MHC-II; the chemokine receptors CCR1, CCR2, CCR5, CCR7, and CXCR4; and the transcription levels of *IL12B*, *TNF*, *IL10*, and *TGFB*. The production of IL12p70 was also assessed.

Before maturation, the levels of CD83, CD40 and MHC-II were found to be similar between iDCs produced with the four media. In contrast, iDCs differentiated with AIM-V presented a significantly higher basal expression of the co-stimulatory molecule CD86: vs. X-VIVO 15 $p<0,001$; vs. DendriMACS $p<0,0001$, and vs. RPMI $p<0,0001$ (**Figure 3** and **Figure S3**). In a similar way, cells produced in RPMI were shown to express significantly higher levels of CD80 than X-VIVO 15 iDCs ($p<0,01$) and AIM-V iDCs ($p<0,05$). Although not statistically different, X-VIVO 15 and AIM-V iDCs consistently presented inferior levels of CD80 and CD40 and a slightly higher expression of MHC-I and CD83.

All the culture media supported an increase in the expression of co-stimulatory and MHC molecules upon treatment of cells with the maturation cocktail. However, the observed increases presented distinct magnitudes, with RPMI-differentiated DCs being the ones that strongly respond to the used stimuli. On the other hand, DCs produced with DendriMACS appear to be somehow resistant to maturation, presenting a smaller increase upon stimulation, particularly for CD86 expression. Cells differentiated with X-VIVO 15 and AIM-V, albeit not maturing as effectively as RPMI DCs, substantially increased the expression of CD40, CD80 and CD83.

A switch in chemokine receptor profile is another hallmark of DC maturation, allowing their relocation from inflamed tissues to draining lymph nodes (23). To migrate to lymph nodes, maturing DCs should upregulate CCR7 to respond to the lymphoid chemokines C-C motif ligands 19 and 21 (CCL19 and CCL21), while downregulating CCR1, CCR2, and CCR5. Therefore, the impact of culture media on the expression of CCR1, CCR2, CCR5, CCR7, and CXCR4 was evaluated by flow cytometry. As shown in **Figure 4** and **Figure S4**, analyzed media elicited a distinct basal chemokine receptor profile in iDCs and induced different responses upon maturation. Basal levels of CCR2, CCR5 and CCR7 are significantly higher in cells differentiated in FBS-supplemented RPMI, while no differences

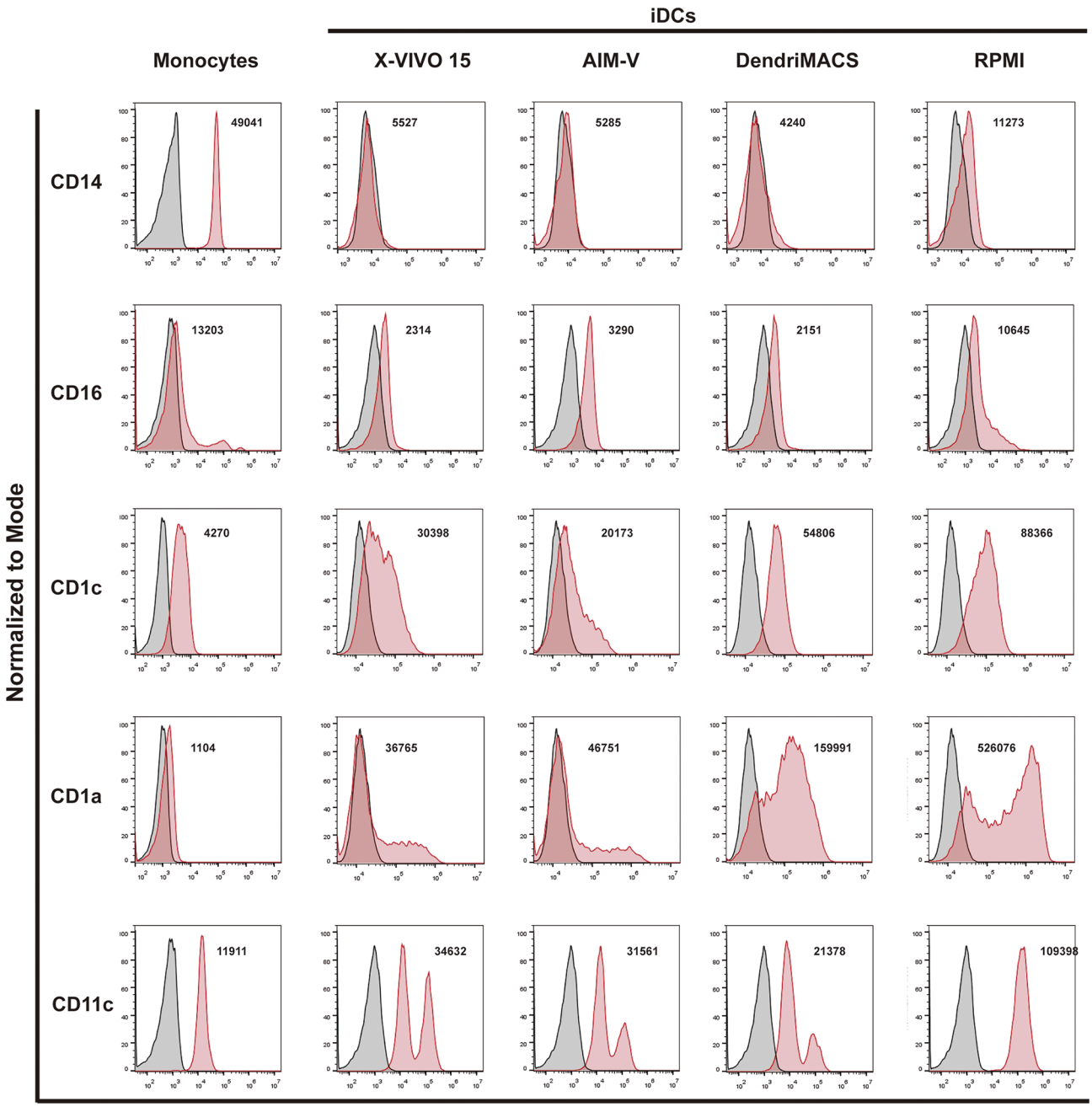


FIGURE 2 | Phenotypic comparison of immature dendritic cells (iDCs) generated in different culture media. Monocytes were cultured with GM-CSF and IL-4 in three different good manufacturing practice (GMP) serum-free media (SFM)—AIM-V, X-VIVO-15, and DendriMACS—and with FBS-supplemented RPMI. After 6 days of culture, expression levels of CD14, CD16, CD1c, CD1a, and CD11c were analyzed by flow cytometry. Viable cells were gated according to their morphological properties. Black line corresponds to isotype control and red line represents specific expression of tested cells. The histograms are representative of at least three independent experiments and the mean fluorescence intensity (MFI) of the performed experiments is presented.

were observed between iDCs produced in SFM. As expected, cell maturation caused a downregulation of CCR1 that was observed for all the media. In contrast, CCR7 is upregulated in SFM cultured cells and slightly downregulated in cells matured in RPMI. Importantly, despite the observed decrease, RPMI mDCS maintained a higher CCR7 expression than any of the SFM conditions (**Figure S4**). Regarding CCR5 expression, it was preserved in X-VIVO 15 and DendriMACS mDCs, decreasing in RPMI mDCs and surprisingly increasing in AIM-V mDCs.

Considering that cytokines produced by DCs are crucial to their immunomodulatory properties, we also characterize the impact of culture media on the transcription levels of *IL12B*,

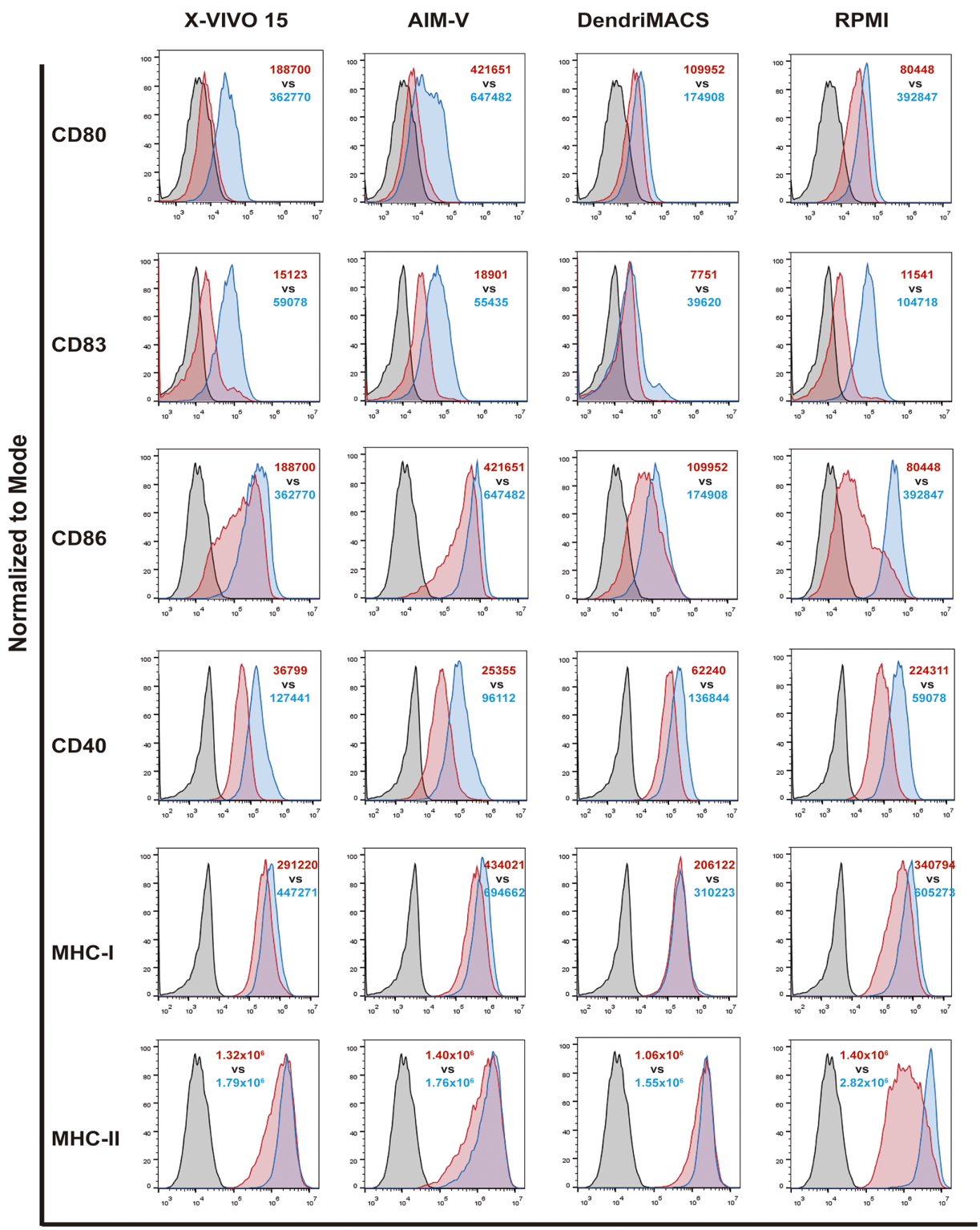


FIGURE 3 | Impact of different culture media on the response of dendritic cells (DCs) to maturation stimuli. DCs differentiated with the four tested media were matured as described in *methods* section. The expression of CD80, CD83, CD86, CD40, MHC-I and MHC-II was assessed by flow cytometry. Black line corresponds to respective isotype control, red line represents specific expression on immature DCs (iDCs) and blue line the expression on mature DCs (mDCs). Final analysis was performed including only viable cells based on their morphological properties. The histograms are representative of at least four independent experiments. In red, MFI values for iDCs and in blue MFI values for mDCs.

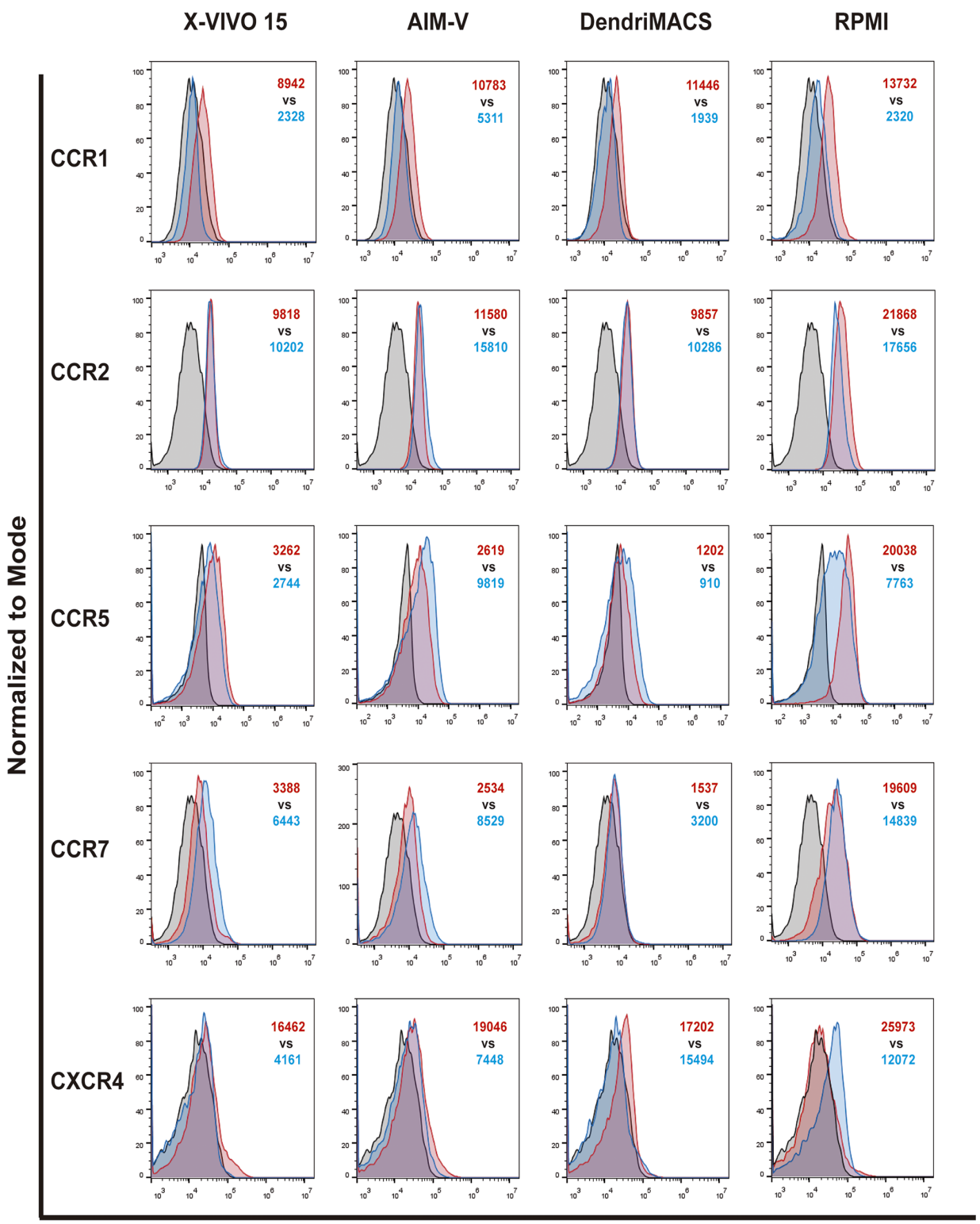


FIGURE 4 | Chemokine receptors profile of immature (iDCs) and mature (mDCs) dendritic cells. CCR1, CCR2, CCR5, CCR7 and CXCR4 expression levels were assessed by flow cytometry. Black line corresponds to respective isotype control, red line represents specific expression in iDCs and blue line the expression on mDCs. Final analysis was performed including only viable cells based on their morphological properties. The histograms are representative of four independent experiments. In red MFI values for iDCs and in blue MFI values for mDCs.

TNF, *IL10*, and *TGFB*, and on the release of IL-12p70 upon maturation. The transcription of anti-inflammatory *IL10* and *TGFB* was not significantly affected, while *IL12B* and *TNF* mRNA levels were strongly upregulated upon maturation in all tested media (**Figure 5A**). Among SFM, X-VIVO 15 and AIM-V supported the strongest increase in *IL12B* and *TNF* transcription, being significantly higher than those observed in DendriMACS mDCs. In accordance with these results, and despite some interindividual variability, DCs differentiated and matured in X-VIVO 15 or AIM-V were found to systematically produce higher amounts of IL-12p70 upon maturation (**Figure 5B**). Taken together, our data clearly indicate that from all the studied SFM, only X-VIVO 15 and AIM-V promoted an effective DC maturation with the used cocktail.

Culture Media Influence the Functional Capacities of Produced DCs

We also sought to address whether the capacities of DC to stimulate T cells were affected by the media used during their production. For this, allogenic mixed leucocyte reactions (MLR) were performed and T cell proliferation, phenotype and IFN-γ production were analyzed. As expected, independently of the used media, T cells that were stimulated with mDCs proliferated more than the T cells without stimulus (alone) (**Figures 6A–C**). Despite not being statistically significant, mDCs cultured in X-VIVO 15 and AIM-V induced a higher proliferation of T cells (79.98%± 4.11; 85.93%±1.62, respectively) than mDCs cultured in DendriMACS and RPMI (66.48%±8.81; 59.25%±9.19, respectively). Looking at each lymphocyte population individually, mDCs cultured in AIM-V induced higher $CD4^+$ T cell proliferation, while mDCs cultured in X-VIVO 15 induced superior proliferation of $CD8^+$ T cells (**Figures 6B, C**). Lymphoid activation antigen CD69 levels were also assessed to infer about T cells activation status (24). Culture media effects were similar to those observed for T cell proliferation with T cells ($CD4^+$ and $CD8^+$) stimulated with mDCs produced in X-VIVO 15 and AIM-V, presenting higher expression of CD69 (**Figures 6D–F**). The capacity of mDCs to polarize T cells toward Th1 or Treg was evaluated by the presence of T-bet^+ and $Foxp3^+CD25^+$ cells, respectively, within the $CD4^+$ T cell population. As shown in **Figures 6G, H**, mDCs cultured in X-VIVO 15 and AIM-V, elicited higher percentages of Th1 cells and a lower polarization of Treg, when compared to mDCs cultured in DendriMACS or RPMI. Accordingly, T cells stimulated with X-VIVO 15 and AIM-V

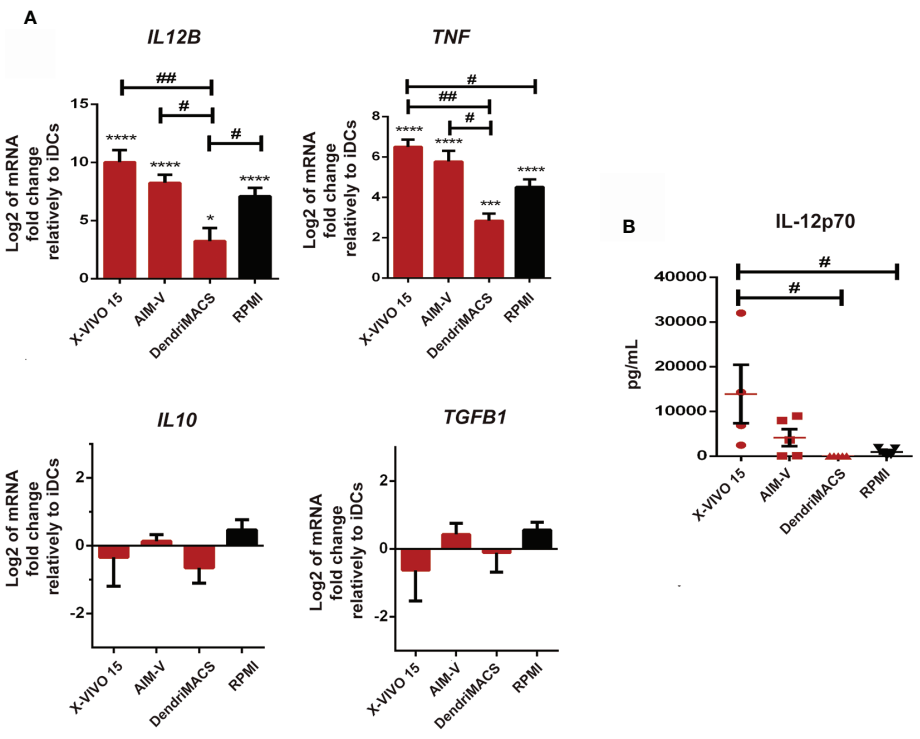


FIGURE 5 | Impact of different culture media on mature dendritic cells (mDCs) transcription levels of *IL12B*, *TNF*, *IL10*, and *TGFB*, and on the production of IL12p70. Immature dendritic cells (iDCs) were maturated with a cocktail of TNF-α, IL-1β, Poly-I:C, and IFN-, for 24 h Then, both cells and culture supernatants were collected for analysis. **(A)** The transcription levels of *IL12B, TNF, IL10*, and *TGFB* were assessed by qPCR. Results are presented as mean log2 values of fold changes relatively to respective iDCs. Each value represents the mean ± SEM from four independent experiments. **(B)** The production of IL-12p70 by mDCs cultured in X-VIVO 15, AIM-V, DendriMACS, and RPMI was determined in culture supernatants by ELISA. Results are presented as mean ± SEM of at least four to five independent experiments. Statistical significance: *$p < 0.05$; ***$p < 0.001$; ****$p < 0,0001$ for iDCs vs mDCs cultured in the same medium; $^{\#}p < 0.05$; $^{\#\#}p < 0.01$ for comparison among mDCs.

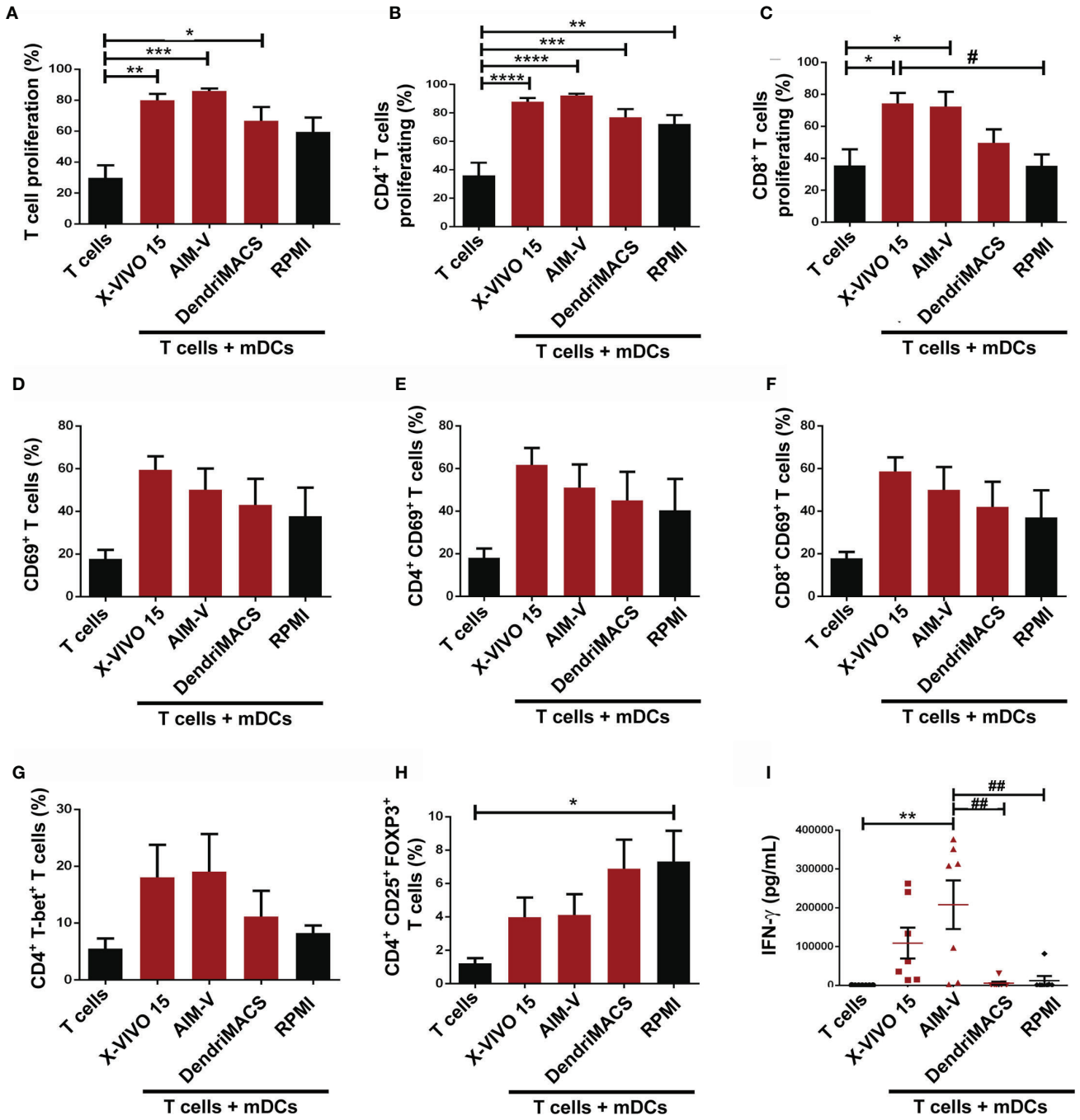


FIGURE 6 | Functional capacities of mDCs generated in X-VIVO 15, AIM-V, DendriMACS and RPMI. **(A–C)** iDCs were treated for 24 h with maturation cocktail and then co-cultured with autologous T cells in a 1:10 ratio. Proliferation of T cells was determined after 5 days of co-culture by analyzing the percentage of total **(A)**, $CD4^+$ **(B)** and $CD8^+$ **(C)** T cells that presented a decrease in CFSE fluorescence (n=4). **(D–F)** Activation of total **(D)**, $CD4^+$**(E)**, and $CD8^+$ **(F)** T cells was assessed by the expression of CD69 activation marker after 18 h of co-culture with mDCs. **(G, H)** The capacity of mDCs to polarize T cells toward Th1 ($CD4^+$T-bet^+) or Treg ($CD4^+CD25^+FoxP3^+$) phenotype was assessed by flow cytometry. Results are expressed as percentage of Th1 **(G)** and Treg **(H)** cells within T lymphocytes. **(I)** The production of IFN-γ was determined by ELISA test in supernatants of 5 days co-cultures. Results are presented as mean ± SEM of at least four independent experiments. Statistical significance: $^*p < 0.05$, $^{**}p < 0.01$, $^{***}p < 0.001$, $^{****}p < 0.0001$ for T cells vs T cells + mDCs from each medium; $^{\#}p < 0.05$; $^{\#\#}p < 0.01$ for comparison among T cells + mDCs.

mDCs were also found to produce significantly higher amounts of IFN-γ, a cytokine canonically produced by Th1 and cytotoxic T-lymphocytes (CTL) (**Figure 6I**). This superior capacity of X-VIVO 15 and AIM-V DCs to activate T cells strongly correlates with their more pronounced maturation status.

Next, we addressed the capacity of DCs to prime and expand antigen-specific $CD8^+$ T cells followed by the analysis of their cytolytic activity over tumor cells. Co-culture of autologous T-cells with Melan-A loaded mDCs differentiated in X-VIVO 15 or AIM-V resulted in superior priming of antigen-specific $CD8^+$ T cells (**Figure 7A**). Accordingly, these $CD8^+$ T cells also shown enhanced cytolytic activity over cancer cells presenting Melan-A (**Figure 7B**). Finally, as DCs and NK cells establish a bidirectional crosstalk that enhances the activation status of both cell type, we analyzed DC maturation and NK activation after their interaction. The interaction with autologous NK cells resulted in enhanced maturation status of X-VIVO 15 and AIM-V mDCs (**Figure S5A**). In turn, mDCs produced in X-VIVO 15 were the more effectives in increasing NK activation markers CD69 and CD25 (**Figure S5B**). This correlates well with cytolytic assays since as shown in **Figures 7C, D**, NK cells co-cultured with X-VIVO 15 or AIM-V mDCs present higher cytolytic activity over Panc-1 and H1650 cancer cells.

DCs Generated in Different Culture Media Have Distinct Metabolic Activity and Composition

To assess the metabolic status of DCs produced in the different media, we performed an NMR metabolomic analysis of conditioned media (exometabolome) and of cell extracts (endometabolome), on day 6 of differentiation. The scores scatter plot resulting from applying principal component analysis (PCA) to the ^{1}H-NMR spectra of media supernatants evidenced a clear separation between groups, indicating

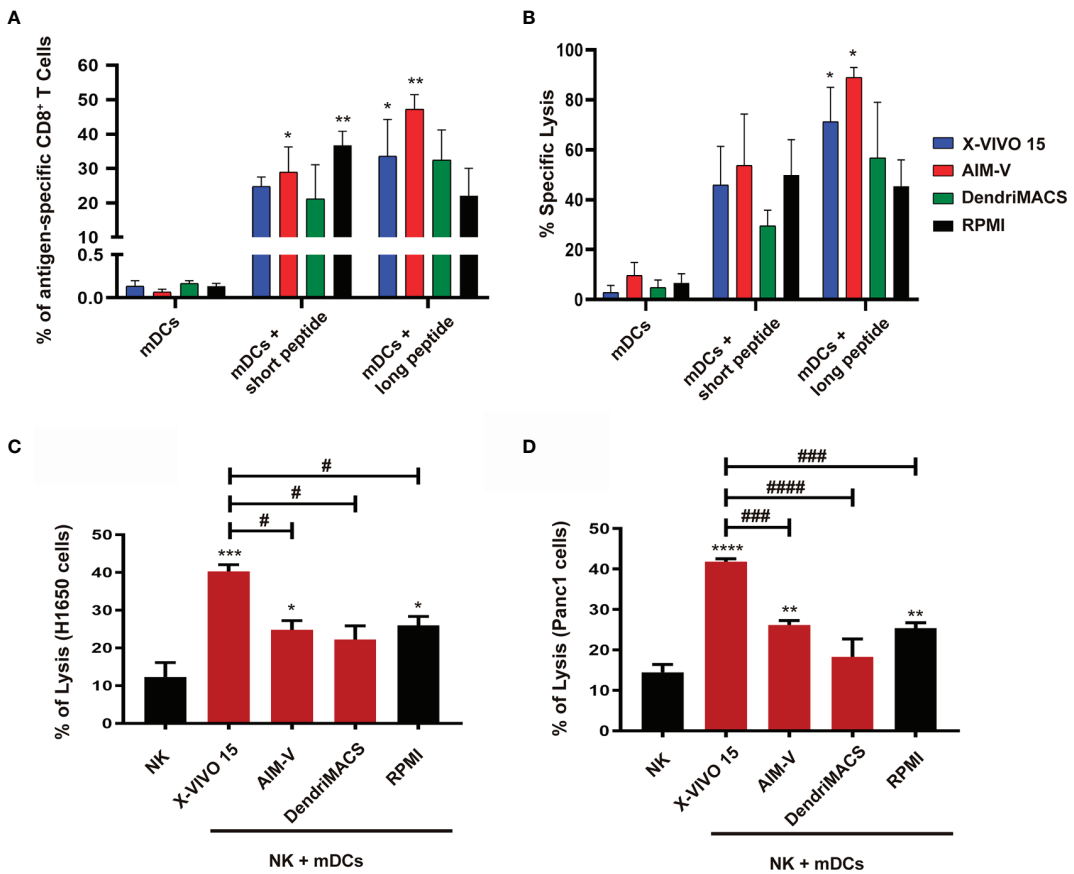


FIGURE 7 | Priming of antigen-specific $CD8^+$T cells and NK cytolytic activity after interaction with mDCs generated in X-VIVO 15, AIM-V, DendriMACS and RPMI. **(A, B)** iDCs were loaded with Melan-A short or long peptides and treated for 24 h with maturation cocktail and then co-cultured with autologous $CD8^+$ and $CD4^+$ cells for 14 days. **(A)** The percentage of primed and expanded Melan-A-specific $CD8^+$ T cells was determined by flow cytometry using Pro5 HLA-A*02:01 – ELAGIGILTV Pentamer—Biotin plus Streptavidin-PE (n=3). **(B)** Primed $CD8^+$ T cells were co-cultured with Melan-A-loaded H1650 lung cancer cell line at 50:1 ratio and their cytolytic activity was determined using LDH release assay (n=3). **(C, D)** iDCs were treated for 24 h with maturation cocktail and then co-cultured with autologous NK cells at a 1:5 ratio. After 24 h, NK cells were co-cultured with H1650 non-small cell lung cancer cell line **(C)** or Panc1 pancreatic cancer cell line **(D)** at 10:1 ratio, and their cytolytic activity was determined using LDH release assay (n=3). Results are presented as mean ± SEM. Statistical significance: $^*p < 0.05$, $^{**}p < 0.01$, $^{***}p < 0.001$, $^{****}p < 0.0001$ for mDCs vs mDCs + peptides or NK cells vs NK cells + mDCs from each medium; $^{\#}p < 0.05$, $^{\#\#\#}p < 0.001$, $^{\#\#\#\#}p < 0.0001$ for comparison among different NK cells + mDCs conditions.

substantial differences in media composition (**Figure 8A**). For a more detailed analysis of cells consumption/excretion behavior, spectral integration was carried out and metabolite variations were calculated by comparing each conditioned media with its acellular counterpart (**Figure 8C**). Pyruvate was the substrate preferred by all cells, being consumed to similar extent from all tested media (~2-fold decrease in cell-conditioned vs. acellular medium). Glutamine and isoleucine were only consumed by cells

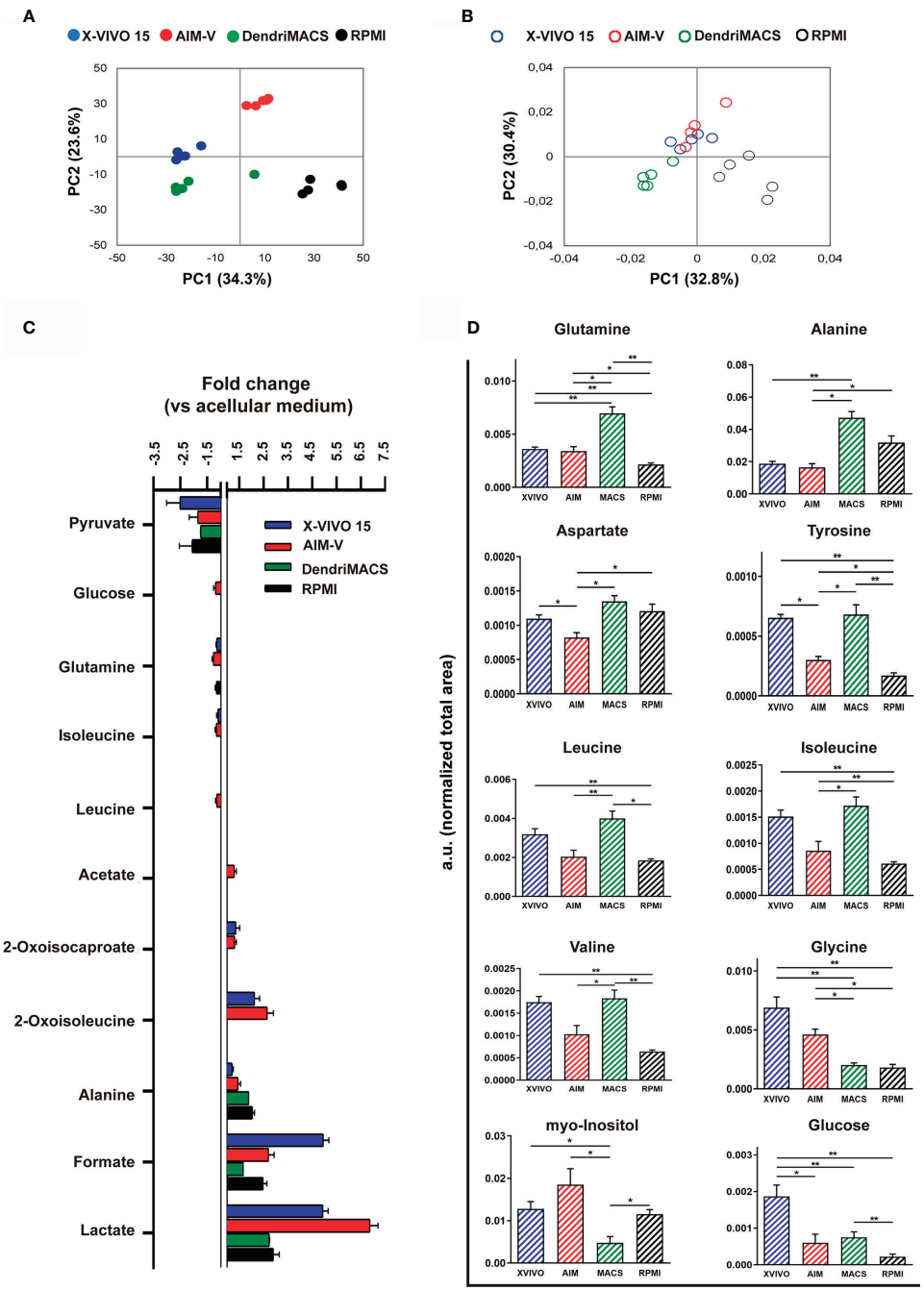


FIGURE 8 | NMR-based metabolomic analysis of immature dendritic cells (iDCs) generated in different media. **(A)** Scores scatter plot obtained by principal component analysis (PCA) of spectral data from the different cell-conditioned media at day 6 of cell differentiation. **(B)** Scores scatter plot obtained by PCA of spectral data recorded for intracellular aqueous extracts of DCs cultured in different media for 6 days. **(C)** Metabolites consumed (negative bars) and excreted (positive bars) during the differentiation of Mo-DCs. Variations are expressed as fold change in relation to acellular media counterparts. **(D)** Relative intracellular levels of metabolites showing significant differences among the tested SFM, as assessed by integration of 1D ^{1}H NMR spectra. Statistical significance: *$p < 0.05$, **$p < 0.01$ for comparison among DCs from the different media.

differentiated in X-VIVO 15 or AIM-V, while AIM-V DCs additionally consumed glucose and leucine. As for metabolites released into the medium, all SFM-differentiated cells excreted lactate, formate and alanine, whereas X-VIVO 15 and AIM-V DCs additionally released 2-oxoisocaproate and 2-oxoisoleucine (catabolic products of leucine and isoleucine). Acetate was excreted by AIM-V DCs only.

NMR analysis of cell extracts further showed DCs generated in different media to have distinct intracellular metabolic profiles. The PCA scores scatter plot (**Figure 8B**) shows that AIM-V and X-VIVO 15 DCs cluster together in the positive side of PC2, while DendriMACS and RPMI DCs, with scores in negative PC2, separate along the PC1 axis. The main quantitative differences between the 4 groups, as assessed by comparing normalized signal areas, are shown in **Figure 8D**. Most differences regarded the levels of amino acids. Among SFM-cultured cells, DendriMACS DCs displayed the highest levels of glutamine, alanine, aspartate, tyrosine, and branched chain amino acids, whereas AIM-V DCs contained the lowest amounts. On the other hand, intracellular levels of glycine were lower in DendriMACS DCs than in AIM-V and X-VIVO 15 DCs. Additionally, AIM-V and X-VIVO 15 DCs contained significantly higher levels of myo-inositol than DendriMACS DCs, while the glucose content was greater in X-VIVO 15 DCs than in all others. Intracellular levels of lactate, glutamate, formate and succinate did not vary significantly between SFM-cultured cells (**Figure S6**).

DISCUSSION

Fully defining culture conditions in which differentiation and maturation occur should be the first step toward the standardization of clinical grade DC production. In order to reduce the variability of a cellular product and to avoid possible immune reactions and transmission of infectious diseases, SFM are commonly used to produce clinical grade DCs (13, 14, 25). However, despite the likely impact of these SFM on the phenotype and functional abilities of produced DCs, very few studies directly compared them (13, 15). Here, we have shown that different SFM elicit a distinct metabolic state on DCs, conditioning cell phenotype, response to maturation stimuli and by consequence their T cell and NK cell immunostimulatory abilities (**Figure 9**). SFM were previously shown to support the

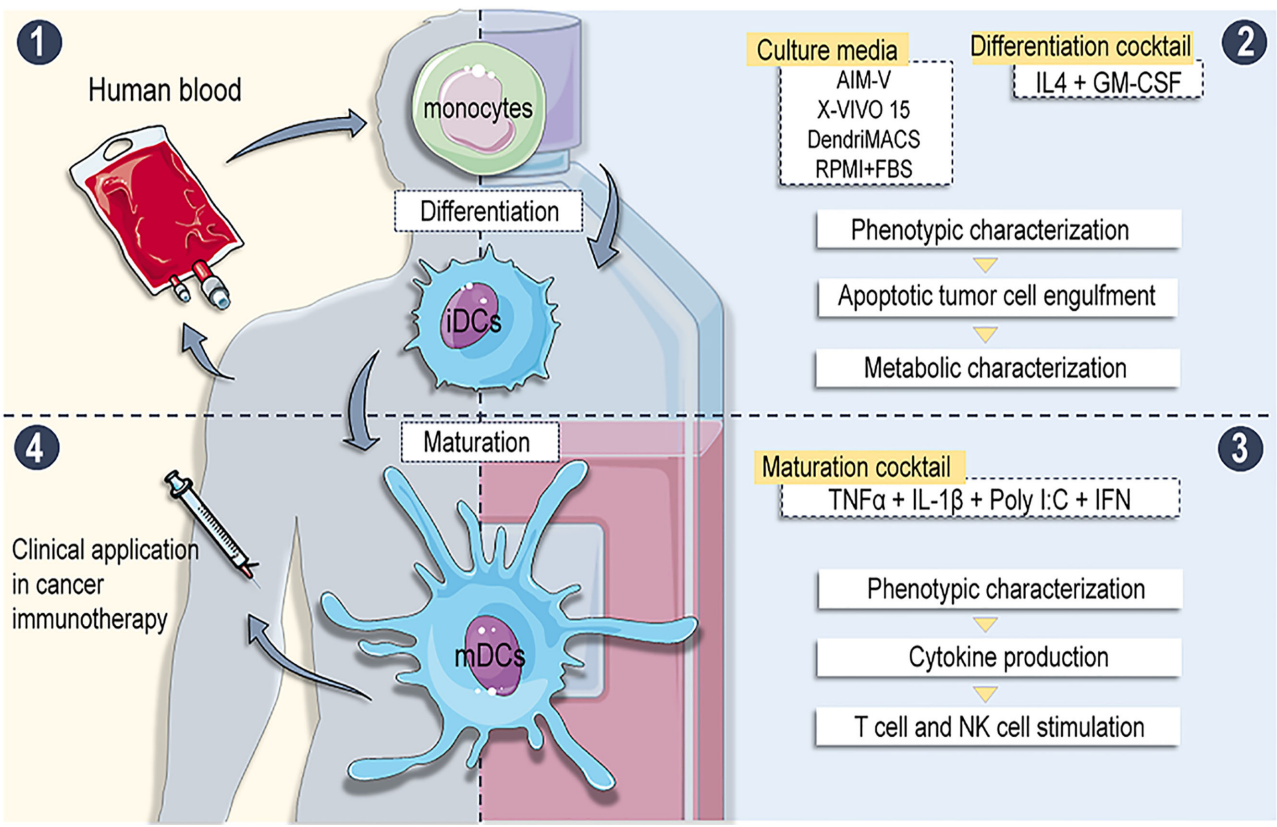


FIGURE 9 | Overview of the work: (1) moDCs were differentiated from buffy coat isolated CD14+ monocytes using different serum free media (SFM) supplemented with IL-4 + GM-CSF. (2) Phenotype, apoptotic tumour engulfment capacity and metabolic profiles were analysed on immature DCs (iDCs). (3) iDCs were matured with alpha DC cocktail and phenotype, cytokine production and T and NK cells stimulatory abilities were assessed. (4) Results: Different SFM generate moDCs with distinct phenotypes and functional abilities. DCs with superior immunostimulatory abilities are produced in media evoking enhanced catabolism of amino acids and glucose. Conclusion: Definition of adequate culture medium is crucial for the production standardization of antitumor DC-based vaccines.

differentiation of $CD14^+$ monocytes into Mo-DCs without major impact in the cell yield and viability (12, 13, 15). In accordance with these observations, no differences were found between the yield obtained in the three tested SFM and FBS-supplemented RPMI. Nonetheless, the capacity of SFM-differentiated iDCs to engulf apoptotic/necrotic cells was clearly compromised. This can be due to the absence of serum bridging molecules, such as complement component C1q, Gas6, Protein S, and milk fat globule-EGF factor 8, that are known to indirectly mediate the recognition of dying cells by phagocytes (26–28). Thus, co-culture with necrotic tumor cells may not be the optimal antigen loading strategy for DCs produced in SFM.

Herein, we demonstrated that the phenotype of iDCs and mainly their behavior upon maturation presented substantial differences between tested media, which is then translated into distinct immunostimulatory capacities. When compared to DendriMACS DCs, cells produced in X-VIVO 15 or AIM-V were found to express higher levels of CD11c, CD86, and MHC-I, while presenting lower levels of CD1a and CD1c. Upon maturation, X-VIVO 15 and AIM-V DCs also expressed higher levels of CD86 and CCR7, presenting an enhanced capacity to secrete IL-12p70. In a previous work, DCs differentiated in serum-supplemented media were shown to present inferior levels of CD1a, when compared to cells differentiated in AIM-V (29). This difference was attributed to the activation of peroxisome proliferator-activated receptor γ (PPARγ) by components of lipoproteins present in serum or FBS. Our results do not corroborate these observations since all SFM elicited significantly lower levels of CD1a vs. FBS-supplemented RPMI. Therefore, lipids used in the formulation of SFM, namely mono- and polyunsaturated fatty acids, may be activating PPARγ in a way that exceeds the effect caused by serum lipoproteins (30). The expression of CD1a has also been positively correlated with a superior capacity of DCs to produce IL-12p70 and to promote Th1 polarization (31, 32). However, this assumption was recently challenged by data showing that genetic polymorphisms affect CD1a expression without compromising DCs Th1 polarizing capacities, or that IL-12p70 secretion and CD1a positivity are dissociated (33, 34). Our results support these latter observations, given that a higher expression of CD1a was found in RPMI and DendriMACS DCs. Nevertheless, these cells marginally produced IL-12p70 upon maturation and were clearly inferior in polarizing IFN-γ–producing T cells.

The low number of DCs present in T cell areas of lymphoid organs after intradermal or subcutaneous injection is pointed as a limiting factor to the efficacy of antitumor DC-based vaccines (35). Additionally, DCs expressing high levels of CCR7, the key regulator of DC migration toward secondary lymphoid tissues, elicit more effective antigen-specific immune responses and lower the required DC dosage during immunization (36, 37). Thus, DCs chemokine profile assumes particular relevance for the success of the clinical approach. In our experimental settings, CCR7 was slightly upregulated upon maturation in all tested SFM. CCR7 modulation on DCs is largely dependent on the stimuli used to mature cells. For instance, prostaglandin E2 (PGE2) was shown to be required for an effective receptor upregulation, with this molecule being part of the most frequently used maturation cocktail in clinical trials (IL1-β, IL-6, TNF-α; and PGE2) (38). However, PGE2 restrains the capacity of Mo-DCs to produce IL-12p70 (39). To surpass this drawback, the maturation cocktail used in this study has been proposed as a good compromise solution between migratory capacity and the production of the cytokine (40). Apart from the upregulation of CCR7, cell migration from peripheral tissues to lymph nodes also requires a coordinated downregulation of inflammatory chemokine receptors, such as CCR1 and CCR5. Accordingly, CCR1 was downregulated after DC maturation, independently of the media used. Surprisingly, DCs differentiated in AIM-V medium presented an increased expression of CCR5 upon maturation. Even though this may hamper the migration of injected DCs toward lymph nodes, it could facilitate their interaction with NK cells (41). This must be carefully contemplated, considering that in pre-clinical studies DC-NK crosstalk has been shown to be crucial for DC-based antitumor vaccines efficacy (42). Indeed, we showed that co-culture of AIM-V and X-VIVO 15 mDCs with autologous NK cells significantly enhanced their cytolytic activity. In accordance with the role played by IL-12p70 on NK cell activation (43), NK-activating capacity of AIM-V and X-VIVO 15 mDCs closely correlates with their higher production of this cytokine. Furthermore, as extensively reported in literature (44–47), we observed that DCs expressing higher levels of CD80, CD83 and CD86 (in our experimental settings those produced in AIM-V or X-VIVO 15) present superior capacity to polarize Th1 subset and to prime antigen-specific $CD8^+$ T cells. Of note, DCs produced in all media tested showed the capacity to internalize and process long Melan-A peptide, cross-presenting resultant antigen on MHC-I molecules. This cross-presenting capacity is of particular relevance if tumor lysates or apoptotic tumor cells were used as antigen source during the production of the DC vaccine (5).

Recently, numerous evidence have demonstrated that cellular metabolism modulates DC functions, as well as their development and differentiation [reviewed in (8, 48)]. Differentiation of monocytes into Mo-DCs relies on the activation of mammalian target of rapamycin (mTOR) complex 1 (mTORC1) (49, 50), being supported by a catabolic metabolism dependent on oxidative phosphorylation (OXPHOS). In turn, upon activation, DCs shift to an aerobic glycolytic state where tricarboxylic acid (TCA) intermediates such as citrate, succinate and fumarate, contribute to the upregulation of co-stimulatory surface molecules, cytokine production and T cell stimulatory capacity (51, 52). In the present study, we have hypothesized that the phenotypical and functional differences observed between DCs produced in the different media could relate to their distinct metabolic status, induced during differentiation. One of the most noticeable differences, as assessed by metabolomics profiling, regarded amino acid metabolism. Unlike DendriMACS DCs, which did not use extracellular amino acids, AIM-V DCs and, to lower extent, X-VIVO 15 DCs were found to consume glutamine and branched chain amino acids (BCAA). Additionally, the

intracellular levels of these and other amino acids were lower in X-VIVO 15 and/or AIM-V DCs, corroborating their higher catabolism. Glutamine consumption and intracellular use (glutaminolysis) likely reflect its anaplerotic channeling into the TCA cycle, to support OXPHOS and energy generation. As for BCAA, their catabolism has been recently reported to exacerbate the inflammatory properties of activated macrophages (53). Therefore, it is plausible to speculate that an increased catabolic rate of valine, leucine, and isoleucine in AIM-V or X-VIVO 15 DCs could contribute to their superior T cell stimulatory abilities. Another major difference between the DC groups compared regarded glucose consumption and intracellular levels. Only DCs differentiating in AIM-V consumed extracellular glucose, while showing the lowest intracellular levels, which, together with prominent lactate excretion, suggest higher glycolytic activity in these cells. This may possibly correlate with the observed higher basal expression of co-stimulatory molecules, as well as with the superior capacity of these cells to acquire a full mature phenotype following cytokine stimulation. Also, it should be noted that lactate, generated by LDH-catalyzed reduction of pyruvate, has been recently shown to be an important carbon source for $CD8^+$ T cells proliferation and activation (54). As all cells took up pyruvate to similar extents, it is likely that higher lactate production and release originates from enhanced glutaminolysis, glycolysis and/or use of intracellular glycogen (55). Furthermore, AIM-V DCs were seen to excrete acetate, which could result from pyruvate, especially in conditions of metabolic overflow (56). Interestingly, acetate has been shown to be required for optimal $CD8^+$ T cell function in the immune system (57). Finally, AIM-V and X-VIVO 15 DCs presented significantly higher intracellular levels of myo-inositol than DendriMACS DCs. This polyalcohol is a precursor molecule for inositol phosphates and other second messengers with important roles in T cell development (58), therefore, its putative relation to DCs immunostimulatory properties should not be ruled out.

CONCLUSION

The present study delivers novel insights into the impact of culture conditions in the production of clinical grade DCs. Our data show that DC phenotype and functional abilities, such as the capacity to activate autologous NK cells and to prime antigen-specific $CD8^+$ T cells, are strongly influenced by the GMP SFM used during DC differentiation and correlate with evoked metabolic status. Definition of culture conditions is therefore a critical step in the production of DCs for clinical application in cancer immunotherapy.

DATA AVAILABILITY STATEMENT

The data used and analysed in the current study are available from the corresponding author on reasonable request.

ETHICS STATEMENT

Buffy coats were provided by the Portuguese Blood and Transplantation Institute (IPST) following an established protocol allowing access to buffy coats for scientific research with academic purposes only. The buffy coats were not specifically obtained for the present study and were provided without any personal detail from the donor.

AUTHOR CONTRIBUTIONS

MAC and BMN designed and conceived the study. JC, MAC, LM, CL, AT, and DF performed the experiments, acquired, and analyzed data. JC, MAC, LM, ID, and BMN interpreted data. JC and MAC wrote the original draft of the manuscript and BMN, CG, AF, and MTC made the final revisions and editing. All authors contributed to the article and approved the submitted version.

FUNDING

This work was developed within the scope of iBiMED (UIDB/04501/2020) and CICECO-Aveiro Institute of Materials (UIDB/50011/2020 & UIDP/50011/2020), financed by national funds through the Foundation for Science and Technology (FCT). Funding was received from the project ImmunoDCs@CancerStemCells: Cellular Immunotherapy toward the elimination of cancer stem cells (Ref.: POCI-01-0247-FEDER-033532), co-funded by the European Regional Development Fund (FEDER), Competitiveness and Internationalization Operational Program (COMPETE2020) and Own Revenues of the University of Coimbra. João Calmeiro and Luís Mendes are supported by the FCT through individual PhD fellowships (PD/BDE/135076/2017; PD/BD/147220/2019). The NMR spectrometer is part of the National NMR Network (PTNMR), partially supported by Infrastructure Project N° 022161 (co-financed by FEDER through COMPETE 2020, POCI and PORL and FCT through PIDDAC).

ACKNOWLEDGMENTS

We thank Prof. Dr. Sebastian Amigorena (Unit Director), Dr. Antonela Merlotti and Dr. Yago Arribas, all from Institute Curie in Paris (Unit 932—Immunity and Cancer), for the valuable in-house training of João Calmeiro and for insight knowledge on DC-T cell cytotoxicity assays.

SUPPLEMENTARY MATERIAL

The Supplementary Material for this article can be found online at: https://www.frontiersin.org/articles/10.3389/fimmu.2020.593363/full#supplementary-material

REFERENCES

1. Collin M, Bigley V. Human dendritic cell subsets: an update. *Immunology* (2018) 154:3–20. doi: 10.1111/imm.12888
2. Mastelic-Gavillet B, Balint K, Boudousquie C, Gannon PO, Kandalaft LE. Personalized dendritic cell vaccines-recent breakthroughs and encouraging clinical results. *Front Immunol* (2019) 10:766. doi: 10.3389/fimmu.2019.00766
3. Constantino J, Gomes C, Falcão A, Neves BM, Cruz MT. Dendritic cell-based immunotherapy: a basic review and recent advances. *Immunol Res* (2017) 65:798–810. doi: 10.1007/s12026-017-8931-1
4. Calmeiro J, Carrascal M, Gomes C, Falcão A, Cruz MT, Neves BM. Biomaterial-based platforms for in situ dendritic cell programming and their use in antitumor immunotherapy. *J Immunother Cancer* (2019) 7:238. doi: 10.1186/s40425-019-0716-8
5. Constantino J, Gomes C, Falcão A, Cruz MT, Neves BM. Antitumor dendritic cell-based vaccines: lessons from 20 years of clinical trials and future perspectives. *Transl Res* (2016) 168:74–95. doi: 10.1016/j.trsl.2015.07.008
6. Saxena M, Balan S, Roudko V, Bhardwaj N. Towards superior dendritic-cell vaccines for cancer therapy. *Nat BioMed Eng* (2018) 2:341–6. doi: 10.1038/s41551-018-0250-x
7. Cintolo JA, Datta J, Mathew SJ, Czerniecki BJ. Dendritic cell-based vaccines: barriers and opportunities. *Future Oncol* (2012) 8:1273–99. doi: 10.2217/fon.12.125
8. Wculek SK, Khouili SC, Priego E, Heras-Murillo I, Sancho D. Metabolic Control of Dendritic Cell Functions: Digesting Information. *Front Immunol* (2019) 10:775:775. doi: 10.3389/fimmu.2019.00775
9. Mackensen A, Dräger R, Schlesier M, Mertelsmann R, Lindemann A. Presence of IgE antibodies to bovine serum albumin in a patient developing anaphylaxis after vaccination with human peptide-pulsed dendritic cells. *Cancer Immunol Immunother* (2000) 49:152–6. doi: 10.1007/s002620050614
10. Loudovaris M, Hansen M, Suen Y, Lee SM, Casing P, Bender JG. Differential Effects of Autologous Serum on CD34 $^{+}$ or Monocyte-Derived Dendritic Cells. *J Hematother Stem Cell Res* (2001) 10:569–78. doi: 10.1089/15258160152509172
11. Ratta M, Fagnoni F, Curti A, Vescovini R, Sansoni P, Oliviero B, et al. Dendritic cells are functionally defective in multiple myeloma: the role of interleukin-6. *Blood* (2002) 100:230–7. doi: 10.1182/blood.V100.1.230
12. Romani N, Reider D, Heuer M, Ebner S, Kämpgen E, Eibl B, et al. Generation of mature dendritic cells from human blood An improved method with special regard to clinical applicability. *J Immunol Methods* (1996) 196:137–51. doi: 10.1016/0022-1759(96)00078-6
13. Napoletano C, Pinto D, Bellati F, Taurino F, Rahimi H, Tomao F, et al. Nuti M. A Comparative Analysis of Serum and Serum-free Media for Generation of Clinical Grade DCs. *J Immunother* (2007) 30:567–76. doi: 10.1097/CJI.0b013e318046f396
14. Peng JC, Thomas R, Nielsen LK. Generation and maturation of dendritic cells for clinical application under serum-free conditions. *J Immunother* (2005) 28:599–609. doi: 10.1097/01.cji.0000175491.21099.04
15. Royer P-J, Tanguy-Royer S, Ebstein F, Sapede C, Simon T, Barbieux I, et al. Culture Medium and Protein Supplementation in the Generation and Maturation of Dendritic Cells. *Scand J Immunol* (2006) 63:401–9. doi: 10.1111/j.1365-3083.2006.001757.x
16. Neves BM, Rosa SC, Martins JD, Silva A, Gonçalo M, Lopes MC, et al. Development of an in Vitro Dendritic Cell-Based Test for Skin Sensitizer Identification. *Chem Res Toxicol* (2013) 26:368–78. doi: 10.1021/tx300472d
17. Carrola J, Bastos V, Jarak I, Oliveira-Silva R, Malheiro E, Daniel-da-Silva AL, et al. Metabolomics of silver nanoparticles toxicity in HaCaT cells: structure–activity relationships and role of ionic silver and oxidative stress. *Nanotoxicology* (2016) 10:1105–17. doi: 10.1080/17435390.2016.1177744
18. Kostidis S, Addie RD, Morreau H, Mayboroda OA, Giera M. Quantitative NMR analysis of intra- and extracellular metabolism of mammalian cells: A tutorial. *Anal Chim Acta* (2017) 980:1–24. doi: 10.1016/J.ACA.2017.05.011
19. Mendes LF, Gaspar VM, Conde TA, Mano JF, Duarte IF. Flavonoid-mediated immunomodulation of human macrophages involves key metabolites and metabolic pathways. *Sci Rep* (2019) 9:14906. doi: 10.1038/s41598-019-51113-z
20. Wishart DS, Feunang YD, Marcu A, Guo AC, Liang K, Vázquez-Fresno R, et al. HMDB 4.0: the human metabolome database for 2018. *Nucleic Acids Res* (2018) 46:D608–17. doi: 10.1093/nar/gkx1089
21. Berben L, Sereika SM, Engberg S. Effect size estimation: Methods and examples. *Int J Nurs Stud* (2012) 49:1039–47. doi: 10.1016/J.IJNURSTU.2012.01.015
22. Carrascal MA, Severino PF, Guadalupe Cabral M, Silva M, Ferreira JA, Calais F, et al. Sialyl Tn-expressing bladder cancer cells induce a tolerogenic phenotype in innate and adaptive immune cells. *Mol Oncol* (2014) 8:753–65. doi: 10.1016/j.molonc.2014.02.008
23. Tiberio L, Del Prete A, Schioppa T, Sozio F, Bosisio D, Sozzani S. Chemokine and chemotactic signals in dendritic cell migration. *Cell Mol Immunol* (2018) 15:346–52. doi: 10.1038/s41423-018-0005-3
24. Simms PE, Ellis TM. Utility of flow cytometric detection of CD69 expression as a rapid method for determining poly- and oligoclonal lymphocyte activation. *Clin Diagn Lab Immunol* (1996) 3:301–4.
25. de Vries IJM, Eggert AAO, Scharenborg NM, Vissers JLM, Lesterhuis WJ, Boerman OC, et al. Phenotypical and Functional Characterization of Clinical Grade Dendritic Cells. *J Immunother* (2002) 25:429–38. doi: 10.1097/00002371-200209000-00007
26. Païdassi H, Tacnet-Delorme P, Garlatti V, Darnault C, Ghebrehiwet B, Gaboriaud C, et al. C1q binds phosphatidylserine and likely acts as a multiligand-bridging molecule in apoptotic cell recognition. *J Immunol* (2008) 180:2329–38. doi: 10.4049/jimmunol.180.4.2329
27. Hanayama R, Tanaka M, Miwa K, Shinohara A, Iwamatsu A, Nagata S. Identification of a factor that links apoptotic cells to phagocytes. *Nature* (2002) 417:182–7. doi: 10.1038/417182a
28. Wu Y, Singh S, Georgescu M-M, Birge RB. A role for Mer tyrosine kinase in αvβ5 integrin-mediated phagocytosis of apoptotic cells. *J Cell Sci* (2005) 118:539–53. doi: 10.1242/jcs.01632
29. Gogolak P, Rethi B, Szatmari I, Lanyi A, Dezso B, Nagy L, et al. Differentiation of CD1a– and CD1a+ monocyte-derived dendritic cells is biased by lipid environment and PPARγ. *Blood* (2007) 109:643–52. doi: 10.1182/blood-2006-04-016840
30. Kliewer SA, Sundseth SS, Jones SA, Brown PJ, Wisely GB, Koble CS, et al. Fatty acids and eicosanoids regulate gene expression through direct interactions with peroxisome proliferator-activated receptors alpha and gamma. *Proc Natl Acad Sci U S A* (1997) 94:4318–23. doi: 10.1073/pnas.94.9.4318
31. Cernadas M, Lu J, Watts G, Brenner MB. CD1a expression defines an interleukin-12 producing population of human dendritic cells. *Clin Exp Immunol* (2009) 155:523–33. doi: 10.1111/j.1365-2249.2008.03853.x
32. Chang CC, Wright A, Punnonen J, Gauchat JF, de Vries JE. Monocyte-derived CD1a+ and CD1a- dendritic cell subsets differ in their cytokine production profiles, susceptibilities to transfection, and capacities to direct Th cell differentiation. *J Immunol* (2000) 165:3584–91. doi: 10.4049/jimmunol.165.7.3584
33. Seshadri C, Shenoy M, Wells RD, Hensley-McBain T, Andersen-Nissen E, McElrath MJ, et al. Human CD1a deficiency is common and genetically regulated. *J Immunol* (2013) 191:1586–93. doi: 10.4049/jimmunol.1300575
34. Mester B, Bauer E, Wood CE, Hermans IF, Gasser O. Expression of CD1a and Type-1 Polarization Are Dissociated in Human Monocyte-Derived Dendritic Cells. *PloS One* (2015) 10:e0140432. doi: 10.1371/journal.pone.0140432
35. Verdijk P, Aarntzen EHJG, Lesterhuis WJ, Boullart ACI, Kok E, van Rossum MM, et al. Limited amounts of dendritic cells migrate into the T-cell area of lymph nodes but have high immune activating potential in melanoma patients. *Clin Cancer Res* (2009) 15:2531–40. doi: 10.1158/1078-0432.CCR-08-2729
36. Okada N, Mori N, Koretomo R, Okada Y, Nakayama T, Yoshie O, et al. Augmentation of the migratory ability of DC-based vaccine into regional lymph nodes by efficient CCR7 gene transduction. *Gene Ther* (2005) 12:129–39. doi: 10.1038/sj.gt.3302358
37. González FE, Ortiz C, Reyes M, Dutzan N, Patel V, Pereda C, et al. Melanoma cell lysate induces CCR7 expression and in vivo migration to draining lymph nodes of therapeutic human dendritic cells. *Immunology* (2014) 142:396–405. doi: 10.1111/imm.12264
38. Scandella E, Men Y, Gillessen S, Förster R, Groettrup M. Prostaglandin E2 is a key factor for CCR7 surface expression and migration of monocyte-derived dendritic cells. *Blood* (2002) 100:1354–61. doi: 10.1182/blood-2001-11-0017
39. Jongmans W, Tiemessen DM, van Vlodrop IJH, Mulders PFA, Oosterwijk E. Th1-polarizing capacity of clinical-grade dendritic cells is triggered by Ribomunyl but is compromised by PGE2: the importance of maturation

cocktails. *J Immunother* (2005) 28:480–7. doi: 10.1097/01.cji.0000171290.78495.66
40. Okada H, Kalinski P, Ueda R, Hoji A, Kohanbash G, Donegan TE, et al. Induction of CD8+ T-cell responses against novel glioma-associated antigen peptides and clinical activity by vaccinations with {alpha}-type 1 polarized dendritic cells and polyinosinic-polycytidylic acid stabilized by lysine and carboxymethylcellulose in. *J Clin Oncol* (2011) 29:330–6. doi: 10.1200/JCO.2010.30.7744
41. Böttcher JP, Bonavita E, Chakravarty P, Blees H, Cabeza-Cabrerizo M, Sammicheli S, et al. NK Cells Stimulate Recruitment of cDC1 into the Tumor Microenvironment Promoting Cancer Immune Control. *Cell* (2018) 172:1022–37.e14. doi: 10.1016/j.cell.2018.01.004
42. Bouwer AL, Saunderson SC, Caldwell FJ, Damani TT, Pelham SJ, Dunn AC, et al. NK Cells Are Required for Dendritic Cell-Based Immunotherapy at the Time of Tumor Challenge. *J Immunol* (2014) 192:2514–21. doi: 10.4049/jimmunol.1202797
43. Ferlazzo G, Pack M, Thomas D, Paludan C, Schmid D, Strowig T, et al. Distinct roles of IL-12 and IL-15 in human natural killer cell activation by dendritic cells from secondary lymphoid organs. *Proc Natl Acad Sci* (2004) 101:16606–11. doi: 10.1073/pnas.0407522101
44. Pufnock JS, Cigal M, Rolczynski LS, Andersen-Nissen E, Wolfl M, McElrath MJ, et al. Priming CD8+ T cells with dendritic cells matured using TLR4 and TLR7/8 ligands together enhances generation of CD8+ T cells retaining CD28. *Blood* (2011) 117:6542–51. doi: 10.1182/blood-2010-11-317966
45. Schuurhuis DH, Laban S, Toes REM, Ricciardi-Castagnoli P, Kleijmeer MJ, van der Voort EIH, et al. Immature Dendritic Cells Acquire Cd8+Cytotoxic T Lymphocyte Priming Capacity upon Activation by T Helper Cell–Independent or–Dependent Stimuli. *J Exp Med* (2000) 192:145–50. doi: 10.1084/jem.192.1.145
46. Jonuleit H, Giesecke-Tuettenberg A, Tüting T, Thurner-Schuler B, Stuge TB, Paragnik L, et al. A comparison of two types of dendritic cell as adjuvants for the induction of melanoma-specific T-cell responses in humans following intranodal injection. *Int J Cancer* (2001) 93:243–51. doi: 10.1002/ijc.1323
47. McIlroy D, Gregoire M. Optimizing dendritic cell-based anticancer immunotherapy: maturation state does have clinical impact. *Cancer Immunol Immunother* (2003) 52:583–91. doi: 10.1007/s00262-003-0414-7
48. He Z, Zhu X, Shi Z, Wu T, Wu L. Metabolic Regulation of Dendritic Cell Differentiation. *Front Immunol* (2019) 10:410. doi: 10.3389/fimmu.2019.00410
49. Szatmari I, Töröcsik D, Agostini M, Nagy T, Gurnell M, Barta E, et al. PPARgamma regulates the function of human dendritic cells primarily by altering lipid metabolism. *Blood* (2007) 110:3271–80. doi: 10.1182/blood-2007-06-096222
50. Morita M, Gravel S-P, Hulea L, Larsson O, Pollak M, St-Pierre J, et al. mTOR coordinates protein synthesis, mitochondrial activity and proliferation. *Cell Cycle* (2015) 14:473–80. doi: 10.4161/15384101.2014.991572
51. Pearce EJ, Everts B. Dendritic cell metabolism. *Nat Rev Immunol* (2015) 15:18–29. doi: 10.1038/nri3771
52. Krawczyk CM, Holowka T, Sun J, Blagih J, Amiel E, DeBerardinis RJ, et al. Toll-like receptor-induced changes in glycolytic metabolism regulate dendritic cell activation. *Blood* (2010) 115:4742–9. doi: 10.1182/blood-2009-10-249540
53. Papathanassiu AE, Ko J-H, Imprialou M, Bagnati M, Srivastava PK, Vu HA, et al. BCAT1 controls metabolic reprogramming in activated human macrophages and is associated with inflammatory diseases. *Nat Commun* (2017) 8:16040. doi: 10.1038/ncomms16040
54. Rundqvist H, Veliça P, Barbieri L, Gameiro PA, Cunha PP, Gojkovic M, et al. Lactate potentiates differentiation and expansion of cytotoxic T cells. *bioRxiv* (2019) 571745. doi: 10.1101/571745
55. Thwe PM, Pelgrom LR, Cooper R, Beauchamp S, Reisz JA, D'Alessandro A, et al. Cell-Intrinsic Glycogen Metabolism Supports Early Glycolytic Reprogramming Required for Dendritic Cell Immune Responses. *Cell Metab* (2017) 26:558–67.e5. doi: 10.1016/j.cmet.2017.08.012
56. Liu X, Cooper DE, Cluntun AA, Warmoes MO, Zhao S, Reid MA, et al. Acetate Production from Glucose and Coupling to Mitochondrial Metabolism in Mammals. *Cell* (2018) 175:502–513.e13. doi: 10.1016/j.cell.2018.08.040
57. Balmer ML, Ma EH, Bantug GR, Grählert J, Pfister S, Glatter T, et al. Memory CD8 + T Cells Require Increased Concentrations of Acetate Induced by Stress for Optimal Function. *Immunity* (2016) 44:1312–24. doi: 10.1016/j.immuni.2016.03.016
58. Huang YH, Sauer K. Lipid signaling in T-cell development and function. *Cold Spring Harb Perspect Biol* (2010) 2:a002428. doi: 10.1101/cshperspect.a002428

Conflict of Interest: JS and MC were employed by Tecnimede Group.

The authors declare that the research was conducted in the absence of any commercial or financial relationships that could be construed as a potential conflict of interest.

Copyright © 2021 Calmeiro, Mendes, Duarte, Leitão, Tavares, Ferreira, Gomes, Serra, Falcão, Cruz, Carrascal and Neves. This is an open-access article distributed under the terms of the Creative Commons Attribution License (CC BY). The use, distribution or reproduction in other forums is permitted, provided the original author(s) and the copyright owner(s) are credited and that the original publication in this journal is cited, in accordance with accepted academic practice. No use, distribution or reproduction is permitted which does not comply with these terms.

frontiers in Immunology

ORIGINAL RESEARCH
published: 09 February 2021
doi: 10.3389/fimmu.2020.618428

Discordance Between the Predicted Versus the Actually Recognized CD8+ T Cell Epitopes of HCMV pp65 Antigen and Aleatory Epitope Dominance

Alexander A. Lehmann[1], *Ting Zhang*[1], *Pedro A. Reche*[2] *and Paul V. Lehmann*[1]*

[1] *Research and Development, Cellular Technology Ltd., Shaker Heights, OH, United States,* [2] *Laboratorio de Inmunomedicina & Inmunoinformatica, Departamento de Immunologia & O2, Facultad de Medicina, Universidad Complutense de Madrid, Madrid, Spain*

CD8+ T cell immune monitoring aims at measuring the size and functions of antigen-specific CD8+ T cell populations, thereby providing insights into cell-mediated immunity operational in a test subject. The selection of peptides for *ex vivo* CD8+ T cell detection is critical because within a complex antigen exists a multitude of potential epitopes that can be presented by HLA class I molecules. Further complicating this task, there is HLA class I polygenism and polymorphism which predisposes CD8+ T cell responses towards individualized epitope recognition profiles. In this study, we compare the actual CD8+ T cell recognition of a well-characterized model antigen, human cytomegalovirus (HCMV) pp65 protein, with its anticipated epitope coverage. Due to the abundance of experimentally defined HLA-A*02:01-restricted pp65 epitopes, and because *in silico* epitope predictions are most advanced for HLA-A*02:01, we elected to focus on subjects expressing this allele. In each test subject, every possible CD8+ T cell epitope was systematically covered testing 553 individual peptides that walk the sequence of pp65 in steps of single amino acids. Highly individualized CD8+ T cell response profiles with aleatory epitope recognition patterns were observed. No correlation was found between epitopes' ranking on the prediction scale and their actual immune dominance. Collectively, these data suggest that accurate CD8+ T cell immune monitoring may necessitate reliance on agnostic mega peptide pools, or brute force mapping, rather than electing individual peptides as representative epitopes for tetramer and other multimer labeling of surface antigen receptors.

Keywords: epitope prediction, brute force epitope mapping, high throughput, ImmunoSpot, ELISPOT

OPEN ACCESS

Edited by:
Graham Pawelec,
University of Tübingen, Germany

Reviewed by:
Mark R. Wills,
University of Cambridge, United Kingdom
Niels A. W. Lemmermann,
Johannes Gutenberg University Mainz, Germany

***Correspondence:**
Paul V. Lehmann
paul.lehmann@immunospot.com

Specialty section:
This article was submitted to Vaccines and Molecular Therapeutics, a section of the journal Frontiers in Immunology

Received: *16 October 2020*
Accepted: *22 December 2020*
Published: *09 February 2021*

Citation:
Lehmann AA, Zhang T, Reche PA and Lehmann PV (2021) Discordance Between the Predicted Versus the Actually Recognized CD8+ T Cell Epitopes of HCMV pp65 Antigen and Aleatory Epitope Dominance. Front. Immunol. 11:618428. doi: 10.3389/fimmu.2020.618428

INTRODUCTION

T cell immune monitoring has a long and successful track record in murine models in which defined experimental conditions, small model antigens, and work with inbred mouse strains expressing few restriction elements (MHC molecules) simplified the task (1). The magnitude of scope is entirely different when the outbred human population is to be studied, largely due to the immense diversity

in complexity restriction elements (human leukocyte antigens, HLA) and the of the antigenic systems, such as viruses. To comprehensively monitor T cell immunity to SARS-CoV-2, for example, this virus' entire proteome, 9,871 amino acids long (2), would need to be considered. In this report, we confined ourselves to a single protein of HCMV, pp65, which is "only" 561 amino acid long, and to subjects who shared a common HLA-A*02:01 restriction element, but differed in the remaining HLA class I alleles.

Monitoring CD4+ T cell immunity is relatively simple. When the test antigen of interest is added as a protein to peripheral blood mononuclear cells (PBMC), the antigen presenting cells (APC) contained in the PBMC will acquire, process, and present the antigen (3). Unfortunately, this is not the case for *ex vivo* CD8+ T cell detection. CD8+ T cells evolved to recognize antigens actively bio-synthetized within host cells, as opposed to antigens that APC acquire from their surroundings. Thereby CD8+ T cells can survey ongoing protein synthesis in the cells of the body, permitting them to identify virally-infected or malignant cells, so as to kill them. During protein synthesis, defective byproducts also arise that are degraded by the proteasome into peptide fragments. Such peptides are loaded onto HLA class I molecules, and transported to the cell surface to be displayed to CD8+ T cells (4). Protein antigens are not suited to recall *in vivo*-primed CD8+ T cells within PBMC because exogenously added proteins are not efficiently presented to CD8+ T cells in the context of class I molecules. Instead, the CD8+ T cell epitopes need to be added as 8–11 amino acid long peptides that they can bind directly to cell surface expressed HLA class I molecules. From this requirement the need arises to select the "right" peptides for *ex vivo* CD8+ T cell immune monitoring: those very same epitopes that have induced a CD8+ T cell response *in vivo*. Missing the "right" peptides, or only partially covering them, has the consequence that the antigen-specific CD8+ T cell repertoire could go partially or entirely undetected.

Selecting the "right" peptides for CD8+ T cell immune monitoring is an inherently intricate task. HLA class I molecules are encoded by three genetic loci, HLA-A, HLA-B, and HLA-C, for which a multitude of alleles exist in the human population (5). Each allelic HLA class I molecule has a unique peptide binding specificity (6). As there are barely two humans with an identical HLA-type, there should be barely two humans who present the same array of epitopes. Protecting the species, T cell epitope recognition evolved to be highly individualized (7). Peptide selection for comprehensive CD8+ T cell immune monitoring must therefore account for the unique HLA allele composition in each test subject.

A mainstream effort for identifying the "right" peptides for CD8+ T cell monitoring is reliant upon *in silico* epitope predictions. As the peptide binding motifs for most HLA alleles are well-defined, predictions can be made as far as which peptide sequence of an antigen can bind to a given HLA allele, thus constituting a potential T cell epitope. Search engines have been made available to the scientific community to rank peptide sequences for their predicted binding strength to most HLA alleles, thus narrowing in on a finite set of epitopes. A critical assumption for epitope predictions is that peptides that rank high in their respective HLA allele binding score will be those that are being targeted most by CD8+ T cells. The data presented in this study challenge this hypothesis supporting the conclusions reached by Mei et al. (8).

Beyond doubt, a peptide needs to be able to bind to an HLA allele to be a candidate for T cell recognition. However, whether a peptide sequence of a protein antigen that has HLA-binding potential indeed becomes an epitope recognized by T cells is defined by many additional factors (9). Limitations exist on the level of antigen presentation, including whether that exact peptide is indeed generated through natural antigen processing, and whether it is produced in quantities that can outcompete other peptides, including self-peptides, for binding to the respective HLA molecules. It has been shown that different class I alleles present in an individual can compete with each other for epitope dominance (10). Limitations also exist on the level of the pre-immune T cell repertoire available to engage in antigen recognition. The duration and abundance of epitope presentation will also affect the ensuing CD8+ T cell response, being regulated both by a virus' replication biology, and the host's ability to control the virus. The CD8+ T cell response is dynamic (11). Therefore, it can be expected that only a fraction of peptides with HLA class I binding properties will elicit strong CD8+ T cell responses, becoming dominant epitopes. Other presented peptides might induce a weaker, subdominant, barely detectable, cryptic, or no CD8+ T cell responses at all. As all antigen-specific CD8+ T cells can be expected to contribute equally to the host's defense, irrespective of their fine specificity, comprehensive immune monitoring must not focus on a single or few epitopes, but should instead accommodate all epitopes of an antigen targeted by CD8+ T cells in an individual in order to assess the entire antigen-specific T cell pool.

Next to predictions *in silico*, experimentally verified epitopes have been used as a guide to select peptides for CD8+ T cell immune monitoring. Over the years, T cell lines and clones specific for many viral antigens have been isolated and their epitope specificity compiled in databases (12, 13). Selection of such previously verified epitopes for immune monitoring is based on the assumption that epitope recognition, including epitope hierarchy, is constant in subjects who express the corresponding HLA allele. In other words, if an HLA-X-restricted peptide Y has been identified as an immune dominant epitope in an HLA-X positive subject Z, this peptide Y will also be immune dominant in HLA-X positive subjects V and W. Such predictable immune dominance prevails in simple murine models when inbred mice are studied that express minimal restriction element diversity (14). However, predictable epitope dominance is lost as soon as restriction element diversity rises through interbreeding these inbred mouse strains. In such F1 mice, aleatory epitope recognition prevails (15): T cells in each F1 mouse respond in an unpredictable, dice-like fashion (*alea* means dice in Latin) to epitopes to which the parental strains responded predictably. Aleatory epitope dominance may also apply to humans due to

their diverse restriction element makeup (16). Therefore, in the present study of HCMV pp65 epitope recognition in HLA-A*02:01-positive individuals, we also compare the peptides that the CD8+ T cells actually target in our cohort with previously verified epitopes.

The third approach for CD8+ T cell immune monitoring is not to select peptides at all, but to systematically test all possible peptides of the antigen. This can be done by using mega peptide pools consisting of hundreds of peptides that cover entire proteins of a virus. By necessity, this approach has become standard recently in the first real world challenge on clinical T cell immune monitoring: trying to study T cell immunity induced by SARS-CoV-2 infection. This crude approach is simple and practical, yet permits comprehensive assessment of the entire expressed antigen-specific T cell repertoire in outbred populations, without requiring customization to HLA types of individuals, but it does not reveal the epitope specificity of the antigen-reactive T cells.

In this study, we applied an agnostic approach in which all possible peptides were tested individually on each subject in a "brute force" high-throughput manner (17). The ability to test hundreds, even thousands of peptides individually on a subject is a recent technological advancement. The hurdles that needed to be overcome included limitations in PBMC numbers available from a subject, access to extensive custom peptide libraries, high-throughput-capable T cell assay platforms, and automated data analysis. We have developed and report here large-scale epitope mapping strategies that can be readily adopted even in small academic laboratories operating on tight budgets. Empowered by the ability to experimentally verify CD8+ T cell epitope utilization at the highest possible resolution in the well-studied HCMV pp65 T cell immune monitoring model, we set out to compare the epitopes actually recognized with those that are predicted, or assumed to be recognized based on existing data.

A protein of HCMV, pp65 is as far as CD8+ T cell recognition goes arguably one of the best studied model antigens: over the decades, 31 epitopes have been experimentally verified for the HLA-A2 allele alone (these are listed in **Supplementary Table 1**, including the corresponding references). Moreover, while the understanding of the rules for peptide binding to most HLA alleles is overall advanced, they are by far best established for HLA-A2. In this study, therefore we focus on the actual CD8+ T cell recognition of pp65 epitopes in HLA-A2 positive subjects, asking the question whether previously defined epitopes or binding predictions suffice to guide the selection of individual peptides for immune monitoring purposes. We assume that lessons learned from the best studied model antigen have implications for still less characterized foreign antigens, such as those of the SARS-CoV-2 virus, or tumor/self-antigens. We draw attention to how incomplete our appreciation of an individual's expressed epitope space currently is even when it comes to a well-studied foreign antigen. Epitope utilization in anti-self/cancer antigen recognition can be expected to underly the same rules, plus T cell repertoire limitations caused by negative selection by abundantly presented self-peptides. Our data suggest that neither epitope predictions, nor reliance on known epitopes suffice, but rather that the agnostic route is best suited for comprehensive CD8+ T cell immune monitoring for foreign antigens, and by inference, tumor antigens as well.

HLA multimers (tetramers, pentamers, dextramers) are frequently used for CD8+ T cell monitoring. Consisting of HLA molecules loaded with a peptide epitope, multimers constitute the T cell-receptor (TCR) ligand that can be used to selectively stain antigen-specific T cells (18). This technique is invaluable for the in-depth phenotypic analysis of the antigen-specific T cells *via* flow cytometry (19), but its limitation is that it requires epitope utilization to be predictable, either based on previously defined, or on in silico predicted epitopes. The data communicated in the following call into question whether such predictions are accurate even in the case of the arguably best-defined model antigen, pp65. We argue that the agnostic use of peptide libraries is needed for reliable CD8+ T cell monitoring, along with the utilization of techniques that are suited for work with such mega peptide pools, including ELISPOT, ICS, and the AID tests.

MATERIALS AND METHODS

Peripheral Blood Mononuclear Cells

PBMC from healthy adult human donors were from CTL's ePBMC library (CTL, Shaker Heights, OH, USA). The PBMC had been collected by HemaCare Blood Donor Center (Van Nuys, CA) under HemaCare's IRB and sold to CTL identifying donors by code only while concealing the subjects' identities. The donors' age, sex, ethnicity, and HLA type are shown in **Supplementary Table 2**. HLA typing was contracted to the University of Oklahoma Health Science Center (Oklahoma City, OK). The ten subjects for this study were selected according to their HCMV-positive status. The frozen cells were thawed following an optimized protocol (20) resulting in viability > 90% for all samples. The PBMC were resuspended in CTL-Test™ Medium (from CTL), developed for low background and high signal performance in ELISPOT assays. The number of PBMC plated into the ImmunoSpot® (ELISPOT) experiments was 3×10^5 PBMC per well.

Peptides and Antigens

Five hundred fifty-three nonamer peptides, spanning the entire amino acid (a.a.) sequence of the HCMV pp65 protein in steps of single a.a. were purchased from JPT (Berlin, Germany) as a FastTrack CD8+ T cell epitope library. These peptides were not further purified following their synthesis; however, individual peptides were analyzed by JPT using LC-MS. The average purity of these peptides was 56%. These peptides were delivered as lyophilized powder with each peptide present in a dedicated well of a 96-well plate, distributed across a total of six 96-well plates. Individual peptides were first dissolved in 50 µl DMSO, followed by addition of 200 µl of CTL-Test™ Medium so as to generate a "primary peptide stock solution" at 100 µg peptide/ml with 20% v/v DMSO. From each of these wells, a "secondary, 10X peptide

stock solution" was prepared using a 96-well multichannel pipette, in which peptides were at a concentration of 2 µg/ml, with DMSO diluted to 0.4%. On the day of testing, 20 µl from each well was transferred "en block", with a 96-well multichannel pipette into pre-coated ImmunoSpot® assay plates containing 80 µl CTL-Test™ Medium. Finally, 100 µl of PBMC (containing 3×10^5 cells) in CTL-Test™ Medium was added resulting in a test peptide concentration of 0.2 µg/ml with DMSO present at 0.04% v/v.

UV-inactivated entire HCMV virions (HCMV Grade 2 antigen from CTL) at 10 µg/ml was used to recall HCMV-specific CD4 cells. CPI (from CTL) was used as a positive control because, unlike CEF peptides, CPI elicits T cell recall responses in all healthy donors (21). CPI is a combination of protein antigens derived from CMV, influenza and parainfluenza viruses, and was used at a final concentration of 6 µg/ml in ImmunoSpot® assays.

Human IFN-γ ImmunoSpot® Assays

Single-color enzymatic ImmunoSpot® kits from CTL were used for the detection of antigen-induced IFNγ-producing CD8+ T cells. Peptides or pp65 were plated at the above specified concentrations into capture antibody-precoated assay plates in a volume of 100 µl per well. These plates with the antigen were stored in a CO_2 incubator for less than 1 h until the PBMC were thawed and ready for plating. The PBMC were added at 3×10^5 cells/well in 100 µl CTL-Test™ Medium followed by a 24 h activation culture at 37°C and 9% CO_2. Thereafter the cells were removed, IFNγ detection antibody was added, and the plate-bound cytokine was visualized by enzyme-catalyzed substrate precipitation. After washing, the plates were air-dried prior to scanning and counting of spot forming units (SFU). ELISPOT plates were analyzed using an ImmunoSpot® S6 Reader, by CTL. For each well, SFU were automatically calculated by the ImmunoSpot® Software using its Autogate™ function (22). The data are expressed as SFU per 3×10^5 PBMC, whereby each SFU corresponds to the cytokine footprint of an individual IFNγ-producing T cell (23).

Statistical Analysis

As SFU counts follow Gaussian (normal) distribution among replicate wells, the use of parametric statistics is appropriate to identify positive and negative responses, respectively (24). The 553 individual peptides of the pp65 nonamer peptide library were tested in single wells. For these peptides, the threshold for a positive response was set at SFU counts exceeding 3 SD of the mean SFU count detected in 18 replicate media control wells, the latter defining the background noise of the test system. This cut off criterion for weak (cryptic) responses renders the likelihood for false positive results at 0.3%. Dominant responses were defined by exceeding 10 SD, and subdominant responses between 5 and 10 SD of the negative control. Simple linear regressions were preformed to examine relationships between variables.

HLA-Binding Predictions

We assessed peptide-HLA I presentation by predicting peptide-HLA I binding using HLA I allele-specific profile motif matrices (25). We considered that a given peptide binds to a specific HLA I molecule when its binding score ranks within the top 3% percentile of the binding scores computed for 1,000 random 9-mer peptides (average amino acid composition of proteins in the SwissProt database). Peptide binding to experimentally defined HLA-A*02:01 restricted epitopes was predicted using netMHCIpan (25) an IEDB analysis resource (12), reporting percentile binding score. The lower the percentile binding score the better the binding. We selected netMHCIpan because it is the NIH's official recommended site that was created based on the consensus of earlier epitope prediction algorithms. Moreover, netMHCIpan allows to target more MHC I molecules for peptide binding predictions than any other method.

Previously Defined Epitopes

Epitope data for HLA-A2-restricted CD8+ T cell recognition was obtained from IEDB (12) with the following search settings: positive response only; host human; MHC I allele, HLA-A*0201, source species HCVM, source antigen: pp65. Only peptides 9 a.a. long were considered.

RESULTS AND DISCUSSION

Experimental Design

Systematic CD8+ T cell epitope mapping for the HCMV pp65 protein requires 553 nonamer peptides to be tested individually on PBMC of single subjects. Due to the magnitude of this scope, such data have not been reported so far except for a recent feasibility study from our own group (17). We took advantage of the fact that ImmunoSpot® assays require as few as 300,000 PBMC per antigen stimulation condition, and that these assays lend themselves to high-throughput testing and analysis. Utilizing only 173 million PBMC per subject, we therefore could test individually 553 nonamer HCMV pp65 peptides, along with 18 negative control replicate wells to establish the background noise, and the CPI positive control in triplicate.

Nonamer peptides were selected because the peptide binding groove of HLA class I molecules accommodates peptides 8–11 amino acid (aa) in length, with the most common peptide size being 9 aa residues (3). In contrast, HLA class II molecules present longer peptides (26). As such, the usage of nonamer peptides in our assays permitted preferential activation of CD8+ T cells (Some nonamer peptides can bind to HLA II molecules but there are only few CD4 T cell epitopes known that comprise of nonamers). Moreover, because the peptide binding groove of HLA class I molecules is closed on both ends (3), it is intolerant for frame shifts. The peptide library was designed therefore to walk the pp65 protein in steps of single a.a. with each nonamer peptide overlapping by 8 a.a. with the previous one (**Supplementary Figure 1**). Importantly, this approach enabled systematic coverage of every possible CD8+ T cell epitope within the pp65 antigen. By utilizing similar peptide libraries that are one or two amino acids shorter or longer than nine we possibly may have gained even more high-resolution data on epitope-reactive CD8+ T cells but for feasibility reasons such comparisons have been deferred.

To reduce assay variables, all peptides used in this study were from the same vendor, and were synthetized, stored, dissolved, and tested in the same way. Moreover, all the peptides were tested on each PBMC donor in a single experiment, which rendered the peptides the only assay variable.

Standard IFNγ ImmunoSpot® assays with 24 h antigen exposure of PBMC were performed; a time period required for blast transformation and CD8+ T cell activation-driven IFNγ secretion to occur, but too short to permit CD8+ T cell proliferation or differentiation during the cell culture. Thus, we measured at single-cell resolution the frequencies of antigen-specific IFNγ-producing CD8+ T cells as they occurred *in vivo* at isolation of the PBMC. This approach, therefore permitted us to firmly measure within each PBMC sample the number of CD8+ T cells responding to each peptide, and thus to compare the frequencies of peptide-reactive CD8+ T cells to establish epitope hierarchies for each donor. Moreover, adding up all peptide-induced IFNγ SFU permits one to assess the cumulative magnitude of the antigen-specific CD8+ T cell population in each donor, in turn allowing for determination of the relative percentage of antigen-specific CD8+ T cells targeting individual epitopes in each test subject.

Such actual measurements of the epitope-specific CD8+ T cells were then compared to a) the recognition of published HLA-A*02:01-restricted epitopes, and b) epitope predictions not only for HLA-A*02:01, an allele that all 10 test subjects shared by design, but also for all other class I molecules expressed by the test subjects.

Epitope scans of this type do not permit to define the activation/differentiation states/lineages of the CD8+ T cells that recognize them. As most functional CD8+ memory/effector T cells secrete IFN-γ, however, screening for IFN-γ should be well suited for detecting epitopes that are targeted by CD8+ T cells (19). Once the number of possible peptides has been narrowed from hundreds to a couple per donor, it becomes possible to narrow in on such peptide-reactive CD8+ T cell populations, e.g.by studying their phenotype by multimers, or by testing their (co-) secretion of other cytokines and effector molecules by multicolor FluoroSpot (27).

Highly Variable HCMV pp65 Epitope Recognition Patterns in HLA-A*02:01 Positive Subjects

Eighteen replicate wells containing media alone were included for all 10 individuals in our HCMV positive, HLA-A*02:01 positive cohort in order to firmly establish the background noise of the respective PBMC. The mean and standard deviation (SD) of this negative control is shown for all subjects in **Table 1**, also specifying the cut off values used for analyzing the peptide-induced SFU counts. The 533 individual pp65 nonamer peptides were also tested on each subjects' PBMC, and the resulting peptide-induced SFU-counts graded: peptides triggering SFU counts larger than 3 and less or equal to 5 SD over the medium control were considered weakly positive or cryptic (highlighted in beige in **Table 1**). Of note, with the mean plus 3 SD definition utilized in this study, the chance for a datapoint being false positive was negligible, less than 0.3%. Peptides triggering SFU counts more than 5 and less than or equal 10 SD over the medium background (highlighted in yellow) were labeled subdominant, and peptides eliciting SFU counts exceeding 10 SD over the medium control were called dominant (and are labeled in orange in **Table 1**). We also introduced a fourth category for peptides that recalled CD8+ T cells in frequencies exceeding 100 SFU/300,000 PBMC, calling them super-dominant epitopes (shown in red in **Table 1**).

Table 1 lists peptides that induced at least one dominant or super-dominant recall response in at least one of the ten test subjects in our cohort. Only for these 56 select peptides of the 553 tested are SFU counts shown for the ten donors. Additionally, a color-coding system was utilized in **Table 1** to delineate whether the peptide recalled a super-, dominant, subdominant, cryptic, or no response in the test subject.

As revealed by the color code at a glance, epitope recognition followed highly individual patterns, that are closer dissected below.

Multiple HCMV pp65 Epitopes Are Recognized in Each HLA-A*02:01 Positive Subject

As **Table 1** lists only super- and dominant recall responses (>10 SD over background), in **Supplementary Table 3** we list 58 additional peptides that induced subdominant recall responses (5–10 SD over the background) in at least one of the ten test subjects in our cohort. At a glance, the color code reveals that these peptides are also recognized in a highly individualized pattern. Peptides that recalled cryptic responses (3–5 SD over background) are not listed individually, but their number is specified for each test subject in **Table 2**, along with the number of subdominant, and dominant and super-dominant epitopes recognized in each donor. Adding up the number of epitopes in all four categories permits one to establish the cumulative number of CD8+ T cell epitopes recognized in each subject, which varied between 5 and 47 HCMV pp65-derived peptides in this cohort ($\bar{x} = 29 \pm 17$). Thus, of the 553 peptides covering the 561 amino acid long pp65 protein, between 1% and 8% ($\bar{x} = 5\,\%$) of the peptides constituted a CD8+ T cell epitope in each individual, but for the entire cohort 114 peptides (21% of 553 peptides tested) were needed to recall all dominant (56 peptides) and subdominant (58 peptides) CD8+ T cell epitopes. These data draw attention to how critical it is for immune monitoring to hit the right peptides—those few super-dominant aleatory epitopes that the majority of CD8+ T cells target. The number of CD8+ T cells recognizing cryptic, subdominant and dominant epitopes, in spite of the numbers of such epitopes, does not add up in most subjects to the repertoire that is directed against the few super-dominant epitopes.

In the feasibility study for this paper (**Tables 1** and **2** of our publication (17) we studied HCMV negative subjects, finding no

TABLE 1 | HCMV ppp65 epitope recognition by CD8+ T cells in HCMV positive, HLA-A*02:01 positive subjects.

Peptides Tested		Individual Subjects' CD8+ T Cell Response (SFU per 300,000 PBMC)									
Peptide Name	**Sequence**	**ID 1**	**ID 2**	**ID 3**	**ID 4**	**ID 5**	**ID 6**	**ID 7**	**ID 8**	**ID 9**	**ID 10**
pp65:018-026	ISGHVLKAV	0	2	2	0	7	1	72	11	0	6
pp65:030-038	GDTPVLPHE	0	2	3	1	2	2	5	9	1	32
pp65:065-073	STPCHRGDN	16	0	0	44	0	1	1	5	0	1
pp65:070-078	RGDNQLQVQ	2	0	2	2	0	2	84	28	2	5
pp65:095-103	HNPTGRSIC	15	0	20	0	0	1	2	10	1	1
pp65:097-105	PTGRSICPS	0	0	41	1	21	0	9	5	0	2
pp65:103-121	CPSQEPMSI	15	0	6	2	1	0	5	11	2	7
pp65:106-114	QEPMSIYVY	14	0	16	5	0	0	2	13	1	3
pp65:107-108	EPMSIYVYA	0	0	17	2	2	0	2	403	1	1
pp65:114-121	YALPLKMLN	22	1	7	0	3	2	23	14	0	3
pp65:115-123	ALPLKMLNI	13	0	5	7	2	0	6	22	6	2
pp65:116-124	LPLKMLNIP	71	0	7	14	2	3	5	18	5	2
pp65:119-127	KMLNIPSIN	5	0	6	102	2	1	21	10	0	0
pp65:139-148	HRHLPVADA	13	1	1	18	1	1	6	9	5	3
pp65:141-149	HLPVADAVI	7	0	1	0	26	0	5	8	0	3
pp65:142-150	LPVADAVIH	11	0	2	10	0	0	0	6	10	1
pp65:144-152	VADAVIHAS	1	2	5	0	44	1	2	3	3	6
pp65:149-157	IHASGKQMW	0	0	525	1	2	0	1	2	2	2
pp65:151-158	ASGKQMWQA	20	0	2	3	0	1	7	6	1	0
pp65:152-160	SGKQMWQAR	23	0	9	7	0	1	10	9	3	1
pp65:155-163	QMWQARLTV	1	1	7	1	10	2	33	13	5	0
pp65:175-183	WKEPDVYYT	1	0	2	0	144	0	1	7	0	1
pp65:188-196	FPTKDVALR	1	1	1	5	6	1	695	3	13	1
pp65:203-211	ELVCSMENT	118	0	0	2	1	1	21	3	7	1
pp65:208-216	MENTRATKM	1	1	71	7	5	1	0	14	11	3
pp65:221-229	DQYVKVYLE	1	1	7	1	76	0	0	10	6	0
pp65:228-236	LESFCEDVP	0	0	2	6	10	1	1	2	0	5
pp65:250-258	VEEDLTMTR	3	0	3	6	13	3	2	2	2	1
pp65:251-259	EEDLTMTRN	0	1	1	2	1	2	107	1	3	2
pp65:262-270	PFMRPHERN	0	1	161	5	0	2	6	3	9	1
pp65:267-275	HERNGFTVL	0	0	3	0	0	0	6	2	0	46
pp65:270-278	NGFTVLCPK	0	2	10	0	1	0	5	9	7	310
pp65:273-281	TVLCPKNMI	1	0	9	62	0	2	7	2	3	2
pp65:284-292	PGKISHIML	11	0	0	11	2	7	6	7	10	18
pp65:320-328	LMNGQQIFL	14	2	10	17	1	0	21	2	1	21
pp65:324-332	QQIFLEVQA	343	0	5	3	3	0	6	5	1	8
pp65:325-333	QIFLEVQAI	398	1	6	16	5	1	1	13	0	7
pp65:328-336	LEVQAIRET	0	5	810	7	1	1	7	10	5	21
pp65:390-398	EGAAQGDDD	0	0	5	56	0	0	7	13	2	6
pp65:395-403	GDDDVWTSG	2	0	3	10	0	0	14	98	1	2
pp65:417-425	TPRVTGGGA	0	0	3	32	0	1	10	2	558	2
pp65:418-426	PRVTGGGAM	1	0	6	6	0	0	6	11	192	0
pp65:430-438	STSAGRKRK	3	1	0	89	1	0	34	18	11	7
pp65:431-439	TSAGRKRKS	0	0	8	9	0	1	92	17	3	2
pp65:465-473	EEDTDEDSD	0	1	11	54	1	1	5	6	7	7
pp65:482-490	FTWPPWQAG	0	21	1	14	1	1	3	3	10	3
pp65:492-500	LARNLVPMV	21	2	5	6	0	0	2	1	5	0
pp65:495-503	NLVPMVATV	60	303	1	100	97	148	287	674	14	318

(Continued)

TABLE 1 | Continued

Peptides Tested		Individual Subjects' CD8+ T Cell Response (SFU per 300,000 PBMC)									
Peptide Name	**Sequence**	**ID 1**	**ID 2**	**ID 3**	**ID 4**	**ID 5**	**ID 6**	**ID 7**	**ID 8**	**ID 9**	**ID 10**
pp65:503-511	VQGQNLKYQ	2	1	512	1	0	1	5	3	5	0
pp65:511-519	QEFFWDAND	2	1	6	9	0	0	8	17	1	95
pp65:512-520	EFFWDANDI	0	28	5	10	1	1	8	13	17	61
pp65:513-521	FFWDANDIY	1	25	5	6	0	1	2	8	8	100
pp65:514-522	FWDANDIYR	0	2	2	1	0	1	10	13	10	44
pp65:521-529	YRIFAELEG	2	1	80	5	0	0	28	7	1	5
pp65:524-532	FAELEGVWQ	2	16	6	8	1	7	24	8	11	6
pp65:544-552	QDALPGPCI	2	6	5	3	15	5	13	5	2	2
Negative Controls and Cut Off Values for Response Categories	$\bar{x}$	1.0	0.8	4.2	3.9	3.9	1.8	6.5	8.4	5.4	3.2
	σ	1.0	1.3	3.6	4.4	0.5	2.4	5.6	5.6	3.7	2.7
	$\bar{x}$*3σ	3.9	4.6	14.9	17.1	5.5	8.8	23.3	25.2	16.6	11.3
	$\bar{x}$*5σ	5.8	7.2	22.1	25.9	6.5	13.5	34.4	36.3	24.0	16.8
	$\bar{x}$*10σ	10.7	13.7	40.0	47.8	9.1	25.3	62.4	64.2	42.5	30.3
	>100 SFU	>100 SFU	>100 SFU	>100 SFU	>100 SFU	>100 SFU	>100 SFU	>100 SFU	>100 SFU	>100 SFU	>100 SFU

*Ten subjects' PBMC at 300,000 cells per well were challenged with a library of 553 nonamer peptides that systematically covered all possible CD8+ T cell epitopes of the HCMV ppp65 antigen. An IFN-γ ImmunoSpot assay was performed with the spot forming units (SFU) elicited by each peptide recorded. The mean and SD for 18 negative control media wells, and the cut-off values for the color- coded response categories are specified on the bottom of this Table. Only peptides that induced at least one dominant (orange) or super-dominant (red) recall response in at least one subject are listed. Peptides that have been described as HLA-A*02:01 restricted nonamer epitopes in the literature are highlighted in green.*

TABLE 2 | HCMV ppp65 epitope category distribution in HCMV positive, HLA-A*02:01 positive subjects.

	Test Subjects' CD8+ T Cells Specific for Epitopes									
	ID 1	**ID 2**	**ID 3**	**ID 4**	**ID 5**	**ID 6**	**ID 7**	**ID 8**	**ID 9**	**ID 10**
Cryptic Epitopes										
Number	11	23	32	24	6	2	14	3	8	21
Cum. SFU	12.10	18.67	67.15	92.50	3.04	0.39	58.40	11.53	21.57	56.12
% of total SFU	1.02%	4.41%	3.02%	13.54%	0.73%	0.24%	4.03%	1.04%	2.89%	5.09%
Subdominant Epitopes										
Number	14	8	5	17	6	2	6	0	1	16
Cum. SFU	45	35	63	230	14	21	194	0	7	132
% of total SFU	4%	8%	3%	34%	3%	13%	13%	0%	1%	12%
Dominant Epitopes										
Number	15	4	3	4	9	0	3	1	0	5
Cum. SFU	281	72	147	193	263	0	178	73	0	221
% of total SFU	24%	17%	7%	28%	63%	0%	12%	7%	0%	20%
Super Dominant Epitopes										
Number	3	1	4	2	1	1	3	2	2	3
Cum. SFU	847	298	1948	168	139	139	1019	1027	717	694
% of total SFU	71%	70%	88%	25%	33%	86%	70%	92%	96%	63%
Total Epitopes Recognized	43	36	44	47	22	5	26	6	11	45
Cumulative Spec. SFU	1185	424	2226	683	418	161	1450	1111	746	1103

The number of cryptic, subdominant, dominant and super-dominant epitopes, as defined in the text, are shown for the individual test subjects, along with the sum of epitopes in each category (Total Epitopes Recognized) for each PBMC donor. The absolute number of CD8+ T cells targeting peptides in each category (Cum. SFU) is also shown. From the number of all pp65-specific CD8+ T cells detected in each subject (Cumulative Spec. SFU) the percentage of CD8+ T cells targeting peptides in each of the four response categories has been calculated (% of total SFU). The SFU counts shown are after subtracting the mean + 3 SD specificity cut off value. Because SFU counts for the cryptic category frequently were at the cut-off value, or barely exceeded it, they shown with two decimal places.

significant HCMV peptide-triggered IFN-γ spot formation. Confirming this notion, in a detailed study dedicated to chance cross-reactivity in various antigenic systems, we also did not find evidence for such (28). These data suggest that chance cross-reactivity does not play a role in the dominant and super-dominant HCMV responses we report here.

The Majority of the pp65-Specific CD8+ T Cell Repertoire Targets Super-Dominant Epitopes

As T cells recognize processed peptides of antigens there is no reason to assume that a T cell specific for one peptide of the antigen will contribute differently to host defense than T cells recognizing

TABLE 3 | CD8+ T cell recognition of predicted high HLA-A*02:01 -binding peptides.

Peptide Tested			Individual Subjects' CD8+ T Cell Response (SFU per 300,000 PBMC)									
pp65 Rank	**Percentile Binding Score**	**Peptide Name**	**ID 1**	**ID 2**	**ID 3**	**ID 4**	**ID 5**	**ID 6**	**ID 7**	**ID 8**	**ID 9**	**ID 10**
1	0.06	pp65:495-503	60	303	1	100	97	148	287	674	14	318
2	0.07	pp65:522-530	5	6	1	9	0	8	5	11	8	10
3	0.11	pp65:040-048	0	1	0	7	3	0	5	13	2	1
4	0.15	pp65:120-128	8	0	0	2	2	0	9	15	3	8
5	0.15	pp65:340-348	6	7	5	6	0	2	1	2	5	21
6	0.17	pp65:320-328	14	2	3	17	1	0	21	2	1	21
7	0.17	pp65:347-355	0	0	10	23	0	0	3	14	1	3
8	0.19	pp65:349-357	1	1	13	15	1	0	1	9	1	6
9	0.23	pp65:014-022	1	1	15	3	5	0	3	24	8	8
10	0.33	pp65;218-226	0	0	7	2	0	0	6	25	5	0
11	0.33	pp65:112-120	0	0	0	3	2	1	6	5	17	1
12	0.38	pp65:155-163	1	1	5	1	10	2	33	13	5	0
13	0.57	pp65:491-499	1	0	5	2	1	2	7	2	7	3
14	0.61	pp65:290-298	2	9	10	14	5	1	3	6	5	9
15	0.71	pp65:425-433	2	0	10	2	1	1	8	7	1	2
16	0.76	pp65:082-090	2	0	2	10	0	0	10	13	0	1
17	0.82	pp65:115-123	13	0	1	7	2	0	6	22	6	2
18	0.82	pp65:286-294	1	2	2	16	8	1	0	3	5	13
19	0.85	pp65:105-113	2	0	2	2	0	0	2	8	1	1
20	1.4	pp65:312-320	5	2	3	1	3	0	5	2	3	2
21	1.4	pp65:216-224	0	0	1	2	1	2	22	7	5	2
22	1.4	pp65:274-282	0	0	8	25	1	3	6	13	2	0
23	1.4	pp65:227-235	0	0	3	5	0	2	5	6	5	2
24	1.5	pp65:318-326	2	1	1	25	0	0	3	1	0	8
25	1.5	pp65:296-304	1	0	2	8	2	0	9	11	1	9
26	1.6	pp65:110-118	8	0	3	18	3	0	5	2	5	10
27	1.6	pp65:042-050	1	0	0	6	3	1	5	5	0	3
28	1.6	pp65:054-062	1	0	1	9	0	0	1	18	3	13
29	2	pp65:186-194	2	2	0	1	1	2	5	5	18	7
30	2	pp65:319-327	0	0	3	15	0	1	1	2	0	1
Negative Controls and Cut Off Values for Response Categories		$\bar{x}$	1.0	0.8	4.2	3.9	3.9	1.8	6.5	8.4	5.4	3.2
		σ	1.0	1.3	3.6	4.4	0.5	2.4	5.6	5.6	3.7	2.7
		$\bar{x}$*3σ	3.9	4.6	14.9	17.1	5.5	8.8	23.3	25.2	16.6	11.3
		$\bar{x}$*5σ	5.8	7.2	22.1	25.9	6.5	13.5	34.4	36.3	24.0	16.8
		$\bar{x}$*10σ	10.7	13.7	40.0	47.8	9.1	25.3	62.4	64.2	42.5	30.3
		>100 SFU	>100 SFU	>100 SFU	>100 SFU	>100 SFU	>100 SFU	>100 SFU	>100 SFU	>100 SFU	>100 SFU	>100 SFU

*All 553 nonamer pp65 peptides in our library were run on the netMHCIpan search engine of the IEDB Analysis Resource for predicting their binding to the HLA-A*02:01 allele, resulting in "pp65 Rank" shown, with the top binder peptide ranked No. 1. The 30 highest ranking peptides are listed. Additionally, an Percentile Binding Score that compares a peptide's binding relative to the binding scores computed for 1,000 random nonamer peptides, reporting the percentile binding score, is also listed. A lower percentile binding score denotes better peptide binding to the HLA-A*02:01 allele. Peptides that have been described as HLA-A*02:01 restricted nonamer epitopes in the literature are highlighted in green and the color-coded response categories defined in* ***Table 1*** *were applied.*

another. Immune monitoring therefore needs to assess all antigen-specific CD8+ T cells irrespective of their fine specificity. In our systematic assessment of CD8+ T cell immunity to pp65, we defined this number as the sum of all SFU counts elicited by the individual epitopes in a subject. This cumulative number of pp65-specific CD8+ T cells is shown for each subject in **Table 2** as "Cum. Spec. SFU". From this number, one can calculate what percentage of the pp65-specific CD8 + T cells occurs in each of the four response categories. As seen in **Table 2**, although the number of super-dominant epitopes was low in each subject (between 4 and 1), in eight of ten donors the majority of pp65-specific CD8+ T cells targeted these super-dominant epitopes. The percentage of CD8+ T cells specific for individual dominant and super-dominant epitopes is shown in **S. Table 4**.

CD8+ T Cells Target pp65 Epitopes in an Aleatory Manner

The data in **Table 1** and **Supplementary Table 3** show that each subject in our cohort displayed a unique CD8+ T cell epitope recognition pattern. This might come as a surprise, as all these subjects were HLA-A*02:01 positive, and one might have expected that among the epitopes recognized there should be at least a shared subset, those restricted by the HLA-A*02:01 allele. To narrow our investigation on such HLA-A*02:01-restricted epitopes, we searched the IEDB database for HLA-A*02:01-restricted nonamer epitopes identifying 31 that have been experimentally verified so far: these are listed in **Supplementary Table 4** with the corresponding reference citations. With the exception of the epitope, $pp65_{495\text{-}503}$, of all these 31 previously defined HLA-A*02:01-restricted epitopes five peptides recalled super-dominant CD8+ T cells responses in only two of the 10 test subjects, while seven additional peptides triggered occasional dominant recall responses. The rest of the 31 previously defined peptides elicited sporadic subdominant (n=4), cryptic (n=6) or no recall responses (n=8) at all. Importantly, donors who did not respond strongly or at all to these previously defined epitopes responded vigorously to other peptides of pp65 (**Table 1**). These previously defined HLA-A*02:01—restricted peptides were therefore also targeted in a dice like, aleatory manner in HLA-A*02:01 positive subjects.

Only one previously defined HLA-A*02:01—restricted epitope, $pp65_{495\text{-}503}$, induced a dominant, or super-dominant recall response in eight of 10 subjects in our cohort (**Table 1** and **Supplementary Table 1**). However, this peptide was not targeted in two donors (ID3# and ID#9) who exhibited responses to other pp65-derived peptides in a super-dominant fashion. Intrigued by this finding, we tested 42 additional (52 in total) HCMV positive, HLA-A*02:01 positive subjects for their recall response to the $pp65_{495\text{-}503}$ peptide. As shown in **Supplementary Figure 2**, the numbers of CD8+ T cells responding to the $pp65_{495\text{-}503}$ peptide did not correlate ($r^2 = 0.01$) to the numbers of T cells recalled by inactivated HCMV virus; which primarily activates HCMV-specific CD4+ T cells. Even though all these subjects have developed T cell immunity to HCMV, about one fourth of them either did not respond to the $pp65_{495\text{-}503}$ peptide, or displayed a low frequency of $pp65_{495\text{-}503}$-specific CD8+ T cells. This finding is consistent with the notion that the CD8+ T cell response to $pp65_{495\text{-}503}$ peptide is also aleatory. Interestingly, although the HLA-A*02:01 restriction element was shared by all test subjects in our cohort, and despite the $pp65_{495\text{-}503}$ peptide being displayed *in vivo via* natural processing and presentation, in some individuals this epitope triggered a super-dominant CD8+ T cell response while in other subjects it did not induce a detectable respond at all. Moreover, in yet other donors, the magnitude of the CD8+T cell response induced by this peptide was anywhere between these two extremes. However, the higher prevalence of recognition for this epitope ($pp65_{495\text{-}503}$) compared to other previously defined HLA-A*02:01-restricted epitopes might have an unexpected reason: in addition to HLA-A*02:01, $pp65_{495\text{-}503}$ received a top binding score for several additional HLA-class I alleles (see next).

HLA Binding Scores Are Unreliable Predictors of Actual CD8+ T Cell Epitope Utilization

The participation of the other HLA class I alleles, beyond the shared HLA-A*02:01 restriction element, might explain the highly individual CD8+ T cell response pattern observed in our cohort. Based on extensive knowledge on the peptide binding properties of individual HLA alleles, reference search engines have been established that permit in silico predictions of which peptides fit the binding criteria of a given allele, and moreover, the strength of peptide binding can also be ranked. It has been widely anticipated that such in silico models will suffice to predict epitope utilization. In particular, when there is the need to select one or a few candidate epitopes, e.g. for multimer analysis, it is tempting to pick peptides that have the highest predicted binding score for the HLA allele of interest. In the following we address the validity of such an approach from three angles.

In the first two approaches we focused on predictions for HLA-A*02:01, the most studied HLA allele that is shared by all subjects in our cohort. We introduced into the netMHCIpan (25) search engine of the IEDB analysis resource (12) the individual sequences of our pp65 nonamer peptide library, resulting in the predicted pp65 ranking shown in **Table 3** (in which only the top 30 predicted peptides of 553 are shown). In Approach 1, we compared this *in silico* predicted epitope hierarchy for pp65 with the actual peptide recognition we detected in our cohort. As can be seen in **Table 3**, $pp65_{495\text{-}503}$ ranked as the top binder, and indeed induced a CD8+ T cell response in the majority of our HLA-A*02:01 positive cohort (albeit in an aleatory manner, see above). Most of the other predicted peptides with high HLA-A*02:01 binding scores recalled CD8+T cells in low frequencies, and in an aleatory manner with each of these predicted peptides eliciting SFU in only one or two of the 10 test subjects. Except for the $pp65_{495\text{-}503}$ peptide, none of the super-dominant, and few of the dominant responses were recalled by these top 30 HLA-A*02:01 binding peptides (compare with **Table 1**). One might rightfully argue that this is because those dominant peptides were restricted by, and are binders of alternative class I molecules present in our cohort. We will address this hypothesis below, in Approach 3.

In Approach 2, we looked up the predicted HLA-A*02:01 binding scores for those peptides that have been identified experimentally as HLA-A*02:01-restricted pp65 epitopes. In **Supplementary Table 1** these peptides have been listed according to their predicted HLA-A*02:01 binding ranking along with CD8+ T cell recall responses they induced in our HLA-A*02:01 positive cohort. With the exception of the $pp65_{495\text{-}503}$ peptide, none of these peptides were among the predicted top 20 binders. Seeking for a correlation between the predicted HLA-A*02:01 binding of these peptides, and their actual immune dominance, these data are also represented graphically in **Supplementary Figure 3**. No significant correlation was seen. The fact, however, that these peptides were targeted by CD8+ T cells in HLA-A*02:01 positive subjects establishes that immune dominant epitopes do not need to rank high in peptide binding

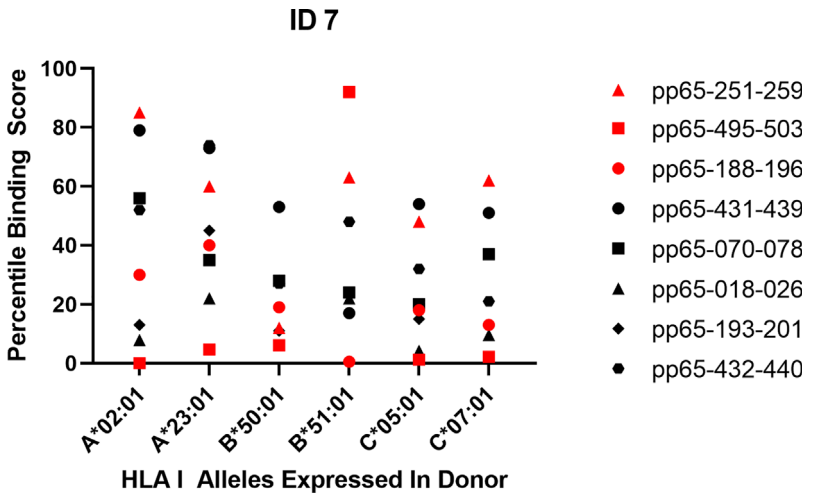


FIGURE 1 | Predicted vs. actual pp65 epitope recognition by CD8+ T cells. Data are shown for subject ID 7 expressing the specified HLA alleles and responding to the listed peptides. Super-dominant responses are shown as red data points, dominant responses in black and weaker responses are not represented. The raw data for the peptide-induced SFU counts are listed in **Table 1**. The corresponding Percentile Binding Score as established by the netMHCIpan search engine is shown comparing a peptide's binding relative to the binding scores computed for 1,000 random nonamer peptides. A lower percentile binding score denotes better peptide binding to the specified HLA allele.

score. The score apparently needs to be just high enough to enable stable HLA allele binding.

Proteasome cleavage and TAP binding predictions can enhance CD8+ T cell epitope discrimination in silico as compared with peptide-MHC I binding predictions alone (29). These data suggest, however, that such refinements to epitope predictions might not suffice to improve the ability to foretell actually recognized epitopes. All 31 peptides in **Supplementary Table 1** are previously experimentally defined HLA-A*02:01-restricted epitopes. All of these peptides therefore passed proteasome and TAP selection. As there are no major known polymorphisms at the level of the proteasome or TAP binding, such are unlikely to contribute to the aleatory epitope recognition pattern observed for previously defined peptides. Therefore, rather than differences in antigen presentation, T cell repertoires and downstream repertoire selection processes are likely to explain the highly individualized epitope hierarchies seen in individuals.

In Approach 3, we matched binding predictions for all super-dominant and dominant epitopes detected in each of the 10 subjects with all HLA class I alleles expressed in the subject. The results shown for Subject ID 7 in **Figure 1** are fully representative for all other subjects in our cohort (see **Supplementary Figure 4**). For donor ID 7 three super-dominant epitopes were identified; these are represented by the red symbols. One is peptide 251–259 (the red triangle) that does not rank as a strong binder for any of the class I alleles present in this individual (a low "percentile binding score" on the Y axis of the graph means strong predicted binding). Based on the binding score the super-dominant status of this peptide could not have been predicted, and in this case the binding score also does not suggest what the restriction element might be. Peptide 495–503 (the red square) is also super dominant in this donor. It shows strong binding (a low score) for all class I alleles expressed in this individual, likely explaining its immunogenicity, but also suggesting that multiple restriction elements are involved (and that picking just one of them for a multimer is likely to underrepresent the 495–503-specific CD8 + T cell repertoire in this subject). Peptide 188–196 (the red dot) is also a super dominant epitope in donor ID 7. This peptide shows a high predicted binding score for the B*51:01 allele suggesting that as the restriction element. When designing B*51:01 multimers for immune monitoring for this donor, the 188–196 peptide would have been a hit—but why would one select one B allele over another B allele, neglecting all other loci and alleles, and if one did select top binders for each, most would be a miss. This erratic pattern carries through for all other dominant epitopes in this subject (the black symbols in **Figure 1**) and in all the other nine subjects we studied (**Supplementary Figure 4**). Few of the actually targeted CD8+ T cell epitopes ranked amongst the top binders for the class I alleles expressed in these respective subjects, and many super-dominant peptides ranked low. A binding score oriented in silico model would not have sufficed to predict the hierarchy of actual epitope recognition.

All three of our above approaches suggest that, at least in the case of CD8+ T cell immunity induced by HCMV infection against its pp65 antigen, in silico predicted high binding scores for a specific HLA class I allele neither predict whether those peptides will indeed induce a CD8+ T cell response, nor the magnitude of it. This finding raises the question how generalizable it is. Mei et al.'s recent report (8) suggests that it may be generalizable as they came to the same conclusion

studying the prediction performance of databases containing 21,101 experimentally verified epitopes across 19 HLA class I alleles.

CONCLUDING REMARKS

The scope of this study was to experimentally query whether CD8+ T cell epitope recognition for a prototypic foreign antigen follows immune dominance patterns that permit to predict the peptides recognized so immune monitoring can focus on them. We studied HCMV pp65 antigen recognition by CD8+ T cells in HCMV infected subjects at the highest possible resolution, testing every potential epitope and measuring the numbers of all epitope-specific CD8+ T cells. Our data show that fixed epitope hierarchies do not exist even in an HLA-A*02:01 allele matched cohort. Instead, different super-dominant and dominant epitopes were targeted by the individual test subjects (**Table 1**). Previously defined epitopes, and peptides predicted to be high HLA-A*02:01 binders also were also targeted in some, but not other individuals, if at all (**Supplementary Table 1** and **Table 3**). If generalizable, the notion of such unpredictable, aleatory epitope recognition patterns in individuals makes it obsolete for CD8+ T cell immune monitoring to rely on testing a select few predicted or previously defined peptides. Rather, comprehensive CD8+T cell immune monitoring must be all inclusive, accommodating all potential epitopes on all restriction elements of each test subject. Such can be accomplished by brute force epitope mapping, as we did here, or by the use of mega peptide pools.

Brute force epitope mapping might be required as the first step towards high definition CD8+ T cell monitoring, permitting the personalization od multimers. It identifies the few individually variable super dominant epitopes in an individual against which the vast majority of CD8+ T cells are directed (**Table 2**). In a second step, the effector lineages/differentiation states of these CD8+ T cells then can be closer characterized either by studying either their phenotype (19), and/or functions (27), whereby both steps can be pursued sequentially testing aliquots of cryopreserved PBMC. For the first step in this study we used 300,000 PBMC per well so as gain a high-resolution picture of epitope utilization detecting even low frequency CD8+ T cells. For testing 553 individual peptides at 300,000 PBMC we needed 173 million PBMC that can be readily obtained from healthy donors, but less so from diseased individuals and children. When epitope mapping aims at detecting super-dominant and dominant peptides only, this can be accomplished with substantially less PBMC. As the numbers of peptide-triggered SFU counts vs. the number of PBMC plated per well show a linear relationship between one million and 100,000 PBMC per well in regular 96-well plates (30), the results provided here could have been obtained with 58 million PBMC testing each peptide individually at 100,000 PBMC/well (however, no longer reliably detecting all subdominant and cryptic epitopes, however), and with e.g. one-fifth of that (12 million PBMC) if the peptides are tested in matrices (31). ELISPOT assay can be further miniaturized to 384-well format requiring one third of PBMC per well compared to the 96-well format (the membrane surface of the 384-well plate is one-third that of the 96-well plate), thus, only four million PBMC could suffice for the agnostic mapping of super dominant and dominant epitopes for an antigen the size of pp65 (30).

The highly individualized nature of CD8+ T cell epitope recognition might also be accommodated by the agnostic use of mega peptide pools. Those presently available consist of 15-mer peptides that walk the protein sequence with gaps of four amino acids and contain up to 200 peptides per pool. In a feasibility study towards this publication (17) we tested such a pp65 peptide pool (15-mers, 4 a.a. gaps, 138 peptides) along with the 9-mer epiScan. The number of peptide pool-triggered IFN-γ producing (CD4+ and CD8+) T cells approximated the number of all 9-mer peptide-induced CD8+ T cells when the latter were added up. However, for several theoretical reasons we are reluctant to propose the use of such 15-mer peptide pools for CD8+ T cell immune monitoring. First, 15-mer peptides are ideal for binding to HLA class II molecules stimulating CD4+ T cells, but they cannot directly bind to class I molecules whose peptide-binding grove is closed on both ends thus not only prevents the direct accommodation of peptides this long. One possibility for a 15-mer peptide to provide a CD8+ T cell epitope is that the peptide is cross presented —a process that is dependent on a subtype of dendritic cells that is too rare in PBMC (32) to be a prevalent APC type in *in vitro* recall assays. Another possibility is that peptidases present in the PBMC culture trim the 15-mer peptide to a length that can be accommodated by class I molecules, or that there are shorter byproducts of the 15-mer peptide synthesis present that can bind directly, or both. Thus, to the extent CD8+ T cells are recalled by 15-mer peptide pools, such recall can be expected to occur under highly suboptimal conditions. In addition, covering the protein sequence in steps of 11 a.a. leaves considerable gaps in CD8+ T cell epitope coverage which is of additional concern as the closed peptide binding grove of class I molecules renders peptide binding intolerant to frame shifts in the anchor residues of an epitope. Mega peptide pools ideal for CD8+ T cell monitoring would consist of 9-mer peptides that cover the protein sequence in steps of single amino acids.

While in silico epitope ranking may have limited value in predicting immune dominant peptides, it should be helpful for narrowing in on the subset of peptides on an antigen that has sufficient HLA-allele binding affinity to constitute an epitope. As it is impractical to tailor a multitude of variable peptides to each individual's HLA-type, it might be more realistic for immune monitoring to develop rules for identifying peptides that do not bind to any HLA class I allele, so as to exclude those peptides from testing. Being able to narrow in on peptides should be helpful, as the ultimate goal of immune monitoring is to assess the CD8+ T cell response to the entire proteome of complex antigenic systems, such as all protein antigens of viruses and tumors.

DATA AVAILABILITY STATEMENT

The raw data supporting the conclusions of this article will be made available by the authors, without undue reservation.

ETHICS STATEMENT

Ethical review and approval were not required for the study on human participants in accordance with the local legislation and institutional requirements. The patients/participants provided their written informed consent to participate in this study.

AUTHOR CONTRIBUTIONS

Experiments were designed by AL, PL and PR. Experimental data were generated by AL with TZ contributing. This publication serves as part of AL's doctoral thesis to be submitted to the Universidad Complutense de Madrid, Madrid, Spain. All authors contributed to the article and approved the submitted version.

FUNDING

This study was funded by the R&D budget of Cellular Technology Limited.

ACKNOWLEDGEMENTS

We thank Ruliang Li of Cellular Technology Limited for expert technical assistance, Greg A. Kirchenbaum and Alexey Y. Karulin for valuable discussions, and Diana R. Roen for editorial assistance.

SUPPLEMENTARY MATERIAL

The Supplementary Material for this article can be found online at: https://www.frontiersin.org/articles/10.3389/fimmu.2020.618428/full#supplementary-material

Supplementary Table 1 | Actual recognition of previously identified HLA-A*02:01-restricted nonamer epitopes in our HCMV positive, HLA-A*02:01 positive cohort. The listed peptides have been identified in the IEDB database as HLA-A*02:01-restricted epitopes and the corresponding publications are specified. All 553 nonamer pp65 peptides in our library were run on IEDB's netMHCIpan search engine for predicting their binding to the HLA-A*02:01 allele, resulting in the "pp65 Rank" shown, with the top binding peptide ranked No. 1. The corresponding Percentile Binding Score is shown comparing each peptide's binding relative to the binding scores computed for 1,000 random nonamer peptides. A lower percentile binding score denotes better peptide binding to HLA-A*02:01. Otherwise, the legend to **Table 1** applies. Following references cited in the table refer to the bibliography (17, 33–50).

Supplementary Table 2 | HLA class I allotypes and other characteristics of human subjects tested in this study.

Supplementary Table 3 | Subdominant pp65 epitopes recognized in our cohort of ten HCMV positive, HLA-A*02:01 positive subjects. Peptides that elicited CD8+ T cell recall responses between 5 and 10 SD over the media background in at least one of the test subjects are highlighted in yellow. Cryptic recall responses (SD 3–5 over background) triggered by these peptides are highlighted in beige. Peptides that elicited SFU counts exceeding 10 SD over background are not shown in this table, as they are listed in **Table 1**. Peptides that only elicited cryptic recall responses (mean plus 3–5 SD) are not shown here, but are summarized in **Table 2**. Otherwise the legend to **Table 1** applies.

Supplementary Table 4 | Percentage of pp65-specific CD8+ T cells targeting individual epitopes. The total number of pp65-specific CD8+ T cells was calculated from the sum of SFU triggered by all epitopes in each subject as detailed in **Table 2**. The percentages of Cumulative Specific SFU counts elicited by individual peptides in each test subjects are shown. For the corresponding absolute SFU counts see **Table 1**. Otherwise, the legend to **Table 1** applies.

Supplementary Figure 1 | Schematic representation of brute force CD8+ T cell epitope mapping. The amino acid sequence of the protein, illustrated on the top, is covered with nonamer peptides that walk the sequence in steps of single amino acids.

Supplementary Figure 2 | Frequency of HCMV $pp65_{495\text{-}503}$ peptide-specific CD8+ T cells vs. HCMV grade 2 antigen-reactive T cells. Fifty-two subjects were selected from the ePBMC database for being HLA-A*02:01 positive and responding to HCMV Grade 2 antigen with more than 100 SFU/300,000 PBMC. Each of these subjects' PBMC (represented by a dot) were re-tested in an ImmunoSpot assay for the numbers of SFU triggered by HCMV Grade 2 antigen (shown on the X axis), and the numbers of SFU elicited by the $pp65_{495\text{-}503}$ peptide (shown on the Y axis). No significant relationship was found by analysis through a simple linear regression.

Supplementary Figure 3 | HLA-A*02:01 binding ranking of previously defined HLA-A*02:01 restricted nonamer pp65 peptides vs. the SFU counts they induced in our cohort of HCMV positive, HLA-A*02:01 positive subjects. The numeric SFU data shown in **S. Table 1** are plotted relative to their Percentile Binding Score as established run on the netMHCIpan search engine for predicting their binding to the HLA-A*02:01 allele. No significant relationship was found by analysis through a simple linear regression.

Supplementary Figure 4 | Predicted vs. actual pp65 epitope recognition by CD8+ T cells. Data are shown for the subjects specified in each panel. For each subject his/her HLA class I alleles are specified (in the case of homozygosity the allele is listed once). Peptides that induced super-dominant responses in that individual are shown as red data points, dominant responses in black and weaker responses are not represented. The raw data for the peptide-induced SFU counts are listed in **Table 1**. The IEBD Rank shown for each peptide and allele was established using the netMHCIpan search engine predicting the peptides' binding score to the respective HLA allele, whereby a lower Percentile Binding Score binding score denotes better peptide binding.

REFERENCES

1. Sercarz EE, Lehmann PV, Ametani A, Benichou G, Miller A, Moudgil K. Dominance and crypticity of T cell antigenic determinants. *Annu Rev Immunol* (1993) 11:729–66. doi: 10.1146/annurev.iy.11.040193.003501
2. Fernandes JD, Hinrichs AS, Clawson H, Gonzalez JN, Lee BT, Nassar LR, et al. The UCSC SARS-CoV-2 Genome Browser. *Nat Genet* (2020) 52:991–8. doi: 10.1038/s41588-020-0700-8
3. Neefjes J, Jongsma ML, Paul P, Bakke O. Towards a systems understanding of MHC class I and MHC class II antigen presentation. *Nat Rev Immunol* (2011) 11:823–36. doi: 10.1038/nri3084

4. Antón LC, Yewdell JW. Translating DRiPs: MHC class I immunosurveillance of pathogens and tumors. *J Leukocyte Biol* (2014) 95:551–62. doi: 10.1189/jlb.1113599
5. Williams TM. Human leukocyte antigen gene polymorphism and the histocompatibility laboratory. *J Molec Diagnostics* (2001) 3:98–104. doi: 10.1016/S1525-1578(10)60658-7
6. Reche PA, Reinherz EL. Sequence variability analysis of human class I and class II MHC molecules: functional and structural correlates of amino acid polymorphisms. *J Molec Biol* (2003) 331:623–41. doi: 10.1016/S0022-2836(03)00750-2
7. Nagy ZA, Lehmann PV, Falcioni F, Muller S, Adorini L. Why peptides? Their possible role in the evolution of MHC-restricted T-cell recognition. *Immunol Today* (1989) 10:132–8. doi: 10.1016/0167-5699(89)90247-8
8. Mei S, Li F, Leier A, Marquez-Lago TT, Giam K, Croft NP, et al. A comprehensive review and performance evaluation of bioinformatics tools for HLA class I peptide-binding prediction. *Brief Bioinform* (2020) 21:1119–35. doi: 10.1093/bib/bbz051
9. Yewdell JW. Confronting complexity: real-world immunodominance in antiviral CD8+ T cell responses. *Immunity* (2006) 25:533–43. doi: 10.1016/j.immuni.2006.09.005
10. Lacey SF, Villacres MC, La Rosa C, Wang Z, Longmate J, Martinez J, et al. Relative dominance of HLA-B*07 restricted CD8+ T-Lymphocyte immune responses to human cytomegalovirus pp65 in persons sharing HLA-A*02 and HLA-B*07 alleles. *Hum Immunol* (2003) 64:440–52. doi: 10.1016/S0198-8859(03)00028-4
11. Khan N, Best D, Bruton R, Nayak L, Rickinson AB, Moss PAH. T cell recognition patterns of immunodominant cytomegalovirus antigens in primary and persistent infection. *J Immunol* (2007) 178:4455–65. doi: 10.4049/jimmunol.178.7.4455
12. Dhanda SK, Mahajan S, Paul S, Yan Z, Kim H, Jespersen MC, et al. IEDB-AR: immune epitope database-analysis resource in 2019. *Nucleic Acids Res* (2019) 47(W1):W502–w6. doi: 10.1093/nar/gkz452
13. Reche PA, Zhang H, Glutting JP, Reinherz EL. EPIMHC: a curated database of MHC-binding peptides for customized computational vaccinology. *Bioinformatics* (2005) 21:2140–1. doi: 10.1093/bioinformatics/bti269
14. Chen W, Antón LC, Bennink JR, Yewdell JW. Dissecting the multifactorial causes of immunodominance in class I-restricted T cell responses to viruses. *Immunity* (2000) 12:83–93. doi: 10.1016/S1074-7613(00)80161-2
15. Moudgil KD, Wang J, Yeung VP, Sercarz EE. Heterogeneity of the T cell response to immunodominant determinants within hen eggwhite lysozyme of individual syngeneic hybrid F1 mice: implications for autoimmunity and infection. *J Immunol* (1998) 161:6046–53.
16. Lehmann PV, Lehmann AA. Aleatory epitope recognition prevails in human T cell responses? *Crit Rev Immunol* (2020) 40:225–35. doi: 10.1615/CritRevImmunol.2020034838
17. Lehmann PV, Suwansaard M, Zhang T, Roen DR, Kirchenbaum GA, Karulin AY, et al. Comprehensive evaluation of the expressed CD8+ T Cell epitope space using high-throughput epitope Mapping. *Front Immunol* (2019) 10:655. doi: 10.3389/fimmu.2019.00655
18. Altman JD, Davis MM. MHC-peptide tetramers to visualize antigen-specific T cells. *Curr Protoc Immunol* (2003) 53:17.3.1–.3.33. doi: 10.1002/0471142735.im1703s53
19. Apetoh L, Smyth MJ, Drake CG, Abastado J-P, Apte RN, Ayyoub M, et al. Consensus nomenclature for CD8+ T cell phenotypes in cancer. *OncoImmunology* (2015) 4:e998538. doi: 10.1080/2162402X.2014.998538
20. Ramachandran H, Laux J, Moldovan I, Caspell R, Lehmann PV, Subbramanian RA. Optimal thawing of cryopreserved peripheral blood mononuclear cells for use in high-throughput human immune monitoring studies. *Cells* (2012) 1:313–24. doi: 10.3390/cells1030313
21. Schiller A, Zhang T, Li R, Duechting A, Sundararaman S, Przybyla A, et al. A positive control for detection of functional CD4 T cells in PBMC: The CPI pool. *Cells* (2017) 6:47. doi: 10.3390/cells6040047
22. Sundararaman S, Karulin A, BenHamouda N, Gottwein J, Laxmanan S, Levine S, et al. Log-Normal ELISPOT spot size distribution permits count harmonization among different laboratories. *J Immunother Cancer* (2014) 2 (Suppl 3):P156–P. doi: 10.1186/2051-1426-2-S3-P156
23. Hesse MD, Karulin AY, Boehm BO, Lehmann PV, Tary-Lehmann M. A T cell clone's avidity is a function of its activation state. *J Immunol* (2001) 167:1353–61. doi: 10.4049/jimmunol.167.3.1353
24. Karulin AY, Caspell R, Dittrich M, Lehmann PV. Normal distribution of CD8 + T-cell-derived ELISPOT counts within replicates justifies the reliance on parametric statistics for identifying positive responses. *Cells* (2015) 4:96–111. doi: 10.3390/cells4010096
25. Reynisson B, Alvarez B, Paul S, Peters B, Nielsen M. NetMHCpan-4.1 and NetMHCIIpan-4.0: improved predictions of MHC antigen presentation by concurrent motif deconvolution and integration of MS MHC eluted ligand data. *Nucleic Acids Res* (2020) 48(W1):W449–w54. doi: 10.1093/nar/gkaa379
26. Rock KL, Reits E, Neefjes J. Present yourself! By MHC class I and MHC class II molecules. *Trends Immunol* (2016) 37:724–37. doi: 10.1016/j.it.2016.08.010
27. Hanson J, Roen DR, Lehmann PV. Four color ImmunoSpot® assays for Identification of effector T-cell lineages. *Methods Molec Biol* (2018) 1808:51–62. doi: 10.1007/978-1-4939-8567-8_5
28. Lehmann AA, Kirchenbaum GA, Zhang T, Reche PA, Lehmann PV. Deconvoluting the T cell response to SARS-CoV-2: specificity versus chance- and cognate cross-reactivity. Preprint. *bioRxiv* (2020) 2020.11.29.402677. doi: 10.1101/2020.11.29.402677
29. Desai DV, Kulkarni-Kale U. T-cell epitope prediction methods: an overview. *Methods Molec Biol* (2014) 1184:333–64. doi: 10.1007/978-1-4939-1115-8_19
30. Hanson J, Sundararaman S, Caspell R, Karacsony E, Karulin AY, Lehmann PV. ELISPOT assays in 384-well format: up pto 30 data points with one million cells. *Cells* (2015) 4:71–83. doi: 10.3390/cells4010071
31. Anthony DD, Lehmann PV. T-cell epitope mapping using the ELISPOT approach. *Methods* (2003) 29:260–9. doi: 10.1016/S1046-2023(02)00348-1
32. Jongbloed SL, Kassianos AJ, McDonald KJ, Clark GJ, Ju X, Angel CE, et al. Human CD141+ (BDCA-3)+ dendritic cells (DCs) represent a unique myeloid DC subset that cross-presents necrotic cell antigens. *J Exp Med* (2010) 207:1247–60. doi: 10.1084/jem.20092140
33. Schalich J, Vytvytska O, Zauner W, Fischer MB, Buschle M, Aichinger G, et al. Analysis of the human cytomegalovirus pp65-directed T-cell response in healthy HLA-A2-positive individuals. *Biol Chem* (2008) 389:551–9. doi: 10.1515/BC.2008.065
34. Newell EW, Sigal N, Nair N, Kidd BA, Greenberg HB, Davis MM. Combinatorial tetramer staining and mass cytometry analysis facilitate T-cell epitope mapping and characterization. *Nat Biotechnol* (2013) 31:623–9. doi: 10.1038/nbt.2593
35. Klinger M, Pepin F, Wilkins J, Asbury T, Wittkop T, Zheng J, et al. Multiplex identification of antigen-specific T cell receptors using a combination of immune assays and immune receptor sequencing. *PLoS One* (2015) 10(10): e0141561. doi: 10.1371/journal.pone.0141561
36. Provenzano M, Sais G, Bracci L, Egli A, Anselmi M, Viehl CT, et al. A HCMV pp65 polypeptide promotes the expansion of CD4+ and CD8+ T cells across a wide range of HLA specificities. *J Cell Molec Med* (2009) 13:2131–47. doi: 10.1111/j.1582-4934.2008.00531.x
37. Hanley PJ, Melenhorst JJ, Nikiforow S, Scheinberg P, Blaney JW, Demmler-Harrison G, et al. CMV-specific T cells generated from naïve T cells recognize atypical epitopes and may be protective in vivo. *Sci Transl Med* (2015) 7 (285):285ra63. doi: 10.1126/scitranslmed.aaa2546
38. Lee S, Park JB, Kim EY, Joo SY, Shin EC, Kwon CH, et al. Monitoring of cytomegalovirus-specific CD8+ T-cell response with major histocompatibility complex pentamers in kidney transplant recipients. *Transplant Proc* (2011) 43:2636–40. doi: 10.1016/j.transproceed.2011.05.051
39. Kondo E, Akatsuka Y, Kuzushima K, Tsujimura K, Asakura S, Tajima K, et al. Identification of novel CTL epitopes of CMV-pp65 presented by a variety of HLA alleles. *Blood* (2004) 103:630–8. doi: 10.1182/blood-2003-03-0824
40. Elkington R, Walker S, Crough T, Menzies M, Tellam J, Bharadwaj M, et al. Ex vivo profiling of CD8+ T-cell responses to human cytomegalovirus reveals broad and multispecific reactivities in healthy virus carriers. *J Virol* (2003) 77:5226–40. doi: 10.1128/JVI.77.9.5226-5240.2003
41. Zhong J, Rist M, Cooper L, Smith C, Khanna R. Induction of pluripotent protective immunity following immunisation with a chimeric vaccine against human cytomegalovirus. *PLoS One* (2008) 3(9):e3256. doi: 10.1371/journal.pone.0003256
42. Rist M, Cooper L, Elkington R, Walker S, Fazou C, Tellam J, et al. Ex vivo expansion of human cytomegalovirus-specific cytotoxic T cells by

recombinant polyepitope: implications for HCMV immunotherapy. *Eur J Immunol* (2005) 35:996–1007. doi: 10.1002/eji.200425746
43. Solache A, Morgan CL, Dodi AI, Morte C, Scott I, Baboonian C, et al. Identification of three HLA-A*0201-restricted cytotoxic T cell epitopes in the cytomegalovirus protein pp65 that are conserved between eight strains of the virus. *J Immunol* (1999) 163:5512–8.
44. Hamel Y, Rohrlich P, Baron V, Bonhomme D, Rieux-Laucat F, Necker A, et al. Characterization of antigen-specific repertoire diversity following in vitro restimulation by a recombinant adenovirus expressing human cytomegalovirus pp65. *Eur J Immunol* (2003) 33:760–8. doi: 10.1002/eji.200323628
45. Khan N, Hislop A, Gudgeon N, Cobbold M, Khanna R, Nayak L, et al. Herpesvirus-specific CD8 T cell immunity in old age: cytomegalovirus impairs the response to a coresident EBV infection. *J Immunol* (2004) 173:7481–9. doi: 10.4049/jimmunol.173.12.7481
46. Godard B, Gazagne A, Gey A, Baptiste M, Vingert B, Pegaz-Fiornet B, et al. Optimization of an elispot assay to detect cytomegalovirus-specific CD8+ T lymphocytes. *Hum Immunol* (2004) 65:1307–18. doi: 10.1016/j.humimm.2004.06.006
47. Ouyang Q, Wagner WM, Zheng W, Wikby A, Remarque EJ, Pawelec G. Dysfunctional CMV-specific CD8(+) T cells accumulate in the elderly. *Exper Gerontol* (2004) 39(4):607–13. doi: 10.1016/j.exger.2003.11.016
48. Ravkov EV, Myrick CM, Altman JD. Immediate early effector functions of virus-specific CD8+CCR7+ memory cells in humans defined by HLA and CC chemokine ligand 19 tetramers. *J Immunol* (2003) 170:2461–8. doi: 10.4049/jimmunol.170.5.2461
49. Nastke MD, Herrgen L, Walter S, Wernet D, Rammensee HG, Stevanović S. Major contribution of codominant CD8 and CD4 T cell epitopes to the human cytomegalovirus-specific T cell repertoire. *Cell Molec Life Sci* (2005) 62:77–86. doi: 10.1007/s00018-004-4363-x
50. Zhang SQ, Ma KY, Schonnesen AA, Zhang M, He C, Sun E, et al. High-throughput determination of the antigen specificities of T cell receptors in single cells. *Nat Biotechnol* (2018) 36:1156–9. doi: 10.1038/nbt.4282

Conflict of Interest: AL, TZ, and PL are employees of Cellular Technology Limited (CTL), a company that specializes on immune monitoring *via* ELISPOT testing, producing high-throughput-suitable readers, test kits, and offering GLP-compliant contract research.

The remaining author declares that the research was conducted in the absence of any commercial or financial relationships that could be construed as a potential conflict of interest.

Copyright © 2021 Lehmann, Zhang, Reche and Lehmann. This is an open-access article distributed under the terms of the Creative Commons Attribution License (CC BY). The use, distribution or reproduction in other forums is permitted, provided the original author(s) and the copyright owner(s) are credited and that the original publication in this journal is cited, in accordance with accepted academic practice. No use, distribution or reproduction is permitted which does not comply with these terms.

frontiers in Immunology

REVIEW
published: 12 February 2021
doi: 10.3389/fimmu.2020.620374

Dendritic Cell-Based Immunotherapy in Lung Cancer

Dieter Stevens[1,2], *Joline Ingels*[3], *Sandra Van Lint*[2,5], *Bart Vandekerckhove*[3,4,5] *and Karim Vermaelen*[1,2,5*]

[1] Respiratory Medicine - Thoracic Oncology Cluster, Ghent University Hospital, Ghent, Belgium, [2] Respiratory Medicine - Tumor Immunology Laboratory, Ghent University, Ghent, Belgium, [3] Department of Diagnostic Sciences, Ghent University Hospital, Ghent, Belgium, [4] GMP Cell Therapy Unit, Department of Regenerative Medicine, Ghent University Hospital, Ghent, Belgium, [5] Cancer Research Institute Ghent, Ghent University, Ghent, Belgium

Lung cancer remains the leading cause of cancer-related death worldwide. The advent of immune checkpoint inhibitors has led to a paradigm shift in the treatment of metastatic non-small cell and small cell lung cancer. However, despite prolonged overall survival, only a minority of the patients derive clinical benefit from these treatments suggesting that the full anti-tumoral potential of the immune system is not being harnessed yet. One way to overcome this problem is to combine immune checkpoint blockade with different strategies aimed at inducing or restoring cellular immunity in a tumor-specific, robust, and durable way. Owing to their unique capacity to initiate and regulate T cell responses, dendritic cells have been extensively explored as tools for immunotherapy in many tumors, including lung cancer. In this review, we provide an update on the nearly twenty years of experience with dendritic cell-based immunotherapy in lung cancer. We summarize the main results from the early phase trials and give an overview of the future perspectives within this field.

Keywords: dendritic cell, cancer vaccine, lung cancer, immunotherapy, tumor antigen, immune checkpoint blockade

OPEN ACCESS

Edited by:
Stephanie E. B. McArdle, Nottingham Trent University, United Kingdom

Reviewed by:
Cristina Maccalli, Sidra Medicine, Qatar
Laura Rogers, Mayo Clinic, United States

***Correspondence:**
Karim Vermaelen
karim.vermaelen@ugent.be

Specialty section:
This article was submitted to Vaccines and Molecular Therapeutics, a section of the journal Frontiers in Immunology

Received: *22 October 2020*
Accepted: *29 December 2020*
Published: *12 February 2021*

Citation:
Stevens D, Ingels J, Van Lint S, Vandekerckhove B and Vermaelen K (2021) Dendritic Cell-Based Immunotherapy in Lung Cancer. Front. Immunol. 11:620374. doi: 10.3389/fimmu.2020.620374

INTRODUCTION

Lung cancer is the leading cause of cancer-related mortality worldwide, with 1.8 million deaths estimated in 2018 (1). Non-small cell lung cancer (NSCLC) represents 85% of all cases, while small cell lung cancer (SCLC) accounts for approximately 15% of all lung cancers. Treatment depends on tumor stage at diagnosis and comprises surgery, radiotherapy and chemotherapy in early stages, and

Abbreviations: Ad, adenovirus; AE, adverse event; AKT, activated killer T cell; APC, antigen presenting cell; ATRA, all-trans retinoic acid; CEA, carcinoembryonic antigen; CIK, cytokine-induced killer cell; CR, complete response; CRC, colorectal cancer; CRT, chemoradiotherapy; CTA, cancer-testis antigen; CTL, cytotoxic T lymphocyte; CTLA-4, cytotoxic T lymphocyte-associated antigen 4; DC, dendritic cell; DCTCMF, dendritic cell/T cell-derived maturation factor; DTH, delayed-type hypersensitivity; ELISPOT, enzyme-linked immune absorbent spot; G-CSF, granulocyte colony-stimulating factor; GM-CSF, granulocyte/macrophage colony-stimulating factor; HR, hazard ratio; HER2, human epidermal growth factor receptor 2; HLA, human leucocyte antigen; ICB, immune checkpoint blocker/blockade; IFN, interferon; IL, interleukin; i.d., intradermal; i.v., intravenous; JAK, Janus kinase; KHL, keyhole limpet hemocyanin; MAGE, melanoma Antigen; MDSC, myeloid-derived suppressor cell; MHC, major histocompatibility complex; MST, median survival time; MUC1, mucin 1; NSCLC, non-small cell lung cancer; ORR, objective response rate; OS, overall survival; PBMC, peripheral blood monocyte; PD, progressive disease; PD-1, programmed cell death protein 1; PD-L1, programmed death-ligand 1; PFS, progression-free survival; PGE2, prostaglandin E2; PR, partial response; QOL, quality of life; RCT, randomized controlled trial; RT, radiotherapy; s.c., subcutaneous; SCLC, small cell lung cancer; SD, stable disease; SOCS1, suppressor of cytokine signaling 1; TAA, tumor-associated antigens; TLR, toll-like receptor; TME, tumor microenvironment; TNF, tumor necrosis factor; TNM, tumor node metastasis; Treg, t-regulatory; TRT, thoracic radiotherapy; WT1, wilms tumor protein 1.

palliative treatments in metastatic disease. Since almost three quarter of the patients are diagnosed with stage III or IV disease and a significant number of patients relapse systemically after a curative treatment, prognosis remains poor with an estimated 5-year overall survival (OS) of only 18% (2).

Immune checkpoint blockade with drugs that target the programmed cell death protein pathway (PD-1/PD-L1) has changed the therapeutic landscape of locally advanced and metastatic lung cancer. Several randomized controlled trials have shown promising results with checkpoint inhibitors alone (3), or in combination with chemotherapy (4–7). PD-1/PD-L1 inhibitors such as nivolumab, pembrolizumab and atezolizumab are now approved for the first and second line treatment of metastatic NSCLC (without actionable driver mutations) and SCLC, and as a maintenance treatment after chemoradiotherapy in inoperable stage III NSCLC (durvalumab). In addition, trials with checkpoint inhibitors as adjuvant or neo-adjuvant therapy in resectable lung cancer are now underway and the results are eagerly awaited.

Despite better outcomes in terms of OS, only a minority of the patients derive clinical benefit from these treatments. In metastatic NSCLC, more than 40% to 50% of the subjects do not respond to immune checkpoint blockade when given in the first line (3, 4, 6). In the second or higher line setting, the objective response rate (ORR) is even lower (< 20%) (8–11). These results suggest that the full anti-tumoral potential of the immune system is not being harnessed yet, possibly explained by immune evasion mechanisms developed by the tumor to escape from immune destruction (12, 13). One way to overcome this problem is to combine immune checkpoint inhibition with other strategies aimed at inducing or restoring cellular immunity such as cancer vaccination (14, 15).

The goal of therapeutic cancer vaccines is to instruct the patient's own immune system to kill cancer cells and to induce immunological memory against later disease relapse (16–18). In contrast to immune checkpoint blockade, which impacts the full T cell repertoire including self-reactive lymphocytes which translates into substantial toxicity, cancer vaccines expose the patient's immune system to a unique selection of relevant antigenic targets resulting in a highly tumor-focused immune response (17, 18). A limitation of this strategy is that the ability of such vaccines to activate patient's T cells depends on the characteristics and level of activation of local dendritic cells (DCs), which are frequently dysfunctional in patients with advanced cancer (17). Hence, vaccines by themselves have failed to show any clinical benefit in NSCLC so far (19–23).

Cell-based approaches that involve patient's *ex vivo*-generated antigen presenting cells (APCs) such as DC-based vaccines avoid the reliance on endogenous APCs and are nowadays one of the most advanced forms of cancer immunotherapy (17). DCs, first identified by Ralph Steinman in 1973 (24), are recognized as the most potent APCs and play a pivotal role in the initiation, programming, and regulation of tumor-specific immune responses (25, 26). They are seeded in all tissues and continuously sample their environment for danger signals and antigens such as those derived from evolving cancer cells. DCs are unique in initiating *de novo* immune responses by processing the captured antigen to peptides and presenting these peptides to naive T cells in lymphoid tissues on major histocompatibility complex (MHC) molecules (26, 27).

Classical DC-based "vaccines" consist of DCs derived *in vitro* from autologous peripheral blood monocytes (PBMCs), exposed to activating factors for maturation and subsequently loaded with tumor-associated antigens (TAAs) (**Figure 1**) (28). These cells are then injected into the patient, a process that has been repeatedly shown to be safe and feasible (27, 29). Alternatively, naturally circulating DCs can be isolated and activated thereby avoiding lengthy *ex vivo* culture periods (30). The selection of tumor antigens for loading onto DCs is crucial to maximize the likelihood of eliciting a strong and tumor-directed immune response. Different sources of TAAs can be used and include cancer cell line lysate, whole tumor lysate, tumor-derived peptides, (synthetic) protein antigen(s), mRNA(s) encoding selected tumor antigen(s), autologous whole-tumor-derived mRNA or antigens packaged within viral vectors (18, 29, 31).

CLINICAL USE OF DCS IN ONCOLOGY: TRACK RECORD AND CRITICAL FACTORS

In the field of cancer medicine, DC vaccination has been extensively studied in melanoma patients, as well as in patients with prostate cancer, glioma and renal cell carcinoma, with a favorable safety profile (i.e., no grade 3 or 4 toxicities), but with an ORR that seldom exceeds 15% (32–34). Paradoxically, findings from early-phase trials indicate that DC vaccination might improve survival, advocating implementation of alternative surrogate endpoints to assess the therapeutic effectiveness of DC-based immunotherapy (32).

Still, a major gap exists between the large amount of preclinical data on the exceptional immunogenic power of DCs, and the modest clinical effects in treated cancer patients. The evolving insights into the complex biology of the DC system confront us with a staggering list of parameters that should be adjusted in order to achieve optimal clinical usability. These parameters not only relate to "tweakable" biological properties of the cells, but also to more down-to-earth aspects such as route of administration, dose and frequency of administration, integration into a combinatorial approach, manufacturing, distribution logistics, and costs.

Perhaps one of the most critical factors in DC therapy, yet least systematically investigated is the choice of antigenic targets. This component varies considerably between clinical studies within the same cancer indication, with antigen selections largely made empirically in absence of any solid underlying rationale. Cancer antigens fall into the following different classes: 1) mutated antigens or neo-antigens originating from genomic alterations in cancer cells (single-nucleotide variations and indels), 2) cancer-germline (formerly cancer-testis) antigens whose expression is epigenetically suppressed in normal tissues except for gonadal cells, placenta and many cancers, 3) "differentiation" antigens, which are self-proteins shared between the cancer and the normal

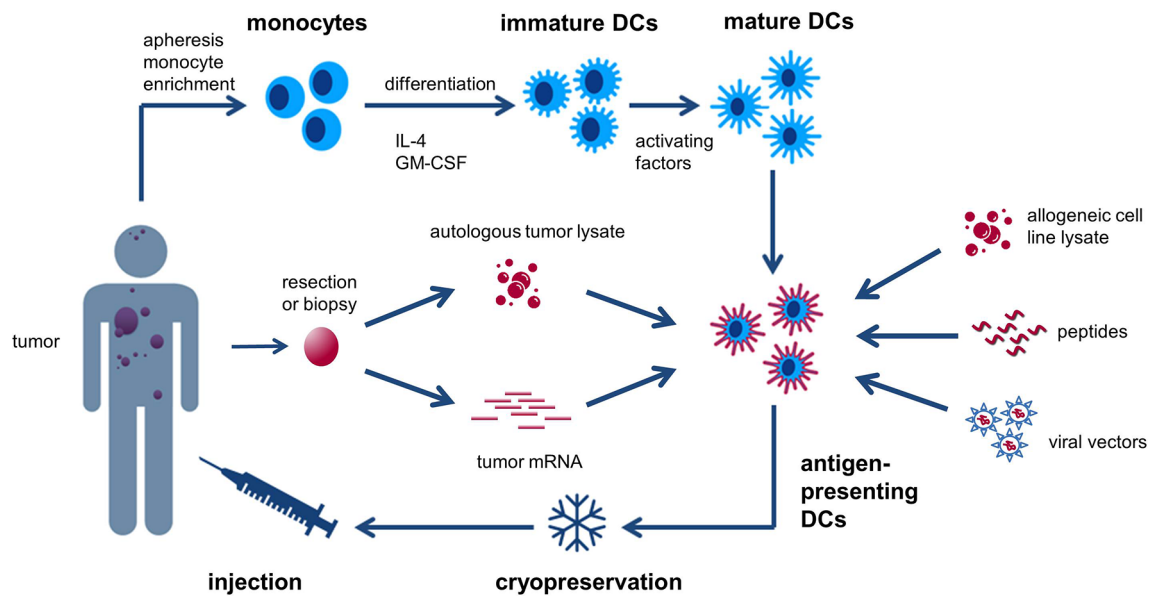


FIGURE 1 | Generic recipe of classical monocyte-derived dendritic cells (DCs). Monocytes are obtained from the patient's peripheral blood and cultured with IL-4 and GM-CSF to generate immature DCs. These cells are subsequently exposed to activating factors for maturation and loaded with tumor-associated antigens (TAAs). The antigen-loaded DCs are then cryopreserved and injected back into the patient. Different sources of TAAs can be used and include cancer cell line lysate, whole tumor lysate, tumor-derived peptides, (synthetic) protein antigen(s), mRNA(s) encoding selected tumor antigen(s), autologous whole-tumor-derived mRNA, or antigens packaged within viral vectors.

tissue from where it originated (e.g., CD20, Melan-A, PSA, CEA), 4) overexpressed shared antigens, which are present in normal tissues and aberrantly overexpressed in tumor cells (e.g., HER2, survivin, WT1), and finally viral oncoproteins, which are expressed in certain virus-induced cancers (e.g., HPV-E6/E7, EBV LMP-1). In addition, some tumor antigens derive their immunogenicity by means of aberrant post-translational modifications, as is the case for the MUC-1 glycoprotein where the tumor-restricted form is strongly hypo-glycosylated. Of all these categories, neo-antigens, cancer-germline antigens and viral oncoproteins are the most attractive targets for DC-based immunotherapy given the highest cancer-restricted expression, and the fact that the natural T cell repertoire has not been tolerized against them. Regardless of the type of antigen used, a major caveat is that studies or databases documenting mRNA expression in a given tumor often do not provide information on protein levels. Moreover, protein expression does not guarantee adequate presentation of antigen-derived peptides on MHC molecules, and if presented, whether these peptides will find a corresponding T cell repertoire with sufficient affinity.

Lung cancer (both NSCLC and SCLC), being a textbook example of a carcinogen-induced tumor, frequently features a high tumor mutational burden, offering opportunities for neoantigen-targeted vaccination approaches. Lung cancers are also rich in cancer-germline antigens [e.g., MAGE-A3 (22)], a number of differentiation antigens (e.g., CEA), and overexpressed shared antigens (e.g., survivin, WT1, MUC1), all being present in variable amounts across different patients. Viral oncoproteins are typically absent in human lung cancers. As we will discuss in the next section, the large majority of completed DC therapy trials in lung cancer made use of shared or tumor-associated antigens (TAAs), a few of the studies also incorporated cancer-germline antigens, and none of the published reports have described a patient-individualized neoantigen approach to date.

DC-BASED IMMUNOTHERAPIES IN LUNG CANCER

In lung cancer, the role of DC-based immunotherapy has yet to be defined. Since the early 2000s, several, mostly non- randomized clinical trials (RCTs) with DC immunotherapy have been conducted, each typically involving a small number of patients and very heterogeneous designs. Over the same timeframe, the lung cancer therapeutic landscape has experienced dramatic changes, with the emergence of oncogene-targeted small molecules, and later immune checkpoint inhibitors. In this review we aim to give an overview of these DC therapy trials which we categorized into four parts: DC therapy in NSCLC, DC/CIK cell therapy in NSCLC, AKT-DC therapy in NSCLC, and DC therapy in SCLC (**Tables 1** and **2**). We will examine the clinical and immunological outcome as well as safety of DC-based immunotherapy in lung cancer, while also discussing the potential challenges of the different vaccine approaches such as the choice of antigens and DC subset, the use of adjuvants and the route, dose and frequency of administration. Next, we will give some future perspectives in how DCs might be used in clinical practice.

TABLE 1 | Overview of trials with dendritic cell (DC)-based immunotherapy in lung cancer.

Reference	Study population	N	Trial phase	DC subset	Maturation factors	Antigen selection and formulation	Vaccination protocol
DC therapy in NSCLC							
Fong et al. (35)	Metastatic CRC or NSCLC expressing CEA	12 (2 with NSCLC)	Phase 1	Flt3-mobilized circulating DCs Mature	N/A	CEA peptide	a) 2 vaccinations b) 1-month interval c) i.v. injection d) Maximum dose of 10^9 cells per vaccination
Itoh et al. (36)	Metastatic digestive tract or lung cancer expressing CEA	10 (2 with lung cancer)	Phase 1	moDCs Immature	N/A	CEA peptide	a) 10 vaccinations b) 2-week interval c) i.d. and s.c. injection at the same site in the inguinal region d) Total dose of 2.7×10^7 cells to 1.6×10^8 cells e) IFN-α and TNF-α
Nair et al. (37)	Metastatic cancer	3 (1 with NSCLC)	Phase 1	moDCs Immature	N/A	CEA RNA or autologous tumor RNA	a) 4 vaccinations b) 4-week interval c) i.v. and i.d. d) 3×10^6 cells (i.v.) and 1×10^6 cells (i.d.) per vaccination
Kontani et al. (38)	Advanced or metastatic breast or lung cancer	14 (8 with lung cancer)	Phase 1	moDCs Mature	N/A	MUC1 antigen or tumor lysate	a) 3 to 12 vaccinations b) 2-week interval c) s.c. or intrapleural d) $4–10 \times 10^6$ cells per vaccination
Hirschowitz et al. (39, 40)	Stage I-IIIB NSCLC	16	Phase 1	moDCs Mature	DCTCMF IFN-γ	Apoptotic bodies of an allogeneic NSCLC cell line that overexpressed HER2/neu, CEA, WT1, MAGE-2, and survivin	a) 2 vaccinations b) 1-month interval c) i.d. injection in the thigh d) Average dose of 9.1×10^7 and 8.2×10^7 cells per vaccination respectively
Ueda et al. (41)	Metastatic gastrointestinal or lung adenocarcinoma expressing CEA	18 (5 with lung cancer)	Phase 1	moDCs Immature	N/A	CEA peptide	a) Median number of 9 vaccinations (range, 5–39) b) 2-week interval c) i.d. and s.c. injection at the same site in the inguinal region d) $0.5–5 \times 10^7$ cells per vaccination
Chang et al. (42)	Stage IV NSCLC with malignant pleural effusion	8	Phase 1	moDCs Mature	TNF-α	Tumor cell lysate derived from malignant pleural effusion specimens	a) 6 vaccinations b) 1-week interval for the first 4 vaccinations, then twice biweekly c) i.n. injection under sonographic guidance d) Dose not mentioned
Morse et al. (43)	Metastatic cancer expressing CEA	14 (3 with NSCLC)	Phase 1	moDCs Immature	N/A	Fowlpox virus encoding CEA and a triad of costimulatory molecules (rF-CEA(6D)-TRICOM)	a) 4 (first cohort) or 8 vaccinations (second cohort) b) triweekly c) s.c. and i.d. injection in the same limb d) Dose not mentioned

(Continued)

TABLE 1 | Continued

Reference	Study population	N	Trial phase	DC subset	Maturation factors	Antigen selection and formulation	Vaccination protocol
Hirschowitz et al. (44)	Stage I-IIIB NSCLC	14	Phase 1	moDCs Immature	N/A	Apoptotic bodies of an allogeneic NSCLC cell line that overexpressed HER2/neu, CEA, WT1, MAGE-2, and survivin	a) 2 vaccinations b) 1-month interval c) i.d. injection in the thigh d) Average dose of 8.2×10^7 and 7.9×10^7 cells per vaccination respectively
Mayordomo J et al. (45)	Metastatic cancer	15 (2 with NSCLC)	Phase 1	moDCs Immature	N/A	Autologous tumor lysate	a) 3 vaccinations b) 3-week interval c) i.v. injection d) Median dose of 6.2×10^7 cells per vaccination e) IL-2, INF-α and GM-CSF
Um et al. (46)	Stage IIIB-IV NSCLC	15	Phase 1	moDCs Mature	TNF-α IL-1 IL-6 PGE2	Autologous tumor lysate	a) 3 vaccinations and after verification of tolerability 2 subsequent vaccinations b) 2-week interval for the first 3 vaccinations and 1-month interval for the subsequent 2 vaccinations c) i.d. injection d) Maximum dose of 12×10^6 cells per vaccination
Perroud et al. (47)	Stage IIIB-IV NSCLC	5	Phase 1	moDCs Mature	IFN-γ	WT1 peptide CEA peptide MAGE-1 peptide HER-2 peptide	a) 2 vaccinations b) 2-week interval c) s.c. and i.v. injection in separate arms d) 5×10^7 cells per vaccination
Takahashi et al. (48)	Locally advanced or metastatic NSCLC	62	Retrospective analysis	moDCs Mature	OK-432 PGE2	Autologous tumor lysate or peptide antigens (WT1, MUC1, CEA) according to the HLA-A pattern.	a) Median number of 10 vaccinations (range, 4–31) b) Biweekly c) i.d. injection near the axillar and/or inguinal lymph nodes d) 1×10^7 cells per vaccination
Hu et al. (49)	Stage IIIB-IV NSCLC	27	Phase 1	moDCs Immature	N/A	Autologous tumor lysate	a) Number of vaccinations not mentioned b) 3-week interval c) i.d. injection d) Average dose of 1×10^7 cells per vaccination
Takahashi et al. (50)	Locally advanced or metastatic NSCLC	260	Retrospective analysis	moDCs Mature	OK-432 PGE2	WT1 peptide MUC1 peptide	a) Median number of 7 vaccinations (range, 5–34) b) Biweekly c) i.d. injection near the axillar and/or inguinal lymph nodes d) 1×10^7 cells per vaccination e) OK-432
Li et al. (51)	Stage I-IIIB NSCLC	16	Phase 1	moDCs Mature	IL-1β IL-6 TNF-α IFN-γ PGE2 Poly I:C	rMAGE-3 peptide rSurvivin peptide	a) 2 vaccinations b) 1-month interval c) i.d. d) 9.1×10^7 cells and 8.2×10^8 cells per vaccination respectively

(Continued)

TABLE 1 | Continued

Reference	Study population	N	Trial phase	DC subset	Maturation factors	Antigen selection and formulation	Vaccination protocol
Lee et al. (52)	Stage III-IV NSCLC	16	Phase 1	moDCs Immature	N/A	Viral vector (Ad.CCL21-DC)	a) 2 vaccinations b) 1-week interval c) CT- or bronchoscopy guided i.t. injection d) Maximum dose of 3×10^7 cells per vaccination
Teramoto et al. (53)	Stage IIIB-IV NSCLC	40	Retrospective analysis	moDCs Mature	OK-432	MUC1 peptide	a) range, 1–42 vaccinations b) 2-week interval c) s.c. injection d) 1×10^7 cells per vaccination
Ge et al. (54)	Resected stage I-IIIA NSCLC	15	Phase 1	moDCs Mature	Flagellin SOSC1-specific small interfering RNA	MUC1 peptide Survivin peptide	a) 3 vaccinations b) 1-week interval c) i.v. injection d) 1×10^6,1×10^7 or 8×10^7 cells per vaccination
DC/CIK therapy in NSCLC							
Li et al. (55)	Stage I-IIIA NSCLC	84 (42 received DC/CIK)	Phase 1/2	moDCs Mature	N/A	Autologous tumor lysate	a) 4 vaccinations b) 1-month interval c) i.v. injection d) Average dose of 13×10^9 cells per vaccination
Zhong et al. (56)	Stage IIIB-IV NSCLC expressing CEA	28 (14 patients received DC/CIK)	Phase 1/2	moDCs Immature	N/A	CEA peptide	a) 4 vaccinations b) 1-month interval c) i.v. injection d) Average dose of 8.1×10^6 cells per vaccination
Shi et al. (57)	Stage IIIB-IV NSCLC	60 (30 patients received DC/CIK)	RCT	moDCs Mature	GM-CSF TNF IL-6	N/A	a) 4-vaccinations b) 1-week interval c) s.c. injection d) Dose not mentioned
Yang et al. (58)	Stage IIIB-IV NSCLC	102 (61 patients received DC/CIK)	Paired cohort study	moDCs Immature	N/A	Autologous tumor lysate	a) 4 vaccinations b) 1-month interval c) i.v. injection d) Average dose of 12.5×10^9 cells per vaccination
Shi et al. (59)	Stage IIIB-IV NSCLC with EGFR exon 19 and/or 21 mutation	54 (26 patients received DC/CIK)	RCT	moDCs Immature	N/A	Autologous tumor lysate	a) 8 vaccinations b) 1-week interval c) s.c. injection d) Dose not mentioned
Zhao et al. (60)	Resected stage I-III NSCLC (arm 1) or metastatic NSCLC (arm 2)	50	Phase 1	moDCs Mature	TNF-α	Human A549 or SK-MES-1 lung cancer cell lysate	a) 4 vaccinations b) 1-week interval c) s.c. (DC) and i.v. injection (DC/CIK) d) 1.5×10^7 cells per vaccination
Zhu et al. (61)	Stage IIIB NSCLC	65 (30 received DC/CIK)	RCT	moDCs Mature	TNF-α	None	a) 4 vaccinations b) 3-week interval c) i.v. injection d) Dose not mentioned

(Continued)

TABLE 1 | Continued

Reference	Study population	N	Trial phase	DC subset	Maturation factors	Antigen selection and formulation	Vaccination protocol
Zhang et al. (62)	Stage IIIB-IV NSCLC	99	Retrospective analysis	moDCs Immature	N/A	Human SK-MES-1 and human SPC-A-1 lung cancer cell lysate	a) 6 vaccinations b) 1-week interval c) i.v. injection (first 3 doses) and i.d. injection (last 3 doses) d) 1×10^7 cells per vaccination
Zhang et al. (63)	Stage III-IV NSCLC	82 (21 received DC/CIK)	Phase 2	moDCs Mature	TNF-α	MUC1 peptide	a) 4 vaccinations b) 1-week interval c) s.c. injection d) 1×10^7 cells per vaccination
Song et al. (64)	Resected stage IIB-IIIA NSCLC	169	Phase 2	moDCs Mature	N/A	Human A549 or SK-MES-1 lung cancer cell lysate	a) 5 vaccinations within 2 weeks per cycle b) 12-24 week-interval (1–2 cycles) or 4–12 week interval (3–5 cycles) c) i.v. (DC/CIK) and s.c. injection (DC) d) 20×10^6 cells per vaccination
Chen et al. (65)	Advanced solid tumors	37 (5 with NSCLC)	Phase 1	moDCs Mature	TNF-α	N/A	a) Median number of 12 vaccinations (range, 3–26) b) 1-week interval for the first 4 doses, then 2-week interval thereafter c) i.v. injection d) Average dose of 8.8×10^9 cells per vaccination
AKT-DC therapy in NSCLC							
Kimura et al. (66)	Resected stage III-IV NSCLC with N2 disease	31	Phase 2	DCs obtained from tissue cultures of TDLNs Mature	N/A	N/A	a) Median number of 11 courses (range, 2–18) b) 2-month interval c) i.v. injection d) Mean dose of 7.07×10^9 cells per course e) IL-2
Kimura et al. (67, 68)	Resected stage IB-IV NSCLC	103 (50 received AKT-DC)	Phase 3 RCT	DCs obtained from tissue cultures of TDLNs Mature	N/A	N/A	a) Median number of 15 courses b) 1-month interval for the first 6 months, and 2-month interval thereafter c) i.v. injection d) Mean dose of 10, 2×10^9 cells per course
DC therapy in SCLC							
Chiappori et al. (69)	Extensive disease SCLC	54	Phase 1/2	moDCs Mature	N/A	p53 viral vector (Ad.p53)	a) 3 vaccinations and if no PD after reassessment 3 subsequent vaccinations b) 2-week interval for the first 3 vaccinations and 4-week interval for the subsequent 3 vaccinations c) i.d. injection d) Maximum dose of 5×10^6 cells per vaccination

(Continued)

TABLE 1 | Continued

Reference	Study population	N	Trial phase	DC subset	Maturation factors	Antigen selection and formulation	Vaccination protocol
Chiappori et al. (70, 71)	Extensive disease SCLC	69 (51 received DC vaccine)	Phase 2 RCT	moDCs Mature	N/A	p53 viral vector (Ad.p53)	a) 3 vaccinations and if no PD after reassessment 3 subsequent vaccinations b) 2-week interval for the first 3 vaccinations and 4-week interval for the subsequent 3 vaccinations c) i.d. injection d) Average dose of 2–5 × 10^6 cells per vaccination.

a) number of vaccinations.
b) dose interval.
c) route of administration.
d) number of DCs injected.
e) adjuvants used.
Ad-CCL21-DC, dendritic cells transduced with an adenoviral vector expressing the CCL21 gene; Ad.p53, dendritic cells transduced with an adenoviral vector expressing p53; anti-PD-1, anti-programmed death-1; CCL21, chemokine ligand 21; CEA, carcinoembryonic antigen; CIK cell, cytokine induced killer cell; CRC, colorectal cancer; DCTCMF, dendritic cell/T cell-derived maturation factor; GM-CSF, granulocyte-macrophage colony-stimulating factor; HER-2, human epidermal growth factor receptor 2; HLA, human leucocyte antigen; i.d., intradermal; IL, interleukin; i.n., intranodal; IFN-α, interferon-alpha; IFN-γ, interferon-gamma; i.t., intratumoral; i.v., intravenous; MAGE-1, melanoma-associated antigen-1; MAGE-2, melanoma-associated antigen-2; moDCs, monocyte derived dendritic cells; MUC1, mucin 1; N, number of patients; N/A, not applicable; NSCLC, non-small cell lung cancer; PGE2, prostaglandin E2; RCT, randomized controlled trial; rMAGE-3, recombinant melanoma-associated antigen-3; rSurvivin, recombinant Survivin; s.c., subcutaneous; TDLN, tumor-draining lymph node; TNF-α, tumor necrosis factor-alpha; WT1, wilms tumor protein I.

DC Therapy in NSCLC

The earliest study in this field was performed by Fong and coworkers in patients with metastatic or recurrent cancer who had abnormal or rising serum carcinoembryonic antigen (CEA) levels (35). CEA is a 180-kDa membrane intercellular adhesion glycoprotein that is overexpressed in several malignancies including NSCLC. Twelve patients with either colorectal cancer (CRC) or NSCLC underwent peripheral blood leukapheresis after prior administration of Flt3 ligand, a hematopoietic growth factor known to expand DCs *in vivo*. DCs were subsequently harvested and loaded with a nonapeptide derived from a human leucocyte antigen (HLA)-A0201-specific peptide of CEA, as well as with keyhole limpet hemocyanin (KLH), a protein with adjuvant properties that also allows to monitor therapy-induced immune responses. Patients were injected intravenously (i.v.) with progressively increasing doses of antigen-exposed DCs with a maximum of 10^9 cells. Adverse events (AEs) were mild self-limited rigors and fever (7/12), as well as mild diarrhea (5/12). Vaccination elicited a CEA-specific immune response in seven patients. Two out of twelve patients experienced dramatic tumor regression, one patient had a mixed response, and two had stable disease (SD). Clinical responses correlated significantly with the expansion of CD8+ T cells.

A similar CEA-targeted DC vaccination strategy was used by the group of Itoh and Ueda et al. (36, 41). The first study enrolled ten patients with advanced digestive tract or lung cancer expressing CEA (36). PBMCs were harvested from peripheral blood by leukapheresis after five days of priming with granulocyte colony-stimulating factor (G-CSF) and cultured with granulocyte/macrophage colony-stimulating factor (GM-CSF) and interleukin 4 (IL-4) to generate DCs. The DCs showed an immature phenotype and were loaded with CEA652, a nonapeptide restricted to HLA-A24, which is present in 60% of the Japanese population. Patients received repeated intradermal (i.d.) and subcutaneous (s.c.) injections up to a cumulative dose ranging from 2.7 × 10^7 to 1.6 × 10^8 DCs. Seven patients also received adjuvant interferon-alpha (IFN-α) and tumor necrosis factor-alpha (TNF-α) twice a week during the vaccination period. No severe toxicity was observed. A positive response to delayed-type hypersensitivity (DTH) skin test was seen in two patients. One of the two demonstrated also a CEA-specific immune response. Two patients, of which one with stage IV lung cancer, had SD for 6 and 9 months respectively, associated with a continuous decrease of serum CEA in the first patient. Clinical and immunological responses were only observed in patients treated with adjuvant use of IFN-α and TNF-α so it is not known whether these responses could be attributed to the DC vaccine. In a follow-up study, 18 patients (five patients with lung cancer) were enrolled and treated using the same immunization protocol, without cytokine adjuvants (41). The vaccine was well tolerated and no toxicity was observed. Although no tumor shrinkage occurred in any patient, long-term SD or marked decreases in the serum CEA level were observed in some subjects. A positive skin response to CEA652-pulsed DCs and a positive *in vitro* cytotoxic T-lymphocyte (CTL) response to CEA652 peptide

TABLE 2 | Clinical and immunological outcomes of dendritic cell (DC)-based immunotherapy in lung cancer.

Reference	Safety	ORR*	Survival	Immune response	Comments
DC therapy in NSCLC					
Fong et al. (35)	Grade 1 or 2 transfusion reaction in 7 patients Grade 1 or 2 diarrhea in 5 patients	0/2 (0%)	N/A	CEA-specific CD8+ T cell immunity was seen in 7/12 patients (58.3%).	Objective responses were observed in 2 patients, both with CRC.
Itoh et al. (36)	Grade 1 local reaction at the injection site in 2 patients	0/2 (0%)	N/A	A positive response to DTH skin test was seen in 2/10 patients (20%) of which 1 patient with lung cancer. A CEA-specific CTL response was seen in 1/10 patients (10%).	A continuous decrease of serum CEA was observed in 1 patient with lung cancer. Two patients had SD (1 patient with lung cancer). Clinical and immunological responses were only observed in patients treated with adjuvant use of INF-α and TNF-α.
Nair et al. (37)	No toxicities	0/1 (0%)	N/A	A CEA specific and tumor antigen-specific CTL response was seen in the patient with NSCLC. The tumor specific immune response was greater than the CEA specific immune response.	
Kontani et al. (38)	Fever in 7 patients	2/8 (25%)	The MST was significantly longer in MUC positive patients versus MUC negative patients (16.8 vs. 3.8 months; p = 0.0101)	A positive response to DTH skin test was seen in 5/9 patients (55.6%). A MUC1-specific CTL response was seen in 3/7 patients (42.9%).	Two patients with lung cancer had a PR. The patients who acquired tumor-specific immunity responded to treatment, i.e., reduction in tumor marker levels and disappearance of malignant pleural effusions.
Hirschowitz et al. (39, 40)	No serious AEs Grade 1 local reaction at the injection site in 10 patients Grade 1 fatigue in 3 patients	N/A	N/A	An antigen-specific immune response was seen in 6/16 patients (37.5%).	Favorable and unfavorable clinical outcomes were independent of measured immunologic responses. Five patients had disease recurrence or progression of which 3 patients died of PD.
Ueda et al. (41)	No toxicities	0/5 (0%)	Survival time ranged from 3 to 46+ months with a median of 8 months.	A positive response to DTH skin test was seen in 5/11 patients (45.5%). A CEA-specific CTL response was seen in 6/11 patients (54.5%).	Three of the 5 patients with lung cancer had prolonged and/or marked decreases in serum CEA levels after therapy.
Chang et al. (42)	No grade 2 to 4 AEs	1/8 (12.5%)	N/A	Minor to moderate increases in T cell responses against tumor antigens were observed in 6/8 patients (75%).	Two patients had SD. The 2 patients who had longer disease control also had better T cell responses.
Morse et al. (43)	No grade 3 or 4 AEs	0/3 (0%)	N/A	A CEA-specific immune response among both CD4+ and CD8+ T cells was seen in all evaluable patients (100%). There was a trend for a greater peak frequency of CEA-specific T cells among those with either a minor response or SD.	One patient had a significant decrease in the CEA level and a minor regression in a retroperitoneal and supraclavicular adenopathy. Five other patients were stable trough at least one cycle of immunization.
Hirschowitz et al. (44)	Local reactions at the injection site in most subjects (not specified)	N/A	N/A	A clear immune response was seen in 9/14 patients (64.2%).	Five patients had disease recurrence or progression of which 3 patients died of progressive disease. Three of 5 patients with PD showed no immunological response.
Mayordomo et al. (45)	Fever in 6 patients Asthenia in 11 patients	0/2 (0%)	Survival time ranged from 0 to 29+ months with a median of 7 months.	A positive response to DTH skin test was seen in 9/15 patients (60%)	Seven patients, of which 1 with NSCLC, had SD for > 3 months, and 7 other patients had PD. Time to progression ranged from 0 to 10 months with a median of 3 months.
Um et al. (46)	No grade 3 or 4 AEs Grade 1 fever in 1 patient	0/8 (0%)	N/A	An increase in the percentage of CD8+ cells expressing INF-γ was seen in 5/9 patients (55.6%).	There were mixed responses that fulfill PD definition but demonstrated some clinical benefit in 2 patients.

(Continued)

TABLE 2 | Continued

Reference	Safety	ORR*	Survival	Immune response	Comments
Perroud et al. (47)	Grade 2 fatigue and chills in 1 patient	N/A	Survival time ranged from 82 to 277 days from the last dose of the vaccine with a median of 112 days.	An improvement in the specific immune response after immunization was seen in all patients (100%) but was short lasting.	From the last dose of the vaccine, the time to disease progression ranged between 1 and 82 days.
Takahashi et al. (48)	No serious AEs Grade 1 fever in 13 patients Grade 2 fever in 2 patients Grade 1 local reaction at the injection site in 26 patients	5/62 (8.1%)	MST = 12 months	N/A	Standard chemotherapy regimens were continued in 36 patients during DC vaccination. DCR was seen in 50% of the patients. Better survival was found in patients with ECOG-PS 0 or 1 and in patients who received > 5 vaccinations.
Hu et al. (49)	Grade 1 fever in 5 patients	3/27 (11.1%)	Median OS = 10.5 months Median PFS = 4.5 months	N/A	
Takahashi et al. (50)	N/A	29/260 (11.2%)	MST = 13,8 months The survival rates from the first vaccination were 53.5% after 1 year, 36.1% after 2 years, and 8.8% after 5 years.	N/A	185 (71.4%) patients received DC vaccines combined with simultaneous chemotherapy. Patients with an adenocarcinoma had a significantly better prognosis compared to other subtypes (MST 15.3 months vs. 8.8 months; p = 0.003). An erythema reaction at the injection site that was ≥ 30 mm in diameter was correlated most strongly with OS from the first vaccine (MST 20.4 vs. 8.8 months; p<0.001).
Li et al. (51)	No serious AEs Grade 1 temporary exanthema in 1 patient Grade 1 pruritus in 3 patients Grade 1 chills in 1 patient Grade 1 fever in 1 patient Grade 1 fatigue in 1 patient	0/16 (0%)	Survival rates from DC therapy was mentioned in three patients and ranged from 6 to 12 months.	A positive response to DTH skin test was seen in all patients (100%). There was a significant increase in INF-γ expression on day 60 vs. day 0. There was an increasing trend in the mean CD4:CD8 values between day 30 and day 90.	5 patients had disease recurrence or progression of which 3 patients died of stage IV NSCLC.
Lee et al. (52)	Grade 1 flu-like symptoms in 1 patient Grade 1 hemoptysis after each injection in 1 patient Grade 1 nausea in 1 patient Grade 1 fatigue in 1 patient	N/A	MST = 3.9 months	A systemic response against TAA's was seen in 6/16 patients (37.5%). Tumor CD8+T cell infiltration was induced in 54% of subjects. Patients with increased CD8+T cells following vaccination showed significantly increased PD-L1 mRNA expression.	SD was seen in 25% of patients at day 56
Teramoto et al. (53)	Fever in 16 patients Local reaction at the site in 6 patients Acute lung injury in 1 patient	0/28 (0%)	MST = 7.4 months	MUC1-specific cytotoxic immune responses were seen in 7/7 patients (100%).	A higher MST was seen in patients receiving > 6 vaccinations, in patients with adverse events, and in patients with higher percentage of peripheral lymphocytes. The DCR in the group of patients that had received 6 vaccinations was 42.9%.
Ge et al. (54)	No serious AEs Grade 1–2 fever in 6 patients Grade 1–2 fatigue in 5	N/A	N/A	A significant decrease in CD3+ CD4+ CD25+ Foxp3+ T regulatory cell number and increase in TNF-α and IL-6 were seen in 2/15 patients (13.3%).	Two patients showed 15% and 64% decrease in CEA and CYFRA21 respectively. The vaccination with the maximum dose significantly improved QOL when administered at the highest dose.

(Continued)

TABLE 2 | Continued

Reference	Safety	ORR*	Survival	Immune response	Comments
	patients Grade 1–2 myalgia in 6 patients Grade 1–2 chills in 1 patient				In the low dose group: 1 patient had no recurrence, 1 patient had PD and 1 patient had died In de middle dose group: all 3 patients had no recurrence. In the high dose group: 1 patient had died, 1 patient had PD and 7 patients had no recurrence.
DC/CIK therapy in NSCLC					
Li et al. (55)	No grade 3 or 4 AEs	N/A	The 2-year OS was significantly increased in the immune-CT group comparing to the non-immunotherapy group ($p<0.05$).	An increased production of cytokines that have known anti-tumor effects was seen, including IFN-γ, TNF-α and TNF-β, in patients who had no progression, but they were not found in patients who developed recurrence.	The 2-year DFS in the immune-CT group (75.6 ± 7.2%) was higher than that in the CT-group (65.3 ± 8.0%) but there was no significant difference. Immunotherapy was started 1 month after chemotherapy in the chemoimmunotherapy group.
Zhong et al. (56)	Grade 1–3 skin toxicity in 9 patients Grade 1–4 fever in 10 patients	N/A	There was no statistically difference in OS between the chemoimmunotherapy group and chemotherapy group ($p = 0.18$).	N/A	In the chemoimmunotherapy group, CEA level decreased in 3 patients, and remained stable in 9 patients. The median time to progression in de chemoimmunotherapy group was 6.9 months (95% CI: 5.0-8.8) and 5.2 months (95% CI: 3.3-6.0) in the chemotherapy group ($p = 0.03$).
Shi et al. (57)	Fever in 4 patients	1/30 (3.3%)	The PFS was significantly increased in the DC/CIK cell group compared to the control group (3.2 vs. 2.56 months; $p<0.05$).	After treatment, an increase in NK-cells, CD3+ and CD4+ T cells was seen, and a decrease in CD8+ cells.	
Yang et al. (58)	No serious AEs	11/61 (18%)	The 1- and 2-year OS rates were 57.2 and 27% in the chemoimmunotherapy group and were significantly higher than in de chemotherapy group ($p<0.05$).	A significant increase in the secretion of INF-γ and TNF-α was seen, and a decrease in TGF-β. An enhanced antitumor activity was seen, as well as an increased CD3+CD56+ cell ratio.	There was no significant difference in the survival rate between the adenocarcinoma and squamous carcinoma patients.
Shi et al. (72)	Fever in 3 patients Rash in 14 patients Diarrhea in 9 patients	N/A	The PFS was significantly longer in the DC/CIK plus erlotinib group compared to the erlotinib group (5.02 vs. 3.98 months; $p<0.05$). There was no statistically significant difference in median OS between both groups ($p = 0.29$).	An increase in the levels of CD3+, CD4+ and CD8+ T cells was found after therapy in the DC/CIK plus erlotinib group, but not in the erlotinib group.	
Zhao et al. (60)	N/A	N/A	N/A	The serum concentrations of the Th2 cytokines (IL-4 and IL-10) in tumor-bearing patients were significantly higher than those with resected NSCLC before immunotherapy. The post-therapy Th1 cytokine (INF-γ) level in patients with resected NSCLC significantly increased from the pre-therapy level. In tumor-bearing patients, significantly enhanced post-therapy Th2 cytokine (IL-4 and IL-10) levels were found.	
Zhu et al. (61)	Grade 1-2 fever in 5 patients	25/30 (83.5%)	1-year OS was significantly higher in the treatment group than in the control group (83.3% vs. 60.6%; $p<0.05$).	A significant increase of CD3+, CD4+ and CD4+/CD8 + was seen in the treatment group, but not in the control group.	

(Continued)

TABLE 2 | Continued

Reference	Safety	ORR*	Survival	Immune response	Comments
Zhang et al. (62)	Grade 1-2 fever in 30 patients Grade 3 fever in 6 patients Grade 1-2 skin rash in 7 patients	N/A	The OS time was significantly increased in comparing to the non-immunotherapy group (p = 0.03).	A positive response to DTH skin test was seen in 59 patients (60.8%).	Matched patients (N = 408) with NSCLC that did not receive DC-CIK acted as the control group.
Zhang et al. (63)	Grade 1-2 fever in 5 patients Grade 1-2 anorexia in 3 patients Grade 1-2 nausea in 3 patients Grade 1-2 radiation pneumonitis in 4 patients Grade 3 radiation pneumonitis in 3 patients	10/21 (47.6%)	The median PFS was significantly longer in the DC/CIK group than in the control group (330 days vs. 233 days; p = 0.0483). There was no difference in median OS between both groups (p = 0.606).	No difference was seen in the serum levels of IL-2 and INF-γ in the two groups both before and after thoracic radiotherapy. No changes were seen in the levels of CD8+ cells or CD4+ cells. A tendency of a decrease in de CD4+/CD8+ T cell ratio was seen in the control group.	
Song et al. (64)	N/A	N/A	N/A	Decreased levels of circulating Tregs and related immunosuppressive cytokines were seen after increased cycles of DC/CIK treatment.	Recurrence rate was lower in the ≥ 3 cycles group compared to < 3 cycles group (p = 0.022).
Chen et al. (65)	Grade 3-4 AEs in 2 patients Grade 1-2 fever in 8 patients Grade 3-4 fever in 1 patients Grade 1-2 chills in 2 patients Grade 3-4 chills in 1 patients	7/31 (22.5%)	OS = 270 days	PD-L1 expression was induced on autologous tumor cells by tumor-reactive DC-CIK cells and elevated IFN-γ secretion was seen.	Among patients with NSCLC, SD was seen in 1 patient.
AKT-DC therapy in NSCLC					
Kimura et al. (66)	Fever in 78.0% of the courses Chills in 83.4% of the courses Fatigue in 23.0% of the courses Nausea in 17.0% of the courses	N/A	The 2- and 5-year OS rates were 88.9% and 52.9% respectively.	N/A	The 5-year survival rate of the group that received > 5.0×10^{10} cells was better than the group that received less (80.8% vs. 38,5%).
Kimura et al., (67, 68)	Fever in 6.2% of the courses Chills in 6.8% of the courses	N/A	The 2- and 5-year OS rates were 96.0% and 69.4% in group A and 64.7% and 45.1% in group B, respectively, with a HR of 0.474.	The CD8+/CD4+ T cell ratio was higher in the survivors than in the deceased (p = 0.0013).	A higher OS was seen in patients ≤ 55 years (HR 0.0098), male patients (HR 0.474), patients with adenocarcinoma (HR 0.479), patients with stage III cancer (HR 0.399) and patients who did not receive preoperative chemotherapy (HR 0.0483).
DC therapy in SCLC					
Chiappori et al. (69)	Grade 1 arthralgia and myalgia in 9 patients Grade 2 arthralgia in 1 patient Grade 1 fatigue in 5	2/54 (3.7%)	The MST from first vaccination was 8.8 months.	A significant p53-specific immune response was seen in 18/43 patients (41.2%).	Patients with a positive immune response had a trend towards improved survival. 78.6% of the patients with a positive immune response had a clinical response to 2^{nd} line chemotherapy

(Continued)

TABLE 2 | Continued

Reference	Safety	ORR*	Survival	Immune response	Comments
	patients Grade 2 fatigue in 1 patient Grade 1 local reaction at the injection site in 5 patients Grade 1 injection site pain in 4 patients				compared to 33.3% patients with a negative immune response.
Chiappori et al. (70, 71)	Grade 3 fatigue in 1 patient. Grade 3 toxicities in 8 patients receiving vaccine + ATRA	1/45 (2.2%)	Survival from date of enrollment was numerically higher in arm A (12.2 months), than in arm B (6.3) and arm C (6.2) but not statistically different.	Positive immune responses were obtained in 20% of arm B (vaccine alone) and 43.3% of arm C (vaccine + ATRA).	No difference was seen in OS between patients with a positive immune response and those with a negative immune response (9.2 vs. 9.3 months; p = 0.250).

**Only responses in lung cancer patients are mentioned.*

AE, adverse event; AKT, activated killer T cells; ATRA, all-trans-retinoid acid; CEA, carcinoembryonic antigen; CI, confidence interval; CIK, cytokine induced killer; CRC, colorectal cancer; CT, chemotherapy; CTL, cytotoxic T-lymphocyte; DCR, disease control rate; DFS, disease free survival; DTH, delayed-type hypersensitivity; ECOG-PS, Eastern Cooperative Oncology Group-Performance Status; HR, hazard ratio; IL, interleukin; INF-α, interferon-alpha; INF-γ, interferon-gamma; MST, median survival time; N/A, not available; ORR, objective response rate; OS, overall survival; PD, progression of disease; QOL, quality of life; SD, stable disease; TAA, tumor-associated antigen; TNF-α, tumor necrosis factor-alpha; TGF-β, transforming growth factor-beta.

after therapy were seen in most of the patients in whom treatment was clinically effective.

Other studies also selected CEA as the antigen of choice for active immunotherapy with DCs. A phase 1 trial included one patient with metastatic lung adenocarcinoma who underwent four monthly immunizations with autologous DCs transfected with CEA-encoding RNA and total tumor RNA (37). Both CEA-specific and tumor-specific CTL immune responses were seen, of which the latter were greater. The authors conclude that RNA-transfected DCs can induce antigen-specific T cell responses in cancer patients with surgically resected malignancies. Morse and coworkers investigated the safety and clinical and immunological efficacy of a DC vaccine modified with a recombinant Fowlpox vector encoding CEA and a triad of stimulatory molecules [rF-CEA(6D)-TRICOM], injected both i.d. and s.c. (43). 14 patients with metastatic CEA-expressing malignancies were enrolled, of which three with NSCLC. There were no treatment-related grade 3 or 4 AEs. One patient had a significant decrease in the CEA level and a minor regression in a retroperitoneal and supraclavicular adenopathy. Five other patients were stable through at least one cycle of immunization. A CEA-specific immune response among both CD4+ and CD8+ T cells was seen in all evaluable patients. There was a trend towards a greater peak frequency of CEA-specific T cells among those with either a minor response or a SD.

Kontani et al. evaluated the clinical effects of a DC vaccine targeting the TAA mucin 1 (MUC1) in 14 patients with advanced or metastatic breast or lung cancer (38). MUC1 is a glycoprotein that is markedly hypoglycosylated in cancer compared to normal tissues, leading to the exposure of immunogenic epitopes (73). PBMCs were collected from peripheral blood samples and supplemented with IL-4 and GM-CSF. Subsequently, DCs were loaded with MUC1 peptides or tumor lysate obtained from malignant pleural effusion specimens of the patients. DCs were then injected s.c. in the supraclavicular region or intrapleurally, at least three times at 2-week intervals. Fever occurred in seven patients. After vaccination, all the evaluable patients with MUC1-positive cancer acquired antigen-specific immunity compared to only one patient with MUC1-negative cancer. Reductions in tumor sizes or tumor marker levels or disappearance of malignant pleural effusion were seen in seven of nine MUC1-positive cancers. The survival of MUC1-positive patients was significantly longer compared to MUC1-negative patients (16.8 vs. 3.8 months; p = 0.0101). The authors conclude in this study that this tumor antigen can elicit a strong immune response and that DC vaccines targeting MUC1, which is expressed in 60% of the lung cancer patients, are a promising immunotherapy in the treatment of cancer (38). Of note, similar signals of clinical efficacy were observed with other MUC1-targeted vaccine approaches in NSCLC (20, 74).

Some important conclusions can be drawn from the different studies mentioned above. First, DC therapy containing one TAA is well tolerated with only minor side effects observed. For CEA-targeted DC vaccination studies, this is reassuring given the severe pulmonary toxicity observed with CEA-specific CAR T cell therapy, which is related to the expression of this antigen on

normal pulmonary epithelium (75). Second, this vaccination approach appears to elicit an antigen-specific, T cell-mediated immune response in a substantial fraction of lung cancer patients, despite a number of obstacles: 1) the use of a shared TAA for which high levels of immunological tolerance must be overcome, 2) the injection of immature DCs in some trials, and 3) the climate of systemic immune suppression in the advanced cancer patients enrolled. Yet, clinical responses were rare, possibly explained by the fact that only one tumor antigen was targeted. A limitation of peptide-based formulations is that they are HLA-restricted, which necessitates patient selection. This is not the case for other antigen formulations such as mRNA encoding antigens or tumor lysates that were used in some other trials. A remarkable observation from these studies is also that prior mobilization with Flt3 ligand or G-CSF could expand the number of DCs produced. However, because it was not assessed whether higher DC doses also yielded stronger immune responses, the benefit of mobilization of the donor in the DC manufacturing process remains unclear.

In contrast to the aforementioned trials enrolling different tumor types, the first DC vaccination trial exclusively in NSCLC patients was performed by Hirschowitz et al. (39, 40). In this trial, multiple TAAs were targeted simultaneously. Autologous DC vaccines were delivered to 16 individuals with stage IA to IIIB NSCLC treated with surgery, chemoradiation, or multimodality therapy. DCs were generated from CD14+ precursors and pulsed with apoptotic bodies of an allogeneic NSCLC cell line that overexpressed human epidermal growth factor receptor 2 (HER2/neu), CEA, wilms tumor protein 1 (WT1), and survivin. Interestingly, DCs were only "partially" matured. Patients received two i.d. vaccines with 1 month apart (average dose of 9.1×10^7 and 8.2×10^7 cells per immunization respectively). AEs were limited to a mild skin reaction at the injection site (10/16) and minor fatigue for one to two days after injection (3/16). Of the 16 patients, six showed an antigen-specific response and five showed a tumor-antigen independent response. Five individuals had documented disease recurrence or progression of which three succumbed to the disease. One individual with stage IB NSCLC developed a solitary brain metastasis 2 months following the initial vaccine and had no evidence of disease 15 months following metastasectomy. Two patients with unresectable stage III NSCLC showed no signs of disease progression at 35 and 23 months from chemoradiation, respectively. The aforementioned clinical outcomes were independent of measured immunologic responses. The same group conducted a continuation study with similar inclusion criteria and immunization protocol, using an immature DC vaccine (44). 14 patients were enrolled of which seven had undergone surgical resection, with or without adjuvant therapy, and seven with unresectable stage III who had been treated with chemoradiation. Immunologic responses, measured by IFN-γ enzyme-linked immune absorbent spot (ELISPOT), were seen in 3/7 stage III unresectable, and 6/7 stage I/II surgically resected patients. There were no AEs, except for local reactions in most subjects. The authors conclude that immature DCs pulsed with apoptotic tumor cells have similar biologic activity to a matured DC preparation in a similar clinical protocol (44).

Although clinical outcomes were difficult to interpret, probably due to the heterogeneity of the patient population, and not correlating with immunological responses, the studies of Hirschowitz and colleagues have clearly indicated that DC therapy following surgery, chemoradiation or multimodality treatment is safe and can possibly find its role as an adjuvant treatment. A remarkable observation from these clinical trials was that immature DCs were able to elicit immune responses in almost 2/3 of the patients, since it has been appreciated for a long time that these DC subsets rather induce immune tolerance than immune stimulation. A difference with the previous studies is that an allogeneic tumor cell line was used to produce a multivalent vaccine, targeting several TAAs. Yet, the antigenic make-up of the cell line used may not be representative for each patient's tumor.

Further exploiting the idea of targeting multiple antigens, Perroud and coworkers assessed the feasibility, safety and immunologic response of a mature, antigen-pulsed autologous DC vaccine loaded with peptides of WT1, CEA, HER2, and Melanoma Antigen 1 (MAGE-1). The trial enrolled five patients with inoperable stage IIIB and IV NSCLC (47). All patients received prior conventional treatment (chemotherapy with or without radiotherapy). PBMCs, obtained after leukapheresis, were cultured in a medium with GM-CSF and IL-4, and subsequently activated with IFN-γ. Patients received two doses of 5×10^7 DCs administered s.c. and i.v. two times at 2-week intervals. One patient developed grade 2 fatigue and chills following the first dose of the vaccine. A lymphoproliferation assay showed an improvement in the specific immune response after immunization in all patients, with a tendency to wane after the second vaccine dose. Survival from the last dose of the vaccine ranged between 82 and 277 days. Three patients had a longer survival time than expected for their tumor, node and metastasis (TNM) classification. The fact that immune responses were not long lasting possibly indicates that multiple doses of the vaccine are required to achieve clinical efficacy.

Li et al. reported the results of a phase 1 trial enrolling 16 patients with stage I to IIIB NSCLC (51). All had no evidence of progression at the time of enrollment and had completed definitive therapy (surgical, medical or multimodal). DC immunotherapy was generated from the patient's PBMCs and loaded with recombinant survivin and MAGE-3 peptides. To induce DC maturation, a cytokine cocktail consisting of IL-1β, IL-6, TNF-α, IFN-γ, prostaglandin E2 (PGE2), and poly I:C had been added to the culture. A prime immunotherapy (9.1×10^7 cells/dose) and a single boost (8.2×10^7 cells/dose) were administered i.d. 1 month apart. AEs were grade 1 fever, chills and fatigue in one patient, and grade 1 pruritus in three patients. A positive response to DTH skin test was seen in all patients. There was a significant increase in IFN-γ expression on day 60 versus day 0. There was also an increasing trend in the mean CD4:CD8 values between day 30 and day 90; however, the increase was not statistically significant. In total, 5/16 patients experienced disease recurrence or progression, of which three patients succumbed to the disease.

An alternative approach to target multiple antigens simultaneously is to load DCs with autologous tumor cells or

cellular lysates. Chang et al. for example conducted a pilot trial using mature DCs pulsed with necrotic tumor cells enriched from malignant pleural effusion specimens (42). Eight patients with advanced NSCLC were injected with antigen-loaded DCs into the inguinal lymph nodes under ultrasound guidance. No major toxicities occurred. Six patients received all six DC injections. Of these, two patients had SD and one patient had a minor response. Minor to moderate increases in T cell responses against tumor antigens were observed after DC vaccination in six of eight patients. The two patients who had a longer disease control also developed better T cell responses. The immunological and clinical effects of a DC vaccine pulsed with autologous tumor lysate was also assessed by the groups of Mayordomo et al. (45) and Um et al. (46). In the first study, 15 patients with metastatic cancer (two with NSCLC) underwent mononuclear cell apheresis after prior mobilization with GM-CSF. PBMCs were cultured with IL-4 and GM-CSF. DCs were then administered i.v. with a median dose of 6.2×10^7 cells per vaccination. In addition, IL-2, IFN-α, and GM-CSF were co-injected s.c. as an adjuvant for several days. A positive response to DTH skin test was noted in 9/15 patients after the first immunization. Seven patients, of whom one with NSCLC, had SD for more than 3 months and seven other patients experienced disease progression. AEs were mild and included fever immediately after DC infusion in six patients and asthenia in eleven patients. The second study enrolled exclusively subjects with stage IIIB and IV NSCLC. DCs were again loaded with autologous tumor lysate by a combination of electroporation and passive loading. Autologous tumor samples were obtained from bronchoscopic biopsies, surgical samples or lymph node biopsies. The antigen-loaded immature DCs were subsequently activated with TNF-α, IL-1, IL-6, and PGE2. In this phase 1 dose-escalation study, 15 patients were assigned to cohorts that received 3, 6, or 12×10^6 DCs by i.d. injection. The maximum dose of the vaccine was shown to be safe with only one patient experiencing low grade fever. In 5/9 patients, the vaccine resulted in an increased IFN-γ production by peripheral blood CD8+ T cells. However, a relationship between the immunological response and the vaccination dose was not seen. Clinical responses were assessed in eight patients. All had PD. Nevertheless, there were mixed responses that fulfilled PD definition but demonstrated some clinical benefit in two patients.

Again, clinical outcomes were disappointing. A possible explanation is that most of the patients enrolled in these studies suffered from relapsed or refractory cancer with often bulky disease and a worse performance status, which is shown to be less responsive to DC vaccination. Another potential concern may be the high concentration of suppressive factors released from the tumor cells, which may influence DC functionality. Moreover, in the last study, the autologous tumor samples used for making tumor lysate had been obtained before the initiation of chemotherapy. Changes in the tumor antigenicity during treatment could perhaps explain the low clinical efficacy.

In an attempt to circumvent the limitations of typically small sample sizes in DC vaccination trials, the group of Takahashi and coworkers conducted a pooled retrospective analysis of 62 patients from one center. The patients had previously treated inoperable or postoperatively relapsed NSCLC and received activated DCs pulsed with either autologous tumor lysates or peptide antigens (WT1, MUC1, CEA) matched to their HLA-A type (48). The DCs were activated by *in vitro* exposure to OK-432, which is a clinically approved lyophilized mixture of group A Streptococcus pyogenes known to promote functional maturation of DCs, including the capacity to secrete IL-12. The vaccines were injected i.d. near the axillar and/or inguinal lymph nodes with a median of 10 immunizations (range, 4–31). Clinical responses were observed in five patients, of which one patient with a complete response (CR). Another 26 patients developed SD. Median survival time (MST) was 12 months from the first DC vaccination. Of note, standard chemotherapy was continued in 36 patients during DC vaccination. A better OS was found in patients who received more than five vaccinations and those with the best performance status. Multivariate analyses also revealed that the use of WT1 peptides significantly affected OS both from initial diagnosis and from the first vaccination. Furthermore, no serious AEs related to the vaccine were observed. In an extended analysis, 260 patients with locally advanced or metastatic NSCLC at six centers were analyzed (50). All had received five or more WT1 and/or MUC1 peptide-pulsed DC vaccinations once every 2 weeks. In some patients, OK-432 was co-administered i.d. as an immunological adjuvant simultaneously with the vaccine. In the majority of the patients (71.4%), DC vaccination was combined with chemotherapy. MST from first vaccination was 13.8 months (95% CI 11.4–16.8) with 8.8% being alive after five years. Patients with an adenocarcinoma had a significantly better prognosis compared with other subtypes (MST 15.3 vs. 8.8 months; $p = 0.003$). An erythema reaction at the injection site that was ≥ 30 mm in diameter was strongly correlated with OS from the first vaccine (MST 20.4 vs. 8.8 months; $p<0.001$). Another Japanese group retrospectively analyzed data of 40 patients with MUC1-positive NSCLC treated with a MUC1-targeted and OK-432 activated DC-vaccine, exploring predictive biomarkers for clinical responses. All patients had stage IIIB-IV NSCLC that was refractory to standard anticancer therapies (53). The vaccines were injected s.c. in the axilla or supraclavicular fossa every 2 weeks until disease progression. Low-grade fever occurred in 16 patients and local skin reactions in six individuals. No patients achieved an objective response. The MST after initial vaccination was 7.4 months and the 1-year OS was 25%. Patients who received more than six vaccinations had a longer MST and 1-year OS (9.5 months and 39.3% respectively). Interestingly, in the latter group, patients who developed immune-related AEs had a significantly longer MST compared with patients without those AEs (12.6 vs. 6.7 months; $p = 0.042$). In addition, longer survival was also seen in patients with > 20% lymphocytes prior to vaccination (12.6 vs. 4.5 months; $p = 0.014$). All seven patients who had received six vaccinations and were evaluable for immune responses showed an increase in MUC1-specific T cells and a decrease in Tregs.

A major drawback of these studies is however their retrospective design, limiting the interpretation of the results. Since most of the patients also received simultaneous

chemotherapy in the first two studies, and no control group was applied, it is difficult to draw definite conclusions regarding the clinical benefit of the vaccine. Furthermore, it was appreciated that patients receiving more DC vaccines also had better survival outcomes, which is of course interesting since the optimal DC dose and frequency of administration is not yet determined. However, this survival benefit could have been possibly attributed to the better performance status of the patients in the group treated with the highest cumulative dose.

Knowledge of negative feedback pathways controlling inflammatory responses can be exploited to re-engineer DCs. Based on this concept, Ge et al. evaluated the safety and efficacy of a DC vaccine activated using the Toll-like receptor (TLR) agonist flagellin, together with siRNA-mediated silencing of the gene encoding for suppressor of cytokine signaling 1 (SOCS1) (54). SOCS1 has been shown to be a negative regulator of DC activation and IL-12 production, thus restricting the DC's capacity to break immunological tolerance. By analogy to other trials, the DCs were pulsed with peptides of survivin and MUC1. Just as MUC1, survivin is also frequently overexpressed in NSCLC and contributes to oncogenesis. In this phase 1 dose-escalation trial, 15 patients with resected stage I to III NSCLC were i.v. injected with 1×10^6, 1×10^7, or the maximum dose of 1×10^8 DCs at days 7, 14, and 21. The most common AEs were grade 1 flu-like symptoms, which occurred mostly in the group immunized with the maximum dose of the vaccine. A significant decrease in T-regulatory (Treg) cells and increase in TNF-α and IL-6 were seen in two patients. Two patients also showed a 15% and 64% decrease in CEA and CYFRA21, respectively. Interestingly, the patients' quality of life (QOL) was significantly improved in the high-dose group, compared with the low-dose and middle-dose group after treatment. More importantly, in the long-term follow-up after more than four years, only two patients had died, two patients had progressive disease (PD) and 11 patients had still no recurrence. With the use of SOCS1-silencing, this trial is the first in lung cancer to explore targeted genetic re-engineering of DCs to boost immunogenicity. This manipulation did not translate into increased cytokine-mediated toxicity. Still the added value of SOCS1-silencing in terms of clinical outcome cannot be ascertained from this trial as there was no comparator product treated with a control siRNA.

Based on preclinical evidence pointing to a possible synergistic effect between chemotherapy and vaccination (as discussed below), Hu et al. explored the combination of pemetrexed and DCs pulsed with autologous tumor lysate in 27 patients suffering from stage IIIB or IV lung adenocarcinoma who had failed on maintenance gefitinib or erlotinib treatment after platinum-doublet chemotherapy (49). PBMCs were enriched from a 50-ml blood sample using density gradient centrifugation and subsequently cultured in the presence of IL-4 and GM-CSF. DCs were then given i.d. every 3 weeks at day 8 of each chemotherapy cycle. Grade 1 fever after DC therapy was noted in five patients. Other, mostly hematological, toxicities were attributed to chemotherapy. Three patients (11.1%) experienced a partial response (PR). The median progression-free survival (PFS) was 4.5 months and the median OS 10.5 months, which is better than a previous trial with second line pemetrexed in advanced NSCLC (76). Grade 1 fever after DC therapy was noted in five patients. Other, mostly hematological, toxicities were attributed to chemotherapy. This was the first study to prospectively investigate the added value of DC therapy combined with chemotherapy. However, since there was no control group, the real value of DC vaccination in this setting remains to be confirmed.

In contrast to all the trials using systemic injection of DCs, Lee and coworkers explored the intratumoral injection in terms of feasibility, safety and efficacy. In a phase 1 dose escalation study, autologous DCs were administered intratumorally in 16 subjects with stage IIIB and IV NSCLC (52). Interestingly, the DCs were genetically modified by transduction with an adenoviral (Ad) vector expressing the *CCL21* gene (Ad-CCL21-DC). CCL21 is a lymphoid chemokine that strongly attracts effector T cells and DCs and hence facilitates entry into the tumor and *in situ* vaccination. Endpoints were safety and tumor antigen-specific immune responses. Patients enrolled into a given cohort received the same Ad-CCL21-DC dose (1×10^6, 5×10^6, 1×10^7, or 3×10^7 cells/injection) by CT-guided or bronchoscopic intratumoral injection on days 0 and 7. Three patients developed possibly treatment-related AEs (flu-like syndrome, hemoptysis, nausea and fatigue, all grade 1). Twenty-five percent of the patients had SD at day 56. MST was 3.9 months. A systemic response against TAAs was observed in six of 16 patients by means of an IFN-γ ELISPOT assay. Tumor CD8+ T cell infiltration was induced in 7/13 subjects. Interestingly, intratumoral PD-L1 mRNA expression increased significantly with increased CD8+ T cell infiltration following vaccination. The authors of this study suggest that *in situ* vaccination itself increases PD-L1 expression as a result of antigen recognition and CD8+ T cell infiltration at the tumor site. In this way, vaccination may be an effective approach to enhance the efficacy of PD-1/PD-L1 checkpoint inhibitors in "cold" tumors with low PD-L1 expression and/or a lack of CD8+ T cell infiltration (52). Still, the major question remains whether DC-induced T cell infiltration and potential priming at one injected site will induce T cells capable of homing into and controlling other metastatic sites.

DC/CIK Cell Therapy in NSCLC

In recent years, the use of autologous DCs co-cultured with cytokine-induced killer (CIK) cells has been the subject of numerous trials in NSCLC, all of them conducted in the Far-East region (77). CIK cells are a subset of non-MHC restricted natural killer T-lymphocytes with a CD3+ CD56+ phenotype that can proliferate rapidly *in vitro* and display strong cytolytic activities against malignant cells (59). In DC/CIK therapy, the DCs are derived from mononuclear cells obtained by leukapheresis in typical GM-CSF/IL-4-supplemented medium and loaded with antigens (autologous tumor lysate or peptides). CIK cells are generated by culturing PBMCs in medium supplemented with anti-CD3 antibody, recombinant human IL-1a, IFN-γ, and IL-2 (58).

DC/CIK cell therapy has been evaluated in diverse disease settings: as adjuvant therapy combined with chemotherapy in resectable disease, in stage IIIB and IV patients as first line in

combination with chemotherapy, and as a maintenance treatment after first line chemotherapy (55–58, 60, 62, 64, 72). In total, 646 patients were enrolled in these trials. No serious toxicities were observed. Signals of clinical activity were observed in some cases, albeit usually modest and often without statistical significance. Signs of systemic immune activation were reported in patients receiving the experimental arm, including increased numbers of circulating CD8+ and CD4+ T cells, a shift from a Th2 toward a Th1-polarized immune response profile with an increase of the anti-tumoral cytokines IFN-γ, TNF-α, and TNF-β (albeit only in early-stage patients), and a reduction in Tregs after repeated injections of DC/CIK.

A different concept is the combination of DC/CIK cell therapy with thoracic radiotherapy (TRT) or chemoradiotherapy (CRT). The underlying rationale being that radiation-killed tumor cells release tumor antigens and "danger-associated molecular patterns" that can potentially promote DCs to elicit tumor antigen-specific CD8+ T cell responses, which would further consolidate or amplify objective responses and improve survival outcomes (61, 63). The immunogenic effects of radiotherapy are thought to underlie the positive results of MUC1-targeted vaccination and, more convincingly, adjuvant PD-L1 blockade in stage III NSCLC patients treated with chemoradiation (20, 78). In a phase 2 trial, patients with stage III and IV NSCLC received TRT (60 Gy delivered at 2 Gy per fraction) plus MUC1-loaded DC/CIK cell therapy or TRT alone (63). All subjects had previously been treated with two or more cycles of platinum-based doublet chemotherapy without disease progression. Patients that received DC/CIK cells combined with TRT had a longer PFS than those who received TRT alone (330 days vs. 233 days; $p<0.05$), as well as a better ORR (47.6% vs. 24.6%; $p<0.05$). Median OS was not significantly different between the two groups. Zhu et al. conducted a RCT in 63 patients with stage IIIB NSCLC (61). Of these, 30 patients were treated with DC/CIK cell therapy combined with platinum-based doublet CRT. DCs were not loaded with tumor antigens. The ORR was significantly higher in the group treated with DC/CIK and CRT than in the group treated with CRT alone (83.3% vs. 54.5%; $p = 0.014$). One-year survival rate was also better (83.3% vs. 60.6%; $p<0.05$). These studies suggest that combined treatments with DC/CIK cell therapy and (chemo)radiotherapy can enhance tumor responses and prolong survival.

Recently, an interesting variation on the DC/CIK manufacturing process was reported and evaluated in advanced cancer patients, among them five with NSCLC. In a phase 1 trial by Chen et al., DC/CIK cells were further activated *in vitro* by incubation with the anti-PD-1 antibody pembrolizumab, and administered i.v. by repeatedly infusions (65). Patients were progressive after at least one previous course of appropriate anti-tumoral treatment. Of note, grade 3 or 4 treatment-related AEs (fever, chills) were noted in two patients. ORR was 22.5% with a median OS and PFS of 270 and 162 days respectively. Still, the actual added value of *in vitro* activation with anti-PD-1 is not clear from this trial as there was no comparator arm with "standard" DC/CIK infusions.

AKT-DC Therapy in NSCLC

Another form of adoptive immunotherapy involving DCs, although somewhat different from the aforementioned treatments, is a therapy using autologous activated killer T cells and DCs (AKT-DC) obtained from tissue cultures of the tumor-draining lymph nodes of the primary lung tumor. Kimura et al. demonstrated that the tumor-draining lymph nodes of lung cancer patients are a potent source of killer T cells specific to autologous tumor cells, but also of mature DCs, when cultured with low dose IL-2, and that this *in vitro* expansion of T cells could last for up to 2 months (79). Based on this mechanism, a phase 2 trial was conducted evaluating the safety and feasibility of chemo-immunotherapy using these AKT-DCs in post-surgical N2 NSCLC patients (66). 31 patients were enrolled, of which three subjects eventually dropped out. Four courses of chemotherapy were administered along with AKT-DC immunotherapy every 2 months for 2 years. Fever and chills were the most frequent AEs. The 2- and 5-year OS were 88.9% and 52.9%, respectively.

The same group performed a phase 3 RCT investigating the efficacy of adjuvant chemo-immunotherapy with AKT-DC, targeting residual micrometastases, in 103 patients with resected NSCLC (67, 68). Patients were randomly allocated to receive either chemo-immunotherapy (group A) or chemotherapy alone (group B). Those who were assigned to group A received four courses of platinum-based chemotherapy along with AKT-DC immunotherapy for up to two years after surgery. Almost half of the patients treated with immunotherapy had at least one AE, mostly chills and/or fever. The 2- and 5-year OS rates were 96.0% and 69.4% in group A and 64.7% and 45.1% in group B, respectively, with a hazard ratio (HR) of 0.474. Subgroup analysis also showed that younger patients, male patients, patients with adenocarcinoma, patients with stage III cancer and those who did not receive preoperative chemotherapy had a significantly better OS. This study showed that NSCLC patients could benefit from adoptive cellular immunotherapy as an adjuvant to surgery. However, the heterogeneity of the study population was a major limitation.

DC Therapy in SCLC

The stark differences in biological and clinical behavior of SCLC compared to NSCLC are also reflected at the immunological level. As a demonstration, clinical trials to this date show only limited responses to immune checkpoint inhibition in this aggressive tumor, in contrast to NSCLC (80, 81). Also, DC-based immunotherapy trials in SCLC are scarce. Antonia and Chiappori were the first to test the immunological and clinical effects of a cancer vaccine consisting of DCs transduced with an adenovirus expressing p53 (Ad.p53) in patients with extensive disease SCLC (69, 82). The tumor suppressor gene, p53, plays an important role as a regulator of cell growth and differentiation and is mutated in ≥ 90% of the SCLC cases (82). Hence, it is considered as an ideal TAA. Fifty-four patients were enrolled in this phase 1/2 trial. All patients were treated with conventional chemotherapy prior to the immunizations. PBMCs were obtained after leukapheresis and cultured in media supplemented with GM-CSF and IL-4. At the completion of incubation, DCs were subsequently infected with Ad.p53 at a viral particle to cell ratio of 15,000:1. DCs had a mature phenotype. Patients were scheduled to receive three doses of the vaccine i.d. at 2-week intervals. Those who did not progress

after three immunizations underwent a second leukapheresis and received three additional doses of the vaccine, but this time once a month. The number of injected DCs was limited to 5×10^6 cells. p53-specific T cell responses were observed in 18/43 (41.8%) patients by IFN-γ ELISPOT assays. AEs associated with the vaccine were infrequent and mostly mild, with one patient experiencing grade 2 fatigue and one patient grade 2 arthralgia. Two patients achieved a PR and 13 patients had SD. Remarkably, a high rate of ORRs to second line chemotherapy was seen in patients with a positive immune response (78.6%) compared to patients with a negative immune response (33.3%). This is higher than expected based on previous trials with paclitaxel in patients with extensive SCLC (83, 84). Median OS was 8.8 months from the time of first vaccination. Patients with a positive immune response to vaccination had a trend towards an improved survival (MST 12.6 vs. 8.2 months; p = 0.131).

The same group subsequently conducted a randomized phase 2 trial involving 69 patients with extensive SCLC who were responsive to therapy or had non-progressive disease after first-line conventional chemotherapy (70, 71). Subjects were randomized into three arms: arm A (control group), arm B (Ad.p53-DC vaccine only), or arm C (Ad.p53-DC vaccine plus All-trans retinoic acid (ATRA)). The rationale to use ATRA is that it decreases systemic levels of myeloid-derived suppressor cells (MDSCs), which have potent immunosuppressive activity. The same immunization protocol was applied as the previous study. The vaccine was found to be safe with one patient experiencing grade 3 fatigue in arm B and eight patients experiencing grade 3 toxicities in arm C. Positive immune responses were obtained in 3/15 of the patients in arm B and 10/23 patients in arm C. The ORRs to second-line chemotherapy were 15.4%, 16.7%, and 23.8%, respectively for arms A, B and C with no survival differences between the different arms. These ORRs were lower than in the previous studies with the same vaccine. Surprisingly, survival from date of enrollment was numerically higher in the control arm than in de treatment arms (12.2, 6.3, and 6.2 months, respectively). A major limitation of this study was the high dropout rate which prevented patients from completing at least one cycle of salvage chemotherapy. Despite this limitation, some conclusions can also be drawn. First, the safety of the Ad.p53-DC vaccine was confirmed and second, the vaccine was able to elicit a specific cytotoxic T cell response in 20-40% of the patients with extensive SCLC, possibly influenced by the co-administration of ATRA. However, this did not translate into clinical responses, which were poor. The higher-than-expected response rate to second line paclitaxel in the first trial is encouraging and paves the way to combinatorial approaches of chemotherapy with immunotherapy to improve clinical efficacy.

DISCUSSION

For almost 20 years, long before the introduction of checkpoint inhibitors, DCs have been studied as a form of immunotherapy in lung cancer patients. This was based on a large body of preclinical data demonstrating the power of DCs to elicit *de novo* cytotoxic T cell responses, and the presence of different classes of TAAs in lung cancer. Evidence, mostly from phase 1 clinical trials, indicates that DC-based immunotherapy is safe and well tolerated with minor side effects depending on the route of administration. Local reactions (e.g., erythema) are a commonly reported AE after cutaneous injection, while systemic side-effects such as fever, chills and fatigue can be triggered as well. These AEs are mostly mild and transient. Severe toxicities rarely occur when DC-based immunotherapy is given solely. This is in contrast to the sometimes serious AEs seen with checkpoint inhibitors. Moreover, even in DC therapies incorporating whole tumor preparations, hence containing a substantial fraction of self-antigens, no clinically significant signs of auto-immunity have been reported so far.

Active immunotherapy involving DCs aims at eliciting cellular immunity in a tumor-specific and robust way. Data from the aforementioned early-phase trials demonstrate that antigen-specific immune responses can be observed in a significant number of patients, even in individuals with metastatic disease. However, positive immune responses as measured by a DTH skin test correlate only imperfectly with clinical outcomes, as shown in other tumor types (85, 86). In addition, these immunological responses tend to abate after the last injected dose.

Despite their proven immunogenicity, DC-based immunotherapy delivers low response rates, with 9.3% (40/432) of the lung cancer patients achieving an objective response. This is comparable to the ORR of second-line docetaxel in metastatic NSCLC (albeit with much less toxicity) and is lower than second-line PD-1/PD-L1 immunotherapy in the same, unselected population (8–11). In SCLC, traditionally considered as a "cold" tumor, the ORR is even lower (3.0%). However, higher ORRs were obtained when DC-based vaccination is combined with CIK cell therapy and/or concurrent chemotherapy (31.2%). Since most of the trials were not designed to assess OS, survival data of DC vaccination in lung cancer patients are scarce and anecdotal. Moreover, a remarkable observation in the DC vaccination field is the disconnect between clinical response and survival, as seen with sipuleucel-T, the FDA-approved DC vaccine for castration-resistant prostate cancer.

A typical limitation of the published studies is the small number of patients and the lack of a control group in almost all clinical trials. Another complicating factor is the huge variability in the methods used. This comprises differences in the type and formulation of TAAs, the DC maturation state at the time of vaccination, different use of co-delivered immunostimulants, as well as variations in the route and frequency of DC injection and dose of the vaccine. Ideally, each of these parameters needs to be optimized in order to improve the clinical efficacy of DC therapy (**Figure 2**).

Different antigen formulations have been used in DC therapy for lung cancer, with tumor-derived peptides (single or combination) and undefined antigen preparations such as autologous tumor cells or cellular lysates being the most frequently used sources. While the use of peptides imposes restrictions in terms of the HLA-type of the target patient population, this is not the case for antigen preparations which also have the advantage to potentially target a

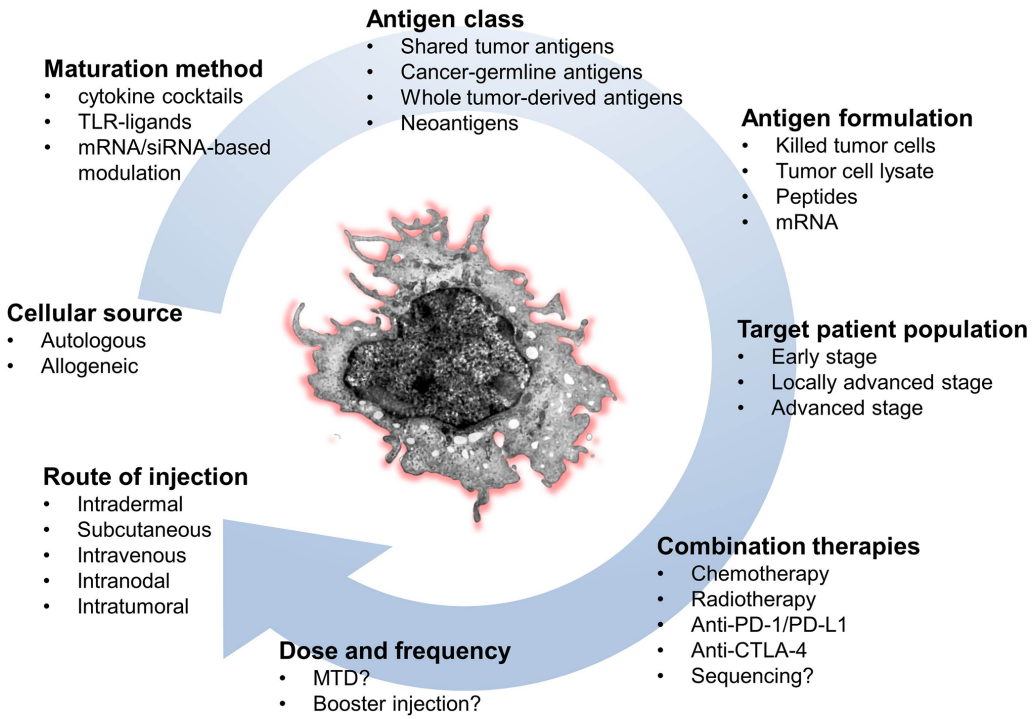


FIGURE 2 | Key parameters to optimize the success of DC-based immunotherapy. CTLA-4, cytotoxic T lymphocyte-associated antigen 4; DC, dendritic cell; MTD, maximum tolerated dose; PD-1, programmed cell death protein 1; PD-L1, programmed death-ligand 1.

much broader antigenic repertoire corresponding more closely to the patient's tumor. A limitation in this approach is the often limited access to autologous tumor material for antigen extraction, as is the case in metastatic lung cancer. Furthermore, in some clinical trials, immature DCs were used in the vaccination protocol. While immunological responses were occasionally observed, immature DCs are primarily inducers of immunological tolerance, which is obviously unwanted in the setting of cancer immunotherapy. To achieve maturation, DCs can be exposed to a myriad of molecular combinations. However not all of them can be easily implemented in a clinical-grade production process, either due to stability, toxicity concerns and/or cost. In addition, strong stimuli can lead to the phenomenon of DC "exhaustion" whereby the capacity to produce the type-1 polarizing cytokine IL-12 is lost by the time the cells reach T cells *in vivo*. Also, inflammatory stimuli can trigger counterregulatory expression of checkpoint molecules such as PD-L1. We have shown that a widely used clinical-grade DC maturation cocktail composed of TNF-α, IL-1β, IL-6, and PGE2 induces high levels of surface PD-L1, which rises even further after cryopreservation and thawing, an effect presumably due to the prostaglandin (87, 88).

The impact of the route of DC injection has also been insufficiently addressed so far. Many trials have used the i.d. or s.c. route of injection, as it is very safe and feasible. However, a disadvantage of this route of administration is that the majority of DCs remain stuck at the injection site and will fail to migrate to the T cell rich areas within draining lymph nodes (89). Direct intranodal administration of DCs has been tested in melanoma, however it is technically challenging, while being not superior in terms of evoked immune responses (90). A much more predictable biodistribution can be achieved by i.v. injection, where the totality of the dose encounters the pulmonary vascular bed first, with subsequent distribution to the spleen and liver, as shown in a unique imaging study on human subjects (91). Preclinical experiments have shown that the "lung vascular filter" acts as a site where robust T cell-mediated immune responses can be efficiently evoked (92). The fact that the human lung represents a reservoir of around 10 billion resident T cells (93) raises the likelihood of productive interactions with antigen-carrying DCs injected intravenously. In addition, the route of DC injection can have an impact on the trafficking pattern of primed T cells, as shown in preclinical studies (94). Whereas an s.c. injection will program elicited T cells to home towards the skin, i.v. injection of DCs induces splenic CD8+ T cells capable of homing towards hematogenic metastases, which is especially relevant for lung cancer. Interestingly, in a therapeutic DC vaccination phase 1 trial in advanced melanoma comparing several ratios of i.v. versus i.d. injection, the data suggest that the i.v. rather than the i.d. injection route could be pivotal for the exceptional objective responses observed (95). Importantly, despite the potential of activated DCs to secrete large amounts of inflammatory cytokines and chemokines, none of the trials using i.v. injection have observed life-threatening toxicity events. A different strategy is the intratumoral injection of DCs, the idea being that relevant tumor antigens are present in abundance, and

that T cells can then be primed *in situ*. One study using *CCL21* gene-modified DCs delivered into lung tumors documented systemic antigen-specific CD8+ T cell responses in a fraction of the patients (52). This is surprising considering the strongly immunosuppressive microenvironment in lung tumors, shown to corrupt the function of DCs and T cells alike (96). Also, intratumoral injection is technically challenging and not feasible in every patient.

Finally, the optimal DC dose and injection schedule has not been determined yet. Given the complex and indirect mechanism of action of DC therapy and the imperfect nature of immune responses as surrogate for clinical responses, accurate modelling of a dose-effect relationship has not been achieved yet. What is clear, however, from all the early-phase trials, is that no dose-limiting AEs have been observed to date. Often the maximum dose delivered is practically limited by the production capacity of autologous DC vaccines. Still, one study suggested a better survival in NSCLC patients receiving the highest dose of DCs (54). Two other studies demonstrated a better OS in patients receiving respectively five and six or more vaccinations (48, 53). A bias may be present in these retrospective studies as the group of patients that received fewer vaccinations generally had a worse performance status.

THE WAY FORWARD

Optimizing the Choice of Target Antigens

The choice of target antigens for loading onto DCs is crucial to maximize the likelihood of eliciting a strong and tumor-directed immune response. Ideally, the antigen should meet different criteria: tumor-specific (expressed by cancer cells only), highly immunogenic, and necessary for cancer survival (97).

To date, most of the DC vaccination trials in lung cancer have targeted TAAs, which are self-antigens that are abnormally expressed by cancer cells, but may be present in normal cells as well. Since TAAs are shared with normal tissues, they can display limited immunogenicity due to central and peripheral tolerance, hence affecting the clinical efficacy of the vaccine. This can be partly circumvented by targeting more than one cancer antigen which will induce a broader immune response (98), as was the case in several of the abovementioned trials. However, the detectable immune responses that were evoked by the DC vaccine in these trials were often not powerful enough to translate into clinical effectiveness.

Development of personalized cancer vaccines based on neoantigens has become a new approach in cancer immunotherapy (99, 100). Neoantigens are tumor specific antigens that arise as a consequence of non-synonymous somatic mutations in the tumor cell genome (100). As their expression is tumor-restricted, in contrast to TAAs, these antigens are not subject to central tolerance and are potentially recognized by high avidity T cells. Hence, these antigens are ideal targets for DC vaccines. Neoantigens can be identified and selected using whole exome sequencing of tumor and blood cell DNA and bioinformatics algorithms. In a murine lung carcinoma model, neoantigen-pulsed DC vaccines were superior to neoantigen-adjuvant vaccines in activating immune responses and inhibiting tumor growth (101). A first demonstration of this approach in human subjects was provided in a phase 1 trial in metastatic melanoma, showing a remarkable induction of *de novo* T cell responses after vaccination with personalized tumor neoantigen-loaded DCs. Several phase 1 clinical trials are currently exploring neoantigen-targeted DC vaccines in lung cancer (**Table 3**), including a study from our group in surgically resected NSCLC (MIDRIX^{NEO}-LUNG/NCT04078269), as well as in lung cancer patients who failed on standard anticancer therapies (NCT03 871205). A major drawback for neoantigen-targeted vaccination is the lengthy and complex process leading up to the identification of potential neo-epitopes, which precludes implementation in patients with advanced or progressing disease. Also, the lack of standardization of *in silico* neo-epitope identification pipelines, with different algorithms producing diverging target lists, is a concern. One workaround consists of harvesting and profiling the "real" HLA-bound mutanome-derived peptides from tumor cells using advanced mass-spectrometric methods (102). This however requires access to large tumor samples which is a challenge in some clinical settings.

Selecting the Right Patients

Autologous cell therapies such as DC-based immunotherapies are labor-intensive and expensive to produce, and scaling-out to address a large patient population is difficult. Affordability of these therapies will be an important issue and challenge for both manufacturers and healthcare providers (103). Hence, a crucial question is which patients will derive most clinical benefit from these treatments. In early stage and locally advanced disease, treatable with curative intent (low tumor burden), the goal of DC-based immunotherapy is primarily to induce immunological memory to prevent later disease relapse (prophylactic vaccination). However, to show any therapeutic efficacy in this patient population, large and lengthy randomized trials are needed. In patients with metastatic disease on the other hand, DC-based immunotherapy actually aims to control the existing tumor (therapeutic vaccination). Considering the delayed antitumor effect and the systemic immunosuppression that is proportionate to the tumor load, patients with rapidly progressive or bulky tumors are unlikely to be appropriate candidates for DC vaccination, unless combinations with other systemic therapies are applied. In order to make DC therapy a viable option in clinical practice, biomarkers to enrich for responders/exclude non-responders upfront must imperatively be developed. Matching the targets loaded into the vaccine with the antigen expression pattern in the tumor is an obvious step. In addition, one can envision to exclude patients whose tumor biopsies harbor immune escape features such as loss-of-function or truncating mutations in Janus kinase (JAK) 1/2 or β2-microglobulin respectively, as vaccine-elicited T lymphocytes will fail to recognize and destroy the escape variants.

Using the Right Combination Partner

Combination with other treatment modalities, such as chemotherapy, radiotherapy and especially immune checkpoint inhibition, may be the key to the success of DC-based

TABLE 3 | Current clinical trials exploring dendritic cell (DC)-based immunotherapy in lung cancer.

Clinical trial I.D.	Study title	Interventions	Phase
NCT04078269	MIDRIXNEO-LUNG Dendritic Cell Vaccine in Patients With Non-small Cell Lung Cancer	Biological: Dendritic cell immunotherapyBiological: Antigen-specific DTHBiological: Control DTH	Phase 1
NCT04082182	MIDRIX4-LUNG Dendritic Cell Vaccine in Patients With Metastatic Non-small Cell Lung Cancer	Biological: Dendritic cell immunotherapyBiological: Antigen-specific DTHBiological: Control DTH	Phase 1
NCT03406715	Combination Immunotherapy-Ipilimumab-Nivolumab-Dendritic Cell p53 Vac – Patients With Small Cell Lung Cancer (SCLC)	Drug: NivolumabDrug: IpilimumabBiological: Dendritic Cell based p53 Vaccine	Phase 2
NCT04199559	Evaluating Combination Therapy using Autologous Dendritic Cells Pulsed With Antigen Peptides and Nivolumab for Subjects With Advanced Non-small Cell Lung Cancer	Drug: Autologous dendritic cells pulsed with antigen	Phase 1
NCT03371485	AST-VAC2 Vaccine in Patients With Non-small Cell Lung Cancer	Biological: AST-VAC2	Phase 1
NCT03360630	Anti-PD-1 Alone or Combined With Autologous Cell Therapy in Advanced NSCLC	Biological: Anti-PD-1 plus DC-CIKBiological: Anti-PD-1 alone	Phase 1
NCT03970746	Safety, Immunogenicity and Preliminary Clinical Activity Study of PDC*lung01 Cancer Vaccine in NSCLC	Biological: PDC*lung01Drug: Keytruda Injectable ProductDrug: Alimta Injectable Product	Phase 1/2
NCT04147078	Personalized DC Vaccine for Postoperative Cancer	Biological: DC vaccine subcutaneous administration	Phase 1
NCT03546361	Intratumoral Administration of CCL21-gene Modified Dendritic Cell With Intravenous Pembrolizumab for Advanced NSCLC	Genetic: Ad-CCL21-DC 1×10^7 Genetic: Ad-CCL21-DC 3×10^7 Genetic: Ad-CCL21-DC 0.05×10^7Drug: Pembrolizumab Genetic: Ad-CCL21-DC ExD	Phase 1
NCT03735290	A study to Evaluate the Safety and Effectiveness of ILIxadencel Administered Into Tumors in Combination With Checkpoint Inhibitor (CPI) in Patients With Advanced Cancer	Biological: ilixadencelDrug: Pembrolizumab	Phase 1/2
NCT03047525	Study of DC-CTL Combined With CIK for Advanced Solid Tumor	Biological: Cytokine-induced Killer Cells	Phase 1/2
NCT02470468	Evaluation of Safety and Efficacy of DCVAC/LuCa (immunotherapy of Lung Cancer) in Patients With Metastatic Lung Cancer	Biological: DCVAC add on to SOCBiological: DCVAC and immune enhancers add on to SOCOther: Standard of Care Chemotherapy	Phase 1/2
NCT03871205	Neoantigen-primed DC Vaccines Therapy for Refractory Lung Cancer	Biological: Neoantigen loaded DC vaccine	Phase 1
NCT04147078	Personalized DC Vaccine for Postoperative Cancer	Biological: DC vaccine subcutaneous administration	Phase 1

Database search (ClinicalTrials.gov) was restricted to clinical trials that are active or will be activated in the near future.

immunotherapy and is currently the subject of several clinical trials (**Table 3**). In principle, all combinatorial strategies aiming to potentiate cancer vaccines in general are applicable to DC therapy in particular (see (18) for an extensive review).

The combination of DC therapy with chemotherapy may seem less suitable due to the immunosuppressive effects of the latter. However, it has become clear that cytotoxic drugs do also have several immune-potentiating effects, not only by inducing immunogenic cell death (104), but also by some ancillary effects on both cancer cells and immune cells present within the tumor3 microenvironment (TME) (105). Chemotherapy can for instance reduce systemic levels of MDSCs and Tregs, which are important factors of lymphocyte suppression in metastatic cancer patients. It was previously shown that vaccination in between platinum-containing chemotherapy cycles can indeed boost antigen-specific T cell responses (106), which is attributed to the MDSC-depleting effect of myelotoxic platinum salts. In addition, chemotherapeutics can also promote antitumor immune responses by upregulating the expression of tumor antigens and MHC class I molecules on the tumor, thereby increasing the capacity for antigen presentation (105). As such, chemotherapy could improve the efficacy of DC-based immunotherapy by rendering tumor cells more susceptible for immune-mediated killing elicited by the DC vaccine (107). Finally, different classes of chemotherapeutics can directly affect DC biology, resulting in upregulated costimulatory molecule expression and increased antigen presentation. For some chemotherapeutics such as taxanes, the effects are mediated by TLR triggering (108). To date, combinatorial approaches of chemotherapy and DC-based immunotherapy (mostly DC/CIK cell therapy) have been investigated only sporadically in lung cancer. A relevant and very recent study in NSCLC is SLU01, a phase 1/2 randomized, open-label, multicenter trial evaluating the clinical efficacy and safety of DCVAC/LuCa added to standard first-line chemotherapy (paclitaxel and carboplatin) and immune-enhancers (IFN-α and hydroxychloroquine) in patients with stage IV NSCLC (NCT02470468). Preliminary results, presented in abstract form (109), demonstrated a better OS in patients receiving the combination therapy versus chemotherapy alone (15.5 vs. 11.8 months, HR 0.55, 95% CI 0.33–0.93; p = 0.0232).

An emerging research topic is the complex interplay between radiotherapy (RT) and the immune system, since it was appreciated that RT can mediate tumor regression outside the radiation field. This phenomenon, called the "abscopal effect", is shown to be the result of an immune-mediated mechanism (110, 111). The advent of immunotherapies, especially immune checkpoint inhibitors, has created special interest in strategies that combine RT with immunotherapeutic agents. RT can enhance systemic antitumor immune responses by several immunomodulatory mechanisms (112), which were already briefly mentioned earlier in this review. In this way, RT could act synergistically with DC-vaccination and thus improve clinical outcomes. Preclinical tumor models have indeed shown potent local and systemic antitumor responses when direct intratumoral administration of DCs was combined with RT (113, 114). The first modest signs of clinical efficacy in humans were demonstrated in

small clinical trials involving patients with digestive tumors and high-risk soft tissue sarcomas (115–117), whereas evidence in lung cancer is limited only to some studies with DC/CIK cell therapy.

Given the spectacular emergence of immune checkpoint blockers (ICBs) in the lung cancer therapeutic landscape, questions inevitably arise as to the role of DC vaccination in this setting. Although ICBs, more specifically PD-1/PD-L1 inhibitors, can sometimes trigger dramatic durable responses, the majority of lung cancer patients still experiences disease progression within a year of treatment. This is not surprising given the fact that anti-PD-1 antibodies, the most commonly used ICBs in lung cancer, only "fix" one specific step in the cancer immunity cycle, which is alleviating T cell paralysis in the TME. Upstream of this, a whole sequence of events leading up to the induction of tumor-homing cytotoxic T cells is operated by DCs, which are known to be dysfunctional within cancer-bearing hosts. Hence, adoptive transfer of fully functional *ex vivo* generated DCs can be seen as an ideal complement to checkpoint inhibition, as a fitting illustration of "pushing the gas pedal" while also "releasing the brakes" (118). ICB failure is often a manifestation of an "immune cold" tumor, i.e., a phenotype characterized by a lack of T cell priming against tumor antigens and consequently an absence of tumor-infiltrating T cells. DC therapy can turn a "cold" into a "hot" tumor through its capacity to prime and generate a *de novo* tumor antigen-specific T cell population. In addition, expanding insights into the mechanisms of action of ICBs could help to design better DC-based therapeutic approaches. The emerging knowledge that exhausted T cells consist of a multi-stage and dynamic group of lymphocytes is extremely relevant in this context. Differences in abundance and distribution of these T cell subsets could underlie differential responsiveness to ICBs, as only "progenitor exhausted" T cells can be expanded by this therapy (119). It raises the question whether DC vaccination may replenish the immune system with the type of progenitor T cells that is amenable to rescue by anti-PD-1 blockade. New insights in the mechanism of action of anti-PD-L1 ICBs are also emerging, mostly diverting the traditional focus from T cell/cancer cell interactions in the TME. As recently reported, anti-PD-L1 ICBs may achieve much of its effect by blocking PD-L1/PD-1 interactions in lymph node-resident DC-T cell clusters, rather than at the level of the tumor (120). Also, adoptively transferred activated DCs express variable levels of surface PD-L1, such that the anti-PD-L1 combination partner must be judiciously chosen. On one hand the combination can indeed result in boosting of T cell responses. However PD-L1-blockade may also be detrimental to DC-mediated T cell priming as PD-L1 protects DCs from cytotoxic T cells during antigen-specific cognate interactions (121). At worse, an anti-PD-L1 ICB with a specific IgG subtype could in theory trigger elimination of the injected DCs through antibody-dependent cytotoxicity. Finally, although CTLA-4 blockade as such is not part of the standard-of-care in lung cancer, its capacity to boost T cell priming could make it an ideal partner in a DC-based combinatorial approach. Clinical evidence for this type of combination was already provided in a phase 1 trial in advanced melanoma patients, where a DC vaccine combined with ipilimumab resulted in remarkably high ORRs (122).

Clinical data supporting the combination of DC therapy and ICBs is not yet available in lung cancer, however several early-phase trials are already addressing this issue (NCT03406715, NCT03360630, NCT03970746, NCT03546361, and NCT03970746). Of these, PDC-LUNG-101 (NCT03970746) seems promising, evaluating the safety, clinical efficacy and immunogenicity of PDC*lung01, a peptide-pulsed allogeneic plasmacytoid DC line in combination with pembrolizumab in patients with metastatic NSCLC. Still many questions remain unanswered such as which class of immune checkpoint inhibition is most suited (anti-PD-1/PD-L1/CTLA4)?. Choosing the correct sequencing could also be critical as preclinical data suggest that PD-1 inhibition can induce a population of T cells that are refractory to subsequent stimulation by a vaccine (123). Additional factors may come into play as our understanding of ICB mechanism of action grows. Of note, accumulating data around the role of the gut microbiome in shaping responses to ICBs (124) may sooner or later impact the way we design cancer vaccination combinatorial studies, including DC immunotherapy.

CONCLUSION

DC-based immunotherapy is safe and well-tolerated and can elicit antitumor immune responses in many patients with lung cancer, with occasional yet remarkable objective responses despite the predominant immunosuppressive climate in the metastatic setting. Combining DC-based immunotherapy with other anticancer therapies, such as chemotherapy, radiotherapy and/or checkpoint inhibition, can potentially improve their effectiveness. Alternatively, a choice of antigens based on neoepitopes with proven expression by the tumor cells may not merely induce immune responses but could result in clinical responses. Clinical trials to prove these hypotheses are underway and the results are eagerly awaited. Additional challenges for the future of DC therapy are determining the adequate dose, frequency, and duration of treatment, improving the choice of target antigens, and finding biomarkers to select potential responders upfront. Finally, identifying the most synergistic combinatorial regimen can hold the real key to long term disease control and survival in this lethal disease.

AUTHOR CONTRIBUTIONS

DS and KV wrote the manuscript. JI, SVL and BV read and corrected where needed. DS and KV took part in the discussion leading up to the manuscript. All authors contributed to the article and approved the submitted version.

FUNDING

KV is supported by an FWO Senior Clinical Investigator Grant. JI received a University BOF (Bijzonder Onderzoeksfonds) grant.

REFERENCES

1. Bray F, Ferlay J, Soerjomataram I, Siegel RL, Torre LA, Jemal A. Global cancer statistics 2018: GLOBOCAN estimates of incidence and mortality worldwide for 36 cancers in 185 countries. *CA: A Cancer J Clin* (2018) 68:394–424. doi: 10.3322/caac.21492
2. Siegel RL, Miller KD, Jemal A. Cancer statistics, 2018. *CA: A Cancer J Clin* (2018) 68:7–30. doi: 10.3322/caac.21442
3. Reck M, Rodriguez-Abreu D, Robinson AG, Hui R, Csoszi T, Fulop A, et al. Pembrolizumab versus Chemotherapy for PD-L1-Positive Non-Small-Cell Lung Cancer. *N Engl J Med* (2016) 375:1823–33. doi: 10.1056/NEJMoa1606774
4. Gandhi L, Rodríguez-Abreu D, Gadgeel S, Esteban E, Felip E, De Angelis F, et al. Pembrolizumab plus Chemotherapy in Metastatic Non–Small-Cell Lung Cancer. *N Engl J Med* (2018) 378:2078–92. doi: 10.1056/NEJMoa1801005
5. Horn L, Mansfield AS, Szczęsna A, Havel L, Krzakowski M, Hochmair MJ, et al. First-Line Atezolizumab plus Chemotherapy in Extensive-Stage Small-Cell Lung Cancer. *N Engl J Med* (2018) 379:2220–9. doi: 10.1056/NEJMoa1809064
6. Paz-Ares L, Luft A, Vicente D, Tafreshi A, Gümüş M, Mazières J, et al. Pembrolizumab plus Chemotherapy for Squamous Non–Small-Cell Lung Cancer. *N Engl J Med* (2018) 379:2040–51. doi: 10.1056/NEJMoa1810865
7. Paz-Ares L, Dvorkin M, Chen Y, Reinmuth N, Hotta K, Trukhin D, et al. Durvalumab plus platinum-etoposide versus platinum-etoposide in first-line treatment of extensive-stage small-cell lung cancer (CASPIAN): a randomised, controlled, open-label, phase 3 trial. *Lancet* (2019) 394:1929–39. doi: 10.1016/S0140-6736(19)32222-6
8. Borghaei H, Paz-Ares L, Horn L, Spigel DR, Steins M, Ready NE, et al. Nivolumab versus Docetaxel in Advanced Nonsquamous Non-Small-Cell Lung Cancer. *N Engl J Med* (2015) 373:1627–39. doi: 10.1056/NEJMoa1507643
9. Brahmer J, Reckamp KL, Baas P, Crino L, Eberhardt WE, Poddubskaya E, et al. Nivolumab versus Docetaxel in Advanced Squamous-Cell Non-Small-Cell Lung Cancer. *N Engl J Med* (2015) 373:123–35. doi: 10.1056/NEJMoa1504627
10. Herbst RS, Baas P, Kim DW, Felip E, Perez-Gracia JL, Han JY, et al. Pembrolizumab versus docetaxel for previously treated, PD-L1-positive, advanced non-small-cell lung cancer (KEYNOTE-010): a randomised controlled trial. *Lancet* (2016) 387:1540–50. doi: 10.1016/S0140-6736(15)01281-7
11. Rittmeyer A, Barlesi F, Waterkamp D, Park K, Ciardiello F, Von Pawel J, et al. Atezolizumab versus docetaxel in patients with previously treated non-small-cell lung cancer (OAK): a phase 3, open-label, multicentre randomised controlled trial. *Lancet* (2017) 389:255–65. doi: 10.1016/S0140-6736(16)32517-X
12. Muenst S, Laubli H, Soysal SD, Zippelius A, Tzankov A, Hoeller S. The immune system and cancer evasion strategies: therapeutic concepts. *J Intern Med* (2016) 279:541–62. doi: 10.1111/joim.12470
13. O'Donnell JS, Teng MWL, Smyth MJ. Cancer immunoediting and resistance to T cell-based immunotherapy. *Nat Rev Clin Oncol* (2019) 16:151–67. doi: 10.1038/s41571-018-0142-8
14. van der Burg SH, Arens R, Ossendorp F, van Hall T, Melief CJ. Vaccines for established cancer: overcoming the challenges posed by immune evasion. *Nat Rev Cancer* (2016) 16:219–33. doi: 10.1038/nrc.2016.16
15. Villanueva N, Bazhenova L. New strategies in immunotherapy for lung cancer: beyond PD-1/PD-L1. *Ther Adv Respir Dis* (2018) 12:1–29. doi: 10.1177/1753466618794133
16. Albright C, Garst J. Vaccine therapy in non—small-cell lung cancer. *Curr Oncol Rep* (2007) 9:241–6. doi: 10.1007/s11912-007-0029-9
17. Kalinski P, Urban J, Narang R, Berk E, Wieckowski E, Muthuswamy R. Dendritic cell-based therapeutic cancer vaccines: what we have and what we need. *Future Oncol* (2009) 5:379–90. doi: 10.2217/fon.09.6
18. Vermaelen K. Vaccine Strategies to Improve Anti-cancer Cellular Immune Responses. *Front Immunol* (2019) 10:8. doi: 10.3389/fimmu.2019.00008
19. Brunsvig PF, Kyte JA, Kersten C, Sundstrom S, Moller M, Nyakas M, et al. Telomerase Peptide Vaccination in NSCLC: A Phase II Trial in Stage III Patients Vaccinated after Chemoradiotherapy and an 8-Year Update on a Phase I/II Trial. *Clin Cancer Res* (2011) 17:6847–57. doi: 10.1158/1078-0432.CCR-11-1385
20. Butts C, Socinski MA, Mitchell PL, Thatcher N, Havel L, Krzakowski M, et al. Tecemotide (L-BLP25) versus placebo after chemoradiotherapy for stage III non-small-cell lung cancer (START): a randomised, double-blind, phase 3 trial. *Lancet Oncol* (2014) 15:59–68. doi: 10.1016/S1470-2045(13)70510-2
21. Nemunaitis J, Jahan T, Ross H, Sterman D, Richards D, Fox B, et al. Phase 1/2 trial of autologous tumor mixed with an allogeneic GVAX® vaccine in advanced-stage non-small-cell lung cancer. *Cancer Gene Ther* (2006) 13:555–62. doi: 10.1038/sj.cgt.7700922
22. Vansteenkiste JF, Cho BC, Vanakesa T, De Pas T, Zielinski M, Kim MS, et al. Efficacy of the MAGE-A3 cancer immunotherapeutic as adjuvant therapy in patients with resected MAGE-A3-positive non-small-cell lung cancer (MAGRIT): a randomised, double-blind, placebo-controlled, phase 3 trial. *Lancet Oncol* (2016) 17:822–35. doi: 10.1016/S1470-2045(16)00099-1
23. Thomas A, Giaccone G. Why has active immunotherapy not worked in lung cancer? *Ann Oncol* (2015) 26:2213–20. doi: 10.1093/annonc/mdv323
24. Steinman RM, Cohn ZA. Identification of a novel cell type in peripheral lymphoid organs of mice. *J Exp Med* (1973) 137:1142–62. doi: 10.1084/jem.137.5.1142
25. Melief CJM. Cancer Immunotherapy by Dendritic Cells. *Immunity* (2008) 29:372–83. doi: 10.1016/j.immuni.2008.08.004
26. Steinman RM, Banchereau J. Taking dendritic cells into medicine. *Nature* (2007) 449:419–26. doi: 10.1038/nature06175
27. Palucka K, Banchereau J. Cancer immunotherapy *via* dendritic cells. *Nat Rev Cancer* (2012) 12:265–77. doi: 10.1038/nrc3258
28. Schuler G, Schuler-Thurner B, Steinman RM. The use of dendritic cells in cancer immunotherapy. *Curr Opin Immunol* (2003) 15:138–47. doi: 10.1016/s0952-7915(03)00015-3
29. Cranmer LD, Trevor KT, Hersh EM. Clinical applications of dendritic cell vaccination in the treatment of cancer. *Cancer Immunol Immunother* (2004) 53:275–306. doi: 10.1007/s00262-003-0432-5
30. Wimmers F, Schreibelt G, Skåld AE, Figdor CG, De Vries IJM. Paradigm Shift in Dendritic Cell-Based Immunotherapy: From *in vitro* Generated Monocyte-Derived DCs to Naturally Circulating DC Subsets. *Front Immunol* (2014) 5:165. doi: 10.3389/fimmu.2014.00165
31. Huber A, Dammeijer F, Aerts JGJV, Vroman H. Current State of Dendritic Cell-Based Immunotherapy: Opportunities for *in vitro* Antigen Loading of Different DC Subsets? *Front Immunol* (2018) 9:2804. doi: 10.3389/fimmu.2018.02804
32. Anguille S, Smits EL, Lion E, van Tendeloo VF, Berneman ZN. Clinical use of dendritic cells for cancer therapy. *Lancet Oncol* (2014) 15:e257–67. doi: 10.1016/S1470-2045(13)70585-0
33. Carreno BM, Magrini V, Becker-Hapak M, Kaabinejadian S, Hundal J, Petti AA, et al. A dendritic cell vaccine increases the breadth and diversity of melanoma neoantigen-specific T cells. *Science* (2015) 348:803–8. doi: 10.1126/science.aaa3828
34. Draube A, Klein-González N, Mattheus S, Brillant C, Hellmich M, Engert A, et al. Dendritic Cell Based Tumor Vaccination in Prostate and Renal Cell Cancer: A Systematic Review and Meta-Analysis. *PLoS One* (2011) 6:e18801. doi: 10.1371/journal.pone.0018801
35. Fong L, Hou Y, Rivas A, Benike C, Yuen A, Fisher GA, et al. Altered peptide ligand vaccination with Flt3 ligand expanded dendritic cells for tumor immunotherapy. *Proc Natl Acad Sci* (2001) 98:8809–14. doi: 10.1073/pnas.141226398
36. Itoh T, Ueda Y, Kawashima I, Nukaya I, Fujiwara H, Fuji N, et al. Immunotherapy of solid cancer using dendritic cells pulsed with the HLA-A24-restricted peptide of carcinoembryonic antigen. *Cancer Immunol Immunother* (2002) 51:99–106. doi: 10.1007/s00262-001-0257-z
37. Nair SK, Morse M, Boczkowski D, Ian Cumming R, Vasovic L, Gilboa E, et al. Induction of Tumor-Specific Cytotoxic T Lymphocytes in Cancer Patients by Autologous Tumor RNA-Transfected Dendritic Cells. *Ann Surg* (2002) 235:540–9. doi: 10.1097/00000658-200204000-00013
38. Kontani K, Taguchi O, Ozaki Y, Hanaoka J, Sawai S, Inoue S, et al. Dendritic cell vaccine immunotherapy of cancer targeting MUC1 mucin. *Int J Mol Med* (2003) 12:493–502. doi: 10.3892/ijmm.12.4.493
39. Hirschowitz EA. Autologous Dendritic Cell Vaccines for Non-Small-Cell Lung Cancer. *J Clin Oncol* (2004) 22:2808–15. doi: 10.1200/JCO.2004.01.074

40. Yannelli JR, Sturgill J, Foody T, Hirschowitz E. The large scale generation of dendritic cells for the immunization of patients with non-small cell lung cancer (NSCLC). *Lung Cancer* (2005) 47:337–50. doi: 10.1016/j.lungcan.2004.08.008
41. Ueda Y, Itoh T, Nukaya I, Kawashima I, Okugawa K, Yano Y, et al. Dendritic cell-based immunotherapy of cancer with carcinoembryonic antigen-derived, HLA-A24-restricted CTL epitope: Clinical outcomes of 18 patients with metastatic gastrointestinal or lung adenocarcinomas. *Int J Oncol* (2004) 24:909–17. doi: 10.3892/ijo.24.4.909
42. Chang G-C, Lan H-C, Juang S-H, Wu Y-C, Lee H-C, Hung Y-M, et al. A pilot clinical trial of vaccination with dendritic cells pulsed with autologous tumor cells derived from malignant pleural effusion in patients with late-stage lung carcinoma. *Cancer* (2005) 103:763–71. doi: 10.1002/cncr.20843
43. Morse MA. Phase I Study of Immunization with Dendritic Cells Modified with Fowlpox Encoding Carcinoembryonic Antigen and Costimulatory Molecules. *Clin Cancer Res* (2005) 11:3017–24. doi: 10.1158/1078-0432.CCR-04-2172
44. Hirschowitz EA, Foody T, Hidalgo GE, Yannelli JR. Immunization of NSCLC patients with antigen-pulsed immature autologous dendritic cells. *Lung Cancer* (2007) 57:365–72. doi: 10.1016/j.lungcan.2007.04.002
45. Mayordomo JI, Andres R, Isla MD, Murillo L, Cajal R, Yubero A, et al. Results of a pilot trial of immunotherapy with dendritic cells pulsed with autologous tumor lysates in patients with advanced cancer. *Tumori* (2007) 93:26–30. doi: 10.1177/030089160709300106
46. Um S-J, Choi YJ, Shin H-J, Son CH, Park Y-S, Roh MS, et al. Phase I study of autologous dendritic cell tumor vaccine in patients with non-small cell lung cancer. *Lung Cancer* (2010) 70:188–94. doi: 10.1016/j.lungcan.2010.02.006
47. Perroud MW, Honma HN, Barbeiro AS, Gilli SC, Almeida MT, Vassallo J, et al. *Mature autologous dendritic cell vaccines in advanced non-small cell lung cancer: a phase I pilot study*. Journal of Experimental & Clinical Cancer Research (2011) 30:65. doi: 10.1186/1756-9966-30-65
48. Takahashi H, Okamoto M, Shimodaira S, Tsujitani S-I, Nagaya M, Ishidao T, et al. Impact of dendritic cell vaccines pulsed with Wilms' tumour-1 peptide antigen on the survival of patients with advanced non-small cell lung cancers. *Eur J Cancer* (2013) 49:852–9. doi: 10.1016/j.ejca.2012.11.005
49. Hu RH, Shi SB, Qi JL, Tian J, Tang XY, Liu GF, et al. Pemetrexed plus dendritic cells as second-line treatment for patients with stage IIIB/IV non-small cell lung cancer who had treatment with TKI. *Med Oncol* (2014) 31:63. doi: 10.1007/s12032-014-0063-z
50. Takahashi H, Shimodaira S, Ogasawara M, Ota S, Kobayashi M, Abe H, et al. Lung adenocarcinoma may be a more susceptive subtype to a dendritic cell-based cancer vaccine than other subtypes of non-small cell lung cancers: a multicenter retrospective analysis. *Cancer Immunol Immunother* (2016) 65:1099–111. doi: 10.1007/s00262-016-1872-z
51. Li D, He S. MAGE3 and Survivin activated dendritic cell immunotherapy for the treatment of non-small cell lung cancer. *Oncol Lett* (2018) 15:8777–83. doi: 10.3892/ol.2018.8362
52. Lee JM, Lee M-H, Garon E, Goldman JW, Salehi-Rad R, Baratelli FE, et al. Phase I Trial of Intratumoral Injection ofCCL21Gene–Modified Dendritic Cells in Lung Cancer Elicits Tumor-Specific Immune Responses and CD8+T-cell Infiltration. *Clin Cancer Res* (2017) 23:4556–68. doi: 10.1158/1078-0432.CCR-16-2821
53. Teramoto K, Ozaki Y, Hanaoka J, Sawai S, Tezuka N, Fujino S, et al. Predictive biomarkers and effectiveness of MUC1-targeted dendritic-cell-based vaccine in patients with refractory non-small cell lung cancer. *Ther Adv Med Oncol* (2017) 9:147–57. doi: 10.1177/1758834016678375
54. Ge C, Li R, Song H, Geng T, Yang J, Tan Q, et al. Phase I clinical trial of a novel autologous modified-DC vaccine in patients with resected NSCLC. *BMC Cancer* (2017) 17:884. doi: 10.1186/s12885-017-3859-3
55. Li H, Wang C, Yu J, Cao S, Wei F, Zhang W, et al. Dendritic cell-activated cytokine-induced killer cells enhance the anti-tumor effect of chemotherapy on non-small cell lung cancer in patients after surgery. *Cytotherapy* (2009) 11:1076–83. doi: 10.3109/14653240903121252
56. Zhong R, Teng J, Han B, Zhong H. Dendritic cells combining with cytokine-induced killer cells synergize chemotherapy in patients with late-stage non-small cell lung cancer. *Cancer Immunol Immunother* (2011) 60:1497–502. doi: 10.1007/s00262-011-1060-0
57. Shi SB, Ma TH, Li CH, Tang XY. Effect of maintenance therapy with dendritic cells: cytokine-induced killer cells in patients with advanced non-small cell lung cancer. *Tumori* (2012) 98:314–9. doi: 10.1700/1125.12398
58. Yang L, Ren B, Li H, Yu J, Cao S, Hao X, et al. Enhanced antitumor effects of DC-activated CIKs to chemotherapy treatment in a single cohort of advanced non-small-cell lung cancer patients. *Cancer Immunol Immunother* (2013) 62:65–73. doi: 10.1007/s00262-012-1311-8
59. Gao X, Mi Y, Guo N, Xu H, Xu L, Gou X, et al. Cytokine-Induced Killer Cells As Pharmacological Tools for Cancer Immunotherapy. *Front Immunol* (2017) 8:774. doi: 10.3389/fimmu.2017.00774
60. Zhao P, Bu X, Wei X, Sun W, Xie X, Li C, et al. Dendritic cell immunotherapy combined with cytokine-induced killer cells promotes skewing toward Th2 cytokine profile in patients with metastatic non-small cell lung cancer. *Int Immunopharmacol* (2015) 25:450–6. doi: 10.1016/j.intimp.2015.02.010
61. Zhu XP, Xu YH, Zhou J, Pan XF. A clinical study evaluating dendritic and cytokine-induced killer cells combined with concurrent radiochemotherapy for stage IIIB non-small cell lung cancer. *Genet Mol Res* (2015) 14:10228–35. doi: 10.4238/2015.August.28.6
62. Zhang L, Yang X, Sun Z, Li J, Zhu H, Li J, et al. Dendritic cell vaccine and cytokine-induced killer cell therapy for the treatment of advanced non-small cell lung cancer. *Oncol Lett* (2016) 11:2605–10. doi: 10.3892/ol.2016.4273
63. Zhang L, Xu Y, Shen J, He F, Zhang D, Chen Z, et al. Feasibility study of DCs/CIKs combined with thoracic radiotherapy for patients with locally advanced or metastatic non-small-cell lung cancer. *Radiat Oncol* (2016) 11:60. doi: 10.1186/s13014-016-0635-5
64. Song H, Liu S, Zhao Z, Sun W, Wei X, Ma X, et al. Increased cycles of DC/CIK immunotherapy decreases frequency of Tregs in patients with resected NSCLC. *Int Immunopharmacol* (2017) 52:97–202. doi: 10.1016/j.intimp.2017.09.014
65. Chen C-L, Pan Q-Z, Weng D-S, Xie C-M, Zhao J-J, Chen M-S, et al. Safety and activity of PD-1 blockade-activated DC-CIK cells in patients with advanced solid tumors. *OncoImmunology* (2018) 7:e1417721. doi: 10.1080/2162402X.2017.1417721
66. Kimura H, Iizasa T, Ishikawa A, Shingyouji M, Yoshino M, Kimura M, et al. Prospective phase II study of post-surgical adjuvant chemo-immunotherapy using autologous dendritic cells and activated killer cells from tissue culture of tumor-draining lymph nodes in primary lung cancer patients. *Anticancer Res* (2008) 28:1229–38.
67. Kimura H, Matsui Y, Ishikawa A, Nakajima T, Iizasa T. Randomized controlled phase III trial of adjuvant chemoimmunotherapy with activated cytotoxic T cells and dendritic cells from regional lymph nodes of patients with lung cancer. *Cancer Immunol Immunother* (2018) 67:1231–8. doi: 10.1007/s00262-018-2180-6
68. Kimura H, Matsui Y, Ishikawa A, Nakajima T, Yoshino M, Sakairi Y. Randomized controlled phase III trial of adjuvant chemo-immunotherapy with activated killer T cells and dendritic cells in patients with resected primary lung cancer. *Cancer Immunol Immunother* (2015) 64:51–9. doi: 10.1007/s00262-014-1613-0
69. Chiappori AA, Soliman H, Janssen WE, Antonia SJ, Gabrilovich DI. INGN-225: a dendritic cell-based p53 vaccine (Ad.p53-DC) in small cell lung cancer: observed association between immune response and enhanced chemotherapy effect. *Expert Opin Biol Ther* (2010) 10:983–91. doi: 10.1517/14712598.2010.484801
70. Chiappori AA, Williams CC, Gray JE, Tanvetyanon T, Haura EB, Creelan BC, et al. Randomized-controlled phase II trial of salvage chemotherapy after immunization with a TP53-transfected dendritic cell-based vaccine (Ad.p53-DC) in patients with recurrent small cell lung cancer. *Cancer Immunol Immunother* (2019) 68:517–27. doi: 10.1007/s00262-018-2287-9
71. Iclozan C, Antonia S, Chiappori A, Chen D-T, Gabrilovich D. Therapeutic regulation of myeloid-derived suppressor cells and immune response to cancer vaccine in patients with extensive stage small cell lung cancer. *Cancer Immunol Immunother* (2013) 62:909–18. doi: 10.1007/s00262-013-1396-8
72. Shi SB, Tang XY, Tian J, Chang CX, Li P, Qi JL. Efficacy of erlotinib plus dendritic cells and cytokine-induced killer cells in maintenance therapy of advanced non-small cell lung cancer. *J Immunother* (2014) 37:250–5. doi: 10.1097/CJI.0000000000000015

73. Cascio S, Finn O. Intra- and Extra-Cellular Events Related to Altered Glycosylation of MUC1 Promote Chronic Inflammation, Tumor Progression, Invasion, and Metastasis. *Biomolecules* (2016) 6:39. doi: 10.3390/biom6040039
74. Quoix E, Lena H, Losonczy G, Forget F, Chouaid C, Papai Z, et al. TG4010 immunotherapy and first-line chemotherapy for advanced non-small-cell lung cancer (TIME): results from the phase 2b part of a randomised, double-blind, placebo-controlled, phase 2b/3 trial. *Lancet Oncol* (2016) 17:212–23. doi: 10.1016/S1470-2045(15)00483-0
75. Thistlethwaite FC, Gilham DE, Guest RD, Rothwell DG, Pillai M, Burt DJ, et al. The clinical efficacy of first-generation carcinoembryonic antigen (CEACAM5)-specific CAR T cells is limited by poor persistence and transient pre-conditioning-dependent respiratory toxicity. *Cancer Immunol Immunother* (2017) 66:1425–36. doi: 10.1007/s00262-017-2034-7
76. Hanna N, Shepherd FA, Fossella FV, Pereira JR, De Marinis F, von Pawel J, et al. Randomized phase III trial of pemetrexed versus docetaxel in patients with non-small-cell lung cancer previously treated with chemotherapy. *J Clin Oncol* (2004) 22:1589–97. doi: 10.1200/JCO.2004.08.163
77. Wang S, Wang Z. Efficacy and safety of dendritic cells co-cultured with cytokine-induced killer cells immunotherapy for non-small-cell lung cancer. *Int Immunopharmacol* (2015) 28:22–8. doi: 10.1016/j.intimp.2015.05.021
78. Antonia SJ, Villegas A, Daniel D, Vicente D, Murakami S, Hui R, et al. Overall Survival with Durvalumab after Chemoradiotherapy in Stage III NSCLC. *N Engl J Med* (2018) 379:2342–50. doi: 10.1056/NEJMoa1809697
79. Kimura H, Dobrenkov K, Iida T, Suzuki M, Ando S, Yamamoto N. Tumor-draining lymph nodes of primary lung cancer patients: a potent source of tumor-specific killer cells and dendritic cells. *Anticancer Res* (2005) 25:85–94.
80. Antonia SJ, López-Martin JA, Bendell J, Ott PA, Taylor M, Eder JP, et al. Nivolumab alone and nivolumab plus ipilimumab in recurrent small-cell lung cancer (CheckMate 032): a multicentre, open-label, phase 1/2 trial. *Lancet Oncol* (2016) 17:883–95. doi: 10.1016/S1470-2045(16)30098-5
81. Chung HC, Piha-Paul SA, Lopez-Martin J, Schellens JHM, Kao S, Miller WHJr, et al. Pembrolizumab After Two or More Lines of Previous Therapy in Patients With Recurrent or Metastatic SCLC: Results From the KEYNOTE-028 and KEYNOTE-158 Studies. *J Thorac Oncol* (2020) 15:618–27. doi: 10.1016/j.jtho.2019.12.109
82. Antonia SJ, Mirza N, Fricke I, Chiappori A, Thompson P, Williams N, et al. Combination of p53 cancer vaccine with chemotherapy in patients with extensive stage small cell lung cancer. *Clin Cancer Res* (2006) 12:878–87. doi: 10.1158/1078-0432.CCR-05-2013
83. Smit EF, Fokkema E, Biesma B, Groen HJ, Snoek W, Postmus PE. A phase II study of paclitaxel in heavily pretreated patients with small-cell lung cancer. *Br J Cancer* (1998) 77:347–51. doi: 10.1038/bjc.1998.54
84. Yamamoto N, Tsurutani J, Yoshimura N, Asai G, Moriyama A, Nakagawa K, et al. Phase II study of weekly paclitaxel for relapsed and refractory small cell lung cancer. *Anticancer Res* (2006) 26:777–81.
85. Aarntzen EHJG, Figdor CG, Adema GJ, Punt CJA, De Vries IJM. Dendritic cell vaccination and immune monitoring. *Cancer Immunol Immunother* (2008) 57:1559–68. doi: 10.1007/s00262-008-0553-y
86. Lesterhuis WJ, De Vries IJM, Schuurhuis DH, Boullart ACI, Jacobs JFM, De Boer AJ, et al. Vaccination of colorectal cancer patients with CEA-loaded dendritic cells: antigen-specific T cell responses in DTH skin tests. *Ann Oncol* (2006) 17:974–80. doi: 10.1093/annonc/mdl072
87. Brabants E, Heyns K, De Smet S, Devreker P, Ingels J, De Cabooter N, et al. An accelerated, clinical-grade protocol to generate high yields of type 1-polarizing messenger RNA-loaded dendritic cells for cancer vaccination. *Cytotherapy* (2018) 20:1164–81. doi: 10.1016/j.jcyt.2018.06.006
88. Prima V, Kaliberova LN, Kaliberov S, Curiel DT, Kusmartsev S. COX2/mPGES1/PGE2pathway regulates PD-L1 expression in tumor-associated macrophages and myeloid-derived suppressor cells. *Proc Natl Acad Sci* (2017) 114:1117–22. doi: 10.1073/pnas.1424355112
89. Verdijk P, Aarntzen EH, Lesterhuis WJ, Boullart AC, Kok E, van Rossum MM, et al. Limited amounts of dendritic cells migrate into the T-cell area of lymph nodes but have high immune activating potential in melanoma patients. *Clin Cancer Res* (2009) 15:2531–40. doi: 10.1158/1078-0432.CCR-08-2729
90. Bol KF, Figdor CG, Aarntzen EH, Welzen ME, Van Rossum MM, Blokx WA, et al. Intranodal vaccination with mRNA-optimized dendritic cells in metastatic melanoma patients. *OncoImmunology* (2015) 4:e1019197. doi: 10.1080/2162402X.2015.1019197
91. Morse MA, Coleman RE, Akabani G, Niehaus N, Coleman D, Lyerly HK. Migration of human dendritic cells after injection in patients with metastatic malignancies. *Cancer Res* (1999) 59:56–8.
92. Willart MA, Jan de Heer H, Hammad H, Soullie T, Deswarte K, Clausen BE, et al. The lung vascular filter as a site of immune induction for T cell responses to large embolic antigen. *J Exp Med* (2009) 206:2823–35. doi: 10.1084/jem.20082401
93. Purwar R, Campbell J, Murphy G, Richards WG, Clark RA, Kupper TS. Resident memory T cells (T(RM)) are abundant in human lung: diversity, function, and antigen specificity. *PLoS One* (2011) 6:e16245. doi: 10.1371/journal.pone.0016245
94. Mullins DW, Sheasley SL, Ream RM, Bullock TN, Fu YX, Engelhard VH. Route of immunization with peptide-pulsed dendritic cells controls the distribution of memory and effector T cells in lymphoid tissues and determines the pattern of regional tumor control. *J Exp Med* (2003) 198:1023–34. doi: 10.1084/jem.20021348
95. Wilgenhof S, Van Nuffel AM, Benteyn D, Corthals J, Aerts C, Heirman C, et al. A phase IB study on intravenous synthetic mRNA electroporated dendritic cell immunotherapy in pretreated advanced melanoma patients. *Ann Oncol* (2013) 24:2686–93. doi: 10.1093/annonc/mdt245
96. Pyfferoen L, Brabants E, Everaert C, De Cabooter N, Heyns K, Deswarte K, et al. The transcriptome of lung tumor-infiltrating dendritic cells reveals a tumor-supporting phenotype and a microRNA signature with negative impact on clinical outcome. *Oncoimmunology* (2017) 6:e1253655. doi: 10.1080/2162402X.2016.1253655
97. Hollingsworth RE, Jansen K. Turning the corner on therapeutic cancer vaccines. *NPJ Vaccines* (2019) 4:7. doi: 10.1038/s41541-019-0103-y
98. Lybaert L, Vermaelen K, De Geest BG, Nuhn L. Immunoengineering through cancer vaccines - A personalized and multi-step vaccine approach towards precise cancer immunity. *J Control Rel* (2018) 289:125–45. doi: 10.1016/j.jconrel.2018.09.009
99. Mastelic-Gavillet B, Balint K, Boudousquie C, Gannon PO, Kandalaft LE. Personalized Dendritic Cell Vaccines—Recent Breakthroughs and Encouraging Clinical Results. *Front Immunol* (2019) 10:766. doi: 10.3389/fimmu.2019.00766
100. Peng M, Mo Y, Wang Y, Wu P, Zhang Y, Xiong F, et al. Neoantigen vaccine: an emerging tumor immunotherapy. *Mol Cancer* (2019) 18:128. doi: 10.1186/s12943-019-1055-6
101. Zhang R, Yuan F, Shu Y, Tian Y, Zhou B, Yi L, et al. Personalized neoantigen-pulsed dendritic cell vaccines show superior immunogenicity to neoantigen-adjuvant vaccines in mouse tumor models. *Cancer Immunol Immunother* (2020) 69:135–45. doi: 10.1007/s00262-019-02448-z
102. Ebrahimi-Nik H, Michaux J, Corwin WL, Keller GL, Shcheglova T, Pak H, et al. Mass spectrometry driven exploration reveals nuances of neoepitope-driven tumor rejection. *JCI Insight* (2019) 5:e129152. doi: 10.1172/jci.insight.129152
103. Lopes AG SA, Frohlich B. Cost Analysis of Cell Therapy Manufacture: Autologous Cell Therapies, Part 1. *BioProcess Int* (2018) 16:S3–8.
104. Ghiringhelli F, Apetoh L, Tesniere A, Aymeric L, Ma Y, Ortiz C, et al. Activation of the NLRP3 inflammasome in dendritic cells induces IL-1beta-dependent adaptive immunity against tumors. *Nat Med* (2009) 15:1170–8. doi: 10.1038/nm.2028
105. Chen G, Emens LA. Chemoimmunotherapy: reengineering tumor immunity. *Cancer Immunol Immunother* (2013) 62:203–16. doi: 10.1007/s00262-012-1388-0
106. Welters MJ, van der Sluis TC, van Meir H, Loof NM, van Ham VJ, van Duikeren S, et al. Vaccination during myeloid cell depletion by cancer chemotherapy fosters robust T cell responses. *Sci Transl Med* (2016) 8:334ra52. doi: 10.1126/scitranslmed.aad8307
107. van Gulijk M, Dammeijer F, Aerts J, Vroman H. Combination Strategies to Optimize Efficacy of Dendritic Cell-Based Immunotherapy. *Front Immunol* (2018) 9:2759. doi: 10.3389/fimmu.2018.02759
108. Truxova I, Hensler M, Skapa P, Halaska MJ, Laco J, Ryska A, et al. Rationale for the Combination of Dendritic Cell-Based Vaccination Approaches With Chemotherapy Agents. *Int Rev Cell Mol Biol* (2017) 330:115–56. doi: 10.1016/bs.ircmb.2016.09.003

109. Havel L, Kolek V, Pesek M, Cernovská M, Bartunkova J, Spisek R, et al. Dendritic-cell vaccine (DCVAC) with first-line chemotherapy in patients with stage IV NSCLC: Final analysis of phase II, open label, randomized, multicenter trial. *J Clin Oncol* (2019) 37:9039. doi: 10.1200/JCO.2019.37.15_suppl.9039
110. Demaria S, Formenti SC. The abscopal effect 67 years later: from a side story to center stage. *Br J Radiol* (2020) 93:20200042. doi: 10.1259/bjr.20200042
111. Demaria S, Ng B, Devitt ML, Babb JS, Kawashima N, Liebes L, et al. Ionizing radiation inhibition of distant untreated tumors (abscopal effect) is immune mediated. *Int J Radiat Oncol Biol Phys* (2004) 58:862–70. doi: 10.1016/j.ijrobp.2003.09.012
112. Ferrara TA, Hodge JW, Gulley JL. Combining radiation and immunotherapy for synergistic antitumor therapy. *Curr Opin Mol Ther* (2009) 11:37–42.
113. Akutsu Y, Matsubara H, Urashima T, Komatsu A, Sakata H, Nishimori T, et al. Combination of direct intratumoral administration of dendritic cells and irradiation induces strong systemic antitumor effect mediated by GRP94/gp96 against squamous cell carcinoma in mice. *Int J Oncol* (2007) 31:509–15.
114. Teitz-Tennenbaum S, Li Q, Rynkiewicz S, Ito F, Davis MA, McGinn CJ, et al. Radiotherapy potentiates the therapeutic efficacy of intratumoral dendritic cell administration. *Cancer Res* (2003) 63:8466–75.
115. Chi KH, Liu SJ, Li CP, Kuo HP, Wang YS, Chao Y, et al. Combination of conformal radiotherapy and intratumoral injection of adoptive dendritic cell immunotherapy in refractory hepatoma. *J Immunother* (2005) 28:129–35. doi: 10.1097/01.cji.0000154248.74383.5e
116. Finkelstein SE, Iclozan C, Bui MM, Cotter MJ, Ramakrishnan R, Ahmed J, et al. Combination of External Beam Radiotherapy (EBRT) With Intratumoral Injection of Dendritic Cells as Neo-Adjuvant Treatment of High-Risk Soft Tissue Sarcoma Patients. *Int J Radiat OncologyBiologyPhysics* (2012) 82:924–32. doi: 10.1016/j.ijrobp.2010.12.068
117. Wang C, Pu J, Yu H, Liu Y, Yan H, He Z, et al. A Dendritic Cell Vaccine Combined With Radiotherapy Activates the Specific Immune Response in Patients With Esophageal Cancer. *J Immunother* (2017) 40:71–6. doi: 10.1097/CJI.0000000000000155
118. Versteven M, Van den Bergh JMJ, Marcq E, Smits ELJ, Van Tendeloo VFI, Hobo W, et al. Dendritic Cells and Programmed Death-1 Blockade: A Joint Venture to Combat Cancer. *Front Immunol* (2018) 9:394. doi: 10.3389/fimmu.2018.00394
119. Beltra JC, Manne S, Abdel-Hakeem MS, Kurachi M, Giles JR, Chen Z, et al. Developmental Relationships of Four Exhausted CD8(+) T Cell Subsets Reveals Underlying Transcriptional and Epigenetic Landscape Control Mechanisms. *Immunity* (2020) 52:825–41.e8. doi: 10.1016/j.immuni.2020.04.014
120. Dammeijer F, van Gulijk M, Mulder EE, Lukkes M, Klaase L, van den Bosch T, et al. The PD-1/PD-L1-Checkpoint Restrains T cell Immunity in Tumor-Draining Lymph Nodes. *Cancer Cell* (2020) 38:685–700.e8. doi: 10.1016/j.ccell.2020.09.001
121. Mohsenzadegan M, Peng RW, Roudi R. Dendritic cell/cytokine-induced killer cell-based immunotherapy in lung cancer: What we know and future landscape. *J Cell Physiol* (2020) 235:74–86. doi: 10.1002/jcp.28977
122. Wilgenhof S, Corthals J, Heirman C, van Baren N, Lucas S, Kvistborg P, et al. Phase II Study of Autologous Monocyte-Derived mRNA Electroporated Dendritic Cells (TriMixDC-MEL) Plus Ipilimumab in Patients With Pretreated Advanced Melanoma. *J Clin Oncol* (2016) 34:1330–8. doi: 10.1200/JCO.2015.63.4121
123. Verma V, Shrimali RK, Ahmad S, Dai W, Wang H, Lu S, et al. PD-1 blockade in subprimed CD8 cells induces dysfunctional PD-1(+)CD38(hi) cells and anti-PD-1 resistance. *Nat Immunol* (2019) 20:1231–43. doi: 10.1038/s41590-019-0441-y
124. Routy B, Le Chatelier E, Derosa L, Duong CPM, Alou MT, Daillère R, et al. Gut microbiome influences efficacy of PD-1–based immunotherapy against epithelial tumors. *Science* (2018) 359:91–7. doi: 10.1126/science.aan3706

Conflict of Interest: The authors declare that the research was conducted in the absence of any commercial or financial relationships that could be construed as a potential conflict of interest.

Copyright © 2021 Stevens, Ingels, Van Lint, Vandekerckhove and Vermaelen. This is an open-access article distributed under the terms of the Creative Commons Attribution License (CC BY). The use, distribution or reproduction in other forums is permitted, provided the original author(s) and the copyright owner(s) are credited and that the original publication in this journal is cited, in accordance with accepted academic practice. No use, distribution or reproduction is permitted which does not comply with these terms.

frontiers in Immunology

REVIEW
published: 17 February 2021
doi: 10.3389/fimmu.2020.615240

Cancer Vaccines: Adjuvant Potency, Importance of Age, Lifestyle, and Treatments

Stefania Cuzzubbo[1,2], *Sara Mangsbo*[3,4], *Divya Nagarajan*[5], *Kinana Habra*[6,7], *Alan Graham Pockley*[7,8] *and Stephanie E. B. McArdle*[7,8*]

[1] Université de Paris, PARCC, INSERM U970, 75015, Paris, France, [2] Laboratoire de Recherches Biochirurgicales (Fondation Carpentier), Assistance Publique-Hôpitaux de Paris (AP-HP), Hôpital Européen Georges Pompidou, Paris, France, [3] Ultimovacs AB, Uppsala, Sweden, [4] Department of Pharmaceutical Biosciences, Science for Life Laboratory, Uppsala University, Uppsala, Sweden, [5] Department of Immunology, Genetics and Clinical pathology Rudbeck laboratories, Uppsala University, Uppsala, Sweden, [6] The School of Science and Technology, Nottingham Trent University, Nottingham, United Kingdom, [7] The John van Geest Cancer Research Centre, School of Science and Technology, Nottingham Trent University, Nottingham, United Kingdom, [8] Centre for Health, Ageing and Understanding Disease (CHAUD), School of Science and Technology, Nottingham Trent University, Nottingham, United Kingdom

OPEN ACCESS

Edited by:
Brian J. Czerniecki, Moffitt Cancer Center, United States

Reviewed by:
Sylvie Bertholet, GSK Vaccines, United States
Dennis Klinman, National Institutes of Health (NIH), United States

***Correspondence:**
Stephanie E. B. McArdle
Stephanie.mcardle@ntu.ac.uk

Specialty section:
This article was submitted to Cancer Immunity and Immunotherapy, a section of the journal Frontiers in Immunology

Received: *08 October 2020*
Accepted: *23 December 2020*
Published: *17 February 2021*

Citation:
Cuzzubbo S, Mangsbo S, Nagarajan D, Habra K, Pockley AG and McArdle SEB (2021) Cancer Vaccines: Adjuvant Potency, Importance of Age, Lifestyle, and Treatments. Front. Immunol. 11:615240. doi: 10.3389/fimmu.2020.615240

Although the discovery and characterization of multiple tumor antigens have sparked the development of many antigen/derived cancer vaccines, many are poorly immunogenic and thus, lack clinical efficacy. Adjuvants are therefore incorporated into vaccine formulations to trigger strong and long-lasting immune responses. Adjuvants have generally been classified into two categories: those that 'depot' antigens (e.g. mineral salts such as aluminum hydroxide, emulsions, liposomes) and those that act as immunostimulants (Toll Like Receptor agonists, saponins, cytokines). In addition, several novel technologies using vector-based delivery of antigens have been used. Unfortunately, the immune system declines with age, a phenomenon known as immunosenescence, and this is characterized by functional changes in both innate and adaptive cellular immunity systems as well as in lymph node architecture. While many of the immune functions decline over time, others paradoxically increase. Indeed, aging is known to be associated with a low level of chronic inflammation—inflamm-aging. Given that the median age of cancer diagnosis is 66 years and that immunotherapeutic interventions such as cancer vaccines are currently given in combination with or after other forms of treatments which themselves have immune-modulating potential such as surgery, chemotherapy and radiotherapy, the choice of adjuvants requires careful consideration in order to achieve the maximum immune response in a compromised environment. In addition, more clinical trials need to be performed to carefully assess how less conventional form of immune adjuvants, such as exercise, diet and psychological care which have all be shown to influence immune responses can be incorporated to improve the efficacy of cancer vaccines. In this review, adjuvants will be discussed with respect to the above-mentioned important elements.

Keywords: cancer vaccine, adjuvant, immunotherapy, inflamm-aging, microbiota, immunosenescence

INTRODUCTION

Therapeutic cancer vaccines represent an attractive strategy to stimulate protective anti-tumor immunity in combination with standard therapies. Cumulative data have confirmed the efficacy of cancer vaccines in many murine tumor models, as well as in phase I and II clinical trials. In view of these promising results, numerous clinical trials are ongoing. **Figures 1** and **2** summarize open cancer vaccine trials, distinguished by trial phase, cancer type and vaccine type (**Figure 1**) and by adjuvant and combinatorial treatments used (**Figure 2**). However, cancer vaccines have not yet achieved significant clinical efficacy in

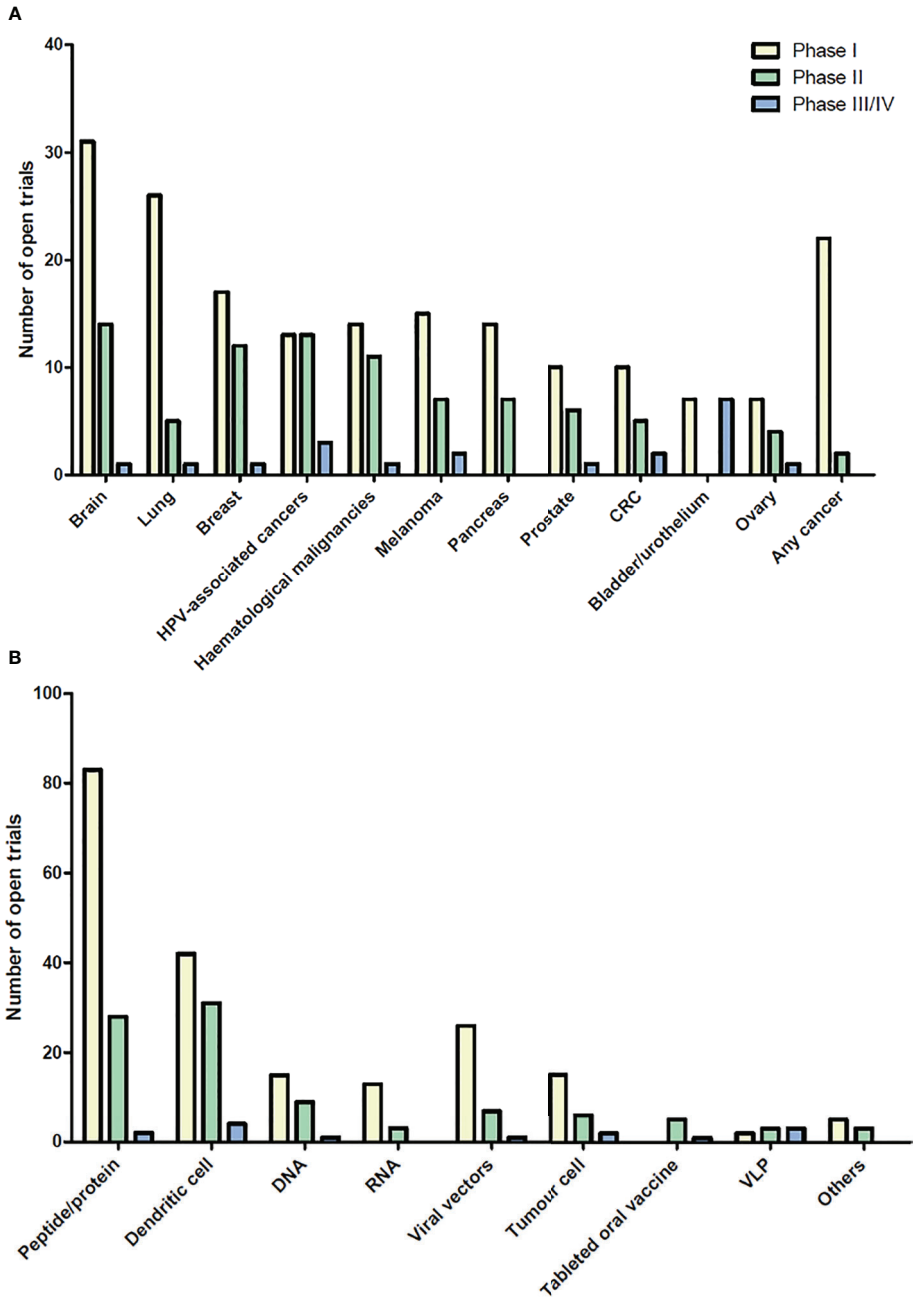


FIGURE 1 | Open cancer vaccine trials. Cancer vaccine trials listed as open at ClinicalTrials.gov on August 2020. The number of trials for each cancer type **(A)** and for each vaccine type **(B)** are shown in the bar graph subdivided into phase I, II, and III/IV. Viral vector vaccines include adenovirus and poxvirus, but also trials using yeast-loaded antigens and one using Salmonella-loaded antigens. Cancers with less than 5 open clinical trials are not shown. "*In situ* vaccinations" (intralesional injection of immune- modulatory molecules) are not included in these graphs. HPV, Human Papilloma Virus; CRC, colorectal cancer; VLP, virus like particle.

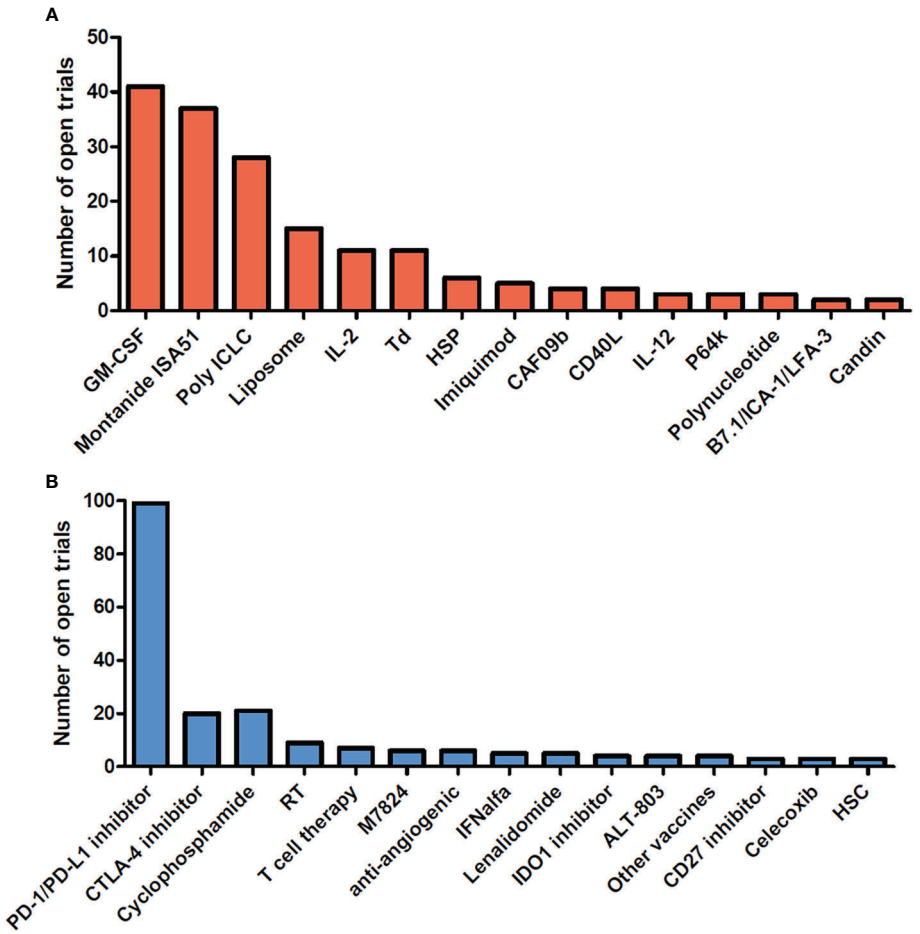


FIGURE 2 | Adjuvants and combinatorial immunomodulatory therapies being used in cancer vaccine trials. Cancer vaccine trials listed as open at ClinicalTrials.gov on August 2020. The number of trials using each adjuvant **(A)** and associating each immunomodulatory therapy with the cancer vaccine **(B)** are shown in the bar graph. Adjuvants and combinatorial therapies used in less than 2 clinical trials are not shown. GM-CSF, Granulocyte-macrophage colony-stimulating factor; IL-2, interleukin-2; Td, Tetanus/diphtheria toxoid; HSP, heat shock protein; CAF09b, cationic liposomes (DDA-MMG1) with complex bound synthetic double-stranded RNA (Poly(I:C)2); IL-12, Interleukin- 12; P64k, Neisseria meningitides protein; PD-1, Programmed cell death 1; PD-L1, Programmed cell death ligand 1; CTLA-4, cytotoxic T-lymphocyte-associated protein 4; RT, radiotherapy; M7824, fusion protein composed of a human IgG1 monoclonal antibody against PD-L1 fused with 2 extracellular domains of TGF-βRII; IFNalfa, Interferon alfa; IDO1, indoleamine 2,3-dioxygenase 1; ALT-803, IL-15 superagonist; Other vaccines, Salmonella, pneumococcal vaccines; HSC, hematopoietic stem cells.

phase III trials (**Table 1**). Indeed, clinical responses have been rather anecdotal (48, 49). The reasons for those failed trials are not fully understood but are most likely related to the stage of the disease treated, an inherent difficulty to mount a strong cellular immune response to non-live vaccine entities when older and the choice of antigens, adjuvant and the suppressive nature of the tumor microenvironment. Among these reasons, the difficulty of achieving strong cellular immune responses is likely a major factor to consider. In contrast to prophylactic vaccines against infectious agents that usually trigger humoral responses, therapeutic cancer vaccines aim to promote T cell immune responses for effectiveness. Moreover, very limited considerations have been given to the pharmacokinetic profile of the antigen/adjuvant administration strategy and, consequently, the required durable and effective long-term $CD4^+$ and $CD8^+$ T cell responses are not achieved. As mentioned, the developed tumor microenvironment is typically immunosuppressive and is characterized by the presence of exhausted T and NK cells and the accumulation of several suppressive immune cells, such as T regulatory cells, T helper type-2 (Th2) $CD4^+$ T cells, tumor-associated macrophages (TAMs), and myeloid-derived suppressor cells (MDSCs) (50–53), in addition to which the activation state of T cells will be regulated by co-inhibitory pathways. However, the approval of the first cancer vaccine (Provenge®) in 2010 spurred hope (54), as did the reported clinical effects and efficacy of checkpoint inhibitors in some advanced cancer patients. However, global availability of the former is limited as the EMA approval was withdrawn in 2015 (55) and the clinical efficacy of the latter is restricted to a few cancers. Nonetheless, many combination strategies involving immune-based therapies and checkpoint inhibition approaches are currently being tested in phase III

TABLE 1 | Completed phase 3 cancer vaccine trials.

Vaccine	Clinical trial (NCT number)	Cancer	Vaccine type	Antigen target	Adjuvant	Associated treatment	Control arm	Results: immunological response (from phase II and III)	Results: clinical efficacy? (from phase III)	References
Peptide vaccine	01989572	Melanoma	Peptide	tyrosinase, gp100, MART-1	Montanide ISA-51 GM-CSF	/	GM-CSF or Placebo	Cell-mediated (CD8)	No (PFS and OS)	(1)
MDX-1379	00094653	Melanoma	Peptide	gp100	Montanide ISA-51	+/- Ipilimumab	Placebo + ipilimumab	NA	No (OS) longer survival with Ipilimumab	(2)
gp100:209-217 (210M) peptide vaccine	00019682	Melanoma	Peptide	gp100	IL-2	/	IL-2	Cell-mediated (no correlation with OS)	Yes (PFS and ORR)	(3)
GSK1572932A	00796445	Melanoma	Peptide	MAGE-A3	AS15	/	Placebo	Antibody-mediated	No (PFS)	(4)
GM2-KLH	00005052	Melanoma	Ganglioside	Ganglioside GM2	QS-21 KLH	/	Observation	NA	No (PFS and OS) Detrimental outcome	(5)
CancerVax (CANVAXIN)	00052156 00052130	Melanoma	Allogeneic tumor cell	/	BCG	/	Placebo + BCG	NA	No (PFS and OS) Detrimental outcome	(6, 7)
Melanoma vaccine	01861938	Melanoma	Allogeneic tumor cell (expressing HLA A2/4-1BB ligand)	/	BCG	Cyclophosphamide	/	Cell-mediated (CD8)	Pending	(8)
Melacine	–	Melanoma	Allogeneic tumor cell lysate	/	Detox	/	Observation	Cell-mediated (CD8)	No (PFS and OS) Survival benefit in HLA-A2 and –Cw3 population	(9)
GSK1572932A	00480025	NSCL	Peptide	MAGE-A3	AS15	/	Placebo	Antibody-mediated (100%)	No (PFS)	(10)
Tecemotide (L-BLP25)	00409188	NSCL	Peptide	MUC1	Liposome	cyclophosphamide	Placebo and cyclophosphamide	Cell-mediated (no correlation with OS)	No (OS) Survival benefit in patients who received chemoRT and tecemotide	(11, 12)
rEGF-P64K/ Montanide ISA-51	00516685 01444118	NSCL	Protein	EGF	Montanide ISA-51 P64k	cyclophosphamide	Best supportive care	Antibody-mediated	Yes (OS)	(13)
Lucanix TM	00676507	NSCL	Allogenic tumor cells (transfected with TGF-β2)	/	/	/	Placebo	Cell- and antibody-mediated	No (PFS and OS); Positive trend in previously irradiated and early treated patients	(14, 15)
TG4010	00415818	NSCL	MVA (encoding MUC1 and IL-2)	MUC1	IL-2 (encoded by MVA)	Cisplatin and gemcitabine	Cisplatin and gemcitabine	Cell-mediated (CD8)	Pending From phase IIb study part: positive trend (PFS)	(16)
TG4010	01383148	NSCL	MVA (encoding MUC1 and IL-2)	MUC1	IL-2 (encoded by MVA)	Standard chemotherapy and bevacizumab if prescribed	Placebo + standard chemotherapy and bevacizumab if prescribed	Cell-mediated (CD8) (correlation with OS)	Pending From phase IIb study part: longer PFS and OS in patients with low peripheral baseline of activated lymphocytes (CD16+ CD56+ CD69+)	(17, 18)
Racotumomab	01460472	NSCL	Anti-idiotypic antibody	NeuGcGM3	Alum	/	Best supportive care	Antibody-mediated	Pending From phase IIb study part: Yes (PFS and OS)	(19)

(Continued)

TABLE 1 | Continued

Vaccine	Clinical trial (NCT number)	Cancer	Vaccine type	Antigen target	Adjuvant	Associated treatment	Control arm	Results: immunological response (from phase II and III)	Results: clinical efficacy? (from phase III)	References
BEC2	00003279 00006352 00037713	SCLC	Anti-idiotypic antibody	GD-3	BCG	/	Best supportive care	Antibody-mediated (no correlation with OS)	No (PFS and OS)	(20, 21)
GVAX®	00089856	Prostate	Allogenic tumor cells (secreting GM-CSF)	/	GM-CSF	/	Docetaxel and prednisone	NA	No (survival)	ClinicalTrials.gov
Sipuleucel-T/ Provenge	00005947	Prostate	DC	PAP	GM-CSF	/	Placebo	Cell- and antibody-mediated	Yes (OS) No significant difference in PFS	(22)
Sipuleucel-T/ Provenge	00065442	Prostate	DC	PAP	GM-CSF	/	Placebo	Cell- and antibody-mediated	Yes (OS) No significant difference in PFS	(23)
Sipuleucel-T/ Provenge	00779402	Prostate	DC	PAP	GM-CSF	/	Placebo	Pending	Not significant difference in time to biochemical failure Pending for OS results	(24)
DCVAC	02111577	Prostate	DC	/	/	Docetaxel and prednisone	Placebo + docetaxel and prednisone	Pending	Pending	ClinicalTrials.gov
PROSTVAC	01322490	Prostate	Poxviral vector (transfected with PSA and TRICOM)	PSA	TRICOM +/- GM-CSF	/	Placebo +/- GM-CSF	No (no detectable antibody responses to PSA)	No (PFS and OS)	(25, 26)
Intravesical BCG	00002990	Bladder	*in situ* vaccination	/	BCG	/	Different doses of BCG	/	No (OS)	(27)
intravesical BCG	00002490	Bladder	*in situ* vaccination	/	BCG	/	RT or mitomycin C	NA	No survival benefit with RT (versus BCG or chemotherapy)	(28)
Intravesical BCG	01442519	Bladder	*in situ* vaccination	/	BCG	Electromotive mitomycin	BCG alone	NA	Yes (PFS, OS) in BCG+ mitomycin group	(29)
Intravesical BCG	00330707	Bladder	*in situ* vaccination	/	BCG +/- IFN α	/	/	NA	Higher recurrence in patients with CIS, NRAMP1 D543N G:G, and the (GT)n allele 3 genotypes	(30)
GV1001 (TELOVAC)	00425360	Pancreas	Peptide	Telomerase	GM-CSF	Gemcitabine and capecitabine	Gemcitabine and capecitabine	Cell-mediated (CD4)	No (OS) on overall population, approved indication in South Korea using eotaxin levels as biomarker for patient stratification	(31)
HyperAcute-pancreatic (Algenpantucel-L)	01072981	Pancreas	Allogenic tumor cells (expressing murine α -gal epitopes)	/	/	Gemcitabine +/- 5FU chemoradiation	Gemcitabine +/- 5FU chemoradiation	Pending	Pending	(32)
PANVAC-VF	00088660	Pancreas	poxvirus vector (expressing CEA, MUC1 and TRICOM)	CEA, MUC1	GM-CSF	/	Best supportive care or palliative chemotherapy	Cell-mediated	Pending	(33)
FNHLId1	00091676	NHL	Protein	Ig idiotype	KLH GM-CSF	/	KLH + GM-CSF	Cell-mediated (CD4 and CD8)	Yes (PFS)	(34, 35)

(Continued)

TABLE 1 | Continued

Vaccine	Clinical trial (NCT number)	Cancer	Vaccine type	Antigen target	Adjuvant	Associated treatment	Control arm	Results: immunological response (from phase II and III)	Results: clinical efficacy? (from phase III)	References
FavId (Mitumprotimut-T)	00089115	NHL	Protein	Ig idiotype	KLH GM-CSF	Previous rituximab	Placebo + GM-CSF	Cell- (72%) and antibody- (20%) mediated	No (PFS and ORR)	(36, 37)
MyVax	00017290	NHL	Protein	Ig idiotype	KHL GM-CSF	Previous chemotherapy	KLH + GM-CSF	Antibody-mediated (41%)	No (PFS)	(38)
DCVax-L	00045968	GBM	DC	/	/	/	Placebo	Pending	Pending	(39)
Rindopepimut	01480479	GBM	Peptide	EGFRvIII	KLH GM-CSF	Temozolomide	KLH + temozolomide	Antibody-mediated	No (OS)	(40)
NeuVax	01479244	Breast	Peptide	HER2	GM-CSF	/	Placebo and GM-CSF	NA	No (PFS)	(41)
THERATOPE	00003638	Breast	Peptide	Sialyl-Tn	KLH Detox-B	cyclophosphamide	KLH-vaccine and cyclophosphamide	Antibody-mediated (correlation with OS)	No (PFS and OS)	(42, 43)
HSPPC-96/ vitespen	00033904	RCC	Autologous tumor-derived HSPPC-96	/	/	/	Observation	NA	No (PFS)	(44)
IMA901	01265901	RCC	Peptide	TUMAPs	GM-CSF	Cyclophosphamide and Sunitinib	Sunitinib	Cell-mediated (CD8) (no correlation with OS)	No (OS)	(45)
BCG	00427570	CRC	*in situ* vaccination	/	BCG	/	Observation or chemotherapy	NA	Yes (OS) compared to observation	(46)
Gardasil	02087384	Anus	VLP	HPV-6, 11, 16, 18	Alum	/	Placebo	Pending	Pending	ClinicalTrials .gov
Abagovomab	00418574	Ovary	anti-idiotypic antibody	CA-125	/	/	Placebo	Antibody-mediated	No (PFS and OS)	(47)

Phase 3 cancer vaccine trials listed as completed at ClinicalTrials.gov on August 2020. Immune responses results are reported as published in phase III data when available or in phase II respective data of the same vaccine and same authors group. 5FU, 5-fluoruracil; BCG, Bacillus Calmette–Guérin; CA-125, carcinoma antigen 125; CEA, Carcinoembryonic antigen; CRC, colorectal carcinoma; Detox, detoxified Freund's adjuvant; DC, dendritic cell; EGF, epidermal growth factor; GBM, glioblastoma; GM-CSF, Granulocyte-macrophage colony-stimulating factor; HER2, human epidermal growth factor receptor 2; HSPPC-96, Heat Shock Protein Peptide Complex-96; HPV, human papillomavirus; IL-2, Interleukin-2; Ig, immunoglobulin; KLH, keyhole limpet hemocyanin; MUC1, Mucin 1; MVA, modified vaccinia virus Ankara; NSCLC, non-small cell lung cancer; ORR, objective response rate; OS, overall survival; PAP, Prostatic acid phosphatase; PFS, progression free survival; PSA, Prostate-specific antigen; SCLC, small cell lung cancer; RCC, renal cell carcinoma; RT, radiotherapy; TGF-β2, Transforming growth factor-beta 2; TUMAP, PLIN2, APOL1, CCND1, GUCY1A3, PRUNE2, MET, MUC1, RGS5, MMP7, HBcAg; TRICOM, B7.1 + ICAM-1, InterCellularAdhesion Molecule-1 + LFA-3, Leukocyte function-associated antigen-3; VLP, virus like particle.

trials (**Table 1**, **Figure 2B**). In relation to the suppressive environment, a key factor is to initiate vaccination in tumor indications early on in the disease, non-metastatic, as the lesion size may impact the effectiveness of the treatment (56). This strategy is however hampered by lack of end-points that facilitates studies that fall within a time-frame that can be viable for the industry sponsored clinical trials.

Another potentially confounding issue with regards to the efficacy of cancer vaccines is age, given that the median age of cancer diagnosis is 66 years, and the immune system is known to decline with age. This phenomenon, known as immunosenescence, is characterized by functional changes in both innate and adaptive cellular immunity as well as in lymph node architecture. While many of the immune functions decline over time, others paradoxically increase. Indeed, aging is known to be associated with a low, but persistent level inflammation. "Inflamm-aging" also leads to dysregulation of innate and adaptive immune cells (57–59).

It is therefore essential that the choice of adjuvants is carefully optimized for each vaccine formulation, as well as for each patient, in order to break immune tolerance and achieve maximum immune responses and clinical efficacy, even in such a compromised environment. Most cancer antigens are poorly immunogenic and adjuvants are required to (i) prolong the antigen availability at the injection site ("depot" effect); (ii) activate the innate immunity; (iii) direct the immune response toward T helper type-1 (Th1) responses; and (iv) to mitigate the tumor/associated immune suppression (60, 61). Based on function, classical adjuvants have generally been divided into two categories: the immunostimulatory adjuvants (cytokines, Toll-Like receptor agonists, saponins …) and "depot" adjuvants (e.g. mineral salts such as aluminum hydroxide, emulsions, liposomes). Although practical, this classification is today rather simplistic since some delivery systems can also activate innate immunity by creating local proinflammatory reactions (62). Novel RNA-based vaccines have an inherited adjuvant capacity that has also been associated with problematic toxicity, handled by elegant design and formulation (63). As such RNA-based vectors, which have had so far been developed for cancer treatment, are now in a record development program reaching the society in response to the COVID-19 pandemic. This also sets the scene for many novel indications ahead (64, 65).

In this review, adjuvants approved for human use will be discussed with respect to the above-mentioned elements. Importantly, new forms of adjuvants including exercise, microbiota and the psychological status of the patient prior to immunization will also be discussed.

IMMUNOSTIMULATORY ADJUVANTS

Immunostimulant adjuvants likely constitute the most promising strategy to potentiate immune responsiveness in elderly cancer patients. Numerous defects in the innate and adaptive immune system have been indeed described in elderly individuals. Age-related reductions in levels of major histocompatibility (MHC) class II expression as well as dysregulation of cellular signaling in human and murine monocytes compromise the efficiency of antigen presentation to T cells (66–68). Studies on peripheral blood mononuclear cells (PBMCs) from elderly donors have also revealed that aged dendritic cells (DCs) have a reduced capacity for producing inflammatory cytokines in response to inflammatory stimuli, and particularly to several Toll-like receptor (TLR) ligands, as well as an impaired ability to present antigens to T cells (59, 69–71). Alongside defects in innate immune potential, numerous reports have described the phenomenon of T cell immunosenescence, an event which primarily results from thymic involution which leads to a contraction of the naïve T cell compartment and a predominance of terminally differentiated memory T cells in the periphery (72, 73). Other studies suggest that chronic latent infections, such as cytomegalovirus (CMV), could also play a crucial role in T cell immunosenescence in the $CD4^+$ T cell compartment, as well as in the naïve and memory $CD8^+$ T cell compartments (74, 75). Permanent CMV infection stimulates the expansion of CMV-specific memory $CD8^+$ T cells and could thus impact on the ability of an individual's T cells to elicit a response against new antigens (76). Additionally, the chronic inflamm-aging status observed with age has been associated with diminished expression of the costimulatory receptor CD28 on T cells because of persistently increased levels of TNF-α (77–79). CD28 is vital for efficient T cell activation, reduced levels of which have been correlated with poor immune responses after vaccination among older people (80, 81).

Cytokines

The use of cytokines in cancer immunotherapy and specifically in cancer vaccine formulations is becoming more prevalent as they can elicit both cellular and humoral immune responses. IFN-α, IFN-γ, IL-2, IL-12, IL-15, IL-18, IL-21 have especially demonstrated immunological efficacy when used as part of a vaccine adjuvant strategy (50). However, to date, GM-CSF (granulocyte macrophage colony-stimulating factor) is the immunostimulatory cytokine which has been most widely used in clinical vaccine trials (**Figure 2A**). GM-CSF has been reported to induce strong T cell responses as well as to inhibit tumor growth in both whole tumor cell and peptide vaccines in preclinical studies (82) by recruiting and activating antigen-presenting cells (APCs) at the injection site. However, GM-CSF as vaccine adjuvant has delivered conflicting results in clinical trials. In some trials, GM-CSF has shown only weak effects in potentiating immune response of cancer vaccine (83, 84) and in others no additional positive effect was reported when associated with Montanide (85, 86). However, the only FDA approved cancer vaccine, Provenge®, bases the adjuvant effect on a fusion protein that contains GM-CSF and reported an OS benefit in patients with metastatic castrate-resistant prostate cancer. However, in phase II and III trials testing Provenge®, the exact role/influence of GM-CSF over clinical efficacy was not thoroughly investigated. In addition, two trials containing GM-CSF in the vaccine formulation resulted in decreased cell-mediated immune responses and shorter survival of patients with melanoma (87, 88), however it is also possible that in this

instance the choice of antigen as well as formulation have had an impact on the results. Indeed, lower doses of GM-CSF in water formulations could shape the lymph node differently compared to a montanide based formulation. Interestingly, daily doses of GM-CSF over 100 μg/day given repeatedly have been reported to promote the expansion of myeloid-derived suppressor cells (MDSCs) and inhibit T-cell function (89). While GM-CSF as an adjuvant in prime/boost administration given at lower doses has shown good adjuvant capabilities and is an adjuvant commonly used in many vaccine formulations due to the expanded knowledge of the adjuvant (**Table 1**, **Figure 2A**).

Systemic use of cytokines such as IL-2 or GM-CSF in combination with other immunotherapies have also shown clinical efficacy (3, 90). It is therefore extremely important to optimize the schedule, formulation and the dose of cytokine in order to avoid/limit systemic side-effects.

Toll-Like Receptor Ligands

The stimulation of professional APCs such as neutrophils, B cells, macrophages and DCs is an efficient approach to boost the efficacy of cancer vaccines, especially in immunocompromised individuals, such as cancer patients and more generally the elderly. However, as indicated above, age-related deficiencies in monocyte and macrophage function mediated by functional dysregulation of cellular signaling, and specifically of Toll-like receptor (TLR) pathway have been described. Activation of APCs relies upon stimulation of pathogen recognition receptors (PRRs) by conserved pathogen-associated molecular patterns (PAMPs) expressed on microbes, or endogenous danger-associated molecular patterns (DAMPs) released by injured cells. TLRs recognizing PAMPs and DAMPs under physiological conditions are expressed either on the cell membrane (TLR1, -2, -4, -5, -6, and -10) or on endosomal membranes within the cell (TLR3, -7, -8, and -9) according to the ligand - membrane TLRs bind lipids and proteins whereas intracellular TLRs bind nucleic acids (91, 92). PRR activation induces the release of chemokines and inflammatory cytokines, the recruitment of innate and adaptive immune cells, and stimulation of the APCs themselves *via* the induction of costimulatory molecule expression, including B7.1 (CD80), B7.2 (CD86) and CD40.

Studies on peripheral blood mononuclear cells (PBMCs) from elderly donors have shown that that aged DCs have a diminished ability in producing cytokines in response to inflammatory stimuli, and particularly to TLR1/2 and TLR7/TLR9 ligands, as well as an impaired capacity for presenting antigens to T cells (69–71). Such deficiencies have been associated with a decreased activity of PI3K that results in aberrant activation of NF-kB and therefore a weak, but chronic inflammatory state characterized by continuous release of IL-6 and TNF-α cytokines (93), the so-called phenomenon of inflamm-aging. The overall result is a compromised ability of DCs to orchestrate an efficient adaptive immune response in elderly individuals (59).

In view of these defects on DCs, TLR ligands which mimic PAMPs represent promising adjuvant candidates for cancer vaccines in elderly individuals. Synthetic TLR3, TLR7 and TLR9 agonists are likely the best candidates, as they mimic viral RNA and DNA PAMPs (94) which generally generate robust cytolytic $CD8^+$ T-cell responses (95, 96). Specifically, TLR3 recognizes viral dsRNA and their synthetic analog Poly I:C (97, 98); TLR7 binds viral ssRNA, whereas TLR9 interacts with unmethylated CpG DNA from bacteria and viruses (91, 92). Three TLR ligands are FDA-approved for cancer therapy: Bacillus Calmette-Guérin (BCG), a TLR2/4 ligand, the TLR4 ligand monophosphoryl lipid A (MPLA) and the TLR7 agonist imiquimod. However, many other TLR agonists have proven their efficacy in pre-clinical and clinical studies.

The use of TLR agonists constitutes an efficient way to boost the efficacy and potency of cancer vaccines thanks also to their interaction with other immune and non-immune cells which can express TLRs, including T-cells and cancer cells. Indeed, poly I:C (TLR3 agonist) has been reported to stimulate the proliferation and survival of both CD4 and CD8 T cells in a CF-kB-dependent manner (99, 100). Additionally, in human $CD4^+$ Th cells, the stimulation of TLR7/8 and TLR5 by resiquimod and flagellin increases IFN-γ, IL-2, and IL-10 release and enhances proliferation in an APC-independent manner (101). Other studies have shown similar effects of TLR9 stimulation on the survival and proliferation of $CD4^+$ and $CD8^+$ T-cells. This effect was mediated by NF-kB signaling and was associated with increased expression of the anti-apoptotic protein Bcl-xL (99). Furthermore, TLR9 stimulation of $CD4^+$ T-cells can render them resistant to the immunosuppressive effects of regulatory T cells (Tregs) (102, 103).

Beside APCs and T cells, TLRs are also expressed by a multitude of cancer cells. Their direct effect on cancer cells is not completely defined, and probably much less important than their immune effects. The activation of TLR2 and TLR4 in cancer cells has been linked to tumor-promoting effects by promoting vascularization and cell invasion *via* the induction of COX-2, PGE2 and IL-8 (104, 105). Similar to TLR2 and TLR4, TLR7/TLR8 overexpression in lung cancer cells has been associated with pro-tumor effects through the activation of NF-kB and resulting in upregulation of inflammatory cytokines, the anti-apoptotic Bcl-2, the angiogenic VEGFR2 and several chemokine receptors associated with cell migration (106). TLR3 stimulation by Poly I:C or BCG has been implicated in promoting tumor cell death in a multitude of cancers, including breast cancer, colon cancer, bladder cancer, head and neck carcinoma, pharynx carcinoma, hepatocellular carcinoma, lung cancer and melanoma. TLR3 polymorphisms have also been linked to an increased risk of several cancers such as nasopharyngeal carcinoma, breast cancer, cervical cancer, and Hodgkin's disease (107). However, TLR3 activation has been reported to induce cancer progression as well by the induction of VEGF, MMP9 and uPAR *via* Myc- and MAPK signaling (108). TLR5 signaling on cancer cells has been reported to inhibit tumor growth in various cancers, including breast cancer (109), head and neck cancer (110) and colon cancer (111). On the contrary, TLR5 stimulation in gastric cancer cells, notably by H. pylori, has been reported to increase IL-8 production, tumor cell proliferation as well as TNF-α expression levels that can support the suppressive effects of Treg cells (112, 113). Depending upon tumor cell types, TLR9 activation

can stimulate or inhibit tumor cell proliferation (114–118) or induce caspase-dependent apoptosis (119, 120). The TLR9 agonist CpG-ODN has proved to be moderately effective in glioblastoma patients when injected intratumorally (121, 122).

In summary, various TLRs can be expressed on numerous cancer cell types and TLR3 and TLR5 appear to be the most promising adjuvants for combining direct anti-tumor properties with immunostimulant effects on APCs and T cells. However, the final effect of each TLR agonist relies on its immunostimulant properties. Therefore, the choice of the TLR agonist should be primarily driven by its ability to trigger T cell response in humans, which should be defined on a case-by-case basis for a given antigen.

Saponins

Saponin adjuvants are extracts from the plant *Quillaja saponaria* and possess potent inflammatory properties. QS-21 is the most commonly used adjuvant in vaccine formulations (123) and its immunogenicity has been attributed to the triterpene aldehyde group, which is capable of triggering the ASC/NALP3 inflammasome signaling and thus stimulating the conversion from precursor to activated forms of IL-1 β and IL-18 (124). The adjuvant QS-21 has been reported to elicit robust T-helper 1, $CD8^+$ T cell and humoral responses in preclinical studies. Besides such immunogenic properties, QS-21 strongly activates the inflammasome thus causing cell membrane lysis and apoptosis of APCs (124). QS21 has also been tested in clinical trials, mostly as adjuvant of cancer vaccines targeting ganglioside antigens and, despite strong humoral responses, no significant cellular immune responses were observed. Its efficacy in cancer vaccine appears thus limited.

QS-21 has also been used as part of more complex vaccine formulations combining multiple adjuvants, for instance ISCOMATRIX incorporating the saponin adjuvant with antigens in a micellar structure (125), and AS01 and AS15 combining QS-21 with MPL (126).

Stimulator of Interferon Genes Agonists

Stimulator of Interferon Genes (STINGs) are transmembrane proteins that induce a robust Type I IFNγ response upon activation and are expressed at the highest levels by T cells. STING activation can lead specifically to T cell apoptosis since DCs or macrophages do not exhibit such sensitivity (127). STING agonists are combined with adjuvant systems that specifically target myeloid cells (128) and are capable of reprogramming MDSCs towards a DC-like phenotype expressing IL-2 and co-stimulatory molecules (129). However, differential binding properties of these agonists to human and murine cells poses a challenge for the development of clinical strategies.

Ideally, implementation of STING agonists in cancer vaccines should be combined with potent adjuvant/delivery systems such as liposomes or polymeric nanoparticles or inorganic materials to minimize systemic dissemination that can cause toxic cytokine storm and limited bioavailability.

Currently, ADU-S100 and MK-1454 are being tested along with immune checkpoint inhibitors (ICIs) in early phase clinical trials in patients with advanced/metastatic solid tumors or lymphomas (NCT03172936, NCT03010176). Both require accessible lesions for intratumor injections to avoid systemic toxicity.

DELIVERY SYSTEM AS ADJUVANTS

The classical classification of delivery systems and immunostimulant adjuvants is practical, but not dichotomic since several adjuvants can act as a delivery platform for antigens, while also having some immunomodulating properties. Adjuvants traditionally classified in this category mainly act by improving antigen stability, preventing antigen degradation and finally optimizing its processing and presentation to T cells. The most important delivery system adjuvants and their mechanisms are described below.

Mineral Salts

Alum is by far the most used adjuvant in approved human vaccines against various infectious organisms (130). Aluminum-based adjuvants are traditionally classified as a delivery system type because their depot effect at the injection site leads to a slow release of the antigens. However, recent reports showed that alum is also capable of stimulating the innate immune response by activating the NLRP3/NALP3 inflammasome complex and triggering the release of uric acid (131, 132).

The adjuvant effect of alum in vaccines against infectious agents essentially results from an induction of a sustained Th2 response, as characterized by antibody production, but generally fails to mount a strong cellular (Th1)-based immune responses that are necessary for robust protective anti-tumor immunity. Hence, the use of aluminum-based adjuvants in cancer vaccines is of limited use (130). However, studies have been able to show that alum can also induce a cytotoxic immune response (133), as well as a clinical efficacy in cancer patients in terms of survival (racotumomab-alum vaccine directed against NeuGcGM3 tumor-associated ganglioside) (19). In addition, recent studies have shown that alum can elicit robust immune responses and have anti-tumor efficacy (in terms of inhibited tumor growth and prolonged survival) when used in nanoscale (134). Nano-aluminum adjuvants can indeed carry more antigens and more efficiently present them to antigen-presenting cells (APCs) in lymph nodes compared to traditional aluminum salt adjuvants which tend, instead, to remain at the injection site because of their positive charge and large particle size (135, 136).

Emulsions

Emulsions are typically classified as water-in-oil (W/O) or oil-in-water (O/W) formulations and mainly act as delivery system of antigens in the injection site, thereby allowing a slow and prolonged release of the latter. Nevertheless, they also have some immune adjuvant properties by inducing local inflammation and promoting the recruitment of APCs as well as their phagocytic uptake of antigen (137–139).

Complete Freund's adjuvant (CFA) was the first water-in-oil emulsion to be developed (1930). CFA is a highly potent adjuvant which contains heat-killed mycobacteria but induces

a strong local inflammation that often leads to ulceration at the site of injection. Given its adverse effects, CFA is not permitted for use in humans.

Incomplete Freund's adjuvant (IFA) is also a W/O emulsion, but without mycobacteria. IFA induces more manageable adverse events than CFA and is the "golden standard" of this group of adjuvants for assessing the immunogenicity of antigens in mice. IFA has proven to induce both cellular and humoral immune responses (140–143) and its human equivalent, Montanide ISA-51, has been and continues to be widely used in peptide cancer vaccine formulations in many trials (melanoma, renal carcinoma) (144, 145) (**Figure 2A**). Other studies, however, have shown negative effects of IFA and, more generally, of all W/O emulsions. The slow persistent release of the antigen coupled with the local inflammation induced by the emulsion itself can actually result in the sequestration of primed $CD8^+$ T cells at the injection site, when using short peptides, leading to limited T cell homing to the tumor and T cell tolerance (146–149). In addition, W/O emulsions are usually associated with Toll-Like receptor (TLR) agonists and numerous studies have reported a detrimental effect of W/O emulsion on T cell responses triggered by TLR agonists (150).

MF59 is an O/W squalene-based emulsion that is currently licensed for human influenza vaccines (151, 152). As for other adjuvants historically included in this group, MF59 also appears capable of triggering cellular and humoral responses. Indeed, MF59 can promote leukocyte recruitment by inducing macrophages and dendritic cells to secrete several chemokines. MF59 has proven to be effective in elderly subjects in human trials and is currently used in a flu vaccine for individuals > 65 years. The use of MF59 is limited in cancer vaccine strategies because of the primal Th2 response. However, in combination with CpG ODN (cytosine guanine dinucleotide oligodeoxynucleotides, TLR9 agonist), MF59 has proven to induce effective anti-tumor responses in several murine cancer models (94, 153).

Liposomes

Liposomes are phospholipid vesicles which are used as delivery carriers for antigen or also immunostimulatory adjuvants (154, 155). Allison and Gregoriadis, in 1974–1976 innovated the liposomes and since then all their derivative nanovesicles have become important delivery systems for vaccines. Positively charged liposomes have been reported to trigger more potent immune responses compared to negatively charged liposomes. This efficacy is attributed to both more efficient phagocytosis of positively charged liposomes by APCs (156) and reduced lysosomal degradation of antigens because of a higher pH (157). The key advantages of liposomes are their versatility, plasticity, biocompatibility, and biodegradability. Various choices for the composition and preparation can be achieved from a selection of lipids to target the desired charge, size, distribution, traveling and location of antigens or adjuvants for cancer vaccines (155). However, using liposomes for human applications is restricted due to the lack of stable manufacturing of vaccine-grade liposomes and their high cost (155, 158). To resolve these obstacles in co-formulation, a manufacturable, synergistic anionic liposome platform with TLR4/TLR7 agonists ready for use in clinical trials has been developed (159).

Many animal models using liposomes as delivery agents have shown that liposomal cancer vaccines have superior efficacy over the non-liposomal vaccines (158, 160, 161). In mice challenged with Lewis lung carcinoma cells, liposomal vaccines combining basic fibroblast growth factor and the adjuvant monophosphoryl lipid A (MPLA) induced tumor-specific antibodies and Th1-type immune responses (160). Liposomal delivery of the lipid antigen α-galactosylceramide induced anti-tumor immunity that was protective against lung metastases in 65% of B16 F10-tumor-bearing mice, by activating the NKT cells in the spleen (161). Park et al., developed a peptide-CpG-liposome complex vaccine which was proven to efficiently elicit humoral responses (anti-hTM4SF5 antibodies) and inhibit cancer growth in various murine tumor models (pancreatic cancer, metastatic hepatocellular cancer, colon cancer, lung metastasis model) (162). Liposomal vaccines have also been reported to elicit strong cytotoxic T lymphocyte (CTL) responses against tumor-associated peptides, as in the case of Lip-DOPE-P5-MPL, where the P5 peptide was encapsulated in a complex of 5 lipids (DMPC, DMPG, cholesterol, DOPE and MPLA) conjugated with maleimide-PEG2000-DSPE (163). In a mouse model of neuroblastoma, liposomal delivery of CpG ODNs has been shown to elicit potent anti-tumor effects, whereas the CpG-alone group failed (119). Liposomes were also proven to increase the uptake and stimulation of APCs leading to anti-tumor efficacy when used as delivery system of DNA or RNA complexes in mice (164). Recently, a novel lipopolyplex vector (multi-LP) was proposed for the *in vivo* delivery of mRNA by incorporating the immune adjuvant α-galactosylceramide (α-GalCer) and a multivalent cationic lipid to target the dendritic cells (DCs) without cell-specific functionalization or ligands (165).

In addition to the above, several clinical trials using liposomes as carrier system for vaccine have reported safety, capability of inducing prolonged antigen-specific $CD4^+$ and $CD8^+$ T cell responses, as well as prolonged survival in various cancers, including non-small-cell lung carcinoma (NSCLC) (166), melanoma (167, 168), follicular lymphoma (169) ovarian (170), breast and prostate cancers (171).

In conclusion, liposomes are versatile delivery systems which can load antigens, proteins, peptides, nucleic acids, and carbohydrates, as well as for the formulation of new types of vaccines targeting the lymphatic system or specific APCs such as macrophages or DCs.

Virosomes

Virosomes are spheres of natural or synthetic phospholipids (liposomes) incorporated into which are virus envelope phospholipids and viral spike proteins. They were identified in 1975, but the first virosome-based vaccine in humans was Inflexal V for influenza in 2009 (158). Virosome-based vaccines are currently commercialized as preventive vaccines for HPV16 and 18-related cancers (Cervarix™ and Gardasil®) (172, 173). Virosomes were widely utilized in cancer vaccines because they are incapable of replicating and therefore are not infectious but retain the ability of the parenting virus while carrying tumor-specific antigens to the APCs to induce immunity (174). Thus, virosomes increase the tumor-specific

antibody and T cell responses (175, 176), as has been observed in phase I clinical trial on metastatic breast cancer patients (177, 178). The main advantages of virosomes as efficient prophylactic and therapeutic agents are tissue targeting, immune activation and potentiation. Application of virosomes in cancer vaccine will open a new prospective with multiple safe advantages as a unique delivery system (179–181). Recently, adding magnetic agents to HA-virosomes has been proposed as a ground-breaking innovative platform for treating cerebral tumors by enabling targeting using an external magnetic field from a magnetic helmet (182).

Nanoparticles

Nanoparticle carriers have the advantage to specifically target the APCs by various formations and strategies. The main types of nanoparticle adjuvants under development include metals, carbon nanotubes and polymers.

Metallic nanoparticles have various advantages over polymers and liposomes thanks to their multifunctional properties such as their small particle size, superparamagnetic properties and biocompatibility. Metallic nanoparticles such as γFe2O3, Al2O3, TiO2, ZnO, and SiO2 enhance immune responses mainly by acting as antigen carriers that deliver directly to APCs. Specifically, γFe2O3 with a positive surface charge can be absorbed by proteins with negative charge, promote the immune response and enable labeling and tracking cells at the same time. Enhancing the cross-presentation ability of DCs and T cell activation confers great potential on superparamagnetic iron oxide nanoparticles as adjuvants. However, the mechanisms are still not well defined (183). Gold nanoparticle platforms have been more widely applied in tumor models, challenges with regards to approval from the Food and Drug Administration (FDA) remain a challenge for translating these into the clinical setting (184). Recently, gold nanoparticle surfaces were coated with high cargo density of polyelectrolyte multilayers or peptides to promote the antigen-specific T cell response (184, 185).

Carbon nanotubes are extensively used in cancer therapeutics due to their large surface area and good conjugation and encapsulation properties. In the field of cancer vaccines, carbon nanotubes have been especially proven to enhance the embryonic stem cell-based cancer vaccine response in murine colon cancer model (MC38) (186). Despite the encouraging results in pre-clinical studies, the use of carbon nanotubes in humans has been hampered by their potential toxicity. Conflicting data is indeed reported on carbon nanotubes biocompatibility and biodegradability (187).

Although *polymeric particles* have been used in product development for several decades, they have not until relatively recently been considered for vaccine development. However, PLGA (poly lactic-co-glycolic acid) nanoparticles have now been approved for human use by the FDA and the European Medicines Agency (EMA) after being considered as the most nontoxic and slowly degraded vaccine delivery system (188) for target-specific and controlled delivery of drugs, peptides, proteins, antibodies and genes in cancer. Linear polyethyleneimine was recently developed for chemical coupling of protein/peptide ligands to form nano-polyplexes with plasmid DNA or RNA which deliver the nucleic acids into the targeted cells without associated toxicity to healthy cells (189). The delivery of DNA and mRNA using such an approach has a number of advantages, including being safer alternatives to viral vectors, colloidal stability (190, 191) can be exploited using injection-free gene delivery systems (192–194), and the ability to modify with targeting moieties like mannose (195).

In addition to the main nanoparticles above-mentioned, other promising nanoparticles are under development as adjuvants in cancer vaccines. For instance, to enhance the tumor penetration capability, positively charged nanoparticles based on the most abundant polysaccharide in nature (chitosan) have been developed over two decades of research on very complex optimized systems. Also, synthetic melanin nanoparticles have been reported to be an innovative adjuvant for cancer vaccines, in that they efficiently localize to draining lymphoid tissues and exhibit strong immunostimulant properties when loaded with both short and long peptides in mice (196). A melanin-based vaccine in combination with a TLR9 has also proved to be a strong anti-tumor efficacy in cancer murine models and compares favorably with the classical formulation of IFA and TLR9 agonist (197).

Current nanoparticle-based strategies in cancer vaccination and immunotherapy vary. Therapeutic nanomaterials enhance the efficacy of cancer vaccines by increasing the lymphatic delivery of specific antigens or by combining targeting approaches with stimulating materials to synergize and/or modulate immune activation. Primarily, the nanocarriers load the adjuvants by hydrophobic or electrostatic interactions which elevate the immunogenicity of tumor antigens (198). The potential co-delivery of antigens and adjuvants such as TLR ligands to DCs can boost the induction of protective anti-tumor immunity. Thus, the therapeutic cancer vaccine becomes essentially a nano-package of antigen, adjuvant and nano-carriers. For instance, the aliphatic polyesters PLGA and poly-ϵ-caprolactone (PCL) have proven to be efficient vectors for increasing their uptake by DCs due to their critical size, surface charge, surface functionalization and route of administration (199, 200). However, the efficacy of such an approach was proven in minimal residual disease conditions instead of the typical clinical condition of large bulky tumors. The co-delivery of adjuvants with nano-based formulations enhances the cross-presentation and/or skews the immune responses to the desired $CD4^+$ T helper phenotypes. Specifically, cancer nano-vaccines co-deliver peptides and TLR9 agonists (201, 202), and gold nanoparticles the anionic TLR3 agonist poly I:C co-delivered with cationic antigen peptides (185). In addition, nanoparticles can support a combinational use of adjuvants to permit exploitation of synergy among certain TLR agonists (159, 203–205). A significant therapeutic example in a late-stage murine melanoma model has been combining the peptide epitope of tyrosine-related protein 2 (Trp2) and CpG-based nano-vaccine with siRNA against TGF-β, which is one of the major cytokines responsible for induction and maintenance of an immunosuppressive tumor microenvironment (206). Effective

cross-presentation was promoted using pH-sensitive delivery systems that retain their cargo under the physiological conditions and release antigens in the endosomal microenvironment (~pH 6) (207, 208). Alternatively, an oxidation-sensitive polymersome can respond to the oxidative environment of endosomes to trigger the delivery of antigens and adjuvants in the cytosol (209). Furthermore, modification of liposomes with a cell-penetrating peptide or gold nanoparticles with tumor antigens has also been shown to promote cross-presentation (210, 211).

Although several vaccination strategies have been tested *in vivo*, therapeutic benefits remain mixed and a huge gap between material research, preclinical experimentation and clinical reality remains. Further research into the use of PLGA are warrantied to bridge this gap (199). The delivery of whole-cell cancer vaccines has been accomplished using a PLGA matrix containing tumor lysate as the source of tumor antigens, granulocyte macrophage colony-stimulating factor (GM-CSF) for recruitment of DCs *in situ*, and CpG for DC activation. This PLGA matrix elicited antigen-specific $CD8^+$ T cells and increased both prophylactic and therapeutic anti-tumor efficacy (212). Alternatively, plasma membranes of tumor cells have been extracted and coated onto polymeric nanoparticle cores along with the TLR4 agonist MPLA as a tumor cell-mimicking cancer vaccine (198).

Although targeted delivery to DCs and the induction of $CD8^+$ T cell responses can be achieved using nano-vaccines consisting of CD40 Ab-modified nanoparticles (213), the efficiencies of DC-targeting and induction of adaptive immune responses require optimization as different DC subsets have characteristic sites of tissue residence, receptor expression profiles and functions (214). Moreover, targeting distinctive tissue sites such as murine lymphoid tissue-resident $CD8^+$ DCs and, for human, $CD141^+$BDCA-3^+ DCs and Langerhans cells requires further study for nano-vaccines (215, 216). The efficient draining of nanoparticle carriers to lymphoid tissues has been qualitatively and quantitatively demonstrated using fluorescent or contrast agent-based imaging. For example, a polyester nanoparticle system loaded with ovalbumin (OVA) has been labeled with a near-infrared probe (216), and PLGA nanoparticles have been designed to carry iron oxide particles conjugated with fluorophore-labeled peptide antigen (217). Additionally, synthetic melanin nanoparticles have efficiently localized to the draining lymphoid tissues and have potent immunostimulant properties when loaded with short or long peptides in murine models (196, 197). Delivery systems having different particle sizes composition, morphology, and surface chemistry of particles are promising candidates to be translated into clinics to confirm delivery to the draining lymphatics (218).

Novel Biomolecule-Based Targeting Strategies

To induce tumor immunity, Fc gamma receptor (FcgR) targeting strategies coupled with antigens have been explored for the purpose of activating both $CD8^+$ and $CD4^+$ T cells. FcgR cross-linking to improve T cell priming can be achieved *via* the formation of immune complexes *in vivo* (219). For vaccine purposes, the conjugating of a universal tetanus-derived synthetic peptide (minimal tetanus toxin epitope, MTTE) with viral or tumor derived antigens - also in the form of synthetic peptides - can facilitate immune complex formation and FcgR cross-linking which results in DC and T cell activation (220, 221). Alternative strategies to target DCs include fusion strategies based on IgG scaffolds that introduce antigen epitopes in the CDR region and vaccine delivery using a DNA based vector system with the aim to target the high affinity FcgRI (222, 223). The goal and advantage of these technologies is to provide a single drug entity which can harness both the adjuvant and targeting of the antigen to APCs, as well as the potential antigen half-life extension that the methodology provides. It also ensures that HLA/peptide off-rate is not the determining factor for antigen delivery to the lymph node. The challenges presented by these approaches are the species differences in the receptor and immunology biology as well as the costly production of, for example, antibody-based therapies, if used as such.

COMBINATORIAL STRATEGIES TO IMPROVE CANCER VACCINE EFFICACY IN THE IMMUNOSUPPRESSIVE CONTEXT OF CANCER PATIENTS

Combining Different Adjuvants to Induce More Extensive Immune Responses

The ideal adjuvant for a cancer vaccine formulation should (i) protect antigens from degradation, (ii) stimulate efficient uptake of the antigens by APCs, (iii) activate these APCs to efficiently present the antigen to T cells in order to trigger a strong Th1/CTL response and long-term memory T cells. One single adjuvant may not provide all of these effects at the same time. Thus, a combination of a delivery system adjuvant and an immunostimulant adjuvant is commonly chosen for cancer vaccine formulation (**Figure 3**). For instance, montanide (for depot effect) and a TLR ligand (for APC stimulation) constitutes a common combination of adjuvants for anti-cancer vaccine (224). Based on preclinical studies, combining several TLR agonists or anti-CD40 antibodies with a TLR ligand could potentiate the adjuvant effect by activating different APCs simultaneously and further inducing more extensive $CD8^+$ T cell responses (225–227). However, the realization that formulations and the design of the antigen can negatively influence the expansion of a systemic immune response is of importance and should trigger in depth characterization of both the design and physiochemical properties of vaccine components, and the pharmacokinetic profiles and administration dose and schedule, to achieve proper anti-tumor responses.

Another strategy to enhance the efficacy of cancer vaccines could be combining it with systemic immunostimulatory agents such as cytokines, especially IL-2 or GM-CSF. Systemic IL-2 in combination with gp100 peptide-vaccine in patients with melanoma has delivered significant efficacy in terms of

objective response and progression-free survival compared to IL-2 monotherapy. However, at such high doses, IL-2 caused numerous toxicities if not formulated correctly (3).

Blocking VEGF to Restore Tumor Vessels and Promote T Cell Homing to Tumors

Following the induction of peripheral immune response by cancer vaccine, specific anti-cancer T cells need to penetrate the tumor to attack cancer cells. Unfortunately, the tumor vasculature is reported to express reduced levels of leukocyte adhesion molecules, such as intercellular adhesion molecule-1 (ICAM-1) and vascular cell adhesion molecule-1 (VCAM-1), and an aberrant overexpression of immune checkpoints including PD-L1, the death receptors FasL and TRAIL, and IDO, all of which impede the infiltration and function of activated T cells into/in the tumor microenvironment (228).

Anti-angiogenic treatments such as bevacizumab (vascular endothelial growth factor—VEGF—inhibitor) have been reported to restore a normal vasculature within tumors and increase the expression levels of ICAM-1 (229). Additionally, VEGF has also been proven to inhibit T cell and DC activation (230, 231). Therefore, combining an anti-angiogenic treatment such as bevacizumab (VEGF inhibitor) with vaccine seems a valid strategy to enhance the anti-cancer T cells (triggered by the vaccine) homing to tumor. Other molecules such as all-trans retinoic acids, anti-inflammatory triterpenoid, tyrosine kinase inhibitors (sunitinib), IL-12 and anti-IL-6R antibodies, anti-CSF-1R, anti-CCL2 have been reported to reduce tumor infiltration by MDSCs and improve the efficacy of cancer vaccines (232–237). Finally, STING agonists possess the ability to convert MDSCs from a suppressive into a type-1 immune profile (129).

Depletion of Immunosuppressive Leucocyte Populations by Combining Chemotherapy With Cancer Vaccines

Chemotherapy has long been considered to conflict with immunotherapies due to its leucocyte depleting effect. However, several peripheral and intratumoral leucocyte populations have immunosuppressive properties, thus reducing the efficacy of tumor-reactive cytotoxic T lymphocytes CTLs. A therapeutic strategy could thus rely on combining therapeutic cancer vaccine with leucocyte-depleting chemotherapeutics that target such populations.

Regulatory T (T reg) cells are particularly known for inhibiting CTL functions through the release of the anti-inflammatory IL-10, FGF-B and adenosine as well as the 'consumption' of IL-2 in the microenvironment, thereby reducing its availability for T cells. Combining cancer vaccines with molecules that can reduce the number of Treg cells, such as cyclophosphamide or low dose temozolomide (TMZ) thus constitutes another valid approach to improve the efficacy of anti-tumoral CTLs (126, 238, 239). Several studies indicate that 3–7 days after these chemotherapies may be the best timing to administer the cancer vaccine (84, 240, 241).

MDSCs represent another immunosuppressive leukocyte population frequently found in the tumor microenvironment which can limit the efficacy of anti-tumoral CTLs. Several myeloablative chemotherapeutics are known to decrease both

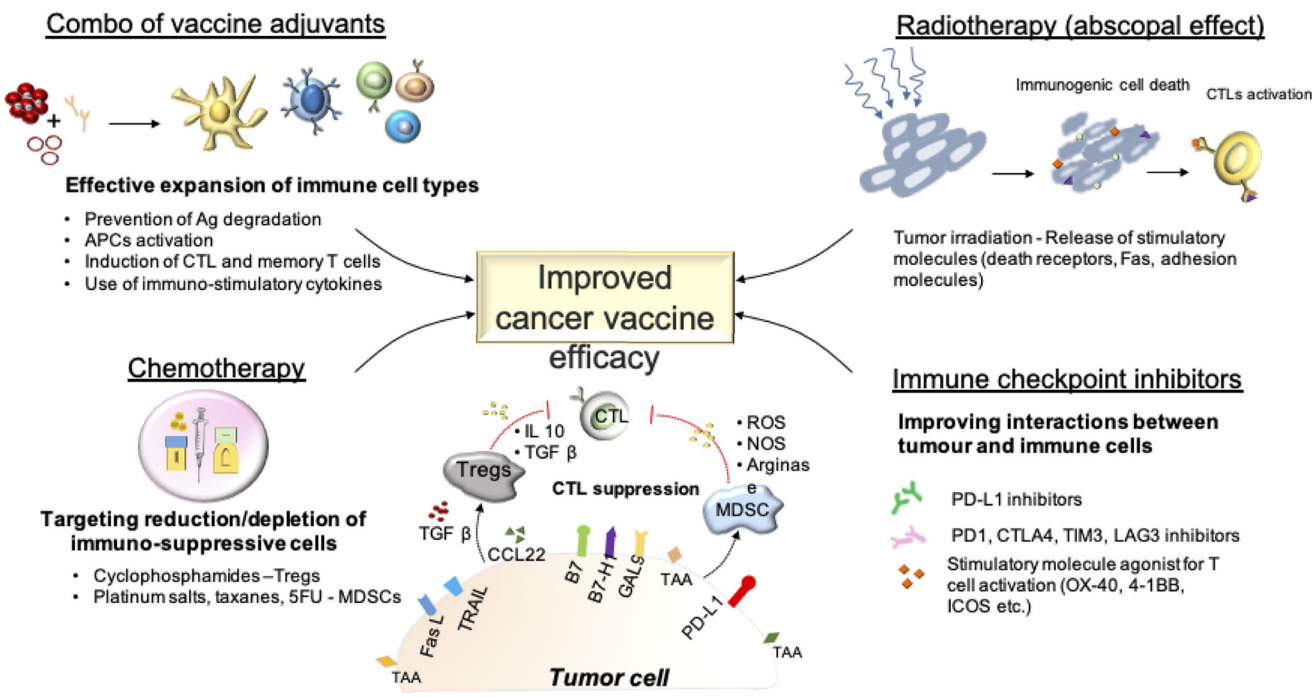


FIGURE 3 | Improving the efficacy of cancer vaccines: Combinational approaches.

peripheral and intra-tumor MDSCs, such as platinum salts, taxanes, gemcitabine, 5-Fluorouracil (242–244). The rationale of combining chemotherapy with therapeutic cancer vaccines to deplete MDSCs and boost vaccine-induced CTL responses has been reported in several studies (84, 238, 245). Specifically, in carboplatin-paclitaxel regimen the normalization of myeloid cells begins 2 weeks after the second cycle of chemotherapy and the administration of cancer vaccine at this point resulted in stronger vaccine-induced responses in preclinical and clinical studies (246–249).

Other studies reported improved anti-tumor responses also when chemotherapeutic agents were given simultaneously with the vaccination, as in the case of metronomic cyclophosphamide (170) or association of cyclophosphamide, paclitaxel and docetaxel (250). Given these results, the optimal schedule may be starting with chemotherapy cycles and following with concomitant chemotherapy and vaccination.

Enhancing Cytotoxic T Lymphocyte Function by Combining Cancer Vaccines With Immune Checkpoint Inhibitors

Immune checkpoint inhibitors (ICIs), including antibodies against programmed cell death protein-1 (PD-1) or its ligand (PDL-1) and cytotoxic T-lymphocyte antigen-4 (CTLA-4) have proven to enhance anti-tumor immunity and efficacy in several cancers. However, a large subset of patients does not benefit from ICI therapy, with a reported objective response rate for anti-PD1 varying from almost absent (pancreatic cancer, glioma, microsatellite-stable colon adenocarcinoma) to 15–30% for most cancers, and 50–80% for few cancers including melanoma, Hodgkin lymphoma, squamous cell carcinoma and Merkel carcinoma (251). This low response rate observed in most cancers is likely related to a limited specific T cell response developed against cancer cells, especially for tumors with a low mutational burden. Therefore, combining a cancer vaccine, which can elicit specific T cell responses, and ICIs represents an attractive therapeutic option. Based on positive results in preclinical models (252–254), several clinical trials are now evaluating novel personalized vaccines against neoepitopes specific of each patient in combination with ICIs (NCT02950766, NCT02897765, NCT03289962) (**Figures 2B** and **3**). However, few studies address the point of the choice of a specific molecule. One preclinical study reported that anti-4-1BB antibody was superior to achieve anti-tumor efficacy in combination with peptide cancer vaccine compared with other immunomodulating antibodies (255). Also, the timing of combination therapy is rarely discussed in clinical trials, but some reports suggest that immune checkpoint inhibitors better synergize with the vaccine when administered at the time of the boost rather than at the prime (256).

Combining Cancer Vaccine With Radiotherapy to Favor Antigen-Presentation by Cancer Cells

Numerous studies have shown the immunogenic properties of radiotherapy. Tumor irradiation can indeed induce immunogenic cell death (ICD) (257, 258) and thus lead to tumor regression even at distance sites, the so-called abscopal effect (259, 260). Additionally, radiotherapy has been reported to stimulate the expression of several molecules in cancer cells including MHC class I, death receptors, adhesion molecules, Fas, thus promoting CTL-mediated killing (261, 262). Therefore, combinatorial strategies of irradiation with the therapeutic cancer vaccine also constitute an attractive treatment option (263–265) (**Figures 2B** and **3**). However, radiotherapy is also responsible of reducing tumor infiltrating effector cells during the radiation regimen (266). Yet, the ultimate effect of radiotherapy synergizing with cancer vaccines is partly due to the vessel normalization that allows a better infiltration of T cells enhanced by the vaccine (267). Another preclinical study reported the best efficacy of vaccine when is administered 5 weeks after radiotherapy (268). In light of these findings, the combinatorial strategy of radiotherapy and cancer vaccine has more potential to succeed when radiotherapy is given first, followed by the vaccine (269).

UNDERSTANDING AND MANIPULATING THE PATIENTS' "LIFE-STYLE" TO INCREASE VACCINE POTENCY

Although life expectancy has increased in Europe over the last 30 years, the so called "healthy life expectancy" has not, and many suffer from some form of chronic disease in the last 9–11 years of their life after the age of 65. In fact, 85% of deaths are caused by chronic diseases such as cancer, cardiovascular disease, chronic respiratory disease, diabetes, and mental illness, with 70 to 80% of healthcare costs being dedicated to the treatment and management of these conditions and diseases. Moreover, whereas cardiovascular diseases are the main cause of death after the age of 65, cancer remains the first and second cause of death before and after the age of 65 respectively. Risk factors known to be involved in chronic disease include repeat infections, obesity, diet, tobacco, radiation and environmental factors, all of which induce chronic disease through the induction of inflammation. Correctly regulated acute inflammation is the normal response to pathogens, irritants or damaged tissue, whereas chronic inflammation results from a failure to completely eliminate the pathogens, the inability to enzymatically remove the irritant, the body turning against self-proteins. However, chronic inflammation can also be the results of recurrent acute inflammation. In recent years, the importance of the microbiota has been revealed, including alterations during chronic inflammation. Furthermore, more recent work has highlighted how a disturbed microbiota cannot only play a part in exacerbating inflammation but can drive the process. For example, in immunotherapy against cancer, studying a patient's intestinal microbiota composition can be used to stratify patients into "responders" *versus* "non-responder" according to their intestinal microbiota composition (270, 271). Indeed, in the study from V. Gopalakrishnan et al., 2018 (271), patients with metastatic melanoma who responded

to anti-PD1 treatment, with longer progression-free survival, were found to have a higher diversity of bacteria as well as a significantly higher number of the *Ruminococcaceae* family in their fecal microbiota. Interestingly, the prevalence of this family of bacteria increases during alcohol abstinence and inversely correlates with intestinal permeability (272). This species has also been shown to have *in vitro* and *in vivo* anti-inflammatory properties (273). Importantly, similar studies in mice have demonstrated that response to treatment could be transferred from responders to non-responders *via* fecal transplantation into tumor-bearing germ-free mice (271). However, other studies have shown the importance of other bacteria such as *Bifidobacterium longum*, *Collinsella aerofaciens*, and *Enterococcus faecium*, and *Akkermansia muciniphila* the latter being systematically found in higher number in patients with advanced melanoma who respond to anti-PD-L1 treatment (274), whereas patients with advanced urothelial carcinoma, non-small cell lung cancer, and renal cell carcinoma who received antibiotics before, during and after treatment all experienced reduced progression-free survival and lower overall survival rates, thereby demonstrating the importance of not disturbing the microbiota (275).

Most cancer vaccines, including cancer vaccines, will require some form of adjuvant to either induce/boost a response, increase the speed of the response, allow for a more reduce dose to be used and/or reduce the number of immunizations. In view of the importance/influence the microbiota on a person's overall wellbeing and the immune system in particular, it is of prime importance to understand ways to improve this biodiversity, as well as to increase the number of "beneficial" bacteria present in the patient's intestinal microbiota before, during and after vaccination. Increasing the diversity of bacteria within the intestinal flora has been shown to improve metabolic and immunological functions (276). No clear data is available about cancer vaccine, but the efficacy of vaccination against several pathogen has been clearly correlated with microbiota. Microbiota can indeed act as a natural vaccine adjuvant and specifically as ligand for different TLRs. Flagellin (TLR5 ligand) from microbiota seems to play a crucial role since levels of TLR5 have been correlated to the magnitude of humoral response (277). Recently, microbiota has also been reported to enhance anti-tumor response when used as a real cancer vaccine adjuvant in a murine model [EGFR vIII-expressing Listeria vaccine, (278)].

In light of these results, the use of probiotics, or novel genetically modified bacteria, may improve the efficacy of cancer vaccine. In addition, the microbiota is sensitive and will respond to physiological changes taking place in the host due to internal and external factors such as lifestyle, exercise, diet and the physiology of the host and this, in turn, will influence the well-being of the host. Exercise has already been shown to have a role in reducing the risk of cancer, and to be associated with a lower incidence of cancer and a lower risk of recurrence (279, 280). These effects and associations have been linked with the ability of exercise to influence immune cells such as NK, T cells, B cells and DCs, all of which have been found at a higher density within the tumors of animals who had been allowed to freely use an exercise wheel (281). Out of all these cells, NK cells (which express the highest number of β-adrenergic receptors) were the most sensitive to exercise, in that they were recruited within minutes after the start of exercise (282). These effects were shown to be driven, at least in part, by exercise-induced increases in catecholamine production (282). Moreover, the relationships between the hypothalamic-pituitary-adrenal (HPA) axis, the autonomic nervous system and the immune system and its effect on the microbiota have previously been neglected and certainly never been taken into account prior to, or during cancer vaccine treatment. Yet, this Gut-Brain axis is bi-directional whereby gut-microflora and brain communicate and are influenced by each other's signals *via* neural, endocrine, humoral and immune links. Therefore, as highlighted above, activities such as exercise which increases the level of neurotransmitters such as catecholamines, and the consumption of certain food such dietary fibers which will increase the production of short chain fatty acids such as butyrate, generated by anaerobic bacteria during fermentation which in turn will influence the production of neuropeptide such as NPY, will have a significant impact on the activation or suppression of certain immune cells. Butyrate itself is a histone deacetylase inhibitor that has been shown to suppress tumor growth (283–285). NPY receptors are widely expressed on immune cells, especially Y1R, which exists on almost every type of immune cells, and have an important yet diverse role on the immune system, having both negative as well as activator functions (286) [For a full review on the immunomodulatory activity of NPY please read Chen et al. (287)]. Targeting selectively certain neuropeptide receptors will therefore open more drug development to improve vaccine potency as well as offer novel vaccine deliver system.

NPY levels often increase during stress responses, and NPY receptors are shown to be overexpressed by many well-innervated cancers such as prostate cancer, the trans-differentiation of which into aggressive neuroendocrine prostate cancer (NEPC) after a long period of androgen-deprivation-therapy (ADT) treatments often leads to metastasis progression and incurable disease. NEPC expresses high levels of β2-adrenergic receptors (ADRs) which can be activated by adrenergic signals triggered by depression or chronic stress, which is prevalent in men with prostate cancer. Improving the efficacy of immunotherapies will therefore require approaches to attenuate the immunosuppressive nature of the tumor microenvironment (TME), increase the biodiversity and the number of "good" bacteria as well take into account the impact of depression and chronic stress.

Although the precise mechanisms underlying such intricate connections are only now starting to be elucidated there is absolutely no doubt that they will need to be carefully assessed if one wants to achieve optimum vaccine efficacy. However, most of the scientific vaccine community is now focused on the microbiota, forgetting the rest of the axis.

Therefore, future successful cancer therapy as well as vaccination strategies may be those that approach the therapy

using both an effective vaccine but also include therapeutic strategies that influence the life-style impacting the immune system.

CONCLUSIONS

Therapeutic vaccines represent an attractive strategy to stimulate the immune system against cancer in combination with standard therapies. However, multiple cancer vaccines have not yet achieved significant clinical efficacy. Their limited efficacy is certainly in part related to the poor immunogenicity of the vaccine itself in many cases, but also to the difficulty of inducing an effective immune response in the compromised immune system of cancer patients. Indeed, cancer cells successfully grow by establishing an immunosuppressive tumor microenvironment to protect themselves from host's immune attack. To add to this the median age of cancer patients is 66 years old and the immune system is known to become less efficient and more dysregulated as people age. However, while on the one hand the immune system declines over time, a phenomenon known as immunosenescence, aging is also known to be associated with a low, but persistent level of inflammation, inflamm-aging, which also leads to dysregulation of innate and adaptive immune cells. Therefore, the choice of adjuvants in vaccine formulations needs careful optimization for each vaccine as well as for each patient if the maximum immune response and clinical efficacy in such a compromised condition is to be achieved. Globally, given the crucial role of CD8+ T cells in tumor control, adjuvants capable of eliciting cellular response, rather than humoral, are certainly preferable. Indeed, levels of CD8+ T cells induced after cancer vaccine have been correlated with tumor regression in both murine and clinical studies (256, 288). More specifically, promising adjuvants are those that proved to favor dendritic cells maturation (the principal APC in tumor context) and cross-presentation. Among the formers, STINGs and TLR agonists (especially CpG, albeit more in mice than in human and poly I:C) demonstrated the most encouraging results. The induction of DC maturation is in fact a crucial point in vaccine strategy to avoid self-antigens tolerance. In addition, given the defects on DCs described in elderly individuals, TLR ligands likely represent the most promising immunomostimulatory adjuvant candidates for cancer vaccines in these patients. Beside the maturation of DCs, the ideal vaccine formulation should also favor the cross-presentation of antigens to CD8+ T cells by DCs. In that respect, several vectors are under development. Although live vectors from virus or bacteria can efficiently induce cross-presentation of antigens, the vector itself being immunogenic, elicits an immune response. Therefore, after the first dose of vaccine, the subsequent boost doses need to use different vectors in order to overcome the neutralization of vectorized vaccine by host immunity. Consequently, this approach has limited prospects in clinical practice. Other not live vectors showed interesting results in mice, such as liposomes, virosomes or nanoparticles. They have the advantage of being able to deliver different source of antigens (RNA, DNA, proteins, peptides, …) and adjuvants and also be immunostimulatory by assembling both molecules in a package and carry it to secondary lymphoid organs. Compared to classic depot adjuvants such as IFA or MF59, these vectors, allow antigens to reach directly the lymph nodes in order to induce a more efficient cross-presentation between DCs and T cells. The use of these adjuvants may thus overcome the detrimental effect that some study reported for W/O emulsions, related to the persistent release of antigen and the inflammation in the injection site. In fact, if in one hand the slow release of antigen may promote a stronger immune response, on the other hand it can lead to T cell anergy if DCs are immatures or T cell sequestration at the injection site has occurred. However, although very promising, vector adjuvants have not yet demonstrated convincing efficacy in humans.

In the light of these results, not-depot adjuvants are thus preferable, but the schedule of this particular type of vaccination is still a crucial point, and unfortunately not directly addressed in clinical trials and only rarely in pre-clinal studies. A too short period between boost and priming vaccinations might indeed lead to immunological tolerance against the antigens. In a mouse model, Wick *et al.* reported a decline of response from 30% to 15% (circulating specific T cells) by day 10 of daily vaccinations with a formulation using poly I:C and OVA protein (289). Another study by Stark *et al.* showed similar results in a B16-OVA melanoma model using a vaccine formulation with archae liposoms (archaeosomes) (290). In this study, the authors vaccinated mice with a regular interval of 0, 21, 42, 72 and 110 days and a decline of response was seen after the third dose. However, beside the potency of immunological response (amount of specific T cells) induced at the time of vaccination, it is also important to achieve a prolonged tumor protection. This latter has been particularly correlated with a central memory phenotype ($CD62L^{high}$) of vaccine-induced T cells, rather than effector memory ($CD62L^{low}$). In that respect, interestingly, in the prophylactic model of Stark *et al.* even if a single dose of vaccine triggered a lower frequency of antigen-specific CD8 T cells than multiple doses, the late tumor protection was similar (tumor challenge on day 323). These results highlight the importance of the quality of the immunological response besides the quantity.

Lastly, different combinatorial approaches are being explored trying to enhance the efficacy of the vaccine. Despite the numerous encouraging results in pre-clinical studies, clinical responses to cancer vaccine as monotherapy have been rather anecdotal so far and they are mostly reported in case of pre-neoplastic lesions or low tumor burden. However, the goal of a therapeutic cancer vaccine should be to improve survival in patients with advanced cancers. In this common situation, the immune response elicited by the vaccine needs to be particularly strong to face the suppressive nature of the tumor microenvironment and more generally the immunocompromised system of the patients in this context, associating different adjuvants, especially an immunostimulatory molecule with a vector adjuvant, may certainly improve the efficacy of the vaccine. In addition, combining cancer vaccine with other treatments is more likely to succeed, but early intervention may also be of value. Several combinatorial strategies are being explored, such as with anti-

angiogenic treatments to promote T cell homing to tumors, with immune checkpoint inhibitors to enhance CTL function, and also with standard anti-cancer therapies such as chemotherapy to deplete immunosuppressive leucocyte populations, and radiotherapy to favor antigen-presentation by cancer cells. As mentioned, a crucial point, rarely addressed in clinical trials, is the optimal timing of such therapies. In the light of the synergic mechanism specifically involved, therapies acting through the clearance of immunosuppressive cells such as radiotherapy and chemotherapy should be given prior to vaccination, whereas immunostimulatory agents enhancing the anti-tumor response of the vaccine should be administered concomitantly with the vaccine (preferentially at the boost dose) as in the case of immune checkpoint inhibitors. It may also be favorable to use vaccines in combination with early surgical intervention as the size of the lesion may hamper effective infiltration into the tumor. If the early intervention is used, then therapy effects could be achieved without a risk for immune suppression. Also, the host is less likely to have been negatively impacted by the tumor, immobilization and/or toxic drugs, making the patient more likely to still have a healthy and functional immune system.

In addition to these more traditional approaches, more clinical trials should consider implementing changes in the diet/exercise/stress level of the patients, while the patients are recovering from other more aggressive form of treatments (chemotherapy, radiotherapy) in order to re-establish a functional more effective immune system prior to the administration of a vaccine and carefully monitor the effect these will have on the diversity/quantity of their microbiome and their immune status, before and after vaccination in order to assess their impact and overall benefit for the patients.

AUTHOR CONTRIBUTIONS

SC, KH, and SMc wrote the initial draft, with DN, SMa, and AP making significant contribution. All authors discussed and reviewed the content.

ACKNOWLEDGMENTS

The authors' laboratories are financially supported by the John and Lucille van Geest Foundation, PROSTaid, and Plan Cancer 2018 «Soutien pour la formation à la recherche translationnelle en cancérologie».

REFERENCES

1. Lawson DH, Lee S, Zhao F, Tarhini AA, Margolin KA, Ernstoff MS, et al. Randomized, Placebo-Controlled, Phase III Trial of Yeast-Derived Granulocyte-Macrophage Colony-Stimulating Factor (GM-CSF) Versus Peptide Vaccination Versus GM-CSF Plus Peptide Vaccination Versus Placebo in Patients With No Evidence of Disease After Complete Surgical Resection of Locally Advanced and/or Stage IV Melanoma: A Trial of the Eastern Cooperative Oncology Group-American College of Radiology Imaging Network Cancer Research Group (E4697). *J Clin Oncol* (2015) 33(34):4066–76. doi: 10.1200/JCO.2015.62.0500
2. Hodi FS, O'Day SJ, McDermott DF, Weber RW, Sosman JA, Haanen JB, et al. Improved survival with ipilimumab in patients with metastatic melanoma. *N Engl J Med* (2010) 363(8):711–23. doi: 10.1056/NEJMoa1003466
3. Schwartzentruber DJ, Lawson DH, Richards JM, Conry RM, Miller DM, Treisman J, et al. gp100 peptide vaccine and interleukin-2 in patients with advanced melanoma. *N Engl J Med* (2011) 364(22):2119–27. doi: 10.1056/NEJMoa1012863
4. Dreno B, Thompson JF, Smithers BM, Santinami M, Jouary T, Gutzmer R, et al. MAGE-A3 immunotherapeutic as adjuvant therapy for patients with resected, MAGE-A3-positive, stage III melanoma (DERMA): a double-blind, randomised, placebo-controlled, phase 3 trial. *Lancet Oncol* (2018) 19 (7):916–29. doi: 10.1016/S1470-2045(18)30254-7
5. Eggermont AM, Suciu S, Ruka W, Marsden J, Testori A, Corrie P, et al. EORTC 18961: Post-operative adjuvant ganglioside GM2-KLH21 vaccination treatment vs observation in stage II (T3-T4N0M0) melanoma: 2nd interim analysis led to an early disclosure of the results. [Abstract]. *J Clin Oncol* (2008) 26(Suppl 15):A–9004. doi: 10.1200/jco.2008.26.15_suppl.9004
6. Hoshimoto S, Faries MB, Morton DL, Shingai T, Kuo C, Wang HJ, et al. Assessment of prognostic circulating tumor cells in a phase III trial of adjuvant immunotherapy after complete resection of stage IV melanoma. *Ann Surg* (2012) 255(2):357–62. doi: 10.1097/SLA.0b013e3182380f56
7. Faries MB, Mozzillo N, Kashani-Sabet M, Thompson JF, Kelley MC, DeConti RC, et al. Long-Term Survival after Complete Surgical Resection and Adjuvant Immunotherapy for Distant Melanoma Metastases. *Ann Surg Oncol* (2017) 24 (13):3991–4000. doi: 10.1245/s10434-017-6072-3
8. Engelstein R, Merims S, Eisenberg G, Cohen J, Frank S, Hamburger T, et al. Immune Monitoring of Patients Treated With a Whole-Cell Melanoma Vaccine Engineered to Express 4-1BBL. *J Immunother* (2016) 39(8):321–8. doi: 10.1097/CJI.0000000000000138
9. Carson WE3, Unger JM, Sosman JA, Flaherty LE, Tuthill RJ, Porter MJ, et al. Adjuvant vaccine immunotherapy of resected, clinically node-negative melanoma: long-term outcome and impact of HLA class I antigen expression on overall survival. *Cancer Immunol Res* (2014) 2(10):981–7. doi: 10.1158/2326-6066.CIR-14-0052
10. Vansteenkiste JF, Cho BC, Vanakesa T, De Pas T, Zielinski M, Kim MS, et al. Efficacy of the MAGE-A3 cancer immunotherapeutic as adjuvant therapy in patients with resected MAGE-A3-positive non-small-cell lung cancer (MAGRIT): a randomised, double-blind, placebo-controlled, phase 3 trial. *Lancet Oncol* (2016) 17(6):822–35. doi: 10.1016/S1470-2045(16)00099-1
11. Butts C, Murray N, Maksymiuk A, Goss G, Marshall E, Soulières D, et al. Randomized phase IIB trial of BLP25 liposome vaccine in stage IIIB and IV non-small-cell lung cancer. *J Clin Oncol* (2005) 23:6674–81. doi: 10.1200/JCO.2005.13.011
12. Butts C, Socinski MA, Mitchell PL, Thatcher N, Havel L, Krzakowski M, et al. Tecemotide (L-BLP25) versus placebo after chemoradiotherapy for stage III non-small-cell lung cancer (START): a randomised, double-blind, phase 3 trial. *Lancet Oncol* (2014) 15:59–68. doi: 10.1016/S1470-2045(13)70510-2
13. Rodriguez PC, Popa X, Martínez O, Mendoza S, Santiesteban E, Crespo T, et al. A phase III clinical trial of the epidermal growth factor vaccine CIMAvax-EGF as switch maintenance therapy in advanced non-small cell lung cancer patients. *Clin Cancer Res* (2016) 22(15):3782–90. doi: 10.1158/1078-0432.CCR-15-0855
14. Nemunaitis J, Dillman RO, Schwarzenberger PO, Senzer N, Cunningham C, Cutler J, et al. Phase II study of belagenpumatucel-L, a transforming growth factor beta-2 antisense gene-modified allogeneic tumor cell vaccine in non-small-cell lung cancer. *J Clin Oncol* (2006) 24(29):4721–30. doi: 10.1200/JCO.2005.05.5335
15. Giaccone G, Bazhenova LA, Nemunaitis J, Tan M, Juhász E, Ramlau R, et al. A phase III study of belagenpumatucel-L, an allogeneic tumour cell vaccine, as maintenance therapy for non-small cell lung cancer. *Eur J Cancer* (2015) 51 (16):2321–9. doi: 10.1016/j.ejca.2015.07.035
16. Quoix E, Ramlau R, Westeel V, Papai Z, Madroszyk A, Riviere A, et al. Therapeutic vaccination with TG4010 and first-line chemotherapy in advanced non-small-cell lung cancer: a controlled phase 2B trial. *Lancet Oncol* (2011) 12(12):1125–33. doi: 10.1016/S1470-2045(11)70259-5

17. Quoix E, Lena H, Losonczy G, Forget F, Chouaid C, Papai Z, et al. TG4010 immunotherapy and first-line chemotherapy for advanced non-small-cell lung cancer (TIME): results from the phase 2b part of a randomised, double-blind, placebo-controlled, phase 2b/3 trial. *Lancet Oncol* (2016) 17 (2):212–23. doi: 10.1016/S1470-2045(15)00483-0
18. Tosch C, Bastien B, Barraud L, Grellier B, Nourtier V, Gantzer M, et al. Viral based vaccine TG4010 induces broadening of specific immune response and improves outcome in advanced NSCLC. *J Immunother Cancer* (2017) 570 (1):70. doi: 10.1186/s40425-017-0274-x
19. Alfonso S, Valdes-Zayas A, Santiesteban ER, Flores YI, Areces F, Hernandez M, et al. A randomized, multicenter, placebo-controlled clinical trial of racotumomab-alum vaccine as switch maintenance therapy in advanced non-small lung cancer patients. *Clin Cancer Res* (2014) 20(14):3660–1. doi: 10.1158/1078-0432.CCR-13-1674
20. Giaccone G, Debruyne C, Felip E, Chapman PB, Grant SC, Millward M, et al. Phase III study of adjuvant vaccination with Bec2/bacille Calmette–Guerin in responding patients with limited-disease small-cell lung cancer (European organisation for research and treatment of cancer 08971-08971B; silva study). *J Clin Oncol* (2005) 23(28):6854–64. doi: 10.1200/JCO.2005.17.186
21. Bottomley A, Debruyne C, Felip E, Millward M, Thiberville L, D'Addario G, et al. Symptom and quality of life results of an international randomised phase III study of adjuvant vaccination with Bec2/BCG in responding patients with limited disease small-cell lung cancer. *Eur J Cancer* (2008) 44(15):2178–84. doi: 10.1016/j.ejca.2008.06.036
22. Higano CS, Schellhammer PF, Small EJ, Burch PA, Nemunaitis J, Yuh L, et al. Integrated data from 2 randomized, double-blind, placebo-controlled, phase 3 trials of active cellular immunotherapy with sipuleucel-T in advanced prostate cancer. *Cancer* (2009) 115(16):3670–9. doi: 10.1002/cncr.24429
23. Kantoff PW, Higano CS, Shore ND, Berger ER, Small EJ, Penson DF, et al. Sipuleucel-T immuno-therapy for castration-resistant prostate cancer. *N Engl J Med* (2010) 363:411–22. doi: 10.1056/NEJMoa1001294
24. Beer TM, Bernstein GT, Corman JM, Glode LM, Hall SM, Poll WL, et al. Randomized Trial of Autologous Cellular Immunotherapy with Sipuleucel-T in Androgen-Dependent Prostate Cancer. *Clin Cancer Res* (2011) 17 (13):4558–67. doi: 10.1158/1078-0432.CCR-10-3223
25. Gulley JL, Borre M, Vogelzang NJ, Ng S, Agarwal N, Parker CC, et al. Phase III Trial of PROSTVAC in Asymptomatic or Minimally Symptomatic Metastatic Castration-Resistant Prostate Cancer. *J Clin Oncol* (2019) 37(13):1051–61. doi: 10.1200/JCO.18.02031
26. Kantoff PW, Schuetz TJ, Blumenstein BA, Glode LM, Bilhartz DL, Wyand M, et al. Overall survival analysis of a phase II randomized controlled trial of a Poxviral-based PSA-targeted immunotherapy in metastatic castration-resistant prostate cancer. *J Clin Oncol* (2010) 28(7):1099–105. doi: 10.1200/JCO.2009.25.0597
27. Cambier S, Sylvester RJ, Collette L, Gontero P, Brausi MA, van Andel G, et al. EORTC Nomograms and Risk Groups for Predicting Recurrence, Progression, and Disease-specific and Overall Survival in Non-Muscle-invasive Stage Ta-T1 Urothelial Bladder Cancer Patients Treated with 1-3 Years of Maintenance Bacillus Calmette-Guérin. *Eur Urol* (2016) 69(1):60–9. doi: 10.1016/j.eururo.2015.06.045
28. Harland SJ, Kynaston H, Grigor K, Wallace DM, Beacock C, Kockelbergh R, et al. A randomized trial of radical radiotherapy for the management of pT1G3 NXM0 transitional cell carcinoma of the bladder. *J Urol* (2007) 178(3 Pt 1):807–13. doi: 10.1016/j.juro.2007.05.024. discussion 813.
29. Di Stasi SM, Giannantoni A, Giurioli A, Valenti M, Zampa G, Storti L, et al. Sequential BCG and electromotive mitomycin versus BCG alone for high-risk superficial bladder cancer: a randomised controlled trial. *Lancet Oncol* (2006) 7(1):43–51. doi: 10.1016/S1470-2045(05)70472-1
30. Chiong E, Kesavan A, Mahendran R, Chan YH, Sng JH, Lim YK, et al. NRAMP1 and hGPX1 gene polymorphism and response to bacillus Calmette-Guérin therapy for bladder cancer. *Eur Urol* (2011) 59(3):430–7. doi: 10.1016/j.eururo.2010.11.031
31. Middleton G, Silcocks P, Cox T, Valle J, Wadsley J, Propper D, et al. Gemcitabine and capecitabine with or without telomerase peptide vaccine GV1001 in patients with locally advanced or metastatic pancreatic cancer (TeloVac): an open-label, randomised, phase 3 trial. *Lancet Oncol* (2014) 15 (8):829–40. doi: 10.1016/S1470-2045(14)70236-0
32. Hardacre JM, Mulcahy M, Small W, Talamonti M, Obel J, Krishnamurthi S, et al. Addition of algenpantucel-L immunotherapy to standard adjuvant therapy for pancreatic cancer: a phase 2 study. *J Gastrointest Surg* (2013) 17 (1):94–100. doi: 10.1007/s11605-012-2064-6. discussion p. 100-1.
33. Madan RA, Arlen PM, Gulley JL. PANVAC-VF: poxviral-based vaccine therapy targeting CEA and MUC1 in carcinoma. *Expert Opin Biol Ther* (2007) 7(4):543–54. doi: 10.1517/14712598.7.4.543
34. Schuster SJ, Neelapu SS, Gause BL, Janik JE, Muggia FM, Gockerman JP, et al. Vaccination with patient-specific tumor-derived antigen in first remission improves disease-free survival in follicular lymphoma. *J Clin Oncol* (2011) 29 (20):2787–94. doi: 10.1200/JCO.2010.33.3005
35. Bendandi M, Gocke CD, Kobrin CB, Benko FA, Sternas LA, Pennington R, et al. Complete molecular remissions induced by patient-specific vaccination plus granulocyte-monocyte colony-stimulating factor against lymphoma. *Nat Med* (1999) 5:1171–77. doi: 10.1038/13928
36. Freedman A, Neelapu SS, Nichols C, Robertson MJ, Djulbegovic B, Winter JN, et al. Placebo-controlled phase III trial of patient-specific immunotherapy with mitumprotimut-T and granulocyte-macrophage colony-stimulating factor after rituximab in patients with follicular lymphoma. *J Clin Oncol* (2009) 27(18):3036–43. doi: 10.1200/JCO.2008.19.8903
37. Koç ON, Redfern C, Wiernik PH, Rosenfelt F, Winter JN, Carter WD, et al. A phase 2 trial of immunotherapy with mitumprotimut-T (Id-KLH) and GM-CSF following rituximab in follicular B-cell lymphoma. *J Immunother* (2010) 33(2):178–84. doi: 10.1097/CJI.0b013e3181bfcea1
38. Levy R, Ganjoo KN, Leonard JP, Vose JM, Flinn IW, Ambinder RF, et al. Active idiotypic vaccination versus control immunotherapy for follicular lymphoma. *J Clin Oncol* (2014) 32(17):1797–803. doi: 10.1200/JCO.2012.43.9273
39. Liau LM, Ashkan K, Tran DD, Campian JL, Trusheim JE, Cobbs CS, et al. First results on survival from a large Phase 3 clinical trial of an autologous dendritic cell vaccine in newly diagnosed glioblastoma. *J Transl Med* (2018) 16(1):142. doi: 10.1186/s12967-018-1507-6. Erratum in: J Transl Med (2018) 16(1):179.
40. Weller M, Butowski N, Tran DD, Recht LD, Lim M, Hirte H, et al. Rindopepimut with temozolomide for patients with newly diagnosed, EGFRvIII-expressing glioblastoma (ACT IV): a randomised, double-blind, international phase 3 trial. *Lancet Oncol* (2017) 18(10):1373–85. doi: 10.1016/S1470-2045(17)30517-X
41. Mittendorf EA, Lu B, Melisko M, Price Hiller J, Bondarenko I, Brunt AM, et al. Efficacy and Safety Analysis of Nelipepimut-S Vaccine to Prevent Breast Cancer Recurrence: A Randomized, Multicenter, Phase III Clinical Trial. *Clin Cancer Res* (2019) 25(14):4248–54. doi: 10.1158/1078-0432.CCR-18-2867
42. Miles D, Roché H, Martin M, Perren TJ, Cameron DA, Glaspy J, et al. Phase III multicenter clinical trial of Sialyl-TN (STn)-keyhole limpet hemocyanin (KLH) vaccine for metastatic breast cancer patients. *Oncologist* (2011) 16:1092–100. doi: 10.1634/theoncologist.2010-0307
43. Ibrahim NK, Murray JL, Zhou D, Mittendorf EA, Sample D, Tautchin M, et al. Survival Advantage in Patients with Metastatic Breast Cancer Receiving Endocrine Therapy plus Sialyl Tn-KLH Vaccine: Post Hoc Analysis of a Large Randomized Trial. *J Cancer* (2013) 4(7):577–84. doi: 10.7150/jca.7028
44. Wood C, Srivastava P, Bukowski R, Lacombe L, Gorelov AI, Gorelov S, et al. An adjuvant autologous therapeutic vaccine (HSPPC-96; vitespen) versus observation alone for patients at high risk of recurrence after nephrectomy for renal cell carcinoma: a multicentre, open-label, randomised phase III trial. *Lancet* (2008) 372(9633):145–54. doi: 10.1016/S0140-6736(08)60697-2
45. Rini BI, Stenzl A, Zdrojowy R, Kogan M, Shkolnik M, Oudard S, et al. IMA901, a multipeptide cancer vaccine, plus sunitinib versus sunitinib alone, as first-line therapy for advanced or metastatic renal cell carcinoma (IMPRINT): a multicentre, open-label, randomised, controlled, phase 3 trial. *Lancet Oncol* (2016) 17(11):1599–611. doi: 10.1016/S1470-2045(16)30408-9
46. Smith RE, Colangelo L, Wieand HS, Begovic M, Wolmark N. Randomized trial of adjuvant therapy in colon carcinoma: 10-year results of NSABP protocol C-01. *J Natl Cancer Inst* (2004) 96(15):1128–32. doi: 10.1093/jnci/djh220
47. Sabbatini P, Harter P, Scambia G, Sehouli J, Meier W, Wimberger P, et al. Abagovomab as maintenance therapy in patients with epithelial ovarian cancer: a phase III trial of the AGO OVAR, COGI, GINECO, and GEICO–

the MIMOSA study. *J Clin Oncol* (2013) 31(12):1554–61. doi: 10.1200/JCO.2012.46.4057
48. Rosenberg SA, Yang JC, Restifo NP. Cancer immunotherapy: moving beyond current vaccines. *Nat Med* (2004) 10:909–15. doi: 10.1038/nm1100
49. Obeid JM, Hu Y, Singluff C. Vaccines, adjuvants and dendritic cells activators – Current status and future challenges. *Semin Oncol* (2015) 42(4):549–61. doi: 10.1053/j.seminoncol.2015.05.006
50. Bowen WS, Svrivastaka AK, Batra L, Barsoumian H, Shirwan H. Current challenges for cancer adjuvant development. *Expert Rev Vaccines* (2018) 17 (3):207–15. doi: 10.1080/14760584.2018.1434000
51. Fernandez A, Oliver L, Alvarez R, Fernandez LE, Lee KP, Mesa C. Adjuvants and myeloid-derived suppressor cells: enemies or allies in therapeutic cancer vaccination. *Hum Vaccin Immunother* (2014) 10(11):3251–60. doi: 10.4161/hv.29847
52. Flores -Borja F, Irshad S, Gordon P, Wong F, Sheriff I, Tutt A, et al. Crosstalk between Innate Lymphoid Cells and Other Immune Cells in the Tumor Microenvironment. *J Immunol Res* (2016) 2016:7803091. doi: 10.1155/2016/7803091
53. Taylor JG, Gribben JG. Microenvironment abnormalities and lymphomagenesis: Immunological aspects. *Semin Cancer Biol* (2015) 34:36–45. doi: 10.1016/j.semcancer.2015.07.004
54. Cheever MA, Higano CS. PROVENGE (Sipuleucel-T) in prostate cancer: the first FDA-approved therapeutic cancer vaccine. *Clin Cancer Res* (2011) 17 (11):3520–6. doi: 10.1158/1078-0432.CCR-10-3126
55. Jarosławski S, Toumi M. Sipuleucel-T (Provenge(®))-Autopsy of an Innovative Paradigm Change in Cancer Treatment: Why a Single-Product Biotech Company Failed to Capitalize on its Breakthrough Invention. *BioDrugs* (2015) 29(5):301–7. doi: 10.1007/s40259-015-0140-7
56. Welters MJ, Kenter GG, de Vos van Steenwijk PJ, Löwik MJ, Berends-van der Meer DM, Essahsah F, et al. Success or failure of vaccination for HPV16-positive vulvar lesions correlates with kinetics and phenotype of induced T-cell responses. *Proc Natl Acad Sci USA* (2010) 107(26):11895–9. doi: 10.1073/pnas.1006500107
57. Franceschi C, Bonafè M, Valensin S, Olivieri F, De Luca M, Ottaviani E, et al. Inflamm-aging. An evolutionary perspective on immunosenescence. *Ann N Y Acad Sci* (2000) 908:244–54. doi: 10.1111/j.1749-6632.2000.tb06651.x
58. Xia S, Zhang X, Zheng S, Khanabdali R, Kalionis B, Wu J, et al. An update on inflamm-aging: mechanisms, prevention, and treatment. *J Immunol Res* (2016) 2016:8426874. doi: 10.1155/2016/8426874
59. Crooke SN, Ovsyannikova IG, Poland GA, Kennedy RB. Immunosenescence: A systems-level overview of immune cell biology and strategies for improving vaccine responses. *Exp Gerontol* (2019) 124:110632. doi: 10.1016/j.exger.2019.110632
60. Lim YT. Vaccine adjuvant materials for cancer immunotherapy and control of infectious disease. *Clin Exp Vaccine Res* (2015) 4:54–8. doi: 10.7774/cevr.2015.4.1.54
61. Marciani DJ. Vaccine adjuvants: role and mechanisms of action in vaccine immunogenicity. *Drug Discovery Today* (2003) 8:934–43. doi: 10.1016/s1359-6446(03)02864-2
62. De Souza Apostolico J, Santos Lunardelli VA, Coirada FC, Boscardin SB, Santoro Rosa D. Adjuvants: classification, modus operandi, and licensing. *J Immunol Res* (2016) 2016:1459394. doi: 10.1155/2016/1459394
63. Kranz LM, Diken M, Haas H, Kreiter S, Loquai C, Reuter KC, et al. Systemic RNA delivery to dendritic cells exploits antiviral defence for cancer immunotherapy. *Nature* (2016) 534(7607):396–401. doi: 10.1038/nature18300
64. Walsh EE, Frenck RW Jr, Falsey AR, Kitchin N, Absalon J, Gurtman A, et al. Safety and Immunogenicity of Two RNA-Based Covid-19 Vaccine Candidates. *N Engl J Med* (2020) 383(25):2439–50. doi: 10.1056/NEJMoa2027906. NEJMoa2027906.
65. Pastor F, Berraondo P, Etxeberria I, Frederick J, Sahin U, Gilboa E, et al. An RNA toolbox for cancer immunotherapy. *Nat Rev Drug Discovery* (2018) 17 (10):751–67. doi: 10.1038/nrd.2018.132
66. Herrero C, Marques L, Lloberas J, Celada A. IFN-gamma-dependent transcription of MHC class II IA is impaired in macrophages from aged mice. *J Clin Invest* (2001) 107(4):485–93. doi: 10.1172/JCI11696
67. Herrero C, Sebastian C, Marques L, Comalada M, Xaus J, Valledor AF, et al. Immunosenescence of macrophages: reduced MHC class II gene expression. *Exper Gerontol* (2002) 37(2-3):389–94. doi: 10.1016/s0531-5565(01)00205-4
68. Villanueva JL, Solana R, Alonso MC, Pena J. Changes in the expression of HLA-class II antigens on peripheral blood monocytes from aged humans. *Dis Markers* (1990) 8(2):85–91.
69. Sridharan A, Esposo M, Kaushal K, Tay J, Osann K, Agrawal S, et al. Age-associated impaired plasmacytoid dendritic cell functions lead to decreased CD4 and CD8 T cell immunity. *Age (Dordr)* (2011) 33(3):363–76. doi: 10.1007/s11357-010-9191-3
70. Nyugen J, Agrawal S, Gollapudi S. Gupta S.Impaired functions of peripheral blood monocyte subpopulations in aged humans. *J Clin Immunol* (2010) 30 (6):806–13. doi: 10.1007/s10875-010-9448-8
71. van Duin D, Mohanty S, Thomas V, Ginter S, Montgomery RR, Fikrig E, et al. Age-associated defect in human TLR-1/2 function. *J Immunol* (2007) 178 (2):970–5. doi: 10.4049/jimmunol.178.2.970
72. Goronzy JJ, Fang F, Cavanagh MM, Qi Q, Weyand CM. Naive T cell maintenance and function in human aging. *J Immunol* (2015) 194(9):4073–80. doi: 10.4049/jimmunol.1500046
73. Nikolich-Zugich J. Ageing and life-long maintenance of T cell subsets in the face of latent persistent infections. *Nat Rev Immunol* (2008) 8(7):512–22. doi: 10.1038/nri2318
74. Pawelec G, Derhovanessian E. Role of CMV in immune senescence. *Virus Res* (2011) 157(2):175–9. doi: 10.1016/j.virusres.2010.09.010
75. Wertheimer AM, Bennett MS, Park B, Uhrlaub JL, Martinez C, Pulko V, et al. Aging and cytomegalovirus infection differentially and jointly affect distinct circulating T cell subsets in humans. *J Immunol* (2014) 192(5):2143–55. doi: 10.4049/jimmunol.1301721
76. Kim J, Kim AR, Shin EC. Cytomegalovirus infection and memory T cell inflation. *Immune Netw* (2015) 15(4):186–90. doi: 10.4110/in.2015.15.4.186
77. Bryl E, Vallejo AN, Matteson EL, Witkowski JM, Weyand CM, Goronzy JJ. Modulation of CD28 expression with anti-tumor necrosis factor alpha therapy in rheumatoid arthritis. *Arthritis Rheum* (2005) 52(10):2996–3003. doi: 10.1002/art.21353
78. Goronzy JJ, Li G, Yu M, Weyand CM. Signaling pathways in aged T cells - a reflection of T cell differentiation, cell senescence and host environment. *Semin Immunol* (2012) 24(5):365–72. doi: 10.1016/j.smim.2012.04.003
79. Lewis DE, Merched-Sauvage M, Goronzy JJ, Weyand CM, Vallejo AN. Tumor necrosis factor-alpha and CD80 modulate CD28 expression through a similar mechanism of T cell receptor-independent inhibition of transcription. *J Biol Chem* (2004) 279(28):29130–8. doi: 10.1074/jbc.M402194200
80. Goronzy JJ, Fulbright JW, Crowson CS, Poland GA, O'Fallon WM, Weyand CM. Value of immunological markers in predicting responsiveness to influenza vaccination in elderly individuals. *J Virol* (2001) 75(24):12182–7. doi: 10.1128/JVI.75.24.12182-12187.2001
81. Moro-Garcia MA, Alonso-Arias R, Lopez-Larrea C. When aging reaches CD4+ T cells: phenotypic and functional changes. *Front Immunol* (2013) 4:107. doi: 10.3389/fimmu.2013.00107
82. Dranoff G, Jaffee E, Lazenby A, Golumbek P, Levitsky H, Brose K, et al. Vaccination with irradiated tumor cells engineered to secrete murine granulocyte-macrophage colony-stimulating factor stimulates potent, specific, and long-lasting anti-tumor immunity. *Proc Natl Acad Sci USA* (1993) 90(8):3539–43. doi: 10.1073/pnas.90.8.3539
83. Hoeller C, Michielin O, Ascierto PA, Szabo Z, Blank CU. Systematic review of the use of granulocyte-macrophage colony- stimulating factor in patients with advanced melanoma. *Cancer Immunol Immunother* (2016) 65(9):1015–34. doi: 10.1007/s00262-016-1860-3
84. Walter S, Weinschenk T, Stenzl A, Zdrojowy R, Pluzanska A, Szczylik C, et al. Multipeptide immune response to cancer vaccine IMA901 after single- dose cyclophosphamide associates with longer patient survival. *Nat Med* (2012) 18 (8):1254–61. doi: 10.1038/nm.2883
85. Weber J, Sondak VK, Scotland R, Phillip R, Wang F, Rubio V, et al. Granulocyte-macrophage-colony-stimulating factor added to a multipeptide vaccine for resected Stage II melanoma. *Cancer* (2003) 97(1):186–200. doi: 10.1002/cncr.11045
86. Slingluff CL Jr, Petroni GR, Olson WC, Smolkin ME, Ross MI, Haas NB, et al. Effect of granulocyte/macrophage colony-stimulating factor on circulating CD8 + and CD4 + T cell responses to a multipeptide melanoma vaccine: outcome of a multicenter randomized trial. *Clin Cancer Res* (2009) 15 (22):7036–44. doi: 10.1158/1078-0432.CCR-09-1544

87. Slingluff CL, Petroni GR, Smolkin ME, Chianese-Bullock KA, Smith K, Murphy C, et al. Immunogenicity for $CD8^+$ and $CD4^+$ T cells of two formulations of an incomplete Freund's adjuvant for multipeptide melanoma vaccines. *J Immunother* (2010) 33(6):630–8. doi: 10.1097/CJI.0b013e3181e311ac
88. Faries MB, Hsueh EC, Ye X, Hoban M, Morton DL. Effect of granulocyte/macrophage colony-stimulating factor on vaccination with an allogeneic whole-cell melanoma vaccine. *Clin Cancer Res* (2009) 15(22):7029–35. doi: 10.1158/1078-0432.CCR-09-1540
89. Parmiani G, Castelli C, Pilla L, Santinami M, Colombo MP, Rivoltini L. Opposite immune functions of GM-CSF administered as vaccine adjuvant in cancer patients. *Ann Oncol* (2007) 18(2):226–32. doi: 10.1093/annonc/mdl158
90. Hodi FS, Lee S, McDermott DF, Rao UN, Butterfield LH, Tarhini AA, et al. Ipilimumab plus sargramostim vs ipilimumab alone for treatment of metastatic melanoma: a randomized clinical trial. *JAMA* (2014) 312 (17):1744–53. doi: 10.1001/jama.2014.13943
91. Rakoff-Nahoum S, Medzhitov R. Toll-like receptors and cancer. *Nat Rev Cancer* (2009) 9(1):57–63. doi: 10.1038/nrc2541
92. So EY, Ouchi T. The application of Toll like receptors for cancer therapy. *Int J Biol Sci* (2010) 6(7):675–81. doi: 10.7150/ijbs.6.675
93. Agrawal A, Gupta S. Impact of aging on dendritic cell functions in humans. *Ageing Res Rev* (2011) 10(3):336–45. doi: 10.1016/j.arr.2010.06.004
94. Maynard SK, Marshall JD, MacGill RS, Yu L, Cann JA, Cheng LI, et al. Vaccination with synthetic long peptide formulated with CpG in an oil-in-water emulsion induces robust E7-specific CD8 T cell responses and TC-1 tumor eradication. *BMC Cancer* (2019) 19(1):540. doi: 10.1186/s12885-019-5725-y
95. Speiser DE, Liénard D, Rufer N, Rubio-Godoy V, Rimoldi D, Lejeune F, et al. Rapid and strong human CD8+ T cell responses to vaccination with peptide, IFA, and CpG oligodeoxynucleotide 7909. *J Clin Invest* (2005) 115(3):739–46. doi: 10.1172/JCI23373
96. Baumgaertner P, Costa Nunes C, Cachot A, Maby-El Hajjami H, Cagnon L, Braun M, et al. Vaccination of stage III/IV melanoma patients with long NY-ESO-1 peptide and CpG-B elicits robust CD8(+) and CD4(+) T cell responses with multiple specificities including a novel DR7-restricted epitope. *Oncoimmunology* (2016) 5(10):e1216290. doi: 10.1080/2162402X.2016.1216290
97. Hennessy EJ, Parker AE, O'Neill LA. Targeting Toll-like receptors: emerging therapeutics? *Nat Rev Drug Discovery* (2010) 9(4):293–307. doi: 10.1038/nrd3203
98. Yoneda K, Sugimoto K, Shiraki K, Tanaka J, Beppu T, Fuke H, et al. Dual topology of functional Toll-like receptor 3 expression in human hepatocellular carcinoma: differential signaling mechanisms of TLR3-induced NF-κB activation and apoptosis. *Int J Oncol* (2008) 33(5):929–36. doi: 10.3892/ijo_00000080
99. Gelman AE, Zhang J, Choi Y, Turka LA. Toll-like receptor ligands directly promote activated CD4+ T cell survival. *J Immunol* (2004) 172(10):6065–73. doi: 10.4049/jimmunol.172.10.6065
100. Seki E, Tsutsui H, Tsuji NM, Hayashi N, Adachi K, Nakano H, et al. Critical roles of myeloid differentiation factor 88-dependent proinflammatory cytokine release in early phase clearance of Listeria monocytogenes in mice. *J Immunol* (2002) 169(7):3863–8. doi: 10.4049/jimmunol.169.7.3863
101. Caron G, Duluc D, Frémaux I, Jeannin P, David C, Gascan H, et al. Direct stimulation of human T cells via TLR5 and TLR7/8: flagellin and R-848 up-regulate proliferation and IFN-gamma production by memory CD4+ T cells. *J Immunol* (2005) 175(3):1551–7. doi: 10.4049/jimmunol.175.3.1551
102. Gelman AE, Larosa DF, Zhang J, Walsh PT, Choi Y, Oriol Sunyer J, et al. The adaptor molecule MyD88 activates PI-3 kinase signaling in CD4+ T cells and enables CpG oligodeoxynucleotide-mediated costimulation. *Immunity* (2006) 25:783–93. doi: 10.1016/j.immuni.2006.08.023
103. LaRosa DF, Gelman AE, Rahman AH, Zhang J, Turka LA, Walsh PT. CpG DNA inhibits CD4+CD25+ Treg suppression through direct MyD88-dependent costimulation of effector CD4+ T cells. *Immunol Lett* (2007) 108:183–8. doi: 10.1016/j.imlet.2006.12.007
104. Fukata M, Abreu MT. Role of Toll-like receptors in gastrointestinal malignancies. *Oncogene* (2008) 27(2):234–43. doi: 10.1038/sj.onc.1210908
105. Kaczanowska S, Joseph AM, Davila E. TLR agonists: our best frenemy in cancer immunotherapy. *J Leukoc Biol* (2013) 93(6):847–63. doi: 10.1189/jlb.1012501
106. Cherfils-Vicini J, Platonova S, Gillard M, Laurans L, Validire P, Caliandro R, et al. Triggering of TLR7 and TLR8 expressed by human lung cancer cells induces cell survival and chemoresistance. *J Clin Invest* (2010) 120(4):1285–97. doi: 10.1172/JCI36551
107. Kutikhin AG. Association of polymorphisms in TLR genes and in genes of the Toll-like receptor signaling pathway with cancer risk. *Hum Immunol* (2011) 72(11):1095–116. doi: 10.1016/j.humimm.2011.07.307
108. Matijevic Glavan T, Cipak Gasparovic A, Vérillaud B, Busson P, Pavelic J. Toll-like receptor 3 stimulation triggers metabolic reprogramming in pharyngeal cancer cell line through Myc, MAPK, and HIF. *Mol Carcinog* (2017) 56(4):1214–26. doi: 10.1002/mc.22584
109. Cai Z, Sanchez A, Shi Z, Zhang T, Liu M, Zhang D. Activation of Toll-like receptor 5 on breast cancer cells by flagellin suppresses cell proliferation and tumor growth. *Cancer Res* (2011) 71(7):2466–75. doi: 10.1158/0008-5472.CAN-10-1993
110. Rydberg C, Mansson A, Uddman R, Riesbeck K, Cardell LO. Toll-like receptor agonists induce inflammation and cell death in a model of head and neck squamous cell carcinomas. *Immunology* (2009) 128(1 Suppl):e600–11. doi: 10.1111/j.1365-2567.2008.03041.x
111. Rhee SH, Im E, Pothoulakis C. Toll-like receptor 5 engagement modulates tumor development and growth in a mouse xenograft model of human colon cancer. *Gastroenterology* (2008) 135(2):518–28. doi: 10.1053/j.gastro.2008.04.022
112. Schmausser B, Andrulis M, Endrich S, Muller-Hermelink HK, Eck M. Toll-like receptors TLR4, TLR5 and TLR9 on gastric carcinoma cells: an implication for interaction with Helicobacter pylori. *Int J Med Microbiol* (2005) 295(3):179–85. doi: 10.1016/j.ijmm.2005.02.009
113. Kumar PS, Brandt S, Madassery J, Backert S. Induction of TLR-2 and TLR-5 expression by Helicobacter pylori switches cagPAI-dependent signalling leading to the secretion of IL-8 and TNF-α. *PloS One* (2011) 6(5):e19614. doi: 10.1371/journal.pone.0019614
114. Bhattacharya D, Yusuf N. Expression of Toll-like receptors on breast tumors: taking a toll on tumor microenvironment. *Int J Breast Cancer* (2012) 2021:716564. doi: 10.1155/2012/716564
115. Samara KD, Antoniou KM, Karagiannis K, Margaritopoulos G, Lasithiotaki I, Koutala E, et al. Expression profiles of Toll-like receptors in non-small cell lung cancer and idiopathic pulmonary fibrosis. *Int J Oncol* (2012) 40 (5):1397–404. doi: 10.3892/ijo.2012.1374
116. Tanaka J, Sugimoto K, Shiraki K, Tameda M, Kusagawa S, Nojiri K, et al. Functional cell surface expression of Toll-like receptor 9 promotes cell proliferation and survival in human hepatocellular carcinomas. *Int J Oncol* (2010) 37(4):805–14. doi: 10.3892/ijo_00000730
117. Kundu SD, Lee C, Billips BK, Habermacher GM, Zhang Q, Liu V, et al. The Toll-like receptor pathway: a novel mechanism of infection-induced carcinogenesis of prostate epithelial cells. *Prostate* (2008) 68(2):223–9. doi: 10.1002/pros.20710
118. Wang C, Cao S, Yan Y, Ying Q, Jiang T, Xu K, et al. TLR9 expression in glioma tissues correlated to glioma progression and the prognosis of GBM patients. *BMC Cancer* (2010) 10:415. doi: 10.1186/1471-2407-10-415
119. Brignole C, Marimpietri D, Di Paolo D, Perri P, Morandi F, Pastorino F, et al. Therapeutic targeting of TLR9 inhibits cell growth and induces apoptosis in neuroblastoma. *Cancer Res* (2010) 70(23):9816–26. doi: 10.1158/0008-5472.CAN-10-1251
120. Li X, Liu D, Liu X, Jiang W, Zhou W, Yan W, et al. CpG ODN107 potentiates radiosensitivity of human glioma cells via TLR9-mediated NF-κB activation and NO production. *Tumour Biol* (2012) 33(5):1607–18. doi: 10.1007/s13277-012-0416-1
121. Carpentier A, Metellus P, Ursu R, Zohar S, Lafitte F, Barrié M, et al. Intracerebral administration of CpG oligonucleotide for patients with recurrent glioblastoma: a phase II study. *Neuro Oncol* (2010) 12:401–8. doi: 10.1093/neuonc/nop047
122. Ursu R, Carpentier A, Metellus P, Lubrano V, Laigle-Donadey F, Capelle L, et al. Intracerebral injection of CpG oligonucleotide for patients with de novo glioblastoma-A phase II multicentric, randomised study. *Eur J Cancer* (2017) 73:30–7. doi: 10.1016/j.ejca.2016.12.003
123. Ragupathi G, Gardner JR, Livingston PO, Gin DY. Natural and synthetic saponin adjuvant QS-21 for vaccines against cancer. *Expert Rev Vaccines* (2011) 10:463–70. doi: 10.1586/erv.11.18
124. Marty-Roix R, Vladimer GI, Pouliot K, Weng D, Buglione-Corbett R, West K, et al. Identification of QS-21 as an inflammasome-activating molecular

component of saponin adjuvants. *J Biol Chem* (2016) 291:1123–36. doi: 10.1074/jbc.M115.683011
125. Davis ID, Chen W, Jackson H, Parente P, Shackleton M, Hopkins W, et al. Recombinant NY-ESO-1 protein with ISCOMATRIX adjuvant induces broad integrated antibody and CD4(+) and CD8(+) T cell responses in humans. *Proc Natl Acad Sci USA* (2004) 101:10697–702. doi: 10.1073/pnas.0403572101
126. Vermaelen K. Vaccine strategies to improve anti-cancer cellular immune responses. *Front Immunol* (2019) 10:8. doi: 10.3389/fimmu.2019.00008
127. Gulen MF, Koch U, Haag SM, Schuler F, Apetoh L, Villunger A, et al. Signalling strength determines proapoptotic functions of STING. *Nat Commun* (2017) 8:427. doi: 10.1038/s41467-017-00573-w
128. Hanson MC, Crespo MP, Abraham W, Moynihan KD, Szeto GL, Chen SH, et al. Nanoparticulate STING agonists are potent lymph node-targeted vaccine adjuvants. *J Clin Invest* (2015) 125:2532–46. doi: 10.1172/JCI79915
129. Chandra D, Quispe-Tintaya W, Jahangir A, Asafu-Adjei D, Ramos I, Sintim HO, et al. STING ligand c-di-GMP improves cancer vaccination against metastatic breast cancer. *Cancer Immunol Res* (2014) 2(9):901–10. doi: 10.1158/2326-6066.CIR-13-0123
130. Hogenesch H. Mechanism of immunopotentiation and safety of aluminum adjuvants. *Front Immunol* (2012) 3:406:406. doi: 10.3389/fimmu.2012.00406
131. Eisenbarth SC, Colegio OR, O'Connor W, Sutterwala FS, Flavell RA. Crucial role for the Nalp3 inflammasome in the immunostimulatory properties of aluminium adjuvants. *Nature* (2008) 453(7198):1122–6. doi: 10.1038/nature06939
132. Kool M, Petrilli V, De Smedt T, Rolaz A, Hammad H, van Nimwegen M, et al. Cutting edge: alum adjuvant stimulates inflammatory dendritic cells through activation of the NALP3 inflammasome. *J Immunol* (2008) 181 (6):3755–9. doi: 10.4049/jimmunol.181.6.3755
133. MacLeod MK, McKee AS, David A, Wang J, Mason R, Kappler JW, et al. Vaccine adjuvants aluminum and monophosphoryl lipid A provide distinct signals to generate protective cytotoxic memory CD8 T cells. *Proc Natl Acad Sci USA* (2011) 108(19):7914–9. doi: 10.1073/pnas.1104588108
134. Gan J, Du G, He C, Jiang M, Mou X, Xue J, et al. Tumor cell membrane enveloped aluminum phosphate nanoparticles for enhanced cancer vaccination. *J Control Release* (2020) 10:S0168–3659(20)30383-7. doi: 10.1016/j.jconrel.2020.07.008
135. Sun B, Ji Z, Liao YP, Wang M, Wang X, Dong J, et al. Engineering an effective immune adjuvant by designed control of shape and crystallinity of aluminum oxyhydroxide nanoparticles. *ACS Nano* (2013) 7(12):10834–49. doi: 10.1021/nn404211j
136. Wang ZB, Xu J. Better adjuvants for better vaccines: progress in adjuvant delivery systems, modifications, and adjuvant-antigen codelivery. *Vaccines* (2020) 8:128. doi: 10.3390/vaccines8010128
137. Aucouturier J, Dupuis L, Ganne V. Adjuvants designed for veterinary and human vaccines. *Vaccine* (2001) 19:2666.7. doi: 10.1016/s0264-410x(00)00498-9
138. Aucouturier J, Dupuis L, Deville S, Ascarateil S, Ganne V. Montanide ISA 720 and 51: a new generation of water in oil emulsions as adjuvants for human vaccines. *Expert Rev Vaccines* (2002) 1:111.8. doi: 10.1586/14760584.1.1.111
139. Iseki K, Matsunaga H, Komatsu N, Suekane S, Noguchi M, Itoh K, et al. Evaluation of a new oil adjuvant for use in peptide-based cancer vaccination. *Cancer Sci* (2010) 101:2110. doi: 10.1111/j.1349-7006.2010.01653.x
140. van Doorn E, Liu H, Huckriede A, Hak E. Safety and tolerability evaluation of the use of Montanide ISA™51 as vaccine adjuvant: A systematic review. *Hum Vaccin Immunother* (2016) 12(1):159–69. doi: 10.1080/21645515.2015.1071455
141. Okada H, Butterfield LH, Hamilton RL, Hoji A, Sakaki M, Ahn BJ, et al. Induction of robust type-I CD8+ T cell responses in WHO grade 2 low-grade glioma patients receiving peptide-based vaccines in combination with poly-ICLC. *Clin Cancer Res* (2015) 21:286. doi: 10.1158/1078-0432.CCR-14-1790
142. Wada H, Isobe M, Kakimi K, Mizote Y, Eikawa S, Sato E, et al. Vaccination with NY-ESO-1 overlapping peptides mixed with Picibanil OK-432 and montanide ISA-51 in patients with cancers expressing the NY-ESO-1 antigen. *J Immunother* (2014) 37(2):84–92. doi: 10.1097/CJI.0000000000000017
143. Zandberg DP, Rollins S, Goloubeva O, Morales RE, Tan M, Taylor R, et al. A phase I dose escalation trial of MAGE-A3- and HPV16-specific peptide immunomodulatory vaccines in patients with recurrent/metastatic (RM) squamous cell carcinoma of the head and neck (SCCHN). *Cancer Immunol Immunother* (2015) 64(3):367–79. doi: 10.1007/s00262-014-1640-x
144. Slingluff CLJr, Yamshchikov G, Neese P, Galavotti H, Eastham S, Engelhard VH, et al. Phase I trial of a melanoma vaccine with gp100(280-288) peptide and tetanus helper peptide in adjuvant: immunologic and clinical outcomes. *Clin Cancer Res* (2001) 7(10):3012–24.
145. Gibney GT, Kudchadkar RR, DeConti RC, Thebeau MS, Czupryn MP, Tetteh L, et al. Safety, correlative markers, and clinical results of adjuvant nivolumab in combination with vaccine in resected high-risk metastatic melanoma. *Clin Cancer Res* (2015) 21(4):712–20. doi: 10.1158/1078-0432.CCR-14-2468
146. Bijker MS, van den Eeden SJ, Franken KL, Melief CJ, Offringa R, van der Burg SH. CD8+ CTL priming by exact peptide epitopes in incomplete Freund's adjuvant induces a vanishing CTL response, whereas long peptides induce sustained CTL reactivity. *J Immunol* (2007) 179(8):5033–40. doi: 10.4049/jimmunol.179.8.5033
147. Hailemichael Y, Dai Z, Jaffarzad N, Ye Y, Medina MA, Huang XF, et al. Persistent antigen at vaccination sites induces tumor-specific $CD8^+$T cell sequestration, dysfunction and deletion. *Nat Med* (2013) 19(4):465–72. doi: 10.1038/nm.3105
148. Schaefer JT, Patterson JW, Deacon DH, Smolkin ME, Petroni GR, Jackson EM, et al. Dynamic changes in cellular infiltrates with repeated cutaneous vaccination: A histologic and immunophenotypic analysis. *J Transl Med* (2010) 8:79. doi: 10.1186/1479-5876-8-79
149. Salerno EP, Shea SM, Olson WC, Petroni GR, Smolkin ME, McSkimming C, et al. Activation, dysfunction and retention of T cells in vaccine sites after injection of incomplete Freund's adjuvant, with or without peptide. *Cancer Immunol Immunothe* (2013) 62(7):1149–59. doi: 10.1007/s00262-013-1435-5
150. Kuball J, de Boer K, Wagner E, Wattad M, Antunes E, Weeratna RD, et al. Pitfalls of vaccinations with WT1-, Proteinase3- and MUC1-derived peptides in combination with Montanide ISA51 and CpG7909. *Cancer Immunol Immunother* (2011) 60(2):161–71. doi: 10.1007/s00262-010-0929-7
151. Schultze V, D'Agosto V, Wack A, Novicki D, Zorn J, Hennig R. Safety of MF59 adjuvant. *Vaccine* (2008) 26(26):3209–22. doi: 10.1016/j.vaccine.2008.03.093
152. Brito LA, O'Hagan DT. Designing and building the next generation of improved vaccine adjuvants. *J Control Release* (2014) 190:563–79. doi: 10.1016/j.jconrel.2014.06.027
153. Yang M, Yan Y, Fang M, Wan M, Wu X, Zhang X, et al. MF59 formulated with CpG ODN as a potent adjuvant of recombinant HSP65-MUC1 for inducing anti-MUC1+ tumor immunity in mice. *Int Immunopharmacol* (2012) 13(4):408–16. doi: 10.1016/j.intimp.2012.05.003
154. Bolhassani A, Safaiyan S, Rafati S. Improvement of different vaccine delivery systems for cancer therapy. *Mol Cancer* (2011) 10:3. doi: 10.1186/1476-4598-10-3
155. Temizoz B, Kuroda E, Ishii KJ. Vaccine adjuvants as potential cancer immunotherapeutics. *Int Immunol* (2016) 28(7):329–38. doi: 10.1093/intimm/dxw015
156. He H, Lu Y, Qi J, Zhu Q, Chen Z, Wu W. Adapting liposomes for oral drug delivery. *Acta Pharm Sin B* (2019) 9(1):36–48. doi: 10.1016/j.apsb.2018.06.005
157. Gao J, Ochyl LJ, Yang E, Moon JJ. Cationic liposomes promote antigen cross-presentation in dendritic cells by alkalizing the lysosomal pH and limiting the degradation of antigens. *Int J Nanomed* (2017) 12:1251–64. doi: 10.2147/IJN.S125866
158. Schwendener RA. Liposomes as vaccine delivery systems: a review of the recent advances. *Ther Adv Vaccines* (2014) 2(6):159–82. doi: 10.1177/2051013614541440
159. Fox CB, Sivananthan SJ, Duthie MS, Vergara J, Guderian JA, Moon E, et al. A nanoliposome delivery system to synergistically trigger TLR4 AND TLR7. *J Nanobiotechnol* (2014) 12:17. doi: 10.1186/1477-3155-12-17
160. Zhong Z, Wei X, Qi B, Xiao W, Yang L, Wei Y, et al. A novel liposomal vaccine improves humoral immunity and prevents tumor pulmonary metastasis in mice. *Int J Pharm* (2010) 399(1-2):156–62. doi: 10.1016/j.ijpharm.2010.07.053
161. Nakamura T, Yamazaki D, Yamauchi J, Harashima H. The nanoparticulation by octaarginine-modified liposome improves α-galactosylceramide-mediated antitumor therapy via systemic

administration. *J Control Release* (2013) 171(2):216–24. doi: 10.1016/j.jconrel.2013.07.004
162. Park S, Kim D, Wu G, Jung H, Park JA, Kwon HJ, et al. A peptide-CpG-DNA-liposome complex vaccine targeting TM4SF5 suppresses growth of pancreatic cancer in a mouse allograft model. *OncoTargets Ther* (2018) 11:8655–72. doi: 10.2147/OTT.S186606
163. Shariat S, Badiee A, Jalali SA, Mansourian M, Yazdani M, Mortazavi SA, et al. P5 HER2/neu-derived peptide conjugated to liposomes containing MPL adjuvant as an effective prophylactic vaccine formulation for breast cancer. *Cancer Lett* (2014) 355:54–60. doi: 10.1016/j.canlet.2014.09.016
164. Mai H, Fan W, Wang Y, Cai Y, Li X, Chen F, et al. Intranasal administration of miR-146a agomir rescued the pathological process and cognitive impairment in an AD Mouse Model. *Mol Ther Nucleic Acids* (2019) 18:681–95. doi: 10.1016/j.omtn.2019.10.002
165. Guevara ML, Jilesen Z, Stojdl D, Persano S. Codelivery of mRNA with α-galactosylceramide using a new lipopolyplex formulation induces a strong antitumor response upon intravenous administration. *ACS Omega* (2019) 4 (8):13015–26. doi: 10.1021/acsomega.9b00489
166. Butts C, Maksymiuk A, Goss G, Soulieres D, Marshall E, Cormier Y, et al. Updated survival analysis in patients with stage IIIB or IV non-small-cell lung cancer receiving BLP25 liposome vaccine (L-BLP25): Phase IIB randomized, multicenter, open-label trial. *J Cancer Res Clin Oncol* (2011) 137(9):1337–42. doi: 10.1007/s00432-011-1003-3
167. Kruit WH, Suciu S, Dreno B, Mortier L, Robert C, Chiarion-Sileni V, et al. Selection of immunostimulant AS15 for active immunization with MAGE-A3 protein: Results of a randomized phase II study of the European Organisation for Research and Treatment of Cancer Melanoma Group in Metastatic Melanoma. *J Clin Oncol* (2013) 31(19):2413–20. doi: 10.1200/JCO.2012.43.7111
168. McQuade JL, Homsi J, Torres-Cabala CA, Bassett R, Popuri RM, James ML, et al. A phase II trial of recombinant MAGE-A3 protein with immunostimulant AS15 in combination with high-dose Interleukin-2 (HDIL2) induction therapy in metastatic melanoma. *BMC Cancer* (2018) 18(1):1274. doi: 10.1186/s12885-018-5193-9
169. Neelapu SS, Baskar S, Gause BL, Kobrin CB, Watson TM, Frye AR, et al. Human Autologous Tumor-Specific T cell Responses Induced by Liposomal Delivery of a Lymphoma Antigen. *Clin Cancer Res* (2004) 10(24):8309–17. doi: 10.1158/1078-0432.CCR-04-1071
170. Berinstein NL, Karkada M, Oza AM, Odunsi K, Villella JA, Nemunaitis JJ, et al. Survivin-targeted immunotherapy drives robust polyfunctional T cell generation and differentiation in advanced ovarian cancer patients. *Oncoimmunology* (2015) 4(8):e1026529. doi: 10.1080/2162402X.2015.1026529
171. Berinstein NL, Karkada M, Morse MA, Nemunaitis JJ, Chatta G, Kaufman H, et al. First-in-man application of a novel therapeutic cancer vaccine formulation with the capacity to induce multi-functional T cell responses in ovarian, breast and prostate cancer patients. *J Transl Med* (2012) 10:156. doi: 10.1186/1479-5876-10-156
172. Harper DM, Franco EL, Wheeler CM, Moscicki AB, Romanowski B, Roteli-Martins CM, et al. Sustained efficacy up to 4. 5 years of a bivalent L1 virus-like particle vaccine against human papillomavirus types 16 and 18: Follow-up from a randomised control trial. *Lancet* (2006) 367(9518):1247–55. doi: 10.1016/S0140-6736(06)68439-0
173. Dawar M, Deeks S, Dobson S. Human papillomavirus vaccines launch a new era in cervical cancer prevention. *CMAJ* (2007) 177(5):456–61. doi: 10.1503/cmaj.070771
174. Adamina M, Guller U, Bracci L, Heberer M, Spagnoli GC, Schumacher R. Clinical applications of virosomes in cancer immunotherapy. *Expert Opin Biol Ther* (2006) 6(11):1113–21. doi: 10.1517/14712598.6.11.1113
175. Banday AH, Jeelani S, Hruby VJ. Cancer vaccine adjuvants - - recent clinical progress and future perspectives. *Immunopharmacol Immunotoxicol* (2015) 37(1):1–11. doi: 10.3109/08923973.2014.971963
176. Cusi MG. Applications of influenza virosomes as a delivery system. *Hum Vaccin* (2006) 2(1):1–7. doi: 10.4161/hv.2.1.2494
177. Wiedermann U, Wiltschke C, Jasinska J, Kundi M, Zurbriggen R, Garner-Spitzer E, et al. A virosomal formulated Her-2/neu multi-peptide vaccine induces Her-2/neu-specific immune responses in patients with metastatic breast cancer: A phase I study. *Breast Cancer Res Treat* (2010) 119(3):673–83. doi: 10.1007/s10549-009-0666-9
178. Wiedermann U, Davis AB, Zielinski CC. Vaccination for the prevention and treatment of breast cancer with special focus on Her-2/neu peptide vaccines. *Breast Cancer Res Treat* (2013) 138(1):1–12. doi: 10.1007/s10549-013-2410-8
179. Liu H, Tu Z, Feng F, Shi H, Chen K, Xu X. Virosome, a hybrid vehicle for efficient and safe drug delivery and its emerging application in cancer treatment. *Acta Pharm* (2015) 65(2):105–16. doi: 10.1515/acph-2015-0019
180. Shaikh SN, Raza S, Ansari MA, Khan G, Athar SHM. Overview on virosomes as a novel carrier for drug delivery. *JDDT [Internet]* (2019) 8(6-s):429–34. doi: 10.22270/jddt.v8i6-s.2163
181. Ngandeu Neubi GM, Opoku-Damoah Y, Gu X, Han Y, Zhou J, Ding Y. Bio-inspired drug delivery systems: an emerging platform for targeted cancer therapy. *Biomater Sci* (2018) 6(5):958–73. doi: 10.1039/C8BM00175H
182. Lucarini G, Sbaraglia F, Vizzoca A, Cinti C, Ricotti L, Menciassi A. Design of an innovative platform for the treatment of cerebral tumors by means of erythro-magneto-HA-virosomes. *BioMed Phys Eng Express* (2020) 6:45005. doi: 10.1088/2057-1976/ab89f1
183. Mou Y, Xing Y, Ren H, Cui Z, Zhang Y, Yu G, et al. The Effect of Superparamagnetic Iron Oxide Nanoparticle Surface Charge on Antigen Cross-Presentation. *Nanoscale Res Lett* (2017) 12(1):52. doi: 10.1186/s11671-017-1828-z
184. Evans ER, Bugga P, Asthana V, Drezek R. Metallic Nanoparticles for Cancer Immunotherapy. *Mater Today (Kidlington)* (2018) 21(6):673–85. doi: 10.1016/j.mattod.2017.11.022
185. Zhang P, Chiu YC, Tostanoski LH, Jewell CM. Polyelectrolyte Multilayers Assembled Entirely from Immune Signals on Gold Nanoparticle Templates Promote Antigen-Specific T Cell Response. *ACS Nano* (2015) 9(6):6465–77. doi: 10.1021/acsnano.5b02153
186. Sheikhpour M, Golbabaie A, Kasaeian A. Carbon nanotubes: A review of novel strategies for cancer diagnosis and treatment. *Mater Sci Eng C Mater Biol Appl* (2017) 76:1289–304. doi: 10.1016/j.msec.2017.02.132
187. Hassan HAFM, Diebold SS, Smyth LA, Walters AA, Lombardi G, Al-Jamal KT. Application of carbon nanotubes in cancer vaccines: Achievements, challenges and chances. *J Control Release* (2019) 297:79–90. doi: 10.1016/j.jconrel.2019.01.017
188. Nevagi RJ, Skwarczynski M, Toth I. Polymers for subunit vaccine delivery. *Eur Polym J* (2019) 114:397–410. doi: 10.1016/j.eurpolymj.2019.03.009
189. Rödl W, Taschauer A, Schaffert D, Wagner E, Ogris M. Synthesis of Polyethylenimine-Based Nanocarriers for Systemic Tumor Targeting of Nucleic Acids. In: M Ogris and H Sami, editors. *Nanotechnology for Nucleic Acid Delivery. Methods in Molecular Biology*. New York, NY: Humana Press (2019). vol 1943. doi: 10.1007/978-1-4939-9092-4_6
190. Shu D, Shu Y, Haque F, Abdelmawla S, Guo P. Thermodynamically stable RNA three-way junctions as platform for constructing multifunctional nanoparticles for delivery of therapeutics. *Nat Nanotechnol* (2011) 6 (10):658–67. doi: 10.1038/nnano.2011.105
191. Douglas SM, Dietz H, Liedl T, Högberg B, Graf F, Shih WM. Self-assembly of DNA into nanoscale three-dimensional shapes. *Nature* (2009) 459 (7245):414–8. doi: 10.1038/nature08016
192. Phua KKL, Staats HF, Leong KW, Nair SK. Intranasal mRNA nanoparticle vaccination induces prophylactic and therapeutic anti-tumor immunity. *Sci Rep* (2014) 4:5128. doi: 10.1038/srep05128
193. Liu Z, Lv D, Liu S, Gong J, Wang D, Xiong M, et al. Alginic acid-coated chitosan nanoparticles loaded with legumain DNA vaccine: effect against breast cancer in mice. *PloS One* (2013) 8(4):e60190. doi: 10.1371/journal.pone.0060190
194. Hu Y, Xu B, Xu J, Shou D, Liu E, Gao J, et al. Microneedle-assisted dendritic cell-targeted nanoparticles for transcutaneous DNA immunization. *Polym Chem* (2015) 6:373–9. doi: 10.1039/C4PY01394H
195. Perche F, Benvegnu T, Berchel M, Lebegue L, Pichon C, Jaffrès PA. Enhancement of dendritic cells transfection in vivo and of vaccination against B16F10 melanoma with mannosylated histidylated lipopolyplexes loaded with tumor antigen messanger RNA. *Nanomedecine* (2011) 7(4):445–53. doi: 10.1016/j.nano.2010.12.010
196. Carpentier AF, Geinguenaud F, Tran T, Sejalon F, Martin A, Motte L, et al. Synthetic melanin bound to subunit vaccine antigens significantly enhances CD8+ T cell responses. *PloS One* (2017) 12(7):e0181403. doi: 10.1371/journal.pone.0181403

197. Cuzzubbo S, Banissi C, Rouchon MS, Tran T, Tanchot C, Tartour E, et al. The adjuvant effect of melanin is superior to incomplete Freund's adjuvant in subunit/peptide vaccines in mice. *Cancer Immunol Immunother* (2020) 69 (12):2501–12. doi: 10.1007/s00262-020-02631-7
198. Fan Y, Moon JJ. Nanoparticle drug delivery systems designed to improve cancer vaccines and immunotherapy. *Vaccines (Basel)* (2015) 3(3):662–85. doi: 10.3390/vaccines3030662
199. Silva JM, Videira M, Gaspar R, Préat V, Florindo HF. Immune system targeting by biodegradable nanoparticles for cancer vaccines. *J Control Release* (2013) 168(2):179–99. doi: 10.1016/j.jconrel.2013.03.010
200. Akagi T, Baba M, Akashi M. Biodegradable nanoparticles as vaccine adjuvants and delivery systems: Regulation of immune responses by nanoparticle-based vaccine. Polymers in Nanomedicine. In: S Kunugi and T Yamaoka, editors. *Advances in Polymer Science, vol 247*. Berlin, Heidelberg: Springer (2011). p. 31–64. doi: 10.1007/12_2011_150
201. Wilson JT, Keller S, Manganiello MJ, Cheng C, Lee CC, Opara C, et al. pH-Responsive nanoparticle vaccines for dual-delivery of antigens and immunostimulatory oligonucleotides. *ACS Nano* (2013) 7(5):3912–25. doi: 10.1021/nn305466z
202. De Titta A, Ballester M, Julier Z, Nembrini C, Jeanbart L, Van Der Vlies AJ, et al. Nanoparticle conjugation of CpG enhances adjuvancy for cellular immunity and memory recall at low dose. *Proc Natl Acad Sci USA* (2013) 110 (49):19902–7. doi: 10.1073/pnas.1313152110
203. Pradhan P, Qin H, Leleux J, Gwak D, Sakamaki I, Kwak LW, et al. The effect of combined IL10 siRNA and CpG ODN as pathogen-mimicking microparticles on Th1/Th2 cytokine balance in dendritic cells and protective immunity against B cell lymphoma. *Biomaterials* (2014) 35 (21):5491–504. doi: 10.1016/j.biomaterials.2014.03.039
204. Silva JM, Zupancic E, Vandermeulen G, Oliveira VG, Salgado A, Videira M, et al. In vivo delivery of peptides and Toll-like receptor ligands by mannose-functionalized polymeric nanoparticles induces prophylactic and therapeutic anti-tumor immune responses in a melanoma model. *J Control Release* (2015) 198:91–103. doi: 10.1016/j.jconrel.2014.11.033
205. Ni Q, Zhang F, Liu Y, Wang Z, Yu G, Liang B, et al. A bi-adjuvant nanovaccine that potentiates immunogenicity of neoantigen for combination immunotherapy of colorectal cancer. *Sci Adv* (2020) 6(12): eaaw6071. doi: 10.1126/sciadv.aaw6071
206. Xu Z, Wang Y, Zhang L, Huang L. Nanoparticle-delivered transforming growth factor-β siRNA enhances vaccination against advanced melanoma by modifying tumor microenvironment. *ACS Nano* (2014) 8(4):3636–45. doi: 10.1021/nn500216y
207. Yuba E, Tajima N, Yoshizaki Y, Harada A, Hayashi H, Kono K. Dextran derivative-based pH-sensitive liposomes for cancer immunotherapy. *Biomaterials* (2014) 35(9):3091–101. doi: 10.1016/j.biomaterials.2013.12.024
208. Keller S, Wilson JT, Patilea GI, Bern HB, Convertine AJ, Stayton PS. Neutral Neutral polymer micelle carriers with pH-responsive, endosome-releasing activity modulate antigen trafficking to enhance CD8+ T cell responses. *J Control Release* (2014) 191:24–33. doi: 10.1016/j.jconrel.2014.03.041
209. Scott E, Stano A, Gillard M, Maio-Liu AC, Swartz MA, Hubbell JA. Dendritic cell activation and T cell priming with adjuvant-and antigen-loaded oxidation-sensitive polymersomes. *Biomaterials* (2012) 33(26):6211–9. doi: 10.1016/j.biomaterials.2012.04.060
210. Ahn S, Lee IH, Kang S, Kim D, Choi M, Saw PE, et al. Gold nanoparticles displaying tumor-associated self-antigens as a potential vaccine for cancer immunotherapy. *Adv Health Mater* (2014) 3(8):1194–9. doi: 10.1002/adhm.201300597
211. Nakamura T, Ono K, Suzuki Y, Moriguchi R, Kogure K Harashima H. Octaarginine-modified liposomes enhance cross-presentation by promoting the c-terminal trimming of antigen peptide. *Mol Pharm* (2014) 11(8):2787–95. doi: 10.1021/mp500147y
212. Ali OA, Huebsch N, Cao L, Dranoff G, Mooney DJ. Infection-mimicking materials to program dendritic cells in situ. *Nat Mater* (2009) 8(2):151–8. doi: 10.1038/nmat2357
213. Cruz L, Rosalia RA, Kleinovink JM, Rueda F, Löwik CWGM, Ossendorp F. Targeting nanoparticles to CD40, DEC-205 or CD11c molecules on dendritic cells for efficient CD8+ T cell response: A comparative study. *J Control Release* (2014) 192:209–18. doi: 10.1016/j.jconrel.2014.07.040
214. Sehgal K, Dhodapkar K, Dhodapkar MV. Targeting human dendritic cells in situ to improve vaccines. *Immunol Lett* (2014) 162(1 Pt A):59–67. doi: 10.1016/j.imlet.2014.07.004
215. Jongbloed S, Kassianos AJ, McDonald KJ, Clark GJ, Ju X, Angel CE, et al. Human CD141+ (BDCA-3)+ dendritic cells (DCs) represent a unique myeloid DC subset that cross-presents necrotic cell antigens. *J Exp Med* (2010) 207(6):1247–60. doi: 10.1084/jem.20092140
216. Joffre OP, Segura E, Savina A, Amigorena S. Cross-presentation by dendritic cells. *Nat Rev Immunol* (2012) 12(8):557–69. doi: 10.1038/nri3254
217. Cruz LJ, Tacken PJ, Zeelenberg IS, Srinivas M, Bonetto F, Weigelin E, et al. Tracking targeted bimodal nanovaccines: Immune responses and routing in cells, tissue, and whole organism. *Mol Pharm* (2014) 11(12):4299–313. doi: 10.1021/mp400717r
218. Irvine DJ, Hanson MC, Rakhra K, Tokatlian T. Synthetic nanoparticles for vaccines and immunotherapy. *Chem Rev* (2015) 115(19):11109–46. doi: 10.1021/acs.chemrev.5b00109
219. Yin W, Gorvel L, Zurawski S, Li D, Ni L, Duluc D, et al. Functional specialty of CD40 and dendritic dell surface lectins for exogenous antigen presentation to CD8(+) and CD4(+) T cells. *EBioMedicine* (2016) 5:46–58. doi: 10.1016/j.ebiom.2016.01.029
220. Fletcher EAK, van Maren W, Cordfunke R, Dinkelaar J, Codee JDC, van der Marel G, et al. Formation of immune complexes with a tetanus-derived B cell epitope boosts human T cell responses to covalently linked peptides in an ex vivo blood loop system. *J Immunol* (2018) 201(1):87–97. doi: 10.4049/jimmunol.1700911
221. Mangsbo SM, Fletcher EAK, van Maren WWC, Redeker A, Cordfunke RA, Dillmann I, et al. Linking T cell epitopes to a common linear B cell epitope: A targeting and adjuvant strategy to improve T cell responses. *Mol Immunol* (2018) 93:115–24. doi: 10.1016/j.molimm.2017.11.004
222. Patel PM, Ottensmeier CH, Mulatero C, Lorigan P, Plummer R, Pandha H, et al. Targeting gp100 and TRP-2 with a DNA vaccine: Incorporating T cell epitopes with a human IgG1 antibody induces potent T cell responses that are associated with favourable clinical outcome in a phase I/II trial. *Oncoimmunology* (2018) 7(6):e1433516. doi: 10.1080/2162402X.2018.1433516
223. Metheringham RL, Pudney VA, Gunn B, Towey M, Spendlove I, Durrant LG. Antibodies designed as effective cancer vaccines. *MAbs* (2009) 1(1):71–85. doi: 10.4161/mabs.1.1.7492
224. Gouttefangeas C, Rammensee HG. Personalized cancer vaccines: adjuvants are important, too. *Cancer Immunol Immunoth* (2018) 67(12):1911–8. doi: 10.1007/s00262-018-2158-4
225. Gutjahr A, Papagno L, Nicoli F, Lamoureux A, Vernejoul F, Lioux T, et al. Cutting edge: a dual TLR2 and TLR7 ligand induces highly potent humoral and cell-mediated immune responses. *J Immunol* (2017) 198(11):4205–9. doi: 10.4049/jimmunol.1602131
226. Ahonen CL, Doxsee CL, McGurran SM, Riter TR, Wade WF, Barth RJ, et al. Combined TLR and CD40 triggering induces potent CD8 + T cell expansion with variable dependence on type I IFN. *J Exp Med* (2004) 199(6):775– 784. doi: 10.1084/jem.20031591
227. Cho HI, Celis E. Optimized peptide vaccines eliciting extensive CD8 T cell responses with therapeutic antitumor effects. *Cancer Res* (2009) 69 (23):9012–9. doi: 10.1158/0008-5472.CAN-09-2019
228. Lanitis E, Irving M, Coukos G. Targeting the tumor vasculature to enhance T cell activity. *Curr Opin Immunol* (2015) 33:55–63. doi: 10.1016/j.coi.2015.01.011
229. Buckanovich RJ, Facciabene A, Kim S, Benencia F, Sasaroli D, Balint K, et al. Endothelin B receptor mediates the endothelial barrier to T cell homing to tumors and disables immune therapy. *Nat Med* (2008) 14(1):28–36. doi: 10.1038/nm1699
230. Ohm JE, Gabrilovich DI, Sempowski GD, Kisseleva E, Parman KS, Nadaf S, et al. VEGF inhibits T cell development and may contribute to tumor-induced immune suppression. *Blood* (2003) 101(12):4878–86. doi: 10.1182/blood-2002-07-1956
231. Gabrilovich DI, Ishida T, Nadaf S, Ohm JE, Carbone DP. Antibodies to vascular endothelial growth factor enhance the efficacy of cancer immunotherapy by improving endogenous dendritic cell function. *Clin Cancer Res* (1999) 5:2963–70.

232. Kusmartsev S, Cheng F, Yu B, Nefedova Y, Sotomayor E, Lush R, et al. All-trans-retinoic acid eliminates immature myeloid cells from tumor-bearing mice and improves the effect of vaccination. *Cancer Res* (2003) 63 (15):4441–9.
233. Nagaraj S, Youn JI, Weber H, Iclozan C, Lu L, Cotter MJ, et al. Anti-inflammatory triterpenoid blocks immune suppressive function of MDSCs and improves immune response in cancer. *Clin Cancer Res* (2010) 16 (6):1812–23. doi: 10.1158/1078-0432.CCR-09-3272
234. Sumida K, Wakita D, Narita Y, Masuko K, Terada S, Watanabe K, et al. Anti-IL-6 receptor mAb eliminates myeloid-derived suppressor cells and inhibits tumor growth by enhancing T cell responses. *Eur J Immunol* (2012) 42 (8):2060–72. doi: 10.1002/eji.201142335
235. Kerkar SP, Goldszmid RS, Muranski P, Chinnasamy D, Yu Z, Reger RN, et al. IL-12 triggers a programmatic change in dysfunctional myeloid-derived cells within mouse tumors. *J Clin Invest* (2011) 121(12):4746–57. doi: 10.1172/JCI58814
236. Priceman SJ, Sung JL, Shaposhnik Z, Burton JB, Torres-Collado AX, Moughon DL, et al. Targeting distinct tumor-infiltrating myeloid cells by inhibiting CSF-1 receptor: combating tumor evasion of antiangiogenic therapy. *Blood* (2010) 115(7):1461–71. doi: 10.1182/blood-2009-08-237412
237. Pienta KJ, Machiels J-P, Schrijvers D, Alekseev B, Shkolnik M, Crabb SJ, et al. Phase 2 study of carlumab (CNTO 888), a human monoclonal antibody against CC-chemokine ligand 2 (CCL2), in metastatic castration-resistant prostate cancer. *Invest New Drugs* (2013) 31(3):760–8. doi: 10.1007/s10637-012-9869-8
238. Ghiringhelli F, Menard C, Puig PE, Ladoire S, Roux S, Martin F, et al. Metronomic cyclophosphamide regimen selectively depletes CD4+CD25+ regulatory T cells and restores T and NK effector functions in end stage cancer patients. *Cancer Immunol Immunother* (2007) 56(5):641–8. doi: 10.1007/s00262-006-0225-8
239. Banissi C, Ghiringhelli F, Chen L, Carpentier AF. Treg depletion with a low-dose metronomic temozolomide regimen in a rat glioma model. *Cancer Immunol Immunother* (2009) 58(10):1627–34. doi: 10.1007/s00262-009-0671-1
240. Camisaschi C, Filipazzi P, Tazzari M, Casati C, Beretta V, Pilla L, et al. Effects of cyclophosphamide and IL-2 on regulatory CD4+ T-cell frequency and function in melanoma patients vaccinated with HLA-class I peptides: impact on the antigen-specific T-cell response. *Cancer Immunol Immunother* (2013) 62:897–908. doi: 10.1007/s00262-013-1397-7
241. Murahashi M, Hijikata Y, Yamada K, Tanaka Y, Kishimoto J, Inoue H, et al. Phase I clinical trial of a five-peptide cancer vaccine combined with cyclophosphamide in advanced solid tumors. *Clin Immunol* (2016) 166-167:48–58. doi: 10.1016/j.clim.2016.03.015
242. Anani W, Shurin MR. Targeting myeloid-derived suppressor cells in cancer. *Adv Exp Med Biol* (2017) 1036:105–28. doi: 10.1007/978-3-319-67577-0_8
243. Kodumudi KN, Woan K, Gilvary DL, Sahakian E, Wei S, Djeu JY. A novel chemoimmunomodulating property of docetaxel: suppression of myeloid-derived suppressor cells in tumor bearers. *Clin Cancer Res* (2010) 16 (18):4583–94. doi: 10.1158/1078-0432.CCR-10-0733
244. Vincent J, Mignot G, Chalmin F, Ladoire S, Bruchard M, Chevriaux A, et al. 5-Fluorouracil selectively kills tumor-associated myeloid-derived suppressor cells resulting in enhanced T cell-dependent antitumor immunity. *Cancer Res* (2010) 70(8):3052–61. doi: 10.1158/0008-5472.CAN-09-3690
245. Machiels JP, Reilly RT, Emens LA, Ercolini AM, Lei RY, Weintraub D, et al. Cyclophosphamide, doxorubicin, and paclitaxel enhance the antitumor immune response of granulocyte/macrophage-colony stimulating factor-secreting whole-cell vaccines in HER-2/neu tolerized mice. *Cancer Res* (2001) 61(9):3689–97.
246. van Poelgeest MI, Welters MJ, van Esch EM, Stynenbosch LF, Kerpershoek G, van Persijn van Meerten EL, et al. HPV16 synthetic long peptide (HPV16-SLP) vaccination therapy of patients with advanced or recurrent HPV16-induced gynecological carcinoma, a phase II trial. *J Transl Med* (2013) 11:88. doi: 10.1186/1479-5876-11-88
247. Antonia SJ, Mirza N, Fricke I, Chiappori A, Thompson P, Williams N, et al. Combination of p53 cancer vaccine with chemotherapy in patients with extensive stage small cell lung cancer. *Clin Cancer Res* (2006) 12:878–87. doi: 10.1158/1078-0432.CCR-05-2013
248. Wu X, Feng QM, Wang Y, Shi J, Ge HL, Di W. The immunologic aspects in advanced ovarian cancer patients treated with paclitaxel and carboplatin chemotherapy. *Cancer Immunol Immunother* (2010) 59:279–91. doi: 10.1007/s00262-009-0749-9
249. Welters MJ, van der Sluis TC, van Meir H, Loof NM, van Ham VJ, van Duikeren S, et al. Vaccination during myeloid cell depletion by cancer chemotherapy fosters robust T-cell responses. *Sci Transl Med* (2016) 8:334ra52. doi: 10.1126/scitranslmed.aaf0746
250. Tagliamonte M, Petrizzo A, Napolitano M, Luciano A, Arra C, Maiolino P, et al. Novel metronomic chemotherapy and cancer vaccine combinatorial strategy for hepatocellular carcinoma in a mouse model. *Cancer Immunol Immunother* (2015) 64:1305–14. doi: 10.1007/s00262-015-1698-0
251. Esfahani K, Roudaia L, Buhlaiga N, Del Rincon SV, Papneja N, Miller WH. A review of cancer immunotherapy: from the past, to the present, to the future. *Curr Oncol* (2020) 27(Suppl 2):S87–97. doi: 10.3747/co.27.5223
252. Quezada SA, Peggs KS, Curran MA, Allison JP. CTLA4 blockade and GM-CSF combination immunotherapy alters the intratumor balance of effector and regulatory T cells. *J Clin Invest* (2006) 116(7):1935–45. doi: 10.1172/JCI27745
253. Karyampudi L, Lamichhane P, Scheid AD, Kalli KR, Shreeder B, Krempski JW, et al. Accumulation of memory precursor CD8 T cells in regressing tumors following combination therapy with vaccine and anti-PD-1 antibody. *Cancer Res* (2014) 74(11):2974–85. doi: 10.1158/0008-5472.CAN-13-2564
254. Soares KC, Rucki AA, Wu AA, Olino K, Xiao Q, Chai Y, et al. PD-1/PD-L1 blockade together with vaccine therapy facilitates effector T cell infiltration into pancreatic tumors. *J Immunother* (2015) 38(1):1–11. doi: 10.1097/CJI.0000000000000062
255. Bartkowiak T, Singh S, Yang G, Galvan G, Haria D, Ai M, et al. Unique potential of 4-1BB ag-onist antibody to promote durable regression of HPV+ tumors when combined with an E6/E7 peptide vaccine. *Proc Natl Acad Sci USA* (2015) 112(38):E5290–9. doi: 10.1073/pnas.1514418112
256. Tran T, Blanc C, Granier C, Saldmann A, Tanchot C, Tartour E. Therapeutic cancer vaccine: building the future from lessons of the past. *Semin Immunopathol* (2019) 41(1):69–85. doi: 10.1007/s00281-018-0691-z
257. Obeid M, Tesniere A, Ghiringhelli F, Fimia GM, Apetoh L, Perfettini J-L, et al. Calreticulin exposure dictates the immunogenicity of cancer cell death. *Nat Med* (2007) 13(1):54–61. doi: 10.1038/nm1523
258. Golden EB, Pellicciotta I, Demaria S, Barcellos-Hoff MH, Formenti SC. The convergence of radiation and immunogenic cell death signaling pathways. *Front Oncol* (2012) 2:88. doi: 10.3389/fonc.2012.00088
259. Demaria S, Ng B, Devitt ML, Babb JS, Kawashima N, Liebes L, et al. Ionizing radiation inhibition of distant untreated tumors (abscopal effect) is immune mediated. *Int J Radiat Oncol Biol Phys* (2004) 58(3):862–70. doi: 10.1016/j.ijrobp.2003.09.012
260. Postow MA, Callahan MK, Barker CA, Yamada Y, Yuan J, Kitano S, et al. Immunologic correlates of the abscopal effect in a patient with melanoma. *N Engl J Med* (2012) 366(10):925–31. doi: 10.1056/NEJMoa1112824
261. Reits EA, Hodge JW, Herberts CA, Groothuis TA, Chakraborty M, Wansley EK, et al. Radiation modulates the peptide repertoire, enhances MHC class I expression, and induces successful antitumor immunotherapy. *J Exp Med* (2006) 203(5):1259–71. doi: 10.1084/jem.20052494
262. Chakraborty M, Abrams SI, Camphausen K, Liu K, Scott T, Coleman N, et al. Irradiation of tumor cells up-regulates Fas and enhances CTL lytic activity and CTL adoptive immunotherapy. *J Immunol* (2003) 170(12):6338–47. doi: 10.4049/jimmunol.170.12.6338
263. Chakraborty M, Abrams SI, Coleman CN, Camphausen K, Schlom J, Hodge JW. External beam radiation of tumors alters phenotype of tumor cells to render them susceptible to vaccine-mediated T cell killing. *Cancer Res* (2004) 64(12):4328–37. doi: 10.1158/0008-5472.CAN-04-0073
264. Demaria S, Bhardwaj N, McBride WH, Formenti SC. Combining radiotherapy and immunotherapy: a revived partnership. *Int J Radiat Oncol Biol Phys* (2005) 63(3):655–66. doi: 10.1016/j.ijrobp.2005.06.032
265. Apetoh L, Ladoire S, Coukos G, Ghiringhelli F. Combining immunotherapy and anticancer agents: the right path to achieve cancer cure? *Ann Oncol* (2015) 26(9):1813–23. doi: 10.1093/annonc/mdv209
266. Filatenkov A, Baker J, Mueller AM, Kenkel J, Ahn GO, Dutt S, et al. Ablative tumor radiation can change the tumor immune cell microenvironment to induce durable complete remissions. *Clin Cancer Res* (2015) 21(16):3727–39. doi: 10.1158/1078-0432.CCR-14-2824
267. Mondini M, Nizard M, Tran T, Mauge L, Loi M, Clémenson C, et al. Synergy of radiotherapy and a cancer vaccine for the treatment of HPV-associated

head and neck Cancer. *Mol Cancer Ther* (2015) 14(6):1336–45. doi: 10.1158/1535-7163.MCT-14-1015
268. Adler AJ, Marsh DW, Yochum GS, Guzzo JL, Nigam A, Nelson WG, et al. CD4(+) T cell tolerance to parenchymal self-antigens requires presentation by bone marrow-derived antigen-presenting cells. *J Exp Med* (1998) 187 (10):1555–64. doi: 10.1084/jem.187.10.1555
269. Aliru ML, Schoenhals JE, Venkatesulu BP, Anderson CC, Barsoumian HB, Younes AI, et al. Radiation therapy and immunotherapy: what is the optimal timing or sequencing? *Immunotherapy* (2018) 10(4):299–316. doi: 10.2217/imt-2017-0082
270. Zheng Y, Wang T, Tu X, Huang Y, Zhang H, Tan D, et al. Gut microbiome affects the response to anti-PD-1 immunotherapy in patients with hepatocellular carcinoma. *J Immunother Cancer* (2019) 7:193. doi: 10.1186/s40425-019-0650-9
271. Gopalakrishnan V, Spencer CN, Nezi L, Reuben A, Andrews MC, Karpinets TV. et.al., Gut microbiome modulates response to anti–PD-1 immunotherapy in melanoma patients. *Science* (2018) 359(6371):97–103. doi: 10.1126/science.aan4236
272. Madsen K, Cornish A, Soper P, Mckaigney C, Jijon H, Yachimec C, et al. Probiotic bacteria enhance murine and human intestinal epithelial barrier function. *Gastroenterology* (2001) 121:580–91. doi: 10.1053/gast.2001.27224
273. Sokol H, Pigneur B, Watterlot L, Lakhdari O, Bermúdez-Humarán LG, Gratadoux JJ, et al. Faecali bacterium prausnitzii is an anti-inflammatory commensal bacterium identified by gut microbiota analysis of Crohn disease patients. *Proc Natl Acad Sci USA* (2008) 105(43):16731–6. doi: 10.1073/pnas.0804812105
274. Matson V, Fessler J, Bao R, Chongsuwat T, Zha Y, Alegre MS, et al. The commensal microbiome is associated with anti-PD-1 efficacy in metastatic melanoma patients. *Science* (2018) 359(6371):104–8. doi: 10.1126/science.aao3290
275. Routy B, Le Chatelier E, Derosa L, Duong CPM, Alou MT, Daillère R, et al. Gut microbiome influences efficacy of PD-1-based immunotherapy against epithelial tumors. *Science* (2018) 359(6371):91–7. doi: 10.1126/science.aan3706
276. Eckburg PB, Bik EM, Bernstein CN, Purdom E, Dethlefsen L, Sargent M, et al. Diversity of the human intestinal microbial flora. *Science* (2005) 308 (5728):1635–43. doi: 10.1126/science.1110591
277. Oh JZ, Ravindran R, Chassaing B, Carvalho FA, Maddur MS, Bower M, et al. TLR5-mediated sensing of gut microbiota is necessary for antibody responses to seasonal influenza vaccination. *Immunity* (2014) 41:478–92. doi: 10.1016/j.immuni.2014.08.009
278. Zebertavage L, Bambina S, Shugart J, Alice A, Zens KD, Lauer P, et al. A microbial-based cancer vaccine for induction of EGFRvIII-specific CD8+ T cells and anti-tumor immunity. *PloS One* (2019) 14:e0209153. doi: 10.1371/journal.pone.0209153
279. McTiernan A. Mechanisms linking physical activity with cancer. *Nat Rev Cancer* (2008) 8(3):205–11. doi: 10.1038/nrc2325
280. Ballard-Barbash R, Friedenreich CM, Courneya KS, Siddiqi SM, McTiernan A, Alfano CM. Physical activity, biomarkers, and disease outcomes in cancer survivors: a systematic review. *J Natl Cancer Inst* (2012) 104(11):815–40. doi: 10.1093/jnci/djs207
281. Pedersen L, Idorn M, Olofsson GH, Nookaew I, Hansen RH, Johannesen HH. Voluntary running suppresses tumor growth through epinephrine- and IL-6-dependent NK cell mobilization and redistribution. *Cell Metab* (2016) 23(3):554–62. doi: 10.1016/j.cmet.2016.01.011
282. Timmons BW, Cieslak T. Human natural killer cell subsets and acute exercise: a brief review. *Exerc Immunol Rev* (2008) 14:8–23.
283. McBain JA, Eastman A, Nobel CS, Mueller GC. Apoptotic death in adenocarcinoma cell lines induced by butyrate and other histone deacetylase inhibitors. *Biochem Pharmacol* (1997) 53(9):1357–68. doi: 10.1016/s0006-2952(96)00904-5
284. Jan G, Belzacq AS, Haouzi D, Rouault A, Metivier D, Kroemer G, et al. Propionibacteria induce apoptosis of colorectal carcinoma cells via short-chain fatty acids acting on mitochondria. *Cell Death Differ* (2002) 9(2):179–88. doi: 10.1038/sj.cdd.4400935
285. Wei W, Sun W, Yu S, Yang Y, Ai L. Butyrate production from high-fiber diet protects against lymphoma tumor. *Leuk Lymphoma* (2016) 57(10):2401–8. doi: 10.3109/10428194.2016.1144879
286. Wheway J, Mackay CR, Newton RA, Sainsbury A, Boey D, Herzog H, et al. A fundamental bimodal role for neuropeptide Y1 receptor in the immune system. *J Exp Med* (2005) 202(11):1527–38. doi: 10.1084/jem.20051971
287. Chen WC, Liu YB, Liu WF, Zhou YY, He HF, Lin S. Neuropeptide Y Is an Immunomodulatory Factor: Direct and Indirect. *Front Immunol* (2020) 11:580378. doi: 10.3389/fimmu.2020.580378
288. Becker JC, Andersen MH, Hofmeister-Muller V, Wobser M, Frey L, Sandig C, et al. Survivin-specific T-cell reactivity correlates with tumor response and patient survival: a phase-II peptide vaccination trial in metastatic melanoma. *Cancer Immunol Immunother* (2012) 61(11):2091–103. doi: 10.1007/s00262-012-1266-9. 2012/ 05/09 edn.
289. Wick DA, Martin SD, Nelson BH, Webb JR. Profound CD8+ T cell immunity elicited by sequential daily immunization with exogenous antigen plus the TLR3 agonist poly(I:C). *Vaccine* (2011) 29(5):984–93. doi: 10.1016/j.vaccine.2010.11.036
290. Stark FC, McCluskie MJ, Krishnan L. Homologous Prime-Boost Vaccination with OVA Entrapped in Self-Adjuvanting Archaeosomes Induces High Numbers of OVA-Specific $CD8^+$ T Cells that Protect Against Subcutaneous B16-OVA Melanoma. *Vaccines (Basel)* (2016) 4(4):44. doi: 10.3390/vaccines4040044

Conflict of Interest: SMa is the Chief Development Officer at Ultimovacs AB, a company that develops cancer vaccines and holds patent applications within the field of cancer vaccines. SMa is also the founder of Immuneed AB and Vivologica AB. AP is the Chief Executive Officer of multimmune GmbH, a company that develops cancer "theranostics" based on tumor expression of membrane Hsp70.

The remaining authors declare that the research was conducted in the absence of any commercial or financial relationships that could be construed as a potential conflict of interest.

Copyright © 2021 Cuzzubbo, Mangsbo, Nagarajan, Habra, Pockley and McArdle. This is an open-access article distributed under the terms of the Creative Commons Attribution License (CC BY). The use, distribution or reproduction in other forums is permitted, provided the original author(s) and the copyright owner(s) are credited and that the original publication in this journal is cited, in accordance with accepted academic practice. No use, distribution or reproduction is permitted which does not comply with these terms.

frontiers in Oncology

REVIEW
published: 29 March 2021
doi: 10.3389/fonc.2021.626463

Prophylactic Cancer Vaccines Engineered to Elicit Specific Adaptive Immune Response

*Davis W. Crews, Jenna A. Dombroski and Michael R. King**

Department of Biomedical Engineering, Vanderbilt University, Nashville, TN, United States

Vaccines have been used to prevent and eradicate different diseases for over 200 years, and new vaccine technologies have the potential to prevent many common illnesses. Cancer, despite many advances in therapeutics, is still the second leading causes of death in the United States. Prophylactic, or preventative, cancer vaccines have the potential to reduce cancer prevalence by initiating a specific immune response that will target cancer before it can develop. Cancer vaccines can include many different components, such as peptides and carbohydrates, and be fabricated for delivery using a variety of means including through incorporation of stabilizing chemicals like polyethylene glycol (PEG) and pan-DR helper T-lymphocyte epitope (PADRE), fusion with antigen-presenting cells (APCs), microneedle patches, and liposomal encapsulation. There are currently five cancer vaccines used in the clinic, protecting against either human papillomavirus (HPV) or hepatitis B virus (HBV), and preventing several different types of cancer including cervical and oral cancer. Prophylactic cancer vaccines can promote three different types of adaptive responses: humoral (B cell, or antibody-mediated), cellular (T cell) or a combination of the two types. Each vaccine has its advantages and challenges at eliciting an adaptive immune response, but these prophylactic cancer vaccines in development have the potential to prevent or delay tumor development, and reduce the incidence of many common cancers.

Keywords: cancer, vaccine, adaptive immune response, prophylactic vaccine, biomaterials

OPEN ACCESS

Edited by:
Alan Graham Pockley, multimmune GmbH, Germany

Reviewed by:
Michele Sommariva, University of Milan, Italy
Songdong Meng, Chinese Academy of Sciences, China

****Correspondence:***
Michael R. King
mike.king@vanderbilt.edu

Specialty section:
This article was submitted to Cancer Immunity and Immunotherapy, a section of the journal Frontiers in Oncology

Received: *05 November 2020*
Accepted: *11 March 2021*
Published: *29 March 2021*

Citation:
Crews DW, Dombroski JA and King MR (2021) Prophylactic Cancer Vaccines Engineered to Elicit Specific Adaptive Immune Response. Front. Oncol. 11:626463. doi: 10.3389/fonc.2021.626463

INTRODUCTION

Vaccines have improved the human condition since Edward Jenner developed the first vaccine to prevent smallpox over 200 years ago, paving the way for the prevention and even eradication of many common ailments (1). Cancer is the second leading cause of death in the United States, with 1.89 million people projected to be diagnosed with cancer in 2021 alone (2, 3). While there are many successful therapeutics for cancer treatment, advances in prophylactic vaccination against cancer have been limited.

Preventative, or prophylactic, cancer vaccines have the potential to reduce cancer prevalence and improve prognosis by inducing an immune response to prevent the development of specific cancers. Currently, five vaccines are used in clinical practice and approved by the FDA. These vaccines

protect against two cancer-promoting viral infections, hepatitis B (HBV) and human papillomavirus (HPV) (4). HPV is a sexually transmitted infection, with several of its forms associated with different types of cancers, the most common being cervical and oral cancer. Individuals vaccinated with the HPV vaccine are protected from cancer by preventing HPV development; since HPV can promote the onset of cervical cancer, HPV prevention is expected to lead to its decline (4). In Scotland, women vaccinated for HPV showed an 89% reduction in cervical intraepithelial neoplasia (CIN) grade 3 or worse when compared to non-vaccinated women. Similar reductions were shown in CIN grade 1 and grade 2 (5). Furthermore, vaccination against HBV, a risk factor for hepatocellular cancer, of infants in Taiwan has shown reduced cancer prevalence. Rates of hepatocellular cancer in vaccinated Taiwanese children age 6-14 years fell approximately 70% (4).

While preventative vaccines are commonly implemented, preventative vaccines designed to protect against cancer are a relatively new development. The goal of preventative cancer vaccines is not to treat, but to prevent the development of a tumor. Cancer vaccines are often defined as therapeutic vaccines, which are different from prophylactic vaccines in that they elicit an immune response to an existing tumor and to residual cancer cells following other treatments (6). Therapeutic vaccines against cancer elicit immune responses following the onset of disease. For example, proposed therapeutic vaccines against breast cancer can target human epidermal growth factor receptor 2 (HER2), utilizing T cells to elicit a targeted immune response (7). While strides are being made in therapeutic vaccines for cancer, many different strategies have been proposed for the development of prophylactic cancer vaccines (**Figure 1**).

Preventative vaccines offer many advantages over therapeutic treatments in terms of health and cost benefits. Preventative treatments reduce morbidity and mortality, and current vaccines from childhood vaccines like Tdap (Tetanus, diphtheria, pertussis) to influenza vaccines have led to economic benefits in low- and middle-income countries (8). Successfully engineered cancer vaccines could decrease health care costs associated with cancer. It has been estimated that the total cost of cancer in the United States would increase 34% in just fifteen years, from $183 billion in 2015 to $246 billion in 2030 (9). Thus, decreasing the cost of cancer treatments through preventative vaccines could result in dramatic decreases in healthcare costs associated with cancer.

Vaccines have demonstrated the ability to successfully eradicate previously common diseases, controlling the spread of 12 diseases, such as smallpox and yellow fever (10). Disease eradication is a common and efficient way to improve public health (10). The successful development of preventative cancer vaccines could decrease the prevalence of cancer, reducing cancer-related deaths. HPV vaccines have already reduced the prevalence of cervical cancer. In Scotland, an 89% reduction in grade 3 or worse cervical intraepithelial neoplasia (CIN) was seen for women vaccinated at 12-13 years old (5). Cervical cancer prevention with HPV vaccines provide promise that vaccines can be developed for other cancers to achieve similar results. Several possible strategies for cancer prevention will be discussed in this review, with each presenting distinct advantages and challenges (**Table 1**). Age-related immune decline is seen across all vaccine engineering strategies as a major challenge.

Role of the Immune System in Cancer

A unique aspect of cancer is its ability to survive in the presence of an immune system, making immunotherapy a challenging yet promising therapeutic for cancer. This property stems from two essential hallmarks of cancer: tumor-promoting inflammation and avoiding immune destruction (39). Tumors utilize the immune system by generating an inflammatory response conducive to tumor growth (39). The tumor microenvironment (TME) consists of neoplastic tissue, which is highly disorganized and grows uncontrollably (40). Neoplastic progression is supported by inflammation of cytokines like interleukin-1 (IL-1) and tumor necrosis factor (TNF) (41, 42). Necrotic cells within the TME stimulate proliferation of neighboring cells through the release of IL-1α, and angiogenesis is driven by IL-1β (43, 44). IL-18 induces vascular cell adhesion expression, supporting invasion and metastasis (45). TNF-α promotes tumor development by regulating factors such as cytokines, chemokines, adhesion molecules, and matrix metalloproteinases (MMPs) (46).

Tumors evade immune detection, and therefore destruction, through a variety of means including regulatory cells, down-modulating antigen presentation, tolerance, and immune suppression (39, 47). Not only does the hypoxic tumor promote regulatory T cell (Treg) homing to the TME, but tumor-derived CD4+CD25+FoxP3+ Tregs have been found to be more suppressive of cytotoxic lymphocytes (CTLs) than normal Tregs (48–50). Tumors are able to evade CTL recognition by down-modulating essential components of antigen processing and presentation such as the MHC I pathway (47). Tolerance is induced by tumor cells, since they do not express co-stimulatory molecules that are needed to activate T cells or antigen-presenting cells (APCs) (51). Furthermore, CTLA-4 and PD-1 are upregulated on cancer cells, inhibiting a T cell response (52). The combination of these various traits of cancer contribute to the difficulty of the immune system to independently stop tumor development, making a prophylactic vaccine a useful approach for cancer prevention.

Cancer Vaccines and the Immune System

The goal of a prophylactic cancer vaccine is to elicit an adaptive primary immune response, to allow for a rapid and strong secondary response if carcinogenesis occurs (53, 54). The mechanism behind these preventative vaccines can be viewed as specific immunity to modified self-antigens, therefore producing an immune response to cells that have undergone malignant transformation (55). Cancer vaccines can be developed to recognize and prevent cancer-promoting viruses or neoantigens, which are peptides found on tumor cells that are associated with spontaneous cancers (56).

Microbes and other foreign bodies included in a vaccine alert the host immune system *via* presentation of Damage-Associated

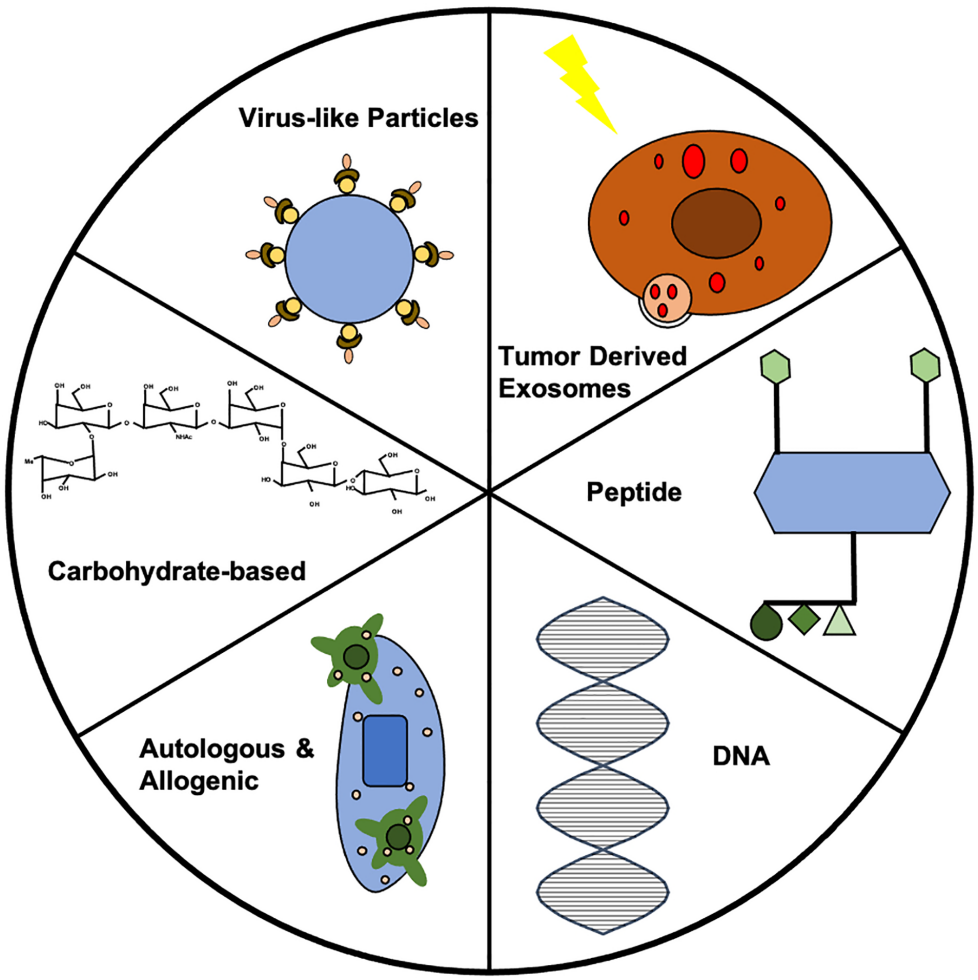


FIGURE 1 | Summary of vaccine strategies. Each vaccine strategy has potential for use in prophylactic cancer vaccines. Further investigation into each strategy could lead to clinically-relevant prophylactic cancer vaccines. In this figure, the VLP represents the HER2-VLP, which has elevated levels of anti-HER2 antibody to protect against breast cancer. The carbohydrate displayed is the chemical structure of Globo H, which has often been used in therapeutic vaccines, but shows potential for prophylactic vaccine development. The allogenic vaccine displays dendritic cells (DCs) recognizing the tumor antigen, which can allow for immune cell activation. The double helix of DNA is the building block for all DNA vaccines. The peptide vaccine shows four epitopes engineered for display, which caused upregulation of CD4+ and CD8+ T cells in addition to increases in IgG antibodies in vaccinated mice. The exosome shows TEX synthesis *via* radiotherapy that prevented breast cancer *via* CD8+.

Molecular Patterns (DAMPs), which cause innate immune cells such as APCs to produce cytokines necessary for activating T cells (**Figure 2**). This activation can result in the production of effector or memory T cells, or facilitate the activation of B cells, ultimately leading to lasting immunity (53). By producing this adaptive response, a vaccine develops memory for protection from an antigen (54). Adaptive immune responses can consist of T cell-mediated cellular responses, B cell-mediated humoral responses, or combinations of the two (57). By activating T and B cells, a vaccine is able to produce memory T and B cells, which are essential for stopping another attack or antigen exposure (57). These memory cells proliferate, causing a stronger, faster response upon a second exposure (54).

While there are many preventative cancer vaccines being developed in the research setting, there are only five clinically-relevant cancer vaccines, three for HBV and two for HPV (4). These vaccines are successful because they avoid major issues in the development of a therapeutic vaccine: an immunosuppressive tumor microenvironment, low immunogenicity of the antigen, and a disease with high incidence (58). Successful prophylactic cancer vaccines take advantage of the immune system to provide lasting benefits of cancer prevention. Cancer vaccines can be used to prevent the formation of virally onset cancers or spontaneous cancers by initiating immune responses against a virus or neoantigen target.

Safety Concerns and Challenges of Prophylactic Cancer Vaccines

It is essential that preventative vaccines, given to healthy patients, do not cause any adverse side effects such as an autoimmune

TABLE 1 | Advantages and disadvantages of different prophylactic cancer vaccine strategies currently being investigated.

Vaccine Strategy	Advantages	Disadvantages
Virus-like Particles	Overcome B cell tolerance (11) Humoral and cellular responses (12)	Must be highly stable for proper downstream applications (13)
Carbohydrate-based	Ease of synthesis (14) target unique glycans (15) Humoral and cellular responses (16)	Poor immunogenicity (17)
Peptide	High stability against degradation *in vivo* (18) Ease of synthesis (19) Humoral and cellular responses (20, 21)	Inefficient immune response (22)
Lipid Nanoparticle	Overcome genetic material degradation (23) Easily synthesized (24)	Difficult to evaluate and predict *in vivo* effectiveness to identify proper dosage and side effects (24)
DNA	Stable at ambient temperatures (25) Ease of preparation (25) Humoral and cellular responses (26)	Inadequate immunogenicity (27)
Tumor-Derived Exosomes	Play natural role in tumor progression (28)	Primarily cellular response (29)
mRNA	Low manufacturing cost (30) Potential high potency Possible non-invasive administration (31)	*In vivo* stability (30) Primarily cellular response (31)
Autologous Tumor Cell	Personalized formulations (32) Humoral and cellular responses (33)	Requires patient tumor cells (32) Mainly therapeutic currently (34)
Allogenic Tumor Cell	Clinical trials for therapeutic version (35) Humoral and cellular responses (36, 37)	Limited current effectiveness (38) Mainly therapeutic currently (38)

response (59). Therefore, high risk individuals—those with increased risk of a specific cancer—are often the best candidates for such vaccines (59). Patients with syndromes such as hereditary non-polyposis colorectal cancer (HNPCC) have a genetic predisposition for specific cancers, motivating the development of a viable preventive measure (60). Since many of the prophylactic vaccines developed involve unnecessary exposure to cancer antigens, these vaccines must be engineered to ensure antigens do not increase cancer risk. This could also pose a problem for public acceptance and successful implementation of prophylactic cancer vaccines into the clinic. Other safety concerns include off-target effects and toxicity related to any possible vaccine materials (61). Successful engineering of prophylactic vaccines must consider the issue of safety earlier in development than therapeutic vaccines, as preventative vaccines are intended for healthy individuals.

There are several challenges that prophylactic vaccines must overcome that are described in this review. These obstacles include poor immunogenicity of common vaccine formulations, and poor stability *in vivo*. Furthermore, prophylactic vaccine trials may need to be proceeded by therapeutic vaccine development, as vaccine dosages for healthy clinical trial participants must be low. Immune system decline in elderly patients is another challenge faced by prophylactic cancer vaccines, as adaptive immunity is paramount to vaccine success. With 70% of cancer-related deaths occurring in patients 65 and older, this poses a significant problem that must be addressed (62).

HUMORAL CANCER VACCINES

Humoral, or antibody-mediated, vaccines invoke B cell responses to prevent disease and have the ability to last for decades, a goal of preventative cancer vaccines. For instance, smallpox vaccines can cause the maintenance of vaccinia-specific IgG+ memory B cells for more than 50 years (63). Another benefit of humoral vaccines is the possibility for secondary tumor antigen targeting. One phenomenon, known as epitope or antigen spreading, is an important concept in vaccine development, where an immune response develops for epitopes that are different than the disease-causing epitope, allowing for more complete and robust protection from disease (64, 65). Studies have shown epitope spread can increase the effectiveness of previously developed therapeutic cancer vaccines (66). For example, the FDA approved therapeutic autologous immunotherapy vaccine for metastatic castration-resistant prostate cancer, Sipuleucel-T, facilitates T cell priming and also results in elevated levels of antigen spread. This results in higher levels of IgG against secondary tumor antigen, increasing overall survival (64). Epitope spread has also been associated with tumor regression (67). In one study, highly specific intramolecular epitope spreading was partly responsible for preventative effects of a vaccine against KRAS-induced lung cancer (68).

Humoral vaccines offer other advantages in the form of neutralization and antibody-dependent cellular cytotoxicity (ADCC). These mechanisms protect cells from viral infection instead of controlling previously infected cells. Neutralizing antibodies function by binding to the virus, alerting the immune system to the presence of a foreign body and preventing the virus from infecting a cell (69). Antibody neutralization of the virus HPV can prevent infection by multiple mechanisms, such as prevention of cell surface binding and disruption of virus internalization (70). Humoral protection *via* neutralization of oncoviruses is an effective strategy to prevent some cancers, such as cervical cancer. ADCC, which utilizes innate immune cells to provide antitumor activity by linking antibodies to target cells, is also a vital part of the humoral response. Natural killer cells play a

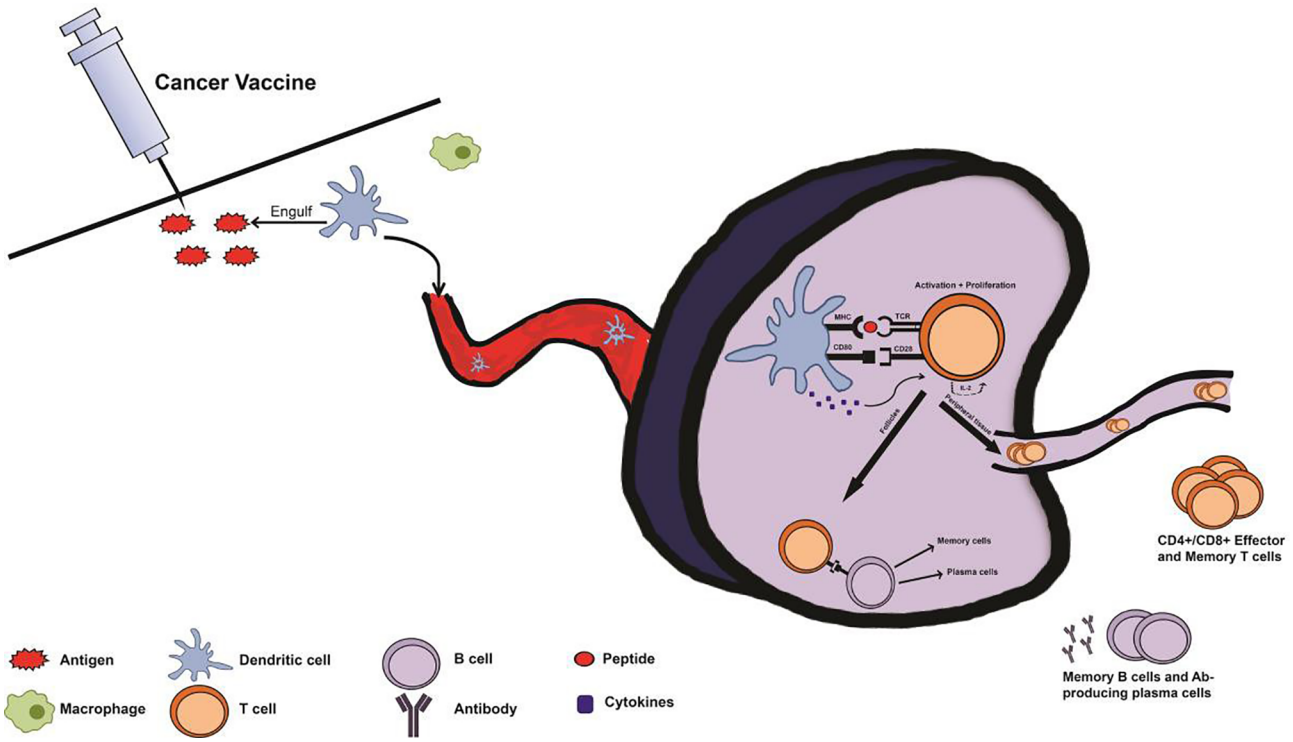


FIGURE 2 | Immune system response with prophylactic cancer vaccine administration. Following administration of a cancer vaccine, antigen-presenting cells (APCs) from the innate immune system such as macrophages and dendritic cells (DCs) recognize the injected antigen as foreign *via* pattern recognition receptors (PRRs), and uptake the antigen. Subsequently, the APCs transport the antigen, migrating to a lymph node and processing and presenting the antigen *via* major histocompatibility complex (MHC) pathway. Once in the lymph node, an immune synapse will form as the APC presents the antigen to an immature T cell at the T cell receptor (TCR). T cells will be activated by this interaction, with the aid of cytokines and co-stimulatory signals from the APC. Upon activation, T cells proliferate *via* IL-2 production and differentiate into effector T cells depending on cytokines and MHC type from the APC. These T cells can then contribute to the activation of B cells or travel to distant sites as effector or memory T cells. This primary response following vaccination produces memory cells so that secondary exposure to cancer-associated antigens results in a rapid and robust secondary immune response.

major role in ADCC, as they are responsible for provoking the immune response and direct cytotoxicity of cells infected by a virus and tumor cells (71). One study found that the success of a preventative human immunodeficiency virus (HIV) vaccine could be partially attributed to an ADCC response (72). Several cancer vaccines, including a MUC1-based cancer vaccine, have successfully elicited an ADCC response (73).

Verifying successful humoral response requires accurate quantification of antibodies and protein expression in patient plasma and tissue samples. Research has shown that many patients have a natural immunity to mesothelin, a glycoprotein expressed in several common cancers. ELISA analysis of IgG antibodies in patient serum and immunohistochemistry analysis of mesothelin protein expression of tumor specimens can be used to evaluate the effectiveness of vaccines and find potential antigen targets (74). A significant disadvantage of humoral vaccines stems from elderly patients having particularly weak humoral immune responses. Aging is associated with decreased B cell levels, which are essential for humoral vaccine success. *In vitro* and *in vivo* studies on tetanus toxoid showed decreases in IgG secretion in elderly patients, with younger patients not only having more B cells, but more potent B cells (75). Following immunization, younger patients also displayed elevated IgG levels for up to a year, while elderly patients returned to baseline levels after only 6 months (75). Since the age distribution of cancer patients skews toward the elderly, this is particularly concerning for the development of humoral cancer vaccines. Thus, when engineering cancer vaccines, especially for cancers originating from the lung, prostate and colon, which are common in elderly patients, it is vital to consider decreased humoral response (76).

Virus-Like Particles

Virus-like particles (VLPs) are protein structures with multiple subunits (13). Several VLPs have been engineered to prevent cancer by eliciting a humoral immune response, often through increasing IgG levels. In the past, VLPs have been used to treat many different viruses, as VLPs closely resemble the structure of the virus it is being used to prevent but lack virus-specific genetic material (13, 77). Specifically, commercially available vaccines against HPV are VLP-based, including Cervarix and Gardasil, in addition to the HBV vaccine (78). However, stability remains a

large concern for VLP vaccine development, as VLP vaccine success depends on downstream effects leading to a need for high stability (13). VLPs have been investigated to treat viruses. Future VLP vaccines must consider the issue of safety earlier in development than therapeutic vaccines, as preventative vaccines are intended for healthy individuals.

A VLP vaccine has been engineered to treat and prevent human epidermal growth factor receptor-2 (HER2)-positive breast cancers (11). To synthesize this VLP, S2 insect cells were transfected to express SpyCatcher-HER2 fusion antigen and incubated with Spytagged VLPs for a stable antigen coating. Transgenic mice, which can spontaneously develop HER2-positive mammary carcinoma, were vaccinated with this HER2-VLP. Vaccinated mice showed no tumor growth until one year of age, while untreated mice developed tumors after only two months. Elevated levels of anti-HER2 antibody were found in vaccinated mice for at least 24 weeks (11). HER2-VLP induced a stronger antibody response and provided better protection against tumor onset than a previously studied DNA vaccine, which had been more effective than passive administration of trastuzumab in HER2 transgenic mice. Furthermore, the anti-HER2 antibodies induced by the vaccine showed comparable affinity to that of monoclonal antibody (mAb) trastuzumab, a HER2-targeting antibody, and the vaccine showed decreased tumor onset when compared to mAb trastuzumab passive administration. The HER2-VLP vaccine inhibited not only tumor onset, but tumor growth, suggesting both preventative and therapeutic effects achieved by the vaccine (11).

Importantly, the HER2-VLP vaccine overcame B cell tolerance, a phenomenon which occurs when B cells die to prevent autoreactive antibody synthesis and is a frequent obstacle for humoral vaccine development (79). VLP vaccines can overcome this issue since they exhibit multivalent display of self-antigen (11). One study demonstrated that multivalent VLP induced higher IgG titers and overcame the effects of anergy (80). This outcome is likely due to VLP multivalency increasing the ability to create stable signaling domains, causing an increase in B cell activation (80). Using anti-HER2 antibodies from the mice, IgG antibodies elicited strong binding to HER2-positive human tumor cell lines, but no binding was detected on HER2-negative cell lines.

Carbohydrate-Based Vaccines

Using carbohydrate structures to induce an immune response is a promising direction in the field of vaccines (15). Cell-surface glycans are targeted by carbohydrate-based vaccines (15). While most carbohydrate-based vaccines are currently limited to therapeutics for infectious diseases, applications for preventative cancer vaccines have been proposed and studied (15). Specifically, the hexasaccharide Globo H (GH) has been proposed to both treat and prevent cancer (81). Globo H is a carbohydrate located on the outer membrane of epithelial cells and is often overexpressed in a variety of tumor specimens, including breast, ovarian, and lung cancer (82). Huang et al. proposed synthesizing a GH and linking it to a carrier protein as a therapeutic treatment for SSEA4-expressing breast cancers (81). Although this is strictly therapeutic, mice treated with this vaccine elicited IgG antibodies against the SSEA4 ganglioside, which can be overexpressed in breast cancer (81).

GH can be synthesized *via* glycal chemistry, one-pot synthesis or enzymatic synthesis. Among these methods, enzymatic synthesis is the cheapest and easiest, and requires enzymes overexpressed in *Escherichia coli* (14). Using sugar nucleotide regeneration and glycosyltransferases, GH can be synthesized in just three steps (14). The GH vaccine engineered by Danishefsky et al. not only induces anti-GH antibodies, but also anti-SSEA3 and anti-SSEA4 antibodies. These three glycoproteins are overexpressed on over 16 cancer types (83). Additionally, a glycolipid adjuvant was designed, which targeted CD1d receptors found on dendritic and B cells to cause a shift to IgG production. This process induces a switch from IgM, which is usually the sole response induced by carbohydrate-based vaccines (83). While this vaccine functions currently as a therapeutic, Danishefsky et al. indicate the possibility of using this vaccine in a preventative manner. The proposed design lays a framework for successful engineering of future carbohydrate-based vaccines. Unique glycan markers associated with cancer can be identified for use as a target, and then a carbohydrate compound can be designed using chemical and immunological processes to effectively leverage the target for cancer prevention (83).

A common problem with carbohydrate vaccines is poor immunogenicity of tumor-associated carbohydrate antigens (TACAs). Sialyl-TN (STn) is an oncofetal antigen found in specific cancers and has been used as an adjuvant to boost the immunogenicity of TACAs (17). One study couples three fluoro-substituted STn analogues to the metalloprotein keyhole limpet hemocyanin (KLH). Fluorine-modified STn compounds can be used to increase immunogenicity and thereby increase the strength of the immune response (84). Previously, it has been shown that 4-KLH, a fluorine-modified STn antigen, results in increased IgG levels when compared to anti-modified-STn (85). Both therapeutic and preventative effects were observed *in vivo*. 4-KLH-vaccinated mice inoculated with colorectal cancer showed increased anti-STn antibodies when compared to a 1-KLH vaccine. 4-KLH also showed some preventative effects when compared to the control (84). This result could provide the framework for STn-KLH vaccines as a means to prevent cancer formation when used with the proposed fluorine modification strategy.

Lipid Nanoparticle Vaccines

Lipid nanoparticle (LNP) vaccines have the potential to effectively deliver genetic information for cancer prevention. Delivery of mRNA and DNA to the body has potential to prevent cancer, but degradation is often a problem for delivery of naked genetic material (23). Use of LNPs can help overcome these problems for preventative cancer vaccines. LNPs are easily synthesized and can protect mRNA or DNA from degradation (24). However, there are challenges associated with LNP vaccine development. Assays to effectively predict *in vivo* responses do

not currently exist, as current assays only measure second-order effects. LNPs may complete their goal successfully, but if certain pathways are not activated, these effects will be undetectable to current assays. This presents challenges when evaluating different formulations, dosages, and side effects (24).

CELLULAR CANCER VACCINES

Cellular vaccines induce CD8+ and CD4+ T cell activity (57). For many successful vaccines, memory T cell induction is vital to eliciting a sufficient immune response to stop disease formation. This response requires large-scale changes in both the properties and number of T cells (86). The idea for cellular vaccines against cancer originated from successful T cell-mediated vaccines for viral infections. T cell-mediated vaccines can have both preventative and therapeutic benefits. For example, a vaccine engineered to prevent HPV and cervical cancer development induces CD8+ T cells, which provides lasting protection against HPV and associated diseases (87). While engineering new vaccines, it is important to consider that a sufficient dose is required to induce a T cell response strong enough to prevent disease, so a high dosage must not be toxic. Another concern with engineering cellular vaccines is overexertion of T cells (88). An overexerted immune system can cause T cell exhaustion, and ultimately, dysfunction. T cell exhaustion is the result of sustained expression of inhibitory receptors, low effector function, and an altered transcriptional state. It leads to decreased immune control of tumors and infections, and poor memory formation (88). Exhaustion can occur during chronic infection and cancer, making it a significant problem that must be addressed when engineering cellular vaccines against cancer (88). Another concern with cellular vaccines, as with humoral vaccines, is age-associated decline. T cell-mediated immunity declines with age due to alterations in the thymus, signal transduction and HLA Class II expression on monocytes (89–91). Aging is also associated with decreased T cell reactivity to foreign antigens (89). Despite these concerns, the successful engineering of preventative cellular vaccines against oncogenic viral infections, which cause 15% of cancers worldwide, offers promise for similar solutions to cancer prevention (92).

Peptide Vaccines

Peptide vaccines use engineered short peptide fragments to induce a specific immune response (22, 93). Longer amino acid chains may also be used, but shorter chains are most common (93). Peptide vaccines can be engineered to have stability against degradation *in vivo* and are cost effective and easy to synthesize (18, 19). Nevertheless, they suffer from poor immunogenicity (22). A peptide vaccine designed to prevent breast cancer was formulated with stabilizing chemical pan DR epitope (PADRE), a carrier epitope used to engineer synthetic and recombinant vaccines (94). A nanoliposomal vaccine was designed using DOPE-containing liposomes and engineered with three different peptides (AE36, E75, and E75-AE36) used in combination with PADRE. Vaccinated mice showed higher CD4+ and CD8+ T cell induction when compared to mice treated with liposomal short peptides without PADRE and mice treated with non-liposomal peptides. Furthermore, increased IFN-γ levels were observed, which promotes adaptive immune mechanisms (95, 96). IFN-γ also plays a role in promoting tumor surveillance, although the exact mechanism is unknown. Previous studies have hypothesized that IFN-γ may even be the basis for immune surveillance. Nevertheless, it is clear that IFN-γ plays a role in directing tumor surveillance to chemically-induced tumors, as well as tumors caused by genetic defects (96).

Transmembrane protein GP2 has also been explored for use in peptide vaccines (97). GP2 vaccines have been explored as viable means to prevent breast cancer reoccurrence for HER2/*neu*+ patients. A polymorphism leading to a mutant GP2 protein called 2VGP2 was found at codon 655 of the HER2/neu protein and has been identified as a common mutation associated with higher risk of breast cancer (98). Autologous DCs from blood samples from HLA-A2 breast cancer patients were pulsed with synthesized GP2 and used to stimulate T cells *in vitro*. Cytotoxicity experiments showed killing of breast and ovarian cancer cells *via* GP2-stimulated CD8+ T cells. These experiments confirm GP2 immunogenicity and show its potential as a peptide vaccine against HER2/*neu*+ breast cancer (99).

A KRAS-targeting peptide vaccine has been engineered to prevent lung cancer. KRAS is considered a proto-oncogene, with mutant KRAS a common driver of cancer (100). A KRAS peptide vaccine was developed with four peptides corresponding to different regions of the protein, and CpG, R848, and anti-CD40 were used as adjuvants. This vaccine increased IFN-γ and granzyme B levels in CD8+ T cells, and when combined with avasimibe, resulted in infiltration of CD8+ T cells in tumors and prevented KRAS-driven lung tumorigenesis. Thus, this vaccine may be a starting point to develop vaccines to prevent premalignant lung legions with mutant KRAS from progressing to malignant lesions (101).

DNA Vaccines

DNA vaccines are appealing due to the ability to mimic natural infections, ease of production, and stability at ambient temperatures (25). Several DNA vaccines have been developed to prevent prostate cancer but have had mixed results in clinical trials, DNA vaccines often failing due to inadequate immunogenicity (27, 102). A DNA vaccine was proposed to prevent castration resistant prostate cancer (CRPC), using RALA/pPSCA nanoparticles (NP) incorporated into a dissolvable microneedle (MN) patch. RALA codes for Ras-related protein Ral-A, a protein implicated in several cancers, and pPSCA is a plasmid encoding prostate stem cell antigen. RALA/pPSCA-loaded MNs caused endogenous production of prostate stem cell antigen, and induced a response against TRAMP-C1 tumors *ex vivo* and anti-tumor immunity *in vivo*. In prophylactic experiments, unvaccinated mice developed palpable tumors within seven days of tumor implantation, whereas vaccinated

mice showed delayed tumor growth. On average, tumor development took 16.2 days for RALA/pPSCA-loaded MNs-treated mice, with one mouse remaining tumor free through the duration of the experiment. This study shows that the use of microneedles to administer a DNA vaccine could be a promising strategy to prevent cancer formation (26).

Tumor-Derived Exosomes

Exosomes are microvesicles released by cells in physiological and pathological settings; exosomes are enclosed by a lipid bilayer with proteins from the origin cell. These cargo exosomes can assist in tumor progression and cancer metastasis by delivering parental cell proteins and nucleic acids to target cells (28). The proteins or nucleic acids in cargo exosomes that contain antigens associated with the parental cancer cells could, therefore, become targets for prophylactic vaccination. Tumor growth is promoted by tumor-derived exosomes (TEX), exosomes released from tumor cells. They signal to both cancerous and normal cells throughout the body and play a role in cancer progression (103). A vaccine against breast cancer has been engineered using TEX. TSA, a BALB/c mouse-derived mammary carcinoma, was exposed to Sham radiotherapy (RT) to develop TEX (104, 105). A vaccine of TEX from untreated cells (UT-TEX) was also used. The RT-TEX vaccine induced a tumor-specific CD8+ response, with 2 of 6 mice vaccinated showing no tumor growth and 4 showing reduced tumor growth compared to UT-TEX-vaccinated mice. RT-TEX-vaccinated mice had a higher number of CD8+ T cells in the tumor, many of which were specific to an immunodominant antigen in the tumor. This supports the idea that TEX produced *via* irradiated cancer cells is a viable strategy for cancer prevention (29).

mRNA Vaccines

mRNA vaccines have the advantage of low-cost manufacturing and potential for high potency. However, stability *in vivo* is a large concern for successful engineering of mRNA vaccines against cancer (30). Even so, mRNA-based vaccines independent of VLP carriers are in development. Previous methods have injected DCs transfected with mRNA with promising results, but this method is costly (106). Another study recommended nasal administration of an mRNA vaccine for the prevention of cancer. Nasal administration is promising due to its non-invasive format and high patient compliance. Tests were performed for nasal administration of naked and nanoparticle encapsulated mRNA for tumor prevention using a mouse model. The mRNA was encoding for a tumor antigen. While the naked mRNA administration did not prevent tumor growth, nasal administration of mRNA encapsulated in nanoparticles was effective for tumor prevention. Therapeutic effects were also observed in additional experiments. Splenocytes recovered from the mice revealed anti-cancer CD8+ T cells in mice treated with the encapsulated mRNA vaccine. As one of the few mRNA vaccine studies available for cancer vaccination, this study shows possible effectiveness of mRNA vaccines for cancer prevention in addition to showing possible effectiveness of nasal administration of prophylactic and therapeutic cancer vaccines (31).

COMBINED CELLULAR AND HUMORAL CANCER VACCINES

As discussed above, there are advantages to both humoral and cellular vaccines. However, many vaccines induce both a humoral and cellular immune response. Vaccines can cause a biased immune response toward one type of adaptive immunity while inducing both T and B cell immunity (36). The benefit of a combined humoral and cellular response can be seen in many non-cancer vaccines. For instance, for influenza prevention, the trivalent live attenuated influenza vaccine (LAIV) induces both B cell and T cell responses. Conversely, the trivalent inactivated influenza vaccine (TIV), which only invokes a T cell response, has been found to be immunologically inferior (20).

Combined Peptide Vaccines

While many peptide vaccines induce only a cellular immune response, others can induce both humoral and cellular responses. A mimotope peptide-based vaccine was developed using BAT monoclonal antibodies, which have immune modulatory and anti-tumor effects (20). Mimotopes are peptides that can bind to an antibody directed against a certain antigen (21). For this vaccine, BAT-binding peptides A and B were used as mimotopes. Vaccinated mice displayed increased IgG antibody production, which competed with BAT binding on Daudi cells, a human B lymphoblast. The IgG antibodies caused similar immune stimulation to BAT, indicating a humoral component to the vaccine. The observed cellular response included increased cytolytic activity, and the vaccine prevented tumor growth *in vivo* in a mouse model (20).

A self-adjuvanting multivalent glycolipopeptide (GLP) has also been developed as a vaccine (21). The GLP vaccines display four components on a molecular delivery system: TACA B cell epitope, CD4+ Th peptide epitope, CD8+ CTL peptide epitope, and immunoadjuvant palmitic acid. This GLP vaccine was administered in combination with PADRE and regioselectively addressable functionalized template molecules (RAFT). *In vivo*, vaccinated mice did not develop tumors over a 90-day period, while unvaccinated mice developed tumors around 35 days after tumor inoculation. Serum collected from BALB/c mice showed IgG antibodies specific to breast cancer, and upregulation of CD4+ and CD8+ T cells, indicating both humoral and cellular responses (21).

Another combined peptide vaccine has undergone clinical trials for the prevention of colorectal cancer. A MUC1-poly-ICLC vaccine has been tested for patients with advanced adenomatous polyps, which are a precursor to colorectal cancer. MUC1 is a glycoprotein and tumor-associated antigen (TAA) for colorectal cancer. Around 43% of patients showed elevated anti-MUC1 IgG levels following vaccination, and long-term memory was observed. T cell response and memory were also measured following a booster vaccine (107). Thus, this vaccine formulation could be useful for prophylactic vaccination in some patients with advanced adenomatous polyps (108).

A vaccine for patients with ductal carcinoma *in situ* (DCIS) has been developed to prevent progression. DCIS is often

associated with HER-2/*neu* overexpression. Patients were given 4 doses of the Her-2/*neu*-pulsed dendritic cells. This vaccine resulted in lower HER-2/*neu* expression and T and B lymphocyte accumulation in the breast. Tumorlytic antibodies were observed. This vaccine lowered HER-2/*neu* expression in addition to decreasing residual DCIS following resection. These results suggest possible prophylactic value for this vaccine formulation (109).

Virus-Like Particles

VLPs have been studied as a way to induce a combined humoral and cellular response. An mRNA-based VLP was developed to target prostate cancer, which has shown responsiveness to mRNA-based vaccines in previous studies (110, 111). Obtaining sufficient *in vivo* potency for nucleic acid vaccines has been difficult, as repeated use of viral vectors results in a dampened immune response (112). A recombinant bacteriophage MS2 mRNA-based VLP was developed using pESC yeast epitope tagging vectors, and PEG precipitation for synthesis to induce both a humoral and cellular response (12). VLP-vaccinated C57BL/6 mice exhibited elevated levels of IgG antibodies and increased antigen-specific cytotoxic T lymphocytes. Further investigation found that the initial Th2 response was converted to Th1 by target proteins. Mice were injected with TRAMP-C2 cells, a murine model of prostate cancer, and vaccinated mice were effectively protected from tumor development (12). This vaccine offers many advantages when compared to other nucleic acid vaccines, such as easy preparation using recombinant protein technology, and production of a strong humoral and cellular response.

Carbohydrate-Based Vaccines

Carbohydrate-based vaccines have been engineered to induce a combined humoral and cellular response. A fluoro-substituted STn analogue was coupled with a nontoxic cross-reactive material of diphtheria toxin 107 (F-Stn-CRM197) for cancer prevention. When combined with Freund's adjuvant, F-STn-CRM197 had significantly higher IFN-γ- and IL-4-releasing splenocytes compared to control. Vaccinated mice showed elevated levels of anti-STn IgG antibodies, which were further elevated with Freund's adjuvant. The F-STn-CRM197 vaccine increased cellular and humoral immune responses when compared to a STn-CRM197 vaccine. This immune response resulted in increased cancer cell lysis. The data of Song et al. suggests the utility of this vaccine as a cancer prophylactic, building a basis for future carbohydrate-based cancer vaccine development (16).

Autologous Tumor Cell Vaccines

Autologous tumor cell vaccines are derived from a patient's own tumor, and although this personalized formulation has been exclusively therapeutic, it holds potential as building blocks for preventative vaccines (32). Agenus' autologous tumor cell vaccine, AutoSynVax, has controlled tumor growth and produced lasting immune responses in recent pre-clinical and phase I clinical trials (34). While this vaccine is therapeutic, the development of autologous tumor cell vaccines to prevent recurrence is underway to prevent cancer recurrence in the setting of high-risk cancer patients. For instance, the use of autologous induced pluripotent stem cells (iPSCs) has been proposed for the development of an autologous tumor cell vaccine (33). Mice vaccinated with iPSCs combined with a CpG adjuvant were inoculated with B16F0 melanoma cells four weeks later. Vaccinated mice showed decreased tumor progression, and spleen analysis revealed increased tumor-specific effector and memory helper T cells. Additionally, there were more mature APCs found in the vaccinated group. While antibody analyses were not included in the study, increased IgG responses were measured in therapeutic experiments, indicating the possibility that this formulation could successfully induce both a humoral and cellular response. This study showed that prophylactic immunization with non-genetically engineered iPSC-based vaccines produce immune responses to melanoma. These vaccines have the potential for tumor immunity to a larger number of cancer types, which is supported by the large number of tumor antigens presented. Both humoral and cellular effects were observed. The use of autologous iPSCs was suggested as they may provide an accurate and personalized panel of a patient's tumor immunogens (33).

Allogenic Tumor Cell Vaccine

Allogenic tumor cell vaccines differ from autologous vaccines in that they are derived from another patient's cells. Melacine, an allogenic tumor cell vaccine for treatment of melanoma, has undergone phase I, II, and III clinical trials, and survival benefits for patients were observed (35). The overall success of allogenic tumor cell vaccines has been limited to therapeutic immunotherapy (38). A preventative vaccine has been proposed using a vaccine derived from the fusion of allogenic DCs with tumor cells (36). DC-tumor fusion vaccines allow for the presentation of a broad spectrum of tumor-associated antigens (113). This vaccine was engineered using PEG-mediated fusion between DCs and inactive gastric cancer cells. The fused cell (FC) vaccine was combined with CTLs to prevent gastric cancer. Vaccinated mice showed slowed tumor growth compared to the control, with 9 of 10 remaining tumor-free and surviving for 90 days. The vaccine successfully induced cytotoxic T lymphocyte cloning through induction of antigenic determinants, resulting in anti-tumor effects. Furthermore, IL-7 and IL-15 levels increased following immunization, indicating immune memory formation.Elevated levels of IFN- γ and IL-10, which enhance B cell survival and antibody production, were observed. This study verified antigen-presenting and tumor-targeting effects from DC-based tumor vaccines and provides a template for future vaccine development (36).

Our group recently fabricated a preventative vaccine for triple-negative breast cancer (37). This vaccine was developed by sonicating 4T1 breast cancer cells and delivering the tumor nano-lysate (TNL) to BALB/c mice *via* tail vein injection 10 d before 4T1 tumor inoculation. Tumor growth and metastasis were significantly delayed, and survival was increased for mice in the vaccinated group compared to the unvaccinated group. While the TNL-vaccinated mice ultimately developed tumors, the success of this simple process motivates future

studies to engineer similar vaccines to produce a preventative response (37).

DNA Vaccines

The idea of DNA vaccines has received much attention over the past decade (114). A DNA vaccine to induce both cellular and humoral responses *in vivo* has been proposed to prevent HPV infection, specifically high risk HPV16 and 18, or HPV16-E7-expressing tumors (115). These viruses, encoding for oncoproteins E6 and E7, promote cervical cancer development (116). The proposed polynucleotide vaccine uses a designed DNA sequence coding for an E6/E7 fusion protein. Vaccinated mice had complete tumor prevention when injected with TC-1 cells, a tumor cell line derived from primary lung epithelial cells that are E6- and E7-expressing (117). Vaccination resulted in an E7-specific antibody response that lasted at least five months. E6- and E7-specific T cells could be identified after 5 months (115). Despite the many obstacles to successful DNA vaccines, this vaccine serves as evidence that the use of prophylactic cancer vaccines is possible and should be further studied (115).

CONCLUSIONS

Preventative vaccines have helped to eradicate many diseases. Cancer remains one of the leading causes of death and healthcare burden in the United States. The development of prophylactic cancer vaccines has the potential to save lives and reduce healthcare costs by going beyond treating cancer to preventing it altogether. These vaccines are currently in a variety of development stages, from concept design and research, to implementation, and clinical practice.

Some of these vaccines produce humoral or cellular immune responses, with associated advantages and disadvantages. While, humoral vaccines allow for long-term immune protection and may be used to target secondary tumor antigens, B cell tolerance can limit their effectiveness. Cellular vaccines can have both preventative and therapeutic benefits, but T cell exhaustion is a common problem that needs to be addressed. Engineered vaccines that induce both humoral and cellular immune responses could represent an innovative solution to address these shortcomings. However, all cancer vaccines must consider age-related immune decline, a problem magnified by the elevated age distribution of cancer patients. Aging is associated with decreased B cell prevalence and potency, attenuating the effectiveness of humoral immune responses. Furthermore, multifactorial phenomenon, including changes to the thymus, cause a decrease in T cell reactivity, resulting in reduced cellular immunity. These challenges require new, innovative solutions. One possible solution is combining cancer vaccine administration with immune augmentation treatments. Vaccinated patients with high-risk of cancer development may be given continuing doses, with increasing frequency as they age.

Many strategies have been discussed in this review to prevent tumor development *via* cellular, humoral or a combined immune response. VLPs and carbohydrate-based vaccines have been designed to induce humoral responses or a combined humoral and cellular immune response. VLP vaccines are able to overcome B cell tolerance due to their multivalent display of self-antigens, but stability must be addressed. Carbohydrate-based vaccines, which have the advantage of targeting unique glycan markers, often show poor immunogenicity. Peptide vaccines and DNA vaccines are able to induce a cellular response or a combination of humoral and cellular. Peptide vaccines are usually engineered to have high stability against degradation *in vivo* and are easy to synthesize but suffer from inefficient immune responses. DNA vaccines are easy to produce and stable, but exhibit inadequate immunogenicity. mRNA vaccines have the potential for high potency but lack *in vivo* stability. Autologous and allogeneic tumor cell vaccines utilize both cellular and humoral immunity, but most current uses are therapeutic in nature. Maximizing the potential of the immune system may be necessary to successfully engineer preventative cancer vaccines, requiring the utilization of both humoral and cellular immunity. Further research into these strategies will lead to improved prophylactic cancer vaccines.

Despite the benefits of each type of vaccine, DNA and mRNA vaccines are garnering increased attention. With new technologies being developed, it seems that DNA and mRNA vaccines may offer the most promise for future research. DNA and mRNA vaccines may be developed to specifically target tumor antigens and promote specific immune responses against tumor onset. New technologies in LNPs and other nanomaterial carriers may help overcome stability problems associated with mRNA vaccines, increasing potency of the vaccine.

Currently, there are very few prophylactic cancer vaccines on the market. Gardasil and Cervarix prevent HPV, while Energix-B, Recombivax HB and Hiberix-B prevent HBV; these two viruses are commonly associated with cancer development (118). These vaccines have been highly successful, and the number of cervical cancer patients has decreased as vaccination has become more prevalent. Following these successful viral vaccines, there is great potential in preventing cancers caused by viruses, which account for 15% of all cancers. Development of vaccines to prevent the remaining 85% of cancer types is underway. However, significant obstacles remain in the development of vaccines for these cancers not caused by viruses. While vaccines against HPV and HBV stop cancer through viral protection, preventing cancers with no known viral etiology will be much more challenging. Researchers must identify viable targets, engineer successful delivery mechanisms, and find long-lasting immune effects. Many current technologies allow for preventative success in non-human tests, but one of the major problems will be finding solutions at clinically relevant doses. Further issues include prevention of immune response to self-antigens. This challenge may be overcome by identifying cancer-specific membrane expression or pre-malignant tumor properties to target. One possible way to overcome this issue is through targeting of neoantigens, a type of tumor-specific antigen, as they are recognized as non-self by the immune system (56). Another possible target includes tumor-associated

TABLE 2 | Summary of the most promising prophylactic cancer vaccine formulations and possible antigens and targets associated with each vaccine strategy.

Vaccine Strategy	Example Vaccines Developed	Antigens/Targets
Virus-like Particles	Cervarix and Gardasil – Commercially available vaccines for HPV (78) HER2-VLP Vaccine – Vaccine for HER2-Postive breast cancer (79) MS2 mRNA-based VLP – Vaccine for prostate cancer (12)	HER2 – protein (79)
Carbohydrate-based	4-KLH Vaccine – Vaccine for colorectal cancer targeting STn (84)	Sialyl-TN – oncofetal antigen (17)
Peptide	KRAS-targeting Peptide Vaccine – Vaccine for lung cancer (100) MUC1-poly-ICLC Vaccine – Vaccine for colorectral cancer (107)	KRAS – proto-oncogene (100) MUC1- glycoprotein and TAA (107)
DNA	RALA-pPSCA-loaded MNs – Vaccine for CRPC (26) HPV Polynucleotide Vaccine – Vaccine for HPV16 and HPV18 (115)	Ral-A – protein (26) E6/E7 – oncoprotein (116)
Tumor-derived Exosomes	RT-TEX Vaccine – Vaccine for mammary carcinoma (29)	Multiple targets (29)
mRNA	Nasal Encapsulated mRNA Vaccine – Vaccine encoding for tumor antigen (31) MS2 mRNA-based VLP – Vaccine for prostate cancer (12)	Multiple targets (12, 31)
Allogenic Tumor Cell	Tumor Nano-Lysate Vaccine – Vaccine for triple-negative breast cancer (37)	Multiple targets (37)

antigens, although those are more difficult since they are also found in healthy cells. Finding possible targets to prevent tumor onset is critical for successful vaccine development for spontaneous cancers (**Table 2**).

Despite these obstacles, current research points to vaccine strategies that could be viable for cancer prevention. Success in animal models offers a promising template for clinical development. Several strategies discussed in this review seem viable for future development; additional insights may come by engineering solutions that combine multiple approaches. However, the benefits of prophylactic vaccine development justify these difficulties. Prophylactic cancer vaccines could be administered to high-risk groups. For example, those with familial risk of triple-negative breast cancer would be ideal candidates for vaccination with a breast cancer vaccine. Patients with hereditary non-polyposis colorectal cancer (HNPCC), a genetic predisposition to colorectal cancer, would also make ideal candidates for vaccination. Successful development of prophylactic cancer vaccines will lead to new challenges: when to administer vaccines, ideal vaccine patients, and proper monitoring of vaccine success in patients. Eliciting strong and lasting immune response is critical for the success of prophylactic vaccine implementation. Furthermore, immune responses must be directed at targets unique to tumor cells during the early stages of carcinogenesis. Likely, vaccines with the most success will elicit both humoral and cellular responses as they work together to strengthen anti-tumor response upon tumor onset. This will include T cell memory, antibody generation, and possible responses by other immune cells, such as dendritic cells. Vaccines can be engineered to induce these responses. Successful immune induction will likely include engineered peptides or carbohydrates combined with stabilizing chemicals. Development and fabrication of both primary components and stabilizing chemicals, such as PEG, PADRE, or liposomal encapsulations, could lead to the prevention of spontaneous cancer formation.

With a foundation for preventative cancer vaccines established, and approved vaccines to prevent two cancer-associated viruses, there is hope that more types of cancer will be prevented by engineering vaccines to evoke a specific immune response. Targeting and promoting the adaptive immune system to respond to a preventative, anti-cancer vaccine will be crucial to the adoption of more successful, prophylactic cancer vaccines.

AUTHOR CONTRIBUTIONS

DC and JD wrote the article, and MK edited it. All authors contributed to the article and approved the submitted version.

REFERENCES

1. Riedel S. Jenner and the History of Smallpox and Vaccination. *Baylor Univ Med Cent Proc* (2005) 18(1):21–5. doi: 10.1080/08998280.2005.11928028
2. CDC National Health Report Highlights CS251163.
3. Siegel RL, Miller KD, Fuchs HE, Jemal A. Cancer statistics, 2021. *CA Cancer J Clin* (2021) 71(1):7–33. doi: 10.3322/caac.21654
4. Tsai H. Clinical cancer chemoprevention: From the hepatitis B virus (HBV) vaccine to the human papillomavirus (HPV) vaccine. *Taiwan J Obstet Gynecol* (2015) 54(2):112–5. doi: 10.1016/j.tjog.2013.11.009
5. Palmer T, Wallace L, Pollock KG, Cuschieri K, Robertson C, Kavanagh K, et al. Prevalence of cervical disease at age 20 after immunisation with bivalent HPV vaccine at age 12-13 in Scotland: retrospective population study. *Int J Gynecol Cancer* (2019) 365:l1161. doi: 10.1136/bmj.l1161
6. Jou J, Harrington KJ, Zocca MB, Ehrnrooth E, Cohen EEW. The Challenging Landscape of Therapuetic Cancer Vaccines – Novel Platforms and Neoantigen Identification. *Clin Cancer Res* (2021) 27 (3):689–703. doi: 10.1158/1078-0432.CCR-20-0245
7. Disis N, Coveler, Bates N. Progress in the development of a therapeutic vaccine for breast cancer. *Breast Cancer Targets Ther* (2010) 2:25. doi: 10.2147/BCTT.S6956
8. Ozawa S, Mirelman A, Stack ML, Walker DG, Levine OS. Cost-effectiveness and economic benefits of vaccines in low- and middle-income countries: A systematic review. *Vaccine* (2012) 31(1):96–108. doi: 10.1016/j.vaccine.2012.10.103
9. Mariotto AB, Enewold L, Zhao J, Zeruto CA, Yabroff KR. Medical Care Costs Associated with Cancer Survivorship in the United States. *Cancer Epidemiol Biomarkers Prev* (2020) 29(7):1304–12. doi: 10.1158/1055-9965.EPI-19-1534
10. Plotkin SA, Orenstein WA, Offit PA. *Vaccines. 5th*. Philadelphia, PA, USA: Saunders Elsevier (2008). p. 1.
11. Palladini A, Thrane S, Janitzek CM, Pihl J, Clemmensen SB, de Jongh WA, et al. Virus-like particle display of HER2 induces potent anti-cancer responses. *Oncoimmunology* (2018) 7(3):e1408749. doi: 10.1080/2162402X.2017.1408749
12. Li J, Sun Y, Jia T, Zhang R, Zhang K, Wang L. Messenger RNA vaccine based on recombinant MS2 virus-like particles against prostate cancer. *Int J Cancer* (2014) 134(7):1683–94. doi: 10.1002/ijc.28482

13. Zeltins A. Construction and characterization of virus-like particles: A review. *Mol Biotechnol* (2013) 53(1):92–107. doi: 10.1007/s12033-012-9598-4
14. Tsai TI, Lee HY, Chang SH, Wang CH, Tu YC, Lin YC, et al. Effective sugar nucleotide regeneration for the large-scale enzymatic synthesis of globo H and SSEA4. *J Am Chem Soc* (2013) 135(39):14831–9. doi: 10.1021/ja4075584
15. Nishat S, Andreana P. Entirely Carbohydrate-Based Vaccines: An Emerging Field for Specific and Selective Immune Responses. *Vaccines* (2016) 4(2):19. doi: 10.3390/vaccines4020019
16. Song C, Zheng XJ, Guo H, Cao Y, Zhang F, Li Q, et al. Fluorine-modified sialyl-Tn-CRM197 vaccine elicits a robust immune response. *Glycoconj J* (2019) 36(5):399–408. doi: 10.1007/s10719-019-09884-0
17. Munkley J. The role of sialyl-Tn in cancer. *Int J Mol Sci* (2016) 17(3):275. doi: 10.3390/ijms17030275
18. Skwarczynski M, Toth I. Peptide-based synthetic vaccines. *Chem Sci* (2016) 7 (2):842–54. doi: 10.1039/C5SC03892H
19. Kumai T, Kobayashi H, Harabuchi Y, Celis E. Peptide vaccines in cancer — old concept revisited. *Curr Opin Immunol* (2017) 45:1–7. doi: 10.1016/j.coi.2016.11.001
20. Xing Cheng HJ, Zengel JR, Suguitan ALJr, Xu Q, Wang W, Lin J. Evaluation of the Humoral and Cellular Immune Responses Elicited by the Live Attenuated and Inactivated Influenza Vaccines and Their Roles in Heterologous Protection in Ferrets. *J Infect Dis* (2013) 208(4):594–602. doi: 10.1093/infdis/jit207
21. Renaudet O, BenMohamed L, Dasgupta G, Bettahi I, Dumy P. Towards a Self- Adjuvanting Multivalent B and T cell Epitope Containing Synthetic Glycolipopeptide Cancer Vaccine. *ChemMedChem* (2008) 3(5):737–41. doi: 10.1002/cmdc.200700315
22. Li W, Joshi MD, Singhania S, Ramsey KH, Murthy AK. Peptide vaccine: Progress and challenges. *Vaccines* (2014) 2(3):515–36. doi: 10.3390/vaccines2030515
23. Hobernik D, Bros M. DNA vaccines—How far from clinical use? *Int J Mol Sci* (2018) 19(11):3605. doi: 10.3390/ijms19113605
24. Reichmuth AM, Oberli MA, Jeklenec A, Langer R, Blankschtein D. mRNA vaccine delivery using lipid nanoparticles. *Ther Deliv* (2016) 7(5):319–34. doi: 10.4155/tde-2016-0006
25. Porter KR, Raviprakash K. DNA Vaccine Delivery and Improved Immunogenicity,"87. *Curr Issues Mol Biol* (2017) 22:129–38. doi: 10.21775/cimb.022.129
26. Cole G, Ali AA, McErlean E, Mulholland EJ, Short A, McCrudden CM, et al. DNA vaccination via RALA nanoparticles in a microneedle delivery system induces a potent immune response against the endogenous prostate cancer stem cell antigen. *Acta Biomater* (2019) 96:480–90. doi: 10.1016/j.actbio.2019.07.003
27. Cole G, McCaffrey J, Ali AA, McCarthy HO. DNA vaccination for prostate cancer: Key concepts and considerations. *Cancer Nanotechnol* (2015) 6(1):2. doi: 10.1186/s12645-015-0010-5
28. Zhang Z, Dombroski JA, King MR. Engineering of Exosomes to Target Cancer Metastasis. *Cell Mol Bioengineer* (2020) 13(1):1–16. doi: 10.1007/s12195-019-00607-x
29. Diamond JM, Vanpouille-Box C, Spada S, Rudqvist NP, Chapman JR, Ueberheide BM, et al. Exosomes Shuttle TREX1-Sensitive IFN-Stimulatory dsDNA from Irradiated Cancer Cells to DCs. *Cancer Immunol Res* (2018) 6 (8):910–20. doi: 10.1158/2326-6066.CIR-17-0581
30. Pardi N, Hogan MJ, Porter FW, Weissman D. mRNA vaccines-a new era in vaccinology. *Nat Rev Drug Discov* (2018) 17(4):261–79. doi: 10.1038/nrd.2017.243
31. Phua KKL, Staats HF, Leong KW, Nair SK. Intranasal mRNA nanoparticle vaccination induces prophylactic and therapeutic anti-tumor immunity. *Sci Rep* (2014) 4:5128. doi: 10.1038/srep05128
32. Dummy A. *Autologous tumor cell vaccine*. Washington DC, USA: National Cancer Institute (2020).
33. Kooreman NG, Kim Y, de Almeida PE, Termglinchan V, Diecke S, Shao NY, et al. Autologous iPSC-Based Vaccines Elicit Anti-tumor Responses *In vivo*. *Cell Stem Cell* (2018) 22(4):501–13.e7. doi: 10.1016/j.stem.2018.01.016
34. Dummy A. *Safety and Tolerability Study of AutoSynVaxTM Vaccine in Subjects With Advanced Cancer*. (2020). ClinicalTrials.gov Identifier: NCT02992977.
35. Sondak VK, Sosman JA. Results of clinical trials with an allogeneic melanoma tumor cell lysate vaccine: Melacine®. *Semin Cancer Biol* (2003) 13(6):409–15. doi: 10.1016/j.semcancer.2003.09.004
36. Li C, Liang S, Zhang C, Liu Y, Yang M, Zhang J, et al. Allogenic dendritic cell and tumor cell fused vaccine for targeted imaging and enhanced immunotherapeutic efficacy of gastric cancer. *Biomaterials* (2015) 54:177–87. doi: 10.1016/j.biomaterials.2015.03.024
37. Dombroski JA, Jyotsana N, Crews DW, Zhang Z, King MR. Fabrication and Characterization of Tumor Nano-Lysate as a Preventative Vaccine for Breast Cancer. *Langmuir* (2020) 36(23):6531–9. doi: 10.1021/acs.langmuir.0c00947
38. Srivatsan S, Patel JM, Bozeman EN, Imasuen IE, He S, Daniels D, et al. Allogeneic tumor cell vaccines: The promise and limitations in clinical trials. *Hum Vaccines Immunother* (2014) 10(1):52–63. doi: 10.4161/hv.26568
39. Hanahan D, Weinberg RA. Hallmarks of Cancer : The Next Generation. *Cell* (2011) 144(5):646–74. doi: 10.1016/j.cell.2011.02.013
40. Comito G, Ippolito L, Chiarugi P, Cirri P. Nutritional Exchanges Within Tumor Microenvironment: Impact for Cancer Aggressiveness. *Front Oncol* (2020) 10:396. doi: 10.3389/fonc.2020.00396
41. Dinarello CA. The paradox of pro-inflammatory cytokines in cancer. *Cancer Metastasis Rev* (2006) 25:307–13. doi: 10.1007/s10555-006-9000-8
42. Coussens LM, Werb Z. Inflammation and cancer. *Nature* (2002) 420 (6917):860–7. doi: 10.1038/nature01322
43. Grivennikov SI, Greten FR, Karin M. Immunity, inflammation, and cancer. *Cell* (2010) 140(6):883–99. doi: 10.1016/j.cell.2010.01.025
44. Voronov E, Shouval DS, Krelin Y, Cagnano E, Benharroch D, Iwakura Y, et al. IL-1 is required for tumor invasiveness and angiogenesis. *Proc Natl Acad Sci USA* (2003) 100(5):2645–50. doi: 10.1073/pnas.0437939100
45. Kim K, Song H, Kim TS, Yoon D, Kim CW, Bang SI, et al . Interleukin-18 is a critical factor for vascular endothelial growth factor- enhanced migration in human gastric cancer cell lines. *Oncogene* (2007) 26(10):1468–76. doi: 10.1038/sj.onc.1209926
46. Balkwill F. Tumor necrosis factor or tumor promoting factor? *Cytokine Growth Factor Rev* (2002) 13:135–41. doi: 10.1016/s1359-6101(01)00020-x
47. Vinay DS, Ryan EP, Pawelec G, Talib WH, Stagg J, Elkord E, et al. Immune evasion in cancer : Mechanistic basis and therapeutic strategies, *Semin Cancer Biol* (2015) 35:S185–98. doi: 10.1016/j.semcancer.2015.03.004
48. Jacobs J, Nierkens S, Figdor C, de Vries I, Adema G. Regulatory T cells in melanoma: the final hurdle towards effective immunotherapy? *Lancet Oncol* (2002) 13(1):e32–42. doi: 10.1016/S1470-2045(11)70155-3
49. Li Y, Patel SP, Roszik J, Qin Y. Hypoxia-Driven Immunosuppressive Metabolites in the Tumor Microenvironment: New Approaches for Combinational Immunotherapy. *Front Oncol* (2018) 9:1591. doi: 10.3389/fimmu.2018.01591
50. Gasparoto TH, Malaspina TSS, Benevides L, de Melo EJF Jr., Costa MRSN, Damante JH, et al. Patients with oral squamous cell carcinoma are characterized by increased frequency of suppressive regulatory T cells in the blood and tumor 23. microenvironment. *Cancer Immunol Immunother* (2010) 59:819–28. doi: 10.1007/s00262-009-0803-7
51. Staveley-O'Carroll K, Sotomayor E, Montgomery J, Borrello I, Hwang L, Fein S, et al. Induction of antigen-specific T cell anergy: An early event in the course of tumor progression. *Proc Natl Acad Sci USA* (1998) 95(3):1178– 83. doi: 10.1073/pnas.95.3.1178
52. Seidel JA, Otsuka A, Kabashima K. Anti-PD-1 and Anti-CTLA-4 Therapies in Cancer: Mechanisms of Action, Efficacy, and Limitations. *Front Oncol* (2018) 8:86. doi: 10.3389/fonc.2018.00086
53. Tsung K, Norton JA. In situ vaccine, immunological memory and cancer cure. *Hum Vaccines Immunother* (2016) 12(1):117–9. doi: 10.1080/21645515.2015.1073427
54. Pulendran B, Ahmed R. Immunological mechanisms of vaccination. *Natur Immunol* (2011) 12(6):509–17. doi: 10.1038/ni.2039
55. Cramer DW, Titus-Ernstoff L, McKolanis JR, Welch WR, Vitonis AF, Berkowitz RS, et al. Conditions Associated with Antibodies Against the Tumor-Associated Antigen MUC1 and Their Relationship to Risk for Ovarian Cancer. *Cancer Epidemiol Biomarkers Prev* (2005) 14(5):1125–31. doi: 10.1158/1055-9965.EPI-05-0035
56. Jiang T, Shi T, Zhang H, Hu J, Song Y, Wei J, et al. Tumor neoantigens: from basic research to clinical applications. *J Hematol Oncol* (2019) 12(1):93. doi: 10.1186/s13045-019-0787-5

57. Amanna IJ, Slifka MK. Contributions of humoral and cellular immunity to vaccine- induced protection in humans. *Virology* (2011) 411(2):206–15. doi: 10.1016/j.virol.2010.12.016
58. Hollingsworth RE, Jansen K. Turning the corner on therapeutic cancer vaccines,"31. *NPJ Vaccines* (2019) 4:7. doi: 10.1038/s41541-019-0103-y
59. Maeng HM, Berzofsky JA. Strategies for developing and optimizing cancer vaccines. *F1000 Res* (2019) 8:Faculty Rev–654. doi: 10.12688/f1000research.18693.1
60. Majumder S, Shah R, Elias J, Manoharan M, Shah P, Kumari A, et al. A cancer vaccine approach for personalized treatment of Lynch Syndrome. *Sci Rep* (2018) 8:12122. doi: 10.1038/s41598-018-30466-x
61. Zhang R, Billingsley MM, Mitchell MJ. Biomaterials for vaccine-based cancer immunotherapy. *J Controlled Release* (2018) 292:256–76. doi: 10.1016/j.jconrel.2018.10.008
62. Cinar D, Tas D. Cancer in the elderly. *North Clin Istanbul* (2015) 2(1):73–80. doi: 10.14744/nci.2015.72691
63. Amanna IJ, Slifka MK, Crotty S. Immunity and immunological memory following smallpox vaccination. *Immunol Rev* (2006) 211(1):320–37. doi: 10.1111/j.0105-2896.2006.00392.x
64. Thakurta DG, Sheikh NA, Fan LQ, Kandadi H, Meagher TC, Hall SJ, et al. Humoral immune response against nontargeted tumor antigens after treatment with sipuleucel-T and its association with improved clinical outcome. *Clin Cancer Res* (2015) 21(16):3619–30. doi: 10.1158/1078-0432.CCR-14-2334
65. Powell AM, Black MM. Epitope spreading: Protection from pathogens, but propagation of autoimmunity? *Clin Exp Dermatol* (2001) 26(5):427–33. doi: 10.1046/j.1365-2230.2001.00852.x
66. Gulley JL, Madan RA, Pachynski R, Mulders P, Sheikh NA, Trager J, et al. Role of Antigen Spread and Distinctive Characteristics of Immunotherapy in Cancer Treatment. *J Natl Cancer Institute* (2017) 109(3):djw261. doi: 10.1093/jnci/djw261
67. Nakagawa M, Greenfield W, Moerman-Herzog A, Coleman HN. Cross-reactivity, epitope spreading, and de novo immune stimulation are possible mechanisms of cross- protection of nonvaccine human papillomavirus (HPV) types in recipients of HPV therapeutic vaccines. *Clin Vaccine Immunol* (2015) 22(7):679–87. doi: 10.1128/CVI.00149-15
68. Pan J, Zhang Q, Sei S, Shoemaker RH, Lubet RA, Wang Y, You M, et al. Immunoprevention of KRAS-driven lung adenocarcinoma by a multipeptide vaccine. *Oncotarget* (2017) 8(47):82689–99. doi: 10.18632/oncotarget.19831
69. Klasse PJ. Neutralization of Virus Infectivity by Antibodies: Old Problems in New Perspectives. *Adv Biol* (2014) 2014:1–24. doi: 10.1155/2014/157895
70. Day PM, Thompson CD, Buck CB, Pang Y-YS, Lowy DR, Schiller JT. Neutralization of Human Papillomavirus with Monoclonal Antibodies Reveals Different Mechanisms of Inhibition. *J Virol* (2007) 81(16):8784–92. doi: 10.1128/JVI.00552-07
71. Lo Nigro C, Macagno M, Sangiolo D, Bertolaccini L, Aglietta M, Merlano MC. NK- mediated antibody-dependent cell-mediated cytotoxicity in solid tumors: biological evidence and clinical perspectives. *Ann Transl Med* (2019) 7(5):105–5. doi: 10.21037/atm.2019.01.42
72. Gray GE, Huang Y, Grunenberg N, Laher F, Roux S, Anderson-Nissen E, et al. Immune correlates of the Thai RV144 HIV vaccine regimen in South Africa. *Sci Transl Med* (2019) 11(510):eaax1880. doi: 10.1126/scitranslmed.aax1880
73. Supekar NT, Lakshminarayanan V, Capicciotti CJ, Sirohiwal A, Madsen CS, Wolfert MA, et al. Synthesis and Immunological Evaluation of a Multicomponent Cancer Vaccine Candidate Containing a Long MUC1 Glycopeptide. *ChemBioChem* (2018) 19(2):121–5. doi: 10.1002/cbic.201700424
74. Ho M, Hassan R, Zhang J, Wang QC, Onda M, Bera T, Pastan I, et al. Humoral immune response to mesothelin in mesothelioma and ovarian cancer patients. *Clin Cancer Res* (2005) 11(10):3814–20. doi: 10.1158/1078-0432.CCR-04-2304
75. Burns EA, Lum LG, L'Hommedieu G, Goodwin JS. Specific Humoral Immunity in the Elderly: *in vivo* and *in vitro* Response to Vaccination. *J Gerontol* (1993) 48(6):B231–6. doi: 10.1093/geronj/48.6.b231
76. Cinar D, Tas D. Cancer in the Elderly. *North Clin Istanbul* (2015) 2(1):73. doi: 10.14744/nci.2015.72691
77. Shang W, Liu J, Yang J, Hu Z, Rao X. Dengue virus-like particles: Construction and application. *Appl Microbiol Biotechnol* (2012) vol94 (1):39–46.
78. Mohsen MO, Zha L, Cabral-Miranda G, Bachmann MF. Major findings and recent advances in virus–like particle (VLP)-based vaccines. *Semin Immunol* (2017) 34:123–32. doi: 10.1016/j.smim.2017.08.014
79. Marrack P, Kappler J. B cell tolerance. *Semin Immunol* (1990) 2(1):45–9.
80. Chackerian B, Durfee MR, Schiller JT. Virus-Like Display of a Neo-Self Antigen Reverses B Cell Anergy in a B Cell Receptor Transgenic Mouse Model. *J Immunol* (2008) 180(9):5816–25. doi: 10.4049/jimmunol.180.9.5816
81. Huang YL, Hung JT, Cheung SKC, Lee HY, Chu KC, Li ST, et al. Carbohydrate-based vaccines with a glycolipid adjuvant for breast cancer. *Proc Natl Acad Sci USA* (2013) 110(7):2517–22. doi: 10.1073/pnas.1222649110
82. Eller CH, Chao TY, Singarapu KK, Ouerfelli O, Yang G, Markley JL, et al. Human cancer antigen Globo H is a cell-surface ligand for human ribonuclease 1. *ACS Cent Sci* (2015) 1(4):181–90. doi: 10.1021/acscentsci.5b00164
83. Danishefsky SJ, Shue YK, Chang MN, Wong CH. Development of Globo-H Cancer Vaccine. *Acc Chem Res* (2015) 48(3):643–52. doi: 10.1021/ar5004187
84. Song C, Zheng XJ, Liu CC, Zhou Y, Ye XS. A cancer vaccine based on fluorine- modified sialyl-Tn induces robust immune responses in a murine model. *Oncotarget* (2017) 8(29):47330–43. doi: 10.18632/oncotarget.17646
85. Yang F, Zheng XJ, Huo CX, Wang Y, Zhang Y, Ye XS. Enhancement of the immunogenicity of synthetic carbohydrate vaccines by chemical modifications of STn antigen. *ACS Chem Biol* (2011) 6(3):252–9. doi: 10.1021/cb100287q
86. Salerno-Gonçalves R, Sztein MB. Cell-mediated immunity and the challenges for vaccine development. *Trends Microbiol* (2006) 14(12):536–42. doi: 10.1016/j.tim.2006.10.004
87. Yang A, Peng S, Farmer E, Zeng Q, Cheng MA, Pang X, et al. Enhancing antitumor immunogenicity of HPV16-E7 DNA vaccine by fusing DNA encoding E7-antigenic peptide to DNA encoding capsid protein L1 of Bovine papillomavirus. *Cell Biosci* (2017) 7(1):1–10. doi: 10.1186/s13578-017-0171-5
88. Wherry EJ. T cell exhaustion. *Nat Immunol* (2011) 12(6):492–9. doi: 10.1038/ni.2035
89. Chakravarti B, Abraham GN. Aging and T-cell-mediated immunity. *Mech Ageing Dev* (1999) 108)(3):183–206. doi: 10.1016/s0047-6374(99)00009-3
90. Steinmann GG. Changes in the human thymus during aging. *Curr Topics Pathol* (1986) 75:43–88. doi: 10.1007/978-3-642-82480-7_2
91. Villanueva JL, Solana R, Alonso MC, Peña J. Changes in the expression of HLA- class II antigens on peripheral blood monocytes from aged humans. *Dis Markers* (1990) 8(2):85–91.
92. Hudnall SD. Viruses and Human Cancer. *J Biol Med* (2014) 79(3–4):115–22. doi: 10.1007/978-1-4939-0870-7
93. Slingluff CL. The present and future of peptide vaccines for cancer: Single or multiple, long or short, alone or in combination? *Cancer J* (2011) 17(5):343–50. doi: 10.1097/PPO.0b013e318233e5b2
94. Rosa DS, Tzelepis F, Cunha MG, Soares IS, Rodrigues MM. The pan HLA DR-binding epitope improves adjuvant-assisted immunization with a recombinant protein containing a malaria vaccine candidate. *Immunol Lett* (2004) 92(3):259–68. doi: 10.1016/j.imlet.2004.01.006
95. Zamani P, Teymouri M, Nikpoor AR, Navashenaq JG, Gholizadeh Z, Darban SA, et al. Nanoliposomal vaccine containing long multi-epitope peptide E75-AE36 pulsed PADRE-induced effective immune response in mice TUBO model of breast cancer. *Eur J Cancer* (2020) 129:80–96. doi: 10.1016/j.ejca.2020.01.010
96. Kaplan DH, Shankaran V, Dighe AS, Stockert E, Aguet M, Old LG, et al. Demonstration of an interferon γ-dependent tumor surveillance system in immunocompetent mice. *Proc Natl Acad Sci USA* (1998) 95(13):7556–61. doi: 10.1073/pnas.95.13.7556
97. Peiper M, Goedegebuure PS, Linehan DC, Ganguly E, Douville CC, Eberlein TJ. The HER2/neu-derived peptide p654-662 is a tumor-associated antigen in human pancreatic cancer recognized by cytotoxic T lymphocytes. *Eur J Immunol* (1997) 27(5):1115–23. doi: 10.1002/eji.1830270511

98. Dawen Xie WZ, Shu X-O, Deng Z, Wen W-Q, Kim E. Creek, Qi Dai, Yu-Tang Gao, Fan Jin, "Population-Based, Case-Control Study of HER2 Genetic Polymorphism and Breast Cancer Risk. *J Natl Cancer Inst* (2008) 37(5):1–9. doi: 10.1093/jnci/92.5.412
99. Mittendorf EA, Storrer CE, Foley RJ, Harris K, Jama Y, Shriver CD, et al. Evaluation of the HER2/neu -derived peptide GP2 for use in a peptide-based breast cancer vaccine trial. *Cancer* (2006) 106(11):2309–17. doi: 10.1002/cncr.21849
100. Pantsar T. The current understanding of KRAS protein structure and dynamics. *Comput Struct Biotechnol J* (2020) 18:189–98. doi: 10.1016/j.csbj.2019.12.004
101. Pan J, et al. Potentiation of Kras peptide cancer vaccine by avasimibe, a cholesterol modulator. *EBioMedicine* (2019) 49:72–81. doi: 10.1016/j.ebiom.2019.10.044
102. Li L, Petrovsky N. Molecular mechanisms for enhanced DNA vaccine immunogenicity. *Expert Rev Vaccines* (2016) 15(3):313–29. doi: 10.1586/14760584.2016.1124762
103. Whiteside TL. Tumor-Derived Exosomes and Their Role in Cancer Progression. *Adv Clin Chem* (2016) 74:103–41. doi: 10.1016/bs.acc.2015.12.005
104. Giovanni CD, Antonio Rosato PZ, Santa SD, Zoso A, Giacomelli S, Milan G, et al. The Cytotoxic T-Lymphocyte Response against a Poorly Immunogenic Mammary Adenocarcinoma Is Focused on a Single Immunodominant Class I Epitope Derived from the gp70 Env Product of an Endogenous Retrovirus. *Cancer Res* (2003) 63(9):2158–63.
105. Vanpouille-Box C, Alard A, Aryankalayil MJ, Sarfraz Y, Diamond JM, Schneider RJ, et al. DNA exonuclease Trex1 regulates radiotherapy-induced tumour immunogenicity. *Nat Commun* (2017) 8(1):15618. doi: 10.1038/ncomms15618
106. Phua KKL, Leong KW, Nair SK. Transfection efficiency and transgene expression kinetics of mRNA delivered in naked and nanoparticle format. *J Control Release* (2013) 166(3):227–33. doi: 10.1016/j.jconrel.2012.12.029
107. Kimura T, McKolanis JR, Dzubinski LA, Islam K, Potter DM, Salazar AM, et al. MUC1 Vaccine for Individuals with Advanced Adenoma of the Colon: A Cancer Immunoprevention Feasibility Study". *Cancer Prev Res (Philadelphia Pa)* (2013) 6(1):18–26. doi: 10.1158/1940-6207.CAPR-12-0275
108. Dummy A. *Study of the MUC1 Peptide-Poly-ICLC Adjuvant Vaccine in Individuals With Advanced Colorectal Adenoma*. Bethesda, MD, USA: US National Library of Medicine (2019) ClinicalTrials.gov Identifier: NCT00773097
109. Czerniecki BJ, Koski GK, Koldovsky U, Xu S, Cohen PA, Mick R, et al. Targeting HER-2/neu in Early Breast Cancer Development Using Dendritic Cells with Staged Interleukin-12 Burst Secretion. *Cancer Res* (2007) 67(4):1842–52. doi: 10.1158/0008-5472.can-06-4038
110. Kübler H, Scheel B, Gnad-Vogt U, Miller K, Schultze-Seemann W, vom Dorp F, et al. Self-adjuvanted mRNA vaccination in advanced prostate cancer patients: a first-in-man phase I/IIa study. *J Immunother Cancer* (2015) 3(1):26. doi: 10.1186/2Fs40425-015-0068-y
111. Martinon F, Krishnan S, Lenzen G, Magne R, Gomard E, Guillet JG, et al. Induction of virus-specific cytotoxic T lymphocytes *in vivo* by liposome-entrapped mRNA. *Eur J Immunol* (1993) 23(7):1719–22. doi: 10.1002/eji.1830230749
112. Ulmer JB, Mason PW, Geall A, Mandl CW. RNA-based vaccines. *Vaccine* (2012) 30(30):4414–8. doi: 10.1016/j.vaccine.2012.04.060
113. Tan C, Dannull J, Nair SK, Ding E, Tyler DS, Pruitt SK, et al. Local secretion of IL-12 augments the therapeutic impact of dendritic cell tumor cell fusion vaccination. *J Surg Res* (2013) 185(2):904–11. doi: 10.1016/j.jss.2013.06.045
114. Porter KR, Raviprakash K. DNA Vaccine Delivery and Improved Immunogenicity. *Curr Issues Mol Biol* (2017) 22:129–38. doi: 10.21775/cimb.022.129
115. Chandra J, Dutton JL, Li B, Woo WP, Xu Y, Tolley LK, et al. DNA Vaccine Encoding HPV16 Oncogenes E6 and E7 Induces Potent Cell-mediated and Humoral Immunity Which Protects in Tumor Challenge and Drives E7-expressing Skin Graft Rejection. *J Immunother* (2017) 40(2):62–70. doi: 10.1097/CJI.0000000000000156
116. Saranath D, Khan Z, Tandle AT, Dedhia P, Sharma B, Contractor R, et al. HPV16/18 prevalence in cervical lesions/cancers and p53 genotypes in cervical cancer patients from India. *Gynecol Oncol* (2002) 86(2):157–62. doi: 10.1006/gyno.2002.6735
117. Liu D-W, Tsao YP, Hsieh CH, Hsieh JT, Kung JT, Chiang CL, et al. Induction of CD8 T Cells by Vaccination with Recombinant Adenovirus Expressing Human Papillomavirus Type 16 E5 Gene Reduces Tumor Growth. *J Virol* (2000) 74(19):9083–9. doi: 10.1128/JVI.74.19.9083-9089.2000
118. *U.S. Vaccine Names*. GA, USA: CDC (2019).

Conflict of Interest: The authors declare that the research was conducted in the absence of any commercial or financial relationships that could be construed as a potential conflict of interest.

Copyright © 2021 Crews, Dombroski and King. This is an open-access article distributed under the terms of the Creative Commons Attribution License (CC BY). The use, distribution or reproduction in other forums is permitted, provided the original author(s) and the copyright owner(s) are credited and that the original publication in this journal is cited, in accordance with accepted academic practice. No use, distribution or reproduction is permitted which does not comply with these terms.

frontiers in Immunology

REVIEW
published: 30 March 2021
doi: 10.3389/fimmu.2021.627932

Cancer Vaccines, Adjuvants, and Delivery Systems

Samantha J. Paston[1], *Victoria A. Brentville*[1], *Peter Symonds*[1] *and Lindy G. Durrant*[2]*

[1] Biodiscovery Institute, Scancell Limited, Nottingham, United Kingdom, [2] Biodiscovery Institute, University of Nottingham, Faculty of Medicine and Health Sciences, Nottingham, United Kingdom

Vaccination was first pioneered in the 18th century by Edward Jenner and eventually led to the development of the smallpox vaccine and subsequently the eradication of smallpox. The impact of vaccination to prevent infectious diseases has been outstanding with many infections being prevented and a significant decrease in mortality worldwide. Cancer vaccines aim to clear active disease instead of aiming to prevent disease, the only exception being the recently approved vaccine that prevents cancers caused by the Human Papillomavirus. The development of therapeutic cancer vaccines has been disappointing with many early cancer vaccines that showed promise in preclinical models often failing to translate into efficacy in the clinic. In this review we provide an overview of the current vaccine platforms, adjuvants and delivery systems that are currently being investigated or have been approved. With the advent of immune checkpoint inhibitors, we also review the potential of these to be used with cancer vaccines to improve efficacy and help to overcome the immune suppressive tumor microenvironment.

Keywords: adjuvant, peptide vaccine, DNA vaccine, cancer, vaccine

OPEN ACCESS

Edited by:
Pål Johansen,
University of Zurich, Switzerland

Reviewed by:
Kwong Tsang,
Precision Biologics, Inc., United States
Steve Pascolo,
University of Zurich, Switzerland

***Correspondence:**
Lindy G. Durrant
lindy.durrant@nottingham.ac.uk

Specialty section:
This article was submitted to Vaccines and Molecular Therapeutics, a section of the journal Frontiers in Immunology

Received: *10 November 2020*
Accepted: *12 March 2021*
Published: *30 March 2021*

Citation:
Paston SJ, Brentville VA, Symonds P and Durrant LG (2021) Cancer Vaccines, Adjuvants, and Delivery Systems. Front. Immunol. 12:627932. doi: 10.3389/fimmu.2021.627932

INTRODUCTION

The potential to develop a cancer vaccine has been extensively researched in both humans and animal models, the majority of these vaccines are therapeutic vaccines that aim to activate the immune system to recognize and kill established tumors. A prophylactic vaccine that prevents cancers caused by the Human Papillomavirus [Types 6, 11, 16, 18] has been approved and in the UK, children aged 12-13-years-old are routinely offered this vaccine. Developing a therapeutic cancer vaccine has been more problematic with many encouraging results in preclinical studies not translating into the clinic. To date the FDA has only approved one vaccine, sipuleucel-T, that is used to treat metastatic castration-resistant prostate cancer in a limited group of nearly asymptomatic patients (1). There are number of reasons for these failures such as the immune suppressive TME, lack of a robust T cell responses, sub optimal vaccine formulations, delivery, adjuvants and identifying the best patients to target. The ideal setting for a cancer vaccine to work is in patients following surgical resection, chemotherapy or radiotherapy, all of which stimulate an immune response themselves. Vaccination at this stage and in combination with a checkpoint inhibitor will provide the best setting to induce a potent anti-tumor immune response.

Over the last couple of decades, a better understanding of the tumor microenvironment (TME) and immune suppressive mechanisms have opened a number of new avenues that can be explored and has led to the next generation of new cancer therapies. The immune suppressive TME is a major obstacle to the success of any cancer vaccine with the description of immunologically "cold" tumors that on their own do not appear to be immunogenic with an absence of tumor infiltrating lymphocytes (TILs). In contrast "hot" tumors are immunogenic and have induced an immune response that has resulted in the infiltration of TILs but are not able to function due to the presence of various checkpoint molecules such as PD-1, CTLA-4, LAG-3, TIM-3 or the presence of immune suppressive cells such as regulatory T cells, myeloid-derived suppressor cells (MDSCs), M2 macrophages, regulatory natural killer (NK) T cells or cytokines such as transforming growth factor-beta [TGFβ], IL-10, and IL-13 (2, 3). The success of any cancer vaccine relies on overcoming the immune suppressive TME and converting "cold" tumors into "hot" tumors and therefore inducing a robust tumor specific immune response that can kill cancer cells.

TARGET ANTIGENS

The choice of antigen to target in any cancer vaccine is extremely important to the efficacy of the vaccine in the clinic. The ideal antigen should be specifically expressed on cancer cells with no expression on normal cells, ideally the antigen should be necessary for cell survival and be highly immunogenic.

Tumor antigens fall into two broad categories, the tumor associated antigens (TAAs) and tumor-specific antigens (TSAs). Within each category a number of different types of tumor antigens have been described and are summarized in **Table 1**. The cancer germline antigens (also called cancer testis antigens) are the most studied group of cancer antigens, historically they were attractive antigens to target due to their expression only on germ cells of immune-privileged organs and high expression on tumor cells. The most common cancer germline antigens that are targeted include MAGE (4, 5), NY-ESO1 (6), GAGE (7, 8) and BAGE (9), both T cell and antibody responses to these antigen have been detected in patients.

The differentiation antigens are expressed on normal and tumor cells from the same tissue, targeting such antigens requires careful consideration to any potential toxicity to the normal tissue. Differentiation antigens include the melanoma antigens Melan A/MART-1 (10, 11), gp100 (12), tyrosinase (13), the prostate antigen prostate specific antigen (PSA) (14, 15) and the colon antigen carcinoembryonic antigen (CEA) (16, 17).

The overexpressed antigens are generally expressed at low levels on normal cells but are over expressed on tumor cells, there are many antigens that fall into this group including HER2 (18), hTERT (19, 20), p53 (21), survivin (22–25), MUC1 (26), WT1 (27), cyclin B (28, 29) and many more. Targeting over expressed antigens can be challenging, preclinical studies need to ensure that normal low-level expressing cells are not targeted by the vaccine induced immune response.

The oncogenic viral antigens are expressed on virus infected cells that have subsequently undergone malignant transformation. Oncogenic viral antigens have been targeted in both prophylactic vaccines such as HPV but also in therapeutic vaccines to treat existing malignancies. The most commonly targeted oncogenic viral antigens in this group include EBV LMP-1 and LMP-2A (30–32), HPV E6/E7 (33), HTLV-1 Tax (34).

The last group of cancer antigens are those antigens that are mutated, these mutations can be generated at the gene level or as a result of post translational modifications leading to the generation of a new peptide. In the last couple of years there has been a renewed effort in generating vaccines that target mutated antigens, in particular the neoantigens. There are very few mutated antigens described where the mutated peptide is shared across patients or cancer types, the most studied shared mutations are KRAS (35), NRAS (36), epitopes from BCR-ABL translocation (Chronic myeloid leukemia) (37, 38), ETV6 (acute myeloid leukemia) (39), NPM/ALK (anaplastic large cell lymphomas) (40, 41) and ALK (neuroblastoma) (42, 43). A number of groups are developing personalized vaccines that target neoantigens identified from the patient's tumor, very few if any of these mutations are shared epitopes and therefore any

TABLE 1 | Different types of tumor antigens.

	Class of tumor antigen	Description	Tumor specificity	Example of tumor antigen
Tumor Specific Antigens (TSA)	Cancer Germline antigens	Expression on healthy cells limited to testes, fetal ovaries and trophoblasts. Expressed on a wide a variety of cancer types.	High	MAGE, NY-ESO-1, GAGE, BAGE
	Tumor specific mutated antigens	Mutations resulting in the generation of a new peptide. Mutations can be generated at the gene level, from chromosome translocations or due post translational modification.	High	KRAS, p53, NRAS, BCR-ABL translocation, ETV6, NPM/ALK, ALK.
	Oncogenic viral antigens	Abnormal expression on cells infected with an oncovirus.	High	EBV LMP-1/LMP-2A, HPV E6/E7, HTLV-1 Tax
Tumor associated Antigens (TAA)	Tissue Differentiation antigens	Antigen expressed on tumor cells and normal cells.	Low	Melan A/MART-1, gp100, Tyrosinase, PSA, CEA.
	Overexpressed antigens	Antigen over expressed on tumor cells and normal level of expression on healthy cells.	Low	HER2, hTERT, p53, Survivin, MUC1, WT1, cyclin B.

generated vaccine is only specific to the individual. Neoantigens are immunogenic because they harbor mutations, they have escaped central tolerance and are recognized as "non self" by the adaptive immune system (44). Despite the higher immunogenicity of neoantigen's only 1-2% of T cells recognize these antigens (45). The poor immunogenicity of many tumors means that designing an effective neoantigen tumor vaccine will need to overcome these challenges.

The post translational modified cancer antigens are another group of antigens, they are not subject to thymic deletion and are therefore attractive vaccine candidates. A number of different post-translational modifications have been described that generate tumor specific epitopes including glycopeptides (46), phosphopeptides (47, 48) and citrullinated peptides (49). Cancer cells often exhibit different phosphorylation patterns leading to the generation of phosphorylated antigens, these make attractive vaccine candidates (47, 48, 50). Phosphorylated epitopes can be naturally processed and presented on the cell surface in association with MHC class I molecules for recognition by CD8+ T cells (50–52). Unregulated signaling cascades in tumor cells often lead to an increase in protein phosphorylation within the cell which in turn leads to the generation of phosphopeptides (52). Phosphopeptides have been identified by mass spectrometry analysis of tumor biopsies and cancer cell lines (53). Engelhard et al. (53) identified two phosphorylated peptides derived from the insulin receptor substrate 2 (IRS2) protein and breast cancer anti-estrogen resistance 3 (BCAR3). The ISR2 protein is overexpressed in many cancer types and *in vivo* has been shown to enhance metastasis (54–56), BCAR3 is associated cellular migration and resistance to therapeutic anti-estrogens in breast cancer cells (57, 58). Phosphopeptides restricted by HLA-*02:01 were identified by mass spectrometry and included in a phase 1 clinical trial (NCT01846143) in patients with resected stage IIA–IV melanoma. All patients had treatment related adverse events, but none were grade 3-4, T cell responses were induced to the phosphorylated IRS2 (1097-1105) peptide in 5/12 patients and to the phosphorylated BCAR3 (126-134) peptide in 2/12 patients. This trial showed that phosphopeptides are safe and induced an immune response in some patients, however, with the advent of immune checkpoint inhibitors future studies will need to define and enhance the immune response induced to these peptides.

Our own research has focused on epitopes that are citrullinated in tumor cells. Citrullination is a post translation modification where positive charged arginine residues are converted into neutrally charged citrulline in a process catalyzed by the Ca^{2+} dependent peptidyl arginine deaminase (PADI) enzymes (59, 60) (**Figure 1**). This modification can impact the protein structure and induce changes that result in protein denaturation potentially altering the structure and the function of the protein (61, 62). We have detected T cell responses to citrullinated peptides in healthy donors (60) suggesting that the T cells recognizing them are positively and not negatively selected in the thymus. In healthy cells the PADI enzymes are maintained in an inactive state due to low concentrations of Ca^{2+} (34), in double membrane vesicles

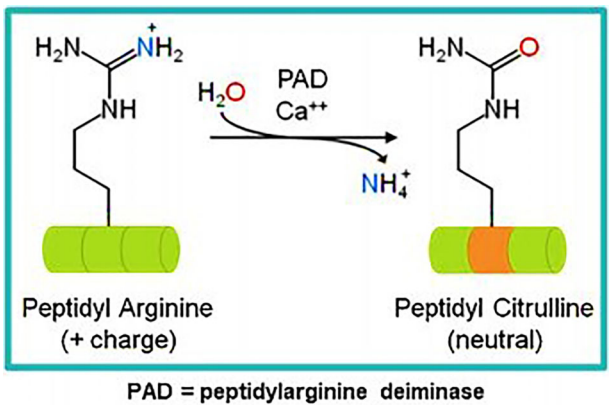


FIGURE 1 | Schematic of the citrullination or deamidation of arginine.

within viable cells the calcium concentrations can be high leading to the activation of the PADI enzymes. Citrullination can occur within autophagosomes as a result of autophagy, here high calcium levels activate PADI enzymes that then citrullinate engulfed proteins from the cytoplasm (36, 37), this process is induced in stressed cells (17) such as cancer cells. During stress induced autophagy and in the presence of inflammation citrullinated peptides can be presented on major histocompatibility complex (MHC) class II molecules for recognition by CD4+ T cells (63). During inflammation many cytokines are produced, the majority are proinflammatory that result in the upregulation of MHC class II expression that then activates CD4+ T cells (**Figure 2**).

A number of studies performed in autoimmune patients have demonstrated that CD4+ T cell responses can be detected to citrullinated proteins such as the intermediate filament protein vimentin and the glycolytic enzyme enolase (64–68). In ovarian cancer patients we have demonstrated the presence of CD4+ T cell responses to citrullinated peptides derived from α-enolase and vimentin (60). The constitutive expression of MHC class II is mainly restricted to APCs such as DCs, B cells and macrophages but other cells such thymic epithelia cells and activated T cells can also express MHC class II (69). The expression of MHC class II on most other cells can be induced by interferon gamma (IFNγ) present in the local vicinity. The expression of MHC class II is controlled by the Class II Major Histocompatibility complex transactivator (CIITA) which is regulated by four different promoters, promoter I is active in myeloid cells, promoter III in lymphocytes and promoter IV is necessary for responsiveness to IFNγ (70), the function of promoter II is unknown, transcripts from this promoter are rare and therefore its function has not been pursued. Most tumors in the presence of inflammation and IFNγ will express MHC class II, if citrullinated peptides are then generated in response to stress or autophagy these can then be loaded onto MHC class II for presentation on the surface of tumor cells.

We have focused on citrullinated vimentin and α-enolase as attractive cancer vaccine targets. Vimentin is an intermediate

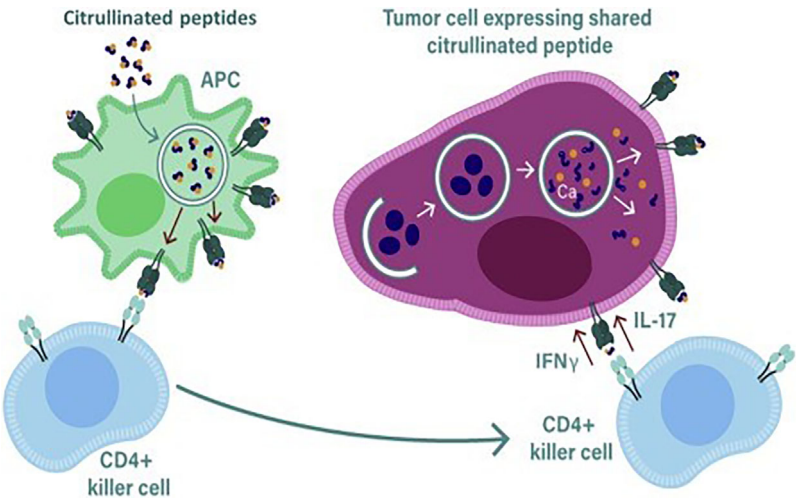


FIGURE 2 | During stress induced autophagy and in the presence of inflammation citrullinated peptides can be presented on major histocompatibility complex (MHC) class II molecules for recognition by CD4+ T cells. During inflammation many cytokines are produced, the majority are proinflammatory that result in the upregulation of MHC class II expression that then activates CD4+ T cells. Primed killer CD4 T cells enter the tumor and are reactivated by APCs presenting citrullinated peptides from tumors allowing recognition and lysis by the killer CD4 T cells.

filament protein that is known to be citrullinated and overexpressed in a wide range of cancers (71–76), particularly during EMT (77). The glycolytic enzyme α-Enolase (ENO1) catalyzes the final step in glycolysis (78). Many tumors switch to generating their energy *via* glycolysis in a process termed the "Warburg effect" and therefore overexpress ENO1, a wide range of tumors overexpress ENO1 (79–82). Due to its ubiquitous expression, ENO1 is often degraded during autophagy; previous studies have also shown that ENO1 can be citrullinated (65, 83). We have shown that these citrullinated peptides are recognized and presented to CD4+ T cells by both MHC class II HLA-DR4 and HLA-DP4 molecules (49, 84, 85). HLA transgenic mice vaccinated with citrullinated vimentin and α-enolase peptides linked to an adjuvant (Modi-1 vaccine) can stimulate CD4+ T cells (49, 64, 86) and generate potent anti-tumor responses resulting in tumor regression and eradication with no associated toxicity (49, 87). We have also shown that healthy donors have a repertoire of T cells that can be detected following stimulation with the citrullinated vimentin and α-enolase peptides showing that citrullinated peptides can be presented in the thymus allowing positive selection and resulting in specific T cell repertoires capable of recognizing these peptides (87). Our preclinical data shows that citrullinated vimentin and α-enolase are promising candidate vaccine targets and as a vaccine have generated impressive anti-tumor responses in preclinical murine models.

ADJUVANTS

Antigens alone in a vaccine are poor inducers of the adaptive immune response. In the absence of an adjuvant antigens targeted to immature DCs in the absence of inflammation or any microbial stimulation induce tolerance instead of a potent immune response (88). Adjuvants need to attract immune cells to the site of injection while also promoting cell mediated trafficking of antigen to draining lymph nodes and triggering the activation of APCs.

Current Vaccine Adjuvants

The water-in-oil emulsions such as Montanide ISA 720 and Montanide ISA-51 have been widely adopted as adjuvants, they form a depot at the injection site, this results in the trapping of the soluble antigens preventing their rapid trafficking to local lymph nodes, this induces inflammation and the gradual release of the antigen. In a clinical trial Montanide ISA-51 was shown to induce both CD4+ and CD8+ T cell responses in patients vaccinated with long peptides of the oncoproteins E6 and E7 (89).

New vaccine adjuvants have been developed that target specific components of the immune system to generate a more robust and longer lasting immune response. Newer adjuvants that consist of Pathogen-associated molecular pattern molecules (PAMPs) are now being used, these provide a danger signal that is recognized by pattern recognition receptors (PRRs) inducing an immune response. Innate cells express PPRs, these receptors include the Toll-like receptors (TLRs), nucleotide binding oligomerization domain like receptors and the mannose receptor. TLR agonists are increasingly being used as a vaccine adjuvant, they mimic microbial stimulation and have been shown to increase vaccine efficacy (90) particularly for cancers (91). Lymph node targeted TLR agonists have shown a direct relationship between the magnitude of CD8+ T cell responses and the amount of TLR agonist accumulated in draining lymph nodes, demonstrating the importance of providing sufficient inflammatory signals during immunization (92). A number of

TLR agonists are currently in trial as adjuvants for cancer vaccines, one of the most commonly used TLR agonist is polyinosinic–polycytidylic acid with polylysine and carboxymethylcellulose (Poly-ICLC) a TLR3 agonist (93), others include monophosphoryl lipid A (MPLA) a TLR4 agonist (94, 95), imiquimod a TLR7 agonist (96, 97), resiquimod a TLR7 and TLR8 agonist (98, 99), CpG oligodeoxynucleotide (CpG ODN) a TLR9 agonist (90, 100, 101).

New Emerging Vaccine Adjuvants

Other newer adjuvants are also being investigated to increase the efficacy of a cancer vaccine, these include the CD40 agonists, these directly target the antigen to the early endosomes of DCs and mediate cross presentation. Although CD40 agonist antibodies have not been extensively studied in clinical trials as a vaccine adjuvant, they have been studied independently as monotherapy (102). A number of preclinical mouse models have shown that CD40 agonists can be used in combination with TLR agonists in a vaccination strategy (103, 104), whether this translates into clinical efficacy is still to be determined.

Another class of potential adjuvants is the Stimulator of interferon genes protein (STING) agonists. STING is a transmembrane protein located in the endoplasmic reticulum (105), its activation triggers a type I interferon response in response to intracellular DNA (106). STING agonists include synthetic cyclic dinucleotide derivatives and cyclic di-guanosine monophosphate, these have all shown anti-tumor activity in mice (107, 108). STING expression is highest on T cells and STING activation can lead to T cell apoptosis, such effects are not seen with macrophages and DCs (109). To use a STING agonist in a cancer vaccine it would need to be combined with an adjuvant or delivery system that targets only myeloid cells *in vivo* (110) preventing T cell apoptosis. STING agonists do induce some systemic toxicity and to overcome this intratumoral injection is the preferred route of administration. In addition, preclinical studies of STING agonists have been complicated by their differential binding properties in murine and human cells (111). The potential toxicity of STING agonists and lack of specific targeting could limit their use as adjuvants in a cancer vaccine.

In addition to using pathogen derived molecules as adjuvants a number of cytokines have also been shown to act as an adjuvant. Immunostimulatory cytokines such as IL-2 (112, 113), IFN (114), IL-12 (115, 116) and granulocyte-macrophage colony stimulating factor (GM-CSF) (117–119) have all been investigated, although recent studies have focused mainly on their application in cellular based therapies and vaccines. GM-CSF is the most studied immunostimulatory factor and has been included in numerous cancer vaccine trials (120). In preclinical studies GM-CSF looked a very promising candidate, it helps recruit DCs to the injection site, it can promote the maturation of DCs and antigen presentation resulting in an enhanced adaptive immune response (117). However, in clinical trials GM-CSF has generated disappointing results with only a few trials having shown a clinical benefit, the results across the majority of trials have been inconsistent. Preclinical studies indicated that GM-CSF could expand MDSCs resulting in the suppression of cell mediated anti-tumor responses (118). The effect of GM-CSF was also observed in clinical trials where a low dose of GM-CSF induced the expansion of CD14 positive, HLA-DR low/negative myeloid cells. In another study GM-CSF was used with incomplete Freund's adjuvant and resulted in a low T cell response when compared to vaccine adjuvant without GM-CSF (119). Despite these results a number of clinical trials are currently underway using GM-CSF as an adjuvant component.

We have previously described our Modi-1 peptide vaccine (60), this vaccine comprises of two citrullinated vimentin peptides, as well as a citrullinated peptide from α-enolase, each peptide is conjugated to the TLR1/2 ligand adjuvant AMPLIVANT® (ISA Pharmaceuticals BV, Leiden, the Netherlands). In preclinical studies we have shown that by combining a peptide vaccine with a TLR ligand adjuvant promotes a Th1 response that is capable of inducing a potent anti-tumor response in tumor bearing mice (60). The CD4+ but not CD8+ T cells were essential for the generation of the anti-tumor response, depleting CD4+ T cells abrogated this response and a corresponding increase in CD4+ tumor-infiltrating lymphocytes (TILs) was associated with tumor regression (60). A comparison of different Toll-like receptor (TLR)-stimulating adjuvants showed that Modi-1 induced strong Th1 responses when combined with GM-CSF, TLR9/TLR4, TLR9, TLR3, TLR1/2 and TLR7 agonists. The strongest response was observed with TLR1/2 AMPLIVANT® adjuvant. The AMPLIVANT® adjuvant is already being used in an ongoing study evaluating two HPV-16 peptides in patients with head and neck squamous cell carcinoma (NCT02821494). These results highlight the importance of screening a range of adjuvants and doses to find the optimal adjuvant and dose to induce a potent immune response. The Modi-1 vaccine will enter a Phase 1/2 clinical trial in 2021.

DELIVERY SYSTEMS

Electroporation and Gene Gun Vaccine Delivery

There have been significant improvements in optimizing vaccine administration routes to overcome poor cellular uptake. Also improvements with delivery and plasmid design have improved the efficacy of DNA vaccines in both pre-clinical and clinical studies (121). One strategy for improving the uptake of plasmid DNA into antigen presenting cells (APCs) is by using electroporation. Electroporation delivers small electrical pulses that causes transient pores to form in the cell membrane. During the period of membrane destabilization plasmid DNA present in the extracellular environment around the target cell gains access to the intracellular compartment (122). Following the transfer of DNA into the cell the membrane then reseals. The transient increase in the permeability of the target cell membrane enhances the uptake of plasmid DNA (123). Electroporation increases DNA uptake by over a 1000-fold and has an adjuvant effect due to local tissue damage and the resulting stimulation of proinflammatory cytokine in the local vicinity (124, 125). A

number of DNA vaccines currently in clinical trials are using electroporation to delivery DNA plasmids, the ability of these plasmids to induce an immune response has been demonstrated in prostate cancer and melanoma (126). Another similar strategy is using a gene gun to deliver plasmid DNA that is coated with a heavy metal, typically gold particle are used, APCs at the injection site are bombarded with plasmid coated particles. The gene gun strategy reduces the amount of DNA required by 100-1,000 (127); some promising preclinical data has led to phase 1 and 2 clinical trials in head and neck squamous cell carcinoma and cervical cancer (128). Electroporation is also being used to deliver plasmid DNA in the infectious disease field, there are a number of COVID-19 DNA vaccines currently in in clinical trial (WHO landscape report Dec 2020) that use DNA plasmids encoding the Spike antigen and using electroporation as a delivery system (NCT04445389, NCT04447781, NCT04642638, NCT04627675). The main disadvantages of a DNA vaccine is when electroporation is used as a delivery system, electroporation can cause considerable pain and anxiety on administration and not suitable for mass vaccination programs, alternative delivery systems are currently being pursued.

Nanoparticle Vaccine Delivery Systems

Nanoparticle based drug delivery platforms offer an alternative vehicle for delivering drugs that have previously suffered from pharmacokinetic limitations including poor bioavailability, a short half-life or poor solubility. A variety of nanoparticles have been explored as delivery systems or as adjuvants, such as polymeric nanoparticles, liposomes, micelles, carbon nanotubes, mesoporous silica nanoparticles, gold nanoparticles and virus nanoparticles, that can all be used alone or in combination (129). Liposomes are a popular nanoparticle vaccine delivery system, they are versatile and can be constructed with a variety of different properties by changing the lipid composition, charge, size and surface properties (130–132). Nanoparticle based drug delivery platforms use well-known lipid carriers to deliver biotherapeutic encoding tumor antigens directly into APCs such as dendritic cells. The targeting of APCs in the lymphoid compartments is accomplished by using well-known lipid carriers such as DOTMA, DOTAP, DOPE and cholesterol and by adjusting negative net charge of the nanoparticles to provide optimal drug delivery. Cationic liposomes are mainly composed of the lipids DOTMA and DOPE that form colloidally stable nanoparticles of reproducible particle size (200–400 nm) with an excess of positive charge preventing excessive aggregation (133). Liposomes can increase the immunogenicity of target antigens for cancer vaccines and have been used to deliver RNA, DNA and antigens. Hydrophilic and lipophilic antigens can be loaded into liposomes, the hydrophilic antigens are trapped in the aqueous inner space and the lipophilic components are inserted into the lipid bilayer by adsorption or chemical attachment. Liposomes have been utilized to improve lymph node trafficking of small molecule adjuvants to the lymph node (134)

BioNTech have developed a lipid-based nanoparticle formulation called Lipoplex. Lipoplex has been used to provide efficient targeting of RNA to dendritic cells. The optimized Lipoplex:RNA formulation uses a charge ratio of 1.3:2, this was found to effectively target RNA to the spleen, form monodisperse and stable particles and was fully resistant to degradation by mouse serum at 37°C (135). In addition to targeting APCs, liposomes can also protect the RNA to be delivered from extracellular ribonucleases and mediates efficient uptake and expression by DCs and macrophages located in various lymphoid compartments. Lipoplex complexed with RNA encoding tumor antigens has also been shown to induce strong effector and memory T cells responses and mediate IFNα dependent rejection of progressive tumors (135). Vaccines using Lipoplex complexed with RNA induce and mobilize both the adaptive and innate immune responses mimicking an antiviral response.

Sahin et al. (136) recently conducted at phase 1 trial (NCT02410733) in melanoma patients who received melanoma FixVac (BNT111) an intravenously administered liposomal RNA (RNA-LPX) vaccine that targets four tumor associated antigens (NY-ESO-1, MAGE-A3, tyrosinase and TPTE) (135). Interim analysis (136) has shown that melanoma FixVac when used alone or in combination with the checkpoint inhibitor PD-1 mediates durable responses in patients with unresectable melanoma and with prior experience with a checkpoint inhibitor. FixVac induced clinical responses and potent CD4+ and CD8+ T cell responses could be detected with the cytotoxic T cell responses in some patients reaching the same level as reported for patients on T cell therapy trials. The completion date for this trial is estimated for December 2021, so far 119 patients (as of August 2020) have been enrolled.

Self-Assembling Peptides

Self-assembling peptides can also be used as a delivery system to deliver antigens to target cells. Self-assembling peptides can spontaneously form into ordered structures in response to changes in pH, solvent, co-assembling molecules, temperature and ionic strength (137, 138). They can have a diverse range of properties and can be manufactured to form nanomicelles, nanovesicles, nanofibers, nanotubes, nanoribbons and hydrogels (139). Self-assembling peptide deliver systems have a number of advantages over liposomes or nanoparticles including high drug loading, low drug leakage, biodegradability and are highly permeable to target cell membranes. The particle size is important for vaccine delivery and can impact the efficiency of uptake by APCs, with smaller particles (20-200 nm) being more immunogenic but there is no optimal size and this should be optimized for each vaccine candidate (140–142). The smaller particle size is thought to improve uptake into DCs and also the lymphatic system, in addition to size the shape, stability and ability to display multiple antigen can also improve immunogenicity. Self-assembling peptides can be designed to provide vaccines with the desired properties to enable efficient delivery to the target cell.

A delivery system based on modified cell penetrating peptide (CPP) based gene vectors, the Glycosaminoglycan (GAG)-binding enhanced transduction (GET) delivery system has been used to enhance delivery of nucleic acids for lung gene therapy and bone

regeneration *in vivo* (143, 144). The GET peptides (143–150) are multi-domain sequences comprising of a heparan sulphate (HS) cell targeting sequence fused to a CPP for improved membrane association and synergistically enhanced intracellular delivery of therapeutic cargoes (145). GET peptides can deliver self-reporting cargo (monomeric red fluorescent protein; mRFP) into difficult to transduce cell types including mesenchymal stem cells (MSCs), human embryonic stem cells (hESCs) and human induced pluripotent stem cells (hiPSCs). Delivery involves a heparin sulphate (HS) cell targeting system fused to a CPP and an endosomal escape peptide and a system which stabilizes particles to prevent aggregation and promote diffusion and cell uptake by PEGylation. The tripeptide complexes the DNA into nanoparticles and can be delivered by simple intramuscular injection. This tripeptide formulation has achieved exceptional results in DNA delivery applications in particular in lung, brain, and has huge potential in vaccine delivery.

GENETIC VACCINES

DNA Vaccines

DNA vaccines have a number of advantages, they are simple to design, relatively low production costs, good stability (stable at + 2-8°C) and solubility, can be rapidly modified, it is a versatile platform that can have many applications including in infectious diseases and oncology. DNA vaccines were first shown to be immunogenic in the 1990s (151–153), they are an attractive cancer vaccine platform (154) and this led to a flood in preclinical and clinical trials. Plasmid DNA vaccines can be designed to act as both an antigen and adjuvant (155), unmethylated DNA containing cytosine-guanine rich regions can act as an adjuvant stimulating an immune response (156). DNA vectors have a negatively charged backbone and have a low molecular weight, therefore naked DNA often suffers from poor cellular uptake resulting in poor antigen production (157–159). With a significant improvement in our knowledge of cancer immunology particular the TME and immune suppression the reasons for the failures of early DNA vaccines are now better understood.

In addition to improving the delivery of plasmid DNA the vector itself can also be modified to specifically target epitopes directly to APCs. In preclinical models we have previously demonstrated that a DNA plasmid encoding T cell epitopes within the complementarity determining regions of a human IgG1 antibody (ImmunoBody®) (160), when administered with electroporation (EP) stimulates high avidity T cell responses (161). ImmunoBody® works by the direct uptake of the DNA into APCs, it is then transcribed, translated and processed, with epitopes being presented on the cell surface in combination with MHC. ImmunoBody® can also be taken up by both antigen presenting cells and non-antigen presenting cells and the transcribed antibody protein secreted. The secreted antibody is internalized *via* the high affinity FcγR1 receptor (CD64) on antigen presenting cells, it is then processed, and epitopes cross presented on MHC class I. The combination of direct and cross presentation induces T cells with sufficiently high avidity to eradicate established tumors in preclinical models (160). Immunization with ImmunoBody® DNA vectors induces high frequency and avidity of T cell responses that are superior when compared to those induced by immunization with DNA encoding full-length antigen or when using peptides or peptide loaded onto dendritic cells (161–164). The first ImmunoBody® in the SCIB series, SCIB1, targets four epitopes from the melanoma-associated antigens TRP2 and gp100, our second vaccine, SCIB2, incorporates several epitopes derived from the NY-ESO-1 cancer testis antigen. A first-in-human study performed by Patel et al. used SCIB1 ImmunoBody® that incorporated HLA-A*02:01 restricted epitopes from gp100 and TRP-2 in addition to HLA-DR*04:01 and HLA-DR7/DR53/DQ6 restricted epitopes from gp100. In a cohort of 15 melanoma patients SCIB1 was shown to be safe (165). In this trial 7/15 patients had stable disease, 5/20 fully resected patients experienced disease recurrence and 1 patient had measurable disease, all patients were still alive at the last observation time of 37 months. A phase 2 study in melanoma patients receiving pembrolizumab is now recruiting (ClinicalTrials.gov Identifier: NCT04079166).

RNA Vaccines

The RNA vaccine platform has the advantage that RNA does not integrate into the host cell genome and thus avoids potential safety concerns, it is also quick to manufacture and can encode multiple epitopes. RNA is single stranded and therefore has a built-in adjuvant function through TLR7 and TLR8 stimulation. However, RNA is very susceptible to cellular degradation, to overcome this in clinical trials it has either been injected directly into inguinal lymph nodes or delivered using a nanoparticle delivery system that protects the RNA. RNA is particularly susceptible to degradation by RNases, to improve transfection and avoid degradation many groups have used delivery systems such as nanoparticles and liposomes (135, 166–170). RNA has an advantage over DNA in that it only needs to be delivered to the cytoplasm for translational into protein unlike DNA that needs to enter the nucleus for transcription.

The first clinical trials using RNA was performed by Weide et al. (171, 172) in patients with metastatic melanoma. In a phase 1 trial in 15 melanoma patients (171) the intradermal administration of naked mRNA was shown to be safe. In a phase 1/2 trial (172) 21 patients received i.d. injections of protamine stabilized mRNA coding for Melan-A, Tyrosinase, gp100, Mage-A1, Mage-A3 and survivin; GM-CSF was used as an adjuvant and half the patients also had keyhole limpet hemocyanin added to the vaccine. The number of clinical responses to the vaccine in this trial was low with only 1 promising clinical response observed in a patient with measurable disease. In a phase 1/2 trial performed by Rittig et al. in 30 patients with stage IV renal cell cancer (173), naked mRNA coding for TAA's was administered intradermally. This trial demonstrated that vaccination was safe and well tolerated and induced clinical responses in 16 patients; this trial also demonstrated that vaccination induced CD4 and CD8 T cell responses as determined by IFNγ ELISpot and Cr-release assays. The results from these trials demonstrated that vaccination with

RNA was feasible and safe. With improvements to trial design, frequency, and route of administration the RNA vaccine platform is progressing through clinical trials in the fields of cancer and infectious diseases. For COVID-19 two RNA vaccines (Tozinameran from Pfizer–BioNTech and mRNA-1273 from Moderna) have now been approved by national health regulators.

In a study performed by Sahin et al. the use of an RNA vaccine encoding neoantigens was explored (174) in melanoma patients. In this study neoantigens were identified by comparative exome analysis in tumors from thirteen patients with stage III and IV melanoma. Mutations were selected for incorporation into the vaccine based firstly on the predicted binding score for HLA class II and secondly based on the predicted binding score for HLA class I. For each patient two synthetic RNAs were synthesized incorporating the identified mutations. The RNA vaccine was produced within 68 days (range 49 to 102 days), following analytical testing they were released within 103 days (range 89 to 160 days). RNA vaccines work in a similar way to the long peptide vaccines, the RNA is translated into protein which is then processed into long peptides by APCs, these peptides are then loaded onto MHC class I or class II molecules and presented on the cell surface to prime and activate T cells. This study demonstrated the clinical feasibility and safety of RNA neo-epitope vaccines. In this study 8/13 patients had no tumors develop during the monitoring period and neoantigen specific T cells could be detected in the peripheral blood of these patients. The use of many neoantigen epitopes in a vaccine reduces the risk of single antigen loss variants (175), however, in this study the outgrowth of B2M deficient tumor cells in one patient demonstrates the complexity of the TME and the selective pressures that drive resistance to therapy.

VIRAL VECTOR VACCINES

Viral vectors have been used in both the gene therapy and vaccine fields. Viral vectors have the advantage of being recognized as foreign by the immune system, inducing potent innate and adaptive immune responses resulting in the induction of strong and durable immune responses. Viral vectors enable the presentation of intracellular antigens incorporated into the vector such as cancer antigens, viral antigens, or a specific gene for gene therapy.

The most commonly used viral vectors are derived from adenoviruses, poxviruses and alpha viruses. The majority of viral vectors are replication defective or attenuated versions, these are preferred from a safety point of view. Viral vectors have a very good safety record with many approved in the infectious disease field such a recently approved Ebola vaccine and COVID-19 vaccines that use adenovirus virus vectors. A disadvantage of the viral vectors is their ability to also induce immune responses that also neutralizes the vector preventing further repeat immunizations. Pre-existing immunity to measles and adenovirus can be problematic limiting the effectiveness and ability to boost responses when adenovirus or measles virus vectors are used. A prime boost vaccine regime is commonly used, and a number of different strategies have been used to overcome the problem with pre-exiting immunity. Strategies using a non-human specific virus such as the replication-defective chimpanzee adenovirus (ChAd68 serotype), or using different vectors derived from different viruses for the prime and boost immunization or using different vaccine platforms for the prime and boost immunizations can all avoid problems associated with pre-existing immunity to the virus vector. A common combination is the use of a DNA prime and a viral vector boost. Another commonly used combination is the Modified Vaccinia virus Ankara (MVA) and Adenovirus (Ad) vectors, both vectors induce potent immune responses that when used in combination in a prime boost regime these responses are further enhanced (176, 177). These strategies have all been used successfully in the infectious disease field, particularly more recently to target SARS-CoV-2, where 40 viral vector vaccines are currently being assessed in preclinical studies, an additional 19 vaccines are currently in clinical trials and another 4 vaccines have already received approval from regulatory authorities (178).

A number of different viral vectors have been used for cancer vaccines (179); with some having progressed into clinical trials. In clinical trials the efficacy of cancer vaccines using viral vectors have not delivered the same results as those generated in the infectious disease field. The immunosuppressive TME and selection of the best cancer antigen to target is problematic and impacts all cancer vaccine platforms. To overcome central tolerance and the immune suppressive TME a cancer vaccine would need multiple boosts in order to induce and sustain a potent immune response, however, this can be problematic due to anti-vector immunity. In preclinical and clinical studies, a prime-boost approach using a recombinant vaccinia vector and a recombinant avipox virus have been successfully used, and multiple boosts using recombinant avipox such as fowlpox is possible. Preclinical and clinical studies have shown that multiple booster vaccinations using a fowlpox does not induce host anti-vector immune responses (180, 181). Both viruses have been shown to be safe, vaccinia was used in the smallpox vaccine that has been delivered to over 1 billion people worldwide. Avipox is an avian virus that is unable to replicate in mammals. Both vectors do not integrate into DNA and successfully infect APCs thus stimulate potent immune responses.

The TRICOM vaccine platform uses the recombinant vaccinia virus (rV-) for the prime and recombinant avipox (fowlpox, rF-) for multiple booster vaccinations. Each vector contains one or more TAAs and transgenes for the costimulatory molecules CD80, ICAM1 and LFA-3. In a phase 2 clinical trial, 125 men with metastatic castration-resistant prostate cancer received a vaccinia virus encoding PSA in combination with GM-CSF followed by six subsequent boosts using a fowlpox virus encoding PSA (PROSTVAC-VF) (182). The results from this phase 2 trial was encouraging with a 10-month improvement in overall survival compared to the empty vector control group (183). Unfortunately, these results were not seen in a large phase 3 study and the study was subsequently stopped (184). It is likely that despite the activation of specific T cells they were either not

potent or unable to overcome the immunosuppressive TME (184). Trials are now ongoing to see if combining PROSTVAC-VF/TRICOM with check point inhibitors can improve clinical responses (NCT02933255, NCT04020094, NCT03532217, and NCT03315871).

PEPTIDE VACCINES

The number of peptide vaccines being explored has increased due to the discovery of neoantigens. Targeting neoantigens is a personalized therapy and the rapid synthesis of peptides makes the peptides vaccines an attractive platform. Almost half of the clinical trials currently recruiting (as of August 2020) that target neoantigens are using peptide vaccines, with the RNA and DNA vaccine platforms also represented (**Figure 3**). Following administration the peptides included in a vaccine need to be presented on antigen presenting cells (APCs) in order to trigger an adaptive immune response. To efficiently prime an immune response the coadministration of an adjuvant is required to activate the immune system to kill tumor cells expressing the peptide (185–187). Tumor antigens need to be processed and the resulting peptides presented on the cell surface in association with MHC class I or class II molecules. Cancer specific T cells in the TME need to recognize the relevant peptides and kill tumor cells expressing them. The key to the success of a peptide vaccine relies on the correct choice of peptides to include and the best adjuvant to use to generate a local immune response and promote antigen trafficking to local draining lymph nodes. Bioinformatic applications and algorithm prediction program are commonly used to define peptides capable of binding MHC I or MHC class II molecules. Identification of peptides bound to the MHC molecules on the cell surface can be achieved *via* mass spectrometry (MS) analysis. Combining data from MS analysis, epitope predicting algorithms and gene expression data help to predict the best candidate peptides to include in a vaccine.

A vaccine needs to stimulate both CD4+ and CD8+ specific T cells. The majority of peptide vaccines use longer peptides typically 20-30mers, these are likely to contain nested CD8+ T cell epitopes in addition to longer CD4 T cell epitopes and therefore are able to stimulate both CD4+ and CD8+ T cells. In addition, multi-peptide vaccines are often used, incorporating many peptides meaning that many antigens can be targeted, increasing the chances of overcoming any antigen loss on the tumor cells. A number of peptide vaccines targeting neoantigens have been developed by a number of groups, this personalized therapy can target a patient's individual tumor. Ott et al. (188) used whole-exome sequencing (WES) and RNA-sequencing (RNA-Seq) to identify neoantigens from six stage III/IV melanoma patients. Using NetMHCpan (v2.4) a list of peptides that bind to MHC class I was generated, synthesized peptides were between 15 to 30 amino acids in length and thus capable of stimulating CD4+ and CD8+ T cells. Patients were immunized with 30 peptides given in combination with poly-ICLC. This vaccine-induced polyfunctional CD4+ and CD8+ T cells targeting 58/97 and 15/97 neoantigens respectively across the patients. At 25 months post vaccination 4 patients had no recurrence while 2 patients had progressive disease that was successfully treated with anti-PD-1 therapy.

A number of early peptide-based cancer vaccine trials primarily focused on short peptides from tumor associated antigens, and did not include any delivery system or longer peptide formulations (189). The majority of these trials failed when reaching phase 3 trials, a number of additional reasons for these failures include adjuvant selection, timing of vaccination and peptide formulation (120). Peptide vaccines do generate an immune response but as a monotherapy they can struggle to show efficacy in the clinic. Kimura et al. immunized 39 patients with premalignant colon adenomas with a MUC1 peptide vaccine, they showed the peptides were immunogenic however in 22 patients there was a lack of a response which correlated with a high number of myeloid derived suppressor cells in the TME pre vaccination (190). In another two trials in melanoma and ovarian cancer patients (191, 192), a mixture of peptides were used to immunize patients, vaccination induced an immune response which was associated with some favorable outcomes. The majority of peptide vaccines did not generate an immune response that was robust enough to see any significant clinical benefit (189). These early studies highlighted the need to further optimize peptide vaccines, either by better targeting, better adjuvants or used in combination to overcome the immunosuppressive TME.

Peptide-Adjuvant Conjugate Vaccines

The administration of free adjuvant with antigens in a cancer vaccine can result in their dissociation following injection and subsequently do not enter the lymphatic system. Adjuvants can be rapidly degraded (193) reducing the amount that reaches the target cells resulting in suboptimal antigen priming and immune response. Free adjuvant in the circulation can also induce autoimmunity (194) or toxicity. The co-delivery of adjuvant with antigens is required to induce a potent immune response while avoiding any autoimmunity or toxicity, as already described a delivery system can be used to deliver the adjuvant and antigen, alternatively the adjuvant and antigen can be linked to improve targeting.

The direct conjugation of a peptide to an adjuvant is gaining increasing attention, particularly from groups targeting neoantigens. Previous reports have described the direct conjugation of peptides to TLR ligands can enhance the immune response by directly targeting the peptide and adjuvant to the same APC (195–199). Peptides can be linked to hydrophobic carriers such as lipids (92), fatty acids (200) and TLR agonists (196, 201, 202) for more efficient delivery to APCs and subsequently lymph nodes. A recent preclinical study performed by Lynn et al. (203) used a peptide platform based on charge modified TLR-7/8a peptide conjugates, these conjugates self-assemble into nanoparticles of uniform size which is independent of the peptide antigen composition. This platform is used to conjugate identified neoantigen peptides, these peptides would possess a variety of properties, such a platform would be able to incorporate peptides with a wide range of characteristics. Neoantigen peptides were predicted (179 peptides) from three murine tumor models, vaccination of mice induced a CD8+ T cell

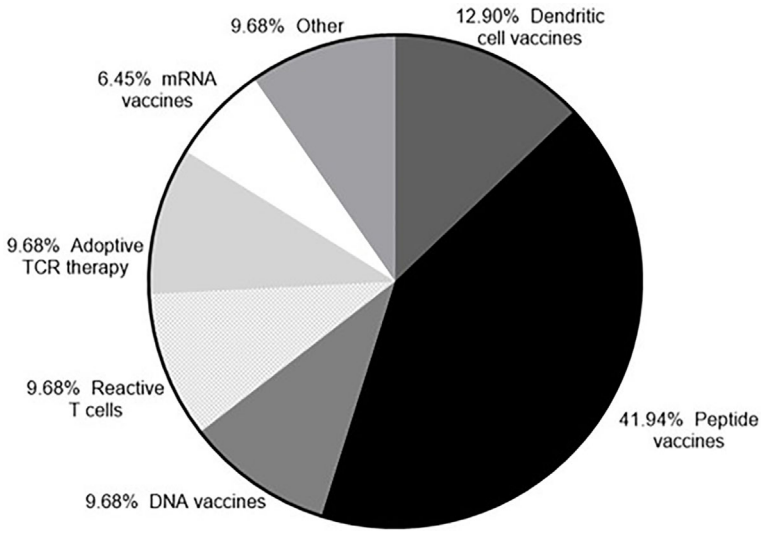


FIGURE 3 | Neoantigens currently in clinical trial. According to clinicaltrials.gov (as of 23rd September 2020) there are currently 33 clinical trials recruiting that target neoantigens.

response with approximately 50% of the peptides being recognized, this led to enhanced tumor clearance.

We have directly conjugated citrullinated peptides from vimentin and α-enolase (Vim28-49cit, Vim415-433cit and Eno241-260cit) to the TLR1/2 ligand AMPLIVANT®. The direct linkage of a TLR agonist to a peptide can enhances the immunogenicity of the vaccine (196–199). In HLA-DR4 and DP4 transgenic mice vaccination with the conjugated peptides induced a high frequency of specific T cells. The direct conjugation of the Vim28cit, Vim415cit and Eno241cit peptides to the TLR1/2 ligand Amplivant® reduced the peptide-equivalent dose required to induce immune responses by at least 1 log without the loss anti-tumor responses (60). These results demonstrate that the linkage of a TLR ligand to a peptide enhances the immune response and supports the development and application of these peptide/TLR ligand linked conjugates in a clinical setting.

Peptide vaccines have many advantages, they can be chemically synthesized, manufactured at large scale and cost effective (204) when compared to other cancer therapies. In pre-clinical and clinical studies they have been shown to be safe and well tolerated (204, 205). Peptide vaccines should include peptides that target multiple antigens to generate a polyclonal antigen T cell response (206–208). Like DNA and RNA vaccines the use of a delivery system can help improve the targeting and stability of peptides used in a vaccine which reduces any potential off target effects (209–212). The production of conjugated peptide vaccines can be problematic for some peptides, particularly hydrophobic peptides that tend to form aggregates that complicate manufacturing and when injected they form injection site depots leading suboptimal immune responses (213). The conjugation of peptides with adjuvants improves the delivery of both components to APCs which may be needed to induce T cell priming (203, 214). Peptide conjugates used in combination with other therapies have a huge potential. A peptide conjugate vaccine can specifically target APCs and that has the advantage of being dose sparing, in combination with a checkpoint inhibitor to relieve immunosuppression in the TME this would provide the best opportunity for these vaccines to work in the clinic.

VACCINES IN COMBINATION WITH OTHER THERAPIES

Immune checkpoint inhibitors constitute an important breakthrough positively influencing treatment outcomes in cancer patients. Cancer vaccines have the potential to induce potent immune responses but are hampered as tumor cells possess a variety of immune evasions mechanisms that interfere with the function of T cells (215–220). Upon activation, T cells migrate and accumulate in the TME where they can induce tumor cell killing, however, tumors have evolved multiple mechanisms that can dampen or inhibit T cell mediated killing. Tumor cells can alter the antigen processing machinery, secrete immunosuppressive factors that kill the T cells or activate pathways that induce tolerance rendering any tumor therapy ineffective (221). The identification of the key regulators of the immune response has led to the generation of new therapies that have the potential to reverse some of the immune suppression in the TME. Immune checkpoint inhibitors are cell surface receptors that regulate the immune response, they enable self-tolerance while preventing over activation of the immune system resulting in autoimmune disease (222). In the TME the expression of checkpoint receptors suppresses T cell activation and thus provides the tumor with a growth advantage (223). The

cytotoxic T lymphocyte protein 4 (CTLA-4) and programmed cell death protein 1 (PD-1) are the best characterised checkpoint receptors in the immunotherapy field, others have been described that are emerging from preclinical studies and entering the clinic.

The checkpoint receptor, PD-1, is expressed on activated T cells and overexpressed on exhausted T cells (90). There are two PD-1 ligands, PD-L1 and PD-L2, PD-L1 is expressed on many cells including immune cells, epithelial cells, endothelial cells and tumor cells (88, 91). PD-L2 is expressed on professional antigen presenting cells including DCs and macrophages (224). The binding of PD-1 on T cells to PD-L1 expressed on a tumor cell or PD-L2 expressed on an APC leads to TCR downregulation, resulting in lower secretion of TNF-α, IFN-γ, and IL-2 (92). The expression of CTLA-4 is induced upon T cell activation and competes with the costimulatory molecule CD28 for its co-stimulatory ligands. CTLA-4 suppresses the early activation of naïve and memory T cells by competing with CD28 (88–90), PD-1 inhibits T cell function at a later activation stage by down regulating TCR expression. Monoclonal antibodies that block CTLA-4 (223), PD-1 (225) or PD-L1 (226) pathways remove the inhibition of T cell function (227) and have made significant clinical impacts. Antibodies that specifically block the CTLA-4 or PD-1/PD-L1 pathway have the potential to remove T cell immune suppression enabling the successful recognition and killing of tumor cells.

Checkpoint blockade has shown promising results in clinical trials and have gained approval for an increasing number of cancers including melanoma, renal-cell carcinoma (RCC), advanced non-small-cell lung cancer (NSCLC), classic Hodgkin's lymphoma (HL), bladder carcinoma, Merkel cell carcinoma, head and neck cancer, and more recently, solid tumors with mismatch repair-deficiency. PD-1 and CTLA-4 inhibit T cell responses at different stages and by different mechanisms, it is therefore tempting to block both pathways in order to overcome immune suppression. Clinical trials in melanoma patients that have combined PD-1 and CTLA-4 blockade have shown improved clinical responses, however, these have come at a cost with an increase in toxicities being reported (228–230). The combination of anti CTLA-4 and anti PD-1 is now approved as the first line therapy for advanced melanoma patients; however, the toxicities have limited the use of this combination, trials are ongoing to vary the dose and interval of dosing to reduce toxicity.

Many cancer vaccines currently in clinical trials are combined with a checkpoint inhibitor such as CTLA-4, PD-1 or PD-L1 inhibitors, which are offered as standard treatment for an increasing number of cancers. A couple of comparative studies have shown that the combination of a tumor vaccine with a checkpoint inhibitor is more effective than monotherapy (231, 232). Less than 50% of patients respond to checkpoint inhibitors (233–235), there are several other factors that can lead to immune suppression in the TME, such as the action of T-regulatory cells, myeloid-derived suppressor cells (MDSCs), tumor associated macrophages and immunosuppressive DCs (236). For a vaccine to show efficacy in the clinic it is likely a combination with another form of therapy is required to improve tumor specific T cell function in the TME.

In preclinical murine models using the ImmunoBody® vaccine SCIB2 a synergistic effect was observed when given in combination with anti-PD-1 (**Figure 4**) (237). The synergistic effect was also observed with SCIB1 when given with anti-PD1 (163, 237). These results demonstrate that a cancer vaccine on its own will not achieve the expected results in the clinic without combining with other therapies aimed at modifying the TME by reducing immune suppression and also improving T cell trafficking into the tumor.

The first line treatment for the majority of cancer indications is radiotherapy or chemotherapy. These traditional treatments are not targeted therapies but the damage they cause to tumors results in the release of more antigens from the tumor cells. Damage to tissue surrounding a tumor can also induce the recruitment of T cells into the vicinity, this is particularly valuable when the tumor mutational burden (TMB) is low (238). A number of clinical trials are using either radiotherapy or chemotherapy to enhance the immune response to a vaccine. Radiotherapy can enhance the recruitment of T cells into tumor tissue and increase the intensity of specific anti-tumor immune responses (239). Other studies have shown that some chemotherapeutic drugs can enhance the antitumor activity of tumor vaccines (140, 141) and adoptively transferred T cells (137, 138). A vaccine combined with immune checkpoint inhibitors or traditional treatments can induce stronger anti-tumor responses (188), as such the majority of tumor vaccines in clinical trials are in combination with other therapies. The majority of cancer patients will be offered first line standard of care treatment prior to being offered alternative therapies or participation in a clinical trial.

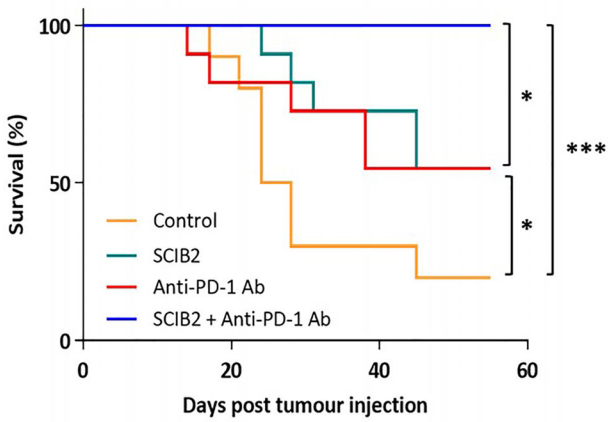


FIGURE 4 | Survival of HHDII mice challenged with 5 x10^4 tumor cells and immunized with SCIB2 and anti-PD-1 antibody alone or in combination. Control vs SCIB2 (*p = 0.037); Control vs anti-PD-1 antibody (p = 0.111); Control vs SCIB2 and anti-PD-1 antibody (***p = 0.0003); SCIB2 vs SCIB2 and anti-PD-1 (* = 0.0177); anti-PD-1 antibody vs SCIB2 and anti-PD-1 (*P = 0.0177). Lack of survival was defined as tumor size > 528 mm^3. Each curve represents at least 10 mice per group.

TUMOR MICROENVIRONMENT AND TUMOR INDUCED IMMUNE SUPPRESSION

Tumors evolve and change, they are heterogenous and genetically unstable. Tumors generate many mutations overtime, some are cloned, altered or lost in the tumor genome. Advances in sequencing technology now allows the analysis of a resected tumor or biopsy, the data gathered is a snapshot of a single tumor or part of a tumor at a specific time and does not provide information regarding the overall heterogeneity in the tumor (240, 241). This is a particular problem with the development of a personalized vaccine targeting a neoantigen, the information gained *via* biopsy or resection may represent a mutated tumor subclone or the neoantigen may be not expressed in the whole tumor or metastatic tumors compromising the effectiveness of the vaccine (242). The ideal mutations to target are driver mutations, these are critical for the growth of the tumor and are usually expressed in every tumor cell. However, the number of driver mutations can be low, for example in melanoma only 8% neoantigens are driver mutations (243). The degree of tumor heterogeneity will vary between patients, indications, and tumors. Improving our understanding of tumor heterogeneity will help identify the best epitopes to include in a cancer vaccine and targeting more than one antigen with help overcome tumor heterogeneity. The cancer vaccines targeting neoantigens address this heterogeneity by targeting more than one neoantigen and also addressing potential antigen loss.

Another factor that significantly contributes to the success immunotherapy is the TMB, studies by Rooney et al. demonstrated that the TMB correlated with immune responses (244). Tumors with high TMB, such as melanoma and NSCLC have a higher response rate to immunotherapy compared to tumors with a low TMB, however, this is not the case with all tumors. Pediatric tumors generally have fewer somatic mutations, a study performed by Zamora et al. showed that tumors from children with acute lymphoblastic leukemia had a low TMB but they could still induce a strong anti-tumor response (245). A number of clinical trials are underway for cancer indications that have an unmet need, poor survival and also have a low TMB e.g. glioblastoma and pancreatic cancer. Hopefully the results from these trials will help with our understanding of how to target tumors with a low TMB.

The TME consists of many different cell types including immune and stromal cells, vasculature, extracellular matrix and a variety of cytokines and chemokines. The extracellular matrix is made up of cells from endothelial, mesenchymal and haematopoietic origins. Changes in the TME impact the trafficking of TILs and efficacy of cancer vaccines that have induced specific T cells but are unable to traffic into the tumor.

Tumors have a number of mechanisms that have evolved to suppress anti-tumor immune responses. Apart from checkpoint mediators such as PD-1 and CTLA-4 a number of cell types have been identified that contribute to immune tolerance and evasion in the TME, Myeloid-derived suppressor cells (MDSCs), T regs, tumor associated macrophages (TAMs) and cancer associated fibroblasts all contribute to this immune suppression (246). MDSCs are a type of regulatory cell that are found within the TME (246, 247), they produce nitric oxide, cytokines and reactive oxygen species that can suppress T cells. MDSCs play a critical role in tumor invasion, metastasis and angiogenesis (248, 249). The presence of MDSCs in the TME correlates with poor overall survival and progression free survival (250). In a murine model of rhabdomyosarcoma, the trafficking of MDSCs was inhibited and subsequently an enhanced response to anti-PD-1 therapy was observed (251). In addition to MDSCs the presence of Tregs in the TME in many cancer types is also associated with a poor prognosis (252). Tregs are critical for the maintenance of cell tolerance, they suppress T cell responses by binding IL-2 therefore limiting the amount of free IL-2 available to drive T cell proliferation and activation (253). Tregs express CTLA-4 and can produce immunosuppressive cytokines that further contribute to the immune suppressive TME (252). The TAMs, in particular the M2 macrophages are another cell type that can contribute to the immune suppressive TME (254). The M2 macrophages can promote tumor growth by stimulating tumor cell motility, angiogenesis, and immune evasion (255). Murine studies have demonstrated that the depletion of macrophages reduces tumor growth and also by inhibiting the myeloid growth factor signaling pathway in macrophages overcome resistance to checkpoint inhibitors in a pancreatic cancer murine model (256, 257). The depletion or inhibition of MDSCs, Tregs or TAMs all have the potential to improve anti-tumor responses induced by vaccination or a cellular therapy, however, the impact of depleting these cells in the periphery as well as the tumor increases the potential to induce autoimmunity.

Within the TME the most abundant stromal cells are the cancer associated fibroblasts (CAF), these have been shown to play a role in tumorigenesis, angiogenesis, metastasis, drug resistance, immunosuppression, extracellular matrix (ECM), remodeling and maintenance of cancer stemness (258–264). Different subtypes of CAFs exist each capable of secreting a number of cytokines and chemokines such as TGF-β, IL-6, IL-8, IL-13, $CXCL_{12}$, $CXCL_{14}$, and VEGF that inhibit anti-tumor immune responses. Some CAFs also express PD-L1/PD-L2 or produce metabolites or enzymes such as indoleamine-2,3-dioxygenase (IDO), arginase (Arg), adenosine, and tryptase that recruit Tregs, mast cells and TAMs. CAFs can also contribute to the integrity of tumors, they can synthesize components that make up the ECM such as collagen, fibronectin, matrix metalloproteinases and can contribute to ECM stiffness and thus prevent T cell infiltration. The role of CAFs in cancer progression makes them a promising target for cancer therapy. There have been a few studies looking at anti-CAF based therapies, however in a murine CAR T cell-based study targeting the fibroblast marker FAP, toxicity was observed due to expression of FAP on other tissues (265). Other studies are looking at depleting CAFs, blocking their function or altering their function.

Cytokines and chemokines within the TME can also induce an immune suppressive TME and reduce T cells responses. One of the most studied cytokines is transforming growth factor beta (TGF-β). TGF-β signaling has a massive impact in the TME

where it can influence cell growth, differentiation and apoptosis while also inhibiting T cells responses and upregulating Tregs (266). In patients with colon cancer TGF-β tends to suppress cell growth but in advanced stages of the disease the presence of cells expressing members of TGF-β superfamily tend to have a poor prognosis. In murine models the inhibition of TGF-β reverses its immunosuppressive effects and improves the activity of T cells also rendering tumors suspectable to treatment with checkpoint blockade (267, 268). In addition to cytokines in the TME, chemokines such as CXCR2 and CXCR4 that bind to MDSCs and Tregs respectively contribute to tumor immune evasion. In murine models the inhibition of CXCR2 and CXCR4 in combination with anti-PD-1 reversed immune evasion (251, 269). Targeting cytokines and chemokines in TME could be a good cancer immunotherapy strategy that will help change the immune suppressive environment by preventing the recruitment and activation of Tregs, TAMs and MDSCs.

Cancer cells can also lose surface antigens as an immune evasion mechanism following natural or therapy induced selective pressure. Antigen loss has been observed for CD19 in acute lymphocytic leukemia and CD20 in chronic lymphocytic leukemia. Antigen loss is a common reason for resistance to therapy and subsequent relapse. To address the problem with potential antigen loss we have targeted two antigens in our Modi-1 and SCIB1 vaccines, with SCIB1 also inducing high avidity T cells that are capable of responding to a lower number of MHC: peptide complexes on tumor cells. In addition to antigen loss, tumors can also decrease MHC class I expression rendering the immune response powerless. The downregulation of MHC class I has been observed in both human and murine tumors (270–272). The majority of early primary tumors express MHC class I but this profile often changes as the tumor progresses and escape immune surveillance (273). The percentage of cancers that have HLA class I loss, total loss, haplotype loss or allelic loss can range from 65-90% (274, 275). We have addressed MHC class I loss by incorporating both MHC class I and class II peptides in our SCIB1 vaccine, our Modi-1 vaccine only includes MHC class II restricted peptides.

CONCLUSIONS

A large number of cancer vaccines have failed to show clinical efficacy, this can be due to the tumor's own mechanisms of immune evasion and escape that have evolved including antigen loss, MHC loss, the presence of immune suppressive cells or soluble factors in the TME and lack of a robust anti-tumor immune response (276–279) and also due to the inability of the cancer vaccines to induce sufficiently high avidity T cell responses to efficiently destroy tumors. Early cancer vaccines were primarily focused on stimulating CD8+ T cell responses against tumor associated antigens often using short minimal epitope sequences, T cells recognizing these antigens are highly tolerized and subsequently these vaccines fail in the clinic. The incorporation of CD4+ T cell epitopes into peptides, RNA or DNA vaccine platforms is essential to induce specific CD4+ and CD8+ T cell responses. Targeting non self or mutated tumor antigens will induce high avidity T cells responses when delivered with optimal adjuvant and delivery systems, as such the neoantigens and post translational modified antigens currently show the most promise.

Generating a neoantigen vaccine can be costly both in terms of time and money, the peptide vaccines are personalized and require a significant amount of bioinformatics input to generate the best candidate neoepitopes. The Modi-1 vaccine is not a personalized therapy and is broadly applicable to many patients and cancer types, it is cheaper to manufacture when compared to other platforms and in addition has no time delay constraints that is associated with the production of neoepitope vaccines.

The vaccine platform and the delivery systems used have undergone a huge number of improvements over the last decade. Many new adjuvants have emerged or are currently being investigated in order to improve the immune response at the injection site while also increasing antigen trafficking to the lymph nodes. The majority of cancer vaccines are currently using TLR agonists as adjuvants, these have also been conjugated to peptides or included in nanoparticles to improve targeting. Other adjuvants such as STING, CD40 agonist and GM-CSF are currently being investigated in clinical trials. The correct selection of an adjuvant is key to the ability of the vaccine to induce a robust immune response. We have previously screened a number of different potential adjuvants to use in our Modi-1 vaccine, this included CpG (TLR9), MPLA (TLR4), CpG/MPLA (TLR9/TLR4), GM-CSF, imiquimod (TLR7), Poly I:C (TLR3) or TLR1/2 (AMPLIVANT®). Preclinical studies have shown that when AMPLIVANT® is given in combination with the Modi-1 peptides it induced the strongest anti-tumor response (60). This highlights the importance of determining the best delivery and targeting approach for a vaccine that generates the strongest immune response while reducing any possible toxicity.

With our ImmunoBody® platform we have modified a DNA vector by engineering T cell epitopes into the IgG1 CDR regions (163), the Fc region of the antibody targets the high affinity Fc receptor CD64 that is expressed on activated APCs. The SCIB DNA vaccines allow both direct- and cross-presentation of epitopes by targeting dendritic cells, and are able to generate high avidity CD8+ T cells that efficiently eradicate tumors.. Vaccination with SCIB1 induces high frequency and high avidity specific T cells (165).

Improvement with vaccine delivery systems has led to the generation of nanoparticles, self-assembling peptides, and needle free delivery systems. Electroporation was used to administer SCIB1 in our phase 1 clinical trial, and has been used to deliver other cancer and infectious disease vaccines. However, the pain on administration using electroporation and the requirement for specialized vaccine delivery instrument have limited their use, these newer delivery systems provide better alternatives. Liposomes are increasingly being used as delivery system, they are versatile, incorporating small drug candidates or antigens in the form of RNA or peptides, and have a good safety profile. Liposomes do require optimization in order to determine the optimal charge/size of the particle to incorporate their cargo and deliver it across the cell membrane. The targeting of cancer

antigens to improve the local immune response and trafficking to lymph nodes can be achieved through either the linking of peptide to adjuvant, incorporating the antigen into nanoparticles or by modifying genetic vectors eg ImmunoBody® platform.

There are a number of challenges to address in the development of a successful cancer vaccine, we have tried to address a number of these challenges with our SCIB1, SCIB2 and Modi-1 vaccines. The SCIB1 vaccine is currently in phase 2 trials in combination with anti-PD-1 therapy, and the Modi-1 vaccine will be entering clinical trials in 2021. The success of any cancer vaccine does not rely only on the ability of the vaccine to induce a robust immune response but also on the modification of the immune suppressive TME to enable the successful trafficking of T cells and the ability of these T cells to recognize and kill tumor cells. The tumor size, TMB and previous treatments will all influence the success of a cancer vaccine and this will vary among patients and cancer types. With huge improvements in the cancer vaccine field and a better knowledge of the TME with time cancer vaccines will start to show good clinical efficacy.

AUTHOR CONTRIBUTIONS

SP wrote the review article. VB and PS contributed and analyzed the data. LD proof read the review and conceived the ideas and work around the Modi-1 and Immunobody vaccine platforms. All authors contributed to the article and approved the submitted version.

FUNDING

This work was funded by Scancell Ltd.

REFERENCES

1. Kantoff PW, Higano CS, Shore ND, Berger ER, Small EJ, Penson DF, et al. Sipuleucel-T immunotherapy for castration-resistant prostate cancer. *N Engl J Med* (2010) 363(5):411–22. doi: 10.1056/NEJMoa1001294
2. Berzofsky JA, Terabe M, Wood LV. Strategies to use immune modulators in therapeutic vaccines against cancer. *Semin Oncol* (2012) 39(3):348–57. doi: 10.1053/j.seminoncol.2012.02.002
3. Parchment RE, Voth AR, Doroshow JH, Berzofsky JA. Immuno-pharmacodynamics for evaluating mechanism of action and developing immunotherapy combinations. *Semin Oncol* (2016) 43(4):501–13. doi: 10.1053/j.seminoncol.2016.06.008
4. van der Bruggen P, Traversari C, Chomez P, Lurquin C, De Plaen E, Van den Eynde B, et al. A gene encoding an antigen recognized by cytolytic T lymphocytes on a human melanoma. *Science* (1991) 254(5038):1643–7. doi: 10.1126/science.1840703
5. De Plaen E, Arden K, Traversari C, Gaforio JJ, Szikora JP, De Smet C, et al. Structure, chromosomal localization, and expression of 12 genes of the MAGE family. *Immunogenetics* (1994) 40(5):360–9. doi: 10.1007/BF01246677
6. Chen YT, Scanlan MJ, Sahin U, Tureci O, Gure AO, Tsang S, et al. A testicular antigen aberrantly expressed in human cancers detected by autologous antibody screening. *Proc Natl Acad Sci U S A* (1997) 94 (5):1914–8. doi: 10.1073/pnas.94.5.1914
7. De Backer O, Arden KC, Boretti M, Vantomme V, De Smet C, Czekay S, et al. Characterization of the GAGE genes that are expressed in various human cancers and in normal testis. *Cancer Res* (1999) 59(13):3157–65.
8. Van den Eynde B, Peeters O, De Backer O, Gaugler B, Lucas S, Boon T. A new family of genes coding for an antigen recognized by autologous cytolytic T lymphocytes on a human melanoma. *J Exp Med* (1995) 182 (3):689–98. doi: 10.1084/jem.182.3.689
9. Boel P, Wildmann C, Sensi ML, Brasseur R, Renauld JC, Coulie P, et al. BAGE: a new gene encoding an antigen recognized on human melanomas by cytolytic T lymphocytes. *Immunity* (1995) 2(2):167–75. doi: 10.1016/S1074-7613(95)80053-0
10. Coulie PG, Brichard V, Van Pel A, Wolfel T, Schneider J, Traversari C, et al. A new gene coding for a differentiation antigen recognized by autologous cytolytic T lymphocytes on HLA-A2 melanomas. *J Exp Med* (1994) 180 (1):35–42. doi: 10.1084/jem.180.1.35
11. Kawakami Y, Eliyahu S, Delgado CH, Robbins PF, Rivoltini L, Topalian SL, et al. Cloning of the gene coding for a shared human melanoma antigen recognized by autologous T cells infiltrating into tumor. *Proc Natl Acad Sci U S A* (1994) 91(9):3515–9. doi: 10.1073/pnas.91.9.3515
12. Kawakami Y, Eliyahu S, Delgado CH, Robbins PF, Sakaguchi K, Appella E, et al. Identification of a human melanoma antigen recognized by tumor-infiltrating lymphocytes associated with in vivo tumor rejection. *Proc Natl Acad Sci U S A* (1994) 91(14):6458–62. doi: 10.1073/pnas.91.14.6458
13. Brichard V, Van Pel A, Wolfel T, Wolfel C, De Plaen E, Lethe B, et al. The tyrosinase gene codes for an antigen recognized by autologous cytolytic T lymphocytes on HLA-A2 melanomas. *J Exp Med* (1993) 178(2):489–95. doi: 10.1084/jem.178.2.489
14. Watt KW, Lee PJ, M'Timkulu T, Chan WP, Loor R. Human prostate-specific antigen: structural and functional similarity with serine proteases. *Proc Natl Acad Sci U S A* (1986) 83(10):3166–70. doi: 10.1073/pnas.83.10.3166
15. Lilja H. A kallikrein-like serine protease in prostatic fluid cleaves the predominant seminal vesicle protein. *J Clin Invest* (1985) 76(5):1899–903. doi: 10.1172/JCI112185
16. Ilantzis C, DeMarte L, Screaton RA, Stanners CP. Deregulated expression of the human tumor marker CEA and CEA family member CEACAM6 disrupts tissue architecture and blocks colonocyte differentiation. *Neoplasia* (2002) 4(2):151–63. doi: 10.1038/sj.neo.7900201
17. Bajenova O, Chaika N, Tolkunova E, Davydov-Sinitsyn A, Gapon S, Thomas P, et al. Carcinoembryonic antigen promotes colorectal cancer progression by targeting adherens junction complexes. *Exp Cell Res* (2014) 324(2):115–23. doi: 10.1016/j.yexcr.2014.04.007
18. Yarden Y. Biology of HER2 and its importance in breast cancer. *Oncology* (2001) 61(Suppl 2):1–13. doi: 10.1159/000055396
19. Huang FW, Hodis E, Xu MJ, Kryukov GV, Chin L, Garraway LA. Highly recurrent TERT promoter mutations in human melanoma. *Science* (2013) 339(6122):957–9. doi: 10.1126/science.1229259
20. Meyerson M, Counter CM, Eaton EN, Ellisen LW, Steiner P, Caddle SD, et al. hEST2, the putative human telomerase catalytic subunit gene, is up-regulated in tumor cells and during immortalization. *Cell* (1997) 90(4):785–95. doi: 10.1016/S0092-8674(00)80538-3
21. Levine AJ. p53, the cellular gatekeeper for growth and division. *Cell* (1997) 88(3):323–31. doi: 10.1016/S0092-8674(00)81871-1
22. Andersen MH, Svane IM, Becker JC, Straten PT. The universal character of the tumor-associated antigen survivin. *Clin Cancer Res* (2007) 13(20):5991–4. doi: 10.1158/1078-0432.CCR-07-0686
23. Andersen MH, thor SP. Survivin–a universal tumor antigen. *Histol Histopathol* (2002) 17(2):669–75. doi: 10.14670/HH-17.669
24. Adida C, Haioun C, Gaulard P, Lepage E, Morel P, Briere J, et al. Prognostic significance of survivin expression in diffuse large B-cell lymphomas. *Blood* (2000) 96(5):1921–5. doi: 10.1182/blood.V96.5.1921
25. Schmidt SM, Schag K, Muller MR, Weck MM, Appel S, Kanz L, et al. Survivin is a shared tumor-associated antigen expressed in a broad variety of malignancies and recognized by specific cytotoxic T cells. *Blood* (2003) 102 (2):571–6. doi: 10.1182/blood-2002-08-2554

26. Lau SK, Weiss LM, Chu PG. Differential expression of MUC1, MUC2, and MUC5AC in carcinomas of various sites: an immunohistochemical study. *Am J Clin Pathol* (2004) 122(1):61–9. doi: 10.1309/9R6673QEC06D86Y4
27. Miwa H, Beran M, Saunders GF. Expression of the Wilms' tumor gene (WT1) in human leukemias. *Leukemia* (1992) 6(5):405–9.
28. Koziol JA, Zhang JY, Casiano CA, Peng XX, Shi FD, Feng AC, et al. Recursive partitioning as an approach to selection of immune markers for tumor diagnosis. *Clin Cancer Res* (2003) 9(14):5120–6.
29. Suzuki H, Graziano DF, McKolanis J, Finn OJ. T cell-dependent antibody responses against aberrantly expressed cyclin B1 protein in patients with cancer and premalignant disease. *Clin Cancer Res* (2005) 11(4):1521–6. doi: 10.1158/1078-0432.CCR-04-0538
30. Epstein MA, Achong BG, Barr YM. Virus Particles in Cultured Lymphoblasts from Burkitt's Lymphoma. *Lancet* (1964) 1(7335):702–3. doi: 10.1016/S0140-6736(64)91524-7
31. Hjalgrim H, Askling J, Rostgaard K, Hamilton-Dutoit S, Frisch M, Zhang JS, et al. Characteristics of Hodgkin's lymphoma after infectious mononucleosis. *N Engl J Med* (2003) 349(14):1324–32. doi: 10.1056/NEJMoa023141
32. zur Hausen H, Schulte-Holthausen H, Klein G, Henle W, Henle G, Clifford P, et al. EBV DNA in biopsies of Burkitt tumours and anaplastic carcinomas of the nasopharynx. *Nature* (1970) 228(5276):1056–8. doi: 10.1038/2281056a0
33. Munoz N, Bosch FX, de Sanjose S, Herrero R, Castellsague X, Shah KV, et al. Epidemiologic classification of human papillomavirus types associated with cervical cancer. *N Engl J Med* (2003) 348(6):518–27. doi: 10.1056/NEJMoa021641
34. Uchiyama T, Yodoi J, Sagawa K, Takatsuki K, Uchino H. Adult T-cell leukemia: clinical and hematologic features of 16 cases. *Blood* (1977) 50 (3):481–92. doi: 10.1182/blood.V50.3.481.481
35. Chu NJ, Armstrong TD, Jaffee EM. Nonviral oncogenic antigens and the inflammatory signals driving early cancer development as targets for cancer immunoprevention. *Clin Cancer Res* (2015) 21(7):1549–57. doi: 10.1158/1078-0432.CCR-14-1186
36. Omholt K, Platz A, Kanter L, Ringborg U, Hansson J. NRAS and BRAF mutations arise early during melanoma pathogenesis and are preserved throughout tumor progression. *Clin Cancer Res* (2003) 9(17):6483–8.
37. Nowell PC, Hungerford DA. Chromosome studies on normal and leukemic human leukocytes. *J Natl Cancer Inst* (1960) 25:85–109.
38. Rowley JD. Letter: A new consistent chromosomal abnormality in chronic myelogenous leukaemia identified by quinacrine fluorescence and Giemsa staining. *Nature* (1973) 243(5405):290–3. doi: 10.1038/243290a0
39. Golub TR, Barker GF, Lovett M, Gilliland DG. Fusion of PDGF receptor beta to a novel ets-like gene, tel, in chronic myelomonocytic leukemia with t(5;12) chromosomal translocation. *Cell* (1994) 77(2):307–16. doi: 10.1016/0092-8674(94)90322-0
40. Morris SW, Kirstein MN, Valentine MB, Dittmer KG, Shapiro DN, Saltman DL, et al. Fusion of a kinase gene, ALK, to a nucleolar protein gene, NPM, in non-Hodgkin's lymphoma. *Science* (1994) 263(5151):1281–4. doi: 10.1126/science.8122112
41. Shiota M, Fujimoto J, Semba T, Satoh H, Yamamoto T, Mori S. Hyperphosphorylation of a novel 80 kDa protein-tyrosine kinase similar to Ltk in a human Ki-1 lymphoma cell line, AMS3. *Oncogene* (1994) 9 (6):1567–74.
42. Bresler SC, Weiser DA, Huwe PJ, Park JH, Krytska K, Ryles H, et al. ALK mutations confer differential oncogenic activation and sensitivity to ALK inhibition therapy in neuroblastoma. *Cancer Cell* (2014) 26(5):682–94. doi: 10.1016/j.ccell.2014.09.019
43. Janoueix-Lerosey I, Lequin D, Brugieres L, Ribeiro A, de Pontual L, Combaret V, et al. Somatic and germline activating mutations of the ALK kinase receptor in neuroblastoma. *Nature* (2008) 455(7215):967–70. doi: 10.1038/nature07398
44. Yadav M, Jhunjhunwala S, Phung QT, Lupardus P, Tanguay J, Bumbaca S, et al. Predicting immunogenic tumour mutations by combining mass spectrometry and exome sequencing. *Nature* (2014) 515(7528):572–6. doi: 10.1038/nature14001
45. Karpanen T, Olweus J. The Potential of Donor T-Cell Repertoires in Neoantigen-Targeted Cancer Immunotherapy. *Front Immunol* (2017) 8:1718. doi: 10.3389/fimmu.2017.01718
46. Ryan SO, Vlad AM, Islam K, Gariepy J, Finn OJ. Tumor-associated MUC1 glycopeptide epitopes are not subject to self-tolerance and improve responses to MUC1 peptide epitopes in MUC1 transgenic mice. *Biol Chem* (2009) 390(7):611–8. doi: 10.1515/BC.2009.070
47. Depontieu FR, Qian J, Zarling AL, McMiller TL, Salay TM, Norris A, et al. Identification of tumor-associated, MHC class II-restricted phosphopeptides as targets for immunotherapy. *Proc Natl Acad Sci U S A* (2009) 106 (29):12073–8. doi: 10.1073/pnas.0903852106
48. Cobbold M, De La Pena H, Norris A, Polefrone JM, Qian J, English AM, et al. MHC class I-associated phosphopeptides are the targets of memory-like immunity in leukemia. *Sci Transl Med* (2013) 5(203):203ra125. doi: 10.1126/scitranslmed.3006061
49. Brentville VA, Metheringham RL, Gunn B, Symonds P, Daniels I, Gijon M, et al. Citrullinated Vimentin Presented on MHC-II in Tumor Cells Is a Target for CD4+ T-Cell-Mediated Antitumor Immunity. *Cancer Res* (2016) 76(3):548–60. doi: 10.1158/0008-5472.CAN-15-1085
50. Zarling AL, Obeng RC, Desch AN, Pinczewski J, Cummings KL, Deacon DH, et al. MHC-restricted phosphopeptides from insulin receptor substrate-2 and CDC25b offer broad-based immunotherapeutic agents for cancer. *Cancer Res* (2014) 74(23):6784–95. doi: 10.1158/0008-5472.CAN-14-0043
51. Zarling AL, Ficarro SB, White FM, Shabanowitz J, Hunt DF, Engelhard VH. Phosphorylated peptides are naturally processed and presented by major histocompatibility complex class I molecules in vivo. *J Exp Med* (2000) 192 (12):1755–62. doi: 10.1084/jem.192.12.1755
52. Zarling AL, Polefrone JM, Evans AM, Mikesh LM, Shabanowitz J, Lewis ST, et al. Identification of class I MHC-associated phosphopeptides as targets for cancer immunotherapy. *Proc Natl Acad Sci U S A* (2006) 103(40):14889–94. doi: 10.1073/pnas.0604045103
53. Engelhard VH, Obeng RC, Cummings KL, Petroni GR, Ambakhutwala AL, Chianese-Bullock KA, et al. MHC-restricted phosphopeptide antigens: preclinical validation and first-in-humans clinical trial in participants with high-risk melanoma. *J Immunother Cancer* (2020) 8(1). doi: 10.1136/jitc-2019-000262
54. Dearth RK, Cui X, Kim HJ, Hadsell DL, Lee AV. Oncogenic transformation by the signaling adaptor proteins insulin receptor substrate (IRS)-1 and IRS-2. *Cell Cycle* (2007) 6(6):705–13. doi: 10.4161/cc.6.6.4035
55. Dearth RK, Cui X, Kim HJ, Kuiatse I, Lawrence NA, Zhang X, et al. Mammary tumorigenesis and metastasis caused by overexpression of insulin receptor substrate 1 (IRS-1) or IRS-2. *Mol Cell Biol* (2006) 26 (24):9302–14. doi: 10.1128/MCB.00260-06
56. Gorgisen G, Gulacar IM, Ozes ON. The role of insulin receptor substrate (IRS) proteins in oncogenic transformation. *Cell Mol Biol (Noisy-le-grand)* (2017) 63(1):1–5. doi: 10.14715/cmb/2017.63.1.1
57. Riggins RB, Quilliam LA, Bouton AH. Synergistic promotion of c-Src activation and cell migration by Cas and AND-34/BCAR3. *J Biol Chem* (2003) 278(30):28264–73. doi: 10.1074/jbc.M303535200
58. Schrecengost RS, Riggins RB, Thomas KS, Guerrero MS, Bouton AH. Breast cancer antiestrogen resistance-3 expression regulates breast cancer cell migration through promotion of p130Cas membrane localization and membrane ruffling. *Cancer Res* (2007) 67(13):6174–82. doi: 10.1158/0008-5472.CAN-06-3455
59. Cantarino N, Musulen E, Valero V, Peinado MA, Perucho M, Moreno V, et al. Downregulation of the Deiminase PADI2 Is an Early Event in Colorectal Carcinogenesis and Indicates Poor Prognosis. *Mol Cancer Res* (2016) 14(9):841–8. doi: 10.1158/1541-7786.MCR-16-0034
60. Brentville VA, Metheringham RL, Daniels I, Atabani S, Symonds P, Cook KW, et al. Combination vaccine based on citrullinated vimentin and enolase peptides induces potent CD4-mediated anti-tumor responses. *J Immunother Cancer* (2020) 8(1). doi: 10.1136/jitc-2020-000560
61. Witalison EE, Thompson PR, Hofseth LJ. Protein Arginine Deiminases and Associated Citrullination: Physiological Functions and Diseases Associated with Dysregulation. *Curr Drug Targets* (2015) 16(7):700–10. doi: 10.2174/1389450116666150202160954
62. Alghamdi M, Alasmari D, Assiri A, Mattar E, Aljaddawi AA, Alattas SG, et al. An Overview of the Intrinsic Role of Citrullination in Autoimmune Disorders. *J Immunol Res* (2019) 2019:7592851. doi: 10.1155/2019/7592851
63. Ireland JM, Unanue ER. Autophagy in antigen-presenting cells results in presentation of citrullinated peptides to CD4 T cells. *J Exp Med* (2011) 208 (13):2625–32. doi: 10.1084/jem.20110640

64. Feitsma AL, van der Voort EI, Franken KL, el Bannoudi H, Elferink BG, Drijfhout JW, et al. Identification of citrullinated vimentin peptides as T cell epitopes in HLA-DR4-positive patients with rheumatoid arthritis. *Arthritis Rheum* (2010) 62(1):117–25. doi: 10.1002/art.25059
65. Gerstner C, Dubnovitsky A, Sandin C, Kozhukh G, Uchtenhagen H, James EA, et al. Functional and Structural Characterization of a Novel HLA-DRB1*04:01-Restricted alpha-Enolase T Cell Epitope in Rheumatoid Arthritis. *Front Immunol* (2016) 7:494. doi: 10.3389/fimmu.2016.00494
66. Gerstner C, Dubnovitsky A, Sandin C, Kozhukh G, Uchtenhagen H, James EA, et al. Corrigendum: Functional and Structural Characterization of a Novel HLA-DRB1*04:01-Restricted alpha-Enolase T Cell Epitope in Rheumatoid Arthritis. *Front Immunol* (2017) 8:1236. doi: 10.3389/fimmu.2017.01236
67. James EA, Rieck M, Pieper J, Gebe JA, Yue BB, Tatum M, et al. Citrulline-specific Th1 cells are increased in rheumatoid arthritis and their frequency is influenced by disease duration and therapy. *Arthritis Rheumatol* (2014) 66 (7):1712–22. doi: 10.1002/art.38637
68. Snir O, Rieck M, Gebe JA, Yue BB, Rawlings CA, Nepom G, et al. Identification and functional characterization of T cells reactive to citrullinated vimentin in HLA-DRB1*0401-positive humanized mice and rheumatoid arthritis patients. *Arthritis Rheum* (2011) 63(10):2873–83. doi: 10.1002/art.30445
69. Seliger B, Kloor M, Ferrone S. HLA class II antigen-processing pathway in tumors: Molecular defects and clinical relevance. *Oncoimmunology* (2017) 6 (2):e1171447. doi: 10.1080/2162402X.2016.1171447
70. Lhuillier C, Rudqvist NP, Elemento O, Formenti SC, Demaria S. Radiation therapy and anti-tumor immunity: exposing immunogenic mutations to the immune system. *Genome Med* (2019) 11(1):40. doi: 10.1186/s13073-019-0653-7
71. Coppola D, Fu L, Nicosia SV, Kounelis S, Jones M. Prognostic significance of p53, bcl-2, vimentin, and S100 protein-positive Langerhans cells in endometrial carcinoma. *Hum Pathol* (1998) 29(5):455–62. doi: 10.1016/S0046-8177(98)90060-0
72. Fuyuhiro Y, Yashiro M, Noda S, Kashiwagi S, Matsuoka J, Doi Y, et al. Clinical significance of vimentin-positive gastric cancer cells. *Anticancer Res* (2010) 30(12):5239–43.
73. Gilles C, Polette M, Piette J, Delvigne AC, Thompson EW, Foidart JM, et al. Vimentin expression in cervical carcinomas: association with invasive and migratory potential. *J Pathol* (1996) 180(2):175–80. doi: 10.1002/(SICI)1096-9896(199610)180:2<175::AID-PATH630>3.0.CO;2-G
74. Gustmann C, Altmannsberger M, Osborn M, Griesser H, Feller AC. Cytokeratin expression and vimentin content in large cell anaplastic lymphomas and other non-Hodgkin's lymphomas. *Am J Pathol* (1991) 138(6):1413–22.
75. Williams AA, Higgins JP, Zhao H, Ljunberg B, Brooks JD. CD 9 and vimentin distinguish clear cell from chromophobe renal cell carcinoma. *BMC Clin Pathol* (2009) 9:9. doi: 10.1186/1472-6890-9-9
76. Yamamoto Y, Izumi K, Otsuka H. An immunohistochemical study of epithelial membrane antigen, cytokeratin, and vimentin in papillary thyroid carcinoma. Recognition of lethal and favorable prognostic types. *Cancer* (1992) 70(9):2326–33. doi: 10.1002/1097-0142(19921101)70:9<2326::AID-CNCR2820700919>3.0.CO;2-D
77. Palena C, Fernando RI, Litzinger MT, Hamilton DH, Huang B, Schlom J. Strategies to target molecules that control the acquisition of a mesenchymal-like phenotype by carcinoma cells. *Exp Biol Med (Maywood)* (2011) 236 (5):537–45. doi: 10.1258/ebm.2011.010367
78. Miles LA, Dahlberg CM, Plescia J, Felez J, Kato K, Plow EF. Role of cell-surface lysines in plasminogen binding to cells: identification of alpha-enolase as a candidate plasminogen receptor. *Biochemistry* (1991) 30 (6):1682–91. doi: 10.1021/bi00220a034
79. Cappello P, Tomaino B, Chiarle R, Ceruti P, Novarino A, Castagnoli C, et al. An integrated humoral and cellular response is elicited in pancreatic cancer by alpha-enolase, a novel pancreatic ductal adenocarcinoma-associated antigen. *Int J Cancer* (2009) 125(3):639–48. doi: 10.1002/ijc.24355
80. Fu QF, Liu Y, Fan Y, Hua SN, Qu HY, Dong SW, et al. Alpha-enolase promotes cell glycolysis, growth, migration, and invasion in non-small cell lung cancer through FAK-mediated PI3K/AKT pathway. *J Hematol Oncol* (2015) 8:22. doi: 10.1186/s13045-015-0117-5
81. Principe M, Ceruti P, Shih NY, Chattaragada MS, Rolla S, Conti L, et al. Targeting of surface alpha-enolase inhibits the invasiveness of pancreatic cancer cells. *Oncotarget* (2015) 6(13):11098–113. doi: 10.18632/oncotarget.3572
82. Zhao M, Fang W, Wang Y, Guo S, Shu L, Wang L, et al. Enolase-1 is a therapeutic target in endometrial carcinoma. *Oncotarget* (2015) 6 (17):15610–27. doi: 10.18632/oncotarget.3639
83. Lundberg K, Kinloch A, Fisher BA, Wegner N, Wait R, Charles P, et al. Antibodies to citrullinated alpha-enolase peptide 1 are specific for rheumatoid arthritis and cross-react with bacterial enolase. *Arthritis Rheum* (2008) 58(10):3009–19. doi: 10.1002/art.23936
84. Brentville VA, Symonds P, Cook KW, Daniels I, Pitt T, Gijon M, et al. T cell repertoire to citrullinated self-peptides in healthy humans is not confined to the HLA-DR SE alleles; Targeting of citrullinated self-peptides presented by HLA-DP4 for tumour therapy. *Oncoimmunology* (2019) 8(5):e1576490. doi: 10.1080/2162402X.2019.1576490
85. Cook K, Daniels I, Symonds P, Pitt T, Gijon M, Xue W, et al. Citrullinated alpha-enolase is an effective target for anti-cancer immunity. *Oncoimmunology* (2018) 7(2):e1390642. doi: 10.1080/2162402X.2017.1390642
86. Durrant LG, Metheringham RL, Brentville VA. Autophagy, citrullination and cancer. *Autophagy* (2016) 12(6):1055–6. doi: 10.1080/15548627.2016.1166326
87. Brentville VA, Vankemmelbeke M, Metheringham RL, Durrant LG. Post-translational modifications such as citrullination are excellent targets for cancer therapy. *Semin Immunol* (2020) 47:101393. doi: 10.1016/j.smim.2020.101393
88. Mellman I, Steinman RM. Dendritic cells: specialized and regulated antigen processing machines. *Cell* (2001) 106(3):255–8. doi: 10.1016/S0092-8674(01)00449-4
89. Kenter GG, Welters MJ, Valentijn AR, Lowik MJ, Berends-van der Meer DM, Vloon AP, et al. Vaccination against HPV-16 oncoproteins for vulvar intraepithelial neoplasia. *N Engl J Med* (2009) 361(19):1838–47. doi: 10.1056/NEJMoa0810097
90. Maisonneuve C, Bertholet S, Philpott DJ, De Gregorio E. Unleashing the potential of NOD- and Toll-like agonists as vaccine adjuvants. *Proc Natl Acad Sci U S A* (2014) 111(34):12294–9. doi: 10.1073/pnas.1400478111
91. Yang Y, Huang CT, Huang X, Pardoll DM. Persistent Toll-like receptor signals are required for reversal of regulatory T cell-mediated CD8 tolerance. *Nat Immunol* (2004) 5(5):508–15. doi: 10.1038/ni1059
92. Liu H, Moynihan KD, Zheng Y, Szeto GL, Li AV, Huang B, et al. Structure-based programming of lymph-node targeting in molecular vaccines. *Nature* (2014) 507(7493):519–22. doi: 10.1038/nature12978
93. Ammi R, De Waele J, Willemen Y, Van Brussel I, Schrijvers DM, Lion E, et al. Poly(I:C) as cancer vaccine adjuvant: knocking on the door of medical breakthroughs. *Pharmacol Ther* (2015) 146:120–31. doi: 10.1016/j.pharmthera.2014.09.010
94. Vosika GJ, Barr C, Gilbertson D. Phase-I study of intravenous modified lipid A. *Cancer Immunol Immunother* (1984) 18(2):107–12. doi: 10.1007/BF00205743
95. Johnson AG, Tomai M, Solem L, Beck L, Ribi E. Characterization of a nontoxic monophosphoryl lipid A. *Rev Infect Dis* (1987) 9(Suppl 5):S512–6. doi: 10.1093/clinids/9.Supplement_5.S512
96. Diebold SS, Kaisho T, Hemmi H, Akira S, Reis e Sousa C. Innate antiviral responses by means of TLR7-mediated recognition of single-stranded RNA. *Science* (2004) 303(5663):1529–31. doi: 10.1126/science.1093616
97. Lee J, Chuang TH, Redecke V, She L, Pitha PM, Carson DA, et al. Molecular basis for the immunostimulatory activity of guanine nucleoside analogs: activation of Toll-like receptor 7. *Proc Natl Acad Sci U S A* (2003) 100 (11):6646–51. doi: 10.1073/pnas.0631696100
98. Heil F, Hemmi H, Hochrein H, Ampenberger F, Kirschning C, Akira S, et al. Species-specific recognition of single-stranded RNA via toll-like receptor 7 and 8. *Science* (2004) 303(5663):1526–9. doi: 10.1126/science.1093620
99. Jurk M, Kritzler A, Schulte B, Tluk S, Schetter C, Krieg AM, et al. Modulating responsiveness of human TLR7 and 8 to small molecule ligands with T-rich phosphorothiate oligodeoxynucleotides. *Eur J Immunol* (2006) 36(7):1815–26. doi: 10.1002/eji.200535806
100. Krug A, Rothenfusser S, Hornung V, Jahrsdorfer B, Blackwell S, Ballas ZK, et al. Identification of CpG oligonucleotide sequences with high induction of

IFN-alpha/beta in plasmacytoid dendritic cells. *Eur J Immunol* (2001) 31 (7):2154–63. doi: 10.1002/1521-4141(200107)31:7<2154::AID-IMMU2154>3.0.CO;2-U

101. Kranzer K, Bauer M, Lipford GB, Heeg K, Wagner H, Lang R. CpG-oligodeoxynucleotides enhance T-cell receptor-triggered interferon-gamma production and up-regulation of CD69 via induction of antigen-presenting cell-derived interferon type I and interleukin-12. *Immunology* (2000) 99 (2):170–8. doi: 10.1046/j.1365-2567.2000.00964.x
102. Vonderheide RH, Glennie MJ. Agonistic CD40 antibodies and cancer therapy. *Clin Cancer Res* (2013) 19(5):1035–43. doi: 10.1158/1078-0432.CCR-12-2064
103. McWilliams JA, Sanchez PJ, Haluszczak C, Gapin L, Kedl RM. Multiple innate signaling pathways cooperate with CD40 to induce potent, CD70-dependent cellular immunity. *Vaccine* (2010) 28(6):1468–76. doi: 10.1016/j.vaccine.2009.11.071
104. Nimanong S, Ostroumov D, Wingerath J, Knocke S, Woller N, Gurlevik E, et al. CD40 Signaling Drives Potent Cellular Immune Responses in Heterologous Cancer Vaccinations. *Cancer Res* (2017) 77(8):1918–26. doi: 10.1158/0008-5472.CAN-16-2089
105. Dubensky TW Jr, Kanne DB, Leong ML. Rationale, progress and development of vaccines utilizing STING-activating cyclic dinucleotide adjuvants. *Ther Adv Vaccines* (2013) 1(4):131–43. doi: 10.1177/2051013613501988
106. Ishikawa H, Barber GN. STING is an endoplasmic reticulum adaptor that facilitates innate immune signalling. *Nature* (2008) 455(7213):674–8. doi: 10.1038/nature07317
107. Corrales L, Glickman LH, McWhirter SM, Kanne DB, Sivick KE, Katibah GE, et al. Direct Activation of STING in the Tumor Microenvironment Leads to Potent and Systemic Tumor Regression and Immunity. *Cell Rep* (2015) 11 (7):1018–30. doi: 10.1016/j.celrep.2015.04.031
108. Chandra D, Quispe-Tintaya W, Jahangir A, Asafu-Adjei D, Ramos I, Sintim HO, et al. STING ligand c-di-GMP improves cancer vaccination against metastatic breast cancer. *Cancer Immunol Res* (2014) 2(9):901–10. doi: 10.1158/2326-6066.CIR-13-0123
109. Gulen MF, Koch U, Haag SM, Schuler F, Apetoh L, Villunger A, et al. Signalling strength determines proapoptotic functions of STING. *Nat Commun* (2017) 8(1):427. doi: 10.1038/s41467-017-00573-w
110. Hanson MC, Crespo MP, Abraham W, Moynihan KD, Szeto GL, Chen SH, et al. Nanoparticulate STING agonists are potent lymph node-targeted vaccine adjuvants. *J Clin Invest* (2015) 125(6):2532–46. doi: 10.1172/JCI79915
111. Conlon J, Burdette DL, Sharma S, Bhat N, Thompson M, Jiang Z, et al. Mouse, but not human STING, binds and signals in response to the vascular disrupting agent 5,6-dimethylxanthenone-4-acetic acid. *J Immunol* (2013) 190(10):5216–25. doi: 10.4049/jimmunol.1300097
112. Kim H, Kwon B, Sin JI. Combined stimulation of IL-2 and 4-1BB receptors augments the antitumor activity of E7 DNA vaccines by increasing Ag-specific CTL responses. *PLoS One* (2013) 8(12):e83765. doi: 10.1371/journal.pone.0083765
113. Pavlenko M, Roos AK, Lundqvist A, Palmborg A, Miller AM, Ozenci V, et al. A phase I trial of DNA vaccination with a plasmid expressing prostate-specific antigen in patients with hormone-refractory prostate cancer. *Br J Cancer* (2004) 91(4):688–94. doi: 10.1038/sj.bjc.6602019
114. Sikora AG, Jaffarzad N, Hailemichael Y, Gelbard A, Stonier SW, Schluns KS, et al. IFN-alpha enhances peptide vaccine-induced CD8+ T cell numbers, effector function, and antitumor activity. *J Immunol* (2009) 182(12):7398–407. doi: 10.4049/jimmunol.0802982
115. Gajewski TF, Fallarino F, Ashikari A, Sherman M. Immunization of HLA-A2 + melanoma patients with MAGE-3 or MelanA peptide-pulsed autologous peripheral blood mononuclear cells plus recombinant human interleukin 12. *Clin Cancer Res* (2001) 7(3 Suppl):895s–901s.
116. Lee P, Wang F, Kuniyoshi J, Rubio V, Stuges T, Groshen S, et al. Effects of interleukin-12 on the immune response to a multipeptide vaccine for resected metastatic melanoma. *J Clin Oncol* (2001) 19(18):3836–47. doi: 10.1200/JCO.2001.19.18.3836
117. Dranoff G. GM-CSF-based cancer vaccines. *Immunol Rev* (2002) 188:147–54. doi: 10.1034/j.1600-065X.2002.18813.x
118. Serafini P, Carbley R, Noonan KA, Tan G, Bronte V, Borrello I. High-dose granulocyte-macrophage colony-stimulating factor-producing vaccines impair the immune response through the recruitment of myeloid suppressor cells. *Cancer Res* (2004) 64(17):6337–43. doi: 10.1158/0008-5472.CAN-04-0757
119. Slingluff CL Jr, Petroni GR, Olson WC, Smolkin ME, Ross MI, Haas NB, et al. Effect of granulocyte/macrophage colony-stimulating factor on circulating CD8+ and CD4+ T-cell responses to a multipeptide melanoma vaccine: outcome of a multicenter randomized trial. *Clin Cancer Res* (2009) 15 (22):7036–44. doi: 10.1158/1078-0432.CCR-09-1544
120. Wong KK, Li WA, Mooney DJ, Dranoff G. Advances in Therapeutic Cancer Vaccines. *Adv Immunol* (2016) 130:191–249. doi: 10.1016/bs.ai.2015.12.001
121. Fioretti D, Iurescia S, Fazio VM, Rinaldi M. DNA vaccines: developing new strategies against cancer. *J BioMed Biotechnol* (2010) 2010:174378. doi: 10.1155/2010/174378
122. Becker SM, Kuznetsov AV. Local temperature rises influence in vivo electroporation pore development: a numerical stratum corneum lipid phase transition model. *J Biomech Eng* (2007) 129(5):712–21. doi: 10.1115/1.2768380
123. Roos AK, Eriksson F, Timmons JA, Gerhardt J, Nyman U, Gudmundsdotter L, et al. Skin electroporation: effects on transgene expression, DNA persistence and local tissue environment. *PLoS One* (2009) 4(9):e7226. doi: 10.1371/journal.pone.0007226
124. Chiarella P, Massi E, De Robertis M, Sibilio A, Parrella P, Fazio VM, et al. Electroporation of skeletal muscle induces danger signal release and antigen-presenting cell recruitment independently of DNA vaccine administration. *Expert Opin Biol Ther* (2008) 8(11):1645–57. doi: 10.1517/14712598.8.11.1645
125. van Drunen Littel-van den Hurk S, Hannaman D. Electroporation for DNA immunization: clinical application. *Expert Rev Vaccines* (2010) 9(5):503–17. doi: 10.1586/erv.10.42
126. Tiptiri-Kourpeti A, Spyridopoulou K, Pappa A, Chlichlia K. DNA vaccines to attack cancer: Strategies for improving immunogenicity and efficacy. *Pharmacol Ther* (2016) 165:32–49. doi: 10.1016/j.pharmthera.2016.05.004
127. Nguyen-Hoai T, Pezzutto A, Westermann J. Gene Gun Her2/neu DNA Vaccination: Evaluation of Vaccine Efficacy in a Syngeneic Her2/neu Mouse Tumor Model. *Methods Mol Biol* (2015) 1317:17–37. doi: 10.1007/978-1-4939-2727-2_2
128. Trimble C, Lin CT, Hung CF, Pai S, Juang J, He L, et al. Comparison of the CD8+ T cell responses and antitumor effects generated by DNA vaccine administered through gene gun, biojector, and syringe. *Vaccine* (2003) 21 (25-26):4036–42. doi: 10.1016/S0264-410X(03)00275-5
129. Wen R, Banik B, Pathak RK, Kumar A, Kolishetti N, Dhar S. Nanotechnology inspired tools for mitochondrial dysfunction related diseases. *Adv Drug Delivery Rev* (2016) 99(Pt A):52–69. doi: 10.1016/j.addr.2015.12.024
130. Cao J, Wang R, Gao N, Li M, Tian X, Yang W, et al. A7RC peptide modified paclitaxel liposomes dually target breast cancer. *Biomater Sci* (2015) 3 (12):1545–54. doi: 10.1039/C5BM00161G
131. Li MH, Yu H, Wang TF, Chang ND, Zhang JQ, Du D, et al. Tamoxifen embedded in lipid bilayer improves the oncotarget of liposomal daunorubicin in vivo. *J Mater Chem B* (2014) 2(12):1619–25. doi: 10.1039/c3tb21423k
132. Nguyen TX, Huang L, Gauthier M, Yang G, Wang Q. Recent advances in liposome surface modification for oral drug delivery. *Nanomed (Lond)* (2016) 11(9):1169–85. doi: 10.2217/nnm.16.9
133. Pires P, Simoes S, Nir S, Gaspar R, Duzgunes N, Pedroso de Lima MC. Interaction of cationic liposomes and their DNA complexes with monocytic leukemia cells. *Biochim Biophys Acta* (1999) 1418(1):71–84. doi: 10.1016/S0005-2736(99)00023-1
134. Detienne S, Welsby I, Collignon C, Wouters S, Coccia M, Delhaye S, et al. Central Role of CD169(+) Lymph Node Resident Macrophages in the Adjuvanticity of the QS-21 Component of AS01. *Sci Rep* (2016) 6:39475. doi: 10.1038/srep39475
135. Kranz LM, Diken M, Haas H, Kreiter S, Loquai C, Reuter KC, et al. Systemic RNA delivery to dendritic cells exploits antiviral defence for cancer immunotherapy. *Nature* (2016) 534(7607):396–401. doi: 10.1038/nature18300
136. Sahin U, Oehm P, Derhovanessian E, Jabulowsky RA, Vormehr M, Gold M, et al. An RNA vaccine drives immunity in checkpoint-inhibitor-treated

melanoma. *Nature* (2020) 585(7823):107–12. doi: 10.1038/s41586-020-2537-9
137. Cui H, Webber MJ, Stupp SI. Self-assembly of peptide amphiphiles: from molecules to nanostructures to biomaterials. *Biopolymers* (2010) 94(1):1–18. doi: 10.1002/bip.21328
138. Mandal D, Nasrolahi Shirazi A, Parang K. Self-assembly of peptides to nanostructures. *Org Biomol Chem* (2014) 12(22):3544–61. doi: 10.1039/C4OB00447G
139. Rudra JS, Tian YF, Jung JP, Collier JH. A self-assembling peptide acting as an immune adjuvant. *Proc Natl Acad Sci U S A* (2010) 107(2):622–7. doi: 10.1073/pnas.0912124107
140. Foged C. Subunit vaccines of the future: the need for safe, customized and optimized particulate delivery systems. *Ther Deliv* (2011) 2(8):1057–77. doi: 10.4155/tde.11.68
141. Xiang SD, Scholzen A, Minigo G, David C, Apostolopoulos V, Mottram PL, et al. Pathogen recognition and development of particulate vaccines: does size matter? *Methods* (2006) 40(1):1–9. doi: 10.1016/j.ymeth.2006.05.016
142. Irvine DJ, Swartz MA, Szeto GL. Engineering synthetic vaccines using cues from natural immunity. *Nat Mater* (2013) 12(11):978–90. doi: 10.1038/nmat3775
143. Osman G, Rodriguez J, Chan SY, Chisholm J, Duncan G, Kim N, et al. PEGylated enhanced cell penetrating peptide nanoparticles for lung gene therapy. *J Control Release* (2018) 285:35–45. doi: 10.1016/j.jconrel.2018.07.001
144. Raftery RM, Walsh DP, Blokpoel Ferreras L, Mencia Castano I, Chen G, LeMoine M, et al. Highly versatile cell-penetrating peptide loaded scaffold for efficient and localised gene delivery to multiple cell types: From development to application in tissue engineering. *Biomaterials* (2019) 216:119277. doi: 10.1016/j.biomaterials.2019.119277
145. Dixon JE, Osman G, Morris GE, Markides H, Rotherham M, Bayoussef Z, et al. Highly efficient delivery of functional cargoes by the synergistic effect of GAG binding motifs and cell-penetrating peptides. *Proc Natl Acad Sci U S A* (2016) 113(3):E291–9. doi: 10.1073/pnas.1518634113
146. Eltaher HM, Yang J, Shakesheff KM, Dixon JE. Highly efficient intracellular transduction in three-dimensional gradients for programming cell fate. *Acta Biomater* (2016) 41:181–92. doi: 10.1016/j.actbio.2016.06.004
147. Abu-Awwad HAM, Thiagarajan L, Dixon JE. Controlled release of GAG-binding enhanced transduction (GET) peptides for sustained and highly efficient intracellular delivery. *Acta Biomater* (2017) 57:225–37. doi: 10.1016/j.actbio.2017.04.028
148. Thiagarajan L, Abu-Awwad HAM, Dixon JE. Osteogenic Programming of Human Mesenchymal Stem Cells with Highly Efficient Intracellular Delivery of RUNX2. *Stem Cells Transl Med* (2017) 6(12):2146–59. doi: 10.1002/sctm.17-0137
149. Markides H, Newell KJ, Rudorf H, Ferreras LB, Dixon JE, Morris RH, et al. Ex vivo MRI cell tracking of autologous mesenchymal stromal cells in an ovine osteochondral defect model. *Stem Cell Res Ther* (2019) 10(1):25. doi: 10.1186/s13287-018-1123-7
150. Spiliotopoulos A, Blokpoel Ferreras L, Densham RM, Caulton SG, Maddison BC, Morris JR, et al. Discovery of peptide ligands targeting a specific ubiquitin-like domain-binding site in the deubiquitinase USP11. *J Biol Chem* (2019) 294(2):424–36. doi: 10.1074/jbc.RA118.004469
151. Tang DC, DeVit M, Johnston SA. Genetic immunization is a simple method for eliciting an immune response. *Nature* (1992) 356(6365):152–4. doi: 10.1038/356152a0
152. Ulmer JB, Donnelly JJ, Parker SE, Rhodes GH, Felgner PL, Dwarki VJ, et al. Heterologous protection against influenza by injection of DNA encoding a viral protein. *Science* (1993) 259(5102):1745–9. doi: 10.1126/science.8456302
153. Wang B, Ugen KE, Srikantan V, Agadjanyan MG, Dang K, Refaeli Y, et al. Gene inoculation generates immune responses against human immunodeficiency virus type 1. *Proc Natl Acad Sci U S A* (1993) 90(9):4156–60. doi: 10.1073/pnas.90.9.4156
154. Melief CJ, van Hall T, Arens R, Ossendorp F, van der Burg SH. Therapeutic cancer vaccines. *J Clin Invest* (2015) 125(9):3401–12. doi: 10.1172/JCI80009
155. Kojima Y, Xin KQ, Ooki T, Hamajima K, Oikawa T, Shinoda K, et al. Adjuvant effect of multi-CpG motifs on an HIV-1 DNA vaccine. *Vaccine* (2002) 20(23-24):2857–65. doi: 10.1016/S0264-410X(02)00238-4
156. Klinman DM, Yamshchikov G, Ishigatsubo Y. Contribution of CpG motifs to the immunogenicity of DNA vaccines. *J Immunol* (1997) 158(8):3635–9.
157. Lee SH, Danishmalik SN, Sin JI. DNA vaccines, electroporation and their applications in cancer treatment. *Hum Vaccin Immunother* (2015) 11(8):1889–900. doi: 10.1080/21645515.2015.1035502
158. Yang B, Jeang J, Yang A, Wu TC, Hung CF. DNA vaccine for cancer immunotherapy. *Hum Vaccin Immunother* (2014) 10(11):3153–64. doi: 10.4161/21645515.2014.980686
159. Kuang H, Ku SH, Kokkoli E. The design of peptide-amphiphiles as functional ligands for liposomal anticancer drug and gene delivery. *Adv Drug Deliv Rev* (2017) 110-111:80–101. doi: 10.1016/j.addr.2016.08.005
160. Metheringham RL, Pudney VA, Gunn B, Towey M, Spendlove I, Durrant LG. Antibodies designed as effective cancer vaccines. *MAbs* (2009) 1(1):71–85. doi: 10.4161/mabs.1.1.7492
161. Pudney VA, Metheringham RL, Gunn B, Spendlove I, Ramage JM, Durrant LG. DNA vaccination with T-cell epitopes encoded within Ab molecules induces high-avidity anti-tumor CD8+ T cells. *Eur J Immunol* (2010) 40(3):899–910. doi: 10.1002/eji.200939857
162. Brentville VA, Metheringham RL, Gunn B, Durrant LG. High avidity cytotoxic T lymphocytes can be selected into the memory pool but they are exquisitely sensitive to functional impairment. *PLoS One* (2012) 7(7):e41112. doi: 10.1371/journal.pone.0041112
163. Xue W, Brentville VA, Symonds P, Cook KW, Yagita H, Metheringham RL, et al. SCIB1, a huIgG1 antibody DNA vaccination, combined with PD-1 blockade induced efficient therapy of poorly immunogenic tumors. *Oncotarget* (2016) 7(50):83088–100. doi: 10.18632/oncotarget.13070
164. Saif JM, Vadakekolathu J, Rane SS, McDonald D, Ahmad M, Mathieu M, et al. Novel prostate acid phosphatase-based peptide vaccination strategy induces antigen-specific T-cell responses and limits tumour growth in mice. *Eur J Immunol* (2014) 44(4):994–1004. doi: 10.1002/eji.201343863
165. Patel PM, Ottensmeier CH, Mulatero C, Lorigan P, Plummer R, Pandha H, et al. Targeting gp100 and TRP-2 with a DNA vaccine: Incorporating T cell epitopes with a human IgG1 antibody induces potent T cell responses that are associated with favourable clinical outcome in a phase I/II trial. *Oncoimmunology* (2018) 7(6):e1433516. doi: 10.1080/2162402X.2018.1433516
166. Lu D, Benjamin R, Kim M, Conry RM, Curiel DT. Optimization of methods to achieve mRNA-mediated transfection of tumor cells in vitro and in vivo employing cationic liposome vectors. *Cancer Gene Ther* (1994) 1(4):245–52.
167. Wasungu L, Hoekstra D. Cationic lipids, lipoplexes and intracellular delivery of genes. *J Control Release* (2006) 116(2):255–64. doi: 10.1016/j.jconrel.2006.06.024
168. Little SR, Lynn DM, Ge Q, Anderson DG, Puram SV, Chen J, et al. Poly-beta amino ester-containing microparticles enhance the activity of nonviral genetic vaccines. *Proc Natl Acad Sci U S A* (2004) 101(26):9534–9. doi: 10.1073/pnas.0403549101
169. Phua KK, Leong KW, Nair SK. Transfection efficiency and transgene expression kinetics of mRNA delivered in naked and nanoparticle format. *J Control Release* (2013) 166(3):227–33. doi: 10.1016/j.jconrel.2012.12.029
170. Su X, Fricke J, Kavanagh DG, Irvine DJ. In vitro and in vivo mRNA delivery using lipid-enveloped pH-responsive polymer nanoparticles. *Mol Pharm* (2011) 8(3):774–87. doi: 10.1021/mp100390w
171. Weide B, Carralot JP, Reese A, Scheel B, Eigentler TK, Hoerr I, et al. Results of the first phase I/II clinical vaccination trial with direct injection of mRNA. *J Immunother* (2008) 31(2):180–8. doi: 10.1097/CJI.0b013e31815ce501
172. Weide B, Pascolo S, Scheel B, Derhovanessian E, Pflugfelder A, Eigentler TK, et al. Direct injection of protamine-protected mRNA: results of a phase 1/2 vaccination trial in metastatic melanoma patients. *J Immunother* (2009) 32(5):498–507. doi: 10.1097/CJI.0b013e3181a00068
173. Rittig SM, Haentschel M, Weimer KJ, Heine A, Muller MR, Brugger W, et al. Intradermal vaccinations with RNA coding for TAA generate CD8+ and CD4+ immune responses and induce clinical benefit in vaccinated patients. *Mol Ther* (2011) 19(5):990–9. doi: 10.1038/mt.2010.289
174. Sahin U, Derhovanessian E, Miller M, Kloke BP, Simon P, Lower M, et al. Personalized RNA mutanome vaccines mobilize poly-specific therapeutic immunity against cancer. *Nature* (2017) 547(7662):222–6. doi: 10.1038/nature23003

175. Matsushita H, Vesely MD, Koboldt DC, Rickert CG, Uppaluri R, Magrini VJ, et al. Cancer exome analysis reveals a T-cell-dependent mechanism of cancer immunoediting. *Nature* (2012) 482(7385):400–4. doi: 10.1038/nature10755
176. Wang HB, Kondo A, Yoshida A, Yoshizaki S, Abe S, Bao LL, et al. Partial protection against SIV challenge by vaccination of adenovirus and MVA vectors in rhesus monkeys. *Gene Ther* (2010) 17(1):4–13. doi: 10.1038/gt.2009.122
177. Bliss CM, Bowyer G, Anagnostou NA, Havelock T, Snudden CM, Davies H, et al. Assessment of novel vaccination regimens using viral vectored liver stage malaria vaccines encoding ME-TRAP. *Sci Rep* (2018) 8(1):3390. doi: 10.1038/s41598-018-21630-4
178. WHO. *W.H.o., The COVID-19 candidate vaccine landscape and tracker.* (2021). Available at: https://www.who.int/publications/m/item/draft-landscape-of-covid-19-candidate-vaccines.
179. Larocca C, Schlom J. Viral vector-based therapeutic cancer vaccines. *Cancer J* (2011) 17(5):359–71. doi: 10.1097/PPO.0b013e3182325e63
180. Marshall JL, Gulley JL, Arlen PM, Beetham PK, Tsang KY, Slack R, et al. Phase I study of sequential vaccinations with fowlpox-CEA(6D)-TRICOM alone and sequentially with vaccinia-CEA(6D)-TRICOM, with and without granulocyte-macrophage colony-stimulating factor, in patients with carcinoembryonic antigen-expressing carcinomas. *J Clin Oncol* (2005) 23 (4):720–31. doi: 10.1200/JCO.2005.10.206
181. Capone S, Reyes-Sandoval A, Naddeo M, Siani L, Ammendola V, Rollier CS, et al. Immune responses against a liver-stage malaria antigen induced by simian adenoviral vector AdCh63 and MVA prime-boost immunisation in non-human primates. *Vaccine* (2010) 29(2):256–65. doi: 10.1016/j.vaccine.2010.10.041
182. DiPaola RS, Plante M, Kaufman H, Petrylak DP, Israeli R, Lattime E, et al. A phase I trial of pox PSA vaccines (PROSTVAC-VF) with B7-1, ICAM-1, and LFA-3 co-stimulatory molecules (TRICOM) in patients with prostate cancer. *J Transl Med* (2006) 4:1. doi: 10.1186/1479-5876-4-1
183. Kantoff PW, Gulley JL, Pico-Navarro C. Revised Overall Survival Analysis of a Phase II, Randomized, Double-Blind, Controlled Study of PROSTVAC in Men With Metastatic Castration-Resistant Prostate Cancer. *J Clin Oncol* (2017) 35(1):124–5. doi: 10.1200/JCO.2016.69.7748
184. Gulley JL, Borre M, Vogelzang NJ, Ng S, Agarwal N, Parker CC, et al. Phase III Trial of PROSTVAC in Asymptomatic or Minimally Symptomatic Metastatic Castration-Resistant Prostate Cancer. *J Clin Oncol* (2019) 37 (13):1051–61. doi: 10.1200/JCO.18.02031
185. Butterfield LH. Cancer vaccines. *BMJ* (2015) 350:h988. doi: 10.1136/bmj.h988
186. Zahm CD, Colluru VT, McNeel DG. Vaccination with High-Affinity Epitopes Impairs Antitumor Efficacy by Increasing PD-1 Expression on CD8(+) T Cells. *Cancer Immunol Res* (2017) 5(8):630–41. doi: 10.1158/2326-6066.CIR-16-0374
187. Mahdavi M, Moreau V, Kheirollahi M. Identification of B and T cell epitope based peptide vaccine from IGF-1 receptor in breast cancer. *J Mol Graph Model* (2017) 75:316–21. doi: 10.1016/j.jmgm.2017.06.004
188. Ott PA, Hu Z, Keskin DB, Shukla SA, Sun J, Bozym DJ, et al. An immunogenic personal neoantigen vaccine for patients with melanoma. *Nature* (2017) 547(7662):217–21. doi: 10.1038/nature22991
189. Pol J, Bloy N, Buque A, Eggermont A, Cremer I, Sautes-Fridman C, et al. Trial Watch: Peptide-based anticancer vaccines. *Oncoimmunology* (2015) 4 (4):e974411. doi: 10.4161/2162402X.2014.974411
190. Kimura T, McKolanis JR, Dzubinski LA, Islam K, Potter DM, Salazar AM, et al. MUC1 vaccine for individuals with advanced adenoma of the colon: a cancer immunoprevention feasibility study. *Cancer Prev Res (Phila)* (2013) 6 (1):18–26. doi: 10.1158/1940-6207.CAPR-12-0275
191. Morse MA, Secord AA, Blackwell K, Hobeika AC, Sinnathamby G, Osada T, et al. MHC class I-presented tumor antigens identified in ovarian cancer by immunoproteomic analysis are targets for T-cell responses against breast and ovarian cancer. *Clin Cancer Res* (2011) 17(10):3408–19. doi: 10.1158/1078-0432.CCR-10-2614
192. Reed CM, Cresce ND, Mauldin IS, Slingluff CL Jr, Olson WC. Vaccination with Melanoma Helper Peptides Induces Antibody Responses Associated with Improved Overall Survival. *Clin Cancer Res* (2015) 21(17):3879–87. doi: 10.1158/1078-0432.CCR-15-0233
193. Sands H, Gorey-Feret LJ, Cocuzza AJ, Hobbs FW, Chidester D, Trainor GL. Biodistribution and metabolism of internally 3H-labeled oligonucleotides. I. Comparison of a phosphodiester and a phosphorothioate. *Mol Pharmacol* (1994) 45(5):932–43.
194. Kreutz M, Giquel B, Hu Q, Abuknesha R, Uematsu S, Akira S, et al. Antibody-antigen-adjuvant conjugates enable co-delivery of antigen and adjuvant to dendritic cells in cis but only have partial targeting specificity. *PLoS One* (2012) 7(7):e40208. doi: 10.1371/journal.pone.0040208
195. Zom GG, Filippov DV, van der Marel GA, Overkleeft HS, Melief CJ, Ossendorp F. Two in one: improving synthetic long peptide vaccines by combining antigen and adjuvant in one molecule. *Oncoimmunology* (2014) 3 (7):e947892. doi: 10.4161/21624011.2014.947892
196. Zom GG, Khan S, Britten CM, Sommandas V, Camps MG, Loof NM, et al. Efficient induction of antitumor immunity by synthetic toll-like receptor ligand-peptide conjugates. *Cancer Immunol Res* (2014) 2(8):756–64. doi: 10.1158/2326-6066.CIR-13-0223
197. Zom GG, Welters MJ, Loof NM, Goedemans R, Lougheed S, Valentijn RR, et al. TLR2 ligand-synthetic long peptide conjugates effectively stimulate tumor-draining lymph node T cells of cervical cancer patients. *Oncotarget* (2016) 7(41):67087–100. doi: 10.18632/oncotarget.11512
198. Heit A, Schmitz F, O'Keeffe M, Staib C, Busch DH, Wagner H, et al. Protective CD8 T cell immunity triggered by CpG-protein conjugates competes with the efficacy of live vaccines. *J Immunol* (2005) 174(7):4373–80. doi: 10.4049/jimmunol.174.7.4373
199. Wille-Reece U, Wu CY, Flynn BJ, Kedl RM, Seder RA. Immunization with HIV-1 Gag protein conjugated to a TLR7/8 agonist results in the generation of HIV-1 Gag-specific Th1 and CD8+ T cell responses. *J Immunol* (2005) 174 (12):7676–83. doi: 10.4049/jimmunol.174.12.7676
200. Cho HI, Barrios K, Lee YR, Linowski AK, Celis E. BiVax: a peptide/poly-IC subunit vaccine that mimics an acute infection elicits vast and effective anti-tumor CD8 T-cell responses. *Cancer Immunol Immunother* (2013) 62 (4):787–99. doi: 10.1007/s00262-012-1382-6
201. Ignacio BJ, Albin TJ, Esser-Kahn AP, Verdoes M. Toll-like Receptor Agonist Conjugation: A Chemical Perspective. *Bioconjug Chem* (2018) 29(3):587–603. doi: 10.1021/acs.bioconjchem.7b00808
202. Lu BL, Williams GM, Verdon DJ, Dunbar PR, Brimble MA. Synthesis and Evaluation of Novel TLR2 Agonists as Potential Adjuvants for Cancer Vaccines. *J Med Chem* (2020) 63(5):2282–91. doi: 10.1021/acs.jmedchem.9b01044
203. Lynn GM, Sedlik C, Baharom F, Zhu Y, Ramirez-Valdez RA, Coble VL, et al. Peptide-TLR-7/8a conjugate vaccines chemically programmed for nanoparticle self-assembly enhance CD8 T-cell immunity to tumor antigens. *Nat Biotechnol* (2020) 38(3):320–32. doi: 10.1038/s41587-019-0390-x
204. Li W, Joshi MD, Singhania S, Ramsey KH, Murthy AK. Peptide Vaccine: Progress and Challenges. *Vaccines (Basel)* (2014) 2(3):515–36. doi: 10.3390/vaccines2030515
205. Nascimento IP, Leite LC. Recombinant vaccines and the development of new vaccine strategies. *Braz J Med Biol Res* (2012) 45(12):1102–11. doi: 10.1590/S0100-879X2012007500142
206. Slingluff CL Jr. The present and future of peptide vaccines for cancer: single or multiple, long or short, alone or in combination? *Cancer J* (2011) 17 (5):343–50. doi: 10.1097/PPO.0b013e318233e5b2
207. Chianese-Bullock KA, Lewis ST, Sherman NE, Shannon JD, Slingluff CL Jr. Multi-peptide vaccines vialed as peptide mixtures can be stable reagents for use in peptide-based immune therapies. *Vaccine* (2009) 27(11):1764–70. doi: 10.1016/j.vaccine.2009.01.018
208. Li AW, Sobral MC, Badrinath S, Choi Y, Graveline A, Stafford AG, et al. A facile approach to enhance antigen response for personalized cancer vaccination. *Nat Mater* (2018) 17(6):528–34. doi: 10.1038/s41563-018-0028-2
209. Kuai R, Ochyl LJ, Bahjat KS, Schwendeman A, Moon JJ. Designer vaccine nanodiscs for personalized cancer immunotherapy. *Nat Mater* (2017) 16 (4):489–96. doi: 10.1038/nmat4822
210. Tan ML, Choong PF, Dass CR. Recent developments in liposomes, microparticles and nanoparticles for protein and peptide drug delivery. *Peptides* (2010) 31(1):184–93. doi: 10.1016/j.peptides.2009.10.002
211. Zhai Y, Su J, Ran W, Zhang P, Yin Q, Zhang Z, et al. Preparation and Application of Cell Membrane-Camouflaged Nanoparticles for Cancer Therapy. *Theranostics* (2017) 7(10):2575–92. doi: 10.7150/thno.20118

212. Zhang R, Leeper CN, Wang X, White TA, Ulery BD. Immunomodulatory vasoactive intestinal peptide amphiphile micelles. *Biomater Sci* (2018) 6 (7):1717–22. doi: 10.1039/C8BM00466H
213. Hailemichael Y, Dai Z, Jaffarzad N, Ye Y, Medina MA, Huang XF, et al. Persistent antigen at vaccination sites induces tumor-specific CD8(+) T cell sequestration, dysfunction and deletion. *Nat Med* (2013) 19(4):465–72. doi: 10.1038/nm.3105
214. Wille-Reece U, Flynn BJ, Lore K, Koup RA, Kedl RM, Mattapallil JJ, et al. HIV Gag protein conjugated to a Toll-like receptor 7/8 agonist improves the magnitude and quality of Th1 and CD8+ T cell responses in nonhuman primates. *Proc Natl Acad Sci U S A* (2005) 102(42):15190–4. doi: 10.1073/pnas.0507484102
215. Jin K, Wang S, Zhang Y, Xia M, Mo Y, Li X, et al. Long non-coding RNA PVT1 interacts with MYC and its downstream molecules to synergistically promote tumorigenesis. *Cell Mol Life Sci* (2019) 76(21):4275–89. doi: 10.1007/s00018-019-03222-1
216. Tang Y, He Y, Zhang P, Wang J, Fan C, Yang L, et al. LncRNAs regulate the cytoskeleton and related Rho/ROCK signaling in cancer metastasis. *Mol Cancer* (2018) 17(1):77. doi: 10.1186/s12943-018-0825-x
217. Wang M, Zhao J, Zhang L, Wei F, Lian Y, Wu Y, et al. Role of tumor microenvironment in tumorigenesis. *J Cancer* (2017) 8(5):761–73. doi: 10.7150/jca.17648
218. Wei F, Wu Y, Tang L, He Y, Shi L, Xiong F, et al. BPIFB1 (LPLUNC1) inhibits migration and invasion of nasopharyngeal carcinoma by interacting with VTN and VIM. *Br J Cancer* (2018) 118(2):233–47. doi: 10.1038/bjc.2017.385
219. Wu Y, Wei F, Tang L, Liao Q, Wang H, Shi L, et al. Herpesvirus acts with the cytoskeleton and promotes cancer progression. *J Cancer* (2019) 10(10):2185–93. doi: 10.7150/jca.30222
220. Xia M, Zhang Y, Jin K, Lu Z, Zeng Z, Xiong W. Communication between mitochondria and other organelles: a brand-new perspective on mitochondria in cancer. *Cell Biosci* (2019) 9:27. doi: 10.1186/s13578-019-0289-8
221. Joyce JA, Fearon DT. T cell exclusion, immune privilege, and the tumor microenvironment. *Science* (2015) 348(6230):74–80. doi: 10.1126/science.aaa6204
222. Jung K, Choi I. Emerging Co-signaling Networks in T Cell Immune Regulation. *Immune Netw* (2013) 13(5):184–93. doi: 10.4110/in.2013.13.5.184
223. Pardoll DM. The blockade of immune checkpoints in cancer immunotherapy. *Nat Rev Cancer* (2012) 12(4):252–64. doi: 10.1038/nrc3239
224. Sharpe AH, Wherry EJ, Ahmed R, Freeman GJ. The function of programmed cell death 1 and its ligands in regulating autoimmunity and infection. *Nat Immunol* (2007) 8(3):239–45. doi: 10.1038/ni1443
225. Hodi FS, O'Day SJ, McDermott DF, Weber RW, Sosman JA, Haanen JB, et al. Improved survival with ipilimumab in patients with metastatic melanoma. *N Engl J Med* (2010) 363(8):711–23. doi: 10.1056/NEJMoa1003466
226. Topalian SL, Hodi FS, Brahmer JR, Gettinger SN, Smith DC, McDermott DF, et al. Safety, activity, and immune correlates of anti-PD-1 antibody in cancer. *N Engl J Med* (2012) 366(26):2443–54. doi: 10.1056/NEJMoa1200690
227. Brahmer JR, Tykodi SS, Chow LQ, Hwu WJ, Topalian SL, Hwu P, et al. Safety and activity of anti-PD-L1 antibody in patients with advanced cancer. *N Engl J Med* (2012) 366(26):2455–65. doi: 10.1056/NEJMoa1200694
228. Das R, Verma R, Sznol M, Boddupalli CS, Gettinger SN, Kluger H, et al. Combination therapy with anti-CTLA-4 and anti-PD-1 leads to distinct immunologic changes in vivo. *J Immunol* (2015) 194(3):950–9. doi: 10.4049/jimmunol.1401686
229. Gubin MM, Zhang X, Schuster H, Caron E, Ward JP, Noguchi T, et al. Checkpoint blockade cancer immunotherapy targets tumour-specific mutant antigens. *Nature* (2014) 515(7528):577–81. doi: 10.1038/nature13988
230. Rotte A. Combination of CTLA-4 and PD-1 blockers for treatment of cancer. *J Exp Clin Cancer Res* (2019) 38(1):255. doi: 10.1186/s13046-019-1259-z
231. Ali OA, Lewin SA, Dranoff G, Mooney DJ. Vaccines Combined with Immune Checkpoint Antibodies Promote Cytotoxic T-cell Activity and Tumor Eradication. *Cancer Immunol Res* (2016) 4(2):95–100. doi: 10.1158/2326-6066.CIR-14-0126
232. Karyampudi L, Lamichhane P, Scheid AD, Kalli KR, Shreeder B, Krempski JW, et al. Accumulation of memory precursor CD8 T cells in regressing tumors following combination therapy with vaccine and anti-PD-1 antibody. *Cancer Res* (2014) 74(11):2974–85. doi: 10.1158/0008-5472.CAN-13-2564
233. Rotte A, Jin JY, Lemaire V. Mechanistic overview of immune checkpoints to support the rational design of their combinations in cancer immunotherapy. *Ann Oncol* (2018) 29(1):71–83. doi: 10.1093/annonc/mdx686
234. Tarhini A. Immune-mediated adverse events associated with ipilimumab ctla-4 blockade therapy: the underlying mechanisms and clinical management. *Scientifica (Cairo)* (2013) 2013:857519. doi: 10.1155/2013/857519
235. Michot JM, Bigenwald C, Champiat S, Collins M, Carbonnel F, Postel-Vinay S, et al. Immune-related adverse events with immune checkpoint blockade: a comprehensive review. *Eur J Cancer* (2016) 54:139–48. doi: 10.1016/j.ejca.2015.11.016
236. Bakdash G, Buschow SI, Gorris MA, Halilovic A, Hato SV, Skold AE, et al. Expansion of a BDCA1+CD14+ Myeloid Cell Population in Melanoma Patients May Attenuate the Efficacy of Dendritic Cell Vaccines. *Cancer Res* (2016) 76(15):4332–46. doi: 10.1158/0008-5472.CAN-15-1695
237. Xue W, Metheringham RL, Brentville VA, Gunn B, Symonds P, Yagita H, et al. SCIB2, an antibody DNA vaccine encoding NY-ESO-1 epitopes, induces potent antitumor immunity which is further enhanced by checkpoint blockade. *Oncoimmunology* (2016) 5(6):e1169353. doi: 10.1080/2162402X.2016.1169353
238. Zhang B, Bowerman NA, Salama JK, Schmidt H, Spiotto MT, Schietinger A, et al. Induced sensitization of tumor stroma leads to eradication of established cancer by T cells. *J Exp Med* (2007) 204(1):49–55. doi: 10.1084/jem.20062056
239. Lugade AA, Moran JP, Gerber SA, Rose RC, Frelinger JG, Lord EM. Local radiation therapy of B16 melanoma tumors increases the generation of tumor antigen-specific effector cells that traffic to the tumor. *J Immunol* (2005) 174 (12):7516–23. doi: 10.4049/jimmunol.174.12.7516
240. de Bruin EC, McGranahan N, Mitter R, Salm M, Wedge DC, Yates L, et al. Spatial and temporal diversity in genomic instability processes defines lung cancer evolution. *Science* (2014) 346(6206):251–6. doi: 10.1126/science.1253462
241. Gerlinger M, Horswell S, Larkin J, Rowan AJ, Salm MP, Varela I, et al. Genomic architecture and evolution of clear cell renal cell carcinomas defined by multiregion sequencing. *Nat Genet* (2014) 46(3):225–33. doi: 10.1038/ng.2891
242. McGranahan N, Favero F, de Bruin EC, Birkbak NJ, Szallasi Z, Swanton C. Clonal status of actionable driver events and the timing of mutational processes in cancer evolution. *Sci Transl Med* (2015) 7(283):283ra54. doi: 10.1126/scitranslmed.aaa1408
243. Schumacher TN, Schreiber RD. Neoantigens in cancer immunotherapy. *Science* (2015) 348(6230):69–74. doi: 10.1126/science.aaa4971
244. Rooney MS, Shukla SA, Wu CJ, Getz G, Hacohen N. Molecular and genetic properties of tumors associated with local immune cytolytic activity. *Cell* (2015) 160(1-2):48–61. doi: 10.1016/j.cell.2014.12.033
245. Zamora AE, Crawford JC, Allen EK, Guo XJ, Bakke J, Carter RA, et al. Pediatric patients with acute lymphoblastic leukemia generate abundant and functional neoantigen-specific CD8(+) T cell responses. *Sci Transl Med* (2019) 11(498). doi: 10.1126/scitranslmed.aat8549
246. Khaled YS, Ammori BJ, Elkord E. Myeloid-derived suppressor cells in cancer: recent progress and prospects. *Immunol Cell Biol* (2013) 91 (8):493–502. doi: 10.1038/icb.2013.29
247. Gabrilovich DI, Nagaraj S. Myeloid-derived suppressor cells as regulators of the immune system. *Nat Rev Immunol* (2009) 9(3):162–74. doi: 10.1038/nri2506
248. Yang L, DeBusk LM, Fukuda K, Fingleton B, Green-Jarvis B, Shyr Y, et al. Expansion of myeloid immune suppressor Gr+CD11b+ cells in tumor-bearing host directly promotes tumor angiogenesis. *Cancer Cell* (2004) 6 (4):409–21. doi: 10.1016/j.ccr.2004.08.031
249. Yang L, Huang J, Ren X, Gorska AE, Chytil A, Aakre M, et al. Abrogation of TGF beta signaling in mammary carcinomas recruits Gr-1+CD11b+ myeloid cells that promote metastasis. *Cancer Cell* (2008) 13(1):23–35. doi: 10.1016/j.ccr.2007.12.004
250. Meyer C, Cagnon L, Costa-Nunes CM, Baumgaertner P, Montandon N, Leyvraz L, et al. Frequencies of circulating MDSC correlate with clinical outcome of melanoma patients treated with ipilimumab. *Cancer Immunol Immunother* (2014) 63(3):247–57. doi: 10.1007/s00262-013-1508-5

251. Highfill SL, Cui Y, Giles AJ, Smith JP, Zhang H, Morse E, et al. Disruption of CXCR2-mediated MDSC tumor trafficking enhances anti-PD1 efficacy. *Sci Transl Med* (2014) 6(237):237ra67. doi: 10.1126/scitranslmed.3007974
252. Shang B, Liu Y, Jiang SJ, Liu Y. Prognostic value of tumor-infiltrating FoxP3+ regulatory T cells in cancers: a systematic review and meta-analysis. *Sci Rep* (2015) 5:15179. doi: 10.1038/srep15179
253. Tanaka A, Sakaguchi S. Regulatory T cells in cancer immunotherapy. *Cell Res* (2017) 27(1):109–18. doi: 10.1038/cr.2016.151
254. Simpson TR, Li F, Montalvo-Ortiz W, Sepulveda MA, Bergerhoff K, Arce F, et al. Fc-dependent depletion of tumor-infiltrating regulatory T cells co-defines the efficacy of anti-CTLA-4 therapy against melanoma. *J Exp Med* (2013) 210(9):1695–710. doi: 10.1084/jem.20130579
255. Du X, Tang F, Liu M, Su J, Zhang Y, Wu W, et al. A reappraisal of CTLA-4 checkpoint blockade in cancer immunotherapy. *Cell Res* (2018) 28(4):416–32. doi: 10.1038/s41422-018-0011-0
256. Dominguez GA, Condamine T, Mony S, Hashimoto A, Wang F, Liu Q, et al. Selective Targeting of Myeloid-Derived Suppressor Cells in Cancer Patients Using DS-8273a, an Agonistic TRAIL-R2 Antibody. *Clin Cancer Res* (2017) 23(12):2942–50. doi: 10.1158/1078-0432.CCR-16-1784
257. Schmid MC, Avraamides CJ, Dippold HC, Franco I, Foubert P, Ellies LG, et al. Receptor tyrosine kinases and TLR/IL1Rs unexpectedly activate myeloid cell PI3kgamma, a single convergent point promoting tumor inflammation and progression. *Cancer Cell* (2011) 19(6):715–27. doi: 10.1016/j.ccr.2011.04.016
258. Kalluri R. The biology and function of fibroblasts in cancer. *Nat Rev Cancer* (2016) 16(9):582–98. doi: 10.1038/nrc.2016.73
259. Bartoschek M, Oskolkov N, Bocci M, Lovrot J, Larsson C, Sommarin M, et al. Spatially and functionally distinct subclasses of breast cancer-associated fibroblasts revealed by single cell RNA sequencing. *Nat Commun* (2018) 9 (1):5150. doi: 10.1038/s41467-018-07582-3
260. Cirri P, Chiarugi P. Cancer associated fibroblasts: the dark side of the coin. *Am J Cancer Res* (2011) 1(4):482–97.
261. Madar S, Goldstein I, Rotter V. 'Cancer associated fibroblasts'–more than meets the eye. *Trends Mol Med* (2013) 19(8):447–53. doi: 10.1016/j.molmed.2013.05.004
262. Valcz G, Sipos F, Tulassay Z, Molnar B, Yagi Y. Importance of carcinoma-associated fibroblast-derived proteins in clinical oncology. *J Clin Pathol* (2014) 67(12):1026–31. doi: 10.1136/jclinpath-2014-202561
263. Ohlund D, Elyada E, Tuveson D. Fibroblast heterogeneity in the cancer wound. *J Exp Med* (2014) 211(8):1503–23. doi: 10.1084/jem.20140692
264. Paraiso KH, Smalley KS. Fibroblast-mediated drug resistance in cancer. *Biochem Pharmacol* (2013) 85(8):1033–41. doi: 10.1016/j.bcp.2013.01.018
265. Tran E, Chinnasamy D, Yu Z, Morgan RA, Lee CC, Restifo NP, et al. Immune targeting of fibroblast activation protein triggers recognition of multipotent bone marrow stromal cells and cachexia. *J Exp Med* (2013) 210 (6):1125–35. doi: 10.1084/jem.20130110
266. Najafi M, Farhood B, Mortezaee K. Contribution of regulatory T cells to cancer: A review. *J Cell Physiol* (2019) 234(6):7983–93. doi: 10.1002/jcp.27553
267. Tauriello DVF, Palomo-Ponce S, Stork D, Berenguer-Llergo A, Badia-Ramentol J, Iglesias M, et al. TGFbeta drives immune evasion in genetically reconstituted colon cancer metastasis. *Nature* (2018) 554 (7693):538–43. doi: 10.1038/nature25492
268. Mariathasan S, Turley SJ, Nickles D, Castiglioni A, Yuen K, Wang Y, et al. TGFbeta attenuates tumour response to PD-L1 blockade by contributing to exclusion of T cells. *Nature* (2018) 554(7693):544–8. doi: 10.1038/nature25501
269. Chen Y, Ramjiawan RR, Reiberger T, Ng MR, Hato T, Huang Y, et al. CXCR4 inhibition in tumor microenvironment facilitates anti-programmed death receptor-1 immunotherapy in sorafenib-treated hepatocellular carcinoma in mice. *Hepatology* (2015) 61(5):1591–602. doi: 10.1002/hep.27665
270. Garrido F, Cabrera T, Concha A, Glew S, Ruiz-Cabello F, Stern PL. Natural history of HLA expression during tumour development. *Immunol Today* (1993) 14(10):491–9. doi: 10.1016/0167-5699(93)90264-L
271. Marincola FM, Jaffee EM, Hicklin DJ, Ferrone S. Escape of human solid tumors from T-cell recognition: molecular mechanisms and functional significance. *Adv Immunol* (2000) 74:181–273. doi: 10.1016/S0065-2776(08)60911-6
272. Seliger B, Cabrera T, Garrido F, Ferrone S. HLA class I antigen abnormalities and immune escape by malignant cells. *Semin Cancer Biol* (2002) 12(1):3–13. doi: 10.1006/scbi.2001.0404
273. Garrido F, Algarra I. MHC antigens and tumor escape from immune surveillance. *Adv Cancer Res* (2001) 83:117–58. doi: 10.1016/S0065-230X(01)83005-0
274. Garrido F, Ruiz-Cabello F, Cabrera T, Perez-Villar JJ, Lopez-Botet M, Duggan-Keen M, et al. Implications for immunosurveillance of altered HLA class I phenotypes in human tumours. *Immunol Today* (1997) 18 (2):89–95. doi: 10.1016/S0167-5699(96)10075-X
275. Koopman LA, Corver WE, van der Slik AR, Giphart MJ, Fleuren GJ. Multiple genetic alterations cause frequent and heterogeneous human histocompatibility leukocyte antigen class I loss in cervical cancer. *J Exp Med* (2000) 191(6):961–76. doi: 10.1084/jem.191.6.961
276. Garrido F. MHC/HLA Class I Loss in Cancer Cells. *Adv Exp Med Biol* (2019) 1151:15–78. doi: 10.1007/978-3-030-17864-2_2
277. Ignatov T, Gorbunow F, Eggemann H, Ortmann O, Ignatov A. Loss of HER2 after HER2-targeted treatment. *Breast Cancer Res Treat* (2019) 175(2):401–8. doi: 10.1007/s10549-019-05173-4
278. Sampson JH, Heimberger AB, Archer GE, Aldape KD, Friedman AH, Friedman HS, et al. Immunologic escape after prolonged progression-free survival with epidermal growth factor receptor variant III peptide vaccination in patients with newly diagnosed glioblastoma. *J Clin Oncol* (2010) 28(31):4722–9. doi: 10.1200/JCO.2010.28.6963
279. Khong HT, Wang QJ, Rosenberg SA. Identification of multiple antigens recognized by tumor-infiltrating lymphocytes from a single patient: tumor escape by antigen loss and loss of MHC expression. *J Immunother* (2004) 27 (3):184–90. doi: 10.1097/00002371-200405000-00002

Conflict of Interest: LD is CSO and shareholder in Scancell Ltd. SP, VB, and PS are employees of Scancell Ltd.

The authors declare that this study was funded by Scancell Ltd. The funder was involved in the study design, collection, analysis, interpretation of data, the writing of this article and the decision to submit it for publication.

Copyright © 2021 Paston, Brentville, Symonds and Durrant. This is an open-access article distributed under the terms of the Creative Commons Attribution License (CC BY). The use, distribution or reproduction in other forums is permitted, provided the original author(s) and the copyright owner(s) are credited and that the original publication in this journal is cited, in accordance with accepted academic practice. No use, distribution or reproduction is permitted which does not comply with these terms.

frontiers in Immunology

REVIEW
published: 14 April 2021
doi: 10.3389/fimmu.2021.617365

Immune Modulation Plus Tumor Ablation: Adjuvants and Antibodies to Prime and Boost Anti-Tumor Immunity *In Situ*

Renske J. E. van den Bijgaart[1†], *Fabian Schuurmans*[1†], *Jurgen J. Fütterer*[2,3], *Marcel Verheij*[1], *Lenneke A. M. Cornelissen*[1] *and Gosse J. Adema*[1*]

[1] Radiotherapy & OncoImmunology Laboratory, Department of Radiation Oncology, Radboud University Medical Center, Nijmegen, Netherlands, [2] Department of Medical Imaging, Radboud University Medical Center, Nijmegen, Netherlands, [3] Department of Robotics and Mechatronics, University of Twente, Enschede, Netherlands

OPEN ACCESS

Edited by:
Alan Graham Pockley, Nottingham Trent University, United Kingdom

Reviewed by:
Graham Robert Leggatt, The University of Queensland, Australia
Yona Keisari, Tel Aviv University, Israel

***Correspondence:**
Gosse J. Adema
gosse.adema@radboudumc.nl

[†]These authors have equally contributed to this work

Specialty section:
This article was submitted to Cancer Immunity and Immunotherapy, a section of the journal Frontiers in Immunology

Received: 14 October 2020
Accepted: 22 March 2021
Published: 14 April 2021

Citation:
van den Bijgaart RJE, Schuurmans F, Fütterer JJ, Verheij M, Cornelissen LAM and Adema GJ (2021) Immune Modulation Plus Tumor Ablation: Adjuvants and Antibodies to Prime and Boost Anti-Tumor Immunity In Situ. Front. Immunol. 12:617365. doi: 10.3389/fimmu.2021.617365

In situ tumor ablation techniques, like radiotherapy, cryo- and heat-based thermal ablation are successfully applied in oncology for local destruction of tumor masses. Although diverse in technology and mechanism of inducing cell death, ablative techniques share one key feature: they generate tumor debris which remains *in situ*. This tumor debris functions as an unbiased source of tumor antigens available to the immune system and has led to the concept of *in situ* cancer vaccination. Most studies, however, report generally modest tumor-directed immune responses following local tumor ablation as stand-alone treatment. Tumors have evolved mechanisms to create an immunosuppressive tumor microenvironment (TME), parts of which may admix with the antigen depot. Provision of immune stimuli, as well as approaches that counteract the immunosuppressive TME, have shown to be key to boost ablation-induced anti-tumor immunity. Recent advances in protein engineering have yielded novel multifunctional antibody formats. These multifunctional antibodies can provide a combination of distinct effector functions or allow for delivery of immunomodulators specifically to the relevant locations, thereby mitigating potential toxic side effects. This review provides an update on immune activation strategies that have been tested to act in concert with tumor debris to achieve *in situ* cancer vaccination. We further provide a rationale for multifunctional antibody formats to be applied together with *in situ* ablation to boost anti-tumor immunity for local and systemic tumor control.

Keywords: tumor ablation, immune activation, *in situ* cancer vaccination, multifunctional antibodies, combination therapy

INTRODUCTION

Vaccines have been extremely successful in preventing infectious diseases by training the immune system to recognize and destroy pathogens. Conventional vaccines comprise of antigen(s) often supplemented with immune adjuvants to support the induction of an effective immune response. Besides, adjuvants can function as a slow release system, ensuring prolonged and continuous

presentation and stimulation of the immune system (1). The application of vaccines to cancer is an obvious extension of their utility, and many diverse vaccination strategies are under development. An interesting novel approach is the *in vivo* loading and activation of dendritic cells (DCs) with tumor antigens released following *in situ* tumor ablation.

Tumor ablation techniques are successfully applied for the treatment of different malignancies. Although diverse in technology and mechanism of action, all ablative techniques lead to *in situ* availability of ablated tumor material (**Figure 1A**). The tumor debris released upon ablation functions as an antigen depot representing the tumors' antigenic repertoire. Together with the simultaneous release of bioactive molecules, such as damage-associated molecular patterns (DAMPs), this has led to the concept of *in situ* cancer vaccination. Indeed, tumor antigens were observed in DCs residing in draining lymph nodes (dLNs) following ablation (2). Immune responses induced by ablation as stand-alone treatment are documented, however, tend to be incapable of evoking robust sustainable anti-tumor immunity. This is further evidenced by the scarce reports of spontaneous regression of untreated distant metastatic sites following ablation, the so-called 'abscopal effect' (3, 4). Therefore, it has been proposed by us and others to initiate and boost ablation-induced anti-tumor immunity by combining ablation with immune activation strategies (5–7). An outstanding question in the field remains which immune activation strategies effectively combine with *in situ* tumor ablation.

Examples of immune activation strategies that are mostly applied together with tumor ablation include stimulation with pattern recognition receptor (PRR) agonists, adjuvants and agonistic antibodies. However, tumors have evolved mechanisms to create an immunosuppressive tumor microenvironment (TME), parts of which may admix with the antigen depot upon ablation. Development of a successful *in situ* cancer vaccine thus requires immune activation strategies to boost immunity and approaches that counteract the

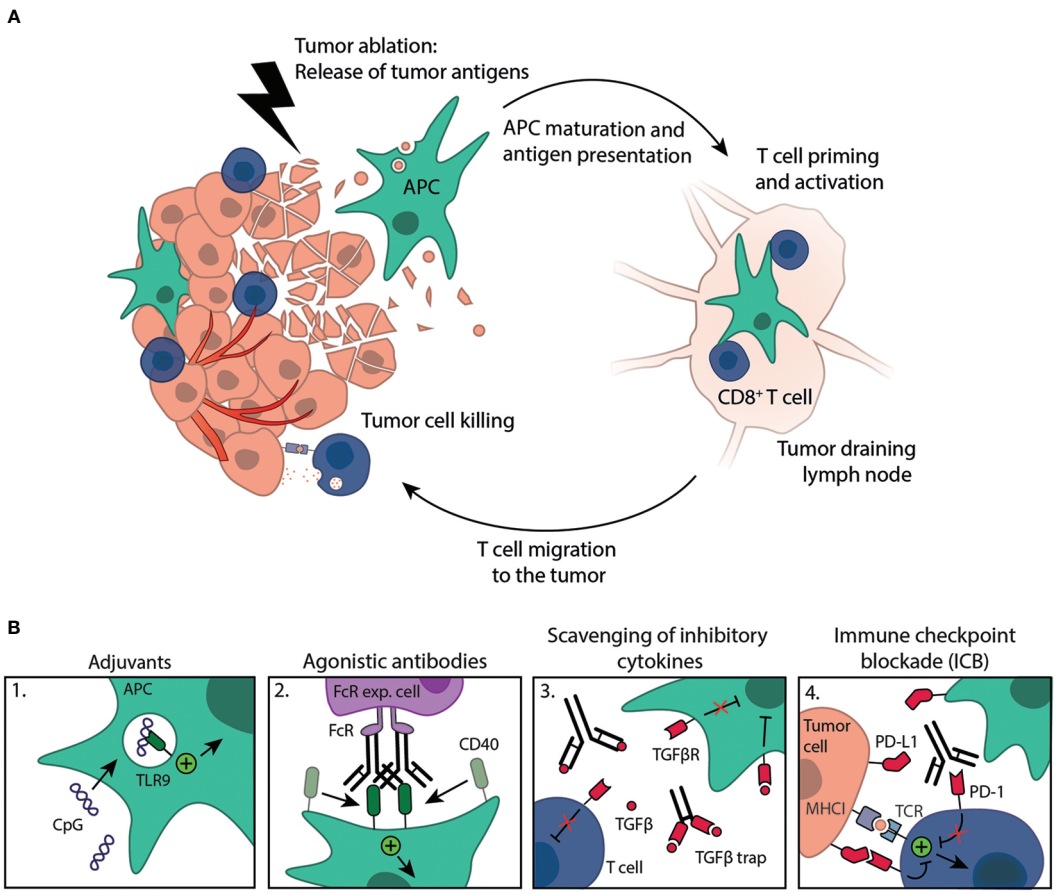


FIGURE 1 | Immune activation strategies plus tumor ablation to create *in situ* cancer vaccines. **(A)** Tumor ablation results in the release of tumor antigens available for uptake by antigen-presenting cells (APC), such as DCs. These antigens are (cross-)presented on MHC molecules to T cells in the dLN, resulting in T cell priming and activation. Activated T cells subsequently migrate to the destructed tumor, as well as distant metastases, where they kill remaining tumor cells. **(B)** Immune response induction is boosted by exogenous administration of immune stimulating compounds like 1. adjuvants (e.g. CpG) or 2. agonistic antibodies (e.g. anti-CD40 mAb, crosslinking by Fc-receptor expressing cells) that can work synergistically with tumor ablation in creating effective, mature DCs. Furthermore, several approaches can be exploited to counteract the immunosuppressive TME, such as 3. scavenging of inhibitory cytokines (e.g. anti-TGFβ mAb or TGFβ trap) or 4. immune checkpoint blockade (ICB, e.g. anti-PD-1 mAb), both to enhance the anti-tumor immune response.

immunosuppressive TME like monoclonal antibodies (mAbs) against inhibitory immune checkpoints, inhibition of immunosuppressive cells like regulatory T cells (Treg) or myeloid derived suppressor cells (MDSC) or by scavenging anti-inflammatory cytokines, such as transforming growth factor beta (TGFβ).

Delivery of these immunomodulators to the relevant locations, i.e. the tumor and tumor dLNs, is often essential for enhancing anti-tumor specific immune responses following ablation. Targeting also mitigates potential toxic side-effects. Antibodies can exhibit tumor targeting abilities, either through their specificity for tumor antigens or ablation-associated factors, such as extracellular DNA and histones. Recent advances in antibody engineering enabled the creation of novel antibody formats with multiple functions, such as bispecific antibodies and protein-linked antibodies (8). Multifunctional antibodies create new opportunities to enhance anti-tumor immunity following *in situ* tumor ablation techniques.

Here, we review immune activation strategies and approaches that counteract the immunosuppressive TME that have been combined with *in situ* tumor ablation. Furthermore, we postulate new combination strategies involving multifunctional antibody formats to be applied together with *in situ* ablation to boost the anti-tumor immunity for local and systemic tumor control.

IN SITU TUMOR ABLATION

During the last decades, there has been widespread interest in the development and refinement of ablation techniques for local treatment of cancers. The primary goal of tumor ablation is to destroy malignant cells within a designated volume through the local deposition of energy *via* different approaches, e.g. ionizing radiation or extreme temperatures. Radiotherapy (RT) has been a strong pillar in cancer therapy and the majority of cancer patients undergo RT at one point during treatment (9). The anti-tumor efficacy of RT has been attributed to its capacity to induce DNA damage, as well as through increased recognition of tumor cells by the immune system. Stereotactic ablative body radiotherapy (SABRT) allows for the delivery of ablative radiation doses. An exciting development in radiation oncology is the magnetic resonance linear accelerator (MR-Linac) which enables high precision ablative RT under real-time MR-guidance, providing better target control while sparing the surrounding healthy tissues including LNs (10). MR-guided RT is a promising tool to answer key questions in the field of immuno-radiobiology, and will help to understand how to bring dose and fractionation schedules into an immunologically active range.

Different from RT, most other tumor ablation techniques rely on extreme temperatures for cellular destruction. Cryoablation applies extremely cold temperatures, whereas heat-based thermal ablation modalities, including radiofrequency ablation (RFA), microwave ablation (MWA), laser ablation and thermal high-intensity focused ultrasound (HIFU) employ different sources of energy to heat the target region (7, 11). Cells in the core of the ablation zone are subjected to lethal temperatures; up to -180°C for cryoablation inducing hypothermic necrosis and >60°C for thermal ablation resulting in protein denaturation and coagulative necrosis. Cells in the periphery of the ablation zones are exposed to sublethal temperatures and either undergo apoptotic cell death or are able to recover from reversible injury (12). In contrast to thermal HIFU ablation, HIFU can be used to generate mechanical damage as a result of acoustic cavitation, with minimal thermal damage, also known as (boiling) histotripsy or mechanical HIFU (12–14).

Besides their ability to kill tumor cells, ablation modalities unveil an array of tumor antigens. Several studies have emphasized the importance of neoantigens arising due to tumor-specific DNA mutations in the recognition of tumor cells by the immune system (15, 16). Each ablation technique results in a unique tumor antigenic fingerprint. Heat-based thermal ablation results in protein denaturation and coagulative necrosis, possibly reducing the availability of intact tumor antigens for the immune system. Furthermore, the coagulative necrosis destroys the structure and vasculature of tumors, thereby affecting the ability of immune cells to reach and interact with the antigen depot (17). Mechanical HIFU, on the other hand, will result in complete liquification of the tissue, which is effectively removed *via* drainage or absorbed as part of the physiologic healing response (18, 19). For cryoablation it has been reported that many native antigen structures are preserved (20). Furthermore, cryoablation has shown to induce polyclonality and intra-tumoral T cell repertoire remodeling (21). How each ablation technique affects handling and processing of antigenic materials by antigen-presenting cells (APCs) and which ablation technique results in the most effective release of immunogenic (neo)antigens remains to be investigated.

During efforts of the body to clear this tumor debris, there is a time frame in which the immune system can be triggered towards antigens from the antigen depot (**Figure 1A**). In fact, the presence of the antigen depot is a prerequisite for the development of an anti-tumor immune response, as protective immunity failed to develop upon surgical removal of cryoablated tumors (2). Cytokines and endogenous danger signals, such as DAMPs, are readily released from the ablated tumor, which may contribute to immune activation. On the other hand, ablation will also lead to a physiological wound healing response that regulates and maintains immunological tolerance toward the damaged tissue. In practice, ablation induced immunomodulation alone appears (often) insufficient to generate consistent protective anti-tumor immunity. Therefore, interest has shifted towards exploring the potential synergy between ablative techniques and immune activation strategies. Strong systemic immunity will be critical for controlling residual disease at the site of ablation and for eradicating distant metastases.

ANTIGEN PRESENTING CELLS AND IMMUNE ACTIVATING STRATEGIES

DCs, the most potent APCs of the immune system, have the unique ability to initiate and direct immune responses. DCs in the vicinity of or recruited to the local ablation site acquire and

process tumor antigens, and subsequently present them to naïve T cells (22). Alternatively, tumor antigens may passively enter the circulation or lymphatics and can be transported to LNs where they can be taken up by LN-resident DCs. DCs can cross-present peptides derived from such extracellular antigens to MHC I restricted $CD8^+$ T cells. In addition to the initial interaction between the TCR and MHC-molecules on DCs, co-stimulation (signal 2) and cytokines (signal 3) are important for initiation of antigen-specific T cells. Thus, proper DC maturation is essential for efficient immune response induction. The ability to load and mature DCs directly *in situ* by tumor ablation plus immune activation is thus an appealing strategy to develop a cancer vaccine.

Adjuvants

Adjuvants can boost the magnitude and duration of the adaptive immune response. One of the ways through which adjuvants act is by serving as, or inducing, DAMPs and/or pathogen-associated molecular patterns (PAMPs) that trigger PRRs on immune cells resulting in their activation. Alternatively, adjuvants can function as slow release system. Although numerous different adjuvants exist, we will focus on nucleic acid-sensing PRR agonists, as well as the potential of saponin-based adjuvants (SBAs) applied in combination with *in situ* tumor ablation.

Toll-Like Receptor (TLR) Agonists

TLR triggering is one of the most potent inducers of DC maturation *in vivo* as evidenced by their capacity to upregulate co-stimulatory molecules and enhanced production of pro-inflammatory cytokines needed for DC-mediated T cell priming. The nucleic acid-sensing TLRs include TLR9, TLR3 and TLR7/8. CpG oligodeoxynucleotides (CpG) are short unmethylated single stranded-synthetic DNA molecules, which were one of the first adjuvants to be combined with *in situ* tumor ablation (2). Pioneering work combining CpG with cryoablation in a B16OVA melanoma model showed the induction of long-term immune memory, evidenced by a 50% survival of mice subjected to a re-challenge. The survival benefit was absent in the single treatment groups. Additional studies showed the anti-tumor effect is dependent on plasmacytoid DCs (pDCs), which stimulate the ability of conventional type 1 DCs (cDC1s) to prime naïve $CD8^+$ T cells (23, 24). A prerequisite for the synergy between cryoablation and CpG is the co-localization of the antigen and CpG within a DC. Therefore, the timing and location of CpG administration relative to the release of tumor antigens by tumor ablation is of importance for protective anti-tumor immunity (25, 26). The beneficial effects of CpG with cryoablation have also been observed in a mammary adenocarcinoma model (27). CpG combinations with other ablative therapies, such as RT and HIFU, have also proven successful (28–30). Interestingly, the combination of thermal HIFU ablation of mammary adenocarcinoma tumors with CpG plus anti-PD-1 increased the number of unique CDR3 rearrangements in the T cell repertoire at distal tumors, indicating the generation of T cells specific for a broad range of different tumor antigens (30).

The synthetic dsRNA analog polyinosinic-polycytidylic acid (Poly-IC) is a ligand for TLR3 and has shown promising preclinical results in combination with a minimal 9 Gy single dose RT. The combination treatment greatly reduced tumor growth at primary and abscopal sites and enhanced survival in different mouse models (31–33). The Poly-IC plus RT combination treatment of A20 lymphoma tumors plus intra-tumoral (i.t.) FLT3L injections further increased DC recruitment and synergistically induced adaptive anti-tumor immunity (33). Mechanistic studies revealed that RT increased serum levels of high mobility group box 1 (HMGB1), a known DAMP *in vivo*. HMGB1 potentiated the Poly-IC induced DC maturation, demonstrating the potential of DAMP plus TLR adjuvant combination strategies (33).

TLR7/8 agonists gained fame through Imiquimod, an adjuvant formulation topically applied in the treatment of skin cancers (34). Topical Imiquimod application, as well as systemic administration (encapsulated in nanoparticles (NP)), in combination with cryoablation or RT, resulted in improved tumor control at primary and distant sites in numerous murine cancer models (35–38). As with CpG, TLR7 agonists are believed to act primarily through activation of pDCs (39). The results of a phase I/II clinical trial investigating the efficacy of topical imiquimod application to breast cancers skin metastases in conjunction with RT are currently on their way (NCT01421017). Altogether, TLR agonists can be employed as powerful adjuvants along with ablation to generate effective anti-tumor immunity.

STING Agonists

DNA normally resides in the nucleus and mitochondria; hence, its presence in the cytoplasm serves as a danger signal. This aberrant localization of DNA is sensed by the DNA binding enzyme cyclic GMP-AMP synthase (cGAS). Upon recognition, cGAS dimerizes and stimulates the production of cyclic-GMP-AMP (cGAMP) which can directly bind stimulator of interferon genes (STING) resulting in type I interferon (IFN) production (40). Cytoplasmic DNA sensing through the cGAS-STING pathway plays a pivotal role in APC activation following phagocytosis (41).

Synthetic analogues of 2'3'-cGAMP, a stable variant of the second messenger produced by cGAS are used as STING-activating agents. Combinations of such analogues with ablative therapy are scarce and limited to one study by Deng et al. which showed i.t. injection of 2'3'-cGAMP in combination with a single 20 Gy RT dose greatly reduced tumor growth compared to either treatment alone and resulted in complete tumor rejection in 70% of the mice (42). Besides cGAMP analogues, an interesting discovery are the STING activating properties of PC7A nanovaccine, which consist of E7 peptide or OVA peptide-loaded micelle NPs binding to STING (43). Half of the mice treated with the combination of PC7A and 20 Gy RT were tumor free 60 days after tumor inoculation, compared to none of the mice from the single treatment groups. Treatment efficacy showed to be depended on STING signaling and increased tumor reactive $CD8^+$ T cells were observed (43). RT induces cytoplasmic DNA and micronuclei formation which can

activate the cGAS/STING pathway. It has been shown that cGAS/STING dependent DNA sensing in DCs is essential in triggering adaptive immunity following RT (42). Other studies, however, report that also cancer cell intrinsic cGAS activation can be important in the induction of an adaptive immune response following RT. cGAMP produced by cancer cells was shown to be transported to DCs *via* gap junctions, resulting in STING activation in these DCs and subsequent type I IFN production (44). One explanation for the beneficial effect of exogenous STING ligand administration on top of RT induced activation could be the numerous regulatory mechanisms that control cGAS-STING pathway activation. TREX1 is a RT inducible dsDNA exonuclease that attenuates the STING signaling cascade (45). More recently, BAF and C9orf72 have been implicated in the regulation of myeloid STING activation (46, 47). It would therefore be interesting to determine if these regulatory mechanisms are upregulated following tumor ablation and whether stimulation of the cGAS/STING pathway upon ablation would be beneficial to achieve an *in situ* cancer vaccine.

However, some degree of caution should be taken as tumor cell intrinsic cGAS/STING activation has been linked to metastases formation (48). This highlights that an appropriate balance and possibly myeloid cell specific STING pathway activation may be required for optimal anti-tumor immunity.

Saponin-Based Adjuvants

Antigen cross-presentation by DCs is crucial for $CD8^+$ T cell mediated anti-tumor immunity. Although most conventional adjuvants are unable to boost $CD8^+$ T cell responses, SBAs are known to be superior in inducing antigen cross-presentation by DCs (1). Cryoablation with co-injection of SBAs, leads to an extremely potent systemic anti-tumor response. These effects are dependent on the ability of SBAs to induce cross-presentation, specifically in $CD11b^+$ DCs (49). Additional administration of CpG with SBAs following cryoablation created a highly effective *in situ* cancer vaccine and resulted in the generation of multifunctional T cells able to produce high amounts of pro-inflammatory cytokines (50). The exact mechanism through which SBAs induce cross-presentation remains elusive, although lipid bodies are found to play a crucial role (49). Interestingly, monocyte-derived $CD11b^+$ DCs have been implicated to be better in the activation and induction of memory $CD8^+$ T cells as compared to cDC1 (51, 52). Therefore, SBAs might be specifically potent in inducing long term immune memory. Besides cryoablation also other ablation therapies, such as RT and HIFU, are of interest for their potential synergy with SBAs.

Altogether, adjuvants are suitable candidates to be applied with tumor ablation to generate an *in situ* cancer vaccine (**Figure 1B1**). More detailed knowledge about effective adjuvant-ablation strategies, such as correct timing and the involved immune subsets, is required to efficiently prime and boost anti-tumor immunity.

Agonistic Antibodies

DCs can further be activated by cell-cell contact and subsequent signaling *via* members of the immunoglobulin domain-containing receptor family, especially the tumor necrosis factor (TNF) receptor family, such as CD40/CD40 ligand (CD40L) and CD27/CD70. CD40 engagement on DCs by CD40L expressed by $CD4^+$ T helper cells or agonistic CD40 mAbs trigger DC activation to provide signals for the licensing and expansion of $CD8^+$ cytotoxic T cells (53, 54). CD40 agonistic mAbs have shown synergistic effects in combination with RT. Addition of agonistic anti-CD40 mAb to 10 Gy RT increased survival of mice inoculated with EG7 tumors to 80% as compared to 40% (anti-CD40) and 20% (RT) for the monotherapy regimens (55). All surviving mice treated with the combination therapy were resistant to a subsequent re-challenge, indicative for immune memory. Similar results have been achieved using a Panc02 tumor model where combination therapy not only limited primary tumor growth, but also growth of an untreated contralateral tumor (56). In the latter model, agonistic CD40 therapy worked best when combined with a hypo-fractionated RT regimen (5 Gy single dose). Moreover, timing of anti-CD40 mAb administration relative to RT treatment was crucial for its efficacy as administration prior to RT did not show beneficial effects (57). TLR agonists, such as CpG and Poly-IC, are known to upregulate the expression of CD40 on human pDCs as well as myeloid DCs (58, 59). Poly-IC is especially interesting as in combination with anti-CD40 mAb it induced the highest percentage of OVA-specific T cells relative to other TLR agonists (60). This can possibly be explained by the upregulation of CD70, the ligand for the T cell co-stimulatory receptor CD27, following stimulation with Poly-IC and anti-CD40 mAb (61). It would therefore be interesting to investigate the efficacy of the triple combination of agonistic mAbs plus adjuvants and ablative therapies.

Besides DCs, also T cells express multiple co-stimulatory receptors, including CD27, OX40 and CD137 (4-1BB). Ligation of these receptors delivers co-stimulatory signals necessary for full T cell activation (62–65). RT induces upregulation of OX40 expression on $CD4^+$ and $CD8^+$ T cells as well as CD137 on $CD8^+$ tumor infiltrating T cells and thus works in concert with agonistic OX40 or CD137 therapy (66–68). CD137 expressing $CD8^+$ T cells are also highly positive for PD-1, and RT plus agonistic CD137 therapy benefits from additional anti-PD-1 mAbs to block negative feedback by PD-L1 (69). Combining multiple different immune activation strategies which complement each other is an appealing approach to further stimulate the immune response. Noteworthy, combinations of CpG plus RT, agonistic OX40 mAbs plus RT as well as CpG plus agonistic OX40 mAbs have shown synergistic effects in their ability to limit tumor growth, making the combination of CpG, agonistic OX40 with RT or other ablative therapies an interesting approach to explore (29, 70, 71).

To date, all agonistic antibodies investigated have shown promising results in combination with RT and the addition of adjuvants might further improve their function (**Figure 1B2**). Whether these agonistic antibodies also synergize with other ablative modalities remains to be determined.

COUNTERACTING THE IMMUNOSUPPRESSIVE TME

Tumors have evolved several mechanisms to instigate an immunosuppressive TME, parts of which may admix with the antigen depot upon ablation. Successful *in situ* cancer vaccines may, in addition to immune activation strategies, also require approaches that counteract the immunosuppressive microenvironment. Immune suppression networks consist of immune suppressive cells including Tregs and MDSCs, immunosuppressive cytokines like TGFβ and IL-10, as well as enhancement of co-inhibitory molecules such as CTLA-4 or PD-1 on T cells. Targeting immunosuppressive cells has emerged as important approach to counteract the immunosuppressive TME, which is discussed in detail elsewhere (72–74). In the next sections, we will discuss strategies to counteract the immunosuppressive molecules, with a focus on cytokine and immune checkpoint blockade, applied together with *in situ* tumor ablation.

Immunosuppressive Cytokines

Immune suppressive cytokines, such as TGFβ and IL-10, are a major obstacle in generating effective anti-tumor immunity. They are often produced by tumor cells and immune suppressive cell subsets, such as Tregs and MDSC (75). RT is known to increase the amount of active TGFβ. TGFβ is initially produced in its latent form containing a pro-domain, dissociation of this domain makes the protein become active. Oxygen radicals produced following RT promote this dissociation resulting in more active TGFβ (76, 77). Thermal ablation at temperatures above 65 °C can lead to denaturation of proteins, potentially including part of immune suppressive cytokines, such as TGFβ or IL-10. Strategies that block inhibitory signaling through antagonistic antibodies, as well as scavenging of inhibitory cytokines themselves are ways to alleviate their inhibitory function (**Figure 1B3**).

Scavenging of TGFβ using antibodies limits growth of treated and untreated tumors following 5 x 6 Gy RT (78). This combination therapy increased DC maturation evidenced by an increase in $CD40^+CD70^+$ DCs. Furthermore, the combination increased the production of IFNγ by dLN-derived $CD8^+$ T cells following *ex vivo* tumor antigen stimulation. Lastly, the percentage of PD-1^+ and PD-L1/2^+ cells in the tumor increased upon combination therapy, highlighting the induction of additional immune escape mechanisms. Inclusion of anti-PD-1 mAbs indeed further improved tumor control. Other successful TGFβ neutralizing approaches include recombinant TGFβ receptor (TGFβR) fused to an Fc-tail (79). The mechanism behind the anti-tumor effect of TGFβ scavenging is not solely immune mediated as TGFβ has pleiotropic functions, such as in wound healing and DNA repair, which could play a role with the anti-tumor effect (80, 81).

The cytokine IL-10 inhibits macrophage pro-inflammatory cytokine production, limits DC antigen presentation, and dampens T and NK cells effector function (82). Interestingly, some studies, however, report an increase in intra-tumoral cytotoxic $CD8^+$ T cells upon IL-10 delivery to the tumor (83). This can be explained by the ability of IL-10 to limit IFN-γ production by DCs, which is crucial for activation induced T cell apoptosis (84). All in all, efficacy of scavenging or blockade of anti-inflammatory factors will probably dependent on the choice of ablative therapy and state of the immune response when applied.

Immune Checkpoints

To shift the balance of the TME away from immunosuppression, mAbs can be applied to block inhibitory immune checkpoint receptors or their ligands (85). Relieving immunosuppression of adaptive immune cells has been extensively studied, and mAbs targeting CTLA-4 or PD-1/PD-L1 can enhance T cell immunity generated by ablation (**Figure 1B4**). CTLA-4 blockade allows CD80 and CD86 co-stimulatory molecules to be available for CD28, lowering the threshold for T cell activation (86). Anti-CTLA-4 mAbs also cause intra-tumoral Treg depletion or modulation of their suppressive functions (87, 88). CTLA-4 blockade synergized with different forms of thermal tumor ablation, resulting in significant amounts of active tumor-specific T cells and the ability to reject secondary or re-challenged tumors (89–91). Data from a pilot study conducted in breast cancer patients that received cryoablation and anti-CTLA-4 mAb showed good tolerability and promising efficacy (92). In the line of relieving immunosuppression, Treg depletion using anti-CD25 mAb enhances the anti-tumor response after RT, RFA and cryoablation, indicated by the increased presence of IFNy producing T cells after combination therapy in case of the latter two (89, 93, 94). Currently various clinical trials are ongoing testing the potential of *in situ* ablation and checkpoint blockade in different solid malignancies.

PD-L1 is often highly expressed on tumor cells and tumor associated myeloid cells. PD-L1 can be induced by pro-inflammatory cytokines and is frequently upregulated in response to *in situ* tumor ablation (95, 96). Engagement of PD-1^+ T cells with its ligands leads to suppression of T cell effector mechanisms and mAbs that block the PD-1/PD-L1 axis are aimed at reinvigorating these exhausted T cells. RFA treatment of a localized tumor increased T cell infiltration in a distant tumor in both tumor-bearing mice as well as human patients (97). However, these tumors quickly overcame T cell cytotoxicity by inhibiting infiltrating T cells *via* upregulation of PD-L1 expression. In the murine setting, combining RFA with anti-PD-1 mAbs increased the tumor antigen-specific T cell response, and synergistically inhibited growth of distant tumors (97). Strikingly, incomplete RFA tumor ablation limited the efficacy of anti-PD-1 immunotherapy (98). The authors demonstrated that incomplete ablation induced local inflammation and resulted in accumulation of immunosuppressive myeloid cells in the residual tumor, which inhibited T cell functionality. Targeting the CCL2/CCR2 pathway, responsible for the recruitment of these immunosuppressive myeloid cells, enhanced anti-tumor immunity in the residual tumor, and thereby overcame the resistance to anti-PD-1 therapy.

Synergy between adaptive immune checkpoint blockade and RT has been demonstrated in multiple different preclinical tumor models (95, 99–102). However, RT dose and fractionation regimens as well as the timing of checkpoint blockade administration in conjunction with RT that would result in the most optimal anti-tumor immune response differ and warrant further study (103). Several other promising novel adaptive immune checkpoint molecules are actively being investigated, including TIM-3, LAG-3, TIGIT and VISTA (104), which could also be potential targets.

Recent studies have indicated that tumor cells exploit sialoglycan–Siglec interactions to modulate cytotoxic T cell as well as myeloid cell function, contributing to an immunosuppressive TME (105). Interference with the sialoglycan-Siglec axis by inhibiting the sialic acid synthesis pathway resulted in enhanced anti-tumor immunity and limited tumor outgrowth (106). Next to Siglec receptors, studies have highlighted innate immune checkpoints as interesting therapeutic targets. One of these checkpoints is the signal-regulatory protein α (SIRPα)-CD47 axis. CD47 is often overexpressed on tumor cells and interacts with SIRPα on myeloid cells to trigger a 'don't eat me' signal (107). Blocking SIRPα-CD47 interactions alleviates inhibitory signaling resulting in improved tumor cell clearance. Besides, murine models suggest that adaptive immunity contributes to tumor control upon targeting the SIRPα-CD47 pathway (108–110). This can be a direct effect of the SIRPα-CD47 pathway on T cell function or an indirect mechanism by which SIRPα-CD47 pathway blockade affects the capacity of myeloid cells to activate T cells. Interestingly, efficacy of CD47 blockade was shown to largely depend on DNA sensing, specifically in DCs (41). Interference with sialoglycan–Siglec interactions as well as innate immune checkpoints should be further explored in the context of *in situ* tumor destruction.

FUTURE PERSPECTIVE: MULTIFUNCTIONAL ANTIBODY DEVELOPMENT AND *IN SITU* TUMOR ABLATION

The tumor exists in a dynamic microenvironment that co-influences anti-tumor immune responses. Strategies that simultaneously modulate multiple key processes in the anti-tumor immune response will likely work synergistically. Recent advances in antibody engineering have resulted in new antibody formats that can exert distinct effector functions (111). Besides, multifunctional antibodies can be used to direct immunomodulators specifically to the relevant locations, limiting systemic exposure and increasing tumor specificity. Multifunctional antibodies come in various molecular varieties, ranging from linked Fab fragments to full antibodies with an Fc-tail to preserve native antibody functions, such as antibody-dependent cellular cytotoxicity (ADCC)/phagocytosis, complement-mediated lysis and improved circulation half-life (111). Multifunctionality can be achieved by combining different antibody variable domains, recognizing different epitopes, e.g. bispecific antibodies. Alternatively, receptors or immuno-modulatory molecules can be attached to antibodies *via* protein-linkers, acquiring multiple specificity in a different manner. Most of these multifunctional antibody formats are in (pre)clinical development and not yet applied in context with tumor ablation. We will here review antibody formats that could be beneficial in combination with tumor ablation to create an *in situ* cancer vaccine (**Figure 2**).

Bispecific antibodies come in various flavors and can target different antigens either on the same cell or on two different cell types. Most known bispecific antibodies in preclinical and clinical development are engaging T cells, binding CD3 and a relevant tumor antigen, to induce tumor cell killing (111). Alternatively, bispecific antibodies harboring an agonistic arm and a tumor targeting arm are developed (112, 113). These bispecific agonistic antibodies ensure tumor localization and allow cross-linking without the need for Fc-receptors to exert its agonistic function (**Figure 2.1**). Instead they rely on a tumor antigen for cross-linking, making activation fully tumor cell dependent. For example, the bispecific antibody LB-1, which is specific for the tumor antigen MSLN and mouse CD40 showed preferential DC activation *in vitro* only when cultured with MSLN expressing tumor cells. *In vivo* application limited tumor growth of an MSLN expressing tumor to a similar extent as a conventional agonistic anti-CD40 mAb. The bifunctional molecule, however, showed less systemic activation and toxicity as compared to anti-CD40 therapy (112, 113). In addition to these there are also bispecific agonistic antibody constructs targeting two co-stimulatory receptors at once, CD137 and OX40, or a co-stimulatory receptor (OX40) and immune checkpoint (CTLA-4) (114, 115).

The success of immune checkpoint mAbs prompted the development of bispecific immune checkpoint formats, such as the PD-L1xErbB2 antibody (**Figure 2.2**). This bispecific antibody reduced tumor growth and increased tumor rejection rate compared to the combination of anti-PD-L1 and anti-ErbB2 mAb therapy, which was dependent on $CD8^+$ T cells and IFNγ (116). The bispecific antibody was constructed with a mIgG2a Fc backbone and the authors describe that ADCC and complement action could be potential mechanisms (116). Alternatively, bispecific antibodies binding two distinct immune checkpoints, such as PD-1/PD-L1, CTLA-4, LAG-3 or TIM-3 are also interesting options to explore (117, 118). Besides, innate immune checkpoints are explored in bispecific antibody formats. Bispecific mAbs consisting of a low-affinity anti-CD47 arm combined with a high-affinity tumor antigen arm ensure that blockade of CD47 only occurs on tumor cells, which co-express both antigens, resulting in improved phagocytosis of target cells and leaving healthy CD47 expressing cells unharmed (119). Bispecific antibodies show potent anti-tumor activity and warrant further study in combination with ablation. As Siglec receptors are regarded as novel immune checkpoints, it would be interesting to explore Siglec targeting antibodies in bi- or multispecific formats.

Alternatively, multispecificity can be achieved through the linking of recombinant receptors/ligands or immunomodulatory molecules to antibodies. To this end, endogenous SIRPα domains are engrafted to a tumor antigen specific antibody (120, 121).

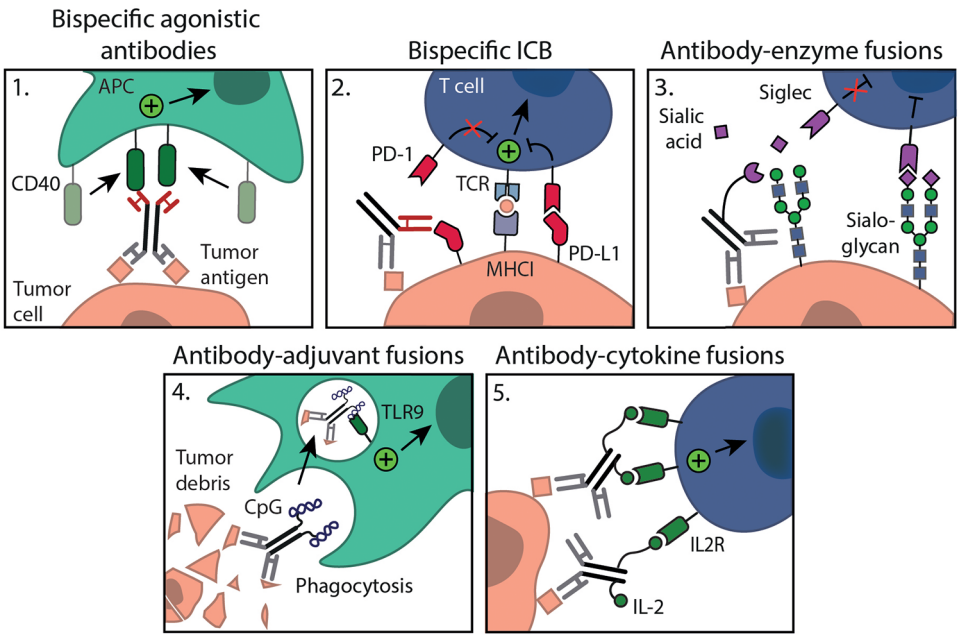


FIGURE 2 | Multifunctional antibody formats for combination with *in situ* tumor ablation. Administration of 1. bispecific agonistic antibodies (e.g. anti-MSLN-CD40) or 4. antibody-adjuvant fusions (e.g. chTNT3-CpG) will lead to local APC activation. Interventions such as 2. bispecific ICB (e.g. PD-L1xErbB2 antibody) may further stimulate myeloid as well as T cell immunity specifically within the TME; 3. antibody-enzyme fusions allow tumor specific sialoglycan degradation (e.g. anti-HER2 mAb-sialidase); 5. antibody-cytokine fusions (e.g. anti-GD2-IL2) will result in targeted cytokine delivery ensuring local immune cell activation, all are aimed at relieving local immunosuppression.

Binding of the antibody to tumor antigen specific cells allows binding of the SIRPα domain to CD47 on these same cells. Thereby, the interaction of CD47 with endogenous SIRPα expressed on myeloid cells is prevented, restoring the phagocytic capacity of myeloid cells (120, 121). In the context sialoglycan–Siglec axis, a recently developed multifunctional antibody consisting of a sialic acid-cleaving enzyme (sialidase) fused to an anti-HER2 antibody, aims to degrade sialoglycans in a tumor-specific manner (**Figure 2.3**) (122). In a syngeneic orthotopic $HER2^+$ breast cancer model, anti-HER2 antibody-sialidase conjugates delayed tumor growth and enhanced immune infiltration, leading to prolonged survival of mice. Using the $HER2^+$ B16D5 melanoma tumor model and Siglec-$E^{-/-}$ mice, the authors showed that the effect was dependent on functional Siglec-E, a receptor highly expressed on tumor-infiltrating myeloid cells (122). These studies indicate that multifunctional antibodies aimed at reversing the immunosuppressive TME are potentially effective. Also, immune activation strategies, such as adjuvants can be incorporated into mAb conjugates (**Figure 2.4**). One such antibody is chTNT3-CpG, which is specific for extracellular DNA/histones (123), often present following ablative therapy. Systemic intraperitoneal (i.p.) administration of chTNT3-CpG resulted in delayed tumor development in both the Colon 26 adenocarcinoma and B16 tumor model, whereas i.p. administration of the chTNT3 antibody or CpG alone failed to show efficacy, again showing the added value of tumor targeting capacities of multifunctional mAbs (123).

Trafficking of APCs to the ablation site where they can capture and process antigens for (cross-) presentation is of importance for an *in situ* cancer vaccine. To this end, antibodies conjugated with DC growth factors, such as GM-CSF or FLT3L, are of interest to expand and redirect DC subsets to the ablation site (124, 125). In fact, preclinical data showed that FLT3L in combination with RT in a mammary carcinoma model can help boost the abscopal effect (126). GM-CSF has been coupled to anti-HER2/neu and demonstrated anti-tumor activity in a HER2/neu expressing colon adenocarcinoma model (127). Several other cytokines including interleukin 2 (IL-2), IL-12 and type I IFN have been fused to antibodies (**Figure 2.5**). The use of antibody-cytokine fusions has to potential to concentrate the cytokines at the tumor site, reducing side effects that are observed with systemic pro-inflammatory cytokine administration. IL-2, an important cytokine in the regulation of adaptive T cell responses, has been fused to diverse antibodies targeting relevant tumor proteins, such as hu14.18-IL2 targeting disialoganglioside GD2, huKS-IL2 targeting EpCAM, L19-IL2 targeting fibronectin and NHS-IL2 targeting histone/DNA complexes. IL-2 fusion antibodies were shown to improve responses to *in situ* tumor ablation, resulting in marked tumor reduction (128–130) and curative abscopal effects (131), mediated by $CD8^+$ T cells.

Preclinical research demonstrated that combination of 12 Gy RT together with five i.t. injections of hu14.18-IL2 on days 6 to 10 after RT eradicates constitutively GD2 expressing B78 melanoma tumors (132). In the ~70% of mice that were rendered disease-free upon combination therapy, 90% rejected a re-challenge with $GD2^{high}$ B78 melanoma cells. This response of RT and hu14.18-IL2 in melanoma could be augmented by addition of anti-CTLA-4 mAb (133). A recent study further pursued the combination of hu14.18-IL2 and RT as *in situ* cancer vaccination strategy. Voeller et al. demonstrated that neither RT plus hu14.18-IL2 therapy nor the addition of anti-CTLA-4 mAb to the combined therapy regimen caused significant growth inhibition in a $GD2^{high}$ non-immunogenic 9464D neuroblastoma model (134). These observations suggest that the antibody-cytokine mediated therapeutic effect is tumor type dependent. Addition of the adjuvant CpG and anti-CD40 co-stimulatory agonist to the RT, ½ dose hu14.18-IL2 (due to concern for significant toxicities) and anti-CTLA-4 mAb, improved tumor control and 80% achieved complete tumor regression. A clinical phase II study recently demonstrated that hu14.18-IL2 given in combination with GM-CSF and the differentiation inducing agent isotretinoin is safe and tolerable, and showed anti-tumor activity in patients with relapsed/refractory neuroblastoma (135). Several other IL2-antibody fusions have advanced to clinical trials, including huKS-IL2 (136), NHS-IL2 (128) and L19-IL2 (137). The combination of RT (5 x 4 Gy) followed by NHS-IL2 after first-line chemotherapy in metastatic non-small cell lung cancer (NSCLC) patients was well tolerated (128). A phase II trial will investigate the combination of SABRT and L19-IL2 therapy in metastatic NSCLC patients (137).

IL-12, an important $CD8^+$ T cell and NK cell cytokine, has been fused to the anti-NHS antibody recognizing histone/DNA complexes. Enhanced tumor uptake of radiolabeled NHS-hIL12 was observed upon RT ablation in rhabdomyosarcoma xenografts (138). Fallon et al. showed that 0.36 Gy RT combined with subcutaneous NHS conjugated with murine IL-12 resulted in superior tumor growth inhibition compared to either treatment alone in a murine LLC lung and MC38 colorectal cancer model (139). Studies combining other ablation types with NHS antibody cytokine fusions are not reported, however would be worthwhile to explore.

Besides interleukins, other pro-inflammatory cytokines, such as type I IFNs, have been coupled to various antibodies. IFNβ fused to anti-EGFR mAb limited growth of mouse EGFR-expressing B16 tumors which were unresponsive to anti-EGFR mAb therapy (140). Furthermore, multifunctional antibodies that simultaneously aim at activating the immune system and counteracting the immunosuppressive TME are promising for future cancer vaccine developments. To this end, anti-PD-L1 was armed with IFNα to simultaneously target both PD-L1 and the IFN-receptor. In different models, anti-PD-L1-IFNα could control advanced tumors as opposed to IFNα-Fc or anti-PD-L1 monotherapy (141). In addition, multifunctional antibodies aimed at blockade of different immunosuppressive pathways are developed, such as the fusion protein M7824, comprising the extracellular domain of human TGFβRII (TGFβ scavenging/trap) linked to the human anti-PD-L1 heavy chain. Combination therapy with M7824 (intravenous, day 2) and RT (3.6 Gy per day, days 0-3) reduced primary as well as untreated secondary tumor growth relative to either treatment alone, indicating the induction of an abscopal effect (142). A phase I trial of M7824 showed a manageable safety profile in patients with heavily pretreated advanced solid tumors and encouraging treatment efficacy (143). Overall, multifunctional antibodies can be created by linking different immunomodulatory molecules with tumor or immune targeting mAbs. Proof-of-concept preclinical studies suggest therapeutic potential of different multifunctional antibody formats and clinical trials showed tolerability and safety. We anticipate that these multifunctional antibodies can work in concert with *in situ* tumor ablation and highlight them as a promising therapeutic strategy to explore.

CONCLUSION

In situ tumor ablation techniques allow for (neo)antigen loading of DCs without prior knowledge of tumor antigens or epitopes as in conventional DC vaccination. The induction of an efficient immune responses following ablation, however, requires addition of immune stimuli to eradicate local tumors and metastases and to provide long-term protection. Numerous immune activating strategies have shown to be suitable to act in concert with ablation generated tumor debris to achieve *in situ* cancer vaccination. More detailed knowledge about how effective immune activation strategies can work in concert with tumor ablation, such as timing and dose, is required to guide rationale ablation combination strategies. Although *in situ* ablation plus immune activating strategies ensure that the immune system is well instructed and initiated, the immunosuppressive environment that immune cells encounter upon arrival at the TME is still a potential bottleneck. Therefore, additional removal of inhibitory influences provides the possibility to further boost anti-tumor immune responses and enhance *in situ* ablation efficacy.

Multifunctional antibodies stimulating immune activation as well as counteracting immunosuppression can simultaneously affect multiple key processes in the anti-tumor immune response. They hold great promise for targeted cancer treatment with limited systemic toxicities and deserve further exploration as potential strategy to achieve a successful *in situ* cancer vaccine.

AUTHOR CONTRIBUTIONS

RB, FS and GA wrote the manuscript. JF, MV and LC reviewed the manuscript. All authors contributed to the article and approved the submitted version.

FUNDING

This work was supported by the foundation 'Villa Joep', a Radboud Institute for Molecular Life Sciences (RIMLS) PhD grant awarded to GA and a grant from the Dutch Cancer Foundation (KWF) awarded to GA (KUN2015-7604).

REFERENCES

1. Ho NI. Huis In 't Veld LGM, Raaijmakers TK, Adema GJ. Adjuvants Enhancing Cross-Presentation by Dendritic Cells: The Key to More Effective Vaccines? *Front Immunol* (2018) 9:2874. doi: 10.3389/fimmu.2018.02874
2. den Brok MH, Sutmuller RP, Nierkens S, Bennink EJ, Toonen LW, Figdor CG, et al. Synergy between in situ cryoablation and TLR9 stimulation results in a highly effective in vivo dendritic cell vaccine. *Cancer Res* (2006) 66 (14):7285–92. doi: 10.1158/0008-5472.can-06-0206
3. Soanes WA, Ablin RJ, Gonder MJ. Remission of metastatic lesions following cryosurgery in prostatic cancer: immunologic considerations. *J Urol* (1970) 104(1):154–9. doi: 10.1016/s0022-5347(17)61690-2
4. Formenti SC, Demaria S. Systemic effects of local radiotherapy. *Lancet Oncol* (2009) 10(7):718–26. doi: 10.1016/S1470-2045(09)70082-8
5. Alteber Z, Azulay M, Cafri G, Vadai E, Tzehoval E, Eisenbach L. Cryoimmunotherapy with local co-administration of ex vivo generated dendritic cells and CpG-ODN immune adjuvant, elicits a specific antitumor immunity. *Cancer Immunol Immunother CII* (2014) 63(4):369–80. doi: 10.1007/s00262-014-1520-4
6. den Brok MH, Nierkens S, Wagenaars JA, Ruers TJ, Schrier CC, Rijke EO, et al. Saponin-based adjuvants create a highly effective anti-tumor vaccine when combined with in situ tumor destruction. *Vaccine* (2012) 30(4):737–44. doi: 10.1016/j.vaccine.2011.11.080
7. van den Bijgaart RJ, Eikelenboom DC, Hoogenboom M, Futterer JJ, den Brok MH, Adema GJ. Thermal and mechanical high-intensity focused ultrasound: perspectives on tumor ablation, immune effects and combination strategies. *Cancer Immunol Immunother CII* (2017) 66 (2):247-58. doi: 10.1007/s00262-016-1891-9
8. Brinkmann U, Kontermann RE. The making of bispecific antibodies. *mAbs* (2017) 9(2):182–212. doi: 10.1080/19420862.2016.1268307
9. Begg AC, Stewart FA, Vens C. Strategies to improve radiotherapy with targeted drugs. *Nat Rev Cancer* (2011) 11(4):239–53. doi: 10.1038/nrc3007
10. Hall WA, Paulson ES, van der Heide UA, Fuller CD, Raaymakers BW, Lagendijk JJW, et al. The transformation of radiation oncology using real-time magnetic resonance guidance: A review. *Eur J Cancer* (2019) 122:42–52. doi: 10.1016/j.ejca.2019.07.021
11. Keisari Y. Tumor abolition and antitumor immunostimulation by physico-chemical tumor ablation. *Front Biosci (Landmark Ed)* (2017) 22:310–47. doi: 10.2741/4487
12. Hoogenboom M, Eikelenboom D, den Brok MH, Veltien A, Wassink M, Wesseling P, et al. In vivo MR guided boiling histotripsy in a mouse tumor model evaluated by MRI and histopathology. *NMR BioMed* (2016) 29 (6):721–31. doi: 10.1002/nbm.3520
13. Khokhlova VA, Fowlkes JB, Roberts WW, Schade GR, Xu Z, Khokhlova TD, et al. Histotripsy methods in mechanical disintegration of tissue: towards clinical applications. *Int J Hyperthermia* (2015) 31(2):145–62. doi: 10.3109/02656736.2015.1007538
14. Hoogenboom M, Eikelenboom DC, van den Bijgaart RJE, Heerschap A, Wesseling P, den Brok MH, et al. Impact of MR-guided boiling histotripsy in distinct murine tumor models. *Ultrason Sonochem* (2017) 38:1–8. doi: 10.1016/j.ultsonch.2017.02.035
15. Matsushita H, Vesely MD, Koboldt DC, Rickert CG, Uppaluri R, Magrini VJ, et al. Cancer exome analysis reveals a T-cell-dependent mechanism of cancer immunoediting. *Nature* (2012) 482(7385):400–4. doi: 10.1038/nature10755
16. Castle JC, Kreiter S, Diekmann J, Lower M, van de Roemer N, de Graaf J, et al. Exploiting the mutanome for tumor vaccination. *Cancer Res* (2012) 72 (5):1081–91. doi: 10.1158/0008-5472.CAN-11-3722
17. Bandyopadhyay S, Quinn TJ, Scandiuzzi L, Basu I, Partanen A, Tome WA, et al. Low-Intensity Focused Ultrasound Induces Reversal of Tumor-Induced T Cell Tolerance and Prevents Immune Escape. *J Immunol* (2016) 196(4):1964–76. doi: 10.4049/jimmunol.1500541
18. Hoogenboom M, Eikelenboom D, den Brok MH, Heerschap A, Futterer JJ, Adema GJ. Mechanical high-intensity focused ultrasound destruction of soft tissue: working mechanisms and physiologic effects. *Ultrasound Med Biol* (2015) 41(6):1500–17. doi: 10.1016/j.ultrasmedbio.2015.02.006
19. Hall TL, Kieran K, Ives K, Fowlkes JB, Cain CA, Roberts WW. Histotripsy of rabbit renal tissue in vivo: temporal histologic trends. *J Endourol* (2007) 21 (10):1159–66. doi: 10.1089/end.2007.9915
20. Shao Q, O'Flanagan S, Lam T, Roy P, Pelaez F, Burbach BJ, et al. Engineering T cell response to cancer antigens by choice of focal therapeutic conditions. *Int J Hyperthermia* (2019) 36(1):130–8. doi: 10.1080/02656736.2018.1539253
21. Page DB, Yuan J, Redmond D, Wen YH, Durack JC, Emerson R, et al. Deep Sequencing of T-cell Receptor DNA as a Biomarker of Clonally Expanded TILs in Breast Cancer after Immunotherapy. *Cancer Immunol Res* (2016) 4 (10):835–44. doi: 10.1158/2326-6066.CIR-16-0013
22. den Brok MH, Nierkens S, Figdor CG, Ruers TJ, Adema GJ. Dendritic cells: tools and targets for antitumor vaccination. *Expert Rev Vaccines* (2005) 4 (5):699–710. doi: 10.1586/14760584.4.5.699
23. Nierkens S, den Brok MH, Garcia Z, Togher S, Wagenaars J, Wassink M, et al. Immune adjuvant efficacy of CpG oligonucleotide in cancer treatment is founded specifically upon TLR9 function in plasmacytoid dendritic cells. *Cancer Res* (2011) 71(20):6428–37. doi: 10.1158/0008-5472.CAN-11-2154
24. Noubade R, Majri-Morrison S, Tarbell KV. Beyond cDC1: Emerging Roles of DC Crosstalk in Cancer Immunity. *Front Immunol* (2019) 10:1014. doi: 10.3389/fimmu.2019.01014
25. Nierkens S, den Brok MH, Sutmuller RP, Grauer OM, Bennink E, Morgan ME, et al. In vivo colocalization of antigen and CpG [corrected] within dendritic cells is associated with the efficacy of cancer immunotherapy. *Cancer Res* (2008) 68(13):5390–6. doi: 10.1158/0008-5472.can-07-6023
26. Nierkens S, den Brok MH, Roelofsen T, Wagenaars JA, Figdor CG, Ruers TJ, et al. Route of administration of the TLR9 agonist CpG critically determines the efficacy of cancer immunotherapy in mice. *PloS One* (2009) 4(12):e8368. doi: 10.1371/journal.pone.0008368
27. Veenstra JJ, Gibson HM, Littrup PJ, Reyes JD, Cher ML, Takashima A, et al. Cryotherapy with concurrent CpG oligonucleotide treatment controls local tumor recurrence and modulates HER2/neu immunity. *Cancer Res* (2014) 74(19):5409–20. doi: 10.1158/0008-5472.can-14-0501
28. Xu A, Zhang L, Yuan J, Babikr F, Freywald A, Chibbar R, et al. TLR9 agonist enhances radiofrequency ablation-induced CTL responses, leading to the potent inhibition of primary tumor growth and lung metastasis. *Cell Mol Immunol* (2019) 16(10):820–32. doi: 10.1038/s41423-018-0184-y
29. Monjazeb AM, Kent MS, Grossenbacher SK, Mall C, Zamora AE, Mirsoian A, et al. Blocking Indolamine-2,3-Dioxygenase Rebound Immune Suppression Boosts Antitumor Effects of Radio-Immunotherapy in Murine Models and Spontaneous Canine Malignancies. *Clin Cancer Res Off J Am Assoc Cancer Res* (2016) 22(17):4328–40. doi: 10.1158/1078-0432.ccr-15-3026
30. Chavez M, Silvestrini MT, Ingham ES, Fite BZ, Mahakian LM, Tam SM, et al. Distinct immune signatures in directly treated and distant tumors result from TLR adjuvants and focal ablation. *Theranostics* (2018) 8 (13):3611–28. doi: 10.7150/thno.25613
31. Blair TC, Bambina S, Alice AF, Kramer GF, Medler TR, Baird JR, et al. Dendritic Cell Maturation Defines Immunological Responsiveness of Tumors to Radiation Therapy. *J Immunol* (2020) 204(12):3416–24. doi: 10.4049/jimmunol.2000194
32. Yoshida S, Shime H, Takeda Y, Nam JM, Takashima K, Matsumoto M, et al. Toll-like receptor 3 signal augments radiation-induced tumor growth retardation in a murine model. *Cancer Sci* (2018) 109: (4):956–65. doi: 10.1111/cas.13543
33. Hammerich L, Marron TU, Upadhyay R, Svensson-Arvelund J, Dhainaut M, Hussein S, et al. Systemic clinical tumor regressions and potentiation of PD1 blockade with in situ vaccination. *Nat Med* (2019) 25(5):814–24. doi: 10.1038/s41591-019-0410-x
34. Schon MP, Schon M. TLR7 and TLR8 as targets in cancer therapy. *Oncogene* (2008) 27(2):190–9. doi: 10.1038/sj.onc.1210913
35. Chen Q, Chen J, Yang Z, Xu J, Xu L, Liang C, et al. Nanoparticle-Enhanced Radiotherapy to Trigger Robust Cancer Immunotherapy. *Adv Mater* (2019) 31(10):e1802228. doi: 10.1002/adma.201802228
36. Dewan MZ, Vanpouille-Box C, Kawashima N, DiNapoli S, Babb JS, Formenti SC, et al. Synergy of topical toll-like receptor 7 agonist with radiation and low-dose cyclophosphamide in a mouse model of cutaneous breast cancer. *Clin Cancer Res Off J Am Assoc Cancer Res* (2012) 18 (24):6668–78. doi: 10.1158/1078-0432.ccr-12-0984
37. Dovedi SJ, Adlard AL, Ota Y, Murata M, Sugaru E, Koga-Yamakawa E, et al. Intravenous administration of the selective toll-like receptor 7 agonist DSR-

29133 leads to anti-tumor efficacy in murine solid tumor models which can be potentiated by combination with fractionated radiotherapy. *Oncotarget* (2016) 7(13):17035–46. doi: 10.18632/oncotarget.7928
38. Redondo P, del Olmo J, Lopez-Diaz de Cerio A, Inoges S, Marquina M, Melero I, et al. Imiquimod enhances the systemic immunity attained by local cryosurgery destruction of melanoma lesions. *J Invest Dermatol* (2007) 127 (7):1673–80. doi: 10.1038/sj.jid.5700777
39. Takagi H, Arimura K, Uto T, Fukaya T, Nakamura T, Choijookhuu N, et al. Plasmacytoid dendritic cells orchestrate TLR7-mediated innate and adaptive immunity for the initiation of autoimmune inflammation. *Sci Rep* (2016) 6:24477. doi: 10.1038/srep24477
40. Motwani M, Pesiridis S, Fitzgerald KA. DNA sensing by the cGAS–STING pathway in health and disease. *Nat Rev Genet* (2019) 20(11):657–74. doi: 10.1038/s41576-019-0151-1
41. Xu MM, Pu Y, Han D, Shi Y, Cao X, Liang H, et al. Dendritic Cells but Not Macrophages Sense Tumor Mitochondrial DNA for Cross-priming through Signal Regulatory Protein α Signaling. *Immunity* (2017) 47(2):363–73.e5. doi: 10.1016/j.immuni.2017.07.016
42. Deng L, Liang H, Xu M, Yang X, Burnette B, Arina A, et al. STING-Dependent Cytosolic DNA Sensing Promotes Radiation-Induced Type I Interferon-Dependent Antitumor Immunity in Immunogenic Tumors. *Immunity* (2014) 41(5):843–52. doi: 10.1016/j.immuni.2014.10.019
43. Luo M, Liu Z, Zhang X, Han C, Samandi LZ, Dong C, et al. Synergistic STING activation by PC7A nanovaccine and ionizing radiation improves cancer immunotherapy. *J Controlled Release Off J Controlled Release Soc* (2019) 300:154–60. doi: 10.1016/j.jconrel.2019.02.036
44. Schadt L, Sparano C, Schweiger NA, Silina K, Cecconi V, Lucchiari G, et al. Cancer-Cell-Intrinsic cGAS Expression Mediates Tumor Immunogenicity. *Cell Rep* (2019) 29(5):1236–48.e7. doi: 10.1016/j.celrep.2019.09.065
45. Vanpouille-Box C, Alard A, Aryankalayil MJ, Sarfraz Y, Diamond JM, Schneider RJ. DNA exonuclease Trex1 regulates radiotherapy-induced tumour immunogenicity. *Nat Commun* (2017) 8:15618. doi: 10.1038/ncomms15618
46. Guey B, Wischnewski M, Decout A, Makasheva K, Kaynak M, Sakar MS, et al. BAF restricts cGAS on nuclear DNA to prevent innate immune activation. *Science* (2020) 369(6505):823–8. doi: 10.1126/science.aaw6421
47. McCauley ME, O'Rourke JG, Yáñez A, Markman JL, Ho R, Wang X, et al. C9orf72 in myeloid cells suppresses STING-induced inflammation. *Nature* (2020) 585(7823):96–101. doi: 10.1038/s41586-020-2625-x
48. Bakhoum SF, Ngo B, Laughney AM, Cavallo JA, Murphy CJ, Ly P, et al. Chromosomal instability drives metastasis through a cytosolic DNA response. *Nature* (2018) 553(7689):467–72. doi: 10.1038/nature25432
49. den Brok MH, Büll C, Wassink M, de Graaf AM, Wagenaars JA, Minderman M, et al. Saponin-based adjuvants induce cross-presentation in dendritic cells by intracellular lipid body formation. *Nat Commun* (2016) 7(1):13324. doi: 10.1038/ncomms13324
50. Raaijmakers TK, van den Bijgaart RJE, den Brok MH, Wassink M, de Graaf A, Wagenaars JA, et al. Tumor ablation plus co-administration of CpG and saponin adjuvants affects IL-1 production and multifunctional T cell numbers in tumor draining lymph nodes. *J ImmunoTher Cancer* (2020) 8(1):e000649. doi: 10.1136/jitc-2020-000649
51. Shin K-S, Jeon I, Kim B-S, Kim I-K, Park Y-J, Koh C-H, et al. Monocyte-Derived Dendritic Cells Dictate the Memory Differentiation of CD8+ T Cells During Acute Infection. *Front Immunol* (2019) 10:1887. doi: 10.3389/fimmu.2019.01887
52. Wakim LM, Waithman J, van Rooijen N, Heath WR, Carbone FR. Dendritic cell-induced memory T cell activation in nonlymphoid tissues. *Science* (2008) 319(5860):198–202. doi: 10.1126/science.1151869
53. Vonderheide RH. CD40 Agonist Antibodies in Cancer Immunotherapy. *Annu Rev Med* (2020) 71:47–58. doi: 10.1146/annurev-med-062518-045435
54. Schoenberger SP, Toes RE, van der Voort EI, Offringa R. Melief CJ. T-cell help for cytotoxic T lymphocytes is mediated by CD40-CD40L interactions. *Nature* (1998) 393(6684):480–3. doi: 10.1038/31002
55. Dovedi SJ, Lipowska-Bhalla G, Beers SA, Cheadle EJ, Mu L, Glennie MJ, et al. Antitumor Efficacy of Radiation plus Immunotherapy Depends upon Dendritic Cell Activation of Effector CD8+ T Cells. *Cancer Immunol Res* (2016) 4(7):621–30. doi: 10.1158/2326-6066.CIR-15-0253
56. Yasmin-Karim S, Bruck PT, Moreau M, Kunjachan S, Chen GZ, Kumar R, et al. Radiation and Local Anti-CD40 Generate an Effective in situ Vaccine in Preclinical Models of Pancreatic Cancer. *Front Immunol* (2018) 9:2030. doi: 10.3389/fimmu.2018.02030
57. Rech AJ, Dada H, Kotzin JJ, Henao-Mejia J, Minn AJ, Twyman-Saint Victor C, et al. Radiotherapy and CD40 Activation Separately Augment Immunity to Checkpoint Blockade in Cancer. *Cancer Res* (2018) 78(15):4282–91. doi: 10.1158/0008-5472.CAN-17-3821
58. Hellman P, Eriksson H. Early activation markers of human peripheral dendritic cells. *Hum Immunol* (2007) 68(5):324–33. doi: 10.1016/j.humimm.2007.01.018
59. Krug A, Towarowski A, Britsch S, Rothenfusser S, Hornung V, Bals R, et al. Toll-like receptor expression reveals CpG DNA as a unique microbial stimulus for plasmacytoid dendritic cells which synergizes with CD40 ligand to induce high amounts of IL-12. *Eur J Immunol* (2001) 31 (10):3026–37. doi: 10.1002/1521-4141(2001010)31:10<3026::aid-immu3026>3.0.co;2-h
60. Ahonen CL, Doxsee CL, McGurran SM, Riter TR, Wade WF, Barth RJ, et al. and CD40 triggering induces potent CD8+ T cell expansion with variable dependence on type I IFN. *J Exp Med* (2004) 199(6):775–84. doi: 10.1084/jem.20031591
61. Sanchez PJ, McWilliams JA, Haluszczak C, Yagita H, Kedl RM. Combined TLR/CD40 Stimulation Mediates Potent Cellular Immunity by Regulating Dendritic Cell Expression of CD70 In Vivo. *J Immunol* (2007) 178(3):1564–72. doi: 10.4049/jimmunol.178.3.1564
62. Weinberg AD, Rivera MM, Prell R, Morris A, Ramstad T, Vetto JT, et al. Engagement of the OX-40 receptor in vivo enhances antitumor immunity. *J Immunol* (2000) 164(4):2160–9. doi: 10.4049/jimmunol.164.4.2160
63. Piconese S, Valzasina B, Colombo MP. OX40 triggering blocks suppression by regulatory T cells and facilitates tumor rejection. *J Exp Med* (2008) 205 (4):825–39. doi: 10.1084/jem.20071341
64. Roberts DJ, Franklin NA, Kingeter LM, Yagita H, Tutt AL, Glennie MJ, et al. Control of established melanoma by CD27 stimulation is associated with enhanced effector function and persistence, and reduced PD-1 expression of tumor infiltrating CD8(+) T cells. *J Immunother (Hagerstown Md 1997)* (2010) 33(8):769–79. doi: 10.1097/CJI.0b013e3181ee238f
65. Eskiocak U, Guzman W, Wolf B, Cummings C, Milling L, Wu H-J, et al. Differentiated agonistic antibody targeting CD137 eradicates large tumors without hepatotoxicity. *JCI Insight* (2020) 5(5):e133647. doi: 10.1172/jci.insight.133647
66. Yokouchi H, Yamazaki K, Chamoto K, Kikuchi E, Shinagawa N, Oizumi S, et al. Anti-OX40 monoclonal antibody therapy in combination with radiotherapy results in therapeutic antitumor immunity to murine lung cancer. *Cancer Sci* (2008) 99(2):361–7. doi: 10.1111/j.1349-7006.2007.00664.x
67. Niknam S, Barsoumian HB, Schoenhals JE, Jackson HL, Yanamandra N, Caetano MS, et al. Radiation Followed by OX40 Stimulation Drives Local and Abscopal Antitumor Effects in an Anti-PD1-Resistant Lung Tumor Model. *Clin Cancer Res Off J Am Assoc Cancer Res* (2018) 24(22):5735–43. doi: 10.1158/1078-0432.ccr-17-3279
68. Rodriguez-Ruiz ME, Rodriguez I, Garasa S, Barbes B, Solorzano JL, Perez-Gracia JL, et al. Abscopal Effects of Radiotherapy Are Enhanced by Combined Immunostimulatory mAbs and Are Dependent on CD8 T Cells and Crosspriming. *Cancer Res* (2016) 76(20):5994–6005. doi: 10.1158/0008-5472.CAN-16-0549
69. Verbrugge I, Hagekyriakou J, Sharp LL, Galli M, West A, McLaughlin NM, et al. Radiotherapy increases the permissiveness of established mammary tumors to rejection by immunomodulatory antibodies. *Cancer Res* (2012) 72 (13):3163–74. doi: 10.1158/0008-5472.CAN-12-0210
70. Sagiv-Barfi I, Czerwinski DK, Levy S, Alam IS, Mayer AT, Gambhir SS, et al. Eradication of spontaneous malignancy by local immunotherapy. *Sci Trans Med* (2018) 10(426):eaan4488. doi: 10.1126/scitranslmed.aan4488
71. Buhtoiarov IN, Lum HD, Berke G, Sondel PM, Rakhmilevich AL. Synergistic Activation of Macrophages via CD40 and TLR9 Results in T Cell Independent Antitumor Effects. *J Immunol* (2006) 176(1):309–18. doi: 10.4049/jimmunol.176.1.309
72. Lindau D, Gielen P, Kroesen M, Wesseling P, Adema GJ. The immunosuppressive tumour network: myeloid-derived suppressor cells,

regulatory T cells and natural killer T cells. *Immunology* (2013) 138(2):105–15. doi: 10.1111/imm.12036
73. Umansky V, Adema GJ, Baran J, Brandau S, Van Ginderachter JA, Hu X, et al. Interactions among myeloid regulatory cells in cancer. *Cancer Immunol Immunother* (2019) 68(4):645–60. doi: 10.1007/s00262-018-2200-6
74. Butt AQ, Mills KH. Immunosuppressive networks and checkpoints controlling antitumor immunity and their blockade in the development of cancer immunotherapeutics and vaccines. *Oncogene* (2014) 33(38):4623–31. doi: 10.1038/onc.2013.432
75. Vesely MD, Kershaw MH, Schreiber RD, Smyth MJ. Natural innate and adaptive immunity to cancer. *Annu Rev Immunol* (2011) 29:235–71. doi: 10.1146/annurev-immunol-031210-101324
76. Barcellos-Hoff MH, Derynck R, Tsang ML, Weatherbee JA. Transforming growth factor-beta activation in irradiated murine mammary gland. *J Clin Invest* (1994) 93(2):892–9. doi: 10.1172/jci117045
77. Jobling MF, Mott JD, Finnegan MT, Jurukovski V, Erickson AC, Walian PJ, et al. Isoform-specific activation of latent transforming growth factor beta (LTGF-beta) by reactive oxygen species. *Radiat Res* (2006) 166 (6):839–48. doi: 10.1667/rr0695.1
78. Vanpouille-Box C, Diamond JM, Pilones KA, Zavadil J, Babb JS, Formenti SC, et al. TGFβ Is a Master Regulator of Radiation Therapy-Induced Antitumor Immunity. *Cancer Res* (2015) 75(11):2232–42. doi: 10.1158/0008-5472.can-14-3511
79. Zhu H, Gu X, Xia L, Zhou Y, Bouamar H, Yang J, et al. A Novel TGFβ Trap Blocks Chemotherapeutics-Induced TGFβ1 Signaling and Enhances Their Anticancer Activity in Gynecologic Cancers. *Clin Cancer Res Off J Am Assoc Cancer Res* (2018) 24(12):2780–93. doi: 10.1158/1078-0432.ccr-17-3112
80. Penn JW, Grobbelaar AO, Rolfe KJ. The role of the TGF-beta family in wound healing, burns and scarring: a review. *Int J Burns Trauma* (2012) 2 (1):18–28.
81. Bouquet F, Pal A, Pilones KA, Demaria S, Hann B, Akhurst RJ, et al. TGFβ1 inhibition increases the radiosensitivity of breast cancer cells in vitro and promotes tumor control by radiation in vivo. *Clin Cancer Res Off J Am Assoc Cancer Res* (2011) 17(21):6754–65. doi: 10.1158/1078-0432.ccr-11-0544
82. Mannino MH, Zhu Z, Xiao H, Bai Q, Wakefield MR, Fang Y. The paradoxical role of IL-10 in immunity and cancer. *Cancer Lett* (2015) 367 (2):103–7. doi: 10.1016/j.canlet.2015.07.009
83. Mumm JB, Emmerich J, Zhang X, Chan I, Wu L, Mauze S, et al. IL-10 Elicits IFNγ-Dependent Tumor Immune Surveillance. *Cancer Cell* (2011) 20 (6):781–96. doi: 10.1016/j.ccr.2011.11.003
84. Qiao J, Liu Z, Dong C, Luan Y, Zhang A, Moore C, et al. Targeting Tumors with IL-10 Prevents Dendritic Cell-Mediated CD8+ T Cell Apoptosis. *Cancer Cell* (2019) 35(6):901–15.e4. doi: 10.1016/j.ccell.2019.05.005
85. Sharma P, Allison JP. Immune checkpoint targeting in cancer therapy: toward combination strategies with curative potential. *Cell* (2015) 161 (2):205–14. doi: 10.1016/j.cell.2015.03.030
86. Wei SC, Duffy CR, Allison JP. Fundamental Mechanisms of Immune Checkpoint Blockade Therapy. *Cancer Discovery* (2018) 8(9):1069–86. doi: 10.1158/2159-8290.CD-18-0367
87. Wang XY, Zuo D, Sarkar D, Fisher PB. Blockade of cytotoxic T-lymphocyte antigen-4 as a new therapeutic approach for advanced melanoma. *Expert Opin Pharmacother* (2011) 12(17):2695–706. doi: 10.1517/14656566.2011.629187
88. Simpson TR, Li F, Montalvo-Ortiz W, Sepulveda MA, Bergerhoff K, Arce F, et al. Fc-dependent depletion of tumor-infiltrating regulatory T cells co-defines the efficacy of anti-CTLA-4 therapy against melanoma. *J Exp Med* (2013) 210(9):1695–710. doi: 10.1084/jem.20130579
89. den Brok MH, Sutmuller RP, Nierkens S, Bennink EJ, Frielink C, Toonen LW, et al. Efficient loading of dendritic cells following cryo and radiofrequency ablation in combination with immune modulation induces anti-tumour immunity. *Br J Cancer* (2006) 95(7):896–905. doi: 10.1038/sj.bjc.6603341
90. Waitz R, Solomon SB, Petre EN, Trumble AE, Fasso M, Norton L, et al. Potent induction of tumor immunity by combining tumor cryoablation with anti-CTLA-4 therapy. *Cancer Res* (2012) 72(2):430–9. doi: 10.1158/0008-5472.CAN-11-1782
91. Zhang L, Wang J, Jiang J, Zhang M, Shen J. CTLA-4 Blockade Suppresses Progression of Residual Tumors and Improves Survival After Insufficient Radiofrequency Ablation in a Subcutaneous Murine Hepatoma Model. *Cardiovasc Intervent Radiol* (2020) 43(9):1353–61. doi: 10.1007/s00270-020-02505-6
92. McArthur HL, Diab A, Page DB, Yuan J, Solomon SB, Sacchini V, et al. A Pilot Study of Preoperative Single-Dose Ipilimumab and/or Cryoablation in Women with Early-Stage Breast Cancer with Comprehensive Immune Profiling. *Clin Cancer Res Off J Am Assoc Cancer Res* (2016) 22(23):5729–37. doi: 10.1158/1078-0432.CCR-16-0190
93. Ji D, Song C, Li Y, Xia J, Wu Y, Jia J, et al. Combination of radiotherapy and suppression of Tregs enhances abscopal antitumor effect and inhibits metastasis in rectal cancer. *J Immunother Cancer* (2020) 8(2):e000826. doi: 10.1136/jitc-2020-000826
94. Oweida AJ, Darragh L, Phan A, Binder D, Bhatia S, Mueller A, et al. STAT3 Modulation of Regulatory T Cells in Response to Radiation Therapy in Head and Neck Cancer. *J Natl Cancer Inst* (2019) 111(12):1339–49. doi: 10.1093/jnci/djz036
95. Deng L, Liang H, Burnette B, Beckett M, Darga T, Weichselbaum RR, et al. Irradiation and anti-PD-L1 treatment synergistically promote antitumor immunity in mice. *J Clin Invest* (2014) 124(2):687–95. doi: 10.1172/JCI67313
96. Eranki A, Srinivasan P, Ries M, Kim A, Lazarski CA, Rossi CT, et al. High-Intensity Focused Ultrasound (HIFU) Triggers Immune Sensitization of Refractory Murine Neuroblastoma to Checkpoint Inhibitor Therapy. *Clin Cancer Res Off J Am Assoc Cancer Res* (2020) 26(5):1152–61. doi: 10.1158/1078-0432.CCR-19-1604
97. Shi L, Chen L, Wu C, Zhu Y, Xu B, Zheng X, et al. PD-1 Blockade Boosts Radiofrequency Ablation-Elicited Adaptive Immune Responses against Tumor. *Clin Cancer Res Off J Am Assoc Cancer Res* (2016) 22(5):1173–84. doi: 10.1158/1078-0432.CCR-15-1352
98. Shi L, Wang J, Ding N, Zhang Y, Zhu Y, Dong S, et al. Inflammation induced by incomplete radiofrequency ablation accelerates tumor progression and hinders PD-1 immunotherapy. *Nat Commun* (2019) 10(1):5421. doi: 10.1038/s41467-019-13204-3
99. Twyman-Saint Victor C, Rech AJ, Maity A, Rengan R, Pauken KE, Stelekati E, et al. Radiation and dual checkpoint blockade activate non-redundant immune mechanisms in cancer. *Nature* (2015) 520(7547):373–7. doi: 10.1038/nature14292
100. Dewan MZ, Galloway AE, Kawashima N, Dewyngaert JK, Babb JS, Formenti SC, et al. Fractionated but not single-dose radiotherapy induces an immune-mediated abscopal effect when combined with anti-CTLA-4 antibody. *Clin Cancer Res Off J Am Assoc Cancer Res* (2009) 15(17):5379–88. doi: 10.1158/1078-0432.CCR-09-0265
101. Demaria S, Kawashima N, Yang AM, Devitt ML, Babb JS, Allison JP, et al. Immune-mediated inhibition of metastases after treatment with local radiation and CTLA-4 blockade in a mouse model of breast cancer. *Clin Cancer Res Off J Am Assoc Cancer Res* (2005) 11(2 Pt 1):728–34.
102. Dovedi SJ, Adlard AL, Lipowska-Bhalla G, McKenna C, Jones S, Cheadle EJ, et al. Acquired resistance to fractionated radiotherapy can be overcome by concurrent PD-L1 blockade. *Cancer Res* (2014) 74(19):5458–68. doi: 10.1158/0008-5472.CAN-14-1258
103. Murray D, McBride WH, Schwartz JL. Radiation biology in the context of changing patterns of radiotherapy. *Radiat Res* (2014) 182(3):259–72. doi: 10.1667/RR13740.1
104. Qin S, Xu L, Yi M, Yu S, Wu K, Luo S. Novel immune checkpoint targets: moving beyond PD-1 and CTLA-4. *Mol Cancer* (2019) 18(1):155. doi: 10.1186/s12943-019-1091-2
105. van de Wall S, Santegoets KCM, van Houtum EJH, Bull C, Adema GJ. Sialoglycans and Siglecs Can Shape the Tumor Immune Microenvironment. *Trends Immunol* (2020) 41(4):274–85. doi: 10.1016/j.it.2020.02.001
106. Bull C, Boltje TJ, Balneger N, Weischer SM, Wassink M, van Gemst JJ, et al. Sialic Acid Blockade Suppresses Tumor Growth by Enhancing T-cell-Mediated Tumor Immunity. *Cancer Res* (2018) 78(13):3574–88. doi: 10.1158/0008-5472.CAN-17-3376
107. Veillette A, Chen J. SIRPalpha-CD47 Immune Checkpoint Blockade in Anticancer Therapy. *Trends Immunol* (2018) 39(3):173–84. doi: 10.1016/j.it.2017.12.005
108. Liu X, Pu Y, Cron K, Deng L, Kline J, Frazier WA, et al. CD47 blockade triggers T cell-mediated destruction of immunogenic tumors. *Nat Med* (2015) 21(10):1209–15. doi: 10.1038/nm.3931

109. Tseng D, Volkmer JP, Willingham SB, Contreras-Trujillo H, Fathman JW, Fernhoff NB, et al. Anti-CD47 antibody-mediated phagocytosis of cancer by macrophages primes an effective antitumor T-cell response. *Proc Natl Acad Sci USA* (2013) 110(27):11103–8. doi: 10.1073/pnas.1305569110
110. Soto-Pantoja DR, Terabe M, Ghosh A, Ridnour LA, DeGraff WG, Wink DA, et al. CD47 in the tumor microenvironment limits cooperation between antitumor T-cell immunity and radiotherapy. *Cancer Res* (2014) 74 (23):6771–83. doi: 10.1158/0008-5472.CAN-14-0037-T
111. Labrijn AF, Janmaat ML, Reichert JM, Parren PWHI. Bispecific antibodies: a mechanistic review of the pipeline. *Nat Rev Drug Discov* (2019) 18 (8):585–608. doi: 10.1038/s41573-019-0028-1
112. Lu L, Liu N, Fan K, Zhang G, Li C, Yan Y, et al. A tetravalent single chain diabody (CD40/HER2) efficiently inhibits tumor proliferation through recruitment of T cells and anti-HER2 functions. *Mol Immunol* (2019) 109:149–56. doi: 10.1016/j.molimm.2019.03.001
113. Ye S, Cohen D, Belmar NA, Choi D, Tan SS, Sho M, et al. A Bispecific Molecule Targeting CD40 and Tumor Antigen Mesothelin Enhances Tumor-Specific Immunity. *Cancer Immunol Res* (2019) 7(11):1864–75. doi: 10.1158/2326-6066.cir-18-0805
114. Gaspar M, Pravin J, Rodrigues L, Uhlenbroich S, Everett KL, Wollerton F, et al. CD137/OX40 Bispecific Antibody Induces Potent Antitumor Activity that Is Dependent on Target Coengagement. *Cancer Immunol Res* (2020) 8 (6):781–93. doi: 10.1158/2326-6066.cir-19-0798
115. Kvarnhammar AM, Veitonmäki N, Hägerbrand K, Dahlman A, Smith KE, Fritzell S, et al. The CTLA-4 x OX40 bispecific antibody ATOR-1015 induces anti-tumor effects through tumor-directed immune activation. *J ImmunoTher Cancer* (2019) 7(1):103. doi: 10.1186/s40425-019-0570-8
116. Mittal D, Vijayan D, Neijssen J, Kreijtz J, Habraken M, Van Eenennaam H, et al. Blockade of ErbB2 and PD-L1 using a bispecific antibody to improve targeted anti-ErbB2 therapy. *Oncoimmunology* (2019) 8(11):e1648171. doi: 10.1080/2162402X.2019.1648171
117. LaMotte-Mohs R, Shah K, Smith D, Gorlatov S, Ciccarone V, Tamura J, et al. MGD013, a bispecific PD-1 x LAG-3 Dual-Affinity Re-Targeting (DART®) protein with T-cell immunomodulatory activity for cancer treatment. *Cancer Res* (2016) 76(Suppl. 14):3217.
118. Kraman M, Faroudi M, Allen NL, Kmiecik K, Gliddon D, Seal C, et al. FS118, a Bispecific Antibody Targeting LAG-3 and PD-L1, Enhances T-Cell Activation Resulting in Potent Antitumor Activity. *Clin Cancer Res Off J Am Assoc Cancer Res* (2020) 26(13):3333–44. doi: 10.1158/1078-0432.CCR-19-3548
119. Dheilly E, Moine V, Broyer L, Salgado-Pires S, Johnson Z, Papaioannou A, et al. Selective Blockade of the Ubiquitous Checkpoint Receptor CD47 Is Enabled by Dual-Targeting Bispecific Antibodies. *Mol Ther* (2017) 25 (2):523–33. doi: 10.1016/j.ymthe.2016.11.006
120. Piccione EC, Juarez S, Tseng S, Liu J, Stafford M, Narayanan C, et al. SIRPalpha-Antibody Fusion Proteins Selectively Bind and Eliminate Dual Antigen-Expressing Tumor Cells. *Clin Cancer Res Off J Am Assoc Cancer Res* (2016) 22(20):5109–19. doi: 10.1158/1078-0432.CCR-15-2503
121. Ponce LP, Fenn NC, Moritz N, Krupka C, Kozik JH, Lauber K, et al. SIRPalpha-antibody fusion proteins stimulate phagocytosis and promote elimination of acute myeloid leukemia cells. *Oncotarget* (2017) 8(7):11284–301. doi: 10.18632/oncotarget.14500
122. Gray MA, Stanczak MA, Mantuano NR, Xiao H, Pijnenborg JFA, Malaker SA, et al. Targeted glycan degradation potentiates the anticancer immune response in vivo. *Nat Chem Biol* (2020) 16(12):1376–84. doi: 10.1038/s41589-020-0622-x
123. Jang JK, Khawli LA, Canter DC, Hu P, Zhu TH, Wu BW, et al. Systemic delivery of chTNT-3/CpG immunoconjugates for immunotherapy in murine solid tumor models. *Cancer Immunol Immunother CII* (2016) 65(5):511–23. doi: 10.1007/s00262-016-1813-x
124. Merad M, Sugie T, Engleman EG, Fong L. In vivo manipulation of dendritic cells to induce therapeutic immunity. *Blood* (2002) 99(5):1676–82. doi: 10.1182/blood.v99.5.1676
125. Pulendran B, Banchereau J, Burkeholder S, Kraus E, Guinet E, Chalouni C, et al. Flt3-ligand and granulocyte colony-stimulating factor mobilize distinct human dendritic cell subsets in vivo. *J Immunol* (2000) 165(1):566–72. doi: 10.4049/jimmunol.165.1.566
126. Demaria S, Ng B, Devitt ML, Babb JS, Kawashima N, Liebes L, et al. Ionizing radiation inhibition of distant untreated tumors (abscopal effect) is immune mediated. *Int J Radiat Oncol Biol Phys* (2004) 58(3):862–70. doi: 10.1016/j.ijrobp.2003.09.012
127. Dela Cruz JS, Trinh KR, Morrison SL, Penichet ML. Recombinant anti-human HER2/neu IgG3-(GM-CSF) fusion protein retains antigen specificity and cytokine function and demonstrates antitumor activity. *J Immunol* (2000) 165(9):5112–21. doi: 10.4049/jimmunol.165.9.5112
128. van den Heuvel MM, Verheij M, Boshuizen R, Belderbos J, Dingemans AM, De Ruysscher D, et al. NHS-IL2 combined with radiotherapy: preclinical rationale and phase Ib trial results in metastatic non-small cell lung cancer following first-line chemotherapy. *J Transl Med* (2015) 13:32. doi: 10.1186/s12967-015-0397-0
129. Johnson EE, Yamane BH, Buhtoiarov IN, Lum HD, Rakhmilevich AL, Mahvi DM, et al. Radiofrequency ablation combined with KS-IL2 immunocytokine (EMD 273066) results in an enhanced antitumor effect against murine colon adenocarcinoma. *Clin Cancer Res Off J Am Assoc Cancer Res* (2009) 15 (15):4875–84. doi: 10.1158/1078-0432.CCR-09-0110
130. Zegers CM, Rekers NH, Quaden DH, Lieuwes NG, Yaromina A, Germeraad WT, et al. Radiotherapy combined with the immunocytokine L19-IL2 provides long-lasting antitumor effects. *Clin Cancer Res Off J Am Assoc Cancer Res* (2015) 21(5):1151–60. doi: 10.1158/1078-0432.CCR-14-2676
131. Rekers NH, Olivo Pimentel V, Yaromina A, Lieuwes NG, Biemans R, Zegers CML, et al. The immunocytokine L19-IL2: An interplay between radiotherapy and long-lasting systemic anti-tumour immune responses. *Oncoimmunology* (2018) 7(4):e1414119. doi: 10.1080/2162402X.2017.1414119
132. Morris ZS, Guy EI, Francis DM, Gressett MM, Werner LR, Carmichael LL, et al. In Situ Tumor Vaccination by Combining Local Radiation and Tumor-Specific Antibody or Immunocytokine Treatments. *Cancer Res* (2016) 76 (13):3929–41. doi: 10.1158/0008-5472.CAN-15-2644
133. Morris ZS, Guy EI, Werner LR, Carlson PM, Heinze CM, Kler JS, et al. Tumor-Specific Inhibition of In Situ Vaccination by Distant Untreated Tumor Sites. *Cancer Immunol Res* (2018) 6(7):825–34. doi: 10.1158/2326-6066.CIR-17-0353
134. Voeller J, Erbe AK, Slowinski J, Rasmussen K, Carlson PM, Hoefges A, et al. Combined innate and adaptive immunotherapy overcomes resistance of immunologically cold syngeneic murine neuroblastoma to checkpoint inhibition. *J Immunother Cancer* (2019) 7(1):344. doi: 10.1186/s40425-019-0823-6
135. Shusterman S, Naranjo A, Van Ryn C, Hank JA, Parisi MT, Shulkin BL, et al. Antitumor Activity and Tolerability of hu14.18-IL2 with GMCSF and Isotretinoin in Recurrent or Refractory Neuroblastoma: A Children's Oncology Group Phase II Study. *Clin Cancer Res Off J Am Assoc Cancer Res* (2019) 25(20):6044–51. doi: 10.1158/1078-0432.CCR-19-0798
136. Connor JP, Cristea MC, Lewis NL, Lewis LD, Komarnitsky PB, Mattiacci MR, et al. A phase 1b study of humanized KS-interleukin-2 (huKS-IL2) immunocytokine with cyclophosphamide in patients with EpCAM-positive advanced solid tumors. *BMC Cancer* (2013) 13:20. doi: 10.1186/1471-2407-13-20
137. Lieverse RIY, Van Limbergen EJ, Oberije CJG, Troost EGC, Hadrup SR, Dingemans AC, et al. Stereotactic ablative body radiotherapy (SABR) combined with immunotherapy (L19-IL2) versus standard of care in stage IV NSCLC patients, ImmunoSABR: a multicentre, randomised controlled open-label phase II trial. *BMC Cancer* (2020) 20(1):557. doi: 10.1186/s12885-020-07055-1
138. Eckert F, Schmitt J, Zips D, Krueger MA, Pichler BJ, Gillies SD, et al. Enhanced binding of necrosis-targeting immunocytokine NHS-IL12 after local tumour irradiation in murine xenograft models. *Cancer Immunol Immunother* (2016) 65(8):1003–13. doi: 10.1007/s00262-016-1863-0
139. Fallon J, Tighe R, Kradjian G, Guzman W, Bernhardt A, Neuteboom B, et al. The immunocytokine NHS-IL12 as a potential cancer therapeutic. *Oncotarget* (2014) 5(7):1869–84. doi: 10.18632/oncotarget.1853
140. Yang X, Zhang X, Fu ML, Weichselbaum RR, Gajewski TF, Guo Y, et al. Targeting the tumor microenvironment with interferon-beta bridges innate and adaptive immune responses. *Cancer Cell* (2014) 25(1):37–48. doi: 10.1016/j.ccr.2013.12.004

141. Liang Y, Tang H, Guo J, Qiu X, Yang Z, Ren Z, et al. Targeting IFNalpha to tumor by anti-PD-L1 creates feedforward antitumor responses to overcome checkpoint blockade resistance. *Nat Commun* (2018) 9(1):4586. doi: 10.1038/s41467-018-06890-y
142. Lan Y, Zhang D, Xu C, Hance KW, Marelli B, Qi J, et al. Enhanced preclinical antitumor activity of M7824, a bifunctional fusion protein simultaneously targeting PD-L1 and TGF-beta. *Sci Transl Med* (2018) 10(424):eaan5488. doi: 10.1126/scitranslmed.aan5488
143. Strauss J, Heery CR, Schlom J, Madan RA, Cao L, Kang Z, et al. Phase I Trial of M7824 (MSB0011359C), a Bifunctional Fusion Protein Targeting PD-L1 and TGFbeta, in Advanced Solid Tumors. *Clin Cancer Res Off J Am Assoc Cancer Res* (2018) 24(6):1287–95. doi: 10.1126/scitranslmed.aan5488

Conflict of Interest: The authors declare that the research was conducted in the absence of any commercial or financial relationships that could be construed as a potential conflict of interest.

Copyright © 2021 van den Bijgaart, Schuurmans, Fütterer, Verheij, Cornelissen and Adema. This is an open-access article distributed under the terms of the Creative Commons Attribution License (CC BY). The use, distribution or reproduction in other forums is permitted, provided the original author(s) and the copyright owner(s) are credited and that the original publication in this journal is cited, in accordance with accepted academic practice. No use, distribution or reproduction is permitted which does not comply with these terms.

frontiers in Immunology

REVIEW
published: 14 April 2021
doi: 10.3389/fimmu.2021.642316

Clinical Experience and Recent Advances in the Development of *Listeria*-Based Tumor Immunotherapies

Mariam Oladejo[1], *Yvonne Paterson*[2] *and Laurence M. Wood*[1]*

[1] *Immunotherapeutics and Biotechnology, Texas Tech University Health Sciences Center, Abilene, TX, United States,*
[2] *Microbiology, Perelman School of Medicine, University of Pennsylvania, Philadelphia, PA, United States*

The promise of tumor immunotherapy to significantly improve survival in patients who are refractory to long-standing therapies, such as chemotherapy and radiation, is now being realized. While immune checkpoint inhibitors that target PD-1 and CTLA-4 are leading the charge in clinical efficacy, there are a number of other promising tumor immunotherapies in advanced development such as *Listeria*-based vaccines. Due to its unique life cycle and ability to induce robust CTL responses, attenuated strains of *Listeria monocytogenes* (*Lm*) have been utilized as vaccine vectors targeting both infectious disease and cancer. In fact, preclinical studies in a multitude of cancer types have found *Listeria*-based vaccines to be highly effective at activating anti-tumor immunity and eradicating tumors. Several clinical trials have now recently reported their results, demonstrating promising efficacy against some cancers, and unique challenges. Development of the *Lm*-based immunotherapies continues with discovery of improved methods of attenuation, novel uses, and more effective combinatorial regimens. In this review, we provide a brief background of *Listeria monocytogenes* as a vaccine vector, discuss recent clinical experience with *Listeria*-based immunotherapies, and detail the advancements in development of improved *Listeria*-based vaccine platforms and in their utilization.

Keywords: *Listeria monocytogenes*, tumor immunotherapy, cancer vaccines, tumor antigens, vaccine vectors, clinical trials

OPEN ACCESS

Edited by:
Stephanie E. B. McArdle, Nottingham Trent University, United Kingdom

Reviewed by:
Rodabe N. Amaria, University of Texas MD Anderson Cancer Center, United States
Graham Robert Leggatt, The University of Queensland, Australia

***Correspondence:**
Laurence M. Wood
laurence.wood@ttuhsc.edu

Specialty section:
This article was submitted to Cancer Immunity and Immunotherapy, a section of the journal Frontiers in Immunology

Received: *15 December 2020*
Accepted: *26 February 2021*
Published: *14 April 2021*

Citation:
Oladejo M, Paterson Y and Wood LM (2021) Clinical Experience and Recent Advances in the Development of Listeria-Based Tumor Immunotherapies. Front. Immunol. 12:642316. doi: 10.3389/fimmu.2021.642316

INTRODUCTION

Tumor immunotherapy has gained rapid acceptance as an effective therapeutic strategy in the treatment of numerous malignancies. A multitude of methods to boost the anti-tumor immune response have been utilized including administration of purified immune system components to the use of microorganisms, such as attenuated bacteria and oncolytic viral particles, and have emerged as tools in the fight against cancer. While therapeutics that unleash the anti-tumor response by blocking inhibitory signaling pathways such as PD-1/PD-L1 have demonstrated the promise of tumor immunotherapy, immunotherapies that stimulate a specific anti-tumor response such as Sipuleucel-T, the first FDA-approved therapeutic cancer vaccine (1), have also provided a proof of

concept for that approach. In fact, numerous cancer vaccines are currently in different stages of clinical trials with promising results (2).

Due to the challenge of overcoming tolerance within the tumor microenvironment, considerable effort has been directed towards stimulating the immune system to mount a robust response against these cells by targeting tumor-associated antigens (TAAs) and tumor-specific antigens (TSAs) (2). Necessary characteristics of an effective cancer vaccine are proficient antigen delivery, limited impact on normal healthy tissue, and the ability to elicit a robust anti-tumor immune response. In this regard, *Listeria monocytogenes*, a facultative gram-positive bacterium is an attractive platform for development of cancer vaccines due its ability to activate and deliver tumor antigens selectively to antigen-presenting cells, resulting in a robust anti-tumor cell-mediated immune response (3). It is these attributes of *Lm* that has driven significant development, in both academia and industry, of *Lm*-based tumor immunotherapies with several candidates in various stages of clinical development (**Table 1**). Therefore, in this review, our focus will be on the use of *Lm* as a

TABLE 1 | Clinical Trials for *LC*-based Vaccines in Tumor Immunotherapy.

Trial Status	*Lm*-based Vaccine	Targeted Antigen(s)	Disease	Trial Phase	Enrollment	NCT Number*
Active	ADXS-NEO	Multiple personalized antigens	Multiple Cancers	Phase 1	5	NCT03265080
	ADXS-HPV	HPV16 E7	Cervical Cancer	Phase 3	450	NCT02853604
	ADXS-PSA	PSA	Prostate Cancer	Phase 1/2	51	NCT02325557
	ADXS-HPV	HPV16 E7	Cervical, Head and Neck Cancer	Phase 1/2	66	NCT02291055
	ADXS-HPV	HPV16 E7	Oropharyngeal Cancer	Phase 2	15	NCT02002182
	ADXS-HOT LUNG	Multiple antigens (hotspot mutations)	Non-Small-Cell Lung Cancer	Phase 1/2	74	NCT03847519
	CRS-207	Mesothelin	Pancreatic Cancer	Phase 2	63	NCT03190265
	CRS-207	Mesothelin	Pancreatic Cancer	Phase 2	70	NCT03006302
Completed, Withdrawn, Terminated	ADXS31-164	Her2	HER2-Expressing Solid Tumors	Phase 1/2	12	NCT02386501
	ADXS-HPV	HPV16 E7	Anal, Rectal Cancer	Phase 2	51	NCT02399813
	ADXS-HPV	HPV16 E7	Anal Cancer	Phase 1/2	11	NCT01671488
	ADXS-HPV	HPV16 E7	Cervical Cancer	Phase 1/2	25	NCT02164461
	ADXS-HPV	HPV16 E7	Cervical Cancer	Phase 2	54	NCT01266460
	CRS-207	Mesothelin	Pancreatic Cancer	Phase 2	303	NCT02004262
	ADU-623	EGFRvIII, NY-ESO-1	Astrocytic Tumors, Glioblastoma Multiforme, Anaplastic Astrocytoma, Brain Tumor	Phase 1	11	NCT01967758
	ANZ-100 (CRS-100)	N/A	Carcinoma and Liver Metastases	Phase 1	9	NCT00327652
	JNJ-64041809	Multiple prostate antigens	Prostate Cancer	Phase 1	26	NCT02625857
	ADXS-HPV	HPV16 E7	Cervical Intraepithelial Neoplasia	Phase 2	81	NCT01116245
	ADXS-HPV	HPV16 E7	Oropharyngeal Carcinoma	Phase 1	2	NCT01598792
	pLADD	Multiple personalized antigens	Colorectal Cancer	Phase 1	28	NCT03189030
	CRS-207	Mesothelin	Malignant Pleural Mesothelioma	Phase 1	60	NCT01675765
	CRS-207	Mesothelin	Malignant Pleural Mesothelioma	Phase 2	10	NCT03175172
	CRS-207	Mesothelin	Pancreatic Cancer	Phase 2	93	NCT02243371
	CRS-207	Mesothelin	Gastric, Gastroesophageal Junction, Esophageal Cancers	Phase 2	5	NCT03122548
	CRS-207	Mesothelin	Malignant Epithelial Mesothelioma, Pancreatic, Ovarian, Non-Small-Cell Lung Cancer	Phase 1	17	NCT00585845
	CRS-207	Mesothelin	Ovarian, Fallopian, Peritoneal Cancer	Phase 1/2	35	NCT02575807
	CRS-207	Mesothelin	Pancreatic Cancer	Phase 2	93	NCT01417000
	JNJ-64041757	EGFRvIII, Mesothelin	Non-Small-Cell Lung Cancer	Phase 1	18	NCT02592967
	JNJ-64041757	EGFRvIII, Mesothelin	Lung Cancer	Phase 1/2	12	NCT03371381
	ADXS-HPV	HPV16 E7	Non-Small-Cell Lung Cancer	Phase 2	124	NCT02531854
	JNJ-64041809	Multiple prostate antigens	Prostate Cancer	Phase 2	0	NCT02906605

**Additional clinical trial information for each study available at https://clinicaltrials.gov/ct2/home.*

tumor immunotherapy vaccine platform including a review of recent advancements in construction of improved *Lm*-based tumor immunotherapies, efficacy of *Lm*-based tumor immunotherapies in combination with other anti-cancer treatment modalities, and the current clinical experience with *Lm*-based tumor immunotherapies.

DEVELOPMENT OF INACTIVATED AND ATTENUATED BACTERIA AS TUMOR IMMUNOTHERAPEUTICS

Evidence that bacteria can harness the immune system to elicit therapeutic efficacy against malignancies dates to the early twentieth century. While William Coley laid a solid foundation for modern bacterial immunotherapy, there are other notable scientists whose work predated even his discoveries. In 1851, Belgian surgeon Didot pioneered the use of a syphilis vaccination to treat inoperable cancer (4). In 1868, Busch, a German scientist, reported the efficacy of erysipelas infection in treatment of sarcoma in a crudely performed clinical study (5–7). Two decades later in 1882, Friedrich Fehleisen discovered *Streptococcus pyogenes* to be the causative agent of erysipelas and noticed that infection with this bacterium caused transplanted tumors to melt away (5, 6, 8). It was armed with these observations and the serendipitous recovery of a German immigrant with an inoperable neck sarcoma, that William Coley embarked on the challenging but foundational work of tumor immunology (9). His belief that a component or "factor" from the microbes, rather than the whole live microorganism, is responsible for the oncolytic activity he observed led to the creation of his Coley toxins, a mixture of heat killed *Streptococcus pyogenes* and *Serratia mersacems* (9). In fact, this novel therapy was reported to result in partial or complete remissions in many difficult-to-treat patients (10, 11). However, given our limited understanding of immunology at the time, the mechanisms that would explain the efficacy of this strategy were unclear, thereby limiting the continued development of Coley's toxins. Eventually, the advent of radiotherapy and chemotherapy that could be more easily standardized relegated this novel therapeutic strategy, comprised of killed or inactivated bacteria, to the background. As our understanding of the immune system has matured, there has been renewed interest in the use of attenuated, inactivated, and killed bacteria to stimulate anti-tumor immunity.

USE OF *LISTERIA MONOCYTOGENES* AS A TUMOR IMMUNOTHERAPEUTIC TO ELICIT TUMOR SPECIFIC IMMUNITY

Unlike the approach taken by Coley, whose toxins non-specifically resulted in an anti-tumor response, current approaches focus on achieving complete and durable antitumor immunity through induction of tumor-specific immune responses. To elicit this tumor-specific immunity, the strategy employed by most tumor immunotherapies is to activate cytotoxic T lymphocytes (CTLs) that recognize peptides from tumor-specific and/or tumor-associated antigens presented on MHC Class I and target tumor cells for lysis (12). In fact, CTL-mediated tumor cell destruction occurs commonly in a process called immunosurveillance, in which the immune system recognizes and eliminates malignant cells prior to clinical detection (13). Unfortunately, some malignant cells can escape immune-mediated destruction and develop into a clinically relevant tumor. The tumors that have escaped immunosurveillance have been able to achieve this, in part, by fostering the development of an immunosuppressive microenvironment that impedes the function and survival of responding lymphocytes, including cytotoxic T lymphocytes. In order to overcome this immunosuppressive microenvironment, various strategies have been employed to enhance the activation and mobilization of CTLs in the tumor environment such as the use of oncolytic viruses, dendritic cell vaccines, adoptive cell therapy, and microbial vectors for the targeting of TAAs (14–16). Each of these strategies has their own advantages and disadvantages. Aside from the important consideration of toxicity in the use of oncolytic viruses, off target viral replication and development of neutralizing antibodies may prevent recurrent use of this strategy. Bacterial vectors such as *Streptococcus pyogenes*, *Clostridium novyi*, *Salmonella enterica*, and *Listeria monocytogenes* (17–20), are all vectors that have been used in cancer immunotherapy and do not pose this significant drawback of preexisting neutralizing immunity. However, what differentiates *Listeria monocytogenes* from its vaccine peers and makes it a superior vector for delivery of cancer antigens is its unique life cycle. *Lm* is readily taken up by macrophages in the course of an infection and, once within a phagocytic compartment, expresses and secretes a cytolysin, Listeriolysin O (LLO) (21). LLO, along with bacterial phospholipases, disrupts the integrity of the phagosome and allows *Lm* to escape into the cytosol and elude destruction in the phagolysosome (22). Once in the cytosol, *Lm* proliferates and secretes additional virulence factors that propel it within the cell and into adjacent cells in order to propagate the infection (23). It is this life cycle that makes *Lm* an ideal candidate to deliver antigen to both the MHC I and II pathways, activating $CD4^+$ T cells and, most importantly for tumor-lytic responses, cytotoxic $CD8^+$ T cells (24). In fact, infection with *Lm* elicits a robust and long-lasting immunological memory response that provides protection against infection upon future exposure to the pathogen (25–27).

In addition to its unique life cycle, *Lm* affords a number of advantages as a vector for tumor immunotherapy. Previous studies found that antigens encoded by *Lm* constructs are more efficiently delivered to the protein processing and presentation machinery than those encoded by other bacterial vectors (28). Further, *Lm* vectors have the ability to break immunologic tolerance, *via* reduction of immunosuppressive myeloid-derived suppressor cells (MDSCs) and regulatory T cells (Tregs) within the tumor microenvironment. Finally, in addition to selective uptake in the spleen and liver of infected subjects, *Lm* displays a specific tropism for primary and metastatic tumors (29, 30). These attractive features, including the ease of manipulation and attenuation of this organism, have been harnessed by various

groups in development of attenuated strains of *Lm*, expressing a wide variety of tumor antigens. We have extensively discussed the various ways by which these attenuated strains are generated, and the antigens that have been delivered by this therapeutic platform (31). Described below, are the more recent *Lm* construction trends as well as the use of these various constructs in combination therapy depicted in **Figure 1** that are currently being tested in various preclinical and clinical trials (**Figure 1**).

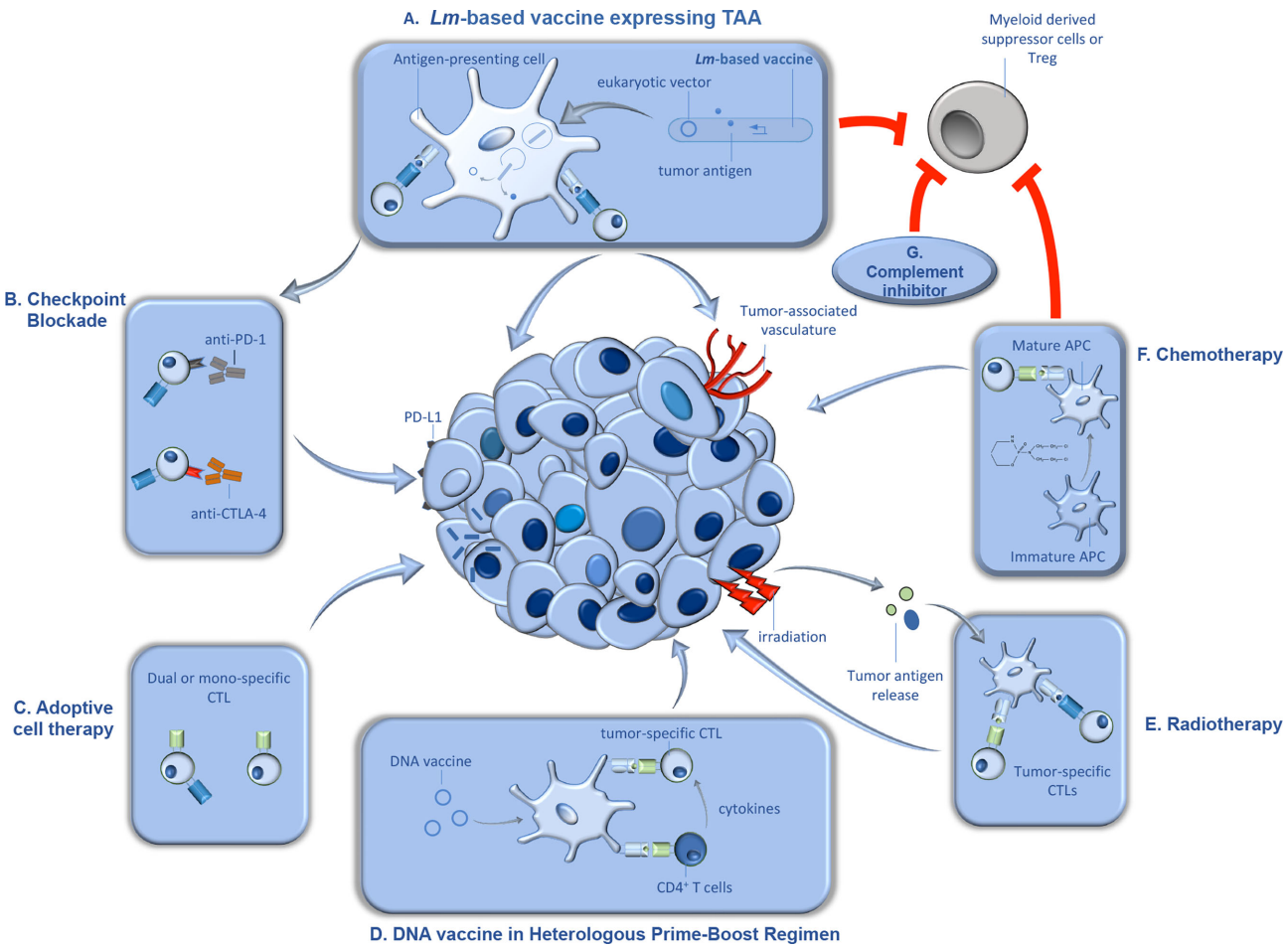


FIGURE 1 | Synergistic therapeutic approaches with *Lm*-based vaccines in tumor immunotherapy. *Lm*-based vaccines have found therapeutic success in preclinical models of cancer for decades, and recent studies demonstrated significant promise for this type of active tumor immunotherapy in clinical trials. Further, recent studies suggest that the anti-tumor efficacy of *Lm*-based vaccines can be significantly improved when utilized in combination with synergistic anti-cancer therapeutics. In this figure, we detail some of the anti-cancer therapeutics that demonstrated efficacy in combination *Lm*-based vaccines along with their proposed mechanism(s) of action. **(A)** Upon administration, attenuated *Lm* vaccines infect antigen presenting cells in secondary lymphoid organs and gain entry to the cytosol, wherein they produce and secrete tumor antigen and/or release eukaryotic expression vectors encoding for tumor antigen. Once delivered by *Lm*, the tumor antigens go through processing and presentation to naïve tumor-specific $CD4^+$ and $CD8^+$ cytotoxic T lymphocytes (CTLs). Tumor-specific CTLs, activated through the action of *Lm*-based vaccines, migrate to the tumor microenvironment (TME) and lyse tumor cells and/or cells associated with the tumor vasculature. Importantly, *Lm*-based vaccines can also reduce immunosuppression within the TME by reducing tumor-associated MDSCs and Tregs. **(B)** Upon continuous activation, tumor-specific CTLs can become exhausted, characterized by the upregulation of inhibitory molecules such as programmed cell death protein 1 (PD-1) and cytotoxic T-lymphocyte-associated protein 4 (CTLA-4). Antibody-mediated blockade of inhibitory molecules results in enhanced T cell function and synergy with *Lm*-based vaccine anti-tumor responses. **(C)** Dual or mono-specific adoptively transferred CTLs targeting both tumor antigens and/or *Lm*-derived antigens work in concert with *Lm*-based vaccines, delivered intratumorally, through increasing the breadth of the anti-tumor T cell response. **(D)** *Lm*-based vaccines have also been found to be effective in heterologous prime-boost approaches. DNA-based tumor vaccines, used as either prime or boost in a heterologous prime-boost vaccination schedule with *Lm*-based vaccines, induce robust expansion of Th1 helper T cells that produce cytokines in support of responses by tumor-specific CTLs. **(E)** Further, radiation can synergize with *Lm*-based vaccines, in part, by causing direct tumor death, resulting in release of tumor antigens which are processed and presented by APCs to tumor-specific T cells. **(F)** Chemotherapeutic agents such as cyclophosphamide can also synergize with *Lm*-based vaccines, in part, by facilitating maturation of APCs. However, cyclophosphamide can also reduce immunosuppressive cell types, Tregs and MDSCs, in the TME allowing for improved anti-tumor efficacy by the anti-tumor responses induced by *Lm*-based vaccines. **(G)** Similarly, inhibition of complement signaling can synergize with *Lm*-based vaccines, in part, through limiting recruitment of MDSCs and Tregs to the TME.

CLINICAL EXPERIENCE WITH *LM*-BASED VACCINES FOR CANCER

With the clinical experience of *Lm*-based vaccines in oncology going well beyond a decade, the promise and further challenges are now being realized regarding their place in the future oncologists toolkit. Below, we summarize clinical studies that have recently published their findings for an array of cancers. Importantly, these studies only scratch the surface of clinical studies regarding the efficacy of *Lm*-based vaccines for cancer that are currently underway or not yet peer-reviewed and published as summarized in **Table 1**.

HPV-Associated Cancers

As the development of *Lm*-based vaccine vectors matured in the late 1990's, the focus of constructing novel vectors progressed from those that targeted model tumor antigens, in order to better understand the platform, to the incorporation of clinically relevant tumor antigens. One of the first *Lm*-based vaccines to incorporate a clinically relevant tumor antigen targeted Human papillomavirus (HPV)-associated cancers (3). While most individuals clear infections with HPV, in certain individuals that are unable to clear the infection, chronic infection with high-risk strains of HPV, such as HPV 16 and 18, can increase their risk of developing cancer (32). Infection with high-risk HPV is particularly problematic in women as it can result in carcinoma of the cervix (33). However, high-risk strains of HPV are also associated with head and neck cancers among others (34). In HPV-associated cancers, constitutive expression of the HPV oncoproteins, E6 and E7, is required to maintain the malignant phenotype (35). Therefore, this necessary expression by the tumor cells, and the lack of central tolerance to these viral antigens, make these oncoproteins particularly attractive targets for *Lm*-based tumor immunotherapy.

In the initial preclinical study documenting the development of *Lm*-based vaccines targeting HPV-associated cancers, there were two vaccines constructed, *Lm*-E7 and *Lm*-LLO-E7 (3). While *Lm*-E7 expressed and secreted HPV 16 E7, generated E7-specific CTLs, and demonstrated anti-tumor efficacy, this was insufficient to cure a majority of mice with established tumors expressing E7. However, administration with an *Lm* construct that expressed and secreted HPV 16 E7 genetically fused to a truncated non-hemolytic form of Listeriolysin O (tLLO) did result in complete eradication of E7-expressing tumors in all experimental mice. The adjuvant-like properties of tLLO have since been elucidated and the vast majority of *Lm*-based vaccines in clinical and preclinical testing genetically fuse the tumor antigen to either tLLO or a truncated form of another *Lm*-derived protein with adjuvant-like properties, ActA (36–39).

The first clinical use of *Lm* -LLO-E7 (also known as ADXS-HPV and as ADXS11-001), or any *Lm*-based therapy in cancer patients, was a Phase I clinical trial in women with cervical cancer that had failed previous front-line therapy including surgery, chemotherapy, and radiation (40). The patients were enrolled into three groups of 5 with each group receiving two intravenous doses ranging from 10^9 colony-forming units (CFU) of *Lm*-LLO-E7 to 10^{10} CFU given 22 days apart. As would be expected with intravenous (i.v.) administration of *Lm*, all of the patients experienced adverse events (AE) including fever, chills, nausea, and vomiting with 40% experiencing severe grade 3 AEs but none of the patients experienced a life-threatening grade 4 adverse event (AE) due to the treatment. Dose-limiting toxicities occurred in the group receiving the highest dose with one patient requiring antibiotics to mitigate a fever. In terms of efficacy, nearly half of the patients were reported to have stable disease with one receiving a possible partial response and the median overall survival was 347 days. These results warranted further investigation as they demonstrated that *Lm*-based vaccines have a safety profile that is likely more favorable than salvage chemotherapy and efficacy that may improve upon current treatment modalities.

Following the promising safety profile of *Lm*-LLO-E7 observed in the Phase I clinical trial, two Phase II trials were commenced to further characterize its safety and efficacy in patients with recurrent cervical cancer. In the first trial, 109 patients were separated into two groups with one receiving only 10^9 CFU *Lm*-LLO-E7 and the second group receiving *Lm*-LLO-E7 along with cisplatin (41). While the *Lm*-LLO-E7 group received three i.v. administrations each separated by roughly one month, the *Lm*-LLO-E7 + cisplatin group received their initial dose of *Lm*-LLO-E7 and then waited 4 weeks to receive their 5 weekly doses of cisplatin and finally the second dose of *Lm*-LLO-E7. The rationale for this staggered administration of *Lm*-LLO-E7 and cisplatin was to promote treatment synergy while limiting any possible suppressive effect of cisplatin on the immune response to *Lm*-LLO-E7. However, the addition of cisplatin to *Lm*-LLO-E7 did not have a significant impact on efficacy. The overall response rates (ORR) were comparable between the groups with an ORR of 17.1% for the *Lm*-LLO-E7 group and 14.7% for the *Lm*-LLO-E7 +cisplatin group. Similarly, median overall survival (OS) were not statistically significant with 8.28 and 8.78 months in the *Lm*-LLO-E7 and *Lm*-LLO-E7+ cisplatin groups, respectively. In terms of safety, the difference between these two arms was more pronounced with more AEs observed in the *Lm*-LLO-E7+cisplatin group (429) than the *Lm*-LLO-E7 alone group (275) but most of these AEs were mild to moderate in severity (80.4%). These results informed the second Phase II trial for cervical cancer funded by the NCI, wherein, there was only a single arm receiving three doses of *Lm*-LLO-E7 only in the first stage, with some patients receiving an additional three doses in a second stage (42). Treatment-related AE types and frequencies were similar to previous trials with nearly all patients experiencing at least one and 38% experiencing a grade 3 AE. In addition, 4% of patients (2) experienced a grade 4 AE that consisted of sepsis and cytokine release syndrome. In terms of efficacy, the median OS was 6.1 months and the 12-month OS rate was 38% which met the study goal of 35%, a dramatic improvement on the historical 12-month OS of 21% in a similar patient population. This trial along with other ADXS-HPV trials were placed on temporary hold when evidence of listeriosis was observed in a patient 31 months after the last administration. This was believed to be due to persistence

associated with biofilm formation on prosthetic material at recent fracture sites in the patient (43). These Phase II trials demonstrated that *Lm*-LLO-E7 is tolerated relatively well in comparison to other treatment modalities and has significant promise to extend the lifespan of a poorly treated patient population.

The results from the Phase I and Phase II clinical trials of *Lm*-LLO-E7 in cervical cancer resulted in the commencement of a Phase III clinical trial, AIM2CERV (NCT02853604). While AIM2CERV is still ongoing and results have not yet been published, the recruitment of new patients has been halted by its sponsor, Advaxis Inc., in order to allocate resources to the development of other promising upcoming vaccine platforms. However, clinical trials are still ongoing with *Lm*-LLO-E7 to evaluate the efficacy of *Lm*-LLO-E7 in other HPV-associated cancers, but the halt of AIM2CERV suggests it may take longer than previously anticipated before possible FDA approval and wide availability of *Lm*-LLO-E7.

In addition to cervical cancer, a recent study reported promising results with *Lm*-LLO-E7 in another HPV-associated cancer, anal cancer (44). In this Phase 1/2 clinical trial, patients with non-metastatic anal cancer were administered *Lm*-LLO-E7 once before and three times after receiving chemoradiation consisting of mitomycin C, 5-fluorouracil, and daily image-guided radiation therapy. While most patients experienced only low-grade AEs due to the *Lm*-based vaccine, two patients did experience grade 3 chills/rigor but all AEs were managed and resolved within 24 hrs. The clinical response was also highly promising as all 9 patients experienced complete responses by trial end (42 months) with only one patient progressing to metastatic disease six months post-trial. This study suggests *Lm*-LLO-E7 may have a promising future as part of a front-line therapeutic regimen in the treatment of HPV-associated cancers beyond cervical cancer.

Pancreatic Cancer

Pancreatic ductal cell carcinoma (PDAC) is one of the most challenging malignancies to treat with the most effective current treatments being surgery and chemotherapy (45). Unfortunately, while the advancement of immunotherapy in oncology, particularly immune checkpoint inhibition (ICI), has brought about significant survival benefits to many cancer patients, PDAC patients have not been afforded the same benefit (46). PDAC expresses TAAs such as mesothelin but is poorly infiltrated by T cells and is considered an immunologically "cold" tumor (47–49). As *Lm*-based vaccines have been found to modulate the tumor microenvironment (TME) and make it more amenable to anti-tumor immune responses (50), significant effort has been expended to determine the promise of this vaccine platform in the treatment of PDAC. To target mesothelin-expressing PDAC, an *Lm*-based vaccine was constructed that expressed and secreted human mesothelin genetically fused to the first 100 residues of ActA, ActAN100, in a highly attenuated strain of *Lm*, LADD (51). This mesothelin-targeting *Lm*-based vaccine (*Lm*-Mesothelin, CRS-207) was initially brought into the clinic in a Phase I trial with several cancer types that all express mesothelin, including PDAC (52). Study subjects received at least one i.v. administration of CRS-207 at a particular dose ranging from 10^8 to 10^{10} CFUs. The vaccine was generally well tolerated with the majority of patients experiencing grade 2 or less AEs. However, a number of patients experienced grade 3 AEs and at least 2 grade 4 AEs at the highest doses. Therefore, the maximum tolerated dose was determined to be 10^9 CFUs. While the study was not powered to assess efficacy, 37% of patients survived beyond 15 months. Interestingly, the patients with longer survival had a more robust T cell response to the vaccine.

Due to the promising data from the Phase I clinical trial, three separate Phase II clinical trials were commenced to evaluate the efficacy and safety of CRS-207 in PDAC. The first Phase IIa trial with 90 patients assessed the efficacy of cyclophosphamide (Cy), a chemotherapeutic drug that limits peripheral tolerance, in combination with GVAX, a tumor vaccine consisting of irradiated allogeneic PDAC cells lines secreting GM-CSF (Arm B) or a heterologous prime boost regimen with Cy/GVAX with CRS-207 (Arm A) (53). The heterologous prime boost regimen, Cy/GVAX+CRS-207, was superior to the Cy/GVAX only treatment regimen, in terms of median OS (6.1 vs. 3.9 months) and in terms of 12-month survival (24% vs. 12%). In fact, mesothelin-specific $CD8^+$ T cell responses were observed earlier with Cy/GVAX+CRS-207 than Cy/GVAX only suggesting that the expected synergy of the prime boost approach was realized in terms of both efficacy and anti-tumor immune response. The most common AEs were associated with injection site reactions but a majority of patients also experienced fever, chills, and gastrointestinal symptoms. The most prevalent severe AE (grade 3-4) was lymphopenia that was observed in 44% of patients. However, one patient did develop systemic listeriosis 12 days post administration that resolved after receiving i.v. penicillin (54). The promising results demonstrate the ability of an *Lm*-based vaccine to synergize with another vaccine strategy, in this case Cy/GVAX, in a heterologous prime boost regimen, thereby, providing strong rationale for the continued exploration of the ability of immunotherapy to increase survival in PDAC.

Unlike the first Phase IIa clinical trial with CRS-207, the second trial (ECLIPSE study) included groups to assess the therapeutic efficacy of CRS-207 by itself in comparison to standard-of-care chemotherapy and a CRS-207+Cy/GVAX combination treatment regimen (55). The primary group in this study was patients given each of these interventions as a third+ line therapy. In this population, the median OS of chemotherapy alone was 4.6 months vs. 3.7 months with the Cy/GVAX+CRS-207 regimen. Interestingly, the CRS-207 alone treatment group had a median OS of 5.4 months suggesting some promise as a therapy in PDAC but these differences in median OS were not significant between any of the treatment groups. In a smaller group of patients when each of these treatment regimens were given as a second line therapy, there was no significant difference in median OS but the chemotherapy treatment arm had the highest median OS. The lower median OS in this trial compared to the first Phase II trial with CRS-207 was likely due to the patients in this trial having more advanced disease. As with the previous CRS-207 studies, treatment related severe AEs were

minimal with the majority of AEs being low-grade. This trial again demonstrates the challenges of demonstrating efficacy in PDAC and suggested that a different approach may be required to demonstrate the promise of *Lm*-based vaccines in this disease.

As the previous Phase II studies with CRS-207 suggested, a new therapeutic approach would be required to demonstrate that it is capable of improving PDAC patient survival. As ICI therapy has been found to synergize with *Lm*-based vaccine approaches preclinically, a third Phase II trial with CRS-207 was conducted in PDAC patients that included anti-hPD-1 blockading antibody, nivolumab, along with Cy/GVAX+CRS-207 (Arm A) in comparison to Cy/GVAX+CRS-207 alone (Arm B) (56). The median OS for each arm was similar at 5.9 and 6.1 months for Arm A and Arm B, respectively. While the addition of nivolumab did not appear to improve median OS in patients receiving Cy/GVAX+CRS-207, some other parameters such as disease control rate and 12- and 18-month survival were improved beyond Cy/GVAX+CRS-207 alone. Interestingly, in the patients receiving nivolumab, long-term survival was correlated with increased $CD8^+$ T cell infiltration into tumors and a reduction in likely immunosuppressive tumor-associated myeloid cells. However, nivolumab treatment did result in more AEs in patients but these were as expected in ICI therapy with 2.2% of patients, all in Arm A, discontinuing treatment due to treatment-related AEs. This study again highlights the enormous challenges of improving survival in PDAC patients. While the Phase II clinical studies with CRS-207 in PDAC did not meet their primary efficacy endpoints, they have advanced our knowledge and experience with *Lm*-based vaccines in a particularly difficult-to-treat patient population that will hopefully inspire additional studies with improved treatment regimens.

Malignant Pleural Mesothelioma

Malignant pleural mesothelioma is a rare disease caused by exposure to asbestos with a high mortality rate (57). The previous first line therapy for MPM was pemetrexed with cisplatin that afforded patients a median OS of 14.1 months, until the recent approval of nivolumab and ipilumimab that raised median OS to 18.1 months in the Checkmate-743 Phase III trial (58, 59). The clinical success of ICI therapy in MPM suggests that it is a disease that is receptive to immunotherapies such as *Lm*-based vaccines. As CRS-207 targets mesothelin, a tumor antigen highly expressed in MPM, a Phase I clinical trial was conducted to determine safety and tolerability of CRS-207 in combination with pemetrexed and cisplatin. In contrast to its efficacy on PDAC, 89% of patients receiving CRS-207 in combination with pemetrexed and cisplatin experienced tumor reduction (60). While the median OS was comparable to chemotherapy at 14.7 months, the OS rate at 1 year of 64.9% was more comparable to ICI-treated MPM patients. As a correlate to this promising efficacy, percentages of functional $CD8^+$ T cells increased and immunosuppressive M2 macrophages decreased in tumors over the course of treatment. AEs were similar to previous trials with CRS-207 and there was no additive effect with the addition of chemotherapy. While only a Phase I study with less than 40 patients, the promising results provide a strong rationale for the continued assessment of CRS-207 in MPM and possibly in combination with the recently FDA-approved ICI therapeutics to determine any synergistic potential.

Non-Small Cell Lung Cancer

Lung cancer is responsible for more deaths worldwide than any other form of cancer with non-small cell lung cancer (NSCLC) accounting for the vast majority (61–63). Effective therapeutic options are lacking for NSCLC as even ICI therapy provides relatively limited benefits compared to other cancers, with a 5-year survival of 15-25% (64, 65). Due to the previously reported ability of *Lm*-based immunotherapies to reduce immunosuppression in the TME and activate tumor-specific immunity, a Phase Ib/2 trial was commenced to determine the safety and effectiveness of *Lm*-based vaccination alone or *Lm*-based vaccination in combination with ICI in NSCLC (66). The bivalent *Lm*-based vaccine utilized in these trials, JNJ-75, expresses NSCLC-associated antigens, both EGFRvIII and mesothelin, on the LADD vector platform, and was previously developed by Aduro Biotech as ADU-214 (31). As a monotherapy, 18 patients received JNJ-75 administered twice i.v. in either 10^8 or 10^9 CFUs/dose. Each dosage of JNJ-75 was well tolerated with no dose-limiting toxicity, and the expected pyrexia and chills with duration no longer than 24hrs. Similar safety data was seen in the combination study where all 12 patients received 10^9 CFUs of JNJ-75 along with 240mg nivolumab. In total, only 6 treatment-related serious AEs (grade 3 or higher) were observed and bacterial shedding was not found in blood, fecal, or urine samples at 4hrs, 2 days, and 4 days-post administration. In terms of clinical response, 44% of patients had stable disease as the best overall response while one patient had a partial response in a target lesion identified at the beginning of the trial but still had overall disease progression. In the combination trial, the best overall response was stable disease in 4 patients but the trial was stopped early and efficacy data was limited. In the monotherapy study, levels of serum proinflammatory cytokines were elevated and activation of T cells and NK cells was increased at 24hrs post administration with cytokine levels returning to baseline at 48hrs. Further, the magnitude of mesothelin-specific T cells responses was limited compared to recall responses to tetanus toxoid and influenza. While stable disease was observed in some patients and there was clear evidence of inflammatory responses, the overall lack of significant clinical benefit to patients suggests that JNJ-75 alone or in combination with nivolumab will not proceed to further with clinical development.

Osteosarcoma

Osteosarcoma is a highly aggressive form of cancer that overwhelmingly affects children and primarily manifests in the long bones prior to metastasizing to vital organs (67). The standard of care currently consists of resection of the lesion or amputations of the affected limb and chemotherapy (68). However, many patients experience recurrence of the disease due to the seeding of micrometastases prior to primary tumor resection (69). Much like in breast cancer, a proportion of pediatric osteosarcoma patients have lesions that highly express the EGFR family receptor, HER2/neu, that correlates with poor prognosis (70). Importantly, a Phase Ib clinical trial

has recently completed utilizing a human Her2/neu-targeting *Lm*-based vaccine, ADXS31-164, for adult patients with Her2/neu-expressing tumors (NCT02386501). This vaccine has now been licensed for development in the pediatric osteosarcoma setting by OS Therapies in conjunction with the NCI Children's Oncology Group. While human clinical studies have not yet begun targeting human osteosarcoma with *Lm*-based immunotherapy, the promise of this therapeutic approach in humans may be predicted by the recently completed and published results from clinical trials in canines for osteosarcoma utilizing ADXS31-164. Canine osteosarcoma is highly aggressive much like the human disease in terms of prognosis and treatment (71). In fact, a significant proportion of canine osteosarcomas overexpress the tumor antigen Her2/neu much like their human counterparts (70, 72). Since human Her2 and canine Her2 have >90% homology and the *Lm*-based vaccine targeting human Her2/neu, ADXS31-164, had already been developed and successfully tested in mice, a small Phase I clinical trial consisting of 18 client-owned dogs was performed to determine the safety, tolerability, and efficacy of the *Lm*-based vaccine targeting Her2/neu, ADXS31-164, in canine osteosarcoma (73, 74). For this trial, dogs were treated with three doses of ADXS31-164 once every three weeks following standard of care amputation and carboplatin adjuvant chemotherapy. AEs were generally low-grade, transient, and independent of ADXS31-164 dosage. Strikingly, the 1, 2, and 3-year survival rates for ADXS31-164 treated dogs were 77.8%, 67%, and 56%, respectively. This is in stark contrast to dogs in a historical control group treated with standard of care amputation and adjuvant chemotherapy with 1, 2, and 3-year survival rates of 55%, 28%, and 22%, respectively. In addition to increased survival, Her2-specific T cell responses were also observed in 83% of the dogs in the study. Based on the promising results of this study, ADXS31-164 was granted conditional approval by the USDA and the study was continued and expanded. In fact, a subsequent study of ADXS31-164 consisting of 50 dogs with osteosarcoma was recently reported. The study protocol mimicked the early Phase I trial and the observed AEs generally confirmed the low-grade and transient nature of those reported in the first study (75). However, 4 dogs did develop listeriosis, a finding not observed in the initial trial. The severity of the listeriosis varied between the animals with some requiring antibiotic treatment. One animal presented with an extrapleural mass that cultured positive for ADXS31-164 three weeks after receiving the final vaccine dose, and required surgery to remove the chest abscess (76). Unfortunately, the study was unable to report efficacy data due to 30% of the dogs discontinuing treatment, an inability to complete follow-up evaluations, and concurrent or subsequent therapies after ADXS31-164 treatment that complicated analysis.

Future of *Listeria* in the Clinic

Clinical trials continue for a number of *Lm*-based vaccines (**Table 1**). However, with the discontinuation of the AIM2CERV Phase III trial, it may take longer than previously anticipated before an *Lm*-based vaccine is widely available for use in oncology. While the safety profile of *Lm*-based vaccines has been very tolerable in comparison to chemotherapy and other forms of immunotherapy, the recent rare reports of listeriosis after final dosing in both humans and dogs may be a challenge in a small number of patients going forward (43, 76). As current trials already incorporate a regimen of antibiotics subsequent to dosing with *Lm*-based vaccines, this regimen may need to be modified and extended in order to mitigate the possible risk of listeriosis. Further, development of even more attenuated vaccine strains described below may help further mitigate this risk and, along with the combination of synergistic therapies, may spur greater clinical success for future *Lm*-based vaccines.

NEW TRENDS IN *LM* VACCINE CONSTRUCTS

For more than two decades, *Listeria monocytogenes* has proven itself to be a highly promising vector for tumor immunotherapy in numerous preclinical studies (31). While the currently available platforms have demonstrated promising performance in clinical trials, none has yet been approved for clinical use by the FDA, thus there is continued interest in engineering newer, safer and more effective *Listeria monocytogenes*-based vaccine platforms (77–79). In addition, while numerous clinical studies have confirmed an excellent safety profile for *Lm*-based vaccines in healthy individuals and oncology patients, there have been some concerns regarding the ability of current clinical strains to persist in patients (40, 43, 52, 66, 76, 80). Described below are the recent advances at overcoming these challenges and improving the safety and efficacy of *Lm*-based immunotherapies

Enhanced Attenuation Methods

While infection with the virulent wild-type strain of *Listeria monocytogenes* can lead to the formation of robust memory T cell responses, several studies have found that attenuated strains of *Lm* actually result in improved immune memory and protective responses (81, 82). The methods utilized to attenuate *Lm* primarily revolve around deletion of non-essential virulence genes that allow for sufficient infectivity and antigen production but limit the potential for severe infection, a necessary concern when the patient population for tumor immunotherapy may already suffer from immune deficiency (83). In fact, the *Lm*-based vaccines currently or previously in clinical trials have all contained some form of deletion of virulence genes such as *actA* or *prfA* (31). While the safety of these attenuated *Lm* platforms has been demonstrated in multiple trials, further modifications that enhance attenuation and improve therapeutic efficacy of *Lm*-based vaccines continue.

One such advancement is the development of suicidal strains that are programmed to lose viability once the antigenic cargo has been delivered to an antigen-presenting cell (84). The need for these suicidal vaccines stems from instances where, despite attenuation, persistence of *Lm* vaccine constructs has been observed following the administration of live *Lm* vaccines (43, 85). Early work in the development of a *Listeria* suicide strain utilized an *Lm* construct that produced a phage lysin under the

control of the ActA promoter so that the suicide switch would be engaged once *Lm* gained entry to the cytosol of an APC and delivered its cargo (84). A similar approach by Souders et al., that we discuss further in 1.4.4, found a dramatic reduction in death of infected APCs by a suicidal strain of *Lm* while still retaining the ability to successfully deliver a eukaryotic plasmid for expression of tumor antigen (79). Recently, this concept of an *Lm*-based suicidal vector for tumor immunotherapy was advanced with the development of a new vector, *Listeria monocytogenes* recombinase-induced intracellular death (*Lm*-RIID). This strain features Aduro's live-attenuated double deletion *Lm* vaccine (LADD) that has been further modified by the introduction of loxP sites adjacent to essential genes, as well as a gene for Cre recombinase that is inserted under the *actA* locus (78). In bacterial growth media, *Lm*-RIID proliferates and functions normally, however, once it infects host cells and gains entry to the cytosol, Cre-recombinase is produced and excises the essential genes flanked by loxP sites. The loss of these essential genes ultimately results in loss of viability for the bacterium, while still allowing sufficient time for it to produce and secrete the necessary tumor antigens within the cytosol. This construct has demonstrated efficacy similar to the LADD platform in mouse tumor models, inducing a robust anti-tumor immune response, and a substantial reduction in tumor burden. In combination with anti-PD-1 therapy, it conferred maximal protection against tumor growth and regression in a lung metastasis model. Perhaps the most interesting characteristic about this platform is its excellent safety profile. Although the enhanced attenuation of *Lm*-RIID did result in reduced immunogenicity in direct comparison to existing platforms, it was shown to be more immunogenic than the killed but metabolically active (KBMA) strain and similarly effective to the live, attenuated, double-deleted (LADD) platform (78). Of note, also, is the recombinant suicidal *Listeria monocytogenes* strain (*rsΔ2*) described by Sinha et al. (77) that undergoes autolysis upon entry into the cytosol but produces and delivers both protein antigen and a eukaryotic expression vector encoding the same antigen to an infected cell. This novel suicidal *Lm* vaccine induced both humoral and cell cytolytic responses to the model antigen, ovalbumin, when delivered both intramuscularly and orally. Importantly, delivery of only the eukaryotic expression plasmid encoding for the antigen by *rsΔ2* resulted in blunted responses compared to the vector that delivered *Lm*-produced protein antigen and the eukaryotic expression vector. These novel suicidal *Lm*-based vaccine vectors demonstrate that, while improvements may still be desired to match their anti-tumor efficacy to previously-developed live *Lm*-based vectors, their effectiveness when given orally, enhanced level of safety, and their greater level of versatility to deliver both protein and nucleic acid cargo demonstrates great promise for them as clinical vectors for tumor immunotherapy.

Listeria as a Targeted Radionuclide Therapeutic (TRT) Platform

The combination of *Lm*-based immunotherapy with radiotherapy has shown promise as a synergistic treatment regimen in a preclinical model for melanoma (86). However, there are still challenges to discover the most efficient sequence of treatment administration for both the *Lm* vaccine and radiotherapy, i.e. concurrently or sequentially, and the off-target effects of radiotherapy on healthy tissue may complicate the timing and number of treatments (87, 88). To overcome these challenges, a recent study utilized a previously engineered *Lm*-based vaccine platform that specifically homes to and replicates within tumors as a vector for tumor-specific delivery of radiotherapy (29). Targeted radionuclide therapeutics (TRT) have shown potential in clinical trials as observed by various radionuclide/antibody conjugates that have been effective in treatment of malignancies such as glioblastoma (89) To accomplish this, a tumor-trophic *Lm*-based vector was incubated with anti-*Listeria* antibodies labeled with radionuclide, ^{188}Re, thereby creating a tumor-targeting radiotherapy platform (30). This generated a radioactive attenuated *Lm* strain with high viability, stability, and infectivity. When this radioactive *Lm*-based therapy was administered in a murine pancreatic cancer model, radioactive^{188}Re specifically accumulated in the tumors and metastatic lesions, further confirming the ability of *Lm* to act as a tumor-specific vector. Interestingly, while there was accumulation of this radioactive *Lm* in both kidney and liver, no histopathological damage and change in liver function was observed one week after the last treatment, suggesting that the highly proliferative tumor cells in metastases are more susceptible to the consequences of radiation-induced DNA damage than normal tissues (30).

However, a limitation of this strategy is the difficulty in generating this antibody dependent *Lm* radionuclide construct. This limitation was overcome in a more recent strategy that utilized radioactive phosphate ^{32}P to generate a novel TRT *Lm* construct. This simple but elegant method involved starving the attenuated *Lm* in saline followed by culturing in media supplemented with ^{32}P (29). The simplicity of this method allows for greater reproducibility and, more importantly, generation of an *Lm* construct that is more viable and stable without losing the incorporated radionuclide. This *Lm*-TRT also specifically homed to the tumor and metastatic sites in a pancreatic cancer model while demonstrating more effectiveness than its precursor. Interestingly, the major side effect associated with the use of ^{32}P in cancer therapy, accumulation in the bone marrow, was not seen with *Lm*-^{32}P used as a TRT. As this approach has only been assessed preclinically in a difficult-to-treat pancreatic cancer model, application of this technology to additional cancer models that are more amenable to immunotherapy may provide even more promising results.

Incorporation of *Lm*-Derived Products Into Nanovaccine Platforms

As development continues in safer and more effective live *Lm*-based vaccines, other groups have focused on utilizing specific products or proteins from *Listeria monocytogenes* to improve the immunogenicity of nanoparticle-based vaccine platforms (90, 91). Much like *Lm*, nanoparticle-based vaccines, comprised of liposomes and/or metal particles, have the ability to selectively deliver cargo to professional antigen presenting cells, and

accumulate within primary and metastatic tumors (92). In fact, a recently developed nanovaccine utilized the adjuvant properties of LLO to enhance the efficacy of a gold nanoparticle-based vaccine in preclinical development for metastatic melanoma (90). Gold nanoparticles are utilized in tumor nanovaccines due to their small size, ability to disseminate widely throughout the tissues, and ability to specifically accumulate at tumor sites (93). The gold nanoparticle-based vaccine, GNP-$LLO_{91\text{-}99}$, was constructed by incorporating gold nanoparticles with β-D glucose, which increases tumor oxidative stress, and a $H2k^d$-restricted epitope peptide derived from LLO, $LLO_{91\text{-}99}$. GNP-$LLO_{91\text{-}99}$ induced a robust production of inflammatory cytokines, a reduction in the intratumoral Treg and MDSC populations, and increased infiltration of LLO and tumor-specific $CD8^+$ T cells into the tumor. Surprisingly, GNP-$LLO_{91\text{-}99}$ was more effective at reducing melanoma tumor burden as a monotherapy, than ICI therapy. However, the combination of GNP-$LLO_{91\text{-}99}$ with anti-PD-1 and anti-CTLA-4 antibodies resulted in synergistic efficacy and complete tumor regression (90) Of note, the melanoma model in this study, B16F10, is performed in the $H2^b$-restricted C57BL/6 mice while the LLO-derived peptide within GNP-$LLO_{91\text{-}99}$ is well characterized as an $H2K^d$-restricted LLO epitope suggesting further investigation is warranted to fully understand its mechanism(s) of adjuvancy.

Another utilization of *Lm*-derived components in a nanovaccine involves the use of purified LLO in combination with liposomal nanoparticles (91). While liposomes are effective carriers of antigens for delivery to APCs (94), it was hypothesized that the lytic properties of LLO may allow for improved cytosolic release of liposomal cargo after uptake. The LLO-liposome nanoparticle-based vaccine consisted of a liposome, loaded with recombinant OVA protein, as a model tumor antigen, and recombinant LLO (91). When compared against a liposomal nanoparticle-based vaccine containing only ovalbumin, the incorporation of LLO into the nanovaccine resulted in enhanced presentation of the immunodominant CTL epitope, SIINFEKL, by APCs, improved OVA-specific cytolytic and humoral responses, a dramatic delay in growth of OVA-expressing melanoma tumors, and improved survival.

While the different types of nanovaccines have widely divergent compositions and chemistry, the incorporation of *Lm*-based components appears to dramatically improve their immunogenicity and anti-tumor efficacy (90, 91). These studies suggest that the utilization of *Lm* for tumor immunotherapy may not necessitate the need for the whole organism but just purified listerial components with unique properties to eventuate a safe but effective anti-tumor response.

Listeria as a Gene Delivery Vector

Due to the cellular tropism of *Lm* and its ability to gain entry to the cytosol after infection, it is uniquely capable as a vector for gene delivery (84, 95, 96). In a process called bactofection, bacteria can be engineered to deliver eukaryotic expression vectors containing genes encoding for enzymes or protein antigens to an infected cell (97). In fact, previous studies have found *Listeria monocytogenes* to be a suitable vector for bactofection (84, 96, 98). Souders et al. performed the first demonstration that this ability of *Lm* to perform bactofection could be utilized in tumor immunotherapy (79). In this study, an *Lm*-based bactofection construct platform was made by engineering *Lm* to include a suicide cassette that expresses a phage lysin under the control of the *actA* promoter, and a eukaryotic expression system containing the HPV16 E7 tumor antigen. Upon infection of APCs, the *Lm* bactofection construction, *Lm*-V2, escaped into the cytosol and underwent autolysis while delivering the E7 expression vector. *Lm*-V2 allowed for proficient expression of the E7 tumor antigen and induced E7-specific CTLs that infiltrated E7-expressing tumors and delayed tumor growth. While *Lm*-V2 did not produce as robust an anti-tumor response as the *Lm*-LLO-E7 vector that secreted E7 protein in the cytosol and did not undergo autolysis, it served as a proof-of-concept for a strategy that would ensure safety as a primary feature (79). Schoen et al. also demonstrated the utility of *Lm* as a vector for bactofection of antigens in a study where, instead of a CMV-driven expression vector, they introduced mRNA encoding for OVA (99). Upon infection of APCs *in vitro*, this vector was able to facilitate the activation of OVA-specific CTLs. While no *in vivo* experiments were performed in this study, they also demonstrated the ability of *Lm* to deliver nucleic acids to tumor cells upon infection. This strategy of utilizing *Lm* as a vector for bactofection of tumor cells was furthered by work from Pijkeren et al. that described the development of an *Lm*-based bactofection vector engineered to release a eukaryotic expression plasmid encoding luciferase subsequent to antibiotic administration (100, 101). *In vitro* infection and intratumoral infection *in vivo* of this bactofection construct did result in robust luciferase expression after antibiotic treatment suggesting *Lm* may also find utility as a tumor-selective delivery vector for nucleic acids.

While *Lm* is certainly capable as a vector for gene therapy to deliver nucleic acid cargo and facilitate protein expression in a target cell, current constructs are still not as effective at delivering antigen than *Lm* constructs that encode and secrete protein directly (102). Thus, since this would limit the ability to maximally present antigens, the ability of these various constructs to elicit robust antigen-specific $CD8^+$ and $CD4^+$T cell responses is currently limited and this technology will likely require further development prior to its successful entry into clinical trials.

COMBINATION THERAPIES WITH *LM*

Lm-based vaccines alone stimulate robust immune responses, increase immune infiltrates into tumors, and result in durable anti-tumor responses in many preclinical models of cancer (31). However, the heterogeneity of tumors and the TME in humans remains a major obstacle in obtaining effective responses to many cancer therapeutics in the broader population (103). One approach to overcome the detrimental effect of tumor heterogeneity on drug sensitivity is to utilize a combination therapy approach that consists of multiple drugs with

complementary mechanisms of action (104). We describe in detail below combination therapy approaches utilizing *Lm*-based vaccines that have shown promise in treatment of cancers in the clinic and preclinically.

Lm in Combination With Immune Checkpoint Inhibitors (ICIs)

One mechanism by which a tumor can escape immune-mediated destruction is by enhancing the expression of immune checkpoint molecules on T cells such as PD-1 and CTLA-4 (105). While effector T cells can transiently express these molecules during activation or prolonged activation, high levels of these molecules are associated with an exhausted T cell phenotype, thereby limiting their tumor lytic potential (106), Since the anti-tumor efficacy of *Lm*-based vaccines is through induction of potent tumor-specific $CD8^+$ T cells, maintaining their functionality is necessary for an effective immunotherapeutic platform (3). In fact, blockading antibodies that act as immune checkpoint inhibitors (ICI) dramatically enhance the functionality of anti-tumor T cell responses, an attribute that has revolutionized the treatment of various solid tumors (105, 107). Therefore, combination of these agents with *Lm*-based immunotherapeutics, which are able to induce potent and effective CTLs that infiltrate the TME may lead to even greater survival in cancer patients.

Thus far, various preclinical studies have found a synergistic effect in the combination of *Lm*-based therapeutics with ICIs (108–111). The initial study demonstrating synergy between anti-PD-1 blockading antibodies and the anti-tumor efficacy of *Lm*-based vaccines was by Mkrtichyan et al. (110). This study utilized the well-characterized *Lm*-LLO-E7 vaccine and assessed the ability of ICI to improve anti-tumor responses against the TC-1 tumor model for HPV-associated cancers. While they did find a synergistic anti-tumor effect by combining *Lm*-LLO-E7 with anti-PD-1 antibody, the dosage of *Lm*-LLO-E7 was approximately 5-fold lower and less effective than previous studies which may have better revealed the synergistic effect of these two therapeutics (110). Further support for this finding was found in a study assessing the efficacy of an *Lm*-based vaccine in combination with PD-1 blockade in a preclinical model of pancreatic ductal adenocarcinoma (PDAC) (109). PDAC is a highly heterogeneous solid tumor that is categorized as a "cold" tumor with limited immune cell tumor infiltrates making it less receptive to ICI treatment alone. However, utilizing an *Lm*-based construct expressing Annexin A2 (*Lm*-ANXA2), a relevant PDAC tumor antigen, Kim et al., demonstrated that sequential treatment with *Lm*-ANXA2 followed by PD-1 blockade resulted in an increase in overall survival of PDAC-bearing mice compared with either *Lm*-ANXA2 or anti-PD-1 therapy alone. Moreover, this therapeutic strategy elicited strong ANXA2-specific immune responses in the TME as evidenced by increase production of IFNγ, an observation not found in the group receiving anti-PD-1 alone (109) In addition to PDAC and HPV-associated cancers, *Lm*-based vaccines have also been reported to synergize with ICI in a particularly challenging malignancy with low survival rates, hepatocellular carcinoma (HCC). In fact, unlike many other cancers, ICI has limited efficacy and can even lead to hyperprogression in some patients (112, 113). Interestingly, an *Lm*-based vaccine expressing a multivalent HCC tumor antigen, Lmdd-MPFG, can induce PD-L1 expression, the ligand for PD-1, in HCC tumor cells suggesting that it may synergize with ICI therapy (108). When Lmdd-MPFG was administered along with anti-PD-1 antibody, it resulted in significantly reduced tumor burden as compared to PD-1 blockade or *Lm* vaccine treatment alone. While Lmdd-MPFG alone did result in significant anti-tumor efficacy, PD-1 blockade alone did not, mirroring clinical experience, and suggesting that the *Lm*-based vaccine sensitized HCC to ICI. Further evidence suggested that the ability of Lmdd-MPFG to polarize TAMs to the M1 phenotype played a role in the sensitization of HCC to PD-1 blockade (108). In addition to ICI synergizing with *Lm*-based vaccines in a therapeutic setting, it has also been found to enhance protection against tumor challenge in an murine model of melanoma expressing ovalbumin, B16F10-OVA (111). While administration of the *Lm*-based vaccine expressing $OVA_{257\text{-}264}$ fused to ActAN100, *Lm*-OVA, provided significant protection against subsequent challenge with B16F10-OVA, up to 30% of mice developed tumors. The authors hypothesized that this could be due to the induction of peripheral tolerance mechanisms such as immune checkpoints that allow tumor escape. Therefore, approximately 2 months after *Lm*-based vaccination, mice were challenged with tumor, and received ICI (either anti-PD-1, anti-CTLA-4, or anti-PD-L1) every 10 days subsequently, in order to maintain anti-tumor T cell function. Each of the ICI antibodies enhanced the anti-tumor effect of *Lm*-OVA. More strikingly, there was significantly more mice remaining tumor-free after the addition of checkpoint blockade compared to vaccination with *Lm*-OVA alone. The data from these studies suggest that the efficacy of *Lm* vaccines can be enhanced by ICI therapy but *Lm* vaccination can also sensitize previously "cold" tumors, such as PDAC, to the powerful potential of ICI therapy (108, 111).

Use of checkpoint inhibitors in combination with *Lm* therapy is also being currently evaluated in various phases of clinical trials (**Table 1**). As we discussed in section 1.3.2, a Phase II study has demonstrated the positive immunomodulatory effect of the combination therapy of CRS-207 (*Lm*-mesothelin) with nivolumab (anti-PD-1) on the TME in the treatment of human PDAC (56).

Lm Combination With Adoptive Cell Therapy (ReACT Cells)

Adoptive cell therapy (ACT) is the use of engineered or naturally occurring immune cells for the treatment of cancer (114). This strategy has enjoyed unprecedented success in oncotherapy, with high response rates in hematopoietic malignancies and melanoma (114). However, this strategy comes with serious limitations and drawbacks that make its use limited in the therapy of solid tumors (115). One of the most significant challenges is that the TME is an immunosuppressive environment with elevated levels of anti-inflammatory

cytokines, inhibitory receptor ligands, and immunosuppressive cell types such as MDSCs that impede the activation, proliferation and differentiation of anti-tumor immune cells (116). Due to their ability to modulate the TME and reduce peripheral tolerance mechanisms, *Lm*-based vaccines may be uniquely able to overcome the limitations of this therapeutic strategy and enhance the efficacy of ACT (50). While *Lm* improves the ability of immune cells to infiltrate into the TME, *Lm* is also able to infect MDSCs which specifically home to the TME and likely mitigate immunosuppression within the tumor (117). Xin et al., has developed an approach that utilizes *Lm*-based vaccines to enhance ACT and overcome the immunosuppressive TME in a strategy named Reenergized ACT (ReACT). To advance their work, they utilized mono-specific and dual-specific $CD8^+$ T cells that recognize a tumor antigen, gp100, or both a tumor antigen and an *Lm*-derived antigen, OVA, respectively. After allowing for tumors to establish, mice were administered mono or dual-specific $CD8^+$ T cells followed by intratumoral injection of the *Lm*-OVA vaccine. Surprisingly, mice receiving only CTLs did not respond and less than 10% of mice receiving only tumor-specific CTLs and i.t. *Lm*-OVA responded, In contrast, 69% of mice receiving both i.t. *Lm*-OVA injection and dual-specific CTLs that recognize the tumor and *Lm*-derived antigens responded and eradicated their tumors. This method also resulted in greater tumor infiltration and function of the transferred CTLs and reduced expression of immune checkpoint molecules by CTLs. In the TME, MDSCs and Tregs made up a lower percentage of overall tumor cells in each of the *Lm*-treated groups but only the dual-specific CTLs with *Lm* treatment group had a higher Teff/Treg ratio and lower absolute Tregs than other treatment groups (14, 15). As loss of the targeted antigen is associated with therapeutic resistance in ACT, broadening of the anti-tumor response through epitope spreading to additional tumor antigens should result in a more durable anti-tumor response (118, 119). In fact, this therapeutic strategy did lead to epitope spreading that induced long-lasting endogenous memory cells that provided protection against subsequent challenge (14). In this preclinical model of melanoma, the only adverse events associated with ReACT was limited to mild vitiligo at the primary tumor injection site (14).

Lm in Heterologous Vaccination Schedules

Heterologous prime boost involves the administration of the same antigens using different vaccine vector platforms to generate a more robust immune response than a homologous prime boost vaccine regimen (120, 121). *Lm*-based vaccines are particularly effective at generating robust responses when used as a booster or primer in combination with various vaccine vectors including viruses, DNA and peptides (122–125). In a preclinical study that involved the use of a DNA vaccine encoding the prostate-specific antigen prostatic acid phosphatase (PAP) along with an attenuated *Lm* vaccine, LADD-PAP, greater antitumor efficacy was seen in the prime boost regimen as compared to the DNA vaccine only regimen or the LADD-PAP only regimen (122). This heterologous vaccination schedule interestingly led to the induction of more $CD4^+$ T cells, which may have played a role in the enhanced antitumor immune response. Enhanced cellular immune responses were observed with a heterologous prime boost regimen consisting of an EGFRvIII peptide vaccine, PEPvIII, and an *Lm*-based vaccine targeting EGFRvIII, *Lm*-EGFRvIIIx5, which resulted in greater induction of EGFR-specific $CD8^+$ T cells than either vaccine alone (125). Interestingly, this enhanced EGFR-specific CTL response was only observed when the *Lm*-EGFRvIIIx5 was given as a booster to a previous peptide immunization. *Lm*-based vaccines have also been found to boost anti-tumor immunity when delivered in heterologous prime boost regimens with viral vectors (123, 124). In a prophylactic study, mice receiving a modified vaccinia Ankara vaccine expressing human p53, MVA-p53, followed by an *Lm*-based vaccine expressing human p53, *LmddA*-LLO-p53, resulted in greater anti-tumor protection against the murine breast cancer model, 4T1p53 (124). Further, the use of an *Lm*-based vaccine targeting the model tumor antigen chicken ovalbumin, *Lm*-OVA, prior to boosting with an oncolytic Maraba virus, MRB-OVA, resulted in a greater reduction in B16F10-OVA melanoma tumor growth, more tumor-free mice, and greater overall survival than mice receiving an adenovirus-based vaccine as the priming agent (123). Most importantly, this incorporation of *Lm*-based vaccines into heterologous prime boost approaches for cancer immunotherapy has already been found effective in a clinical trial. As we previously discussed, in a Phase II trial in PDAC patients, CRS-207 (*Lm*-mesothelin) in combination with Cy/GVAX improved median overall survival and enhanced induction of mesothelin specific $CD8^+$ T cells as compared to Cy/GVAX alone (53).

Lm in Combination With Radiotherapy

Radiation therapy (RT) has been a mainstay therapeutic option for nearly a century in the treatment of various forms of malignancies (126). However, recent work has found that RT does not solely disrupt tumor cell division but has immunostimulatory effects in the TME (127). RT helps trigger the release of tumor antigens, improve presentation of tumor antigens to T cells, and induces an inflammatory response in the TME that results in elevated IFNγ levels and reduced immunosuppression (86, 128). However, despite all these attractive features of RT, resistance and recurrence still occur through multiple mechanisms (129). In order to improve the efficacy of RT, a recent study utilized a combination of RT and *Lm*-OVA in the B16-OVA melanoma model (86). This approach resulted in an increase in the activated T cells infiltrating the TME and a more robust response in the combination therapy than in the use of *Lm* or RT alone. One possible explanation for the observed synergy was that both the *Lm* vaccine and the RT seem to activate different components of the immune system (86). A similar synergistic effect of RT and *Lm*-based vaccines was observed in a murine model of prostate cancer. In this study, an *Lm*-based vaccine expressing human prostate antigen (PSA) in combination with RT resulted in synergistic induction of PSA-specific splenic T cell responses and therapeutic anti-tumor efficacy (130).

In an effort to improve on the efficacy and specific delivery of the lethal radiation therapy to the tumors and metastasis, the Gravekamp group has developed an elegant method to use *Lm* as a delivery vector for radioisotopes directly to tumors. In this study using *Lm* infused with ^{32}Phosphorous (L*m*-^{32}P), this group was able to demonstrate that *Lm*-^{32}P specifically homes to the TME in a mouse model for PDAC (29). The DNA damage caused by the radioisotope coupled with the antitumor efficacy of *Lm* itself makes this platform very potent and promising in cancer therapy.

Lm in Combination With Inhibitors of Complement Signaling

The complement cascade is well characterized to play a crucial role in the innate immune response to pathogens (131). However, evidence over the past decade demonstrates that the complement pathway and its components can also regulate adaptive immunity, particularly anti-tumor T cell responses (132). In fact, complement is highly activated in tumors and this activation results in T cell dysfunction and blunted anti-tumor responses (133). Importantly, a small molecule inhibitor of the C5a receptor (C5aR1), PMX53, enhances infiltration and function of tumor-infiltrating T cells leading to tumor regression in mouse cancer models (134). Therefore, inhibition of complement signaling may make the TME more amenable to anti-tumor T cells and synergize with an *Lm*-based vaccine. In a recent study, this synergistic potential was confirmed by demonstrating that treatment with PMX53 synergized with tumor vasculature targeting *Lm*-based vaccines to significantly reduce primary tumor growth and reduce lung metastases in a murine model of metastatic breast cancer, 4T1 (135). Furthermore, this synergistic potential was correlated with reduced levels of MDSCs and Tregs in the lungs of tumor-bearing mice and enhanced maturation of lung-associated dendritic cells.

Lm in Combination With Traditional Chemotherapy

Chemotherapy remains the gold standard for the treatment of various forms of cancers. Chemotherapy may also synergize with and augment the activity of immunotherapies, such as *Lm*-based vaccines, by inducing direct cell death that results in release and presentation of tumor antigens and maturation of dendritic cells (136, 137). Chemotherapy, such as low-dose cyclophosphamide, can also significantly reduce the Treg population in the TME (138). In fact, in a murine model of hepatic metastases, animals treated with attenuated *Lm* along with low dose cyclophosphamide had reduced levels of Tregs in the TME and spleen and a dramatic increase in overall survival (139). The Treg-depleting properties of cyclophosphamide were also found to enhance the efficacy of an *Lm*-based vaccine in the challenging KPC mouse model for PDAC (140, 141). In this study, Treg depletion by cyclophosphamide was further enhanced by addition of anti-CD25 depleting antibody in combination with an *Lm*-based vaccine targeting a 25 amino acid region of Kras^{G12D}, LM-Kras. In KPC mice less than 2 months old, the combination of LM-Kras and cyclophosphamide/anti-CD25 was found to significantly delay progression of precancerous pancreatic lesions to PDAC and enhance survival in comparison to LM-Kras or cyclophosphamide/anti-CD25 alone. T cell infiltration and Th1 responses in the pancreas were also enhanced in the group receiving LM-Kras and cyclophosphamide/anti-CD25 in comparison to LM-Kras alone. While it is not possible to dissect the exact contribution of cyclophosphamide in the efficacy of LM-Kras in this study, much like another PDAC study that included cyclophosphamide in all treatment groups (109). These results provide additional pre-clinical evidence that chemotherapy will likely have an important role to play in effective treatment regimens with *Lm*-based vaccines. In humans, several clinical trials have incorporated chemotherapeutic agents, such as cyclophosphamide, pemetrexed and cisplatin, along with *Lm*-based vaccines into their treatment regimen (41, 44, 53, 55, 56, 60). As yet, evidence from these clinical trials suggest some chemotherapy regimens may provide a clinical benefit in combination with *Lm*-based vaccines (53, 60) while others have found mixed or negligible benefit from this combination (41).

Conclusion

The recent results reported from several clinical trials demonstrate the promising future of *Lm*-based tumor immunotherapies but also reveal challenges that educate the future development of the platform (41, 42, 60). Numerous improvements to the platform have already been reported in preclinical studies that would not be evident in the clinical results as they are mostly utilizing first-generation *Lm*-based constructs (29, 30, 78). Even with the use of these first generation constructs, promising clinical responses have been reported in several cancers including cervical cancer, malignant pleural mesothelioma, and canine osteosarcoma (74). As results from clinical and preclinical studies demonstrate, improvements to therapeutic efficacy may be realized utilizing *Lm*-based vaccines in heterologous prime boost regimens with other vectors and by combination with synergistic therapeutic strategies such as ACT and ICI (14, 53, 108, 110, 122, 123, 134). However, there still remain several challenges going forward to realize the full potential of Lm-based vaccines. As a recent clinical trial suggests, *Lm*-based vaccines may not significantly benefit from combination with particular chemotherapies that suppress immunity and increase risk of adverse events (41). Further, while rarely observed in clinical trials as yet, the incidence of listeriosis in humans and dogs may justify additional study into the variables contributing to this risk (43, 76). Nevertheless, improvements to clinical safety may be realized with the adoption of recently developed suicide strains, such as *Lm*-RIID, that would dramatically reduce the risk of listeriosis (78). As with other current vaccine platforms, treatment resistance due to immune escape will also likely be an ongoing challenge, particularly due to many of the current vaccines targeting a single tumor antigen (142, 143). While not yet published, improvements to the antigens targeted by *Lm*-based vaccines such as the multivalent ADXS-HOT platform targeting

immunogenic hotspot mutations and the patient-personalized ADXS-NEO platform will likely bring improvements in efficacy, in part by limiting immune escape. Finally, recent advancements in leveraging its tumor-trophic potential suggest that attenuated *Lm*-based therapeutics can provide multiple separate but effective anti-tumor mechanisms which, if fully leveraged, may also mitigate therapeutic resistance (14, 15, 29, 30, 117, 144). With our improved understanding of its clinical performance and the continued development of the platform, the future is promising for *Lm*-based therapeutics.

AUTHOR CONTRIBUTIONS

MO, drafting. YP, revision. LW, drafting and revision. All authors contributed to the article and approved the submitted version.

FUNDING

National Institutes of Health 1R15CA216205-01 (LW).

REFERENCES

1. Kantoff PW, Higano CS, Shore ND, Berger ER, Small EJ, Penson DF, et al. Sipuleucel-T immunotherapy for castration-resistant prostate cancer. *N Engl J Med* (2010) 363(5):411–22. doi: 10.1056/NEJMoa1001294
2. Hollingsworth RE, Jansen K. Turning the corner on therapeutic cancer vaccines. *NPJ Vaccines* (2019) 4:7. doi: 10.1038/s41541-019-0103-y
3. Gunn GR, Zubair A, Peters C, Pan ZK, Wu TC, Paterson Y. Two *Listeria monocytogenes* vaccine vectors that express different molecular forms of human papilloma virus-16 (HPV-16) E7 induce qualitatively different T cell immunity that correlates with their ability to induce regression of established tumors immortalized by HPV-16. *J Immunol* (2001) 167 (11):6471–9. doi: 10.4049/jimmunol.167.11.6471
4. Didot A. Essai sur la prophylaxie du cancer par la syphilization artificielle. *Bull Acad Roy Belge* (1851) 1852(11):100–72.
5. Hall SS. *A commotion in the blood : life, death, and the immune system. 1st ed* Vol. xiv. . New York: Henry Holt (1997). 544 p.
6. Oelschlaeger TA. Bacteria as tumor therapeutics? *Bioeng Bugs* (2010) 1 (2):146–7. doi: 10.4161/bbug.1.2.11248
7. Busch W. Aus der Sitzung der medicinischen Section vom 13 November 1867. *Berl Klin Wochenschr* (1868) 5:137.
8. Fehleisen F. Ueber die Züchtung der Erysipelkokken auf künstlichem Nährboden und ihre Übertragbarkeit auf den Menschen. *Dtsch Med Wochenschr* (1882) 8(31):553–4. doi: 10.1055/s-0029-1196806
9. Coley WB. The Diagnosis and Treatment of Bone Sarcoma. *Glasgow Med J* (1936) 126(2):49–86.
10. McCarthy EF. The toxins of William B. Coley and the treatment of bone and soft-tissue sarcomas. *Iowa Orthop J* (2006) 26:154–8.
11. Coley WBII. Contribution to the Knowledge of Sarcoma. *Ann Surg* (1891) 14 (3):199–220. doi: 10.1097/00000658-189112000-00015
12. Durgeau A, Virk Y, Corgnac S, Mami-Chouaib F. Recent Advances in Targeting CD8 T-Cell Immunity for More Effective Cancer Immunotherapy. *Front Immunol* (2018) 9:14. doi: 10.3389/fimmu.2018.00014
13. Dunn GP, Bruce AT, Ikeda H, Old LJ, Schreiber RD. Cancer immunoediting: from immunosurveillance to tumor escape. *Nat Immunol* (2002) 3(11):991–8. doi: 10.1038/ni1102-991
14. Xin G, Khatun A, Topchyan P, Zander R, Volberding PJ, Chen Y, et al. Pathogen-Boosted Adoptive Cell Transfer Therapy Induces Endogenous Antitumor Immunity through Antigen Spreading. *Cancer Immunol Res* (2020) 8(1):7–18. doi: 10.1158/2326-6066.CIR-19-0251
15. Xin G, Schauder DM, Jing W, Jiang A, Joshi NS, Johnson B, et al. Pathogen boosted adoptive cell transfer immunotherapy to treat solid tumors. *Proc Natl Acad Sci U S A* (2017) 114(4):740–5. doi: 10.1073/pnas.1614315114
16. Overwijk WW, Theoret MR, Finkelstein SE, Surman DR, de Jong LA, Vyth-Dreese FA, et al. Tumor regression and autoimmunity after reversal of a functionally tolerant state of self-reactive CD8+ T cells. *J Exp Med* (2003) 198(4):569–80. doi: 10.1084/jem.20030590
17. Minton NP. Clostridia in cancer therapy. *Nat Rev Microbiol* (2003) 1 (3):237–42. doi: 10.1038/nrmicro777
18. Barbé S, Van Mellaert L, Theys J, Geukens N, Lammertyn E, Lambin P, et al. Secretory production of biologically active rat interleukin-2 by Clostridium acetobutylicum DSM792 as a tool for anti-tumor treatment. *FEMS Microbiol Lett* (2005) 246(1):67–73. doi: 10.1016/j.femsle.2005.03.037
19. Wood LM, Guirnalda PD, Seavey MM, Paterson Y. Cancer immunotherapy using *Listeria monocytogenes and* listerial virulence factors. *Immunol Res* (2008) 42(1-3):233–45. doi: 10.1007/s12026-008-8087-0
20. Agrawal N, Bettegowda C, Cheong I, Geschwind J-F, Drake CG, Hipkiss EL, et al. Bacteriolytic therapy can generate a potent immune response against experimental tumors. *Proc Natl Acad Sci U S A* (2004) 101(42):15172–7. doi: 10.1073/pnas.0406242101
21. Mengaud J, Chenevert J, Geoffroy C, Gaillard JL, Cossart P. Identification of the structural gene encoding the SH-activated hemolysin of *Listeria monocytogenes*: listeriolysin O is homologous to streptolysin O and pneumolysin. *Infect Immun* (1987) 55(12):3225–7. doi: 10.1128/IAI.55.12.3225-3227.1987
22. Poussin MA, Goldfine H. Involvement of *Listeria monocytogenes* phosphatidylinositol-specific phospholipase C and host protein kinase C in permeabilization of the macrophage phagosome. *Infect Immun* (2005) 73 (7):4410–3. doi: 10.1128/IAI.73.7.4410-4413.2005
23. Tilney LG, Portnoy DA. Actin filaments and the growth, movement, and spread of the intracellular bacterial parasite, *Listeria monocytogenes*. *J Cell Biol* (1989) 109(4 Pt 1):1597–608. doi: 10.1083/jcb.109.4.1597
24. Brunt LM, Portnoy DA, Unanue ER. Presentation of *Listeria monocytogenes* to CD8+ T cells requires secretion of hemolysin and intracellular bacterial growth. *J Immunol* (1990) 145(11):3540–6. doi: 10.1084/jem.175.6.1531
25. Tufail S, Badrealam KF, Owais M, Zubair S. Illuminating the Petite Picture of T Cell Memory Responses to *Listeria monocytogenes*. *BioMed Res Int* (2013) 2013:121684. doi: 10.1155/2013/121684
26. Orme IM. Active and memory immunity to *Listeria monocytogenes* infection in mice is mediated by phenotypically distinct T-cell populations. *Immunology* (1989) 68(1):93–5.
27. D'Orazio SEF. Innate and Adaptive Immune Responses during *Listeria monocytogenes* Infection. *Microbiol Spectr* (2019) 7(3):21–2. doi: 10.1128/microbiolspec.GPP3-0065-2019
28. Stark FC, Sad S, Krishnan L. Intracellular Bacterial Vectors That Induce CD8 (+) T Cells with Similar Cytolytic Abilities but Disparate Memory Phenotypes Provide Contrasting Tumor Protection. *Cancer Res* (2009) 69 (10):4327. doi: 10.1158/0008-5472.CAN-08-3160
29. Chandra D, Selvanesan BC, Yuan Z, Libutti SK, Koba W, Beck A, et al. 32-Phosphorus selectively delivered by *listeria to* pancreatic cancer demonstrates a strong therapeutic effect. *Oncotarget* (2017) 8(13):20729–40. doi: 10.18632/oncotarget.15117
30. Quispe-Tintaya W, Chandra D, Jahangir A, Harris M, Casadevall A, Dadachova E, et al. Nontoxic radioactive *Listeria*(at) is a highly effective therapy against metastatic pancreatic cancer. *Proc Natl Acad Sci U S A* (2013) 110(21):8668–73. doi: 10.1073/pnas.1211287110
31. Wood LM, Paterson Y. Attenuated *Listeria monocytogenes*: a powerful and versatile vector for the future of tumor immunotherapy. *Front Cell Infect Microbiol* (2014) 4:51–. doi: 10.3389/fcimb.2014.00051
32. Roden RBS, Stern PL. Opportunities and challenges for human papillomavirus vaccination in cancer. *Nat Rev Cancer* (2018) 18(4):240–54. doi: 10.1038/nrc.2018.13
33. McCredie MR, Sharples KJ, Paul C, Baranyai J, Medley G, Jones RW, et al. Natural history of cervical neoplasia and risk of invasive cancer in women with cervical intraepithelial neoplasia 3: a retrospective cohort study. *Lancet Oncol* (2008) 9(5):425–34. doi: 10.1016/S1470-2045(08)70103-7

34. Gillison ML, Alemany L, Snijders PJ, Chaturvedi A, Steinberg BM, Schwartz S, et al. Human papillomavirus and diseases of the upper airway: head and neck cancer and respiratory papillomatosis. *Vaccine* (2012) 30(Suppl 5): F34–54. doi: 10.1016/j.vaccine.2012.05.070
35. Pal A, Kundu R. Human Papillomavirus E6 and E7: The Cervical Cancer Hallmarks and Targets for Therapy. *Front Microbiol* (2019) 10:3116. doi: 10.3389/fmicb.2019.03116
36. Wallecha A, Wood L, Pan ZK, Maciag PC, Shahabi V, Paterson Y. *Listeria monocytogenes*-derived listeriolysin O has pathogen-associated molecular pattern-like properties independent of its hemolytic ability. *Clin Vaccine Immunol* (2013) 20(1):77–84. doi: 10.1128/CVI.00488-12
37. Wood LM, Pan ZK, Shahabi V, Paterson Y. *Listeria*-derived ActA is an effective adjuvant for primary and metastatic tumor immunotherapy. *Cancer Immunol Immunother* (2010) 59(7):1049–58. doi: 10.1007/s00262-010-0830-4
38. Peng X, Treml J, Paterson Y. Adjuvant properties of listeriolysin O protein in a DNA vaccination strategy. *Cancer Immunol Immunother* (2007) 56 (6):797–806. doi: 10.1007/s00262-006-0240-9
39. Lauer P, Hanson B, Lemmens EE, Liu W, Luckett WS, Leong ML, et al. Constitutive Activation of the PrfA regulon enhances the potency of vaccines based on live-attenuated and killed but metabolically active *Listeria monocytogenes* strains. *Infect Immun* (2008) 76(8):3742–53. doi: 10.1128/IAI.00390-08
40. Maciag PC, Radulovic S, Rothman J. The first clinical use of a live-attenuated *Listeria monocytogenes* vaccine: a Phase I safety study of Lm-LLO-E7 in patients with advanced carcinoma of the cervix. *Vaccine* (2009) 27 (30):3975–83. doi: 10.1016/j.vaccine.2009.04.041
41. Basu P, Mehta A, Jain M, Gupta S, Nagarkar RV, John S, et al. A Randomized Phase 2 Study of ADXS11-001 *Listeria monocytogenes*-Listeriolysin O Immunotherapy With or Without Cisplatin in Treatment of Advanced Cervical Cancer. *Int J Gynecol Cancer* (2018) 28(4):764–72. doi: 10.1097/IGC.0000000000001235
42. Huh WK, Brady WE, Fracasso PM, Dizon DS, Powell MA, Monk BJ, et al. Phase II study of axalimogene filolisbac (ADXS-HPV) for platinum-refractory cervical carcinoma: An NRG oncology/gynecologic oncology group study. *Gynecol Oncol* (2020) 158(3):562–9. doi: 10.1016/j.ygyno.2020.06.493
43. Fares E, McCloskey CB, Gutierrez A, Princiotta M, Salinas LJ, Drevets DA. Vaccine strain *Listeria monocytogenes* bacteremia occurring 31 months after immunization. *Infection* (2019) 47(3):489–92. doi: 10.1007/s15010-018-1249-7
44. Safran H, Leonard KL, Perez K, Vrees M, Klipfel A, Schechter S, et al. Tolerability of ADXS11-001 Lm-LLO *Listeria*-Based Immunotherapy With Mitomycin, Fluorouracil, and Radiation for Anal Cancer. *Int J Radiat Oncol Biol Phys* (2018) 100(5):1175–8. doi: 10.1016/j.ijrobp.2018.01.004
45. Seufferlein T, Ettrich TJ. Treatment of pancreatic cancer-neoadjuvant treatment in resectable pancreatic cancer (PDAC). *Transl Gastroenterol Hepatol* (2019) 4:21. doi: 10.21037/tgh.2019.03.05
46. Royal RE, Levy C, Turner K, Mathur A, Hughes M, Kammula US, et al. Phase 2 trial of single agent Ipilimumab (anti-CTLA-4) for locally advanced or metastatic pancreatic adenocarcinoma. *J Immunother* (2010) 33(8):828–33. doi: 10.1097/CJI.0b013e3181eec14c
47. Blando J, Sharma A, Higa MG, Zhao H, Vence L, Yadav SS, et al. Comparison of immune infiltrates in melanoma and pancreatic cancer highlights VISTA as a potential target in pancreatic cancer. *Proc Natl Acad Sci U S A* (2019) 116(5):1692–7. doi: 10.1073/pnas.1811067116
48. Teng MW, Ngiow SF, Ribas A, Smyth MJ. Classifying Cancers Based on T-cell Infiltration and PD-L1. *Cancer Res* (2015) 75(11):2139–45. doi: 10.1158/0008-5472.CAN-15-0255
49. Le K, Wang J, Zhang T, Guo Y, Chang H, Wang S, et al. Overexpression of Mesothelin in Pancreatic Ductal Adenocarcinoma (PDAC). *Int J Med Sci* (2020) 17(4):422–7. doi: 10.7150/ijms.39012
50. Wallecha A, Singh R, Malinina I. *Listeria monocytogenes* (Lm)-LLO immunotherapies reduce the immunosuppressive activity of myeloid-derived suppressor cells and regulatory T cells in the tumor microenvironment. *J Immunother* (2013) 36(9):468–76. doi: 10.1186/2051-1426-1-S1-O18
51. Brockstedt DG, Giedlin MA, Leong ML, Bahjat KS, Gao Y, Luckett W, et al. *Listeria*-based cancer vaccines that segregate immunogenicity from toxicity. *Proc Natl Acad Sci U S A* (2004) 101(38):13832–7. doi: 10.1073/pnas.0406035101
52. Le DT, Brockstedt DG, Nir-Paz R, Hampl J, Mathur S, Nemunaitis J, et al. A live-attenuated *Listeria* vaccine (ANZ-100) and a live-attenuated *Listeria* vaccine expressing mesothelin (CRS-207) for advanced cancers: phase I studies of safety and immune induction. *Clin Cancer Res* (2012) 18(3):858–68. doi: 10.1158/1078-0432.CCR-11-2121
53. Le DT, Wang-Gillam A, Picozzi V, Greten TF, Crocenzi T, Springett G, et al. Safety and survival with GVAX pancreas prime and *Listeria Monocytogenes*-expressing mesothelin (CRS-207) boost vaccines for metastatic pancreatic cancer. *J Clin Oncol* (2015) 33(12):1325–33. doi: 10.1200/JCO.2014.57.4244
54. Denham JD, Lee DH, Castro M, Pandya S, Aslam S, Nanjappa S, et al. Two cases of disseminated infection following live organism anti-cancer vaccine administration in cancer patients. *Int J Infect Dis* (2018) 72:1–2. doi: 10.1016/j.ijid.2018.04.004
55. Le DT, Picozzi VJ, Ko AH, Wainberg ZA, Kindler H, Wang-Gillam A, et al. Results from a Phase IIb, Randomized, Multicenter Study of GVAX Pancreas and CRS-207 Compared with Chemotherapy in Adults with Previously Treated Metastatic Pancreatic Adenocarcinoma (ECLIPSE Study). *Clin Cancer Res* (2019) 25(18):5493–502. doi: 10.1158/1078-0432.CCR-18-2992
56. Tsujikawa T, Crocenzi T, Durham JN, Sugar EA, Wu AA, Onners B, et al. Evaluation of Cyclophosphamide/GVAX Pancreas Followed by *Listeria*-mesothelin (CRS-207) With or Without Nivolumab in Patients with Pancreatic Cancer. *Clin Cancer Res* (2020) 26:3578–88. doi: 10.1158/1078-0432.CCR-19-3978
57. Rossini M, Rizzo P, Bononi I, Clementz A, Ferrari R, Martini F, et al. New Perspectives on Diagnosis and Therapy of Malignant Pleural Mesothelioma. *Front Oncol* (2018) 8:91. doi: 10.3389/fonc.2018.00091
58. Disselhorst MJ, Quispel-Janssen J, Lalezari F, Monkhorst K, de Vries JF, van der Noort V, et al. Ipilimumab and nivolumab in the treatment of recurrent malignant pleural mesothelioma (INITIATE): results of a prospective, single-arm, phase 2 trial. *Lancet Respir Med* (2019) 7(3):260–70. doi: 10.1016/S2213-2600(18)30420-X
59. Vogelzang NJ, Rusthoven JJ, Symanowski J, Denham C, Kaukel E, Ruffie P, et al. Phase III study of pemetrexed in combination with cisplatin versus cisplatin alone in patients with malignant pleural mesothelioma. *J Clin Oncol* (2003) 21(14):2636–44. doi: 10.1200/JCO.2003.11.136
60. Hassan R, Alley E, Kindler H, Antonia S, Jahan T, Honarmand S, et al. Clinical Response of Live-Attenuated, *Listeria monocytogenes* Expressing Mesothelin (CRS-207) with Chemotherapy in Patients with Malignant Pleural Mesothelioma. *Clin Cancer Res* (2019) 25(19):5787–98. doi: 10.1158/1078-0432.CCR-19-0070
61. Bray F, Ferlay J, Soerjomataram I, Siegel RL, Torre LA, Jemal A. Global cancer statistics 2018: GLOBOCAN estimates of incidence and mortality worldwide for 36 cancers in 185 countries. *CA Cancer J Clin* (2018) 68 (6):394–424. doi: 10.3322/caac.21492
62. Ferlay J, Colombet M, Soerjomataram I, Mathers C, Parkin DM, Pineros M, et al. Estimating the global cancer incidence and mortality in 2018: GLOBOCAN sources and methods. *Int J Cancer* (2019) 144(8):1941–53. doi: 10.1002/ijc.31937
63. Molina JR, Yang P, Cassivi SD, Schild SE, Adjei AA. Non-small cell lung cancer: epidemiology, risk factors, treatment, and survivorship. *Mayo Clin Proc* (2008) 83(5):584–94. doi: 10.4065/83.5.584
64. Topalian SL, Hodi FS, Brahmer JR, Gettinger SN, Smith DC, McDermott DF, et al. Five-Year Survival and Correlates Among Patients With Advanced Melanoma, Renal Cell Carcinoma, or Non-Small Cell Lung Cancer Treated With Nivolumab. *JAMA Oncol* (2019) 5(10):1411–20. doi: 10.1001/jamaoncol.2019.2187
65. Garon EB, Hellmann MD, Rizvi NA, Carcereny E, Leighl NB, Ahn MJ, et al. Five-Year Overall Survival for Patients With Advanced NonSmall-Cell Lung Cancer Treated With Pembrolizumab: Results From the Phase I KEYNOTE-001 Study. *J Clin Oncol* (2019) 37(28):2518–27. doi: 10.1200/JCO.19.00934
66. Brahmer JR, Johnson ML, Cobo M, Viteri S, Sarto JC, Sukari A, et al. JNJ-64041757 (JNJ-757), a Live, Attenuated, Double-Deleted *Listeria monocytogenes*-Based Immunotherapy, in Patients With Non-Small Cell

Lung Cancer: Results From 2 Phase 1 Studies. *JTO Clin Res Rep* (2020) 2:100103. doi: 10.1016/j.jtocrr.2020.100103
67. Jafari F, Javdansirat S, Sanaie S, Naseri A, Shamekh A, Rostamzadeh D, et al. Osteosarcoma: A comprehensive review of management and treatment strategies. *Ann Diagn Pathol* (2020) 49:151654. doi: 10.1016/j.anndiagpath.2020.151654
68. Link MP, Goorin AM, Miser AW, Green AA, Pratt CB, Belasco JB, et al. The effect of adjuvant chemotherapy on relapse-free survival in patients with osteosarcoma of the extremity. *N Engl J Med* (1986) 314(25):1600–6. doi: 10.1056/NEJM198606193142502
69. Dahlin DC, Coventry MB. Osteogenic sarcoma. A study of six hundred cases. *J Bone Joint Surg Am* (1967) 49(1):101–10. doi: 10.2106/00004623-196749010-00008
70. Onda M, Matsuda S, Higaki S, Iijima T, Fukushima J, Yokokura A, et al. ErbB-2 expression is correlated with poor prognosis for patients with osteosarcoma. *Cancer* (1996) 77(1):71–8. doi: 10.1002/(SICI)1097-0142(19960101)77:1<71::AID-CNCR13>3.0.CO;2-5
71. Simpson S, Dunning MD, de Brot S, Grau-Roma L, Mongan NP, Rutland CS. Comparative review of human and canine osteosarcoma: morphology, epidemiology, prognosis, treatment and genetics. *Acta Vet Scand* (2017) 59(1):71. doi: 10.1186/s13028-017-0341-9
72. Flint AF, U'Ren L, Legare ME, Withrow SJ, Dernell W, Hanneman WH. Overexpression of the erbB-2 proto-oncogene in canine osteosarcoma cell lines and tumors. *Vet Pathol* (2004) 41(3):291–6. doi: 10.1354/vp.41-3-291
73. Shahabi V, Seavey MM, Maciag PC, Rivera S, Wallecha A. Development of a live and highly attenuated *Listeria monocytogenes*-based vaccine for the treatment of Her2/neu-overexpressing cancers in human. *Cancer Gene Ther* (2011) 18(1):53–62. doi: 10.1038/cgt.2010.48
74. Mason NJ, Gnanandarajah JS, Engiles JB, Gray F, Laughlin D, Gaurnier-Hausser A, et al. Immunotherapy with a HER2-Targeting *Listeria* Induces HER2-Specific Immunity and Demonstrates Potential Therapeutic Effects in a Phase I Trial in Canine Osteosarcoma. *Clin Cancer Res* (2016) 22(17):4380–90. doi: 10.1158/1078-0432.CCR-16-0088
75. Musser ML, Berger EP, Tripp CD, Clifford CA, Bergman PJ, Johannes CM. Safety evaluation of the canine osteosarcoma vaccine, live *Listeria* vector. *Vet Comp Oncol* (2020) 19(1):92–8. doi: 10.1111/vco.12642
76. Musser ML, Berger EP, Parsons C, Kathariou S, Johannes CM. Vaccine strain *Listeria monocytogenes* abscess in a dog: a case report. *BMC Vet Res* (2019) 15(1):467. doi: 10.1186/s12917-019-2216-y
77. Sinha S, Kuo C-Y, Ho JK, White PJ, Jazayeri JA, Pouton CW. A suicidal strain of *Listeria monocytogenes* is effective as a DNA vaccine delivery system for oral administration. *Vaccine* (2017) 35(38):5115–22. doi: 10.1016/j.vaccine.2017.08.014
78. Hanson WG, Benanti EL, Lemmens EE, Liu W, Skoble J, Leong ML, et al. A Potent and Effective Suicidal *Listeria* Vaccine Platform. *Infect Immun* (2019) 87(8):e00144–19. doi: 10.1128/IAI.00144-19
79. Souders NC, Verch T, Paterson Y. In vivo bactofection: *listeria* can function as a DNA-cancer vaccine. *DNA Cell Biol* (2006) 25(3):142–51. doi: 10.1089/dna.2006.25.142
80. Angelakopoulos H, Loock K, Sisul DM, Jensen ER, Miller JF, Hohmann EL. Safety and shedding of an attenuated strain of *Listeria monocytogenes* with a deletion of actA/plcB in adult volunteers: a dose escalation study of oral inoculation. *Infect Immun* (2002) 70(7):3592–601. doi: 10.1128/IAI.70.7.3592-3601.2002
81. Starks H, Bruhn KW, Shen H, Barry RA, Dubensky TW, Brockstedt D, et al. *Listeria monocytogenes* as a vaccine vector: virulence attenuation or existing antivector immunity does not diminish therapeutic efficacy. *J Immunol* (2004) 173(1):420–7. doi: 10.4049/jimmunol.173.1.420
82. Olino K, Wada S, Edil BH, Pan X, Meckel K, Weber W, et al. Tumor-associated antigen expressing *Listeria monocytogenes* induces effective primary and memory T-cell responses against hepatic colorectal cancer metastases. *Ann Surg Oncol* (2012) 19(Suppl 3):S597–607. doi: 10.1245/s10434-011-2037-0
83. Golub SH, O'Connell TX, Morton DL. Correlation of in vivo and in vitro assays of immunocompetence in cancer patients. *Cancer Res* (1974) 34(8):1833–7.
84. Dietrich G, Bubert A, Gentschev I, Sokolovic Z, Simm A, Catic A, et al. Delivery of antigen-encoding plasmid DNA into the cytosol of macrophages by attenuated suicide *Listeria monocytogenes*. *Nat Biotechnol* (1998) 16(2):181–5. doi: 10.1038/nbt0298-181
85. Sacco JJ, Evans M, Harrington KJ, Man S, Powell N, Shaw RJ, et al. Systemic listeriosis following vaccination with the attenuated *Listeria monocytogenes* therapeutic vaccine, ADXS11-001. *Hum Vaccin Immunother* (2016) 12(4):1085–6. doi: 10.1080/21645515.2016.1154248
86. Lim JY, Brockstedt DG, Lord EM, Gerber SA. Radiation therapy combined with *Listeria monocytogenes*-based cancer vaccine synergize to enhance tumor control in the B16 melanoma model. *Oncoimmunology* (2014) 3:e29028. doi: 10.4161/onci.29028
87. Burdett S, Rydzewska L, Tierney J, Fisher D, Parmar MK, Arriagada R, et al. Postoperative radiotherapy for non-small cell lung cancer. *Cochrane Database Syst Rev* (2016) 10:CD002142. doi: 10.1002/14651858.CD002142.pub4
88. Marmagkiolis K, Finch W, Tsitlakidou D, Josephs T, Iliescu C, Best JF, et al. Radiation Toxicity to the Cardiovascular System. *Curr Oncol Rep* (2016) 18(3):15. doi: 10.1007/s11912-016-0502-4
89. Speer TW. *Targeted Radionuclide Therapy*. Philadelphia: Wolters Kluwer Health/Lippincott Williams & Wilkins (2012).
90. Terán-Navarro H, Calderon-Gonzalez R, Salcines-Cuevas D, García I, Marradi M, Freire J, et al. Pre-clinical development of *Listeria*-based nanovaccines as immunotherapies for solid tumours: insights from melanoma. *Oncoimmunology* (2018) 8(2):e1541534–e. doi: 10.1080/2162402X.2018.1541534
91. Mandal M, Lee K-D. Listeriolysin O-liposome-mediated cytosolic delivery of macromolecule antigen in vivo: enhancement of antigen-specific cytotoxic T lymphocyte frequency, activity, and tumor protection. *Biochim Biophys Acta (BBA) - Biomembranes* (2002) 1563(1):7–17. doi: 10.1016/S0005-2736(02)00368-1
92. Matsumura Y, Maeda H. A new concept for macromolecular therapeutics in cancer chemotherapy: mechanism of tumoritropic accumulation of proteins and the antitumor agent smancs. *Cancer Res* (1986) 46(12 Pt 1):6387–92.
93. Jain S, Hirst DG, O'Sullivan JM. Gold nanoparticles as novel agents for cancer therapy. *Br J Radiol* (2012) 85(1010):101–13. doi: 10.1259/bjr/59448833
94. La-Beck NM, Liu X, Wood LM. Harnessing Liposome Interactions With the Immune System for the Next Breakthrough in Cancer Drug Delivery. *Front Pharmacol* (2019) 10:220. doi: 10.3389/fphar.2019.00220
95. Yu YA, Shabahang S, Timiryasova TM, Zhang Q, Beltz R, Gentschev I, et al. Visualization of tumors and metastases in live animals with bacteria and vaccinia virus encoding light-emitting proteins. *Nat Biotechnol* (2004) 22(3):313–20. doi: 10.1038/nbt937
96. Pilgrim S, Stritzker J, Schoen C, Kolb-Maurer A, Geginat G, Loessner MJ, et al. Bactofection of mammalian cells by *Listeria monocytogenes*: improvement and mechanism of DNA delivery. *Gene Ther* (2003) 10(24):2036–45. doi: 10.4161/bbug.1.6.13146
97. Pálffy R, Gardlík R, Hodosy J, Behuliak M, Reško P, Radvánský J, et al. Bacteria in gene therapy: bactofection versus alternative gene therapy. *Gene Ther* (2006) 13(2):101–5. doi: 10.1038/sj.gt.3302635
98. Krusch S, Domann E, Frings M, Zelmer A, Diener M, Chakraborty T, et al. *Listeria monocytogenes* mediated CFTR transgene transfer to mammalian cells. *J Gene Med* (2002) 4(6):655–67. doi: 10.1002/jgm.313
99. Schoen C, Kolb-Mäurer A, Geginat G, Löffler D, Bergmann B, Stritzker J, et al. Bacterial delivery of functional messenger RNA to mammalian cells. *Cell Microbiol* (2005) 7(5):709–24. doi: 10.1111/j.1462-5822.2005.00507.x
100. Tangney M, van Pijkeren JP, Gahan CGM. The use of *Listeria monocytogenes* as a DNA delivery vector for cancer gene therapy. *Bioeng Bugs* (2010) 1(4):284–7. doi: 10.4161/bbug.1.4.11725
101. van Pijkeren JP, Morrissey D, Monk IR, Cronin M, Cronin M, Rajendran S, et al. A novel *Listeria monocytogenes*-based DNA delivery system for cancer gene therapy. *Hum Gene Ther* (2010) 21(4):405–16. doi: 10.1089/hum.2009.022
102. Loeffler DIM, Schoen CU, Goebel W, Pilgrim S. Comparison of Different Live Vaccine Strategies In Vivo for Delivery of Protein Antigen or Antigen-Encoding DNA and mRNA by Virulence-Attenuated *Listeria monocytogenes*. *Infect Immun* (2006) 74(7):3946. doi: 10.1128/IAI.00112-06
103. Dagogo-Jack I, Shaw AT. Tumour heterogeneity and resistance to cancer therapies. *Nat Rev Clin Oncol* (2018) 15(2):81–94. doi: 10.1038/nrclinonc.2017.166

104. Zhang J, Adrian FJ, Jahnke W, Cowan-Jacob SW, Li AG, Iacob RE, et al. Targeting Bcr-Abl by combining allosteric with ATP-binding-site inhibitors. *Nature* (2010) 463(7280):501–6. doi: 10.1038/nature08675
105. Gong J, Chehrazi-Raffle A, Reddi S, Salgia R. Development of PD-1 and PD-L1 inhibitors as a form of cancer immunotherapy: a comprehensive review of registration trials and future considerations. *J Immunother Cancer* (2018) 6 (1):8. doi: 10.1186/s40425-018-0316-z
106. Wherry EJ. T cell exhaustion. *Nat Immunol* (2011) 12(6):492–9. doi: 10.1038/ni.2035
107. Li K, Tian H. Development of small-molecule immune checkpoint inhibitors of PD-1/PD-L1 as a new therapeutic strategy for tumour immunotherapy. *J Drug Targeting* (2019) 27(3):244–56. doi: 10.1080/1061186X.2018.1440400
108. Xu G, Feng D, Yao Y, Li P, Sun H, Yang H, et al. *Listeria*-based hepatocellular carcinoma vaccine facilitates anti-PD-1 therapy by regulating macrophage polarization. *Oncogene* (2020) 39(7):1429–44. doi: 10.1038/s41388-019-1072-3
109. Kim VM, Blair AB, Lauer P, Foley K, Che X, Soares K, et al. Anti-pancreatic tumor efficacy of a *Listeria*-based, Annexin A2-targeting immunotherapy in combination with anti-PD-1 antibodies. *J Immunother Cancer* (2019) 7 (1):132. doi: 10.1186/s40425-019-0601-5
110. Mkrtichyan M, Chong N, Abu Eid R, Wallecha A, Singh R, Rothman J, et al. Anti-PD-1 antibody significantly increases therapeutic efficacy of *Listeria monocytogenes* (Lm)-LLO immunotherapy. *J Immunother Cancer* (2013) 1:15. doi: 10.1186/2051-1426-1-15
111. Gilley RP, Dube PH. Checkpoint blockade inhibitors enhances the effectiveness of a *Listeria monocytogenes*-based melanoma vaccine. *Oncotarget* (2020) 11(7):740–54. doi: 10.18632/oncotarget.27490
112. Kim CG, Kim C, Yoon SE, Kim KH, Choi SJ, Kang B, et al. Hyperprogressive disease during PD-1 blockade in patients with advanced hepatocellular carcinoma. *J Hepatol* (2021) 74(2):350–9. doi: 10.1016/j.jhep.2020.08.010
113. Finn RS, Ryoo BY, Merle P, Kudo M, Bouattour M, Lim HY, et al. Pembrolizumab As Second-Line Therapy in Patients With Advanced Hepatocellular Carcinoma in KEYNOTE-240: A Randomized, Double-Blind, Phase III Trial. *J Clin Oncol* (2020) 38(3):193–202. doi: 10.1200/JCO.19.01307
114. Rosenberg SA, Restifo NP. Adoptive cell transfer as personalized immunotherapy for human cancer. *Science* (2015) 348(6230):62–8. doi: 10.1126/science.aaa4967
115. D'Ippolito E, Schober K, Nauerth M, Busch DH. T cell engineering for adoptive T cell therapy: safety and receptor avidity. *Cancer Immunol Immunother* (2019) 68(10):1701–12. doi: 10.1007/s00262-019-02395-9
116. Labani-Motlagh A, Ashja-Mahdavi M, Loskog A. The Tumor Microenvironment: A Milieu Hindering and Obstructing Antitumor Immune Responses. *Front Immunol* (2020) 11:940. doi: 10.3389/fimmu.2020.00940
117. Jahangir A, Chandra D, Quispe-Tintaya W, Singh M, Selvanesan BC, Gravekamp C. Immunotherapy with *Listeria* reduces metastatic breast cancer in young and old mice through different mechanisms. *Oncoimmunology* (2017) 6(9):e1342025. doi: 10.1080/2162402X.2017.1342025
118. Sotillo E, Barrett DM, Black KL, Bagashev A, Oldridge D, Wu G, et al. Convergence of Acquired Mutations and Alternative Splicing of CD19 Enables Resistance to CART-19 Immunotherapy. *Cancer Discov* (2015) 5 (12):1282–95. doi: 10.1158/2159-8290.CD-15-1020
119. Walsh SR, Simovic B, Chen L, Bastin D, Nguyen A, Stephenson K, et al. Endogenous T cells prevent tumor immune escape following adoptive T cell therapy. *J Clin Invest* (2019) 129(12):5400–10. doi: 10.1172/JCI126199
120. Lu S. Heterologous prime-boost vaccination. *Curr Opin Immunol* (2009) 21 (3):346–51. doi: 10.1016/j.coi.2009.05.016
121. Liu J, Ewald BA, Lynch DM, Denholtz M, Abbink P, Lemckert AA, et al. Magnitude and phenotype of cellular immune responses elicited by recombinant adenovirus vectors and heterologous prime-boost regimens in rhesus monkeys. *J Virol* (2008) 82(10):4844–52. doi: 10.1128/JVI.02616-07
122. Johnson LE, Brockstedt D, Leong M, Lauer P, Theisen E, Sauer JD, et al. Heterologous vaccination targeting prostatic acid phosphatase (PAP) using DNA and *Listeria* vaccines elicits superior anti-tumor immunity dependent on CD4+T cells elicited by DNA priming. *Oncoimmunology* (2018) 7(8):2–10. doi: 10.1080/2162402X.2018.1456603
123. Aitken AS, Roy DG, Martin NT, Sad S, Bell JC, Bourgeois-Daigneault MC. Brief Communication; A Heterologous Oncolytic Bacteria-Virus Prime-Boost Approach for Anticancer Vaccination in Mice. *J Immunother* (2018) 41(3):125–9. doi: 10.1097/CJI.0000000000000208
124. Ishizaki H, Song GY, Srivastava T, Carroll KD, Shahabi V, Manuel ER, et al. Heterologous prime/boost immunization with p53-based vaccines combined with toll-like receptor stimulation enhances tumor regression. *J Immunother* (2010) 33(6):609–17. doi: 10.1097/CJI.0b013e3181e032c6
125. Zebertavage L, Bambina S, Shugart J, Alice A, Zens KD, Lauer P, et al. A microbial-based cancer vaccine for induction of EGFRvIII-specific CD8+ T cells and anti-tumor immunity. *PloS One* (2019) 14(1):e0209153. doi: 10.1371/journal.pone.0209153
126. Connell PP, Hellman S. Advances in radiotherapy and implications for the next century: a historical perspective. *Cancer Res* (2009) 69(2):383–92. doi: 10.1158/0008-5472.CAN-07-6871
127. Kumari S, Mukherjee S, Sinha D, Abdisalaam S, Krishnan S, Asaithamby A. Immunomodulatory Effects of Radiotherapy. *Int J Mol Sci* (2020) 21(21):11–7. doi: 10.3390/ijms21218151
128. Garnett-Benson C, Hodge JW, Gameiro SR. Combination regimens of radiation therapy and therapeutic cancer vaccines: mechanisms and opportunities. *Semin Radiat Oncol* (2015) 25(1):46–53. doi: 10.1016/j.semradonc.2014.07.002
129. Barker HE, Paget JT, Khan AA, Harrington KJ. The tumour microenvironment after radiotherapy: mechanisms of resistance and recurrence. *Nat Rev Cancer* (2015) 15(7):409–25. doi: 10.1038/nrc3958
130. Hannan R, Zhang H, Wallecha A, Singh R, Liu L, Cohen P, et al. Combined immunotherapy with *Listeria monocytogenes*-based PSA vaccine and radiation therapy leads to a therapeutic response in a murine model of prostate cancer. *Cancer Immunol Immunother* (2012) 61(12):2227–38. doi: 10.1007/s00262-012-1257-x
131. Merle NS, Noe R, Halbwachs-Mecarelli L, Fremeaux-Bacchi V, Roumenina LT. Complement System Part II: Role in Immunity. *Front Immunol* (2015) 6:257. doi: 10.3389/fimmu.2015.00257
132. Markiewski MM, DeAngelis RA, Benencia F, Ricklin-Lichtsteiner SK, Koutoulaki A, Gerard C, et al. Modulation of the antitumor immune response by complement. *Nat Immunol* (2008) 9(11):1225–35. doi: 10.1038/ni.1655
133. Wang Y, Sun SN, Liu Q, Yu YY, Guo J, Wang K, et al. Autocrine Complement Inhibits IL10-Dependent T-cell-Mediated Antitumor Immunity to Promote Tumor Progression. *Cancer Discov* (2016) 6 (9):1022–35. doi: 10.1158/2159-8290.CD-15-1412
134. Reese B, Silwal A, Daugherity E, Daugherity M, Arabi M, Daly P, et al. Complement as Prognostic Biomarker and Potential Therapeutic Target in Renal Cell Carcinoma. *J Immunol* (2020) 205(11):3218–29. doi: 10.4049/jimmunol.2000511
135. Ghouse SM, Vadrevu SK, Manne S, Reese B, Patel J, Patel B, et al. Therapeutic Targeting of Vasculature in the Premetastatic and Metastatic Niches Reduces Lung Metastasis. *J Immunol* (2020) 204(4):990–1000. doi: 10.4049/jimmunol.1901208
136. Nowak AK, Robinson BWS, Lake RA. Synergy between Chemotherapy and Immunotherapy in the Treatment of Established Murine Solid Tumors. *Cancer Res* (2003) 63(15):4490.
137. Nowak AK, Lake RA, Marzo AL, Scott B, Heath WR, Collins EJ, et al. Induction of Tumor Cell Apoptosis In Vivo Increases Tumor Antigen Cross-Presentation, Cross-Priming Rather than Cross-Tolerizing Host Tumor-Specific CD8 T Cells. *J Immunol* (2003) 170(10):4905. doi: 10.4049/jimmunol.170.10.4905
138. Le DT, Jaffee EM. Regulatory T-cell modulation using cyclophosphamide in vaccine approaches: a current perspective. *Cancer Res* (2012) 72(14):3439–44. doi: 10.1158/0008-5472.CAN-11-3912
139. Yoshimura K, Laird LS, Chia CY, Meckel KF, Slansky JE, Thompson JM, et al. Live attenuated *Listeria monocytogenes* effectively treats hepatic colorectal cancer metastases and is strongly enhanced by depletion of regulatory T cells. *Cancer Res* (2007) 67(20):10058–66. doi: 10.1158/0008-5472.CAN-07-0573
140. Keenan BP, Saenger Y, Kafrouni MI, Leubner A, Lauer P, Maitra A, et al. A *Listeria* vaccine and depletion of T-regulatory cells activate immunity against early stage pancreatic intraepithelial neoplasms and prolong

survival of mice. *Gastroenterology* (2014) 146(7):1784–94 e6. doi: 10.1053/j.gastro.2014.02.055
141. Hingorani SR, Wang L, Multani AS, Combs C, Deramaudt TB, Hruban RH, et al. Trp53R172H and KrasG12D cooperate to promote chromosomal instability and widely metastatic pancreatic ductal adenocarcinoma in mice. *Cancer Cell* (2005) 7(5):469–83. doi: 10.1016/j.ccr.2005.04.023
142. Beatty GL, Gladney WL. Immune escape mechanisms as a guide for cancer immunotherapy. *Clin Cancer Res* (2015) 21(4):687–92. doi: 10.1158/1078-0432.CCR-14-1860
143. Singh R, Paterson Y. Immunoediting sculpts tumor epitopes during immunotherapy. *Cancer Res* (2007) 67(5):1887–92. doi: 10.1158/0008-5472.CAN-06-3960
144. Kim SH, Castro F, Paterson Y, Gravekamp C. High efficacy of a *Listeria*-based vaccine against metastatic breast cancer reveals a dual mode of action. *Cancer Res* (2009) 69(14):5860–6. doi: 10.1158/0008-5472.CAN-08-4855

Conflict of Interest: YP has a financial interest in Advaxis, Inc., a vaccine and therapeutic company that has licensed or has an option to license all patents from the University of Pennsylvania that concern the use of *Listeria monocytogenes* or listerial products as vaccines.

The remaining authors declare that the research was conducted in the absence of any commercial or financial relationships that could be construed as a potential conflict of interest.

Copyright © 2021 Oladejo, Paterson and Wood. This is an open-access article distributed under the terms of the Creative Commons Attribution License (CC BY). The use, distribution or reproduction in other forums is permitted, provided the original author(s) and the copyright owner(s) are credited and that the original publication in this journal is cited, in accordance with accepted academic practice. No use, distribution or reproduction is permitted which does not comply with these terms.

frontiers in Oncology

ORIGINAL RESEARCH
published: 28 June 2021
doi: 10.3389/fonc.2021.636977

A Novel HAGE/WT1-ImmunoBody® Vaccine Combination Enhances Anti-Tumour Responses When Compared to Either Vaccine Alone

*Rukaia Almshayakhchi[1,2], Divya Nagarajan[1,2], Jayakumar Vadakekolathu[1,2], Barbara-Ann Guinn[3], Stephen Reeder[1,2], Victoria Brentville[4], Rachael Metheringham[4], A. Graham Pockley[1,2], Lindy Durrant[4] and Stephanie McArdle[1,2]**

[1] John van Geest Cancer Research Centre, School of Science and Technology, Nottingham Trent University, Nottingham, United Kingdom, [2] Centre for Health, Ageing and Understanding Disease, School of Science and Technology, Nottingham Trent University, Nottingham, United Kingdom, [3] Department of Biomedical Sciences, University of Hull, Hull, United Kingdom, [4] Scancell Ltd, Biodiscovery Institute, University of Nottingham, Nottingham, United Kingdom

OPEN ACCESS

Edited by:
Sophia N. Karagiannis, King's College London, United Kingdom

Reviewed by:
Satu Mustjoki, University of Helsinki, Finland
Ali Roghanian, University of Southampton, United Kingdom

***Correspondence:**
Stephanie McArdle
stephanie.mcardle@ntu.ac.uk

Specialty section:
This article was submitted to Cancer Immunity and Immunotherapy, a section of the journal Frontiers in Oncology

Received: 02 December 2020
Accepted: 14 May 2021
Published: 28 June 2021

Citation:
Almshayakhchi R, Nagarajan D, Vadakekolathu J, Guinn BA, Reeder S, Brentville V, Metheringham R, Pockley AG, Durrant L and McArdle S (2021) A Novel HAGE/WT1-ImmunoBody® Vaccine Combination Enhances Anti-Tumour Responses When Compared to Either Vaccine Alone. Front. Oncol. 11:636977. doi: 10.3389/fonc.2021.636977

Many cancers, including myeloid leukaemia express the cancer testis antigen (CTA) DDX43 (HAGE) and/or the oncogene Wilms' tumour (WT1). Here we demonstrate that HAGE/WT1-ImmunoBody® vaccines derived T-cells can kill *ex-vivo* human CML cell lines expressing these antigens and significantly delay B16/HHDII$^+$/DR1$^+$/HAGE$^+$/WT1$^+$ tumour growth in the HHDII/DR1 mice and prolonged mouse survival in the prophylactic setting in comparison to non-immunised control mice. We show that immunisation of HHDII/DR1 mice with HAGE- and WT1-ImmunoBody® DNA vaccines in a prime-boost regime in two different flanks induce significant IFN-γ release by splenocytes from treated mice, and a significant level of cytotoxicity against tumour targets expressing HAGE/WT1 *in vitro*. More importantly, the combined HAGE/WT1 ImmunoBody® vaccine significantly delayed tumour growth in the B16/HHDII$^+$/DR1$^+$/HAGE$^+$/WT1$^+$ tumour model and prolonged mouse survival in the prophylactic setting in comparison to non-immunised control mice. Overall, this work demonstrates that combining both HAGE- and WT1-ImmunoBody® into a single vaccine is better than either vaccine alone. This combination vaccine could be given to patients whose cancer expresses HAGE and WT1 in parallel with existing therapies in order to decrease the chance of disease progression and relapse.

Keywords: WT1, ImmunoBody®, immunotherapy, HAGE, cancer vaccine combination, HHDII/DR1 mice

Abbreviations: Allo-SCT, allogeneic-stem cell transplantation; HAGE, helicase antigen; DDX43, DEAD-Box Helicase 43; WT1, Wilms tumour; CML, chronic myeloid leukaemia; TKIs, tyrosine kinase inhibitors; ER, endoplasmic reticulum; FCS, Foetal calf serum; β2m, beta2 microglobulin; TAPs, transporter-associated proteins; DMSO, Dimethyl sulfoxide; BFA, Brefeldin A; RT-qPCR, Real-time quantitative polymerase chain reaction; CT, cycle threshold; MFI, mean fluorescence intensity; FIR, fluorescence intensity ratio; PI, propidium iodide; FITC, fluorescein isothiocyanate; ^{51}Cr, ^{51}Chromium; ELISpot, Enzyme-linked immunospot; IVS, *in vitro* peptide re-stimulation; PD-1, programmed death-1; shRNA, Short hairpin RNA.

INTRODUCTION

The role of a cancer vaccine is to stimulate cellular immune responses that effectively lead to anti-tumour cytotoxic T-lymphocyte (CTL) responses. We have previously shown that DNA vaccines in which antigenic epitopes are encoded within an antibody framework can lead to T cell responses and delayed tumour growth (1). ImmunoBody(R) vaccines have entered Phase I clinical trials (2) and demonstrated safety as well as immune responses in 23/25 evaluable melanoma patients. Previous studies have incorporated epitopes from a single antigen to stimulate anti-tumour responses (3) but few have used epitope combinations that could widen the applicability of vaccines to stimulate both CD4+ and CD8+ T cell responses and recognise multiple tumour cell populations (2).

The oncogene Wilm's Tumour (WT1) has been found to play a role in normal kidney, genital tract and eye development and be mutated in some Wilms' tumours. In addition it has been found to be elevated in uterine leiomyosarcoma and carcinosarcomas (4) as well as epithelial ovarian cancer (5). However it is frequently used as a marker of minimal residual disease in chronic myeloid and acute leukaemia (6) having been found to be overexpressed in malignant but not healthy haematopoietic cells. WT1 is one of a number of leukaemia associated antigens that have been considered as promising targets for immunotherapy because of their ability to elicit specific immune responses against antigen-bearing cancerous cells while sparing normal tissues. A National Cancer Institute pilot project by Cheever et al. (7), developed a priority-ranked list of cancer vaccine target antigens based on predefined and weighted criteria for the 'ideal' antigen. Although no single antigen met all of the top subcriteria such as therapeutic function, immunogenicity and having already been in clinical trials, WT1 was identified as the top ranked antigen for these criteria and WT1 is overexpressed in most *de novo* acute myeloid leukaemia (AML) cases (8) and in chronic myeloid leukaemia (CML) (9). More specifically WT1 was shown to be expressed in 50–100% cases of blast crisis but not in chronic or accelerated phase cases (10).

HAGE is a cancer-testis antigen (CTA), a member of a family of HAGE was found to be expressed in (12/16) 75% of carcinomas (11) and in 57% of CML patient samples at diagnosis (12). Expression of HAGE, like many CTAs (13, 14), is limited in healthy tissues except immunologically protected sites such as the testis and placenta, making it an excellent target for immunotherapy due to its low associated risk of effective treatment causing damage to healthy tissues.

Leukaemia, and CML in particular, have gained a special attention in the field of the immunotherapy due to the fact that the circulating tumour cells are readily accessible to immune attack. Furthermore, the disease has a well-defined carcinogenesis pathway that allows for the development of immunotherapies targeting particular and well characterised targets. CML is a clonal myeloproliferative disorder resulting from malignant transformation of the primitive haematopoietic stem cell (HSC). The disease is characterised by the formation of a fusion gene, called *BCR/ABL1* which encodes a chimeric protein that has a constitutive oncogenic tyrosine kinase (TK) activity. Targeting this enzyme using tyrosine kinase inhibitors (TKIs) such as imatinib (15), which is often the first line 'gold standard' therapeutic approach, has significantly improved the clinical outcome for patients with CML. Despite this, 35-40% of patients with CML on TKIs develop resistance (16), often due to the clonal outgrowth of CML cells harbouring BCR-ABL point mutations (recently reviewed in (17). These findings demonstrate that most TKIs are not curative, but merely put CML stem cells into a state of autophagy (18). However, the pathognomonic molecular characteristics of CML and the particular nature of cancer-host immune cells interaction in CML, as well as the advantageous immunomodulatory effects of the imatinib therapy (19), all offer a favourable setting in which immunotherapeutic strategies could be added with synergistic effect. Indeed, active immunotherapeutic strategies that enhance T cell responses against specific antigens in patients on imatinib therapy could increase the number of patients experiencing relapse-free survival following cessation of imatinib.

Using data from CML single cell (SC) gene expression downloaded from GEO database (Acc. No. GSE76312 (20),) we were able to demonstrate that both HAGE and WT1 genes were expressed in CML cancer stem cells but not in HSC cells highlighting the specific tumour cell expression of these antigens (**Supplementary Figure 1**). Thus it made sense to assess the capacity of two sequences, one derived from DDX43 (HAGE) and the other from WT1, to generate effective anti-tumour immune responses in a humanised HHDRII/DR1 mouse model and determine the ability the ImmunoBody® DNA delivery system (1) to induce tumour-specific cell death. Although ImmunoBody® DNA can be administered *via* intradermal, intravenous, intramuscular, subcutaneous or intraperitoneal routes (21), the standard method is the intradermal route using a gene gun device in mice, and i.m. injection combined with electroporation in humans (2). The overall goal of this study was to evaluate the capacity of a combined HAGE/WT1 sequence-based vaccine to eliminate/prevent the growth of HAGE/WT1 expressing tumours. We hypothesised that combining both HAGE and WT1 vaccines would be more effective against cancerous cells expressing both antigens through the reduced chance of escape variants, and also that such a vaccine could be used against a wider range of cancers that express either, or both of these antigens.

This study has therefore explored and compared the following aspects; the immunogenicity of HAGE and WT1 derived ImmunoBody® vaccines individually and in combination in HHDII/DR1 mice, the capacity of the vaccines given individually and in combination to induce activated cytotoxic T cells that can specifically recognise and kill HAGE/WT1-expressing targets *in vitro*, and finally, the *in vivo* capability of the combined vaccine to induce tumour rejection using $HAGE^{+}$/$WT1^{+}$ expressing humanised B16 cells as a "Proof-of-Concept" in tumour challenge experiments.

MATERIALS AND METHODS

Animals

HHDII-DR1 double transgenic mice expressing human α1 and α2 chains of HLA-A*0201 chimeric with α3 chain of H-2Dd

allele (HHDII), also expressing HLA-DRB*0101, and knocked out for the expression of murine MHC class I (H-2b) and II (I-Ab) were provided by Dr. Lone (CNRS, Orleans, France). Animal use and care was in accordance with EU Directive 2010/63/EU and UK Home Office Code of Practice for the housing and care of animals bred, supplied, or used for scientific purposes. The studies were undertaken with UK Home Office approval. Females aged between 6-8 weeks were used for this study. Three mice per group were used to assess the immunogenicity of the vaccine in at least two independent studies, whereas a minimum of 10 mice per group were used for tumour model experiments.

Cell Lines and Growth Condition

The Transporter-Associated Proteins (TAP) deficient, HLA-A2+ lymphoblastoid suspension cell line, T2 (22), was a gift from Dr. J. Bartholomew (Paterson Institute, Manchester, UK). The CML derived cell line K562 was purchased from ATCC, the KCL-22 CML cell line was kindly provided by Anthony Nolan (UK, https://www.anthonynolan.org). T2 cells, KCL-22 and TCC-S cells were cultured in the Roswell Park Memorial Institute (RPMI) 1640 medium (SLS/Lonza, BE12-167F) containing 10% (v/v) foetal bovine serum (FBS, Life Technologies, 10270106) and 2mM L-Glutamine (SLS/Lonza, BE17-605E). K562 cells were cultured in Iscove's modified Dulbecco's medium (IMDM, SLS/Lonza, BE12-722F) containing 10% (v/v) FBS.

For the tumour implant model, the B16F1 (murine melanoma) cell line was knocked out for both murine endogenous MHC class I and II by Zinc Finger Nuclease (ZFN) technology and stably transfected with plasmids encoding both HHDII and HLA-DR1 molecules. Cells were grown in RPMI 1640 supplemented with 10% (v/v) FBS, 1% L-Glutamine, 300µg/mL Hygromycin (Insight Biotechnology, Middlesex, UK) and 500µg/mL Geneticin (Insight Biotechnology). The cells were further transfected with luciferase and HAGE constructs (23). In this study, the cells were referred to as $_{h}$B16/HAGE^{+}/Luc^{+}, and maintained in RPMI-1640 medium supplemented with 10% (v/v) FBS, 1% L-Glutamine, 300µg/mL hygromycin and 550µg/mL zeocin (Thermo Fisher Scientific, U.K.) to retain luciferase gene expression, and 1µg/mL puromycin (Thermo Fisher Scientific) to retain HAGE gene expression. The HEK293T human embryonic kidney cell line (Thermo Fisher Scientific) was maintained in DMEM (SLS/Lonza, Yorkshire, U.K.) containing 10% (v/v) FBS and 2mM L-Glutamine - these cells were routinely used for viral gene transduction. All cells were maintained in a 37°C incubator with 5% (v/v) CO_2.

Epitope Prediction

The WT1 protein sequence was screened for peptides that have binding affinity to HLA-A2 and HLA-DR1 molecules using a web-based algorithm (www.syfpeithi.de) (24) and peptides selected according to their binding score. A 15 amino acid long peptide (VRDLNALLPAVPSLG) derived from the WT1 protein was chosen. The HAGE 30mer sequence used in this study (QTGTGKTLCYLMPGFIHLVLQPSLKGQRNR) has previously been studied by our group (23), and the same class I and class II HAGE-derived peptides were used herein. All peptides were synthesised by GenScript Ltd (Piscataway, USA), with a minimum purity of 80%. All peptides were reconstituted in 100% (v/v) dimethyl sulfoxide (DMSO) to a stock concentration of 10mg/mL and stored at -80°C in small aliquots to minimise the number of freeze/thaw cycles.

Peptide Binding Affinity Assay

A T2 peptide-binding assay was performed to evaluate the binding affinity of the HAGE and WT1 class I peptide sequences to the HLA-A2 molecules, as predicted by SYFPEITHI software. T2 cells are an HLA-A2 human lymphoblast suspension cell line that have been genetically modified to produce mutated non-functional TAPs that are necessary to transport MHC class I restricted peptides into the endoplasmic reticulum (ER). This defect results in a failure to present internal TAP-dependant peptides and instead MHC molecules leave the ER and the Golgi compartments empty, leading to a 70–80% reduction of HLA-A2 expression on T2 cell surface. These empty molecules are not stable and are quickly recycled. However, the empty HLA-A2 molecules on the surface of cells can be stabilised by addition of exogenous peptides for which they have an affinity (25). T2 cells are therefore frequently used to validate the binding of exogenously administered peptides. Briefly, in a sterile 96-well rounded-bottom plate, T2 cells were plated at 0.5×10^{6} cells/100µL in serum-free RPMI medium supplemented with 3µg/mL human β2m (Sigma-Aldrich, Hertfordshire, U.K.) in the presence of varying concentrations of HAGE and WT1 class I peptides or with DMSO as negative controls and then incubated at 26°C overnight. T2 cells were then harvested, washed and stained with an APC-conjugated human HLA-A2 monoclonal antibody (BioLegend, 343308, Clone: BB7.2) for 30 minutes at 4°C. Cells were then washed and stained with propidium iodide (PI, Sigma-Aldrich) to exclude dead cells, and then immediately run to assess HLA-A2 expression using a Beckman Coulter Gallios™ flow cytometer and Kaluza™ data acquisition and analysis software.

Brefeldin A Decay Assay (BFA)

A BFA decay assay was performed to evaluate the stability of the class I peptide-HLA-A2 complex on the cell surface. For this, T2 cells were seeded in a 96-well rounded-bottom plate at a concentration of 1×10^{6} cells/100 µL in a serum-free RPMI medium containing 3µg/mL human β2m. Cells were cultured with either the candidate peptides at a final concentration of 50µg (as determined by T2 binding assay) or with DMSO as a negative control and incubated at 26°C overnight. The next day, one batch of cells was washed and incubated with 10µg/mL BFA (BioLegend, 420601) for 1 hour at 37°C (Time 0) and thereafter every two hours until 8 hours. After each incubation, cells were transferred into 12x75 mm polycarbonate tubes, washed and stained with an APC-conjugated human HLA-A2 monoclonal antibody (BioLegend, 343308, Clone: BB7.2) for 30 minutes at 4° C and analysed using the flow cytometer. Dead cells were excluded by staining with LIVE/DEAD™ viability dye (Invitrogen) or PI (Sigma-Aldrich).

The stability of peptide-HLA-A2 complex was assessed by calculating the DC_{50} value, which is defined as the time required

for a 50% reduction in the level of MFI recorded at time 0 (26), the longer the time for this to happen, the more stable the complex. The DC_{50} was calculated according to the formula: (MFI at a given time point/MFI at time 0) X100%. T2 cells incubated in the absence of peptide, but in the presence of the same concentrations of DMSO were used as negative controls.

Target Cell Line Preparation: Gene Knock-In and Knock Down

The CML derived cell lines, K562, KCL-22 and TCC-S were genetically engineered to either over express HAGE and/or WT1 proteins or HAGE and/or WT1 expression was silenced. K562 cells constitutively express low levels of HLA and were electroporated with the pcDNA-3.1/HHDII gene using SF cell line 4D Nucleofection™ Xkit/Amaxa according to manufacturer's instructions. Positively transfected cells were selected using 2000μg/mL of G418. K562/HHDII$^+$ cells and KCL-22 cells were transduced with HAGE using a PLenti.Puro/HAGE plasmid. An empty plasmid control PLenti.Puro/empty vector, was used as a vector control. Cells were selected with 1μg/mL puromycine and 2000μg/mL G418 in a 24-well plate at 37°C in 5% (v/v) CO_2. Gene silencing was performed using short hairpin RNA (shRNA) sequences targeting the human WT1 (MISSION shRNA/Sigma-Aldrich in TCC-S cells

(WT1.shRNA$_1$,TRCN0000010466,CGGATGAACTTAGGAGCCACCTTCTCGAGAAGGTGGCTCCTAAGTTCATCTTTTTG and WT1.shRNA$_2$, TRCN0000040064,

CCGGGCAGTGACAATTTATACCAAACTCGAGTTTGGTATAAATTGTCACTGCTTTTTG).

After have being transduced, cells were selected with 1μg/mL puromycin and assessed for either HAGE or WT1 expression using Western blot and RT-qPCR.

Real-Time Quantitative Polymerase Chain Reaction (RT-qPCR)

RT-qPCR was used to assess the expression of the genes of interest in target cells. Briefly, total RNA was isolated from cell lines using a RNeasy Mini Kit (Qiagen, Lancashire, UK), following the manufacturer's instructions. The quantity and purity of the produced RNA was evaluated using a NanoDrop™ 8000 Spectrophotometer (ThermoFisher Scientific). 2μg of RNA was then reverse transcribed into cDNA using Promega M-MLV Reverse Transcriptase. For each qPCR reaction, 1μL of cDNA (diluted 1:1 in ddH_2O) was mixed with 6.75μL of SYBR™ Green Supermix (Bio-Rad, 172-5124), 0.5μL (5pmol) of the forward, 0.5μL (5pmol) of the reverse primer (Sigma-Aldrich) and 3.25μL of molecular grade water. Each sample was run in triplicate on a Rotor-Gene Q real-time PCR cycler (Qiagen). **Table 1** below summarises primer pair sequences and annealing temperatures used in the PCR reaction. It also shows the HAGE-codon optimised pair primers which were used to detect the transduced HAGE gene in the modified cells. Expression levels of each genes were calculated using comparative CT method (27).

Protein Assay and Western Blot Analysis

Immunoblotting was performed to detect HAGE and/or WT1 expression in target cells. Briefly, CML cells were washed twice with cold DPBS, lysed in bromophenol blue free-Laemmli lysis buffer containing 0.125M Tris-HCl (pH 6.8), 4% (w/v) SDS, and 20% (v/v) glycerol and 10% (v/v) 2-mercaptoethanol. Cells were then boiled for 15 minutes at 95°C to denature proteins. To determine the quantity of protein in the lysates obtained, a protein assay (Bio-Rad, 500-0116) was performed following the manufacturer's protocol, wherein standards were prepared by serial dilutions of bovine serum albumin (BSA) diluted in bromophenol blue free-Laemmli lysis buffer. A pre-calculated volume of sample containing 30μg of protein was loaded onto on Tris/glycine SDS-polyacrylamide gels alongside 5μL of marker ladder (Precision Plus Protein™, Bio-Rad, Hertfordshire, UK). The proteins on gels were then transferred onto Amersham Hybond-P PVDF membranes (GE Healthcare, Life science, UK) for 60 minutes at 100V at 4°C. The membranes were then blocked with TBS-Tween-20 (TBST) containing 5% (w/v) Marvel milk powder under a constant agitation for 1 hour at room temperature. After being thoroughly washed, membranes were blotted with primary antibodies at a concentration recommended by the manufacturer's instructions (rabbit anti-human WT1 antibody, Abcam, Ab89901) and (rabbit anti-human DDX43 antibody, Sigma-Aldrich, HPA031381) and kept rocking overnight at 4°C. The next day, the membrane was washed 5 times with TBST, for 5 minutes each, and incubated in horseradish peroxidase (HRP)-conjugated secondary antibodies; HRP-conjugated anti-rabbit IgG antibody (Cell Signaling Technology, 70745, 1:1000) and HRP-conjugated anti-mouse IgG (Cell Signaling Technology, 70765). At the same time, Precision Protein™ Strep-Tactin™ HRP-conjugate, (Bio-Rad, 161-0380) was also added. Membranes were kept under a constant agitation for 2 hours at room

TABLE 1 | Primers and annealing temperatures used in RT-qPCR assay.

Primers	Sequence	Annealing Temp
WT1 forward	GACTCATACAGGTGAAAAGC	58°C
WT1 reverse	GAGTTTGGTCATGTTTCTCTG	58°C
DDX43 forward	CAACACCTATTCAGTCACAG	58°C
DDX43 reverse	GACCAGATGAATAAATCCAGG	58°C
GUSB forward	ACTGAACAGTCACCGAC	58°C
GUSB reverse	AAACATTGTGACTTGGCTAC	58°C
HAGE forward (codon optimised)	CCACATGCACTTTCGACGAT	58°C
HAGE reverse (codon optimised)	ATTCCTGGTCGGTTCCTCTG	58°C

temperature. After giving an additional five washes, membranes were developed using Clarity™ Western ECL Substrate (Bio-Rad, 170-5061) and luminescence was detected by G:BOX XT4: Chemiluminescence and Fluorescence Imaging System (Syngene). For each sample, mouse anti β-actin was used as a loading control (Sigma-Aldrich, A5441).

Phenotypic Analysis of Target Cell Lines

Surface staining was performed to characterise target cells phenotypically to detect HLA-A2 expression using an (APC-conjugated anti-human HLA-A2 antibody (BioLegend, 343308, Clone: BB7.2). Phenotypic analysis was also performed to assess the success of HHDII gene transfection using an FITC-conjugated anti-human β2m antibody (Sigma-Aldrich, SAB4700012, Clone: β2M-01). Cells were incubated with PI immediately prior to running the samples. At the end of the assay, cells were re-suspended in Beckman Coulter Isoton II™ diluent and analysed immediately on the Beckman Coulter Gallios™ flow cytometer.

DNA Vaccine-Bullet Preparation

Expression vectors encoding HAGE- and WT1-ImmunoBody® (28) were coated onto 1.0μm gold microcarriers, as per the manufacturer's instructions. In brief, 200μL of 0.05M spermidine containing 16.6mg of gold was mixed with 36μg of the ImmunoBody® DNA. After giving the sample a short sonication, 200μL of 1M $CaCl_2$ was then added in a dropwise manner to the mixture while vertexing, and then the DNA-gold complex was kept for 10 minutes at the room temperature. The pellet was then re-suspended in 2mL of 0.025mg/mL Polyvinylpyrrolidone after being washed twice with anhydrous ethanol. After this, and while the tube was sonicating, the sample was syringed into dried Tefzel™ tubing and kept standing in a Tubing Prep Station for five minutes. Without disturbing the gold, the ethanol was then gradually taken off using a syringe. Nitrogen gas was turned on while the tube was kept spinning for 7-10 minutes inside the station. When completely dried out, the tube was detached from the station and cut by a guillotine. Bullets were kept at 4°C until used.

Immunisation Programme

HHDII/DR1 mice were immunised with DNA bullet containing 1μg of either HAGE DNA ImmunoBody® which encodes the HAGE 30-mer sequence [QTGTGKTLCYLMPGFIH LVLQPSLKGQRNR] or WT1 ImmunoBody® which encodes the WT1 15-mer sequence [VRDLNALLPAVPSLG] or both, administered by gene gun device on Day 1, 7 and 14. On Day 21, mice were culled and splenocytes were immediately harvested and used in an IFN-γ Enzyme-Linked ImmunoSpot (ELISpot) assay.

Ex Vivo IFN-γ ELISpot Assay

The immunogenicity of either HAGE or WT1 peptides was determined using splenocytes harvested from immunised mice in an *ex vivo* IFN-γ ELISpot assay (ELISpot kit for mouse IFN-γ/ MABTECH, 3321-2A). The assay was performed as previously described (29). Briefly $0.5x10^6$ of freshly isolated splenocytes were seeded per well in triplicates into the pre-coated IFN-γ ELISpot plate along with 1μg/mL of either HLA class I or 10μg/mL of HLA class II HAGE/WT1 derived peptides, cells were then incubated at 37°C in a 5% (v/v) CO_2 incubator for 48 hours. The plates were then washed and biotinylated detection antibody against mouse IFN-γ was then added and incubated for 2 hours at room temperature. Plates were then washed followed by the addition of alkaline phosphatase (AP)-conjugated streptavidin, after which they were incubated for 60 minutes at room temperature. Plates were washed, development solution (BCIP/NBT, Bio-Rad) added left in dark at room temperature until spots could be seen. Once spots developed, the reaction was stopped by rinsing the plates under tap water. Plates were then left to dry and the spots were quantified using an ELISpot plate reader (Cellular Technology Limited). Staphylococcal enterotoxin-B (SEB), was used as a positive control, and unstimulated splenocytes (cells alone) were used as a negative control for every ELISpot assay. Animals were scored as having a positive reaction when the number of spots in the cells alone wells did not reach more than 20 spots and when the response in the peptide containing wells were at least twice that of standard deviation of the mean of the control wells.

Chromium (^{51}Cr) Release Cytotoxicity Assay

Splenocytes derived from vaccinated mice were cultured for 7 days with mitomycin-C treated peptide pulsed LPS blast cells as previously written (29). Briefly, LPS blast cells were prepared using splenocytes extracted from naïve mice and stimulated with LPS and dextran sulphate in a T75 flask. After 48 hours, cells from LPS blasts were harvested and treated with mitomycin-C. Following the incubation, cells were washed and counted and incubated with immunogenic HLA class I peptides, as determined by the *ex vivo* IFN-γ ELISpot assay for 90 minutes at 37°C. The peptide-pulsed LPS cells were then washed and co-cultured with freshly isolated splenocytes from immunised mice at a ratio (1) LPS (5): splenocytes in the presence of β-mercaptoethanol and murine IL-2 (mIL-2, Sigma-Aldrich, I0523, 50U/mL) at 37°C for 6 days. After incubation, LPS blast/T cells were then harvested, washed and counted to be ready for co-culture with ^{51}Cr-labelled target cells.

Target cells were labelled with 1.85Mbq of ^{51}Cr in a water bath at 37°C for one hour. Cells were then washed twice and rested for another hour at 37°C in 1mL of medium. Meanwhile, *in vitro* stimulated T cells were harvested and counted. Effector cells and target cells were plated in a 96-well rounded-bottom plate at a final volume of 200μL at different effector: target ratios of 100:1, 50:1, 25:1 and 12.5:1. Maximum and spontaneous release were set up in 4 replicates using 1% (w/v) SDS and plain medium, respectively. After 24 hours of co-culture of the effector and target cells at 37°C in 5% (v/v) CO_2 incubator, 50μL supernatants were transferred to 96-well Luma plates to be dried on the plate. The ^{51}Cr release was measured using a TopCount Microplate scintillation counter (beta scintillation counting) and the percentage of specific cytotoxicity was calculated using the following equation:

$$\text{Percentage of cytotoxicity} = \frac{(\text{Experimental release} - \text{Spontaneous release})}{(\text{Maximum release} - \text{Spontaneous release})}$$

In Vitro Peptide Re-Stimulation (IVS) of the Murine Splenocytes

Fresh splenocytes isolated from vaccinated animals were stimulated with either HAGE 30-mer long peptides, WT1 15-mer long peptides or both, at a concentration of 1μg/mL in the presence of β-mercaptoethanol and 50U/mL mIL-2 for 7 days at 37°C in a 5% (v/v) CO_2 incubator. Cells were then washed and counted using a NucleoCounter™ (Chemometec).

Tumour Model

In the prophylactic setting, mice were immunised with 1μg of gold-coated HAGE-ImmunoBody® DNA in one flank and 1μg of gold-coated WT1-ImmunoBody® DNA into the contralateral flank simultaneously once, on 3 consecutive weeks (Day-1, -7 and -14). On Day-21, mice received $0.75x10^6$ $_hB16/HAGE^+/Luc^+$. In the therapeutic setting, $0.75x10^6$ $_hB16/HAGE^+/Luc^+$ cells were first implanted and the next day mice received the double vaccine which was then followed by two additional injections 7- and 14 days post tumour implantation. A control group of mice received the same dose of tumour cells, but no vaccines. Animals were monitored twice weekly and tumour growth assessed by callipers until a palpable tumour was detected. Mice were then monitored twice weekly by *in vivo* imaging until termination. For each imaging session, luciferin was administered intraperitoneally at 150mg/kg, and anaesthesia induction began 10 minutes afterwards. All mice were anaesthetised with an appropriate concentration of isoflurane and imaged using the IVIS Lumina III system (Perkin Elmer). Mice were sacrificed when the tumour volume reached a maximum of $1.2cm^2$ for the prophylactic group and 1.5 cm^2 for the therapeutic group or show clinical signs.

Processing of B16 Tumour Tissue

Tumour Volume and Weight

Once threshold endpoints were reached, tumours were dissected, weighed and scaled. Tumour volume was measured applying the formula: Π/6 (length X width^2). Approximatively 1g of tumour was excised and enzymatically digested to study tumour-infiltrating lymphocytes (TILs), the remaining tumour was snap-frozen in liquid nitrogen.

Isolation of Tumour Infiltrating Lymphocytes (TILs)

Briefly, 1g of tumour tissue was excised from B16 tumours, chopped into small pieces using scissors and incubated with 5mL of RPMI containing 1mg/mL of collagenase-I (Sigma-Aldrich, C0130). The mixture was kept shaking at 37°C for 30 minutes to help tumour dissociation. Thereafter, the suspensions were filtered through a 70-μm filter, washed with PBS to remove the dissociation medium and re-suspended in 5mL of T cell medium. Cells ($1x10^6$) were then stained for CD8 (APC/Cy7™-conjugated anti-mouse CD8a, BioLegend, 100714, Clone: 53-6.7), CD4 (Alexa-Fluor™ 700-conjugated anti-mouse CD4, BioLegend, 100430, Clone: GK1.5), CD3 (Brilliant Violet™ 421-conjugated anti-mouse CD3, 100228, Clone: 17A2) and PD-1 (APC-conjugated anti-mouse CD279 (PD-1), 135210, Clone: 29F.1 A12), as well as ZOMBIE™ or LIVE/DEAD™ Yellow™ viability stains to exclude dead cells. TILs were then analysed by a flow cytometry.

STATISTICAL ANALYSIS

Data were analysed with GraphPad Prism7 software. The Mann-Whitney U-test was used for comparisons of two non-parametric datasets and one-way ANOVA or two-way ANOVA tests with *post hoc* testing using Tukey's multiple comparison were used for multigroup comparisons. For tumour challenge studies, the survival proportion was evaluated by both the Gehan-Breslow-Wilcoxon test and the log-rank test. For each test, P-value (probability value) was calculated, and was found to be significant if *p-value=<0.05, very significant if **p-value=<0.01 and highly significant in case ***p-value=<0.001 or ****p-value =<0.0001.

RESULTS

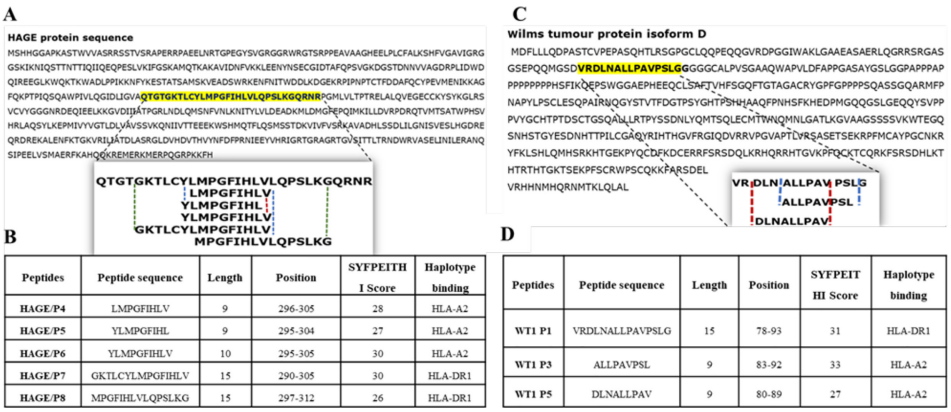
Prediction of Peptide Binding to HLA-A2 and HLA-DR1

The immunogenic region of the HAGE antigen was previously identified in our group using combination approaches of matrix-screening method of overlapping peptides and reverse immunology. It has been found that a 30-mer peptide sequence [QTGTGKTLCYLMPGFIHLVLQPSLKGQRNR]/[position: 286-316] derived from the HAGE protein is associated with high immunogenicity, as detected using an *ex-vivo* IFN-γ ELISpot assay (22). From that sequence, various short peptides were predicted to bind to HLA class I (HLA-A2) and HLA class II (HLA-DR1) using the freely available software SYFPEITHI, **Tables 2A, B**. Only HLA-A2 and HLA-DR1 restricted peptides were selected to be used in the HLA-A2/DR1 double transgenic mice (HHDII/DR1). Similarly, a 15 amino acid HLA-DR1 binding peptide [VRDLNALLPAVPSLG] derived from the WT1 protein containing two known HLA-A2 9-mer (30) was initially assessed for its binding affinity using the SYFPEITHI database (**Tables 2C, D**).

In Vitro Peptide-HLA-A*0201 Molecule Affinity and Stability

Several factors influence the capacity of peptide-MHC complexes to stimulate T cells, of which the primary two are the affinity of peptides for the MHC molecules and the cell surface stability of the peptide-MHC complex (31, 32). Although scoring of peptide binding to HLA-A2 *via* the computer algorithm predictions is useful, its accuracy is less than 70–80% (33). Therefore, the strength and stability of the interaction between the respective HAGE and WT1 class I peptides and the HLA-A2 molecules were assessed experimentally using peptide-

TABLE 2 | Class I and class II peptides sequence derived from the entire length of the HAGE and WT1 proteins.



Peptides	Peptide sequence	Length	Position	SYFPEITHI Score	Haplotype binding
HAGE/P4	LMPGFIHLV	9	296-305	28	HLA-A2
HAGE/P5	YLMPGFIHL	9	295-304	27	HLA-A2
HAGE/P6	YLMPGFIHLV	10	295-305	30	HLA-A2
HAGE/P7	GKTLCYLMPGFIHLV	15	290-305	30	HLA-DR1
HAGE/P8	MPGFIHLVLQPSLKG	15	297-312	26	HLA-DR1

Peptides	Peptide sequence	Length	Position	SYFPEITHI Score	Haplotype binding
WT1 P1	VRDLNALLPAVPSLG	15	78-93	31	HLA-DR1
WT1 P3	ALLPAVPSL	9	83-92	33	HLA-A2
WT1 P5	DLNALLPAV	9	80-89	27	HLA-A2

The entire HAGE protein sequence of 648 amino acid length, from which the long 30-mer (yellow highlighted in A) and other short 9-15-mer peptides derived from the long 30-mer are shown in A&B. This length was fully copied from NCBI website/FASTA, available at: https://www.ncbi.nlm.nih.gov/protein/Q9NXZ2.2?report=fasta. Whereas the entire WT1 protein sequence of 522 amino acid length (Isoform-D), from which the long 15-mer (yellow highlighted in C) and the two others short peptide derivatives are illustrated in C&D. This length was fully copied from NCBI website/FASTA available at: https://www.ncbi.nlm.nih.gov/protein/NP_077744.4?report=fasta.

HLA-A2 T2 binding and stability assays, respectively. Overall, data in (**Figure 1**) (A, B) demonstrate that the intensity of HLA-A2 expression as measured by Mean Fluorescence Intensity (MFI) progressively increases in a dose-dependent manner in comparison with the control (MFI produced by cells that were treated with matched doses of DMSO vehicle control), indicating a successful peptide-MHC engagement, apart from WT1/P5 which did not increase the MFI, thereby reflecting its poor binding affinity toward HLA-A2 molecules. In addition, the Fluorescence Intensity Ratio (FIR) was calculated for each peptide concentration using the MFI of HLA-A2 expressed by T2 cells incubated with peptides and the MFI of HLA-A2 expressed by T2 cells that were incubated in the absence of peptide, but with the same concentrations of DMSO as background level of HLA-A2 molecules present on the surface of T2 cells. A summary of the results is shown in **Table 3**. Peptides with FIR=1 were categorised as being non-binders, 1<FIR ≤ 1.5 as weak binders, 1.5<FIR<2 as moderate binders and 2≤FIR as strong binders. All HAGE peptides demonstrated strong binding affinity towards HLA-A2 molecules, from 30μg/mL onwards (**Figure 1A** and **Table 3**). WT1 peptide, P3, was found to be a strong binder even at 10μg/mL, whereas WT1/P5 exhibited the least binding affinity with a score of 1 (non-binder) at 10 μg/mL, and only weak binding capability (1.4 to 1.5) at the higher concentrations (**Figure 1B** and **Table 3**).

The persistence of the peptide-HLA class I complex on the cell surface was assessed in a time course manner using a Brefeldin A (BFA) assay (**Figures 1C, D**). BFA has a trap effect by obstructing anterograde transport of vesicles from the ER to the Golgi apparatus, thereby preventing peptide-MHC proteins from being transported to the cell surface. Results in **Figures 1C** show that there is a steady, time-dependent reduction in the level of MFI in all complexes within the first hours of study, but that the reduction stopped after 6 hours. With regards of the DC_{50} value, all HAGE and WT1/P3-HLA-A2 complexes on the T2 cell surface were stable as their DC_{50} values were all more than 8 hours (**Figure 1D**). However, WT1/P5-HLA-A2 complex exhibited a poor stability, as DC_{50} value fell before 6 hours.

Immunogenicity of HAGE- and WT1-ImmunoBody® Vaccines

To determine the immunogenicity of the HAGE (30mer) and WT1 (15mer) sequences and whether the predicted HLA-A2 and HLA-DR1 derived from these sequences were endogenously processed, HHDII/DR1 mice were immunised with either HAGE-ImmunoBody® or WT1-ImmunoBody® constructs on Day- 0, -7 and -14 (**Figure 2A**). On Day 21, animals were culled, and their respective spleens harvested and assessed in an *ex-vivo* IFNγ ELISpot assay. Results in **Figure 2B** confirms the immunogenicity of two class I peptides (HAGE/P5 and HAGE/P6) and one class II (HAGE/P7) in comparison to cell alone (cells that did not receive any peptide) as reflected by the high number of IFN-γ producing cells (*P-value<0.0001, n=3)*. Whereas, HAGE/P4 and HAGE/P8 peptides did not produce any IFN-γ, indicating that these peptides were not endogenously produced and presented to T cells *in vivo*. WT1-specific responses induced by a novel WT1 DNA ImmunoBody® vaccine was also assessed and the results in **Figure 2C** demonstrate the immunogenicity of WT1/P1 and WT1/P3, and the poor immunogenicity of WT1/P5.

In Vitro Recognition and Killing of CML Targets Expressing HLA-A2, HAGE and WT1 Antigens by Dual Vaccine-Induced T Cells

K562, KCL-22 and TCC-S CML cell line-derived targets were assessed for HLA-A2 expression. Histograms in **Figure 3B** shows that that only a small percentage of K562 cells naturally express HLA-A2, whereas a high percentage of KCL-22 and TCC-S cells are HLA-A2 positive (**Figures 3A, B**). Therefore, K562 cells were

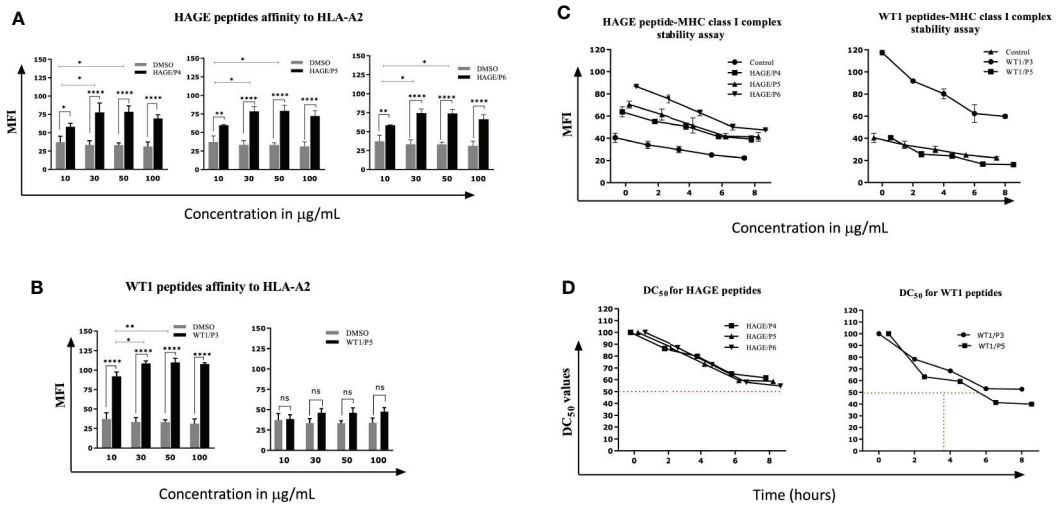


FIGURE 1 | *In vitro* determination of the HAGE and WT1 peptides-HLA-A*0201 molecule affinity and stability. The affinity of class I HAGE peptides (HAGE/P4, HAGE/P5 and HAGE/P6) shown in **(A)** and WT1 peptides (WT1/P3 and WT/P5) shown in **(B)** to bind HLA-A2 molecules in comparison to controls (DMSO-treated cells) was determined using the T2 binding assay. T2 cells were incubated with 10, 30, 50 and 100µg/mL peptide in serum-free media containing 3µg/mL human β2m overnight in a 26°C incubator. Cells were stained with an anti-HLA-A2 antibody and propidium iodide (PI), and then immediately analysed using a flow cytometer. Values are expressed as the mean ± SD of three independent experiments and the level of significance was determined using Two Way ANOVA, followed by Tukey's multiple comparisons test. Results indicate that all peptides were strong binders to MHC class I with the exception of WT1/P5. The binding stability (measured by MFI) of class I HAGE peptides and WT1 peptides shown in **(C)** in comparison to cells that were incubated with the same concentration of DMSO. DC_{50} for these peptides is shown in **(D)**. T2 cells in serum-free medium containing human β2m at 3µg/mL were incubated with 50µg/mL of the respective peptides overnight and assessed in a time course analysis for HLA-A2 expression using a flow cytometer. Values are expressed as the mean ± SD of two independent experiments. All peptide-HLA complexes studied are stable on the T2 cells surface as their DC_{50} values were > 8 hours, apart from the WT1/P5- HLA-A2 complex which shows poor stability as there was a drop in DC_{50} value earlier between 5-6 hours. *p-value=<0.05, significant; **p-value=<0.01, very significant and ****p-value=<0.0001, highly significant, ns, not significant.

electroporated with PcDNA-3.1/HHDII construct encoding the chimeric HLA-A2 gene (HHDII). **Figure 3C** demonstrates the success of HHDII transfection of K562 cells.

The constitutive expression at mRNA and protein levels of both HAGE and WT1 was then determined in all CML targets using RT-qPCR and Western blotting (**Figures 3D, E**). All cell lines expressed WT1 mRNA and protein, whereas HAGE mRNA and protein expression was only detected in TCC-S cells. Therefore, both K562/HHDII$^+$ and KCL-22 cells were then transduced with PLenti-Puro/HAGE plasmid construct, followed by antibiotic selection using puromycin to maintain HAGE expression in addition to G418, for K562/HHDII, to maintain HHDII gene expression. Post selection, the success of the transduction was demonstrated at mRNA and protein levels using RT-qPCR and Western blot (**Figures 3F, G**).

TCC-S cells were found to express HLA-A2, WT1 and HAGE proteins. It was expected that knockdown of WT1 in these cells could establish a negative control for WT1 expressing TCC-S (wild-type) upon assessing the responsiveness of WT1-specific CTLs in the cytotoxicity assay. Data in **Figure 3H** demonstrate the outcome of WT1 knockdown in TCC-S at protein level using two WT1.shRNA sequences in comparison with cells that were transfected with the lentiviral carrying the empty vector (PLKO.1.Puro), as a control vector. Although both sequences of shRNA were successful in significantly inhibiting WT1 protein expression, the WT1.shRNA.1 appeared to be more efficient than

TABLE 3 | Categorisation of the binding affinity of class I HAGE- and WT1-derived peptides toward HLA-A2 molecules, as assessed using the T2 binding assay.

Peptides	FIR obtained from various HAGE and WT1 peptide doses			
10µg/mL	30µg/mL	50µg/mL	100µg/mL	
HAGE/P4	1.8 (moderate)	2.3 (strong)	2.4 (strong)	2.3 (strong)
HAGE/P5	1.9 (moderate)	2.4 (strong)	2.4 (strong)	2.3 (strong)
HAGE/P6	1.8 (moderate)	2.3 (strong)	2.3 (strong)	2.2 (strong)
WT1/P3	2.6 (strong)	3.3 (very strong)	3.4 (very strong)	3.5 (very strong)
WT1/P5	1.0 (non)	1.4 (weak)	1.4 (weak)	1.5 (weak)

Serial doses were used to assess peptides binding affinity toward HLA-A using flow cytometry, peptides were then categorised for being a strong, moderate, and weak HLA-A2 binder according to Fluorescence Intensity Ratio (FIR).

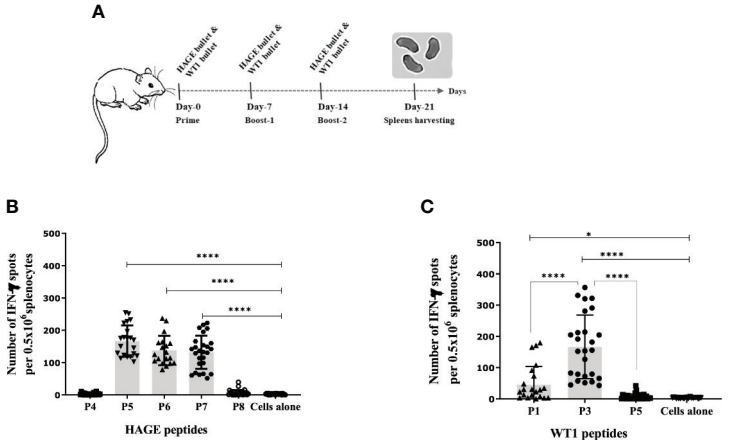


FIGURE 2 | Immunogenicity of HAGE- and WT1-ImmunoBody® vaccines, as determined using the IFN-γ ELISpot assay. Schematic presentation of ImmunoBody® immunisation regime is demonstrated in **(A)** where a prime-boost strategy was applied to assess the immunogenicity of HAGE-and WT1- ImmunoBody® administered in separate sets of mice. In this programme, each mouse received a total of three injections at 7-day intervals and spleens were then harvested on Day-21 for IFN-γ ELISpot assay. The level of IFN-γ produced by fresh 0.5x10^6 splenocytes harvested from a group of mice immunised and boosted with HAGE-ImmunoBody® **(B)** and WT1- ImmunoBody® vaccine **(C)** were assessed using the ELISpot assay. Values are expressed as the mean ± SD of at least 8 independent experiments (3 mice/group) and the level of significance was assessed using One Way ANOVA followed by Dunnett's multiple comparisons test. Results in **(B)** demonstrate the potent immunogenicity of the two class I peptides; HAGE/P5 and HAGE/P6 and one class II; HAGE/P7 in comparison to cells alone, whereas the class I HAGE/P4 and class II HAGE/P8 are shown to be poorly immunogenic. Results in **(C)** demonstrate the potent immunogenicity of WT1/P3, mild immunogenicity of WT1/P1 and poor immunogenicity of WT1/P5 in comparison with the absence of peptide 'cells alone'. *p-value=<0.05, significant and ****p-value=<0.0001, highly significant.

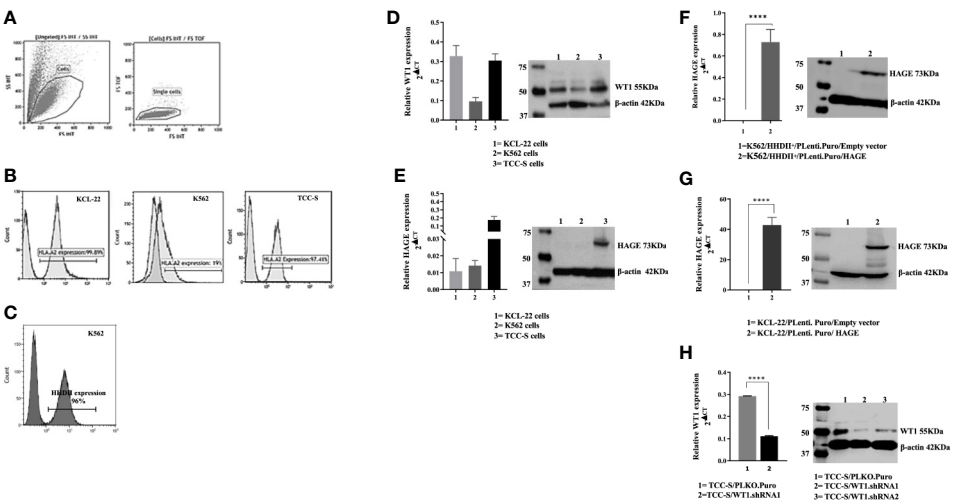


FIGURE 3 | HLA-A2, HAGE and WT1 expression in target cells: **(A)** Representative gating strategy used for the analysis of the surface expression of HLA-A2 on targets, as assessed by flow cytometry. Live cells were first gated according to their Side Scatter and Forward Scatter profile, and then single cells were selected, avoiding doublets. **(B)** The level of surface HLA-A2 expression was determined on basis of fluorescence intensity depicted by a shift to the right of the histogram in comparison to unstained samples. **(C)** Overlay histogram illustrates HLA-A2 surface expression on the targets in comparison to a negative control (non-stained sample). The constitutive expression of WT1 and HAGE by KCL-22, K562 and TCC-S cell lines using RT-qPCR and Western blot shown in **(D, E)**. HAGE is transcribed at low levels in KCL-22 and K562 cells, but protein level are high. In contrast, TCC-S cells have constitutively high HAGE transcript and protein levels. WT1 was expressed by all cells studied as detectable by transcription and and protein levels. The Success of transfection; knock-in and knockdown, seen in **(F–H)** Values of PCR are expressed as the mean ± SD of two independent experiments. The doublet on WT1 seen in the Western blot might represent WT1 isoforms resulting from an alternative splicing event. ****p-value=<0.0001, highly significant.

WT1.shRNA.2, and therefore the WT1.shRNA.1 clone was used in the cytotoxicity assay. All the modified cell types were periodically checked for the maintenance of the transduced genes.

Once all the target cells had successfully been "engineered" to express the correct HLA-A haplotype and/or antigens the ability of the vaccine induced cells to recognised and kill them was assessed. Briefly, splenocytes harvested from animals immunised with either HAGE-ImmunoBody® alone, WT1-Immunobody® alone or both were co-cultured *in vitro* with mitomycin-C treated and peptide-pulsed LPS blasts at ratio of 1:5 (LPS blast: T cell) for 6 days. Cells were then plated with ^{51}Cr labelled K562 cells at various target: effector ratios (1:100, 1:50, 1:25, and 1:12.5) for 24 hours at 37°C. Supernatants were then transferred onto Luma plates and read using a TopCount beta scintillation counter.

Figure 4 shows that *in vitro* expanded cells from all vaccinated mice were able to specifically recognise and kill all the target cells expressing the antigen against which the mice were vaccinated, **Figure 4** (A1, A2) (B1, B2) (C1, C2). Moreover, cells derived from the mice immunised with both HAGE- and WT1-ImmunoBody® vaccines could consistently kill significantly more target cells expressing both antigens indicative of a synergistic effect achieved with the combined vaccines **Figure 4** (A3, A4) (B3, B4) (C3, C4) *(P-value<0.0001, n=3)* in almost all ratios used.

In our previous studies, the B16/murine MHC knockout/HHDII+/DR1+ murine melanoma cell line was shown to constitutively express the murine WT1 protein (data not shown). Herein, these cells (with/without HAGE) were used as targets to assess the capability of HAGE- and WT1-ImmunoBody® vaccines derived cells to provoke *in vitro* killing activity. **Figure 4D** highlights the significant difference in the lysis produced by each indicated group against these cells. Here again, a statistically significant difference was found between the killing of B16 cells expressing HAGE (almost 50%) and HAGE-negative B16 (20%) at 1:100 ratio (shown in D1), whereas no differences in killing were found against these two targets when the effector cells used were derived from mice immunised with only WT1 (shown in D2), since both express murine WT1. This indicates that the WT1 peptide used in this study was endogenously processed naturally and presented on the surface of the B16 cells and was recognised by cytotoxic T lymphocytes (CTLs). Again, as for the other targets, a significantly higher percentage of B16/HAGE$^+$ cells was killed when the CTLs used were derived from mice immunised with the combined approach (**Figure 4D**, at almost 60%) than when they were derived from mice immunised with either HAGE or WT1 vaccine individually (50% and 45%, respectively). This difference is shown to be a statistically significance at 1:100 (target: effector ratio) (*P-value=0.0032, n=3* and *P-value=0.0002, n=3*) in HAGE and WT1 groups, respectively.

Overall, these findings demonstrate that the sequences contain within HAGE- and WT1-ImmunoBody® derived vaccines either individually or in combination was

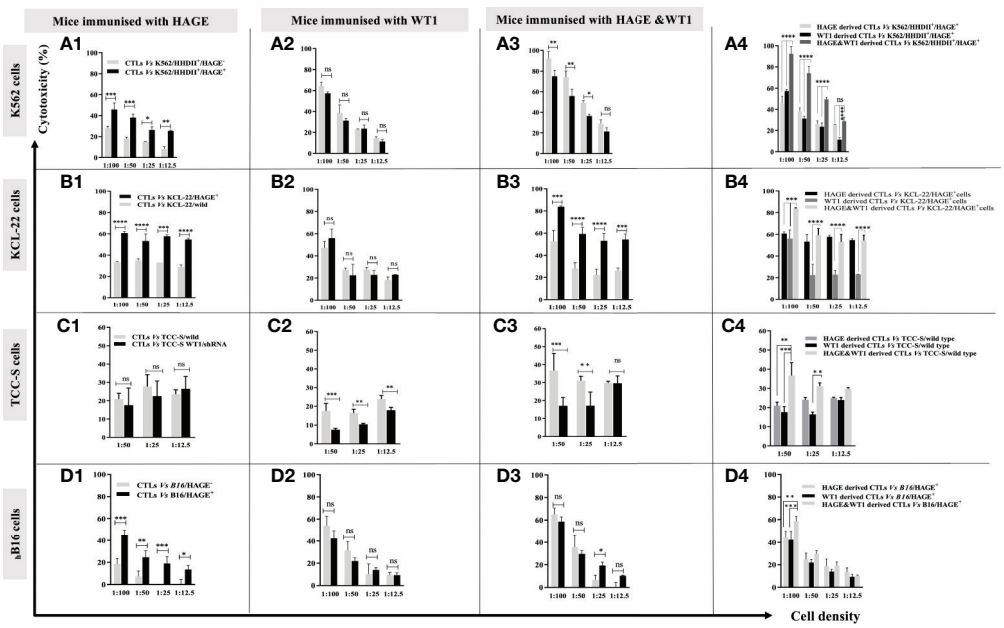


FIGURE 4 | Specific *in vitro* killing of target cells by vaccine induced CTLs, as assessed by 51Cr release assay. Splenocytes from mice immunised with HAGE, WT1 and combined, were co-cultured in vitro with mitomycin-C treated and peptide-pulsed LPS T cells for 6 days and then plated with ^{51}Cr labelled-targets at various ratios for 24 hours at 37°C, followed by measuring ^{51}Cr in the medium. Values are expressed as the mean ± SD of three independent experiments (3 mice/group) and the level of differences between groups were assessed using Two Way ANOVA followed by Tukey's multiple comparisons test. Results demonstrate that the percentage of lysis generated from combined vaccine is higher than the individual vaccines. P*-value < 0.05, **p-value < 0.01, ***p-value < 0.001, ****P-value < 0.0001 versus the corresponding control group. NS, not significant.

endogenously processed and displayed on the surface of antigen presenting cells (APCs) in association with HLA-A2 molecules leading to the development of professional CTLs which are able of specifically recognising and killing antigen-expressing target cells. They also indicate that the combination approach improves CTL responses.

Efficacy of the Combined HAGE/WT1 ImmunoBody® Vaccines in HHDII/DR1 Mice Bearing the Aggressive $_h$B16/HAGE$^+$/Luc$^+$ Tumour

The efficacy of the combined HAGE/WT1 ImmunoBody® vaccines was then tested in both prophylactic and therapeutic settings in female HHDII/DR1 mice (n=10/group) using the aggressive $_h$B16/HAGE$^+$/Luc$^+$ tumour. In the prophylactic setting, mice were first immunised with both HAGE- and WT1-ImmunoBody® vaccines 3 times, a week apart, and on Day 21 mice were then challenged with subcutaneous injection of $_h$B16/HAGE$^+$/Luc$^+$ cells, as shown in **Figure 5A**1. In the therapeutic setting, mice were first implanted with the same dose of $_h$B16/HAGE$^+$/Luc$^+$ cells, followed by immunisation the next day, and then received two more injections of the dual HAGE/WT1 ImmunoBody® vaccines 7 days apart. The control group received no vaccine (**Figures 5A2, A3**).

Details of bioluminescence images and mice culling per session are shown in **Supplementary Figure 2**. Mice that did not receive the vaccines had to be sacrificed as early as Day 39 post-implantation due to tumour size endpoints, whereas tumour growth was delayed in mice that combined vaccines in comparison to the controls (**Figure 5**). Indeed, at around day-46 post-implantation, the number of surviving mice was 8/10 (80%) for the prophylactic group and 6/10 (60%) for the therapeutic group, in comparison with only 1/10 (10%) for the control group. Tumour growth, as measure by the total luminescence flux for each group was recorded and plotted in **Figure 5B**. Eventually, 4 mice from prophylactic group (Mouse-6, Mouse-7, Mouse-9 and Mouse-10) and one mouse from the therapeutic group (Mouse-24) were the last mice to be culled. The study was then terminated on Day 56 post-implantation before the tumours reached their end point size. This was purposely done in order to be able to perform immune characterisation of the tumour

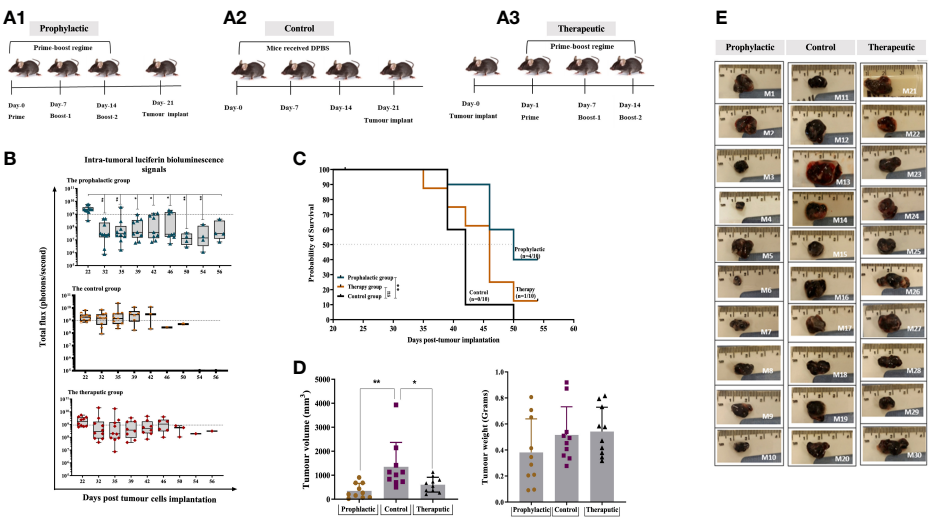


FIGURE 5 | Combined HAGE/WT1 ImmunoBody® vaccines significantly delay tumour growth in tumour challenge experiment. Schematic representation of the in vivo experimental design is shown in **(A)** where three groups of mice were used in this study using prime- boost regime. In the prophylactic setting, mice were received the vaccine then challenged with hB16/HAGE$^+$/Luc$^+$ cells on Day-21, whereas, in the therapeutic setting, tumour cells were implanted, followed by vaccination in the determined days. The control group of mice received DPBS instead of the vaccine. Intra-tumoural luciferin bioluminescent signals in the vaccinated HHDII/DR1 mice bearing the aggressive hB16/HAGE$^+$/Luc$^+$ tumour in comparison to the control are shown in **(B)**. The figure demonstrates the prophylactic and therapeutic efficacy of the combined HAGE/WT1 ImmunoBody® vaccines, wherein luciferin bioluminescent signals were detected in all groups as a total flux measured by photons/second. Data shows that the total flux in the prophylactic group and therapeutic declined in comparison with the control, and that both treatment settings led to prolong mice survival rate. Most mice from the control group were culled after Day-39 post transplantation session whereas mice in the vaccinated groups survive while they were holding small size tumour. Post-culled hB16/HAGE$^+$/Luc$^+$ tumour weight and volume are shown in **(C, D)**. For each indicated group, tumour weight in grams and tumour volume in mm3 were determined, and post-culled tumour images highlighted the tumour size shown in **(D)**. Mice were euthanized when tumour size reached endpoint threshold (12 mm2 for the prophylactic setting and 15 mm2 for the therapeutic setting). **(E)** Data in these graphs are expressed as the mean ± SD, and the level of the significance was determined using one-way ANOVA analysis followed by Dunnett's multiple comparisons test. Survival analysis demonstrates the antitumor efficacy of the combined HAGE/WT1 ImmunoBody® vaccines in vaccinated tumour bearing mice. Results shows that the combined HAGE/WT1 vaccines is significantly protective in the prophylactic group in comparison to the control group at **P-value<0.01, but not in the therapeutic setting. The significance of the difference was evaluated by both Gehan-Breslow-Wilcoxon test and log-rank test. The total number of mice is 30, (10/group). *p-value=<0.05, significant; **p-value=<0.01, very significant, ns, not significant.

infiltrating lymphocytes extracted from the growing tumour and performed functional assay on splenocytes extracted from these mice.

Interestingly, although the total luminescence flux signals, as expected, were very similar on Day 22 (one day post-transplant), 10 days later, a statistically difference between the size of the tumours for the prophylactic group and those for the control was detected. Thereafter, the size of the tumour in the prophylactic group and for the therapeutic group remained below the $1x10^9$ threshold for the majority of the tumours. However, by Day 39, tumours in a distinct group consisting of 4 mice separated from the rest of the prophylactic group, continued to grow until they had to be culled on Day 46. In the future, it would be important to re-immunise animals showing such a trend before their tumour became too large. It is also evident from the data that for 7 out of the 10 mice that received the vaccine after tumour implantation, the tumour first regressed below the $1x10^9$ threshold, whereas the size of the tumours from the control group was, for the majority, above or very near this value (with the exception of one mouse), but then by Day-39 these increased again. This demonstrates the ability of the combined vaccines to delay the growth of the tumour, but there would likely be a requirement for further vaccination on Day-39 or additional interventions, such as checkpoint inhibitor. The survival proportion in **Figure 5C** clearly demonstrates that the combined HAGE/WT1 ImmunoBody® vaccines were able to significantly delay the aggressive growth of B16 melanoma cells and increases the overall survival in the prophylactic setting in comparison to the control at ***P-value<0.01*. However, this level of efficacy was not shown in the therapeutic group.

Tumour volume and weight were measured as soon as animals were culled. Data in **Figure 5D** demonstrates that there was a significance difference in the tumour volume in the prophylactic and therapeutic group compared to the control (*P-value =0.003, n=10* and *P-value= 0.0271, n=10*), respectively, which indicates a shrinkage of the tumour, probably due to the activation of anti-B16 CTLs.

The Combined HAGE/WT1 ImmunoBody® Vaccine Provokes *In Vivo* Anti-Tumour Effector T Cell Function in HHDII/DR1 Mice Bearing $_h$B16/HAGE$^+$/Luc$^+$ Tumour

Until Day 56 post-implantation, all mice were sacrificed due to tumour size reaching the endpoint threshold, except for Mouse-6, Mouse-7, Mouse-9 and Mouse-10 from the prophylactic group and Mouse-24 from the therapeutic group. However, it was decided to terminate the study to enable the analysis of TILs and perform functional assays, such as IFN-γ ELISpot.

The immune response generated in these mice was compared with that of the IFN-γ response assessed in a set of mice culled earlier in the study, (Mouse-11, Mouse-13, Mouse-15 and Mouse-16) from the control group and one mouse from the therapeutic group (Mouse-22). Interestingly, comparing data in **Figure 6A1** *versus* **A2**, IFN-γ production was significantly greater in the surviving mice than those which were culled early in the study due to their tumour size reaching the end point. Vaccinated mice which had to be sacrificed early in the study due to tumour size (such as mouse-22) lacked the development of a specific anti-tumour immune response and therefore could not maintain tumour growth in a similar pattern as the control. IFN-γ production from spleens of these mice was also assessed after 1week *in vitro* stimulation (IVS) using the IFN-γ ELISpot assay. As demonstrated in **Figure 6A3**, IFN-γ secretion was significantly increased after IVS in comparison with those obtained straight *ex-vivo* demonstrating that these cells can be further expanded *in vitro* after *in vivo* priming.

Phenotypical Characterisation of T Cells and TILs From Mice Bearing $_h$B16/HAGE$^+$/Luc$^+$ Tumour

The profile of tumour-infiltrating lymphocytes (TILs) was assessed and compared with T cells extracted from spleens from tumour bearing mice. After each culling, a small piece of tissue was immediately digested and stained with anti-mouse CD3, CD4, CD8a and CD279 PD-1 antibodies. Thereafter, samples were assessed by flow cytometry and analysed according to the gating strategy shown **Figure 6B**. **Figures 6C, D** demonstrates the expression pattern of CD3$^+$, CD4$^+$, CD8$^+$ and PD-1 on TILs and T cells from freshly isolated splenocytes from tumour bearing mice in both treatment settings in comparison to the control group. From these data, the following points can be concluded; firstly, the majority of CD3$^+$ T cells recruited in spleens were CD4$^+$ cells, whereas the majority of CD3$^+$ T cells in all tumours studied were CD8$^+$ cells, indicating a reversal in the CD4$^+$/CD8$^+$ ratio of TILs in comparison with those derived from the spleens. Although this trend was observed regardless of whether the mice were vaccinated, the percentage of CD8$^+$ T cells within the tumour of the prophylactic and therapeutic mice was significantly higher than the control at ****P-value= 0.0003* and **P-value= 0.0323*, respectively, indicating that the combined vaccines were able to recruit more CD8$^+$ cells in the vaccinated group in both the prophylactic and therapeutic settings. Secondly, more than 60% of CD4$^+$ and CD8$^+$ TILs expressed PD-1 compared to 5-10% in the spleens, suggesting that T cells of both types CD4$^+$ and CD8$^+$ in the tumour microenvironment have been jeopardised by immunosuppressive elements, PD-1, which might be induced by immune immunosuppressive cells in the hostile B16 microenvironment. Finally, the percentage of CD4$^+$PD-1$^+$ cells in the tumour was higher in the prophylactic group at ***P-value= 0.0046* than the control.

DISCUSSION

Although the choice of antigen and peptide sequence remain crucial elements for the success of peptide-based vaccines, the adjuvant and/or delivery system and route of delivery used with these also play an important role in the intensity and duration of the response. It is now well established that long peptide vaccines are preferred to single CD8 epitopes due to their capacity to harbour multiple CD8$^+$ and CD4$^+$ T cell epitopes and bind to a wider range of HLA-haplotypes, thereby increasing their efficiency at generating durable

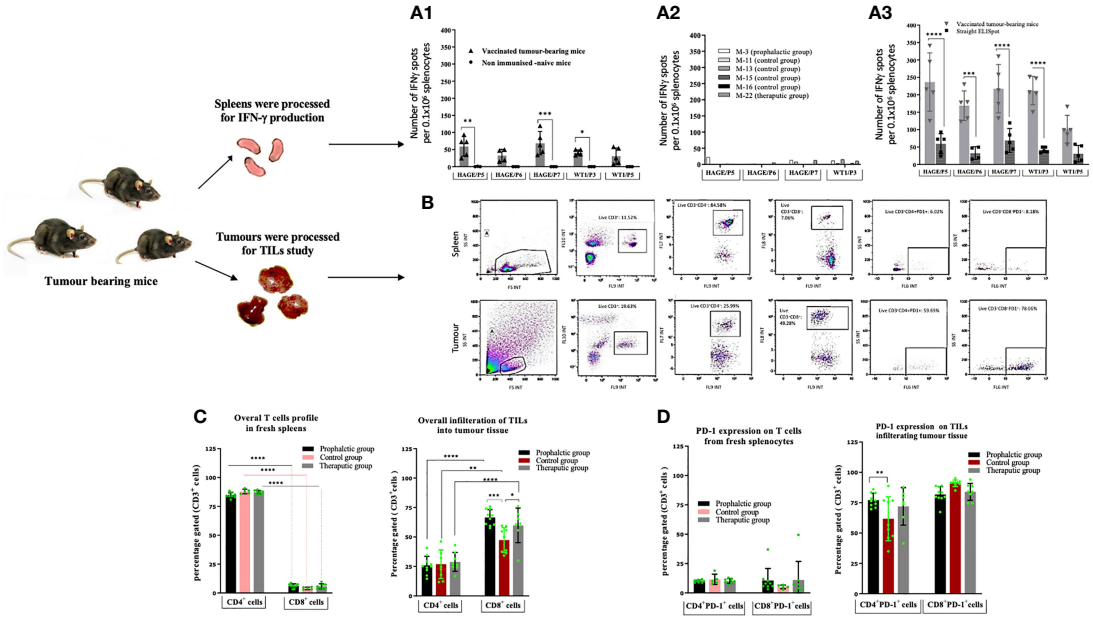


FIGURE 6 | Number of IFN-gamma symbol producing cells can be further expanded *in vitro*. Tumour induced PD-1 expression on T-cells. *Ex vivo* IFN-gamma symbol ELISpot analysis on splenocytes derived from HHDII/DR1 tumour bearing mice vaccinated by the combined HAGE/WT1 ImmunoBody® vaccines shown in **(A)**. Result of direct ELISpot assay on fresh splenocytes derived from the last surviving tumour-bearing mice from the prophylactic group (Mouse-6 ,Mouse-7 , Mouse-9 and Mouse-10) and one mice from therapeutic group (Mouse-24) shown in **(A1)** versus samples from mice culled earlier shown in **(A2)**, cells were harvested and plated at a density of 0.5x106 cells/well and re-stimulated with 1μg/mL of short peptides for 48hours. Results demonstrate that IFN-gamma symbol is much greater in the surviving mice than the control. These splenocytes were also assessed in vitro after one-week stimulation using IVS assay, wherein, cells were incubated at a density of 0.1x106 cells/well with 1ug/mL short peptides shown in **(A3)**. Results reveal that there was a significance induction of IFN-gamm symbol secretion after 1-week IVS. Data plotted as an average of spots/mouse, expressed as the mean ± SD of all 5 mice and the level of the significance was assessed using two-way ANOVA. Cells were processed and incubated with anti-mouse FcR block at 1μg/test for 15 minutes at 4°C and then stained with surface antibody; anti-CD3, -CD4, -CD8, -PD-1 and LIVE/DEAD YellowTM stain for 30 minutes at 4°C, cells were then assessed by a flow cytometry. Overall profile of T cells derived from spleens and TILs harvested from vaccinated and non-vaccinated tumour-bearing mice were analysed according to the gating strategy shown in **(B)** and the results are presented in **(C)** (for the % of T-cells) and **(D)** (for the % of PD1+). Data are expressed as the means± SD of at around 10 mice/group and the level of significance were assessed by two-way ANOVA followed by Dunnett's multiple comparisons test. Data demonstrate an inversed CD4:CD8 ratio derived from tumour in comparison to spleens and demonstrates PD-1 upregulation in the T cells derived from tumour tissues. *p-value=<0.05, significant; **p-value=<0.01, very significant; ***p-value=<0.001 and ****p-value=<0.0001, highly significant, ns, not significant

anti-tumour responses (34, 35). In addition, the targeting of multiple antigens, and epitopes therein, reduces the risk of escape variants. HAGE and WT1, have both been shown to be immunogenic (36, 37), with the HAGE long 30-mer peptide sequence [QTGTGKTLCYLMPGFIHLVLQPSLKGQRNR] having been found to be immunogenic and to encompass several immunogenic class I and class II restricted epitopes that bind to HLA-A2 and HLA-DR1 haplotypes (23). The superiority of ImmunoBody® over peptide immunisation has previously been demonstrated using several different antigens including HAGE (23, 28). Hence, the present study focused on the use of two ImmunoBody® vaccines - HAGE-ImmunoBody® and WT1-ImmunoBody® vaccine. In a similar manner, a 15 amino acid peptide [VRDLNALLPAVPSLG] derived from the WT1 protein contained two known and previously published HLA-A2 9-mers, and was selected so the efficacy of the WT1 vaccine could be studied. Here the combination of both HAGE and WT1 HLA-A2 restricted epitopes were evaluated for their MHC binding affinity *in vitro* using a T2 binding assay. Results showed that all HAGE HLA-A2 restricted peptides; HAGE/P4, HAGE/P5, and HAGE/P6 were able to stabilise HLA-A2, as was reflected by the high FIRs which correlated with the SYFPEITHI software predication of high binders. Likewise, the binding affinity of WT1 peptides to HLA-A2 was experimentally studied. WT1/P3 was found to be a very strong HLA-A2 binder, which would reasonably be expected to activate WT-1 specific T cells *in vitro* and *in vivo*. On the other hand, although WT1/P5 has a predicted SYFPEITHI score of 27, it exhibited low binding capability to HLA-A2 which was not improved with higher peptides concentrations. It was therefore categorised as being a weak HLA-A2 binder. However, while a high peptide binding affinity to MHC is associated with high frequency peptide-MHC complex production, it does not necessarily mean that these complexes will induce potent T cell activation, as in some instances peptide-MHC complexes are relatively unstable and subject to rapid recycling and endocytosis, thereby hindering T cell recognition and subsequent killing. In addition, it has been reported that the peptide-MHC stability, more than the peptide-MHC binding affinity, is linked to T cell activation (38). It was

therefore decided to study the stability of the respective peptide-MHC complex on T2 cells using DC_{50} as an indicator (the time required for a 50% reduction in the MFI), such that the higher the DC_{50} the more stable is the interaction between peptide and MHC. This study revealed that all HAGE-HLA and WT1-HLA complexes were associated with rapid dissociation within the first 6 hours of the experiment, as reflected by the drop in the MFI values, however this decline seemed to stop thereafter. As far as the DC_{50} value is concerned, the results indicated that all complexes were technically stable, as there was less than 50% reduction in MFI in comparison to time zero during the time range of the experiment (>8 hours), except for WT1/P5-HLA-A2 complex which showed poor stability as its DC_{50} value was between 5-6 hours. Collectively, the feasibility of using the candidate peptides for future experiments was validated, as they were associated with strong binding affinity toward HLA molecules as well as potential resistance to the dissociation, except for WT1/P5 which demonstrated low binding and early dissociation from HLA-A2 molecules.

The endogenous presentation of these peptide after vaccination of HHDII/DR1 mice with HAGE-ImmunoBody® and WT1-ImmunoBody® were then assessed using direct *ex vivo* IFN-γ ELISpot in order to determine the frequency of T cell responses. Class I HAGE/P5, HAGE/P6 and class II HAGE/P7 epitopes were all associated with high T cell responses. However, no specific IFN-γ response was detected for the class I peptide HAGE/P4, indicating this peptide may not be endogenously processed, despite being a strong and stable HLA-A2 binder. WT1/P3 epitope was found to elicit high number of IFN-γ producing cells in response to WT1-ImmunoBody® vaccination while WT1/P5 peptide was not recognised by the vaccine-induced splenocytes as indicated by a lack of IFN-γ production.

The capability of HAGE/WT1-ImmunoBody® induced T cells to recognise and kill HAGE and WT1 expressing leukaemia cells was then assessed using *in vitro* cytotoxicity assays. For this purpose, three CML cell lines were chosen, K562, KCL-22 and TCC-S cells. TCC-S and KCL-22 cells were found to express HLA-A2, unlike K562, therefore the latter was transfected with the chimeric HHDII construct to be compatible with HHDII/DR1 mice. In addition, as both K562 and KCL-22 cells do not express HAGE, they were transduced with the HAGE construct. All cell lines expressed WT1. TCC-S cells were the only cells found to express HAGE, WT1 and HLA-A2. Some of these cells were transfected with shRNA for WT1 to produce TCC-S-HAGE^{+}/WT1^{Low} cells. Splenocytes derived from HAGE/WT1-ImmunoBody® vaccinated animals were stimulated once *in vitro*. These splenocytes were able to recognise and kill targets in an antigen dependant manner. Interestingly, although the number of IFN-γ producing cells generated with either vaccine alone was similar to those generated when both were used simultaneously, the combined vaccine led to a significant increase in cell killing compared to either vaccines alone. Importantly, the level of HAGE protein detected in the transduced cell lines was similar to that of the naturally HAGE expressing TCC-S cells.

In the absence of an available murine CML model that can be used in the HLA transgenic mice we tested the efficacy of this combination in *in vivo* tumour challenge experiments, wherein a pre-defined dose of the modified $_{h}$B16/HAGE^{+}/Luc^{+} cells, which also endogenously express WT1, was injected subcutaneously as a "Proof-of-Concept" to form tumour. The combination vaccines were assessed in prophylactic and therapeutic trial. This melanoma-derived tumour model is obviously far from ideal being a solid tumour with a very different tumour microenvironment to that of a blood-derived cancer. Therefore one should be careful in translating the findings obtained here to leukaemia. Nonetheless, results showed that the combination of HAGE- and WT1-ImmunoBody® was able to significantly delay tumour growth and prolong mouse survival when compared to mice in the control group. Indeed, mice that did not receive the vaccines exhibited faster growing tumours than those that received the vaccines and had to be sacrificed earlier due to the endpoint tumour size being reached. Interestingly, while the vast majority of mice in the prophylactic group developed a slow growing tumour, a distinct group of four mice exhibited faster tumour growth and these had to be culled earlier than the remaining six mice. Having seen such pattern of tumour development detected by bioluminescent imaging, it would be important, in the future, to continue administering the vaccines to the animals showing such a trend before the tumour size becomes too big. The mice in the therapeutic group exhibited a reduction in tumour size while the immunisation regime was ongoing, but as soon as the last injection of the vaccine was performed, the tumour started to grow, highlighting the fine balance between the efficacy of the vaccine and the increasing immunosuppression of the microenvironment as described by Schreiber's group (39).

Comparing the outcomes of the present study with our previous studies using either HAGE- or WT1-ImmunoBody® vaccination programme as a monotherapy (data not shown), the combined HAGE/WT1 ImmunoBody® vaccines used herein were found to further improve the delay in the tumour growth in pre-immunised mice, but also and importantly, to delay tumour growth in a significant proportion of mice even when the vaccines were used after tumour implantation. Significance was not achieved when either vaccine was used on their own. These observations highlight the importance of incorporating epitopes from both HAGE and WT1 epitopes in future immunotherapy strategies. Moreover, this novel combination was found to induce notable HAGE- and WT1-specific T cells in the tumour bearing mice which were culled later in the experiment. This was in comparison to the mice that were euthanised early in the study in order to assess the IFN-γ ELISpot assay on splenocytes derived from the immunised mice so examination could occur before too much immunosuppression could interfere with the results.

Immunophenotypic analysis on TILs and splenocytes isolated from mice from different groups using flow cytometry demonstrated a clear reverse in the CD4^{+}/CD8^{+} ratio of TILs in comparison with those derived from the spleens. Whereas the

majority of $CD3^+$ T cells in the spleens were $CD4^+$ (80%), more than 75% of them were $CD8^+$ T cells in the tumours. The high percent of recruited $CD8^+$ cells were found in both vaccinated and non-vaccinated mice, thereby indicating that B16 tumour cells were being recognised as non-self probably due to the presence of HAGE and the luciferase reporter gene; the latter has been reported to induce immunogenicity in mice tumours (40, 41). However, the frequency of $CD8^+$ TILs isolated from mice that were vaccinated with combined vaccines in the prophylactic and the therapeutic settings was significantly higher than those derived from the control group, indicating that these cells were the principal T cell type involved in controlling tumour growth.

We also noted that the $CD4^+$ and $CD8^+$ TILs that trafficked through the $_h$B16/HAGE$^+$/Luc$^+$ tumour model exhibited a remarkable upregulation of PD-1 that was independent of the immunisations. PD-1 expression is promptly induced on T cell after TCR activation (42), and this expression is temporary, and declines when immunogen is cleared. PD-1 is, however, maintained and becomes persistently expressed on antigen-specific T cells in cancer or chronic disease (43) leading to functional impairment of $CD8^+$ T-cells (44). As B16 expresses PD-L1 (PD-1 ligand), it is possible that the PD-1/PD-L1 pathway was activated and that this could be attributed to the modest efficacy noticed in the therapeutic setting. However, the prophylactic setting demonstrated significant benefits in terms of prolonged mouse survival and resistance to tumour growth, despite the upregulation of PD-1 on TILs. This suggests the occurrence of other mechanisms that could enable the combined vaccines in the prophylactic treatment to overcome PD-1/PD-L1 pathway activity. Because of the modest response seen in the therapeutic setting, we would recommend the incorporation of anti-PD-1/anti-PD-L1 in combination with novel vaccines to study whether a further enhancement of the anti-tumour effect that could be obtained.

CONCLUSIONS

The present study revealed that the combined HAGE and WT1 vaccine was more effective than either vaccine alone, demonstrating the superiority of combination HAGE- and WT1- ImmunoBody® vaccines. CTLs generated using this combination were also shown to specifically recognise and kill relevant targets.

The WT1 sequence used in this study was completely human and differs from the murine WT1 by a single amino-acid. Although this had no consequence when used in double transgenic mice, the same vaccine failed to generate any detectable immune responses in syngeneic C57BL/6 mice (Joshua Pearson, personal communication).

Although the observed delayed growth of the implanted tumour cells was only significant in the prophylactic study, these results also showed that the mice would have benefitted from a more sustained vaccination strategy. Moreover, the fact that B16 cells are PD-L1 positive and that $CD3^+$ T cells were also positive for PD-1, means that one should consider continued vaccinations post-tumour implantation, as well as consider the inclusion of anti-PD-1 antibody therapy.

Overall, the data presented herein support the development of vaccine strategies based on a combination of both HAGE- and WT1-ImmunoBody® vaccines which could be further improved with the use of immune checkpoint inhibitors.

DATA AVAILABILITY STATEMENT

The original contributions presented in the study are included in the article/**Supplementary Material**. Further inquiries can be directed to the corresponding author.

ETHICS STATEMENT

Pre-clinical studies were approved by the Home Office under the Animals (Scientific Procedures) Act under two Project Licences (PPL): 1. 40/3563 valid until the 5th December 2016 2. PB26CF602, granted on the 28th of November 2016 and valid until the 28th of November 2021.

AUTHOR CONTRIBUTIONS

RA and SM contributed to the conception and design of the study. RA preformed the experiments. RA, SM, DN and JV contributed to the development of the methodology. SM and SR helped by labelling targets with chromium, RA and SM analysed the data and wrote the paper. VB, RM and LD provide the vaccines. AP and B-aG revised and corrected the manuscript. All authors contributed to the article and approved the submitted version.

ACKNOWLEDGMENTS

The authors thank Mrs. Anne Schneider for her assistance in this study. We would like to also thank The Higher Committee for Education Development in Iraq for funding. Thanks should also go to Adam McVicar, Andrew Marr, Joseph Lenton and Murrium Ahmad for technical support.

SUPPLEMENTARY MATERIAL

The Supplementary Material for this article can be found online at: https://www.frontiersin.org/articles/10.3389/fonc.2021.636977/full#supplementary-material

Supplementary Figure 1 | HAGE and WT1 expression in CML stem cells and normal stem cells. CML single cell (SC) gene expression data was downloaded from GEO database (Acc. No. GSE76312, Giustacchini et al 2017), All data from single cell CML cell line were removed from the matrix prior to the analysis. Single cell gene

expression data was available for 1964 patient derived CML cells and 232 Normal Hematopoietic cells (HSC). Gene expression values (RPKM) of CD34, CD38, HAGE and WT1 genes were extracted from the data matrix and matched up with the patient identities and clinical information. Values greater than 1RPKM were considered as a positive expression. Both HAGE and WT1 expression on single cells was shown to vary within patients with some cells express very high level of HAGE while others do not. No expression was detected in HSC cells for both WT1 and HAGE expression highlightinh their tumour cell specific expression.

Supplementary Figure 2 | Sequential, real-time in vivo analysis of tumour burden in live animals assessed by Perkin Elmer IVIS Lumina III system. The figure reflects intra-tumoral luciferin bioluminescence signals in anesthetised HHDII/DR1 mice bearing $_{h}$B16/HAGE^{+}/Luc^{+} tumour. Images from different groups point out a decline in tumour size and prolonged mice survival in vaccinated group in comparison with control. Colours overlying mice represent the rate of photons emission of the luciferin per second, wherein, red refers to the highest photons density and violet corresponding to the least detectable emission.

REFERENCES

1. Metheringham RL, Pudney VA, Gunn B, Towey M, Spendlove I, Durrant LG. Antibodies Designed as Effective Cancer Vaccines. *MAbs* (2009) 1(1):71–85. doi: 10.4161/mabs.1.1.7492
2. Patel PM, Ottensmeier CH, Mulatero C, Lorigan P, Plummer R, Pandha H, et al. Targeting gp100 and TRP-2 With a DNA Vaccine: Incorporating T Cell Epitopes With a Human IgG1 Antibody Induces Potent T Cell Responses That are Associated With Favourable Clinical Outcome in a Phase I/II Trial. *Oncoimmunology* (2018) 7 (6):e1433516. doi: 10.1080/2162402X.2018.1433516
3. Xue W, Metheringham RL, Brentville VA, Gunn B, Symonds P, Yagita H, et al. SCIB2, an Antibody DNA Vaccine Encoding NY-ESO-1 Epitopes, Induces Potent Antitumor Immunity Which is Further Enhanced by Checkpoint Blockade. *Oncoimmunology* (2016) 5(6):e1169353. doi: 10.1080/2162402X.2016.1169353
4. Coosemans A, Nik SA, Caluwaerts S, Lambin S, Verbist G, Van Bree R, et al. Upregulation of Wilms' Tumour Gene 1 (WT1) in Uterine Sarcomas. *Eur J Cancer* (2007) 43(10):1630–7. doi: 10.1016/j.ejca.2007.04.008
5. Shimizu M, Toki T, Takagi Y, Konishi I, Fujii S. Immunohistochemical Detection of the Wilms' Tumor Gene (WT1) in Epithelial Ovarian Tumors. *Int J Gynecol Pathol* (2000) 19(2):158–63. doi: 10.1097/00004347-200004000-00010
6. Inoue K, Ogawa H, Sonoda Y, Kimura T, Sakabe H, Oka Y, et al. Aberrant Overexpression of the Wilms Tumor Gene (WT1) in Human Leukemia. *Blood* (1997) 89(4):1405–12. doi: 10.1158/1078-0432.CCR-09-0737
7. Cheever MA, Allison JP, Ferris AS, Finn OJ, Hastings BM, Hecht TT, et al. The prioritization of cancer antigens: a national cancer institute pilot project for the acceleration of translational research. *Clin Cancer Res* (2009) 15 (17):5323–37. doi: 10.1158/1078-0432.CCR-09-0737
8. Cilloni D, Gottardi E, De Micheli D, Serra A, Volpe G, Messa F, et al. Quantitative Assessment of WT1 Expression by Real Time Quantitative PCR may be a Useful Tool for Monitoring Minimal Residual Disease in Acute Leukemia Patients. *Leukemia* (2002) 16(10):2115–21. doi: 10.1038/sj.leu.2402675
9. Rosenfeld C, Cheever MA, Gaiger A. WT1 in Acute Leukemia, Chronic Myelogenous Leukemia and Myelodysplastic Syndrome: Therapeutic Potential of WT1 Targeted Therapies. *Leukemia* (2003) 17(7):1301–12. doi: 10.1038/sj.leu.2402988
10. Miyagi T, Ahuja H, Kubota T, Kubonishi I, Koeffler HP, Miyoshi I. Expression of the Candidate Wilm's Tumor Gene, WT1, in Human Leukemia Cells. *Leukemia* (1993) 7(7):970–7.
11. Mathieu MG, Linley AJ, Reeder SP, Badoual C, Tartour E, Rees RC, et al. HAGE, a Cancer/Testis Antigen Expressed At the Protein Level in a Variety of Cancers. *Cancer Immun* (2010) 10:2.
12. Adams SP, Sahota SS, Mijovic A, Czepulkowski B, Padua RA, Mufti GJ, et al. Frequent Expression of HAGE in Presentation Chronic Myeloid Leukaemias. *Leukemia* (2002) 16:2238–42. doi: 10.1038/sj.leu.2402732
13. Almeida LG, Sakabe NJ, deOliveira AR, Silva MC, Mundstein AS, Cohen T, et al. Ctdatabase: A Knowledge-Base of High-Throughput and Curated Data On Cancer-Testis Antigens. *Nucleic Acids Res* (2009) 37(Database issue): D816–9. doi: 10.1093/nar/gkn673
14. Bruggeman JW, Koster J, Lodder P, Repping S, Hamer G. Massive Expression of Germ Cell-Specific Genes is a Hallmark of Cancer and a Potential Target for Novel Treatment Development. *Oncogene* (2018) 37:5694–700. doi: 10.1038/s41388-018-0357-2
15. Druker BJ, Guilhot F, O'Brien SG, Gathmann I, Kantarjian H, Gattermann N, et al. Five-Year Follow-Up of Patients Receiving Imatinib for Chronic Myeloid Leukemia. *N Engl J Med* (2006) 355(23):2408–17. doi: 10.1056/NEJMoa062867
16. Hochhaus A, Larson RA, Guilhot F, Radich JP, Branford S, Hughes TP, et al. Long-Term Outcomes of Imatinib Treatment for Chronic Myeloid Leukemia. *N Engl J Med* (2017) 376(10):917–27. doi: 10.1056/NEJMoa1609324
17. Massimino M, Stella S, Tirro E, Pennisi MS, Vitale SR, Puma A, et al. Abl1-Directed Inhibitors for CML: Efficacy, Resistance and Future Perspectives. *Anticancer Res* (2020) 40(5):2457–65. doi: 10.21873/anticanres.14215
18. Dikic I, Elazar Z. Mechanism and Medical Implications of Mammalian Autophagy. *Nat Rev Mol Cell Biol* (2018) 19(6):349–64. doi: 10.1038/s41580-018-0003-4
19. Zitvogel L, Rusakiewicz S, Routy B, Ayyoub M, Kroemer G. Immunological Off-Target Effects of Imatinib. *Nat Rev Clin Oncol* (2016) 13(7):431–46. doi: 10.1038/nrclinonc.2016.41
20. Giustacchini A, Thongjuea S, Barkas N, Woll PS, Povinelli BJ, Booth CAG, et al. Single-Cell Transcriptomics Uncovers Distinct Molecular Signatures of Stem Cells in Chronic Myeloid Leukemia. *Nat Med* (2017) 23(6):692–702. doi: 10.1038/nm.4336
21. Doria-Rose NA, Haigwood NL. DNA Vaccine Strategies: Candidates for Immune Modulation and Immunization Regimens. *Methods* (2003) 31 (3):207–16. doi: 10.1016/s1046-2023(03)00135-x
22. Salter RD, Cresswell P. Impaired Assembly and Transport of HLA-A and -B Antigens in a Mutant TxB Cell Hybrid. *EMBO J* (1986) 5(5):943–9. doi: 10.1002/j.1460-2075.1986.tb04307.x
23. Nagarajan D, Pearson J, Brentville V, Metheringham R, Ahmad M, Durrant L, et al. ImmunoBody®-HAGE Derived Vaccine Induces Immunity to HAGE and Delays the Growth and Metastasis of HAGE-expressing Tumours In Vivo. *Immunol Cell Biol* (2021).
24. Rammensee H, Bachmann J, Emmerich NP, Bachor OA, Stevanovic S. SYFPEITHI: Database for MHC Ligands and Peptide Motifs. *Immunogenetics* (1999) 50(3-4):213–9. doi: 10.1007/s002510050595
25. van der Burg SH, Visseren MJ, Brandt RM, Kast WM, Melief CJ. Immunogenicity of Peptides Bound to MHC Class I Molecules Depends on the MHC-peptide Complex Stability. *J Immunol* (1996) 156(9):3308–14.
26. Chen F, Zhai MX, Zhu YH, Qi YM, Zhai WJ, Gao YF. In Vitro and In Vivo Identification of a Novel Cytotoxic T Lymphocyte Epitope From Rv3425 of Mycobacterium Tuberculosis. *Microbiol Immunol* (2012) 56(8):548–53. doi: 10.1111/j.1348-0421.2012.00470.x
27. Schmittgen TD, Livak KJ. Analyzing Real-Time PCR Data by the Comparative C(T) Method. *Nat Protoc* (2008) 3(6):1101–8. doi: 10.1038/nprot.2008.73
28. Pudney VA, Metheringham RL, Gunn B, Spendlove I, Ramage JM, Durrant LG. DNA Vaccination With T-cell Epitopes Encoded Within Ab Molecules Induces High-Avidity Anti-Tumor CD8+ T Cells. *Eur J Immunol* (2010) 40 (3):899–910. doi: 10.1002/eji.200939857
29. Saif JM, Vadakekolathu J, Rane SS, McDonald D, Ahmad M, Mathieu M, et al. Novel Prostate Acid Phosphatase-Based Peptide Vaccination Strategy Induces Antigen-Specific T-cell Responses and Limits Tumour Growth in Mice. *Eur J Immunol* (2014) 44(4):994–1004. doi: 10.1002/eji.201343863
30. Pinilla-Ibarz J, May RJ, Korontsvit T, Gomez M, Kappel B, Zakhaleva V, et al. Improved Human T-cell Responses Against Synthetic HLA-0201 Analog Peptides Derived From the WT1 Oncoprotein. *Leukemia* (2006) 20 (11):2025–33. doi: 10.1038/sj.leu.2404380
31. Baker BM, Gagnon SJ, Biddison WE, Wiley DC. Conversion of a T Cell Antagonist Into an Agonist by Repairing a Defect in the TCR/peptide/MHC Interface: Implications for TCR Signaling. *Immunity* (2000) 13(4):475–84. doi: 10.1016/s1074-7613(00)00047-9
32. Holler PD, Kranz DM. Quantitative Analysis of the Contribution of TCR/pepMHC Affinity and CD8 to T Cell Activation. *Immunity* (2003) 18(2):255–64. doi: 10.1016/s1074-7613(03)00019-0

33. Dao T, Korontsvit T, Zakhaleva V, Jarvis C, Mondello P, Oh C, et al. An Immunogenic WT1-derived Peptide That Induces T Cell Response in the Context of HLA-A*02:01 and HLA-A*24:02 Molecules. *Oncoimmunology* (2017) 6(2):e1252895. doi: 10.1080/2162402X.2016.1252895
34. Melief CJ, van der Burg SH. Immunotherapy of Established (Pre)Malignant Disease by Synthetic Long Peptide Vaccines. *Nat Rev Cancer* (2008) 8(5):351–60. doi: 10.1038/nrc2373
35. Slingluff CLJr. The Present and Future of Peptide Vaccines for Cancer: Single or Multiple, Long or Short, Alone or in Combination? *Cancer J* (2011) 17 (5):343–50. doi: 10.1097/PPO.0b013e318233e5b2
36. Mathieu MG, Knights AJ, Pawelec G, Riley CL, Wernet D, Lemonnier FA, et al. HAGE, a Cancer/Testis Antigen With Potential for Melanoma Immunotherapy: Identification of Several MHC Class I/II HAGE-Derived Immunogenic Peptides. *Cancer Immunol Immunother* (2007) 56(12):1885–95. doi: 10.1007/s00262-007-0331-2
37. Sugiyama H. Wt1 (Wilms' Tumor Gene 1): Biology and Cancer Immunotherapy. *Jpn J Clin Oncol* (2010) 40(5):377–87. doi: 10.1093/jjco/hyp194
38. Harndahl M, Rasmussen M, Roder G, Dalgaard Pedersen I, Sorensen M, Nielsen M, et al. Peptide-MHC Class I Stability is a Better Predictor Than Peptide Affinity of CTL Immunogenicity. *Eur J Immunol* (2012) 42(6):1405–16. doi: 10.1002/eji.201141774
39. Dunn GP, Old LJ, Schreiber RD. The Three Es of Cancer Immunoediting. *Annu Rev Immunol* (2004) 22:329–60. doi: 10.1146/annurev.immunol.22.012703.104803
40. Contag CH, Ross BD. It's Not Just About Anatomy: In Vivo Bioluminescence Imaging as an Eyepiece Into Biology. *J Magn Reson Imaging* (2002) 16(4):378–87. doi: 10.1002/jmri.10178
41. Hollingshead MG, Bonomi CA, Borgel SD, Carter JP, Shoemaker R, Melillo G, et al. A Potential Role for Imaging Technology in Anticancer Efficacy Evaluations. *Eur J Cancer* (2004) 40(6):890–8. doi: 10.1016/j.ejca.2003.12.018
42. Chikuma S, Terawaki S, Hayashi T, Nabeshima R, Yoshida T, Shibayama S, et al. Pd-1-mediated Suppression of IL-2 Production Induces CD8+ T Cell Anergy In Vivo. *J Immunol* (2009) 182(11):6682–9. doi: 10.4049/jimmunol.0900080
43. Youngblood B, Oestreich KJ, Ha SJ, Duraiswamy J, Akondy RS, West EE, et al. Chronic Virus Infection Enforces Demethylation of the Locus That Encodes PD-1 in Antigen-Specific CD8(+) T Cells. *Immunity* (2011) 35(3):400–12. doi: 10.1016/j.immuni.2011.06.015
44. Brentville VA, Metheringham RL, Gunn B, Durrant LG. High Avidity Cytotoxic T Lymphocytes can be Selected Into the Memory Pool But They are Exquisitely Sensitive to Functional Impairment. *PloS One* (2012) 7(7): e41112. doi: 10.1371/journal.pone.0041112

Conflict of Interest: LD is a director and shareholder of Scancell Ltd and is a named inventor on the ImmunoBody patents. VB and RM were employed by Scancell Ltd.

The remaining authors declare that the research was conducted in the absence of any commercial or financial relationships that could be construed as a potential conflict of interest.

Copyright © 2021 Almshayakhchi, Nagarajan, Vadakekolathu, Guinn, Reeder, Brentville, Metheringham, Pockley, Durrant and McArdle. This is an open-access article distributed under the terms of the Creative Commons Attribution License (CC BY). The use, distribution or reproduction in other forums is permitted, provided the original author(s) and the copyright owner(s) are credited and that the original publication in this journal is cited, in accordance with accepted academic practice. No use, distribution or reproduction is permitted which does not comply with these terms.

Advantages of publishing in Frontiers

OPEN ACCESS
Articles are free to read for greatest visibility and readership

FAST PUBLICATION
Around 90 days from submission to decision

HIGH QUALITY PEER-REVIEW
Rigorous, collaborative, and constructive peer-review

TRANSPARENT PEER-REVIEW
Editors and reviewers acknowledged by name on published articles

Frontiers
Avenue du Tribunal-Fédéral 34
1005 Lausanne | Switzerland

Visit us: www.frontiersin.org
Contact us: frontiersin.org/about/contact

REPRODUCIBILITY OF RESEARCH
Support open data and methods to enhance research reproducibility

DIGITAL PUBLISHING
Articles designed for optimal readership across devices

FOLLOW US
@frontiersin

IMPACT METRICS
Advanced article metrics track visibility across digital media

EXTENSIVE PROMOTION
Marketing and promotion of impactful research

LOOP RESEARCH NETWORK
Our network increases your article's readership